# EPIGENETIC VARIATION INFLUENCES ON LIVESTOCK PRODUCTION AND DISEASE TRAITS

EDITED BY: Eveline M. Ibeagha-Awemu, Hélène Kiefer, Stephanie McKay and George E. Liu

PUBLISHED IN: Frontiers in Genetics and Frontiers in Cell and Developmental Biology



frontiers Research Topics



# frontiers

**Frontiers eBook Copyright Statement**

The copyright in the text of individual articles in this eBook is the property of their respective authors or their respective institutions or funders. The copyright in graphics and images within each article may be subject to copyright of other parties. In both cases this is subject to a license granted to Frontiers.

The compilation of articles constituting this eBook is the property of Frontiers.

Each article within this eBook, and the eBook itself, are published under the most recent version of the Creative Commons CC-BY licence. The version current at the date of publication of this eBook is CC-BY 4.0. If the CC-BY licence is updated, the licence granted by Frontiers is automatically updated to the new version.

When exercising any right under the CC-BY licence, Frontiers must be attributed as the original publisher of the article or eBook, as applicable.

Authors have the responsibility of ensuring that any graphics or other materials which are the property of others may be included in the CC-BY licence, but this should be checked before relying on the CC-BY licence to reproduce those materials. Any copyright notices relating to those materials must be complied with.

Copyright and source acknowledgement notices may not be removed and must be displayed in any copy, derivative work or partial copy which includes the elements in question.

All copyright, and all rights therein, are protected by national and international copyright laws. The above represents a summary only. For further information please read Frontiers' Conditions for Website Use and Copyright Statement, and the applicable CC-BY licence.

ISSN 1664-8714
ISBN 978-2-88976-533-1
DOI 10.3389/978-2-88976-533-1

## About Frontiers

Frontiers is more than just an open-access publisher of scholarly articles: it is a pioneering approach to the world of academia, radically improving the way scholarly research is managed. The grand vision of Frontiers is a world where all people have an equal opportunity to seek, share and generate knowledge. Frontiers provides immediate and permanent online open access to all its publications, but this alone is not enough to realize our grand goals.

## Frontiers Journal Series

The Frontiers Journal Series is a multi-tier and interdisciplinary set of open-access, online journals, promising a paradigm shift from the current review, selection and dissemination processes in academic publishing. All Frontiers journals are driven by researchers for researchers; therefore, they constitute a service to the scholarly community. At the same time, the Frontiers Journal Series operates on a revolutionary invention, the tiered publishing system, initially addressing specific communities of scholars, and gradually climbing up to broader public understanding, thus serving the interests of the lay society, too.

## Dedication to Quality

Each Frontiers article is a landmark of the highest quality, thanks to genuinely collaborative interactions between authors and review editors, who include some of the world's best academicians. Research must be certified by peers before entering a stream of knowledge that may eventually reach the public - and shape society; therefore, Frontiers only applies the most rigorous and unbiased reviews.
Frontiers revolutionizes research publishing by freely delivering the most outstanding research, evaluated with no bias from both the academic and social point of view. By applying the most advanced information technologies, Frontiers is catapulting scholarly publishing into a new generation.

## What are Frontiers Research Topics?

Frontiers Research Topics are very popular trademarks of the Frontiers Journals Series: they are collections of at least ten articles, all centered on a particular subject. With their unique mix of varied contributions from Original Research to Review Articles, Frontiers Research Topics unify the most influential researchers, the latest key findings and historical advances in a hot research area! Find out more on how to host your own Frontiers Research Topic or contribute to one as an author by contacting the Frontiers Editorial Office: frontiersin.org/about/contact

# EPIGENETIC VARIATION INFLUENCES ON LIVESTOCK PRODUCTION AND DISEASE TRAITS

Topic Editors:
**Eveline M. Ibeagha-Awemu,** Agriculture and Agri-Food Canada (AAFC), Canada
**Hélène Kiefer,** INRAE Centre Jouy-en-Josas, France
**Stephanie McKay,** University of Vermont, United States
**George E. Liu,** United States Department of Agriculture, United States

**Citation:** Ibeagha-Awemu, E. M., Kiefer, H., McKay, S., Liu, G. E., eds. (2022). Epigenetic Variation Influences on Livestock Production and Disease Traits. Lausanne: Frontiers Media SA. doi: 10.3389/978-2-88976-533-1

# Table of Contents


06 ***Editorial: Epigenetic Variation Influences on Livestock Production and Disease Traits***
Eveline M. Ibeagha-Awemu, Hélène Kiefer, Stephanie McKay and George E. Liu

10 ***Thermal Manipulation During Embryogenesis Impacts H3K4me3 and H3K27me3 Histone Marks in Chicken Hypothalamus***
Sarah-Anne David, Anaïs Vitorino Carvalho, Coralie Gimonnet, Aurélien Brionne, Christelle Hennequet-Antier, Benoît Piégu, Sabine Crochet, Nathalie Couroussé, Thierry Bordeau, Yves Bigot, Anne Collin and Vincent Coustham

21 ***Epigenetic Reprogramming During Somatic Cell Nuclear Transfer: Recent Progress and Future Directions***
Xiangyu Wang, Jiadan Qu, Jie Li, Hongbin He, Zhonghua Liu and Yanjun Huan

34 ***Sperm DNA Hypomethylation Proximal to Reproduction Pathway Genes in Maturing Elite Norwegian Red Bulls***
Abdolrahman Khezri, Birgitte Narud, Else-Berit Stenseth, Teklu Tewoldebrhan Zeremichael, Frøydis Deinboll Myromslien, Robert C. Wilson, Rafi Ahmad and Elisabeth Kommisrud

48 ***Accelerating Onset of Puberty Through Modification of Early Life Nutrition Induces Modest but Persistent Changes in Bull Sperm DNA Methylation Profiles Post-puberty***
Jean-Philippe Perrier, David A. Kenny, Aurélie Chaulot-Talmon, Colin J. Byrne, Eli Sellem, Luc Jouneau, Anne Aubert-Frambourg, Laurent Schibler, Hélène Jammes, Patrick Lonergan, Sean Fair and Hélène Kiefer

63 ***The Profiling of DNA Methylation and Its Regulation on Divergent Tenderness in Angus Beef Cattle***
Chunping Zhao, Guanyu Ji, José A. Carrillo, Yaokun Li, Fei Tian, Ransom L. Baldwin VI, Linsen Zan and Jiuzhou Song

75 ***Integrated Transcriptome and Histone Modification Analysis Reveals NDV Infection Under Heat Stress Affects Bursa Development and Proliferation in Susceptible Chicken Line***
Ganrea Chanthavixay, Colin Kern, Ying Wang, Perot Saelao, Susan J. Lamont, Rodrigo A. Gallardo, Gonzalo Rincon and Huaijun Zhou

93 ***Parental Effects on Epigenetic Programming in Gametes and Embryos of Dairy Cows***
Chongyang Wu and Marc-André Sirard

106 ***Genome-Wide DNA Methylation Analysis of Mammary Gland Tissues From Chinese Holstein Cows With* Staphylococcus aureus *Induced Mastitis***
Mengqi Wang, Yan Liang, Eveline M. Ibeagha-Awemu, Mingxun Li, Huimin Zhang, Zhi Chen, Yujia Sun, Niel A. Karrow, Zhangping Yang and Yongjiang Mao

123 ***Genome-Wide Assessment of DNA Methylation in Chicken Cardiac Tissue Exposed to Different Incubation Temperatures and $CO_2$ Levels***
Ryan J. Corbett, Marinus F. W. te Pas, Henry van den Brand, Martien A. M. Groenen, Richard P. M. A. Crooijmans, Catherine W. Ernst and Ole Madsen

137 ***Putative Epigenetic Biomarkers of Stress in Red Blood Cells of Chickens Reared Across Different Biomes***
Fábio Pértille, Adriana Mercia Guaratini Ibelli, Maj El Sharif, Mirele Daiana Poleti, Anna Sophie Fröhlich, Shiva Rezaei, Mônica Corrêa Ledur, Per Jensen, Carlos Guerrero-Bosagna and Luiz Lehmann Coutinho

157 ***Whole Transcriptome Analysis Identifies the Taxonomic Status of a New Chinese Native Cattle Breed and Reveals Genes Related to Body Size***
Xiao-Dong Zheng, Jin Cheng, Wen-Juan Qin, Nyamsuren Balsai, Xuan-Jian Shang, Meng-Ting Zhang and Hong-Quan Chen

168 ***Genetic Determinism Exists for the Global DNA Methylation Rate in Sheep***
Dominique Hazard, Florence Plisson-Petit, Carole Moreno-Romieux, Stéphane Fabre and Laurence Drouilhet

179 ***Dysregulated H3K27 Acetylation Is Implicated in Fatty Liver Hemorrhagic Syndrome in Chickens***
Yaling Zhu, Qingjie Zeng, Fang Li, Haoshu Fang, Zhimin Zhou, Tao Jiang, Chao Yin, Qing Wei, Yujie Wang, Jiming Ruan and Jianzhen Huang

194 ***Weaning Induces Stress-Dependent DNA Methylation and Transcriptional Changes in Piglet PBMCs***
Ryan J. Corbett, Andrea M. Luttman, Kaitlin E. Wurtz, Janice M. Siegford, Nancy E. Raney, Laura M. Ford and Catherine W. Ernst

203 ***Impacts of Epigenetic Processes on the Health and Productivity of Livestock***
Mengqi Wang and Eveline M. Ibeagha-Awemu

234 ***The Epigenetics of Gametes and Early Embryos and Potential Long-Range Consequences in Livestock Species—Filling in the Picture With Epigenomic Analyses***
Linkai Zhu, Sadie L. Marjani and Zongliang Jiang

255 ***Environmentally Driven Color Variation in the Pearl Oyster* Pinctada margaritifera *var.* cumingii *(Linnaeus, 1758) Is Associated With Differential Methylation of CpGs in Pigment- and Biomineralization-Related Genes***
Pierre-Louis Stenger, Chin-Long Ky, Céline M. O. Reisser, Céline Cosseau, Christoph Grunau, Mickaël Mege, Serge Planes and Jeremie Vidal-Dupiol

273 ***Methylome Patterns of Cattle Adaptation to Heat Stress***
Marcello Del Corvo, Barbara Lazzari, Emanuele Capra, Ludmilla Zavarez, Marco Milanesi, Yuri Tani Utsunomiya, Adam Taiti Harth Utsunomiya, Alessandra Stella, Guilherme de Paula Nogueira, Josè Fernando Garcia and Paolo Ajmone-Marsan

286 ***Comprehensive Analysis of Transcriptome-wide $m^6A$ Methylome Upon* Clostridium perfringens *Beta2 Toxin Exposure in Porcine Intestinal Epithelial Cells by $m^6A$ Sequencing***
Juanli Zhang, Qiaoli Yang, Jiaojiao Yang, Xiaoli Gao, Ruirui Luo, Xiaoyu Huang, Zunqiang Yan, Pengfei Wang, Wei Wang, Kaihui Xie, Bo Zhang and Shuangbao Gun

*300* ***Integrated Study of Transcriptome-wide m$^6$A Methylome Reveals Novel Insights Into the Character and Function of m$^6$A Methylation During Yak Adipocyte Differentiation***

Yongfeng Zhang, Chunnian Liang, Xiaoyun Wu, Jie Pei, Xian Guo, Min Chu, Xuezhi Ding, Pengjia Bao, Qudratullah Kalwar and Ping Yan

*315* ***Whole Genome Methylation Analysis Reveals Role of DNA Methylation in Cow's Ileal and Ileal Lymph Node Responses to* Mycobacterium avium *subsp.* paratuberculosis *Infection***

Eveline M. Ibeagha-Awemu, Nathalie Bissonnette, Suraj Bhattarai, Mengqi Wang, Pier-Luc Dudemaine, Stephanie McKay and Xin Zhao

*334* ***Integrative Genome-Wide DNA Methylome and Transcriptome Analysis of Ovaries From Hu Sheep With High and Low Prolific***

Xiaolei Yao, Fengzhe Li, Zongyou Wei, M. A. El-Samahy, Xu Feng, Fan Yang and Feng Wang

*348* ***Variability in Global DNA Methylation Rate Across Tissues and Over Time in Sheep***

Laurence Drouilhet, Carole Moreno, Florence Plisson-Petit, Didier Marcon, Stéphane Fabre and Dominique Hazard

frontiers | Frontiers in Genetics

EDITORIAL
published: 15 June 2022
doi: 10.3389/fgene.2022.942747

# Editorial: Epigenetic Variation Influences on Livestock Production and Disease Traits

*Eveline M. Ibeagha-Awemu*[1]*, *Hélène Kiefer*[2,3], *Stephanie McKay*[4] and *George E. Liu*[5]

[1]Sherbrooke Research and Development Centre, Agriculture and Agri-Food Canada, Sherbrooke, QC, Canada, [2]Université Paris-Saclay, UVSQ, INRAE, BREED, Jouy-en-Josas, France, [3]Ecole Nationale Vétérinaire d'Alfort, BREED, Maisons-Alfort, France, [4]Department of Animal and Veterinary Sciences, University of Vermont, Burlington, VT, United States, [5]Animal Genomics and Improvement Laboratory, Agricultural Research Service, United States Department of Agriculture, Beltsville, MD, United States

**Keywords: livestock, DNA/RNA methylation, histone tail modifications, production, reproduction, nutrition, pathogens/health, stress**

## Editorial on the Research Topic

## Epigenetic Variation Influences on Livestock Production and Disease Traits

The epigenome source of variation modulates gene expression without involving changes to the DNA sequence and is an underutilized source of information that may contribute to improved disease management, reproduction, productivity, and environmental adaptation of livestock. The epigenome which comprises DNA methylation, histone tail modifications, chromatin remodeling, and non-coding RNA species that can transmit epigenetic information (e.g. microRNAs and long non-coding RNAs, etc.) responds to environmental factors (nutrition, pathogens, and climate, etc.) to influence the expression of genes and the emergence of specific phenotypes. Increasing evidence indicates that phenotypic expression results from multi-level interactions between the genome, epigenome, environmental factors, and other non-genetic factors. Furthermore, numerous lines of evidence suggest the influence of epigenome variation on livestock production (e.g. milk production), disease traits, reproduction, and environmental adaptation. Given that livestock breeding depends heavily on the interaction between host genetics, environment (e.g. cold or warm climate, nutrition, pathogens, etc.), physiology (e.g. age) and management practices (e.g. type of feed material, form/quantity of feed), many of which impact the epigenome, it is imperative that attention should be given to epigenome characterization and application in livestock breeding and disease management. Therefore, the aim of this Research Topic is to collect research data on the influences of epigenome alterations (DNA methylation, RNA methylation, histone tail modifications and chromatin remodeling) on livestock production traits, to facilitate gainful use of this important source of variation to support continued improvement in livestock traits and disease management. Non-coding RNA data on livestock is already covered by other Research Topics and is excluded from this topic.

This Research Topic collates four review articles and 19 original research articles covering major topics in epigenetics (DNA methylation, RNA methylation, and histone modification) in relation to livestock health, reproduction, production and response to stress and environmental perturbations in many livestock species, including cattle (seven articles), chicken (five articles), sheep (three articles), pig (two articles), yak (one article), and pearl oyster (one article). Although, many livestock species and a broad range of epigenomics alterations are covered, there is a bias towards DNA methylation alterations and more concentration on cattle, highlighting the need to widen/intensify research efforts to include all livestock species as well as address more issues of health and productivity, which is vital for

OPEN ACCESS

**Edited and reviewed by:**
Martino Cassandro,
University of Padua, Italy

***Correspondence:**
Eveline M. Ibeagha-Awemu
eveline.ibeagha-awemu@agr.gc.ca

**Specialty section:**
This article was submitted to Livestock Genomics, a section of the journal Frontiers in Genetics

**Received:** 12 May 2022
**Accepted:** 16 May 2022
**Published:** 15 June 2022

**Citation:**
Ibeagha-Awemu EM, Kiefer H, McKay S and Liu GE (2022) Editorial: Epigenetic Variation Influences on Livestock Production and Disease Traits. Front. Genet. 13:942747. doi: 10.3389/fgene.2022.942747

the effective exploitation of epigenetic information for livestock trait improvement and health management.

The review articles critically examine available epigenetics research data and impacts on livestock health, productivity, reproduction, stress adaptation, and reprograming during somatic cell nuclear transfer. Wang and Ibeagha-Awemu (Wang and Ibeagha-Awemu) present the recent discoveries and evidence on how the epigenetic processes due to DNA methylation, $n^6$ methyladenosine ($m^6A$) RNA methylation, histone modification, and chromatin remodeling impacts the health and productivity of farm animals, particularly cattle, pig, goat, sheep, and poultry. The investigations collated, examined DNA-methylation alterations mostly at the genome-wide scale and to a lesser extent at specific gene regions and addressed animal response to environmental stressors, nutrition, disease pathogens, and developmental processes. They further discuss the application of epigenetics data in livestock health and production and present gaps in livestock epigenetics research. Given increasing evidence that supports the concept that some acquired traits result from environmental exposure during early embryonic and fetal development (i.e., fetal programming), and which can be stamped in the germline as epigenetic information and transmitted to subsequent generations, Zhu et al., discuss the effects of parental environmental exposures on the epigenetics (DNA methylation, histone modification, chromatin remodeling, and non-coding RNAs regulation) of gametes and the early embryo, and available evidence for transgenerational ineritance in livestock (Zhu et al.). In the same light, Wu and Sirard (Wu and Sirard) present available information on the parental non-genetic effects retained in gametes on the development of the early embryo of cows (dairy), paying particular attention to the metabolism of the mother at the time of conception, *in vitro* culture conditions, and parental age relative to puberty. Examining an assisted reproduction technology, somatic cell nuclear transfer, that is commonly used for the production of cloned animals but with the limitation of low cloning efficiency, Wang et al. presents available data proving that incomplete epigenetic reprogramming contributes to the low developmental potential of cloned embryos, and also describes the regulation of epigenetic reprogramming by long non-coding RNAs (Wang et al.).

A majority of the original research articles (65%) investigate how DNA methylation or $m^6A$ RNA methylation alterations play essential roles in the regulation of various livestock traits. Two articles present DNA methylation alterations in response to disease pathogens in cattle. Wang et al. present evidence of significant DNA methylation alterations in mammary gland quarters of Chinese Holsteins challenged with *Staphylococcus aureus* compared with non-challenged quarters of the same animals, as well as significant enrichment of several differentially methylated and expressed genes with immune functions (e.g. *IL6R*, *TNF*, *BTK*, *IL1R2*, and *TNFSF8*) in several immune-related pathways indicative of their involvement in cow's response to *Staphylococcus aureus* infection (Wang et al.). Meanwhile, the role of *Mycobacterium avium subsp paratuberculosis* (MAP) infection on the epigenetic modeling of gut immunity during the progression of Johne's Disease (JD) is presented with evidence of tissue-specific responses to MAP infection with more DNA methylation alterations (more differentially methylated cytosines and differentially methylated regions) in the ileum lymph node tissue than in the ileum tissue of cows with subclinical JD (Ibeagha-Awemu et al.). Five articles discuss the effects of different stressors or environment change on DNA methylation patterns in livestock, such as differential DNA methylation changes due to the effect of different incubation temperatures and $CO_2$ levels in chicken cardiac muscle (Corbett et al.); or due to weaning stress in piglet peripheral blood mononuclear cells (Corbett et al.); or due to heat stress in cattle (Del Corvo et al.); or due to long term stress in chicken red blood cells (Pértille et al.); or due to water depth variation (environment change) in pearl oyster (*Pinctada margaritifera* var. *cumingii*) resulting in shell color variation (Stenger et al.). With regards to product quality, Zhao et al. present the impact of DNA methylation alterations on beef tenderness as well as novel epigenetic data associated with beef quality and further insights into meat science and muscle biology (Zhao et al.). DNA methylation alterations known to influence reproduction traits is the subject of three articles. Perrier et al. report the effects of early life plane of nutrition of Holstein calves on sperm DNA methylation patterns post-puberty (Perrier et al.); while Khezri et al. examine the effect of age and sperm cell condition (fresh or frozen-thawed), demonstrating a significant decrease in the percentage of DNA fragmented sperm cells, and more sperm DNA methylation with increasing age of the bull at differentially methylated regions found between 14 and 17 months of age (Khezri et al.). Examining sheep reproduction traits, Yao et al. demonstrate significant DNA methylation and gene expression changes between high prolificacy (FecBB) and low prolificacy (FecB+) Hu sheep, thereby demonstrating that DNA methylation influences prolificacy capacity by modulating gene expression in the ovaries (Yao et al.). Deviating from a focus on single DNA sites/regions or tissues, Hazard and colleagues show that global DNA methylation rate (GDMR) in blood varies among animals, but is significantly higher in female lambs compared to male lambs, and is moderately heritable and associates significantly with quantitative trait loci harboring genes with known active roles in gene expression (Hazard et al.). Meanwhile, Drouilhet et al. demonstrate significant GDMR variability in sheep blood due to sampling date and breed, and between blood and various tissues (12 somatic tissues and 6 reproductive tissues) (Drouilhet et al.).

In addition to presenting the effects of DNA methylation, the effect of RNA methylation, especially $m^6A$ RNA methylation, also known to participate in post-transcriptional gene regulation, is discussed. Combining methylated RNA immunoprecipitation sequencing (MeRIP-seq) and RNA sequencing (RNA-Seq) data, Zhang and colleagues show that genes with up-regulated $m^6A$ peaks but with decreased expression, are mainly enriched in the Wnt signaling pathway, suggesting that this pathway may be modified by $m^6A$ methylation in *Clostridium perfringens* beta2 toxin-induced porcine intestinal epithelial (IPEC-J2) cells (Zhang et al.). Similarly, Zhang et al. present a positive association between $m^6A$ methylation abundance (MeRIP-seq) and levels of

gene expression (RNA-Seq), as well as a vital role of $m^6A$ methylation in the modulation of gene expression during yak adipocyte differentiation (Zhang et al.).

The effects of histone modifications, the second most studied epigenetic mechanism, is presented in relation to heat stress, disease/disease pathogens and thermal manipulation. Addressing two active histone modifications, H3K4me3 (predominantly marks active promoters) and H3K27ac (marks both active promoters and enhancers), Chanthavixay et al. present higher differences in histone modifications in the bursal of Leghorns compared to Fayoumis chickens in response to treatment with Newcastle disease virus while under chronic heat stress (Chanthavixay et al.), while David and colleagues show that histone marks (H3K4me3 and H3K27me3) known to contribute to environmental memory in eukaryotes, presents higher numbers of differential peaks in the hypothalamus of 35 days old (slaughter age) chickens with implicated peaks found on genes with metabolic, neurodevelopmental, and gene regulation functions, but fewer differences between peaks of the histone marks in muscle tissue in response to thermal stress during embryogenesis (David et al.). Examining liver tissue between healthy and fatty liver hemorrhagic syndrome (FLHS) chickens, Zhu et al. present H3K27ac differential peaks association with multiple known FLHS risk genes with roles in the immune response, and lipid and energy metabolism (Zhu et al.). On a more general note, Zheng et al. present transcriptional changes and the taxonomic status of a new Chinese native cattle known as Wandong (Zheng et al.)

These reports unequivocally present evidence of the involvement of epigenetic marks in defining livestock trait expression and their importance in modulating economically important livestock traits, products, and environmental adaptation. Concerted efforts and more targeted epigenetic research in livestock spanning the exposome (nutrition, disease pathogens, microbiota, chemicals, pollutants, and environmental stress [heat, cold, and climate chane], parental stress, maternal behavior and management practices), species, breeds (genetic variation), and under various conditions will provide a holistic view and understanding of the epigenetic influence on phenotypic variation in livestock production, reproduction, health and environmental adaptation, and gainful exploitation for production and health management.

## AUTHOR CONTRIBUTIONS

EMI-A initiated the Research Topic. HK, SM, and GL co-edited the Research Topic with EMI-A and all authors participated in the editorial process. EMI-A drafted the manuscript. All authors revised and approved the manuscript.

## REFERENCES


Chanthavixay, G., Kern, C., Wang, Y., Saelao, P., Lamont, S. J., Gallardo, R. A., et al. (2020). Integrated Transcriptome and Histone Modification Analysis Reveals NDV Infection under Heat Stress Affects Bursa Development and Proliferation in Susceptible Chicken Line. *Front. Genet.* 11, 567812. doi:10.3389/fgene.2020.567812

Corbett, R. J., Luttman, A. M., Wurtz, K. E., Siegford, J. M., Raney, N. E., Ford, L. M., et al. (2021). Weaning Induces Stress-dependent DNA Methylation and Transcriptional Changes in Piglet PBMCs. *Front. Genet.* 12, 633564. doi:10.3389/fgene.2021.633564

Corbett, R. J., te Pas, M. F. W., van den Brand, H., Groenen, M. A. M., Crooijmans, R. P. M. A., Ernst, C. W., et al. (2020). Genome-Wide Assessment of DNA Methylation in Chicken Cardiac Tissue Exposed to Different Incubation Temperatures and CO2 Levels. *Front. Genet.* 11, 558189. doi:10.3389/fgene.2020.558189

David, S-A., Vitorino Carvalho, A., Gimonnet, C., Brionne, A., Hennequet-Antier, C., Piégu, B., et al. 2019. Thermal Manipulation during Embryogenesis Impacts H3K4me3 and H3K27me3 Histone Marks in Chicken Hypothalamus. *NIH* 10: 01207. doi:10.3389/fgene.2019.01207

Del Corvo, M., Lazzari, B., Capra, E., Zavarez, L., Milanesi, M., Utsunomiya, Y. T., et al. (2021). Methylome Patterns of Cattle Adaptation to Heat Stress. *Front. Genet.* 12, 633132. doi:10.3389/fgene.2021.633132

Drouilhet, L., Moreno, C., Plisson-Petit, F., Marcon, D., Fabre, S., and Hazard, D. (2022). Variability in Global DNA Methylation Rate across Tissues and over Time in Sheep. *Front. Genet.* 13, 791283. doi:10.3389/fgene.2022.791283

Hazard, D., Plisson-Petit, F., Moreno-Romieux, C., Fabre, S., and Drouilhet, L. (2020). Genetic Determinism Exists for the Global DNA Methylation Rate in Sheep. *Front. Genet.* 11, 616960. doi:10.3389/fgene.2020.616960

Ibeagha-Awemu, E. M., Bissonnette, N., Bhattarai, S., Wang, M., Dudemaine, P-L., McKay, S., et al. (2021). Whole Genome Methylation Analysis Reveals Role of DNA Methylation in Cow's Ileal and Ileal Lymph Node Responses to *Mycobacterium avium* Subsp. Paratuberculosis Infection. *Front. Genet.* 12.135 doi:10.3389/fgene.2021.797490

Khezri, A., Narud, B., Stenseth, E.-B., Zeremichael, T. T., Myromslien, F. D., Wilson, R. C., et al. (2020). Sperm DNA Hypomethylation Proximal to Reproduction Pathway Genes in Maturing Elite Norwegian Red Bulls. *Front. Genet.* 11, 922. doi:10.3389/fgene.2020.00922

Perrier, J.-P., Kenny, D. A., Chaulot-Talmon, A., Byrne, C. J., Sellem, E., Jouneau, L., et al. (2020). Accelerating Onset of Puberty through Modification of Early Life Nutrition Induces Modest but Persistent Changes in Bull Sperm DNA Methylation Profiles Post-puberty. *Front. Genet.* 11, 945. doi:10.3389/fgene.2020.00945

Pértille, F., Ibelli, A. M. G., Sharif, M. E., Poleti, M. D., Fröhlich, A. S., Rezaei, S., et al. (2020). Putative Epigenetic Biomarkers of Stress in Red Blood Cells of Chickens Reared across Different Biomes. *Front. Genet.* 11, 508809. doi:10.3389/fgene.2020.508809

Stenger, P.-L., Ky, C.-L., Reisser, C. M. O., Cosseau, C., Grunau, C., Mege, M., et al. (2021). Environmentally Driven Color Variation in the Pearl Oyster Pinctada Margaritifera Var. Cumingii (Linnaeus, 1758) Is Associated with Differential Methylation of CpGs in Pigment- and Biomineralization-Related Genes. *Front. Genet.* 12, 630290. doi:10.3389/fgene.2021.630290

Wang, M., and Ibeagha-Awemu, E. M. (2021). Impacts of Epigenetic Processes on the Health and Productivity of Livestock. *Front. Genet.* 11, 1812. doi:10.3389/fgene.2020.613636

Wang, M., Liang, Y., Ibeagha-Awemu, E. M., Li, M., Zhang, H., Chen, Z., et al. (2020). Genome-Wide DNA Methylation Analysis of Mammary Gland Tissues from Chinese Holstein Cows with *Staphylococcus aureus* Induced Mastitis. *Front. Genet.* 11, 550515. doi:10.3389/fgene.2020.550515

Wang, X., Qu, J., Li, J., He, H., Liu, Z., and Huan, Y. (2020). Epigenetic Reprogramming during Somatic Cell Nuclear Transfer: Recent Progress and Future Directions. *Front. Genet.* 11, 205. doi:10.3389/fgene.2020.00205

Wu, C., and Sirard, M.-A. (2020). Parental Effects on Epigenetic Programming in Gametes and Embryos of Dairy Cows. *Front. Genet.* 11, 557846. doi:10.3389/fgene.2020.557846

Yao, X., Li, F., Wei, Z., Ei-Samahy, M. A., Feng, X., Yang, F., et al. (2022). Integrative Genome-wide DNA Methylome and Transcriptome Analysis of Ovaries from Hu Sheep with High and Low Prolific. *Front. Cell Dev. Biol.* 10, 820558. doi:10.3389/fcell.2022.820558

Zhang, J., Yang, Q., Yang, J., Gao, X., Luo, R., Huang, X., et al. (2021). Comprehensive Analysis of Transcriptome-wide m6A Methylome upon *Clostridium perfringens* Beta2 Toxin Exposure in Porcine Intestinal Epithelial Cells by m6A Sequencing. *Front. Genet.* 12, 689748. doi:10.3389/fgene.2021.689748

Zhang, Y., Liang, C., Wu, X., Pei, J., Guo, X., Chu, M., et al. (2021). Integrated Study of Transcriptome-wide m6A Methylome Reveals Novel Insights into the Character and Function of m6A Methylation during Yak Adipocyte Differentiation. *Front. Cell Dev. Biol.* 9, 689067. doi:10.3389/fcell.2021.689067

Zhao, C., Ji, G., Carrillo, J. A., Li, Y., Tian, F., Baldwin, R. L., et al. (2020). The Profiling of DNA Methylation and its Regulation on Divergent Tenderness in Angus Beef Cattle. *Front. Genet.* 11, 939. doi:10.3389/fgene.2020.00939

Zheng, X.-D., Cheng, J., Qin, W.-J., Balsai, N., Shang, X.-J., Zhang, M.-T., et al. (2020). Whole Transcriptome Analysis Identifies the Taxonomic Status of a New Chinese Native Cattle Breed and Reveals Genes Related to Body Size. *Front. Genet.* 11, 562855. doi:10.3389/fgene.2020.562855

Zhu, L., Marjani, S. L., and Jiang, Z. (2021). The Epigenetics of Gametes and Early Embryos and Potential Long-Range Consequences in Livestock Species-Filling in the Picture with Epigenomic Analyses. *Front. Genet.* 12, 557934. doi:10.3389/fgene.2021.557934

Zhu, Y., Zeng, Q., Li, F., Fang, H., Zhou, Z., Jiang, T., et al. (2021). Dysregulated H3K27 Acetylation Is Implicated in Fatty Liver Hemorrhagic Syndrome in Chickens. *Front. Genet.* 11, 574167. doi:10.3389/fgene.2020.574167

**Conflict of Interest:** The authors declare that the research was conducted in the absence of any commercial or financial relationships that could be construed as a potential conflict of interest.

**Publisher's Note:** All claims expressed in this article are solely those of the authors and do not necessarily represent those of their affiliated organizations, or those of the publisher, the editors and the reviewers. Any product that may be evaluated in this article, or claim that may be made by its manufacturer, is not guaranteed or endorsed by the publisher.

*Copyright © 2022 Kiefer, McKay, Liu and Her Majesty the Queen in Right of Canada, as represented by the Minister of Agriculture and Agri-Food Canada for the contribution of Ibeagha-Awemu. This is an open-access article distributed under the terms of the Creative Commons Attribution License (CC BY). The use, distribution or reproduction in other forums is permitted, provided the original author(s) and the copyright owner(s) are credited and that the original publication in this journal is cited, in accordance with accepted academic practice. No use, distribution or reproduction is permitted which does not comply with these terms.*

frontiers in Genetics

ORIGINAL RESEARCH
published: 26 November 2019
doi: 10.3389/fgene.2019.01207

# Thermal Manipulation During Embryogenesis Impacts H3K4me3 and H3K27me3 Histone Marks in Chicken Hypothalamus

*Sarah-Anne David[1†], Anaïs Vitorino Carvalho[1†], Coralie Gimonnet[1], Aurélien Brionne[1], Christelle Hennequet-Antier[1], Benoît Piégu[2], Sabine Crochet[1], Nathalie Couroussé[1], Thierry Bordeau[1], Yves Bigot[2], Anne Collin[1] and Vincent Coustham[1]**

[1] BOA, INRA, Université de Tours, Nouzilly, France, [2] PRC, CNRS, IFCE, INRA, Université de Tours, Nouzilly, France

OPEN ACCESS

**Edited by:**
Helene Kiefer,
INRA Centre Jouy-en-Josas, France

**Reviewed by:**
Christoph Grunau,
Université de Perpignan Via Domitia, France
Naoko Hattori,
National Cancer Center Research Institute, Japan

***Correspondence:**
Vincent Coustham
vincent.coustham@inra.fr

[†]These authors have contributed equally to this work

**Specialty section:**
This article was submitted to Epigenomics and Epigenetics, a section of the journal Frontiers in Genetics

**Received:** 03 September 2019
**Accepted:** 01 November 2019
**Published:** 26 November 2019

**Citation:**
David S-A, Vitorino Carvalho A, Gimonnet C, Brionne A, Hennequet-Antier C, Piégu B, Crochet S, Couroussé N, Bordeau T, Bigot Y, Collin A and Coustham V (2019) Thermal Manipulation During Embryogenesis Impacts H3K4me3 and H3K27me3 Histone Marks in Chicken Hypothalamus. Front. Genet. 10:1207. doi: 10.3389/fgene.2019.01207

Changes in gene activity through epigenetic alterations induced by early environmental challenges during embryogenesis are known to impact the phenotype, health, and disease risk of animals. Learning how environmental cues translate into persisting epigenetic memory may open new doors to improve robustness and resilience of developing animals. It has previously been shown that the heat tolerance of male broiler chickens was improved by cyclically elevating egg incubation temperature. The embryonic thermal manipulation enhanced gene expression response in muscle (*P. major*) when animals were heat challenged at slaughter age, 35 days post-hatch. However, the molecular mechanisms underlying this phenomenon remain unknown. Here, we investigated the genome-wide distribution, in hypothalamus and muscle tissues, of two histone post-translational modifications, H3K4me3 and H3K27me3, known to contribute to environmental memory in eukaryotes. We found 785 H3K4me3 and 148 H3K27me3 differential peaks in the hypothalamus, encompassing genes involved in neurodevelopmental, metabolic, and gene regulation functions. Interestingly, few differences were identified in the muscle tissue for which differential gene expression was previously described. These results demonstrate that the response to embryonic thermal manipulation (TM) in chicken is mediated, at least in part, by epigenetic changes in the hypothalamus that may contribute to the later-life thermal acclimation.

**Keywords: thermal manipulation, epigenetic, reprogramming, histone post-translational modification, chicken**

## INTRODUCTION

During the last several decades, it became clear that the epigenome of eukaryotes dynamically responds to the environment. Stress, diet, behavior, toxins, and other factors modulate gene expression through epigenetic modifications such as chemical additions to DNA and histones that can be stably maintained during mitotic divisions and do not change the primary DNA sequence (Fresard et al., 2013; David et al., 2017a). Early embryogenesis is a critical window of sensitivity to the environment, and environmentally induced changes can be transmitted during development by subsequent cell divisions. Among the best-studied examples are the persistent epigenetic differences in humans associated with prenatal exposure to famine during the Dutch hunger winter (Heijmans

et al., 2008) and the maternal diet supplemented with folate that induces pseudo-agouti phenotypes in mice (Feil and Fraga, 2012). Early temperature exposure is also known to affect the phenotypes of plants and animals through epigenetic reprogramming. In yeast, histone post-translational modifications, and in particular H3K4 methylation, have emerged as primary actors in the mitotic memory of the environmental stress response (Fabrizio et al., 2019). In plants, the molecular basis of vernalization (the acceleration of flowering by prolonged cold) has been extensively studied and notably involves the quantitative accumulation of trimethylation of histone H3 at lysine 27 (H3K27me3) during cold periods (Coustham et al., 2012). Heat acclimation-mediated cross-tolerance resulting from the enhancement of innate cytoprotective pathways in rats was shown to involve epigenetic mechanisms such as post-translational histone modification and altered levels of chromatin modifiers during the acclimation phase (Horowitz, 2017). In chickens, post-natal heat acclimation during the 3$^{rd}$ or 5$^{th}$ day of life was shown to improve temperature tolerance at 10 days of age through epigenetic changes such as DNA methylation at *BDNF* and histone post-translational modifications at *BDNF*, *Eif2b5* and *HSP70* in the hypothalamus (Yossifoff et al., 2008; Kisliouk et al., 2010; Kisliouk et al., 2011; Kisliouk et al., 2017).

Broiler chickens have long been selected for growth performance traits, with significant progress in genetic selection during the last several decades. However, the huge improvement in chicken body weight and muscle growth has not been associated with a similar increase in visceral organs such as heart and lungs necessary for hyperventilation and heat loss (Havenstein et al., 2003). As a consequence, chickens have became less able to cope with extreme environmental temperatures, as illustrated by the 2003 hot spells in France that resulted in the death of several millions of meat-type chickens (Yahav and McMurtry, 2001; St-Pierre et al., 2003). In order to improve bird thermal tolerance and welfare without impairing growth in later life, a protocol of early exposure to heat during egg embryonic development has been proposed (Piestun et al., 2008). The TM treatment during embryogenesis consists in increasing egg incubation temperature to 39.5°C for 12 h/d, in contrast to a continuous incubation at 37.8°C under standard condition, during a time-window that coincides with the development of the hypothalamic-pituitary-thyroid axis (between E7 and E16; chicken eggs hatch around E21) (Piestun et al., 2008; Loyau et al., 2013). The TM treatment, that can easily be applied by hatcheries, was shown to modify several physiological parameters such as lowering the internal temperature and to improve heat tolerance of broilers during acute heat stress at slaughter age (5 weeks old) with little effect on animal performance (Piestun et al., 2008; Loyau et al., 2013).

To investigate the impact of TM at the molecular level, a muscle transcriptome analysis was performed on TM and control (C) chickens that were either heat challenged or not challenged before sampling at 5 weeks of age (Loyau et al., 2016). Only a few genes (28) were found to be differentially expressed (DE) between C and TM. Interestingly, 759 genes were found to be DE between the heat-challenged TM (32°C for 5h at 35 days of age) and TM individuals that were left at thermally neutral condition (21°C) while only 128 were found to be DE in the comparison between heat-challenged controls and controls left in thermally neutral conditions (Loyau et al., 2016). Hence, a number of genes may have been conditioned to respond to further heat exposure by a mechanism that may involve epigenetic changes. In addition, the analysis showed that 26 genes involved in chromatin organization, remodeling, and gene silencing were DE when TM chickens were exposed to a heat challenge (vs. TM in thermal neutral conditions) (Loyau et al., 2016). We therefore hypothesized that an epigenetic reprogramming induced by the embryonic heat exposure may have modified part of the chromatin landscape thus affecting gene expression in favor of heat acclimation. To test this hypothesis, we performed a whole-genome analysis of H3K4me3 and H3K27me3 histone marks. Both *P. major* muscle and hypothalamus tissues of TM and C chickens were investigated because of the transcriptome changes previously shown and the involvement of brain in postnatal acclimation respectively (Yossifoff et al., 2008). Here, we show that embryonic TM affected H3K4me3 and, to a lesser extent, H3K27me3 in the hypothalamus of 35-day-old chickens whereas the effects were very limited in the muscle. Most differential peaks occurred within the 5' part of genes that were involved in biological functions relevant to neurodevelopmental, metabolic, and gene regulation functions. This study showed that several genes that code for components of the corticotropin-releasing hormone (CRH) signaling pathway were affected at the histone level, suggesting that TM may affect biological processes similar to those affected by the postnatal acclimation model.

# RESULTS

## TM Has a Long-Lasting Impact on the Epigenome of Developing Chickens

TM was applied (or not, for controls) on Cob500 eggs and the reproducibility of the embryonic treatment was compared to previous experiments by measuring cloacal temperature at hatching, as this has been shown to be decreased in TM chickens (Loyau et al., 2015). As expected, we found that cloacal temperature of male TM animals was significantly reduced at hatching (38.7°C in average, n = 54) compared to male controls (38.9°C, n = 68; p-value < 0.05). We then sampled hypothalamus and muscle samples of 35-day-old male TM and C chickens. ChIP followed by Illumina sequencing was performed using antibodies specific to H3K4me3 and H3K27me3 modifications. For hypothalamus samples, ~23 to 75 thousands of peaks were obtained (**Table 1** and **Supplementary Table S1**). As expected, H3K27me3 peaks were broader than H3K4me3 peaks (**Supplementary Figure S1** and **Table S1**). 785 and 148 differential peaks (DP) were identified for H3K4me3 and H3K27me3 respectively in this tissue (**Table 1**). By contrast, only 45 and 20 peaks were found to be DE for H3K4me3 and H3K27me3 respectively in the muscle, representing less than 0.1% of detected peaks. A majority of DP showed reduced signal in TM animals for both marks and tissues (**Table 1**).

We next investigated the distribution of DP. Hypothalamic H3K4me3 DP were found preferentially in genes, near the transcription start sites (TSS), in the first exon and in the first intron (**Figure 1A**). This result is consistent with genome-wide distribution of this mark in all the H3K4me3 peaks detected in the study (**Figure 1B**). Only DP outside of genes appeared underrepresented suggesting that H3K4me3 changes in the hypothalamus of TM

**TABLE 1 |** Summary of ChIP-seq results.Three biological replicates were sequenced per tissue and mark.

| | Hypothalamus | | Muscle *P. major* | |
|---|---|---|---|---|
| | **H3K4me3** | **H3K27me3** | **H3K4me3** | **H3K27me3** |
| Analyzed peaks | 30597 | 23098 | 75943 | 26562 |
| Number of DP | 785 | 148 | 45 | 20 |
| % DP | 2.57 | 0.64 | 0.06 | 0.08 |
| Number of DP up | 147 | 37 | 7 | 4 |
| Number of DP down | 638 | 111 | 38 | 16 |
| Genes containing DP | 975 | 69 | 44 | 17 |

*Reads were mapped against the chicken genome Galgal5, and peaks were detected using PePr for H3K4me3 and epic for H3K27me3. DP, Differential Peaks. Comparisons (DP up, DP down) were calculated as TM vs. control.*

animals occurred preferentially within genes. However, H3K27me3 hypothalamus DP were evenly distributed within the body of genes (**Figure 1A**), likely reflecting the broader size of peaks. However, one quarter of hypothalamus H3K27me3 DP were found outside of genes, which is similar to the genome-wide distribution of this mark in our experiment (**Supplementary Figure S2A**). Muscle distribution of DP was roughly similar to the hypothalamus, with the exception of the H3K4me3 distribution that appeared less skewed toward the 5' end of genes (**Supplementary Figure S2B**).

We next sought to identify DP that were localized within genes (DP genes). For the hypothalamus, we found 975 genes containing at least one H3K4me3 DP (95% unique) and 69 genes containing at least one H3K27me3 DP. Muscle DP were found only in 44 and 17 genes for H3K4me3 and H3K27me3, respectively (**Table 1**). Overall, 25 DP genes (2.5%) were found in at least two conditions (shared between marks and/or tissues; **Figure 1C** and **Table S2**). Notably, eight genes including the *Protocadherin alpha-2*(*PCDHA2*) subunit involved in the establishment and function of specific cell to cell connections in the brain and seven nonannotated genes contained DP in three conditions (**Supplementary Table S2**). Moreover, 17 genes contained DP in two conditions, either in a tissue specific or a mark specific fashion with the exception of another protocadherin (*PCDHA11*) that contained a H3K4me3 DP in the hypothalamus and a H3K27me3 DP in muscle (**Supplementary Table S2**). The complete list of DP genes is provided in **Supplementary Table S2**.

To validate the ChIP-seq data, we performed ChIP-qPCR on biological replicates from the same experiment on a set of H3K4me3 DP in the hypothalamus. Primers were designed within or encompassing DP regions at *CCNF* (*cyclin F*), *CRY2* (*Cryptochrome 2*), *CDKL5* (*Cyclin Dependent Kinase Like 5*), *OCLN* (*Occludin*), and *RGS4* (*Regulator Of G Protein Signaling 4*) with an increase in TM condition. A nondifferential control at the *GAPDH* locus was included in the analysis. We found that H3K4me3 levels were significantly increased in all regions in TM hypothalamus samples from biological replicates thus confirming ChIP-seq data except for *CCNF* that only showed a nonsignificant trend toward an increase (**Figure 1D** and data not shown). To investigate the relationship between DP and gene expression, we also checked the expression of *CCNF*, *CDKL5*, *CRY2,* and *OCLN* by RT-qPCR. However, none of these appeared to be altered by the presence of DP as no transcript level was found significantly altered (**Supplementary Figure S4**).

## Differential Peaks Were Found Preferentially in Neurodevelopmental, Metabolic and Transcriptional Regulator Genes

To gain insights into the biological functions that may be affected by the presence of DP, we performed a functional analysis based on gene ontology (GO) analysis using the ViSEAGO tool (Brionne et al., 2019). Enrichment tests of GO terms associated with biological processes led to the identification of 154 enriched terms among the four list of genes (**Figure 2**, **Table 2**, and **Supplementary Figure S4** and **Table S3**). These terms were grouped into 26 clusters that could be further categorized into four major processes: neurodevelopment (36 GO terms), metabolism (39 GO terms), gene regulation (30 GO terms) and immunity, cellular and other processes (49 GO terms; **Supplementary Table S3**).

Six functional clusters comprised GO terms from different conditions. The 7$^{th}$cluster, associated with gene expression regulation at the protein modification level, was defined by five GO terms corresponding to H3K4me3 DP (four for hypothalamus, one for muscle) and one GO term corresponding to hypothalamic H3K27me3 DP. However, none of the 144 genes defining this cluster were in common between conditions. Moreover, two clusters related to metabolic processes (2 and 23) and one related to cellular processes (21) resulted from GO terms enriched for H3K4me3 DP from both tissues. Finally, two clusters related to cellular processes (17 and 20) resulted from GO terms enriched for both H3K4me3 and H3K27me3 DP in the hypothalamus.

Interestingly, all clusters defining the neurodevelopmental function (10–16) were specific to the H3K4me3 mark and the hypothalamus, suggesting that this mark may contribute to the neurogenic processes of acclimation. This finding was confirmed by an analysis using the Ingenuity Pathway Analysis (IPA) software demonstrating that biological functions associated with hypothalamic H3K4m3 DP were mostly related to the nervous system development, including cellular development, growth and proliferation, as well as the cell-to-cell signaling (**Supplementary Table S4**).

## IPA Canonical Pathway Analysis Revealed an Impact of TM on H3K4me3 in Several Genes Related to the CRH Pathway and Previously Identified in the Postnatal Model

To gain further insights into the molecular mechanisms affected by TM, we investigated the canonical pathways using the IPA software and Fisher's exact test. We focused on the hypothalamic H3K4me3 DP as it was the condition for which most DP were found. The most significantly enriched canonical pathways were mainly related to cellular growth and development such as AMPK signaling and *Oct4* (*Octamer-binding transcription factor 4*) function in embryonic cell, but were also related to the nervous system and behavior with calcium signaling, opioid signaling pathway, and synaptic long-term potential (**Table 3**). Interestingly, the CRH signaling pathway was also significantly enriched ($p$-value < 0.05; **Table 3** and **Supplementary Figure S5**). Molecules identified in this pathway included *ATF2* (Activating transcription factor 2), a transcriptional factor shown to be involved in the maintenance of the chromatin structure following

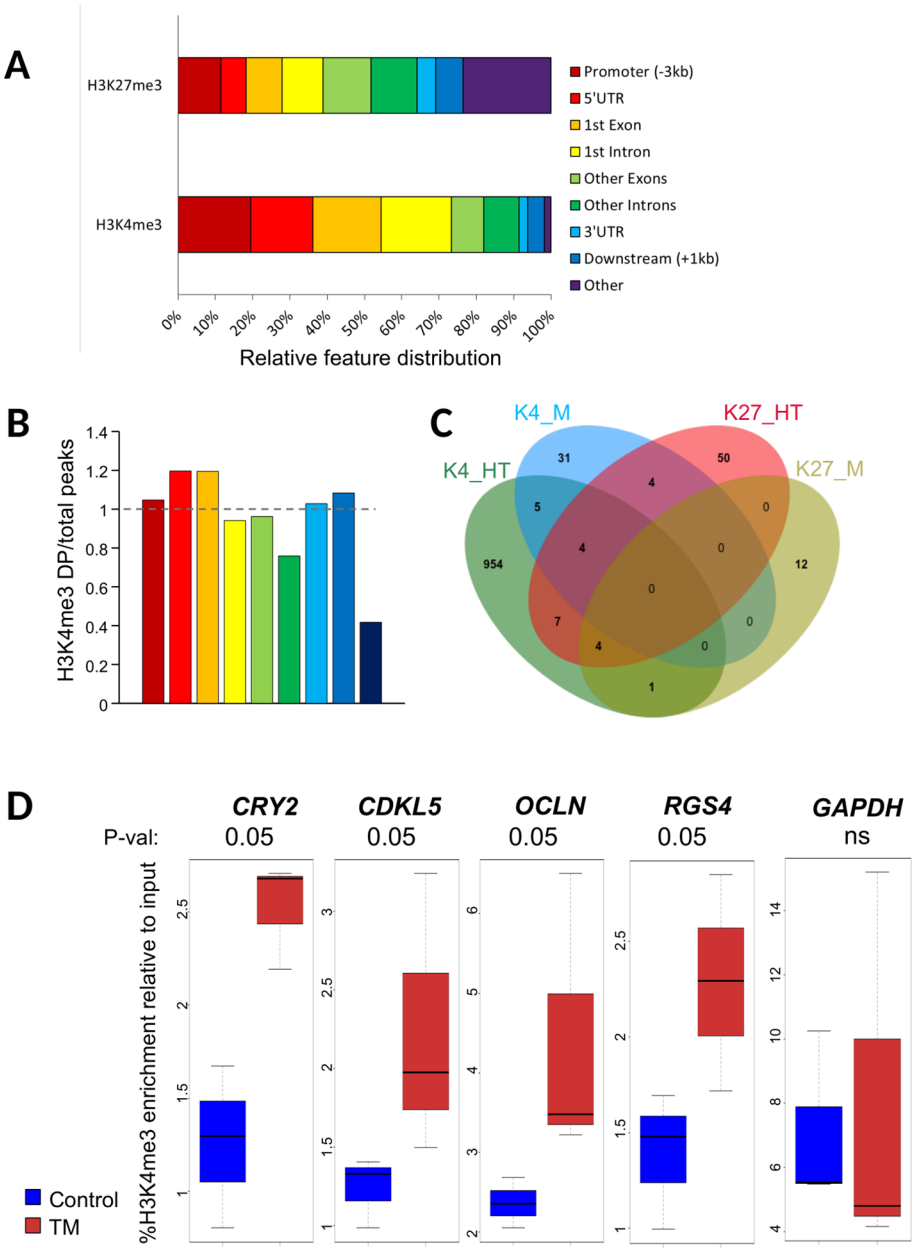



**FIGURE 1 |** Characteristics of differential peaks. **(A)** Percentage of ChIP-seq H3K4me3 differential peaks across genomic features in hypothalamus relative to all differential peaks, obtained using GenomeFeatures. Promoter and downstream regions were defined upstream of Transcription Start and End Sites (TSS and TES, respectively), respectively. **(B)** Barplot showing the ratio for each feature between the percentage of differential peaks (DP) per feature relative to all DP and the percentage of all peaks per feature vs. all peaks for H3K4me3 in hypothalamus. The color legend is the same as in **Figure 1A**. **(C)** Venn diagram showing the number of genes containing a DP that are specific or common for H3K4me3 (K4) and H3K27me3 (K27) marks in hypothalamus (HT) and muscle (M) tissues. **(D)** Box plot of H3K4me3 relative enrichment to input at *CRY2*, *CDKL5*, *OCLN,* and *RGS4* loci in Control (blue) and TM (red) replicates. Box boundaries represent the first and third quartiles. The median is indicated by the bold horizontal line dividing the interquartile range. Upper and lower ticks indicate the 10th and 90th percentiles. Corresponding p-values are indicated at the top of each graph

embryonic stress in Drosophila (Seong et al., 2011), and *CRHR2* (*Corticotropin Releasing Hormone Receptor 2*), a receptor of the CRH hormone shown to be involved in determining later-life stress response of thermally-manipulated chicks (Cramer et al., 2015). In addition, the downstream target *BDNF* (*Brain Derived Neurotrophic Factor*; **Supplementary Figure S5**) was previously reported to be a major epigenetic target of postnatal thermal treatment in chicks (Yossifoff et al., 2008). To explore the impact of H3K4me3 changes of several members of the CRH pathway in TM animals, we measured the gene expression by RT-qPCR of several members of the pathway that contained a DP (*CRHR2*, *ATF2* and *MAPK11* – *Mitogen-Activated Protein Kinase 11*;

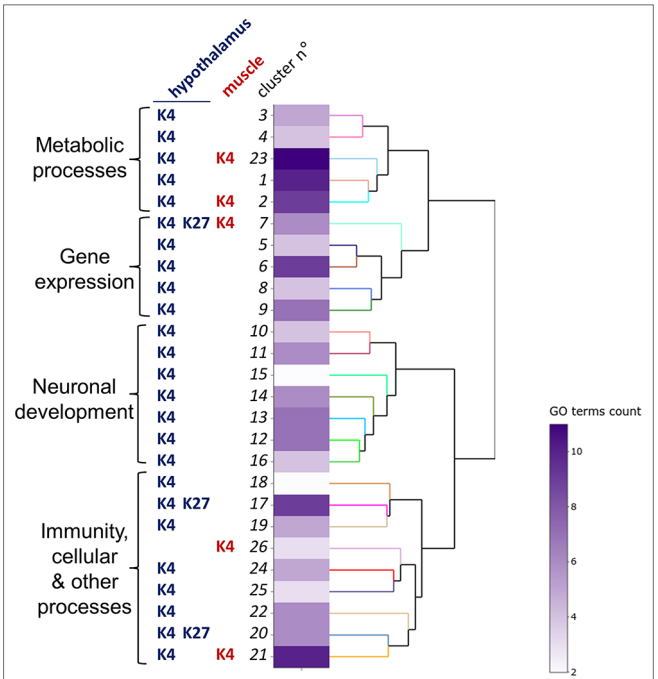



**FIGURE 2 |** Functional analysis of hypothalamus and muscle genes bearing H3K4me3 and H3K27me3 differential peaks.The clustering heatmap plot of functional sets of gene ontology (GO) terms was obtained using ViSEAGO. From left to right are shown the major processes, the conditions defining the clusters (histone marks, tissues) defining the clusters, the cluster number, a heat map with the number of GO terms in each set and a dendrogram based on BMA semantic similarity distance and Ward's clustering criterion

**TABLE 2 |** Description of gene ontology (GO) clusters. For each cluster, the number of GO terms and the common ancestor term are shown

| Cluster | GO Terms (total: 154) | Common ancestor term |
|---|---|---|
| 1 | 10 | Cellular metabolic process |
| 2 | 9 | Regulation of metabolic process |
| 3 | 5 | Regulation of macromolecule metabolic process |
| 4 | 4 | Regulation of macromolecule biosynthetic process |
| 5 | 4 | Regulation of nucleobase-containing compound metabolic process |
| 6 | 9 | Regulation of RNA biosynthetic process |
| 7 | 6 | Organic substance metabolic process |
| 8 | 4 | Nucleobase-containing compound metabolic process |
| 9 | 7 | Cellular biosynthetic process |
| 10 | 4 | Neuron projection morphogenesis |
| 11 | 6 | Anatomical structure morphogenesis |
| 12 | 7 | Gliogenesis |
| 13 | 7 | Cellular developmental process |
| 14 | 6 | System development |
| 15 | 2 | Cerebral cortex cell migration |
| 16 | 4 | Ensheathment of neurons |
| 17 | 9 | Multicellular organismal process |
| 18 | 2 | Positive regulation of muscle hypertrophy |
| 19 | 5 | Negative regulation of biological process |
| 20 | 6 | Microtubule cytosekeleton organization |
| 21 | 10 | Cellular process |
| 22 | 6 | Process |
| 23 | 11 | Biological regulation |
| 24 | 5 | Metal ion transport |
| 25 | 3 | Cytokine secretion |
| 26 | 3 | Protein localization to cell cortex |

**Supplementary Figure S6**). We also investigated the expression of other key members of this pathway or downstream targets that did not contain a DP (*CRHR1, BDNF,* and *CREB1–CAMP Responsive Element Binding Protein 1*). Our results showed that none of these genes showed expression changes at a significance level of 0.05 even though *BDNF* and *CRHR1* showed a trend toward a decrease (both at P = 0.066; **Supplementary Figure S7**). Therefore, while TM appeared to significantly affect H3K4me3 marks for a subset of *CRH* pathway members, we could not demonstrate a clear link with gene expression in the biological replicates assayed.

## Muscle Differential Peaks Did Not Localize Within De Genes Previously Identified

Prior to this study, a chicken transcriptome microarray (accession number GSE70756) was performed to compare *P. major* gene expression profiles of TM and C chickens reared at 21°C and under heat challenge condition at 32°C for 5 h (TM-HC and C-HC, respectively) (Loyau et al., 2016). Among the DE genes in the muscle, 28 were found to be DE between C and TM, 128 between C-HC and C, and 759 between TM-HC and TM. We investigated whether the DP gene list overlapped to these DE gene lists. To that end, the microarray data was reannotated with the Galgal5 annotation used in this study, leading to a similar list of 24, 127, and 724 DE genes included in the analysis for C vs. TM, C-HC vs. C, and TM-HC vs. TM comparisons, respectively (**Supplementary Table S5**). None of the 44 H3K4me3 and 17 H3K27me3 DP genes corresponded to DE genes from all comparisons (**Supplementary Table S4**). We also investigated the presence of DP in candidate genes that were shown to be DE by targeted RT-qPCR approach in the pectoral muscle of TM animals compared to C, including the *DIO3* (*Iodothyronine Deiodinase 3*) and *PGC1-α* (*PPARG Coactivator 1 alpha*) metabolic genes (Loyau et al., 2014). However, none of these DE genes contained a DP in the present analysis (data not shown).

# DISCUSSION

Many studies investigated the impact of embryonic heat treatment in birds (for a review see Loyau et al., 2015) at the phenotypic, metabolic, and gene expression levels, but the molecular mechanisms underlying these changes were not fully understood. Recently, the hypothesis of an epigenetic contribution was raised by the identification of long-term gene expression effects including the alteration of transcript abundance of key epigenetic players (Loyau et al., 2016). Here, we provided the first demonstration of an epigenetic effect induced during embryogenesis in broiler chickens by the genome-wide mapping of two histone marks, H3K4me3 and H3K27me3, selected for their known function in epigenetic memory.

**TABLE 3 |** List of the canonical pathways identified by Ingenuity Pathway Analysis. The 25 significant pathways, with p-value < 0.05, are listed. The number and name of molecules participating in each pathway are shown in the "*n* =" column

| Ingenuity Canonical Pathways | -log(p-value) | *n*= | Molecules |
|---|---|---|---|
| AMPK Signaling | 3.81 | 21 | CHRNA5, ATF2, PPM1B, CAB39, PRKAR2B, PIK3CB, SMARCC1, FOXO6, RAB9B, RAB3A, PPARGC1A, CCND1, SMARCD3, PPP2R5D, CHRNB2, PRKAR1B, PPP2R2B, ELAVL1, PHF10, MAPK11, CHRM4 |
| RAN Signaling | 3.57 | 5 | CSE1L, KPNA4, KPNA6, RAN, RANBP1 |
| Role of Oct4 in Mammalian Embryonic Stem Cell Pluripotency | 2.79 | 7 | RARA, JARID2, BMI1, NR5A2, WWP2, CCNF, KDM5B |
| Geranylgeranyldiphosphate Biosynthesis | 2.69 | 2 | FDPS, GGPS1 |
| Calcium Signaling | 2.68 | 17 | CHRNA5, ATF2, NFATC2, PRKAR2B, CAMK2D, MICU1, TRPC3, CACNA1B, ATP2B1, PPP3CA, ATP2B2, MCU, CHRNB2, PRKAR1B, CACNA2D2, TPM1, RYR2 |
| CDK5 Signaling | 2.47 | 11 | PPP1R14C, KRAS, PRKAR2B, ADCY7, ITGB1, PPP2R5D, PRKAR1B, PPP2R2B, MAPK11, GNAL, MAPK6 |
| Trans, Trans-farnesyl Diphosphate Biosynthesis | 2.22 | 2 | FDPS, GGPS1 |
| BMP Signaling Pathway | 1.83 | 8 | KRAS, ATF2, PRKAR2B, PITX2, TLX2, PRKAR1B, MAPK11, SMURF1 |
| Netrin Signaling | 1.81 | 7 | NFATC2, PRKAR2B, PRKAR1B, CACNA1B, PPP3CA, CACNA2D2, RYR2 |
| GP6 Signaling Pathway | 1.71 | 10 | SCHIP1, COL4A6, LAMC3, PRKD3, KLF12, COL4A5, COL24A1, COL25A1, PIK3CB, PTK2 |
| Cardiac Beta-Adrenergic Signaling | 1.65 | 11 | PPP1R14C, PDE4A, PRKAR2B, ADCY7, PDE4D, PPP2R5D, PRKAR1B, PPP2R2B, AKAP1, PDE10A, RYR2 |
| Opioid Signaling Pathway | 1.62 | 17 | KRAS, ATF2, PRKAR2B, PRKD3, ADCY7, CLTC, CAMK2D, CACNA1B, PPP3CA, GNAL, RGS3, MAPK6, PRKAR1B, CACNA2D2, RGS4, GRK6, RYR2 |
| Sonic Hedgehog Signaling | 1.61 | 4 | GLIS2, PRKAR2B, PRKAR1B, HHIP |
| Corticotropin Releasing Hormone Signaling | 1.6 | 11 | ATF2, GUCY1A2, PRKAR2B, PRKD3, UCN, ADCY7, PRKAR1B, CACNA1B, MAPK11, CACNA2D2, CRHR2 |
| Synaptic Long Term Potentiation | 1.59 | 9 | PPP1R14C, KRAS, GRM2, ATF2, PRKAR2B, PRKD3, CAMK2D, PRKAR1B, PLCL2, PPP3CA |
| Dopamine-DARPP32 Feedback in cAMP Signaling | 1.58 | 12 | PPP1R14C, ATF2, GUCY1A2, PRKAR2B, PRKD3, ADCY7, PPP2R5D, PRKAR1B, PPP2R2B, PLCL2, PPP3CA, KCNJ10 |
| cAMP-Mediated Signaling | 1.55 | 16 | GRM2, ATF2, PDE4A, CNGA4, PRKAR2B, ADCY7, CAMK2D, PPP3CA, GNAL, PDE10A, PDE4D, PRKAR1B, CHRM4, RGS4, AKAP1, DUSP4 |
| RAR Activation | 1.52 | 13 | RARA, PRKAR2B, PRKD3, ADCY7, PIK3CB, SMARCC1, ALDH1A2, PPARGC1A, SMARCD3, PRKAR1B, PHF10, MAPK11, SRA1 |
| Protein Kinase A Signaling | 1.49 | 21 | ATF2, TCF3, PDE4A, NFATC2, CNGA4, PRKAR2B, PRKD3, ADCY7, CAMK2D, PPP3CA, PTK2, PDE10A, ANAPC10, PPP1R14C, PTPRG, PDE4D, PRKAR1B, PLCL2, AKAP1, DUSP4, RYR2 |
| Sperm Motility | 1.48 | 9 | PDE4A, GUCY1A2, CNGA4, PRKAR2B, PRKD3, PDE4D, PRKAR1B, PLCL2, PTK2 |
| Regulation of Cellular Mechanics by Calpain Protease | 1.46 | 6 | KRAS, CNGA4, CCND1, ITGB1, TLN2, PTK2 |
| Synaptic Long Term Depression | 1.44 | 12 | IGF1R, KRAS, GRM2, GUCY1A2, PRKD3, PPP2R5D, PPP2R2B, PLCL2, CACNA1B, CACNA2D2, GNAL, RYR2 |
| ERK/MAPK Signaling | 1.41 | 13 | KRAS, ATF2, PRKAR2B, TLN2, PIK3CB, PTK2, HSPB2, PPP1R14C, ITGB1, PPP2R5D, PRKAR1B, PPP2R2B, DUSP4 |
| Renin-Angiotensin Signaling | 1.4 | 10 | KRAS, ATF2, PRKAR2B, PRKD3, ADCY7, SHC2, PRKAR1B, MAPK11, PIK3CB, PTK2 |
| Mitotic Roles of Polo-Like Kinase | 1.32 | 5 | STAG2, PPP2R5D, PPP2R2B, SMC3, ANAPC10 |

With only 61 DP for both marks, muscle chromatin of TM chickens displayed little changes compared to control animals at 35 days of age. This surprising result, given the large number of DE genes resulting from TM in muscle of heat-challenged broilers identified in a previous study (Loyau et al., 2016), is unlikely to be due to technical limitations given the very high sequencing depth employed in this study, above 74 M uniquely mapped reads for H3K27me3 instead of 40 M as recommended by ENCODE (Landt and Marinov, 2012) and 41 to 61 M uniquely mapped reads for H3K4me3 whereas ENCODE recommends 20 M for this mark in humans (**Supplementary Table S1**). The number of biological replicates (3) was also in agreement with ENCODE recommendations (> 2). Finally, the ChIP muscle preparation was optimized as shown in a previous study (David et al., 2017b) and led to the identification of a large number of peaks (**Table 1**) that were of expected shape and distribution (**Supplementary Table S1** and **Figures S1**, **S2**, and **S8**). Therefore, we are confident in concluding that TM had a limited impact on muscle H3K4me3 and H3K27me3 marks in our study. We previously showed in a transcriptome study based on the same *P. major* muscle tissue from the same Cobb 500 line of the same age and raised in the same experimental unit, that a large number of genes were DE in heat-challenged animals when they were TM. We hypothesized that some of these DE genes may bear epigenetic marks that may condition their response when animals were further exposed to a heat challenge in later life. Among the 61 genes that contained a DP identified in our study, none were found in the transcriptome data reannotated to match the current annotation. This suggests that both H3K4me3 and H3K27me3 marks are unlikely to be directly responsible for the DE genes resulting from TM previously observed in muscle. Whether or not other epigenetic marks or nonepigenetic mechanisms might be involved in long-term muscle TM response remains to be shown.

TM had a much stronger impact on both marks in the hypothalamus of 35-day-old chickens, with about 150 DP for H3K27me3 and 785 for H3K4me3. About 75% of H3K4me3 DP occurred at the 5' end of genes, which is mainly explained by the sharp distribution of this mark around gene TSS. Nonetheless, H3K4me3 DP were underrepresented in intergenic regions, suggesting that TM is likely to preferentially impact H3K4me3 peaks possibly controlling gene expression. We confirmed the differential enrichment identified at four candidate loci by ChIP-qPCR in four biological replicates per condition, suggesting that the epigenetic impact of TM was reproducible within the flock. However, among the five DP genes tested for differential expression by qRT-PCR, none seemed to be altered in expression (**Supplementary Figures S4** and **S7**). Even though H3K4me3 is globally associated with transcriptional activity, many reports also showed that epigenetic marks, in particular when analyzed individually, are not always instructive of transcriptional status (Dong and Weng, 2013; Howe et al., 2017). Instead, TM-induced DP may also promote changes in expression in response to a stimulus (such as heat) rather than a constitutive change in gene expression that may be deleterious for development under normal conditions. For instance, a post-natal heat conditioning of 3-day-old chicks affected the expression of key factors such as *BDNF* an *DNMT3A* (Yossifoff et al., 2008), *EZH2* (Kisliouk et al., 2011), *HSP70* (Kisliouk et al., 2017), *CRH* (Cramer et al., 2015), and *Eif2b5* (Kisliouk et al., 2010) only during a 24-hour heat exposure at 10 days of age but not in control rearing conditions. To test this hypothesis, a new experiment would be required to measure the expression of DP genes in the hypothalamus during a heat challenge at 35 days of age as performed previously (Loyau et al., 2016).

The HSP70 family of chaperone proteins was shown to be involved in the cytoprotection of heat acclimated rats (Horowitz, 2017). In addition, the methylation level of a distal part of the HSP70 promoter was suggested to reflect heat-stress-related epigenetic memory in postnatally heat-conditioned chicks (Kisliouk et al., 2017). All *HSP* and *HSF* were checked for DP in all conditions. None appeared to display a differential peak with the exception of *HSPB2* for which a significantly higher peak of H3K4me3 signal was found in the hypothalamus. Despite not being a member of the HSP70 family, the small HSPB2 chaperone was recently shown to be associated with neuropathies when disregulated (Yu et al., 2018) and thus may play a role in neuron proliferation, a process shown to be important for acclimation (Matsuzaki et al., 2017).

To explore which biological functions may have been impacted by histone mark changes induced by TM, we performed a comprehensive GO analysis including all conditions (mark, tissue). No significantly enriched GO term was found for muscle H3K27me3, likely due to the very low number of DP genes (17) in that condition. Thirty-nine GO terms identified were related to metabolic processes. This is consistent with findings showing that TM was shown to affect the expression of several metabolic regulator genes in muscle (Loyau et al., 2014) and to the fact that heat acclimation is known to impact metabolic rate in several animal models (Collin et al., 2001; Shein et al., 2007; Piestun et al., 2009). Thirty-six GO terms were associated with neuronal development. IPA biological function analysis confirmed an impact of TM on H3K4me3 peaks localized at genes controlling neurodevelopmental functions. This finding is consistent with previous reports in rats showing that neurogenesis plays an important role in the establishment of heat acclimation in this species (Matsuzaki et al., 2009; Shido and Matsuzaki, 2015). Heat exposure of 5-week-old rats was notably shown to induce GABAergic and/or glutamatergic heat-responsive neurons in the preoptic area of the hypothalamus, influencing autonomic thermoregulation in the long term (Matsuzaki et al., 2017). Thirty GO terms were associated with the regulation of gene expression, which is consistent with a previous hypothesis suggesting that heat exposure during embryogenesis may impact the dynamics of chromatin architecture to allow access of the regulatory transcription machinery to favor efficient response of TM birds to heat (Loyau et al., 2016). Interestingly, one functional cluster was shared by both marks and tissues (excluding muscle H3K27me3, for which no GO term was found as stated above). This cluster is associated with gene regulation at the protein modification level (sialylation, peptidyl-methionine modification or ubiquitination) reinforcing the idea that chromatin structure is a key player for long-term acclimation (Loyau et al., 2016). Finally, 49 GO terms were associated with various cellular processes that notably involve immune responsein agreement with previous findings showing that, in the muscle, genes controlling immune or inflammatory responses were found be DE in TM broilers during heat stress in later life (Loyau et al., 2016). Additionally, in rats, heat acclimation was also shown to alter immune functions (Schneider and Zuhl, 2016). Altogether, TM affected the enrichment level of histone marks at a number of genes involved in several functions previously shown to be impacted by the TM or other heat acclimation models.

One interesting finding highlighted by the IPA H3K4me3 DP analysis was the identification, among others, of the CRH signaling pathway as significantly enriched (**Supplementary Figure S5**). The CRH pathway is involved in the neuroendocrine, autonomic, and behavioral stress responses (Kovács, 2013). Several key players of the CRH signaling pathway, including the ones cited below, were identified as bearing a H3K4me3 DP. Among them, *CRHR2* encodes one of the two downstream G protein-coupled receptors of CRH involved in the increase of intracellular cAMP levels (Inda et al., 2017). A downstream target in the pathways identified in our study is *MAPK11*, encoding one of the four p38 MAPKs which was shown to participate to heat acclimation in rats (Horowitz, 2014). A substrate for this enzyme is the transcriptional factor ATF2, and the *ATF2* gene also contained a DP. Remarkably, ATF2 was shown to be involved in heterochromatin formation and heterochromatin disruption following heat stress-induced activation (Seong et al., 2011). ATF2 belongs to the cAMP-responsive element (CRE) family that comprises the transcription factor CREB which target genes include *BDNF*. *BDNF* was reported more than a decade ago to be a key player in the thermal-experience-dependent plasticity of the hypothalamus in the postnatal acclimation model in chicks (Katz and Meiri, 2006). *BDNF* changes in expression were shown to be under the control of epigenetic alterations in the postnatal model (Yossifoff et al., 2008). *BDNF* was not part of the list of DP-containing genes but we tested to see if changes in the CRH pathway may influence its expression in the hypothalamus of TM animals. We therefore tested the gene expression of *CRHR2*,

*ATF2*, *MAPK11* (DP genes) alongside the expression of *CRHR1, CREB1,* and *BDNF*. None of these genes appeared significantly misregulated, but *BDNF* showed a decrease in expression at the significance threshold of 0.1 (**Supplementary Figure S7**) that was replicated twice (data not shown). *CRHR1* also showed a decrease at the same significance threshold. More biological replicates might be necessary to verify this hypothesis. Nonetheless, it is worth mentioning that *BDNF* expression was shown to be increased by heat during postnatal conditioning (Katz and Meiri, 2006), and during a heat challenge following conditioning at 10 days of age (Yossifoff et al., 2008), but not after conditioning in absence of heat challenge. It would therefore be interesting to analyze *BDNF* expression, among other components of the CRH pathway, during or right after a heat exposure as was previously performed (Loyau et al., 2016). Finally, it is worth noting that we previously showed that the corticosterone (stress hormone) response seemed to be reduced in heat stressed TM chickens (vs. TM) compared to heat-stressed control chickens (vs. C) (Loyau et al., 2013). Given the interplay between corticosterone levels and *CRH* expression (Makino et al., 1994), it remains to be shown whether the changes in CRH signaling were induced directly during TM treatment and/or are a consequence of different stress response of TM animals during their lifetime until sampling.

In conclusion, this study provides the first line of evidence that embryonic TM in chicken involves lasting epigenetic changes in the hypothalamus that may contribute to the thermal acclimation of the animals.

# METHODS

## Animals

Experiments were performed in accordance with the legislation governing the ethical treatment of birds and were approved by the French Ministry of Higher Education and the Val De Loire Animal Ethics Committee (Authorization N°APAFIS#4608-201603211212171v2). Cobb 500 eggs were supplied by Hendrix Genetics (Saint-Laurent-de-la-Plaine, France). The 500 eggs were incubated and hatched and animals were raised at the INRA UE1295 PEAT Poultry Experimental Facility (2018, https://doi.org/10.15454/1.5572326250887292E12). Half of the eggs were incubated in TM conditions (39.5°C for 12h/day and 65% RH during E7-16, the rest of the time at 37.8°C and 56% RH) and the other half was incubated in standard condition (37.8°C, 56% RH). The 120 TM chicks and 143 control chicks were hatched, monitored for cloacal temperature using a KIMO KTT-310 probe thermometer (KIMO, Montpon Ménestérol, France) and sexed by venting. Male chickens were raised in four pens (two for TM and two for C) and slaughtered for Pectoralis Major muscle and hypothalamus sampling at 35 days of age. Statistical analysis of temperature at hatching was performed using a Student test. Six animals were used for muscle ChIP-seq experiments (three TM and three C) and six animals were used for hypothalamus ChIP-seq experiments (three TM and three C). For ChIP-qPCR validations, hypothalamus samples from six male animals (three TM and three C; 35 days old) from the same experimental batch were sampled. For RT-qPCR analysis, hypothalamus samples from 10 other male animals (six TM and four C; 35 days old) from the same experimental batch were sampled.

## Chromatin Immunoprecipitation, Library Construction, and Sequencing

Muscle native chromatin immunoprecipitation (ChIP) was performed as previously described (David et al., 2017b). For hypothalamus samples, tissues were ground in a mortar using a pestle both cooled using liquid nitrogen. Ground powder was transferred in 1.5 ml TPX tube containing fixation buffer (1% FA in PBS with 1 X Complete™ protease inhibitors, PBS-C, Roche) for 5 min at room temperature under agitation. The reaction was stopped by adding Glycine to 0,125M final. The samples were centrifuged for 5 min at 3,000 g and washed twice using 1-ml ice-cold PBS-C. Cells were then centrifuged 5 min at 5,000 g and cellular pellets were resuspended in 300 µl sodium Dodecyl Sulphate (SDS) Lysis Buffer (50 mM Tris-HCl pH 8, 10 mM EDTA pH 8, 1% SDS, 10% glycerol, 1 X Complete™ protease inhibitors). Tubes were vortexed 20 s, incubated 10 min on ice and vortexed 20 s again. Lysed nuclei were sonicated using a Bioruptor (Diagenode, Denville, USA) set to high setting (30 s ON, 30 s OFF; 4 × 5 min). Chromatin immunoprecipitation was then performed as previously described (David et al., 2017b) using 5 µl of H3K27me3 antibody (07–449, batch #2506493, Merck-Millipore, Billerica, USA) or 5 µl of H3K4me3 antibody (07–473, batch #JBC188194 for hypothalamus and #2717639 for muscle, Merck-Millipore, Billerica, USA). The Sequencing libraries were prepared using the NEB Next Ultra II DNA Library Prep kit for Illumina (New England Biolabs, Ipswich, USA). Ten ng of H3K27me3 IP DNA, 10 ng of H3K4me3 IP DNA and 100 ng of input DNA were used. For hypothalamus, 10, 7, and 4 cycles of PCR amplification were performed, respectively; for muscle, 7, 8, and 4 cycles of PCR amplification were performed, respectively. Agencourt AMPure XP beads (Beckman Coulter, Brea, USA) were used for the 200-bp size selection of DNA fragments. Library concentration was measured by Qubit™ dsDNA HS Assay Kit (Invitrogen, Carlsbad, USA).

All samples were sequenced by the GenomEast genomic platform (IGBMC, Illkirch, France). Sequencing was realized in single-end read with 50-bp fragments by an Illumina Hi-Seq 4,000 sequencer.

## Bioinformatic and Biostatistic Analyses of Peaks

Sequencing quality was verified by a FASTQC analysis version 0.11.8 (Babraham bioinformatics). All reads were mapped to the version 5 of the chicken reference genome (Gallus gallus 5.0, GenBank assembly accession GCA_000002315.3) using Bowtie 2 version 2.2.6.2 (Langmead and Salzberg, 2012) with default options. Read duplicates were removed using SAMtools version 1.7 (Li et al., 2009). H3K27me3 broad peak detection for both tissues was realized using epic version 0.1.25 (https://github.com/biocore-ntnu/epic), a reimplementation of SICER (Xu et al., 2014) (options: –fragment-size 50–gaps-allowed 2–false-discovery-rate-cutoff 0.05). For hypothalamus samples, H3K4me3 peak detection was realized using PePr (Zhang et al., 2014) (version 1.1.14) and default settings (option: –peaktype = SHARP). For H3K4me3

peaks in muscle samples, PePr window size of peak detection was fixed to 240 bp (options: –peaktype = SHARP -w 240) as peaks were too broad using default settings in this tissue. A union between controls and TM peaks was performed independently for each tissue to include in the analysis peaks specific from each treatment and peaks common between treatments. Counts at union peak level were computed using featureCounts (Liao et al., 2014) version 1.6.2 (options -F SAF -s 0).

Differential peaks (DP) between control and TM samples were identified using edgeR package version 3.20.8 (McCarthy et al., 2012) for the four data sets (H3K27me3 and H3K4me3 from muscle and hypothalamus samples). Raw counts were normalized for library size and peak composition using trimmed mean of M-values method as recommended by Dillies et al. (2013). Descriptive and diagnostic graphs, like MDS-plot, permitted to detect a technological batch effect corresponding to library preparation and sequencing. A generalized linear model was fitted on normalized counts for each peak including batch and challenging factors (TM vs. C). A likelihood ratio test was performed to test the effect of the challenging factor. Raw p-value were adjusted for multiple testing using the Benjamini-Hochberg procedure to control False Discovery Rate (Benjamini and Hochberg, 1995). Peaks with an adjusted p-value less than 0.05 were considered as differential.

Annotation of DP and analysis of their distribution was made with the GenomeFeatures R Package version 0.99 (https://forgemia.inra.fr/aurelien.brionne/GenomeFeatures) for promoter (3 Kbp upstream and 500 bp downstream of TSS), flanking exons (5'UTR, 3'UTR), exons, introns, and downstream (1 Kbp from TES) features on both strands. A DP was considered within a gene when at least 1 bp of the peak overlapped to the gene, from the TSS until the transcriptional end site (TES). Peaks were visualized with Integrative Genome Viewer (Robinson et al., 2011). BigWig files were obtained from bam files using bamCoverage from deepTools suite (Ramírez et al., 2016) version 3.0.0. Normalization factors were calculated by performing a ratio between the bam file which have the smallest number of unique reads aligned per condition and the bam file of interest of the corresponding condition. Then, mean of BigWig files in each condition and each tissue was realized with bigWigMerge and bedGraphToBigWig (UCSC bioinformatic tools (Kent et al., 2010).

## Functional Analysis

Biological interpretations were carried out using the GO public database with the use of Biological Process (BP) category using ViSEAGO R package (Brionne et al., 2019). Associated Gene terms were retrieved from EntrezGene database (Sept. 2018) for *Gallus gallus* and experimental GO terms from orthologous genes were added. Enrichment tests were performed using exact Fisher's test for each mark and tissue (four lists of genes). Enriched GO terms ($p < 0.01$) were grouped into functional clusters using hierarchical clustering based on Wang's semantic similarity between GO terms respecting GO graph topology and Ward's criterion. To go further in the interpretation, these functional clusters were grouped using hierarchical clustering based on BMA distance between sets of GO terms and Ward's criterion.

Ingenuity Pathway Analysis (IPA, Ingenuity Systems, Mountain View, CA; version 377306M, content version 27216297) was used to explore canonical pathways. Core analysis, originally developed to analyze the impacted biological functions from expression data set, was used on identified DP genes with gene symbol and the associated adjusted p-value to discover the impacted molecular and cellular functions.

## ChiP-qPCR

Hypothalamus were mechanically homogenized in 1 ml of 0,1X fixation buffer in PBS with 1 X Complete™ protease inhibitors (Roche) using 5-mm stainless steel beads (Retsch) and a Mixer Mill MM 400 (Retsch, 1 min at 10 Hz). The rest of the experiment was performed as the ChIP-seq experiments previously described using H3K4me3 antibody (07–473, batch #2839113, Merck-Millipore, Billerica, USA). Immunoprecipitated DNA was eluated in 60 µl of TE buffer. A selection of putative candidates was obtained from ChIP-seq DP data. DP selection was based on the adjusted p-value (< 0.05) and a fold change >2 or <0.5. qPCR primers were designed in or around the DP coordinates with NCBI Primer blast (https://www.ncbi.nlm.nih.gov/tools/primer-blast/index.cgi?LINK_LOC=BlastHome) (**Supplementary Table S6**). The qPCR was performed as previously described (David et al., 2017b) on 2 µl of ChIP DNA or 1 µl of input DNA in triplicates with 5 µM of each primer and Takyon No ROX SYBR 2X MasterMix blue dTTP (Eurogentec, Liege, Belgium) following manufacturer's instructions. Reactions were performed on a LightCycler®480 Instrument (Roche Diagnostics, Basel, Switzerland) using the following program: denaturation 5 min at 95°C, 50 amplification cycles (10 s at 95°C, 15 s at 60°C, and 15 s at 72°C), melting curve (5 s at 95°C, 1 min at 65°C, continuous at 95°C) and cooling. Enrichments were determined with the percent input method [100*2^ (adjusted input - Ct (IP)]. Statistical analyses of ChIP-qPCR were performed using R (version 3.5.1) by comparing TM (n = 3) and C (n = 3) enrichment using a Wilcoxon signed rank test with one-sided (alternative hypothesis as less) at the 0.05 level of significance.

## RNA Isolation, Reverse Transcription and Quantitative PCR for Gene Expression

Gene expression was evaluated by reverse transcription followed by real-time PCR as previously described. Total RNA was extracted from hypothalamus of biological replicates using AllPrep RNA/DNA Mini kit (Qiagen), according to the manufacturer's instruction. RNA integrity was verified by electrophoresis on agarose gel. RNA was quantified on a Nanodrop ND-1000 UV-Vis Spectrophotometer.

cDNAs were synthesized from 2 µg of total RNA using the Superscript II enzyme (Invitrogen) and hexamer random primers (Promega) in 20 µl final volume, following the manufacturer's instructions. Quantitative real-time PCR (qPCR) was carried out with Takyon qPCR Kits (Eurogentec) and using a LightCycler®480 Instrument II system (Roche) with 384-well plates (4TI-0382, 4titude).

Three technical replicates were performed for each sample and a standard curve protocol was used to evaluate gene expression.

Primer sequences (**Supplementary Table S7**) were designed with NCBI Primer blast or Primer3Plus (http://www.bioinformatics.nl/cgi-bin/primer3plus/primer3plus.cgi) software. To assess the amplification of the correct cDNA fragments, every PCR product size was checked on a 2% agarose gel and sequenced by Sanger sequencing (Genewiz). Relative expression was normalized to the expression of three reference genes (selected among four reference genes tested): *GAPDH*, *POLR2E,* and *CytB* using geNorm software (Vandesompele et al., 2002). Statistical analyses of gene expression were performed using R (version 3.5.1) by comparing TM (n = 6) and C (n = 4) enrichment using a Wilcoxon signed rank test with two-sided at the 0.05 level of significance.

## DATA AVAILABILITY STATEMENT

The datasets generated for this study can be found in the ChIP-seq data have been deposited in the ArrayExpress database at EMBL-EBI (www.ebi.ac.uk/arrayexpress) under accession number E-MTAB-7297 ("ChIP-seq of H3K4me3 and H3K27me3 histone marks in Pectoralis major muscle of 35 days-old control and thermally-manipulated chickens") and E-MTAB-7300 ("ChIP-seq of H3K4me3 and H3K27me3 histone marks in the hypothalamus of 35 days-old control and thermally manipulated chickens").

## ETHICS STATEMENT

The animal study was reviewed and approved by the French Ministry of Higher Education and the Val De Loire Animal Ethics Committee (Authorization N°APAFIS#4608-201603211212171v2).

## AUTHOR CONTRIBUTIONS

VC, AC, and S-AD designed the experiments. VC, S-AD, AVC, TB, SC, and NC performed the experiments. VC, CG, BP, CH-A, AB, AVC, YB and S-AD analyzed the results. VC, AVC, CG, AB, and CH-A wrote the manuscript. All authors read and approved the final manuscript.

## FUNDING

Studies were made possible by the financial support of INRA Department Animal Physiology and Livestock Systems (PHASE), project STRESSEPIMARK. S-AD PhD work was cofunded by INRA-PHASE and Region Centre-Val de Loire. AVC and CG were funded by the ANR JCJC "QuailHeatE" Research Program (ANR-15-CE02-0009-01).

## ACKNOWLEDGMENTS

The authors wish to thank C. Praud, A. Jacques, Y. Wang, S. Metayer-Coustard, E. Cailleau-Audouin, P. Chartrin, E. Coudert, C. Combémorel, E. Godet, E. Baéza, D. Nyuiadzi (URA, INRA, 37380 Nouzilly, France), and L. Beauclair (PRC, CNRS, IFCE, INRA, Université de Tours, 37380, Nouzilly, France) for their technical support; K. Anger, J. Delaveau, C. Rat, P. Ganier, and O. Callut (UE PEAT, INRA, 37380 Nouzilly, France) for the rearing and care of the animals; and A. Juanchich for GO analysis discussions. We thank P. Arensburger (Cal Poly Pomona, USA) for proofreading the manuscript. Sequencing was performed by the IGBMC Microarray and Sequencing platform, a member of the "France Génomique" consortium (ANR-10-INBS-0009).

## SUPPLEMENTARY MATERIAL

The Supplementary Material for this article can be found online at: https://www.frontiersin.org/articles/10.3389/fgene.2019.01207/full#supplementary-material

## REFERENCES

Benjamini, Y., and Hochberg, Y. (1995). Controlling the False Discovery Rate: a Practical and Powerful Approach to Multiple Testing. *J. R. Stat. Soc Ser. B*. 57 (1), 289–300.

Brionne, A., Juanchich, A., and Hennequet-Antier, C. (2019). ViSEAGO: a Bioconductor package for clustering biological functions using Gene Ontology and semantic similarity. *BioData Min*. 12, 16 doi: 10.1186/s13040-019-0204-1

Collin, A., van Milgen, J., Dubois, S., and Noblet, J. (2001). Effect of high temperature on feeding behaviour and heat production in group-housed young pigs. *Br. J. Nutr*. 86 (1), 63–70 doi: 10.1079/BJN2001356

Coustham, V., Li, P., Strange, A., Lister, C., Song, J., and Dean, C. (2012). Quantitative modulation of polycomb silencing underlies natural variation in vernalization. *Science* 337 (6094), 584–587. doi: 10.1126/science.1221881

Cramer, T., Kisliouk, T., Yeshurun, S., and Meiri, N. (2015). The balance between stress resilience and vulnerability is regulated by corticotropin-releasing hormone during the critical postnatal period for sensory development. *Dev. Neurobiol.* 75, 842–853. doi: 10.1002/dneu.22252

David, S.-A., Mersch, M., Foissac, S., Collin, A., Pitel, F., and Coustham, V. (2017a). Genome-wide epigenetic studies in chicken: a review. *Epigenomes* 1, 20. doi: 10.3390/epigenomes1030020

David, S.-A., Piégu, B., Hennequet-Antier, C., Pannetier, M., Aguirre-Lavin, T., and Crochet, S., et al. (2017b). An assessment of fixed and native chromatin preparation methods to study histone post-translational modifications at a whole genome scale in skeletal muscle tissue. *Biol. Proced. Online* 19. 10. doi: 10.1186/s12575-017-0059-0

Dillies, M. A., Rau, A., Aubert, J., Hennequet-Antier, C., Jeanmougin, M., and Servant, N. (2013). A comprehensive evaluation of normalization methods for Illumina high-throughput RNA sequencing data analysis.*Brief. Bioinform.* 14 (6), 671–683. doi: 10.1093/bib/bbs046

Dong, X., and Weng, Z. (2013). The correlation between histone modifications and gene expression. *Epigenomics* 5 (2), 113–116. doi:10.2217/epi.13.13

Fabrizio, P., Garvis, S., and Palladino, F. (2019). Histone methylation and memory of environmental stress. *Cells* 8 (4), E339. doi: 10.3390/cells8040339

Feil, R., and Fraga, M. F. (2012). Epigenetics and the environment: emerging patterns and implications. *Nat. Rev. Genet.* 13, 97–109. doi: 10.1038/nrg3142

Fresard, L., Morisson, M., Brun, J. M., Collin, A., Pain, B., and Minvielle, F. (2013). Epigenetics and phenotypic variability: some interesting insights from birds. *Genet. Sel. Evol.* 45, 12. doi: 10.1186/1297-9686-45-16

Havenstein, G. B., Ferket, P. R., and Qureshi, M. A. (2003). Growth, livability, and feed conversion of 1957 versus 2001 broilers when fed representative 1957 and 2001 broiler diets. *Poult. Sci.* 82 (10), 1500–1508. doi: 10.1093/ps/82.10.1500

Heijmans, B. T., Tobi, E. W., Stein, A. D., Putter, H., Blauw, G. J., and Susser, E. S., et al. (2008). Persistent epigenetic differences associated with prenatal exposure to famine in humans. *Proc. Natl. Acad. Sci. U. S. A.* 105, 17046–17049. doi: 10.1073/pnas.0806560105

Horowitz, M. (2014). Heat acclimation, epigenetics, and cytoprotection memory. *Compr. Physiol.* 4 (1), 199–230 doi: 10.1002/cphy.c130025

Horowitz, M. (2017). Heat acclimation-mediated cross-tolerance: origins in within-life epigenetics? *Front. Physiol.* 8, 1–10. doi:10.3389/fphys.2017.00548

Howe, F. S., Fischl, H., Murray, S. C., and Mellor, J. (2017). Is H3K4me3 instructive for transcription activation? *Bio Essays*. 39 (1), 1–12 doi: 10.1002/bies.201600095

Inda, C., Armando, N. G., dos Santos Claro, P. A., and Silberstein, S. (2017). Endocrinology and the brain: corticotropin-releasing hormone signaling. *Endocr. Connect*. 6 (6), R99–R120. doi: 10.1530/EC-17-0111

Katz, A., and Meiri, N. (2006). Brain-derived neurotrophic factor is critically involved in thermal-experience-dependent developmental plasticity. *J. Neurosci.* 26, 3899–3907. doi:10.1523/JNEUROSCI.0371-06.2006

Kent, W. J., Zweig, A. S., Barber, G., Hinrichs, A. S., and Karolchik, D. (2010). Bigwig and Bigbed: enabling browsing of large distributed datasets. *Bioinformatics*. 26 (17), 2204–2207. doi: 10.1093/bioinformatics/btq351

Kisliouk, T., Ziv, M., and Meiri, N. (2010). Epigenetic control of translation regulation: Alterations in histone H3 lysine 9 post-translation modifications are correlated with the expression of the translation initiation factor 2B (Eif2b5) during thermal control establishment. *Dev. Neurobiol.* 70, 100–113. doi: 10.1002/dneu.20763

Kisliouk, T., Yosefi, S., and Meiri, N. (2011). MiR-138 inhibits EZH2 methyltransferase expression and methylation of histone H3 at lysine 27, and affects thermotolerance acquisition. *Eur. J. Neurosci.* 33, 224–235. doi: 10.1111/j.1460-9568.2010.07493.x

Kisliouk, T., Cramer, T., and Meiri, N. (2017). Methyl CpG level at distal part of heat-shock protein promoter HSP70 exhibits epigenetic memory for heat stress by modulating recruitment of POU2F1-associated nucleosome-remodeling deacetylase (NuRD) complex. *J. Neurochem.* 141, 358–372. doi: 10.1111/jnc.14014

Kovács, K. J. (2013). CRH: The link between hormonal-, metabolic- and behavioral responses to stress. *J. Chem. Neuroanat*. 54, 25–33. doi: 10.1016/j.jchemneu.2013.05.003

Landt, S., and Marinov, G. (2012). ChIP-seq guidelines and practices of the ENCODE and modENCODE consortia. *Genome Res.* 22 (9), 1813–1831. doi: 10.1101/gr.136184.111

Langmead, B., and Salzberg, S. L. (2012). Fast gapped-read alignment with Bowtie 2.*Nat. Methods*9,357–359. doi: 10.1038/nmeth.1923

Li, H., Handsaker, B., Wysoker, A., Fennell, T., Ruan, J., and Homer, N., et al. (2009). The Sequence Alignment/Map format and SAMtools. *Bioinformatics*. 25 (16), 2078–2079. doi: 10.1093/bioinformatics/btp352

Liao, Y., Smyth, G. K., and Shi, W. (2014). FeatureCounts: an efficient general purpose program for assigning sequence reads to genomic features. *Bioinformatics*. 30 (7), 923–930. doi: 10.1093/bioinformatics/btt656

Loyau, T., Berri, C., Bedrani, L., Métayer-Coustard, S., Praud, C., and Duclos, M. J., et al. (2013). Thermal manipulation of the embryo modifies the physiology and body composition of broiler chickens reared in floor pens without affecting breast meat processing quality. *J. Anim. Sci.* 91, 3674–3685. doi: 10.2527/jas2013-6445

Loyau, T., Berri, C., Crochet, S., Cailleau-Audouin, E., and Sannier, M., et al. (2014). Thermal manipulation during embryogenesis has long-term effects on muscle and liver metabolism in fast-growing chickens. *PloS One* 9 (9), e105339. doi: 10.1371/journal.pone.0105339

Loyau, T., Bedrani, L., Berri, C., Metayer-Coustard, S., Praud, C., and Coustham, V., et al. (2015). Cyclic variations in incubation conditions induce adaptive responses to later heat exposure in chickens: a review. *Animal* 9 (1), 76–85. doi: 10.1017/S1751731114001931

Loyau, T., Hennequet-Antier, C., Coustham, V., Berri, C., Leduc, M., and Crochet, S., et al. (2016). Thermal manipulation of the chicken embryo triggers differential gene expression in response to a later heat challenge. *BMC Genomics* 17, 329. doi: 10.1186/s12864-016-2661-y

Makino, S., Gold, P. W., and Schulkin, J. (1994). Corticosterone effects on corticotropin-releasing hormone mRNA in the central nucleus of the amygdala and the parvocellular region of the paraventricular nucleus of the hypothalamus. *Brain Res.* 640 (1–2), 105–112. doi: 10.1016/0006-8993(94)91862-7

Matsuzaki, K., Katakura, M., Hara, T., Li, G., Hashimoto, M., and Shido, O. (2009). Proliferation of neuronal progenitor cells and neuronal differentiation in the hypothalamus are enhanced in heat-acclimated rats. *Pflugers Arch. Eur. J. Physiol.* 458 (4), 661–673, doi: 10.1007/s00424-009-0654-2

Matsuzaki, K., Katakura, M., Sugimoto, N., Hara, T., Hashimoto, M., and Shido, O. (2017). Neural progenitor cell proliferation in the hypothalamus is involved in acquired heat tolerance in long-term heat-acclimated rats. *PloS One* 12, 1–16. doi: 10.1371/journal.pone.0178787

McCarthy, D. J., Chen, Y., and Smyth, G. K. (2012). Differential expression analysis of multifactor RNA-Seq experiments with respect to biological variation. *Nucleic Acids Res.* 40 (10), 4288–4297 doi: 10.1093/nar/gks042

Piestun, Y., Shinder, D., Ruzal, M., Halevy, O., Brake, J., and Yahav, S. (2008). Thermal manipulations during broiler embryogenesis: effect on the acquisition of thermotolerance. *Poult. Sci.* 87, 1516–1525. doi: 10.3382/ps.2008-00030

Piestun, Y., Halevy, O., and Yahav, S. (2009). Thermal manipulations of broiler embryos–the effect on thermoregulation and development during embryogenesis. *Poultry Sci.* 88 (12), 2677–2688. doi:10.3382/ps.2009-00231

Ramírez, F., Ryan, D. P., Grüning, B., Bhardwaj, V., Kilpert, F., and Richter, A. S., et al. (2016). Deeptools2: a next generation web server for deep-sequencing data analysis. *Nucleic Acids Res.* 44 (W1), W160–W165. doi: 10.1093/nar/gkw257

Robinson, J. T., Thorvaldsdóttir, H., Winckler, W., Guttman, M., Lander, E. S., and Getz, G., et al. (2011). Integrative genomics viewer. *Nat. Biotechnol.* 29 (1), 24–26 doi: 10.1038/nbt.1754

Schneider, S. M., and Zuhl, M. N. (2016). HSP72 Up-regulation with heat acclimation.*Temperature*3,28–30. doi:10.1080/23328940.2016.1148525

Seong, K. H., Li, D., Shimizu, H., Nakamura, R., and Ishii, S. (2011) .Inheritance of stress-induced, ATF-2-dependent epigenetic change. *Cell* 145, 1049–1061. doi: 10.1016/j.cell.2011.05.029

Shein, N. A., Horowitz, M., and Shohami, E. (2007). Heat acclimation: a unique model of physiologically mediated global preconditioning against traumatic brain injury. *Prog. Brain Res.* 161, 353–363. doi: 10.1016/S0079-6123(06)61025-X

Shido, O., and Matsuzaki, K. (2015). Involvement of neurogenesis in the hypothalamic area in establishing long-term heat acclimation in rats. *Temperature*. 2 (3), 362–367. doi:10.1080/23328940.2015.1076591

St-Pierre, N. R., Cobanov, B., and Schnitkey, G. (2003) .Economic Losses from Heat Stress by US Livestock Industries. *J. Dairy Sci.* 86, E52–E77. doi: 10.3168/jds.S0022-0302(03)74040-5

Vandesompele, J., De Preter, K., Pattyn, F., Poppe, B., Van Roy, N., and De Paepe, A., eta al. (2002). Accurate normalization of real-time quantitative RT-PCR data by geometric averaging of multiple internal control genes. *Genome Biol.* 3, RESEARCH0034. doi: 10.1186/gb-2002-3-7-research0034

Xu, S., Grullon, S., Ge, K., and Peng, W. (2014). Spatial clustering for identification of chip-enriched regions (SICER) to map regions of histone methylation patterns in embryonic stem cells. *Methods Mol. Biol.* 1150, 97–111. doi: 10.1007/978-1-4939-0512-6_5

Yahav, S., and McMurtry, J. P. (2001). Thermotolerance acquisition in broiler chickens by temperature conditioning early in life - The effect of timing and ambient temperature. *Poult. Sci.* 80 (12), 1662–1666. doi: 10.1093/ps/80.12.1662

Yossifoff, M., Kisliouk, T., and Meiri, N. (2008). Dynamic changes in DNA methylation during thermal control establishment affect CREB binding to the brain-derived neurotrophic factor promoter. *Eur. J. Neurosci.* 28, 2267–2277. doi: 10.1111/j.1460-9568.2008.06532.x

Yu, L., Petyuk, V. A., Gaiteri, C., Mostafavi, S., Young-Pearse, T., and Shah, R. C., et al. (2018). Targeted brain proteomics uncover multiple pathways to Alzheimer's dementia. *Ann. Neurol.* 84 (1), 78–88. doi: 10.1002/ana.25266

Zhang, Y., Lin, Y. H., Johnson, T. D., Rozek, L. S., and Sartor, M. A. (2014). PePr: a peak-calling prioritization pipeline to identify consistent or differential peaks from replicated ChIP-Seq data. *Bioinformatics* 30 (18), 2568–2575. doi: 10.1093/bioinformatics/btu372

**Conflict of Interest:** The authors declare that the research was conducted in the absence of any commercial or financial relationships that could be construed as a potential conflict of interest.

*Copyright © 2019 David, Vitorino Carvalho, Gimonnet, Brionne, Hennequet-Antier, Piégu, Crochet, Couroussé, Bordeau, Bigot, Collin and Coustham. This is an open-access article distributed under the terms of the Creative Commons Attribution License (CC BY). The use, distribution or reproduction in other forums is permitted, provided the original author(s) and the copyright owner(s) are credited and that the original publication in this journal is cited, in accordance with accepted academic practice. No use, distribution or reproduction is permitted which does not comply with these terms.*

frontiers in Genetics

REVIEW
published: 18 March 2020
doi: 10.3389/fgene.2020.00205

# Epigenetic Reprogramming During Somatic Cell Nuclear Transfer: Recent Progress and Future Directions

*Xiangyu Wang[1†], Jiadan Qu[1†], Jie Li[2†], Hongbin He[3], Zhonghua Liu[4] and Yanjun Huan[1*]*

[1] College of Veterinary Medicine, Qingdao Agricultural University, Qingdao, China, [2] Department of Cadre Health Care, Qingdao Municipal Hospital, Qingdao, China, [3] College of Life Sciences, Shandong Normal University, Jinan, China, [4] College of Life Sciences, Northeast Agricultural University, Harbin, China

Somatic cell nuclear transfer (SCNT) has broad applications but is limited by low cloning efficiency. In this review, we mainly focus on SCNT-mediated epigenetic reprogramming in livestock and also describe mice data for reference. This review presents the factors contributing to low cloning efficiency, demonstrates that incomplete epigenetic reprogramming leads to the low developmental potential of cloned embryos, and further describes the regulation of epigenetic reprogramming by long non-coding RNAs, which is a new research perspective in the field of SCNT-mediated epigenetic reprogramming. In conclusion, this review provides new insights into the epigenetic regulatory mechanism during SCNT-mediated nuclear reprogramming, which could have great implications for improving cloning efficiency.

**Keywords: somatic cell nuclear transfer, cloning efficiency, nuclear reprogramming, epigenetic modification, long non-coding RNA**

OPEN ACCESS

***Edited by:***
*Helene Kiefer,*
*INRA Centre Jouy-en-Josas, France*

***Reviewed by:***
*Nathalie Beaujean,*
*Institut National de Recherche pour l'Agriculture, l'Alimentation et l'Environnement (INRAE), France*
*Masahiro Kaneda,*
*Tokyo University of Agriculture and Technology, Japan*

****Correspondence:***
*Yanjun Huan*
*huanyanjun1982@163.com*

*† These authors have contributed equally to this work*

***Specialty section:***
*This article was submitted to Epigenomics and Epigenetics, a section of the journal Frontiers in Genetics*

***Received:*** *23 October 2019*
***Accepted:*** *21 February 2020*
***Published:*** *18 March 2020*

***Citation:***
*Wang X, Qu J, Li J, He H, Liu Z and Huan Y (2020) Epigenetic Reprogramming During Somatic Cell Nuclear Transfer: Recent Progress and Future Directions. Front. Genet. 11:205. doi: 10.3389/fgene.2020.00205*

## INTRODUCTION

Somatic cell nuclear transfer (SCNT) is an assisted reproduction technology for the generation of cloned mammals that involves the culture of donor somatic cells and oocytes, transplantation of donor cell nuclei into enucleated oocytes, activation of reconstructed embryos, and transfer of cloned embryos into surrogates (**Figure 1**). SCNT enables the reprogramming of terminally differentiated cells into totipotent cells, which has revolutionized our understanding of cell fate determination and development, and has significant value for theoretical research and production applications.

## SCNT IN MAMMALS

The first SCNT mammal was a sheep known as Dolly that was born in 1997 (Wilmut et al., 1997), and since then, SCNT has entered a new era (**Table 1**). A series of cloned mammals, including cow, mouse, goat, pig, and cat, have been produced with this technology (Cibelli et al., 1998; Wakayama et al., 1998; Baguisi et al., 1999; Polejaeva et al., 2000; Chesne et al., 2002; Shin et al., 2002; Galli et al., 2003; Woods et al., 2003; Zhou et al., 2003; Lee et al., 2005; Li et al., 2006; Berg et al., 2007; Shi et al., 2007; Wani et al., 2010). In 2018, the first non-human primate species, the macaque monkey, was successfully cloned by SCNT, further attracting worldwide attention on SCNT technology (Liu et al., 2018; Matoba and Zhang, 2018). Using this

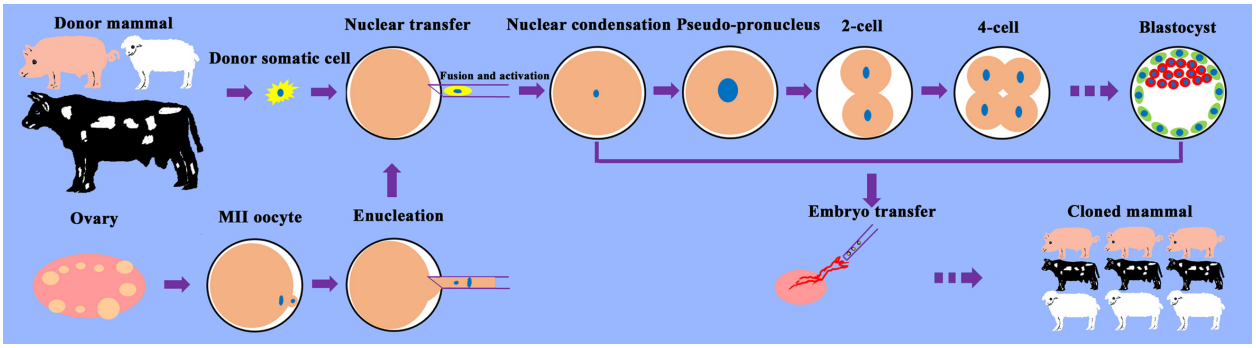



**FIGURE 1 |** Schematic illustration of the SCNT process. Somatic cells from the desired donor mammal are cultured for SCNT. Oocytes are recovered from the ovaries obtained from the slaughterhouse and allowed to mature into metaphase (M)II oocytes. MII oocytes are enucleated, and donor somatic cells are transferred into the perivitelline space of oocytes. After the fusion and activation of cell–cytoplast complexes, the reconstructed cloned embryos begin to develop, undergoing nuclear condensation and nuclear swelling, followed by pseudo-pronucleus, 2-cell, 4-cell, etc. stages and form blastocysts *in vitro*. Cloned embryos are transferred into surrogates and develop into cloned mammals.

technology, a large number of mammals have been successfully produced, showing many potential applications (Campbell et al., 2007; Ogura et al., 2013; Telugu et al., 2017). In agriculture, SCNT can rescue endangered species, protect the genetic resources of commercially important species, and accelerate the propagation of breeding livestock, including pigs, cows, and sheep (Gomez et al., 2009; Keefer, 2015). In combination with genome-modification technologies such as the recently developed clustered regularly interspaced short palindromic repeats (CRISPR)/CRISPR-associated protein 9-mediated genome editing, SCNT can rapidly produce cloned mammals with desirable traits including rapid growth, disease resistance, and good meat quality, thereby cultivating novel varieties, and shortening breeding cycle (Galli et al., 2012; Wells and Prather, 2017; Lee et al., 2020). In biomedicine, SCNT can create a mammary gland bioreactor to produce therapeutic proteins, establish animal models to investigate the pathogenesis of human diseases, and produce genetically modified xenograft organs for patient transplantation (Lotti et al., 2017; Niu et al., 2017; Telugu et al., 2017). SCNT can also generate blastocyst-derived stem cells, namely, nuclear transfer embryonic stem cells (ntESCs), especially human ntESCs, which are isogenic to the donor and do not cause immune rejection when transplanted, thus providing an important tool for organ regeneration (Tachibana et al., 2013). In basic research, SCNT has been used to investigate interactions between the nucleus and cytoplasm, which has enhanced our understanding of the mechanisms of cell fate determination (Long et al., 2014). Moreover, SCNT has promoted the generation and development of induced pluripotent stem cells (iPSCs), which have similar therapeutic applications to ntESCs (Takahashi and Yamanaka, 2006).

## LOW CLONING EFFICIENCY LIMITS THE APPLICABILITY OF SCNT

Although SCNT has been successfully used to clone many species of mammals with significant improvements in cloning efficiency in more than 20 years since the birth of Dolly, the proportion of cloned embryos that develop to full term remains very low, greatly limiting the application of SCNT technology (Czernik et al., 2019). To improve the birth of cloned mammals and cloning efficiency, researchers have investigated the effects of donor cell type, oocyte maturation stage, embryo activation method, etc. on the developmental competence of cloned embryos (**Table 1**), and to some extent, cloning efficiency has been shown to increase through optimizing these parameters (Blelloch et al., 2006; Campbell et al., 2007; Kurome et al., 2013). However, cloning efficiency remains low, the abortion of cloned fetus frequently occurs, and the rate of abnormality or mortality is high. Moreover, developmental defects still occur in cloned mammals even after birth (Campbell et al., 2007; Loi et al., 2016). These phenomena demonstrate that optimizing these technology parameters of SCNT cannot make significant improvements in cloning efficiency and only clarifying the theoretical molecular mechanism underlying SCNT could understand the cause of the poor and abnormal development of cloned embryos. However, SCNT-mediated nuclear reprogramming is still poorly understood, and the key factors determining the developmental potential of cloned embryos remain unclear (Matoba and Zhang, 2018). Therefore, fully and clearly revealing the molecular mechanism underlying SCNT-mediated nuclear reprogramming is needed to enhance the development of cloned embryos.

## INCOMPLETE EPIGENETIC REPROGRAMMING UNDERLIES LOW CLONING EFFICIENCY

During development, totipotent embryos differentiate into pluripotent stem cells and subsequently into differentiated cells. Cell fate determination is largely achieved by activating some genes while suppressing other genes through epigenetic modification such as DNA methylation, histone modification, genomic imprinting, and X chromosome inactivation (XCI) (Reik et al., 2003). These heritable changes in gene expression

**TABLE 1 |** Mammals first cloned by different SCNT-based procedures.

| Mammal | Special procedures | | |
|---|---|---|---|
| | **Donor cells** | **Oocytes** | **Cloned embryos** |
| Sheep | Synchronized adult mammary epithelial cells | Superovulated MII oocytes | General SCNT |
| Cow | Transgenic fetal fibroblast cells | Oocyte maturation *in vitro* | General SCNT |
| Mouse | Adult cumulus cells without *in vitro* culture | Superovulated MII oocytes | Donor cells injected into enucleated oocytes |
| Goat | Synchronized transgenic fetal fibroblast cells | Superovulated MII and TII oocytes | General SCNT |
| Pig | Synchronized adult granulosa cells | Superovulated MII oocytes and zygotes | Double nuclear transfer |
| Cat; ferret | Adult cumulus cells | Oocyte maturation *in vitro* | General SCNT |
| Rabbit | Adult transgenic cumulus cells | Superovulated MII oocytes | General SCNT |
| Mule | Fetal fibroblast cells | Oocyte collection *in vivo* | General SCNT |
| Horse | Adult fibroblast cells | Oocyte maturation *in vitro* | Zona-free manipulation |
| Rat | Synchronized fetal fibroblast cells | Oocyte maturation *in vivo*; blocking oocyte activation | One-step SCNT |
| Dog | Adult fibroblast cells | Oocyte maturation *in vivo* | General SCNT |
| Buffalo | Synchronized fetal fibroblast and adult granulosa cells | Oocyte maturation *in vitro* | General SCNT |
| Red deer | Antlerogenic periosteum, putative bone and fat cells | Oocyte maturation *in vitro* | General SCNT |
| Camel | Adult cumulus cells | Oocyte maturation *in vivo* | General SCNT |
| Macaque monkey | Fetal fibroblast cells | Oocyte maturation *in vivo* | HVJ-E-mediated fusion; embryos with kdm4d injection and TSA treatment |

*General SCNT refers to the fact that donor cell is transferred into the perivitelline space of enucleated MII oocyte and the cell–cytoplast complexes are fused by electrical stimulation and activated by electrical or chemical induction.*

without alterations in genomic DNA sequences occur during the progression from fertilized oocyte to differentiated embryo and also play a key role in embryo development following SCNT (Niemann, 2016). It is thought that the low cloning efficiency, abnormal embryo phenotype, and low viability of animals generated by SCNT are due to incomplete reprogramming of donor nuclei (Yang et al., 2007). Epigenetic changes during the SCNT process are discussed in greater detail below (**Figure 2**).

DNA methylation occurs at cytosine residues in the CpG dinucleotide and is generally associated with transcriptional silencing (Schubeler, 2015). In the life cycle, the genome undergoes DNA methylation maintenance, DNA demethylation, and DNA remethylation, which allows organisms to activate or silence specific genes according to the requirements of organism growth and development (Li and Zhang, 2014). DNA methyltransferases (Dnmts) such as Dnmt1 and Dnmt3 (Dnmt3a, Dnmt3b, and Dnmt3l) are responsible for DNA methylation maintenance and *de novo* DNA methylation (Chen and Zhang, 2019). DNA demethylation occurs through the oxidation-base excision repair pathway. Oxidative DNA demethylation enzymes include ten–eleven translocation (Tet)1, Tet2, Tet3, activation-induced cytidine deaminase, and DNA glycosylases (Ito et al., 2010; Iqbal et al., 2011; Shen et al., 2013). Other pathways also contribute to active DNA demethylation during early embryonic development (Wang et al., 2014). Dnmt1 maintains methyl marks on genomic DNA and ensures that the DNA methylation pattern of offspring cells is identical to that of parental cells (Lyko, 2018). After fertilization, the genome demonstrates a combination of active and passive DNA methylation, and the paternal genomic DNA is actively demethylated while maternal genomic DNA is passively demethylated (Guo et al., 2014). When fertilized embryos develop to the blastocyst or subsequent implantation stage, genomic DNA is remethylated (Reik et al., 2001; Yang et al., 2007). In cloned embryos, the genomic DNA of donor somatic cells is highly methylated and DNA methylation reprogramming (especially DNA demethylation) is necessary for development to proceed normally. The genome also undergoes de-/remethylation during SCNT, but this is delayed and incomplete compared with normal embryos (Bourc'his et al., 2001; Dean et al., 2001; Yang et al., 2007). Tissue-specific and pluripotency-related genes in cloned embryos show low and high DNA methylation levels, respectively (**Figure 2**, DNA methylation) (Ng and Gurdon, 2005; Kremenskoy et al., 2006; Yamazaki et al., 2006; Huan et al., 2014, 2015a). Following zygotic genome activation (ZGA), the erroneous reconstitution of DNA methylation pattern caused by aberrant expression of genes related to DNA methylation reprogramming and, consequently, of key genes required for the normal development of cloned embryos results in low cloning efficiency and abnormalities and death in cloned animals (Bourc'his et al., 2001; Bortvin et al., 2003; Chung et al., 2003; Kiefer et al., 2016; Gao et al., 2018). Thus, a DNA methylation pattern similar to that in normal fertilized embryos is necessary for the successful development of SCNT embryos.

Chromatin structure and histone modification are key factors that regulate gene expression (Sproul et al., 2005; Yi and Kim, 2018). The basic structural unit of chromatin is the nucleosome, a histone octamer consisting of two copies each of H2A, H2B, H3, and H4 wrapped by 146 bp of DNA and H1 as a linker (Kobayashi and Kurumizaka, 2019). Gene expression depends on chromatin accessibility, which is controlled by chromatin remodeling factors and through covalent modification (e.g., acetylation, methylation, and phosphorylation) of amino acids in the histone tail (Qin et al., 2016; Kobayashi and Kurumizaka, 2019). Chromatin accessibility during the SCNT-mediated epigenetic reprogramming has not been extensively investigated as it requires a large number of embryos. Recently, progress is being made in mice owing to technologic advances such as low-input DNase I hypersensitive site (DHS) sequencing and transposase-accessible chromatin sequencing (Wu et al., 2016; Djekidel et al., 2018). DHSs, which are positively correlated with gene expression, are present in

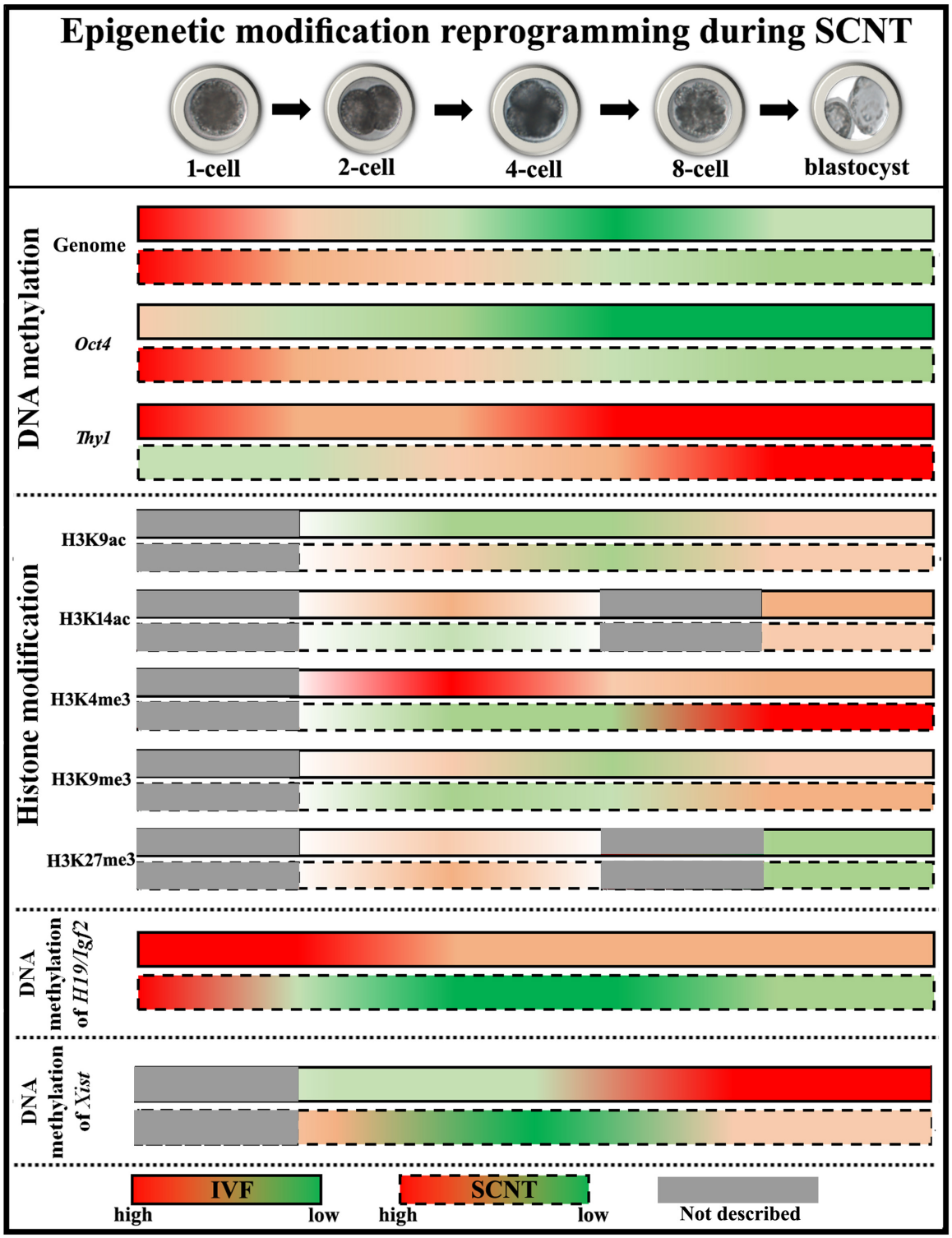



**FIGURE 2 |** Diagram of epigenetic modification changes during SCNT-mediated nuclear reprogramming. The data of pig embryos are adopted to describe epigenetic modification reprogramming. For DNA methylation, cloned embryos demonstrate delayed DNA demethylation and incomplete DNA remethylation of genome (the data shown here represent DNA methylation status at centromeric repeats, which partly reflects genome DNA status), high DNA methylation status of pluripotency-related gene *Oct4*, and low DNA methylation levels of tissue-specific gene *Thy1*, respectively. For histone modifications, low levels of histone acetylation (H3K9ac at the ZGA stage and H3K14ac at the blastocyst stage) and H3K4me3, and high levels of histone methylation (H3K9me3 after ZGA and H3K27me3 at the 2-cell stage) are observed in cloned embryos. For genomic imprinting, DNA methylation of *H19/Igf2* is not maintained during SCNT. For XCI, DNA methylation of *Xist* is not fully established in female cloned embryos.

donor somatic cells and are reprogrammed in cloned embryos. However, specific DHSs of donor somatic cells fail to be reprogrammed to those of embryos, which prevents the binding of chromatin remodeling factors to regulate gene expression in cloned embryos (Djekidel et al., 2018).

Histone acetylation is regulated by histone acetyltransferase (Hat) and histone deacetylase (Hdac). Hat opens up chromatin, which allows transcription factor binding and leads to activation of gene transcription, whereas Hdac promotes gene inactivation (Sun et al., 2003). After fertilization, histone acetylation such as histone H3 acetylation occurs and allows the appropriate expression of genes related to early embryonic development (Rybouchkin et al., 2006; Ziegler-Birling et al., 2016). During SCNT, histone acetylation marks decrease and gradually disappear, for instance, Lys9 acetylation of H3 (H3K9ac) at the ZGA stage and H3K14ac at the blastocyst stage (Rybouchkin et al., 2006; Wee et al., 2006; Liu et al., 2012; Zhai et al., 2018). Histone methylation mainly occurs on lysine and arginine, and involves three methylation patterns including monomethylation, dimethylation, and trimethylation (Izzo and Schneider, 2010). Trimethyl of H3 Lys4 (H3K4me3) and H3K27me3 are the most typical modifications. H3K4me3 is regulated by the Trithorax group (TrxG) complex and is associated with gene activation, while H3K27me3 is mediated by the Polycomb group (PcG) proteins and leads to gene silencing (Liu X. et al., 2016). During SCNT-mediated nuclear reprogramming, H3K4me3 level decreases and H3K27me3 level increases (Cao et al., 2015; Xie et al., 2016; Zhai et al., 2018; Zhou et al., 2019). Another modification, H3K9me3, is catalyzed by suppressor of variegation 39H1/2 (Suv39H1/2) and removed by lysine demethylase (Kdm)4 (Kdm4a, Kdm4b, Kdm4d, and Kdm4e), and can alter chromatin conformation to inhibit gene expression (Ninova et al., 2019). H3K9me3 can be removed in donor somatic cells, but incomplete H3K9me3 demethylation in cloned embryos inhibits their development. Studies have shown that H3K9me3 is enriched in the promoters of genes against SCNT-mediated nuclear reprogramming, suggesting that incomplete H3K9me3 demethylation is an inhibitor of the development of cloned embryos (Matoba et al., 2014; Liu W. et al., 2016; Zhai et al., 2018). These disrupted histone modifications finally affect chromatin accessibility, lead to the disordered expression of genes required for the normal development of cloned embryos, and result in low cloning efficiency (**Figure 2**, Histone modification) (Liu et al., 2012; Xie et al., 2016; Zhai et al., 2018). Several histone variants also exhibit abnormalities such as the delayed change of H1foo (oocyte-specific H1) to somatic H1s, macroH2A expression before the endogenous activation, and the existing replacement of donor cell H3 carrying repressive modification by maternal H3.3 in cloned embryos, which contributes to incomplete SCNT-mediated nuclear reprogramming (Gao et al., 2004; Chang et al., 2010; Wen et al., 2014). Therefore, histone modification is a critical determinant in the development of cloned embryos.

Genomic imprinting, an epigenetically regulated phenomenon that shows monoallelic parent-specific gene expression, is controlled by the differentially methylated region (DMR) or specific histone modifications. The DMR is protected by DNA-binding complexes composed of Dnmt1, zinc finger protein 57, and tripartite motif-containing 28, and the H3K27me3 mark (Barlow and Bartolomei, 2014; Inoue et al., 2017a). In general, paternal and maternal gene imprinting promotes and inhibits, respectively, offspring growth and development (Barlow and Bartolomei, 2014). Therefore, parental imprinted genes compete with or complement each other, and the balance between the expression of paternal and maternal imprinted genes is important for normal developmental progression. H19/insulin-like growth factor (Igf)2 is a typical genomic imprinting locus with the DMR methylated on the paternal allele, on which H19 silencing stimulates IGF2 activity and cell growth. In contrast, H19 on the maternal allele is an inhibitory factor that has a cis-silencing effect on Igf2 expression. Inhibiting Igf2 expression leads to fetal growth retardation, whereas Igf2 overexpression or H19 transcription deficiency results in fetal overgrowth (Sasaki et al., 2000). Genomic imprinting is erased and established during gametogenesis and is maintained throughout the lifetime of an organism (Simon et al., 1999; MacDonald and Mann, 2014). Thus, the restoration of a diploid genome in fertilized embryos and mutually compensatory expression of monoallelic parent-specific imprinted genes ensure normal growth and development of early embryos. However, genomic imprinting is not effectively maintained in cloned embryos, resulting in the aberrant expression of imprinted genes that gives rise to development defects such as placental hypertrophy and fetal abortion and death (**Figure 2**, Genome imprinting) (Mann et al., 2003; Shi et al., 2003; Yang et al., 2007; Wei et al., 2010; Zhang et al., 2014; Huan et al., 2015b). For example, hypomethylated H19/Igf2 imprinting results in increased H19 transcription and suppresses the growth of cloned fetuses, whereas Igf2 overexpression mediated by hypermethylated H19/Igf2 imprinting leads to their overgrowth. Therefore, disrupted genome imprinting during the development of cloned embryos results in developmental abnormalities and death in cloned offspring, constraining the cloning efficiency.

Female mammals have two X chromosomes, whereas only one is present in males. In order to balance gene dosage, female mammals silence one X chromosome through the activity of the Xist gene product, a long non-coding (lnc)RNA on the inactive X chromosome that recruits transcriptional repressors such as PcG proteins (Latham, 2005; Galupa and Heard, 2015). During normal embryonic development of female mammals, both X chromosomes are active and XCI occurs at the blastocyst stage, resulting in random inactivation of the X chromosome in the inner cell mass (ICM). Meanwhile, the paternal X chromosome is inactivated in the trophoblast (Yang et al., 2007; Payer, 2016). During SCNT, the inactivated X chromosome in female donor cells is reactivated during early development of cloned embryos, with XCI occurring at the blastocyst stage. In theory, XCI should occur randomly in the ICM, with the trophoblast exhibiting XCI as in the donor cells. However, irrespective of the sex of cloned embryos, DNA methylation level of Xist is lower than that in fertilized embryos, and the consequent upregulation of Xist expression represses the transcription of numerous X-linked genes (**Figure 2**, XCI) (Xue et al., 2002; Nolen et al., 2005; Inoue et al., 2010; Xu et al., 2013; Yuan et al., 2014; Ruan et al., 2018). Such abnormal XCI has also been detected in the placenta

and carcass of dead cloned animals and could be due to the absence of a H3K27me3 mark in the Xist promoter following SCNT, and H3K9me3 may also determine the expression level of Xist in cloned embryos (Xue et al., 2002; Inoue et al., 2010; Inoue et al., 2017b; Ruan et al., 2018). Therefore, the abnormal XCI pattern seriously affects the development of cloned fetuses and placentas.

As epigenetic modification regulates gene expression, disrupted epigenetic modification during SCNT leads to the abnormal transcription of genes related to development in cloned embryos. The persistently high expression of donor somatic cell-specific genes and failure to activate genes related to embryo development are against SCNT-mediated nuclear reprogramming (Matoba et al., 2014; Liu W. et al., 2016). Therefore, epigenetic modification status determines gene expression levels and the developmental potential of cloned embryos, further suggesting that only the full and effective reconstruction of epigenetic modifications during SCNT-mediated nuclear reprogramming can support the full-term development of cloned embryos.

## STRATEGIES FOR ENHANCING THE DEVELOPMENT OF CLONED EMBRYOS BY IMPROVING EPIGENETIC REPROGRAMMING

Presently, the aim of SCNT-mediated nuclear reprogramming-related research is to improve epigenetic reconstruction in cloned embryos, as the degree of epigenetic reprogramming determines the developmental competence of cloned embryos (Niemann, 2016).

Improving DNA methylation reprogramming has been applied in cloned embryos (Enright et al., 2003; Huan et al., 2015a; Liao et al., 2015). One way in which this is accomplished is by recapitulating the DNA methylation pattern of normal fertilized embryos using DNA-demethylating agents or by Dnmts including Dnmt1 and Dnmt3l gene silencing. The application of DNA demethylation reagents and Dnmts knockdown have successfully ameliorated genome DNA methylation and histone modification in cloned embryos. The nucleoside analog 5-aza-2′-deoxycytidine (5-aza-dC) is incorporated into the genome during DNA replication, inhibiting DNMT1 activity and resulting in DNA hypomethylation (Enright et al., 2003). Genomic DNA hypomethylation by 5-aza-dC treatment has been shown to improve the development of cloned embryos, whereas Dnmt1 or Dnmt3l knockdown in somatic cells or cloned embryos increases gene-specific DNA methylation and histone modification reprogramming and, consequently, developmental competence (Diao et al., 2013; Huan et al., 2015a; Liao et al., 2015; Song et al., 2017b). Additionally, the expression level of Tet3 in oocytes has been shown to be positively correlated with the developmental competence, and Tet3 overexpression in donor cells restores normal DNA hypermethylation and increases the full-term development of cloned embryos (Han et al., 2018). Therefore, ameliorating DNA methylation reprogramming in cloned embryos is a feasible strategy to enhance cloning efficiency.

Modifying histone marks is another approach for increasing the development competence of cloned embryos. Hdac inhibitor treatment increases histone acetylation and opens up the chromatin structure, which facilitates the binding of transcription factors that activate genes involved in early embryonic development. Hdac inhibitors have been used to improve the developmental ability of cloned embryos. For example, trichostatin A (the class I and II Hdac inhibitor), scriptaid (a synthetic Hdac inhibitor with low toxicity), and valproic acid all increase histone acetylation levels, especially H3K9ac and H3K14ac, improve gene expression levels in cloned embryos, and thus enhance SCNT-mediated nuclear reprogramming (Enright et al., 2003; Kishigami et al., 2006; Bui et al., 2011; Costa-Borges et al., 2010; Liu et al., 2012; Zhai et al., 2018). These results suggest that histone acetylation is beneficial for the development of cloned embryos. The increased H3K4me3 has been shown to improve the epigenetic modifications and the developmental efficiency of cloned embryos (Zhai et al., 2018). H3K9me3 has been reported to be a barrier for SCNT-mediated nuclear reprogramming, and removal of H3K9me3 through injection of Kdm4 mRNA activates the appropriate expression of repressed genes and increases the developmental competence of cloned embryos (Antony et al., 2013; Matoba et al., 2014; Chung et al., 2015; Liu et al., 2018; Weng et al., 2019). Importantly, the positive effect of histone acetylation on cloning efficiency could also be mediated through H3K9me3 removal (Matoba et al., 2014). Moreover, the loss of H3K9me3 can also be realized by introducing protamines in the nuclei of donor somatic cells, holding great potential to improve cloning efficiency (Iuso et al., 2015). Additionally, blocking H3K27me3 has been shown to promote nuclear reprogramming and embryonic development following SCNT (Xie et al., 2016; Zhou et al., 2019). Therefore, improvements in histone modification can correct the expression pattern of genes required for the normal development of cloned embryos and greatly enhance cloning efficiency.

Importantly, with the enhanced development of cloned embryos induced by histone modification improvements, genome imprinting in cloned embryos, fetuses, and offspring is also effectively maintained, suggesting that epigenetic modifications form mutually regulatory networks (Cervera et al., 2009; Xu et al., 2013; Huan et al., 2015b; Inoue et al., 2017a). H19 knockdown in abnormal imprinting fetal fibroblasts has also been shown to rescue damaged imprinting and the reduced development of cloned embryos (Song et al., 2017a). Therefore, restoring normal epigenetic marks and expression of imprinted-related genes can directly or indirectly ensure genome imprinting and the normal development of cloned embryos.

Targeting XCI is another strategy for improving developmental potential in SCNT. When Xist is deleted, the pattern of X-linked gene expression is corrected in cloned embryos, and the birth rate of cloned mammals is improved (Inoue et al., 2010; Matoba et al., 2011; Ruan et al., 2018). The inhibition of Xist also results in a remarkable improvement in the development of male cloned embryos (Zeng et al., 2016; Yang et al., 2019). Therefore, Xist deletion or knockdown restores

X-linked gene expression patterns in cloned embryos and increases cloning efficiency.

With the understanding of epigenetic modifications during SCNT, researchers have successfully cloned macaque monkeys (Liu et al., 2018). Therefore, the existing evidence indicates that the epigenetic status of cloned embryos is an important determinant in cloning efficiency, and improving epigenetic modifications can be a good strategy to support the successful long-term development of cloned embryos (**Figure 3**).

## ROLE OF LNCRNAS IN SCNT-MEDIATED EPIGENETIC REPROGRAMMING

An increasing number of studies have shown that the degree of epigenetic reprogramming determines the developmental potential of cloned embryos (Niemann, 2016; Matoba and Zhang, 2018). However, the molecular regulatory network involved in SCNT-mediated epigenetic reprogramming remains unclear. Therefore, exploring the molecular mechanism underlying nuclear reprogramming induced by SCNT and clarifying how highly differentiated somatic cells effectively become pluripotent cloned embryos through the epigenetic reprogramming process are areas of great interest.

LncRNAs are gene transcripts longer than 200 nucleotides that do not encode proteins but nonetheless play a critical role in gene regulation in nearly all physiologic processes, as well as in cell fate determination during development (Pauli et al., 2011; Chen and Zhang, 2016; Wang et al., 2018). A comprehensive and systematic exploration and analysis of lncRNA function has become a frontier in the field of life science (Flynn and Chang, 2014). As mentioned above, H19 and Xist have

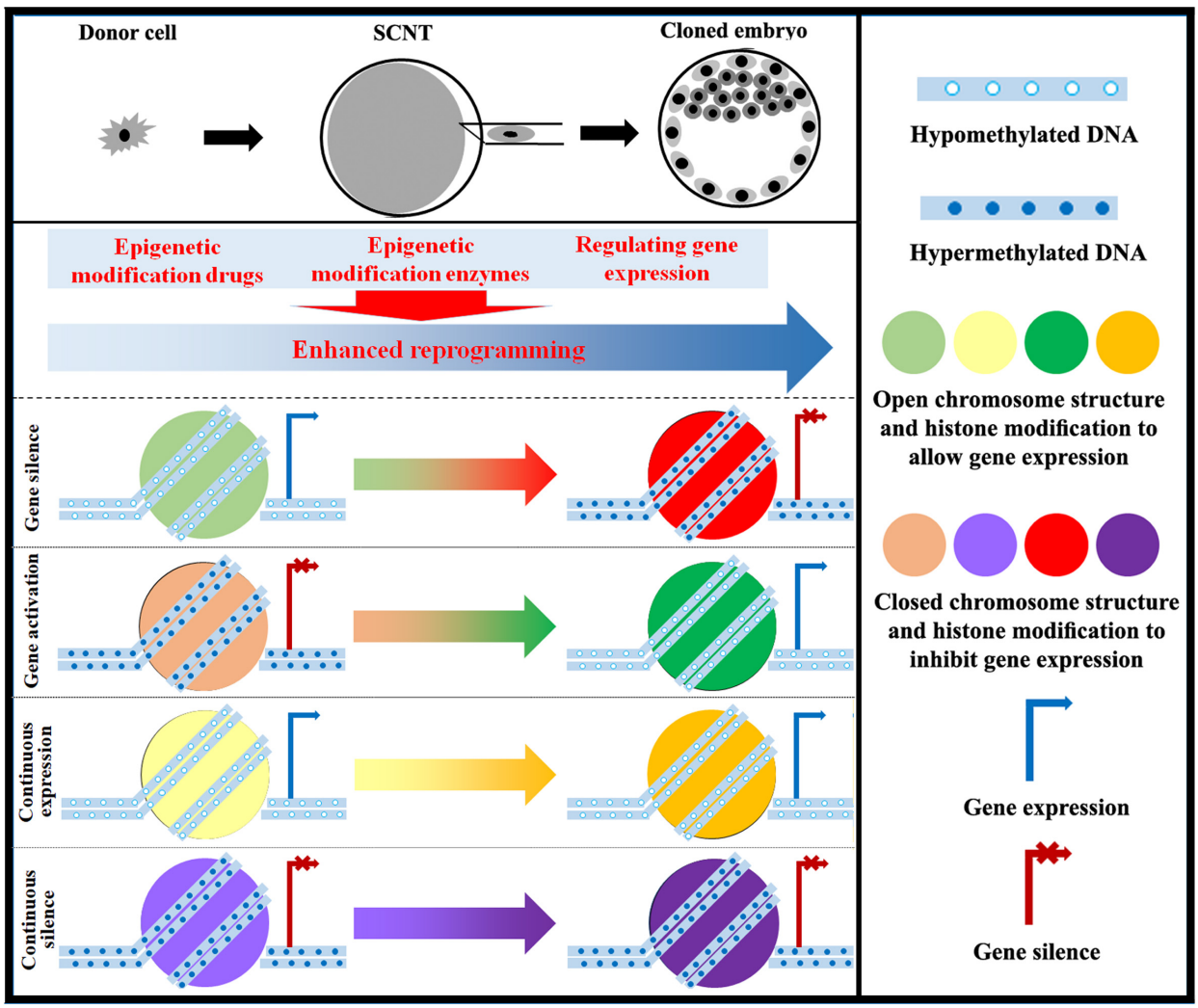



**FIGURE 3 |** Strategy for improving epigenetic reprogramming during SCNT. The application of epigenetic modification drugs and the regulation of enzymes involved in epigenetic modification as well as associated genes can induce changes in DNA methylation, chromosome structure, histone modification, genomic imprinting, and XCI in cloned embryos close to those in normal fertilized embryos. Targeting epigenetic reprogramming to activate or silence genes can yield cloned embryos with high developmental competence.

been shown to regulate the development of cloned embryos, suggesting that lncRNAs play a key role during SCNT-mediated nuclear reprogramming (Inoue et al., 2010; Song et al., 2017a). Exploring the molecular mechanism of lncRNAs in mediating epigenetic reconstruction during SCNT can provide new ideas for improving cloning efficiency.

Recent studies have shown that lncRNAs participate in many epigenetic modification processes, such as DNA methylation, histone modification, genome imprinting and XCI, and regulate the activation or silencing of genes according to cell function requirements (Mercer and Mattick, 2013; Holoch and Moazed, 2015). During DNA methylation reprogramming, lncRNAs can interact with enzymes related to DNA methylation or demethylation (Dnmts and Tets), and determine DNA methylation reconstruction to regulate gene expression. When a gene needs to be activated, lncRNAs recruit DNA demethylation-related enzymes, such as Tets, to the gene promoter and help to achieve gene DNA demethylation, and when a gene needs to be silenced, lncRNAs interact with Dnmts to establish and maintain DNA methylation of a gene promoter (Bao et al., 2015; Hamazaki et al., 2015; Wang et al., 2015; Zhou et al., 2015; Kimura et al., 2017). Therefore, lncRNAs can interact with the DNA methylation reprogramming-related enzymes to regulate DNA methylation reprogramming and regulate gene expression. LncRNAs can also alter gene expression by regulating histone modification. Studies have demonstrated that lncRNAs

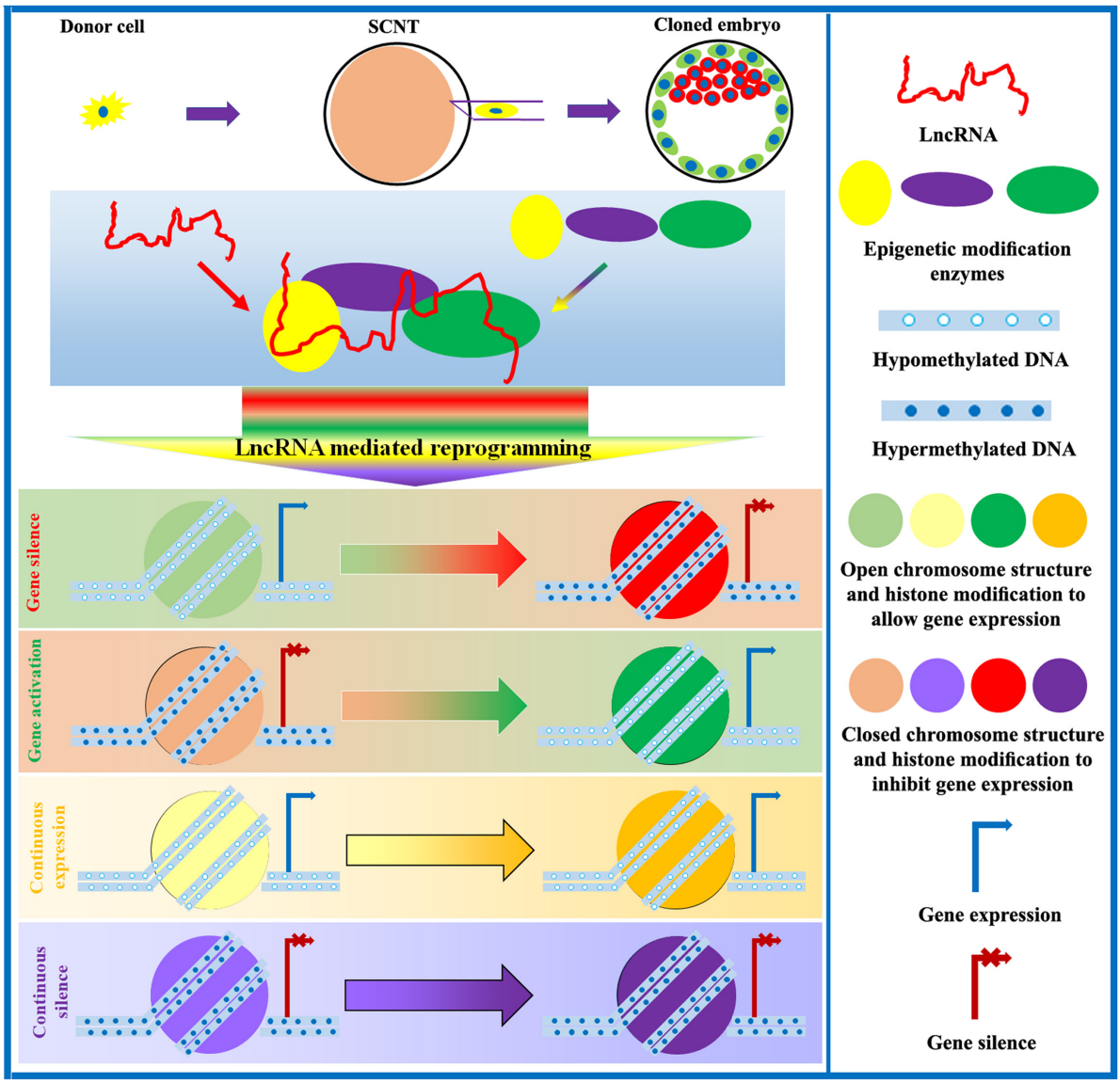



**FIGURE 4 |** Role of lncRNAs in the regulation of SCNT-mediated epigenetic reprogramming. LncRNAs interact with epigenetic modification enzymes to modulate DNA methylation, chromosome structure, histone modification, genomic imprinting, and XCI, thereby controlling gene expression and promoting the development of cloned embryos.

recruit the TrxG proteins to catalyze H3K4me3 and enhance gene transcription or PcG proteins to silence gene expression through H3K27me3 (Tsai et al., 2010; Wang et al., 2011; Liu et al., 2015). LncRNAs are also involved in the regulation of genomic imprinting, as evidenced by the finding that every genomic imprinting center contains at least one lncRNA, such as H19 and Meg3 in the H19/Igf2 and Dlk1/Meg3 imprinting regions, respectively, that regulates monoallelic parental-specific gene expression through epigenetic silencing (Barlow and Bartolomei, 2014). During XCI, Xist has been displayed to recruit PcG protein to certain gene loci, establish H3K27me3 modification and DNA methylation, and lead to gene silencing on the X chromosome (Lee, 2009; Inoue et al., 2017b). Therefore, lncRNAs can determine epigenetic modification construction.

After SCNT, epigenetic and gene expression profiles undergo substantial changes in cloned embryos. Naturally, lots of differentially expressed lncRNAs exist during the development of cloned embryos. However, research on key lncRNAs during the SCNT process is very limited. Encouragingly, the existing studies have suggested that lncRNAs can regulate the developmental competence of cloned embryos (Inoue et al., 2010; Song et al., 2017a; Ruan et al., 2018). Studies of parthenogenetic and semi-cloned mice have shown that these animals also express different levels of H19, which are associated with variable patterns of epigenetic modification and gene expression and influence developmental potential (Kono et al., 2004; Zhong and Li, 2017). Additionally, in iPSCs, lncRNAs are also shown to either promote or inhibit the reconstitution of epigenetic modifications during nuclear reprogramming (Kim et al., 2015). Therefore, lncRNAs could determine the developmental competence of cloned embryos. Given the importance of lncRNAs during SCNT-mediated epigenetic reprogramming, exploring and clarifying the underlying molecular mechanism of lncRNA-mediated epigenetic reprogramming during SCNT could lead to improvements in cloning efficiency (**Figure 4**).

## FUTURE RESEARCH AND THE APPLICATION OF SCNT

It is known to be difficult to produce cloned embryos, and their developmental competence remains poor. Moreover, studies on the factors that regulate epigenetic reprogramming during SCNT, especially those investigating lncRNAs, are still limited. To enhance the developmental potential of cloned embryos, a systematic analysis of the factors and mechanisms involved in SCNT is required. In recent years, with technological advancements, particularly the application of single-cell transcriptome sequencing, great progress has been made in discovering and identifying the reprogramming factors related to the development of cloned embryos. To date, lots of novel genes and lncRNAs have been revealed (Bai et al., 2016; Liu X. et al., 2016; Wu et al., 2018). However, the relevant reprogramming factors, including the emerging lncRNAs that regulate the developmental potential of cloned embryos, have not yet been deeply explored. Therefore, more detailed studies are needed to elucidate the molecular mechanisms underlying SCNT-mediated epigenetic reprogramming in order to improve cloning efficiency.

Efforts to improve cloning efficiency have also promoted the application of SCNT technology. Presently, a series of agriculturally and economically important animals can be cloned, which could not only enable the protection of endangered species but also accelerate the utilization of livestock. Gland bioreactors can be created through SCNT to produce therapeutic proteins. Animal models can also be generated through SCNT to investigate the pathogenesis of human diseases. Moreover, with the CRISPR/Cas9-mediated genome editing technology, SCNT can produce desired animals or models for specific applications. In short, if cloning efficiency is greatly improved, the application of SCNT technology will be more extensive.

## CONCLUSION

SCNT has important theoretical and practical research value. In this review, we present our understanding of SCNT-mediated nuclear reprogramming, especially the factors contributing to low cloning efficiency, and that incomplete epigenetic reprogramming leads to the low developmental potential of cloned embryos. We further demonstrate that the application of epigenetic modification methods can improve cloning efficiency. We also describe the regulation of epigenetic reprogramming by lncRNAs and provide a new research perspective in the field of SCNT-mediated epigenetic reprogramming. The elucidation of these mechanisms has enhanced cloning efficiency and expanded the application of SCNT technology in agriculture, regenerative medicine, and other areas. We believe that with further advances in technology, more molecular mechanisms will be revealed to enhance the development of cloned embryos, and improved cloning efficiency will promote the extensive application of SCNT technology.

## AUTHOR CONTRIBUTIONS

YH designed the manuscript. XW, JQ, and JL wrote the manuscript. YH, HH, and ZL provided the writing guidance and revised the manuscript. All authors read and approved the final manuscript.

## FUNDING

This work was supported by grants from the Key Research and Development Program of Shandong Province (2017NC210007 to YH), the Entrepreneurship and Innovation Leading Talent Program of Qingdao (19-3-2-2-zhc to YH), the Agriculture Variety Project of Shandong Province (2019LZGC011 to YH), the Excellent Youth Innovation Team in Shandong Colleges and Universities (2019KJF005 to YH), the National Natural Science Foundation of China (31602019 to YH), the Open Projects of

Key Laboratory of Animal Cellular and Genetic Engineering of Heilongjiang Province (KF201704 to YH), and the High-level Talent Research Foundation of Qingdao Agricultural University (6631116029 to YH).

## ACKNOWLEDGMENTS

We thank Dr. Jiang Zhu at Tongji University for the manuscript revision and English polishing.

## REFERENCES


Antony, J., Oback, F., Chamley, L. W., Oback, B., and Laible, G. (2013). Transient JMJD2B-mediated reduction of H3K9me3 levels improves reprogramming of embryonic stem cells into cloned embryos. *Mol. Cell. Biol.* 33, 974–983. doi: 10.1128/MCB.01014-12

Baguisi, A., Behboodi, E., Melican, D. T., Pollock, J. S., Destrempes, M. M., Cammuso, C., et al. (1999). Production of goats by somatic cell nuclear transfer. *Nat. Biotechnol.* 17, 456–461.

Bai, L., Li, M., Sun, J., Yang, X., Lu, Y., Lu, S., et al. (2016). RNA-Seq profiling of intact and enucleated oocyte SCNT embryos reveals the role of pig oocyte nucleus in somatic reprogramming. *PLoS One* 11:e0153093. doi: 10.1371/journal.pone.0153093

Bao, X., Wu, H., Zhu, X., Guo, X., Hutchins, A. P., Luo, Z., et al. (2015). The p53-induced lincRNA-p21 derails somatic cell reprogramming by sustaining H3K9me3 and CpG methylation at pluripotency gene promoters. *Cell Res.* 25, 80–92. doi: 10.1038/cr.2014.165

Barlow, D. P., and Bartolomei, M. S. (2014). Genomic imprinting in mammals. *Cold Spring Harb. Perspect. Biol.* 6:a018382. doi: 10.1101/cshperspect.a018382

Berg, D. K., Li, C., Asher, G., Wells, D. N., and Oback, B. (2007). Red deer cloned from antler stem cells and their differentiated progeny. *Biol. Reprod.* 77, 384–394. doi: 10.1095/biolreprod.106.058172

Blelloch, R., Wang, Z., Meissner, A., Pollard, S., Smith, A., and Jaenisch, R. (2006). Reprogramming efficiency following somatic cell nuclear transfer is influenced by the differentiation and methylation state of the donor nucleus. *Stem Cells* 24, 2007–2013. doi: 10.1634/stemcells.2006-0050

Bortvin, A., Eggan, K., Skaletsky, H., Akutsu, H., Berry, D. L., Yanagimachi, R., et al. (2003). Incomplete reactivation of Oct4-related genes in mouse embryos cloned from somatic nuclei. *Development* 130, 1673–1680. doi: 10.1242/dev.00366

Bourc'his, D., Le Bourhis, D., Patin, D., Niveleau, A., Comizzoli, P., Renard, J. P., et al. (2001). Delayed and incomplete reprogramming of chromosome methylation patterns in bovine cloned embryos. *Curr. Biol.* 11, 1542–1546. doi: 10.1016/s0960-9822(01)00480-8

Bui, H. T., Seo, H. J., Park, M. R., Park, J. Y., Thuan, N. V., Wakayama, T., et al. (2011). Histone deacetylase inhibition improves activation of ribosomal RNA genes and embryonic nucleolar reprogramming in cloned mouse embryos. *Biol. Reprod.* 85, 1048–1056. doi: 10.1095/biolreprod.110.089474

Campbell, K. H., Fisher, P., Chen, W. C., Choi, I., Kelly, R. D., Lee, J. H., et al. (2007). Somatic cell nuclear transfer: Past, present and future perspectives. *Theriogenology* 68(Suppl. 1), S214–S231.

Cao, Z., Li, Y., Chen, Z., Wang, H., Zhang, M., Zhou, N., et al. (2015). Genome-wide dynamic profiling of histone methylation during nuclear transfer-mediated porcine somatic cell reprogramming. *PLoS One* 10:e0144897. doi: 10.1371/journal.pone.0144897

Cervera, R. P., Marti-Gutierrez, N., Escorihuela, E., Moreno, R., and Stojkovic, M. (2009). Trichostatin A affects histone acetylation and gene expression in porcine somatic cell nucleus transfer embryos. *Theriogenology* 72, 1097–1110. doi: 10.1016/j.theriogenology.2009.06.030

Chang, C.-C., Gao, S., Sung, L.-Y., Corry, G. N., Ma, Y., Nagy, Z. P., et al. (2010). Rapid elimination of the histone variant MacroH2A from somatic cell heterochromatin after nuclear transfer. *Cell. Reprogram.* 12, 43–53. doi: 10.1089/cell.2009.0043

Chen, L., and Zhang, S. (2016). Long noncoding RNAs in cell differentiation and pluripotency. *Cell Tissue Res.* 366, 509–521. doi: 10.1007/s00441-016-2451-5

Chen, Z., and Zhang, Y. (2019). Role of mammalian DNA methyltransferases in development. *Annu. Rev. Biochem.* doi: 10.1146/annurev-biochem-103019-102815 [Epub ahead of print].

Chesne, P., Adenot, P. G., Viglietta, C., Baratte, M., Boulanger, L., and Renard, J. P. (2002). Cloned rabbits produced by nuclear transfer from adult somatic cells. *Nat. Biotechnol.* 20, 366–369. doi: 10.1038/nbt0402-366

Chung, Y. G., Matoba, S., Liu, Y., Eum, J. H., Lu, F., Jiang, W., et al. (2015). Histone demethylase expression enhances human somatic cell nuclear transfer efficiency and promotes derivation of pluripotent stem cells. *Cell Stem Cell* 17, 758–766. doi: 10.1016/j.stem.2015.10.001

Chung, Y. G., Ratnam, S., Chaillet, J. R., and Latham, K. E. (2003). Abnormal regulation of DNA methyltransferase expression in cloned mouse embryos. *Biol. Reprod.* 69, 146–153. doi: 10.1095/biolreprod.102.014076

Cibelli, J. B., Stice, S. L., Golueke, P. J., Kane, J. J., Jerry, J., Blackwell, C., et al. (1998). Cloned transgenic calves produced from nonquiescent fetal fibroblasts. *Science* 280, 1256–1258. doi: 10.1126/science.280.5367.1256

Costa-Borges, N., Santalo, J., and Ibanez, E. (2010). Comparison between the effects of valproic acid and trichostatin A on the in vitro development, blastocyst quality, and full-term development of mouse somatic cell nuclear transfer embryos. *Cell. Reprogram.* 12, 437–446. doi: 10.1089/cell.2009.0108

Czernik, M., Anzalone, D. A., Palazzese, L., Oikawa, M., and Loi, P. (2019). Somatic cell nuclear transfer: failures, successes and the challenges ahead. *Int. J. Dev. Biol.* 63, 123–130. doi: 10.1387/ijdb.180324mc

Dean, W., Santos, F., Stojkovic, M., Zakhartchenko, V., Walter, J., Wolf, E., et al. (2001). Conservation of methylation reprogramming in mammalian development: aberrant reprogramming in cloned embryos. *Proc. Natl. Acad. Sci. U.S.A.* 98, 13734–13738. doi: 10.1073/pnas.241522698

Diao, Y. F., Naruse, K. J., Han, R. X., Li, X. X., Oqani, R. K., Lin, T., et al. (2013). Treatment of fetal fibroblasts with DNA methylation inhibitors and/or histone deacetylase inhibitors improves the development of porcine nuclear transfer-derived embryos. *Anim. Reprod. Sci.* 141, 164–171. doi: 10.1016/j.anireprosci.2013.08.008

Djekidel, M. N., Inoue, A., Matoba, S., Suzuki, T., Zhang, C., Lu, F., et al. (2018). Reprogramming of chromatin accessibility in somatic cell nuclear transfer is DNA replication independent. *Cell Rep.* 23, 1939–1947. doi: 10.1016/j.celrep.2018.04.036

Enright, B. P., Kubota, C., Yang, X., and Tian, X. C. (2003). Epigenetic characteristics and development of embryos cloned from donor cells treated by trichostatin A or 5-aza-2′-deoxycytidine. *Biol. Reprod.* 69, 896–901. doi: 10.1095/biolreprod.103.017954

Flynn, R. A., and Chang, H. Y. (2014). Long noncoding RNAs in cell-fate programming and reprogramming. *Cell Stem Cell* 14, 752–761. doi: 10.1016/j.stem.2014.05.014

Galli, C., Lagutina, I., Crotti, G., Colleoni, S., Turini, P., Ponderato, N., et al. (2003). Pregnancy: a cloned horse born to its dam twin. *Nature* 424:635. doi: 10.1038/424635a

Galli, C., Lagutina, I., Perota, A., Colleoni, S., Duchi, R., Lucchini, F., et al. (2012). Somatic cell nuclear transfer and transgenesis in large animals: current and future insights. *Reprod. Domest. Anim.* 47, 2–11. doi: 10.1111/j.1439-0531.2012.02045.x

Galupa, R., and Heard, E. (2015). X-chromosome inactivation: new insights into cis and trans regulation. *Curr. Opin. Genet. Dev.* 31, 57–66. doi: 10.1016/j.gde.2015.04.002

Gao, R., Wang, C., Gao, Y., Xiu, W., Chen, J., Kou, X., et al. (2018). Inhibition of aberrant DNA re-methylation improves post-implantation development of somatic cell nuclear transfer embryos. *Cell Stem Cell* 23, doi: 10.1016/j.stem.2018.07.017

Gao, S., Chung, Y. G., Parseghian, M. H., King, G. J., Adashi, E. Y., and Latham, K. E. (2004). Rapid H1 linker histone transitions following fertilization or somatic cell nuclear transfer: evidence for a uniform developmental program in mice. *Dev. Biol.* 266, 62–75. doi: 10.1016/j.ydbio.2003.10.003

Gomez, M. C., Pope, C. E., Ricks, D. M., Lyons, J., Dumas, C., and Dresser, B. L. (2009). Cloning endangered felids using heterospecific donor oocytes and interspecies embryo transfer. *Reprod. Fertil. Dev.* 21, 76–82.

Guo, F., Li, X., Liang, D., Li, T., Zhu, P., Guo, H., et al. (2014). Active and passive demethylation of male and female pronuclear DNA in the mammalian zygote. *Cell Stem Cell* 15, 447–459. doi: 10.1016/j.stem.2014.08.003

Hamazaki, N., Uesaka, M., Nakashima, K., Agata, K., and Imamura, T. (2015). Gene activation-associated long noncoding RNAs function in mouse preimplantation development. *Development* 142, 910–920. doi: 10.1242/dev.116996

Han, C., Deng, R., Mao, T., Luo, Y., Wei, B., Meng, P., et al. (2018). Overexpression of Tet3 in donor cells enhances goat somatic cell nuclear transfer efficiency. *FEBS J.* 285, 2708–2723. doi: 10.1111/febs.14515

Holoch, D., and Moazed, D. (2015). RNA-mediated epigenetic regulation of gene expression. *Nat. Rev. Genet.* 16, 71–84. doi: 10.1038/nrg3863

Huan, Y., Wu, Z., Zhang, J., Zhu, J., Liu, Z., and Song, X. (2015a). Epigenetic modification agents improve gene-specific methylation reprogramming in porcine cloned embryos. *PLoS One* 10:e0129803. doi: 10.1371/journal.pone.0129803

Huan, Y., Zhu, J., Huang, B., Mu, Y., Kong, Q., and Liu, Z. (2015b). Trichostatin A rescues the disrupted imprinting induced by somatic cell nuclear transfer in pigs. *PLoS One* 10:e0126607. doi: 10.1371/journal.pone.0126607

Huan, Y. J., Zhu, J., Wang, H. M., Wu, Z. F., Zhang, J. G., Xie, B. T., et al. (2014). Epigenetic modification agents improve genomic methylation reprogramming in porcine cloned embryos. *J. Reprod. Dev.* 60, 377–382. doi: 10.1262/jrd.2014-062

Inoue, A., Jiang, L., Lu, F., Suzuki, T., and Zhang, Y. (2017a). Maternal H3K27me3 controls DNA methylation-independent imprinting. *Nature* 547, 419–424. doi: 10.1038/nature23262

Inoue, A., Jiang, L., Lu, F., and Zhang, Y. (2017b). Genomic imprinting of Xist by maternal H3K27me3. *Genes Dev.* 31, 1927–1932. doi: 10.1101/gad.304113.117

Inoue, K., Kohda, T., Sugimoto, M., Sado, T., Ogonuki, N., Matoba, S., et al. (2010). Impeding Xist expression from the active X chromosome improves mouse somatic cell nuclear transfer. *Science* 330, 496–499. doi: 10.1126/science.1194174

Iqbal, K., Jin, S. G., Pfeifer, G. P., and Szabo, P. E. (2011). Reprogramming of the paternal genome upon fertilization involves genome-wide oxidation of 5-methylcytosine. *Proc. Natl. Acad. Sci. U.S.A.* 108, 3642–3647. doi: 10.1073/pnas.1014033108

Ito, S., D'Alessio, A. C., Taranova, O. V., Hong, K., Sowers, L. C., and Zhang, Y. (2010). Role of Tet proteins in 5mC to 5hmC conversion, ES-cell self-renewal and inner cell mass specification. *Nature* 466, 1129–1133. doi: 10.1038/nature09303

Iuso, D., Czernik, M., Toschi, P., Fidanza, A., Zacchini, F., Feil, R., et al. (2015). Exogenous expression of human protamine 1 (hPrm1) remodels fibroblast nuclei into spermatid-like structures. *Cell Rep.* 13, 1765–1771. doi: 10.1016/j.celrep.2015.10.066

Izzo, A., and Schneider, R. (2010). Chatting histone modifications in mammals. *Brief. Funct. Genomics* 9, 429–443. doi: 10.1093/bfgp/elq024

Keefer, C. L. (2015). Artificial cloning of domestic animals. *Proc. Natl. Acad. Sci. U.S.A.* 112, 8874–8878. doi: 10.1073/pnas.1501718112

Kiefer, H., Jouneau, L., Campion, E., Rousseau-Ralliard, D., Larcher, T., and Martin-Magniette, M. L. (2016). Altered DNA methylation associated with an abnormal liver phenotype in a cattle model with a high incidence of perinatal pathologies. *Sci. Rep.* 6:38869. doi: 10.1038/srep38869

Kim, D. H., Marinov, G. K., Pepke, S., Singer, Z. S., He, P., Williams, B., et al. (2015). Single-cell transcriptome analysis reveals dynamic changes in lncRNA expression during reprogramming. *Cell Stem Cell* 16, 88–101. doi: 10.1016/j.stem.2014.11.005

Kimura, A. P., Yoneda, R., Kurihara, M., Mayama, S., and Matsubara, S. (2017). A long noncoding RNA, lncRNA-Amhr2, plays a role in Amhr2 gene activation in mouse ovarian granulosa cells. *Endocrinology* 158, 4105–4121. doi: 10.1210/en.2017-00619

Kishigami, S., Mizutani, E., Ohta, H., Hikichi, T., Thuan, N. V., Wakayama, S., et al. (2006). Significant improvement of mouse cloning technique by treatment with trichostatin A after somatic nuclear transfer. *Biochem. Biophys. Res. Commun.* 340, 183–189. doi: 10.1016/j.bbrc.2005.11.164

Kobayashi, W., and Kurumizaka, H. (2019). Structural transition of the nucleosome during chromatin remodeling and transcription. *Curr. Opin. Struct. Biol.* 59, 107–114. doi: 10.1016/j.sbi.2019.07.011

Kono, T., Obata, Y., Wu, Q., Niwa, K., Ono, Y., Yamamoto, Y., et al. (2004). Birth of parthenogenetic mice that can develop to adulthood. *Nature* 428, 860–864. doi: 10.1038/nature02402

Kremenskoy, M., Kremenska, Y., Suzuki, M., Imai, K., Takahashi, S., Hashizume, K., et al. (2006). DNA methylation profiles of donor nuclei cells and tissues of cloned bovine fetuses. *J. Reprod. Dev.* 52, 259–266. doi: 10.1262/jrd.17098

Kurome, M., Geistlinger, L., Kessler, B., Zakhartchenko, V., Klymiuk, N., Wuensch, A., et al. (2013). Factors influencing the efficiency of generating genetically engineered pigs by nuclear transfer: multi-factorial analysis of a large data set. *BMC Biotechnol.* 13:43. doi: 10.1186/1472-6750-13-43

Latham, K. E. (2005). X chromosome imprinting and inactivation in preimplantation mammalian embryos. *Trends Genet.* 21, 120–127. doi: 10.1016/j.tig.2004.12.003

Lee, B. C., Kim, M. K., Jang, G., Oh, H. J., Yuda, F., Kim, H. J., et al. (2005). Dogs cloned from adult somatic cells. *Nature* 436:641. doi: 10.1038/436641a

Lee, J. T. (2009). Lessons from X-chromosome inactivation: long ncRNA as guides and tethers to the epigenome. *Genes Dev.* 23, 1831–1842. doi: 10.1101/gad.1811209

Lee, K., Uh, K., and Farrell, K. (2020). Current progress of genome editing in livestock. *Theriogenology*. doi: 10.1016/j.theriogenology.2020.01.036 [Epub ahead of print].

Li, E., and Zhang, Y. (2014). DNA methylation in mammals. *Cold Spring Harb. Perspect. Biol.* 6:a019133. doi: 10.1101/cshperspect.a019133

Li, Z., Sun, X., Chen, J., Liu, X., Wisely, S. M., Zhou, Q., et al. (2006). Cloned ferrets produced by somatic cell nuclear transfer. *Dev. Biol.* 293, 439–448. doi: 10.1016/j.ydbio.2006.02.016

Liao, H. F., Mo, C. F., Wu, S. C., Cheng, D. H., Yu, C. Y., Chang, K. W., et al. (2015). Dnmt3l-knockout donor cells improve somatic cell nuclear transfer reprogramming efficiency. *Reproduction* 150, 245–256. doi: 10.1530/REP-15-0031

Liu, G. Y., Zhao, G. N., Chen, X. F., Hao, D. L., Zhao, X., Lv, X., et al. (2015). The long noncoding RNA Gm15055 represses Hoxa gene expression by recruiting PRC2 to the gene cluster. *Nucleic Acids Res.* 44, 2613–2627. doi: 10.1093/nar/gkv1315

Liu, L., Liu, Y., Gao, F., Song, G., Wen, J., Guan, J., et al. (2012). Embryonic development and gene expression of porcine SCNT embryos treated with sodium butyrate. *J. Exp. Zool. Part B Mol. Dev. Evol.* 318, 224–234. doi: 10.1002/jez.b.22440

Liu, W., Liu, X., Wang, C., Gao, Y., Gao, R., Kou, X., et al. (2016). Identification of key factors conquering developmental arrest of somatic cell cloned embryos by combining embryo biopsy and single-cell sequencing. *Cell Discov.* 2:16010. doi: 10.1038/celldisc.2016.10

Liu, X., Wang, C., Liu, W., Li, J., Li, C., Kou, X., et al. (2016). Distinct features of H3K4me3 and H3K27me3 chromatin domains in pre-implantation embryos. *Nature* 537, 558–562. doi: 10.1038/nature19362

Liu, Z., Cai, Y., Wang, Y., Nie, Y., Zhang, C., Xu, Y., et al. (2018). Cloning of macaque monkeys by somatic cell nuclear transfer. *Cell* 172, 881–887.e7. doi: 10.1016/j.cell.2018.01.020

Loi, P., Iuso, D., Czernik, M., and Ogura, A. (2016). A new dynamic Era for somatic cell nuclear transfer? *Trends Biotechnol.* 34, 791–797. doi: 10.1016/j.tibtech.2016.03.008

Long, C. R., Westhusin, M. E., and Golding, M. C. (2014). Reshaping the transcriptional frontier: epigenetics and somatic cell nuclear transfer. *Mol. Reprod. Dev.* 81, 183–193. doi: 10.1002/mrd.22271

Lotti, S. N., Polkoff, K. M., Rubessa, M., and Wheeler, M. B. (2017). Modification of the genome of domestic animals. *Anim. Biotechnol.* 28, 198–210. doi: 10.1080/10495398.2016.1261874

Lyko, F. (2018). The DNA methyltransferase family: a versatile toolkit for epigenetic regulation. *Nat. Rev. Genet.* 19, 81–92. doi: 10.1038/nrg.2017.80

MacDonald, W. A., and Mann, M. R. (2014). Epigenetic regulation of genomic imprinting from germ line to preimplantation. *Mol. Reprod. Dev.* 81, 126–140. doi: 10.1002/mrd.22220

Mann, M. R., Chung, Y. G., Nolen, L. D., Verona, R. I., Latham, K. E., and Bartolomei, M. S. (2003). Disruption of imprinted gene methylation and expression in cloned preimplantation stage mouse embryos. *Biol. Reprod.* 69, 902–914. doi: 10.1095/biolreprod.103.017293

Matoba, S., Inoue, K., Kohda, T., Sugimoto, M., Mizutani, E., Ogonuki, N., et al. (2011). RNAi-mediated knockdown of Xist can rescue the impaired postimplantation development of cloned mouse embryos. *Proc. Natl. Acad. Sci. U.S.A.* 108, 20621–20626. doi: 10.1073/pnas.1112664108

Matoba, S., Liu, Y., Lu, F., Iwabuchi, K. A., Shen, L., Inoue, A., et al. (2014). Embryonic development following somatic cell nuclear transfer impeded by persisting histone methylation. *Cell* 159, 884–895. doi: 10.1016/j.cell.2014.09.055

Matoba, S., and Zhang, Y. (2018). Somatic cell nuclear transfer reprogramming: mechanisms and applications. *Cell Stem Cell* 23, 471–485. doi: 10.1016/j.stem.2018.06.018

Mercer, T. R., and Mattick, J. S. (2013). Structure and function of long noncoding RNAs in epigenetic regulation. *Nat. Struct. Mol. Biol.* 20, 300–307. doi: 10.1038/nsmb.2480

Ng, R. K., and Gurdon, J. B. (2005). Maintenance of epigenetic memory in cloned embryos. *Cell Cycle* 4, 760–763. doi: 10.4161/cc.4.6.1743

Niemann, H. (2016). Epigenetic reprogramming in mammalian species after SCNT-based cloning. *Theriogenology* 86, 80–90. doi: 10.1016/j.theriogenology.2016.04.021

Ninova, M., Fejes Toth, K., and Aravin, A. A. (2019). The control of gene expression and cell identity by H3K9 trimethylation. *Development* 146, dev181180. doi: 10.1242/dev.181180

Niu, D., Wei, H. J., Lin, L., George, H., Wang, T., Lee, I. H., et al. (2017). Inactivation of porcine endogenous retrovirus in pigs using CRISPR-Cas9. *Science* 357, 1303–1307. doi: 10.1126/science.aan4187

Nolen, L. D., Gao, S., Han, Z., Mann, M. R., Gie Chung, Y., Otte, A. P., et al. (2005). X chromosome reactivation and regulation in cloned embryos. *Dev. Biol.* 279, 525–540. doi: 10.1016/j.ydbio.2005.01.016

Ogura, A., Inoue, K., and Wakayama, T. (2013). Recent advancements in cloning by somatic cell nuclear transfer. *Philos. Trans. R. Soc. Lond. B Biol. Sci.* 368:20110329. doi: 10.1098/rstb.2011.0329

Pauli, A., Rinn, J. L., and Schier, A. F. (2011). Non-coding RNAs as regulators of embryogenesis. *Nat. Rev. Genet.* 12, 136–149. doi: 10.1038/nrg2904

Payer, B. (2016). Developmental regulation of X-chromosome inactivation. *Semin. Cell Dev. Biol.* 56, 88–99. doi: 10.1016/j.semcdb.2016.04.014

Polejaeva, I. A., Chen, S. H., Vaught, T. D., Page, R. L., Mullins, J., Ball, S., et al. (2000). Cloned pigs produced by nuclear transfer from adult somatic cells. *Nature* 407, 86–90. doi: 10.1038/35024082

Qin, H., Zhao, A., Zhang, C., and Fu, X. (2016). Epigenetic control of reprogramming and transdifferentiation by histone modifications. *Stem Cell Rev. Rep.* 12, 708–720. doi: 10.1007/s12015-016-9682-4

Reik, W., Dean, W., and Walter, J. (2001). Epigenetic reprogramming in mammalian development. *Science* 293, 1089–1093. doi: 10.1126/science.1063443

Reik, W., Santos, F., Mitsuya, K., Morgan, H., and Dean, W. (2003). Epigenetic asymmetry in the mammalian zygote and early embryo: relationship to lineage commitment? *Philos. Trans. R. Soc. Lond. B Biol. Sci.* 358, 1403–1409. doi: 10.1098/rstb.2003.1326

Ruan, D., Peng, J., Wang, X., Ouyang, Z., Zou, Q., Yang, Y., et al. (2018). XIST derepression in active X chromosome hinders pig somatic cell nuclear transfer. *Stem Cell Rep.* 10, 494–508. doi: 10.1016/j.stemcr.2017.12.015

Rybouchkin, A., Kato, Y., and Tsunoda, Y. (2006). Role of histone acetylation in reprogramming of somatic nuclei following nuclear transfer. *Biol. Reprod.* 74, 1083–1089. doi: 10.1095/biolreprod.105.047456

Sasaki, H., Ishihara, K., and Kato, R. (2000). Mechanisms of Igf2/H19 imprinting: DNA methylation, chromatin and long-distance gene regulation. *J. Biochem.* 127, 711–715. doi: 10.1093/oxfordjournals.jbchem.a022661

Schubeler, D. (2015). Function and information content of DNA methylation. *Nature* 517, 321–326. doi: 10.1038/nature14192

Shen, L., Wu, H., Diep, D., Yamaguchi, S., D'Alessio, A. C., Fung, H. L., et al. (2013). Genome-wide analysis reveals TET- and TDG-dependent 5-methylcytosine oxidation dynamics. *Cell* 153, 692–706. doi: 10.1016/j.cell.2013.04.002

Shi, D., Lu, F., Wei, Y., Cui, K., Yang, S., Wei, J., et al. (2007). Buffalos (*Bubalus bubalis*) cloned by nuclear transfer of somatic cells1. *Biol. Reprod.* 77, 285–291. doi: 10.1095/biolreprod.107.060210

Shi, W., Zakhartchenko, V., and Wolf, E. (2003). Epigenetic reprogramming in mammalian nuclear transfer. *Differentiation* 71, 91–113. doi: 10.1046/j.1432-0436.2003.710201.x

Shin, T., Kraemer, D., Pryor, J., Liu, L., Rugila, J., Howe, L., et al. (2002). A cat cloned by nuclear transplantation. *Nature* 415:859. doi: 10.1038/nature723

Simon, I., Tenzen, T., Reubinoff, B. E., Hillman, D., McCarrey, J. R., and Cedar, H. (1999). Asynchronous replication of imprinted genes is established in the gametes and maintained during development. *Nature* 401, 929–932. doi: 10.1038/44866

Song, X., Li, F., Jiang, Z., Sun, Y., Li, H., Gao, S., et al. (2017a). Imprinting disorder in donor cells is detrimental to the development of cloned embryos in pigs. *Oncotarget* 8, 72363–72374. doi: 10.18632/oncotarget.20390

Song, X., Liu, Z., He, H., Wang, J., Li, H., Li, J., et al. (2017b). Dnmt1s in donor cells is a barrier to SCNT-mediated DNA methylation reprogramming in pigs. *Oncotarget* 8, 34980–34991. doi: 10.18632/oncotarget.16507

Sproul, D., Gilbert, N., and Bickmore, W. A. (2005). The role of chromatin structure in regulating the expression of clustered genes. *Nat. Rev. Genet.* 6, 775–781. doi: 10.1038/nrg1688

Sun, J. M., Spencer, V. A., Chen, H. Y., Li, L., and Davie, J. R. (2003). Measurement of histone acetyltransferase and histone deacetylase activities and kinetics of histone acetylation. *Methods* 31, 12–23. doi: 10.1016/s1046-2023(03)00083-5

Tachibana, M., Amato, P., Sparman, M., Nuria Gutierrez, M., Tippner-Hedges, R., Ma, H., et al. (2013). Human embryonic stem cells derived by somatic cell nuclear transfer. *Cell* 153, 1228–1238. doi: 10.1016/j.cell.2013.05.006

Takahashi, K., and Yamanaka, S. (2006). Induction of pluripotent stem cells from mouse embryonic and adult fibroblast cultures by defined factors. *Cell* 126, 663–676. doi: 10.1016/j.cell.2006.07.024

Telugu, B. P., Park, K. E., and Park, C. H. (2017). Genome editing and genetic engineering in livestock for advancing agricultural and biomedical applications. *Mamm. Genome* 28, 338–347. doi: 10.1007/s00335-017-9709-4

Tsai, M. C., Manor, O., Wan, Y., Mosammaparast, N., Wang, J. K., Lan, F., et al. (2010). Long noncoding RNA as modular scaffold of histone modification complexes. *Science* 329, 689–693. doi: 10.1126/science.1192002

Wakayama, T., Perry, A. C., Zuccotti, M., Johnson, K. R., and Yanagimachi, R. (1998). Full-term development of mice from enucleated oocytes injected with cumulus cell nuclei. *Nature* 394, 369–374. doi: 10.1038/28615

Wang, J., Wang, L., Feng, G., Wang, Y., Li, Y., Li, X., et al. (2018). Asymmetric expression of LincGET biases cell fate in two-cell mouse embryos. *Cell* 175, 1887–1901.e18. doi: 10.1016/j.cell.2018.11.039

Wang, K. C., Yang, Y. W., Liu, B., Sanyal, A., Corces-Zimmerman, R., Chen, Y., et al. (2011). A long noncoding RNA maintains active chromatin to coordinate homeotic gene expression. *Nature* 472, 120–124. doi: 10.1038/nature09819

Wang, K. Y., Chen, C. C., and Shen, C. K. (2014). Active DNA demethylation of the vertebrate genomes by DNA methyltransferases: deaminase, dehydroxymethylase or demethylase? *Epigenomics* 6, 353–363. doi: 10.2217/epi.14.21

Wang, L., Zhao, Y., Bao, X., Zhu, X., Kwok, Y. K., Sun, K., et al. (2015). LncRNA Dum interacts with Dnmts to regulate Dppa2 expression during myogenic differentiation and muscle regeneration. *Cell Res.* 25, 335–350. doi: 10.1038/cr.2015.21

Wani, N. A., Wernery, U., Hassan, F. A. H., Wernery, R., and Skidmore, J. A. (2010). Production of the first cloned camel by somatic cell nuclear transfer1. *Biol. Reprod.* 82, 373–379. doi: 10.1095/biolreprod.109.081083

Wee, G., Koo, D. B., Song, B. S., Kim, J. S., Kang, M. J., Moon, S. J., et al. (2006). Inheritable histone H4 acetylation of somatic chromatins in cloned embryos. *J. Biol. Chem.* 281, 6048–6057. doi: 10.1074/jbc.m511340200

Wei, Y., Zhu, J., Huan, Y., Liu, Z., Yang, C., Zhang, X., et al. (2010). Aberrant expression and methylation status of putatively imprinted genes in placenta of cloned piglets. *Cell. Reprogram.* 12, 213–222. doi: 10.1089/cell.2009.0090

Wells, K. D., and Prather, R. S. (2017). Genome-editing technologies to improve research, reproduction, and production in pigs. *Mol. Reprod. Dev.* 84, 1012–1017. doi: 10.1002/mrd.22812

Wen, D., Banaszynski, L. A., Rosenwaks, Z., Allis, C. D., and Rafii, S. (2014). H3.3 replacement facilitates epigenetic reprogramming of donor nuclei in somatic cell nuclear transfer embryos. *Nucleus* 5, 369–375. doi: 10.4161/nucl.36231

Weng, X. G., Cai, M. M., Zhang, Y. T., Liu, Y., Liu, C., and Liu, Z. H. (2019). Improvement in the in vitro development of cloned pig embryos after kdm4a overexpression and an H3K9me3 methyltransferase inhibitor treatment. *Theriogenology*. doi: 10.1016/j.theriogenology.2019.11.027 [Epub ahead of print].

Wilmut, I., Schnieke, A. E., McWhir, J., Kind, A. J., and Campbell, K. H. S. (1997). Viable offspring derived from fetal and adult mammalian cells. *Nature* 385, 810–813. doi: 10.1038/385810a0

Woods, G. L., White, K. L., Vanderwall, D. K., Li, G. P., Aston, K. I., Bunch, T. D., et al. (2003). A mule cloned from fetal cells by nuclear transfer. *Science* 301:1063. doi: 10.1126/science.1086743

Wu, F., Liu, Y., Wu, Q., Li, D., Zhang, L., Wu, X., et al. (2018). Long non-coding RNAs potentially function synergistically in the Cell. Reprogram. of SCNT embryos. *BMC Genomics* 19:631. doi: 10.1186/s12864-018-5021-2

Wu, J., Huang, B., Chen, H., Yin, Q., Liu, Y., Xiang, Y., et al. (2016). The landscape of accessible chromatin in mammalian preimplantation embryos. *Nature* 534:652. doi: 10.1038/nature18606

Xie, B., Zhang, H., Wei, R., Li, Q., Weng, X., Kong, Q., et al. (2016). Histone H3 lysine 27 trimethylation acts as an epigenetic barrier in porcine nuclear reprogramming. *Reproduction* 151, 9–16. doi: 10.1530/REP-15-0338

Xu, W., Li, Z., Yu, B., He, X., Shi, J., Zhou, R., et al. (2013). Effects of DNMT1 and HDAC inhibitors on gene-specific methylation reprogramming during porcine somatic cell nuclear transfer. *PLoS One* 8:e64705. doi: 10.1371/journal.pone.0064705

Xue, F., Tian, X. C., Du, F., Kubota, C., Taneja, M., Dinnyes, A., et al. (2002). Aberrant patterns of X chromosome inactivation in bovine clones. *Nat. Genet.* 31, 216–220. doi: 10.1038/ng900

Yamazaki, Y., Fujita, T. C., Low, E. W., Alarcon, V. B., Yanagimachi, R., and Marikawa, Y. (2006). Gradual DNA demethylation of the Oct4 promoter in cloned mouse embryos. *Mol. Reprod. Dev.* 73, 180–188. doi: 10.1002/mrd.20411

Yang, X., Smith, S. L., Tian, X. C., Lewin, H. A., Renard, J. P., and Wakayama, T. (2007). Nuclear reprogramming of cloned embryos and its implications for therapeutic cloning. *Nat. Genet.* 39, 295–302. doi: 10.1038/ng1973

Yang, X., Wu, X., Yang, Y., Gu, T., Hong, L., Zheng, E., et al. (2019). Improvement of developmental competence of cloned male pig embryos by short hairpin ribonucleic acid (shRNA) vector-based but not small interfering RNA (siRNA)-mediated RNA interference (RNAi) of Xist expression. *J. Reprod. Dev.* 65, 533–539. doi: 10.1262/jrd.2019-070

Yi, S. J., and Kim, K. (2018). Histone tail cleavage as a novel epigenetic regulatory mechanism for gene expression. *BMB Rep.* 51, 211–218. doi: 10.5483/bmbrep.2018.51.5.053

Yuan, L., Wang, A., Yao, C., Huang, Y., Duan, F., Lv, Q., et al. (2014). Aberrant expression of Xist in aborted porcine fetuses derived from somatic cell nuclear transfer embryos. *Int. J. Mol. Sci.* 15, 21631–21643. doi: 10.3390/ijms151221631

Zeng, F., Huang, Z., Yuan, Y., Shi, J., Cai, G., Liu, D., et al. (2016). Effects of RNAi-mediated knockdown of Xist on the developmental efficiency of cloned male porcine embryos. *J. Reprod. Dev.* 62, 591–597. doi: 10.1262/jrd.2016-095

Zhai, Y., Zhang, Z., Yu, H., Su, L., Yao, G., Ma, X., et al. (2018). Dynamic methylation changes of DNA and H3K4 by RG108 improve epigenetic reprogramming of somatic cell nuclear transfer embryos in pigs. *Cell. Physiol. Biochem.* 50, 1376–1397. doi: 10.1159/000494598

Zhang, X., Wang, D., Han, Y., Duan, F., Lv, Q., and Li, Z. (2014). Altered imprinted gene expression and methylation patterns in mid-gestation aborted cloned porcine fetuses and placentas. *J. Assist. Reprod. Genet.* 31, 1511–1517. doi: 10.1007/s10815-014-0320-2

Zhong, C., and Li, J. (2017). Efficient generation of gene-modified mice by haploid embryonic stem cell-mediated semi-cloned technology. *Methods Mol. Biol.* 1498, 121–133. doi: 10.1007/978-1-4939-6472-7_8

Zhou, C., Wang, Y., Zhang, J., Su, J., An, Q., Liu, X., et al. (2019). H3K27me3 is an epigenetic barrier while KDM6A overexpression improves nuclear reprogramming efficiency. *FASEB J.* 33, 4638–4652. doi: 10.1096/fj.201801887R

Zhou, J., Yang, L., Zhong, T., Mueller, M., Men, Y., Zhang, N., et al. (2015). H19 lncRNA alters DNA methylation genome wide by regulating S-adenosylhomocysteine hydrolase. *Nat. Commun.* 6:10221. doi: 10.1038/ncomms10221

Zhou, Q., Renard, J. P., Le Friec, G., Brochard, V., Beaujean, N., Cherifi, Y., et al. (2003). Generation of fertile cloned rats by regulating oocyte activation. *Science* 302:1179. doi: 10.1126/science.1088313

Ziegler-Birling, C., Daujat, S., Schneider, R., and Torres-Padilla, M. E. (2016). Dynamics of histone H3 acetylation in the nucleosome core during mouse pre-implantation development. *Epigenetics* 11, 553–562. doi: 10.1080/15592294.2015.1103424

**Conflict of Interest:** The authors declare that the research was conducted in the absence of any commercial or financial relationships that could be construed as a potential conflict of interest.

*Copyright © 2020 Wang, Qu, Li, He, Liu and Huan. This is an open-access article distributed under the terms of the Creative Commons Attribution License (CC BY). The use, distribution or reproduction in other forums is permitted, provided the original author(s) and the copyright owner(s) are credited and that the original publication in this journal is cited, in accordance with accepted academic practice. No use, distribution or reproduction is permitted which does not comply with these terms.*

frontiers in Genetics

ORIGINAL RESEARCH
published: 11 August 2020
doi: 10.3389/fgene.2020.00922

# Sperm DNA Hypomethylation Proximal to Reproduction Pathway Genes in Maturing Elite Norwegian Red Bulls

*Abdolrahman Khezri*†, Birgitte Narud, Else-Berit Stenseth, Teklu Tewoldebrhan Zeremichael, Frøydis Deinboll Myromslien, Robert C. Wilson, Rafi Ahmad† and Elisabeth Kommisrud*

*Department of Biotechnology, Inland Norway University of Applied Sciences, Hamar, Norway*

OPEN ACCESS

**Edited by:**
*Eveline M. Ibeagha-Awemu, Agriculture and Agri-Food Canada (AAFC), Canada*

**Reviewed by:**
*Shahin Eghbalsaied, Islamic Azad University, Isfahan, Iran*
*Jie Mei, Huazhong Agricultural University, China*

***Correspondence:**
*Abdolrahman Khezri*
*abdolrahman.khezri@inn.no; khezri.vet@gmail.com*

**†ORCID:**
*Abdolrahman Khezri*
*orcid.org/0000-0003-1061-8229*
*Rafi Ahmad*
*orcid.org/0000-0002-0383-7848*

**Specialty section:**
*This article was submitted to Livestock Genomics, a section of the journal Frontiers in Genetics*

**Received:** *27 April 2020*
**Accepted:** *24 July 2020*
**Published:** *11 August 2020*

**Citation:**
*Khezri A, Narud B, Stenseth E-B, Zeremichael TT, Myromslien FD, Wilson RC, Ahmad R and Kommisrud E (2020) Sperm DNA Hypomethylation Proximal to Reproduction Pathway Genes in Maturing Elite Norwegian Red Bulls. Front. Genet. 11:922. doi: 10.3389/fgene.2020.00922*

Genomic selection in modern farming demands sufficient semen production in young bulls. Factors affecting semen quality and production capacity in young bulls are not well understood; DNA methylation, a complicated phenomenon in sperm cells, is one such factors. In this study, fresh and frozen-thawed semen samples from the same Norwegian Red (NR) bulls at both 14 and 17 months of age were examined for sperm chromatin integrity parameters, ATP content, viability, and motility. Furthermore, reduced representation bisulfite libraries constructed according to two protocols, the Ovation® RRBS Methyl-Seq System (Ovation method) and a previously optimized gel-free method and were sequenced to study the sperm DNA methylome in frozen-thawed semen samples. Sperm quality analyses indicated that sperm concentration, total motility and progressivity in fresh semen from 17 months old NR bulls were significantly higher compared to individuals at 14 months of age. The percentage of DNA fragmented sperm cells significantly decreased in both fresh and frozen-thawed semen samples in bulls with increasing age. Libraries from the Ovation method exhibited a greater percentage of read loss and shorter read size following trimming. Downstream analyses for reads obtained from the gel-free method revealed similar global sperm DNA methylation but differentially methylated regions (DMRs) between 14- and 17 months old NR bulls. The majority of identified DMRs were hypomethylated in 14 months old bulls. Most of the identified DMRs (69%) exhibited a less than 10% methylation difference while only 1.5% of DMRs exceeded a 25% methylation difference. Pathway analysis showed that genes annotated with DMRs having low methylation differences (less than 10%) and DMRs having between 10 and 25% methylation differences, could be associated with important hormonal signaling and sperm function relevant pathways, respectively. The current research shows that RRBS in parallel with routine sperm quality analyses could be informative in reproductive capacity of young NR bulls. Although global sperm DNA methylation levels in 14 and 17 months old NR bulls were similar, regions with low and varying levels of DNA methylation differences can be identified and linked with important sperm function and hormonal pathways.

**Keywords: Norwegian Red, bulls, puberty, sperm, DNA methylation, RRBS**

## INTRODUCTION

Epigenetics is a phenomenon where gene expression is regulated without any changes in DNA sequence, rather being modulated via changes in DNA methylation, histone post-translational modification, and interaction of transcriptional factors with small RNAs (Donkin and Barres, 2018). Epigenetic changes in sperm cells are even more complex compared to somatic cells for two main reasons. First, during primary phase of spermatogenesis, where germ cells develop to spermatids, DNA methylation is initially erased, becoming re-established later. Moreover, during spermiogenesis, where spermatids further differentiate to spermatozoa, the majority of histones are gradually replaced by protamines (O'Doherty and McGettigan, 2015; McSwiggin and O'Doherty, 2018). In recent years, different methods have been developed to study DNA methylation. Reduced representation bisulfite sequencing (RRBS) is an efficient and high-throughput method, allowing the study of DNA methylation profiles at single-base resolution, while experiment costs are kept low (Meissner et al., 2005). Previous studies have used RRBS to investigate DNA methylation profile in different bovine somatic tissues as well as bull sperm cells (Zhou et al., 2016; Perrier et al., 2018).

Sexual maturation in bulls is a hormone-regulated process lasting up to 50 weeks of age (Rawlings et al., 2008). Previous research has demonstrated that semen quality is closely correlated with different environmental factors and animal age. For instance, it has been shown that sperm morphology, concentration and motility positively correlated with age in young tropical composite bulls (Fortes et al., 2012) and Austrian Simmental bulls (Fuerst-Waltl et al., 2006). Although several studies reported low methylation levels in different genomic features of bull sperm cells (Perrier et al., 2018; Zhou et al., 2018; Kiefer and Perrier, 2019), the methylation level is dynamic and recent evidence suggests that the bull sperm methylome correlates with age (Lambert et al., 2018).

Norwegian Red (NR) is a highly fertile breed with e.g., low incidence of calving difficulties and mastitis (Refsdal, 2007; Ferris et al., 2014). Historically the NR breeding program was based on progeny testing of sires. However, starting from 2016, genomic selection was implemented in the NR breeding program and top NR elite bulls are today selected based on genomic breeding values. Despite the fact that NR is widely employed for artificial insemination (AI) in Norway and a very good record of genetic information has been build up during the last 40 years, little is known about the NR sperm methylome. In addition, because of short generation intervals due to genomic selection, there is more demand hence more physiological pressure for semen production from young NR bulls. The objective of this research is to determine if sperm DNA methylome could provide additional information to age related sperm quality differences. For this purpose, sperm samples from the same NR bulls at 14 and 17 months of age were used for analyzing chromatin integrity, viability, ATP content, and motility parameters. Furthermore in order to assess the sperm DNA methylome, two different RRBS protocols including Ovation RRBS Methyl-Seq System (as a, simple, fast, and scalable solution) and a gel-free based RRBS protocol which previously was optimized to study boar sperm DNA methylome (Khezri et al., 2019), were implemented.

## MATERIALS AND METHODS

In the present study, the sperm quality traits including chromatin integrity parameters, ATP content, viability and motility parameters were analyzed in semen from NR elite bulls, at both 14 and 17 months of age. Furthermore, following comparison of two different protocols for constructing RRBS libraries, sperm DNA methylation in both age groups was analyzed.

### Semen Collection and Sample Preparation

Bulls in this study, were raised, cared for and fed standardized diet at Geno SA (Geno Breeding and AI Association, Hamar, Norway), AI station. Ejaculates were collected from nine young genomic selected NR bulls with unknown fertility at 14 and 17 months of age and processed by the breeding company Geno SA. Prior to dilution, sperm cell concentration in each ejaculate was calculated using an Accucell® spectrophotometer (IMV Technologies, L'Aigle, France). The semen was diluted in a two-step procedure using Biladyl extender (13500/0004-0006; Minitübe, GmbH, Tiefenbach, Germany). After first dilution, samples were taken for fresh semen analyses and simultaneously used for subjective quality control analysis. Ejaculates with motility above 70% and morphological abnormalities below 20% were further diluted with the glycerol-containing fraction (1:2) to a final concentration of $12 \times 10^6$ sperm cells per insemination dose, filled into 0.25 ml standard French mini straws (IMV, L'Aigle, France), and cryopreserved as previously described (Standerholen et al., 2014). Cryopreserved doses were later prepared for sperm quality analyses and DNA extraction by thawing the semen doses for 1 min in a water bath at 37°C. To minimize the influence of possible variation between straws, semen from two straws/ejaculate were pooled and mixed before analyses.

### Sperm Quality Analyses

#### Sperm Chromatin Integrity Assessment

Sperm chromatin integrity assessment was performed using sperm chromatin structure assay (SCSA) (Evenson and Jost, 2000; Boe-Hansen et al., 2005). Using this assay, two different chromatin integrity parameters, including DNA fragmentation index (DFI) and high DNA stainability index (HDS), were measured.

In brief, both fresh and frozen-thawed semen samples were diluted to $2 \times 10^6$ cells/ml using TNE buffer (10 mM Tris-HCl, 0.1 M NaCl, 1 mM EDTA, pH 7.4). Diluted samples were denatured for 30 s by adding an acid detergent solution (0.38 M NaCl, 80 mM HCl, 0.1% Triton-X 100, pH 1.2). Denatured samples were stained with acridine orange (AO) staining buffer (37 mM citric acid, 0.126 M $Na_2PO_4$, 1.1 mM EDTA, 0.15 M NaCl and 0.6 μg/ml of AO, pH 6.0) and were incubated for 3 min at room temperature. Two technical replicates were considered for each sample and 5000 sperm cells per replicate

were analyzed using a pre-AO saturated flow cytometer equipped with a blue laser (488 nm) (Cell Lab QuantaTM SC MPL flow cytometer, Beckman Coulter, Fullerton, CA, United States). Laser stability was controlled (at the beginning of the experiment and after every fifth sample) using a bull reference sample with pre-identified DFI and by re-setting the mean green and red fluorescence signals to 425 ± 5 and 125 ± 5, respectively. Following AO staining, double- and single-stranded DNA emitted green (collected using a 525 nm band pass filter) and red fluorescence (collected using a 670 nm long pass filter), respectively. The percentage of red and green fluorescence was determined using the FCS Express 6 flow cytometry data analyzer software (*Denovo* Software, Los Angeles, CA, United States). Based on the ratio of red/(red + green), the DFI percentage was calculated. Furthermore, HDS sperm cells, which are considered as sperm cells with an incomplete chromatin condensation, were identified according to a high incorporation of AO into double-stranded DNA.

### Assessment of Sperm Viability

Sperm viability and data analysis were performed using the flow cytometry system described above and Kaluza® software, Version 2.1 (Beckman Coulter Ltd.). Frozen-thawed semen samples were diluted in SP-Talp media (105 mM NaCl, 3.1 mM KCl, 0.4 mM $MgCl_2$, 2.0 mM $CaCl_2{\cdot}2H_2O$, 0.3 mM $NaH_2PO_4{\cdot}H_2O$, 1 mM sodium pyruvate, 21.6 mM sodium lactate, 20 mM Hepes, 20 mM Hepes salt, 5 mM glucose, 50 μg/ml gentamycin) to a concentration of $1 \times 10^6$ sperm cells/ml. Two technical replicates were considered per sample. Sperm suspensions were stained with 0.48 μM propidium iodide (PI, Sigma-Aldrich) and incubated for 10 min prior to flow cytometric analysis. PI fluorescence was detected using a 670 nm long pass filter (FL3), and gating was performed to reveal sperm cells population (based on electronic volume) and percentages of living spermatozoa as previous described (Standerholen et al., 2014).

### Sperm ATP Content

The ATP content was measured in frozen-thawed semen samples using the CellTiter-Glo® Luminescent Cell Viability Assay (Promega; Madison, Wisconsin). A total volume of 60 μl of semen ($3 \times 10^5$ sperm cells) was added to a white 96-well microtiter plate (NUNC®, Denmark) and mixed with 60 μl CellTiter-Glo® reagent. To induce cell lysis, the mixture was gently shaken for 2 min in a rotary shaker (IKA® MS 3 digital, United States), followed by 15 min incubation at room temperature to stabilize the luminescence. The bioluminescence signal was measured in relative luminescence units (RLU) using a FLUOstar OPTIMA multiwell plate reader (BMG LABTECH GmbH, Offenburg, Germany), equipped with MARS data analyzer software (Version 1.10, BMG LABTECH, Germany). Obtained RLU signals were converted to a corresponding ATP value in nM according to a prepared standard curve. ATP values obtained from the average of three technical replicates per sample. Then the value further corrected for the percentage of motile sperm cells before statistical analyses.

### Sperm Motility Analysis

Sperm motility analysis were performed using the SCA evolution CASA system (Microptic SL, Spain), equipped with a phase contrast Eclipse Ci-S/Ci-L microscope (Nikon, Japan), a BASLER Ace acA780-75 gc digital camera (Basler Vision Technologies, Ahrensburg, Germany) and Sperm class analyzer software (v 6.1.0.0). Fresh and thawed semen samples were incubated for 15 min at 37°C, and diluted (1:2) with pre-warmed PBS buffer (37°C) before analysis. A volume of 3 μl of diluted samples was loaded into the chamber of a pre-warmed (37°C) 20 μm depth Leja-4 slide (Leja products, Nieuw-Vennep, the Netherlands). Analyses were performed using two technical replicates per sample, under a 10x objective and on the pre-heated thermal stage (37°C) of the phase contrast microscope. Eight or more microscope fields with at least 800 cells per sample were analyzed. Bull sperm cells were detected based on head area (20–80 $\mu m^2$) and camera setting of 45 frames per sec. The motility parameters measured were total motility, progressive motility, and hyperactive motility. In addition, other information regarding to sperm motion kinetics including curvilinear velocity (VCL, μm/s), straight-line velocity (VSL, μm/s), average path velocity (VAP, μm/s), straightness of the average path [STR (%) = VSL/VAP], linearity of the curvilinear path [LIN (%) = VSL/VCL], Wobble [WOB (%) = VAP/VCL], lateral displacement of sperm head (ALH, μm) and beat cross frequency (BCF, Hz) were obtained. Sperm cells were defined as static and progressive motile if VAP < 10 μm/s and STR > 70μm/s, respectively. Sperm cells with VCL > 80μm/s, ALH > 6.5μm and LIN < 65% were defined as sperm cells with hyperactive motility.

## RRBS Library Preparation

Prior to RRBS library construction, DNA from frozen-thawed sperm samples of seven bulls at, both 14 and 17 months of age, was extracted using a Maxwell 16 Benchtop instrument (Promega Corporation, United States) at Biobank AS, Hamar. Isolated DNA was quantified using Qubit dsDNA BR assay kit (Thermo Fisher Scientific, United States) and further diluted to 20 ng/μl in low TE media [10 mM Tris, pH 8.0 (Calbiochem, United States), 0.1 mM EDTA, pH 8.0 (Calbiochem, United States)]. Libraries for sperm DNA methylation analysis were constructed using the RRBS approach and according to two different RRBS protocols.

### RRBS Library Preparation Using Ovation® RRBS Methyl-Seq System (Ovation Method)

In this method Ovation® RRBS Methyl-Seq System (NuGEN Technologies, San Carlos, CA, United States) was employed and RRBS libraries were constructed using 100 ng genomic DNA, according to the manufacturer's protocol with slight modifications.

Briefly, genomic DNA was digested overnight at 37°C using *Msp*I and Taq α1 enzymes (New England Biolabs, United States). After digestion, AMPure XP beads (Beckman Coulter, United States) were added (2x) and samples were kept at room temperature for 30 min. Then by putting the samples on a side magnet, supernatant was removed and beads were washed twice with 100% EtOH. Dried beads were re-suspended

in 10 μl elution buffer (Qiagen, Germany) and fragmented DNA was ligated with adapters by incubation at 25°C for 30 min followed by 70°C for 10 min. Adapter ligated fragments were final repaired at 60 and 70°C each for 10 min. The fragments were further size selected by adding 1.5x of 20% PEG 8000/2.5 M NaCl (Amresco Inc., United States) followed by incubation for 30 min at room temperature. The supernatant was removed as previously described and after washing the beads twice with 70% EtOH and drying, the beads were re-suspended in 25 μl elution buffer (Qiagen, Germany). Eluted products were subjected to bisulfite conversion using EpiTect kit (QIAGEN, Germany) following the manufacturer's protocol designated for DNA extracted from FFPE tissues. Bisulfite converted DNA, was amplified using 10 cycles of PCR. Amplified libraries were purified by adding 1x SPRI AMPure XP beads followed by incubation for 30 min at room temperature. Supernatant was removed, beads were washed with 70% EtOH and re-suspended in elution buffer. Eluted beads were further placed on a side magnet and purified libraries were transferred to a clean tube.

### RRBS Library Preparation Using a Gel-Free Multiplexed Method (Gel-Free Method)

In this method RRBS libraries were constructed using a gel-free multiplexed technique (Boyle et al., 2012), which we previously optimized it to study boar sperm DNA methylome (Khezri et al., 2019). The protocol was consisted of the following steps.

First, genomic DNA (100 ng) was digested as described in section "RRBS Library Preparation Using Ovation® RRBS Methyl-Seq System (Ovation Method)." Gap filling and A-tailing steps were carried out by adding 1 μl of Klenow fragment (New England Biolabs, United States) along with 1 μl of dNTP mixture containing 10 mM dATP, 1 mM dCTP, and 1 mM dGTP (New England Biolabs, United States) to fragmented DNA. The processed DNA was incubated for 20 min at 30°C followed by 20 min at 37°C. After incubation, fragmented DNA was size selected (300–500 bp) by adding a 2x AMPure XP beads (Beckman Coulter, United States). After incubation in room temperature for 30 min the supernatant was removed as previously described in section "RRBS Library Preparation Using Ovation® RRBS Methyl-Seq System (Ovation Method)" and beads were washed and re-suspended in 20 μl elution buffer (Qiagen, Germany). Adapter ligation was performed by adding 2 μl of NEXTflex™ Bisulfite-Seq barcodes (Bio Scientific Corporation, United States) and ligase mixture to eluted DNA followed by overnight incubation at 16°C. Adapter-ligated DNA again was size selected by adding 1.5x of 20% PEG 8000/2.5 M NaCl (Amresco Inc., United States) followed by incubation at room temperature for 30 min. The product was placed on a side magnet; supernatant was removed, beads were washed two times in 70% EtOH and were re-suspended in 25 μl elution buffer (Qiagen, Germany). Prior to fragment amplification, different PCR amplification cycles (10, 13, 16, and 19 cycles) were tested. PCR products were run on a gradient 4–20% Criterion precast polyacrylamide TBE gel (Thermo Fisher Scientific, United States). Gradient gel further stained with SybrGold (Thermo Fisher Scientific, United States) and the efficiency of protocol were evaluated based on the appearing DNA bands. Later, size selected DNA fragments were bisulfite converted and product was cleaned up according to recommended protocol in the QIAGEN EpiTect kit (Gu et al., 2011). At the last step, converted DNA, PCR amplified using 13 amplification steps (PCR Primer 1: 5′- AATGATACGGCGACCGAGATCTACAC-3′, PCR Primer 2: 5′-CAAGCAGAAGACGGCATACGAGAT-3′) and PCR product (libraries) were further cleaned up using 1x SPRI beads as described earlier for the Ovation method.

## Illumina Sequencing

Eluted RRBS libraries from both protocols were quantified using the PicoGreen dsDNA absorbance method and were sent to Norwegian Sequencing Center. Sequencing was performed using Illumina HiSeq 2500 in the paired-end (2 × 150 bp) mode.

## Bioinformatics Analyses

### Illumina Reads Quality Assessment and Trimming

The quality of paired-end Illumina reads first was assessed using fastQC software (v 0.11.8 for Linux). For reads obtained via the gel-free protocol, Illumina adapters and low-quality sequences (below 20 bp and Phred score of 30) were trimmed using Trim-galore software (v 0.4.4 for Linux) (Martin, 2011). For reads obtained via the Ovation protocol, manufacturer's recommendations were followed for quality control and adapter trimming[1]. Then, additional nucleotides from the 5′ ends of adapter-removed reads, were further trimmed using a NuGEN-developed 'trimRRBSdiversityAdaptCustomers.py' script in Python (2.7.5 for Linux).

### Mapping the Clean Reads With Reference Genome

Bull reference genome (*bosTau 9*) was downloaded from the UCSC database (UCSC, 2018) and was indexed using bismark_genome_preparation option in Bismark (v 0.19.0 for Linux) (Krueger and Andrews, 2011). After initial assessment of libraries (**Table 2**), only reads from the gel-free protocol were mapped to the reference genome. The mapping was carried out using Bismark and bowtie2 aligner (v 2.3.2 for Linux) (Krueger and Andrews, 2011) with following parameters [-n 0 –l 20 and –score-min (L, 0, −0.6)]. All covered Cs were used for calculation of global CpG methylation level in Bismark using following formula:% of global methylation = 100 * number of methylated Cs/number of methylated Cs + number of unmethylated Cs.

### Differential Methylation Analysis

In this study differentially methylated regions were identified between control (17 months old bulls) and test (14 months old bulls) groups. In brief, SAM-sorted alignment files from Bismark were analyzed using the methylKit package (v 1.6.1) (Akalin et al., 2012) in Rstudio (v 1.1.453 for Linux). First, reads containing CpGs with more than 99.9th percentile coverage were filtered out. Every single C was considered to calculate differentially methylated regions (DMRs). For this purpose, the genome was divided in 1000 bp tiles with sliding step 1000 bp, containing at least three mutually covered Cs in the CpG context. Average DNA methylation of each tile was calculated and in order to determine

[1]https://github.com/nugentechnologies/NuMetRRBS

DMRs with *q-value* < 0.05 (filtered DMRs onward), logistic regression with a sliding linear model to correct for multiple comparisons was applied. In this study, hypermethylation and hypomethylation are defined as any positive and negative value for DMRs in the test group compared to the control group, respectively. Later, DMRs were categorized as those with < 10% differential methylation ($DMRs_{<10\%}$), those showing 10–25% ($DMRs_{10-25\%}$) and those exhibiting > 25% methylation differences ($DMRs_{>25\%}$) and were used for downstream analyses.

### Annotation of Differentially Methylated Regions

BED files containing gene and CpG annotation for the *bosTau9* assembly were downloaded from the UCSC table browser (UCSC, 2018). All DMRs with any level of hypo/hyper methylation were annotated with nearest (no specific cut off) transcriptional start site (TSS), genes elements (exons, introns, promoter, intergenic regions) and CpG features (CpG islands, CpG shore, other) using Genomation package (v 1.14.0) in Rstudio. Promoters and CpG shore were defined as ± 1000 bp and ± 2000 bp of the TSS and CpG islands, respectively.

### Pathway Analysis

Corresponding GenBank accession IDs to annotated TSSs, were submitted to DAVID Bioinformatics resources for functional annotation (Huang da et al., 2009) for Gene Ontology (GO) analysis. Gene enrichment for each identified pathway was calculated using Fisher's exact test and *p-value* was Benjamini adjusted for multiple testing and set to 0.05.

## Statistical Analyses

Statistical analyses were performed in Rstudio (v 1.1.383 for windows). In order to compare sperm quality parameters in fresh and frozen-thawed samples from 14 and 17 months old bulls, linear mixed models within the lme4 package were established using quality parameters of sperm cells and bulls age as response and independent variables, respectively. In addition, animals, semen concentration at the time of semen collection and pedigree information were included as random effects. The level of significance (*p-value*) was set to 0.05 except for DFI and HDS where, in order to minimize type I error, *p-values* were Bonferroni adjusted to 0.025. Results were plotted using GraphPad Prism (v 6.01 for Windows, GraphPad Software, San Diego, CA, United States). Venn diagrams were constructed using Venny online platform (Oliveros, 2015). Pathway analysis results were plotted using ggplot2 package (v 3.1.0) in Rstudio (Wickham, 2016).

# RESULTS

## Sperm Quality Analyses in Young Norwegian Red Bulls

Sperm quality analyses results showed that some of the parameters were significantly different between the 14 and 17-months old bulls (**Table 1**). For instance, sperm concentration in 17 months old bulls was significantly higher compared to those 14 months old. Furthermore, both fresh and frozen-thawed samples from 14 months old bulls showed higher DFI compared to the 17 months old group. In addition, fresh sperm cells from 17 months old bulls showed significantly higher HDS (less condensed DNA) compared to those 14 months old. However, no significant changes in HDS between 14 and 17 months. of age were observed in frozen-thawed semen samples. The results further indicated that total sperm motility and progressivity in fresh semen from 17 months old bulls were significantly higher compared to 14 months old bulls. However, in frozen-thawed semen none of the sperm motility parameters was significantly different in bulls 14 months, compared to 17 months of age. Other sperm motion kinetic parameters showed no significance differences between 14 and 17 months old bulls (**Supplementary Table 1**).

## Bioinformatics Analyses of RRBS Data

### Comparison of RRBS Data Obtained Based on Ovation and Gel-Free Protocols

**Table 2** compares the summary statistics for RRBS data obtained from two protocols. Surprisingly, no Illumina adapter contamination was detected for reverse reads in libraries constructed using Ovation method while both forward and reverse reads from RRBS libraries constructed based on gel-free

**TABLE 1 |** An overview of results (mean ± SEM) for different sperm quality parameters analyses for both fresh and frozen-thawed semen samples in 14 months (*n* = 9) and 17 months (*n* = 8) old Norwegian red bulls.

| | Fresh semen | | Frozen-thawed semen | |
|---|---|---|---|---|
| | **14 months** | **17 months** | **14 months** | **17 months** |
| Sperm concentration ($10^6$ cells/ml) | 974 ± 83.80 | 1330 ± 133.40* | NA | NA |
| DFI | 2.78 ± 0.30 | 1.83 ± 0.20* | 2.02 ± 0.13 | 1.64 ± 0.20* |
| HDS | 0.67 ± 0.07 | 0.80 ± 0.10* | 0.64 ± 0.05 | 0.88 ± 0.15 |
| ATP (nM/$10^6$ cells) | NA | NA | 1.22 ± 0.13 | 1.16 ± 0.06 |
| Viability (%) | NA | NA | 62.15 ± 5.32 | 65.64 ± 2.85 |
| Motility (%) | 87.09 ± 1.51 | 98.10 ± 0.30* | 58.45 ± 5.10 | 63.47 ± 2.95 |
| Progressivity (%) | 72.90 ± 2.00 | 87.23 ± 1.00* | 52.16 ± 5.52 | 59.26 ± 3.16 |
| Hyperactivity (%) | 24.34 ± 1.83 | 24.21 ± 3.51 | 10.44 ± 2.24 | 12.50 ± 1.47 |

*Asterisks indicate a significant difference between age in fresh or frozen-thawed samples based on linear mixed model. *p < 0.05 for all parameters except for DFI and HDS, where *p < 0.025 (Bonferroni corrected). NA, data not available; DFI, DNA fragmentation index; HDS, high DNA stainability; nM, nanomolar.*

**TABLE 2 |** An overview of summary statistic for RRBS libraries constructed based on Ovation RRBS Methyl-Seq and our previously optimized method (gel-free method).

| RRBS protocol | Adapter contamination | Read loss after trimming | Reads length (bp) distribution after trimming | |
|---|---|---|---|---|
| Ovation method | Detected only in forward reads | 51% | < 50 | 34% |
| | | | 50–99 | 40% |
| | | | 100–150 | 26% |
| Gel-free method | Detected in both reads | 8% | < 50 | 4% |
| | | | 50–99 | 29% |
| | | | 100–150 | 67% |

*Paired-end reads from both methods were quality checked using fastQC software and trimming for Ovation libraries was performed according to manufacturer's instructions. Read loss percentage was calculated as number of reads after trimming/number of reads before trimming. Bp, base pair.*

method, showed Illumina adapter contamination. After quality control and trimming, 51% of reads were discarded in Ovation libraries, whereas quality control and trimming resulted in only 8% read loss in gel-free method. After trimming, reads with length < 50 bp and 100–150 bp were corresponding to 4 and 67% of all reads in libraries made according to gel-free protocol, respectively. Whereas reads with similar size in Ovation libraries were about 34 and 26% of total reads, respectively. This is particularly important, as longer reads tend to align better with reference genome in Bismark (Tran et al., 2014). Therefore, based on observed differences, we decided to conduct downstream analyses using RRBS libraries constructed based on the gel-free optimized method.

## Basic Statistics of RRBS Libraries Constructed Based on Gel-Free Method

Using an in-house bioinformatics pipeline and after trimming the Illumina reads, 91% of reads were retrieved in libraries constructed based on the gel-free protocol. As shown in **Table 3**, this was equal to an average of 7.7 million reads per sample, 33.1% unique mapping efficiency, 15.9x read coverage and 99.1% conversion rate. Overall, minimum variation was observed between samples from different individuals and age regarding to retrieved clean reads, mapping efficiency, global CpG methylation, and bisulfite conversion rate (**Table 3**). Furthermore, CpG statistic revealed that generated libraries in average covered 4.4 million CpG, with methylation average of 40%. Mixed models indicated that none of mapping efficiency, global CpG methylation level and conversion rate parameters were significantly different ($p < 0.05$) in 14 months compared to 17 months old bulls. Cluster analysis based on methylation value of $CpG_{W1000}$ (i.e., CpGs that have fallen into a 1000 bp tiles across the genome) in each sample, showed that samples are distributed in two main clusters. However, within the main clusters, samples from the same individuals but different age always sub-clustered together (**Figure 1**). Furthermore, Pearson's correlation coefficient based on methylation value of $CpG_{W1000}$ indicated a very high positive correlation between samples in term of global methylation profile (Pearson's correlation coefficient $\geq 0.95$) (**Supplementary Table 2**).

## Differential Methylation Analysis

Differential methylation analysis were performed using a tile-based approach. This resulted in identification of 131,073 DMRs between test (14 months old) and control (17 months old) bulls. However, after setting the level of significance to *q-value* < 0.05, a total number of 6426 DMRs (filtered DMRs) were detected with varying levels of methylation ranging from 0 to 38%. Majority of filtered DMRs (60%) were found to be hypomethylated in the 14 months old group relative to the control group (**Figure 2A**). Distribution of DMRs exhibiting varying degrees of methylation differences in hypomethylation and hypermethylation groups were similar; ∼70% of DMRs showed less than a 10% difference in methylation, and ca. 1.5% of DMRs had over a 25% difference in methylation levels (**Figures 2B,C**).

## Annotation of Differentially Methylated Regions With Gene and CpG Features

In this study, all filtered DMRs with any level of methylation differences ($DMRs_{<10\%}$, $DMRs_{10-25\%}$ and $DMRs_{>25\%}$), were considered for downstream analyses. The filtered DMRs were annotated with gene and CpG features. The analyses showed that, on average, 65% of the filtered DMRs were present in the intergenic regions. Annotation of DMRs in both hypomethylation and hypermethylation groups within promoters and introns showed similar trend. For instance, $DMRs_{<10\%}$ and $DMRs_{>25\%}$ were the major groups that annotated within promoter and intron regions, respectively (**Figure 3A**). For CpG features, on average, over 85% of filtered DMRs in both hypomethylation and hypermethylation groups were annotated within regions outside of CpG islands (CGI)/CpG shores. A majority of annotated DMRs within these external regions exhibited methylation differences exceeding 25%. Only around 15% of filtered DMRs were annotated within CGI/CpG shores and most showed less than a 10% methylation difference (**Figure 3B**).

Next, the nearest transcription start sites (TSSs) to filtered DMRs were extracted (**Figures 4A,B**). This resulted in a greater number of TSSs in the hypomethylation group (2982 TSSs) compared to the hypermethylation group (2129 TSSs). However, in both hypomethylation and hypermethylation groups, a majority of TSSs were associated with $DMRs_{<10\%}$, followed by $DMRs_{10-25\%}$ and $DMRs_{>25\%}$. Furthermore, 474 TSSs associated to $DMRs_{<10\%}$ were annotated with both hypo- and hypermethylated regions. This number for the $DMRs_{10-25\%}$ was 156 TSSs and no commonly annotated TSS was found between hypo- and hypermethylated regions in the $DMRs_{>25\%}$ group (**Supplementary Figure S1** and **Table 3**).

## Pathway Analysis

Genes whose TSSs were annotated with DMRs were first identified and subsequently subjected to pathway analysis. We were particularly interested in genes associated with biological processes and molecular functions related to sexual maturity such as androgen signaling, steroid hormone biosynthesis,

**TABLE 3 |** An overview of basic statistic for RRBS libraries constructed based on the gel-free protocol.

| Sample ID | Total reads | Clean reads after trimming | Read coverage (X) | Unique mapping efficiency (%) | Global CpG methylation (%) | Number of covered CpGs | Bisulfite conversion rate (%) |
|---|---|---|---|---|---|---|---|
| 14 A | 8,092,814 | 7,424,375 | 15.3 | 32.3 | 40.4 | 4,287,779 | 99.2 |
| 17 A | 8,769,052 | 8,037,908 | 16.2 | 29.2 | 38.4 | 4,161,727 | 99.2 |
| 14 B | 8,187,841 | 7,514,351 | 15.4 | 30.5 | 38.0 | 3,867,873 | 99.2 |
| 17 B | 7,916,740 | 7,242,150 | 15.0 | 30.2 | 37.6 | 3,941,237 | 99.2 |
| 14 C | 9,235,837 | 8,452,463 | 17.4 | 33.3 | 40.3 | 4,792,957 | 99.2 |
| 17 C | 8,208,151 | 7,515,657 | 15.3 | 33.0 | 39.9 | 4,267,681 | 99.2 |
| 14 D | 8,608,751 | 7,932,141 | 15.6 | 33.3 | 39.6 | 4,529,706 | 99.3 |
| 17 D | 6,947,434 | 6,395,163 | 12.4 | 32.6 | 39.6 | 3,918,954 | 99.2 |
| 14 E | 7,745,029 | 7,098,249 | 14.6 | 33.9 | 40.2 | 4,230,165 | 99.2 |
| 17 E | 8,179,041 | 7,538,949 | 15.7 | 34.4 | 40.7 | 4,384,431 | 99.2 |
| 14 F | 9,561,827 | 8,631,458 | 18.2 | 33.9 | 41.2 | 4,855,729 | 99.0 |
| 17 F | 11,204,211 | 10,288,338 | 21.6 | 34.8 | 41.4 | 5,383,672 | 98.9 |
| 14 G | 6,739,955 | 6,197,336 | 13.1 | 35.2 | 40.7 | 3,947,850 | 98.8 |
| 17 G | 8,406,205 | 7,643,950 | 16.4 | 37.0 | 42.7 | 4,819,724 | 98.7 |

*Libraries were constructed from sperm DNA collected from the same young Norwegian red bulls (n = 7) at two different ages. Letters A to G prefixed by 14 or 17, indicating different bulls of age 14 and 17 months, respectively. Clean reads were obtained after adapter and low-quality trimming of Illumina sequencing reads (total reads). Read coverage was calculated by number of bp in the clean reads/number of bp at in silico MspI-digested bosTau9 genome. Mapping efficiency shows the percentage of uniquely mapped clean reads with the reference genome. CpG methylation shows the percentage of global methylation in clean reads. Downstream analyses were performed based on all covered CpGs. Bisulfite conversion rate shows the proportion of Cs, which converted to uracil during bisulfite conversion process.*

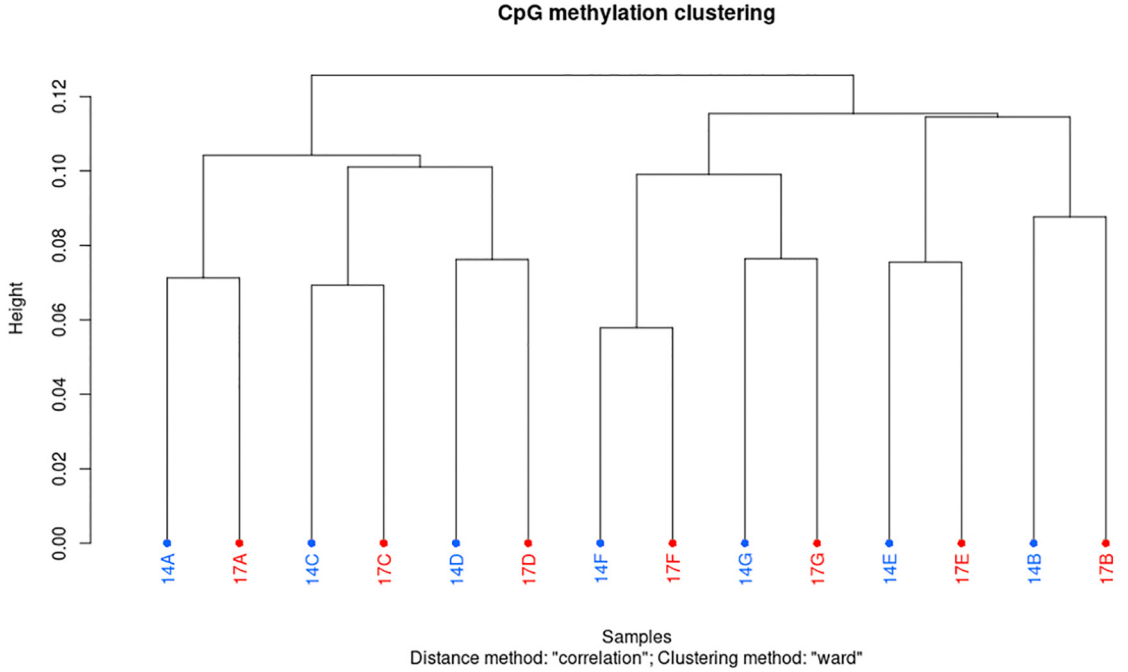



**FIGURE 1 |** Hierarchical clustering of samples based on their $CpG_{W1000}$ methylation levels in sperm DNA from Norwegian red bulls. Letters A to G prefixed by 14 or 17, indicating different bulls of age 14 and 17 months, respectively.

steroid hormone receptor signaling, spermatogenesis and developmental growth. **Figures 5A,B** show that the numbers of such genes were higher in the hypomethylation group compared to the hypermethylation group. Steroid hormone biosynthesis, identified exclusively in hypermethylation group. Moreover, genes whose TSSs were annotated with the $DMRs_{<10\%}$ and $DMRs_{>25\%}$ groups represented those functions to the greatest and least extent, respectively. In both hypo- and hypermethylation groups, functions including spermatogenesis, followed by steroid hormone receptor and energy homeostasis, were represented by the highest numbers of genes (**Supplementary Table 4**).

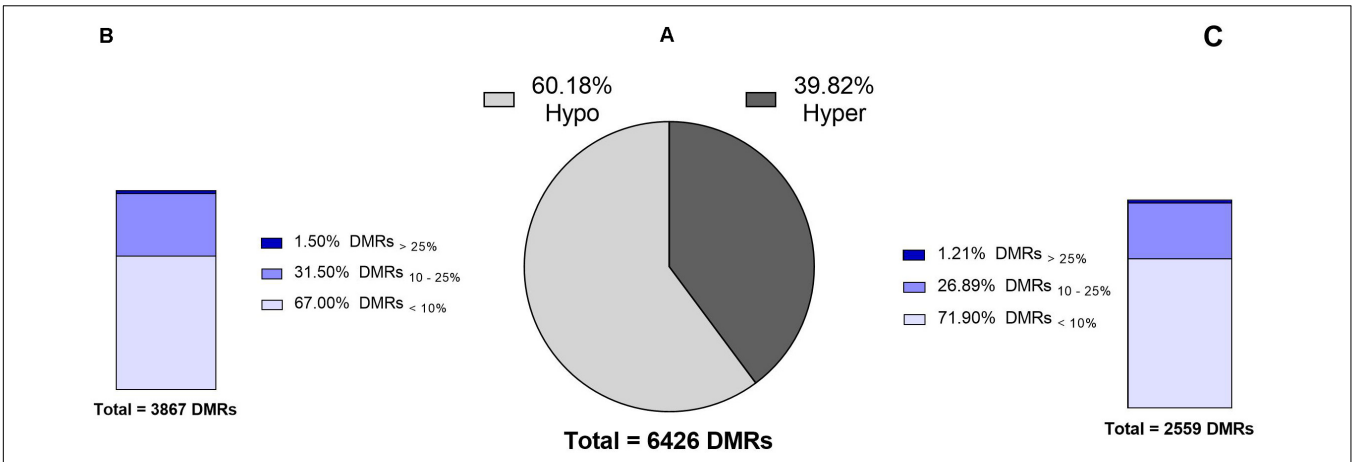



**FIGURE 2 |** Numbers and levels of significant DMRs identified in the sperm DNA methylome between identical 14 months old bulls (test) and 17 months old bulls (control). **(A)** Total number of significant DMRs indicating that 60% are hypomethylated in the test group compared to the control group. **(B,C)** Different levels of hypo- and hypermethylated regions in the test group compared to the control group. Explanation of percentage ranges: $DMRs_{<10\%}$ indicating regions with less than 10% difference in DNA methylation, $DMRs_{10\text{-}25\%}$ indicating regions having between 10 and 25% difference in DNA methylation, $DMRs_{>25\%}$ indicating regions having over 25% difference in DNA methylation.

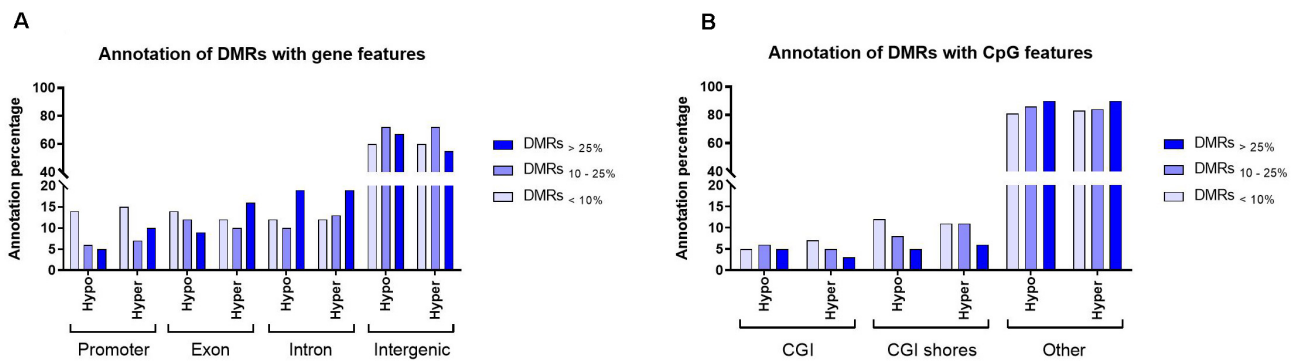



**FIGURE 3 |** An overview of the distribution of filtered DMRs in the *bosTau9* genome. **(A)** Annotation of the hypo- and hypermethylated regions with gene features. **(B)** Annotation of the hypo- and hypermethylated regions with CpG features. Hypo, hypomethylated regions; Hyper, hypermethylated regions; CGI, CpG island. Explanation of percentage ranges: $DMRs_{<10\%}$ indicating regions with less than 10% difference in DNA methylation, $DMRs_{10\text{-}25\%}$ indicating regions having between 10 and 25% difference in DNA methylation, $DMRs_{>25\%}$ indicating regions having over 25% difference in DNA methylation.

As shown in **Figure 6**, similar to biological processes and molecular functions, the majority of identified pathways (49 pathways) were in association with genes annotated with $DMRs_{<10\%}$. Only eight pathways were linked to genes annotated with $DMRs_{10-25\%}$. None of the identified pathways exhibited significant association with $DMRs_{>25\%}$. Some of the hormonal pathways (gonadotropin-releasing hormone, estrogen and oxytocin signaling) and sperm function related pathways (disulfide bond and glycoprotein) were exclusively identified in the hypermethylation group of test samples (14 months old bulls). In other words, genes associated with those pathways were annotated with hypomethylated regions in more mature, 17 months old, bulls. Although the number of annotated TSSs to DMRs (with any level) was higher in hypomethylation groups compared to the hypermethylation groups (**Figure 4**), the number of pathways represented by genes harboring those TSSs showed an opposite trend (**Figure 6**). However, the majority of identified pathways in the $DMRs_{<10\%}$ hypomethylation group exhibited stronger *p-values* (**Figure 6A**).

## DISCUSSION

In this study, sperm quality was assessed in 14 and 17 months old NR bulls. Furthermore, DNA methylation patterns were elucidated in sperm cells from the same individuals using RRBS data generated from comparative library construction where two protocols were tested.

Our results showed that the number of sperm cells in ejaculates from NR bulls significantly increased with aging. These results support previous findings where total sperm count was higher in post-pubertal Holstein bulls compared to 4 months younger bulls (Devkota et al., 2008; Wu et al., 2020). Sperm DFI results (**Table 1**) indicate that DNA integrity

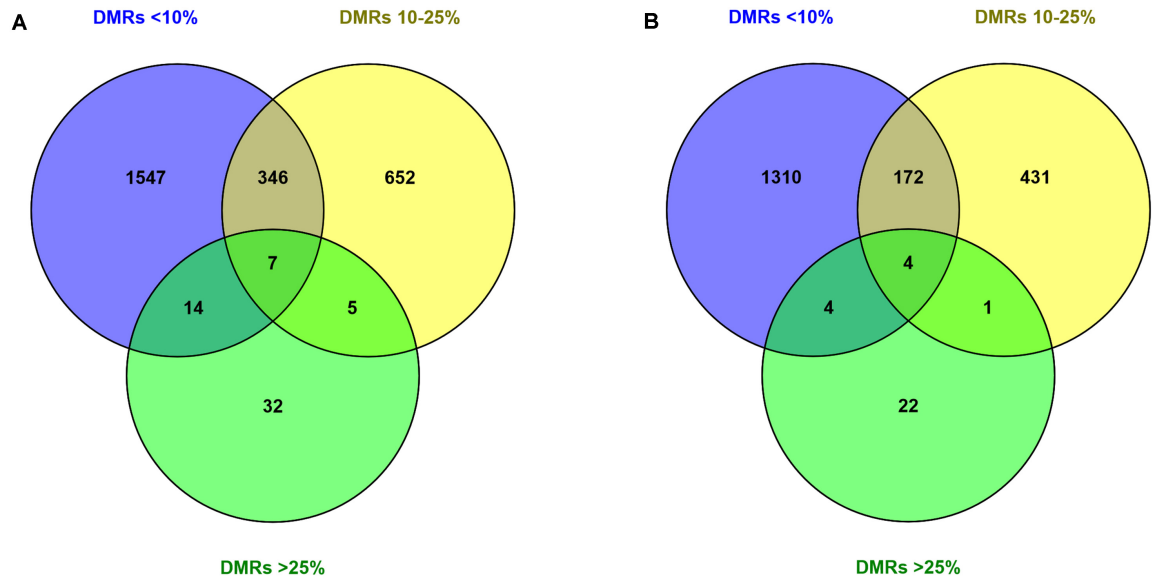



**FIGURE 4 |** Annotation of the filtered DMRs with varying degrees of methylation difference to the nearest TSSs. Numbers inside the circles, showing the number of closest unique TSSs (duplicated TSSs removed) to DMRs in **(A)** hypomethylation and **(B)** hypermethylation groups. Explanation of percentage ranges: $DMRs_{<10\%}$ indicating regions with less than 10% difference in DNA methylation, $DMRs_{10\text{-}25\%}$ indicating regions having between 10 and 25% difference in DNA methylation, $DMRs_{>25\%}$ indicating regions having over 25% difference in DNA methylation.

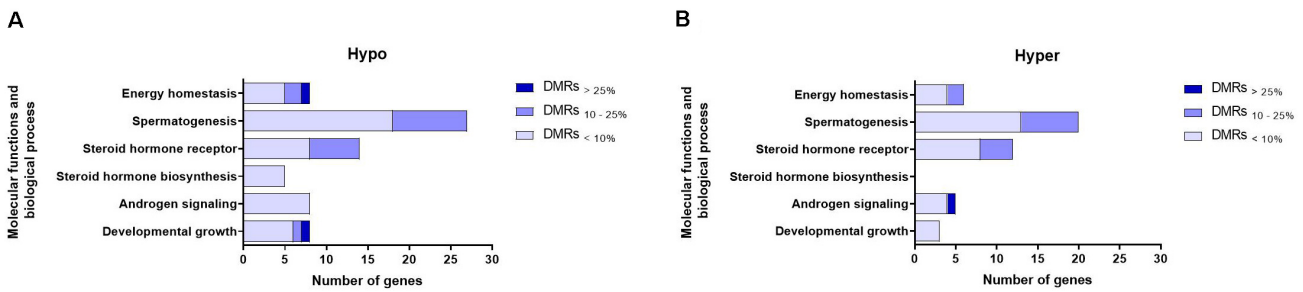



**FIGURE 5 |** Numbers of genes representing different molecular functions and biological processes related to sexual maturation in **(A)** hypomethylated (Hypo) and **(B)** hypermethylated (Hyper) groups and displayed according to their association with DMR-groups exhibiting varying degrees of methylation differences. Explanation of percentage ranges: $DMRs_{<10\%}$ indicating regions with less than 10% difference in DNA methylation, $DMRs_{10\text{-}25\%}$ indicating regions having between 10 and 25% difference in DNA methylation, $DMRs_{>25\%}$ indicating regions having over 25% difference in DNA methylation.

also improves with aging. This can be explained by ongoing sperm nucleus development from 14 to 17 months of age as it has been reported that sperm DNA is more compact in older bulls rendering it less prone to fragmentation (Andrabi, 2007). In addition, sperm DFI was reduced in frozen-thawed semen samples compared to fresh samples in both age groups. It seems possible that sperm cells with higher DFI in fresh semen may not tolerate the cryopreservation process and became degraded during cryopreservation and thawing, hence not falling into the gate defined as sperm cells based on electronic volume in the flowcytometry analysis. However, the observed differences are small and less likely to be of biological importance. The HDS results presented here indicate that the degree of sperm chromatin compactness was reduced in fresh NR ejaculates at 17 compared to 14 months of age. This must, however, be further investigated using a larger number of samples. Furthermore, both total sperm motility and sperm progressivity were significantly increased in fresh semen from bulls of age 17 compared to 14 months. This trend was also observed for frozen-thawed samples, although the changes were not significant. These results are in agreement with observations from previous research where sperm cell motility in fresh samples were positively correlated with increasing age in Holstein bulls (Devkota et al., 2008; Murphy et al., 2018) and Nelore bulls (Reis et al., 2016). Overall, the results from sperm quality analyses show that sperm cells from NR bulls at 17 months of age displayed higher sperm quality compared to 14 months of age. Although sexual maturation lasting up to 50 weeks of age (Rawlings et al., 2008), previous evidences have documented that bull sperm quality increased even after puberty (Brito et al., 2004). Therefore,

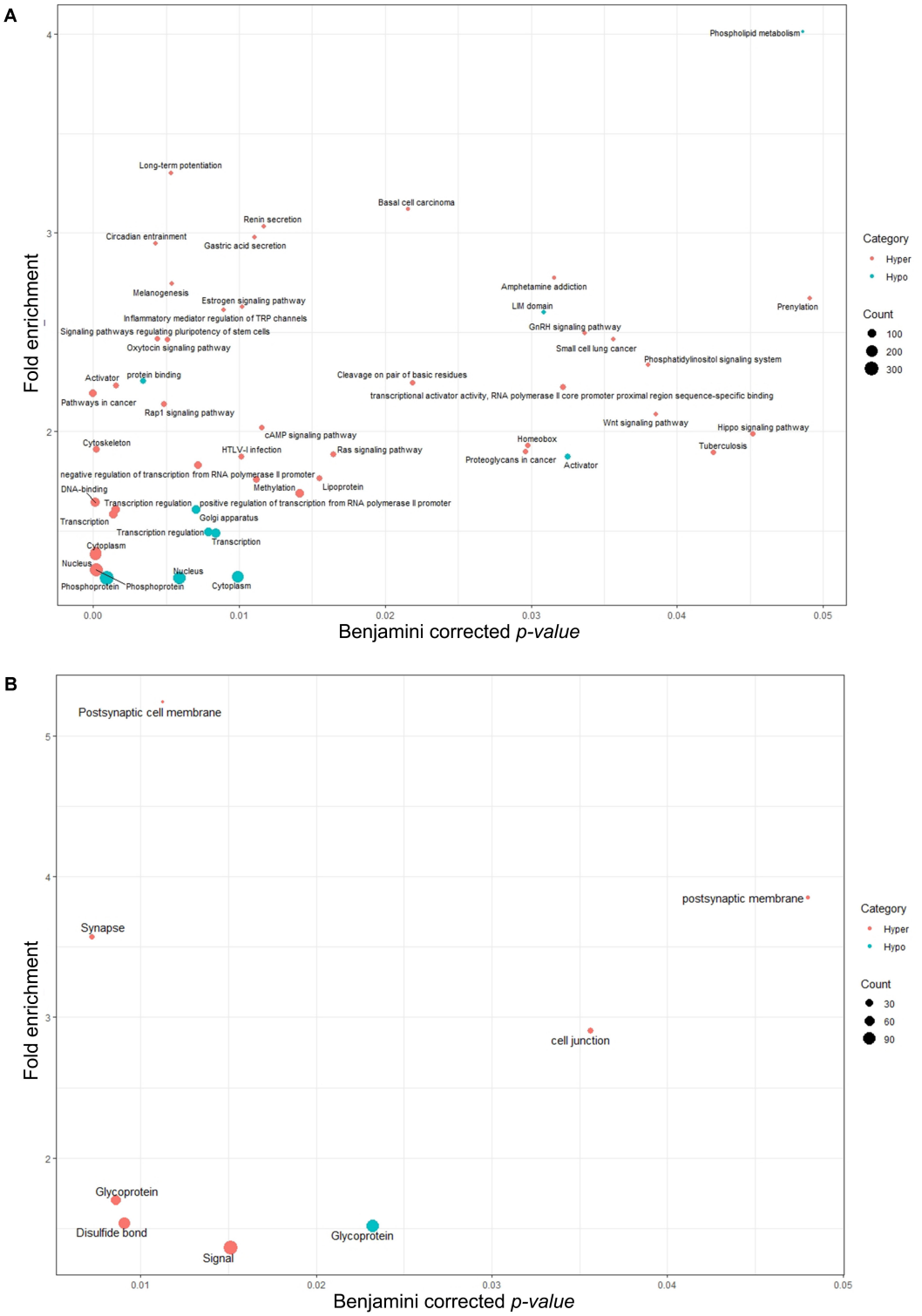



**FIGURE 6 |** Pathway analysis for annotated genes associated with **(A)** filtered DMRs with less than a 10% methylation difference and **(B)** filtered DMRs with a 10–25% methylation difference. No significant pathways were identified for annotated genes associated with DMRs over 25% methylation difference. GO terms are plotted in function of their Benjamini corrected *p*-value (*x*-axis) and fold enrichment (*y*-axis). Gene count size key shows the number of genes involved in that particular pathway. Hypo, hypomethylated regions (referring to TSSs annotated with hypomethylated regions in test group); Hyper, hypermethylated regions (referring to TSSs annotated to hypermethylated regions in test group).

these results are likely to be related to the well-known sexual maturation process.

Read quality control is an important initial step in next generation sequencing data processing. The Trim-galore software has been recommended for trimming the low-quality reads in RRBS libraries (Wreczycka et al., 2017). Although RRBS libraries from the Ovation method were constructed, evaluated and trimmed according to criteria recommended by the manufacturer, surprisingly we did not detect any Illumina adapter sequences in the reverse reads of libraries. This observation might partially be explained by the sequencing technique and source of DNA. Although according to manufacture recommendation, Ovation method is compatible with paired-end sequencing, previous results employing this method, sequenced the libraries in a single-end mode, and not paired-end, mode (Pilsner et al., 2018; Chen et al., 2019; Paul et al., 2019; Rashid et al., 2020). The same studies applied this method to study DNA methylome in rat, mice and humans brain/sperm cells while, according to manufacturer's recommendation, the Ovation method is designed to generate RRBS libraries from human genomic DNA (NuGEN, 2020). Length distribution after trimming also revealed that libraries constructed using the Ovation method had several peaks reflecting different fragment sizes specifically of short length, whereas reads from the gel-free method revealed only one major peak of fragments greater than 130 base pairs long. This is an important factor as it has been shown that longer reads align better and more specifically to a reference genome (Tran et al., 2014). To our knowledge, this was the first time the Ovation® RRBS Methyl-Seq system has been applied to study DNA methylation in bull sperm. However, further work is required to successfully adopt Ovation system for studying the bull sperm DNA methylome.

Basic statistics of sequencing results from the RRBS libraries constructed using the gel-free protocol indicated very consistent and reproducible bisulfite conversion between samples. The average conversion rate of 99.1% is higher and equal to previously published whole genome bisulfite sequencing (WGBS) (Duan et al., 2019) and RRBS results (Jiang et al., 2018) for bull sperm cells, respectively. Although in this study, the *bosTau9* genome was used as the reference genome and some relaxed alignment parameters were applied, the average mapping efficiency of 33.1% was much higher than previously reported results for RRBS libraries in bull sperm cells (Jiang et al., 2018).

Results further indicated a 40% global DNA methylation level in NR bull sperm cells. Previous studies showed that, in general, global DNA methylation level is low in bull sperm cells. For instance, using a luminometric methylation assay an average of 45% (Perrier et al., 2018) and using RRBS, an average of 35% (Jiang et al., 2018) global CpG methylation in bull sperm cells has been reported. Similarly, low global CpG methylation was also reported for ten different cattle tissues using RRBS (Zhou et al., 2016). Previously, we reported an average of 33% of global methylation in boar sperm cells using a gel-free RRBS technique (Khezri et al., 2019). However, it has been shown that global sperm DNA methylation in bulls can reach 75% as documented using WGBS (Zhou et al., 2018). One should keep in mind that the applied RRBS method in this study focuses on a small subset (CpG island) of the compact sperm genome where methylation levels are generally low (Suzuki and Bird, 2008). In addition, differences in global bull sperm DNA methylation described in the literature might be explained by different laboratory techniques, instrumental platforms, bioinformatics workflows, reference genome versions utilized for read alignment and interspecies differences in sperm DNA methylation patterns.

Here, no significant associations between sperm global CpG methylation and age were found. These findings are further supported by Pearson correlation and cluster analyses, where a high positive correlation between samples from both age groups was observed. In addition, samples from both age groups of the same individuals always clustered together, which suggests that, in this study, individual effects on global sperm DNA methylation are probably more pronounced than age effects. Considering uniform condition and environment for raising and feeding the bulls, it is least likely that individual differences in DNA methylation here is driven by environmental factors. However, in addition to environmental factors, it has been shown that individual differences in sperm DNA methylation may be explained by epigenetic polymorphism phenomenon and interindividual genetic diversity (Kiefer and Perrier, 2019). In agreement with global sperm DNA methylome results presented here, previous research reported that DNA methylation levels in bull sperm is dynamic during puberty, becoming stable after the age of 1 year (Lambert et al., 2018). In parallel with global methylation analysis, differential methylation analysis, showed an increasing trend of DNA methylation in the control group (sperm DNA from 17 months old bulls) compared to test group (sperm DNA from 14 months old bulls). Although, 70% of identified differentially methylated regions, displayed less than 10% methylation difference, we believe that this further highlights the possibility of an existing relationship between differentially methylated regions and sexual maturation in NR bulls. This hypothesis is supported by previous studies in Holstein bulls where more methylated regions were found in sperm cells from 16 months bulls compared to 10 months bulls (Lambert et al., 2018). Similar findings were reported in one Japanese black bull (at 14, 19, 28, 54, and 162 months of age), where authors identified eight CpGs that exhibited an age-dependent increase in their methylation levels (Takeda et al., 2019).

The distribution of DMRs demonstrated here showed that the majority lay within intergenic regions and regions outside CpG Islands/CpG shores. Similar trends have been reported in boar (Hwang et al., 2017; Khezri et al., 2019) and bull (Jiang et al., 2018; Perrier et al., 2018) sperm DNA. Previous research has shown that CpG Islands and CpG shores, in parallel with promoters, play an important role in regulation of transcription (Deaton and Bird, 2011; Long et al., 2017). Although only a small percentage of DMRs were annotated with CpG Island/CpG shores and promoters here, the majority of annotated DMRs exhibited less than a 10% methylation difference. This further suggests similar DNA methylation profiles in these regions in sperm samples from NR bulls at age 14 and 17 months.

GO analysis results for the $DMR_{>25\%}$ group further showed that molecular functions/biological processes such as energy

homeostasis, developmental growth and androgen signaling could be driven by Cytochrome B5 Reductase 4 (*CYB5R4*), Phospholipase C Beta 1 (*PLCB1*) and NK3 homeobox 1 (*NKX3-1*) genes, respectively. However, these genes are not specific for reproduction or sexual maturation. For instance, previous research demonstrated that the *CYB5R4* gene could be consider as one of the candidate gene for quantitative trait locus studies for the oleic acid percentage in Japanese Black cattle (Kawaguchi et al., 2019). In other research, the *PLCB1* gene was identified in oxidative stress response and heat tolerance in Dehong humped cattle (Li et al., 2020). Furthermore, the transcription factor *NKX3-1* was proposed as a possible regulator of gene expression in the endometrium of cattle who received n-3 polyunsaturated fatty acid as a feed supplement (Waters et al., 2014). In addition, steroid hormone biosynthesis was the only biological process that was exclusively identified in the $DMR_{<10\%}$ hypomethylation group. Several genes also identified, such as cytochrome P450 superfamily members (*CYP1B1, CYP11A1, and CYP2E1*), steroid 5 alpha-reductase 2 (*SRD5A2*) and steroid sulfatase (*STS*) are annotated to be involve in steroid hormone biosynthesis. Given their annotated molecular functions/associated biological processes, genes identified in this study may contribute to age-dependent reproductive capacity in NR bulls.

Our analyses did not show any significant pathways connected to genes annotated with $DMR_{>25\%}$. These findings are in line with previous research from Holstein bulls, where no significant DMR-associated pathways were found in sperm samples collected at 12 and 16 months of age (Lambert et al., 2018). For the $DMR_{10-25\%}$ group, a total number of eight significant pathways including sperm-relevant pathways such as "disulfide bond" and "glycoprotein" in 14 months old NR bulls were identified. "Disulfide bond" was exclusively identified in the hypermethylation group. It has been shown that disulfide bonds are essential for protamine function and DNA packaging in bull sperm chromatin (Hutchison et al., 2017). Although the number of bulls was limited here, fresh semen samples from 14 months old NR bulls exhibited higher degree of chromatin compaction compared to 17 months old bulls (**Table 1**). These results suggest a possible link between sperm DNA hypermethylation and DNA packaging via protamine function. Similar possible contribution of DNA methylation to nucleosome rigidity via histone function, has previously been suggested in human somatic cells (Choy et al., 2010; Lee and Lee, 2012). Furthermore, the pathway "glycoprotein" was identified in both hypo and hyper $DMR_{10-25\%}$ with a stronger *p-values* in the hypermethylation group. "Glycoproteins" have been identified in the sperm plasma membrane and play an important role in mammalian fertilization (Tecle and Gagneux, 2015). Further research is required to shed light on compositions of sperm glycoproteins during bull sexual maturation. The highest numbers of identified pathways with significant *p-values* were found to be related to genes annotated with $DMR_{<10\%}$. In the study conducted by Lambert et al. (2018), identified DMRs in sperm cells from bulls at 10 and 16 months of age were associated with pathways related to sperm function, including androgen hormone signaling. Here, we identified other hormonal pathways such as GnRH, estrogen and oxytocin signaling pathways, which were exclusively related to $DMR_{<10\%}$. This further emphasizes the importance of hormonal signaling in development and sexual maturation. However, pathway analysis results need to be interpreted with caution for two main reasons. First, it has been recommended to avoid using differential DNA methylation level cut off percentages less than 5% in DMR-analysis due to the minimal effects on gene expression they exercise (Wreczycka et al., 2017). Second, a moderate number of genes annotated with DMRs overlapped between hypo- and hypermethylation groups. How transcriptional regulation can be exerted via TSSs proximal to both hypo- and hypermethylated regions is not clear, especially in sperm cells that are relatively transcriptionally silent. Therefore, further research using transcriptome analysis of *in vitro* produced embryos, fertilized with sperm cells from wider age groups of young NR bulls is recommended.

## CONCLUSION

The purpose of the present research was to study the sperm DNA methylome, in parallel with sperm quality assessment, in similar NR bulls both at 14 and 17 months of age. Although the number of tested bulls were limited, the present study found that with increasing age of young bulls, sperm quality increased. Furthermore, a gel-free, multiplexed method to construct RRBS libraries from frozen-thawed bull sperm cells was found to be reproducible. The current results showed that sperm DNA methylation in 14- and 17-months-old NR bulls was similar globally, while marginally different regionally. Taken all together, identified DMRs even with low levels of methylation differences, in parallel with sperm quality results, offers some useful insight into the reproductive capacity of genomic selected young NR bulls.

## DATA AVAILABILITY STATEMENT

The datasets presented in this study can be found in online repositories. The names of the repository/repositories and accession number(s) can be found below: https://www.ebi.ac.uk/ena, PRJEB37763.

## ETHICS STATEMENT

Ethical review and approval was not required for the animal study because sperm cells that we used in this research routinely collected from bulls owned by breeding company Geno in Norway. However, the bulls were housed and cared for according to international guidelines and regulations for keeping bulls in Norway, at Geno artificial insemination (AI) station, in Hamar, Norway.

## AUTHOR CONTRIBUTIONS

AK performed the sperm motility assay, bioinformatics and biostatistics analyses with inputs from RA as well as RW and

wrote the manuscript. BN, E-BS, and TZ performed and drafted the viability assay, sperm chromatin integrity analysis and ATP content assay, respectively. E-BS prepared RRBS libraries with inputs from RW. FM and EK did conceptualization and original project draft. All authors were involved in the planning of the experiments and provided useful inputs, interpreted the data, read, edited, and approved the manuscript.

## FUNDING

The Research Council of Norway (Project No. 268048) and Regional Research Fund Inland, Norway (Project No. 257606), funded this research work. The funding bodies played no role in the design of the study and collection, analyses, and interpretation of data and in writing the manuscript.

## ACKNOWLEDGMENTS

We kindly thank personnel at Geno AI station for collecting, evaluating, and processing the semen samples. We would also like to thank Janeth Mbuma for the sperm quality analyses she performed on a sub-set of samples. The Norwegian Sequencing Centre (www.sequencing.uio.no), a national technology platform hosted by Oslo University Hospital and the University of Oslo, supported by the Research Council of Norway and the Southeastern Regional Health Authority, provided the sequencing service.

## SUPPLEMENTARY MATERIAL

The Supplementary Material for this article can be found online at: https://www.frontiersin.org/articles/10.3389/fgene.2020.00922/full#supplementary-material

## REFERENCES

Akalin, A., Kormaksson, M., Li, S., Garrett-Bakelman, F. E., Figueroa, M. E., Melnick, A., et al. (2012). methylKit: a comprehensive R package for the analysis of genome-wide DNA methylation profiles. *Genome Biol.* 13:R87. doi: 10.1186/gb-2012-13-10-r87

Andrabi, S. M. H. (2007). Mammalian sperm chromatin structure and assessment of DNA fragmentation. *J. Assist. Reprod. Genet.* 24, 561–569. doi: 10.1007/s10815-007-9177-y

Boe-Hansen, G. B., Ersboll, A. K., Greve, T., and Christensen, P. (2005). Increasing storage time of extended boar semen reduces sperm DNA integrity. *Theriogenology* 63, 2006–2019. doi: 10.1016/j.theriogenology.2004.09.006

Boyle, P., Clement, K., Gu, H., Smith, Z. D., Ziller, M., Fostel, J. L., et al. (2012). Gel-free multiplexed reduced representation bisulfite sequencing for large-scale DNA methylation profiling. *Genome Biol.* 13:R92. doi: 10.1186/gb-2012-13-10-r92

Brito, L. F., Silva, A. E., Unanian, M. M., Dode, M. A., Barbosa, R. T., and Kastelic, J. P. (2004). Sexual development in early- and late-maturing Bos indicus and Bos indicus x *Bos taurus* crossbred bulls in Brazil. *Theriogenology* 62, 1198–1217. doi: 10.1016/j.theriogenology.2004.01.006

Chen, X., Zhang, L., and Wang, C. (2019). Prenatal hypoxia-induced epigenomic and transcriptomic reprogramming in rat fetal and adult offspring hearts. *Sci. Data* 6:238. doi: 10.1038/s41597-019-0253-9

Choy, J. S., Wei, S., Lee, J. Y., Tan, S., Chu, S., and Lee, T.-H. (2010). DNA methylation increases nucleosome compaction and rigidity. *J. Am. Chem. Soc.* 132, 1782–1783. doi: 10.1021/ja910264z

Deaton, A. M., and Bird, A. (2011). CpG islands and the regulation of transcription. *Genes Dev.* 25, 1010–1022. doi: 10.1101/gad.2037511

Devkota, B., Koseki, T., Matsui, M., Sasaki, M., Kaneko, E., Miyamoto, A., et al. (2008). Relationships Among Age, Body Weight, scrotal circumference, semen quality and peripheral testosterone and estradiol concentrations in pubertal and postpubertal holstein bulls. *J. Vet. Med. Sci.* 70, 119–121. doi: 10.1292/jvms.70.119

Donkin, I., and Barres, R. (2018). Sperm epigenetics and influence of environmental factors. *Mo.l Metab.* 14, 1–11. doi: 10.1016/j.molmet.2018.02.006

Duan, J. E., Jiang, Z. C., Alqahtani, F., Mandoiu, I., Dong, H., Zheng, X., et al. (2019). Methylome dynamics of bovine gametes and in vivo early embryos. *Front. Genet.* 10:512. doi: 10.3389/fgene.2019.00512

Evenson, D., and Jost, L. (2000). Sperm chromatin structure assay is useful for fertility assessment. *Methods Cell Sci.* 22, 169–189. doi: 10.1023/a:1009844109023

Ferris, C. P., Patterson, D. C., Gordon, F. J., Watson, S., and Kilpatrick, D. J. (2014). Calving traits, milk production, body condition, fertility, and survival of holstein-friesian and norwegian red dairy cattle on commercial dairy farms over 5 lactations. *J. Dairy Sci.* 97, 5206–5218. doi: 10.3168/jds.2013-7457

Fortes, M. R. S., Holroyd, R. G., Reverter, A., Venus, B. K., Satake, N., and Boe-Hansen, G. B. (2012). The integrity of sperm chromatin in young tropical composite bulls. *Theriogenology* 78, 326–333, 333.e1–.e4. doi: 10.1016/j.theriogenology.2012.02.007

Fuerst-Waltl, B., Schwarzenbacher, H., Perner, C., and Sölkner, J. (2006). Effects of age and environmental factors on semen production and semen quality of Austrian Simmental bulls. *Anim. Reprod. Sci.* 95, 27–37. doi: 10.1016/j.anireprosci.2005.09.002

Gu, H., Smith, Z. D., Bock, C., Boyle, P., Gnirke, A., and Meissner, A. (2011). Preparation of reduced representation bisulfite sequencing libraries for genome-scale DNA methylation profiling. *Nat. Protoc.* 6, 468–481. doi: 10.1038/nprot.2010.190

Huang da, W., Sherman, B. T., and Lempicki, R. A. (2009). Systematic and integrative analysis of large gene lists using DAVID bioinformatics resources. *Nat. Protoc.* 4, 44–57. doi: 10.1038/nprot.2008.211

Hutchison, J. M., Rau, D. C., and DeRouchey, J. E. (2017). Role of disulfide bonds on DNA packaging forces in bull sperm chromatin. *Biophys. J.* 113, 1925–1933. doi: 10.1016/j.bpj.2017.08.050

Hwang, J. H., An, S. M., Kwon, S., Park, D. H., Kim, T. W., Kang, D. G., et al. (2017). DNA methylation patterns and gene expression associated with litter size in Berkshire pig placenta. *PLoS One* 12:e0184539. doi: 10.1371/journal.pone.0184539

Jiang, Z., Lin, J., Dong, H., Zheng, X., Marjani, S. L., Duan, J., et al. (2018). DNA methylomes of bovine gametes and in vivo produced preimplantation embryos. *Biol. Reprod.* 99, 949–959. doi: 10.1093/biolre/ioy138

Kawaguchi, F., Kigoshi, H., Fukushima, M., Iwamoto, E., Kobayashi, E., Oyama, K., et al. (2019). Whole-genome resequencing to identify candidate genes for the QTL for oleic acid percentage in Japanese Black cattle. *Anim. Sci. J.* 90, 467–472. doi: 10.1111/asj.13179

Khezri, A., Narud, B., Stenseth, E.-B., Johannisson, A., Myromslien, F. D., Gaustad, A. H., et al. (2019). DNA methylation patterns vary in boar sperm cells with different levels of DNA fragmentation. *BMC Genomics* 20:897. doi: 10.1186/s12864-019-6307-8

Kiefer, H., and Perrier, J.-P. (2019). DNA methylation in bull spermatozoa: evolutionary impacts, interindividual variability, and contribution to the embryo. *Can. J. Anim. Sci.*100, 1–16. doi: 10.1139/cjas-2019-0071

Krueger, F., and Andrews, S. R. (2011). Bismark: a flexible aligner and methylation caller for Bisulfite-Seq applications. *Bioinformatics* 27, 1571–1572. doi: 10.1093/bioinformatics/btr167

Lambert, S., Blondin, P., Vigneault, C., Labrecque, R., Dufort, I., and Sirard, M. A. (2018). Spermatozoa DNA methylation patterns differ due to peripubertal age

in bulls. *Theriogenology* 106(Suppl. C), 21–29. doi: 10.1016/j.theriogenology.2017.10.006

Lee, J. Y., and Lee, T.-H. (2012). Effects of DNA methylation on the structure of nucleosomes. *J. Am. Chem. Soc.* 134, 173–175. doi: 10.1021/ja210273w

Li, R., Li, C., Chen, H., Li, R., Chong, Q., Xiao, H., et al. (2020). Genome-wide scan of selection signatures in Dehong humped cattle for heat tolerance and disease resistance. *Anim. Genet.* 51, 292–299. doi: 10.1111/age.12896

Long, M. D., Smiraglia, D. J., and Campbell, M. J. (2017). The genomic impact of DNA CpG methylation on gene expression; relationships in prostate cancer. *Biomolecules* 7:15. doi: 10.3390/biom7010015

Martin, M. (2011). Cutadapt removes adapter sequences from high-throughput sequencing reads. *EMBnet. J.* 17, 10–12. doi: 10.14806/ej.17.1.200

McSwiggin, H. M., and O'Doherty, A. M. (2018). Epigenetic reprogramming during spermatogenesis and male factor infertility. *Reproduction* 156, R9–R21. doi: 10.1530/REP-18-0009

Meissner, A., Gnirke, A., Bell, G. W., Ramsahoye, B., Lander, E. S., and Jaenisch, R. (2005). Reduced representation bisulfite sequencing for comparative high-resolution DNA methylation analysis. *Nucleic Acids Res.* 33, 5868–5877. doi: 10.1093/nar/gki901

Murphy, E. M., Kelly, A. K., O'Meara, C., Eivers, B., Lonergan, P., and Fair, S. (2018). Influence of bull age, ejaculate number, and season of collection on semen production and sperm motility parameters in Holstein Friesian bulls in a commercial artificial insemination centre. *J. Anim. Sci.* 96, 2408–2418. doi: 10.1093/jas/sky130

NuGEN, (2020). *User Guide for Ovation$RRBS Methyl-Seq System*. Redwood City, CA: Tecan Genomics, Inc, 1–16.

O'Doherty, A. M., and McGettigan, P. A. (2015). Epigenetic processes in the male germline. *Reprod. Fertil. Dev.* 27, 725–738. doi: 10.1071/RD14167

Oliveros, J. C. (2015). *Venny. An Interactive Tool for Comparing Lists With Venn's Diagrams*. Available online at: https://bioinfogp.cnb.csic.es/tools/venny/index.html (accessed February 13, 2020).

Paul, J. L., Dashtipour, K., Chen, Z., and Wang, C. (2019). DNA methylome study of human cerebellar tissues identified genes and pathways possibly involved in essential tremor. *Precis. Clin. Med.* 2, 221–234. doi: 10.1093/pcmedi/pbz028

Perrier, J. P., Sellem, E., Prezelin, A., Gasselin, M., Jouneau, L., Piumi, F., et al. (2018). A multi-scale analysis of bull sperm methylome revealed both species peculiarities and conserved tissue-specific features. *BMC Genomics* 19:404. doi: 10.1186/s12864-018-4764-0

Pilsner, J. R., Shershebnev, A., Medvedeva, Y. A., Suvorov, A., Wu, H., Goltsov, A., et al. (2018). Peripubertal serum dioxin concentrations and subsequent sperm methylome profiles of young Russian adults. *Reprod. Toxicol.* 78, 40–49. doi: 10.1016/j.reprotox.2018.03.007

Rashid, F., Ramakrishnan, A., Fields, C., and Irudayaraj, J. (2020). Acute PFOA exposure promotes epigenomic alterations in mouse kidney tissues. *Toxicol. Rep.* 7, 125–132. doi: 10.1016/j.toxrep.2019.12.010

Rawlings, N., Evans, A., Chandolia, R., and Bagu, E. (2008). Sexual Maturation in the Bull. *Reprod. Domest. Anim.* 43(Suppl. 2), 295–301. doi: 10.1111/j.1439-0531.2008.01177.x

Refsdal, A. O. (2007). Reproductive performance of Norwegian cattle from 1985 to 2005: trends and seasonality. *Acta Vet. Scand.* 49:5. doi: 10.1186/1751-0147-49-5

Reis, L. S. L. S., Ramos, A. A., Camargos, A. S., and Oba, E. (2016). Integrity of the plasma membrane, the acrosomal membrane, and the mitochondrial membrane potential of sperm in Nelore bulls from puberty to sexual maturity. *Arq. Bras. Med. Vet. Zootec.* 68, 620–628.

Standerholen, F. B., Myromslien, F. D., Kommisrud, E., Ropstad, E., and Waterhouse, K. E. (2014). Comparison of electronic volume and forward scatter principles of cell selection using flow cytometry for the evaluation of acrosome and plasma membrane integrity of bull spermatozoa. *Cytometry A* 85, 719–728. doi: 10.1002/cyto.a.22474

Suzuki, M. M., and Bird, A. (2008). DNA methylation landscapes: provocative insights from epigenomics. *Nat. Rev. Genet.* 9, 465–476. doi: 10.1038/nrg2341

Takeda, K., Kobayashi, E., Nishino, K., Imai, A., Adachi, H., Hoshino, Y., et al. (2019). Age-related changes in DNA methylation levels at CpG sites in bull spermatozoa and in vitro fertilization-derived blastocyst-stage embryos revealed by combined bisulfite restriction analysis. *J. Reprod. Dev.* 65, 305–312. doi: 10.1262/jrd.2018-146

Tecle, E., and Gagneux, P. (2015). Sugar-coated sperm: unraveling the functions of the mammalian sperm glycocalyx. *Mol. Reprod. Dev.* 82, 635–650. doi: 10.1002/mrd.22500

Tran, H., Porter, J., Sun, M.-A., Xie, H., and Zhang, L. (2014). Objective and comprehensive evaluation of bisulfite short read mapping tools. *Adv. Bioinformat.* 2014, 472045–472045. doi: 10.1155/2014/472045

UCSC, (2018). *Table Browser for bosTau 9 Assembly*. Available online at: https://genome.ucsc.edu/cgi-bin/hgTables (accessed September 18, 2019).

Waters, S. M., Coyne, G. S., Kenny, D. A., and Morris, D. G. (2014). Effect of dietary n-3 polyunsaturated fatty acids on transcription factor regulation in the bovine endometrium. *Mol. Biol. Rep.* 41, 2745–2755. doi: 10.1007/s11033-014-3129-2

Wickham, H. (2016). *ggplot2: Elegant Graphics for Data Analysis*. New York, NY: Springer-Verlag.

Wreczycka, K., Gosdschan, A., Yusuf, D., Gruning, B., Assenov, Y., and Akalin, A. (2017). Strategies for analyzing bisulfite sequencing data. *J. Biotechnol.* 261, 105–115. doi: 10.1016/j.jbiotec.2017.08.007

Wu, C., Blondin, P., Vigneault, C., Labrecque, R., and Sirard, M.-A. (2020). The age of the bull influences the transcriptome and epigenome of blastocysts produced by IVF. *Theriogenology* 144, 122–131. doi: 10.1016/j.theriogenology.2019.12.020

Zhou, Y., Connor, E. E., Bickhart, D. M., Li, C., Baldwin, R. L., Schroeder, S. G., et al. (2018). Comparative whole genome DNA methylation profiling of cattle sperm and somatic tissues reveals striking hypomethylated patterns in sperm. *GigaScience* 7:giy039. doi: 10.1093/gigascience/giy039

Zhou, Y., Xu, L., Bickhart, D. M., Abdel Hay, E. H., Schroeder, S. G., Connor, E. E., et al. (2016). Reduced representation bisulphite sequencing of ten bovine somatic tissues reveals DNA methylation patterns and their impacts on gene expression. *BMC Genomics* 17:779. doi: 10.1186/s12864-016-3116-1

**Conflict of Interest:** The authors declare that the research was conducted in the absence of any commercial or financial relationships that could be construed as a potential conflict of interest.

*Copyright © 2020 Khezri, Narud, Stenseth, Zeremichael, Myromslien, Wilson, Ahmad and Kommisrud. This is an open-access article distributed under the terms of the Creative Commons Attribution License (CC BY). The use, distribution or reproduction in other forums is permitted, provided the original author(s) and the copyright owner(s) are credited and that the original publication in this journal is cited, in accordance with accepted academic practice. No use, distribution or reproduction is permitted which does not comply with these terms.*

frontiers in Genetics

ORIGINAL RESEARCH
published: 26 August 2020
doi: 10.3389/fgene.2020.00945

# Accelerating Onset of Puberty Through Modification of Early Life Nutrition Induces Modest but Persistent Changes in Bull Sperm DNA Methylation Profiles Post-puberty

*Jean-Philippe Perrier[1†], David A. Kenny[2], Aurélie Chaulot-Talmon[3,4], Colin J. Byrne[1,2†], Eli Sellem[5], Luc Jouneau[3,4], Anne Aubert-Frambourg[3,4], Laurent Schibler[5], Hélène Jammes[3,4], Patrick Lonergan[6], Sean Fair[1]* and Hélène Kiefer[3,4]*

[1] Laboratory of Animal Reproduction, Department of Biological Sciences, Biomaterials Research Cluster, Bernal Institute, University of Limerick, Limerick, Ireland, [2] Animal and Bioscience Research Department, Animal and Grassland Research and Innovation Centre, Teagasc, Grange, Co. Meath, Ireland, [3] Université Paris-Saclay, UVSQ, INRAE, BREED, Jouy-en-Josas, France, [4] Ecole Nationale Vétérinaire d'Alfort, BREED, Maisons-Alfort, France, [5] R&D Department, ALLICE, Paris, France, [6] School of Agriculture and Food Science, University College Dublin, Dublin, Ireland*

In humans and model species, alterations of sperm DNA methylation patterns have been reported in cases of spermatogenesis defects, male infertility and exposure to toxins or nutritional challenges, suggesting that a memory of environmental or physiological changes is recorded in the sperm methylome. The objective of this study was to ascertain if early life plane of nutrition could have a latent effect on DNA methylation patterns in sperm produced post-puberty. Holstein-Friesian calves were assigned to either a high (H) or moderate (M) plane of nutrition for the first 24 weeks of age, then reassigned to the M diet until puberty, resulting in HM and MM groups. Sperm DNA methylation patterns from contrasted subgroups of bulls in the HM (ejaculates recovered at 15 months of age; $n = 9$) and in the MM (15 and 16 months of age; $n = 7$ and 9, respectively) were obtained using Reduced Representation Bisulfite Sequencing. Both 15 and 16 months were selected in the MM treatment as these bulls reached puberty approximately 1 month after the HM bulls. Hierarchical clustering demonstrated that inter-individual variability unrelated to diet or age dominated DNA methylation profiles. While the comparison between 15 and 16 months of age revealed almost no change, 580 differentially methylated CpGs (DMCs) were identified between the HM and MM groups. Differentially methylated CpGs were mostly hypermethylated in the HM group, and enriched in endogenous retrotransposons, introns, intergenic regions, and shores and shelves of CpG islands. Furthermore, genes involved in spermatogenesis, Sertoli cell function, and the hypothalamic–pituitary–gonadal axis were targeted by differential methylation when HM and MM groups were compared at 15 months of age, reflecting the earlier timing of puberty onset in the HM bulls. In contrast, the genes still differentially methylated in MM bulls at 16 months of age were enriched for ATP-binding molecular

OPEN ACCESS

**Edited by:**
*Simone Eliza Facioni Guimaraes, Universidade Federal de Viçosa, Brazil*

**Reviewed by:**
*Hasan Khatib, University of Wisconsin-Madison, United States*
*Brittney Keel, United States Department of Agriculture, United States*
*Arlindo Moura, Federal University of Ceará, Brazil*

***Correspondence:**
*Sean Fair*
*sean.fair@ul.ie*

**†Present address:**
*Jean-Philippe Perrier, INSERM U1209, CNRS UMR 5309, Institute for Advanced Biosciences, Université Grenoble Alpes, Grenoble, France*
*Colin J. Byrne, School of Veterinary and Life Sciences, Murdoch University, Perth, WA, Australia*

**Specialty section:**
*This article was submitted to Livestock Genomics, a section of the journal Frontiers in Genetics*

**Received:** *05 February 2020*
**Accepted:** *28 July 2020*
**Published:** *26 August 2020*

**Citation:**
*Perrier J-P, Kenny DA, Chaulot-Talmon A, Byrne CJ, Sellem E, Jouneau L, Aubert-Frambourg A, Schibler L, Jammes H, Lonergan P, Fair S and Kiefer H (2020) Accelerating Onset of Puberty Through Modification of Early Life Nutrition Induces Modest but Persistent Changes in Bull Sperm DNA Methylation Profiles Post-puberty. Front. Genet. 11:945. doi: 10.3389/fgene.2020.00945*

function, suggesting that changes to the sperm methylome could persist even after the HM and MM bulls reached a similar level of sexual maturity. Together, results demonstrate that enhanced plane of nutrition in pre-pubertal calves associated with advanced puberty induced modest but persistent changes in sperm DNA methylation profiles after puberty.

**Keywords: Bovine, puberty, spermatozoa, DNA methylation, nutritional programming**

## INTRODUCTION

With the advent of genomic selection, genetically elite dairy bulls can now be reliably identified as sires for use in artificial insemination shortly after birth; however, semen cannot be supplied until after puberty is reached. Earlier onset of puberty in young, genomically selected, high genetic merit dairy bulls will advance the availability of semen, shorten the generation interval, and accelerate genetic improvement. Recent data from our group (Byrne et al., 2018a,b) demonstrated that offering bull calves a high plane of nutrition in early life hastens the age at puberty onset by approximately 1 month. Indeed, our own research and that of others (Harstine et al., 2015; Dance et al., 2016) on Holstein-Friesian bulls has clearly shown that an enhanced plane of nutrition up to 6 months of age does not result in any latent effects on measures of post-pubertal semen quality, including pre- and post-thaw sperm motility, or on the *in vitro* fertilizing ability (Dance et al., 2015, 2016), despite leading to increased scrotal skin thickness (Byrne et al., 2018a) compared to their contemporaries offered a moderate plane of nutrition. In addition to these alterations, thermographic imaging of the testes also highlighted differences in the scrotal surface temperature (Byrne et al., 2018a). There is some evidence for a negative effect of increased dietary energy on semen quality in post-pubertal beef bulls, possibly mediated through increased testicular temperatures (Coulter et al., 1997). However, there is a dearth of information on whether such intensive nutritional regimes negatively affect a bull's post-pubertal semen production when employed in early life. In particular, insight into the biochemical or molecular changes induced by nutrition and affecting sperm cells – in particular those of a more persistent nature which could be transmitted to the next generation – is essential.

Epigenetics refers to the molecular mechanisms that alter gene regulation in a DNA sequence-independent fashion. More specifically, cell differentiation requires a specific transcriptional program that relies on combinations of histone modifications, DNA methylation states and non-coding RNAs. These epigenetic modifications constitute the memory of tissue-specific regulations that are transmitted to the daughter cells through cell divisions (Bird, 2007), and have the potential to record past environmental or physiological changes. The sperm epigenome could therefore provide useful markers of the latent effect of early life nutrition. The production of mature sperm requires sequential and complex reorganization of the epigenomic architecture of sperm cell precursors, which begins during fetal life and is only completed after sexual maturity is reached. Epigenetic reprogramming during fetal development first consists of a genome-wide erasure of DNA methylation marks of primordial germ cells (Popp et al., 2010; von Meyenn and Reik, 2015; Tang et al., 2016). Re-establishment of male germline-specific DNA methylation marks then progressively occurs before birth and during early post-natal life. After puberty and during spermatogenesis, DNA methylation patterns are essentially maintained, whereas profound rearrangements of DNA packaging (histone to protamine replacement, addition of sperm-specific histone variants, and histone post-translational modifications), and significant changes of sperm non-coding RNA content can be observed (Carrell, 2012; McSwiggin and O'Doherty, 2018). Any alterations of these dynamic epigenetic processes by intrinsic or environmental factors can potentially affect fertility, as well as influence the phenotype of the offspring (Chavatte-Palmer et al., 2016; Champroux et al., 2018; Kiefer and Perrier, 2020).

There is growing evidence that physiological, metabolic, and environmental factors, and in particular diet, can have an impact on the sperm methylome. For example, differential DNA methylation patterns in human sperm have been detected between men before and after gastric-bypass induced weight loss (Donkin et al., 2016). Similarly, in the rat, high-fat diet induces modifications in the sperm methylome (de Castro Barbosa et al., 2015), while no diet-related modifications have been found in the sperm of mice challenged with three different diets (control, low protein, and high fat diets; Shea et al., 2015). Depending on the study, mice subjected to low-protein diet or caloric restriction before conception showed either no detectable (Carone et al., 2010) or significant (Martínez et al., 2014; Radford et al., 2014) changes to DNA methylation pattern in their sperm, while a low protein diet during adulthood impacted testicular morphology and lowered the global DNA methylation content of sperm cells (Watkins et al., 2018). In addition, folic acid deficiency resulted in delayed meiotic onset, alterations in the sperm methylome and negative pregnancy outcomes in female mice (Lambrot et al., 2013), while its supplementation induced a decreased sperm count coupled with alterations of DNA methylation pattern of several imprinted genes (Ly et al., 2017). In addition to the direct effects on sperm, recent published studies have demonstrated that alterations of the sperm methylome can potentially affect the offspring metabolic phenotype, such as glucose tolerance or insulin sensitivity (reviewed in Schagdarsurengin and Steger, 2016; Donkin and Barrès, 2018).

We have previously shown that the bovine sperm methylome is unique, being globally hypomethylated compared to that of other mammals (Perrier et al., 2018). While within the context of the livestock industry, a number of studies on DNA methylation patterns have focused on male fertility (Kropp et al., 2017)

or on the effects of various types of dietary supplementation regimen (reviewed by Murdoch et al., 2016), none have examined the existence of residual effects of pre-pubertal diet on sperm DNA methylation profiles after puberty in the bull. The aim of this study was to examine the effect of plane of nutrition during the first 6 months of life and advanced puberty on post-pubertal sperm DNA methylation patterns. We also compared bulls between 15 and 16 months of age, as previous work from our group (Byrne et al., 2018a,b) demonstrated that puberty was advanced by approximately 1 month in bulls fed a high plane of nutrition during the first 6 months of life, allowing us to evaluate how the DNA methylation pattern evolves during the weeks following this critical event.

# MATERIALS AND METHODS

## Animals and Semen Collection

The management of the bulls has been described in detail (Byrne et al., 2018a). Diets were designed using National Research Council (NRC) guidelines (2001). Briefly, autumn-born Holstein-Friesian bull calves were assigned to a high (H) or moderate (M) plane of nutrition for the first 6 months of life. They were offered pre-weaning diets for a minimum of 56 days (corresponding to 247 and 117% of NRC energy and protein requirements for 55 kg calves, for calves on the H and M diets, respectively) and were weaned once they were consuming 1 kg of concentrates for three consecutive days, which happened at a mean (±SD) age of 17 (±4.4) days. After weaning, calves on the H diet received 1200 g of milk replacer and concentrate *ad libitum*, whereas calves on the M diet received 450 g of milk replacer and a maximum of 1 kg of concentrate daily (corresponding to 166 and 98% of NRC energy and protein requirements for 90 kg calves, respectively). All calves were offered grass hay to appetite and had *ad libitum* access to water. At 24 weeks of age, all calves were fed a moderate plane of nutrition consisting of 0.5 kg of concentrate daily and grass to appetite (corresponding to 178% of NRC energy and protein requirements), resulting in the HM and MM groups After puberty, all bulls received 4 kg of concentrates and grass silage *ad libitum* until 60 weeks of age. From 60 weeks of age, all animals were fed concentrate *ad libitum* plus 5 kg of grass silage, until slaughter at 72 weeks of age. The complete composition of diets can be found in **Supplementary Table 1** (chemical composition of milk replacer), **Supplementary Table 2** (composition and chemical analyses of the concentrate), and **Supplementary Table 3** (chemical analysis of forages). To monitor the onset of puberty, animals were weighed weekly pre-weaning and fortnightly post-weaning. The average daily gain pre- and post- weaning can be found in **Supplementary Table 4**

Semen was collected from the bulls on a bi-weekly basis using electro-ejaculation once their scrotal circumference reached 24 cm. Puberty was defined as an ejaculate with >50 million sperm with a progressive motility of >10% (Wolf et al., 1965) in two consecutive ejaculates. Among the HM and MM bulls, those with the most extreme differences in terms of age at puberty were selected for the present study ($n = 9$ bulls per group). Semen was collected at 15 and 16 months of age via electro-ejaculation, resulting in four groups of samples (**Supplementary Table 5**): HM15 ($n = 9$), MM15 ($n = 7$), HM16 ($n = 7$), and MM16 ($n = 9$). Semen was diluted in Bioxcell (IMV), to a concentration of $80 \times 10^6$ per ml. Straws (0.25 ml) were then frozen to -140°C over a 9 min. period (-15.5°C/min) in a programmable freezer (Planar), followed by immersion and storage in liquid nitrogen, pending further analysis.

## Genomic DNA Extraction

One straw of bull semen was used for DNA extraction (∼20 million sperm). After thawing at 37°C, the semen was washed with phosphate-buffered saline (PBS) to remove the extender, then briefly washed with $H_2O$ to eliminate somatic cells that may have contaminated the sample, and incubated overnight at 55°C in 200 µl lysis buffer (10 mM Tris-HCl pH 7.5, 25 mM EDTA, 1% SDS, 75 mM NaCl, 50 mM dithiothreitol and 0.5 µg glycogen) in the presence of 0.2 mg/ml proteinase K. Microscopic examination of all samples before lysis revealed no contamination with somatic cells. After incubation with 25 µg/ml RNAse A for 1 h at 37°C, genomic DNA was extracted twice using phenol and phenol:chloroform (1:1), then ethanol precipitated and washed. The dried pellet was re-suspended in TE buffer (10 mM Tris HCl pH 7.5, 2 mM EDTA) and the DNA concentration was measured using a Qubit 2.0 Fluorometer with the dsDNA BR Assay kit (Invitrogen).

## Reduced Representation Bisulfite Sequencing

Since we previously showed that HM bulls reached puberty one month earlier than MM bulls (Byrne et al., 2018a), the effect of diet and/or earlier puberty was assessed by comparing groups with either identical chronological age (HM15 vs. MM15 comparison) or similar physiological age (HM15 vs. MM16). Reduced Representation Bisulfite Sequencing (RRBS) libraries from HM15, MM15, and MM16 samples were prepared from 200 ng of genomic DNA digested with MspI (Fermentas), as described elsewhere (Gu et al., 2011; Perrier et al., 2018), with the exception that magnetic bead-based size selection was performed using SPRIselect magnetic beads (Beckman-Coulter). Briefly, after ligation to 55 bp methylated Illumina adapters for paired-end sequencing, $H_2O$ was added up to 50 µl, which was followed by the addition of 35 µl magnetic beads. The larger fragments bound to the beads were removed using a magnetic rack according to the manufacturer's instructions, and 85 µl of supernatant containing the smaller fragments were transferred into a new tube. The addition of 25 µl of fresh beads next allowed the selection of fragments ranging from 150 to 400 bp (40–290 bp genomic DNA fragments + adapters). After washing with 85% ethanol, the DNA bound to the beads was eluted in 20 µl EB buffer (Qiagen). The DNA was then converted twice with sodium bisulfite using the EpiTect bisulfite kit (Qiagen) following the manufacturer's instructions. Converted DNA was amplified with Pfu Turbo Cx hotstart DNA polymerase (Agilent) using 14 PCR cycles. The libraries were finally purified using AMPure XP beads (Beckman-Coulter) and sequenced on an Illumina HiSeq4000 sequencer to produce 75 bp paired-end reads (Integragen SA).

All pipetting steps before the final amplification were carried out using an NGS STARlet liquid handling system with four channels (Hamilton).

## Bioinformatics and Statistical Analyses

The sequences displayed the expected nucleotide composition based on MspI digestion and bisulfite conversion according to FastQC quality control[1]. Subsequent quality checks and trimming were carried out using Trim Galore v0.4.0[2] which removed adapter sequences, poor quality bases and reads (Phred score below 20) and reads shorter than 20 nucleotides. High quality reads were aligned to the bovine reference genome (UMD 3.1) in which the sequence of the Y chromosome has been incorporated (GenBank: CM001061.2) using Bismark v0.14.3 in the default mode with Bowtie 1 (Langmead et al., 2009; Krueger and Andrews, 2011). The bisulfite conversion rate was estimated from the unmethylated cytosine added *in vitro* during the end-repair step and was ≥97.9%. The CpGs were then selected based on their coverage by uniquely mapped reads. Only CpGs covered by at least 10 uniquely mapped reads (termed as CpGs10) were retained for subsequent analyses. Each CpG10 was assigned a methylation percentage per sample calculated from Bismark methylation calling: [(reads with "C")/(reads with "C" + reads with "T")] × 100. HM15, MM15, and MM16 groups were compared for the mapping efficiency, coverage, and average methylation at CpGs10 using permutation tests for k independent samples, with Monte-Carlo sampling of 100,000 permutations. For **Figure 1**, correlation hierarchical clustering was computed on the matrix of methylation percentages for each CpG10 covered in at least 4 bulls per group. For each comparison, differentially methylated CpGs (DMCs) were identified using DSS v2.14.0 software in the default mode (Feng et al., 2014), and Independent Hypothesis Weighting for p-value adjustment using alpha parameter set to 5% and the average methylation per group as a covariable (Ignatiadis et al., 2016). A CpG10 was considered as a DMC when it was covered in at least 4 bulls per group, when the adjusted p-value was weaker than 0.1, and the methylation difference between two groups at least 10%. A differentially methylated region (DMR) was constituted by a minimum of three DMCs with a maximum inter-DMC distance of 100 bp.

The annotation of the DMCs, DMRs, and the 1,653,793 CpGs10 was performed as described (Perrier et al., 2018) relative to gene features, CpG density and repetitive elements using an in-house pipeline[3]. The reference files were downloaded at the following sites: ftp://ftp.ensembl.org/pub/release-94/gtf/bos_taurus/Bos_taurus.UMD3.1.94.gtf.gz, http://oct2018.archive.ensembl.org/biomart/ martview/ 2c4d22063af3b241ef9322512fae0cdc [Ensembl Genes 94, Cow genes (UMD3.1)], http://hgdownload.cse.ucsc.edu/goldenPath/bosTau6/database/cpgIslandExt.txt.gz and http://hgdownload.cse.ucsc.edu/goldenPath/bosTau6/database/rmsk.txt.gz. The following criteria were applied: TSS, -100 to +100 bp relative to the transcription start site (TSS); promoter, -2000 to -100 relative to the TSS; TTS: -100 to +100 bp relative to the transcription termination site (TTS); shore, up to 2000 bp from a CpG island (CGI); and shelf, up to 2000 bp from a shore. A site/fragment was considered to belong to a CGI (respective shore and shelf) if an overlap of at least 75% was observed between the site/fragment and the CGI (respective shore and shelf). A site/fragment was considered as being overlapped by a repetitive element whatever the extent of this overlapping. The list of annotated DMCs and DMRs in the three comparisons are available in **Supplementary Table 6**. Genes containing DMCs at a maximal distance of 10 kb were subjected to enrichment analyses with the Database for Annotation, Visualization, and Integrated Discovery (DAVID) using default parameters (Huang et al., 2009), and using the gene list containing the 1,653,793 CpGs10 covered in at least four samples per group as the background. Clusters of terms showing EASE enrichment scores above 1.3 were considered significant.

## Validation by Bisulfite-Pyrosequencing

Bisulfite conversion was performed on 0.5 μg genomic DNA using the EpiTect bisulfite kit (Qiagen). Primers were designed using the Pyromark assay design software and amplifications were performed using the Pyromark PCR kit (Qiagen) according to the manufacturer's instructions. The primers used to amplify each region are listed in **Supplementary Table 7**. The following PCR program was used: 3 min at 94°C followed by 45 cycles of 30 s at 94°C, 1 min at 56°C, 1 min at 72°C, and finally 10 min at 72°C. The reverse primers were 5′-biotinylated for the DMRs included in *ATP10A*, *NEUROG2*, and *SRGAP3*, and the forward primer for the DMR included in *BCL2*. After denaturation and purification, the biotinylated strand of PCR product was used as a template for pyrosequencing with 0.3 μM pyrosequencing primer, using the Pyromark Q24 device and Pyromark Gold Q96 reagents (Qiagen). The pyrosequencing primers are listed in **Supplementary Table 8**. Each CpG was analyzed in duplicate, and inconsistent duplicates (more than 5% difference) were repeated. For each sample, the DNA methylation percentage per CpG was obtained by calculating the mean of all replicates that passed quality control by the Pyromark Q24 software. For **Figure 4A**, correlation significance between the average DNA methylation values per DMR obtained by RRBS and pyrosequencing was tested using Spearman's rank correlation test. For **Figure 4B**, HM and MM groups were compared at each CpG using non-parametric tests suited to small samples (permutation tests for two independent samples, with Monte-Carlo sampling of 100,000 permutations and with correction for the stratification of the population according to the age). All statistics were calculated using R software (R Core Team, 2018).

# RESULTS

## Sequencing Quality Controls

In order to examine the effects of plane of nutrition in the first 6 months of life associated with advanced puberty on bovine sperm DNA methylation patterns post-puberty, we analyzed 25 sperm samples from the HM15, MM15, and MM16

[1]https://www.bioinformatics.babraham.ac.uk/projects/fastqc/

[2]http://www.bioinformatics.babraham.ac.uk/projects/trim_galore/

[3]https://github.com/FAANG/faang-methylation/tree/master/RRBS-toolkit/Annotation

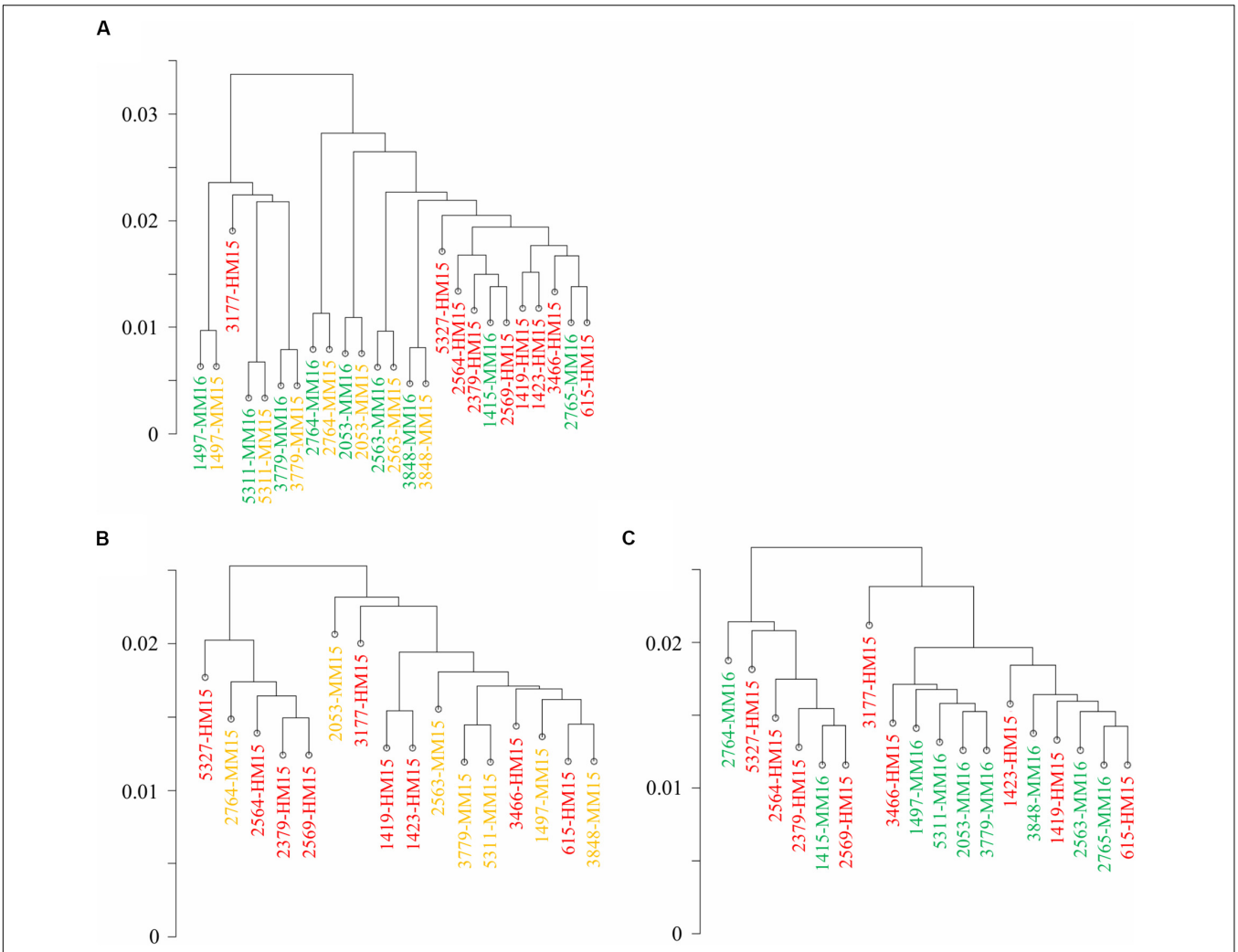



**FIGURE 1 |** Diet and age do not induce genome-wide modifications of the sperm methylome. Correlation clustering was run on the methylation percentages calculated at CpGs covered more than 10 reads in at least four samples per group. Samples belonging to the three groups are shown in different colors (HM15, red; MM15, yellow; and MM16, green). **(A)** Correlation clustering ran on the whole dataset. Unpaired samples, mainly from the HM group, cluster apart (right part). **(B,C)** Correlation clustering run on unpaired samples from HM15 and MM15 groups **(B)** and HM15 and MM16 groups **(C)**. Taken together, the results demonstrate that the inter-bull variability vs. intra-bull similarity appear to have a greater effect on global bull sperm methylome than any latent effect of dietary regimen *per se*.

groups using RRBS (**Supplementary Table 5**). Sequencing of the RRBS libraries generated an average of 37 (±6) million reads per sample (**Table 1**). The average quality score was 38.2 (±0.20), which represents more than 92.4% of bases with a high quality score (Q30 score). The percentage of unique mapping efficiency, although low (on average, 35.3 (±2.7)% uniquely mapped reads), is consistent with what has been previously described in bovine and other ruminant species (Doherty and Couldrey, 2014; Doherty et al., 2016; Perrier et al., 2018), and is due to the significant number of repetitive elements in the bovine genome. Bisulfite conversion rate, monitored using the conversion rate of the unmethylated cytosine added *in vitro* during the end-repair step of library preparation, was on average at 99.4 (±0.7)%. There was no statistically significant difference for any of the above parameters when comparing the different groups of bulls. This eliminated the possibility of technical bias during RRBS library preparation or sequencing that could have affected subsequent results and indicated that the data were of good quality. For the rest of the analysis, we focused on the 58.1 (±4.4)% CpGs that were covered by at least 10 uniquely mapped reads, which we named CpGs10. There was no statistically significant differences between the HM15, MM15, and MM16 groups for the percentages of hypermethylated (DNA methylation >80%), intermediate (DNA methylation in [20–80%]) and hypomethylated (DNA methylation <20%) CpGs10, indicating that neither diet or age difference between 15 and 16 months induce global DNA methylation changes.

## Inter-Bull Variability Unrelated to Age or Diet Shapes DNA Methylation Profiles

Hierarchical clustering revealed two distinct clusters: one essentially composed of paired samples collected at 15 and

**TABLE 1 |** Library characterization, mapping efficiency on the bovine genome (UMD3.1), coverage and average methylation in RRBS libraries.

| | HM15 ($n$ = 9) | MM15 ($n$ = 7) | MM16 ($n$ = 9) |
|---|---|---|---|
| Number of read pairs (million) | 35.1 ± 6.1 | 36.5 ± 7.0 | 39.4 ± 7.5 |
| Average quality score (Phred score) | 38.3 ± 0.2 | 38.2 ± 0.3 | 38.2 ± 0.1 |
| Uniquely mapped reads (%) | 35.5 ± 3.1 | 35.3 ± 2.4 | 35.0 ± 2.9 |
| Ambiguous reads (%) | 52.6 ± 2.8 | 52.5 ± 3.0 | 52.7 ± 2.8 |
| Unmapped reads (%) | 11.9 ± 1.0 | 12.2 ± 0.9 | 12.2 ± 0.8 |
| Bisulfite conversion rate (%) | 99.3 ± 0.7 | 99.4 ± 0.7 | 99.5 ± 0.6 |
| Number of covered CpGs (million) | 3.05 ± 0.1 | 3.08 ± 0.2 | 3.08 ± 0.1 |
| Average coverage per CpG | 24.8 ± 4.6 | 25.1 ± 4.4 | 26.8 ± 4.0 |
| Percentage of CpGs10 | 56.7 ± 5.0 | 57.8 ± 4.7 | 59.8 ± 3.3 |
| Average DNA methylation at CpGs10 (%) | 50.3 ± 1.0 | 50.1 ± 0.9 | 50.5 ± 0.6 |
| Percentage of CpGs10 hypermethylated (DNA methylation > 80%) | 47.1 ± 1.4 | 46.9 ± 0.7 | 47.5 ± 0.6 |
| Percentage of intermediate CpGs10 (DNA methylation in [20%; 80%]) | 7.1 ± 0.5 | 7.3 ± 0.3 | 7.1 ± 0.4 |
| Percentage of CpGs10 hypomethylated (DNA methylation < 20%) | 45.8 ± 1.1 | 45.8 ± 0.8 | 45.5 ± 0.5 |

*Values are mean ± standard error of the means. CpGs10: CpGs covered by at least 10 uniquely mapped reads. Hypermethylated, intermediate and hypomethylated CpGs10 indicate CpGs10 with average methylation percentage >80%, [20%; 80%], and <20%, respectively.*

16 months from 3 bulls and another one comprising the other samples including almost all HM15 samples (**Figure 1A**). However, the clustering of HM samples was not due to the diet. Indeed, six of nine samples from the MM groups clustered together with the HM samples, and the paired MM15/MM16 samples from the same bull all grouped together. Moreover, correlation between independent HM15 samples was lower than that between MM15/MM16 pairs, as reflected by the greater length of the branches separating them on the correlation clustering. To examine the effect of diet and/or advanced puberty more closely, we carried out a new analysis focused on unpaired samples from HM15 and MM15 groups (identical chronological age, **Figure 1B**), and HM15 and MM16 groups (closer physiological age; **Figure 1C**). By suppressing the intra-individual effect, the clustering according to the HM diet disappeared. In conclusion, the hierarchical clustering conducted on all CpGs10 did not allow discrimination of samples according to pre-pubertal nutrition or age, but rather emphasized the similarity of semen samples collected at two close stages from the same individual.

## Stability of Sperm Methylome Between 15 Months and 16 Months of Age

Because the above analyses suggested an important inter-individual variability that could bias the detection of DMCs due to the extreme behavior of some individuals, we next conducted differential analyses using an algorithm described to deal with intra-group inter-individual variability (Feng et al., 2014). To disentangle any confounding effects of age and diet/advanced puberty in the comparison involving HM15 and MM16 samples, we first investigated the impact of the one-month age difference on paired samples of the MM15 and MM16 groups. This resulted in the identification of one unique DMC located in an intron of a gene, *LEMD2* (**Supplementary Table 6**). This demonstrated that DNA methylation profiles are conserved in semen samples collected at 15 and 16 months of age, a result consistent with the absence of difference reported for semen from sexually mature bulls collected at 12 and 16 months of age (Lambert et al., 2018).

## Modest Effect of Diet Associated With Advanced Puberty on Sperm Methylome

We next focused on the latent effect of nutritional regimen employed during calfhood associated with advanced puberty on DNA methylation profiles. Diet-related DMCs and DMRs were identified by pairwise comparisons between HM15 vs. MM15 (identical chronological age), and between HM15 vs. MM16 (similar physiological age; **Figure 2A**). In the HM15 vs. MM15 comparison, there were 491 DMCs and 20 DMRs identified, from which 67.4 and 95.0%, respectively, were found hypermethylated for the HM15 group. Similar results were obtained with the HM15 vs. MM16 comparison. A total of 164 DMCs and 4 DMRs were identified, with 61.6% of the DMCs, and all of the DMRs, being hypermethylated in the HM15 group. Therefore, even though the number of DMCs and DMRs between the HM15 group and the two MM groups was within the same order of magnitude, we identified more than twice as many DMCs in HM15 vs. MM15 compared to HM15 vs. MM16. Nevertheless, these DMCs exhibit the same behavior, i.e., most being hypermethylated in HM15 (particularly the DMRs).

In order to understand why the overlap between HM15 vs. MM15 and HM15 vs. MM16 comparisons was limited in spite of the absence of DNA methylation differences between 15 and 16 months, we generated volcano plots for 580 unique DMCs representing the totality of the DMCs identified between the two comparisons. Although the raw $p$-values were higher and the differences in DNA methylation lower for the HM15 vs. MM16 comparison, the 580 unique DMCs exhibited a similar behavior in both comparisons, with differences above 10% for most of them and a distribution slightly shifted towards positive values indicating more DNA methylation in the HM15 group (**Figure 2B**). We therefore concluded that differences in DNA methylation probably exist between the HM15 and MM16 but do not reach significance thresholds.

To characterize whether specific genomic features are enriched in DMCs, we carried out the annotation of DMCs found for each of the comparisons (**Figure 3A**). Essentially, DMCs from HM15 vs. MM15 and HM15 vs. MM16 were distributed similarly. There were more DMCs in intronic and intergenic regions, along with a depletion in exons, promoter-TSS and UTRs of genes, compared to the background. There was also a depletion in CGIs, together with an enrichment in areas less dense in CpGs such as CpG shores, shelves (for HM15 vs. MM15), and open sea. These results are consistent with the fact that only 17.5% of HM15 vs. MM15 and 9.2% of the HM15 vs. MM16 DMCs participate in the formation of DMRs, meaning that the majority of DMCs are dispersed over the genome. Overall, DMCs tended to be more enriched in repetitive elements compared to the background

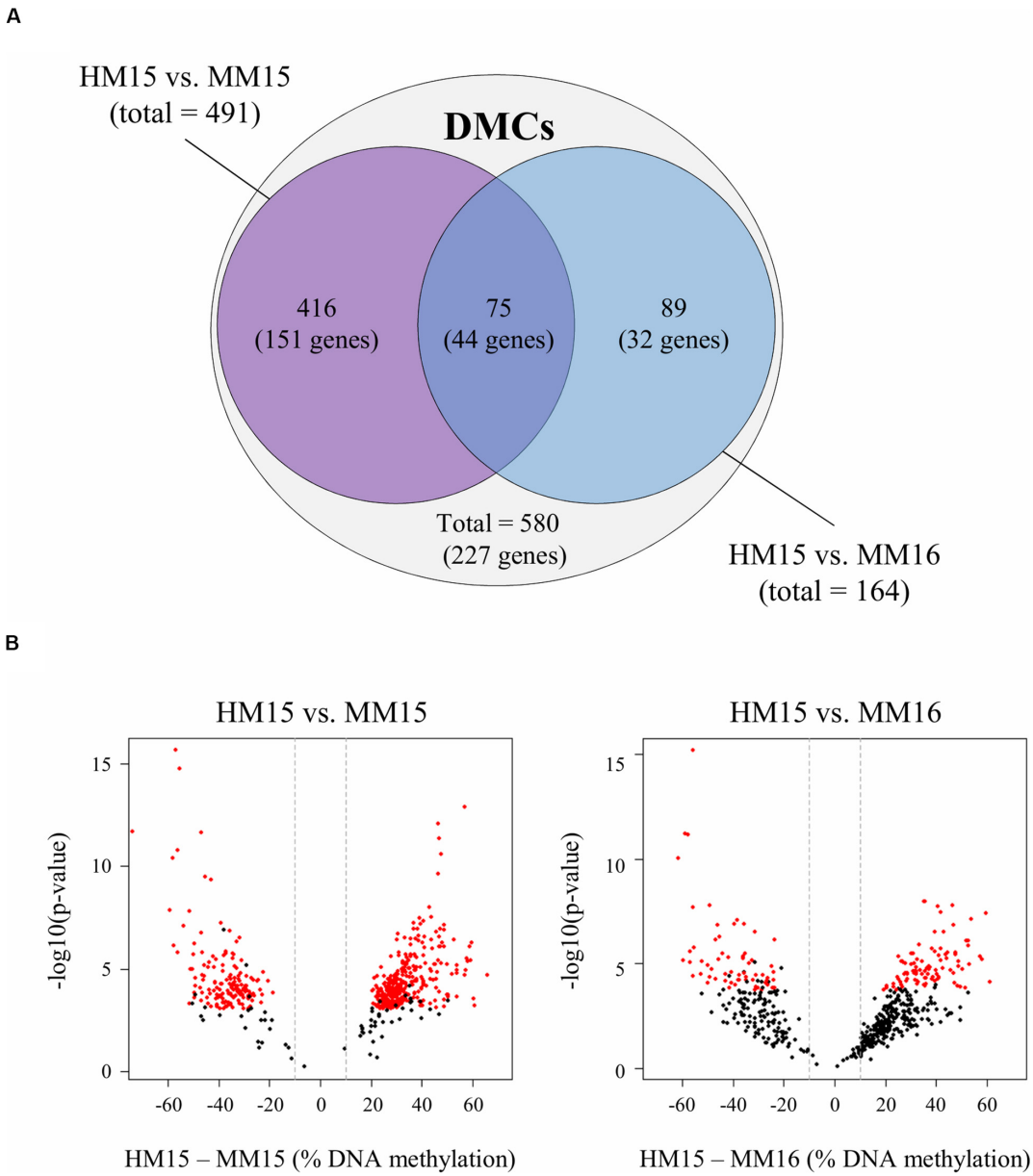



**FIGURE 2 |** Diet-related differentially methylated CpGs (DMCs) identified in sperm from pairwise comparisons between diet groups. **(A)** Venn diagram showing the 491 and 164 DMCs identified between HM15 vs. MM15 and HM15 vs. MM16 groups, respectively. A total of 580 unique DMCs were obtained. Among those DMCs, 75 (12.9%) are in the middle intersection, representing those that are common between both comparisons. DMCs were associated with 227 unique genes, 44 being common between both comparisons. **(B)** Volcano plots showing the variations of raw *p*-values (*y*-axis, -log10 scale) according to the differences in DNA methylation (*x*-axis, HM – MM differences) for the 580 unique DMCs, in the HM15 vs. MM15 (left) and the HM15 vs. MM16 (right) comparisons. The DMCs that passed the significance thresholds (adjusted *p*-value $< 0.1$ and difference in methylation $\geq 10\%$) are indicated in red for each comparison. Most of the 580 unique DMCs, including those that did not reach significance in the HM15 vs. MM16 comparison, showed a similar behavior in both comparison, with a difference in DNA methylation above 10% (indicated by the vertical dashed lines) and a distribution shifted towards positive values indicating a higher methylation in the HM group.

(78.6 and 73.8% of DMCs not associated with repeats for HM15 vs. MM15 and HM15 vs. MM16, respectively, compared to 85.5% for the background), such as LINEs, SINEs and LTRs. On the contrary, DMCs were found depleted in satellites and simple repeats. The lists of DMCs/DMRs, together with their annotation regarding gene features, repetitive elements and CGIs, are available in **Supplementary Table 6**.

We then investigated whether specific Gene Ontology (GO) terms were enriched in genes displaying a different representation in DMCs and background. To this end, genes associated with DMCs were subjected to DAVID analysis. While HM15 vs. MM16 exhibited no specific enrichment, for HM15 vs. MM15 an enrichment just below statistical significance was found for a cluster of terms related to ATP binding (EASE score of 1.2; data

**A**

| | Background | HM15 vs. MM15 | HM15 vs. MM16 |
|---|---|---|---|
| **Number of CpGs** | 1,653,793 | 491 | 164 |
| **Gene annotation (%)** | | | |
| Intron | 26.1 | 36.0 ↑ | 36.0 ↑ |
| Exon | 14.0 | 7.7 ↓ | 11.0 ↓ |
| Promoter | 9.0 | 1.8 ↓ | 1.8 ↓ |
| TSS | 5.1 | 1.0 ↓ | 1.2 ↓ |
| 5'UTR | 3.5 | 1.4 ↓ | 1.2 ↓ |
| 3'UTR | 0.9 | 0.6 = | 0.0 ↓ |
| TTS | 0.7 | 0.6 = | 0.0 ↓ |
| Upstream gene regions | 5.3 | 3.9 ↓ | 2.4 ↓ |
| Downstream gene regions | 6.3 | 5.5 = | 3.7 ↓ |
| Intergenic | 29.2 | 41.3 ↑ | 42.7 ↑ |
| **CpG density annotation (%)** | | | |
| CpG islands | 45.0 | 10.2 ↓ | 12.8 ↓ |
| CpG shores | 17.8 | 17.7 = | 15.9 = |
| CpG shelves | 6.5 | 12.0 ↑ | 7.9 = |
| Open Sea | 30.7 | 60.1 ↑ | 63.4 ↑ |
| **Repeats annotation (%)** | | | |
| DNA | 0.4 | 1.0 ↑ | 1.8 ↑ |
| LINE | 2.4 | 5.7 ↑ | 7.3 ↑ |
| Low complexity | 0.5 | 0.6 = | 0.6 = |
| LTR | 1.4 | 5.9 ↑ | 5.5 ↑ |
| Satellite | 4.0 | 0.0 ↓ | 0.6 ↓ |
| Simple repeat | 2.3 | 1.2 ↓ | 1.2 ↓ |
| SINE | 3.5 | 6.9 ↑ | 9.1 ↑ |
| Not in repeat | 85.5 | 78.6 ↓ | 73.8 ↓ |

**B**

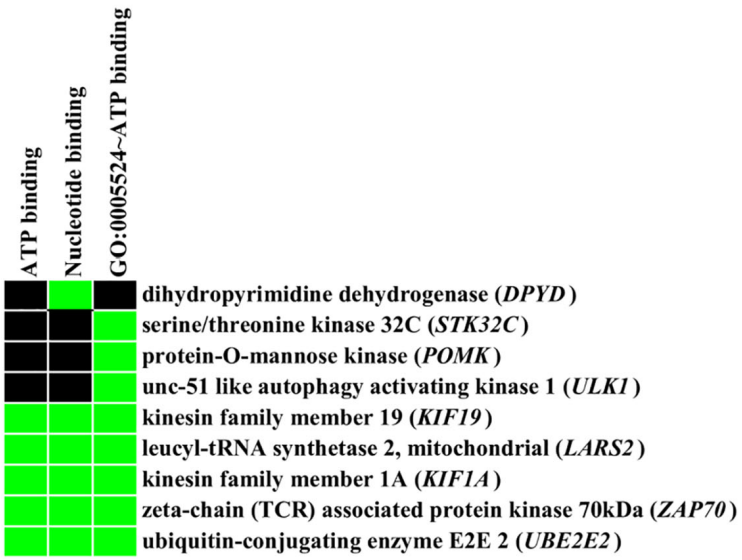



**FIGURE 3 |** Annotation of the diet-related differentially methylated CpGs (DMCs). **(A)** Annotation of DMCs relative to gene features, CpG density and repetitive elements of the genome. Upstream gene regions (resp. downstream gene regions) represent DMCs located 10 kb upstream of the transcription start site (resp. 10 kb downstream of the transcription termination site). Red and green arrows represent a more than 25% decrease or increase in the relative abundance of genomic features compared to the background, respectively. An equal sign represents that the abundance of the element is less than 25% different to the background. **(B)** Results of enrichment analysis using the DAVID functional annotation tool. The analysis has been performed using the genes identified in the intersection between HM15 vs. MM15 and HM15 vs. MM16 comparisons (**Figure 2A**, 44 genes). The list of all genes covered by RRBS was used as the background (18,020 genes). The cluster corresponding to ATP binding molecular function showed an EASE enrichment score of 1.36, considering that scores above 1.3 are significant (Huang et al., 2009). Terms of gene ontology or Uniprot keywords enriched among the DMCs are indicated, as are the genes present in each category. The green color on the heatmap represents a correspondence between a gene and a term.

not shown). Interestingly, using the intersection between HM15 vs. MM15 and HM15 vs. MM16 comparisons (**Figure 2A**), which accounted for only 44 unique genes, this enrichment became significant (EASE score of 1.36; **Figure 3B**).

We also performed an extensive review of the literature for all genes differentially methylated between the HM15 and MM15 samples with Biomart annotation available ("Gene name" column in **Supplementary Table 6**; 174 of 195 genes). Genes relevant to spermatogenesis, sperm function, sexual precocity, gonadal development, and Sertoli cell function and proliferation represented a significant part of all differentially methylated genes (61 over 174) and are listed, together with the corresponding references, in **Supplementary Table 9**. Strikingly, among these 61 genes, only 6 still retained a methylation difference above significance thresholds in the HM15 vs. MM16 comparison. This is significantly lower than expected by chance ($p = 0.02$; Chi-squared test). Together with the DAVID analysis, these results suggest that the genes differentially methylated in the two HM vs. MM comparisons are not involved in the same biological functions. Genes differentially methylated when HM and MM bulls were compared at 15 months of age are involved in functions that may reflect the different timing of puberty onset in the two diet groups. Considering the genes still differentially methylated when the MM bulls reached a similar level of sexual maturity, these puberty-related functions became less represented and an enrichment in GO terms related to ATP binding could be observed.

### RRBS Data Validation by Pyrosequencing

To maximize the number of CpG sites to validate by pyrosequencing, we chose to focus on DMRs (as they each contain multiple DMCs). Among the 20 DMRs identified between HM15 and MM15 groups, eight were associated with six genes (the gene *BCL2* exhibiting three DMRs). Four of these six genes are characterized on the bovine genome and are already described in the literature, and therefore were selected for validation by pyrosequencing: ATPase Phospholipid Transporting 10A (*ATP10A*, related to ATP binding GO term), B-cell CLL/lymphoma 2 (*BCL2*), Neurogenin 2 (*NEUROG2*), and SLIT-ROBO Rho GTPase activating protein 3 (*SRGAP3*). For each sample belonging to the HM15, MM15, and MM16 groups, correlations were calculated between the mean DNA methylation of the DMCs composing DMRs on RRBS, to its pyrosequencing counterparts (**Figure 4A**). We found a significant correlation between RRBS and pyrosequencing data in all of the analyzed regions ($0.80 \leq \text{rho} \leq 0.97$; $p < 0.0001$; Spearman's rank correlation test). This demonstrated that there was a very good agreement between RRBS and pyrosequencing data and validated the data from a technical perspective.

The DNA methylation status of individual DMCs and CpGs included in the DMRs was measured by pyrosequencing (not only on samples from the HM15, MM15 and MM16 groups that were analyzed by RRBS, but also on samples from the HM16 group; **Supplementary Table 5**). Significant DNA methylation differences between HM and MM groups were identified for genes *ATP10A*, *BCL2*, and *SRGAP3*, for all of the assessed DMCs, validating the RRBS data ($p < 0.05$, permutation test; **Figure 4B**), while the differences did not reach significance for *NEUROG2*. For all four genes, pyrosequencing analyses confirmed the lower DNA methylation level in the MM groups at each DMR analyzed and the absence of significant change between 15 and 16 months. For the DMRs included in *BCL2* and *ATP10A*, the HM15 and HM16 groups showed a rather homogenous behavior, with similar median DNA methylation percentages and dispersions (indicated by the size of the boxplot). In contrast, the median DNA methylation percentage was slightly increased in the MM16 group compared with the MM15 group, both MM groups exhibiting more dispersion than the HM groups. This could indicate an evolution of the DNA methylation profile at these loci between 15 and 16 months, in some, but not all, individuals of the MM groups. Consistent with the detection by RRBS of only one DMC in the MM15 vs. MM16 comparison, this tendency towards an increased DNA methylation in MM16 group did not reach statistical significance.

## DISCUSSION

This study demonstrates how early life plane of nutrition associated with advancement in the age of puberty can induce changes in the post-pubertal sperm DNA methylation profile.

A rise in luteinizing hormone (LH), typically occurring between 10 and 20 weeks of age, is an important factor in determining the age at onset of puberty in bulls (Rawlings and Evans, 1995). This initial rise in LH secretion is necessary for differentiation and maturation of testicular Leydig cells, leading to the secretion of testosterone. Secretion of follicle stimulating hormone (FSH) is high post-natally and plays a role in Sertoli cell differentiation, reaching a nadir at 25 weeks of age (Brito, 2014). These mechanisms are essential for the onset of spermatogenesis with sperm usually first observed at 32 weeks of age (Amann, 1983). Therefore, augmentations to nutrition during the first months of life have the potential to affect the future functionality of cells that differentiate during this period. In particular, the total number of Sertoli cells is essentially determined by these events, which has direct consequences on the efficiency of spermatogenesis given that each Sertoli cell can support a definite number of germ cells. In a previous study using the same animal model, it was shown that an enhanced plane of nutrition during the first 6 months of life hastened onset of puberty and sexual maturation by approximately one month in the HM group (Byrne et al., 2018a). The hastened onset of puberty was accompanied by an increase in scrotal circumference and in testosterone concentration (Byrne et al., 2018b), indicating that HM bull testes matured earlier. In addition, at 4 months of age, calves subjected to a high plane of nutrition had greater seminiferous tubule diameter, more mature spermatogenic cells and more Sertoli cells, compared to calves on a low plane of nutrition (English et al., 2018). In agreement with the increased testosterone concentration observed at a later age, calves in the high plane group also exhibited a tendency for greater peripheral LH concentrations. They also exhibited 1,346 differentially expressed genes in the testicular parenchyma, most of which were upregulated and involved in the production of

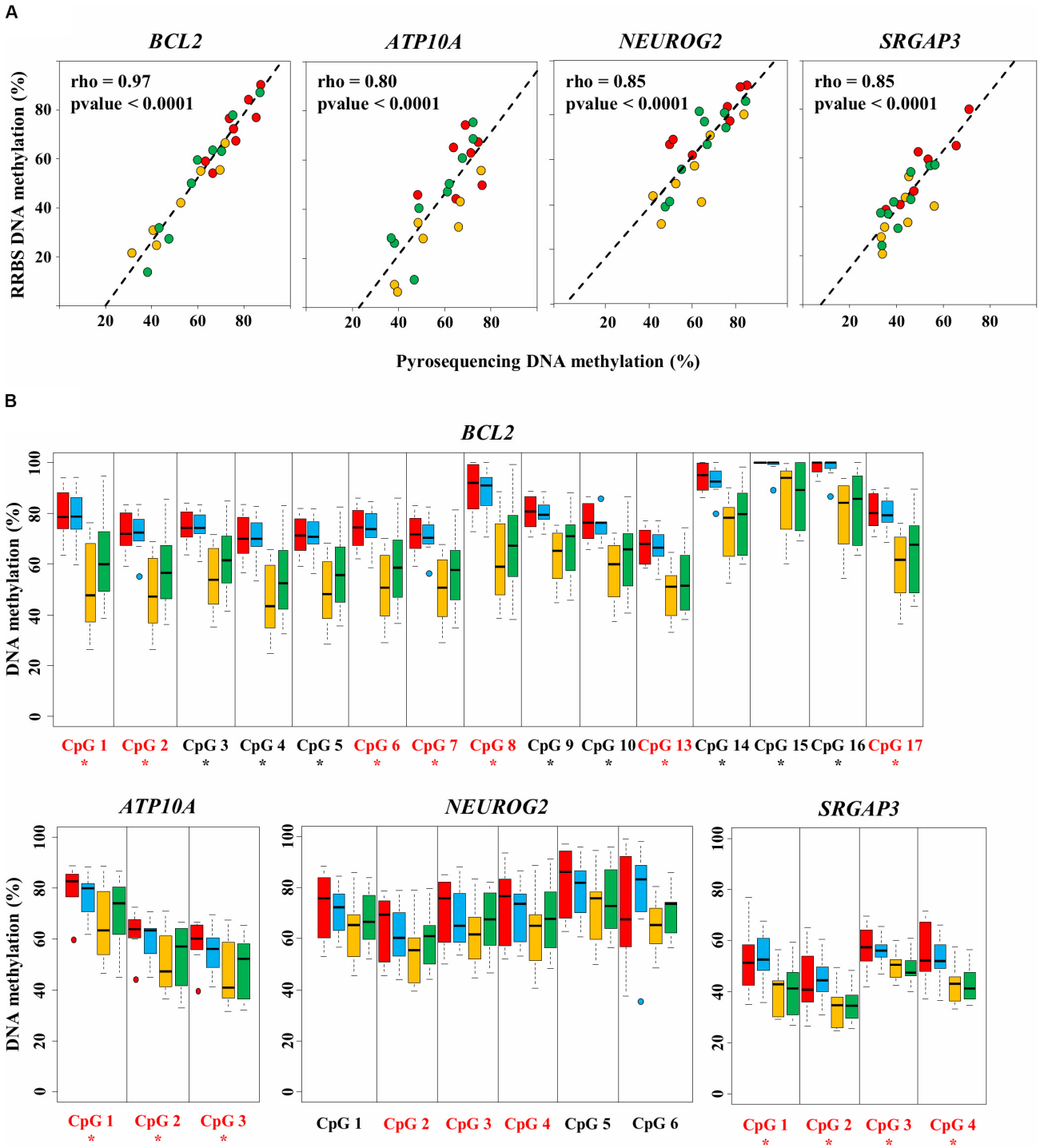



**FIGURE 4 |** Validation of four diet-related differentially methylated regions (DMRs) by bisulfite-pyrosequencing. **(A)** The average methylation rate measured by RRBS is calculated for the differentially methylated CpGs (DMCs) included in the DMR and plotted against the average methylation rate measured by pyrosequencing. Each dot represents one sample from the HM15 ($n$ = 7, in red), MM15 ($n$ = 7, in yellow), and MM16 ($n$ = 9, in green) groups. The least squares lines of best fit and Spearman's rank correlation coefficients rho are indicated. All correlations were highly significant (Spearman's rank correlation test; $p < 0.0001$). **(B)** Methylation percentages of individual CpGs assayed by pyrosequencing in HM15 ($n$ = 7, in red), HM16 ($n$ = 7, in blue), MM15 ($n$ = 7, in yellow), and MM16 ($n$ = 9, in green) groups. For each box, the middle line indicates the median and the edges the 25th/75th percentiles. CpGs are numbered according to their 5′–3′ position along the genome. CpGs found as DMCs by the RRBS analysis are shown in red. Asterisks indicate CpGs at which the methylation percentage measured by pyrosequencing is significantly different between HM and MM groups ($p < 0.05$, permutation test corrected for the stratification according to the age).

androgen or cholesterol biosynthesis. However, once all animals were sexually mature no subsequent modifications in either semen volume or quality were evident when compared to the MM group (Byrne et al., 2018a). These phenomena demonstrate that the enhanced plane of nutrition hastened sexual maturation and the onset of puberty without resulting in obvious latent effects on traditional measures of sperm quality. In contrast, in the present study we observed that HM and MM bulls can be distinguished based on their sperm DNA methylation profile after puberty.

The first observation is that more DMCs, a higher proportion of which were hypermethylated in HM bulls, were identified between the HM15 vs. MM15 groups than between the HM15 vs. MM16 groups, which could be related to the advanced maturity of HM bulls rather than to the diet early in life. Indeed, the MM15 and MM16 samples originated from animals on the same diet; therefore, if the DNA methylation changes solely reflected the direct effect of diet, a similar number of DMCs, with a similar proportion of hypermethylated DMCs would have been expected in the two comparisons between HM and MM bulls. Furthermore, the differential methylation observed between HM15 and MM15 but not between HM15 and MM16 samples targets genes relevant to puberty and may be related to the more advanced maturity of the HM bulls, which is counterbalanced when MM bulls are used one month later. In contrast, the differential methylation still observable in the HM15 vs. MM16 comparison targets other genes and may reflect a long-term memory of the metabolic and physiological consequences induced by HM diet and advanced puberty, that may persist at later stages. The hypothesis that advanced puberty is the main determinant of the DNA methylation patterns we report herein is further supported by the gain of DNA methylation observed in the sperm of sexually mature bulls at 16 months of age compared to when they were 10 months old (Lambert et al., 2018). The quasi absence of DMCs when MM animals were compared at 15 and again at 16 months of age is also consistent with the relative stability of the sperm methylome in sexually mature bulls reported by Lambert et al. (2018). Importantly, it indicates that the lower number of DMCs and proportion of hypermethylated DMCs in the HM15 vs. MM16 comparison (relative to the HM15 vs. MM15 comparison) can be attributed to the difference in sexual maturity rather than in age. Indeed, the MM bulls were already sexually mature at 15 months of age and interval to the second time point (1 month later) may have been too short in duration to expose significant age-related differences, should they exist. Why then, if MM15 and MM16 samples are similar in terms of DNA methylation pattern, did the two comparisons involving HM and MM bulls give rise to different amounts of DMCs, with a limited extent of overlap between the two sets of DMCs? A possible explanation may be related to the experimental design. Only paired samples were considered for the comparison between 15 and 16 months of age, therefore excluding any influence of genetic factors on the compared DNA methylation profiles. In contrast, for the HM vs. MM comparisons, independent samples were used, with no complete overlap between the MM15 and MM16 groups in terms of included bulls due the unavailability of the biological material. Given the limited number of individuals included in this study, we can therefore not exclude that DNA methylation differences at some DMCs rely on genetic polymorphisms, as has been described in humans (Lappalainen and Greally, 2017), and in agreement with the significant inter-bull variability highlighted by the hierarchical clustering run on our RRBS data.

Although the algorithm used to detect differential DNA methylation is highly stringent compared with others (Feng et al., 2014), the number of DMCs identified between HM and MM groups could be considered as modest, with a total of 580 DMCs relative to the 1,653,793 CpGs covered by the RRBS method. However, the genes targeted by differential methylation have compelling relationships with testis development and puberty. Based on these genes, four potential explanations for the advanced sexual maturity of HM bulls induced by enhanced nutrition are detailed below. Firstly, four differentially methylated genes are found in regions with genome-wide association study (GWAS) signals associated with sexual precocity in Nellore cattle (Irano et al., 2016). *ATP10A*, related to the ATP binding GO term that was enriched in our study, is located in a region associated with early pregnancy. Even more interestingly, *SEC23B*, *SRGAP3*, and *LHFPL4* are located in regions associated with scrotal circumference, a trait specifically modified in HM bulls. Of note, *ATP10A* and *SRGAP3* account for two of the 20 DMRs we identified between HM15 and MM15 samples and were analyzed more precisely and validated by pyrosequencing. *ATP10A* is known to be imprinted in humans, but this specificity has not been described in cattle. Interestingly, a lack of *ATP10A* activity in adulthood is related to obesity in humans (Gillessen-Kaesbach et al., 1999) and *SRGAP3* expression is known to be influenced by its DNA methylation status (Gao et al., 2016). Together with our results, these reports indicate that *ATP10A* and *SRGAP3,* as putative candidate genes for sexual precocity, are regulated not only by genetic factors but also by environmental and epigenetic factors. The second compelling piece of evidence for the involvement of the differentially methylated genes in sexual maturity of HM bulls is provided by a study using Yiling goats, a native Chinese breed exhibiting precocious puberty, as a model to investigate the changes in the testis transcriptome that parallel the post-natal development of testis (Bo et al., 2020). In that study, 120 days of age was identified as the transition point at which testis weight dramatically increases and spermatogenesis becomes functional in Yiling goats; two genes targeted by differential methylation in our study, *ALDOB* and *PIGR*, are listed as "hub genes" whose expression is modified during this transition. Although not listed as "hub genes" by Bo et al. (2020), we identified several genes involved in spermatid differentiation or highly expressed post-meiotically, such as *RARB*, *ADCY8*, and *OSBP2* (relevant references are provided in **Supplementary Table 9**). We also identified many differentially methylated genes involved in cytoskeleton remodeling, cilium growth and cell junction, such as *ACTN1*, *GSN*, *MTMR7*, *PACRG*, *TUBB2B*, and *ARC*. Interestingly, the genes differentially expressed during the transition to functional spermatogenesis in Yiling goats are involved in similar functions, suggesting that the methylation changes between HM and MM bulls are the consequence of a different dynamics in the process of testis maturation around puberty. The third potential explanation for the hastened puberty

of HM bulls involves the hypothalamic-pituitary-gonadal axis, which is crucial for puberty and reproductive function. Indeed, our study points to genes directly acting at different levels of this axis, such as *PREP*, *WWOX*, and *CALB2*. *PREP* encodes a prolyl endopeptidase that metabolizes gonadotropin-releasing hormone (GnRH) in the hypothalamus and pituitary gland and could contribute to pulsatile GnRH secretion that precedes the onset of puberty (Yamanaka et al., 1999). The *PREP* gene product is detected in both somatic cells and germ cells of the testis, as well as in sperm; *PREP*-deficient mice exhibit smaller testes, abnormal spermatogenesis and decreased sperm motility (Dotolo et al., 2016). *WWOX*-deficient mice die before puberty, and exhibit reduced expression of *LH* and *FSH* genes in the pituitary gland, abnormal testis development and alteration in the number and size of Leydig cells (Aqeilan et al., 2009). Overexpression of *CALB2* in mouse primary Leydig cells upregulates testosterone production in response to LH signaling (Xu et al., 2018). The differential methylation of these genes may thus reflect a higher degree of stimulation of the hypothalamic–pituitary–gonadal axis in the HM bulls. The fourth potential explanation for hastened testis development in response to enhanced nutrition in HM bulls is related to the balance between proliferation, survival and apoptosis in Sertoli and germ cells, which is highly sensitive to the nutritional status. Indeed, *BCL2*, a well-known antiapoptotic gene that enhances anti-oxidant enzyme activities (Hockenbery et al., 1993), was identified as differentially methylated in our study, as well as two other genes for which a role in the regulation of apoptosis in germ cells has been reported, *CAST* and *NFIX* (references in **Supplementary Table 9**). Differential methylation affects *BCL2* at three regions, among which one has been analyzed in more detail by pyrosequencing. In Sertoli cells of immature animals, *BCL2* contributes to the control of cell proliferation through estrogen signaling (Lucas et al., 2011). Estrogens are synthesized from androgens by the aromatase encoded by *CYP19* that is stimulated by FSH, therefore bridging the hypothalamic-pituitary-gonadal axis with the control of apoptosis in Sertoli cells. *BCL2* is also highly expressed in Sertoli cells of sexually mature animals, which may be essential to promote survival of these cells since they are essentially quiescent after puberty and cannot be replaced (Aslani et al., 2017). Interestingly, in sexually mature sheep exposed to undernutrition, spermatogenesis reversibly regresses due to the alteration of Sertoli cell function that in turn induces apoptosis in germ cells (Guan and Martin, 2017). Likewise, in the sperm of mice fed a low protein diet, genes involved in apoptosis were found hypomethylated, echoing the hypermethylation we report here in the HM groups (Watkins et al., 2018). These reports highlight the link between metabolic status and apoptosis in Sertoli and germ cells. As well as the control of apoptosis, autophagy may also contribute to the larger number of Sertoli cells at a younger age and to the hastened onset of puberty of HM bulls, as suggested by the differential methylation status we observed in two key genes involved in this pathway, *ULK1* and *TFEB*. Autophagy is a stress response pathway that promotes cell survival by providing energy and nutrients through the self-digestion of cellular constituents by lysosomes. *ULK1* encodes a protein kinase that triggers the entry of the cell into the autophagy pathway upon starvation and therefore bridges together energy metabolism with autophagy. Pre-pubertal energy restriction in sheep induces testis autophagy and apoptosis by respectively increasing *ULK1* gene and protein expression and modifying the ratio between *BCL2* and its pro-apoptotic antagonist *BAX* (Pang et al., 2018). *TFEB* encodes a transcription factor that activates the transcription of many genes involved in lysosome biogenesis and autophagy and its expression is tightly regulated during spermatogenesis. During the differentiation of spermatogonia, the activation of autophagy by TFEB facilitates migration towards the lumen of seminiferous tubules through the recycling of adhesion molecules, receptor and matrix proteins (Liu et al., 2018). In contrast, the induction of the meiosis gatekeeper *STRA8* at the onset of meiosis is associated with a repression of autophagy and with *ULK1* and *TFEB* downregulation (Ferder et al., 2019). In Sertoli cells, *TFEB* mediates the initiation of autophagy upon exposure to toxins such as ethanol, in order to promote cell survival and sustain spermatogenesis (Horibe et al., 2017). Interestingly, *ULK1* directly relates autophagy with the mTOR pathway, which regulates many metabolic processes and essential cell functions in response to the nutrient and energy status of the cell (Kim et al., 2011). *RPTOR*, an important player in the mTOR pathway targeted by differential methylation between HM and MM bulls, is necessary for the maintenance and self-renewing population of spermatogonial stem cells, and *RPTOR*-deficient mice are infertile (Serra et al., 2019).

A question to be addressed is the potential impact of these DNA methylation modifications on the phenotype in subsequent generations. Changes in both DNA methylation patterns and expression of genes involved in energy metabolism have been recently reported in embryos generated using the sperm from peripubertal bulls (10 and 12 months of age), relative to those obtained with sperm collected at 16 months of age from the same bulls (Wu et al., 2020). This raises the possibility that part of the methylation changes in HM bulls, which reached sexual maturity earlier than MM bulls, may influence embryo metabolism, which may also have important consequences at later stages of development. For an alteration of DNA methylation pattern to have an effect on gene expression during embryonic development or on offspring phenotype, the alteration needs to escape or to interfere with the reprogramming process occurring after fertilization. Imprinted genes, but also some endogenous retroviruses, escape reprogramming during early embryo development (Seah and Messerschmidt, 2018). In the mouse, a subset of LINE and LTR elements, as well as intergenic regions, are highly methylated in sperm cells and resist genome-wide DNA methylation erasure in the embryo (Wang et al., 2014). It is interesting to note the DMCs we identified were enriched in these genome features, raising the possibility that the hypermethylation observed in HM sperm samples is transmitted to the embryo. Based on these reports, further analyses on DNA methylation patterns and gene expression on embryos from bulls that had undergone hastened puberty onset, and of the resultant offspring, is warranted.

In conclusion, the data presented here demonstrate that a high plane of nutrition during the first 6 months of life in bull calves associated with an advancement in the onset of puberty

induces modest latent modifications of the sperm methylome after puberty. Evidence suggest that these alterations of the sperm methylome reflect advanced puberty onset of the calves rather than plane of nutrition *per se*, with the differences in DNA methylation patterns being reduced when bulls on a high plane of nutrition were compared to older animals on a moderate plane of nutrition. These findings should be replicated on an independent and larger cohort of bulls. The modification of sperm DNA methylation does not appear to have any significant effect on sperm functional parameters routinely assessed pre- and post-thawing in artificial insemination centers; further work needs to be performed to assess any latent effects on fertilizing ability, embryo development, as well as on offspring health.

## DATA AVAILABILITY STATEMENT

The datasets generated for this study can be found in the European Nucleotide Archive (ENA) at EMBL-EBI under accession number PRJEB35837 (https://www.ebi.ac.uk/ena/data/view/PRJEB35837).

## ETHICS STATEMENT

All protocols were in accordance with the Cruelty to Animals Act (Ireland 1876, as amended by European Communities Regulations 2002 and 2005) and the European Community Directive 86/609/EC. All animal procedures performed were conducted under experimental license from the Irish Department of Health and Children.

## AUTHOR CONTRIBUTIONS

J-PP participated in the pyrosequencing experiment, RRBS and pyrosequencing data analysis, and drafted the manuscript. DK, SF, and PL conceived the study and performed critical revision of the manuscript. AC-T performed the RRBS and pyrosequencing experiments. CB participated in the conception of the study, collected the samples, and participated in drafting the manuscript. ES performed experiments and participated in the conception of the study and in the critical reading of the manuscript. LJ and AA-F performed the bioinformatics and statistical analyses of RRBS data. LS and HJ obtained funding and participated in the conception of the study and edited the manuscript. HK coordinated the study and carried out the data analysis and editing of the manuscript. All authors have read and approved the final manuscript.

## FUNDING

This research was made possible by funding from the Irish Department of Agriculture, Food and the Marine under the Research Stimulus Fund (Project 11/S/116), from Science Foundation Ireland under the Investigators Program (Dublin, Ireland; Project 16/IA/4474), and from the French National Research Agency (grant ANR-13-LAB3-0008-01 'SeQuaMol').

## ACKNOWLEDGMENTS

We are grateful to the Genotoul bioinformatics platform Toulouse Midi-Pyrenees (Bioinfo Genotoul) for providing computing and storage resources.

## SUPPLEMENTARY MATERIAL

The Supplementary Material for this article can be found online at: https://www.frontiersin.org/articles/10.3389/fgene.2020.00945/full#supplementary-material

## REFERENCES

Amann, R. P. (1983). Endocrine changes associated with onset of spermatogenesis in Holstein bulls. *J. Dairy Sci.* 66, 2606–2622. doi: 10.3168/jds.S0022-0302(83)82135-3

Aqeilan, R. I., Hagan, J. P., de Bruin, A., Rawahneh, M., Salah, Z., Gaudio, E., et al. (2009). Targeted ablation of the WW domain-containing oxidoreductase tumor suppressor leads to impaired steroidogenesis. *Endocrinology* 150, 1530–1535. doi: 10.1210/en.2008-1087

Aslani, F., Sebastian, T., Keidel, M., Fröhlich, S., Elsässer, H. P., Schuppe, H. C., et al. (2017). Resistance to apoptosis and autophagy leads to enhanced survival in Sertoli cells. *Mol. Hum. Reprod.* 23, 370–380. doi: 10.1093/molehr/gax022

Bird, A. (2007). Perceptions of epigenetics. *Nature* 447, 396–398. doi: 10.1038/nature05913

Bo, D., Jiang, X., Liu, G., Xu, F., Hu, R., Wassie, T., et al. (2020). Multipathway synergy promotes testicular transition from growth to spermatogenesis in early-puberty goats. *BMC Genomics* 21:372. doi: 10.1186/s12864-020-6767-x

Brito, L. F. C. (2014). "Endocrine control of testicular development and initiation of spermatogenesis in bulls," in *Bovine Reproduction*, ed. R. Hopper (Oxford, UK: John Wiley & Sons, Inc.), 30-38. doi: 10.1002/9781118833971.ch4

Byrne, C. J., Fair, S., English, A. M., Cirot, M., Staub, C., Lonergan, P., et al. (2018a). Plane of nutrition pre and post-six months of age in Holstein-Friesian bulls: I. Effects on performance, body composition, age at puberty and post-pubertal semen production. *J. Dairy Sci.* 101, 3447–3459. doi: 10.3168/jds.2017-13719

Byrne, C. J., Fair, S., English, A. M., Urh, C., Sauerwein, H., Crowe, M. A., et al. (2018b). Plane of nutrition before and after 6 months of age in Holstein-Friesian bulls : II. Effects on metabolic and reproductive endocrinology and identification of physiological markers of puberty and sexual maturation. *J. Dairy Sci.* 101, 1–16. doi: 10.3168/jds.2017-13720

Carone, B. R., Fauquier, L., Habib, N., Shea, J. M., Hart, C. E., Li, R., et al. (2010). Paternally induced transgenerational environmental reprogramming of metabolic gene expression in mammals. *Cell* 143, 1084–1096. doi: 10.1016/j.cell.2010.12.008

Carrell, D. T. (2012). Epigenetics of the male gamete. *Fertil. Steril.* 97, 267–274. doi: 10.1016/j.fertnstert.2011.12.036

Champroux, A., Cocquet, J., Henry-Berger, J., Drevet, J. R., and Kocer, A. (2018). A decade of exploring the mammalian sperm epigenome: paternal epigenetic and transgenerational inheritance. *Front. Cell Dev. Biol.* 6:50. doi: 10.3389/fcell.2018.00050

Chavatte-Palmer, P., Tarrade, A., Kiefer, H., Duranthon, V., and Jammes, H. (2016). Breeding animals for quality products: not only genetics. *Reprod. Fertil. Dev.* 28, 94–111. doi: 10.1071/RD15353

Coulter, G. H., Cook, R. B., and Kastelic, J. P. (1997). Effects of dietary energy on scrotal surface temperature, seminal quality, and sperm production

in young beef bulls. *J. Anim. Sci.* 75, 1048–1052. doi: 10.2527/1997.7541048x

Dance, A., Thundathil, J., Blondin, P., and Kastelic, J. P. (2016). Enhanced early-life nutrition of Holstein bulls increases sperm production potential without decreasing postpubertal semen quality. *Theriogenology* 86, 687–694. doi: 10.1016/j.theriogenology.2016.02.022

Dance, A., Thundathil, J., Wilde, R., Blondin, P., and Kastelic, J. P. (2015). Enhanced early-life nutrition promotes hormone production and reproductive development in Holstein bulls. *J. Dairy Sci.* 98, 987–998. doi: 10.3168/jds.2014-8564

de Castro Barbosa, T., Ingerslev, L. R., Alm, P. S., Versteyhe, S., Massart, J., Rasmussen, M., et al. (2015). High-fat diet reprograms the epigenome of rat spermatozoa and transgenerationally affects metabolism of the offspring. *Mol. Metab.* 5, 184–197. doi: 10.1016/j.molmet.2015.12.002

Doherty, R., and Couldrey, C. (2014). Exploring genome wide bisulfite sequencing for DNA methylation analysis in livestock: a technical assessment. *Front. Genet.* 5:126. doi: 10.3389/fgene.2014.00126

Doherty, R., Whiston, R., Cormican, P., Finlay, E. K., Couldrey, C., Brady, C., et al. (2016). The CD4+ T cell methylome contributes to a distinct CD4+ T cell transcriptional signature in Mycobacterium bovis-infected cattle. *Sci. Rep.* 6, 31014. doi: 10.1038/srep31014

Donkin, I., and Barrès, R. (2018). Sperm epigenetics and influence of environmental factors. *Mol. Metab.* 14, 1–11. doi: 10.1016/j.molmet.2018.02.006

Donkin, I., Versteyhe, S., Ingerslev, L. R., Qian, K., Mechta, M., Nordkap, L., et al. (2016). Obesity and bariatric surgery drive epigenetic variation of spermatozoa in humans. *Cell Metab.* 23:369e378. doi: 10.1016/j.cmet.2015.11.004

Dotolo, R., Kim, J. D., Pariante, P., Minucci, S., and Diano, S. (2016). Prolyl endopeptidase (PREP) is associated with male reproductive functions and gamete physiology in mice. *J. Cell. Physiol.* 231, 551–557. doi: 10.1002/jcp.25178

English, A. M., Byrne, C. J., Cormican, P., Waters, S. M., Fair, S., and Kenny, D. A. (2018). Effect of early calf-hood nutrition on the transcriptional regulation of the hypothalamic-pituitary-testicular axis in holstein-friesian bull calves. *Sci. Rep.* 8:16577. doi: 10.1038/s41598-018-34611-4

Feng, H., Conneely, K. N., and Wu, H. (2014). A Bayesian hierarchical model to detect differentially methylated loci from single nucleotide resolution sequencing data. *Nucleic Acids Res.* 42:e69. doi: 10.1093/nar/gku154

Ferder, I. C., Fung, L., Ohguchi, Y., Zhang, X., Lassen, K. G., Capen, D., et al. (2019). Meiotic gatekeeper STRA8 suppresses autophagy by repressing Nr1d1 expression during spermatogenesis in mice. *PLoS Genet.* 15:e1008084. doi: 10.1371/journal.pgen.1008084

Gao, J., Ma, Y., Fu, H. L., Luo, Q., Wang, Z., Xiao, Y. H., et al. (2016). Non-catalytic roles for TET1 protein negatively regulating neuronal differentiation through srGAP3 in neuroblastoma cells. *Prot. Cell* 7, 351–361. doi: 10.1007/s13238-016-0267-4

Gillessen-Kaesbach, G., Demuth, S., Thiele, H., Theile, U., Lich, C., and Horsthemke, B. (1999). A previously unrecognised phenotype characterised by obesity, muscular hypotonia, and ability to speak in patients with Angelman syndrome caused by an imprinting defect. *Eur. J. Hum. Genet.* 7, 638–644. doi: 10.1038/sj.ejhg.5200362

Gu, H., Smith, Z. D., Bock, C., Boyle, P., Gnirke, A., and Meissner, A. (2011). Preparation of reduced representation bisulfite sequencing libraries for genome-scale DNA methylation profiling. *Nat. Protoc.* 6, 468–481. doi: 10.1038/nprot.2010.190

Guan, Y., and Martin, G. B. (2017). Cellular and molecular responses of adult testis to changes in nutrition: novel insights from the sheep model. *Reproduction* 154, R133–R141. doi: 10.1530/REP-17-0061

Harstine, B. R., Maquivar, M., Helser, L. A., Utt, M. D., Premanandan, C., DeJarnette, J. M., et al. (2015). Effects of dietary energy on sexual maturation and sperm production in Holstein bulls. *J. Anim. Sci.* 93, 2759–2766. doi: 10.2527/jas.2015-8952

Hockenbery, D. M., Oltvai, Z. N., Yin, X. M., Milliman, C. L., and Korsmeyer, S. J. (1993). Bcl-2 functions in an antioxidant pathway to prevent apoptosis. *Cell* 75, 241–251. doi: 10.1016/0092-8674(93)80066-n

Horibe, A., Eid, N., Ito, Y., Hamaoka, H., Tanaka, Y., and Kondo, Y. (2017). Upregulated autophagy in sertoli cells of ethanol-treated rats is associated with induction of inducible nitric oxide synthase (iNOS), androgen receptor suppression and germ cell apoptosis. *Int. J. Mol. Sci.* 18:1061. doi: 10.3390/ijms18051061

Huang, W., Sherman, B. T., and Lempicki, R. A. (2009). Systematic and integrative analysis of large gene lists using DAVID bioinformatics resources. *Nat. Protoc.* 4, 44–57. doi: 10.1038/nprot.2008.211

Ignatiadis, N., Klaus, B., Zaugg, J. B., and Huber, W. (2016). Data-driven hypothesis weighting increases detection power in genome-scale multiple testing. *Nat. Methods* 13, 577–580. doi: 10.1038/nmeth.3885

Irano, N., de Camargo, G. M., Costa, R. B., Terakado, A. P., Magalhães, A. F., Silva, R. M., et al. (2016). Genome-wide association study for indicator traits of sexual precocity in nellore cattle. *PLoS One* 11:e0159502. doi: 10.1371/journal.pone.0159502

Kiefer, H., and Perrier, J. P. (2020). DNA methylation in bull spermatozoa: evolutionary impacts, inter individual variability and contribution to the embryo. *Can. J. Anim. Sci.* 100, 1–16. doi: 10.1139/cjas-2019-0071

Kim, J., Kundu, M., Viollet, B., and Guan, K. L. (2011). AMPK and mTOR regulate autophagy through direct phosphorylation of Ulk1. *Nat. Cell Biol.* 13, 132–141. doi: 10.1038/ncb2152

Kropp, J., Carrillo, J. A., Namous, H., Daniels, A., Salih, S. M., Song, J., et al. (2017). Male fertility status is associated with DNA methylation signatures in sperm and transcriptomic profiles of bovine preimplantation embryos. *BMC Genomics* 18:280. doi: 10.1186/s12864-017-3673-y

Krueger, F., and Andrews, S. R. (2011). Bismark: a flexible aligner and methylation caller for Bisulfite-Seq applications. *Bioinformatics* 27, 1571–1572. doi: 10.1093/bioinformatics/btr167

Lambert, S., Blondin, P., Vigneault, C., Labrecque, R., Dufort, I., and Sirard, M. A. (2018). Spermatozoa DNA methylation patterns differ due to peripubertal age in bulls. *Theriogenology* 106, 21–29. doi: 10.1016/j.theriogenology.2017.10.006

Lambrot, R., Xu, C., Saint-Phar, S., Chountalos, G., Cohen, T., Paquet, M., et al. (2013). Low paternal dietary folate alters the mouse sperm epigenome and is associated with negative pregnancy outcomes. *Nat. Commun.* 4:2889. doi: 10.1038/ncomms3889

Langmead, B., Trapnell, C., Pop, M., and Salzberg, S. L. (2009). Ultrafast and memory-efficient alignment of short DNA sequences to the human genome. *Genome Biol.* 10:R25. doi: 10.1186/gb-2009-10-3-r25

Lappalainen, T., and Greally, J. M. (2017). Associating cellular epigenetic models with humans phenotypes. *Nat. Rev. Genet.* 18, 441–451. doi: 10.1038/nrg.2017.32

Liu, Y., Hu, Y., Wang, L., and Xu, C. (2018). Expression of transcriptional factor EB (TFEB) in differentiating spermatogonia potentially promotes cell migration in mouse seminiferous epithelium. *Reprod. Biol. Endocrinol.* 16:105. doi: 10.1186/s12958-018-0427-x

Lucas, T. F., Pimenta, M. T., Pisolato, R., Lazari, M. F., and Porto, C. S. (2011). 17β-estradiol signaling and regulation of Sertoli cell function. *Spermatogenesis* 1, 318–324. doi: 10.4161/spmg.1.4.18903

Ly, L., Chan, D., Aarabi, M., Landry, M., Behan, N. A., MacFarlane, A. J., et al. (2017). Intergenerational impact of paternal lifetime exposures to both folic acid deficiency and supplementation on reproductive outcomes and imprinted gene methylation. *Mol. Hum. Reprod.* 23, 461–477. doi: 10.1093/molehr/gax029

Martínez, D., Pentinat, T., Ribó, S., Daviaud, C., Bloks, V. W., Cebrià, J., et al. (2014). In utero undernutrition in male mice programs liver lipid metabolism in the second-generation offspring involving altered Lxra DNA methylation. *Cell Metab.* 19, 941–951. doi: 10.1016/j.cmet.2014.03.026

McSwiggin, H. M., and O'Doherty, A. M. (2018). Epigenetic reprogramming during spermatogenesis and male factor infertility. *Reproduction* 156, R9–R21. doi: 10.1530/REP-18-0009

Murdoch, B. M., Murdoch, G. K., Greenwood, S., and McKay, S. (2016). Nutritional influence on epigenetic marks and effect on livestock production. *Front. Genet.* 7:182. doi: 10.3389/fgene.2016.00182

Pang, J., Li, F., Feng, X., Yang, H., Han, L., Fan, Y., et al. (2018). Influences of different dietary energy level on sheep testicular development associated with AMPK/ULK1/autophagy pathway. *Theriogenology* 108, 362–370. doi: 10.1016/j.theriogenology.2017.12.017

Perrier, J. P., Sellem, E., Prézelin, A., Gasselin, M., Jouneau, L., Piumi, F., et al. (2018). A multi-scale analysis of bull sperm methylome revealed both species peculiarities and conserved tissue-specific features. *BMC Genomics* 19:404. doi: 10.1186/s12864-018-4764-0

Popp, C., Dean, W., Feng, S., Cokus, S. J., Andrews, S., Pellegrini, M., et al. (2010). Genome-wide erasure of DNA methylation in mouse primordial germ cells is affected by AID deficiency. *Nature* 463, 1101–1105. doi: 10.1038/nature08829

R Core Team (2018). *R: A Language and Environment for Statistical Computing*. Vienna: R Foundation for Statistical Computing.

Radford, E. J., Ito, M., Shi, H., Corish, J. A., Yamazawa, K., Isganaitis, E., et al. (2014). In utero effects. In utero undernourishment perturbs the adult sperm methylome and intergenerational metabolism. *Science* 345, 1255903. doi: 10.1126/science.1255903

Rawlings, N. C., and Evans, A. C. (1995). Androgen negative feedback during the early rise in LH secretion in bull calves. *J. Endocrinol.* 145, 243–249. doi: 10.1677/joe.0.1450243

Schagdarsurengin, U., and Steger, K. (2016). Epigenetics in male reproduction: effect of paternal diet on sperm quality and offspring health. *Nat. Rev. Urol.* 13, 584–595. doi: 10.1038/nrurol.2016.157

Seah, M. K. Y., and Messerschmidt, D. M. (2018). From germline to soma: epigenetic dynamics in the mouse preimplantation embryo. *Curr. Top. Dev. Biol.* 128, 203–235. doi: 10.1016/bs.ctdb.2017.10.011

Serra, N., Velte, E. K., Niedenberger, B. A., Kirsanov, O., and Geyer, C. B. (2019). The mTORC1 component RPTOR is required for maintenance of the foundational spermatogonial stem cell pool in mice. *Biol. Reprod.* 100, 429–439. doi: 10.1093/biolre/ioy198

Shea, J. M., Serra, R. W., Carone, B. R., Shulha, H. P., Kucukural, A., Ziller, M. J., et al. (2015). Genetic and epigenetic variation, but not diet, shape the sperm methylome. *Dev. Cell* 35, 750–758. doi: 10.1016/j.devcel.2015.11.024

Tang, W. W., Kobayashi, T., Irie, N., Dietmann, S., and Surani, M. A. (2016). Specification and epigenetic programming of the human germ line. *Nat. Rev. Genet.* 17, 585–600. doi: 10.1038/nrg.2016.88

von Meyenn, F., and Reik, W. (2015). Forget the parents: epigenetic reprogramming in human germ cells. *Cell* 61, 1248–1251. doi: 10.1016/j.cell.2015.05.039

Wang, L., Zhang, J., Duan, J., Gao, X., Zhu, W., Lu, X., et al. (2014). Programming and inheritance of parental DNA methylomes in mammals. *Cell* 157, 979–991. doi: 10.1016/j.cell.2014.04.017

Watkins, A. J., Dias, I., Tsuro, H., Allen, D., Emes, R. D., Moreton, J., et al. (2018). Paternal diet programs offspring health through sperm- and seminal plasma-specific pathways in mice. *Proc. Natl. Acad. Sci. U.S.A.* 115, 10064–10069. doi: 10.1073/pnas.1806333115

Wolf, F., Almquist, J., and Hale, E. (1965). Prepuberal behavior and puberal characteristics of beef bulls on high nutrient allowance. *J. Anim. Sci.* 24, 761–765. doi: 10.2527/jas1965.243761x

Wu, C., Blondin, P., Vigneault, C., Labrecque, R., and Sirard, M.-A. (2020). The age of the bull influences the transcriptome and epigenome of blastocysts produced by IVF. *Theriogenology* 144, 122–131. doi: 10.1016/j.theriogenology.2019.12.020

Xu, W., Zhu, Q., Liu, S., Dai, X., Zhang, B., Gao, C., et al. (2018). Calretinin participates in regulating steroidogenesis by PLC-$Ca^{2+}$-PKC pathway in leydig cells. *Sci. Rep.* 8:7403. doi: 10.1038/s41598-018-25427-3

Yamanaka, C., Lebrethon, M. C., Vandersmissen, E., Gerard, A., Purnelle, G., Lemaitre, M., et al. (1999). Early prepubertal ontogeny of pulsatile gonadotropin-releasing hormone (GnRH) secretion: I. Inhibitory autofeedback control through prolyl endopeptidase degradation of GnRH. *Endocrinology* 140, 4609–4615. doi: 10.1210/endo.140.10.6971

**Conflict of Interest:** The authors declare that the research was conducted in the absence of any commercial or financial relationships that could be construed as a potential conflict of interest.

*Copyright © 2020 Perrier, Kenny, Chaulot-Talmon, Byrne, Sellem, Jouneau, Aubert-Frambourg, Schibler, Jammes, Lonergan, Fair and Kiefer. This is an open-access article distributed under the terms of the Creative Commons Attribution License (CC BY). The use, distribution or reproduction in other forums is permitted, provided the original author(s) and the copyright owner(s) are credited and that the original publication in this journal is cited, in accordance with accepted academic practice. No use, distribution or reproduction is permitted which does not comply with these terms.*

frontiers in Genetics

ORIGINAL RESEARCH
published: 26 August 2020
doi: 10.3389/fgene.2020.00939

# The Profiling of DNA Methylation and Its Regulation on Divergent Tenderness in Angus Beef Cattle

*Chunping Zhao[1,2], Guanyu Ji[3], José A. Carrillo[2], Yaokun Li[1,2], Fei Tian[2], Ransom L. Baldwin VI[4], Linsen Zan[1]* and Jiuzhou Song[2]**

*[1] College of Animal Science and Technology, Northwest A&F University, Xianyang, China, [2] Department of Animal and Avian Sciences, University of Maryland, College Park, MD, United States, [3] Shenzhen GenDo Health Sci&Tech Ltd., Shenzhen, China, [4] Animal Genomics and Improvement Laboratory, BARC, NEA, USDA, Beltsville, MD, United States*

OPEN ACCESS

**Edited by:**
*Stephanie McKay, University of Vermont, United States*

**Reviewed by:**
*Penny Riggs, Texas A&M University, United States*
*Adriana Mercia Guaratini Ibelli, EMBRAPA Swine and Poultry, Brazil*

***Correspondence:**
*Linsen Zan*
*zanlinsenn@163.com*
*Jiuzhou Song*
*songj88@umd.edu*

**Specialty section:**
*This article was submitted to Livestock Genomics, a section of the journal Frontiers in Genetics*

**Received:** *03 December 2019*
**Accepted:** *28 July 2020*
**Published:** *26 August 2020*

**Citation:**
*Zhao C, Ji G, Carrillo JA, Li Y, Tian F, Baldwin RL VI, Zan L and Song J (2020) The Profiling of DNA Methylation and Its Regulation on Divergent Tenderness in Angus Beef Cattle. Front. Genet. 11:939. doi: 10.3389/fgene.2020.00939*

Beef is an essential food source in the world. Beef quality, especially tenderness, has a significant impact on consumer satisfaction and industry profit. Many types of research to date have focused on the exploration of physiological and developmental mechanisms of beef tenderness. Still, the role and impact of DNA methylation status on beef tenderness have yet to be elucidated. In this study, we exhaustively analyzed the DNA methylation status in divergent tenderness observed in Angus beef. We characterized the methylation profiles related to beef tenderness and explored methylation distributions on the whole genome. As a result, differentially methylated regions (DMRs) associated with tenderness and toughness of beef were identified. Importantly, we annotated these DMRs on the bovine genome and explored bio-pathways of underlying genes and methylation biomarkers in beef quality. Specifically, we observed that the ATP binding cassette subfamily and myosin-related genes were highly methylated gene sets, and generation of neurons, regulation of GTPase activity, ion transport and anion transport, *etc.,* were the significant pathways related with beef tenderness. Moreover, we explored the relationship between DNA methylation and gene expression in DMRs. Some methylated genes were identified as candidate biomarkers for beef tenderness. These results provide not only novel epigenetic information associated with beef quality but offer more significant insights into meat science, which will further help us explore the mechanism of muscle biology.

**Keywords: DNA methylation, MBD-seq, DMR, epigenetic, beef quality**

**Abbreviations:** HTO, high methylated-DNA from tough beef; LTE, low methylated-DNA from tender beef; LTO, low methylated-DNA from tough beef; MTE, medially methylated-DNA from tender beef; MTO, medially methylated-DNA from tough beef; HTE, high methylated-DNA from tender beef.

## INTRODUCTION

Beef constitutes one of the primary food sources worldwide due to its high-quality protein and other nutrients, such as B vitamins, iron, zinc, unsaturated fatty acid, *etc.* (Delgado, 2003; McNeill and Van Elswyk, 2012). Thus, beef composition and quality have always been a principal focal point for both consumers and producers (Galbraith, 2002; Raes et al., 2003). Traditionally, beef quality has been influenced and evaluated by three general criteria: tenderness, juiciness, and flavor (Boleman et al., 1997), of which, juiciness and flavor are subjective and influenced by several factors, such as cooking style, consumer preferences, and ethnic, cultural habits. However, tenderness is one of the most important factors influencing the quality and can be quantitatively and objectively measured by the Warner–Bratzler shear forces (WBSF) (Huffman et al., 1996; Ferraris et al., 2013; Hocquette et al., 2013; Morales et al., 2013; Nogalski et al., 2018). Tenderness is a complex trait influenced by different structural components, such as the myofibrillar mass, sarcoplasmic proteins, intramuscular fat, and connective tissue, *etc*. Besides, many intricate biological processes are also involved, such as rigor development, fiber contraction, proteolysis during aging and meat maturation (Tornberg, 1996; Patten et al., 2008; Nishimura, 2010).

To date, a large number of molecular studies have focused on the exploration of molecular mechanisms responsible for beef tenderness (Zhao et al., 2012a,b, 2014, 2015; Picard et al., 2015; Silva et al., 2016; Enriquez-Valencia et al., 2017; Goncalves et al., 2018; Gagaoua et al., 2019; Leal-Gutierrez et al., 2019). Interestingly, these studies revealed some factors related with beef tenderness and meat quality, such as quantitative trait loci (QTL), single nucleotide polymorphisms (SNPs), copy number variations (CNVs), functional candidate genes, transcripts, and proteins, *etc.* (Zhao et al., 2012b, 2014; Silva et al., 2016; Enriquez-Valencia et al., 2017; Goncalves et al., 2018; Gagaoua et al., 2019; Leal-Gutierrez et al., 2019). In our previous researches, we ascertained that some genes, proteins, miRNAs, and histone modification, namely an epigenetic factor, are demonstrably related with beef tenderness and meat quality (Zhao et al., 2012a,b, 2014, 2015). However, DNA methylation has not been elucidated in the regulation of beef quality traits.

DNA methylation is one of the most studied epigenetic modifications which occurs by covalently attaching a methyl group to the fifth carbon of cytosine residues (Goldberg et al., 2007). It is reported that DNA methylation plays essential roles in diverse processes, including cell proliferation and differentiation, genomic imprinting, embryogenesis, X chromosome inactivation, tumor genesis, *etc.* (Wilson, 2008). Moreover, DNA methylation has been associated with gene repression at specific genome regions and mainly when it occurs in gene promoters (Mendoza-Garces et al., 2013). Much attention has been paid to the figuration of DNA methylation on the whole genome in livestock animals, such as chicken, pig, horse, beef cattle and dairy cattle using methylated DNA immune-precipitation sequencing (MeDIP-seq) (Li et al., 2011, 2012; Huang et al., 2014; Lee et al., 2014; Song et al., 2016); goat and beef cattle using methylated DNA binding domain-sequencing (MBD-seq) (Frattini et al., 2017; Li et al., 2019); sheep using reduced representation bisulfite sequencing (RRBS) (Couldrey et al., 2014), hen using whole-genome bisulfite sequencing (WGBS) (Zhang et al., 2017), etc. These studies identified differentially methylated regions (DMRs) and methylation-regulated genes related to variant phenotypes or different development stages in domestic animals. Intriguingly, one of the studies found that DNA methylation was related to meat quality and tenderness of breast muscle in chicken (Li et al., 2011). However, the DNA methylation analysis of beef quality and tenderness remains unknown.

In the present study, we explored DNA methylation in *longissimus lumborum* with divergent tenderness of inbred Angus cattle. We first depicted the methylation profiles related to beef tenderness and described methylation distributions on the whole genome. We then identified DMRs between those divergent tenderness beef and annotated the DMRs on the bovine genome and subsequently explored the bio-pathways with those underlying genes of DMRs. Finally, we examined the relationships between gene expression and these selected methylated markers. We believe that the results of the study will contribute to excavating epigenetic mechanisms regulating beef quality and provide valuable information for further functional validation and, ultimately, promote the improvement of beef production.

## MATERIALS AND METHODS

### Sample Preparation and Experimental Design

Nineteen Angus cattle were obtained from WYE Angus (Queenstown, MD, United States). They consisted of contemporaneous steers that received the same pelleted forge diet formulated to provide the nutritional requirement. Around 12 months of age, the animals were terminated, and samples of *longissimus lumborum* from the 12–13th rib were collected and aged at 4°C for 14 days. Concurrently, a small piece of fresh tissue samples from the same muscle was obtained and immediately placed in RNAlater solution at −80°C for DNA and RNA extraction. After the aging process, WBSF, crude fat, fatty acid contents, and cooking loss of the samples were measured to evaluate beef tenderness as previously described (Zhao et al., 2012b). Then four samples exhibiting the lowest WBSF were selected as the tender group and four individuals with the greatest WBSF designed as the tough group.

All procedures were approved by the University of Maryland Institutional Animal Care and Use Committee (Protocol # R-07-05). Research performed in this study were in accordance with the relevant guidelines and regulations of the ethics approvals above.

### DNA Extraction and MBD-Seq Library Preparation

Two samples were randomly selected as representatives from four individuals of each group (tender and tough), and

Genomic DNA was extracted using the Wizard Genomic DNA purification kit (Promega, Madison, WI, United States). DNA concentrations were measured by the Qubit dsDNA Broad-Range Assay (Invitrogen, Carlsbad, CA, United States). The MBD-seq method was used to identify methylated DNA regions, and elution of the captured methylated DNA was done separately using three salt gradients, namely the low, medium and high concentrations as our previous publication (Carrillo et al., 2015). MethylCap kit (Diagenode, Denville, NJ, United States) was used to obtain DNA containing methylated CpGs. Briefly, DNA was extracted and sheared into 300–500 bp fragments using the Bioruptor® Sonicator (Diagenode) and then visualized on an agarose gel to verify the size of the resultant segments. A 141.8 μl capture reaction mix containing 12 μl of sheared DNA and lacking the MethylCap protein was prepared. From this preparation, 119 μl of capture reaction mix was incubated with 1 μl of diluted MethylCap protein at 40 rpm on a rotating wheel for 2 h and at 4°C to allow the interaction. The remaining solution (22.8 μl) was used as an input sample. Magnetic beads captured methylated DNA. Unbound DNA was washed off, and the eluted DNA collected. For the elution, 150 μl of the low, medium, and high concentration elution buffer was used serially per capture. These three elutions are corresponding to the high, medium, and low methylation parts of the whole genome, respectively (Brinkman et al., 2010). They were named as HTE (High methylated-DNA from tender beef), HTO (High methylated-DNA from tough beef), MTE (Medially methylated-DNA from tender beef), MTO (Medially methylated-DNA from tough beef), LTE (Low methylated-DNA from tender beef), LTO (Low methylated-DNA from tough beef), respectively. All fractions and input were purified using the MiniElute PCR Purification Kit (QIAGEN, Valencia, CA, United States). Quantitative PCR (qPCR) (iCycleriQ PCR system, Bio-Rad, Hercules, CA, United States) was performed in duplicate for each sample to test the enrichment efficiency. Method $2^{-\Delta\Delta Ct}$ was applied to determine relative fold enrichments and compared enrichment values of a positive *TGFB3* to a negative primer pair *MON2*, between experimental (methyl DNA) and reference (input DNA) samples.

The sequencing libraries were constructed as follows: NEBNext® End Repair Module (NEB, Ipswich, MA, United States) was used for the end repair of the fragmented methylated DNA, a 3′ A was added using DNA Polymerase I, Large (Klenow) Fragment (NEB), then a pair of Solexa adaptors (Illumina, San Diego, CA, United States) was ligated to the repaired ends by T4 ligase (Promega). Filtration in a 2% agarose gel was used to select fragments (DNA plus adaptors) from 300 to 500 bp. PCR enriched purified DNA templates were amplified by Phusion® Hot Start High-Fidelity DNA Polymerase (NEB). After purification, DNA quality was examined. The DNA library was diluted, and the concentration double-checked using the Qubit assay (Life Technologies). A total of 12 libraries were constructed for three gradient-eluted DNA from two replicates of two groups. Finally, the libraries identified by the 6-bp index were sequenced at 50 bp sequence read using an Illumina HiSeq 2000 sequencer.

## MBD-Seq Data Analysis

The raw reads were obtained by Illumina sequencing. We created the clean reads from the dataset by filtering reads contained the adaptor sequence or the reads which had low quality and N bases occupy more than 50% of the read length (Chen et al., 2018). The clean reads were obtained by SOAPnuke and aligned to the cattle reference genome (BosTau8) using the Burrows-Wheeler Aligner (BWA) (Li and Durbin, 2010), allowing up to two nucleotide mismatches to the reference genome per seed and returning only uniquely mapped reads. Replicate sequencing reads (i.e., reads with the same starting position) were counted only once.

Uniquely mapped reads were used to analyze the DNA methylation differential peaks based on a defined model of ChIP-Seq data (MACS2) (Liu, 2014). Peaks were identified by the Poisson test with $p$-value $< 0.01$; then, we modified results by FDR $< 0.01$ for further analysis, and all the other parameters were used as the default (Wang et al., 2018).

We found most of the peaks in the biological replicates overlapped with the merged peaks. Thus, we determined that the data may not be saturated and selected data for the next differential analysis. The peaks from the tender and tough samples were then merged as candidate differentially methylated regions (CDMRs). The reads were counted for each of the CDMRs, and the DESeq Bioconductor package (Anders and Huber, 2010) was used to identify CDMRs with an FDR $< 0.01$ and $|\log_2 FC| > 2$ as final differentially methylated regions (DMRs). Read distributions were normalized using the Reads Per Kilobase per Million (RPKM) mapped reads strategy in 100 bp bins, followed by the analysis of the immune-precipitation-based DNA methylome using a method based on a Bayesian deconvolution strategy (Down et al., 2008). A prior report (Chavez et al., 2010) demonstrated that this normalization strategy improves the correlation to bisulfite sequencing data.

The paired reads were not extended and were placed in bins of 100 bp across the genome. The values of each bin were used to determine the read density or read distribution on the gene element regions. All the details on data analysis can be found in a previous publication (Wang et al., 2018).

## Joint Analysis of MBD-Seq and Gene Expression

Gene expression of the four samples in each group (tender and tough) was assessed with the 4 × 44K Bovine Gene Expression Microarray (Agilent, Santa Clara, CA, United States) as previously described (Zhao et al., 2012b). Pearson correlation was used for correlation analysis between DNA methylation and gene expression. Specifically, the reads density [uniformed by tags per million (TPM) method] of the peaks, which located in the region from transcription start site (TSS) upstream 2000 bp to downstream 2000 bp, were statics to represent the degree of DNA methylation on the genes. Then, three levels of DNA methylation for tender and tough samples were totally counted separately. At last, the difference values between the tender and tough for the three levels of DNA methylation were pairing with the difference of gene expression (beta value for microarray were also

uniformed by TPM method) respectively, and cor.test() in the default functions of R package was used to calculate the Pearson correlation coefficient with default parameters. Specifically, the parameter alternative with two.sided, conf.level = 0.95. The difference value of the DNA methylation and the difference of gene expression were performed by scatter plot.

# RESULTS

## The Meat Quality of *Longissimus Lumborum* From Angus Cattle

A total of 19 Angus cattle were slaughtered, and *longissimus lumborum* samples were collected. The measurement of meat quality traits showed that WBSF values differed significantly for these 19 steers, ranged from 5.81 to 20.70 kg (13.37 ± 5.35 kg), but crude fat, fatty acid contents, and cooking loss varied slightly. To explore the mechanisms of tenderness variation, four samples exhibiting the lowest WBSF (6.03 ± 0.31 kg) were selected to represent the tender group and four samples with the greatest WBSF (20.33 ± 0.53 kg) were designated as the tough group. After further analysis of the meat quality traits between tender and tough groups, we found that crude fat content was also significant between these two groups ($P < 0.05$).

## The DNA Methylation in *Longissimus Lumborum* Muscle of Angus Cattle

To detect the distribution of DNA methylation across the entire genome of *longissimus lumborum* from Angus, MBD-seq was performed in the beef with divergent tenderness, namely tender and tough. By using deep sequencing, we obtained a total of 146271818 raw reads. After filtering the reads of low quality, we aligned those clean reads to the reference genome (bosTau8), and our results reveal that 92.25% of reads were uniquely mapped to the reference (**Supplementary Table S1**). The uniquely mapped reads were 35257025, 52946431, and 46738093 in the high, medium, and low methylated regions, respectively, implying that more proportion of the genome in *longissimus lumborum* of Angus is moderately methylated. Additionally, a total of 63346070 uniquely mapped reads were identified in the tender group while 71595479 in the tough samples (**Supplementary Table S2**).

To check the distribution of DNA methylation, CpG islands (CGIs), promoters, namely the most methylated and functional regions in the genome, were partitioned; average distance cluster analysis was carried out using uniquely mapped reads in these areas normalized with RPKM. All regions were divided into several clusters so as to present differential DNA methylation patterns in CGIs and promoters subtly. The cluster analysis results are shown in **Figures 1A,C**, in which, every two replicates are tightly clustered in the bottom of the dendrogram, and some regions have been overtly divided according to methylation levels. All the high methylated regions were distinctly separated from others, and all the low methylated regions also cluster together in CGIs (**Figure 1A**). In contrast, the DNA methylation of middle and high has closer distance in promoter regions (**Figure 1C**).

To further verify the results of cluster analysis, Principal Components Analysis (PCA) was also performed in CGIs and promoters, respectively. As shown in **Figures 1B,D**, after the analysis of dimension reduced, the top two principal components could distinguish those two elements clearly. The three clusters, namely the high, medium, and low methylated regions, separated along with the first two principal components. Additionally, the two biological replicates were highly consistent in read density in CGIs and promoters, and they had a closer distance in the cluster and PCA. Therefore, the reads from the two replicates in the same condition were merged respectively for further analysis.

## DNA Methylation Profiles of *Longissimus Lumborum*

To obtain the global DNA methylation landscapes in the *longissimus lumborum*, the methylation levels were explored in different genome regions, including the upstream 2 kb, exon, intron, and downstream 2 kb of genes, after the read number was normalized using RPKM method. As shown in **Figure 2A**, the methylation levels dramatically increased in the exons. On the whole genome, the exons showed a much higher methylation level than the other regions, and the global methylation levels of upstream, downstream, intron decreased in turn. Additionally, the methylation levels of HTE and HTO were much higher than those from the medium or low methylated regions.

As reported previously, DNA methylation often occurs in the CGIs of the genome. Therefore, we divided the genome into three parts, namely CGIs, upstream 2 kb of CGIs, and downstream 2 kb of CGIs, to clarify the relationship of DNA methylation and the CpG density. As shown in **Figure 2B**, the methylation levels were found to increase sharply in the CGIs compared to upstream and downstream. Three levels of methylation were successively high (HTE and HTO), medium (MTE and MTO), and low (LTE and LTO), from top to bottom.

To explore the methylation levels on the different components of genes, we examined the read distribution in the promoter, 5′UTR, exon, intron, 3′UTR, repeat elements, CGIs, and CpG shores (CGSs). The introns were observed to have enriched with more unique reads than the other components, and CGSs harbored with more reads than CGIs (**Figure 2C**). Moreover, the 5′ UTR and 3′ UTR were seldom methylated compared to the other components, while numerous reads enriched in the repeat elements. Further, the tough always had more reads than the tender in every element, except in repeat elements, where HTE had more reads than HTO, and LTE had more reads than LTO. Thus, we further explored the distribution of reading in repeat elements. The results showed that LINE/L1, simple repeat, LINE/L2, SINE/MIR exhibited more enriched unique reads (**Figure 2D**). And the read distribution pattern in rRNA was different from other repeat elements, namely that in rRNA most-read enriched in HTO, but in other repeat elements, most reads fell in LTE.

Then DNA methylation enriched regions, namely peaks, were identified through MACS2, a common approach for clustering to enable identification of enriched domains from ChIP-seq data. The details of the peak numbers are shown in **Figure 3A**.

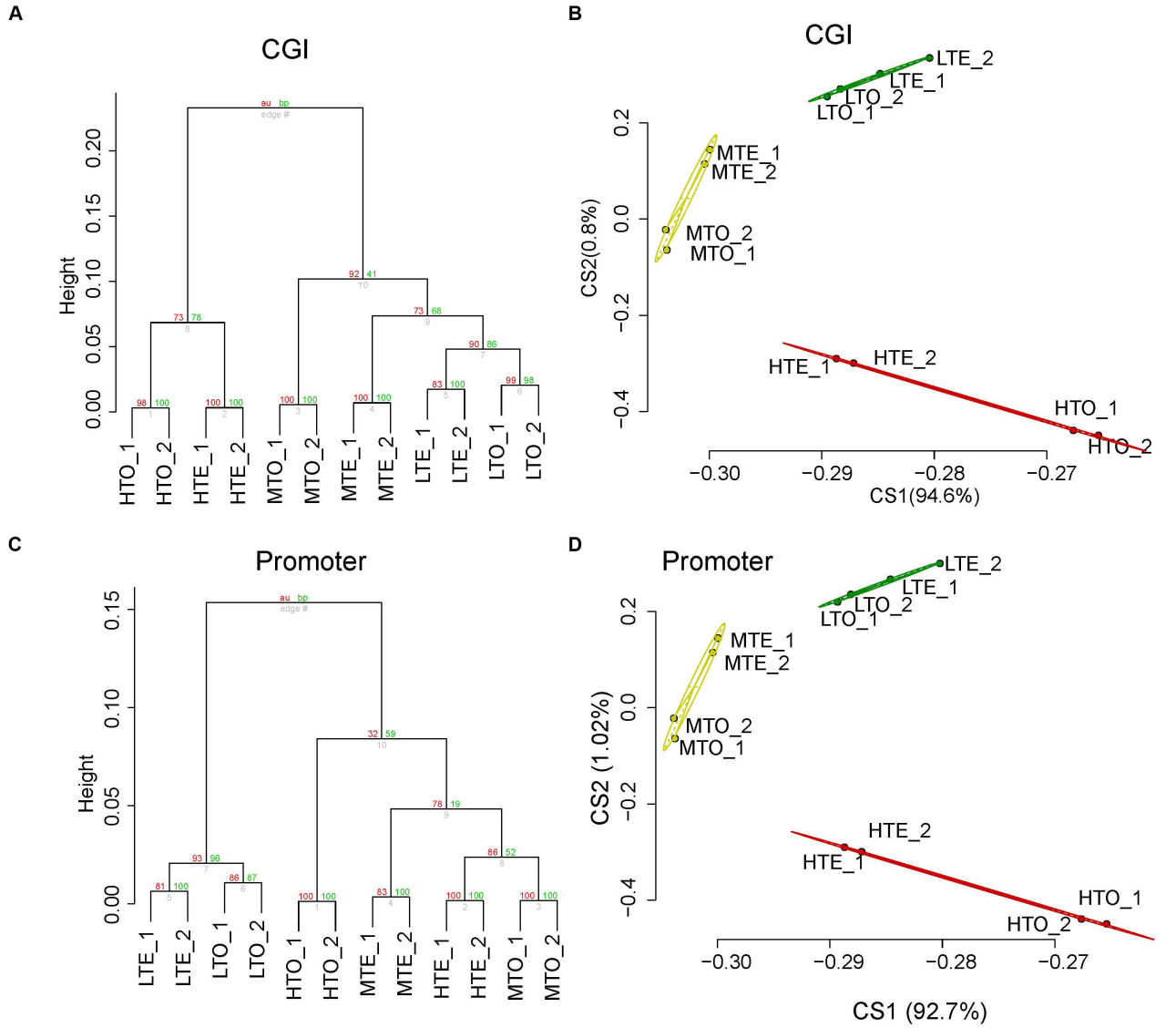



**FIGURE 1 |** Methylation profile analysis of *longissimus lumborum* from cattle on CGI and promoter. **(A)** Unsupervised hierarchical clustering analysis on CGI. **(B)** Principal Component Analysis on CGI. **(C)** Unsupervised hierarchical clustering analysis on promoter. **(D)** Principal Component Analysis on promoter.

More peaks were identified in the low methylated regions (LTE and LTO), and the tough (LTO) enriched more peaks than the tender (LTE) in the low methylated areas, which is the inverse of that observed in the medium and high methylated regions. Additionally, in the tender group, the medium methylated regions (MTE) harbored more peaks (86,678), while in the tough group, the low methylated regions (LTO) enriched more peaks (122,437), implying distinct methylation patterns in these two kinds of beef.

We further explored the distribution of peaks in the different components of the genes in the order of upstream 2 kb, 5′UTR, CDS, intron, 3′UTR, downstream 2 kb, and intergenic region. If a peak spans two components, it is only annotated in the prior one. The peak distribution analysis results showed that around 60% of the peaks are located in the intergenic regions. About 15% of peaks are distributed in the introns and CDS, respectively. The peaks in the upstream, 5′UTR, 3′UTR, and downstream are very scarce (**Figure 3B**). Besides, we refined the peaks distributed in the repeat elements and observed that more than 55% of peaks in the repeat elements are located in simple repeat and 14.01% and 7.23% of peaks in LINE/L1 and SINE/MIR, respectively. Peaks are seldom identified in the other repeat elements (**Figure 3C**). Then to precisely compare the peaks between the tender and tough we calculated the peak ratios in the repeat elements between the two kinds of beef. As shown in **Figure 3D**, in the low methylated zones, more than twofold peaks were observed in the tough in all repeat elements except rRNA with an opposite trend for the medium methylated zones. In the high methylation regions, peak numbers were more equalized between tender and tough groups except for tRNA and DNA/hAT-Tip100, *etc.*

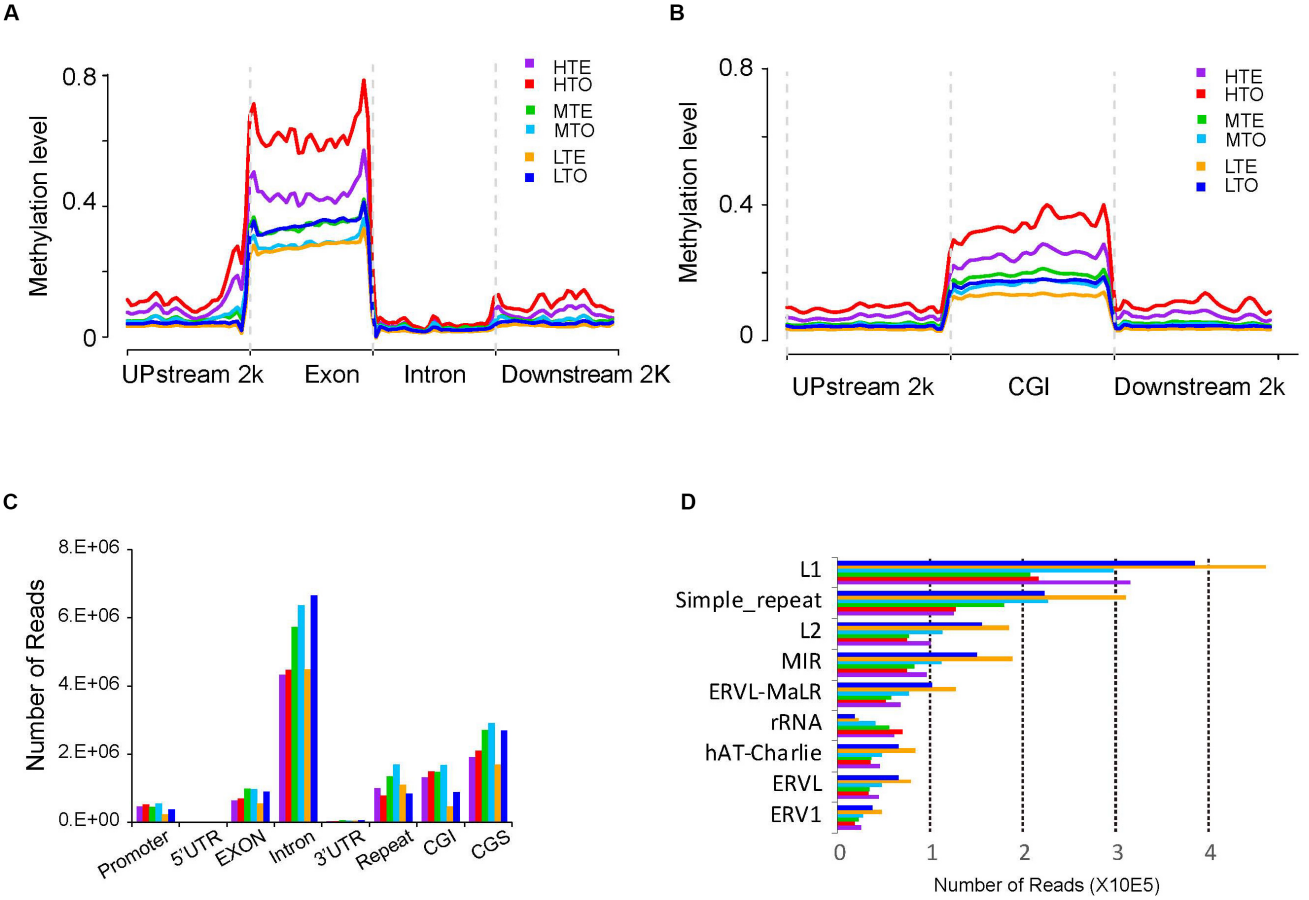



**FIGURE 2 |** Methylation levels and read distributions in each gene elements and repeat elements. Reads were normalized by RPKM (Reads Per Kilobase per Million mapped reads). **(A)** Distribution of 5-mC tag densities on genome. **(B)** Distribution of 5-mC densities on CGIs. **(C)** Read distribution on genome elements. **(D)** Read distribution in repeat elements.

## DNA Methylation Variations Between the Tender and Tough Beef

To explore the relationship between DNA methylation and beef tenderness, we identified differentially methylated regions (DMRs) between the tender and tough groups. A total of 7215 DMRs were identified in three methylated levels. In the high methylated regions, almost half of the 1090 DMRs were up-methylated in the tender beef compared with the tough beef; in the MTE 2531 DMRs were up-methylated and 683 DMRs were down-methylated; in the LTO much more down-methylated DMRs were identified in the tough beef (**Figure 4A**). By separating the peak distribution on the gene components and the repeat elements, we observed more peaks harbored in the MTE for all gene components (upstream, 5′ UTR, exon, intron, 3′ UTR, downstream), while more peaks are enriched in the LTO in all repeat elements except simple repeat (**Figures 4B,C**).

To graphically demonstrate global DNA methylation variations between these two kinds of beef, a macroscopical display of DMRs along chromosomes was represented by a Circos histogram (**Figure 4D**), the inner two cycles represent CGI density and gene density respectively, and the outer cycle represents all chromosomes of a cow with scale at 1 Mb bins. We found that the high CGI density regions also predominately harbored more DMRs in the whole genome. Additionally, the methylation patterns on chromosomes were different among these three methylation levels. For example, in the low methylation level (circle c), DMRs on chromosome 13 were hypomethylated while they were hypermethylated in the medium level (circle b). In contrast, DNA methylation variation patterns between the low and high methylation levels on chromosome 17 were the opposite. Furthermore, in the low methylation level of chromosome 3, 9, 22, 29, DMRs were hypomethylated while methylation patterns were similar in the high and medium methylation levels. Thus, variations in DNA methylation exhibited by the different methylation levels may play distinct roles in beef tenderness.

## The Function Annotation of DMRs Between the Tender and Tough Beef

To explore more deeply the putative mechanisms and biological functions of these DMRs, we identified the DMRs underlying genes. Among these annotated genes, we identified more

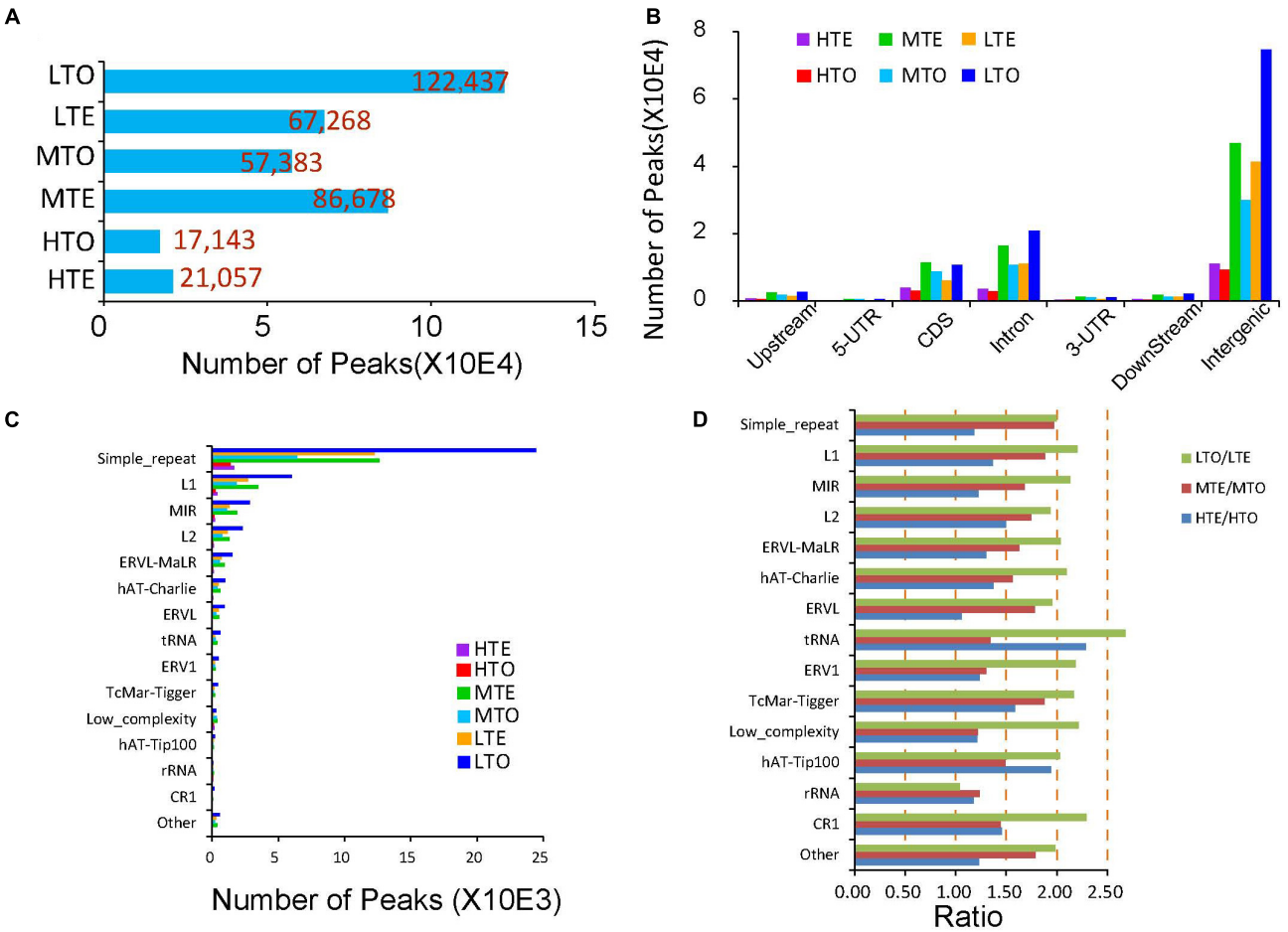



**FIGURE 3 |** Peak distribution in the tender and tough beef. **(A)** Peak numbers in each elute. **(B)** Peak number distribution on gene elements. **(C)** Peak number distribution in repeat elements. **(D)** Comparison of peak numbers in repeat elements between tough and tender beef.

enrichments in ATP binding cassette subfamily and myosin-related genes, such as *ABCA1*, *ABCG1*, *ABCA7*, myosins, myosin heavy chains, myosin light chains, *etc*, which were reported to be involved in fatty acid metabolism and beef tenderness. We annotated these genes by GO term and KEGG pathway analysis. A total of 1242 genes are mapped to the unique Entrez Gene IDs in the high methylated regions, and 960 genes are mapped in the medium and 2154 in the LTO, respectively. The GO term results are interpreted to indicate that DNA methylation differences affect the different biological processes, cellular components, and molecular functions (**Supplementary Figure S1**). In the biological process, DMRs in the high methylated zones involved the generation of neurons, regulation of GTPase activity, *etc.*, and in the medium methylated zones, DMRs functioned in ion transport and anion transport, *etc.*, while in the low methylated zones DMRs played roles in ion transmembrane transport and generation of neurons, *etc.* The KEGG analysis results indicated that the most highly affected pathways for the high and low methylation regions were focal adhesion, Axon guidance, while regulation of actin cytoskeleton was the most important pathway in the medium methylation regions.

## The Relationship of DNA Methylation and Gene Expression in the Tender and Tough Beef

To examine the relationship between DNA methylation and gene activity in the variation of beef tenderness, we evaluated the relative gene expression rate of tender and tough groups using Agilent 4 × 44K bovine microarray. Subsequently, we combined gene expression data with the MBD-seq results. To visualize the relationship on the whole genome, we divided the genome into upstream, exon, intron, and downstream. And we grouped all genes into four categories according to their relative expression (high, medium, low, and silent) and plotted the distribution of DNA methylation in four parts of the genome for each expression category. The results confirmed that the density of methylation in the exons was higher than the introns, downstreams, and upstreams. Additionally, for these four expression categories, genes with lower expression exhibited a higher density of methylation in exons, indicating that the methylation level of exons negatively correlates with gene expression (**Supplementary Figure S2**).

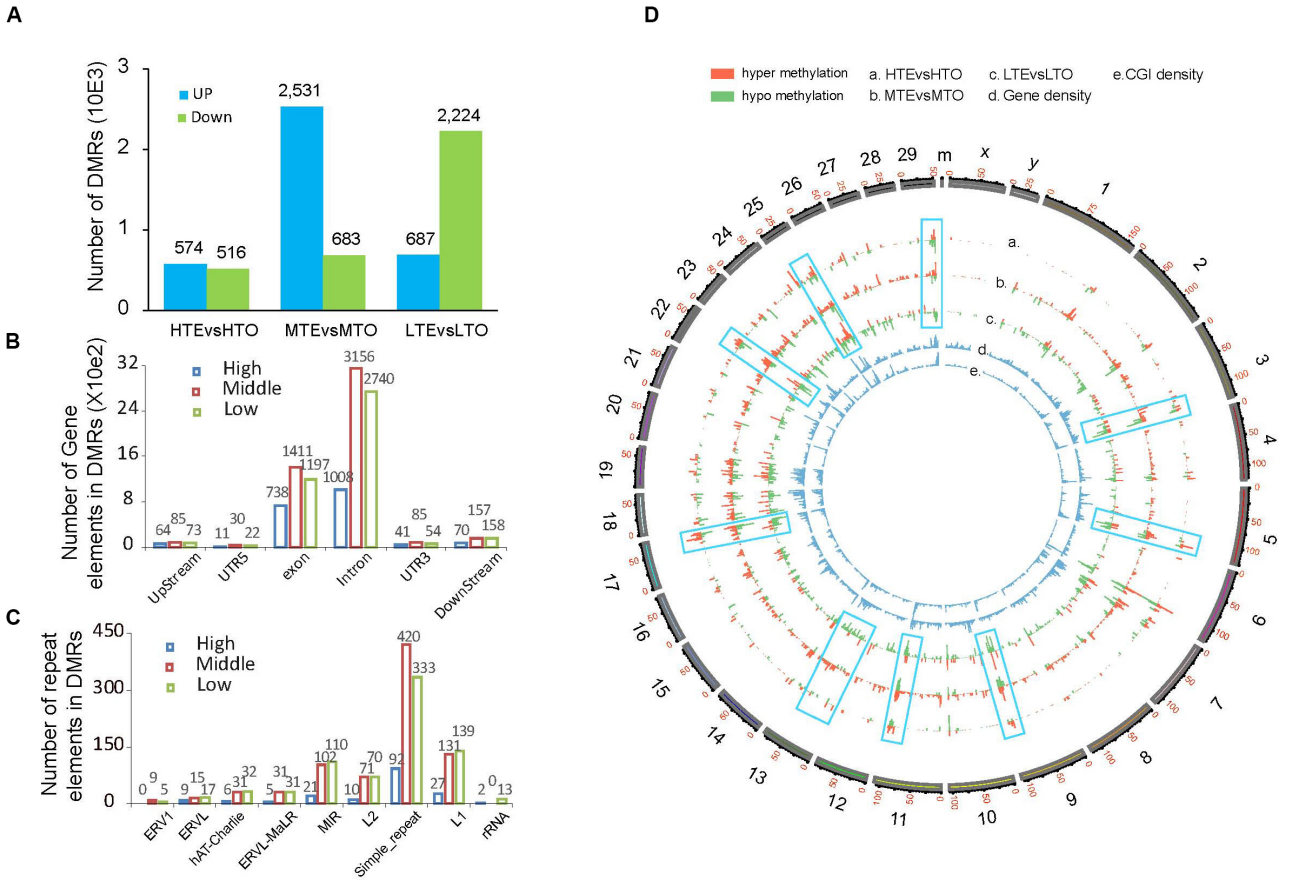



**FIGURE 4 |** DMR distribution between the tender and tough beef. **(A)** Number of DMRs in each elute. **(B)** Number of DMRs in gene elements. **(C)** Number of DMRs in repeat elements. **(D)** Global DMR distribution on the whole chromosome.

Previous research found that methylation on the promoter of genes repressed gene expression. Thus, we plotted the scatter diagram to visualize the relationship of DNA methylation in the promoters and gene expression of these two kinds of beef. Although correlations are very low between gene expression and DNA methylation of the promoters as shown in **Figure 5**, some genes, such as *MYH8, UHRF1*, *LCT, ACVR1B*, *NAALAD2, PLA2G4A*, *BDKRB1,* and *ANTXR1* were identified to exhibit an inverse relationship between expression and methylation. Therefore, these genes may be used as biomarkers of DNA methylation regulating beef tenderness.

## DISCUSSION

Tenderness is one of the most critical factors influencing beef palatability and consumers willingly pay a higher price for beef with guaranteed tenderness. Therefore, consumers' sensory to beef tenderness is a crucial factor in making a purchase decision (Van Wezemael et al., 2014). Tenderness can be evaluated by sensory methods or instrumental methods. Neural methods assessed by expert panels or untrained consumers are time-consuming and expensive. Therefore, there have been many efforts to devise instrumental methods for determining beef tenderness. The most widely used and accepted method is the Warner–Bratzler method because of programming operation and objective results (Yancey et al., 2010). There is a moderate relationship between Warner–Bratzler shear and sensory assessment of beef tenderness (Destefanis et al., 2008; Wright et al., 2018).

Meat quality is a complex trait controlled by many factors, including genetics, epigenetics, and environments. DNA methylation has been reported to play essential roles in muscle biology. It represses transcription by blocking the binding of transcription factors and promoting the formation of an inactive compact chromatin structure (Picard et al., 2014). DNMT1, one of DNMT family members, is differentially expressed in the muscle of pigs with different fat contents, whereas DNMT3b is a known factor affecting beef quality traits (Zhang et al., 2014). It was reported that *MYF6* is highly expressed and hypermethylated in lean pigs compared to high-fat pigs (Nogalski et al., 2018). An SNP in the *ELOVL6* gene is associated with an increase in methylation and a decrease of its expression, which may result in the different fatty acid contents in muscle and backfat (Li and Durbin, 2010). Moreover, methylation on pectoral muscle tissues has a highly significant effect on muscle fiber

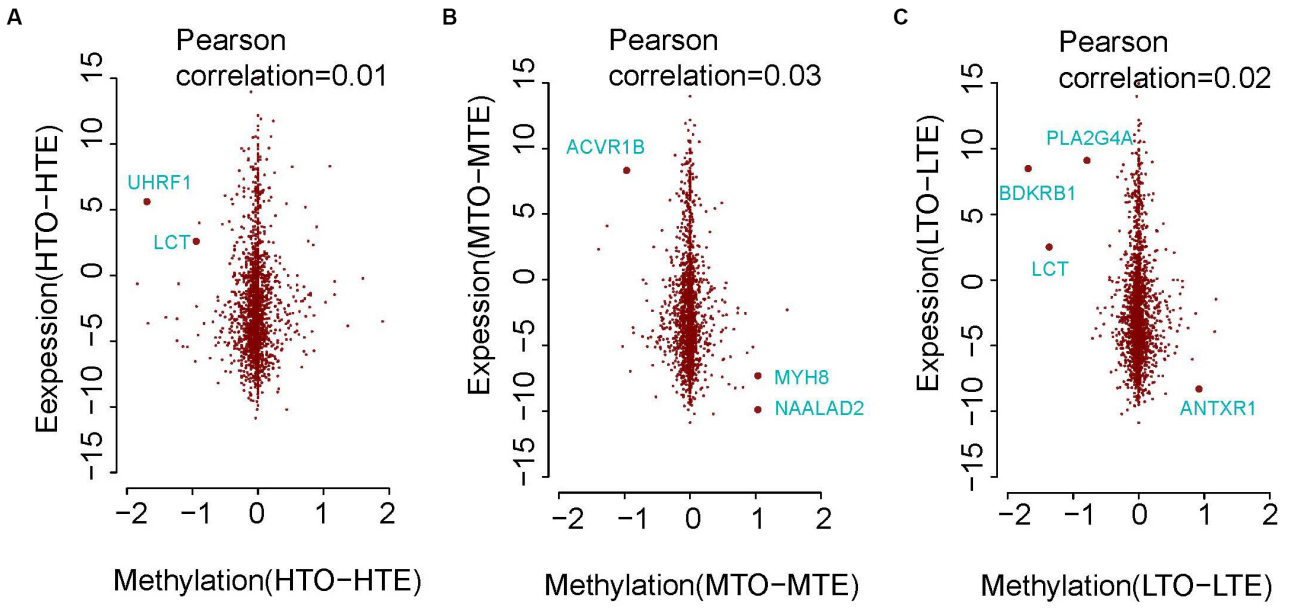



**FIGURE 5 |** The relationship of methylation and gene expression between the tender and tough beef. **(A)** In high methylation regions. **(B)** In medium methylation regions. **(C)** In low methylation regions.

density and drip loss in broilers (Farke et al., 2008). Methylation affected the expression of *FGF2* in the leg muscles of broiler, which is related to myoblast proliferation and meat quality (Anderson et al., 2012). Hypermethylation in the downregulation of *HK-2* and *PFKFB4* decreased glycolytic potential in the psoas major (Goncalves et al., 2018). Additionally, hypomethylation in the upregulation of miR-378 silences the expression of the target genes and promotes capillary biosynthesis in the muscle (Goncalves et al., 2018). Importantly, DNA methylation plays a role during myogenic differentiation. During differentiation of the myoblast global DNA methylation levels increase, and hypermethylation is associated with genes involved in muscle contraction processes (Miyata et al., 2015), and coordinately regulate genes during myogenic differentiation (Miyata et al., 2015; Laker and Ryall, 2016). Collectively, DNA methylation definitely involves in meat quality, and it could be a major epigenetic regulator of beef quality.

MBD-seq, compared to other methods, is a cost-effective way to evaluate DNA methylation on the whole genome. Its strategy is to reduce the complexity of the genome by enrichment of methylated DNA with MethylCap protein against 5-methylcytosine. But it likely produces a bias toward the high-CpG-dense regions because the highly methylated regions are preferentially captured. That was why we performed step-wise elution for the capture of the methylated DNA to stratify the genome into different methylated CpG fractions (Brinkman et al., 2010). DNA fragments with only a few methyl-CpGs are found in the low salt elution, while fragments containing many methyl-CpGs are only eluted at the high-salt. Step-wise elution facilitates the detection of differentially methylated regions not only within the highly CpG dense regions like CpG islands but also in the regions with lower CpG density such as non-CpG islands and other regions. Using this approach, we acquired high sequence coverage during sequencing. We analyzed the data of the high, medium, and low methylated regions, respectively, to assess DNA methylation variations between the tender and tough groups. In the present study, the exons had a much higher degree of methylation than the other regions, and around 60% of the peaks are located in the intergenic regions. Additionally, we observed that the methylation of exons correlates highly and negatively with the gene expression in beef. All these results support our hypothesis that DNA methylation is involved in beef tenderness variation.

In annotation corresponding to DMRs, the ATP binding cassette family is the most important gene sets. This family, also known as the ABC superfamily, encodes proteins that use ATP as an energy resource to transport substrates across the cell membranes. Its members are essential for many processes in the cell and are thought to participate in the absorption and secretion of endogenous and exogenous substances and muscle regeneration (Bunting, 2002). More than 100 ABC transporters are identified from prokaryotes to humans, of which, more than 30 have been reported in cattle. For example, the expression of *ABCB1* and *ABCG2* were detected in the rumen (Anders and Huber, 2010). Researches in cattle found that ABC transporters mainly function on lipid transport. *ABCA1*, *ABCG1*, and *ABCA7* are differentially expressed between the lactation and non-lactating stages, showing species-specific patterns in mammary tissue (Mani et al., 2010). The enhanced expression for *ABCA1* and decreased expression for *ABCA7*, *ABCG2* was observed in bovine mammary tissue during the dry period of lactation (Farke et al., 2008). The presence of *ABCAS*, *ABCA1*, and *ABCG1* are involved in muscle activity and mammary epithelial cells (Dean et al., 2001; Mani et al., 2011). However, very few reports on ABC

transporters were related to beef quality. In our study, A total of 21 members of ATP binding cassette subfamily were identified as being differentially methylated between the tender and tough beef, and they include: *ABCA3*, *ABCA4, ABCA5, ABCA6, ABCA10, ABCA12, ABCA13, ABCB7, ABCB9, ABCB10, ABCC1, ABCC3, ABCC5, ABCC6, ABCC9, ABCD1, ABCD3, ABCD4, ABCF3, ABCG1, ABCG2*. Differential methylation of these ABC transporters may influence the extent of lipid transport and result in fatty acid metabolism of the *longissimus lumborum*, consistent with our previous results that fat contents of the tender and tough beef differ (Zhao et al., 2012b).

Importantly, myosin related genes were another ones differentially methylated between these two kinds of beef. Myosins are a superfamily of motor proteins known for their roles in muscle contraction. The structure and function of myosins are globally conserved across species. Some isoforms of myosins have specialized functions in certain cell types, such as muscle. Some researchers have linked myosins with meat tenderness (Goncalves et al., 2018). Myosin light chain 1 was reported as a potential indicator of proteolysis and tenderness of beef when it is released from myofibrillar fraction during postmortem aging (Anderson et al., 2012). And myosin heavy chain IIX was found inversely related to beef tenderness (Picard et al., 2014). Additionally, *MyHC-I*, *MyHC-IIa,* and *MyHC-IIx* exhibit different expression patterns across various locations of skeletal muscle, and expression levels are negatively related to beef tenderness (Zhang et al., 2014). These, however, are contrary to our previous results that *MYH3* and *MYH8* are positively associated with beef tenderness (Zhao et al., 2012b). Therefore, the relationships between MyHC and tenderness are variable, implying that other environmental or epigenetic factors may play roles in the regulation of MyHC and beef tenderness (Maltin et al., 2003; Chriki et al., 2012). Herein we observed myosin-related genes were differentially methylated between the tender and tough beef. They belong to three categories, namely myosins (*MYO5A, MYO10, MYO15A, MYO16, MYO18B, MYO19, MYO1B, MYO1C, MYO1D, MYO1F, MYO1G, MYO3B, MYO5B, MYO7A, MYO7B, MYO9B*), myosin heavy chains (*MYH10, MYH14, MYH6, MYH7B, MYH8, MYH9*), myosin light chains (*MYL3, MYLK, MYLK4*). *MYH8* was only found differentially methylated while distinctly expressed in the tender and tough beef. The other myosins were not differentially expressed, suggesting that DNA methylation effects may act upon more distal genes, therefore may be too subtle to detect using our approach, or other mechanisms may be involved in.

Many factors influence beef quality and tenderness, such as breeds, production style, sex, slaughtering age, welfare before slaughter, and other environmental impacts, including temperature, humidity, management, nutrition, *etc*. Even in the same animal, meat quality varies among different parts of the carcass. Additionally, postmortem factors, affecting the conversion of muscle to meat, also contribute to the variation of beef tenderness (Maltin et al., 2003; Hocquette et al., 2012; Bonny et al., 2018). Our study was conducted using steers of Angus from one cut of *longissimus lumborum* only. Therefore, further research needs to be conducted to explore the biological effects of epigenetic factors regulating beef quality and tenderness.

## CONCLUSION

In this study, we report the DNA methylome profiling in divergent tenderness of beef. We found that methylations were mainly observed on the intron and exon of genes. Differential patterns of DMRs were identified between the tender and tough beef. Based on the selected DMRs, ATP binding cassette subfamily and myosin-related genes were highly methylated gene sets. Generation of neurons, GTPase activity, ion transport, and anion transport were the most profoundly affected pathways related to beef tenderness. Meanwhile, we also explored the relationship between DNA methylation and gene expression, implying that *MYH8, NAALAD2, PLA2G4A, UHRF1* were the most likely candidate biomarkers for beef tenderness. Overall, this first study of DNA methylome on beef tenderness may provide more in-depth insight into the mechanisms regulating meat quality, which will help us develop new strategies of beef genetics and breeding.

## DATA AVAILABILITY STATEMENT

The datasets generated for this study can be found in The Angus cattle methylome data have been deposited into the NCBI Gene Expression Omnibus (http://www.ncbi.nlm.nih.gov/geo/query/acc.cgi?acc=GSE127215).

## ETHICS STATEMENT

The animal study was reviewed and approved by the University of Maryland Institutional Animal Care and Use Committee (Protocol # R-07-05). Written informed consent was obtained from the owners for the participation of their animals in this study.

## AUTHOR CONTRIBUTIONS

JS conceived and designed the experiments. CZ, YL, JS, and FT performed the experiments. GJ and JC analyzed the data. CZ, GJ, JC, RB, LZ, and JS wrote the manuscript. All the authors contributed to the article and approved the submitted version.

## ACKNOWLEDGMENTS

This work was supported by the Maryland Agricultural Experiment Station (MAES), Jorgensen Endowment Funds, China Postdoctoral Science Foundation (2016M590977), and the Shaanxi Key Research and Development Program (2018ZDXM-NY-046).

## SUPPLEMENTARY MATERIAL

The Supplementary Material for this article can be found online at: https://www.frontiersin.org/articles/10.3389/fgene.2020.00939/full#supplementary-material

## REFERENCES


Anders, S., and Huber, W. (2010). Differential expression analysis for sequence count data.*Genome Biol.* 11, R106. doi: 10.1186/gb-2010-11-10-r106

Anderson, M. J., Lonergan, S. M., and Huff-Lonergan, E. (2012). Myosin light chain 1 release from myofibrillar fraction during postmortem aging is a potential indicator of proteolysis and tenderness of beef. *Meat. Sci.* 90, 345–351. doi: 10.1016/j.meatsci.2011.07.021

Boleman, S. J., Boleman, S. L., Miller, R. K., Taylor, J. F., Cross, H. R., Wheeler, T. L., et al. (1997). Consumer evaluation of beef of known categories of tenderness. *J. Anim. Sci.* 75, 1521–1524.

Bonny, S. P., O'Reilly, R. A., Pethick, D. W., Gardner, G. E., Hocquette, J.-F., and Pannier, L. J. J. O. I. A. (2018). Update of Meat Standards Australia and the cuts based grading scheme for beef and sheepmeat. *J. Integr. Agric.* 17, 1641–1654.

Brinkman, A. B., Simmer, F., Ma, K., Kaan, A., Zhu, J., and Stunnenberg, H. G. (2010). Whole-genome DNA methylation profiling using MethylCap-seq. *Methods* 52, 232–236. doi: 10.1016/j.ymeth.2010.06.012

Bunting, K. D. (2002). ABC transporters as phenotypic markers and functional regulators of stem cells. *Stem Cells* 20, 11–20. doi: 10.1634/stemcells.20-3-274

Carrillo, J. A., He, Y., Luo, J., Menendez, K. R., Tablante, N. L., Zhao, K., et al. (2015). Methylome analysis in chickens immunized with infectious laryngotracheitis vaccine. *PLoS One* 10:e0100476. doi: 10.1371/journal.pone.0100476

Chavez, L., Jozefczuk, J., Grimm, C., Dietrich, J., Timmermann, B., Lehrach, H., et al. (2010). Computational analysis of genome-wide DNA methylation during the differentiation of human embryonic stem cells along the endodermal lineage. *Genome Res.* 20, 1441–1450. doi: 10.1101/gr.110114.110

Chen, Y., Chen, Y., Shi, C., Huang, Z., Zhang, Y., Li, S., et al. (2018). SOAPnuke: a MapReduce acceleration-supported software for integrated quality control and preprocessing of high-throughput sequencing data. *Gigascience* 7, 1–6. doi: 10.1093/gigascience/gix120

Chriki, S., Gardner, G. E., Jurie, C., Picard, B., Micol, D., Brun, J. P., et al. (2012). Cluster analysis application identifies muscle characteristics of importance for beef tenderness. *BMC Biochem.* 13:29. doi: 10.1186/1471-2091-13-29

Couldrey, C., Brauning, R., Bracegirdle, J., Maclean, P., Henderson, H. V., and McEwan, J. C. (2014). Genome-wide DNA methylation patterns and transcription analysis in sheep muscle. *PLoS One* 9:e101853. doi: 10.1371/journal.pone.0101853

Dean, M., Rzhetsky, A., and Allikmets, R. (2001). The human ATP-binding cassette (ABC) transporter superfamily. *Genome Res.* 11, 1156–1166. doi: 10.1101/gr.184901

Delgado, C. L. (2003). Rising consumption of meat and milk in developing countries has created a new food revolution. *J. Nutr.* 133, 3907S–3910S.

Destefanis, G., Brugiapaglia, A., Barge, M. T., and Dal Molin, E. (2008). Relationship between beef consumer tenderness perception and Warner-Bratzler shear force. *Meat. Sci.* 78, 153–156. doi: 10.1016/j.meatsci.2007.05.031

Down, T. A., Rakyan, V. K., Turner, D. J., Flicek, P., Li, H., Kulesha, E., et al. (2008). A Bayesian deconvolution strategy for immunoprecipitation-based DNA methylome analysis. *Nat. Biotechnol.* 26, 779–785. doi: 10.1038/nbt1414

Enriquez-Valencia, C. E., Pereira, G. L., Malheiros, J. M., de Vasconcelos Silva, J., Albuquerque, L. G., de Oliveira, H. N., et al. (2017). Effect of the g.98535683A > G SNP in the CAST gene on meat traits of Nellore beef cattle (Bos indicus) and their crosses with *Bos taurus*. *Meat. Sci.* 123, 64–66. doi: 10.1016/j.meatsci.2016.09.003

Farke, C., Meyer, H. H., Bruckmaier, R. M., and Albrecht, C. (2008). Differential expression of ABC transporters and their regulatory genes during lactation and dry period in bovine mammary tissue. *J. Dairy Res.* 75, 406–414. doi: 10.1017/s002202990800335x

Ferraris, D. C., Libertino, L. M., Rodriguez, G. L., and Hough, G. E. (2013). How thick do consumers' want their meat and how thick do they get it? The case of deep-fried breaded beef. *Food Sci. Technol. Int.* 19, 335–342. doi: 10.1177/1082013212452586

Frattini, S., Capra, E., Lazzari, B., McKay, S. D., Coizet, B., Talenti, A., et al. (2017). Genome-wide analysis of DNA methylation in hypothalamus and ovary of *Capra hircus*. *BMC Genomics* 18:476. doi: 10.1186/s12864-017-3866-4

Gagaoua, M., Terlouw, C., Richardson, I., Hocquette, J. F., and Picard, B. (2019). The associations between proteomic biomarkers and beef tenderness depend on the end-point cooking temperature, the country origin of the panelists and breed. *Meat. Sci.* 157:107871. doi: 10.1016/j.meatsci.2019.06.007

Galbraith, H. (2002). Hormones in international meat production: biological, sociological and consumer issues. *Nutr. Res. Rev.* 15, 293–314. doi: 10.1079/nrr200246

Goldberg, A. D., Allis, C. D., and Bernstein, E. (2007). Epigenetics: a landscape takes shape. *Cell* 128, 635–638.

Goncalves, T. M., de Almeida Regitano, L. C., Koltes, J. E., Cesar, A. S. M., da Silva Andrade, S. C., Mourao, G. B., et al. (2018). Gene co-expression analysis indicates potential pathways and regulators of beef tenderness in nellore cattle. *Front. Genet.* 9:441. doi: 10.3389/fgene.2018.00441

Hocquette, J.-F., Bernard-Capel, C., Vidal, V., Jesson, B., Levéziel, H., Renand, G., et al. (2012). The GENOTEND chip: a new tool to analyse gene expression in muscles of beef cattle for beef quality prediction. *BMC Vet. Res.* 8:135. doi: 10.1186/1746-6148-8-135

Hocquette, J. F., Van Wezemael, L., Chriki, S., Legrand, I., Verbeke, W., Farmer, L., et al. (2013). Modelling of beef sensory quality for a better prediction of palatability. *Meat. Sci.* 97, 316–322. doi: 10.1016/j.meatsci.2013.07.031

Huang, Y. Z., Sun, J. J., Zhang, L. Z., Li, C. J., Womack, J. E., Li, Z. J., et al. (2014). Genome-wide DNA methylation profiles and their relationships with mRNA and the microRNA transcriptome in bovine muscle tissue (*Bos taurine*). *Sci. Rep.* 4:6546.

Huffman, K. L., Miller, M. F., Hoover, L. C., Wu, C. K., Brittin, H. C., and Ramsey, C. B. (1996). Effect of beef tenderness on consumer satisfaction with steaks consumed in the home and restaurant. *J. Anim. Sci.* 74, 91–97.

Laker, R. C., and Ryall, J. G. (2016). DNA methylation in skeletal muscle stem cell specification, proliferation, and differentiation. *Stem Cells Int.* 2016:5725927. doi: 10.1155/2016/5725927

Leal-Gutierrez, J. D., Elzo, M. A., Johnson, D. D., Hamblen, H., and Mateescu, R. G. (2019). Genome wide association and gene enrichment analysis reveal membrane anchoring and structural proteins associated with meat quality in beef. *BMC Genomics* 20:151. doi: 10.1186/s12864-019-5518-3

Lee, J. R., Hong, C. P., Moon, J. W., Jung, Y. D., Kim, D. S., Kim, T. H., et al. (2014). Genome-wide analysis of DNA methylation patterns in horse. *BMC Genomics* 15:598. doi: 10.1186/1471-2164-15-598

Li, H., and Durbin, R. (2010). Fast and accurate long-read alignment with Burrows-Wheeler transform. *Bioinformatics* 26, 589–595. doi: 10.1093/bioinformatics/btp698

Li, M., Wu, H., Luo, Z., Xia, Y., Guan, J., Wang, T., et al. (2012). An atlas of DNA methylomes in porcine adipose and muscle tissues. *Nat. Commun.* 3:850. doi: 10.1038/ncomms1854

Li, Q., Li, N., Hu, X., Li, J., Du, Z., Chen, L., et al. (2011). Genome-wide mapping of DNA methylation in chicken. *PLoS One* 6:e19428. doi: 10.1371/journal.pone.0019428

Li, Y., Carrillo, J. A., Ding, Y., He, Y., Zhao, C., Liu, J., et al. (2019). DNA methylation, microRNA expression profiles and their relationships with transcriptome in grass-fed and grain-fed Angus cattle rumen tissue. *PLoS One* 14:e0214559. doi: 10.1371/journal.pone.0214559

Liu, T. (2014). Use model-based Analysis of ChIP-Seq (MACS) to analyze short reads generated by sequencing protein-DNA interactions in embryonic stem cells. *Methods Mol. Biol.* 1150, 81–95. doi: 10.1007/978-1-4939-0512-6_4

Maltin, C., Balcerzak, D., Tilley, R., and Delday, M. (2003). Determinants of meat quality: tenderness. *Proc. Nutr. Soc.* 62, 337–347.

Mani, O., Korner, M., Ontsouka, C. E., Sorensen, M. T., Sejrsen, K., Bruckmaier, R. M., et al. (2011). Identification of ABCA1 and ABCG1 in milk fat globules and mammary cells–implications for milk cholesterol secretion. *J. Dairy Sci.* 94, 1265–1276. doi: 10.3168/jds.2010-3521

Mani, O., Korner, M., Sorensen, M. T., Sejrsen, K., Wotzkow, C., Ontsouka, C. E., et al. (2010). Expression, localization, and functional model of cholesterol transporters in lactating and nonlactating mammary tissues of murine, bovine, and human origin. *Am. J. Physiol. Regul. Integr. Comp. Physiol.* 299, R642–R654. doi: 10.1152/ajpregu.00723.2009

McNeill, S., and Van Elswyk, M. E. (2012). Red meat in global nutrition. *Meat. Sci.* 92, 166–173. doi: 10.1016/j.meatsci.2012.03.014

Mendoza-Garces, L., Rodriguez-Dorantes, M., Alvarez-Delgado, C., Vazquez-Martinez, E. R., Garcia-Tobilla, P., and Cerbon, M. A. (2013). Differential DNA methylation pattern in the A and B promoters of the progesterone receptor is associated with differential mRNA expression in the female rat hypothalamus during proestrus. *Brain Res.* 1535, 71–77. doi: 10.1016/j.brainres.2013.08.042

Miyata, K., Miyata, T., Nakabayashi, K., Okamura, K., Naito, M., Kawai, T., et al. (2015). DNA methylation analysis of human myoblasts during in vitro myogenic differentiation: de novo methylation of promoters of muscle-related genes and its involvement in transcriptional down-regulation. *Hum. Mol. Genet.* 24, 410–423. doi: 10.1093/hmg/ddu457

Morales, L. E., Griffith, G., Wright, V., Fleming, E., Umberger, W., and Hoang, N. (2013). Variables affecting the propensity to buy branded beef among groups of Australian beef buyers. *Meat. Sci.* 94, 239–246. doi: 10.1016/j.meatsci.2013.02.005

Nishimura, T. (2010). The role of intramuscular connective tissue in meat texture. *Anim. Sci. J.* 81, 21–27. doi: 10.1111/j.1740-0929.2009.00696.x

Nogalski, Z., Pogorzelska-Przybyłek, P., Sobczuk-Szul, M., Nogalska, A., Modzelewska-Kapituła, M., and Purwin, C. (2018). Carcass characteristics and meat quality of bulls and steers slaughtered at two different ages. *Ital. J. Anim. Sci.* 17, 279–288. doi: 10.1080/1828051X.2017.1383861

Patten, L. E., Hodgen, J. M., Stelzleni, A. M., Calkins, C. R., Johnson, D. D., and Gwartney, B. L. (2008). Chemical properties of cow and beef muscles: benchmarking the differences and similarities. *J. Anim. Sci.* 86, 1904–1916. doi: 10.2527/jas.2007-0478

Picard, B., Gagaoua, M., Micol, D., Cassar-Malek, I., Hocquette, J. F., and Terlouw, C. E. (2014). Inverse relationships between biomarkers and beef tenderness according to contractile and metabolic properties of the muscle. *J. Agric. Food Chem.* 62, 9808–9818. doi: 10.1021/jf501528s

Picard, B., Lebret, B., Cassar-Malek, I., Liaubet, L., Berri, C., Le Bihan-Duval, E., et al. (2015). Recent advances in omic technologies for meat quality management. *Meat. Sci.* 109, 18–26. doi: 10.1016/j.meatsci.2015.05.003

Raes, K., Balcaen, A., Dirinck, P., De Winne, A., Claeys, E., Demeyer, D., et al. (2003). Meat quality, fatty acid composition and flavour analysis in Belgian retail beef. *Meat. Sci.* 65, 1237–1246. doi: 10.1016/s0309-1740(03)00031-7

Silva, V. H., Regitano, L. C., Geistlinger, L., Pertille, F., Giachetto, P. F., Brassaloti, R. A., et al. (2016). Genome-wide detection of CNVs and their association with meat tenderness in nelore cattle. *PLoS One* 11:e0157711. doi: 10.1371/journal.pone.0157711

Song, M., He, Y., Zhou, H., Zhang, Y., Li, X., and Yu, Y. (2016). Combined analysis of DNA methylome and transcriptome reveal novel candidate genes with susceptibility to bovine *Staphylococcus aureus* subclinical mastitis. *Sci. Rep.* 6:29390.

Tornberg, E. (1996). Biophysical aspects of meat tenderness. *Meat. Sci.* 43, 175–191.

Van Wezemael, L., De Smet, S., Ueland, O., and Verbeke, W. (2014). Relationships between sensory evaluations of beef tenderness, shear force measurements and consumer characteristics. *Meat. Sci.* 97, 310–315. doi: 10.1016/j.meatsci.2013.07.029

Wang, B., Ji, G., Naeem, H., Wang, J., Kantharidis, P., Powell, D., et al. (2018). The use of targeted next generation sequencing to explore candidate regulators of TGF-beta1's impact on kidney cells. *Front. Physiol.* 9:1755. doi: 10.3389/fphys.2018.01755

Wilson, A. G. (2008). Epigenetic regulation of gene expression in the inflammatory response and relevance to common diseases. *J. Periodontol.* 79, 1514–1519.

Wright, S. A., Ramos, P., Johnson, D. D., Scheffler, J. M., Elzo, M. A., Mateescu, R. G., et al. (2018). Brahman genetics influence muscle fiber properties, protein degradation, and tenderness in an Angus-Brahman multibreed herd. *Meat. Sci.* 135, 84–93. doi: 10.1016/j.meatsci.2017.09.006

Yancey, J. W., Apple, J. K., Meullenet, J. F., and Sawyer, J. T. (2010). Consumer responses for tenderness and overall impression can be predicted by visible and near-infrared spectroscopy, Meullenet-Owens razor shear, and Warner-Bratzler shear force. *Meat. Sci.* 85, 487–492. doi: 10.1016/j.meatsci.2010.02.020

Zhang, M., Liu, Y. L., Fu, C. Y., Wang, J., Chen, S. Y., Yao, J., et al. (2014). Expression of MyHC genes, composition of muscle fiber type and their association with intramuscular fat, tenderness in skeletal muscle of Simmental hybrids. *Mol. Biol. Rep.* 41, 833–840. doi: 10.1007/s11033-013-2923-6

Zhang, M., Yan, F.-B., Li, F., Jiang, K.-R., Li, D.-H., Han, R.-L., et al. (2017). Genome-wide DNA methylation profiles reveal novel candidate genes associated with meat quality at different age stages in hens. *Sci. Rep.* 7:45564.

Zhao, C., Carrillo, J. A., Tian, F., Zan, L., Updike, S. M., Zhao, K., et al. (2015). Genome-wide H3K4me3 analysis in angus cattle with divergent tenderness. *PLoS One* 10:e0115358. doi: 10.1371/journal.pone.0115358

Zhao, C., Tian, F., Yu, Y., Liu, G., Zan, L., Updike, M. S., et al. (2012a). miRNA-dysregulation associated with tenderness variation induced by acute stress in Angus cattle. *J. Anim. Sci. Biotechnol.* 3:12.

Zhao, C., Tian, F., Yu, Y., Luo, J., Hu, Q., Bequette, B. J., et al. (2012b). Muscle transcriptomic analyses in Angus cattle with divergent tenderness. *Mol. Biol. Rep.* 39, 4185–4193.

Zhao, C., Zan, L., Wang, Y., Updike, M. S., Liu, G., Bequette, B. J., et al. (2014). Functional proteomic and interactome analysis of proteins associated with beef tenderness in Angus cattle. *Livestock Sci.* 161, 201–209.

**Conflict of Interest:** GJ was employed by the company Shenzhen GenDo, Co., Ltd.

The remaining authors declare that the research was conducted in the absence of any commercial or financial relationships that could be construed as a potential conflict of interest.

*Copyright © 2020 Zhao, Ji, Carrillo, Li, Tian, Baldwin, Zan and Song. This is an open-access article distributed under the terms of the Creative Commons Attribution License (CC BY). The use, distribution or reproduction in other forums is permitted, provided the original author(s) and the copyright owner(s) are credited and that the original publication in this journal is cited, in accordance with accepted academic practice. No use, distribution or reproduction is permitted which does not comply with these terms.*

frontiers in Genetics

ORIGINAL RESEARCH
published: 25 September 2020
doi: 10.3389/fgene.2020.567812

# Integrated Transcriptome and Histone Modification Analysis Reveals NDV Infection Under Heat Stress Affects Bursa Development and Proliferation in Susceptible Chicken Line

*Ganrea Chanthavixay[1], Colin Kern[1], Ying Wang[1], Perot Saelao[1], Susan J. Lamont[2], Rodrigo A. Gallardo[3], Gonzalo Rincon[4] and Huaijun Zhou[1]**

*[1] Department of Animal Science, University of California, Davis, Davis, CA, United States, [2] Department of Animal Science, Iowa State University, Ames, IA, United States, [3] School of Veterinary Medicine, University of California, Davis, Davis, CA, United States, [4] Zoetis Inc., Parsippany, NJ, United States*

OPEN ACCESS

**Edited by:**
*Eveline M. Ibeagha-Awemu, Agriculture and Agri-Food Canada (AAFC), Canada*

**Reviewed by:**
*Jian Xu, Chinese Academy of Fishery Sciences (CAFS), China*
*Yunliang Jiang, Shandong Agricultural University, China*

***Correspondence:**
*Huaijun Zhou*
*hzhou@ucdavis.edu*

**Specialty section:**
*This article was submitted to Livestock Genomics, a section of the journal Frontiers in Genetics*

**Received:** *30 May 2020*
**Accepted:** *07 September 2020*
**Published:** *25 September 2020*

**Citation:**
*Chanthavixay G, Kern C, Wang Y, Saelao P, Lamont SJ, Gallardo RA, Rincon G and Zhou H (2020) Integrated Transcriptome and Histone Modification Analysis Reveals NDV Infection Under Heat Stress Affects Bursa Development and Proliferation in Susceptible Chicken Line. Front. Genet. 11:567812. doi: 10.3389/fgene.2020.567812*

Two environmental factors, Newcastle disease and heat stress, are concurrently negatively impacting poultry worldwide and warrant greater attention into developing genetic resistance within chickens. Using two genetically distinct and highly inbred layer lines, Fayoumi and Leghorn, we explored how different genetic backgrounds affect the bursal response to a treatment of simultaneous Newcastle disease virus (NDV) infection at 6 days postinfection (dpi) while under chronic heat stress. The bursa is a primary lymphoid organ within birds and is crucial for the development of B cells. We performed RNA-seq and ChIP-seq targeting histone modifications on bursa tissue. Differential gene expression revealed that Leghorn, compared to Fayoumi, had significant down-regulation in genes involved in cell proliferation, cell cycle, and cell division. Interestingly, we also found greater differences in histone modification levels in response to treatment in Leghorns than Fayoumis, and biological processes enriched in associated target genes of H3K27ac and H3K4me1 were similarly associated with cell cycle and receptor signaling of lymphocytes. Lastly, we found candidate variants between the two genetic lines within exons of differentially expressed genes and regulatory elements with differential histone modification enrichment between the lines, which provides a strong foundation for understanding the effects of genetic variation on NDV resistance under heat stress. This study provides further understanding of the cellular mechanisms affected by NDV infection under heat stress in chicken bursa and identified potential genes and regulatory regions that may be targets for developing genetic resistance within chickens.

**Keywords: Newcastle disease virus, heat stress, bursa, RNA-seq, ChIP-seq**

## INTRODUCTION

Infection with the paramyxovirus, Newcastle disease virus (NDV), in chickens has resulted in devastating economic losses across both commercial and backyard poultry farms with mortality rates as high as 100% (Alexander, 2000). The most effective method in preventing and controlling the spread of Newcastle disease (ND) is through biosecurity and vaccines, which when administered effectively can provide up to 100% survival against lethal, velogenic NDV infection in chickens (Stone et al., 1980; Miller et al., 2013). However, vaccination is not a practical option for many farmers in developing countries because vaccination programs are costly, have limited support, and lack proper infrastructure. An additional protective measure that has not been extensively explored is the use of genomics and genetics to improve NDV resistance. Therefore, our efforts have been in identifying genetic variation that is associated with NDV resistance as a method for mitigating the potentially devastating effects of virulent NDV. Variation in NDV resistance has previously been observed between different breeds and lines that were first observed during previous outbreaks (Albiston and Gorrie, 1942).

With global climate change occurring, there is increasing concern about the effects of heat stress. Poultry are experiencing more frequent events of higher temperatures and associated humidity levels, which are likely coupled with detrimental effects of NDV infection. Heat stress is well-known to have negative effects on economic traits such as decreased meat and egg quality and quantity, decreased reproduction, and, in extreme cases, increased mortality (St-Pierre et al., 2003; Mashaly et al., 2004; Barrett et al., 2019; Zaboli et al., 2019). More relevant to our concerns are the effects of heat stress on the immune system. Several studies in chickens under heat stress have provided evidence of increased cell-mediated immunity by stimulating greater numbers of circulating heterophils, which are the predominant leukocyte within birds (Maxwell et al., 1992; Prieto and Campo, 2010). The negative effects of heat stress appear to predominantly be in the humoral and adaptive arm of the immune system. Several studies have shown that heat stress in chickens caused a reduction of antibody levels following vaccination and decreased total white blood cells (Thaxton et al., 1968; Nathan et al., 1976; Maxwell et al., 1992). These results suggest that there is a negative impact that can affect vaccine efficacy or the host's ability to fight infection because B cells are the host's antibody-producing cells and play a large role in building protection against NDV.

The bursa of Fabricius is an organ vital in the development of B cells in avian species. B cells are responsible for producing the host's natural and antigen-specific antibodies, conferring general and broad protection during primary infection and pathogen-specific protection for recurring infections. This essential function of B cells relies on the bursa as a primary lymphoid organ that provides the only site where gene conversion occurs for immunoglobulin (Ig) gene diversification that is critical for producing the B-cell repertoire. At hatching, the bursa is composed almost entirely of B cells (Ko et al., 2018) and continues growing in weight to peak between 5 and 8 weeks posthatching after which involution begins until the organ completely disappears around the age of sexual maturity (∼20–25 weeks) (Ratcliffe and Härtle, 2014). Bursectomy in 2-week-old or younger chicks resulted in reduced hemagglutination inhibition antibody formation to NDV compared to control chicks, illustrating that the bursa plays a significant role in protection against NDV (Matsuda and Bito, 1973). Therefore, exploring the bursal response to NDV infection under heat stress is important for understanding what responses contribute to host resistance.

One of the most important conclusions drawn from reviews of genome-wide association studies (GWAS) is that the majority of trait-associated variants lie within non-coding regions of the genome (Hindorff et al., 2009; Maurano et al., 2012). Even the few studies that performed GWAS for NDV resistance found that most associated single-nucleotide polymorphisms (SNPs) and quantitative trait loci (QTLs) lie within or overlap with non-coding regions (Yonash et al., 2001; Biscarini et al., 2010; Luo et al., 2013; Saelao et al., 2019). Therefore, identification and annotation of genome-wide non-coding regions will aid in identifying regulatory elements and putative causative variants possibly associated with NDV resistance. Here, we performed chromatin immunoprecipitation followed by high-throughput sequencing (ChIP-seq) of histone modifications that have known associations with genome regulatory elements and their state of activities. We selected two active histone modifications: H3K4me3 and H3K27ac, with H3K4me3 predominantly marking active promoters and H3K27ac marking both active promoters and enhancers (Guenther et al., 2007; Mikkelsen et al., 2007; Nègre et al., 2011). H3K4me1 also marks both promoters and enhancers but is not strongly associated with activity and, when appearing on enhancers in the absence of H3K27ac, indicates a poised or primed enhancer (Creyghton et al., 2010; Ernst et al., 2011). H3K27me3 is associated with polycomb-mediated repression, spanning over large repressed regions or regulatory elements (Cao et al., 2002; ENCODE Project Consortium, Birney et al., 2007). To extend our exploration of genome-wide changes within functional genomic regions, transcriptome analysis from RNA-seq was utilized to identify differential gene expression associated with treatment or genetic line in order to identify genes and biological pathways contributing to treatment responses.

The aims of this study were to annotate regulatory elements in chicken bursa and identify genes, regulatory elements, and biological processes of the bursal response contributing to host resistance to NDV infection under heat stress. We took advantage of two genetically distinct and inbred chicken lines, Fayoumi and Leghorn, with Fayoumi being the more relatively resistant line compared to Leghorn as observed through their lower NDV titers and higher NDV-specific antibody levels. Additionally, Fayoumi is hypothesized to be more heat stress–resistant because the line originated from Egypt therefore historically had adapted through natural selection to an environment with higher climate (Wang et al., 2014; Deist et al., 2017; Saelao et al., 2018b). Physiological responses to heat stress have been shown to be significantly different between the two lines, with electrolyte levels appearing to be more well-maintained during heat stress in Fayoumis compared to Leghorns (Wang et al., 2018).

# MATERIALS AND METHODS

## Experimental Design

This study is part of a collaborative project for the Feed the Future Innovation Lab for Genomics to Improve Poultry program[1]. The project involves studying the host genetic contribution to NDV resistance alone and NDV resistance under heat stress, with the latter being the focus of our study and the former at Iowa State University (ISU). The two inbred chicken lines used in this study are Fayoumi (M15.2) and Leghorn (GHs 6), which are maintained at ISU (Ames, IA, United States). The experimental design has been described in previous publications (Saelao et al., 2018a,b; Wang et al., 2018). Upon arriving from ISU, chicks were randomly divided into a non-treated and treated group for each line. Both groups were reared at 29.4°C and 60% humidity until 13 days of age after which the treated group at 14 days of age was subjected to heat stress. Heat stress treatment consisted of 38°C for the first 4 h, after which decreased to 35°C for the remainder of the trial. At 21 days of age, the treated group, while still under heat stress, was inoculated with a total of 200 μL $10^7$ $EID_{50}$ through oral and nasal passages. The non-treated group (25 birds each line) was kept at 25°C and inoculated with phosphate-buffered saline (PBS) at 21 days of age. Four randomly selected birds at each time point were euthanized by $CO_2$. Bursa tissue collected at 6 days postinfection (dpi) was snap-frozen and submerged in RNA*later* for storage in 80°C (Thermo Fisher, Waltham, MA, United States #AM7024). The experiment's procedures were performed according to the guidelines approved by the Institutional Animal Care and Use Committee at the University of California, Davis (IACUC #17853).

## RNA-Seq Experiments

Total RNA (four individuals per group) from bursa tissue stored in RNA*later* was extracted using TRIzol (Thermo Fisher, #15596026), treated with DNase, and purified through ethanol precipitation. Total RNA for each sample was sent to Novogene Co., Ltd. (Beijing, China) where RNA integrity number determined using an Agilent'sBioanalyzer (Agilent Technologies, Santa Clara, CA, United States) was confirmed to be 7 or above. Then, non-directional RNA-seq libraries were prepared and sequenced using Illumina's Hiseq 4000 (Illumina, San Diego, CA, United States) with paired-end 150–base pair (bp) reads.

## RNA-Seq Analysis

Adaptors were trimmed and low-quality reads removed using Trim Galore! (Krueger, 2012) version 0.4.5, with default parameters and aligned using STAR (Dobin et al., 2012) version 2.7.2a to the chicken galGal6 genome assembly and Ensembl annotation 95. Reads were filtered based on alignment quality using SAMtools (Li et al., 2009) version 1.9. **Supplementary Table 1** shows a summary of read alignment for each sample. Raw read counts were obtained using HTSeq (Anders et al., 2014) version 0.9.1, and differential gene analysis was performed with DESeq2 (Love et al., 2014) version 1.22.2 with a design that included treatment group, genetic line, and batch group that refers to the sample prep. Transcript per million expression values were obtained by using StringTie (Pertea et al., 2015) version 2.0.4.

[1] gip.ucdavis.edu

## ChIP-Seq Experiments

ChIP-seq experiments (two biological replicates per group) were performed on 20–30 mg of frozen tissue per sample using the iDeal ChIP-seq kit for Histones (#C01010059) (Diagenode Inc., Denville, NJ, United States). Tissue was homogenized using liquid nitrogen with mortar pestle and then transferred to 1.5-mL microcentrifuge tube containing lysis buffer iL1 from the kit. Cross-linking was performed for 8 min using 1% formaldehyde that was produced from Pierce 16% methanol-free formaldehyde (Thermo Fisher, #28906), quenched with glycine for 10 min, washed twice with PBS, and resuspended in iL1 lysis buffer. After incubating for 20 min on ice, tissue was homogenized with a Dounce homogenizer, centrifuged 5 min at 2,000 × *g*, and resuspended in iL2 buffer for incubation on ice for 10 min. Nuclei were harvested by centrifugation at 2,000 × *g* for 5 min and resuspended in iS1 buffer for incubation on ice for 30 min. All centrifugation steps were performed at 4°C. Chromatin was sheared using the Covaris E220 in snap-cap microTUBEs (Covaris, Inc., Woburn, MA, United States, #520077) for 6 min at 105 W and then 6 min at 140 W. For immunoprecipitation experiments, about 1,000 ng of sheared chromatin (estimated from DNA extraction) was used as input after which the kit protocol was followed with 1 μg of antibody. The antibodies used were from Diagenode Inc.: H3K4me3 (provided in kit), H3K27me3 (#C15410069), H3K27ac (#C15410174), and H3K4me1 (#C15410037). Each sample had ChIP performed for the four histone modifications and an input (no antibody). Libraries were prepared using the NEBNext Ultra DNA library prep kit for Illumina (New England Biolabs, Ipswich, MA, United States, #E7645L), selecting for 150- to 200-bp insert fragment sizes. Libraries were sequenced on Illumina's HiSeq 4000 with single-end 50-bp reads.

## ChIP-Seq Analysis

Adaptors were trimmed and low-quality reads removed using Trim Galore! version 0.4.5 and aligned using BWA (Li and Durbin, 2009) version 0.7.17 to the chicken galGal6 genome. Duplicate reads were marked and removed using SAMtools version 1.9 to eliminate PCR amplification bias. Bam files were converted to tagalign files using BEDtools (Quinlan and Hall, 2010) (version 2.27.1) bamtobed command, which were then input files into MACS2 (Zhang et al., 2008) version 2.1.1 peak caller. For all samples, peak calling included the parameters –to-large and –fix-bimodal. For narrow peaks, which included all modifications except H3K27me3, the cutoff for significance was $q < 0.01$ and included the parameter –call-summits. For broad peaks, the cutoff for significance was $q < 0.05$ and included the parameter –broad. The Jensen–Shannon distance (JSD) quality metric was calculated from the PlotFingerprint command from deepTools 2.0 version 3.3.0 and essentially is a measurement comparing mark sample versus input sample. Measurements should be between 0 and 1, where a higher value indicates a higher-quality library. Pearson correlation plots were produced

using deepTools (**Supplementary Figure 1**). Final read count, number of peak calls, genome coverage, and quality metrics for all individual samples and number of peak calls for each combined group are summarized in **Supplementary Table 2**. Based on the measurements above, we observed that one of the treated Fayoumi samples (1107) appears to be an outlier. Therefore, we removed sample 1107 from further analysis. Combined group peak calls were identified by combining peak calls from both replicates within each group. Peaks that were called in only one replicate but were found to have enrichment in the second replicate were also retained in the combined group peak calls. Pipelines used in this study for peak calling are available at https://github.com/kernco.

## Chromatin State Prediction From ChromHMM

Combined group peak calls were used as the input files for ChromHMM (Ernst and Kellis, 2012) to build a model of state annotations based on the genome-wide combinatorial patterns of the histone modifications across all samples. The most optimal number of chromatin states was determined by creating models between 10 and 16 states using data from all samples and then using only samples within each of the four biological groups. For each state model between 10 and 16, a correlation was calculated for each state between the all-sample model to each of the smaller models created for each of the four groups. An average correlation value was calculated for each state model, and the highest correlation was observed for the 13-state model. The 13-state model was annotated into regulatory regions and their state of activity using several criteria: enrichment around the transcription state site (TSS) and median gene expression as shown in **Supplementary Figure 2**, the known association of each histone modification to regulatory elements and activity prediction as previously described in the introduction, and examples from previously annotated chromatin state modes (Ernst et al., 2011; Roadmap Epigenomics Consortium, Kundaje et al., 2015). In order to assign the promoter regions a chromatin state, a 4,000-bp region centered on the TSS was annotated with the most prevalent overlapping state excluding the low signal/heterochromatin state (state 10). However, the promoter was reassigned to the following states if there was any overlap within the region, which are also ordered by priority if more than two of these occurred: active TSS (state 6), Poised TSS (state 8), and then repressed TSS (state 13).

## Determining Regulatory Regions for Enrichment Analysis

Given the challenge in how to integrate multiple histone marks to determine the regulatory regions that were used to calculate the enrichment levels, we utilized the chromatin state model for this purpose. First, adjacent states were merged using BEDtools (Quinlan and Hall, 2010) version 2.27.1. Then, the co-occurrence of two states were counted and presented as the percentage of a state's total count number in order to observe which chromatin states have a tendency to co-occur together within the same regulatory regions (**Supplementary Figure 3**). Only high confidence states that specifically identified promoters and enhancers were considered; therefore, states 7, 10, and 11 were removed. By looking at the co-occurrence of the states, we observed that in general the active states tend to co-occur together in the same regulatory region and *vice versa* for poised/repressed regions. However, there were still instances where active states co-occur with poised states and, to a lesser degree, repressed states. The co-occurrence analysis, along with visualization of chromatin states and histone peaks on the genome browser (**Supplementary Figure 4**), revealed that multiple chromatin states can characterize one regulatory element and therefore cannot be considered separately for the enrichment analysis when a histone modification peak can overlap multiple chromatin states. For these reasons, adjacent states (excluding states 7, 10, and 11) were merged together, resulting in a total of 45,596 regions that were divided into 15,856 promoter regions and 32,055 distal from promoter regulatory regions (**Supplementary Figure 5**).

## Histone Modification Enrichment Analysis

Enrichment levels for each histone modification were calculated using deepTools' (version 3.3.0) multiBamSummary command to count reads overlapping the regulatory regions produced from merged chromatin states. DESeq2 version 1.22.2 was used to determine differentially enriched regions (DERs) between groups. Normalized read counts were used to produce principal components analysis (PCA) plots (**Figure 5**). Previously, Pearson correlation was used for quality checking ChIP-seq samples because Pearson correlation is more appropriate when comparing samples within a histone modification. Additionally, because the whole genome was utilized to calculate correlation, there will be much more noise that affects the Spearman correlation more than the Pearson correlation. However, when comparing enrichment level fold changes between histone modifications and against gene expression, the measurements are between different assays that may not necessarily be changing at constant rate together, making the Spearman correlation more appropriate for these comparisons.

## Functional Analysis of Differentially Expressed Genes, Regulatory Regions, and Their Associated Target Genes

Associated target genes of DERs were determined by identifying the nearest TSS to each regulatory element. GO terms for biological processes (GO_TERM_BP) and KEGG pathways were identified for differentially expressed genes (DEGs) and associated target genes of DERs using database for annotation, visualization, and integrated discovery (DAVID) (Huang et al., 2007) version 6.8. Ensembl gene IDs were converted to official gene symbols for input into DAVID using Ensembl's Biomart. Significance cutoff was $p < 0.05$. The background chosen was *Homo sapiens* because terms and pathways are much more improved in annotation than *Gallus gallus*, especially for immune-related processes. Additionally, uninformative pathways related to cancer, which were broad and/or unrelated to

the tissue or treatment in the study, were removed from the top 5 pathways shown for the KEGG pathway analysis for Leghorn within-line DEGs. *De novo* transcription factor motif analysis was performed with HOMER (Heinz et al., 2010). The median width of regulatory regions was 2,400 bp; therefore, a 2,400-bp region centered on each DER was used as input for HOMER. Background regions for comparison against the input regions were randomly generated by HOMER.

## Variant Analysis

Whole-genome sequencing data from DNA-seq of Fayoumi and Leghorn birds from Fleming et al. (2016) was used. Adaptors were trimmed and low-quality reads removed using Trim Galore! version 0.4.5 and aligned to the galGal6 reference genome using BWA version 0.7.17. Reads were filtered based on alignment quality ($q < 30$), and duplicate reads were marked with Picard tools were then removed with SAMtools version 1.9. Variant calling of single-nucleotide variants (SNVs) and indels were called using GATK (Van der Auwera et al., 2013) (version 4.1.4.1) HaplotypeCaller command. The ploidy was set to 2, even though the pooled library contained 16 individuals. However, we were only considering homozygous variants between lines; therefore, any heterozygous variants within any individual in a genetic line would have been filtered. Variants were hard-filtered with the following arguments: QD $< 2.0$, FS $> 60.0$, SOR $> 3.0$, MQ $< 40.0$, MQRankSum $< -12.5$, and ReadPosRankSum $< -8.0$. Using BCFtools (Li, 2011) version 1.10.2, variants within each line were filtered if total reads $< 20$, and BEDtools (Quinlan and Hall, 2010) version 2.27.1 was used to identify variants that overlapped exons from the Ensembl galGal6 annotation and regulatory regions used for the histone modification enrichment in this study.

# RESULTS

## Transcriptome Analysis for Treatment and Line Differences

By performing RNA-seq in four groups (combination of two lines and two conditions), four comparisons were made for differential gene analysis on bursa samples from 6 dpi that included within-line comparisons [treated Fayoumis (TF) vs. control Fayoumis (CF) and treated Leghorn (TL) vs. control Leghorn (LC)] and between-line comparisons (CF vs. CL and TF vs. TL).

Within-line comparisons for Fayoumis and Leghorns identified 54 and 1,592 DEGs, respectively (**Supplementary Figure 5A**). Interestingly, DEGs identified in Fayoumis were mostly up-regulated, whereas about two-thirds of DEGs in Leghorns were down-regulated. The top 5 GO terms for biological processes and KEGG pathways for DEGs in within-line comparisons are shown in **Figures 1A,B**. Fayoumis had one significant GO term involving extracellular matrix organization, whereas Leghorns' top 5 GO terms revealed several pathways that appear to be involved in cell cycle (**Figure 1A**). Significant KEGG pathways were found only for the within-line comparison of Leghorns (**Figure 1B**), which also showed pathways related to cell division and cell cycle, as well as other pathways possibly related to heat stress response. In general, considerable down-regulation of DEGs across the top 3 KEGG pathways was observed in the Leghorn line (**Figure 1B**).

The between-line comparisons identified greater numbers of DEGs regardless of treatment (**Supplementary Figure 5B**), illustrating that genetic line was a more influential biological factor in gene expression differences compared to treatment. However, the treated-line comparison produced a greater number of DEGs than the non-treated-line comparison, which alludes to the distinct effects of treatment on each line. Focusing on the genetic line differences due to treatment, the 2,524 DEGs that were specific to the comparison between the treated Fayoumi and treated Leghorn (treated-line comparison) were further explored (**Supplementary Figure 5C**). Separating the DEGs into Fayoumi-biased and Leghorn-biased DEGs (i.e., higher expression in one line), the log2 fold change across all comparisons are presented in **Figure 2A**, the top 5 GO terms are presented in **Figure 2B**, and the top 5 KEGG pathways are presented in **Figure 2C**. Additionally, these DEGs appeared to mainly be due to the changes within Leghorns, where most Fayoumi-biased DEGs or Leghorn-biased DEGs have greater fold changes in expression in the Leghorn within-line comparison (TL vs. CL) compared to the Fayoumi within-line comparison (TF vs. CF) (**Figure 2A**).

The top 5 GO terms and KEGG pathways for Fayoumi-biased and Leghorn-biased DEGs are shown in **Figures 2B,C**. In the top GO terms for Fayoumi-biased DEGs, we again observed processes related to cell division with the addition of those related to mRNA processes, whereas for Leghorn-biased DEGs we observed processes related to various cellular and developmental processes. For the top 5 KEGG pathways with Fayoumi-biased DEGs, we found immune-related KEGG pathways including a very relevant pathway, B-cell receptor signaling pathway, to bursa, which is almost entirely comprised of B cells (Weill et al., 1987; Ko et al., 2018). The top KEGG pathway for the Leghorn-biased DEGs was axon guidance with several other pathways related to cellular processes and interactions such as adherens junction and rap1 signaling pathway.

An interesting pattern was observed in the fold changes of the DEGs specific to the treated-line comparison (TF vs. TL, **Figure 2A**), where a number of those DEGs have a preexisting trend of bias, although not statistically significant (FDR $> 0.05$), toward one line in the comparison between non-treated lines (CF vs. CL). This suggests that for a set of DEGs that have inherently differential expression between the lines, treatment exacerbates the differences in expression between the lines. Exploring this further, we performed *k*-means clustering on the DEGs specific to the treated-line comparison in order to separate the set of DEGs with this specific pattern described above. **Figure 3** shows a heat map of the four clusters with a table that includes descriptions of general regulation patterns observed between lines within a treatment or between treatment groups within a line. The top 2 GO terms and KEGG pathways are also listed for each cluster along with the gene count and -log10 *p*-value. The two clusters that display the specific pattern of interest are clusters 1 and 4. The set of DEGs in cluster 1 show a pattern of Leghorn bias when comparing between non-treated lines (CF

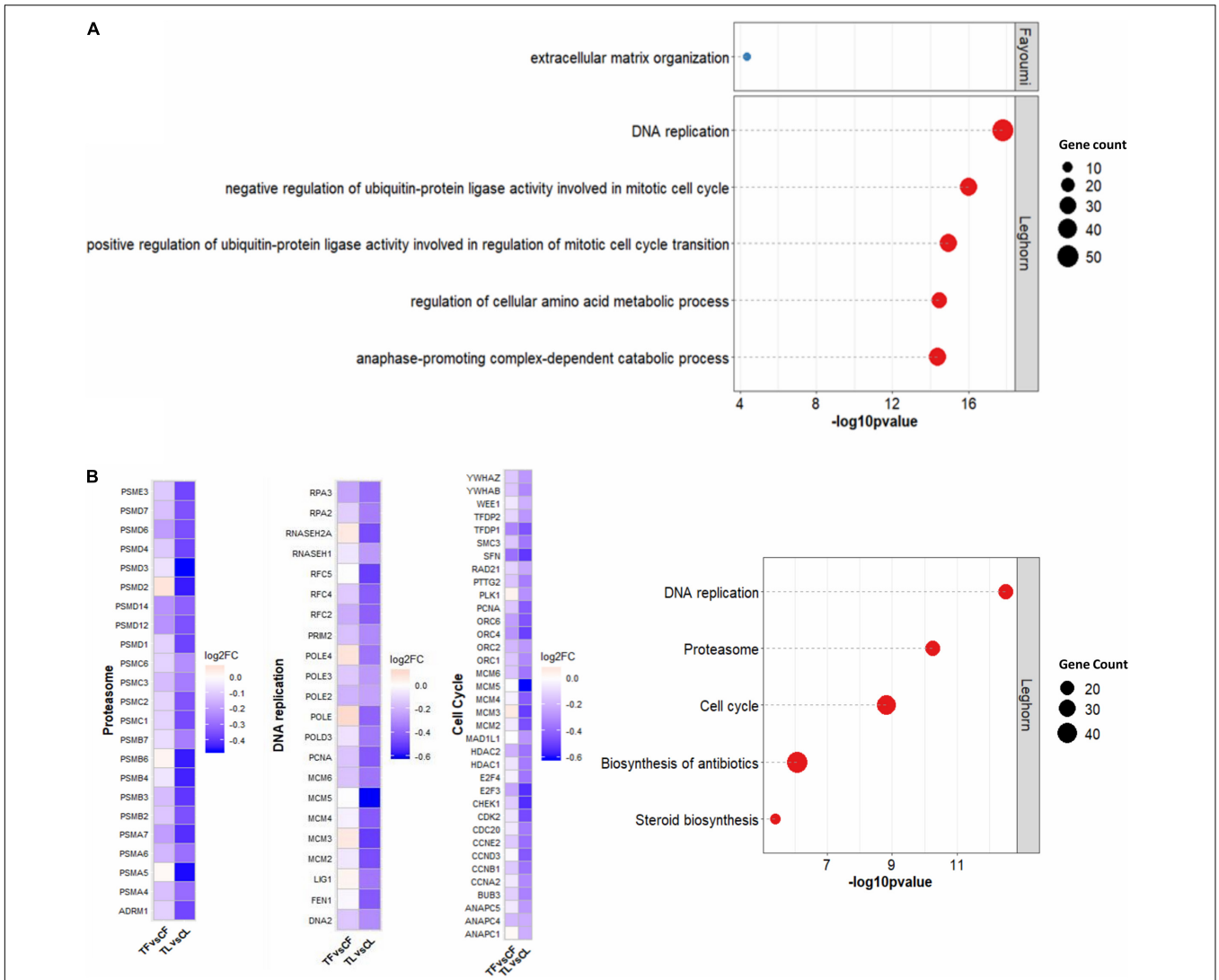



**FIGURE 1 |** Functional analysis of DEGs for within-line comparisons. **(A)** Top 5 GO terms for biological processes. **(B)** Top 5 KEGG pathways on the right were found for Leghorn only and heat map of the log2 fold changes of the DEGs within the top 3 KEGG pathways related to cell proliferation on the left. The number of genes denotes the number of DEGs associated with the term or pathway. Significant GO terms and KEGG pathway were identified by $p < 0.05$ with more than two gene counts. CF, control Fayoumi; TF, treated Fayoumi; CL, control Leghorn; TL, treated.

vs. CL). This magnitude of Leghorn bias then became increased when comparing treated lines (TF vs. TL). Cluster 4 shows a similar pattern except there is a Fayoumi bias. The biological processes in cluster 1 appeared to be more enriched in early development, whereas in cluster 4 the processes relate to cellular processes and immune signaling of lymphocytes. These results suggest that Fayoumis compared to Leghorns may have a more progressed immune cell identity of the bursa that is preserved during treatment.

## Chromatin State Annotation at Promoters of DEGs

To explore the changes in the activation of *cis*-regulatory regions such as promoters and enhancers due to treatment or genetic line differences, we performed replicate ChIP-seq assays for each group in the following four histone modifications: H3K4me3, H3K27ac, H3K4me1, and H3K27me3. Pearson correlation values between the samples showed replicates within groups are highly correlated and clustered by genetic line and treatment (**Supplementary Figure 1**). A summary of the number of peaks called and genome coverage of peaks are provided in **Supplementary Table 2**, alongside the number of aligned and filtered reads and quality metric scores that include FRIP (fraction of reads in peaks) and JSD.

In order to identify and annotate genome-wide *cis*-regulatory elements, we utilized a tool called ChromHMM. The tool allows integration of multiple histone modifications, which increases confidence in more accurate chromatin state annotation, to identify combinatorial patterns that characterize regulatory

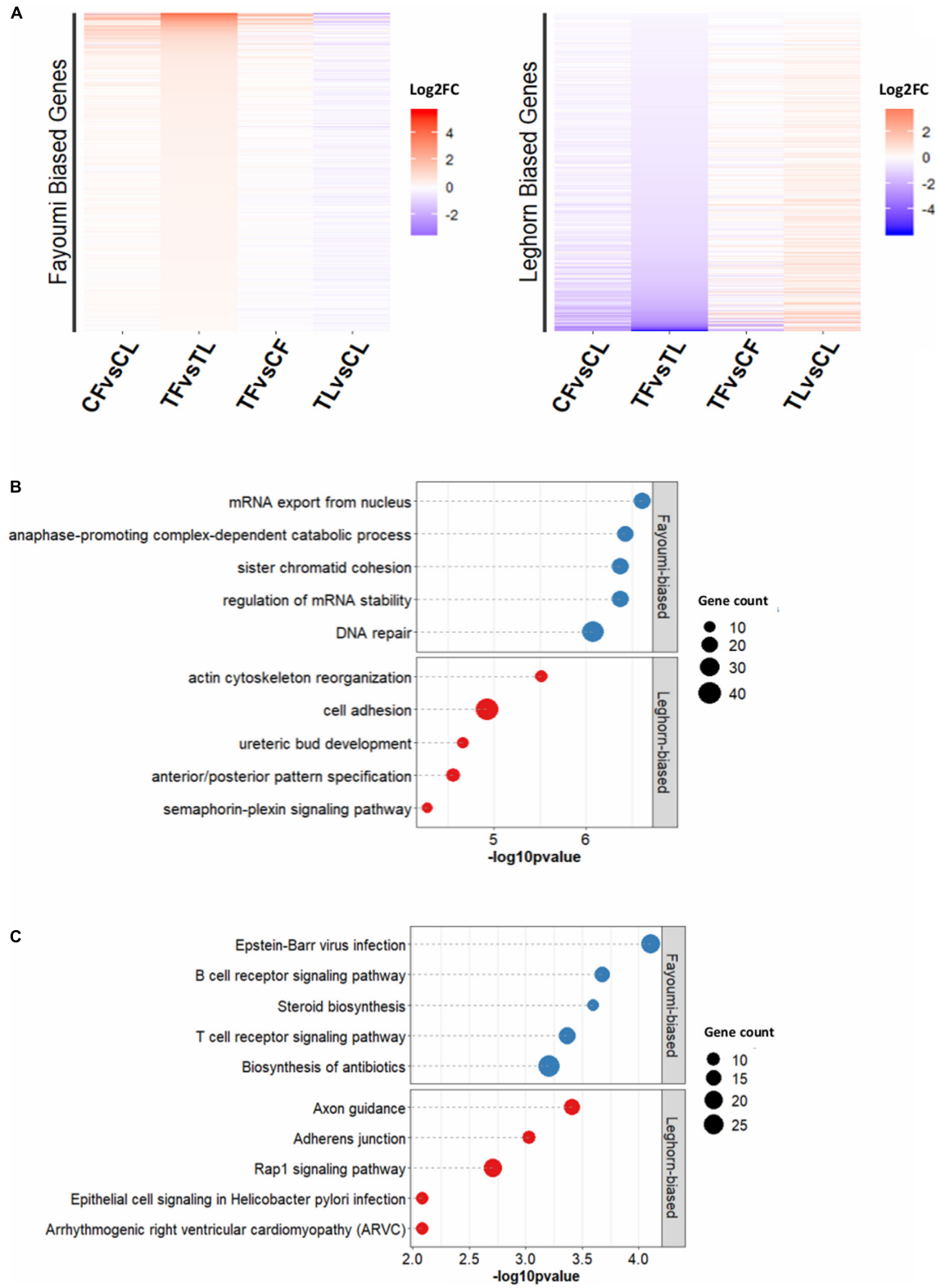
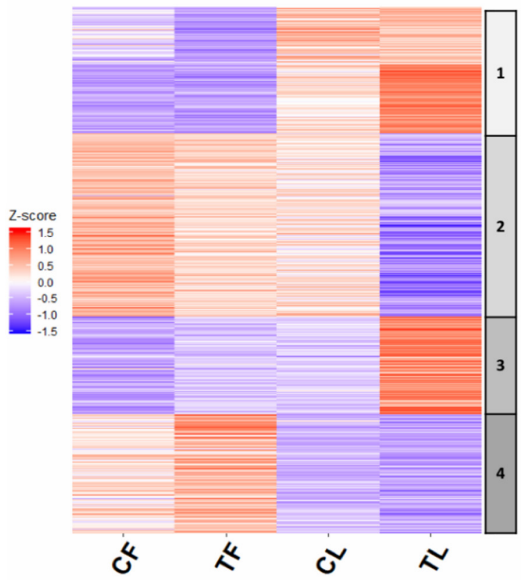



**FIGURE 2 |** Functional analysis of DEGs specific for treated-line comparison. **(A)** Log2FC for Fayoumi-biased and Leghorn-biased DEGs specifically within treated-line comparison compared to control-line comparison. **(B)** The top 5 GO terms for Fayoumi-biased and Leghorn-biased DEGs specific to the treated-line comparison. **(C)** The top 5 KEGG pathways for Fayoumi-biased and Leghorn-biased DEGs specific to treated-line comparison.




| Cluster | Gene Regulation Pattern | Functional Enrichment Terms |
|---|---|---|
| 1 | • Leghorn bias between control lines<br>• Increased Leghorn bias between treated lines<br>• Fayoumi down-regulation or Leghorn up-regulation during treatment | Top 2 GO Terms:<br>• Ureteric bud development (8, 4.64)<br>• Anterior/posterior pattern specific (10, 4.03)<br>Top 2 KEGG pathways:<br>• Vibrio cholerae infection (15, 3.94)<br>• Axon guidance (9, 2.18) |
| 2 | • Fayoumi bias between control lines and treated lines<br>• Down-regulation in both lines during treatment | Top 2 GO Terms:<br>• Anaphase-promoting complex-dependent catabolic process (19, 8.50)<br>• Negative reg. of ubiquitin-protein ligase act. Involved mitotic cell cycle transition (18, 1.16)<br>Top 2 KEGG pathways:<br>• Steroid biosynthesis 98, 4.59)<br>• Proteosome (10, 3.69)<br>***Additionally contains terms related to B cell biology** |
| 3 | • Leghorn bias between control lines and treated lines<br>• Up-regulation in both lines during treatment | Top 2 GO terms:<br>• Focal adhesion assembly (6, 4.11)<br>• Hindlimb morphogenesis (4, 3.45)<br>Top 2 KEGG pathways:<br>• Arrhythmogenic right ventricular cardiomyopathy (6, 1.85)<br>• Amoebiases (7, 1.58) |
| 4 | • Fayoumi bias between control lines<br>• Increased Fayoumi bias between treated lines<br>• Fayoumi up-regulation or Leghorn-downregulation during treatment | Top 2 GO Terms:<br>• Protein phosphorylation (22, 3.04)<br>• DNA repair (14, 2.75)<br>Top 2 KEGG pathways:<br>• T cell receptor signaling pathway (11, 4.52)<br>• ErbB signaling pathway (7, 2.09) |

**FIGURE 3 |** Differentially expressed genes (DEGs) with inherent line biases that increase during treatment show Fayoumi's ability to retain cell-identity development versus Leghorn. The *z* scores were calculated for DEGs that were specific to the treated-line comparison and used in k-means clustering. Five clusters were chosen for the *k*-means clustering, but two clusters with similar gene regulation patterns were combined into cluster 1, resulting in four clusters shown in the heat map above. The chart summarizes the gene pattern regulation of each cluster that describes whether the DEGs had up-regulation or down-regulation between non-treated and treated birds within each line and whether they were Fayoumi-biased or Leghorn-biased for each between-line comparison. The top 2 GO terms and KEGG pathways are shown for each cluster with the number of DEGs enriched in each pathway and –log10 *p*-value. Significant GO terms and KEGG pathway were identified by $p < 0.05$ with more than two gene counts.

regions and the state of activity of regulatory elements for each biological group, thereby facilitating more convenient downstream comparisons of regulatory regions between groups (ENCODE Project Consortium, Birney et al., 2007; Ernst et al., 2011; Roadmap Epigenomics Consortium, Kundaje et al., 2015). A 13-state model was chosen based on criteria explained in Section "Materials and Methods," and the annotation is shown in **Figure 4A**. All 13 states were individually annotated but can generally be categorized into active (red), poised (yellow), and repressed (blue) regulatory elements or regions.

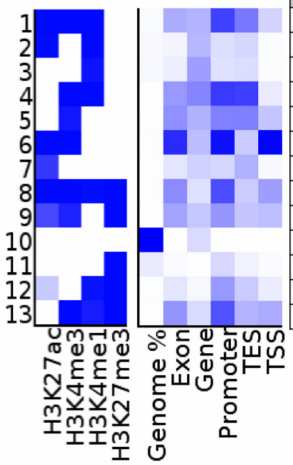
The promoters of all genes were assigned a chromatin state based on the criteria that first prioritize the overlap of specific promoter-enriched states, which if not applicable was then based on the most prevalent state overlap (further described in section "Materials and Methods"). The promoter state of each gene was compared between each group, following the comparisons completed for the gene expression data (**Figure 4B**). The first observation was that promoter states on the majority of DEGs did not change between two groups across all four comparisons. In addition, the majority of DEGs (81%) had active TSS (i.e., chromatin state 6), indicating that regulatory changes due to treatment or genetic line differences occur on constitutively active genes as opposed to regulation of poised or repressed genes (**Figure 5B**). Lastly, most promoter transitions between groups were moderate (i.e., within states of same activity) or to/from poised states (red/blue state to yellow state and *vice versa*) (**Figure 4C**).

The lack of or moderate changes seen in the promoter chromatin states of DEGs between groups may suggest that histone modification changes due to treatment or line differences are not dramatic enough to result in strong chromatin state transitions (i.e., active to silent state and *vice versa*), which are caused by differences in regions either being enriched versus not enriched between groups (i.e., peak calling). Instead, the regions that have assigned peaks in both groups being compared may still have significant changes in levels of enrichment. To explore this scenario, we examined the changes in histone modification enrichment levels at regulatory regions.

## Effects of Treatment and Genetic Line on Histone Modification Enrichment Levels

Histone enrichment levels have previously been shown to be correlated with biologically significant features such as enhancer activity, developmental state, and promoter conservation (Creyghton et al., 2010; Thakurela et al., 2015; Villar et al., 2015). Therefore, we explored the differences in the activity or priming of regulatory elements by measuring changes in enrichment levels of active (H3K4me3 and H3K27ac) or poised (H3K4me1) histone modifications, respectively. Enrichment

**A**




| Total number of states | State Annotation |
|---|---|
| 16582 | Flanking/Active TSS |
| 18625 | Strong enhancer/Flanking active regulatory elements |
| 32503 | Poised/Flanking enhancer |
| 5120 | Flanking/Active TSS |
| 1373 | Flanking/Active TSS |
| 7801 | Active TSS |
| 7177 | Weak active signal |
| 5276 | Poised TSS |
| 2686 | Poised TSS |
| 56332 | No/Low signal |
| 36907 | Repressed regions |
| 9795 | Flanking/Repressed regulatory elements |
| 4348 | Repressed TSS |

**B**

Control Leghorn

| Control Fayoumi | 1 | 2 | 3 | 4 | 5 | 6 | 7 | 8 | 9 | 10 | 11 | 12 | 13 |
|---|---|---|---|---|---|---|---|---|---|---|---|---|---|
| 1 | 67 | 9 | 1 | 4 | 0 | 71 | 0 | 6 | 0 | 1 | 2 | 1 | 0 |
| 2 | 8 | 77 | 14 | 0 | 0 | 11 | 4 | 4 | 1 | 4 | 3 | 1 | 0 |
| 3 | 8 | 14 | 63 | 1 | 3 | 9 | 5 | 1 | 0 | 18 | 7 | 0 | 0 |
| 4 | 0 | 0 | 0 | 2 | 0 | 1 | 0 | 0 | 0 | 1 | 1 | 0 | 0 |
| 5 | 0 | 0 | 0 | 0 | 10 | 9 | 0 | 1 | 0 | 3 | 1 | 0 | 0 |
| 6 | 25 | 2 | 6 | 0 | 3 | 1335 | 3 | 12 | 1 | 7 | 0 | 2 | 1 |
| 7 | 1 | 5 | 3 | 0 | 0 | 2 | 8 | 0 | 0 | 4 | 0 | 0 | 0 |
| 8 | 11 | 1 | 4 | 0 | 0 | 66 | 1 | 402 | 40 | 0 | 7 | 8 | 30 |
| 9 | 0 | 0 | 0 | 0 | 1 | 12 | 0 | 7 | 37 | 1 | 3 | 2 | 1 |
| 10 | 0 | 0 | 17 | 0 | 4 | 5 | 8 | 1 | 2 | 462 | 44 | 0 | 0 |
| 11 | 1 | 2 | 14 | 0 | 5 | 6 | 1 | 7 | 7 | 36 | 168 | 1 | 10 |
| 12 | 0 | 1 | 3 | 0 | 2 | 0 | 1 | 12 | 2 | 1 | 4 | 14 | 3 |
| 13 | 2 | 0 | 0 | 0 | 1 | 2 | 0 | 24 | 1 | 0 | 23 | 0 | 55 |

Treated Leghorn

| Treated Fayoumi | 1 | 2 | 3 | 4 | 5 | 6 | 7 | 8 | 9 | 10 | 11 | 12 | 13 |
|---|---|---|---|---|---|---|---|---|---|---|---|---|---|
| 1 | 28 | 5 | 4 | 2 | 1 | 21 | 0 | 11 | 0 | 0 | 0 | 0 | 0 |
| 2 | 2 | 28 | 6 | 1 | 1 | 2 | 4 | 0 | 0 | 1 | 0 | 1 | 0 |
| 3 | 4 | 13 | 42 | 1 | 0 | 9 | 6 | 1 | 0 | 15 | 7 | 1 | 0 |
| 4 | 0 | 0 | 0 | 1 | 0 | 0 | 0 | 1 | 0 | 0 | 1 | 0 | 0 |
| 5 | 0 | 0 | 0 | 0 | 10 | 22 | 0 | 0 | 2 | 4 | 1 | 0 | 0 |
| 6 | 26 | 3 | 1 | 1 | 0 | 1287 | 0 | 20 | 15 | 1 | 1 | 2 | 1 |
| 7 | 0 | 4 | 0 | 0 | 0 | 3 | 3 | 0 | 0 | 2 | 0 | 0 | 0 |
| 8 | 0 | 0 | 1 | 0 | 0 | 6 | 1 | 183 | 10 | 0 | 2 | 3 | 12 |
| 9 | 0 | 0 | 0 | 0 | 0 | 4 | 1 | 23 | 47 | 0 | 2 | 1 | 2 |
| 10 | 0 | 1 | 14 | 0 | 4 | 3 | 9 | 0 | 1 | 292 | 39 | 0 | 0 |
| 11 | 0 | 0 | 2 | 0 | 0 | 2 | 0 | 10 | 5 | 13 | 91 | 0 | 10 |
| 12 | 0 | 1 | 0 | 0 | 0 | 2 | 0 | 1 | 0 | 0 | 0 | 6 | 1 |
| 13 | 0 | 0 | 0 | 0 | 0 | 1 | 0 | 29 | 3 | 0 | 10 | 2 | 45 |

Control Fayoumi

| Treated Fayoumi | 1 | 2 | 3 | 4 | 5 | 6 | 7 | 8 | 9 | 10 | 11 | 12 | 13 |
|---|---|---|---|---|---|---|---|---|---|---|---|---|---|
| 1 | 1 | 0 | 0 | 0 | 0 | 0 | 0 | 0 | 0 | 0 | 0 | 0 | 0 |
| 2 | 1 | 0 | 0 | 0 | 0 | 0 | 0 | 1 | 0 | 0 | 0 | 0 | 0 |
| 3 | 0 | 0 | 0 | 0 | 0 | 0 | 0 | 1 | 0 | 0 | 1 | 0 | 0 |
| 4 | 0 | 0 | 0 | 0 | 0 | 0 | 0 | 0 | 0 | 0 | 0 | 0 | 0 |
| 5 | 0 | 0 | 0 | 0 | 0 | 0 | 0 | 0 | 0 | 2 | 0 | 0 | 0 |
| 6 | 1 | 1 | 0 | 0 | 1 | 9 | 0 | 2 | 4 | 0 | 0 | 0 | 0 |
| 7 | 0 | 0 | 0 | 0 | 0 | 0 | 0 | 0 | 0 | 0 | 0 | 0 | 0 |
| 8 | 0 | 0 | 0 | 0 | 0 | 0 | 0 | 7 | 1 | 0 | 0 | 0 | 0 |
| 9 | 0 | 0 | 0 | 0 | 0 | 0 | 0 | 1 | 3 | 0 | 1 | 0 | 0 |
| 10 | 0 | 0 | 0 | 0 | 0 | 0 | 0 | 0 | 0 | 8 | 0 | 0 | 0 |
| 11 | 0 | 0 | 0 | 0 | 0 | 0 | 0 | 1 | 0 | 0 | 5 | 0 | 0 |
| 12 | 0 | 0 | 0 | 0 | 0 | 0 | 0 | 0 | 0 | 0 | 0 | 1 | 0 |
| 13 | 0 | 0 | 0 | 0 | 0 | 0 | 0 | 0 | 0 | 0 | 0 | 0 | 1 |

Control Leghorn

| Treated Leghorn | 1 | 2 | 3 | 4 | 5 | 6 | 7 | 8 | 9 | 10 | 11 | 12 | 13 |
|---|---|---|---|---|---|---|---|---|---|---|---|---|---|
| 1 | 15 | 1 | 1 | 0 | 0 | 10 | 0 | 0 | 0 | 0 | 0 | 0 | 0 |
| 2 | 6 | 17 | 3 | 0 | 0 | 1 | 1 | 1 | 0 | 0 | 0 | 0 | 0 |
| 3 | 2 | 4 | 18 | 0 | 0 | 1 | 2 | 0 | 1 | 4 | 1 | 0 | 0 |
| 4 | 0 | 0 | 1 | 1 | 0 | 0 | 0 | 0 | 0 | 0 | 0 | 0 | 0 |
| 5 | 0 | 0 | 0 | 0 | 6 | 1 | 0 | 1 | 1 | 0 | 1 | 0 | 0 |
| 6 | 23 | 5 | 1 | 0 | 4 | 1018 | 1 | 8 | 7 | 0 | 1 | 0 | 0 |
| 7 | 0 | 1 | 0 | 0 | 0 | 0 | 5 | 0 | 0 | 1 | 1 | 0 | 0 |
| 8 | 3 | 0 | 0 | 0 | 0 | 12 | 0 | 120 | 8 | 0 | 4 | 4 | 7 |
| 9 | 0 | 0 | 0 | 0 | 0 | 4 | 1 | 15 | 30 | 1 | 2 | 1 | 2 |
| 10 | 0 | 0 | 6 | 0 | 0 | 0 | 1 | 0 | 0 | 83 | 10 | 0 | 0 |
| 11 | 0 | 0 | 1 | 0 | 0 | 2 | 0 | 3 | 1 | 4 | 57 | 0 | 4 |
| 12 | 0 | 0 | 1 | 0 | 0 | 0 | 0 | 4 | 1 | 1 | 1 | 2 | 0 |
| 13 | 0 | 0 | 0 | 1 | 0 | 0 | 0 | 9 | 0 | 0 | 1 | 1 | 7 |

**C**

**Promoter state comparisons of differential genes of all comparisons**

| DEG comparison | Equivalent promoter states | Different promoter states |
|---|---|---|
| TF vs CF | 35 | 19 |
| TL vs CL | 1379 | 213 |
| CF vs CL | 2700 | 753 |
| TF vs TL specific* | 2063 | 461 |
| Total | 6177 (81%) | 1446 (19%) |

**FIGURE 4 |** The promoter states of differentially expressed genes generally are not different between groups, suggesting enhancers may play a role in modulating expression for these DEGs. **(A)** Annotation of chromatin states are based on promoter enrichment, gene expression correlation, and known associations of histone modifications to regulatory elements and their activity. States are grouped into three main activity groups: active (red), poised (yellow), and repressed (blue). **(B)** Promoter transition tables are shown for the DEGs in each comparison. **(C)** Table summarizing the states that remain the same between two groups or are different between groups is shown in **(A)** and includes the total number of promoters that were the same and were different between two groups. *Numbers shown for TF versus TL comparison refer to DEGs specific to that gene set in comparison to the CF vs. CL gene set. CF, control Fayoumi; TF, treated Fayoumi; CL, control Leghorn; TL, treated Leghorn.

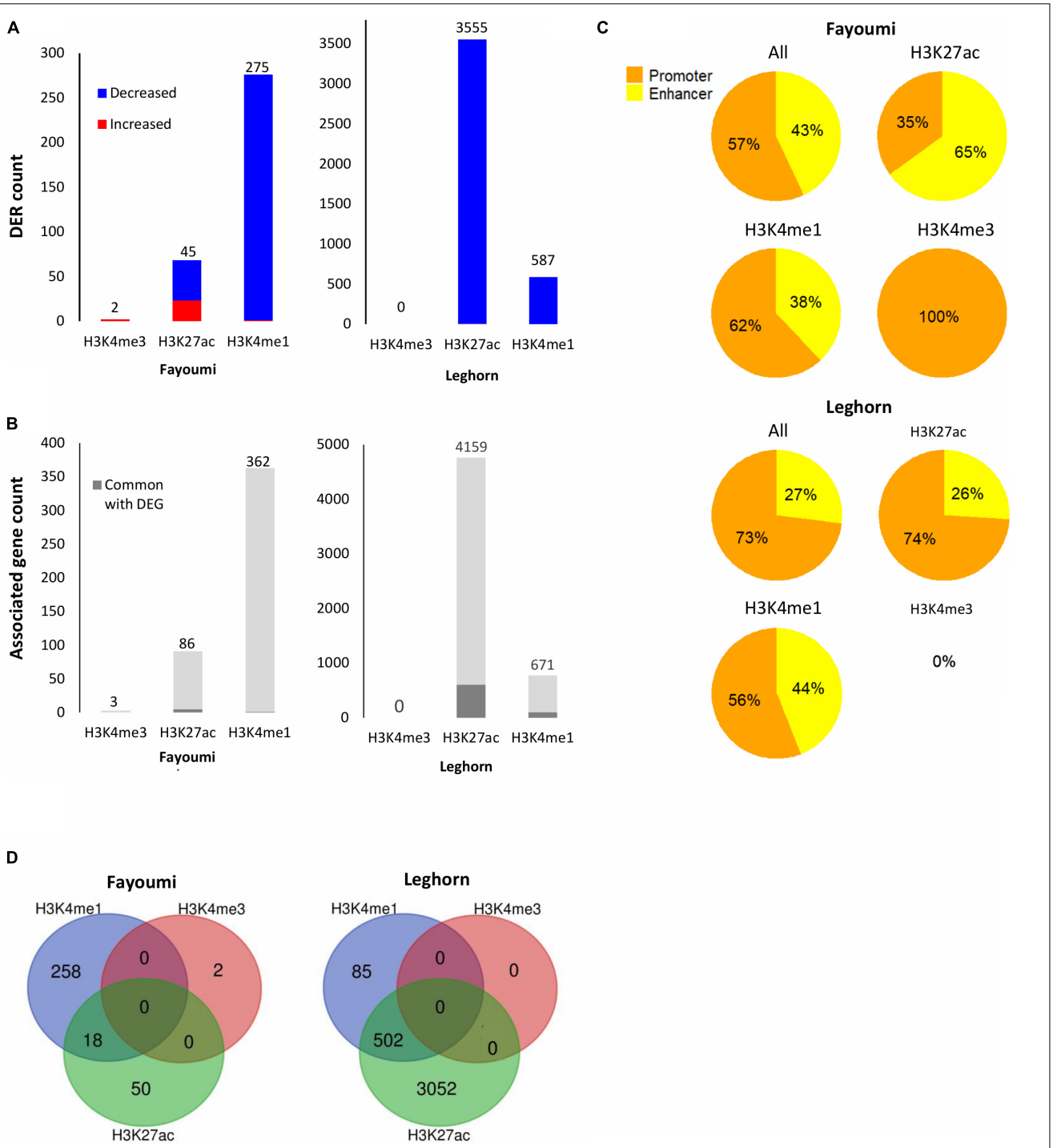



**FIGURE 5 |** Summary of DER analysis for within-line comparisons. **(A)** Stacked bar plots showing the number of DERs with increased or decreased enrichment identified for each within-line comparison across all histone modifications. **(B)** Stacked bar plots showing the number of unique target genes associated with DERs and the number of associated genes that are in common with DEGs of the corresponding differential gene analysis (i.e., within-line Leghorn or Fayoumi). **(C)** Pie charts showing the percentage of promoters or enhancers within the DERs of each histone modification. **(D)** Venn diagrams showing overlap of DERs across histone modifications. No overlap of H3K4me3 DERs was found for either comparison.

levels were calculated by counting reads overlapping regulatory regions, which were determined from the chromatin states (see section "Materials and Methods"), for each histone modification. PCA plots of histone peak depth across samples showed clear clustering by line in all three histone modifications, while clustering by treatment can be observed in only H3K27ac and

H3K4me1 (**Supplementary Figure 6**). The Spearman correlation was calculated between the fold changes of each histone modification enrichment level at promoters and gene expression of DEGs within each comparison (**Supplementary Figure 7**). The correlation with gene expression fold change across all comparisons showed that the greatest positive correlations with expression are with active histone modifications H3K4me3 and even more so with H3K27ac, which suggests that H3K27ac enrichment levels may be the most predictive of changes to gene expression levels among the four histone modification marks. Second, there was moderately positive correlation of expression with H3K4me1, and lastly, there was moderately negative correlation of expression with the repressive mark H3K27me3. On an interesting note, the greatest correlations occurred between histone marks H3K4me3 and H3K27ac, illustrating a biologically close relationship in regulation between the two histone modifications at promoters (Mikkelsen et al., 2007; Villar et al., 2015).

Differentially enriched regions were identified between each group using DESeq2 (FDR $< 0.05$). The numbers of DERs for within-line comparisons are summarized in **Figure 6A**. In both within-line comparisons, the greatest number of DERs appeared in H3K27ac (45 DERs in Fayoumi and 3,555 in Leghorn) and H3K4me1 (275 DERs in Fayoumi and 587 DER in Leghorn), whereas for H3K4me3 there were very few DERs detected (two DERs in Fayoumi and no DERs in Leghorn). This illustrates that H3K27ac and H3K4me1 were the most informative histone modifications among the three when exploring changes in regulatory regions due to treatment. The DER analysis mirrored the observations seen in the DEG analysis in that there appeared to be a larger effect of treatment on Leghorns as indicated by the greater number of DERs. Furthermore, the direction of change is similar, with the majority of the DERs having decreased enrichment due to treatment, reflecting the significant down-regulation of DEGs in Leghorn (**Figure 5A**). There was no complete overlap of DERs between the histone modifications, which illustrates the importance of examining multiple modifications as different indicators of chromatin changes during a response to treatment (**Figure 5D**). Lastly, prediction of target genes for regulatory elements has been determined in previous studies by proximity, which we have similarly implemented by assigning a target gene with the nearest TSS to a DER. We then compared the set of uniquely associated target genes with the set of DEGs from the same comparison group and found that the majority were not common between the two sets of genes (**Figure 5B**). There are several possible explanations for this: (1) the spatial dynamics of regulation results in the target gene not actually being the nearest gene, (2) the temporal dynamics of gene expression changes and histone modifications are not necessarily captured at the same time point, or (3) technical aspects in our assay or analysis. All statements described above were also observed in the between-line comparisons shown in the **Figure 6**, with the exception of one observation. In the between-line DERs, greater than 70% of H3K4me3 DERs overlapped with H3K27ac DERs, but without *vice versa* being true also (**Figure 6D**). These results suggest that between the two active histone modifications, the H3K27ac appears to be more informative by encompassing the majority of regions with H3K4me3 enrichment changes in addition to identifying significant numbers of other regulatory regions affected by treatment or line differences. Although there was moderate correlation of histone modification fold changes at the promoters of DEGs, there was high correlation of the fold changes between the active/poised histone modifications at DERs for both within-line and between-line comparisons, especially with H3K27ac compared to H3K4me3 or H3K3me1 (**Supplementary Figure 8**). This supports the hypothesis that active/poised histone modifications are concurrently regulated together and that changes in H3K27ac enrichment levels reflect its dynamic role in the activity of promoters and enhancers that has previously been shown in other studies (Creyghton et al., 2010; Thakurela et al., 2015).

We were interested in confirming the hypothesis of whether enhancers played a greater role than promoters in the differences seen during treatment or between lines as suggested above with the chromatin state transition analysis of the promoters of DEGs where there were small changes seen between groups (**Figure 4B**). In contrast to what we observed in the chromatin state promoter transition analysis, there were significant changes occurring in promoters where greater numbers of DERs were located in promoters in nearly all comparisons involving treated groups: 57% for within-line Fayoumi, 73% for within-line Leghorn, and 64% for between treated lines (**Figures 5C**, **6C**). However, in the comparison between non-treated lines, we found that the majority of DERs (65%) were enhancers (**Figure 6C**). These observations suggest that inherent line differences are mainly regulated by enhancers, whereas response to treatment is mainly regulated by promoters.

## Functional Analysis of Regions With Histone Enrichment Level Changes

Using the associated target genes of DERs from within-line comparisons, the top 5 enriched GO terms and KEGG pathways are presented for each analysis. For DERs identified for H3K4me1, we found that both within-line analyses have very similar terms and pathways that relate to the immune system and, especially interestingly, are ones relevant to B-cell biology such as B-cell homeostasis, B cell receptor (BCR) signaling, and B-cell activation (**Table 1**). For H3K4me1, nearly all DERs had decreased enrichment with the treatment in both lines, which suggests possible down-regulation of B-cell function and development. For DERs identified for H3K27ac, there was only one enriched GO term in Fayoumi, which related to transcriptional regulation, but for Leghorns, there were many enriched GO terms and pathways that were similar to those found using the Leghorn DEGs such as protein regulation, cell division, and cell cycle (**Table 1**). Interestingly, the BCR pathway was enriched in Leghorn but not in Fayoumi, revealing a possible pathway that illustrates a significant difference in the effect of treatment on Leghorns versus Fayoumi.

We further explored enrichment of transcription factor motifs within H3K27ac DERs in order to identify any potential transcription factors with significant roles in the differences

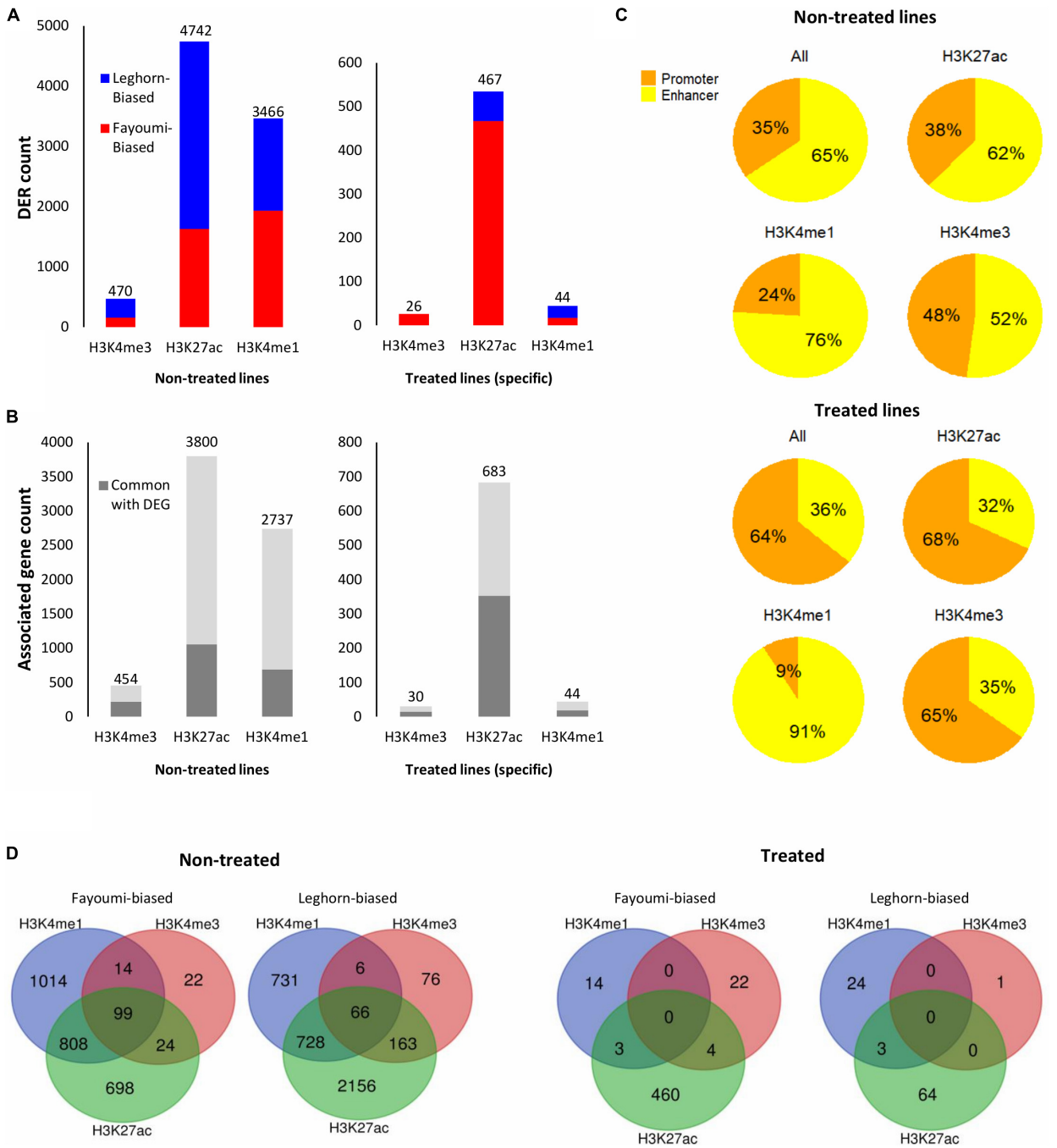



**FIGURE 6 |** Summary of DER analysis for between-line comparisons. **(A)** Stacked bar plots showing the number of DERs with increased or decreased enrichment identified for each between-line comparison across all histone modifications. **(B)** Stacked bar plots showing the number of unique target genes associated with DERs and the number of associated genes that are in common with DEGs of the corresponding differential gene analysis (i.e., between non-treated lines or treated lines). **(C)** Pie charts showing the percentage of promoters or enhancers within the DERs of each histone modification. **(D)** Venn diagrams showing the overlapped DERs with similar line biases across histone modifications within each between-line comparison. DER, differentially enriched region; DEG, differentially expressed gene.

seen for our comparisons. Using only comparisons with larger numbers (>1,000) of DERs (TL vs. CL and CF vs. CL), the top 5 transcription factor motifs (similarity score $\geq$ 0.70) enriched in DERs for the non-treated-line and the within-line Leghorn comparison are presented (**Supplementary Figure 9**). In the non-treated-line comparison, the top 3 motifs belong to transcription factors with critical roles in B-cell development, highlighting possible differences between Leghorn and Fayoumi in their B-cell development in the bursa. The transcription factors enriched in Leghorn H3K27ac DERs have diverse roles

**TABLE 1 |** Treatment causes changes in H3K4me1 within regions that may function in B cell–related processes, and Leghorn has significant enrichment of processes related to bursal development, highlighting susceptible mechanisms to treatment compared to Fayoumi.

| | | Description | Count | −log10 *p*-value |
|---|---|---|---|---|
| **GO terms and KEGG pathways for genes associated with H3K4me1 DERs** | | | | |
| Fayoumi | GO terms BP | B-cell homeostasis | 4 | 2.88 |
| | | Positive regulation of GTPase activity | 17 | 2.76 |
| | | Adaptive immune response | 8 | 2.62 |
| | | B-cell receptor signaling pathway | 5 | 2.36 |
| | | Positive regulation of transcription, DNA-templated | 15 | 2.32 |
| | KEGG pathway | Fc epsilon RI signaling pathway | 6 | 2.71 |
| | | Fcγ R–mediated phagocytosis | 6 | 2.31 |
| | | B-cell receptor signaling pathway | 5 | 1.89 |
| | | HTLV-I infection | 9 | 1.73 |
| | | Glycosaminoglycan biosynthesis—chondroitin sulfate/dermatan sulfate | 3 | 1.55 |
| Leghorn | GO terms BP | Adaptive immune response | 18 | 7.00 |
| | | T-cell activation | 11 | 6.88 |
| | | B-cell receptor signaling pathway | 11 | 6.28 |
| | | B-cell activation | 7 | -0.20 |
| | | Transcription from RNA polymerase II promoter | 28 | 3.92 |
| | KEGG pathway | Fc epsilon RI signaling pathway | 11 | 5.00 |
| | | T-cell receptor signaling pathway | 12 | 4.22 |
| | | Fcγ R–mediated phagocytosis | 11 | 4.18 |
| | | B-cell receptor signaling pathway | 10 | 4.12 |
| | | Primary immunodeficiency | 7 | 3.64 |
| **GO terms and KEGG pathways for genes associated with H3K27ac DERs** | | | | |
| Fayoumi | GO terms BP | Transcription from RNA polymerase II promoter | 5 | 1.85 |
| Leghorn | GO terms BP | Protein phosphorylation | 88 | 10.15 |
| | | Positive regulation of transcription from RNA polymerase II promoter | 151 | 9.25 |
| | | Cell division | 71 | 9.20 |
| | | Positive regulation of transcription, DNA-templated | 92 | 8.79 |
| | | Negative regulation of transcription from RNA polymerase II promoter | 116 | 8.26 |
| | KEGG pathway | B-cell receptor signaling pathway | 30 | 10.95 |
| | | Fc gamma R-mediated phagocytosis | 33 | 10.65 |
| | | Cell cycle | 37 | 8.10 |
| | | Phosphatidylinositol signaling system | 27 | 5.21 |
| | | Chronic myeloid leukemia | 22 | 5.00 |

*GO terms and KEGG pathways were identified to be enriched in the target genes associated with the differentially enriched H3K4me1 and H3K27ac for each line. Significant processes were determined by $p < 0.05$ with gene counts of more than 2. The top 5 GO terms and KEGG pathways are shown for each line along with their gene count and -log10 p-value. BP, biological processes.*

in many cellular functions. ETS-like 1 (ELK1), Yin Yang 1 (YY1), Zinc finger X-chromosomal protein (ZFX), and NDT80 all function in processes that involve cell cycle and division, such proliferation, replication, and meiosis, while interferon regulatory factor 3 (IRF3) functions in type I interferon responses induced by viruses.

## Identifying Potential Functional Variants Between Genetic Lines

To identify variants between the lines that potentially have functional consequences in genetic line differences associated with disease resistance, we identified homozygous variants (SNPs and small indels) between the lines that overlap coding and functional non-coding regions of the genome. After SNPs were filtered by quality, the SNPs were further filtered if they were heterozygous in either line, which allows more confidence that remaining SNPs are fixed among all individuals within each line. The total number of variants called within both lines was 5,808,195, and the total number of variants different between the lines was 3,521,496. **Table 2** summarizes the total variants between lines that overlap genes and regulatory elements including DERs and DEGs identified from between-line comparisons. This reveals that there is a substantial number of candidate variants between lines that may be contributing to line differences, both inherent and in treatment response. **Figure 7** shows an example of candidate variants overlapping the promoter of a DEG between the lines, dihydropyrimidinase-like 3 (*DPYSL3*) gene, which also overlap a DER for H3K27ac between the lines. This example illustrates the potential benefits of the integration of multiple genome-wide assays to identify potential causal variants affecting gene expression between these two lines.

**TABLE 2 |** Variants between the genetic lines overlapping functional genomic regions.

| | Total overlapped variants | % of total variants |
|---|---|---|
| Total within both lines | 5,808,195 | |
| Different between lines | 3,521,496 | 60.63 |
| Total regulatory regions | 239,194 | 6.79 |
| Total promoters | 92,968 | 2.64 |
| Total enhancers | 146,226 | 4.15 |
| Der between non-treated lines | 83,740 | 2.38 |
| DER between treated lines (specific) | 10,596 | 0.30 |
| Total exons | 90,025 | 2.56 |
| DEGs between lines (both treatment groups) | 3,381 | 0.10 |

*Number of variants called within both genetic lines (versus reference galGal6 genome), number of variants different between the genetic lines, and number of variants different between the genetic lines that overlap total functional genomic regions and those different between the lines. Only homozygous variants within both lines were considered. The percentage of total variants is calculated from total variants within both lines.*

## DISCUSSION

To capture changes due to simultaneous NDV infection and heat stress in both genes and regulatory elements, we performed differential analysis on the transcriptome, chromatin state transitions, and differential analysis on the histone modification enrichment levels for bursal tissue collected at 6 dpi from two genetically distinct inbred chicken lines, Fayoumi and Leghorn.

With treatment, differential gene analysis revealed a significant number of gene expression changes in the Leghorn line, but few in the Fayoumi line. Fayoumi showed enrichment in "extracellular matrix organization," which is a biological process ubiquitous across all tissues and essential for proper development and tissue homeostasis (Bonnans et al., 2014). Leghorn displayed multiple enriched terms and pathways, but the ones most intriguing were those related to the housekeeping processes cell cycle and division. The significant down-regulation of these processes (**Figure 1B**) highlighted a potential detrimental effect of the treatment on Leghorns. Cell cycle and cell division are crucial aspects of cell proliferation, which is critical for bursa growth as B cells are rapidly dividing starting before hatch and up to the 4 weeks when the tissues were collected. Therefore, the down-regulation of these processes related to cell proliferation indicates that treatment may be hindering clonal division of B cells within the bursa of the treated birds, but more severely in the treated Leghorns. Previous studies in both chicken and mice suggest that this is more likely a result of the effects of heat stress rather than infection. Chickens that were subjected to heat stress had decreased lymphocyte count or antibody levels (Thaxton et al., 1968; Nathan et al., 1976; Prieto and Campo, 2010). These studies suggested that stress hormones, such as corticosterone or ACTH, which are increased during heat stress, may be the cause of these harmful effects on the humoral arm of the immune system. Indeed, mice under chronic stress from overexpressed corticotropin-releasing hormone from the hypothalamus had significantly decreased total B cells from both primary and secondary lymphoid organs and decreased antibody levels following immunization (Murray et al., 2001). This may explain a potential detrimental impact on B-cell development in bursa for the birds under chronic heat stress in our study.

Integration of chromatin state analysis with DEGs revealed an interesting finding. DEGs due to treatment or line differences had active chromatin state promoters in both groups within a comparison, which suggests that gene expression differences within any comparison mainly result from modulation of constitutively active genes. This phenomenon indicates that they likely play an important role in housekeeping functions. Indeed as described above, the enriched GO terms and KEGG pathways from DEGs identified in comparisons of treated versus non-treated groups for both lines were related to housekeeping processes.

The integration of multiple histone modifications to explore the chicken response to treatment provided a more comprehensive exploration into the biological significance of the effect of genetic variation than just analysis into the transcriptome alone. Both the functional analysis of the differential histone modifications of H3K4me1 and H3K27ac and the transcriptome analysis support the conclusion that treatment seems to affect cell proliferation of the bursa and more so in Leghorns than Fayoumis. As cell proliferation is a housekeeping process, the regulatory element bias toward histone modification enrichment changes in promoters during treatment is reasonable because transcription factors involved in housekeeping functions are enriched in binding sites that are proximal to TSS (Heidari et al., 2014). Moreover, the most significant enriched transcription factor motif in H3K27ac DERs for Leghorns (**Supplementary Figure 8**), which was 73% promoters (**Figure 6C**), was ELK1. Elk1 functions in ERK signaling pathway for positive regulation of the cell cycle and cell proliferation (Shin et al., 2011; Ducker et al., 2019) and has preferential bias for proximal-promoter binding when cobinding with GATA1 (Gerstein et al., 2012).

Exploring the histone modification differences between the two groups highlighted several interesting conclusions in the epigenetic changes due to treatment or line differences. Of the three active/poised histone modifications, the most informative appeared to be H3K27ac, which falls in line with what has previously been demonstrated (Creyghton et al., 2010; Villar et al., 2015; Gorkin et al., 2017; Fu et al., 2018). First, H3K27ac enrichment level fold changes had the highest correlation with fold changes of DEG and fold changes of enrichment levels of the other histone modifications, highlighting the predictive power of H3K27ac enrichment levels. Additionally, only H3K27ac enrichment level changes between the treated and non-treated groups were able to identify regulatory changes in biological processes and pathways uniquely within Leghorn, but not within Fayoumi. These pathways uniquely within Leghorn are very important for B-cell development and function, which may help

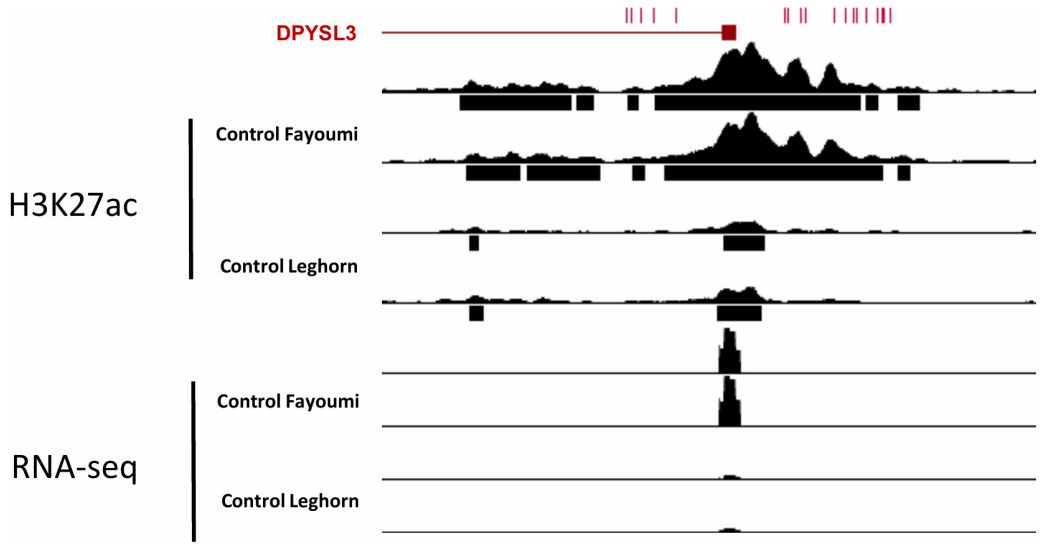



**FIGURE 7 |** Genome browser track of the promoter of DPYSL3 with H3K27ac read pile-up and RNA-seq read pile-up of two biological replicates from control Fayoumi and control Leghorn. Red tick marks on top of the browser represent variants between the genetic lines.

explain Leghorns' susceptibility to treatment. Lastly, the majority of DERs due to treatment occurred in promoters, whereas the majority of DERs due to line differences occurred in enhancers, illustrating a regulatory element bias for either the response to treatment or genetic line differences.

One of the more intriguing findings was that the enriched pathways and processes associated with H3K4me1 DERs between treatment groups for both lines and H3K27ac DERs between treatment groups in Leghorn were related to B-cell biology. The repeated appearance of the "B-cell receptor signaling pathway" enriched in DERs that were all nearly decreased with treatment (**Table 1**) suggests an important mechanism of B-cell development that is being repressed. This ties into the narrative of decreased B-cell proliferation suggested by our study and in previously mentioned chicken and mice studies with heat stress because loss of pre-BCR or BCR signaling arrests early B-cell development, thereby inhibiting maturation (Ferrari et al., 2007), or leads to induced death into mature B cells (Lam et al., 1997). This harmful effect of heat stress on B cells appeared in both lines, but it seems it was more exacerbated in Leghorns because of the greater changes seen in both transcriptome and histone modification analysis.

Leghorns have significantly lower levels of NDV-specific antibody titers compared to Fayoumis (Saelao et al., 2018b), which supports the notion that that Leghorns had more markedly decreased B-cell counts through inhibition of proliferation than Fayoumis. However, one caveat that must be considered is that B cells responsible for producing NDV-specific antibodies were most likely from peripheral tissues rather than from the bursa. This conclusion was drawn from several reasons. First is that a lentogenic strain of NDV will not systemically infect the bursa, which is supported by the fact that we did not detect viral transcripts from the bursa RNA-seq. Second, many B cells within the bursa are still maturing their BCR, the activation of which is necessary for differentiating B cells into secreting NDV-specific antibodies. Lastly, there is little evidence of the bursa acting as a peripheral lymphoid organ (Sorvari et al., 1975; Sorvari and Sorvari, 1978). Nonetheless, our results in the bursa provide an indication of what mechanisms may be affecting B cells throughout the body, including those responding to infection. Another possibility is that the impact of heat stress on bursa may have decreased the migration of B cells to peripheral tissues, thereby decreasing B-cell populations that are able to respond to infection. Our work provides some novel information on the impact of both heat stress and NDV on B-cell development in the bursa and laid the foundation of future studies into exploring the consequences of NDV infection under heat stress on peripheral B cells. Further studies by isolating B cells from multiple secondary lymphoid tissues during heat stress can further confirm our findings and examine our hypothesis regarding the impact of treatment on B-cell development and B-cell response to NDV infection.

The overall goal of our program is to genetically enhance resistance against heat stress and NDV infection in chickens. Therefore, we further explored genetic variants between the two lines that might be contributing to the resistance difference between the two genetic lines. Our analysis revealed a substantial number of variants between the lines that overlapped coding and functional non-coding regions of the genome. There were more variants that overlapped regulatory regions (6.79%) than exonic regions (2.59%), which suggest that the causal variants that affect line differences will most likely lie in functional non-coding regulatory regions as proposed by many GWAS. Indeed, a previous study exploring variants between the genetic lines observed that the majority of those variants were intergenic or intronic (Fleming et al., 2016). To further narrow down putative variants that are associated with line differences, we identified variants that overlapped all DEGs

and DERs identified for between-line comparisons in both treated and non-treated groups. The listed putative variants generated from this study can be used to investigate disease resistance for further functional studies and highlights the advantage of integrating genome-wide multi-omics data that is currently appreciated in multiple projects for different species (ENCODE Project Consortium, Birney et al., 2007; Nègre et al., 2011; Roadmap Epigenomics Consortium, Kundaje et al., 2015), including livestock (Andersson et al., 2015).

Lastly, we speculated that there might be inherent differences between the two lines that allowed Fayoumi to be readily able to receive heat stress and NDV infection without significant genomic changes in response to treatment as shown by the small number of DEGs and DERs (**Supplementary Figures 5A, 6A**). RNA-seq analysis between the lines within treated birds showed that Fayoumi inherently had greater expression than Leghorns in genes involved in immune-related cell identity, suggesting they may have greater progression in bursal development (**Figure 3**). Furthermore, transcription factors such as PU.1, POU2F2, and IRF8 have very important roles in B-cell development and differentiation. These top enriched transcription factors in the H3K27ac DERs between non-treated Fayoumi and Leghorn suggest potential differences in binding activity between the lines, which implicate that B-cell development may vary between the lines. This is unsurprising given that bursal development can differ between lines (MiliĆEviĆ et al., 1986). Further studies collecting phenotypic data such as immune cell profiles and populations using flow cytometry across lymphoid tissues of the two lines are warranted to confirm this hypothesis.

## CONCLUSION

In summary, our study characterized the bursal response of chicken to NDV infection and heat stress and differences in responses between two different inbred chicken lines, Fayoumi and Leghorn. We found down-regulation of many genes within cellular processes such as cell division and cell cycle within Leghorn, suggesting a possible deleterious effect on bursal cell proliferation. The immune-related GO terms and pathways associated with regulatory regions with decreased enrichment levels in H3K27ac and H3K4me1 illuminated other potential mechanisms affected by heat stress and NDV infection. This potential harmful effect of stress on B cells induced by treatment may partly underlie why Leghorns are more susceptible to both heat stress and NDV infection. Further studies are needed to confirm the roles of these potentially significant mechanisms within bursa that play a role for resistance against NDV infection under heat stress. To our knowledge, our study is the first to identify genome-wide regulatory elements in the bursa tissue of chickens and therefore reveals novel insight into the chicken regulatory elements in bursa tissue and provides a great resource for other genomics-related chicken studies.

## DATA AVAILABILITY STATEMENT

The datasets generated for this study can be found in online repositories. The names of the repository/repositories and accession number(s) can be found below: https://www.ebi.ac.uk/ena, PRJEB38599 and https://www.ebi.ac.uk/ena, PRJEB38600.

## ETHICS STATEMENT

The animal study was reviewed and approved by Institutional Animal Care and Use Committee at the University of California, Davis.

## AUTHOR CONTRIBUTIONS

HZ, RG, and SL conceived study idea and developed experimental design. GC generated and analyzed data with guidance from CK. GC, YW, and PS collected the samples. YW assisted in experiments. GR provided technical advice on analysis. GC wrote the manuscript. All authors provided input into manuscript.

## FUNDING

This study was funded by the United States Agency for International Development Feed the Future Innovation Lab for Genomics to Improve Poultry AID-OAA-A-13-00080. The authors declare that this study received funding from Zoetis.

## ACKNOWLEDGMENTS

We thank all the Zhou and Gallardo lab members who helped with the sample collection for the animal trial.

## SUPPLEMENTARY MATERIAL

The Supplementary Material for this article can be found online at: https://www.frontiersin.org/articles/10.3389/fgene.2020.567812/full#supplementary-material

## REFERENCES

Albiston, H. E., and Gorrie, C. J. (1942). Newcastle disease in Victoria. *Aust. Vet. J.* 18, 75–79. doi: 10.1111/j.1751-0813.1942.tb01466.x

Alexander, D. J. (2000). Newcastle disease and other avian paramyoviruses. *Rev. Sci. Tech.* 19, 443–462.

Anders, S., Pyl, P. T., and Huber, W. (2014). HTSeq—a python framework to work with high-throughput sequencing data. *Bioinformatics* 31, 166–169. doi: 10.1093/bioinformatics/btu638

Andersson, L., Archibald, A. L., Bottema, C. D., Brauning, R., Burgess, S. C., Burt, D. W., et al. (2015). Coordinated international action to accelerate genome-to-phenome with FAANG, the functional annotation of animal genomes project. *Genome Biol.* 16:57.

Barrett, N. W., Rowland, K., Schmidt, C. J., Lamont, S. J., Rothschild, M. F., Ashwell, C. M., et al. (2019). Effects of acute and chronic heat stress on the performance, egg quality, body temperature, and blood gas parameters of laying hens. *Poult. Sci.* 98, 6684–6692. doi: 10.3382/ps/pez541

Biscarini, F., Bovenhuis, H., van Arendonk, J. A., Parmentier, H. K., Jungerius, A. P., van der Poel, J. J., et al. (2010). Across-line SNP association study of innate and adaptive immune response in laying hens. *Anim. Genet.* 41, 26–38. doi: 10.1111/j.1365-2052.2009.01960.x

Bonnans, C., Chou, J., and Werb, Z. (2014). Remodelling the extracellular matrix in development and disease. *Nat. Rev. Mol. Cell Biol.* 15, 786–801. doi: 10.1038/nrm3904

Cao, R., Wang, L., Wang, H., Xia, L., Erdjument-Bromage, H., Tempst, P., et al. (2002). Role of histone H3 lysine 27 methylation in polycomb-group silencing. *Science* 298, 1039–1043. doi: 10.1126/science.1076997

Creyghton, M. P., Cheng, A. W., Welstead, G. G., Kooistra, T., Carey, B. W., Steine, E. J., et al. (2010). Histone H3K27ac separates active from poised enhancers and predicts developmental state. *Proc. Natl. Acad. Sci. U.S.A.* 107, 21931–21936. doi: 10.1073/pnas.1016071107

Deist, M. S., Gallardo, R. A., Bunn, D. A., Kelly, T. R., Dekkers, J. C. M., Zhou, H., et al. (2017). Novel mechanisms revealed in the trachea transcriptome of resistant and susceptible chicken lines following infection with newcastle disease virus. *Clin. Vaccine Immunol.* 24:e00027-17.

Dobin, A., Davis, C. A., Schlesinger, F., Drenkow, J., Zaleski, C., Jha, S., et al. (2012). STAR: ultrafast universal RNA-seq aligner. *Bioinformatics* 29, 15–21. doi: 10.1093/bioinformatics/bts635

Ducker, C., Chow, L. K. Y., Saxton, J., Handwerger, J., McGregor, A., Strahl, T., et al. (2019). De-ubiquitination of ELK-1 by USP17 potentiates mitogenic gene expression and cell proliferation. *Nucleic Acids Res.* 47, 4495–4508. doi: 10.1093/nar/gkz166

ENCODE Project Consortium, Birney, E., Stamatoyannopoulos, J. A., Dutta, A., Guigó, R., Gingeras, T. R., et al. (2007). Identification and analysis of functional elements in 1% of the human genome by the ENCODE pilot project. *Nature* 447, 799–816. doi: 10.1038/nature05874

Ernst, J., and Kellis, M. (2012). ChromHMM: automating chromatin-state discovery and characterization. *Nat. Meth.* 9, 215–216. doi: 10.1038/nmeth.1906

Ernst, J., Kheradpour, P., Mikkelsen, T. S., Shoresh, N., Ward, L. D., Epstein, C. B., et al. (2011). Mapping and analysis of chromatin state dynamics in nine human cell types. *Nature* 473, 43–49. doi: 10.1038/nature09906

Ferrari, S., Lougaris, V., Caraffi, S., Zuntini, R., Yang, J., Soresina, A., et al. (2007). Mutations of the Igβ gene cause agammaglobulinemia in man. *J. Exp. Med.* 204, 2047–2051. doi: 10.1084/jem.20070264

Fleming, D. S., Koltes, J. E., Fritz-Waters, E. R., Rothschild, M. F., Schmidt, C. J., Ashwell, C. M., et al. (2016). Single nucleotide variant discovery of highly inbred Leghorn and Fayoumi chicken breeds using pooled whole genome resequencing data reveals insights into phenotype differences. *BMC Genomics* 17:812. doi: 10.1186/s12864-016-3147-7

Fu, S., Wang, Q., Moore, J. E., Purcaro, M. J., Pratt, H. E., Fan, K., et al. (2018). Differential analysis of chromatin accessibility and histone modifications for predicting mouse developmental enhancers. *Nucleic Acids Res.* 46, 11184–11201. doi: 10.1093/nar/gky753

Gerstein, M. B., Kundaje, A., Hariharan, M., Landt, S. G., Yan, K. K., Cheng, C., et al. (2012). Architecture of the human regulatory network derived from ENCODE data. *Nature* 489, 91–100.

Gorkin, D. U., Barozzi, I., Zhang, Y., Lee, A. Y., Li, B., Zhao, Y., et al. (2017). Systematic mapping of chromatin state landscapes during mouse development. *bioRxiv [Preprint]* doi: 10.1101/166652

Guenther, M. G., Levine, S. S., Boyer, L. A., Jaenisch, R., and Young, R. A. (2007). A chromatin landmark and transcription initiation at most promoters in human cells. *Cell* 130, 77–88. doi: 10.1016/j.cell.2007.05.042

Heidari, N., Phanstiel, D. H., He, C., Grubert, F., Jahanbani, F., Kasowski, M., et al. (2014). Genome-wide map of regulatory interactions in the human genome. *Genome Res.* 24, 1905–1917. doi: 10.1101/gr.176586.114

Heinz, S., Benner, C., Spann, N., Bertolino, E., Lin, Y. C., Laslo, P., et al. (2010). Simple combinations of lineage-determining transcription factors prime cis-regulatory elements required for macrophage and B cell identities. *Mol. Cell* 38, 576–589. doi: 10.1016/j.molcel.2010.05.004

Hindorff, L. A., Sethupathy, P., Junkins, H. A., Ramos, E. M., Mehta, J. P., Collins, F. S., et al. (2009). Potential etiologic and functional implications of genome-wide association loci for human diseases and traits. *Proc. Natl. Acad. Sci. U.S.A.* 106, 9362–9367. doi: 10.1073/pnas.0903103106

Huang, D. W., Sherman, B. T., Tan, Q., Collins, J. R., Alvord, W. G., Roayaei, J., et al. (2007). The DAVID gene functional classification tool: a novel biological module-centric algorithm to functionally analyze large gene lists. *Genome Biol.* 8:R183.

Ko, K. H., Lee, I. K., Kim, G., Gu, M. J., Kim, H. Y., Park, B. C., et al. (2018). Changes in bursal B cells in chicken during embryonic development and early life after hatching. *Sci. Rep.* 8:16905.

Krueger, F. (2012). *Trim Galore: a Wrapper Tool Around Cutadapt and FastQC to Consistently Apply Quality and Adapter Trimming to FastQ Files, with some Extra Functionality for MspI-Digested RRBS-Type (Reduced Representation Bisufite-Seq) Libraries*. Available online at: http://www.bioinformatics.babraham.ac.uk/projects/trim_galore/. (accessed April 28, 2016).

Lam, K.-P., Kühn, R., and Rajewsky, K. (1997). In vivo ablation of surface immunoglobulin on mature B cells by inducible gene targeting results in rapid cell death. *Cell* 90, 1073–1083. doi: 10.1016/s0092-8674(00)80373-6

Li, H. (2011). A statistical framework for SNP calling, mutation discovery, association mapping and population genetical parameter estimation from sequencing data. *Bioinformatics* 27, 2987–2993. doi: 10.1093/bioinformatics/btr509

Li, H., and Durbin, R. (2009). Fast and accurate short read alignment with Burrows–Wheeler transform. *Bioinformatics* 25, 1754–1760. doi: 10.1093/bioinformatics/btp324

Li, H., Handsaker, B., Wysoker, A., Fennell, T., Ruan, J., Homer, N., et al. (2009). The sequence alignment/map format and SAMtools. *Bioinformatics* 25, 2078–2079. doi: 10.1093/bioinformatics/btp352

Love, M. I., Huber, W., and Anders, S. (2014). Moderated estimation of fold change and dispersion for RNA-seq data with DESeq2. *Genome Biol.* 15:550.

Luo, C., Qu, H., Ma, J., Wang, J., Li, C., Yang, C., et al. (2013). Genome-wide association study of antibody response to Newcastle disease virus in chicken. *BMC Genet.* 14:42. doi: 10.1186/1471-2156-14-42

Mashaly, M. M., Hendricks, G. L. III, Kalama, M. A., Gehad, A. E., Abbas, A. O., Patterson, P. H., et al. (2004). Effect of heat stress on production parameters and immune responses of commercial laying hens. *Poult. Sci.* 83, 889–894. doi: 10.1093/ps/83.6.889

Matsuda, H., and Bito, Y. (1973). Different effects of bursectomy of chickens on immune response to newcastle disease virus and *Salmonella* pullorum antigens. *Poult. Sci.* 52, 1042–1052. doi: 10.3382/ps.0521042

Maurano, M. T., Humbert, R., Rynes, E., Thurman, R. E., Haugen, E., Wang, H., et al. (2012). Systematic localization of common disease-associated variation in regulatory DNA. *Science* 337, 1190–1195. doi: 10.1126/science.1222794

Maxwell, M. H., Robertson, G. W., Mitchell, M. A., and Carlisle, A. J. (1992). The fine structure of broiler chicken blood cells, with particular reference to basophils, after severe heat stress. *Comp. Haematol. Int.* 2, 190–200. doi: 10.1007/bf00216094

Mikkelsen, T. S., Ku, M., Jaffe, D. B., Issac, B., Lieberman, E., Giannoukos, G., et al. (2007). Genome-wide maps of chromatin state in pluripotent and lineage-committed cells. *Nature* 448, 553–560. doi: 10.1038/nature06008

MiliĆEviĆ, Ž., VujiĆ, D., IsakoviĆ, K., MiĆIĆ, M., and MiliĆEviĆ, N. M. (1986). Involution of bursa of fabricius in male and female chickens: a light microscopic histoquantitative study. *Poult. Sci.* 65, 2318–2323. doi: 10.3382/ps.0652318

Miller, P. J., Afonso, C. L., El Attrache, J., Dorsey, K. M., Courtney, S. C., Guo, Z., et al. (2013). Effects of Newcastle disease virus vaccine antibodies on the shedding and transmission of challenge viruses. *Dev. Comp. Immunol.* 41, 505–513. doi: 10.1016/j.dci.2013.06.007

Murray, S. E., Lallman, H. R., Heard, A. D., Rittenberg, M. B., and Stenzel-Poore, M. P. (2001). A genetic model of stress displays decreased lymphocytes and impaired antibody responses without altered susceptibility to *Streptococcus pneumoniae*. *J. Immunol.* 167, 691–698. doi: 10.4049/jimmunol.167.2.691

Nathan, D. B., Heller, E. D., and Perek, M. (1976). The effect of short heat stress upon leucocyte count, plasma corticosterone level, plasma and leucocyte ascorbic acid content. *Br. Poult. Sci.* 17, 481–485. doi: 10.1080/00071667608416303

Nègre, N., Brown, C. D., Ma, L., Bristow, C. A., Miller, S. W., Wagner, U., et al. (2011). A cis-regulatory map of the *Drosophila* genome. *Nature* 471, 527–531.

Pertea, M., Pertea, G. M., Antonescu, C. M., Chang, T. C., Mendell, J. T., Salzberg, S. L., et al. (2015). StringTie enables improved reconstruction of a transcriptome from RNA-seq reads. *Nat. Biotechnol.* 33, 290–295. doi: 10.1038/nbt.3122

Prieto, M. T., and Campo, J. L. (2010). Effect of heat and several additives related to stress levels on fluctuating asymmetry, heterophil:lymphocyte ratio, and tonic immobility duration in White Leghorn chicks. *Poult. Sci.* 89, 2071–2077. doi: 10.3382/ps.2010-00716

Quinlan, A. R., and Hall, I. M. (2010). BEDTools: a flexible suite of utilities for comparing genomic features. *Bioinformatics* 26, 841–842. doi: 10.1093/bioinformatics/btq033

Ratcliffe, M. J. H., and Härtle, S. (2014). "B cells, the bursa of fabricius and the generation of antibody repertoires," in *Avian Immunology*, 2nd Edn, eds K. A. Schat, B. Kaspers, and P. Kaiser (Boston, MA: Academic Press), 65–89. doi: 10.1016/b978-0-12-396965-1.00004-2

Roadmap Epigenomics Consortium, Kundaje, A., Meuleman, W., Ernst, J., Bilenky, M., Yen, A., et al. (2015). Integrative analysis of 111 reference human epigenomes. *Nature* 518, 317–330.

Saelao, P., Wang, Y., Chanthavixay, G., Gallardo, R. A., Wolc, A., Dekkers, J. C. M., et al. (2019). Genetics and genomic regions affecting response to newcastle disease virus infection under heat stress in layer chickens. *Genes* 10:61. doi: 10.3390/genes10010061

Saelao, P., Wang, Y., Chanthavixay, G., Yu, V., Gallardo, R. A., Dekkers, J. C. M., et al. (2018a). Integrated proteomic and transcriptomic analysis of differential expression of chicken lung tissue in response to NDV infection during heat stress. *Genes* 9:579. doi: 10.3390/genes9120579

Saelao, P., Wang, Y., Gallardo, R. A., Lamont, S. J., Dekkers, J. M., Kelly, T., et al. (2018b). Novel insights into the host immune response of chicken Harderian gland tissue during Newcastle disease virus infection and heat treatment. *BMC Vet. Res.* 14:280. doi: 10.1186/s12917-018-1583-0

Shin, S. Y., Kim, C. G., Lim, Y., and Lee, Y. H. (2011). The ETS family transcription factor ELK-1 regulates induction of the cell cycle-regulatory gene p21Waf1/Cip1 and the BAX gene in sodium arsenite-exposed human keratinocyte HaCaT cells. *J. Biol. Chem.* 286, 26860–26872. doi: 10.1074/jbc.m110.216721

Sorvari, R., and Sorvari, T. E. (1978). Bursal fabricii as a peripheral lymphoid organ. Transport of various materials from the anal lips to the bursal lymphoid follicles with reference to its immunological importance. *Immunology* 32, 499–505.

Sorvari, T., Sorvari, R., Ruotsalainen, P., Toivanen, A., and Toivanen, P. (1975). Uptake of environmental antigens by the bursa of Fabricius. *Nature* 253, 217–219. doi: 10.1038/253217a0

Stone, H. D., Brugh, M., Erickson, G. A., and Beard, C. W. (1980). Evaluation of inactivated newcastle disease oil-emulsion vaccines. *Avian Dis.* 24, 99–111. doi: 10.2307/1589770

St-Pierre, N. R., Cobanov, B., and Schnitkey, G. (2003). Economic losses from heat stress by US livestock industries1. *J. Dairy Sci.* 86, E52–E77.

Thakurela, S., Sahu, S. K., Garding, A., and Tiwari, V. K. (2015). Dynamics and function of distal regulatory elements during neurogenesis and neuroplasticity. *Genome Res.* 25, 1309–1324. doi: 10.1101/gr.190926.115

Thaxton, P., Sadler, C. R., and Glick, B. (1968). Immune response of chickens following heat exposure or injections with ACTH1,2. *Poult. Sci.* 47, 264–266. doi: 10.3382/ps.0470264

Van der Auwera, G. A., Carneiro, M. O., Hartl, C., Poplin, R., Del Angel, G., Levy-Moonshine, A., et al. (2013). From FastQ data to high confidence variant calls: the genome analysis toolkit best practices pipeline. *Curr. Protoc. Bioinformatics* 43, 11.10.1–11.10.33.

Villar, D., Berthelot, C., Aldridge, S., Rayner, T. F., Lukk, M., Pignatelli, M., et al. (2015). Enhancer evolution across 20 mammalian species. *Cell* 160, 554–566. doi: 10.1016/j.cell.2015.01.006

Wang, Y., Lupiani, B., Reddy, S. M., Lamont, S. J., and Zhou, H. (2014). RNA-seq analysis revealed novel genes and signaling pathway associated with disease resistance to avian influenza virus infection in chickens1. *Poult. Sci.* 93, 485–493. doi: 10.3382/ps.2013-03557

Wang, Y., Saelao, P., Chanthavixay, K., Gallardo, R., Bunn, D., Lamont, S. J., et al. (2018). Physiological responses to heat stress in two genetically distinct chicken inbred lines. *Poult. Sci.* 97, 770–780. doi: 10.3382/ps/pex363

Weill, J. C., Leibowitch, M., and Reynaud, C. A. (1987). "Questioning the role of the embryonic bursa in the molecular differentiation of B lymphocytes," in *Differentiation of B Lymphocytes*, eds C. J. Paige and R. H. Gisler (Berlin, Heidelberg: Springer), 111–124.

Yonash, N., Cheng, H. H., Hillel, J., Heller, D. E., and Cahaner, A. (2001). DNA microsatellites linked to quantitative trait loci affecting antibody response and survival rate in meat-type chickens. *Poult. Sci.* 80, 22–28. doi: 10.1093/ps/80.1.22

Zaboli, G., Huang, X., Feng, X., and Ahn, D. U. (2019). How can heat stress affect chicken meat quality? – a review. *Poult. Sci.* 98, 1551–1556. doi: 10.3382/ps/pey399

Zhang, Y., Liu, T., Meyer, C. A., Eeckhoute, J., Johnson, D. S., Bernstein, B. E., et al. (2008). Model-based analysis of ChIP-Seq (MACS). *Genome Biol.* 9:R137.

**Conflict of Interest:** GR was employed by the company Zoetis.

The remaining authors declare that the research was conducted in the absence of any commercial or financial relationships that could be construed as a potential conflict of interest.

*Copyright © 2020 Chanthavixay, Kern, Wang, Saelao, Lamont, Gallardo, Rincon and Zhou. This is an open-access article distributed under the terms of the Creative Commons Attribution License (CC BY). The use, distribution or reproduction in other forums is permitted, provided the original author(s) and the copyright owner(s) are credited and that the original publication in this journal is cited, in accordance with accepted academic practice. No use, distribution or reproduction is permitted which does not comply with these terms.*

frontiers in Genetics

REVIEW
published: 14 October 2020
doi: 10.3389/fgene.2020.557846

# Parental Effects on Epigenetic Programming in Gametes and Embryos of Dairy Cows

*Chongyang Wu and Marc-André Sirard**

*Centre de Recherche en Reproduction, Développement et Santé Intergénérationnelle (CRDSI), Département des Sciences Animales, Faculté des Sciences de l'Agriculture et de l'Alimentation, Université Laval, Québec City, QC, Canada*

The bovine represents an important agriculture species and dairy breeds have experienced intense genetic selection over the last decades. The selection of breeders focused initially on milk production, but now includes feed efficiency, health, and fertility, although these traits show lower heritability. The non-genetic paternal and maternal effects on the next generation represent a new research topic that is part of epigenetics. The evidence for embryo programming from both parents is increasing. Both oocytes and spermatozoa carry methylation marks, histones modifications, small RNAs, and chromatin state variations. These epigenetic modifications may remain active in the early zygote and influence the embryonic period and beyond. In this paper, we review parental non-genetic effects retained in gametes on early embryo development of dairy cows, with emphasis on parental age (around puberty), the metabolism of the mother at the time of conception and *in vitro* culture (IVC) conditions. In our recent findings, transcriptomic signatures and DNA methylation patterns of blastocysts and gametes originating from various parental and IVC conditions revealed surprisingly similar results. Embryos from all these experiments displayed a metabolic signature that could be described as an "economy" mode where protein synthesis is reduced, mitochondria are considered less functional. In the absence of any significant phenotype, these results indicated a possible similar adaptation of the embryo to younger parental age, post-partum metabolic status and IVC conditions mediated by epigenetic factors.

**Keywords: parental age, embryonic development, dairy cows, epigenetics, metabolism, transgenerational inheritance, intergenerational inheritance**

OPEN ACCESS

***Edited by:***
*Stephanie McKay,*
*University of Vermont, United States*

***Reviewed by:***
*George E. Liu,*
*United States Department of Agriculture, United States*
*Shahin Eghbalsaied,*
*Islamic Azad University, Isfahan, Iran*

***Correspondence:**
*Marc-André Sirard*
*marc-andre.sirard@fsaa.ulaval.ca*

***Specialty section:***
*This article was submitted to Livestock Genomics, a section of the journal Frontiers in Genetics*

***Received:*** *30 April 2020*
***Accepted:*** *18 September 2020*
***Published:*** *14 October 2020*

***Citation:***
*Wu C and Sirard M-A (2020) Parental Effects on Epigenetic Programming in Gametes and Embryos of Dairy Cows. Front. Genet. 11:557846. doi: 10.3389/fgene.2020.557846*

## EPIGENETICS: A NEW MEASURE OF THE EFFECTS OF THE ENVIRONMENT ON THE PHENOTYPE

Phenotype is the term that refers to the observable characteristics or traits of an organism. It is determined by the genotype of an organism, and by the growing environment, but precisely predicting the actual outcome for a particular individual is still a challenge (Burga and Lehner, 2012). The idea that phenotype changes caused by environmental alterations can be passed to next generations has existed for centuries (Roberts and Hay, 2019) but only in recent decades the advances in epigenetics knowledge gave us insights to the underlying mechanism of how environment affects the phenotype of an organism. In this review, we will discuss the parental epigenetic effects on programming in gametes and embryos, mainly focusing on dairy cattle.

The definition of epigenetics is evolving to accommodate our increasing knowledge of mechanisms that regulate gene expression. Presently, the widely accepted definition of epigenetics is "heritable changes in gene expression without altering the DNA sequence" with two main characteristics: inheritable and reprogrammable (Allis and Jenuwein, 2016). Inheritability of epigenetics mainly refers to the maintenance of epigenetic modifications in a short term, such as during mitosis of differentiated somatic cells, while reprogramming of epigenetics describes the ability to erase and rebuild modifications in a long term, such as across generations (Ji and Khurana Hershey, 2012). However, reprogrammable epigenetic information does not mean it will be completely removed at each generation, on the contrary, a small portion of epigenetic modifications can be transferred to next generation (intergenerational inheritance) or even beyond them (transgenerational inheritance) (Perez and Lehner, 2019).

The understanding of epigenetics is constantly modulated by the advance in our knowledge of evolution and development (Felsenfeld, 2014). There are four main epigenetic components: DNA methylation, histone modifications, non-coding RNAs, and chromatin state. In contrast to genetic information, epigenetic factors are vulnerable to be influenced by environmental changes. These alterations have been reported to be transgenerationally and/or intergenerationally inherited and affect the phenotype of the subsequent generations (Xavier et al., 2019).

## DNA Methylation

DNA methylation is an epigenetic modification catalyzed by DNA methyltransferases (DNMTs) which transfer the methyl from the donor *s*-adenosyl methionine (SAM) to specific bases (Lyko, 2018). In mammals, DNA methylation predominantly occurs in the dinucleotide sequence 5′CpG3′, generating 5-methylcytosine (5mC) (Lyko, 2018). Most bulk genomic methylation status are steady over lifetime, with minor changes during specific cellular activities (Smith and Meissner, 2013). The two exceptions occur in embryo development, i.e., pre-implantation stage and primordial germ cell (PGC) stage, when most of the CpGs undergo global demethylation and remethylation (Wang et al., 2014). However, in mammals, a small portion of DNA methylation marks are protected from two waves of genome-wide DNA methylation reprogramming, which is not only indispensable for embryogenesis but can also inherit parental acquired traits to next generations (Smith et al., 2014; Wang et al., 2014; Jiang et al., 2018). The dynamic DNA methylome landscape carries important regulatory roles in gene expression, genomic imprinting, embryo development, and chromosome structure (Smith and Meissner, 2013).

## Histone Modifications

Histones are basic proteins in eukaryotic cell nuclei that package DNA into nucleosomes. Different covalent post-translational modifications of histones bind to different genomic elements and have diverse functions in modulating the chromatin structure or recruiting other proteins to regulate gene expression. Modifications such as histone H3 lysine 4 di-/tri-methylation (H3K4me2/me3), H3K36me3, H3K79me3, and histone acetylation are linked to active expression, while H3K9me2/me3, H3K27me3 and histone deacetylation are associated with transcriptional repression (Zhang et al., 2015). During spermatogenesis and maturation, histones are gradually replaced with protamine to reduce the size of the sperm head. However, 1–15% of the histones are retained and are associated with DNA regions accessible soon after fertilization (Siklenka et al., 2015). In contrast, this replacement does not occur in oocytes, but the histones go through spatial and temporal post-translational modifications, including acetylation, methylation, phosphorylation, etc., which is critical for oocyte maturation (Gu et al., 2010) and maternal-to-zygotic transition after fertilization (Dahl et al., 2016; Zheng et al., 2016; Xia et al., 2019). A novel imprinting mechanism was reported to be dependent on maternal H3K27me3 rather than DNA methylation (Inoue et al., 2017).

## Non-coding RNAs

Non-coding RNAs (ncRNAs) are transcripts that are not translated into proteins: such as ribosomal RNA (rRNA), ribozyme, transfer RNA (tRNA), and small nuclear RNA (snRNA). They are involved in the regulation of numerous bioactivities: such as cell proliferation, cell differentiation, cell apoptosis, cell metabolism, and chromosome remodeling. Moreover, ncRNA from both parental gametes are required for normal embryonic development (Yuan et al., 2016; Conine et al., 2018; McJunkin, 2018). Before the embryonic genome activation (EGA), early embryos mainly rely on transcript reservoir from maternal origin, thus the importance of maternal ncRNAs during early embryogenesis is taken for granted. Plenty of maternal ncRNAs were discovered to be involved in EGA, hence transfer maternal environmental influences to offspring (Perez and Lehner, 2019).

Sperm of germline-specific *Dicer* and *Drosha* conditional knockout mice have deficient miRNAs and/or endo-siRNAs profiles (Yuan et al., 2016). Although these sperms could still fertilize wild-type oocytes by intracytoplasmic sperm injection (ICSI), developmental potential of embryos produced were significantly impaired. Injecting wild-type sperm-derived total or small RNAs was able to rescue the developmental deficiency of these embryos (Yuan et al., 2016). Further studies identified that these transcripts especially small non-coding RNAs were gained during later maturation in epididymis (Conine et al., 2018). Embryos generated by ICSI using sperm from caput failed after implantation, while this deficiency could be rescued by microinjection of cauda-specific small RNAs (Conine et al., 2018).

## Chromatin State

Chromatin state is used to describe various conformations of chromatin structure which reflects its dynamic spatial changes during embryo reprogramming and other cellular activities (Zhou and Dean, 2015). Multiple epigenetic factors are involved in determining chromatin state, including histone modification, DNA methylation and non-coding RNAs (Gupta et al., 2010; Kundaje et al., 2015). The complex relationship between epigenetic modifications, chromatin state and transcriptional

activities are still largely unknown, but our understanding of these associations is improving, based on the increasing experimental evidence (Ernst et al., 2011; Ernst and Kellis, 2012, 2017). Basically, genes with higher expression are most likely located at open chromatin regions which are generally modified by active epigenetic marks: such as H3K4me3 on proximal promoters, H3K27-ac on enhancers, and low DNA methylated promoters (Gaspar-Maia et al., 2011; Tian et al., 2011). Repressed expression genes are found in closed chromatin regions bound with inactive epigenetic marks including H3K37me3, hypermethylation at transcription start sites, and long non-coding RNA bound regions (Saxena and Carninci, 2011; Ando et al., 2019; Igolkina et al., 2019). During gametogenesis and embryogenesis, chromatin states undergo extensive remodeling to reach totipotency. However, the erasure is not complete, a complex pattern of 3D interactions between chromatin and transcription factors in both oocytes and sperm can still be transmitted to zygote according to ATAC-seq and ChIP-seq results (Jung et al., 2017, 2019). In bovine, retained histones were also identified by Mnase-seq in spermatozoa and seem required for spermatogenesis and fertilization (Sillaste et al., 2017). Overall, these retained accessible chromatin are indispensable for early embryogenesis and may also be potential candidates to transmit parental effects to next generations.

# REPROGRAMMING AND INHERITANCE OF EPIGENETIC MARKS DURING EMBRYO DEVELOPMENT

## Preimplantation Embryo Development

Throughout mammalian life cycle, individual experiences two waves of global epigenetic reprogramming, during preimplantation stages and germ cell development (Zeng and Chen, 2019). After fertilization, murine parental genomes were both observed to be actively (TETs-dependent) and passively (replication-dependent) demethylated during early embryogenesis, with exception of certain genomic loci, including imprinted genes (Guo F. et al., 2014; Wang et al., 2014). Recent single-cell chromatin overall omic-scale landscape sequencing (scCOOL-seq) of mouse preimplantation embryos further comprehensively described a heterogeneous but highly coordinated features of epigenetic reprogramming (Guo et al., 2017). Global DNA demethylation occurs within 12 h of fertilization, while distinct gene regions were resistant to reprogramming in parental genomes (Guo et al., 2017). Comparable chromatin accessibility was observed between paternal and maternal genomes from the late zygote to the blastocyst stage (Wu et al., 2016; Guo et al., 2017). Genomic regions that are resistant to global epigenetic reprogramming are potential factors to inherit parental environmental influences on offspring, but this requires to be further distinguished from *de novo* modifications after fertilization.

Epigenetic reprogramming during early embryo development is conserved between human and mice, while the kinetics of human embryos is relatively slower (Eckersley-Maslin et al., 2018). In human, major wave of global DNA demethylation was completed at 2-cell stage, and further reduced to 29% as the bottom at blastocyst stage in ICM (Guo H. et al., 2014). Besides imprinted genes, evolutionarily young transposable elements with more active transcription retain their DNA methylation status in early embryos (Guo H. et al., 2014). scCOOL-seq of human preimplantation embryos identified a complex, yet highly ordered epigenetic reprogramming process (Li et al., 2018). In contrary to mice, the paternal genomes in human early embryos are already more open than maternal genomes from the mid-zygote to the 4-cell stage (Li et al., 2018).

In bovine, the genome-wide demethylation is closely related to EGA since the major wave reduction of DNA methylation is completed by the 8-cell stage (Jiang et al., 2018). During that period, promoter methylation is negatively correlated with the expression levels of genes at preimplantation stages; gametes-specific differentially methylated regions (DMRs) are enriched in different regions and demethylated in different manners (Jiang et al., 2018). However, a small portion of DNA methylation will be maintained during the global reprogramming after fertilization, including imprinted genes, which could become a legacy between parental environment effects with offspring phenotype (Jiang et al., 2018). Moreover, dynamic landscape of accessible chromatin in bovine preimplantation embryos were revealed recently by ATAC-seq. Chromatin accessibility is dramatically increased in coordination with EGA and reached to peak in elongating embryos at day 14 (Ming et al., 2020). Combined with bovine transcriptomic and DNA methylation data, accessible promoters were related to genes with high expression and the accessibility is closely related to DNA methylation level and CpG density (Ming et al., 2020). Although the expression of histone modification enzymes was profiled during early embryo development (McGraw et al., 2003; Glanzner et al., 2018), global reprogramming of modified histones throughout bovine preimplantation stages is not known.

## PGC Development

During the two waves, somatic epigenetic modifications in PGCs are erased and established as sex-specific patterns, including the genome-wide DNA methylation reprogramming and chromatin reorganization (Hackett et al., 2013). Less than 10% CpG sites were protected from demethylation in mouse PGC at E13.5, which is predominantly located in long terminal repeats (LTRs) at intergenic regions (Hackett et al., 2013; Wang et al., 2014). However, conflicting results were reported as to whether IAP elements (Intracisternal A-type particle) were resistant to DNA demethylation (Seisenberger et al., 2012; Hackett et al., 2013) or not (Wang et al., 2014). Along with the global DNA demethylation, chromatin structure undergoes actively remodeling by both extensive erasure of various histone modifications and exchange of histone variants (Hajkova et al., 2008). Although genome-wide distribution of retained histone modification is still not clear in mice, it has been identified that several silencing marks, such as H3K9me3 and H4K20me3, were retained on pericentric heterochromatin during PGC development (Magaraki et al., 2017). Diverse piRNAs were expressed in mice PGCs and involved in not

only silencing of transposable elements but also translation regulations (Barreñada et al., 2020), which can be regarded as another transgenerational inheritance factors as reported in *Caenorhabditis elegans* (Ashe et al., 2012).

In human, the lowest DNA methylation was observed in the female PGCs of 10-week embryos, with an average of 6% methylation remaining (Guo et al., 2015). Similar to the observations in mice, the retained loci are particularly enriched in evolutionarily younger and more active repeat and transposable elements (Gkountela et al., 2015; Guo et al., 2015). Moreover, H3K9me3 can escape from global reprogramming to repress the constitutive heterochromatin (Gkountela et al., 2015; Guo et al., 2015), while the involvement of non-coding RNAs in human PGC development is still not clear.

Studies on PGC reprogramming were mainly focusing on model animals and human, although bovine PGCs were already identified and isolated by AP staining in embryos at E18-E39 in 1990s (Lavoir et al., 1994; Wrobel and Süß, 1998). Thus, it is urgently needed to characterize the landscapes of DNA methylation, histone modifications/chromatin states, ncRNAs, etc. during PGC development in bovine. This will enlighten our knowledge of the most extensively reprogramming process in large animals and point out the potential transgenerational inheritance factors which are able to escape from this global erasure.

## THE KNOWN NON-GENETIC PARENTAL INFLUENCES IN MICE AND HUMAN

Due to the vast amount of information conveyed from female gametes to zygotes and the exposure to the uterus environment during pregnancy, epigenetic influences of maternal origin were studied extensively. The effects of maternal nutrition status, age, stress, lifestyle, disease, and others were reported to be transmitted to next generations. However, research on paternal non-genetic effects has been long neglected compared to the numerous studies undertaken on the maternal side. Benefitting from studies to identify the molecules that sperm transfer during fertilization, paternal epigenetic influences are now gaining more and more attention. Here, we will firstly illustrate parental non-genetic effects focusing on mouse and human studies.

### Non-genetic Maternal Effects in Mice

Due to the short lifespan, transgenerational studies of maternal effects in mice are quite common and informative. Pre-conceptional and gestational maternal obesity induced cardiac dysfunction and hypertension in offspring (Loche et al., 2018). Also, exposure to bisphenol A (BPA, an endocrine disruptor) induced metabolic defects transgenerationally up to the F3 offspring (Bansal et al., 2019). However, the phenotype was less severe with increasing generations, probably due to the diluting effects of epigenetic reprogramming during early embryo development (Bansal et al., 2019). Pre-conceptional maternal exposure to cyclophosphamide (an agent for breast cancer therapy) altered DNA methylation levels in F1 and F2 mouse oocytes, resulting in delayed growth in these two generations (Di Emidio et al., 2019).

### Non-genetic Maternal Effects in Human

In humans, the mother condition has a profound impact on offspring across generations through epigenetic modifications. Epidemiological studies demonstrated that F2 generations of mothers who experienced famine periods had a higher tendency toward metabolic disorders (Aiken et al., 2016), partially due to the alteration of methylation levels in genomic DNA and histones (Uchiyama et al., 2018; Zimmet et al., 2018). Maternal age is another factor that can influence the developmental outcomes of progeny. Offspring of younger mothers tended to take more time to get pregnant (Reynolds et al., 2020); while offspring of advanced-age mothers were more likely to have metabolism or neurodevelopmental disorders with reduced methylation levels of several specific CpG sites (Markunas et al., 2016). Hence, epigenetic modifications are involved in the massive non-genetic maternal influence on offspring.

### Non-genetic Paternal Effects in Mice

Several comprehensive studies on paternal epigenetic effects on offspring were generated with the mouse model. The effects of metabolic disorders in male mice (Wei et al., 2014) and toxic exposure (Guerrero-Bosagna et al., 2012) can be transgenerationally inherited by disturbing DNA methylation levels in sperm. Disruption of histone methylation during spermatogenesis resulted in modified chromatin states in sperm and impaired development and survivability over two generations (Siklenka et al., 2015). Transfer RNA-derived small RNAs (tsRNAs), the major component of ncRNAs in mature spermatozoa apparently acquired during the transit in the epididymis (Chen et al., 2016b; Sharma et al., 2018), is believed to mediate paternal diet-induced metabolic disorders in offspring (Chen et al., 2016a; Sharma et al., 2016). These results clearly demonstrated the transgenerational inheritability of paternal epigenetic information in mice.

### Non-genetic Paternal Effects in Human

In human, the paternal contribution to an embryo is required for the embryo development and non-genetic components are involved in the transmission of paternal acquired traits to their children. Alteration of DNA methylation level, histone modifications, non-coding RNA expression and chromatin status were observed in the sperm of men who smokes, are obese, or experience mental stresses indicating an intergenerational inheritance through them (Soubry et al., 2016; Jenkins et al., 2017; Rowold et al., 2017; Dupont et al., 2019). Moreover, some of these aberrant changes were found in the sperm of their offspring and transgenerationally influenced the health of next generation (Soubry et al., 2013; Craig et al., 2017).

# THE KNOWN NON-GENETIC PARENTAL INFLUENCES IN DAIRY CATTLE

## Non-genetic Maternal Effects in Dairy Cattle

In bovine, prenatal maternal conditions were significantly correlated with the daughters' fertility and milk production. For example, daughters of dam that calved early for the first time produced more first-lactation daily milk, had higher body condition score (BCS), but experienced difficulties conceiving (Banos et al., 2007). Meanwhile, gestating dams with higher BCS tended to give birth to calves with higher BCS, had lower return rates, but slightly lower daily milk yields (Banos et al., 2007). The prenatal environment of grand-dam can also somewhat influence the milk production in subsequent daughters potentially in a transgenerationally manner by epigenetic mechanisms (Singh et al., 2012; Gudex et al., 2014). Additionally, the separation of heifers from their mother shortly after birth, which is a widely applied procedure in dairy cow management, will result in stress analogous to the maternal separation and unpredictable maternal stress (MSUS) model in rodents. Thus, this practice makes dairy cows a model to study the non-genetic inheritance of MSUS (Engmann, 2018).

As mentioned above, the maternal metabolic status can influence production and reproductive traits of subsequent generations through non-genetic pathways. However, there is a paucity of studies on the specific mechanisms underlying the effects of the maternal metabolism pre-conception or during gestation on offspring. Recently, embryos from dairy cows experiencing different levels of negative energy balance (NEB) were collected to study the influence of the maternal metabolic environment on the transcriptome and epigenome of early embryos by microarrays (Chaput and Sirard, 2019). Transcriptomic data highlighted that the most significantly affected pathways were metabolism-related: such as protein synthesis (EIF2 Signaling and eIF4, translation factors), mitochondrial function (oxidative phosphorylation and mitochondrial dysfunction), and metabolism (Sirtuin signaling and mTOR Signaling) (Chaput and Sirard, 2019). Gene expression levels do not provide any information about the amount of protein generated, or the extent of further modifications: such as phosphorylation, acylation, and/or methylation. Transcriptomic studies can be used to evaluate the immediate impact of environmental stresses and the embryonic responses (Cagnone and Sirard, 2016). Meanwhile, to study the long-term effects of stressors, studies on epigenetic modifications are required, especially for those regions that are affected according to the transcriptomic results. Using a DNA methylation microarray, 462 DMRs were identified between embryos from cows in high and low NEB, with many of them being located in gene regions, including introns, exons, proximal promoters, promoters, and distal promoters (Chaput and Sirard, 2019). Most of these genic regions, except exons, were more hypermethylated in embryos from cows experiencing severe NEB (Chaput and Sirard, 2019). Functional analysis of DMRs located in gene regions was consistent with transcriptomic results and pointed toward metabolic related pathways (AMPK signaling and mTOR signaling) which are significantly affected by maternal energy deficits (Chaput and Sirard, 2019). As a key switch for keep the energy balance, AMPK were also regulated by small non-coding RNAs to control cellular anabolic and catabolic processes in dairy cows (Mahmoudi et al., 2015). These changes demonstrated the metabolic adaptations of embryos to the maternal gestational environment by the regulation of mitochondrial functions, cell growth, and other protective pathways. These NEB-associated DMRs were retained at the time of the global reprogramming after fertilization, thus it is highly possible that they could affect the phenotype of offspring intergenerationally. The DNA methylation analysis of blood from eight calves produced from high and low BHB mothers resulted in 1675 DMRs ($p < 0.05$) indicating a post-natal legacy. This study highlighted how embryos interact with the maternal environment and the potential for intergenerationally inherited phenotype transmission through epigenetic modifications.

## Non-genetic Paternal Effects in Dairy Cattle

Multiple epigenetic factors conveyed by sperm are affected by the environmental or physical conditions of bulls. Not only maternal and fetal effects influence gestation length, a total of 66,318 DMRs in sperm were correlated with gestation length as well as days to first breeding after calving, somatic cell score, body type, milk production, and other traits (Fang et al., 2019). Reactome pathways analysis further validated that DMRs were mainly related to pregnancy, embryonic development, and lipid metabolism pathways (Fang et al., 2019). Moreover, some of these DMR were mapped to genes that are transcriptionally active during preimplantation stages, suggesting their potential role in early embryo development (Fang et al., 2019). Similarly, age-related DMRs were observed in bovine spermatozoa (Takeda et al., 2017, 2019; Lambert et al., 2018), and 57 of 2223 DMRs (2.56%) were retained in blastocysts (Lambert et al., 2018; Wu et al., 2020). Among the genes that are mapped with these DMRs, some of them were involved in spermatogenesis (FKBP6) and embryonic preimplantation development (AKT2). Chromatin condensation status can also be altered under heat-stress and further influence DNA methylation reprogramming of paternal pronuclei, which may be responsible for the reduced fertilization rates after IVF (Rahman et al., 2014). *In vitro* exposure to Chlorpyrifos, a pesticide, significantly affected bovine sperm DNA methylation patterns, resulted in reduced sperm motility and IVF rates, and increased chromatin structure abnormalities (Pallotta et al., 2019). Although large epidemiologic studies are missing, these changes in the epigenetic marks could potentially alter the phenotype of offspring.

Similar to cows, paternal metabolic status significantly influences semen quality. Enhanced pre-pubertal nutrition elevates the percentage of progressively motile and upregulates mitochondrial function in sperm of post-pubertal dairy bulls

(Johnson et al., 2020). In contrast, low planes of nutrition of young Holstein-Friesian bulls resulted in the retarded onset of puberty (Byrne et al., 2018). Although epigenetic studies related to bull metabolic status is still missing, DNA methylation and histone modifications patterns were both reported to be associated with bull fertility (Verma et al., 2015; Kropp et al., 2017; Kutchy et al., 2018; Capra et al., 2019; Ugur et al., 2019). Functional annotation of these alterations indicate that they might be involved in spermatogenesis and embryo development (Verma et al., 2015; Ugur et al., 2019).

## Effects of *in vitro* Culture Condition in Dairy Cattle

Another tool to study embryo programming is *in vitro* culture (IVC) in different types of environment. Assisted reproductive technologies (ARTs) have been widely used to either overcome reproductive difficulties (for human) or increase the genetic gain of elite sires (for cattle). *In vitro* culture, an indispensable ART procedure, allows zygotes to divide to a transferrable stage at around day 7 for bovine embryos. Each aspect of the IVC medium, including physicochemical, oxidative, and energetic conditions (Summers and Biggers, 2003), has profound effects on embryo development, and these effects could be maintained to adulthood or even subsequent generations. The physiochemical parameters increased osmolality (Etienne and Martin, 1979), decreased local pH (Dagilgan et al., 2015), and heat shock (Sakatani et al., 2008) were all shown to compromise embryo development. Additionally, specific levels of reactive oxygen species (ROS) are required for normal embryo development; however, it is inevitable that embryos will be exposed to higher concentrations of oxygen *in vitro*, which is detrimental as a result of increased $H_2O_2$ production, DNA fragmentation, and mitochondrial dysfunction-induced apoptosis (Van Soom et al., 2002; Harvey et al., 2004; Kitagawa et al., 2004). The presence of nutrients in concentrations that mimic *in vivo* conditions is fundamental to early embryogenesis as demonstrated by the deleterious effects on embryo development of high concentrations of glucose and lipids in the culture medium (Díaz-Ruiz et al., 2008). An excessive inflammatory response was observed in IVC blastocysts, and this could interfere with the embryo-maternal recognition process following transfer (Cagnone and Sirard, 2014). Based on the metabolic pathways affected by culture conditions, embryos can either enhance a Warburg-like effect to adapt to minor stresses or induce apoptosis under severe stress. As a result, even though blastocyst rates may not be significantly impacted in modified media, embryo loss rates may be higher compared to control conditions. Moreover, mitochondrial dysfunction is involved in the embryonic response to IVC stresses which may impact its main role as energy factory, as well as the production of acetyl-CoA and methyl groups associated with one-carbon metabolism (Steegers-Theunissen et al., 2013), which controls histone acetylation and DNA methylation. Thus, suboptimal IVC conditions do disturb the embryonic epigenome which could contribute to the sometime altered phenotype of offspring (Cagnone and Sirard, 2016).

# USING PARENTAL AGE TO ASSESS THE MECHANISMS OF METABOLIC PROGRAMMING

Potential genetically elite sires can be identified a few days postnatally by genomic selection. In combination with ARTs, these approaches greatly reduce generation interval to increase the rate of genetic gain (Kasinathan et al., 2015). Additionally, there is increased demand for the use of juvenile calves or heifers for embryo production in combination with genomic selection and ARTs, which can further shorten generation interval (Landry et al., 2016). However, gametes from young donors are suboptimum compared to those from adults. Recent studies also indicated the potential parental age effects on early embryo development.

## Paternal Age Effects on Semen

On the male side, semen quality and quantity are significantly correlated with the age of the bull (Takeda et al., 2017). The ontogeny of the male reproductive system is initiated during the fetal period and the onset of bull puberty is governed by complex neuroendocrine networks (Plant, 2015) which are responsible for the tight coupling between metabolic status and reproductive system development (Roa et al., 2010). The early transient rise in LH pulsatility marks the initiation of puberty (Evans et al., 1995), which is observed in bull calves between 10 and 20 weeks of age (Rawlings and Evans, 1995). Leydig cells proliferate rapidly with an elevated responsiveness to LH, resulting in increased testosterone concentration to initiate the differentiation of unmatured Sertoli cells and further spermatogenesis (Amann and Walker, 1983). The first unmatured spermatids are generated between 25 and 35 weeks of age, while mature spermatozoa are obvious in seminiferous tubules at 32–40 weeks of age (Abdel-Raouf, 1960; Macmillan and Hafs, 1968; Evans et al., 1996; Bagu et al., 2006). A bull is then considered to have reached puberty when the first ejaculation containing over 50 million spermatozoa with at least 10% progressively motile spermatozoa is observed at around 45 weeks of age (Wolf et al., 1965). Hence, it is expected that semen collected at prepubertal stages is often sub-optimal in terms of sperm concentration, motility, and IVF performance compared to semen collected from adult bulls (Takeda et al., 2017). Moreover, this sub-standard sperm quality is associated with lower body weight in sexually immature bulls (Devkota et al., 2008), indicating that the paternal age effects on reproductive outcome may resemble the restricted diet effects (Brito et al., 2007).

Several studies demonstrated that enhanced early-life nutrition of bull calves positively affects several key metabolic and reproductive hormones related to the hypothalamic-pituitary-gonadal (HPG) axis, as reviewed by Kenny and Byrne (2018), and successfully hastens puberty without interfering with post-pubertal semen quality (Dance et al., 2015, 2016). In the commercial environment (optimized for breeders) setting used for the bulls in our study, semen ejaculated at the age of 10 months performed similarly

to semen from post-pubertal animals regarding sperm concentration, motility, and blastocyst rates; although the semen from younger animals contained fewer spermatozoa (Wu et al., 2020).

To study the epigenetic programming of sperm from young bulls, a new bovine specific platform, EmbryoGENE[1], which can simultaneously evaluate the genome-wide epigenome and transcriptome of small samples, such as sperm, oocytes, and early embryos (Shojaei Saadi et al., 2014), was used to evaluate the influence of environmental and parental effects on embryo development (Salilew-Wondim et al., 2015; Desmet et al., 2016; Pagé-Larivière et al., 2016; Morin-Doré et al., 2017; Tremblay et al., 2018; Chaput and Sirard, 2019; Wu et al., 2020).

Different DNA methylation patterns were observed in sperm collected either from the same bulls at different pubertal stages (Lambert et al., 2018) or from different bulls of different ages (Takeda et al., 2017, 2019). Approximately 69% of the DMRs were located in genic regions, including one associated with the paternally imprinted gene MEST (mesoderm specific transcript) (Lambert et al., 2018). Methylation levels of most DMRs were higher with increasing age (Lambert et al., 2018; Takeda et al., 2019); interestingly, these levels changed rapidly especially at younger ages (Takeda et al., 2019). Network analysis of these DMRs revealed that sperm function related pathways, such as PKA signaling, sperm motility, calcium signaling, and protein G signaling pathways were significantly affected by paternal age (Lambert et al., 2018). Hence, although young bulls can produce functional semen, epigenetic factors transmitted by spermatozoa could potentially impact embryo or offspring development.

## Paternal Age Effects on Embryos

Epigenetic modifications are known to occur as paternal inter or transgenerational inheritance factors (Rando, 2016; Spadafora, 2017; Bošković and Rando, 2018). To further study paternal age effects on embryos, blastocysts were produced by IVF with spermatozoa from the same bulls at different pubertal periods (10, 12, and 16 months) and oocytes from several matched (the same cow for each individual bull) adult cows (Wu et al., 2020). Transcriptomic and epigenetic analysis were performed on four pairs, where the only difference between embryos was the age of the bull. The results revealed elevated mitochondrial dysfunction, suppressed oxidative phosphorylation, and reduced protein synthesis in blastocysts generated from younger bulls suggesting a low energy status in these blastocysts (Wu et al., 2020). Moreover, the affected metabolic and sperm function pathways observed in blastocysts were consistent with the sperm studies mentioned above (Lambert et al., 2018), suggesting paternal age effects on embryos mediated by epigenetic factors in sperm.

## Maternal Age Effects on Oocyte

On the female side, the same selection pressure pushes the breeding industry to collect oocytes from dairy heifers to reduce generational interval and increase genetic gain. It has been reported that *in vitro* produced embryos can be obtained using oocytes from heifers as young as 2–4 months; however, few cumulus oocyte complexes (COCs) could be recovered from non-stimulated heifer ovaries (Majerus et al., 1999; Palma et al., 2001; Kauffold et al., 2005). Even though these COCs had similar performance in maturation, fertilization, and early cleavage rates after IVF compared to COCs from adult cows, reduced blastocyst yields and greater embryo loss following embryo transfer were observed, which may be a consequence of increased apoptosis in embryos from young donors (Zaraza et al., 2010). Ovarian stimulation is widely accepted for generating oocytes of high quality and for increasing blastocyst yields from adult cows (Nivet et al., 2012; Labrecque et al., 2013). More follicles were aspirated from young calves following stimulation, and higher numbers of mature oocytes and cleaved embryos were obtained (Landry et al., 2016). However, there was no difference in the total number of morula or viable embryos from heifers 5–18 months old, due to the significant lower morula and blastocyst rates in heifer groups which neutralized the larger number of oocytes recovered (Landry et al., 2016). Further analysis of granulosa cells collected from heifers demonstrated that cell differentiation, inflammation, and apoptosis pathways were inhibited indicating a suboptimal environment for oocytes in young donors (Landry et al., 2018).

## Maternal Age Effects on Embryos

To further investigate the maternal age effects on embryos, oocytes from the same heifers at different pubertal stages were collected and *in vitro* fertilized with spermatozoa from matched adult bulls (Morin-Doré et al., 2017). Transcriptomic analysis revealed that mitochondrial function was impacted in blastocysts from younger heifers, with inhibited mTOR, NRF2, and PPAR signaling (Morin-Doré et al., 2017). Thus, we can obtain more oocytes and comparable numbers of transferable embryos from young donors following ovarian stimulation; however, young maternal age impairs metabolic functions during early embryo development and may cause embryo loss at later stages or induce offspring health disorders. The identification of genes affected in blastocysts from younger females revealed several gene pathways similarly affected in embryos originating from younger males making the results even more convincing and suggesting that there might be an evolutionary conserved mechanism involved.

# GENOTYPE × ENVIRONMENT INTERACTION

Genotype (G) × Environment (E) interaction is defined as genotype-specific phenotypic responses to different environments (Falconer, 1952). Taking G × E into consideration in dairy cow breeding reduces the error variance and hence increases the accuracy of genetic evaluation of sires and cows compared to classical approach, which considers the effects of genotype and environment only (**Figure 1B**) (Ron and Hillel, 1983). Two formations of G × E interactions can be taken to induce either unchanged ranking, i.e., a

[1]http://emb-bioinfo.fsaa.ulaval.ca/

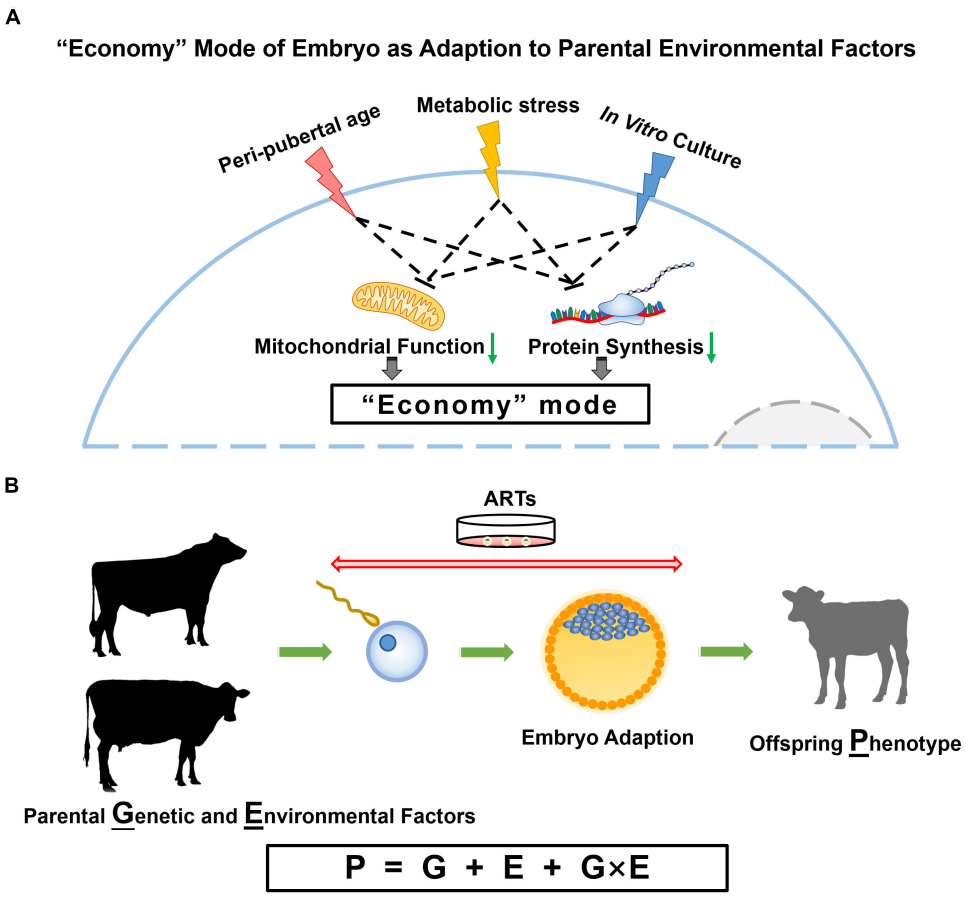



**FIGURE 1 |** Parental influences on embryo and offspring. **(A)** Proposed model for embryo adaption of parental environmental factors. In this model, peri-pubertal age, metabolic status and IVC conditions result in embryos turning to an "economy" mode with slowed down cellular activities, especially the reduced mitochondrial function and protein synthesis. **(B)** The phenotype of offspring is determined by genotype, environment, and the interplay of genetic and environmental factors.

scaling effects, or reranking of sires across environments (Cromie et al., 1998). Plenty of across countries and within a country dairy cattle studies concluded that scale effects, which is due to the unequal scale of differences in sire proofs in the two environments, account majorly for the G × E interaction (McDaniel and Corley, 1967; Stanton et al., 1991; Boettcher et al., 2003). However, emerging evidence using genetic correlation proved the existence of re-ranking effects of G × E interactions, especially between the traits expressed in environments with large differences as reviewed by Hammami et al. (2009b) and Wakchaure et al. (2016). Genetic correlations < 0.80 were observed between milk yield across countries (Ojango and Pollott, 2002; Cerón-Muñoz et al., 2004b; Hammami et al., 2009a), between age at first calving across countries (Cerón-Muñoz et al., 2004a), between two feeding systems within country (Ramírez-Valverde et al., 2010), indicating the presence of genotype by environment interactions and at least some re-ranking of the animals. In this case, the breeders are required to optimize the breeding programs to accommodate the various environments.

Genes may be expressed in different patterns under different environment, and this could be one of the molecular mechanisms of G × E interactions (Hammami et al., 2009b). Epigenetic factors are involved in changing gene expression under varied environments. For example, DNA methylation at promoter regions can affect the binding of transcription factors, small non-coding RNAs can also regulate the transcription and translation in different ways, histone modification and chromatin states can determine the accessibility of chromatin for gene expression. Epigenetic regulation of multiple traits of dairy cow under different environments have been studied broadly and deeply (Singh et al., 2010; Ibeagha-Awemu and Zhao, 2015; Thompson et al., 2020). However, direct study of involvement of epigenetic factors in G × E interactions is still missing. Nevertheless, genomic bias were presented in relation to gene with G × E interactions, as reviewed by Grishkevich and Yanai (2013) based on whole-genome approaches in model organism and concluded that gene having long promoters with high concentration of regulatory motifs showed high correlation with distant-acting loci. Thus, epigenetic variations in different environments are highly possible to be responsible

for G × E interactions effects, while substantial and systematic studies are required.

## CONCLUSION

Epigenetic information conveyed by gametes represent non-genetic factors that may explain why gametes of donors at different ages have similar reproductive performance, but result in different gene expression and DNA methylation patterns in embryos they produced. Counterintuitively, parental nutritional status, age, and IVC environment have similar consequences on embryo programming, i.e., alterations in metabolic pathways, especially mitochondrial signaling, which proves that cellular energy production is central in the response to environmental changes (**Figure 1A**). The most important task now becomes the analysis of post-natal phenotypes to identify the phenotypical consequences of all these epigenetic modifications in offspring. Fortunately, in sub-species like the dairy cow, data are accumulating on the genetic side (G) as more and more animals get genotyped, and on the phenotype (P) side using manual or electronic data generation at the farm. The combination of information from the farm environment (E) with genotype (G) and phenotype (P) information will allow the modeling of optimal environmental conditions for each animal or the optimal genotype for a defined environment (**Figure 1B**).

## AUTHOR CONTRIBUTIONS

M-AS designed the manuscript. CW and M-AS wrote the manuscript. All authors read and approved the final manuscript.

## FUNDING

This work was funded by the Natural Sciences and Engineering Research Council (NSERC grant no. 445230-12), Semex and DairyGen of Canada. CW received studentship support from China Scholarship Council-Université Laval (CSC-UL) joint scholarship.

## ACKNOWLEDGMENTS

The authors would like to thank Sylvie Bilodeau-Goeseels for proofreading this article.

## REFERENCES

Abdel-Raouf, M. (1960). The postnatal development of the reproductive organs in bulls with special reference to puberty. *Acta Endocrinol.* 34(2 Suppl.), 1–109. doi: 10.1530/acta.0.XXXIVS009

Aiken, C. E., Tarry-Adkins, J. L., and Ozanne, S. E. (2016). Transgenerational effects of maternal diet on metabolic and reproductive ageing. *Mamm. Genome* 27, 430–439. doi: 10.1007/s00335-016-9631-1

Allis, C. D., and Jenuwein, T. (2016). The molecular hallmarks of epigenetic control. *Nat. Rev. Genet.* 17, 487–500. doi: 10.1038/nrg.2016.59

Amann, R. P., and Walker, O. A. (1983). Changes in the pituitary-gonadal axis associated with puberty in Holstein bulls. *J. Anim. Sci.* 57, 433–442. doi: 10.2527/jas1983.572433x

Ando, M., Saito, Y., Xu, G., Bui, N. Q., Medetgul-Ernar, K., Pu, M., et al. (2019). Chromatin dysregulation and DNA methylation at transcription start sites associated with transcriptional repression in cancers. *Nat. Commun.* 10:2188. doi: 10.1038/s41467-019-09937-w

Ashe, A., Sapetschnig, A., Weick, E.-M., Mitchell, J., Bagijn, Marloes, P., et al. (2012). piRNAs can trigger a multigenerational epigenetic memory in the germline of *C. elegans*. *Cell* 150, 88–99. doi: 10.1016/j.cell.2012.06.018

Bagu, E., Cook, S., Gratton, C., and Rawlings, N. (2006). Postnatal changes in testicular gonadotropin receptors, serum gonadotropin, and testosterone concentrations and functional development of the testes in bulls. *Reproduction* 132, 403–411. doi: 10.1530/rep.1.00768

Banos, G., Brotherstone, S., and Coffey, M. P. (2007). Prenatal maternal effects on body condition score, female fertility, and milk yield of dairy cows. *J. Dairy Sci.* 90, 3490–3499. doi: 10.3168/jds.2006-809

Bansal, A., Li, C., Xin, F., Duemler, A., Li, W., Rashid, C., et al. (2019). Transgenerational effects of maternal bisphenol: a exposure on offspring metabolic health. *J. Dev. Orig. Health Dis.* 10, 164–175. doi: 10.1017/S2040174418000764

Barreñada, O., Fernández-Pérez, D., Larriba, E., Brieño-Enriquez, M., and del Mazo, J. (2020). Diversification of piRNAs expressed in PGCs and somatic cells during embryonic gonadal development. *RNA Biol.* 17, 1309–1323. doi: 10.1080/15476286.2020.1757908

Boettcher, P. J., Fatehi, J., and Schutz, M. M. (2003). Genotype×environment interactions in conventional versus pasture-based dairies in Canada. *J. Dairy Sci.* 86, 383–389. doi: 10.3168/jds.S0022-0302(03)73617-0

Bošković, A., and Rando, O. J. (2018). Transgenerational epigenetic inheritance. *Annu. Rev. Genet.* 52, 21–41. doi: 10.1146/annurev-genet-120417-031404

Brito, L. F. C., Barth, A. D., Rawlings, N. C., Wilde, R. E., Crews, D. H., Boisclair, Y. R., et al. (2007). Effect of feed restriction during calfhood on serum concentrations of metabolic hormones, gonadotropins, testosterone, and on sexual development in bulls. *Reproduction* 134, 171–181. doi: 10.1530/rep-06-0353

Burga, A., and Lehner, B. (2012). Beyond genotype to phenotype: why the phenotype of an individual cannot always be predicted from their genome sequence and the environment that they experience. *FEBS J.* 279, 3765–3775. doi: 10.1111/j.1742-4658.2012.08810.x

Byrne, C. J., Fair, S., English, A. M., Cirot, M., Staub, C., Lonergan, P., et al. (2018). Plane of nutrition before and after 6 months of age in Holstein-Friesian bulls: I. Effects on performance, body composition, age at puberty, and postpubertal semen production. *J. Dairy Sci.* 101, 3447–3459. doi: 10.3168/jds.2017-13719

Cagnone, G., and Sirard, M.-A. (2014). The impact of exposure to serum lipids during in vitro culture on the transcriptome of bovine blastocysts. *Theriogenology* 81, 712.e3–722.e3. doi: 10.1016/j.theriogenology.2013.12.005

Cagnone, G., and Sirard, M. A. (2016). The embryonic stress response to in vitro culture: insight from genomic analysis. *Reproduction* 152, R247–R261. doi: 10.1530/REP-16-0391

Capra, E., Lazzari, B., Turri, F., Cremonesi, P., Portela, A. M. R., Ajmone-Marsan, P., et al. (2019). Epigenetic analysis of high and low motile sperm populations reveals methylation variation in satellite regions within the pericentromeric position and in genes functionally related to sperm DNA organization and maintenance in *Bos taurus*. *BMC Genomics* 20:940. doi: 10.1186/s12864-019-6317-6

Cerón-Muñoz, M. F., Tonhati, H., Costa, C. N., Maldonado-Estrada, J., and Rojas-Sarmiento, D. (2004a). Genotype×environment interaction for age at first calving in brazilian and colombian holsteins. *J. Dairy Sci.* 87, 2455–2458. doi: 10.3168/jds.S0022-0302(04)73369-X

Cerón-Muñoz, M. F., Tonhati, H., Costa, C. N., Rojas-Sarmiento, D., and Echeverri Echeverri, D. M. (2004b). Factors that cause genotype by environment interaction and use of a multiple-trait herd-cluster model for milk yield of holstein cattle from Brazil and Colombia. *J. Dairy Sci.* 87, 2687–2692. doi: 10.3168/jds.S0022-0302(04)73395-0

Chaput, C., and Sirard, M. A. (2019). Embryonic response to high beta-hydroxybutyrate (BHB) levels in postpartum dairy cows. *Domest. Anim. Endocrinol.* 72:106431. doi: 10.1016/j.domaniend.2019.106431

Chen, Q., Yan, M., Cao, Z., Li, X., Zhang, Y., Shi, J., et al. (2016a). Sperm tsRNAs contribute to intergenerational inheritance of an acquired metabolic disorder. *Science* 351, 397–400. doi: 10.1126/science.aad7977

Chen, Q., Yan, W., and Duan, E. (2016b). Epigenetic inheritance of acquired traits through sperm RNAs and sperm RNA modifications. *Nat. Rev. Genet.* 17, 733–743. doi: 10.1038/nrg.2016.106

Conine, C. C., Sun, F., Song, L., Rivera-Pérez, J. A., and Rando, O. J. (2018). Small RNAs gained during epididymal transit of sperm are essential for embryonic development in mice. *Dev. Cell* 46, 470.e3–480.e3. doi: 10.1016/j.devcel.2018.06.024

Craig, J. R., Jenkins, T. G., Carrell, D. T., and Hotaling, J. M. (2017). Obesity, male infertility, and the sperm epigenome. *Fertil. Steril.* 107, 848–859. doi: 10.1016/j.fertnstert.2017.02.115

Cromie, A., Kelleher, D., Gordon, F., and Rath, M. (1998). Genotype by environment interaction for milk production traits in Holstein Friesian dairy cattle in Ireland. *Interbull. Bull.* 15, 100–104.

Dagilgan, S., Dundar-Yenilmez, E., Tuli, A., Urunsak, I. F., and Erdogan, S. (2015). Evaluation of intracellular pH regulation and alkalosis defense mechanisms in preimplantation embryos. *Theriogenology* 83, 1075–1084. doi: 10.1016/j.theriogenology.2014.12.011

Dahl, J. A., Jung, I., Aanes, H., Greggains, G. D., Manaf, A., Lerdrup, M., et al. (2016). Broad histone H3K4me3 domains in mouse oocytes modulate maternal-to-zygotic transition. *Nature* 537, 548–552. doi: 10.1038/nature19360

Dance, A., Thundathil, J., Blondin, P., and Kastelic, J. (2016). Enhanced early-life nutrition of Holstein bulls increases sperm production potential without decreasing postpubertal semen quality. *Theriogenology* 86, 687.e2–694.e2.

Dance, A., Thundathil, J., Wilde, R., Blondin, P., and Kastelic, J. (2015). Enhanced early-life nutrition promotes hormone production and reproductive development in Holstein bulls. *J. Dairy Sci.* 98, 987–998. doi: 10.3168/jds.2014-8564

Desmet, K. L. J., Van Hoeck, V., Gagné, D., Fournier, E., Thakur, A., O'Doherty, A. M., et al. (2016). Exposure of bovine oocytes and embryos to elevated non-esterified fatty acid concentrations: integration of epigenetic and transcriptomic signatures in resultant blastocysts. *BMC Genomics* 17:1004. doi: 10.1186/s12864-016-3366-y

Devkota, B., Koseki, T., Matsui, M., Sasaki, M., Kaneko, E., Miyamoto, A., et al. (2008). Relationships among age, body weight, scrotal circumference, semen quality and peripheral testosterone and estradiol concentrations in pubertal and postpubertal Holstein bulls. *J. Vet. Med. Sci.* 70, 119–121. doi: 10.1292/jvms.70.119

Di Emidio, G., D'Aurora, M., Placidi, M., Franchi, S., Rossi, G., Stuppia, L., et al. (2019). Pre-conceptional maternal exposure to cyclophosphamide results in modifications of DNA methylation in F1 and F2 mouse oocytes: evidence for transgenerational effects. *Epigenetics* 14, 1057–1064. doi: 10.1080/15592294.2019.1631111

Díaz-Ruiz, R., Avéret, N., Araiza, D., Pinson, B., Uribe-Carvajal, S., Devin, A., et al. (2008). Mitochondrial oxidative phosphorylation is regulated by fructose 1,6-bisphosphate. A possible role in Crabtree effect induction? *J. Biol. Chem.* 283, 26948–26955. doi: 10.1074/jbc.M800408200

Dupont, C., Kappeler, L., Saget, S., Grandjean, V., and Lévy, R. (2019). Role of miRNA in the transmission of metabolic diseases associated with paternal diet-induced obesity. *Front. Genet.* 10:337. doi: 10.3389/fgene.2019.00337

Eckersley-Maslin, M. A., Alda-Catalinas, C., and Reik, W. (2018). Dynamics of the epigenetic landscape during the maternal-to-zygotic transition. *Nat. Rev. Mol. Cell Biol.* 19, 436–450. doi: 10.1038/s41580-018-0008-z

Engmann, O. (2018). Dairy cows – an opportunity in the research field of non-genetic inheritance? *Environ. Epigenet.* 4:dvy014. doi: 10.1093/eep/dvy014

Ernst, J., and Kellis, M. (2012). ChromHMM: automating chromatin-state discovery and characterization. *Nat. Methods* 9, 215–216. doi: 10.1038/nmeth.1906

Ernst, J., and Kellis, M. (2017). Chromatin-state discovery and genome annotation with ChromHMM. *Nat. Protoc.* 12, 2478–2492. doi: 10.1038/nprot.2017.124

Ernst, J., Kheradpour, P., Mikkelsen, T. S., Shoresh, N., Ward, L. D., Epstein, C. B., et al. (2011). Mapping and analysis of chromatin state dynamics in nine human cell types. *Nature* 473, 43–49. doi: 10.1038/nature09906

Etienne, S. E., and Martin, T. G. (1979). Secondary selection differentials for cow productivity traits associated with seven criteria of selecting replacement beef heifers. *J. Anim. Sci.* 49, 26–38. doi: 10.2527/jas1979.49126x

Evans, A., Pierson, R., Garcia, A., McDougall, L., Hrudka, F., and Rawlings, N. (1996). Changes in circulating hormone concentrations, testes histology and testes ultrasonography during sexual maturation in beef bulls. *Theriogenology* 46, 345–357. doi: 10.1016/0093-691x(96)00190-2

Evans, A. C. O., Davies, F. J., Nasser, L. F., Bowman, P., and Rawlings, N. C. (1995). Differences in early patterns of gonadotrophin secretion between early and late maturing bulls, and changes in semen characteristics at puberty. *Theriogenology* 43, 569–578. doi: 10.1016/0093-691x(94)00062-y

Falconer, D. S. (1952). The problem of environment and selection. *Am. Nat.* 86, 293–298. doi: 10.1086/281736

Fang, L., Jiang, J., Li, B., Zhou, Y., Freebern, E., Vanraden, P. M., et al. (2019). Genetic and epigenetic architecture of paternal origin contribute to gestation length in cattle. *Commun. Biol.* 2:100. doi: 10.1038/s42003-019-0341-6

Felsenfeld, G. (2014). A brief history of epigenetics. *Cold Spring Harb. Perspect. Biol.* 6:a018200. doi: 10.1101/cshperspect.a018200

Gaspar-Maia, A., Alajem, A., Meshorer, E., and Ramalho-Santos, M. (2011). Open chromatin in pluripotency and reprogramming. *Nat. Rev. Mol. Cell Biol.* 12, 36–47. doi: 10.1038/nrm3036

Gkountela, S., Zhang, K. X., Shafiq, T. A., Liao, W.-W., Hargan-Calvopiña, J., Chen, P.-Y., et al. (2015). DNA demethylation dynamics in the human prenatal germline. *Cell* 161, 1425–1436. doi: 10.1016/j.cell.2015.05.012

Glanzner, W. G., Rissi, V. B., de Macedo, M. P., Mujica, L. K. S., Gutierrez, K., Bridi, A., et al. (2018). Histone 3 lysine 4, 9, and 27 demethylases expression profile in fertilized and cloned bovine and porcine embryos†. *Biol. Reprod.* 98, 742–751. doi: 10.1093/biolre/ioy054

Grishkevich, V., and Yanai, I. (2013). The genomic determinants of genotype x environment interactions in gene expression. *Trends Genet.* 29, 479–487. doi: 10.1016/j.tig.2013.05.006

Gu, L., Wang, Q., and Sun, Q.-Y. (2010). Histone modifications during mammalian oocyte maturation: dynamics, regulation and functions. *Cell Cycle* 9, 1942–1950. doi: 10.4161/cc.9.10.11599

Gudex, B., Johnson, D., and Singh, K. (2014). Prenatal maternal and possible transgenerational epigenetic effects on milk production. *PLoS One* 9:e98928. doi: 10.1371/journal.pone.0098928

Guerrero-Bosagna, C., Covert, T. R., Haque, M. M., Settles, M., Nilsson, E. E., Anway, M. D., et al. (2012). Epigenetic transgenerational inheritance of vinclozolin induced mouse adult onset disease and associated sperm epigenome biomarkers. *Reprod. Toxicol.* 34, 694–707. doi: 10.1016/j.reprotox.2012.09.005

Guo, F., Li, L., Li, J., Wu, X., Hu, B., Zhu, P., et al. (2017). Single-cell multi-omics sequencing of mouse early embryos and embryonic stem cells. *Cell Res.* 27, 967–988. doi: 10.1038/cr.2017.82

Guo, F., Li, X., Liang, D., Li, T., Zhu, P., Guo, H., et al. (2014). Active and passive demethylation of male and female pronuclear DNA in the mammalian zygote. *Cell Stem Cell* 15, 447–459. doi: 10.1016/j.stem.2014.08.003

Guo, F., Yan, L., Guo, H., Li, L., Hu, B., Zhao, Y., et al. (2015). The transcriptome and DNA methylome landscapes of human primordial germ cells. *Cell* 161, 1437–1452. doi: 10.1016/j.cell.2015.05.015

Guo, H., Zhu, P., Yan, L., Li, R., Hu, B., Lian, Y., et al. (2014). The DNA methylation landscape of human early embryos. *Nature* 511, 606–610. doi: 10.1038/nature13544

Gupta, R. A., Shah, N., Wang, K. C., Kim, J., Horlings, H. M., Wong, D. J., et al. (2010). Long non-coding RNA HOTAIR reprograms chromatin state to promote cancer metastasis. *Nature* 464, 1071–1076. doi: 10.1038/nature08975

Hackett, J. A., Sengupta, R., Zylicz, J. J., Murakami, K., Lee, C., Down, T. A., et al. (2013). Germline DNA Demethylation Dynamics and Imprint Erasure Through 5-Hydroxymethylcytosine. *Science* 339, 448–452.

Hajkova, P., Ancelin, K., Waldmann, T., Lacoste, N., Lange, U. C., Cesari, F., et al. (2008). Chromatin dynamics during epigenetic reprogramming in the mouse germ line. *Nature* 452, 877–881. doi: 10.1038/nature06714

Hammami, H., Rekik, B., Bastin, C., Soyeurt, H., Bormann, J., Stoll, J., et al. (2009a). Environmental sensitivity for milk yield in Luxembourg and Tunisian Holsteins by herd management level. *J. Dairy Sci.* 92, 4604–4612. doi: 10.3168/jds.2008-1513

Hammami, H., Rekik, B., and Gengler, N. (2009b). Genotype by environment interaction in dairy cattle. *Biotechnol. Agron. Soc. Environ.* 13, 155–164.

Harvey, A. J., Kind, K. L., Pantaleon, M., Armstrong, D. T., and Thompson, J. G. (2004). Oxygen-regulated gene expression in bovine blastocysts. *Biol. Reprod.* 71, 1108–1119. doi: 10.1095/biolreprod.104.028639

Ibeagha-Awemu, E. M., and Zhao, X. (2015). Epigenetic marks: regulators of livestock phenotypes and conceivable sources of missing variation in livestock improvement programs. *Front. Genet.* 6:302. doi: 10.3389/fgene.2015.00302

Igolkina, A. A., Zinkevich, A., Karandasheva, K. O., Popov, A. A., Selifanova, M. V., Nikolaeva, D., et al. (2019). H3K4me3, H3K9ac, H3K27ac, H3K27me3 and H3K9me3 histone tags suggest distinct regulatory evolution of open and condensed chromatin landmarks. *Cells* 8:1034.

Inoue, A., Jiang, L., Lu, F., Suzuki, T., and Zhang, Y. (2017). Maternal H3K27me3 controls DNA methylation-independent imprinting. *Nature* 547, 419–424. doi: 10.1038/nature23262

Jenkins, T. G., James, E. R., Alonso, D. F., Hoidal, J. R., Murphy, P. J., Hotaling, J. M., et al. (2017). Cigarette smoking significantly alters sperm DNA methylation patterns. *Andrology* 5, 1089–1099. doi: 10.1111/andr.12416

Ji, H., and Khurana Hershey, G. K. (2012). Genetic and epigenetic influence on the response to environmental particulate matter. *J. Allergy Clin. Immunol.* 129, 33–41. doi: 10.1016/j.jaci.2011.11.008

Jiang, Z., Lin, J., Dong, H., Zheng, X., Marjani, S. L., Duan, J., et al. (2018). DNA methylomes of bovine gametes and in vivo produced preimplantation embryos. *Biol. Reprod.* 99, 949–959. doi: 10.1093/biolre/ioy138

Johnson, C., Dance, A., Kovalchuk, I., Kastelic, J., and Thundathil, J. (2020). Enhanced pre-pubertal nutrition upregulates mitochondrial function in testes and sperm of post-pubertal Holstein bulls. *Sci. Rep.* 10:2235. doi: 10.1038/s41598-020-59067-3

Jung, Y. H., Kremsky, I., Gold, H. B., Rowley, M. J., Punyawai, K., Buonanotte, A., et al. (2019). Maintenance of CTCF- and transcription factor-mediated interactions from the gametes to the early mouse embryo. *Mol. Cell.* 75, 154.e5–171.e5. doi: 10.1016/j.molcel.2019.04.014

Jung, Y. H., Sauria, M. E. G., Lyu, X., Cheema, M. S., Ausio, J., Taylor, J., et al. (2017). Chromatin states in mouse sperm correlate with embryonic and adult regulatory landscapes. *Cell Rep.* 18, 1366–1382. doi: 10.1016/j.celrep.2017.01.034

Kasinathan, P., Wei, H., Xiang, T., Molina, J. A., Metzger, J., Broek, D., et al. (2015). Acceleration of genetic gain in cattle by reduction of generation interval. *Sci. Rep.* 5:8674. doi: 10.1038/srep08674

Kauffold, J., Amer, H. A. H., Bergfeld, U., Weber, W., and Sobiraj, A. (2005). The in vitro developmental competence of oocytes from juvenile calves is related to follicular diameter. *J. Reprod. Dev.* 51, 325–332. doi: 10.1262/jrd.17002

Kenny, D. A., and Byrne, C. J. (2018). Review: the effect of nutrition on timing of pubertal onset and subsequent fertility in the bull. *Animal* 12, s36–s44. doi: 10.1017/S1751731118000514

Kitagawa, Y., Suzuki, K., Yoneda, A., and Watanabe, T. (2004). Effects of oxygen concentration and antioxidants on the in vitro developmental ability, production of reactive oxygen species (ROS), and DNA fragmentation in porcine embryos. *Theriogenology* 62, 1186–1197. doi: 10.1016/j.theriogenology.2004.01.011

Kropp, J., Carrillo, J. A., Namous, H., Daniels, A., Salih, S. M., Song, J., et al. (2017). Male fertility status is associated with DNA methylation signatures in sperm and transcriptomic profiles of bovine preimplantation embryos. *BMC Genomics* 18:280. doi: 10.1186/s12864-017-3673-y

Kundaje, A., Meuleman, W., Ernst, J., Bilenky, M., Yen, A., Heravi-Moussavi, A., et al. (2015). Integrative analysis of 111 reference human epigenomes. *Nature* 518, 317–330. doi: 10.1038/nature14248

Kutchy, N. A., Menezes, E. S. B., Chiappetta, A., Tan, W., Wills, R. W., Kaya, A., et al. (2018). Acetylation and methylation of sperm histone 3 lysine 27 (H3K27ac and H3K27me3) are associated with bull fertility. *Andrologia* 50:e12915. doi: 10.1111/and.12915

Labrecque, R., Vigneault, C., Blondin, P., and Sirard, M.-A. (2013). Gene expression analysis of bovine oocytes with high developmental competence obtained from FSH-stimulated animals. *Mol. Reprod. Dev.* 80, 428–440. doi: 10.1002/mrd.2217

Lambert, S., Blondin, P., Vigneault, C., Labrecque, R., Dufort, I., and Sirard, M.-A. (2018). Spermatozoa DNA methylation patterns differ due to peripubertal age in bulls. *Theriogenology* 106(Suppl. C), 21–29. doi: 10.1016/j.theriogenology.2017.10.006

Landry, D. A., Bellefleur, A.-M., Labrecque, R., Grand, F.-X., Vigneault, C., Blondin, P., et al. (2016). Effect of cow age on the in vitro developmental competence of oocytes obtained after FSH stimulation and coasting treatments. *Theriogenology* 86, 1240–1246. doi: 10.1016/j.theriogenology.2016.04.064

Landry, D. A., Labrecque, R., Grand, F.-X., Vigneault, C., Blondin, P., and Sirard, M.-A. (2018). Effect of heifer age on the granulosa cell transcriptome after ovarian stimulation. *Reprod. Fertil. Dev.* 30, 980–990. doi: 10.1071/RD17225

Lavoir, M.-C., Basrur, P. K., and Betteridge, K. J. (1994). Isolation and identification of germ cells from fetal bovine ovaries. *Mol. Reprod. Dev.* 37, 413–424. doi: 10.1002/mrd.1080370408

Li, L., Guo, F., Gao, Y., Ren, Y., Yuan, P., Yan, L., et al. (2018). Single-cell multi-omics sequencing of human early embryos. *Nat. Cell Biol.* 20, 847–858. doi: 10.1038/s41556-018-0123-2

Loche, E., Blackmore, H. L., Carpenter, A. A., Beeson, J. H., Pinnock, A., Ashmore, T. J., et al. (2018). Maternal diet-induced obesity programmes cardiac dysfunction in male mice independently of post-weaning diet. *Cardiovasc. Res.* 114, 1372–1384. doi: 10.1093/cvr/cvy082

Lyko, F. (2018). The DNA methyltransferase family: a versatile toolkit for epigenetic regulation. *Nat. Rev. Genet.* 19, 81–92. doi: 10.1038/nrg.2017.80

Macmillan, K., and Hafs, H. (1968). Gonadal and extra gonadal sperm numbers during reproductive development of holstein bulls. *J. Anim. Sci.* 27, 697–700. doi: 10.2527/jas1968.273697x

Magaraki, A., van der Heijden, G., Sleddens-Linkels, E., Magarakis, L., van Cappellen, W. A., Peters, A. H. F. M., et al. (2017). Silencing markers are retained on pericentric heterochromatin during murine primordial germ cell development. *Epigenet. Chromatin* 10:11. doi: 10.1186/s13072-017-0119-3

Mahmoudi, A., Zargaran, A., Amini, H.-R., Assadi, A., Vajdi Hokmabad, R., and Eghbalsaied, S. (2015). A SNP in the 3′-untranslated region of AMPKγ1 may associate with serum ketone body and milk production of Holstein dairy cows. *Gene* 574, 48–52. doi: 10.1016/j.gene.2015.07.077

Majerus, V., De Roover, R., Etienne, D., Kaidi, S., Massip, A., Dessy, F., et al. (1999). Embryo production by ovum pick up in unstimulated calves before and after puberty. *Theriogenology* 52, 1169–1179. doi: 10.1016/s0093-691x(99)00209-5

Markunas, C. A., Wilcox, A. J., Xu, Z., Joubert, B. R., Harlid, S., Panduri, V., et al. (2016). Maternal age at delivery is associated with an epigenetic signature in both newborns and adults. *PLoS One* 11:e0156361. doi: 10.1371/journal.pone.0156361

McDaniel, B., and Corley, E. (1967). Relationships between sire evaluations at different herdmate levels. *J. Dairy Sci.* 50, 735–741.

McGraw, S., Robert, C., Massicotte, L., and Sirard, M.-A. (2003). Quantification of histone acetyltransferase and histone deacetylase transcripts during early bovine embryo development1. *Biol. Reprod.* 68, 383–389. doi: 10.1095/biolreprod.102.005991

McJunkin, K. (2018). Maternal effects of microRNAs in early embryogenesis. *RNA Biol.* 15, 165–169. doi: 10.1080/15476286.2017.1402999

Ming, H., Sun, J., Pasquariello, R., Gatenby, L., Herrick, J. R., Yuan, Y., et al. (2020). The landscape of accessible chromatin in bovine oocytes and early embryos. *Epigenetics* doi: 10.1080/15592294.2020.1795602 [Epub ahead of print].

Morin-Doré, L., Blondin, P., Vigneault, C., Grand, F.-X., Labrecque, R., and Sirard, M.-A. (2017). Transcriptomic evaluation of bovine blastocysts obtained from peri-pubertal oocyte donors. *Theriogenology* 93, 111–123. doi: 10.1016/j.theriogenology.2017.01.005

Nivet, A.-L., Bunel, A., Labrecque, R., Belanger, J., Vigneault, C., Blondin, P., et al. (2012). FSH withdrawal improves developmental competence of oocytes in the bovine model. *Reproduction* 143:165. doi: 10.1530/rep-11-0391

Ojango, J. M. K., and Pollott, G. E. (2002). The relationship between Holstein bull breeding values for milk yield derived in both the UK and Kenya. *Livestock Prod. Sci.* 74, 1–12. doi: 10.1016/S0301-6226(01)00282-2

Pagé-Larivière, F., Tremblay, A., Campagna, C., Rodriguez, M. J., and Sirard, M.-A. (2016). Low concentrations of bromodichloromethane induce a toxicogenomic response in porcine embryos in vitro. *Reprod. Toxicol.* 66, 44–55. doi: 10.1016/j.reprotox.2016.09.010

Pallotta, M. M., Barbato, V., Pinton, A., Acloque, H., Gualtieri, R., Talevi, R., et al. (2019). In vitro exposure to CPF affects bovine sperm epigenetic gene methylation pattern and the ability of sperm to support fertilization and embryo development. *Environ. Mol. Mutagen.* 60, 85–95. doi: 10.1002/em.22242

Palma, G. A., Tortonese, D. J., and Sinowatz, F. (2001). Developmental capacity in vitro of prepubertal oocytes. *Anat. Histol. Embryol.* 30, 295–300. doi: 10.1046/j.1439-0264.2001.00324.x

Perez, M. F., and Lehner, B. (2019). Intergenerational and transgenerational epigenetic inheritance in animals. *Nat. Cell Biol.* 21, 143–151. doi: 10.1038/s41556-018-0242-9

Plant, T. M. (2015). Neuroendocrine control of the onset of puberty. *Front. Neuroendocrinol.* 38, 73–88. doi: 10.1016/j.yfrne.2015.04.002

Rahman, M. B., Kamal, M. M., Rijsselaere, T., Vandaele, L., Shamsuddin, M., and Van Soom, A. (2014). Altered chromatin condensation of heat-stressed spermatozoa perturbs the dynamics of DNA methylation reprogramming in the paternal genome after in vitro fertilisation in cattle. *Reprod. Fertil. Dev.* 26, 1107–1116. doi: 10.1071/RD13218

Ramírez-Valverde, R., Peralta-Aban, J. A., Núñez-Domínguez, R., Ruíz-Flores, A., García-Muñiz, J. G., and García-Peniche, T. B. (2010). Genotype by feeding system interaction in the genetic evaluation of Jersey cattle for milk yield. *Animal* 4, 1971–1975. doi: 10.1017/S175173111000128X

Rando, O. J. (2016). Intergenerational transfer of epigenetic information in sperm. *Cold Spring Harb. Perspect. Med.* 6:a022988. doi: 10.1101/cshperspect.a022988

Rawlings, N. C., and Evans, A. C. (1995). Androgen negative feedback during the early rise in LH secretion in bull calves. *J. Endocrinol.* 145, 243–249. doi: 10.1677/joe.0.1450243

Reynolds, T. S., Lynch, C. D., Hade, E. M., Allain, D. C., Westman, J. A., and Toland, A. E. (2020). Maternal age at delivery and fertility of the next generation. *Paediatr. Perinatal Epidemiol.* doi: 10.1111/ppe.12666 [Epub ahead of print].

Roa, J., García-Galiano, D., Castellano, J. M., Gaytan, F., Pinilla, L., and Tena-Sempere, M. (2010). Metabolic control of puberty onset: new players, new mechanisms. *Mol. Cell. Endocrinol.* 324, 87–94. doi: 10.1016/j.mce.2009.12.018

Roberts, A. J., and Hay, E. H. (2019). Multigenerational effects. *Vet. Clin. Food Anim. Pract.* 35, 355–364. doi: 10.1016/j.cvfa.2019.02.009

Ron, M., and Hillel, J. (1983). Genotype x environment interaction in dairy cattle and its role in breeding programmes. TAG. Theoretical and applied genetics. *Theor. Angew. Genet.* 66, 93–99. doi: 10.1007/bf00265180

Rowold, E. D. H., Schulze, L., Van der Auwera, S., and Grabe, H. J. (2017). Paternal transmission of early life traumatization through epigenetics: do fathers play a role? *Med. Hypothes.* 109, 59–64. doi: 10.1016/j.mehy.2017.09.011

Sakatani, M., Yamanaka, K., Kobayashi, S., and Takahashi, M. (2008). Heat shock-derived reactive oxygen species induce embryonic mortality in in vitro early stage bovine embryos. *J. Reprod. Dev.* 54, 496–501. doi: 10.1262/jrd.20017

Salilew-Wondim, D., Fournier, E., Hoelker, M., Saeed-Zidane, M., Tholen, E., Looft, C., et al. (2015). Genome-wide DNA methylation patterns of bovine blastocysts developed in vivo from embryos completed different stages of development in vitro. *PLoS One* 10:e0140467. doi: 10.1371/journal.pone.0140467

Saxena, A., and Carninci, P. (2011). Long non-coding RNA modifies chromatin. *BioEssays* 33, 830–839. doi: 10.1002/bies.201100084

Seisenberger, S., Andrews, S., Krueger, F., Arand, J., Walter, J., Santos, F., et al. (2012). The dynamics of genome-wide DNA methylation reprogramming in mouse primordial germ cells. *Mol. Cell.* 48, 849–862. doi: 10.1016/j.molcel.2012.11.001

Sharma, U., Conine, C. C., Shea, J. M., Boskovic, A., Derr, A. G., Bing, X. Y., et al. (2016). Biogenesis and function of tRNA fragments during sperm maturation and fertilization in mammals. *Science* 351, 391–396. doi: 10.1126/science.aad6780

Sharma, U., Sun, F., Conine, C. C., Reichholf, B., Kukreja, S., Herzog, V. A., et al. (2018). Small RNAs are trafficked from the epididymis to developing mammalian sperm. *Dev. Cell* 46, 481.e6–494.e6. doi: 10.1016/j.devcel.2018.06.023

Shojaei Saadi, H. A., O'Doherty, A. M., Gagne, D., Fournier, E., Grant, J. R., Sirard, M. A., et al. (2014). An integrated platform for bovine DNA methylome analysis suitable for small samples. *BMC Genomics* 15:451. doi: 10.1186/1471-2164-15-451

Siklenka, K., Erkek, S., Godmann, M., Lambrot, R., McGraw, S., Lafleur, C., et al. (2015). Disruption of histone methylation in developing sperm impairs offspring health transgenerationally. *Science* 350:aab2006. doi: 10.1126/science.aab2006

Sillaste, G., Kaplinski, L., Meier, R., Jaakma, Ü, Eriste, E., and Salumets, A. (2017). A novel hypothesis for histone-to-protamine transition in *Bos taurus* spermatozoa. *Reproduction* 153, 241–251.

Singh, K., Erdman, R. A., Swanson, K. M., Molenaar, A. J., Maqbool, N. J., Wheeler, T. T., et al. (2010). Epigenetic regulation of milk production in dairy cows. *J. Mamm. Gland Biol. Neoplasia* 15, 101–112. doi: 10.1007/s10911-010-9164-2

Singh, K., Molenaar, A. J., Swanson, K. M., Gudex, B., Arias, J. A., Erdman, R. A., et al. (2012). Epigenetics: a possible role in acute and transgenerational regulation of dairy cow milk production. *Animal* 6, 375–381. doi: 10.1017/S1751731111002564

Smith, Z. D., Chan, M. M., Humm, K. C., Karnik, R., Mekhoubad, S., Regev, A., et al. (2014). DNA methylation dynamics of the human preimplantation embryo. *Nature* 511, 611–615. doi: 10.1038/nature13581

Smith, Z. D., and Meissner, A. (2013). DNA methylation: roles in mammalian development. *Nat. Rev. Genet.* 14, 204–220. doi: 10.1038/nrg3354

Soubry, A., Guo, L., Huang, Z., Hoyo, C., Romanus, S., Price, T., et al. (2016). Obesity-related DNA methylation at imprinted genes in human sperm: results from the TIEGER study. *Clin. Epigenet.* 8:51. doi: 10.1186/s13148-016-0217-2

Soubry, A., Schildkraut, J. M., Murtha, A., Wang, F., Huang, Z., Bernal, A., et al. (2013). Paternal obesity is associated with IGF2 hypomethylation in newborns: results from a newborn epigenetics Study (NEST) cohort. *BMC Med.* 11:29. doi: 10.1186/1741-7015-11-29

Spadafora, C. (2017). Sperm-mediated transgenerational inheritance. *Front. Microbiol.* 8:2401. doi: 10.3389/fmicb.2017.02401

Stanton, T., Blake, R., Quaas, R., Van Vleck, L. D., and Carabano, M. (1991). Genotype by environment interaction for Holstein milk yield in Colombia, Mexico, and Puerto Rico. *J. Dairy Sci.* 74, 1700–1714.

Steegers-Theunissen, R. P. M., Twigt, J., Pestinger, V., and Sinclair, K. D. (2013). The periconceptional period, reproduction and long-term health of offspring: the importance of one-carbon metabolism. *Hum. Reprod. Update* 19, 640–655. doi: 10.1093/humupd/dmt041

Summers, M. C., and Biggers, J. D. (2003). Chemically defined media and the culture of mammalian preimplantation embryos: historical perspective and current issues. *Hum. Reprod. Update* 9, 557–582. doi: 10.1093/humupd/dmg039

Takeda, K., Kobayashi, E., Akagi, S., Nishino, K., Kaneda, M., and Watanabe, S. (2017). Differentially methylated CpG sites in bull spermatozoa revealed by human DNA methylation arrays and bisulfite analysis. *J. Reprod. Dev.* 63, 279–287. doi: 10.1262/jrd.2016-160

Takeda, K., Kobayashi, E., Nishino, K., Imai, A., Adachi, H., Hoshino, Y., et al. (2019). Age-related changes in DNA methylation levels at CpG sites in bull spermatozoa and in vitro fertilization-derived blastocyst-stage embryos revealed by combined bisulfite restriction analysis. *J. Reprod. Dev.* 65, 305–312. doi: 10.1262/jrd.2018-146

Thompson, R. P., Nilsson, E., and Skinner, M. K. (2020). Environmental epigenetics and epigenetic inheritance in domestic farm animals. *Anim. Reprod. Sci.* 18:106316. doi: 10.1016/j.anireprosci.2020.106316

Tian, Y., Jia, Z., Wang, J., Huang, Z., Tang, J., Zheng, Y., et al. (2011). Global Mapping of H3K4me1 and H3K4me3 reveals the chromatin state-based cell type-specific gene regulation in human treg cells. *PLoS One* 6:e27770. doi: 10.1371/journal.pone.0027770

Tremblay, R., Dufort, I., and Sirard, M.-A. (2018). Metabolic stress induces modifications in the epigenetic program of preimplantation bovine embryos. *Mol. Reprod. Dev.* 85, 117–127. doi: 10.1002/mrd.22941

Uchiyama, R., Kupkova, K., Shetty, S. J., Linford, A. S., Pray-Grant, M. G., Wagar, L. E., et al. (2018). Histone H3 lysine 4 methylation signature associated with human undernutrition. *Proc. Natl. Acad. Sci. U.S.A.* 115, E11264–E11273. doi: 10.1073/pnas.1722125115

Ugur, M. R., Kutchy, N. A., de Menezes, E. B., Ul-Husna, A., Haynes, B. P., Uzun, A., et al. (2019). Retained acetylated histone four in bull sperm associated with fertility. *Front. Vet. Sci.* 6:223. doi: 10.3389/fvets.2019.00223

Van Soom, A., Yuan, Y. Q., Peelman, L. J., de Matos, D. G., Dewulf, J., Laevens, H., et al. (2002). Prevalence of apoptosis and inner cell allocation in bovine embryos cultured under different oxygen tensions with or without cysteine addition. *Theriogenology* 57, 1453–1465. doi: 10.1016/s0093-691x(01)00726-9

Verma, A., Rajput, S., Kumar, S., De, S., Chakravarty, A. K., Kumar, R., et al. (2015). Differential histone modification status of spermatozoa in relation

to fertility of buffalo bulls. *J. Cell. Biochem.* 116, 743–753. doi: 10.1002/jcb.25029

Wakchaure, R., Ganguly, S., and Praveen, K. (2016). Genotype x environment interaction in animal breeding: a review. Biodiversity conservation in changing climate. *Cap* 3, 60–73.

Wang, L., Zhang, J., Duan, J., Gao, X., Zhu, W., Lu, X., et al. (2014). Programming and inheritance of parental DNA methylomes in mammals. *Cell* 157, 979–991.

Wei, Y., Yang, C.-R., Wei, Y.-P., Zhao, Z.-A., Yi, H., Schatten, H., et al. (2014). Paternally induced transgenerational inheritance of susceptibility to diabetes in mammals. *Proc. Natl. Acad. Sci. U.S.A.* 111, 1873–1878. doi: 10.1073/pnas.1321195111

Wolf, F., Almquist, J., and Hale, E. (1965). Prepuberal behavior and puberal characteristics of beef bulls on high nutrient allowance. *J. Anim. Sci.* 24, 761–765. doi: 10.2527/jas1965.243761x

Wrobel, K. H., and Süß, F. (1998). Identification and temporospatial distribution of bovine primordial germ cells prior to gonadal sexual differentiation. *Anat. Embryol.* 197, 451–467. doi: 10.1007/s004290050156

Wu, C., Blondin, P., Vigneault, C., Labrecque, R., and Sirard, M.-A. (2020). The age of the bull influences the transcriptome and epigenome of blastocysts produced by IVF. *Theriogenology* 144, 122–131. doi: 10.1016/j.theriogenology.2019.12.020

Wu, J., Huang, B., Chen, H., Yin, Q., Liu, Y., Xiang, Y., et al. (2016). The landscape of accessible chromatin in mammalian preimplantation embryos. *Nature* 534, 652–657. doi: 10.1038/nature18606

Xavier, M. J., Roman, S. D., Aitken, R. J., and Nixon, B. (2019). Transgenerational inheritance: how impacts to the epigenetic and genetic information of parents affect offspring health. *Hum. Reprod. Update* 25, 519–541. doi: 10.1093/humupd/dmz017

Xia, W., Xu, J., Yu, G., Yao, G., Xu, K., Ma, X., et al. (2019). Resetting histone modifications during human parental-to-zygotic transition. *Science* 365, 353–360. doi: 10.1126/science.aaw5118

Yuan, S., Schuster, A., Tang, C., Yu, T., Ortogero, N., Bao, J., et al. (2016). Sperm-borne miRNAs and endo-siRNAs are important for fertilization and preimplantation embryonic development. *Development* 143, 635–647. doi: 10.1242/dev.131755

Zaraza, J., Oropeza, A., Velazquez, M. A., Korsawe, K., Herrmann, D., Carnwath, J. W., et al. (2010). Developmental competence and mRNA expression of preimplantation in vitro–produced embryos from prepubertal and postpubertal cattle and their relationship with apoptosis after intraovarian administration of IGF-1. *Theriogenology* 74, 75–89. doi: 10.1016/j.theriogenology.2009.11.033

Zeng, Y., and Chen, T. (2019). DNA methylation reprogramming during mammalian development. *Genes* 10:257.

Zhang, T., Cooper, S., and Brockdorff, N. (2015). The interplay of histone modifications – writers that read. *EMBO Rep.* 16, 1467–1481. doi: 10.15252/embr.201540945

Zheng, H., Huang, B., Zhang, B., Xiang, Y., Du, Z., Xu, Q., et al. (2016). Resetting epigenetic memory by reprogramming of histone modifications in mammals. *Mol. Cell.* 63, 1066–1079. doi: 10.1016/j.molcel.2016.08.032

Zhou, L.-Q., and Dean, J. (2015). Reprogramming the genome to totipotency in mouse embryos. *Trends Cell Biol.* 25, 82–91. doi: 10.1016/j.tcb.2014.09.006

Zimmet, P., Shi, Z., El-Osta, A., and Ji, L. (2018). Epidemic T2DM, early development and epigenetics: implications of the Chinese famine. *Nat. Rev. Endocrinol.* 14, 738–746. doi: 10.1038/s41574-018-0106-1

**Conflict of Interest:** The authors declare that the research was conducted in the absence of any commercial or financial relationships that could be construed as a potential conflict of interest.

*Copyright © 2020 Wu and Sirard. This is an open-access article distributed under the terms of the Creative Commons Attribution License (CC BY). The use, distribution or reproduction in other forums is permitted, provided the original author(s) and the copyright owner(s) are credited and that the original publication in this journal is cited, in accordance with accepted academic practice. No use, distribution or reproduction is permitted which does not comply with these terms.*

frontiers in Genetics

ORIGINAL RESEARCH
published: 19 October 2020
doi: 10.3389/fgene.2020.550515

# Genome-Wide DNA Methylation Analysis of Mammary Gland Tissues From Chinese Holstein Cows With *Staphylococcus aureus* Induced Mastitis

*Mengqi Wang[1,2,3], Yan Liang[1], Eveline M. Ibeagha-Awemu[3], Mingxun Li[1,2], Huimin Zhang[2], Zhi Chen[2], Yujia Sun[2], Niel A. Karrow[4], Zhangping Yang[1,2] and Yongjiang Mao[1,2]**

[1] Key Laboratory for Animal Genetics, Breeding, Reproduction and Molecular Design of Jiangsu Province, College of Animal Science and Technology, Yangzhou University, Yangzhou, China, [2] Joint International Research Laboratory of Agriculture and Agri-Product Safety, The Ministry of Education of China, Yangzhou University, Yangzhou, China, [3] Agriculture and Agri-Food Canada, Sherbrooke Research and Development Centre, Sherbrooke, QC, Canada, [4] Centre for Genetic Improvement of Livestock, Department of Animal Biosciences, University of Guelph, Guelph, ON, Canada

OPEN ACCESS

**Edited by:**
Göran Andersson,
Swedish University of Agricultural Sciences, Sweden

**Reviewed by:**
Ying Yu,
China Agricultural University, China
Yachun Wang,
China Agricultural University, China

***Correspondence:**
Yongjiang Mao
cattle@yzu.edu.cn

**Specialty section:**
This article was submitted to Livestock Genomics, a section of the journal Frontiers in Genetics

**Received:** 09 April 2020
**Accepted:** 29 September 2020
**Published:** 19 October 2020

**Citation:**
Wang M, Liang Y, Ibeagha-Awemu EM, Li M, Zhang H, Chen Z, Sun Y, Karrow NA, Yang Z and Mao Y (2020) Genome-Wide DNA Methylation Analysis of Mammary Gland Tissues From Chinese Holstein Cows With Staphylococcus aureus Induced Mastitis. Front. Genet. 11:550515. doi: 10.3389/fgene.2020.550515

*Staphylococcus aureus* intramammary infection is one of the most common causes of chronic mastitis in dairy cows, whose development may be associated with epigenetic changes in the expression of important host defense genes. This study aimed to construct a genome-wide DNA methylation profile of the mammary gland of Chinese Holstein cows ($n$ = 3) following experimentally induced *S. aureus* mastitis, and to explore the potential gene regulatory mechanisms affected by DNA methylation during *S. aureus* mastitis. DNA was extracted from *S. aureus*-positive ($n$ = 3) and *S. aureus*-negative ($n$ = 3) mammary gland quarters and subjected to methylation-dependent restriction-site associated DNA sequencing (Methyl-RAD Seq). Results showed that $C^mCGG$/$C^mCWGG$ DNA methylation sites were unevenly distributed and concentrated on chromosomes 5, 11, and 19, and within intergenic regions and intron regions of genes. Compared with healthy control quarters, 9,181 significantly differentially methylated (DM) $C^mCGG$ sites and 1,790 DM $C^mCWGG$ sites were found in the *S. aureus*-positive quarters ($P < 0.05$, $|\log2FC| > 1$). Furthermore, 363 $C^mCGG$ differently methylated genes (DMGs) and 301 $C^mCWGG$ DMGs (adjusted $P < 0.05$, $|\log2FC| > 1$) were identified. Gene ontology and KEGG enrichment analysis indicated that $C^mCGG$ DMGs are involved in immune response pathways, while the $C^mCWGG$ DMGs were mainly enriched in gene ontology terms related to metabolism. The mRNAs of 526 differentially methylated $C^mCGG$ genes and 124 differentially methylated $C^mCWGG$ genes were also significantly differentially expressed (RNA-Seq data) in the same samples, herein denoted differentially methylated and expressed genes (DMEGs) ($P < 0.05$). Functional enrichment analysis of DMEGs revealed roles related to biological

processes, especially the regulation of immune response to diseases. $C^mCGG$ DMEGs like *IL6R*, *TNF*, *BTK*, *IL1R2*, and *TNFSF8* enriched in several immune-related GO terms and pathways indicated their important roles in host immune response and their potential as candidate genes for *S. aureus* mastitis. These results suggest potential regulatory roles for DNA methylation in bovine mammary gland processes during *S. aureus* mastitis and serves as a reference for future epigenetic regulation and mechanistic studies.

**Keywords: genome-wide DNA methylation, mastitis, *Staphylococcus aureus*, mammary gland tissue, Chinese Holstein**

## INTRODUCTION

Mastitis, which is defined as inflammation of the mammary gland, is one of the most common production-limiting diseases of the dairy industry (Beniæ et al., 2018). Mastitis not only has significant negative impacts on milk production, including decreased milk yield and milk quality (Detilleux et al., 2015), but also influences the reproductive system (Kumar et al., 2017) as well as increases susceptibility to other diseases (Cha et al., 2013). Mastitis is caused by varied pathogens leading to the development of subclinical/chronic (25–65% incidence worldwide) or clinical (∼5% incidence worldwide) infections (Dufour et al., 2012). *Staphylococcus aureus* (*S. aureus*), a Gram positive bacterium, is the major cause of chronic mastitis and accounts for up to 64% of total mastitis cases in Canada (Reksen et al., 2006). *S. aureus* mastitis is usually asymptomatic, persistent, easily reoccurs and some *S. aureus* isolates have developed antibiotic resistance (Makovec and Ruegg, 2003; Jensen et al., 2013). Preventive measures to control the occurrence and spread of *S. aureus* IMI (intramammary infections) are hampered by false-positive bacterial diagnostic tests, sudden outbreaks of IMI and poor therapeutic response to antibiotic treatment (Sampimon et al., 2009).

Mastitis results from the interaction between environment (pathogens) and genetic factors. Attempts to control mastitis through improved farm environment and management practices, and application of antibiotics have not eradicated the disease. The possibility to use genetic selection to improve mastitis resistance was born when heritable genetic variation in the incidence of mastitis was demonstrated (Lush, 1950). However, the use of conventional breeding strategies based on phenotypic selection to eradicate mastitis have shown limited success due to the low heritability of the trait (Emanuelson et al., 1988; Carlén et al., 2004; Koivula et al., 2005; Vallimont et al., 2009). Genomic selection has recently been identified as a complementary or alternative tool for selection to reduce mastitis (Martin et al., 2018; Weigel and Shook, 2018). To support genomic selection, several genome wide association studies (GWAS) have identified genes, markers and quantitative trait loci (QTL) significantly associated with mastitis (Wang X. et al., 2015; Suravajhala and Benso, 2017; Cai et al., 2018; Welderufael et al., 2018; Kurz et al., 2019).

In recent years, attention has been devoted to the study of transcriptome and post-transcriptional regulatory mechanisms of *S. aureus* mastitis, with aim to find additional biomarkers from different perspectives, for use in genomic selection, molecular diagnostics and for therapeutic purposes (Wang et al., 2016; Luoreng et al., 2018; Han, 2019). Furthermore, growing evidence demonstrates that epigenetics also profoundly influence health, growth, development and production traits of cattle (Ibeagha-Awemu and Zhao, 2015; Reynolds et al., 2017; Sun et al., 2019). Several studies have reported the potential contribution of epigenetic mechanisms like DNA methylation (Song et al., 2016; Zhang et al., 2018), histone modification (He et al., 2016) and non-coding RNA (Li et al., 2015; Pu et al., 2017; Ma et al., 2019) to mastitis risk. As the most characterized epigenetic regulatory mechanism, DNA methylation was reported to regulate mammary gland health (Zhang et al., 2018; Chen et al., 2019; Wang et al., 2019). For example, hypermethylation of *CD4* gene promoter was reported to repress its expression during clinical mastitis (Wang et al., 2013; Usman et al., 2016). Genome-wide DNA methylation analysis of peripheral blood lymphocytes identified 1,078 differentially methylated genes between cows with *S. aureus*-mastitis and healthy cows, as well as the potential of *NRG1*, *MST1,* and *NAT9* genes to serve as biomarkers of *S. aureus* mastitis progression (Song et al., 2016). Furthermore, DNA methylation was found to regulate the expression of bovine immune-related genes, including *IL6*, *IL8,* and *TLR4*, in response to lipopolysaccharide-induced mastitis (Korkmaz, 2018). Additionally, abnormal expression of *IL6* was revealed to be due to altered DNA methylation rather than genetic mutation during clinical mastitis (Zhang et al., 2018). Moreover, methylation changes in *NCKAP5* and transposon MTD were associated with the development of *S. aureus* mastitis (Wang et al., 2020), while hypomethylation of global DNA methylation induced by *S. aureus* infection repressed DNA methyltransferase activity in bovine mammary epithelial cells (Wu et al., 2020).

DNA methylation occurs mainly in the form of CpG (addition of methyl group to the fifth position of cytosine base followed by guanosine), and to a lesser extend at non-CpG sites, including CpA, CpT, and CpC. However, the functions of non-CpG sites are not yet elucidated or still controversial (Patil et al., 2014). Methods used for whole genome DNA methylation profiling include whole genome sequencing approaches (e.g., whole genome bisulfite sequencing) and enrichment based immunoprecipitation or enzyme based methods that reduce genome complexity through enzymatic digestion followed by bisulfite treatment and next generation

sequencing (Li et al., 2010). Methyl-RAD Seq is one of such enzymatic based methods that uses methylation-dependent restriction enzymes (FspEI, MspJI, etc.) to reduce genome size and focus the analysis on methylation rich regions (Wang S. et al., 2015). Methyl-RAD Seq has been improved in technological ways making it more advantageous than other enzymatic based methods such as reduced representation bisulfite sequencing (RRBS) (Gu et al., 2011), MeDIP-seq (Taiwo et al., 2012), MethylCap-seq (Brinkman et al., 2010) and MethylSeq (Brunner et al., 2009). $C^mCGG$ and $C^mCWGG$ (W = T or A) are two primary target sites of methylation-dependent restriction enzymes used for some DNA methylation sequencing approaches including Methyl-RAD Seq, providing the data for next-step functional analysis for both CpG and non-CpG sites (Wang S. et al., 2015).

The reports above support the hypothesis that DNA methylation contributes to susceptibility to, or outcome of *S. aureus* mastitis. However, the global DNA methylation pattern of mammary gland tissue from dairy cows infected with *S. aureus* mastitis is ambiguous, and related functional reports are scarce. To further test this hypothesis, the aim of the present study was to profile the genome-wide DNA methylation landscape of mammary gland tissue of Holstein cows, and to identify differentially methylated sites and genes and their potential involvement in the host response to *S. aureus*-induced mastitis. Data from this study is expected to provide reference for further functional studies and mechanistic exploration of epigenetic mechanisms underlying *S. aureus* mastitis and to contribute to improve management of *S. aureus* infection in dairy herd.

# MATERIALS AND METHODS

## Animals and *S. aureus* Challenge

Three primiparous Holstein cows in mid-lactation (142 ± 25 days) and without a history of disease were selected from Yangzhou University Dairy Farm (Jiangsu, China) for this study. Cows were in their first parity and were under routine farm management and feeding regime. The milk somatic cell counts (SCC) of cows was monitored for 3 weeks prior to the experimental IMI challenge. Furthermore, milk samples were collected weekly and cultured at 37°C for 24 h on Aureus ChromoSelect Agar Base Media (HiMedia, Mumbai, India) to detect the presence of *S. aureus*. Only cows negative for *S. aureus* and having a SCC of ≤100,000 cells/mL were used (Rainard et al., 2018). The *S. aureus* strain Rosenbach ATCC®29213™ (ATCC, Manassas, VA, United States) was used for the IMI challenge as described previously (Li et al., 2015). Briefly, 5 mL *S. aureus* suspension ($1 \times 10^7$ CFU, SA treatment) was injected into one mammary gland quarter of each of the three cows, while the same volume of aseptic vehicle phosphate buffer (PBS) solution was injected into another quarter of each of the same three cows (CL treatment). Milk samples were aseptically collected from each quarter just before *S. aureus* IMI challenge and then at 6, 12, 18, and 24 h post IMI challenge. Quantification of SCC and test for the presence of *S. aureus* in milk samples were done as described previously with three experimental repeats for each sample from each sampling time (Li et al., 2015). Mammary gland tissues were surgically collected at 24 h post IMI challenge from each quarter and immediately sectioned into small pieces (around 50 mg) and snap frozen and stored in liquid nitrogen. All the above animal experiments followed the guide of animal welfare and use procedures of Yangzhou University and permission to carry out the study was approved by the Institutional Animal Care and Use Committee of Yangzhou University (NO: 201404018).

## DNA Isolation

DNA was extracted from three *S. aureus* positive mammary tissues (SA treatment) and three control tissues (CL treatment) using QIAamp DNA mini kit (Qiagen Inc., Shanghai, China) according to manufacturer's protocol. The concentration and purification of DNA samples were measured with a NanoDrop ND-1000 (NanoDrop Technologies, Wilmington, DE, United States) and confirmed by agarose gel.

## DNA Methylation Library Construction and Sequencing

Preparation of genome-wide DNA methylation sequencing libraries was carried out according to method reported earlier (Wang S. et al., 2015) using Methyl-RAD Seq method. Briefly, DNA was digested with 4 U FspEI (NEB) at 37°C for 4 h followed by adaptor ligation and PCR amplification. Barcodes were introduced through PCR for multiplex sequencing. The sequences of primers, adaptors and barcodes are listed in **Supplementary Table S1A**. The PCR products were purified using the QIAquick PCR Purification Kit (Qiagen Inc., Shanghai, China), and single-end sequenced (1 × 36 bp) on an Illumina HiSeq 2500 system (Illumina, San Diego, United States). Sequencing was performed to achieve a coverage depth of 10x.

## DNA Methylation Sequencing Data Analysis

The raw sequences were trimmed with Trimmomatic (v 0.36) (Bolger et al., 2014) to remove adaptor sequences. Reads with more than 8% ambiguous bases, or more than 15% bases with a quality score of less than 30 were also trimmed. Clean reads that passed quality control and with expected restriction sites were defined as enzyme reads and were used for subsequent analyses. Sequences containing $C^mCGG$ or $C^mCWGG$ (W = T or A) (methylation on second C) with FspEI restriction sites were extracted from the bovine reference genome UMD 3.1.1 (GCF_000003055.6 *Bos Taurus* UMD 3.1.1) and used as reference for methyl-RAD data analysis. Enzyme reads were mapped to the reference sequences with SOAP (v2.21) (Li et al., 2008) allowing two mismatches (-M 4 -v 2 -r 0). The methylation sites that were found in all SA and/or CL samples and with >3× coverage were retained for further analyses. The normalized read-depth (reads per million, RPM) was used as the unit for relative quantification of level of DNA methylation. SnpEff (v4.3p) (Cingolani et al., 2012) was used to obtain information on untranslated regions (UTR) from the bovine reference genome (UMD 3.1.1). The distribution of mapped enzyme reads to different genic regions {3′ UTR, 5′ UTR, Upstream [2,000 bp

upstream of transcription start site (TSS)], exon, intron and downstream [2,000 bp downstream of transcription termination site (TTS)]} and intergenic regions was achieved with bedtools (v 2.25.0) (Quinlan and Hall, 2010).

## Identification of Differently Methylated Genes and Functional Enrichment Analysis

The methylation level of a gene was represented by the sum of the sequencing reads of all its methylated sites. Differential methylated gene (DMG) analysis was accomplished with EdgeR (v 3.26.4) (Robinson et al., 2010). DMGs meeting the thresholds of adjusted *P*-value $< 0.05$ and $|\log2FC| > 1$ were considered significant. Significantly DMGs were subjected to gene ontology (GO) and Kyoto Encyclopedia of Genes and Genomes (KEGG) pathways functional enrichment analysis with the ClusterProfile (v 3.8) program in R package (Yu et al., 2012).

## Association Analysis of Differently Methylated Genes and Transcriptome Data

The DMGs (adjusted *P*-value $< 0.05$) were filtered against the mRNA transcriptome data of the same samples (Liao, 2014; Chen et al., 2019,b) to select the differentially methylated genes that were also transcriptionally differentially- expressed (adjusted *P*-value $< 0.05$); these will subsequently be referred to as differentially methylated and expressed genes (DMEG). The DMEGs were used for GO and KEGG pathway enrichment with the ClusterProfiler package in R software, and network visualization was performed with ClueGO[1] (Bindea et al., 2009).

## Validation of DNA Methylation by Bisulfite Sequencing PCR (BSP)

To validate the reliability of Methyl-RAD Seq data, bisulfite sequencing PCR (BSP) was used to identify the methylation level of three DMEGs (*CXCR1*, *CDH13*, and *METTL13*). The Methyl primer express (v1.0) was used to design the PCR primers (**Supplementary Table S1B**). Genomic DNA (around 1,000 ng) from each tissue sample was treated with bisulfite sodium using EpiTect Plus Bisulfite kit (Qiagen, Shanghai, China). The BSP reaction was performed in 20 μL, including 1 μL (10 ng) of bisulfite-treated DNA, 1 μL of forward and reverse primer (10 μmoL each), 10 μL of 2 × T5 super PCR MIX (Qingke, Beijing, China) and 7 μL of RNase-free water. The PCR program was as follows: 94°C for 5 min; 40 cycles of 94°C for 5 s, 58°C for 30 s and 72°C for 30 s; and 72°C for 10 min. The PCR product size and purity were confirmed by agarose gel electrophoresis and then cloned into the pMD19-T vector (Shenggong, Shanghai, China). About 20 positive clones for each gene and sample were randomly selected for sequencing (Shenggong, Shanghai, China). The BiO_Analyzer[2] was used to analyze the sequence results.

[1]http://apps.cytoscape.org/apps/cluego

[2]https://biq-analyzer.bioinf.mpi-inf.mpg.de/index.php

## Statistical Analyses

The DNA methylation levels of $C^mCGG$ and $C^mCWGG$ sites between SA and CL groups were compared with Fisher's exact Test implemented in EdgeR (v 3.26.4) program. The enrichment score in the gene ontology (GO) analysis in ClusterProfile (v 3.8) was calculated with the following formula:

$$\text{Enrichment score} = \frac{m}{n} \Big/ \frac{M}{N}$$

Where N represents the number of all genes with GO annotation, *n* is the number of DMGs with GO annotation. M and *m* are the number of all genes and DMGs annotated in a specific GO term, respectively. Hypergeometric contribution test was used to calculate the significance of gene enrichment in each GO term, and adjusted *P*-value $< 0.05$ was considered significant.

# RESULTS

## Induction of Mastitis in Chinese Holstein Cows With *S. aureus*

As compared with the CL treatment (**Figure 1A**), the infected mammary gland quarters of the SA treatment showed significant symptoms of inflammation (redness, swelling and warmness to the touch) at 24 h after *S. aureus* challenge (**Figure 1B**). Furthermore, cows of the SA treatment showed avoidance behavior and refused to be milked when the infected mammary gland quarter was touched. Histological sections of the infected mammary gland quarters showed atrophic acinar wall and damaged acinar structure with lots of impurities gathered in the acini, that could be exfoliated mammary epithelial cells and inflammatory cells (**Figure 1D**) as compared to uninfected quarters (**Figure 1C**).

Compared with CL, the milk yield of SA treatment decreased, with flocculent precipitate and increased SCC ($P < 0.05$) (**Figure 1E**), indicative of mastitis. Bacterial culture revealed that milk samples collected from all the mammary gland quarters before IMI challenge were *S. aureus* negative, whereas after IMI, *S. aureus* was cultured from the SA treatments but not in the CL treatments. In summary, these results confirmed successful induction of *S. aureus*-induced mastitis in the challenged quarters and a healthy state in control quarters.

## Genome-Wide DNA Methylation Profile of Mammary Gland Tissue

The level of genome-wide DNA methylation was analyzed by Methyl-RAD Seq. A total of 81,125,685 raw reads were generated from the six samples, with an average of 13,520,947 raw reads per sample (**Table 1**). Reads that mapped to multiple positions (mapping rates of 67.7 to 70.13% of clean reads) were removed, only uniquely mapped reads (mapping rates of 26.93 to 29.09%) were kept for further analysis. The $C^mCGG$ and $C^mCWGG$ (W = A or T) methylation maps were generated to show the genome-wide DNA methylation distribution in the studied samples (**Figure 2** and **Supplementary Table S2**). The $C^mCGG$ and $C^mCWGG$ methylation sites were unevenly distributed

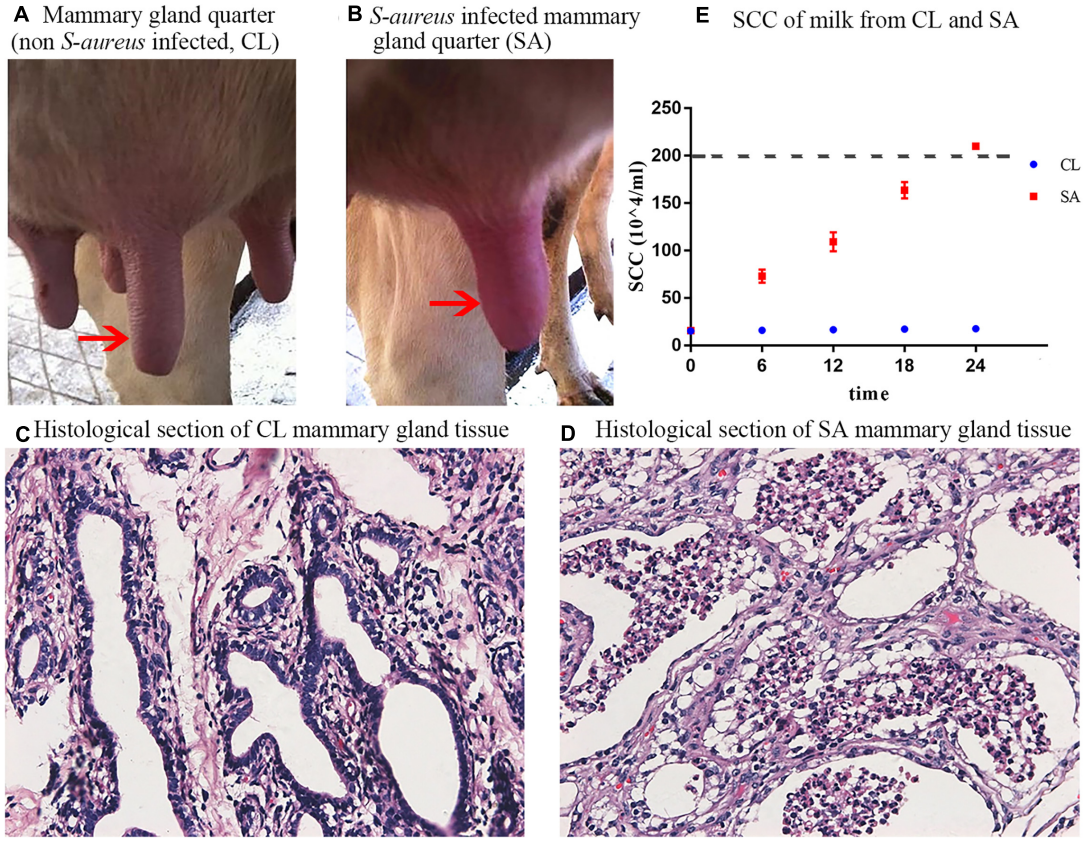



**FIGURE 1 |** Clinical observation and diagnosis of *S. aureus*-induced mastitis. **(A)** Healthy mammary gland quarter; **(B)** Mammary gland quarter with clinical symptoms: red, swollen and indurated, 24 h after *S. aureus* induction; **(C)** Histological section of healthy mammary gland quarter; **(D)** Histological section of *S. aureus*-infected mammary gland quarter, showing atrophic acinar wall and damaged acinar structure with lots of magazines gathered in the acini; **(E)** Individual SCC of milk collected from the healthy (CL group: quarters A1, B1, and C1) and *S. aureus*-infected (SA group: quarters A2, B2, and C2) mammary gland quarters during the 24 h post *S. aureus* induction. The red arrows shows the control **(A)** and challenged **(B)** mammary gland quarters.

**TABLE 1 |** Generated reads and mapping statistics of Methyl-RAD Seq sequence data from *Staphylococcus aureus* induced and healthy udder tissues of Chinese Holstein cows.

| Samples | Raw reads | Clean reads | Error rate | Enzyme reads | Q20 | Q30 | Multi mapped reads | Multi-mapping rate | Unique mapped reads | Unique mapping rate |
|---|---|---|---|---|---|---|---|---|---|---|
| A1 | 13479949 | 13467408 | 0.99907 | 12910973 | 99.87% | 99.67% | 9053897 | 70.13% | 3857076 | 29.87% |
| B1 | 13724935 | 13711869 | 0.999048 | 13251576 | 99.88% | 99.70% | 9151743 | 69.06% | 4099833 | 30.94% |
| C1 | 13411585 | 13398863 | 0.999051 | 12483616 | 99.88% | 99.70% | 8464402 | 67.80% | 4019214 | 32.20% |
| A2 | 14104057 | 14090675 | 0.999051 | 13650097 | 99.88% | 99.69% | 9381653 | 68.73% | 4268444 | 31.27% |
| B2 | 13165243 | 13152778 | 0.999053 | 12812360 | 99.88% | 99.69% | 8932597 | 69.72% | 3879763 | 30.28% |
| C2 | 13239916 | 13226976 | 0.999023 | 12399152 | 99.88% | 99.69% | 8394779 | 67.70% | 4004373 | 32.30% |

*A1, B1, and C1 represents healthy udder tissues of Chinese Holstein cows (CL group); A2, B2, and C2 represents S. aureus mastitis infected udder tissues of Chinese Holstein cows (SA group); Error Rate is the ratio of clean reads to raw reads; Enzyme Reads represent clean reads containing the expected restriction site and that passed quality control. The multi/unique-mapping rate is based on enzyme reads.*

across bovine chromosomes (BTA); BTA with the most $C^mCGG$ methylation sites were BTA 11, 5, and 19, while $C^mCWGG$ methylation sites were most distributed on BTA 5, 11, and 1. Additionally, $C^mCGG$ and $C^mCWGG$ methylation sites were more concentrated at the BTA ends.

To further understand the distribution of DNA methylation sites in the studied mammary gland tissues, gene body, upstream and downstream of genes were analyzed. As shown in **Figure 3**, the methylation level in gene bodies was higher than in the regions before the TSS and after the TTS and a sharp increase was observed around the TSS and a decrease around the TTS. Moreover, the distribution of DNA methylation sites in different functional gene elements showed enrichment in intergenic regions and introns, followed by exons and upstream

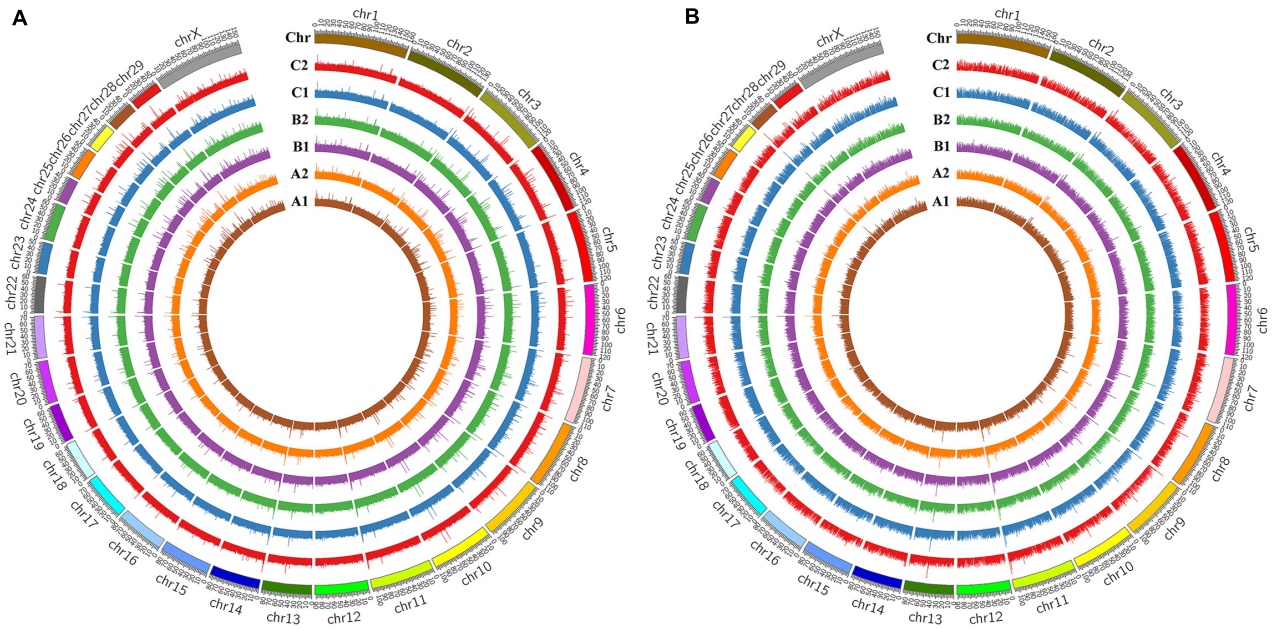



**FIGURE 2 |** DNA methylation profiles of mammary gland tissues from Chinese Holstein cows. **(A)** C$^{m}$CGG methylation map; **(B)** C$^{m}$CWGG methylation map (W = A or T); C$^{m}$CGG means the methylation whose primary target site is C$^{m}$CGG, while C$^{m}$CWGG means the methylation with C$^{m}$CWGG site (W = A/T/H); A1, B1, and C1 indicate the whole genome wide DNA methylation patterns of healthy mammary gland quarters, while A2, B2, and C2 indicate quarters with *S. aureus*-induced mastitis.




**FIGURE 3 |** DNA methylation level across gene in mammary gland quarters from Chinese Holstein cows. TSS, transcriptional start site; TTS, transcriptional termination site; Abscissa represents the gene body, expressed as the percentage of gene length (from 0 to 1),the region of 2000 bp before TSS (from –2000 bp to the start of gene body marked as 0), and 2000 bp after TTS [following the end of gene body (marked as 1) until 2000 bp]. Ordinate represents the average relative DNA methylation level (RPM, reads per million) and different colors means different groups.

regions, while the 3′UTRs and 5′UTRs had less methylation sites (**Figure 4**).

## DNA Methylation Variations Between *S. aureus*-Infected and Non-infected Mammary Gland Quarters

Exploration of the DNA methylation variations between *S. aureus* mastitis and healthy control tissues, showed significant C$^{m}$CGG/C$^{m}$CWGG methylation differences between the two groups (**Figures 5A,B**). A total of 9,181 C$^{m}$CGG methylation sites and 1,790 C$^{m}$CWGG methylation sites were differentially methylated between SA group and CL group (**Supplementary Table S3**). Furthermore, differentially methylated sites were unevenly distributed among chromosomes, with higher density of sites on BTA 5, 11, and 19 (**Supplementary Table S4**). All the methylation sites were annotated to genes to further assess the DNA methylation variations. A total of 363 C$^{m}$CGG DMGs and 301 C$^{m}$CWGG DMGs were obtained (**Supplementary Table S5**), including 28 DMGs common to the two DNA methylation

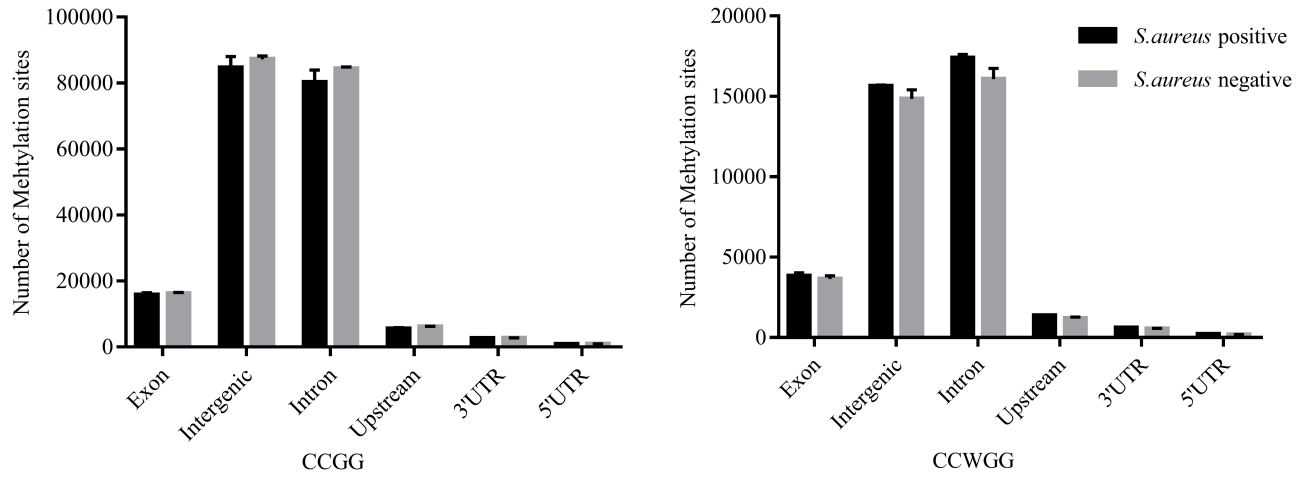



**FIGURE 4 |** The distribution of DNA methylation sites in functional gene elements. Abscissa represents functional gene elements, and upstream represents 2000 bp region before transcriptional start site. Ordinate represents the number of DNA methylation sites.

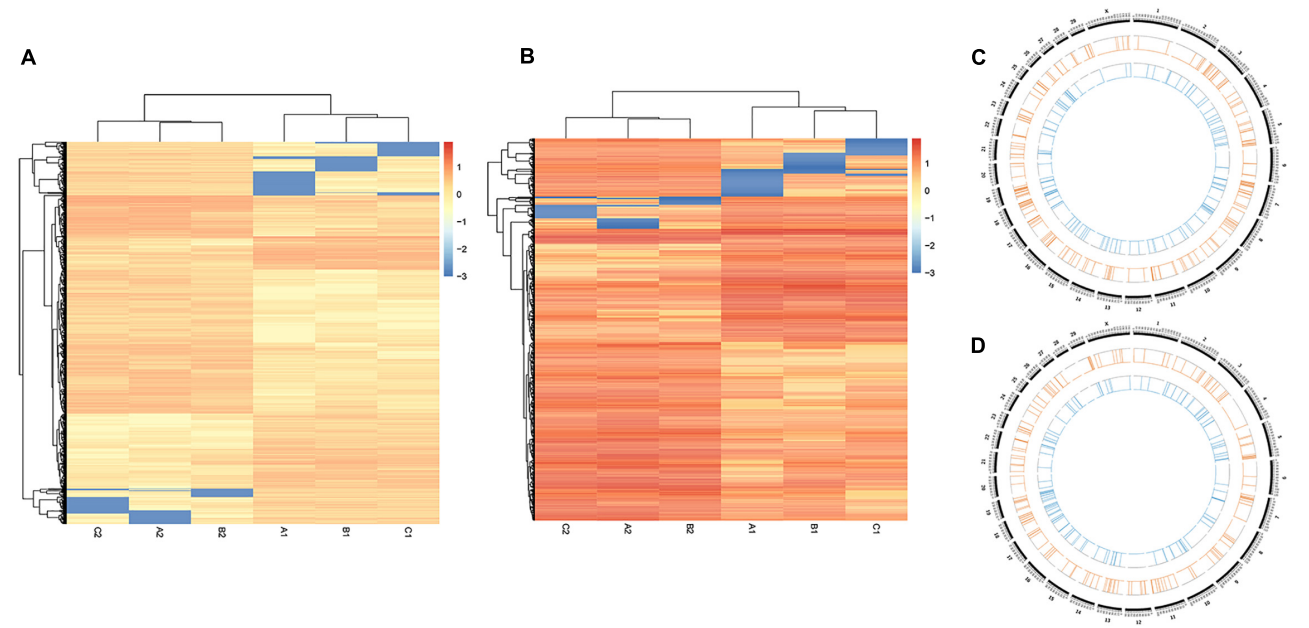



**FIGURE 5 |** Cluster analysis of DNA methylation levels in healthy and *S. aureus*-induced mammary gland tissues. **(A,B)** are the heat maps for C$^{m}$CGG and C$^{m}$CWGG methylation, respectively. The colors and intensity indicate the methylation level in the heat map. For example, highly methylated sites are in red color and hypomethylated sites are in blue color. **(C)** The distribution of C$^{m}$CGG differently methylated genes across chromosomes, while **(D)** shows the distribution of C$^{m}$CWGG differently methylated genes. Blue lines in the inner circle represent genes with significantly down-regulated methylation levels, while the orange lines in the next circle represent genes with significantly up-regulated methylation levels.

types, which showed enrichment on BTA 5, 7, 11, 18, and 19 (**Figures 5C,D** and **Supplementary Table S4**).

## GO and KEGG Pathway Enrichment Analysis of DMGs

Investigation of the potential functions of DMGs through GO and KEGG pathways enrichment analyses revealed that 580 GO terms were significantly enriched by C$^{m}$CGG DMGs, while C$^{m}$CWGG DMGs were significantly enriched in 460 GO terms (adjusted *P*-value $< 0.05$, **Supplementary Table S6**). For the C$^{m}$CGG DMGs, the most significant biological process (BP), cellular component (CC) and molecular function (MF) GO terms were "hematopoietic progenitor cell differentiation" (GO:0002244), and "cytoplasm" (GO:0005737) and "sequence-specific DNA binding," respectively (**Figure 6A**). "Kidney development" (GO:0001822), "integral component of endoplasmic reticulum membrane" (GO:0030176) and

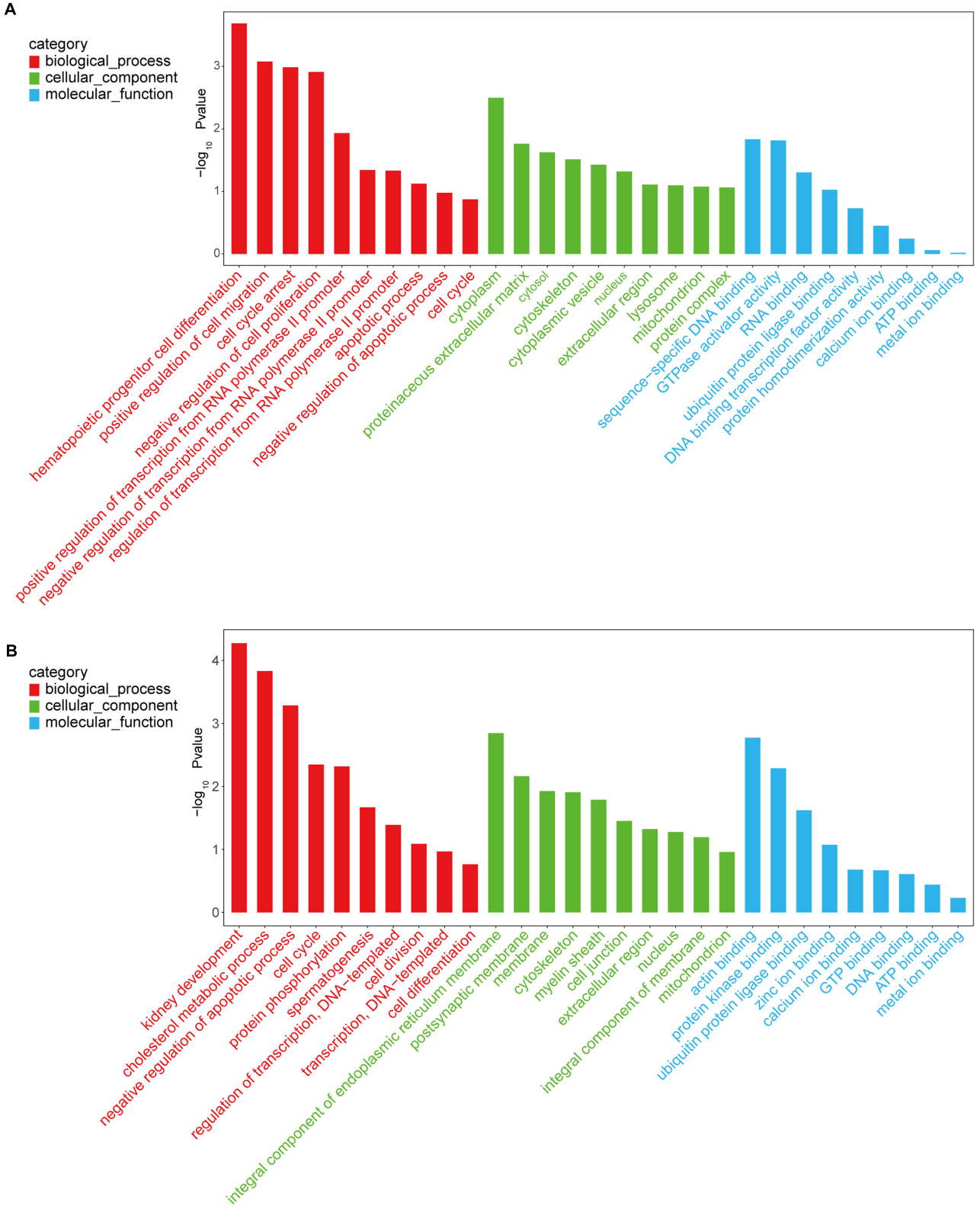



**FIGURE 6 |** Histogram of gene ontology terms enriched by differently methylated genes. **(A)** Histogram of C$^{m}$CGG differently methylated genes; **(B)** Histogram of C$^{m}$CWGG differently methylated genes. Ordinate represents the adjusted *P*-value (-log$_{10}$ *P*-value). Abscissa represents the GO terms. Only the top 10 GO terms of each category are listed in ascending order of adjusted *P*-value.

"actin binding" (GO:0003779) were the most significant BP, CC and MF GO terms enriched by C$^{m}$CWGG DMGs, respectively (**Figure 6B**).

KEGG pathways enrichment analysis identified 40 pathways for the C$^{m}$CGG DMGs and 64 pathways for the C$^{m}$CWGG DMGs (adjusted *P*-value < 0.05) (**Supplementary Table S7**). The top 20 significantly enriched pathways in each category are shown in **Figure 7**. KEGG pathways enriched by C$^{m}$CGG DMGs were mainly related to diseases and the immune response. The most significantly enriched pathways for C$^{m}$CGG DMGs were "asthma" (bta05310), "transcriptional mis-regulation in cancer" (bta05202) and "leishmaniasis" (bta05140). Meanwhile, the C$^{m}$CWGG DMGs enriched KEGG pathways were more related to biosynthesis and metabolism. "N-Glycan biosynthesis" (bta00510), "glycosphingolipid biosynthesis" (bta00601) and "galactose metabolism" (bta00052) were the top most significantly enriched pathways for C$^{m}$CWGG DMGs.

## Co-expression Analysis Between DEGs and DMGs to Identify DMEGs

The next step was to identify DMEGs, this was achieved by cross-comparing the above DMGs with those that were also previously found to be differentially transcriptionally expressed (Liao, 2014; Chen et al., 2019,b). As shown in **Figure 8**, 526 C$^{m}$CGG and 124 C$^{m}$CWGG DMEGs were identified. Functional enrichment of the C$^{m}$CWGG DMEGs indicated that only two GO terms [endochondral bone growth (GO:0003416) and calcium ion transmembrane import into cytosol (GO:0097553)] were significantly enriched by seven DMEGs. There were 430 C$^{m}$CGG DMEGs that were significantly enriched in 480 GO terms (adjusted *P* < 0.05, **Supplementary Table S8A**). The top three most significantly enriched GO terms were "cell adhesion" (GO:0007155), "cell activation" (GO:0001775) and "leukocyte cell-cell adhesion" (GO:0007159). Several enriched (adjusted *P* < 0.05) GO terms were related to cell proliferation, differentiation, migration and adhesion of immune-related cells, such as T cell, lymphocyte and leukocyte, etc (**Table 2** and **Supplementary Table S8A**). Furthermore, GO terms related to the immune response and regulation processes were also enriched by C$^{m}$CGG DMEGs, including "regulation of immune system process" (GO:0002682), "myeloid cell activation involved in immune response" (GO:0002275), etc. Some C$^{m}$CGG DMEGs such as *BTK*, *TNF*, *TNFAIP8L2*, *IL6R*, and *IL18R1*, were enriched in multiple immune processes related GO terms (**Supplementary Table S9**). Meanwhile, 44 KEGG pathways were significantly enriched (adjusted *P* < 0.05) for C$^{m}$CGG DMEGs. "Focal adhesion" (KEGG:04510) was the most significantly enriched pathway (adjusted $P = 2.52 \times 10^{-5}$) (**Figure 9** and **Supplementary Table S8B**). The "T cell receptor signaling pathway" (KEGG:04660), "primary immunodeficiency" (KEGG:05340) and other pathways related to cancers and other diseases were enriched (adjusted *P* < 0.05). A total of 102 immune-related C$^{m}$CGG DMEGs enriched in 82 GO terms and 3 KEGG pathways related to immune response, including *IL6R*, *TNF*, *BTK*, *IL1R2*, and *TNFSF8*, are listed in **Supplementary Tables S9A,B**.

## Validation of Methyl-RAD Seq Data by BSP

To assess the reliability and accuracy of the Methyl-RAD Seq data, the methylation levels in promoter regions of three candidate genes were validated by BSP in the SA and CL treatments. *CXCR1*, *CDH13,* and *METTL13* with high, low and zero methylation levels, respectively, were selected. In general, the BSP results were in good agreement with the Methyl-RAD Seq results. For example, the *CXCR1* gene showed

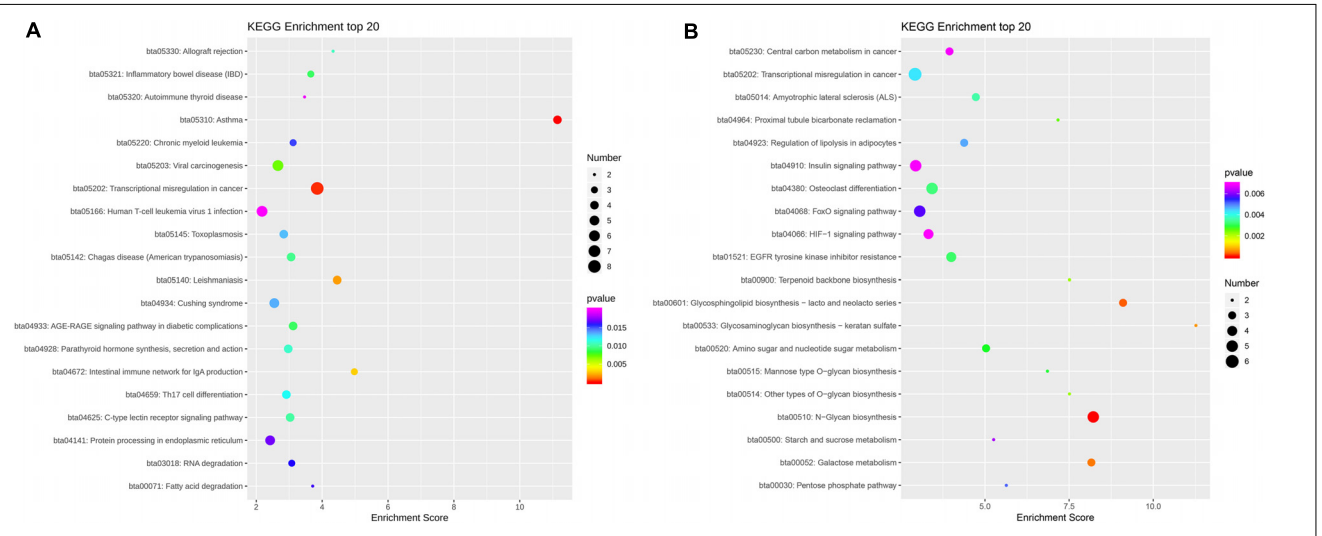



**FIGURE 7 |** Scatter plot of KEGG pathways enriched by differently methylated genes. **(A)** Scatter plot of C$^{m}$CGG differently methylated genes; **(B)** Scatter plot of C$^{m}$CWGG differently methylated genes. Ordinate represents the significantly enriched KEGG pathways. The abscissa represents the corresponding enrichment score. The color of the spot indicates the adjusted *P*-value of each pathways, while the size of the spot indicates the number of differently methylated genes enriched in that pathway. A bigger enrichment score means better enrichment. Only the top 20 KEGG pathways are listed in ascending order of adjusted *P*-value.

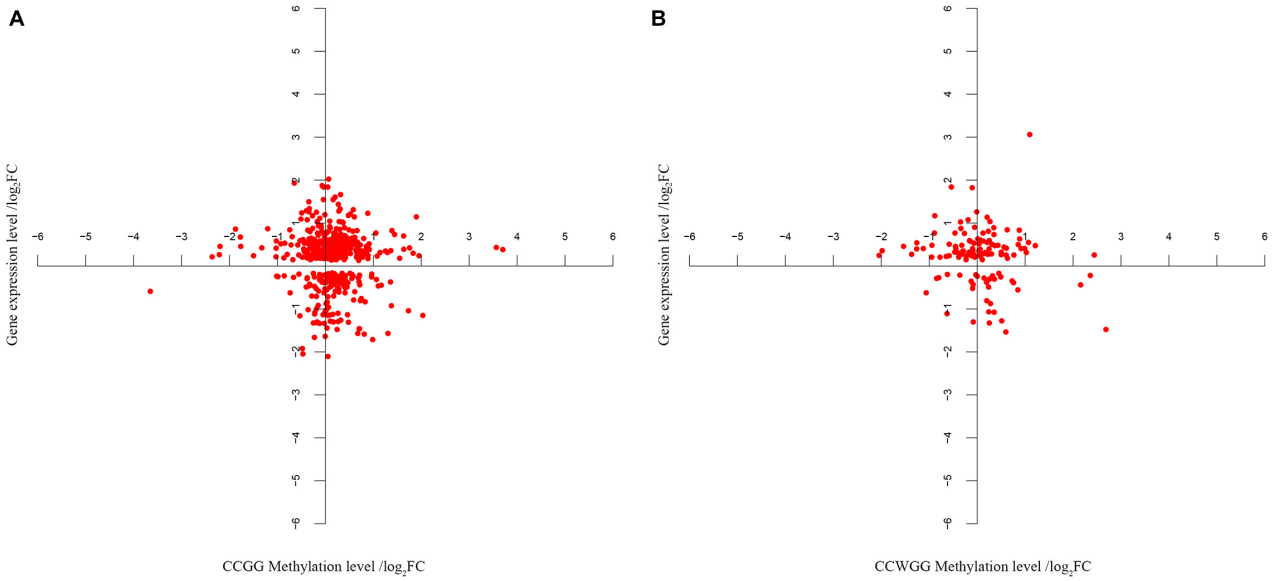



**FIGURE 8 | (A,B)** The co-expression analysis of gene expression and DNA methylation level for DMEGs. Each point in the figure represents one DMEG, the differently methylated gene whose gene expression level is also significantly different in the same tissues. Abscissa indicates the $C^mCGG$ or $C^mCWGG$ methylation level, represented by adjusted fold change ($log_2FC$). Ordinate indicates the gene expression level ($log_2FC$).

high methylation levels (**Figure 10A**), and the *CDH13* gene showed low methylation levels (**Figure 10B**), while the *METTL13* gene was almost completely unmethylated (**Supplementary Figure S1**) according to both methods.

## DISCUSSION

Experimental induction of mastitis by inoculating *S. aureus* into mammary gland quarters has been used to study the transcriptional and post-transcriptional regulatory immune response mechanisms during IMI (Fang et al., 2016; Enger et al., 2019). This strategy was used in this study whereby one mammary gland quarter was inoculated with *S. aureus* to induce mastitis (SA treatment), while one quarter of the same animal was inoculated with PBS and served as the control (CL treatment). Typical clinical symptoms of mastitis were observed in the quarters inoculated with *S. aureus*, such as swelling, redness, warm feeling to the touch, incomplete anatomical structure of acini with exfoliated epithelial cells, as well as significantly increased SCC (>2 million cells/mL) as compared to the healthy PBS quarters, indicating that induction of *S. aureus* mastitis in the SA treatment was successful.

### Global DNA Methylation Pattern of Mammary Gland Tissues Revealed by Methyl-RAD Seq

Methyl-RAD Seq is an improved enzymatic based genome-wide DNA methylation detection method when compared with similar techniques (RRBS, MeDIP Seq, and MethyCap Seq) (Brunner et al., 2009; Taiwo et al., 2012; Huang et al., 2013; Wang S. et al., 2015). Firstly, the process of Methyl-RAD Seq eliminates some enzymatic treatments and purification steps inherent in other methods (RRBS, MeDIP Seq, and MethyCap Seq), which allows application to a wide-range of samples due to it very low DNA input acquirement (about 1 ng). Particularly, the gel purification after DNA digestion is omitted by Methyl-RAD technique, thereby avoiding the denaturation of short fragments (23 or 24 bp) with low melting point in the process of gel electrophoresis (Sanderson et al., 2014). Furthermore, the Methyl-RAD Seq technique is easier and faster, and can be done in a 96-well PCR plate in just 2 days, thus making it an ideal protocol for large-scale methylation detection of numerous samples. Additionally, Methyl-RAD Seq is flexible and users can adjust the label density to meet their specific requirements. Moreover, Methyl-RAD Seq has high specificity, sensitivity and reproducibility with unique abilities to perform qualitative DNA methylation analysis (Huang et al., 2013).

In this study, Methyl-RAD Seq was used for genome-wide DNA methylation profiling of mammary gland tissues of Chinese Holstein cows. Both $C^mCGG$ and $C^mCWGG$ methylation sites were unevenly distributed among chromosomes with higher density on BTA 5 and 11 in the mammary gland tissues. A previous study also reported that *S. aureus*-positive cattle had significantly more methylation sites on BTA 11 than *S. aureus*-negative controls (Song et al., 2016), implying a potential regulatory role of DNA methylation in response to *S. aureus* mastitis. We observed the intergenic and intron regions had more methylation sites (adjusted $P < 0.05$) compared with other functional gene elements, which is in agreement with previous studies in other cattle breeds (Song et al., 2016; Fang et al., 2017; Chen et al., 2019,a). Similar to results obtained with other mammalian species (Gim et al., 2015; Song et al., 2016; Zhang X. et al., 2017; Zhang Y. et al., 2017), the methylation level was

**TABLE 2 |** Top 30 significantly enriched gene ontology terms for $C^mCGG$ DMEGs.

| ID | Term | Category | Term *P*-value | Adjusted Term *P*-value |
|---|---|---|---|---|
| GO:0007155 | Cell adhesion | BP | 3.70E−15 | 2.76E−12 |
| GO:0001775 | Cell activation | BP | 1.05E−11 | 3.91E−09 |
| GO:0007159 | Leukocyte cell-cell adhesion | BP | 1.10E−10 | 2.73E−08 |
| GO:0098609 | Cell-cell adhesion | BP | 2.31E−10 | 4.31E−08 |
| GO:0009611 | Response to wounding | BP | 3.12E−10 | 4.67E−08 |
| GO:0045321 | Leukocyte activation | BP | 7.64E−10 | 9.52E−08 |
| GO:0032879 | Regulation of localization | BP | 1.15E−09 | 1.22E−07 |
| GO:0046649 | Lymphocyte activation | BP | 1.32E−09 | 1.23E−07 |
| GO:0050865 | Regulation of cell activation | BP | 3.43E−09 | 2.85E−07 |
| GO:0042060 | Wound healing | BP | 8.47E−09 | 6.33E−07 |
| GO:0030155 | Regulation of cell adhesion | BP | 1.02E−08 | 6.94E−07 |
| GO:0009986 | Cell surface | CC | 1.23E−08 | 7.66E−07 |
| GO:0042110 | T cell activation | BP | 1.74E−08 | 9.98E−07 |
| GO:0016477 | Cell migration | BP | 3.09E−08 | 1.65E−06 |
| GO:0048856 | Anatomical structure development | BP | 5.26E−08 | 2.62E−06 |
| GO:0022407 | Regulation of cell-cell adhesion | BP | 6.63E−08 | 3.09E−06 |
| GO:0030334 | Regulation of cell migration | BP | 1.19E−07 | 5.25E−06 |
| GO:0002694 | Regulation of leukocyte activation | BP | 1.48E−07 | 6.13E−06 |
| GO:0048870 | Cell motility | BP | 1.69E−07 | 6.32E−06 |
| GO:0043062 | Extracellular structure organization | BP | 1.68E−07 | 6.62E−06 |
| GO:0030198 | Extracellular matrix organization | BP | 2.75E−07 | 9.79E−06 |
| GO:0007596 | Blood coagulation | BP | 4.63E−07 | 1.57E−05 |
| GO:0048869 | cellular developmental process | BP | 4.97E−07 | 1.61E−05 |
| GO:1903037 | Regulation of leukocyte cell-cell adhesion | BP | 7.92E−07 | 2.27E−05 |
| GO:0002682 | Regulation of immune system process | BP | 9.08E−07 | 2.51E−05 |
| GO:0051239 | Regulation of multicellular organismal process | BP | 1.20E−06 | 3.10E−05 |
| GO:0031012 | Extracellular matrix | CC | 1.19E−06 | 3.17E−05 |

*DMEGs, the $C^mCGG$ differently methylated genes with significantly different gene expression level in the same animal model; BP, biological process; CC, cellular component.*

significantly higher in the gene body than its up- and downstream regions.

## Potential Functions of Differentially Methylated Genes

DNA methylation plays an important regulatory role in gene expression, which is also influenced by environmental factors and age (Horvath, 2013; Kanzleiter et al., 2015). It has been noted that knowledge on the spatial and temporal regulation of DNA methylation is necessary for understanding the biology of disease (Bergman and Cedar, 2013; Shin et al., 2015). A total of 9,181 $C^mCGG$ and 1,790 $C^mCWGG$ methylation sites were identified as differently methylated sites in this study, and were annotated to 363 $C^mCGG$ and 301 $C^mCWGG$ DMGs (adjusted *P*-value $< 0.05$ and $|\log2FC| > 1$). The DNA methylation data in this study was compared with the mRNA transcriptome data generated from these same tissues (Liao, 2014; Chen et al., 2019,b) to explore the effects of DNA methylation on gene expression in response to *S. aureus*-mastitis. We found that a total of 526 $C^mCGG$ and 124 $C^mCWGG$ DMGs in this study were also reported as significantly differentially expressed in response to *S. aureus*-induced mastitis (adjusted *P*-value $< 0.05$) (Chen et al., 2019,b), suggesting that DNA methylation may be one of the regulatory mechanisms of gene expression during *S. aureus* IMI.

DNA methylation of some immune-related genes has been associated with mastitis, such as *CXCR1* and *CDH13*. *CXCR1* gene polymorphism was shown to impact milk production and sensitivity to mastitis, and was selected as a candidate marker for improving bovine resistance to mastitis (Verbeke et al., 2015; Pokorska et al., 2016; Siebert et al., 2017). In addition, CpG sites in the promoter region of bovine *CXCR1* were found to potentially affect its gene expression during *S. aureus*-induced mastitis (Mao et al., 2015). Consistent with Mao et al. (2015) the *CXCR1* gene DNA methylation level in this study was higher in the CL treatment than in the SA treatment. This is supported by its upregulated expression in the SA treatment (Liao, 2014), suggesting an important role in response to *S. aureus* mastitis. In contrast, *CDH13* was reported to have important regulatory roles in human cancers based on a significant correlation of DNA methylation in the *CDH13* promoter with the occurrence, development and prognosis of disease (Yang et al., 2016; Ye et al., 2017; Li Y. et al., 2018). Furthermore, the level DNA methylation in the promoter of *CDH13* is often high during cancer processes (Xu et al., 2016; Wang et al., 2018). In this study, the level of

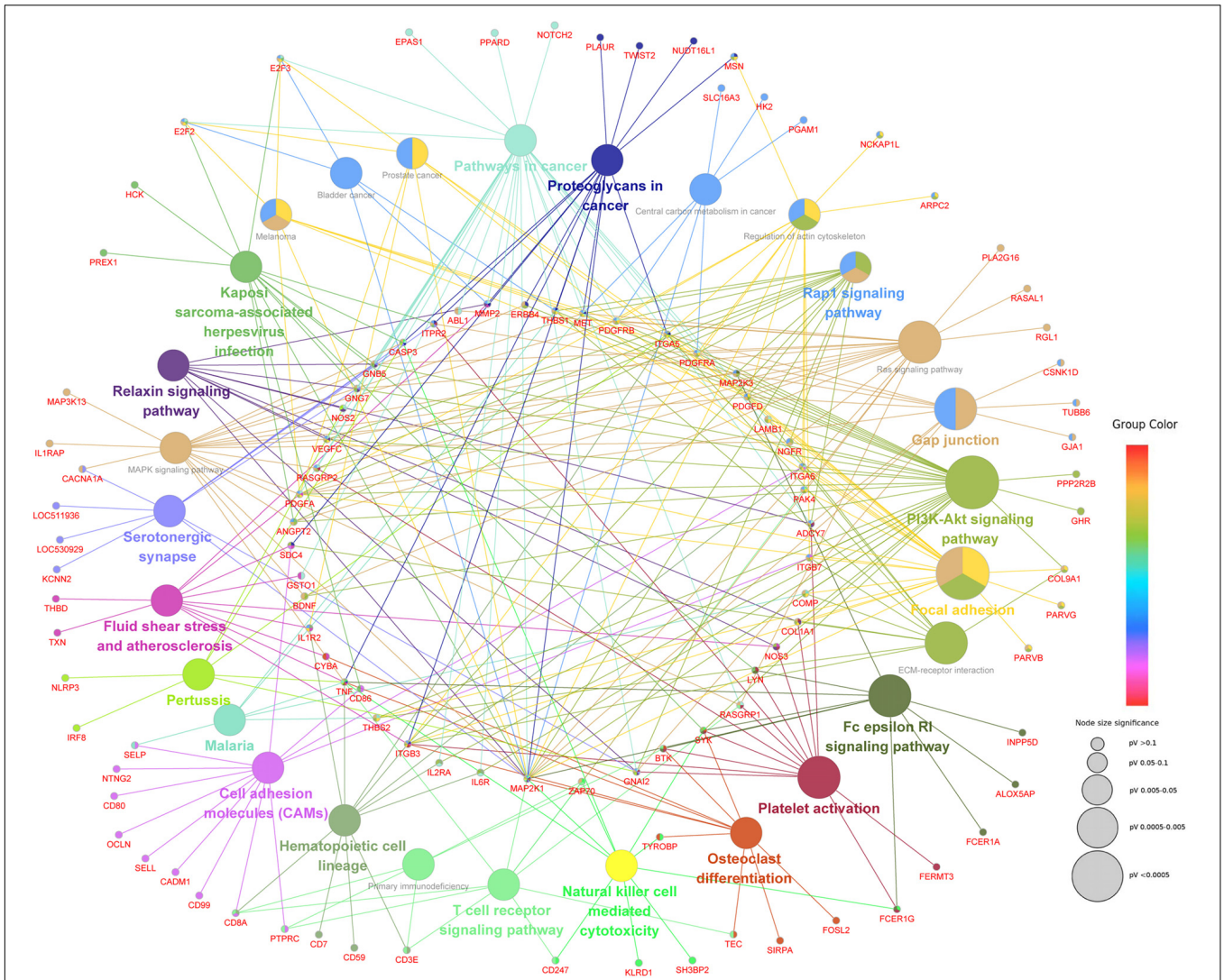



**FIGURE 9 |** The network of KEGG pathways significantly enriched by C$^{m}$CGG DMEGs. Each node represents a KEGG pathway or a C$^{m}$CGG DMEG enriched in the pathway. The color of the node indicates the cluster of KEGG pathways, that more similar colors mean closer clusters with more similar functions. The size of node indicates the adjusted *P*-value of the corresponding pathway, that a bigger size of the node means more significant enrichment.

DNA methylation in *CDH13* was higher in SA treatment than in the CL treatment, suggesting a potential regulatory role during *S. aureus* mastitis.

In addition to *CXCR1* and *CDH13*, DNA methylation levels of other immune-related genes, including *IL6R*, *IL10*, *IL17*, and *NFKBIA*, were also significantly different between SA and CL treatments. Moreover, 102 C$^{m}$CGG DMEGs, including *IL6R*, *TNF*, *BTK*, *IL1R2*, and *TNFSF8* were enriched in several immune-related GO terms, indicating their important roles in host immune response, and their potential as candidate genes for improving resistance to *S. aureus* mastitis. A higher level of DNA methylation in *IL6R* was also previously found in mastitis-infected cows; and it was found to regulate the expression of *IL6R* in part by promoting the inclusion of its alternatively spliced exon 2 (Zhang et al., 2018). In contrast, hypomethylation of *IL10* has been reported to promote the incidence of diseases, including *Escherichia coli*-induced mastitis (Modak et al., 2012) and systemic lupus erythematosus (Lin et al., 2012).

The GO functional enrichment revealed the potential roles of C$^{m}$CWGG DMGs in biological processes related to cholesterol metabolic process and protein phosphorylation, as well as molecular functions related to protein kinase binding and ubiquitin ligase binding (**Figure 8B**). Meanwhile, C$^{m}$CGG DMGs were enriched in several cellular biological processes including cell proliferation, cell differentiation, cell migration, etc., (**Figure 8A**), suggesting their potential regulatory roles in cell development and diverse biological processes. The C$^{m}$CGG DMGs were significantly enriched in KEGG pathways related to infectious diseases, including Leishmaniasis, Toxoplasmosis and American trypanosomiasis (**Figure 9**). *S. aureus* mastitis is a common infectious disease of dairy cows, and enrichment of these disease pathways in this study suggests regulatory roles

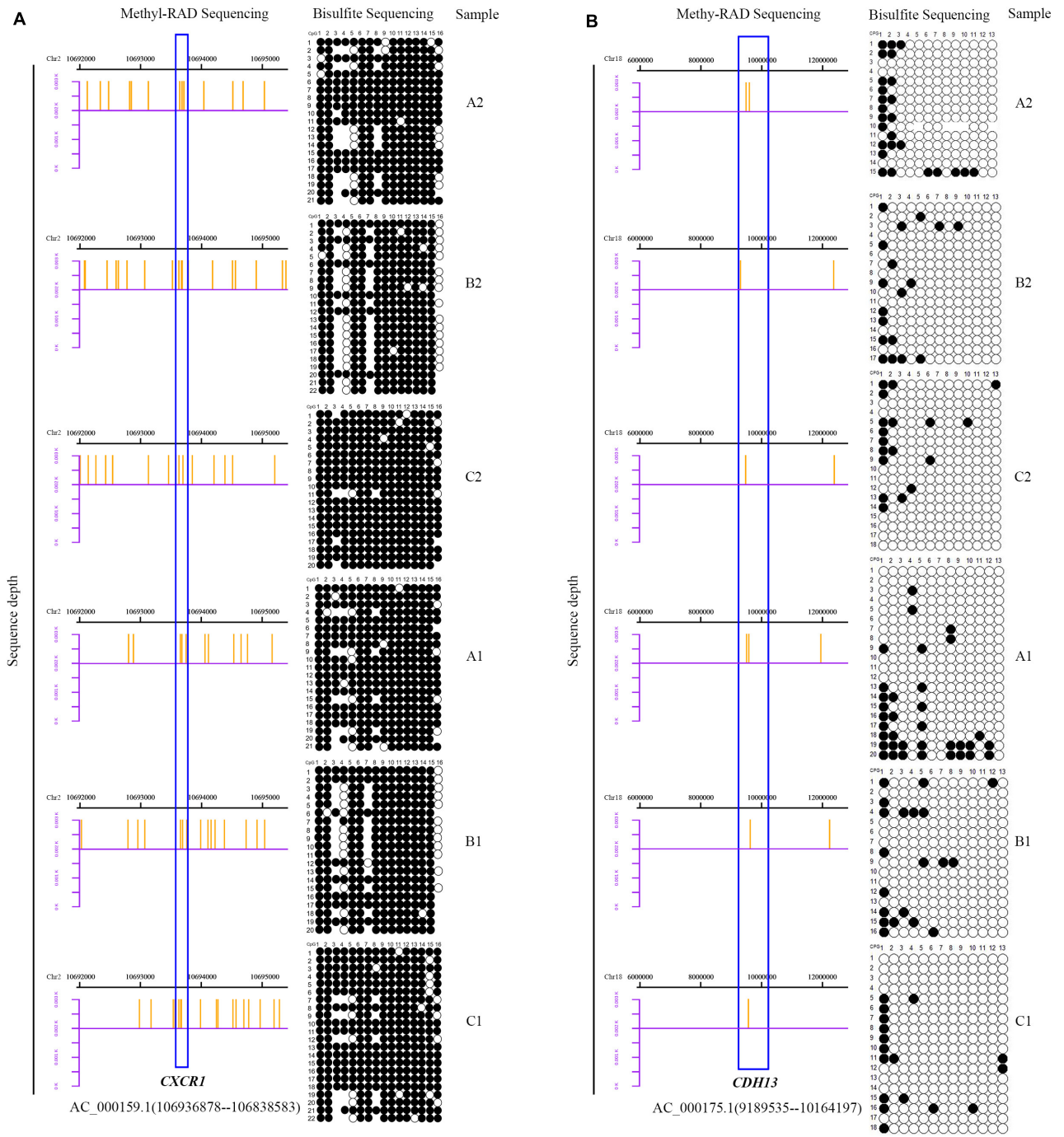



**FIGURE 10 |** Bisulfite sequencing PCR results. Columns represent the CpG sites and rows represent the clones. Black and white points represent methylated and unmethylated CpG sites, respectively. The blank region indicate that the CpG site was not detected by BSP. The distribution of sequencing reads detected by Methyl-RAD Seq for two genes in the mammary gland quarters of SA group (A2, B2, and C2) and CL group (A1, B1, and C1) are to the right of each figure. The blue boxes represent two genes, *CXCR1* [**(A)**, high methylation level] and *CDH13* [**(B)**, low methylation level].

of $C^mCGG$ DMGs in the host response to *S. aureus*-induced mastitis. Furthermore, $C^mCGG$ DMGs were also enriched in KEGG pathways related to the immune response, such as "Intestinal immune network for IgA production," "Th17 cell differentiation," and "C-type lectin receptor signaling pathway." C-type lectin is important for the regulation of innate immune and inflammatory processes (Del Fresno et al., 2018), and is known to influence host antimicrobial immunity (Dambuza and Brown, 2015). Th17 cell differentiation plays an important role in immune regulation of T cell during specific immune processes

(Sordillo, 2011). It was previously reported that Th17 cells showed specific differentiation in *S. aureus*-mastitis (Zhao et al., 2015), and the diseases and immune-related KEGG pathways in the present study further support the importance of Th17 cells in the host immune response to *S. aureus* mastitis and the regulatory roles of $C^mCGG$ DMGs.

Interestingly, several GO terms and KEGG pathways related to cell adhesion were enriched by $C^mCGG$ DMEGs, indicating the important impacts of $C^mCGG$ methylation on the process of cell adhesion. Cell adhesion has been noted to influence immune cell function impacting cell proliferation, differentiation and migration as well as host-pathogen interaction (Samanta and Almo, 2015; Li J. et al., 2018). The $C^mCGG$ DMEGs were enriched in GO terms related to inflammatory response, immune system development, regulation of immune response as well as other immune response-regulating signaling pathways indicating their potential regulatory roles in response to *S. aureus*-infection. In addition, we found that $C^mCGG$ DMEGs were significantly enriched in pathways related to activities of immune cells, such as leukocyte, lymphocyte and T cell, which are important effector cells of the immune system, thus suggesting important roles for these methylated genes in the host immune response to *S. aureus*-mastitis. Lymphocytes are important members of the acquired immune system (Hoekstra et al., 2015) and lymphocyte proliferation and viability are detrimentally affected by *S. aureus* (Nonnecke and Harp, 1988; Hu et al., 2001). T cells activated by monocyte-derived dendritic cells play key roles in immune response to *S. aureus* (Bharathan, 2016). He et al. (2016) also reported that differently expressed genes due to subclinical *S. aureus* mastitis in cattle are involved in the T cell receptor-signaling pathway. These reports are supported by the enriched GO terms related to the immune response regulation and immune system, and KEGG disease and immune related pathways observed in this study.

### Study Limitations and Further Research Prospect

This study constructed the landscape of genome wide DNA methylation of healthy and *S. aureus* infected mammary gland tissues of Holstein dairy cows, providing basic functional prediction of altered methylation sites or genes in relation to *S. aureus* mastitis. However, the relatively small sample size ($n$ = 3) limits the reliability of the data. But a major advantage of the data is the fact that infected and health mammary gland quarters where from the same cows which provided room for valid comparisons of methylated sites and also eliminated the bias due to different genetic constitution of infected and control cows if a different set of challenged and control cows were used. Although the sequencing technology (Methyl-RAD) employed for this study had many advantages, such as higher sensitivity and accuracy, the reliability and reference value, but is still limited because of the short-read output, which normally limits the success of unique mapping. This study has provided a general overview and functional prediction of DNA methylation alterations due to *S. aureus* bacteria but further in-depth analyses are needed. For example, the methylation distribution and alteration at the promotor regions, which has significant impacts on gene expression, deserves more detailed analysis. Furthermore, functional analysis and validation of DMGs should be expand and deepen. More cows and a more reliable sequencing method such as whole genome bisulfite sequencing is expected to further enhance the reliability and reference value of detected methylation sites due to *S. aureus* bacteria.

## CONCLUSION

The genome-wide DNA methylation profile of mammary gland tissues of Chinese Holstein cows with *S. aureus*-induced mastitis was generated by the method of Methyl-RAD Seq, indicating the significantly difference of DNA methylation level between *S. aureus*-challenged and non-challenged quarters. A total of 9,181 $C^mCGG$ sites and 1,790 DM $C^mCWGG$ sites were significantly DM between SA and CL treatments. Furthermore, potential functions of 363 $C^mCGG$ DMGs and 301 $C^mCWGG$ DMGs were related to the regulation of immune response and metabolism during *S. aureus*-infection, respectively. The functional enrichment of 526 $C^mCGG$ DMEGs further revealed the regulatory roles of altered methylation of 102 immune-related $C^mCGG$ DMEGs involved in immune processes and regulation in response to *S. aureus* infection, suggesting their potential as candidate genes for *S. aureus* mastitis. Therefore, these results show that DNA methylation has potential regulatory roles in bovine mammary gland processes during *S. aureus* mastitis and also serves as a reference for future mechanistic studies aiming to better understand the epigenetic regulation of host response to *S. aureus*-induced mastitis.

## DATA AVAILABILITY STATEMENT

Our sequence data have submitted to NCBI (https://dataview.ncbi.nlm.nih.gov/?search=SUB7329711) and accession number is SUB7329711.

## ETHICS STATEMENT

The animal use protocol was reviewed and approved by the animal use and care committee of Yangzhou University.

## AUTHOR CONTRIBUTIONS

MW conducted the experiments, analyzed the data, and drafted the manuscript. ZY and YM designed the experiments and guided the experimental implementation. YL and YS handled the samples and prepared libraries for sequencing. ML, HZ, and ZC were involved in data processing and visualization. EI-A provided inputs in data interpretation and critically reviewed the

initial manuscript draft. NK provided inputs in the discussion. All authors reviewed and approved the final draft.

## FUNDING

The research was financially supported by the National Natural Science Foundation of China (31972555 and 31372286), the Natural Science Foundation of the Jiangsu Higher Education Institutions of China (18KJA230003), the Six Talent Peaks Project in Jiangsu Province (NY-093), the Key Project Foundation of Joint International Research Laboratory of Agriculture and Agri-Product Safety, the Ministry of Education of China (JRK20180014), and the Priority Academic Program Development of Jiangsu Higher Education Institutions (PAPD).

## SUPPLEMENTARY MATERIAL

The Supplementary Material for this article can be found online at: https://www.frontiersin.org/articles/10.3389/fgene.2020.550515/full#supplementary-material

## REFERENCES

Beniæ, M., Maæešiæ, N., Cvetniæ, L., Habrun, B., Cvetniæ, Ž, Turk, R., et al. (2018). Bovine mastitis: a persistent and evolving problem requiring novel approaches for its control-a review. *Vet. Arh.* 88, 535–557. doi: 10.24099/vet.arhiv.0116

Bergman, Y., and Cedar, H. (2013). DNA methylation dynamics in health and disease. *Nat. Struct. Mole. Biol.* 20, 274–281.

Bharathan, M. (2016). *Monocyte Derived Dendritic Cells: Sentinels and Translators of Immune Response to Staphylococcus aureus*. Dissertation, Virginia: Virginia Polytechnic Institute and State University.

Bindea, G., Mlecnik, B., Hackl, H., Charoentong, P., Tosolini, M., Kirilovsky, A., et al. (2009). ClueGO: a Cytoscape plug-in to decipher functionally grouped gene ontology and pathway annotation networks. *Bioinformatics* 25, 1091–1093. doi: 10.1093/bioinformatics/btp101

Bolger, A. M., Lohse, M., and Usadel, B. (2014). Trimmomatic: a flexible trimmer for Illumina sequence data. *Bioinformatics* 30, 2114–2120. doi: 10.1093/bioinformatics/btu170

Brinkman, A. B., Simmer, F., Ma, K., Kaan, A., Zhu, J., and Stunnenberg, H. G. (2010). Whole-genome DNA methylation profiling using MethylCap-seq. *Methods* 52, 232–236. doi: 10.1016/j.ymeth.2010.06.012

Brunner, A. L., Johnson, D. S., Kim, S. W., Valouev, A., Reddy, T. E., Neff, N. F., et al. (2009). Distinct DNA methylation patterns characterize differentiated human embryonic stem cells and developing human fetal liver. *Genome Res.* 19, 1044–1056. doi: 10.1101/gr.088773.108

Cai, Z., Guldbrandtsen, B., Lund, M. S., and Sahana, G. (2018). Prioritizing candidate genes post-GWAS using multiple sources of data for mastitis resistance in dairy cattle. *BMC Genom.* 19:656. doi: 10.1186/s12864-018-5050-x

Carlén, E., Strandberg, E., and Roth, A. (2004). Genetic parameters for clinical mastitis, somatic cell score, and production in the first three lactations of Swedish Holstein cows. *J. Dairy Sci.* 87, 3062–3070. doi: 10.3168/jds.s0022-0302(04)73439-6

Cha, E., Hertl, J., Schukken, Y., Tauer, L., Welcome, F., and Gröhn, Y. (2013). The effect of repeated episodes of bacteria-specific clinical mastitis on mortality and culling in Holstein dairy cows. *J. Dairy Sci.* 96, 4993–5007. doi: 10.3168/jds.2012-6232

Chen, J., Wu., , Y., Sun, Y., Dong, X., Wang, Z., Zhang, Z., et al. (2019). Bacterial Lipopolysaccharide Induced Alterations of Genome-Wide DNA Methylation and Promoter Methylation of Lactation-Related Genes in Bovine Mammary Epithelial Cells. *Toxins* 11:298. doi: 10.3390/toxins11050298

Chen, Z., Chu, S., Xu, X., Jiang, J., and Yang, Z. (2019a). Analysis of longissimus muscle quality characteristics and associations with DNA methylation status in cattle. *Genes Genom.* 41, 1147–1163. doi: 10.1007/s13258-019-00844-4

Chen, Z., Zhou, J., Wang, X., Zhang, Y., Lu, X., Fan, Y., et al. (2019b). Screening candidate microR-15a-IRAK2 regulatory pairs for predicting the response to Staphylococcus aureus-induced mastitis in dairy cows. *J. Dairy Res.* 86, 425–431. doi: 10.1017/s0022029919000785

Cingolani, P., Platts, A., Wang, L. L., Coon, M., Nguyen, T., Wang, L., et al. (2012). A program for annotating and predicting the effects of single nucleotide polymorphisms, SnpEff: SNPs in the genome of Drosophila melanogaster strain w1118; iso-2; iso-3. *Fly* 6, 80–92. doi: 10.4161/fly.19695

Dambuza, I. M., and Brown, G. D. (2015). C-type lectins in immunity: recent developments. *Curr. Opin. Immunol.* 32, 21–27. doi: 10.1016/j.coi.2014.12.002

Del Fresno, C., Iborra, S., Saz-Leal, P., Martínez-López, M., and Sancho, D. (2018). Flexible signaling of myeloid C-type lectin receptors in immunity and inflammation. *Front. Immunol.* 9:804. doi: 10.3389/fimmu.2018.00804

Detilleux, J., Kastelic, J. P., and Barkema, H. W. (2015). Mediation analysis to estimate direct and indirect milk losses due to clinical mastitis in dairy cattle. *Prevent. Vet. Med.* 118, 449–456. doi: 10.1016/j.prevetmed.2015.01.009

Dufour, S., Dohoo, I. R., Barkema, H. W., DesCôteaux, L., DeVries, T., Reyher, K. K., et al. (2012). Manageable risk factors associated with the lactational incidence, elimination, and prevalence of Staphylococcus aureus intramammary infections in dairy cows. *J. Dairy Sci.* 95, 1283–1300. doi: 10.3168/jds.2011-4711

Emanuelson, U., Danell, B., and Philipsson, J. (1988). Genetic parameters for clinical mastitis, somatic cell counts, and milk production estimated by multiple-trait restricted maximum likelihood. *J. Dairy Sci.* 71, 467–476. doi: 10.3168/jds.s0022-0302(88)79576-4

Enger, B., Tucker, H., Nickerson, S., Parsons, C., and Akers, R. (2019). Effects of Staphylococcus aureus intramammary infection on the expression of estrogen receptor α and progesterone receptor in mammary glands of nonlactating cows administered estradiol and progesterone to stimulate mammary growth. *J. Dairy Sci.* 102, 2607–2617. doi: 10.3168/jds.2018-15499

Fang, L., Hou, Y., An, J., Li, B., Song, M., Wang, X., et al. (2016). Genome-wide transcriptional and post-transcriptional regulation of innate immune and defense responses of bovine mammary gland to Staphylococcus aureus. *Front. Cell. Infect. Microbiol.* 6:193. doi: 10.3389/fcimb.2016.00193

Fang, X., Zhao, Z., Yu, H., Li, G., Jiang, P., Yang, Y., et al. (2017). Comparative genome-wide methylation analysis of longissimus dorsi muscles between Japanese black (Wagyu) and Chinese Red Steppes cattle. *PLoS One* 12:e0182492. doi: 10.1371/journal.pone.0182492

Gim, J.-A., Hong, C. P., Kim, D.-S., Moon, J.-W., Choi, Y., Eo, J., et al. (2015). Genome-wide analysis of DNA methylation before-and after exercise in the thoroughbred horse with MeDIP-Seq. *Mole. Cells* 38:210. doi: 10.14348/molcells.2015.2138

Gu, H., Smith, Z. D., Bock, C., Boyle, P., Gnirke, A., and Meissner, A. (2011). Preparation of reduced representation bisulfite sequencing libraries for genome-scale DNA methylation profiling. *Nat. Proto.* 6:468. doi: 10.1038/nprot.2010.190

Han, H. (2019). Identification of several key genes by microarray data analysis of bovine mammary gland epithelial cells challenged with *Escherichia coli* and Staphylococcus aureus. *Gene* 683, 123–132. doi: 10.1016/j.gene.2018.10.004

He, Y., Song, M., Zhang, Y., Li, X., Song, J., Zhang, Y., et al. (2016). Whole-genome regulation analysis of histone H3 lysin 27 trimethylation in subclinical mastitis cows infected by Staphylococcus aureus. *BMC Genom.* 17:565. doi: 10.1186/s12864-016-2947-0

Hoekstra, M. E., Dijkgraaf, F. E., Schumacher, T. N., and Rohr, J. C. (2015). Assessing T lymphocyte function and differentiation by genetically encoded reporter systems. *Trends Immunol.* 36, 392–400. doi: 10.1016/j.it.2015.05.008

Horvath, S. (2013). DNA methylation age of human tissues and cell types. *Genome Biol.* 16, 1–5.

Hu, S., Concha, C., Johannisson, A., Meglia, G., and Waller, K. P. (2001). Effect of Subcutaneous Injection of Ginseng on Cows with Subclinical Staphylococcus aureus Mastitis. *J. Vet. Med. B Infect. Dis. Vet. Publ. Health* 48, 519–528. doi: 10.1111/j.1439-0450.2001.00470.x

Huang, X., Lu, H., Wang, J.-W., Xu, L., Liu, S., Sun, J., et al. (2013). High-throughput sequencing of methylated cytosine enriched by modification-dependent restriction endonuclease MspJI. *BMC Genet.* 14:56. doi: 10.1186/1471-2156-14-56

Ibeagha-Awemu, E. M., and Zhao, X. (2015). Epigenetic marks: regulators of livestock phenotypes and conceivable sources of missing variation in livestock improvement programs. *Front. Genet.* 6:302. doi: 10.3389/fgene.2015.00302

Jensen, K., Günther, J., Talbot, R., Petzl, W., Zerbe, H., Schuberth, H.-J., et al. (2013). *Escherichia coli*-and Staphylococcus aureus-induced mastitis differentially modulate transcriptional responses in neighbouring uninfected bovine mammary gland quarters. *BMC Genom.* 14:36. doi: 10.1186/1471-2164-14-36

Kanzleiter, T., Jähnert, M., Schulze, G., Selbig, J., Hallahan, N., Schwenk, R. W., et al. (2015). Exercise training alters DNA methylation patterns in genes related to muscle growth and differentiation in mice. *Am. J. Physiol. Endocrinol. Metabol.* 308, E912–E920.

Koivula, M., Mäntysaari, E., Negussie, E., and Serenius, T. (2005). Genetic and phenotypic relationships among milk yield and somatic cell count before and after clinical mastitis. *J. Dairy Sci.* 88, 827–833. doi: 10.3168/jds.s0022-0302(05)72747-8

Korkmaz, F. (2018). *An Analysis of Between-Cow Variation in Innate Immunity in Relation to Mastitis Severity*. Graduate College Dissertations Burlington: The University of Vermont.

Kumar, N., Manimaran, A., Kumaresan, A., Jeyakumar, S., Sreela, L., Mooventhan, P., et al. (2017). Mastitis effects on reproductive performance in dairy cattle: a review. *Trop. Anim. Health Product.* 49, 663–673. doi: 10.1007/s11250-017-1253-4

Kurz, J. P., Yang, Z., Weiss, R. B., Wilson, D. J., Rood, K. A., Liu, G. E., et al. (2019). A genome-wide association study for mastitis resistance in phenotypically well-characterized Holstein dairy cattle using a selective genotyping approach. *Immunogenetics* 71, 35–47. doi: 10.1007/s00251-018-1088-9

Li, J., Hsu, H.-C., Mountz, J. D., and Allen, J. G. (2018). Unmasking fucosylation: from cell adhesion to immune system regulation and diseases. *Cell Chem. Biol.* 25, 499–512. doi: 10.1016/j.chembiol.2018.02.005

Li, N., Ye, M., Li, Y., Yan, Z., Butcher, L. M., Sun, J., et al. (2010). Whole genome DNA methylation analysis based on high throughput sequencing technology. *Methods* 52, 203–212. doi: 10.1016/j.ymeth.2010.04.009

Li, R., Li, Y., Kristiansen, K., and Wang, J. (2008). SOAP: short oligonucleotide alignment program. *Bioinformatics* 24, 713–714. doi: 10.1093/bioinformatics/btn025

Li, R., Zhang, C. L., Liao, X. X., Chen, D., Wang, W. Q., Zhu, Y. H., et al. (2015). Transcriptome microRNA profiling of bovine mammary glands infected with Staphylococcus aureus. *Int. J. Mol. Sci.* 16, 4997–5013. doi: 10.3390/ijms16034997

Li, Y., Li, C., Ma, Q., Zhang, Y., Yao, Y., Liu, S., et al. (2018). Genetic variation in CDH13 gene was associated with non-small cell lung cancer (NSCLC): A population-based case-control study. *Oncotarget* 9:881. doi: 10.18632/oncotarget.22971

Liao, X. (2014). *Gene expression profile of Staphylococcus aureus induced mastitis in dairy cows*. China: Yangzhou University.

Lin, S., Hsieh, S., Lin, Y., Lee, C., Tsai, M., Lai, L., et al. (2012). A whole genome methylation analysis of systemic lupus erythematosus: hypomethylation of the IL10 and IL1R2 promoters is associated with disease activity. *Genes Immun.* 13, 214–220. doi: 10.1038/gene.2011.74

Luoreng, Z.-M., Wang, X.-P., Mei, C.-G., and Zan, L.-S. (2018). Comparison of microRNA Profiles between Bovine Mammary Glands Infected with Staphylococcus aureus and *Escherichia coli*. *Int. J. Biol. Sci.* 14:87. doi: 10.7150/ijbs.22498

Lush, J. L. (1950). Inheritance of susceptibility to mastitis. *J. Dairy Sci.* 33, 121–125. doi: 10.3168/jds.s0022-0302(50)91876-5

Ma, S., Tong, C., Ibeagha-Awemu, E. M., and Zhao, X. (2019). Identification and characterization of differentially expressed exosomal microRNAs in bovine milk infected with Staphylococcus aureus. *BMC Genom.* 20:934. doi: 10.1186/s12864-019-6338-1

Makovec, J. A., and Ruegg, D. P. L. (2003). Antimicrobial resistance of bacteria isolated from dairy cow milk samples submitted for bacterial culture: 8,905 samples (1994–2001). *J. Am. Vet. Med. Assoc.* 222, 1582–1589. doi: 10.2460/javma.2003.222.1582

Mao, Y., Zhu, X., Li, R., Chen, D., Xin, S., Zhu, Y., et al. (2015). Methylation analysis of CXCR1 in mammary gland tissue of cows with mastitis induced by Staphylococcus aureus. *Genet. Mole. Res.* 14, 12606–12615. doi: 10.4238/2015.october.19.4

Martin, P., Barkema, H., Brito, L., Narayana, S., and Miglior, F. (2018). Symposium review: novel strategies to genetically improve mastitis resistance in dairy cattle. *J. Dairy Sci.* 101, 2724–2736. doi: 10.3168/jds.2017-13554

Modak, R., Das Mitra, S., Krishnamoorthy, P., Bhat, A., Banerjee, A., Gowsica, B., et al. (2012). Histone H3K14 and H4K8 hyperacetylation is associated with *Escherichia coli*-induced mastitis in mice. *Epigenetics* 7, 492–501. doi: 10.4161/epi.19742

Nonnecke, B. J., and Harp, J. A. (1988). Effects of Staphylococcus aureus on Bovine Mononuclear Leukocyte Proliferation and Viability: Modulation by Phagocytic Leukocytes. *J. Dairy Sci.* 71, 835–842. doi: 10.3168/jds.s0022-0302(88)79624-1

Patil, V., Ward, R. L., and Hesson, L. B. (2014). The evidence for functional non-CpG methylation in mammalian cells. *Epigenetics* 9, 823–828. doi: 10.4161/epi.28741

Pokorska, J., Dusza, M., Kułaj, D., Żukowski, K., and Makulska, J. (2016). Single nucleotide polymorphisms in the CXCR1 gene and its association with clinical mastitis incidence in Polish Holstein-Friesian cows. *Genet. Mole. Res. GMR* 15:15027247

Pu, J., Li, R., Zhang, C., Chen, D., Liao, X., Zhu, Y., et al. (2017). Expression profiles of miRNAs from bovine mammary glands in response to Streptococcus agalactiae-induced mastitis. *J. Dairy Res.* 84, 300–308. doi: 10.1017/S0022029917000437

Quinlan, A. R., and Hall, I. M. (2010). BEDTools: a flexible suite of utilities for comparing genomic features. *Bioinform* 26, 841–842. doi: 10.1093/bioinformatics/btq033

Rainard, P., Foucras, G., Boichard, D., and Rupp, R. (2018). Invited review: low milk somatic cell count and susceptibility to mastitis. *J. Dairy Sci.* 101, 6703–6714. doi: 10.3168/jds.2018-14593

Reksen, O., Sølverød, L., Branscum, A., and Østerås, O. (2006). Relationships between milk culture results and treatment for clinical mastitis or culling in Norwegian dairy cattle. *J. Dairy Sci.* 89, 2928–2937. doi: 10.3168/jds.s0022-0302(06)72565-6

Reynolds, L. P., Ward, A. K., and Caton, J. S. (2017). *Epigenetics and Developmental Programming in Ruminants: Long-Term Impacts on Growth and Development, Biology of domestic animals*. Boca: CRC Press, 85–121.

Robinson, M. D., McCarthy, D. J., and Smyth, G. K. (2010). edgeR: a Bioconductor package for differential expression analysis of digital gene expression data. *Bioinformatics* 26, 139–140. doi: 10.1093/bioinformatics/btp616

Samanta, D., and Almo, S. C. (2015). Nectin family of cell-adhesion molecules: structural and molecular aspects of function and specificity. *Cell. Mole. Life Sci.* 72, 645–658. doi: 10.1007/s00018-014-1763-4

Sampimon, O., Barkema, H. W., Berends, I., Sol, J., and Lam, T. (2009). Prevalence of intramammary infection in Dutch dairy herds. *J. Dairy Res.* 76, 129–136. doi: 10.1017/s0022029908003762

Sanderson, B. A., Araki, N., Lilley, J. L., Guerrero, G., and Lewis, L. K. (2014). Modification of gel architecture and TBE/TAE buffer composition to minimize heating during agarose gel electrophoresis. *Anal. Biochem.* 454, 44–52. doi: 10.1016/j.ab.2014.03.003

Shin, J., Bourdon, C., Bernard, M., Wilson, M. D., Reischl, E., Waldenberger, M., et al. (2015). Layered genetic control of DNA methylation and gene expression: a locus of multiple sclerosis in healthy individuals. *Hum Mole. Genet.* 24, 5733–5745. doi: 10.1093/hmg/ddv294

Siebert, L., Staton, M., Oliver, S., and Pighetti, G. (2017). *Identifying genome associations with unique mastitis phenotypes in response to intramammary Streptococcus uberis challenge*, Doctoral Dissertations Knoxville: The University of Tennessee, 86.

Song, M., He, Y., Zhou, H., Zhang, Y., Li, X., and Yu, Y. (2016). Combined analysis of DNA methylome and transcriptome reveal novel candidate genes with susceptibility to bovine Staphylococcus aureus subclinical mastitis. *Sci. Rep.* 6:29390.

Sordillo, L. M. (2011). New Concepts in the Causes and Control of Mastitis. *J. Mammary Gland Biol. Neopl.* 16, 271–273. doi: 10.1007/s10911-011-9239-8

Sun, X., Li, J., Fu, L., Jiang, J., Zhao, J., and Wang, G. (2019). The Epigenetic Modification in Mammals under Heat Stress. *World J. Vet. Sci.* 1:1005.

Suravajhala, P., and Benso, A. (2017). Prioritizing single-nucleotide polymorphisms and variants associated with clinical mastitis. *Adv. Appl. Bioinform. Chem. AABC* 10:57. doi: 10.2147/aabc.s123604

Taiwo, O., Wilson, G. A., Morris, T., Seisenberger, S., Reik, W., Pearce, D., et al. (2012). Methylome analysis using MeDIP-seq with low DNA concentrations. *Nat. Prot.* 7:617. doi: 10.1038/nprot.2012.012

Usman, T., Yu, Y., and Wang, Y. (2016). CD4 promoter hyper methylation is associated with lower gene expression in clinical mastitis cows and vice versa in the healthy controls. *J. Anim. Sci.* 94, 38–38. doi: 10.2527/jas2016.94supplement438x

Vallimont, J., Dechow, C. D., Sattler, C., and Clay, J. (2009). Heritability estimates associated with alternative definitions of mastitis and correlations with somatic cell score and yield. *J. Dairy Sci.* 92, 3402–3410. doi: 10.3168/jds.2008-1229

Verbeke, J., Piccart, K., Piepers, S., Van Poucke, M., Peelman, L., De Visscher, A., et al. (2015). Somatic cell count and milk neutrophil viability of dairy heifers with specific CXCR1 genotypes following experimental intramammary infection with Staphylococcus chromogenes originating from milk. *Vet J.* 204, 322–326. doi: 10.1016/j.tvjl.2015.04.010

Wang, D., Wei, Y., Shi, L., Khan, M. Z., Fan, L., Wang, Y., et al. (2019). Genome-wide DNA methylation pattern in a mouse model reveals two novel genes associated with Staphylococcus aureus mastitis. *Asian Austr. J. Anim. Sci.* 33, 203–211. doi: 10.5713/ajas.18.0858

Wang, D., Wei, Y., Shi, L., Khan, M. Z., Fan, L., Wang, Y., et al. (2020). Genome-wide DNA methylation pattern in a mouse model reveals two novel genes associated with Staphylococcus aureus mastitis. *Asian Austr. J. Anim. Sci* 33:203. doi: 10.5713/ajas.18.0858

Wang, H.-Q., Yang, C.-Y., Wang, S.-Y., Wang, T., Han, J.-L., Wei, K., et al. (2018). Cell-free plasma hypermethylated CASZ1, CDH13 and ING2 are promising biomarkers of esophageal cancer. *J. Biomed. Res.* 32, 424–433.

Wang, S., Lv, J., Zhang, L., Dou, J., Sun, Y., Li, X., et al. (2015). MethylRAD: a simple and scalable method for genome-wide DNA methylation profiling using methylation-dependent restriction enzymes. *Open Biol.* 5:150130. doi: 10.1098/rsob.150130

Wang, X. G., Ju, Z. H., Hou, M. H., Jiang, Q., Yang, C. H., Zhang, Y., et al. (2016). Deciphering transcriptome and complex alternative splicing transcripts in mammary gland tissues from cows naturally infected with Staphylococcus aureus mastitis. *PLoS One* 11:e0159719. doi: 10.1371/journal.pone.0159719

Wang, X., Ma, P., Liu, J., Zhang, Q., Zhang, Y., Ding, X., et al. (2015). Genome-wide association study in Chinese Holstein cows reveal two candidate genes for somatic cell score as an indicator for mastitis susceptibility. *BMC Genet.* 16:111. doi: 10.1186/s12863-015-0263-3

Wang, X., Zhang, Y., He, Y., Ma, P., Fan, L., Wang, Y., et al. (2013). Aberrant promoter methylation of the CD4 gene in peripheral blood cells of mastitic dairy cows. *Genet. Mol. Res.* 12, 6228–6239. doi: 10.4238/2013.december.4.10

Weigel, K. A., and Shook, G. E. (2018). Genetic selection for mastitis resistance. *Vet. Clin. Food Anim. Pract.* 34, 457–472. doi: 10.1016/j.cvfa.2018.07.001

Welderufael, B. G., Løvendahl, P., De Koning, D.-J., Janss, L. L., and Fikse, W. (2018). Genome-wide association study for susceptibility to and recoverability from mastitis in Danish Holstein cows. *Front. Genet.* 9:141. doi: 10.3389/fgene.2018.00141

Wu, Y., Chen, J., Sun, Y., Dong, X., Wang, Z., Chen, J., et al. (2020). PGN and LTA from Staphylococcus aureus Induced Inflammation and Decreased Lactation through Regulating DNA Methylation and Histone H3 Acetylation in Bovine Mammary Epithelial Cells. *Toxins* 12:238. doi: 10.3390/toxins12040238

Xu, Y., Li, X., Wang, H., Xie, P., Yan, X., Bai, Y., et al. (2016). Hypermethylation of CDH13, DKK3 and FOXL2 promoters and the expression of EZH2 in ovary granulosa cell tumors. *Mole. Med. Rep.* 14, 2739–2745. doi: 10.3892/mmr.2016.5521

Yang, J., Niu, H., Huang, Y., and Yang, K. (2016). A systematic analysis of the relationship of CDH13 promoter methylation and breast cancer risk and prognosis. *PLoS One* 11:e0149185. doi: 10.1371/journal.pone.0149185

Ye, M., Huang, T., Li, J., Zhou, C., Yang, P., Ni, C., et al. (2017). Role of CDH13 promoter methylation in the carcinogenesis, progression, and prognosis of colorectal cancer: a systematic meta-analysis under PRISMA guidelines. *Medicine* 96:e5956. doi: 10.1097/md.0000000000005956

Yu, G., Wang, L.-G., Han, Y., and He, Q.-Y. (2012). clusterProfiler: an R package for comparing biological themes among gene clusters. *OMICS A J. Integr. Biol.* 16, 284–287. doi: 10.1089/omi.2011.0118

Zhang, X., Zhang, S., Ma, L., Jiang, E., Xu, H., Chen, R., et al. (2017). Reduced representation bisulfite sequencing (RRBS) of dairy goat mammary glands reveals DNA methylation profiles of integrated genome-wide and critical milk-related genes. *Oncotarget* 8:115326. doi: 10.18632/oncotarget.23260

Zhang, Y., Li, F., Feng, X., Yang, H., Zhu, A., Pang, J., et al. (2017). Genome-wide analysis of DNA Methylation profiles on sheep ovaries associated with prolificacy using whole-genome Bisulfite sequencing. *BMC Genom.* 18:759. doi: 10.1186/s12864-017-4068-9

Zhang, Y., Wang, X., Jiang, Q., Hao, H., Ju, Z., Yang, C., et al. (2018). DNA methylation rather than single nucleotide polymorphisms regulates the production of an aberrant splice variant of IL6R in mastitic cows. *Cell Stress Chap.* 23, 617–628. doi: 10.1007/s12192-017-0871-0

Zhao, Y., Zhou, M., Gao, Y., Liu, H., Yang, W., Yue, J., et al. (2015). Shifted T helper cell polarization in a murine Staphylococcus aureus mastitis model. *PLoS One* 10:e0134797. doi: 10.1371/journal.pone.0134797

**Conflict of Interest:** The authors declare that the research was conducted in the absence of any commercial or financial relationships that could be construed as a potential conflict of interest.

*Copyright © 2020 Wang, Liang, Ibeagha-Awemu, Li, Zhang, Chen, Sun, Karrow, Yang and Mao. This is an open-access article distributed under the terms of the Creative Commons Attribution License (CC BY). The use, distribution or reproduction in other forums is permitted, provided the original author(s) and the copyright owner(s) are credited and that the original publication in this journal is cited, in accordance with accepted academic practice. No use, distribution or reproduction is permitted which does not comply with these terms.*

frontiers in Genetics

ORIGINAL RESEARCH
published: 28 October 2020
doi: 10.3389/fgene.2020.558189

# Genome-Wide Assessment of DNA Methylation in Chicken Cardiac Tissue Exposed to Different Incubation Temperatures and $CO_2$ Levels

*Ryan J. Corbett[1]*, Marinus F. W. te Pas[2], Henry van den Brand[3], Martien A. M. Groenen[2], Richard P. M. A. Crooijmans[2], Catherine W. Ernst[4] and Ole Madsen[2]**

*[1] Genetics and Genome Sciences Graduate Program, Michigan State University, East Lansing, MI, United States, [2] Animal Breeding and Genomics, Wageningen University & Research, Wageningen, Netherlands, [3] Adaptation Physiology Group, Wageningen University & Research, Wageningen, Netherlands, [4] Department of Animal Science, Michigan State University, East Lansing, MI, United States*

OPEN ACCESS

**Edited by:**
*George E. Liu, United States Department of Agriculture, United States*

**Reviewed by:**
*Shahin Eghbalsaied, Islamic Azad University, Isfahan, Iran*
*Ed Smith, Virginia Tech, United States*

***Correspondence:**
*Ryan J. Corbett*
*corbet35@msu.edu*
*Ole Madsen*
*ole.madsen@wur.nl*

**Specialty section:**
*This article was submitted to Livestock Genomics, a section of the journal Frontiers in Genetics*

**Received:** *01 May 2020*
**Accepted:** *30 September 2020*
**Published:** *28 October 2020*

**Citation:**
*Corbett RJ, te Pas MFW, van den Brand H, Groenen MAM, Crooijmans RPMA, Ernst CW and Madsen O (2020) Genome-Wide Assessment of DNA Methylation in Chicken Cardiac Tissue Exposed to Different Incubation Temperatures and $CO_2$ Levels. Front. Genet. 11:558189. doi: 10.3389/fgene.2020.558189*

Temperature and $CO_2$ concentration during incubation have profound effects on broiler chick development, and numerous studies have identified significant effects on hatch heart weight (HW) as a result of differences in these parameters. Early life environment has also been shown to affect broiler performance later in life; it has thus been suggested that epigenetic mechanisms may mediate long-term physiological changes induced by environmental stimuli. DNA methylation is an epigenetic modification that can confer heritable changes in gene expression. Using reduced-representation bisulfite sequencing (RRBS), we assessed DNA methylation patterns in cardiac tissue of 84 broiler hatchlings incubated at two egg shell temperatures (EST; 37.8°C and 38.9°C) and three $CO_2$ concentrations (0.1%, 0.4%, and 0.8%) from day 8 of incubation onward. We assessed differential methylation between EST treatments and identified 2,175 differentially methylated (DM) CpGs (1,121 hypermethylated, 1,054 hypomethylated at 38.9° vs. 37.8°) in 269 gene promoters and 949 intragenic regions. DM genes (DMGs) were associated with heart developmental processes, including cardiomyocyte proliferation and differentiation. We identified enriched binding motifs among DM loci, including those for transcription factors associated with cell proliferation and heart development among hypomethylated CpGs that suggest increased binding ability at higher EST. We identified 9,823 DM CpGs between at least two $CO_2$ treatments, with the greatest difference observed between 0.8 and 0.1% $CO_2$ that disproportionately impacted genes involved in cardiac muscle development and response to low oxygen levels. Using HW measurements from the same chicks, we performed an epigenome-wide association study (EWAS) for HW, and identified 23 significantly associated CpGs, nine of which were also DM between ESTs. We found corresponding differences in transcript abundance between ESTs in three DMGs (*ABLIM2*, *PITX2*, and *THRSP*). Hypomethylation of an exonic CpG in *PITX2* at 38.9°C was associated with increased

expression, and suggests increased cell proliferation in broiler hatchlings incubated at higher temperatures. Overall, these results identified numerous epigenetic associations between chick incubation factors and heart development that may manifest in long-term differences in animal performance.

**Keywords: DNA methylation, epigenetics, temperature, $CO_2$, heart, chicken**

## INTRODUCTION

Early life environmental parameters have profound effects on broiler chick development and post-hatch performance. Incubation temperature is one of the most important factors influencing embryonic growth, development, and physiology (Ricklefs, 1987; French, 1994; Christensen et al., 1999; Lourens et al., 2005). In studies assessing the effects of incubation egg shell temperature (EST) on organ growth, heart weight (HW) is consistently observed to be negatively correlated with EST (Leksrisompong et al., 2007; Molenaar et al., 2010, 2011; Maatjens et al., 2014, 2016). Mechanisms linking incubation EST and heart development have been proposed; studies have shown that increased incubation temperature decreases the mitotic index of cardiomyocytes (Romanoff, 1960), as well as the concentration of circulating T3, the metabolically active form of thyroid hormone (Kühn et al., 1984; Yahav et al., 1996). Additionally, phenotypic differences in adult broilers associated with differences in early life temperature have been observed. Chicks incubated at a higher EST from embryonic day 7 (E7) to hatch were found to have a higher incidence of ascites mortality at 6 weeks of age (Molenaar et al., 2011; Sözcü and Ipek, 2015). However, broilers exposed to increased temperature early in life exhibited decreased mortality when exposed to heat stress again at 6 weeks of age relative to unexposed animals, suggesting that early heat stress confers thermotolerance that can improve performance upon subsequent exposures (Yahav and Hurwitz, 1996).

In addition to temperature, $CO_2$ concentration during the incubation period has been suggested to be important for regulating chick growth and physiology. Embryos incubated at increased $CO_2$ concentration have been found to exhibit numerous phenotypes; in addition to a significantly greater average HW at hatch (Maatjens et al., 2014), lower blood oxygen levels relative to control chicks have also been observed (Hassanzadeh et al., 2010). Increased incubator $CO_2$ concentration was associated with decreased ascites mortality in broilers later in life (Buys et al., 1998), suggesting long-term effects of early life $CO_2$ exposure. Alterations made to the epigenome have been proposed as one mechanism by which early life environmental differences can manifest in phenotypic differences in adult precocial birds (Tzschentke and Basta, 2002; Nichelmann, 2004), and it has recently been shown that embryonic thermal manipulation induces epigenetic modifications in the hypothalamus of 35-day old broilers (David et al., 2019).

Numerous epigenetic molecular mechanisms including DNA methylation, histone tail modifications, and non-coding RNA interactions have been observed to induce mitotically heritable changes in gene expression without altering DNA sequence (Jaenisch and Bird, 2003; Ibeagha-Awemu and Zhao, 2015). DNA methylation is an epigenetic modification involving the enzymatic addition of a methyl group to the 5-carbon of cytosine rings, producing 5-methylcytosine. Methylation occurs almost exclusively at CpG dinucleotides in vertebrates and has context-specific associations with gene expression. In gene promoters, methylation generally functions to decrease levels of transcription through the alteration of transcription factor (TF) binding sites, the recruitment of transcriptional repressors, or changes in chromatin conformation (Bird and Wolffe, 1999; Greenberg and Bourc'his, 2019). Conversely, gene body methylation is generally associated with increased levels of transcription (Lorincz et al., 2004; Ball et al., 2009; Maunakea et al., 2010), although negative associations have been identified in the context of genic enhancers (Varley et al., 2013). Epigenetic processes are known to be altered in response to environmental perturbations, and this phenomenon has been studied in livestock species in response to heat stress (Hao et al., 2016; Skibiel et al., 2018; Vinoth et al., 2018). Additionally, numerous epigenome-wide association studies (EWAS) have been performed in humans and mice to identify loci at which methylation level is significantly associated with complex and disease traits (Orozco et al., 2015; reviewed in Flanagan, 2015). Bisulfite-sequencing approaches allow for genome-wide assessment of DNA methylation patterns, yet this approach has been underutilized in the chicken thus far (Li et al., 2015; Lee et al., 2017; Zhang et al., 2017, 2018).

In the current study, we assessed DNA methylation patterns in cardiac tissue of broiler chicks incubated at normal or high EST (37.8 or 38.9°C, respectively) and low, medium, or high $CO_2$ concentration (0.1%, 0.4%, 0.8%, respectively) from embryonic day 8 (E8) until hatch. Using reduced representation bisulfite sequencing (RRBS), we tested for differences in CpG methylation rates between EST and $CO_2$ treatments and identified thousands of loci exhibiting differential methylation that are associated with heart development. Additionally, by integrating phenotypic records from the same samples, we performed an EWAS and identified loci at which methylation rate was significantly associated with HW, and many of these sites were within genes with known roles in heart development. Our results provide evidence that EST and $CO_2$ may be influencing heart growth and physiology through changes in cardiac DNA methylation patterns.

# MATERIALS AND METHODS

## Experimental Design and Sample Collection

Heart tissue samples were collected from a 2 × 3 factorial study. Briefly, Cobb 500 broiler eggs were obtained from commercial broiler breeder farms and incubated in six consecutive batches. From day 0 to 8 of incubation (E8), all eggs were incubated at an EST of 37.8°C and 0.1% $CO_2$. At E8 eggs were divided into two ESTs (37.8°C and 38.9°C) and three $CO_2$ concentrations (0.1%, 0.4%, and 0.8% $CO_2$) until hatch. Both EST treatments were applied in all batches, but $CO_2$ treatment application varied between batches. Time until hatch was recorded for each chick, and animals were removed from the incubator 6 h post-hatch. Chicks were then killed by cervical dislocation followed by decapitation. Hearts were removed and stored at −20°C until further analysis. Heart samples derived from the left ventricle of 84 chicks (13 to 15 samples per EST-$CO_2$ combination) were utilized for DNA isolation and RRBS.

## Statistical Analyses of Heart Weight

We tested for the significance of EST, $CO_2$ concentration, and their interaction on HW using analysis of variance (ANOVA). To account for the significantly shorter incubation time of 38.9°C chicks, we constructed a linear model with HW as the response variable and incubation time as a fixed effect, and subsequently used the model residuals as a response variable to test the significance of the environmental parameter main effects and their interaction.

## Sample Processing and Bisulfite Sequencing

DNA and RNA from heart samples were isolated using the AllPrep DNA/RNA Mini Kit (Qiagen) following manufacturer's instructions. The RRBS libraries were prepared with the Ovation RRBS Library construction kit from NuGEN following manufacturer's instructions. Isolated DNA was cut with *Msp*I and a fragment size selection of 20–250 bases was applied. Samples were pooled across 9 flow cell lanes with each pool containing no more than 10 samples, and all pools were sequenced for 161 cycles on a HiSeq 2500 using the TruSeq SBS sequencing kit version 4. Fastq files were generated and demultiplexed with the bcl2fastq v2.17.1.14 Conversion Software (Illumina).

## Bioinformatics Analyses

Raw RRBS FASTQ files were trimmed of adapter sequences using Trim Galore v0.5.0 with Cutadapt v1.8.1 (Babraham Bioinformatics) and the parameters: -a AGATCGGAAGAGC. Reads were subsequently filtered for only those beginning with the expected YGG trinucleotide sequence using a python script provided by NuGEN Technologies[1].

Read alignment was performed using BS-seeker2 v2.1.3 (Guo et al., 2013). An RRBS bowtie2 index was generated from the *Gallus gallus* GRCg6a reference genome assembly using bs_seeker_build.py with the following parameters: –aligner bowtie2 –rrbs –low 10 –up 280. Trimmed reads were subsequently aligned to the RRBS index using bs_seeker2-align.py with the following parameters: –rbbs –low 10 –up 280 –mismatches 0.05 –aligner = bowtie2 –bt2-p 10 –bt–local –bt2-N 1. Binary alignment map (BAM) files were converted to CGmap files using CGmapTools v0.1.2 (Guo et al., 2018), which reports methylation rates for all covered CpGs.

CGmap files were used to calculate sample global methylation rates, and to assess their associations with EST, $CO_2$, and individual CpG methylation rates. We identified an overrepresentation of CpG sites where methylation was significantly correlated with sample global CpG methylation rate (data not shown). We therefore corrected for this factor in subsequent site-specific differential methylation analyses.

## Differential Methylation Analyses

We filtered CGmap files to only include CpGs with coverage of at least 10 reads within a sample. Filtered CGmap files were subsequently converted to CpG report text files for *methylKit* analysis using a custom python script.

Differential methylation analyses were performed using the *methylKit* R package v1.8.1 (Akalin et al., 2012). Briefly, we removed CpGs in the 99.5th percentile of coverage for each sample to remove potential PCR duplicates. For the EST differential methylation analysis (38.9 vs. 37.8°C), CpGs were retained if they were covered in at least 25 samples per EST treatment over all $CO_2$ treatments. A logistic regression model was fitted for each CpG accounting for the covariates of $CO_2$ level and sample mean CpG methylation rate to test if EST had a significant effect on the log odds ratio of the CpG methylation rate. For $CO_2$ differential methylation analyses, CpGs were retained if they were covered in at least 16 samples per $CO_2$ treatment over both EST treatments. Three different analyses were performed to contrast the three different $CO_2$ treatment pairs (0.4 vs. 0.1%, 0.8 vs. 0.4%, and 0.8 vs. 0.1% $CO_2$). Again, a logistic regression model was fitted for each CpG, accounting for covariates of EST and sample mean CpG methylation rate, and testing for the effect of $CO_2$ level. A CpG site was considered significantly differentially methylated (DM) if the difference in methylation rate between treatments was greater than 10% and the corresponding $q$-value was less than 0.05 in both EST and $CO_2$ comparisons.

## CpG Annotation

All analyzed CpGs were annotated with respect to overlap with genes using the genomation R package v1.14.0 (Akalin et al., 2015). We defined promoter CpGs as those within 2 kb upstream or 200 bp downstream of a gene transcription start site (TSS). Intragenic CpGs were defined as CpGs within any other region of a gene, while all remaining CpGs were classified as intergenic. Promoter- and intragenic-DM genes (DMGs) were defined as those with a DM promoter and intragenic CpG, respectively.

To determine if DMGs were disproportionately involved in certain biological processes, gene lists were submitted for gene set enrichment analysis (GSEA) using the Panther database (Thomas et al., 2003, 2006). We submitted promoter- and intragenic-DMG

[1]https://github.com/nugentechnologies/NuMetRRBS

lists separately, and a background list composed of all genes with CpGs covered by our RRBS data was applied. We considered GO terms significantly enriched at FDR < 0.05.

## Motif Enrichment Analysis

We extracted 100 bp genomic sequences centered around EST hyper- and hypomethylated CpGs, as well as 100 bp sequences at 10 k random CpGs included in the DM analysis to use as control sequences. Sequences were uploaded to the MEME suite (Bailey et al., 2009; McLeay and Bailey, 2010) and the Analysis of Motif Enrichment (AME) tool was applied to identify enriched motifs in the Vertebrates (*in vivo* and *in silico*) database among our hyper- and hypomethylated sequences. We utilized the average odds score scoring method and Fisher's exact test to calculate motif enrichment. Motifs were considered significantly enriched at adjusted $p$-value < 0.05 and $E$-value < 0.05. We identified motifs that were uniquely enriched among hyper- or hypomethylated sequences, as well as their corresponding TF. The genes encoding these TFs were submitted to GSEA using the PANTHER database to identify enriched GO terms.

## Epigenome-Wide Association Study

We performed an EWAS to identify significant associations between CpG methylation rates and HW. CpG sites with a methylation rate variance of at least 1 across samples with coverage ≥10 were retained for further analysis. For each CpG site, a linear model was fitted with methylation rate as a response variable and including the fixed effects of sample mean methylation rate and $CO_2$ level. Residual methylation rates were extracted and used for subsequent association analyses. For each CpG site, a linear model was fitted with log2-transformed HW as a response variable, and $CO_2$ concentration, sample mean methylation rate, and CpG methylation rate as fixed effects. Analysis of variance was performed to assess the effect of the CpG methylation rate on HW, and this process was repeated for all sites. Associations were considered significant at $p$ < 1e-5.

## Quantitative Reverse-Transcription PCR

We performed quantitative reverse-transcription PCR (RT-qPCR) on eight DMGs (*TBX1*, *TBX4*, *THRSP*, *PITX2*, *ABLIM2*, *NGB*, *GSC*, and *DAG1*). Total RNA from six samples per EST treatment was reverse transcribed using Superscript II Reverse Transcriptase (Invitrogen). Custom primers were designed for the eight DMGs and two stably methylated genes (*MEAF6* and *SRRM1*), as well as for *YWHAZ* and *RPL13* which have been cited as suitable reference genes in chicken heart (Hassanpour et al., 2018; **Supplementary Table S1**). All assays were performed in singleton on a QuantStudio 5 Real-Time PCR System (Thermo Fisher) using 3.75 ul cDNA template (10 ng total), 1.25 ul of forward and reverse primers, and 6.25 ul MESA BLUE qPCR Master Mix (Eurogentec). Cycling conditions were 50°C for 2 min. and 95°C for 10 min., followed by 40 cycles of 95°C for 15 s and 60°C for 1 min., followed by a melt curve stage of 95°C for 15 s and 60°C for 1 min. and a dissociation step of 95°C for 15 s. Delta Cts (dCts) were obtained for each gene per sample by subtracting the test gene Ct from the geometric mean of the reference gene Cts, and analyses of variance were performed to assess the significance of EST on dCts correcting for sample $CO_2$ concentrations. Fold changes in abundance at 38.9°C relative to 37.8°C were calculated using the 2^-ddCt method.

# RESULTS

## Broiler Chicks Differ Significantly in HW Between ESTs

We measured HW in all broiler chicks 6 h post-hatch. Chicks incubated at 38.9°C exhibited significantly lower HW relative to 37.8°C chicks (**Figure 1**; $F$ = 37.53, $p$ = 3.19E-08). There was no significant effect of $CO_2$ concentration ($F$ = 0.254, $p$ = 0.62) or EST-$CO_2$ interaction ($F$ = 0.257, $p$ = 0.61) on HW. When correcting for the significantly shorter incubation time of 38.9°C chicks ($F$ = 52.79, $p$ = 2.18E-10), the difference in HW between ESTs remained significant ($F$ = 12.75, $p$ = 6.05E-04). These results recapitulate the well-established negative association between incubation EST and HW that has been found in numerous studies (Leksrisompong et al., 2007; Molenaar et al., 2010, 2011; Maatjens et al., 2014, 2016), and provided strong support for the assessment of associated differences in cardiac methylation between ESTs.

## RRBS Reads Capture Predominantly Lowly Methylated Regions of the Chicken Genome

An average of 18.9 million RRBS reads were generated per sample, of which 18.3 million remained after trimming (**Table 1**). Mapping of RRBS reads to the *G. gallus* reference genome resulted in an average unique alignment rate of 73.8%, and an average of 3.1 million CpGs covered at a read depth ≥10X. Global CpG methylation rates across all samples were low on

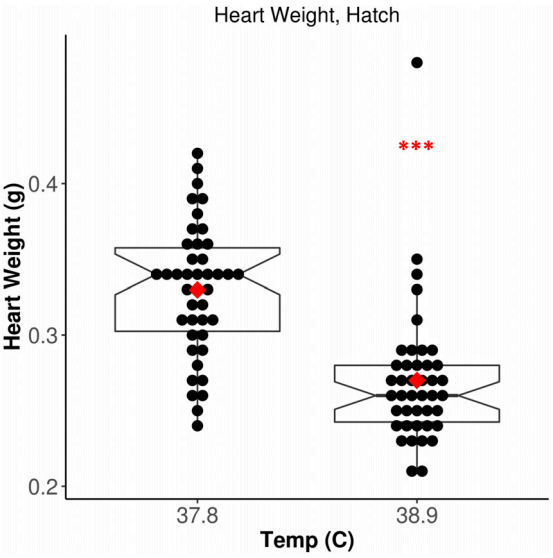



**FIGURE 1 |** Increased EST is associated with significantly lower heart weight. Notched horizontal lines and red dots indicate treatment median and mean values, respectively. ***$p$ < 0.001.

**TABLE 1 |** Summary of RRBS mapping.

| | No. Raw Reads | No. Trimmed Reads | Unique Mapping Rate (%) | CpG Methylation Rate (%) | CHG Methylation Rate (%) | CHH Methylation Rate (%) | CpGs Covered |
|---|---|---|---|---|---|---|---|
| **Mean** | 18.9 M | 18.3 | 73.8 | 17.7 | 0.55 | 0.56 | 3.1 M |
| **Range** | 10.1–34.1 M | 9.6–32.8 M | 77.1–69.9 | 13.8–20.4 | 0.48–0.78 | 0.49–0.77 | 2.3–3.5 M |

average (17.7%), likely due in part to the fact that RRBS targets CpG-rich regions of the genome which are lowly methylated (Meissner et al., 2008). Average CHG and CHH methylation rates were 0.55% and 0.56%, respectively; given the inherently low prevalence of methylation in non-CpG contexts in vertebrates (Ziller et al., 2011), this suggests high bisulfite conversion efficiency of sequenced reads across samples.

A total of 1,874,588 CpG sites were shared across at least 25 samples per EST treatment, and the majority of these (40.56%) were within gene promoters. 35.18% of CpGs were within gene bodies (25.67% in introns and 12.51% in exons), while 21.26% were intergenic. Promoter CpGs exhibited the lowest methylation rate on average (7.76%), with 85% of sites having an average methylation rate less than 10% (**Supplementary Figure S1A**). The percentage of lowly methylated (<10%) CpGs in exons, introns, and intergenic regions was significantly lower – 42.74%, 54.52%, and 51.77%, respectively (**Supplementary Figures S1B–D**). The low methylation observed at a majority of CpGs indicates that many loci covered by our RRBS data are not dynamically methylated in response to the applied environmental conditions, but remain relatively unmethylated regardless of EST or $CO_2$ treatment.

## EST Impacts the Methylation State of Genes Involved in General and Heart-Specific Developmental Processes

We identified a total of 2,175 DM CpGs between EST treatments, of which 1121 were hypermethylated and 1054 hypomethylated at 38.9°C relative to 37.8°C (**Figure 2** and **Supplementary Table S2**). Differential methylation was more likely to occur outside of promoter regions; of the 760,332 promoter CpGs tested, only 285 (0.05%) were DM, while 0.14%, 0.18%, and 0.15% of exonic, intronic, and intergenic CpGs, respectively, were DM. In total 269 genes were promoter-DM (promoter-DMGs; 123 hyper- and 146 hypomethylated), while 949 genes were intragenic-DM (intragenic-DMGs; 526 hyper- and 423 hypomethylated).

DM gene lists were submitted to Panther for GSEA, and we identified uniquely enriched biological processes among different gene sets (**Supplementary Table S3**). We did not identify enriched GO terms when considering hyper- and hypomethylated promoter-DMGs separately, however, when combining the two groups we identified enrichment of the terms "Multicellular Organism Development," "Animal Organ Development," and "Anatomical Structure Development" (**Table 2**). Among promoter-DMGs, several are known to play roles in heart development, including T-box transcription factors 1 and 4 (*TBX1* and *TBX4*) that were hypomethylated at 38.9°C, and two genes involved in thyroid hormone signaling: thyroid hormone receptor alpha (*THRA*) and thyroid hormone responsive (*THRSP*), which were hypo- and hypermethylated, respectively (**Supplementary Figures S2A,B**). As promoter methylation is generally inversely correlated with gene expression, hypomethylation of these gene promoters at 38.9°C is indicative of increased potential for gene activation, while hypermethylation suggests decreased activation.

Intragenic-DMGs were enriched for processes related to cardiac muscle development (**Table 2**). Specifically, hypermethylated intragenic-DMGs were enriched for GO terms such as "Heart Development," "Regulation of Myoblast Differentiation," and "Cardiovascular System Development," while hypomethylated intragenic-DMGs were enriched for terms including "Cell Differentiation," "Cell Adhesion," and "Glycosaminoglycan Metabolic Process." Among genes associated with these GO terms are many involved in cardiomyocyte proliferation and differentiation, including: dystroglycan 1 (*DAG1*, hyper- and hypomethylated; **Supplementary Figure S2C**), paired like homeodomain 2 (*PITX2*, hypomethylated; **Supplementary Figure S2D**), and Erb-B2 receptor tyrosine kinase 2 (*ERBB2*, hypomethylated) and 4 (*ERBB4*, hyper- and hypomethylated). Associations between intragenic methylation and gene expression are context-specific (Varley et al., 2013). Nevertheless, temperature-associated differential methylation within genes involved in heart development demonstrates the potential for corresponding differences in gene expression.

## EST Differential Methylation Impacts Binding Sites for TFs Involved in Cell Proliferation

As methylation is known to affect gene regulation through the alteration of TF binding sites, we sought to identify enriched motifs in the vicinity of DM CpGs between EST treatments. We submitted 100-bp sequences centered on the 2,175 DM CpGs for motif enrichment analysis, and were specifically interested in identifying motifs that were uniquely enriched among hyper- or hypomethylated sequences. We identified 71 motifs for 49 TFs uniquely enriched among hypermethylated regions, and 120 motifs for 81 TFs enriched among hypomethylated regions (**Supplementary Table S4**). Among the most uniquely enriched binding motifs for hypermethylated regions were numerous members of the zinc finger and BTB domain containing (ZBTB) family (ZBTB7C, ZBTB7A, ZBTB7B, and ZBTB49), many of which have been shown to negatively regulate cell proliferation (Jeon et al., 2014; Liu et al., 2014). Among hypermethylated regions, the most uniquely enriched binding motif was for musculin (MSC), which functions as a repressor of the myogenic factor *MYOD* (Zhao and Hoffman, 2006).

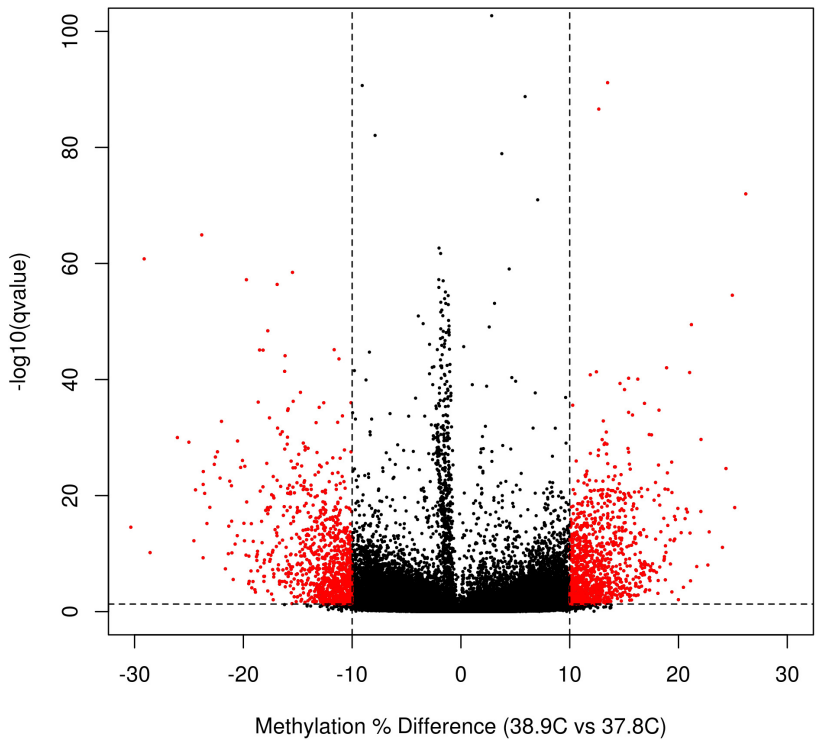



**FIGURE 2 |** Volcano plot of CpG differential methylation between incubation ESTs. Horizontal line indicates the *q*-value threshold for significance (0.05), and vertical lines indicate methylation difference threshold for significance (10% difference between EST treatments).

**TABLE 2 |** Enriched GO terms among DMGs between EST treatments.

| GO term | No. Genes | Enrichment | *P*-value |
|---|---|---|---|
| **Promoter-DMGs** | | | |
| anatomical structure development | 86 | 1.53 | 1.19E-05 |
| animal organ development | 60 | 1.81 | 4.22E-06 |
| multicellular organism development | 84 | 1.61 | 2.06E-06 |
| **Intragenic hypermethylated genes** | | | |
| anatomical structure development | 179 | 1.82 | 1.93E-18 |
| cell differentiation | 131 | 1.95 | 3.15E-11 |
| cardiovascular system development | 29 | 3.04 | 2.71E-07 |
| negative regulation of myoblast differentiation | 5 | 10.21 | 2.37E-04 |
| heart development | 22 | 2.30 | 4.33E-04 |
| regulation of cardiac muscle tissue development | 7 | 4.82 | 9.30E-04 |
| **Intragenic hypomethylated genes** | | | |
| anatomical structure development | 165 | 1.97 | 2.32E-21 |
| cell differentiation | 111 | 1.93 | 1.65E-12 |
| cell adhesion | 36 | 2.53 | 8.86E-07 |
| positive regulation of transcription | 50 | 2.08 | 1.20E-06 |
| glycosaminoglycan metabolic process | 11 | 4.64 | 4.52E-05 |

We submitted the gene IDs for TFs of hyper- and hypomethylated motifs to the PANTHER database for GO enrichment analysis. Uniquely enriched terms among TFs of hypermethylated motifs were not directly related to heart development or function; however, TFs of hypomethylated motifs were uniquely enriched for the GO terms "cardiovascular system development" and "positive regulation of cell population proliferation" (**Table 3**). Genes associated with these terms included several with known roles in positively regulating cardiomyocyte proliferation, including retinoic acid receptor alpha (*RARA*) (Xavier-Neto et al., 2015), T-box transcription factor 20 (*TBX20*) (Lu et al., 2017), lymphoid enhancer binding

factor 1 (*LEF1*) (Ye et al., 2019) and *PITX2*, which was also found to be hypomethylated at 38.9°C. Overall, these results reveal the potential for decreased binding ability (via hypermethylation) of TFs involved in negatively regulating cell proliferation, and increased binding ability (via hypomethylation) of TFs involved in positively regulating cardiomyocyte proliferation at 38.9 vs. 37.8°C.

## $CO_2$ Differential Methylation Impacts Genes Involved in Heart Development and Response to Hypoxia

We identified a total of 9,823 DM CpG between at least one pair of $CO_2$ treatments. Among these, 3,652 were DM between 0.4 and 0.1% $CO_2$ chicks, 4,695 between 0.8 and 0.4% $CO_2$, and 4,482 between 0.8 and 0.1% $CO_2$ (**Table 4** and **Supplementary Table S5**). In each contrast, the higher $CO_2$ treatment was associated with a higher proportion of hypermethylated CpGs, especially when comparing 0.8% $CO_2$ to the other treatments.

DM genes were enriched for more heart- and muscle-specific GO terms when contrasting 0.8% $CO_2$ to either of the other two $CO_2$ treatments (**Table 5** and **Supplementary Table S6**) Among hypermethylated intragenic-DMGs for each of the three contrasts, 18 such GO terms were enriched among the 0.8 vs. 0.1% contrast, while only five and six terms were enriched at 0.4 vs. 0.1% and 0.8 vs. 0.4%, respectively. Among hypomethylated intragenic-DMGs, the 0.8 vs. 0.4% $CO_2$ contrast yielded the greatest number of enriched heart/muscle-related terms ($n$ = 23), while the 0.4 vs. 0.1% and 0.8 vs. 0.1% yielded only three and seven, respectively. Intragenic-DMGs at 0.8% $CO_2$ vs. 0.4% and 0.1% included: *PDLIM7*, whose resulting protein regulates valve annulus size and hemostasis (Krcmery et al., 2013); *TGFB1*, which regulates postnatal cardiomyocyte differentiation (Engelmann et al., 1992); and *ILK*, which has been shown to exhibit protective effects against cardiomyopathy (Hannigan et al., 2007). Additionally, we also identified an enrichment of DMGs associated with response to low oxygen only when comparing 0.8 to 0.1% $CO_2$ (**Table 5**). Hypomethylated intragenic-DMGs were enriched for the GO terms "response to decreased oxygen levels" and "response to hypoxia," and these were not enriched among the DMGs in the other two contrasts.

## EWAS Identifies Methylation Signatures Significantly Associated With HW

Given the significant difference in HW between chicks of different incubation ESTs, we sought to identify CpG sites at which methylation rate was significantly associated with HW. We tested 1,521,346 CpG sites and identified 23 significant associations (**Figure 3** and **Supplementary Table S7**), which represented a modest enrichment in significant $p$-values compared to a random distribution (**Supplementary Figure S3**). Three of these CpGs were within gene promoter regions (in *GFI1*, *SP9,* and *ST6GALNAC4*), 13 were within gene bodies (exons or introns), and seven were in intergenic regions.

Among the 23 significantly associated CpG sites, nine were also significantly DM between EST treatments, and only one site – the hypomethylated CpG in *PITX2* – had a methylation difference greater than 10%. This site was found to be significantly positively correlated with HW ($r$ = 0.60, $p$ = 2.97E-06), along with four other sites: two exonic CpGs in neuroglobin (*NGB*) and goosecoid homeobox (*GSC*), an intronic CpG in calcium voltage-gated channel subunit alpha1 G (*CACNA1G*), and an intergenic CpG. Four hypermethylated CpGs were negatively associated with HW: an exonic CpG in *ENSGALG00000011444*, an intronic CpG in actin binding LIM protein family member 2 (*ABLIM2*), and two intergenic CpGs.

## RT-qPCR Identifies Genes With Coordinated Differences in Gene Methylation and Expression Between EST Treatments

We assessed transcript abundance of eight genes exhibiting differential methylation and/or significant associations with

**TABLE 3 |** Uniquely enriched GO terms among TFs of hypomethylated motifs.

| GO term | No. Genes | Enrichment | $p$-value |
|---|---|---|---|
| embryo development ending in birth or egg hatching | 13 | 5.42 | 8.08E-07 |
| vasculature development | 9 | 4.77 | 1.20E-04 |
| cardiovascular system development | 9 | 4.68 | 1.38E-04 |
| circulatory system development | 12 | 3.79 | 7.37E-05 |
| positive regulation of cell population proliferation | 12 | 3.58 | 1.25E-04 |
| cellular response to stress | 17 | 2.67 | 1.59E-04 |

**TABLE 4 |** Summary of $CO_2$ differential methylation analyses.

| Contrast | DM CpGs | Hypermethylated | Hypomethylated | Promoter hyper/hypo DMGs | Intragenic hyper/hypo DMGs |
|---|---|---|---|---|---|
| 0.4 vs. 0.1% | 3652 | 1951 | 1701 | 124/106 | 524/517 |
| 0.8 vs. 0.4% | 4695 | 2760 | 1935 | 165/156 | 744/514 |
| 0.8 vs. 0.1% | 4482 | 2782 | 1670 | 176/119 | 671/457 |

**TABLE 5 |** Enriched GO terms among $CO_2$ intragenic-DMGs related to heart/muscle development and hypoxic response.

| GO term | 0.4 vs. 0.1 $CO_2$ | | 0.8 vs. 0.4 $CO_2$ | | 0.8 vs. 0.1 $CO_2$ | |
|---|---|---|---|---|---|---|
| | Enr. | *P*-value | Enr. | *P*-value | Enr. | *P*-value |
| **Intragenic-hypermethylated genes** | | | | | | |
| positive regulation of striated muscle cell differentiation | 5.3 | 2.3E-04 | | | 4.7 | 2.5E-04 |
| positive regulation of striated muscle tissue development | 4.5 | 6.5E-04 | | | 4.0 | 7.6E-04 |
| positive regulation of muscle organ development | 4.5 | 6.5E-04 | | | 4.0 | 7.6E-04 |
| cardiac ventricle development | 3.5 | 5.1E-04 | | | 3.2 | 3.5E-04 |
| cardiac chamber development | 3.1 | 4.7E-04 | 2.7 | 5.9E-04 | 2.8 | 5.2E-04 |
| muscle organ development | | | 2.5 | 3.4E-05 | 2.6 | 2.9E-05 |
| muscle structure development | | | 2.2 | 1.6E-05 | 2.4 | 5.2E-06 |
| muscle tissue development | | | 2.1 | 9.7E-04 | | |
| heart development | | | 1.9 | 1.8E-04 | 2.0 | 1.3E-04 |
| cardiovascular system development | | | 2.6 | 5.3E-09 | 2.5 | 1.7E-07 |
| positive regulation of myotube differentiation | | | | | 5.6 | 1.2E-03 |
| positive regulation of striated muscle cell differentiation | | | | | 4.7 | 2.5E-04 |
| positive regulation of muscle cell differentiation | | | | | 4.3 | 5.7E-05 |
| muscle tissue morphogenesis | | | | | 3.9 | 4.4E-04 |
| positive regulation of muscle tissue development | | | | | 3.9 | 8.3E-04 |
| muscle organ morphogenesis | | | | | 3.6 | 8.0E-04 |
| cardiac chamber morphogenesis | | | | | 2.9 | 1.3E-03 |
| cardiac muscle tissue development | | | | | 2.7 | 1.2E-03 |
| **Intragenic-hypomethylated genes** | | | | | | |
| positive regulation of striated muscle tissue development | 4.7 | 5.1E-04 | | | | |
| positive regulation of muscle organ development | 4.7 | 5.1E-04 | | | | |
| mitral valve development | | | 18.4 | 2.8E-05 | | |
| heart valve formation | | | 13.5 | 4.8E-04 | | |
| pulmonary valve morphogenesis | | | 10.1 | 1.2E-03 | | |
| atrioventricular valve development | | | 8.4 | 5.8E-04 | | |
| aortic valve morphogenesis | | | 8.1 | 6.9E-04 | | |
| heart valve morphogenesis | | | 7.3 | 1.1E-05 | 6.5 | 2.0E-04 |
| aortic valve development | | | 7.2 | 1.1E-03 | | |
| cardiac atrium development | | | 7.2 | 3.6E-04 | | |
| semi-lunar valve development | | | 6.8 | 4.8E-04 | | |
| heart valve development | | | 6.5 | 2.5E-05 | 5.8 | 3.7E-04 |
| ventricular septum development | | | 5.3 | 1.1E-04 | | |
| cardiac septum development | | | 4.2 | 1.2E-04 | | |
| cardiac ventricle development | | | 3.6 | 4.3E-04 | | |
| cardiac muscle tissue development | | | 3.3 | 3.2E-04 | | |
| regulation of muscle tissue development | | | 3.3 | 9.4E-04 | | |
| cardiac chamber development | | | 3.2 | 3.9E-04 | | |
| heart morphogenesis | | | 2.7 | 6.0E-04 | 3.0 | 1.5E-04 |
| muscle tissue development | | | 2.4 | 1.2E-03 | | |
| muscle structure development | | | 2.3 | 2.5E-04 | | |
| heart development | | | 2.2 | 1.5E-04 | 2.2 | 6.1E-04 |
| cardiac chamber morphogenesis | | | | | 3.7 | 6.6E-04 |
| cardiovascular system development | | | | | 2.7 | 2.5E-06 |
| cellular response to oxidative stress | | | | | 2.7 | 1.0E-03 |
| response to hypoxia | | | | | 2.7 | 1.1E-04 |
| response to decreased oxygen levels | | | | | 2.6 | 1.7E-04 |
| response to oxygen levels | | | | | 2.4 | 5.5E-04 |

HW via RT-qPCR, to determine if differential methylation was associated with differences in gene expression. We detected quantifiable transcript abundance for all genes except *NGB*, which was undetectable in multiple samples in both EST treatments. Three genes – *ABLIM2*, *PITX2*, and *THRSP* – exhibited significant differences in transcript

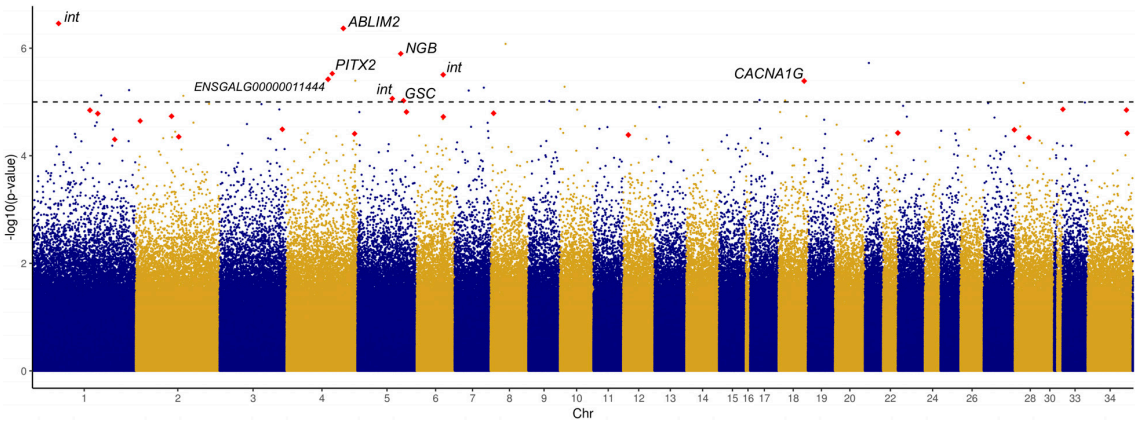



**FIGURE 3 |** Manhattan plot displaying –log10 *p*-values of association between CpG methylation rate and log2-transformed relative heart weight, ordered by chromosome. Red points indicate DM CpGs; significantly associated and DM CpGs are labeled with their corresponding gene ID (int, intergenic).

abundance between EST treatments (**Figure 4**). In all three cases, abundance was higher in the treatment with lower methylation. We observed significantly lower *THRSP* abundance in 38.9°C chicks ($p$ = 0.046), which is consistent with the promoter hypermethylation observed. Abundance of *PITX2*, which contained a hypomethylated CpG in its last exon, was significantly higher in 38.9°C chicks ($p$ = 7.59E-03). *ABLIM2*, containing a hypermethylated intronic CpG, exhibited lower abundance at 38.9°C ($p$ = 1.37E-03). Among the remaining five DMGs, the differences in expression were negatively associated with the differences in methylation for *DAG1*, while the differences were positively associated for *TBX1*, *TBX4*, and *GSC*. We also assessed transcript abundance in two genes that did not exhibit differential methylation (*MEAF6* and *SRRM1*), and did not detect differences in abundance between ESTs. These results have identified candidate genes exhibiting coordinated differences in methylation and expression in the developing chick heart that are associated with incubation EST.

## DISCUSSION

To the best of our knowledge, this study represents the largest epigenome-wide analysis in livestock species, the first EWAS in broiler chickens, and the first study assessing genome-wide DNA methylation between chickens incubated in different environments. RRBS was performed in cardiac tissue collected from broiler chicks in a study that recapitulated the established negative correlation between incubation EST and HW. We observed significantly lower HW in chicks incubated at 38.9 vs. 37.8°C, which was independent of differences in incubation length. The heart appears to be uniquely impacted by incubation EST, a finding that has been observed in numerous studies showing up to 30% lower HW in 38.9°C chicks with no significant differences in organs such as the liver, intestines or stomach (Molenaar et al., 2011; Maatjens et al., 2014, 2016; Nangsuay et al., 2016).

Using RRBS, we assessed methylation at over 3 million CpGs across 84 heart samples. Global methylation rates in these samples were low (13.8–20.4%), due to the fact that a majority of sites exhibited methylation rates less than 10%. RRBS reads are disproportionally derived from CpG dense regions of the genome, which are known to be less methylated than the genome at large (Meissner et al., 2008). However, RRBS data from eight pig tissues revealed an average methylation rate of 41% (Schachtschneider et al., 2011). Thus the low methylation observed in our data may be specific to the species, tissue, or stage of development. To date, whole-genome bisulfite sequencing studies in *G. gallus* and other avian species have reported global CpG methylation rates between 50 and 65% (Li et al., 2015; Derks et al., 2016; Lee et al., 2017; Zhang et al., 2017, 2018), which is lower than the 60–80% that has been reported in mammalian studies. It is possible that the low levels of CpG methylation detected in our data can be attributed to lower CpG methylation rates in avian genomes.

We identified thousands of DM CpGs between ESTs, and annotation of DMGs revealed an enrichment for general and heart-specific developmental processes. While promoter-DMGs were only significantly enriched for processes related to general development, many of these genes are known to be involved in heart development. Among these were two T-box transcription factors, *TBX1* and *TBX4*, that were promoter-hypomethylated at 38.9°C. *TBX1* has been shown to promote cell proliferation and inhibit differentiation of heart cells (Xu et al., 2004; Chen et al., 2009). *TBX4* has been shown to be expressed in the developing heart, and has been hypothesized to play a role in regulating tissue-specific gene expression (Krause et al., 2004). Also among promoter-DMGs were two genes involved in response to thyroid hormone (*THRA*, hypomethylated and *THRSP*, hypermethylated at 38.9°C), which has previously been hypothesized to mediate temperature-driven differences in heart growth. *THRA* is the major thyroid hormone receptor expressed in the heart (Gloss et al., 2001), and *THRA* mutations in zebrafish have been linked to defects in heart development (Marelli et al., 2017). *THRSP* is expressed in chicken cardiac tissue

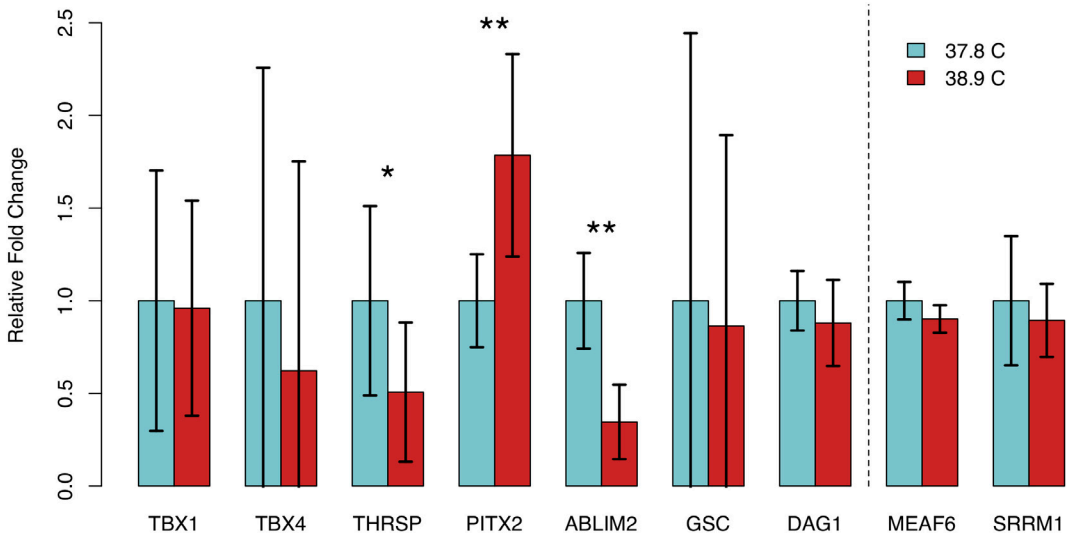



**FIGURE 4 |** Relative fold changes in transcript abundance (38.9°C relative to 37.8°C) for seven expressed genes exhibiting differential methylation and two stably methylated genes between temperature treatments. Error bars indicate standard deviation. *$p < 0.05$, **$p < 0.01$.

(Ren et al., 2017), and research has shown that overexpression of *THRSP* results in decreased levels of genes involved in heart development (Wellberg et al., 2014). Intragenic-DMGs were enriched for GO terms related to heart development. Among these, *DAG1* possessed hypo- and hypermethylated CpGs, and encodes a glycoprotein that has been shown to play an important role in the inhibition of cardiomyocyte proliferation in mice (Morikawa et al., 2017). *PITX2* contained an exonic CpG that was significantly hypomethylated at 38.9°C. This gene encodes a homeobox TF with roles in heart development that have been reviewed extensively (Franco et al., 2017); of note, it has been shown to promote cardiomyocyte proliferation in mice (Tao et al., 2016). *ERBB2* and *ERBB4* encode receptor kinases that have been shown to promote cardiomyocyte proliferation and survival (Zhao et al., 1998). The observed differential epigenetic regulation of genes involved in cardiomyocyte proliferation and differentiation may be contributing to observed differences in HW between chicks of different incubation ESTs.

Furthermore, assessment of enriched binding motifs among DM loci provides evidence that temperature-differential methylation is impacting the developmental trajectories of the chick heart. Methylation is known to reduce the binding potential of TFs by altering binding motif sequences (Yin et al., 2017) At 38.9°C, hypomethylated binding motifs – which would be predicted to be more accessible due to lower methylation levels – were enriched for TFs involved in positive regulation of cardiomyocyte proliferation. Conversely, the binding sites for TFs involved in negative regulation of cell proliferation – namely TFs in the ZBTB family – were the most enriched motifs among hypermethylated regions, which would be expected to be less accessible. The more favorable binding of pro-proliferation TFs in the cardiac methylome of chicks at higher temperatures suggests that observed differences in HW may be associated with differences in rates of differentiation and maturation.

We also identified thousands of DM CpGs between $CO_2$ treatments. Increasing $CO_2$ concentrations above 0.8% during late stages of incubation have benefits in commercial settings such as reduced hatching time variability (van Roovert-Reijrink, 2016). However, continuous incubation in a hypercapnic environment has been shown to increase ascites incidence later in life (Hassanzadeh et al., 2002). Not only did differential methylation at 0.8% $CO_2$ relative to the lower treatments disproportionately affect genes involved in heart development, but contrasting 0.8% with 0.1% $CO_2$ revealed differential methylation of genes that were enriched for hypoxia response GO terms. Such DMGs associated with hypoxia included: *ETS1*, a TF that has been shown to activate hypoxia-inducible genes (Salnikow et al., 2008); *SRC*, encoding a tyrosine kinase that is upregulated in rat cardiomyocytes by hypoxia to activate MAPK signaling pathways (Seko et al., 1996); and *DNM2*, encoding a GTPase and actin-binding protein that has been shown to be downregulated in cardiomyocytes subject to hypoxic conditions (Shi et al., 2014). Hypoxia-inducible genes being specifically overrepresented when comparing extremes for $CO_2$ indicate a cardiac response to differences in gas exchange via differences in gene regulation. Incubation $CO_2$ level was not associated with differences in HW in this study, which has been shown previously (Maatjens et al., 2014). However, $CO_2$ concentration may have observable effects on physiological processes that were not assessed here – including angiogenesis – that may contribute to adverse conditions later in life including increased ascites risk.

Our EWAS revealed a small but significant enrichment of association *p*-values between CpG methylation and HW, suggesting a relationship between gene regulation in the heart and its size at hatch. At the 23 significantly associated CpGs, epigenetic regulation of gene expression by DNA methylation may directly or indirectly affect heart growth. A DM CpG in an exon of *PITX2* was also the most significantly positively

correlated with HW. We identified additional significant CpGs in our EWAS that were also DM, albeit at a difference less than 10%. An intragenic CpG in *ABLIM2* was significantly hypermethylated at 38.9°C and negatively correlated with HW; this gene encodes a actin binding protein that has been shown to be highly expressed in striated muscle and is thought to regulate cytoskeletal signaling pathways (Barrientos et al., 2007). Additionally, an intergenic CpG in *NGB* was significantly hypomethylated and positively correlated with HW. The gene, encoding neuroglobin, was found to be differentially expressed in response to water temperature in Whiteleg shrimp (Wu et al., 2017). However, we did not detect NGB transcript abundance at appreciable levels in our samples, suggesting a limited role at this stage in chick heart development and temperature response. CpGs in these genes, along with those identified in other genes and in intergenic regions, are strong candidates for identifying epigenetic-mediated associations between temperature and heart development.

We identified coordinated changes in methylation and expression for three of the eight tested genes: *ABLIM2*, *PITX2*, and *THRSP*. In all three cases, direction of the difference in gene expression was opposite that of the difference in methylation between ESTs. This inverse relationship was expected at *THRSP*, since the DM CpG was immediately upstream of the TSS in the likely promoter region. Intragenic methylation in *ABLIM2* and *PITX2* were also negatively associated with expression, and this is in contrast to findings in other animal studies that the majority of CpGs in such regions are positively correlated with gene expression. Cases of intragenic methylation being negatively associated with gene expression have been reported by ENCODE (Varley et al., 2013), and they found these CpGs to be enriched in intragenic enhancers. The presence of CpGs in *ABLIM2* and *PITX2* at which methylation rate is inversely correlated with gene expression suggests that these CpGs may be located within gene regulatory elements. To explore this idea, we searched for binding motifs in the genomic regions flanking in DM CpGs in *ABLIM2* and *PITX2*. The *PITX2* DM regions had strong sequence similarity to the Kruppel Like Factor 5 (*KLF5*) binding motif, and this TF has been shown to be upregulated during heat stress in chickens previously (Sun et al., 2015). Additionally, the *ABLIM2* DM regions showed strong sequence similarity to the binding motif of Achaete-Scute Family BHLH Transcription Factor 2 (*ASCL2*), which is a known inhibitor of myogenic differentiation (Wang et al., 2017). While differential expression was not observed for five of the eight tested DMGs, this could be due in part to the limited number of samples that were assayed via qPCR ($n$ = 6/trt) relative to the number assayed via RRBS ($n$ = 42/trt).

Among these three DM and differentially expressed genes, *PITX2* has the most well-established role in heart development, specifically in promoting cardiomyocyte proliferation. In this study, increased EST was associated with both decreased methylation at an exonic CpG in *PITX2* as well as increased *PITX2* transcript abundance. As *PITX2* is known to promote cardiomyocyte proliferation, this suggests an increased proliferative capacity in the hearts of 38.9°C chicks. This conflicts with results reported in Romanoff, 1960, in which increased incubation temperature was associated with a reduced mitotic index from E8 to hatch. However, our results indicate that proliferation in high EST chicks may be increased relative to lower EST chicks as a partial compensatory mechanism immediately following hatch, and that developmental trajectories of hearts at different ESTs continue to be affected even after incubation.

In conclusion, this study has identified differential methylation patterns in the post-hatch chick heart associated with differences in incubation EST and $CO_2$ level, and such differences may be impacting heart growth and development through associated changes in TF binding and gene expression. Future studies should seek to further assess differences in methylation between incubation treatments at later stages of post-hatch life. Additionally, characterizing epigenetic patterns in additional organs responsible for regulating body temperature, including the hypothalamus and thyroid gland, may help in characterizing the mechanisms regulating temperature-driven differences in heart development. Knowledge of such epigenetic signatures influenced by early life environment may benefit animal breeding by serving as predictors of future animal performance.

## DATA AVAILABILITY STATEMENT

The RRBS data is available by the following SRA/ENA accession number PRJEB39999.

## ETHICS STATEMENT

The animal study was reviewed and approved by the Central Animal Experiments Committee (The Hague, Netherlands; approval no. 2016.W-0087).

## AUTHOR CONTRIBUTIONS

OM, MG, and RPC conceived of the study design. HB conducted the incubation study from which heart samples were collected. RJC performed all of the bioinformatics, differential methylation, GO enrichment analyses, as well as the EWAS, and wrote the manuscript. MP and CE contributed intellectually to the interpretation of results. All authors read and approved of the manuscript.

## FUNDING

This study was financially supported by the Dutch Ministry of Economic Affairs (TKI-Toeslag) and the Breed4Food partners Cobb Europe, CRV, Hendrix Genetics, and Topigs Norsvin. RJC was funded under a USDA NIFA NNF Training Grant (#2015-38420-23697). The authors declare that the funders Breed4Food partners Cobb Europe, CRV, Hendrix Genetics and Topigs Norsvin were not involved in the study design, collection, analysis, interpretation of data, the writing of this article or the decision to submit it for publication.

## ACKNOWLEDGMENTS

We thank the Breed4Food EWAS committee for useful discussion during the project and Bert Dibbits for technical laboratory support.

## SUPPLEMENTARY MATERIAL

The Supplementary Material for this article can be found online at: https://www.frontiersin.org/articles/10.3389/fgene.2020.558189/full#supplementary-material

## REFERENCES

Akalin, A., Franke, V., Vlahovíček, K., Mason, C. E., and Schübeler, D. (2015). Genomation: a toolkit to summarize, annotate and visualize genomic intervals. *Bioinformatics* 31, 1127–1129. doi: 10.1093/bioinformatics/btu775

Akalin, A., Kormaksson, M., Li, S., Garrett-Bakelman, F. E., Figueroa, M. E., Melnick, A., et al. (2012). MethylKit: a comprehensive R package for the analysis of genome-wide DNA methylation profiles. *Genome Biol.* 13:R87. doi: 10.1186/gb-2012-13-10-R87

Bailey, T. L., Boden, M., Buske, F. A., Frith, M., Grant, C. E., Clementi, L., et al. (2009). MEME SUITE: tools for motif discovery and searching. *Nucleic Acids Res.* 37, W202–W208. doi: 10.1093/nar/gkp335

Ball, M. P., Li, J. B., Gao, Y., Lee, J.-H., Leproust, E., Park, I.-H., et al. (2009). Targeted and genome-scale methylomics reveals gene body signatures in human cell lines HHS Public access author manuscript. *Nat. Biotechnol.* 27, 361–368. doi: 10.1038/nbt.1533

Barrientos, T., Frank, D., Kuwahara, K., Bezprozvannaya, S., Pipes, G. C. T., Bassel-Duby, R., et al. (2007). Two novel members of the ABLIM protein family, ABLIM-2 and -3, associate with STARS and directly bind F-actin. *J. Biol. Chem.* 282, 8393–8403. doi: 10.1074/jbc.M607549200

Bird, A. P., and Wolffe, A. P. (1999). Methylation-induced repression-belts, braces, and chromatin. *Cell* 99, 451–454. doi: 10.1016/S0092-8674(00)81532-81539

Buys, N., Dewil, E., Gonzales, E., and Decuypere, E. (1998). Avian pathology different CO2 levels during incubation interact with hatching time and ascites susceptibility in two broiler lines selected for different growth rate. *Avian. Pathol.* 27, 605–612. doi: 10.1080/03079459808419391

Chen, L., Fulcoli, F. G., Tang, S., and Baldini, A. (2009). Tbx1 regulates proliferation and differentiation of multipotent heart progenitors. *Circ. Res.* 105, 842–851. doi: 10.1161/CIRCRESAHA.109.200295

Christensen, V. L., Donaldson, W. E., and Nestor, K. E. (1999). Length of the plateau and pipping stages of incubation affects the physiology and survival of turkeys. *Br. Poult. Sci.* 40, 297–303. doi: 10.1080/00071669987737

David, S.-A., Vitorino Carvalho, A., Gimonnet, C., Brionne, A., Hennequet-Antier, C., Piégu, B., et al. (2019). Thermal manipulation during embryogenesis impacts H3K4me3 and H3K27me3 histone marks in chicken hypothalamus. *Front. Genet.* 10:1207. doi: 10.3389/fgene.2019.01207

Derks, M. F. L., Schachtschneider, K. M., Madsen, O., Schijlen, E., Verhoeven, K. J. F., and van Oers, K. (2016). Gene and transposable element methylation in great tit (Parus major) brain and blood. *BMC Genomics* 17:332. doi: 10.1186/s12864-016-2653-y

Engelmann, G. L., Boehm, K. D., Birchenall-Roberts, M. C., and Ruscetti, F. W. (1992). Transforming growth factor-beta1 in heart development. *Mech. Dev.* 38, 85–97. doi: 10.1016/0925-4773(92)90001-Z

Flanagan, J. M. (2015). Epigenome-wide association studies (EWAS): past, present, and future. *Methods Mol. Biol.* 1238, 51–63. doi: 10.1007/978-1-4939-1804-1_3

Franco, D., Sedmera, D., and Lozano-Velasco, E. (2017). Multiple roles of Pitx2 in cardiac development and disease. *J. Cardiovasc. Dev. Dis.* 4:16. doi: 10.3390/jcdd4040016

French, N. A. (1994). Effect of incubation temperature on the gross pathology of turkey embryos. *Br. Poult. Sci.* 35, 363–371. doi: 10.1080/00071669408417701

Gloss, B., Trost, S. U., Bluhm, W. F., Swanson, E. A., Clark, R., Winkfein, R., et al. (2001). Cardiac ion channel expression and contractile function in mice with deletion of thyroid hormone receptor α or β**This work was supported by grant HL-25022 (to W.H.D.) and by operating grants from the Canadian medical research council and the heart and stroke foundation of Canada (to W.G. and R.C.). *Endocrinology* 142, 544–550. doi: 10.1210/endo.142.2.7935

Greenberg, M. V. C., and Bourc'his, D. (2019). The diverse roles of DNA methylation in mammalian development and disease. *Nat. Rev. Mol. Cell Biol.* 20, 590–607. doi: 10.1038/s41580-019-0159-156

Guo, W., Fiziev, P., Yan, W., Cokus, S., Sun, X., Zhang, M. Q., et al. (2013). BS-Seeker2: a versatile aligning pipeline for bisulfite sequencing data. *BMC Genomics* 14:774. doi: 10.1186/1471-2164-14-774

Guo, W., Zhu, P., Pellegrini, M., Zhang, M. Q., Wang, X., and Ni, Z. (2018). CGmapTools improves the precision of heterozygous SNV calls and supports allele-specific methylation detection and visualization in bisulfite-sequencing data. *Bioinformatics* 34, 381–387. doi: 10.1093/bioinformatics/btx595

Hannigan, G. E., Coles, J. G., and Dedhar, S. (2007). Integrin-linked kinase at the heart of cardiac contractility. *Repair Dis. Circ. Res.* 100, 1408–1414. doi: 10.1161/01.RES.0000265233.40455.62

Hao, Y., Cui, Y., and Gu, X. (2016). Genome-wide DNA methylation profiles changes associated with constant heat stress in pigs as measured by bisulfite sequencing. *Sci. Rep.* 6:27507. doi: 10.1038/srep27507

Hassanpour, H., Bahadoran, S., Farhadfar, F., Fallahi Chamali, Z., Nazari, H., and Kaewduangta, W. (2018). Identification of reliable reference genes for quantitative real-time PCR in lung and heart of pulmonary hypertensive chickens. *Poult. Sci.* 97, 4048–4056. doi: 10.3382/ps/pey258

Hassanzadeh, M., Buyse, J., and Decuypere, E. (2002). Further evidence for the involvement of cardiac β-adrenergic receptors in right ventricle hypertrophy and ascites in broiler chickens. *Avian. Pathol.* 31, 177–181. doi: 10.1080/03079450120118676

Hassanzadeh, M., Maddadi, M. S., Mirzaie, S., Assasie, K., and Moayyedian, H. (2010). Partial pressure of carbon dioxide in the venous blood of young birds as a predictor of ascites susceptibility in broiler chickens. *Acta Vet. Hung.* 58, 221–230. doi: 10.1556/AVet.58.2010.2.8

Ibeagha-Awemu, E. M., and Zhao, X. (2015). Epigenetic marks: regulators of livestock phenotypes and conceivable sources of missing variation in livestock improvement programs. *Front. Genet.* 6:302. doi: 10.3389/fgene.2015.00302

Jaenisch, R., and Bird, A. (2003). Epigenetic regulation of gene expression: how the genome integrates intrinsic and environmental signals. *Nat. Genet.* 33, 245–254. doi: 10.1038/ng1089

Jeon, B. N., Kim, M. K., Yoon, J. H., Kim, M. Y., An, H., Noh, H. J., et al. (2014). Two ZNF509 (ZBTB49) isoforms induce cell-cycle arrest by activating transcription of p21/CDKN1A and RB upon exposure to genotoxic stress. *Nucleic Acids Res.* 42, 11447–11461. doi: 10.1093/nar/gku857

Krause, A., Zacharias, W., Camarata, T., Linkhart, B., Law, E., Lischke, A., et al. (2004). Tbx5 and Tbx4 transcription factors interact with a new chicken PDZ-LIM protein in limb and heart development. *Dev. Biol.* 273, 106–120. doi: 10.1016/J.YDBIO.2004.05.024

Krcmery, J., Gupta, R., Sadleir, R. W., Ahrens, M. J., and Misener, S. (2013). Loss of the cytoskeletal protein pdlim7 predisposes mice to heart defects and hemostatic dysfunction. *PLoS One* 8:80809. doi: 10.1371/journal.pone.0080809

Kühn, E. R., Decuypere, E., Colen, L. M., Chadwick, A., Heyns, W., and Michels, H. (1984). "59 Orcadian rhythm of Corticosterone, Prolactin and thyroid hormones in serum and endocrine glands of post-hatch chicks, incubated at different temperatures," in *Proceeding of the 15th International Conference of the International Society for Chronobiology 1982-1983*, Minneapolis, MI.

Lee, I., Rasoul, B. A., Holub, A. S., Lejeune, A., Enke, R. A., and Timp, W. (2017). Whole genome DNA methylation sequencing of the chicken retina, cornea and brain. *Sci. Data* 4:170148. doi: 10.1038/sdata.2017.148

Leksrisompong, N., Romero-Sanchez, H., Plumstead, P. W., Brannan, K. E., and Brake, J. (2007). Broiler Incubation. 1. Effect of elevated temperature during late incubation on body weight and organs of chicks. *Poult. Sci.* 86, 2685–2691. doi: 10.3382/ps.2007-2170

Li, J., Li, R., Wang, Y., Hu, X., Zhao, Y., Li, L., et al. (2015). Genome-wide DNA methylome variation in two genetically distinct chicken lines using MethylC-seq. *BMC Genom.* 16:851. doi: 10.1186/s12864-015-2098-2098

Liu, X. S., Haines, J. E., Mehanna, E. K., Genet, M. D., Ben-Sahra, I., Asara, J. M., et al. (2014). ZBTB7A acts as a tumor suppressor through the transcriptional

repression of glycolysis. *Genes Dev.* 28, 1917–1928. doi: 10.1101/gad.245910.114

Lorincz, M. C., Dickerson, D. R., Schmitt, M., and Groudine, M. (2004). Intragenic DNA methylation alters chromatin structure and elongation efficiency in mammalian cells. *Nat. Struct. Mol. Biol.* 11, 1068–1075. doi: 10.1038/nsmb840

Lourens, A., van den Brand, H., Meijerhof, R., and Kemp, B. (2005). Effect of eggshell temperature during incubation on embryo development, hatchability, and posthatch development. *Poult. Sci.* 84, 914–920. doi: 10.1093/ps/84.6.914

Lu, F., Langenbacher, A., and Chen, J. N. (2017). Tbx20 drives cardiac progenitor formation and cardiomyocyte proliferation in zebrafish. *Dev. Biol.* 421, 139–148. doi: 10.1016/j.ydbio.2016.12.009

Maatjens, C. M., Reijrink, I. A. M., Molenaar, R., van der Pol, C. W., Kemp, B., and van den Brand, H. (2014). Temperature and $CO_2$ during the hatching phase. I. Effects on chick quality and organ development. *Poult. Sci.* 93, 645–654. doi: 10.3382/ps.2013-03490

Maatjens, C. M., Van Roovert-Reijrink, I. A. M., Engel, B., Van Der Pol, C. W., Kemp, B., and Van Den Brand, H. (2016). Temperature during the last week of incubation. I. Effects on hatching pattern and broiler chicken embryonic organ development. *Poult. Sci.* 95, 956–965. doi: 10.3382/ps/pev447

Marelli, F., Carra, S., Rurale, G., Cotelli, F., and Persani, L. (2017). In vivo functional consequences of human THRA variants expressed in the Zebrafish. *Thyroid* 27, 279–291. doi: 10.1089/thy.2016.0373

Maunakea, A. K., Nagarajan, R. P., Bilenky, M., Ballinger, T. J., Dsouza, C., Fouse, S. D., et al. (2010). Conserved role of intragenic DNA methylation in regulating alternative promoters. *Nature* 466, 253–257. doi: 10.1038/nature09165

McLeay, R. C., and Bailey, T. L. (2010). Motif enrichment analysis: a unified framework and an evaluation on ChIP data. *BMC Bioinform.* 11:165. doi: 10.1186/1471-2105-11-165

Meissner, A., Mikkelsen, T. S., Gu, H., Wernig, M., Hanna, J., Sivachenko, A., et al. (2008). Genome-scale DNA methylation maps of pluripotent and differentiated cells. *Nature* 454, 766–770. doi: 10.1038/nature07107

Molenaar, R., Hulet, R., Meijerhof, R., Maatjens, C. M., Kemp, B., and van den Brand, H. (2011). High eggshell temperatures during incubation decrease growth performance and increase the incidence of ascites in broiler chickens. *Poult. Sci.* 90, 624–632. doi: 10.3382/ps.2010-2970

Molenaar, R., Meijerhof, R., van den Anker, I., Heetkamp, M. J. W., van den Borne, J. J. G. C., Kemp, B., et al. (2010). Effect of eggshell temperature and oxygen concentration on survival rate and nutrient utilization in chicken embryos. *Poult. Sci.* 89, 2010–2021. doi: 10.3382/ps.2010-2787

Morikawa, Y., Heallen, T., Leach, J., Xiao, Y., and Martin, J. F. (2017). Dystrophin glycoprotein complex sequesters yap to inhibit cardiomyocyte proliferation HHS public access. *Nature* 547, 227–231. doi: 10.1038/nature22979

Nangsuay, A., Meijerhof, R., Van Den Anker, I., Heetkamp, M. J. W., Morita, V. D. S., Kemp, B., et al. (2016). Effects of breeder age, broiler strain, and eggshell temperature on development and physiological status of embryos and hatchlings. *Poult. Sci.* 95, 1666–1679. doi: 10.3382/ps/pew080

Nichelmann, M. (2004). Perinatal epigenetic temperature adaptation in avian species: comparison of turkey and Muscovy duck. *J. Therm. Biol.* 29, 613–619. doi: 10.1016/j.jtherbio.2004.08.032

Orozco, L. D., Morselli, M., Rubbi, L., Guo, W., Go, J., Shi, H., et al. (2015). Epigenome-wide association of liver methylation patterns and complex metabolic traits in mice. *Cell Metab.* 21, 905–917. doi: 10.1016/j.cmet.2015.04.025

Ren, J., Xu, N., Zheng, H., Tian, W., Li, H., Li, Z., et al. (2017). Expression of thyroid hormone responsive SPOT 14 gene is regulated by estrogen in chicken (*Gallus gallus*). *Sci. Rep.* 7:10243. doi: 10.1038/s41598-017-08452-8456

Ricklefs, R. E. (1987). Comparative analysis of avian embryonic growth. *J. Exp. Zool. Suppl. Publ.* 1, 309–323.

Romanoff, A. L. (1960). *The Avian Embryo: Structure and Functional Development*. New York, NY: Macmillan.

Salnikow, K., Aprelikova, O., Ivanov, S., Tackett, S., Kaczmarek, M., Karaczyn, A., et al. (2008). Regulation of hypoxia-inducible genes by ETS1 transcription factor. *Carcinogenesis* 29, 1493–1499. doi: 10.1093/carcin/bgn088

Schachtschneider, K. M., Madsen, O., Park, C., Rund, L. A., Groenen, M. A. M., and Schook, L. B. (2011). Adult porcine genome-wide DNA methylation patterns support pigs as a biomedical model. *BMC Genom.* 16:743. doi: 10.1186/s12864-015-1938-x

Seko, Y., Tobe, K., Takahashi, N., Kaburagi, Y., Kadowaki, T., and Yazaki, Y. (1996). Hypoxia and hypoxia/reoxygenation activate Src family tyrosine kinases and p21(ras) in cultured rat cardiac myocytes. *Biochem. Biophys. Res. Commun.* 226, 530–535. doi: 10.1006/bbrc.1996.1389

Shi, D., Xie, D., Zhang, H., Zhao, H., Huang, J., Li, C., et al. (2014). Reduction in dynamin-2 is implicated in ischaemic cardiac arrhythmias. *J. Cell. Mol. Med.* 18, 1992–1999. doi: 10.1111/jcmm.12335

Skibiel, A. L., Peñagaricano, F., Amorín, R., Ahmed, B. M., Dahl, G. E., and Laporta, J. (2018). In utero heat stress alters the offspring epigenome. *Sci. Rep.* 8:14609. doi: 10.1038/s41598-018-32975-1

Sözcü, A., and Ipek, A. (2015). Acute and chronic eggshell temperature manipulations during hatching term influence hatchability, broiler performance, and ascites incidence. *Poult. Sci.* 94, 319–327. doi: 10.3382/ps/peu080

Sun, L., Lamont, S. J., Cooksey, A. M., McCarthy, F., Tudor, C. O., Vijay-Shanker, K., et al. (2015). Transcriptome response to heat stress in a chicken hepatocellular carcinoma cell line. *Cell Stress Chaper.* 20, 939–950. doi: 10.1007/s12192-015-0621-620

Tao, G., Kahr, P. C., Morikawa, Y., Zhang, M., Rahmani, M., Heallen, T. R., et al. (2016). Pitx2 promotes heart repair by activating the antioxidant response after cardiac injury. *Nature* 534, 119–123. doi: 10.1038/nature17959

Thomas, P. D., Campbell, M. J., Kejariwal, A., Mi, H., Karlak, B., Daverman, R., et al. (2003). PANTHER: a library of protein families and subfamilies indexed by function. *Genome Res.* 13, 2129–2141. doi: 10.1101/GR.772403

Thomas, P. D., Kejariwal, A., Guo, N., Mi, H., Campbell, M. J., Muruganujan, A., et al. (2006). Applications for protein sequence-function evolution data: mRNA/protein expression analysis and coding SNP scoring tools. *Nucleic Acids Res.* 34, W645–W650. doi: 10.1093/nar/gkl229

Tzschentke, B., and Basta, D. (2002). Early development of neuronal hypothalamic thermosensitivity in birds: influence of epigenetic temperature adaptation. *Comp. Biochem. Physiol. Part A Mol. Integr. Physiol.* 131, 825–832. doi: 10.1016/S1095-6433(02)00020-X

van Roovert-Reijrink, I. (2016). *Incubation Affects Chick Quality*. Available online at: https://www.poultryworld.net/Genetics/Articles/2013/5/Incubation-affects-chick-quality-1183725W/ (accessed April 20, 2019).

Varley, K. E., Gertz, J., Bowling, K. M., Parker, S. L., Reddy, T. E., Pauli-Behn, F., et al. (2013). Dynamic DNA methylation across diverse human cell lines and tissues. *Genome Res.* 23, 555–567. doi: 10.1101/gr.147942.112

Vinoth, A., Thirunalasundari, T., Shanmugam, M., Uthrakumar, A., Suji, S., and Rajkumar, U. (2018). Evaluation of DNA methylation and mRNA expression of heat shock proteins in thermal manipulated chicken. *Cell Stress Chaper.* 23, 235–252. doi: 10.1007/s12192-017-0837-832

Wang, C., Wang, M., Arrington, J., Shan, T., Yue, F., Nie, Y., et al. (2017). Ascl2 inhibits myogenesis by antagonizing the transcriptional activity of myogenic regulatory factors. *Development* 144, 235–247. doi: 10.1242/dev.138099

Wellberg, E. A., Rudolph, M. C., Lewis, A. S., Padilla-Just, N., Jedlicka, P., and Anderson, S. M. (2014). Modulation of tumor fatty acids, through overexpression or loss of thyroid hormone responsive protein spot 14 is associated with altered growth and metastasis. *Breast Cancer Res.* 16:481. doi: 10.1186/s13058-014-0481-z

Wu, M., Chen, N., Huang, C. X., He, Y., Zhao, Y. Z., Chen, X. H., et al. (2017). Effect of low temperature on globin expression, respiratory metabolic enzyme activities, and gill structure of *Litopenaeus vannamei*. *Biochemistry* 82, 844–851. doi: 10.1134/S0006297917070100

Xavier-Neto, J., Sousa Costa, ÂM., Carolina, A., Figueira, M., Donato, C. C., and Neves Do Amaral, F. (2015). Signalling through retinoic acid receptors in cardiac development: doing the right things at the right times HHS public access author manuscript. *Biochim. Biophys. Acta* 1849, 94–111. doi: 10.1016/j.bbagrm.2014.08.003

Xu, H., Morishima, M., Wylie, J. N., Schwartz, R. J., Bruneau, B. G., Lindsay, E. A., et al. (2004). Tbx1 has a dual role in the morphogenesis of the cardiac outflow tract. *Development* 131, 3217–3227. doi: 10.1242/dev.01174

Yahav, S., and Hurwitz, S. (1996). Induction of thermotolerance in male broiler chickens by temperature conditioning at an early age. *Poult. Sci.* 75, 402–406. doi: 10.3382/ps.0750402

Yahav, S., Straschnow, A., Plavnik, I., and Hurwitz, S. (1996). Effects of diurnally cycling versus constant temperatures on chicken growth and food intake. *Br. Poult. Sci.* 37, 43–54. doi: 10.1080/00071669608417835

Ye, B., Li, L., Xu, H., Chen, Y., and Li, F. (2019). Opposing roles of TCF7/LEF1 and TCF7L2 in cyclin D2 and Bmp4 expression and cardiomyocyte cell cycle control during late heart development. *Lab. Investig.* 99, 807–818. doi: 10.1038/s41374-019-0204-202

Yin, Y., Morgunova, E., Jolma, A., Kaasinen, E., Sahu, B., Khund-Sayeed, S., et al. (2017). Impact of cytosine methylation on DNA binding specificities of human transcription factors. *Science* 356:eaaj2239. doi: 10.1126/science.aaj2239

Zhang, M., Yan, F.-B., Li, F., Jiang, K.-R., Li, D.-H., Han, R.-L., et al. (2017). Genome-wide DNA methylation profiles reveal novel candidate genes associated with meat quality at different age stages in hens. *Sci. Rep.* 7:45564. doi: 10.1038/srep45564

Zhang, Z., Du, H., Bai, L., Yang, C., Li, Q., Li, X., et al. (2018). Whole genome bisulfite sequencing reveals unique adaptations to high-altitude environments in Tibetan chickens. *PLoS One* 13:e0193597. doi: 10.1371/journal.pone.0193597

Zhao, P., and Hoffman, E. P. (2006). Musculin isoforms and repression of MyoD in muscle regeneration. *Biochem. Biophys. Res. Commun.* 342, 835–842. doi: 10.1016/j.bbrc.2006.01.188

Zhao, Y. Y., Sawyer, D. R., Baliga, R. R., Opel, D. J., Han, X., Marchionni, M. A., et al. (1998). Neuregulins promote survival and growth of cardiac myocytes: persistence of ErbB2 and ErbB4 expression in neonatal and adult ventricular myocytes. *J. Biol. Chem.* 273, 10261–10269. doi: 10.1074/jbc.273.17.10261

Ziller, M. J., Mü Ller, F., Liao, J., Zhang, Y., and Gu, H. (2011). Genomic distribution and inter-sample variation of Non-CpG methylation across human cell types. *PLoS Genet.* 7:1002389. doi: 10.1371/journal.pgen.1002389

**Conflict of Interest:** The authors declare that the research was conducted in the absence of any commercial or financial relationships that could be construed as a potential conflict of interest.

*Copyright © 2020 Corbett, te Pas, van den Brand, Groenen, Crooijmans, Ernst and Madsen. This is an open-access article distributed under the terms of the Creative Commons Attribution License (CC BY). The use, distribution or reproduction in other forums is permitted, provided the original author(s) and the copyright owner(s) are credited and that the original publication in this journal is cited, in accordance with accepted academic practice. No use, distribution or reproduction is permitted which does not comply with these terms.*

frontiers in Genetics

ORIGINAL RESEARCH
published: 02 November 2020
doi: 10.3389/fgene.2020.508809

# Putative Epigenetic Biomarkers of Stress in Red Blood Cells of Chickens Reared Across Different Biomes

*Fábio Pértille[1,2]*, Adriana Mercia Guaratini Ibelli[3], Maj El Sharif[2], Mirele Daiana Poleti[4], Anna Sophie Fröhlich[2], Shiva Rezaei[2], Mônica Corrêa Ledur[3], Per Jensen[2], Carlos Guerrero-Bosagna[2,5]*† and Luiz Lehmann Coutinho[1]*†*

[1] Animal Biotechnology Laboratory, Animal Science and Pastures Department, University of São Paulo (USP)/"Luiz de Queiroz" College of Agriculture (ESALQ), Piracicaba, Brazil, [2] Avian Behavioural Genomics and Physiology Group, IFM Biology, Linköping University, Linköping, Sweden, [3] Embrapa Suínos e Aves, Concórdia, Brazil, [4] Animal Science Program, Faculty of Animal Science and Food Engineering (FZEA), University of São Paulo (USP), Pirassununga, Brazil, [5] Evolutionary Biology Centre, Department of Organismal Biology, Uppsala University, Uppsala, Sweden

Production animals are constantly subjected to early adverse environmental conditions that influence the adult phenotype and produce epigenetic effects. CpG dinucleotide methylation in red blood cells (RBC) could be a useful epigenetic biomarker to identify animals subjected to chronic stress in the production environment. Here we compared a reduced fraction of the RBC methylome of chickens exposed to social isolation to non-exposed. These experiments were performed in two different locations: Brazil and Sweden. The aim was to identify stress-associated DNA methylation profiles in RBC across these populations, in spite of the variable conditions to which birds are exposed in each facility and their different lineages. Birds were increasingly exposed to a social isolation treatment, combined with food and water deprivation, at random periods of the day from weeks 1–4 after hatching. We then collected the RBC DNA from individuals and compared a reduced fraction of their methylome between the experimental groups using two bioinformatic approaches to identify differentially methylated regions (DMRs): one using fixed-size windows and another that preselected differential peaks with MACS2. Three levels of significance were used ($P \leq 0.05$, $P \leq 0.005$, and $P \leq 0.0005$) to identify DMRs between experimental groups, which were then used for different analyses. With both of the approaches more DMRs reached the defined significance thresholds in BR individuals compared to SW. However, more DMRs had higher fold change values in SW compared to BR individuals. Interestingly, ChrZ was enriched above expectancy for the presence of DMRs. Additionally, when analyzing the locations of these DMRs in relation to the transcription starting site (TSS), we found three peaks with high DMR presence: 10 kb upstream, the TSS itself, and 20–40 kb downstream. Interestingly, these peaks had DMRs with a high presence (>50%) of specific transcription factor binding sites. Three overlapping DMRs were found between the BR and SW population using the most relaxed *p*-value ($P \leq 0.05$). With the

OPEN ACCESS

**Edited by:**
Stephanie McKay,
The University of Vermont,
United States

**Reviewed by:**
Brittney Keel,
U.S. Meat Animal Research Center,
Agricultural Research Service,
United States Department
of Agriculture, United States
Alex Clop,
Centre for Research in Agricultural
Genomics (CRAG), Spain
Xiao Wang,
Technical University of Denmark,
Denmark

***Correspondence:**
Fábio Pértille
fabiopertille@gmail.com
Carlos Guerrero-Bosagna
carlos.guerrero.bosagna@liu.se
Luiz Lehmann Coutinho
llcoutinho@usp.br

† These authors have contributed equally to this work

**Specialty section:**
This article was submitted to
Livestock Genomics,
a section of the journal
Frontiers in Genetics

**Received:** 31 October 2019
**Accepted:** 11 September 2020
**Published:** 02 November 2020

**Citation:**
Pértille F, Ibelli AMG, Sharif ME, Poleti MD, Fröhlich AS, Rezaei S, Ledur MC, Jensen P, Guerrero-Bosagna C and Coutinho LL (2020) Putative Epigenetic Biomarkers of Stress in Red Blood Cells of Chickens Reared Across Different Biomes. Front. Genet. 11:508809. doi: 10.3389/fgene.2020.508809

most stringent *p*-value ($P \leq 0.0005$), we found 7 and 4 DMRs between treatments in the BR and SW populations, respectively. This study is the first approximation to identify epigenetic biomarkers of long-term exposure to stress in different lineages of production animals.

**Keywords: stress, red blood cells, epigenetics, chicken, DNA methylation, animal welfare**

## INTRODUCTION

External influences affecting early life stages (pre- and post-birth) of animals can have enormous consequences on their adult phenotypes (Guerrero-Bosagna and Skinner, 2012). Several environmental factors are reported to affect early development, including environmental chemical compounds, endocrine disrupters (Susiarjo et al., 2013), inorganic chemicals (Kile et al., 2014), nutritional components (Dolinoy et al., 2007; Guerrero-Bosagna et al., 2008), or stress conditions (Fagiolini et al., 2009). Notably, epigenetic processes are substantially affected during early exposures to each of these factors (Guerrero-Bosagna and Skinner, 2012).

Epigenetics is the study of molecules that bind to DNA and can maintain this interaction in a mitotically stable manner (Skinner et al., 2010). Epigenetic modifications can regulate gene expression and are fundamental for all cellular processes. Epigenetic research has permeated several fields of biological research, from molecular to evolutionary biology (Richard and Stein, 2012). However, despite the importance of epigenetic mechanisms in biology in general, epigenetic studies in production animals are incipient, with some studies performed in chickens (Pértille et al., 2017a, 2019; Bélteky et al., 2018; Guerrero-Bosagna et al., 2020), in cattle (Su et al., 2014; Fang et al., 2017; Zhou et al., 2018; Sevane et al., 2019), in sheep (Cao et al., 2017; Capra et al., 2017; Zhang X. et al., 2017; Zhang Y. et al., 2017), and pigs (Gao et al., 2014; Choi et al., 2015; Yuan et al., 2017; Wang and Kadarmideen, 2019, 2020). Among production animals, chickens have recently emerged as a promising model for epigenetic studies (Frésard et al., 2013) following their historical use as a model for translational research with implications for human health and physiology (Kain et al., 2014).

Chickens are livestock animals of great zootechnical interest that are subjected to constant challenges in their production environment. These challenges include extreme temperatures, social disruption, unfamiliar sounds, unfamiliar or uncaring handlers, feed and water restriction injection with antigens, and diseases (Zulkifli, 2013). These exposures cause stress responses involving an initial homeostatic imbalance followed by physiological and behavioral responses (Zulkifli, 2013). Stress leads to immunodepression, reduced performance, and increased susceptibility to diseases (Eberhart and Washburn, 1993; Goerlich et al., 2012). Losses in poultry production are generated by some noticeable phenotypes such as carcass injury and dermatitis (Meluzzi et al., 2008) (which relate to poor rearing conditions) and to other phenotypes that are harder to notice, such as reduction in meat quality (Sandercock et al., 2001). Therefore, poor handling in production animals is an issue concerning not only animal welfare, but also meat quality and human nutrition. Consequently, it is of utmost importance to develop effective and cost-efficient tools to trace prolonged stress caused by poor practices in animal production.

By knowing the physiological and molecular mechanisms behind stress response in animals, it is possible to develop tools for its diagnosis. For example, under stress, alterations in the HPA axis activity result in elevated levels of glucocorticoids (Fallahsharoudi et al., 2015). Consequently, hormonal responses are produced such as changes in testosterone, noradrenaline, adrenaline, prolactin, adrenocorticotrophic hormone, and cortisol (Henry, 1993). Based on this plethora of hormonal changes, stress in animals is usually determined by hormone levels such as cortisol and epinephrine (Ishibashi et al., 2013; Müller et al., 2013). However, the release of stress hormones may show an acute physiological response but may not reflect a prolonged exposure to stress conditions (Henry, 1993). Recently, hair cortisol has been used as a long-term stress indicator (Heimbürge et al., 2019). In addition, salivary cortisol concentrations have also been used as a long-term stress indicator in horses (Peeters et al., 2011). Researchers have also begun to use corticosteroid metabolites in feathers, hair, or feces as a non-invasive metric of prolonged stress in different species (Berk et al., 2016). However, these authors report that procedures measuring hormones are laborious, the interpretation of the results is difficult, and the methods still need to be validated (Berk et al., 2016). Therefore, a major challenge still lies in determining the history of an organism's exposure to stress for prolonged periods. Epigenetic marks in peripheral cells may serve as epigenetic biomarkers of stress history (Provencal et al., 2012; Wang et al., 2012) because in animals constantly subjected to stress it is expected that related hormonal plasmatic changes will leave an epigenomic mark in different cells, including blood cells.

One traceable epigenetic biomarker is the DNA methylation of cytosines in CpG dinucleotides (Feil and Fraga, 2012; Denham et al., 2016). We have recently reported DNA methylation differences in RBC of chickens reared in cages compared to conventional shed systems (Pértille et al., 2017a). However,

**Abbreviations:** ADAMTSL5, thrombospondin type-1 domain-containing protein 6; ADJW, adjacent windows; BR, Brazil; SW, Sweden; C, control animals; CEUA, Ethics Committee on Animal Utilization; CNPq, National Council for Scientific and Technological Development; CONCEA, National Council for the Control of Animal Experimentation; CP, crude protein; DMRs, differentially methylated regions; EMBRAPA, Brazilian Agricultural Research Corporation; FAPESP, São Paulo Research Foundation; FORMAS, Swedish Research Council for Sustainable Development; GBS, genotyping by sequencing; HPA, hypothalamic-pituitary-adrenal; IGF2R, insulin-like growth factor 2; Iset1, input set 1; Iset2, input set 2; MACS2, model-based analysis of ChIP-Seq data version 2; ME, metabolizable energy; MeDIP, methylated DNA immunoprecipitation; minRowSum, minimum sum of counts; mnMAF, minimum minor allele frequency; mnScov, minimum site coverage; mnTCov, minimum taxon/sample coverage; RBC, red blood cells; ROI, regions of interest; S, social isolation treatment; SP, São Paulo; TFBS, transcription factor binding site; THOP, thimet oligopeptidase 1; TMM, trimmed mean of M values; VEP, variant effect predictor.

in this proof-of-concept study we lacked the knowledge of which of these conditions was most stressful for the animals. The broad interest in RBC is due to the fact that they are easily purified and nucleated in birds. This allows us to easily extract DNA specifically from this cell type to study epigenetic changes without multiple cell bias and without producing major stress to the animal. In addition, other features of RBC have been investigated in relation to the physiological condition of organisms, including humans. For example, changes in RBC shape (Mueller et al., 2006) and distribution (Xanthopoulos et al., 2017) have been associated with several coronary, heart, and other systemic diseases in humans. Deformability of RBC is an essential feature of its biological function (Diez-Silva et al., 2010). Despite the importance of these studies in RBC, they are limited to the analysis of their phenotype. Studies in mammalian RBC involving DNA are very limited, since only immature RBCs are nucleated (O'Neill and Reddy, 2011). Therefore, the use of the chicken as a model is advantageous to understanding possible biological mechanisms involving erythrocyte responses in vertebrates.

A robust epigenetic biomarker of stress should be reproducible between animals raised in different environmental conditions (biomes). Thus, the present study is based on three strategies in order to validate and fill the gaps opened by our previous study (Pértille et al., 2017a). The present study involves the exposure of chickens from a genetically controlled population to a known stress. First, we selected one of the most utilized chicken breed lines around the world, i.e., White Leghorn. White Leghorn is a Mediterranean breed widely used throughout the global egg industry. All commercial white egg lineages have originated from line crosses involving the White Leghorn breed (Fulton, 2006). Second, we selected lineages with similar genetic backgrounds and used the same protocol to induce a known common stressor (Yanagita et al., 2011; Goerlich et al., 2012) that involves social isolation and deprivation of food and water stress. Third, the animals were reared in completely different biomes, namely in experimental systems in Sweden and a validation population in Brazil. We compared DNA methylation in a reduced fraction of the RBC genome (obtained by genomic digestion using a restriction enzyme) between individuals in a stress and a non-stress condition and then we compared the effects across the two different biomes.

The results of the present study have an important impact from the point of view of animal welfare. It brings us closer to the identification of epigenetic markers that would test the history of stress that production animals experience in their housing environment.

# MATERIALS AND METHODS

All animal experimental protocols employed in the present study were performed in accordance with international guidelines for animal welfare. In Brazil, the study was approved by the resolution #008/2017 from the CEUA following the CONCEA. In Sweden the study was approved under the license #50-13 from the Regional Committee for Scientific Research on Animals from Linköping, Sweden.

## Animal Rearing and Treatments

This study was conducted using non-beak-trimmed, male White Leghorn chickens (*Gallus gallus domesticus*) aged 0–26 days with normal health status. The experiments were performed with chickens from, and in, different geographic locations. One of the lineages was from Brazil (BR) and the experiment was performed at the Embrapa Swine and Poultry National Research Center, Concórdia/Santa Catarina State. The other population was from Sweden (SW) and the experiment was performed at Linköping University. In Brazil, birds were hatched at the EMBRAPA experimental hatchery, while in Sweden, birds were hatched at a commercial hatchery and immediately brought to a rearing farm. In each location, all birds were housed within the same room, where they were provided with *ad libitum* access to water and to feed provided through tubular feeders in BR, and a chain dispersal system in SW. The commercial diet provided for the laying birds in BR contained 12.1 MJ/kg ME (metabolizable energy) and 21.41% CP (crude protein), while the diet provided to the birds in SW contained 11.3 MJ/kg ME and 15.5% CP. The animals were raised in conventional sheds in BR while in a dark house in SW. Thus, the experimental settings present many differences related to the different biomes (different weather, rearing systems, and diets for each country) and minimize the experimental heterogeneity within the same biome.

A social isolation treatment (S) was performed on 8 out of 14 animals in the SW experiment (6 controls) and on 16 out of 32 animals (16 controls) in the BR experiment.

This treatment consisted in exposing birds of both SW and BR populations to social isolation stress at random times once a day between 4 and 26 days of age. During the treatment, these birds were individually placed in a metal (25 cm × 38 cm × 18 cm) mesh (in SW facilities) or wooden (28 cm × 28 cm × 30 cm) boxes (in the BR facilities). There, they had vocal, but not visual or physical contact with other birds. Thus, during the stress treatment the birds were actually exposed to a combination of stressors: social isolation and deprivation of food and water. The time in the treated box was gradually increased from 1 h during the first week to 2 h during the second and 3 h during the third week. The control animals (C) were not exposed to the sessions of social isolation stress but experienced the same environmental conditions as S animals. Blood samples from the S and C animals were collected 2 h after the last isolation. The same experimental set up has been previously applied (Goerlich et al., 2012) to measure the effects on corticosterone levels and gene expression across generations. Thus, the stress effect induced by this experimental design has already been validated. To account for genetic effects in the BR experiment, we randomly separated complete siblings between the S and C groups, i.e., for each chicken randomly chosen for the S group, one random sibling was chosen for the C group.

## Collection of Biological Material

Two mL of blood were collected in a 2 mL microtube with 20 μL of 0.5 M EDTA from each individual. After blood collection,

each tube was centrifuged at 3,000 rpm for 5 min and the RBC fraction was separated from the whole blood. The upper white and yellow fractions were discarded. After this, the blood samples were frozen at −20°C.

The DNA from the RBC was extracted after digestion with proteinase K (Promega; Madison, United States), precipitation of DNA in absolute ethanol, washing of DNA in 70% ethanol, and re-suspension in ultrapure water. The DNA samples were quantified in a fluorometer (Qubit Fluorometric Quantitation). The DNA quality was evaluated using the Nanodrop 2000c spectrophotometer and the integrity was checked on 1% agarose gels.

## Preparation of Sequencing Libraries

To prepare the sequencing libraries, we used an approach that combines two techniques previously optimized in chickens: GBS (Pértille et al., 2016) and MeDIP (Guerrero-Bosagna and Jensen, 2015). We recently described the optimization of this methodological combination in previous studies (Pértille et al., 2016, 2017a). This approach allows for the parallel identification of genetic and epigenetic differences between experimental groups in the same reduced fraction of the genome across individuals. The general idea of this method is to assess genome wide levels of methylation in a reduced fraction of the genome that is not biased toward CpG islands, using a restriction enzyme unrelated to CpG sites. With our method, we first digest the genome with the *PstI* restriction enzyme (Thermo Scientific; Waltham, MA, United States) in a suitable range (∼450 bp) for Illumina (San Diego, CA, United States) sequencing (Pértille et al., 2016). Illumina sequencing barcodes are then ligated to each end of the digested DNA fragments, allowing the pool of DNA samples to be immunoprecipitated together. Each pooled DNA sample contained different barcodes identifying each individual. The methylated fraction of the sampled DNA is then captured by an anti-methyl-cytosine antibody (Diagenode; Sparta, United States) (Guerrero-Bosagna and Jensen, 2015). After this step, the methylated DNA is amplified using PCR, which is followed by a clean-up of the primer dimers and unbound adapters (Elshire et al., 2011; Poland et al., 2012). The samples are then sent for sequencing. A detailed description of the protocol related to this combination of methods is currently being prepared for publication elsewhere. In BR samples, after connecting the DNA to adapters and barcodes, and pooling the samples, a 50 ng fraction of the DNA pool was taken for immediate amplification by PCR. This portion represents the genetic background of the libraries, which we call inputs. Moreover, after library prep, for the BR samples, each library was quantified by quantitative PCR using the KAPA Library Quantification Kit (Roche; Basel, Switzerland). Sequencing libraries were diluted to 16 pM and clustered using the cBOT (Illumina; San Diego, CA, United States) equipment. Paired-end sequencing with a read length of 100 bp was performed using the HiSeq2500 instrument from Illumina in the BR lab facility. In SW samples, we sent out the libraries to be quantified, clustered, and paired-end sequenced in the Illumina HiSeq2500 platform with a read length of 125 bp at the SNP&SEQ facilities of the SciLifeLab (Uppsala, SE).

## Bioinformatic Analyses

The CASAVA (Illumina) program was used for the initial processing of the samples by converting the ".bcl" (base call files) to ".fastq" extensions, which is compatible with programs used for read alignment. The quality of the reads was checked using FastQC v.0.11.3 (Andrews, 2010). Quality trimming was performed in short read sequences during the data processing using default parameters. For both SNP calling and methylation analyses, quality-trimmed reads were aligned against the chicken reference genome (*Gallus_gallus* 5.0, NCBI) using the Bowtie2 tool v.2-2.3.4.2 (Langmead and Salzberg, 2012) default parameters. The coverage depth of each sequenced file was determined using Samtools v.0.1.19 (Li et al., 2009) with the "depth" option. A TASSEL-GBS Discovery Pipeline was used to process the data and for SNP calling by employing default Tassel v.3.0 (Glaubitz et al., 2014) parameters. For SNP calling, default filtering parameters were applied except for the use of 5% for mnMAF, 70% of mnTCov, and 70% for mnScov. These parameters were applied in accordance with similar studies (Pértille et al., 2016, 2017a,b). An Archaeopteryx tree (Han and Zmasek, 2009) was then plotted using a cladogram generated by a Neighbor Joining distance matrix using the Tassel v.3.0 software. For the identification of differential methylation regions (DMR), uncalled and low quality score bases were eliminated using the process_radtags function in the Stacks v.1.39 (Catchen et al., 2011) program.

After the alignment, the .bam files from each individual were then assigned to one of the experimental groups (S or C). DMRs were then calculated between the two experimental conditions using the MeDIPS package within R (Lienhard et al., 2014) for basic data processing, quality controls, normalization, identification of differential methylated regions (DMRs), and the calculation of fold-changes methylation values among experimental groups. We used MeDIPS with default parameters and the BSgenome.Ggallus.UCSC.galGal5 (package from Bioconductor). In addition, to identify confounding factors related to the input (i.e., copy number variations, CNVs), we tested for differential coverage between the inputs of S and C samples in BR individuals. MeDIPs allows us to include the following parameters: two methylation enriched DNA sets (named MSet S and C) and two input sets (named ISet S and C). When the two methylation-enriched DNA sets are included, MeDIPs calculates DMRs. In addition, when two input sets are included, MeDIPs will identify CNVs between the inputs and match the results to the DMRs identified between the two methylation-enriched sets[1]. This gives an output containing only the DMRs that do not match with the CNVs calculated from the inputs.

Quality control was carried out to confirm the enrichment of the methylated fraction of the genome. This was performed by calculating the average enrichment score. Enrichment scores > 1 are recommended in the literature to denote methylated DNA enrichment, with values around 2 being optimal (Lienhard et al., 2014).

[1]https://www.bioconductor.org/packages/release/bioc/vignettes/MEDIPS/inst/doc/MEDIPS.pdf

We followed the same specific parameters for the MeDIPS package previously used (Pértille et al., 2017a). However, to call DMRs we used two different approaches in which the parameter $P = 0.01$ was used as the threshold for the detection of stacked reads. The first approach was the MeDIPS default in which the genome is divided into ADJW of a pre-defined length size of 100 bp. This differential methylation analysis then uses a weighted trimmed mean of the log expression ratios (TMM) (Robinson and Oshlack, 2010). In the second approach, a pre-selection of the regions later tested in MeDIPS was obtained by comparing the methylation enriched sets (Msets S and C) using the MACS2 peak calling program[2] (Zhang et al., 2008) with default parameters. In MeDIPs, differences between the methylation enriched sets (Msets), or between the input sets (Isets), were tested only on these MACS2-generated regions. MACS2 is a recommended tool to identify sample-wise 'peak specific' methylated regions of variable sizes in experiments using paired controls to determine enrichment against background (Feng et al., 2012; Niazi et al., 2016; Cavalcante et al., 2019). The use of MACS2 contrasts to the division of the genome into small subsequent windows performed by the ADJW approach. Importantly, these peaks, called 'regions of interest' (ROI), were obtained after passing FDR correction ($\leq$0.1). After ROIs were identified, MeDIPs used them to test for DMR. ROIs found differentially methylated by MeDIPS were called ROI-DMRs ($P \leq 0.05$). MACS2 improves the spatial resolution of the predicted sites, uses a dynamic parameter to capture local biases in the genome, and improves the robustness and specificity of the prediction, that are strongly indicated for fold-enrichment experiments (Zhang et al., 2008). Considering that in the BR individuals the sequencing covered a ∼3.5 times larger region than the sequencing of SW individuals, we performed differential weighting of default parameter thresholds for a minimum sum of counts across all samples per window. Therefore, for SW individuals we used the default parameter (minRowSum = 10) and for BR individuals we used a 3.5 times higher value (minRowSum = 35). As a consequence of this differential weighting, a similar number of windows between individuals from Brazil and Sweden were tested using both the ADJW and ROI approaches. For a general visualization of the experimental and bioinformatic workflow see **Figure 1**, and **Supplementary Figure 1**.

The differential genomic windows obtained by the ADJW and ROI analyses were considered as DMRs based on three significance thresholds: $P \leq 0.0005$ DMRs were used for describing genes related to significant DMRs; $P \leq 0.005$ DMRs were used for visualization purposes and to describe overlapping DMRs between the ROI and ADJW approaches; and $P \leq 0.05$ DMRs were used for enrichment pathway analyses, for the detection of overlapping DMRs between the BR and SW lineages, and to calculate distance among neighboring DMRs and between DMRs and their nearest TSS. ROIs that passed a significance threshold level of 0.05 were considered ROI-DMRs. The idea behind using datasets with different levels of significance was to obtain different levels of information. For example, more stringent *p*-values will give a better idea of specific sites to be tested in the future as putative epigenetic biomarkers of stress in RBCs. Less stringent *p*-values will give information of which biological pathways could be influenced by the early stress applied, and also provide DMRs to be tested later as common epigenetic regions altered by the stress in different populations. All DMRs obtained were annotated against the chicken reference genome (*Gallus_gallus* 5.0, NCBI) using the VEP tool (McLaren et al., 2010).

In addition to the VEP annotation, we performed an annotation with R in order to obtain information about the distance between each ROI-DMR and their nearest TSS. For this, we extracted the coordinates from each ROI (from the BR and SW populations) and from the annotated genes from the chicken genome (using the org.Gg.eg.db package). Then, we overlapped the identified ROI with these annotated genes using the Genomic Ranges R package. Next, we performed a functional genomic annotation of the ROIs overlapping with genes. For this, we used the annotatePeak function from the ChIPseeker package (Yu et al., 2015). In this function, we forged a gg_txdb object using the GenomicFeatures and org.Gg.eg.db packages. The latter is the functional annotation database for the chicken genome (BSgenome.Ggallus.UCSC.galGal5). This gg_txdb for *Gallus gallus* was extracted from the transcript metadata TxDB, which contains all the functional annotations available at the UCSC genome browser. For this, we used the function makeTxDBFromUCSC (using the parameter: genome = "galGal5").

After identifying specific features related to DMRs found in each population (BR and SW) we checked the distribution of the identified ROI-DMRs in relation to (i) the nearest ROI-DMR, and (ii) the nearest gene's TSS locations. For this, we considered different chromosomal data subsets: all, autosomal, and Z chromosomes. These distances were categorized in ten, hundred, thousand, and million numerical magnitudes. The analysis includes every distance that was counted at least once. At continuation, we tested whether transcription factor binding site (TFBS) motifs could map to the ROI-DMRs associated to specific peaks of distance in relation to the TSS. This test was performed with the web-based tool PhysBinder[3] (Broos et al., 2013) using the threshold of 'Max. Precision (PPV)' and selecting all the 85 transcription factors available[4], which included all 'Direct Evidence' and 'Putative Associated' factors. The motifs selected as of special interest were those that passed two criteria: TFBS should have hits in all DMRs longer than 100 bp tested (even if non-significant) and should have hits above the threshold (i.e., considered significant) in at least 50% of the DMRs tested.

An overlap analysis to identify DMRs obtained by both methods, i.e., ADJW and ROI (in the two different experiments) was performed by permutation tests ($N = 100$) that determined which peak overlaps were significant. For this, we used the findOverlapsOfPeaks function from the ChIPpeakAnno v3.6.5 R package with default parameters. Venn diagrams were plotted using the *makeVennDiagram* function within the same package.

[2]https://github.com/taoliu/MACS/

[3]http://bioit.dmbr.ugent.be/physbinder/index.php

[4]http://bioit.dmbr.ugent.be/physbinder/models.php

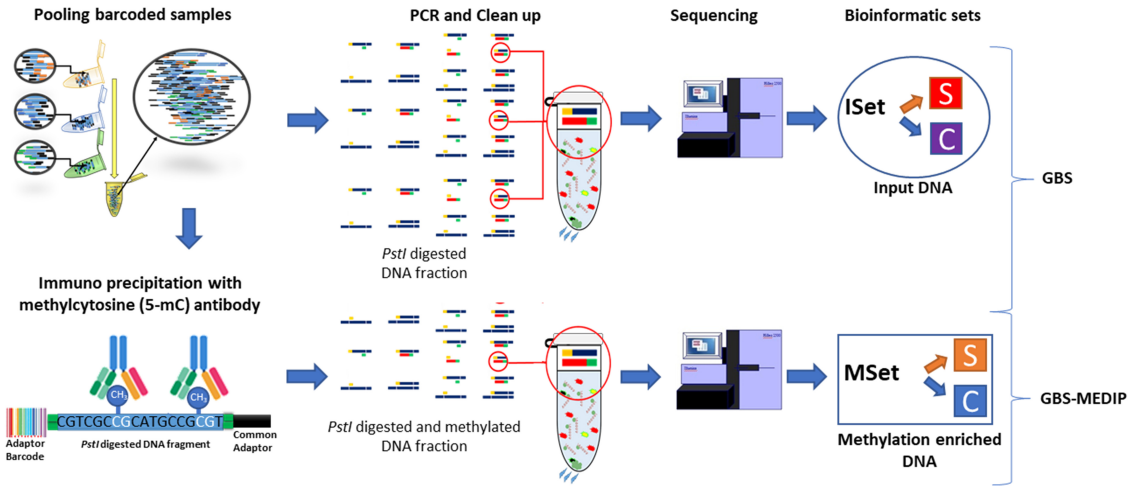



**FIGURE 1 |** Scheme depicting the general experimental workflow of the genetic and methylomic analyses employed and the datasets used for the bioinformatic analyses.

**TABLE 1 |** Average sequencing and alignment statistics for the White Leghorn SW and BR lineages.

| Lineages | Samples | Sample number | Depth ± *SD* | Number of bp sequenced ± *SD* | Breadth (bp sequenced/depth) ± *SD* | % of the *Gal.gal* genome v.5.0 covered ± *SD* |
|---|---|---|---|---|---|---|
| SW | MeDIP average | 14 | 54.7 ± 5.5 | 313,562,292.1 ± 112,051,857.5 | 5,786,017.2 ± 2,201,546.4 | 0.54 ± 0.20 |
| BR | MeDIP average | 32 | 30.2 ± 3.1 | 597,344,785.8 ± 294,204,155.2 | 20,026,886.1 ± 10,085,067.7 | 1.9 ± 0.9 |
| | Input average | 32 | 23.0 ± 3.4 | 741,551,215 ± 186,608,136 | 31,947,116.0 ± 3,230,589.0 | 2.97 ± 0.30 |

The internet-based tool used to identify over-represented pathways related to our gene list was Reactome v72 (Croft et al., 2011). This is an open-source curated bioinformatic database of pathways and reactions from human and other animals[5]. Reactome is capable of accessing a variety of databases that contain previously described biological pathways (e.g., Kegg, Biocarta, Reactome, and Wikipathways).

# RESULTS

## Sequencing and Alignment

The average sequencing and alignment statistics for the individuals investigated in the SW ($N$ = 14) and BR ($N$ = 32) experiments are shown in **Table 1**. More details can be found in **Supplementary Tables 1**, **2**. For BR White Leghorn chickens, we sequenced both the reduced genome ($N$ = 32 and 16/treatment) and its methylated fraction ($N$ = 32 and 16/treatment). The reduced genome, obtained through the GBS approach, was used as the input for genetic background analyses. The individually reduced genomes were used to verify the relatedness among individuals. For SW White Leghorn chickens ($N$ = 14 and 8/treatment) we did not use input DNA, because the idea with this population was only to compare their RBC methylomic response (to social isolation) with BR chickens.

[5]www.reactome.org

## DNA Background

Based on the input DNA of all BR individuals, we identified 93,215 SNPs among them (**Supplementary VFC File 1** online). From these SNPs, a tree showing genetic relatedness was plotted using a cladogram generated by a Neighbor Joining distance matrix (**Figure 2**). The cladogram in **Figure 2** shows that individuals are grouped by family, which is expected because we controlled the genetic background by separating the full siblings between S and C groups. Each individual analyzed was categorized within the expected family cluster (tree branch) according to their genetic relationship. The .bam files generated by the genomic sequences of the individuals were later used for methylomic coverage normalizations.

## CpG Enrichment

For BR individuals, an enrichment score of 1.59 (±0.13) was obtained and, in average, 3.94% of the CpG regions on the *Gallus gallus* genome were covered (**Supplementary Table 3**). For SW individuals we obtained an enrichment score of 2.87 (±0.10) and, in average, 1.18% of the CpG regions on *Gallus gallus* genome were covered (**Supplementary Table 4**). This indicates that in BR genomes approximately 3.33 × (3.94/1.18) more CpG regions were covered than in SW genomes. This difference could be explained by a different procedure conducted in the SW library construction compared to the BR library. In SW libraries, the protein beads containing immunoprecipitated DNA were washed once more than what was previously recommended (Guerrero-Bosagna and Jensen, 2015). Concomitant with the fact that the

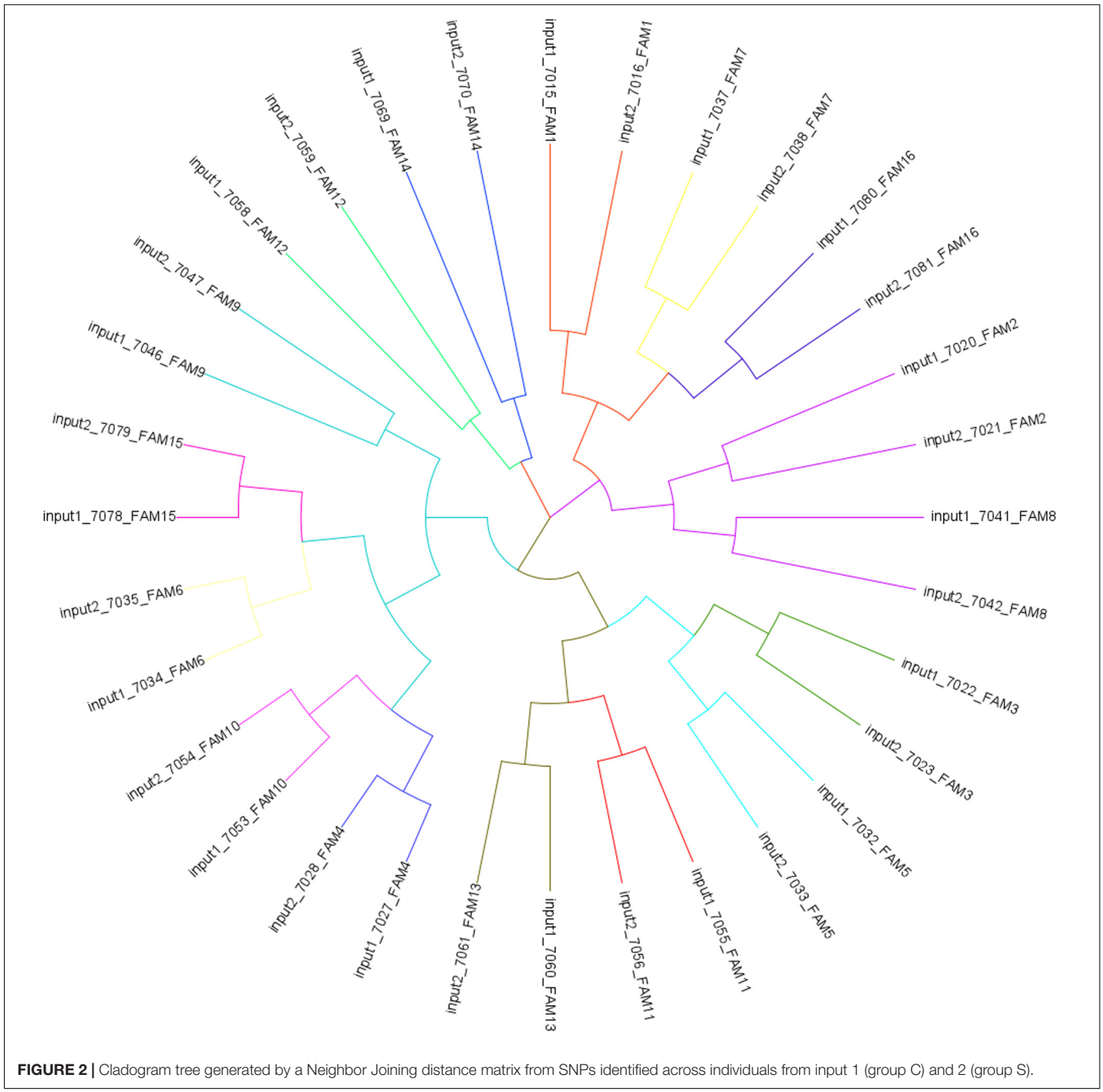



**FIGURE 2 |** Cladogram tree generated by a Neighbor Joining distance matrix from SNPs identified across individuals from input 1 (group C) and 2 (group S).

**TABLE 2 |** Total number of genomic windows sequenced and tested in the BR and SW lineages and number of DMRs identified using different *p*-value thresholds.

| **Test** | | **BR** | **SW** | **BR** | **SW** | **BR** | **SW** | **BR** | **SW** |
|---|---|---|---|---|---|---|---|---|---|
| **minRowSum** | | 35 | 10 | ***P* ≤ 0.0005** | | ***P* ≤ 0.005** | | ***P* ≤ 0.05** | |
| ADJW (100 bps windows) | Total | 10,188,209 | 10,188,209 | 6 | 7 | 38 | 57 | 359 | 561 |
| | Tested | 14,040 | 14,522 | | | | | | |
| ROI (FDR ≤ 0.1) | Total | 73,825 | 12,019 | 4 | 1 | 17 | 6 | 154 | 91 |
| | Tested | 5,058 | 994 | | | | | | |

*Genomic windows were tested when they passed a "minimum sum read count" parameter of 10 for SW and of 35 for BR experiments.*

number of covered regions were lower in SW samples, coverage depth was higher. Consequently, a reduction in false positive and an increase in false negative DMRs is expected to be observed in the SW population.

## Analysis of Differentially Methylated Regions (DMRs)

Three levels of significance were used to identify DMRs between the S and C groups ($P \leq 0.05$, $P \leq 0.005$, and $P \leq 0.0005$). These were then used for different analyses. The number of DMRs obtained with each significance level used is shown in **Table 2**. Windows obtained with the less stringent values of $P \leq 0.005$ and $P \leq 0.05$ were used to investigate overlaps among the different methodologies employed, i.e., ROI and ADJW (**Supplementary Spreadsheet 1**). Additionally, DMRs obtained with $P \leq 0.05$ were selected to identify common DMRs between the two different experiments, since no overlap was obtained with more stringent *p*-values. Although $P \leq 0.05$ will generate more false positives, it can also provide a set of putative regions to be further investigated with other methodologies. Windows obtained with $P \leq 0.0005$ when using the ADJW approach were considered of special relevance in terms of significance and the ADJWs fulfilling this criterion were merged (**Table 3**).

With ADJW we investigated relative DNA methylation changes between experimental groups in 10,188,209 ADJW of 100 bps across the chicken genome. A total of 359 and 561 of these windows were obtained with a threshold of $P \leq 0.0005$ for BR and SW experiments, respectively (**Table 3**). Merging of these adjacent differentially covered windows identified by ADJW between the S and C groups produced 3 DMRs in the SW experiment and 3 DMRs in the BR experiment. Of all DMRs identified by ADJW one passed FDR $\leq 0.05$ (FDR = 0.02), which was identified in the BR population (**Table 3**).

In parallel, with MACS2 we identified 14,040 regions with differential coverage in the methylation enriched genomes between S and C groups in the BR experiment, and 14,533 in the SW experiment (**Table 2**). After testing these regions with the MeDIPS package, 4 and 1 ROI-DMRs were obtained with a threshold of $P \leq 0.0005$ for the BR and SW experiments, respectively (**Table 3**). Of all ROI-DMRs one passed FDR $\leq 0.05$ (FDR = 0.0000034), which was identified in the BR population (**Table 3**). Importantly, this is the same region that was previously identified to pass FDR $\leq 0.05$ with ADJW.

Additionally, in the BR population we tested for artifacts potentially caused by differential coverage of the input between the S and C groups using the inputs as the Iset parameter in the MeDIPs package (Lienhard et al., 2014). These coverage differences could mask or enhance DMR identification. The results were unchanged after using the inputs to control for eventual pre-existing coverage differences. In addition to the ROI-DMRs obtained between the S and C groups with a threshold of $P \leq 0.0005$ (1 in SW and 4 in BR), using a less stringent *p*-value ($P \leq 0.05$) we identified 359 ROI-DMRs in the BR experiment and 561 ROI-DMRs in the SW experiment. About 50% of these ROI-DMRs overlapped with DMRs identified with AJDWs ($P \leq 0.05$). Detailed information of the DMRs above the two thresholds depicted in **Figure 3** are shown in **Tables 3**, **4**. All ROI-DMRs were annotated using the VEP tool. Additionally, "consequences" were plotted using pie charts for a general view of their location in relation to the annotated genes in the chicken genome (including those overlapping test) (**Figure 4**).

With both of these approaches more DMRs reached the defined significance thresholds in BR individuals compared to SW. However, more DMRs had higher fold change values in SW compared to BR individuals. When comparing the two approaches used to call DMRs (**Figure 3**), we observed that the number of DMRs identified with ADJW was 4 times larger than with ROI (**Table 2**). This was probably due to the fragment size analyzed, since with ADJW a fixed 100 bp window was used, while with ROI the average fragment sizes in BR and SW groups were $323 \pm 256$ and $427 \pm 479$ bps, respectively (according to the peak calling). Expectedly, ROI-DMRs tend to encompass larger regions than ADJW-DMRs (fixed in 100 bps). Not surprisingly, when using the ADJW method some DMRs were identified that had no CpGs. The reason for this is that DMRs larger than 100 bp identified by ADJW will be arbitrary divided into 100 bp sub windows and not all of these sub-windows will have a CpG in their composition. Due to this, the ADJWs were merged (see **Table 3**). Additionally, CpG count can equal zero when the CpG is present in the analyzed population but not in the reference genome (see **Table 4**). Another difference is that ROI tended to detect more hypermethylated DMRs in the S vs. C groups than ADJW. With a stringent *p*-value threshold ($p \leq 0.0005$) no overlaps were found. With a less stringent threshold of $P \leq 0.005$, 47.1% of the DMRs identified by ROI overlapped with DMRs identified by ADJW in the BR experiment, while 62.3% of the ROI and ADJW DMRs identified overlapped in the SW experiment. Considering $P \leq 0.05$, this overlap corresponds to 66.7 in BR, and 49.5%, in SW.

To verify the distribution of the DMRs throughout the chicken genome we first constructed a Manhattan plot (right side of **Figure 3**) with the three above-mentioned thresholds of significance. Additionally, we plotted a distribution expectancy of 100,000 random windows across the chicken genome to compare with the observed distribution of the 5,058 and 994 peaks called between S and C groups in BR and SW (ROI peaks) populations, respectively. For this, we used $237.7 \pm 184$ bps mean length, which was the average length of all windows used in our study (ROI peaks for BR and SW). An inverse distribution of the observed DMRs was identified in relation to their random expectation corrected by chromosome size (**Figure 5**). This distribution of DMRs increases toward microchromosomes. We analyzed the sex ChrZ separately because even though it is considered a macrochromosome in chicken (Habermann et al., 2001), it presented the greater proportion of DMRs. Interestingly, the ChrZ was enriched to 2.38× (BR) and 4.47× (SW) above expectancy for the presence of DMRs (**Figure 5**). Additionally, to eliminate any remaining possibility of this being an artifact of our technique, we assessed the number of expected CpGs and *PstI*-digested fragments (ranging from 200 to 600 bps – compatible with our library size) per chromosome in relation to their size. Neither the number of CpGs nor the number of

**TABLE 3 |** Putative stress-induced DMR descriptive statistics and gene annotations for the DMRs found with the ADJW and ROI ($P \leq 0.0005$) analyses in BR and SW populations (SvsC groups).

| S vs. C | Test | Location | Width | logFC | *P*-value | FDR *p*-value | CpGs | % of CpG | Position regarding gene | Gene symbol | ENSEMBL name | Gene strand |
|---|---|---|---|---|---|---|---|---|---|---|---|---|
| BR | ADJW | chr1:61077901-61078200 | 300 | 3.4 | 2.24E-05 | 1.05E-01 | 19 | 6% | Intron/intron | *LRTM2*/*NA* | ENSGALG00000026214/ ENSGALG00000036964 | 1/−1 |
| | | chr6:17299601-17299700 | 100 | 2.1 | 4.77E-04 | 1.00E+00 | 1 | 1% | Intergenic | – | – | – |
| | | *chr28:3263201-3263400 | 200 | 3.5 | 2.33E-06 | 1.64E-02 | 7 | 7% | Upstream gene/downstream gene | *ADAMTSL5*/THOP1 | ENSGALG00000024298/ ENSGALG00000041934 | −1/−1 |
| | ROI | chr9:3693375-3694655 | 1281 | 1.4 | 4.76E-04 | 5.84E-01 | 44 | 3% | Coding sequence, intron | *KY* | ENSGALG00000044975 | −1 |
| | | chr26:3262317-3263255 | 939 | 1.6 | 5.91E-05 | 1.49E-01 | 30 | 3% | Downstream gene | – | ENSGALG00000001480 | −1 |
| | | *chr28:3263299-3263412 | 114 | 3.4 | 3.40E-06 | 1.72E-02 | 9 | 8% | Upstream gene/downstream gene | *ADAMTSL5*/THOP1 | ENSGALG00000024298/ | 1 |
| | | chrZ:7337093-7337617 | 525 | 1.5 | 4.76E-04 | 5.84E-01 | 6 | 1% | Intron | *UBE2R2* | ENSGALG00000041934 | 1 |
| SW | ADJW | chr14:12337401-12337500 | 100 | 3.2 | 1.93E-04 | 4.00E-01 | 3 | 3% | Downstream gene/downstream gene | *CLCN7*/*NA* | ENSGALG00000030826/ ENSGALG00000032279 | −1/1 |
| | | chr20:49301-49600 | 300 | −4.4 | 4.18E-05 | 2.03E-01 | 24 | 8% | Intergenic | – | – | – |
| | | chrZ:70400401-70400700 | 300 | −.5.4 | 1.46E-04 | 3.53E-01 | 2 | 1% | Intergenic | – | – | – |
| | ROI | chr2:66704195-66704415 | 221 | 5.5 | 3.56E-04 | 3.53E-01 | 4 | 2% | Intron | *IRF4* | ENSGALG00000012830 | 1 |

**overlaps among methodologies (ROI and ADJW); "/" separate genes that are associated to the same DMR; NA means information not available. DMRs shown for ADJW represent merged consecutive windows significantly altered.*

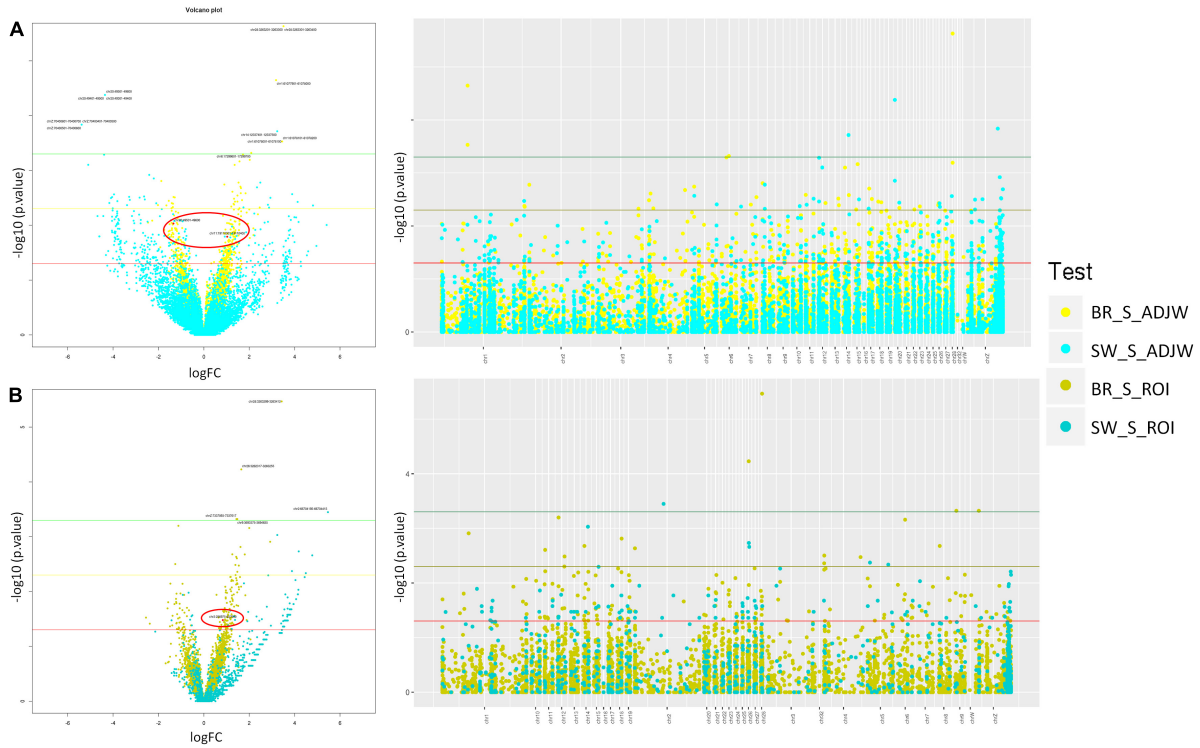



**FIGURE 3 |** Volcano and Manhattan plots showing stress-induced DMRs found in BR and SW lineages using **(A)** ADJW and **(B)** ROI. Thresholds shown correspond to *p*-values 0.05 (red), 0.005 (yellow), and 0.0005 (green). Overlapping windows in Volcano plots are marked in red. Light colors represents ADJW and dark colors represent ROI.

*Pst*I-generated fragments was statistically different than expected (*t*-test $P \leq 0.05$).

In relation to the distances among ROI-DMRs, we found that most distances were concentrated at 1–2 Kbps, 20–30 Kbps, 200–300 Kbps, and 10 Mbps in both populations (**Supplementary Spreadsheet 2** online). Altogether, these peaks represent 52.9% (BR) and 57.9% (SW) of all ROI-DMRs within the respective population.

In relation to the distribution of distances from ROI-DMRs to their nearest TSS, we observed high similarity between the two populations (BR and SW) studied ($r \geq 0.94$). The same trend was observed between the chromosome subsets analyzed (all vs. autosomal and all vs. ChrZ) within each population studied ($r \geq 0.93$). Both distributions of distances between either ROI or ROI-DMRs and their nearest TSS presented a trimodal pattern (**Figure 6** and **Supplementary Spreadsheet 2** online). The highest peaks of these trimodal distributions were located at −10 Kbps, 0 Kbps, and +20 Kbps from the TSS. The exception was the largest distance peak between ROI-DMRs and TSS in the SW population, located at 40 Kbps.

The observation of these peaks of ROI-DMRs in relation to the TSS together with the fact that these peaks were located in regions of potential regulation by transcription factors prompted us to investigate, with the web tool PhysBinder (Broos et al., 2013), the possibility that these peaks could be enriched for specific TFBS. We investigated potential hits of our ROI-DMRs to 85 TFBS motifs (all that were available in PhysBinder). For the ROI-DMR peaks of 10 kb upstream TSS and 20–40 kb downstream the TSS we combined the ROI- DMRs obtained in the BR and in the SW experiment, since the peaks were the same. For the peak at the TSS we performed independent analyses for the BR and the SW experiment since their peaks were slightly different. Interestingly, we found the following TFBS motifs with a high presence (>50%) in these ROI-DMRs: Tfcp2l1, Esrrb, RELA, and Zfx in the peak of −10 kb; Tfcp2l, Esrrb, KLF4, RELA in the peak at the TSS SW; Tfcp2l and Zfx in the peak at the TSS BR; and Tfcp2l1, Esrrb, RELA, and KLF4 in the peak of +20 to 40 kb (**Supplementary Spreadsheet 3**). Of particular interest is the Tfcp2l1 motif, which mapped against nearly 100% of these ROI-DMRs.

After performing an overlap test based on permutations test ($N$ = 100) between the SW and BR ROI-DMRs, we identified two common DMRs with the ADJW approach and one with the ROI approach (**Figure 3**). These three overlapping DMRs between BR and SW were located in Chr 2, 11, and 20. The first was located in an intronic region of a *novel gene*, the second was located in an intronic region of the *DBNDD1* gene and at the 5-prime UTR of the *CDHI* gene, while the third was in an intergenic position (**Table 5**). In addition, we plotted the results of the DMR overlapping test considering a maximum gap of 1 kb for each two peak ranges (**Figure 7**). For better visualization of DMR locations, three Manhattan plots were constructed (**Supplementary Figures 2–4**).

**TABLE 4 |** Descriptive statistics and gene annotations for ROI DMRs found ($P \leq 0.005$) in BR and SW populations (S vs. C groups).

| S vs. C | ROI ~ DMR | Location | Width | LogFC | *P*-value | FDR p-value | CpGs | % of CpG | Position regarding gene | Gene symbol | ENSEMBL name | Gene strand |
|---|---|---|---|---|---|---|---|---|---|---|---|---|
| BR | T | chr1:61077945-61078198 | 254 | 2.9 | 1.23E-03 | 8.91E-01 | 16 | 6% | Intron/intron | *LRTM2*/NA | ENSGALG00000026214/ ENSGALG00000036964 | 1/−1 |
| | T | chr2:189007-189224 | 218 | 1.4 | 2.32E-03 | 1.00E+00 | 11 | 5% | Downstream gene | – | ENSGALG00000043576 | −1 |
| | T | chr4:740034-740180 | 147 | 1.5 | 4.36E-03 | 1.00E+00 | 1 | 1% | Intergenic | – | – | |
| | F | chr4:1212081-1212352 | 272 | −1.3 | 3.15E-03 | 1.00E+00 | 6 | 2% | coding sequence/3 prime UTR | – | ENSGALG00000004475 | 1 |
| | | | | | | | | | Upstream gene/upstream gene | *WNT11B/gga-mir-6658* | ENSGALG00000004401/ ENSGALG00000028208 | 1/−1 |
| | T | chr4:85246930-85247063 | 134 | 1.5 | 3.36E-03 | 1.00E+00 | 0 | 0% | Intron | *CTBP1* | ENSGALG00000039942 | 1 |
| | T | chr6:17299560-17299780 | 221 | 2 | 6.93E-04 | 5.84E-01 | 4 | 2% | Intergenic | – | – | – |
| | F | chr8:5191540-5191738 | 199 | 1.8 | 2.10E-03 | 1.00E+00 | 18 | 9% | Coding sequence, intron | *LMX1A* | ENSGALG00000003424 | 1 |
| | F | chr9:3693375-3694655 | 1281 | 1.4 | 4.76E-04 | 5.84E-01 | 44 | 3% | Coding sequence, intron | *KY* | ENSGALG00000044975 | −1 |
| | F | chr11:1715302-1715998 | 697 | 1.5 | 2.47E-03 | 1.00E+00 | 9 | 1% | Coding sequence, intron | *VAC14* | ENSGALG00000002458 | 1 |
| | F | chr12:2700294-2700543 | 250 | −1.1 | 6.30E-04 | 5.84E-01 | 11 | 4% | Coding sequence, intron | – | ENSGALG00000046133 | 1 |
| | | | | | | | | | Downstream gene | – | ENSGALG00000046133 | 1 |
| | F | chr12:16285799-16286230 | 432 | 1.4 | 4.99E-03 | 1.00E+00 | 7 | 2% | Intron, non -coding transcript | – | ENSGALG00000035037 | 1 |
| | T | chr12:16763013-16763444 | 432 | 1.4 | 3.27E-03 | 1.00E+00 | 16 | 4% | Upstream gene | *PDZRN3* | ENSGALG00000007819 | −1 |
| | T | chr14:4134485-4134909 | 425 | 1.3 | 2.09E-03 | 1.00E+00 | 45 | 11% | Start lost, start retained, 5 prime UTR | *TNRC18* | ENSGALG00000040770 | −1 |
| | F | chr18:10291116-10291837 | 722 | 1.6 | 1.54E-03 | 9.71E-01 | 41 | 6% | Coding sequence, intron | *CACNA1G* | ENSGALG00000007623 | −1 |
| | F | chr26:3262317-3263255 | 939 | 1.6 | 5.91E-05 | 1.49E-01 | 30 | 3% | Downstream gene | – | ENSGALG00000001480 | −1 |
| | T | chr28:3263299-3263412 | 114 | 3.4 | 3.40E-06 | 1.72E-02 | 9 | 8% | Upstream gene/downstream gene | *ADAMTSL5/ THOP1* | ENSGALG00000024298/ ENSGALG00000041934 | 1 |
| | F | chrZ:7337093-7337617 | 525 | 1.5 | 4.76E-04 | 5.84E-01 | 6 | 1% | Intron | *UBE2R2* | ENSGALG00000001668 | 1 |
| SW | F | chr2:66704195-66704415 | 221 | 5.5 | 3.56E-04 | 3.53E-01 | 4 | 2% | Intron | *IRF4* | ENSGALG00000012830 | 1 |
| | T | chr5:5717497-5717944 | 448 | 3.9 | 4.23E-03 | 4.79E-01 | 9 | 2% | Intergenic | – | – | |
| | F | chr5:48281849-48282123 | 275 | 4.5 | 4.61E-03 | 4.79E-01 | 16 | 6% | Intergenic | – | – | |
| | T | chr14:12337347-12337639 | 293 | 3.2 | 9.29E-04 | 4.62E-01 | 10 | 3% | Downstream gene/downstream gene | *CLCN7/NA* | ENSGALG00000030826/ ENSGALG00000032279 | −1 |
| | T | chr26:3554060-3554373 | 314 | 4.2 | 1.85E-03 | 4.79E-01 | 15 | 5% | intron | *RHOC* | ENSGALG00000001569 | −1 |
| | | | | | | | | | Downstream gene/downstream gene | *MOV10/PPM1J* | ENSGALG00000001558/ ENSGALG00000001605 | 1 |
| | T | chr26:4552858-4553138 | 281 | 4.8 | 2.18E-03 | 4.79E-01 | 0 | 0% | Downstream gene | *OPN1MSW* | ENSGALG00000002848 | – |

*T (true) and F (false) when the ROI is overlapped or not, respectively, by an AJDW identified using the same P-value threshold; "/" separate genes that are associated to the same DMR; NA means information not available.*

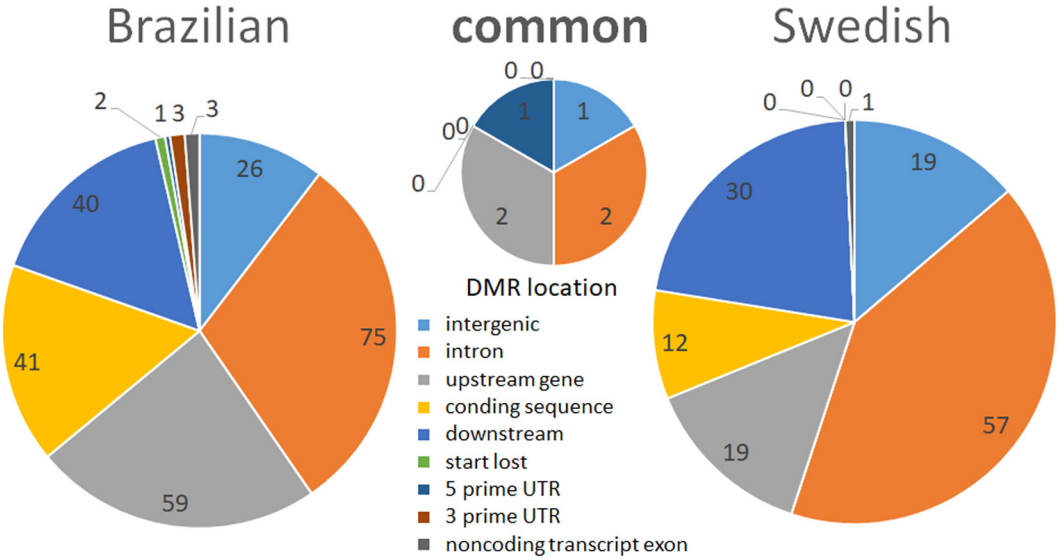



**FIGURE 4 |** Pie charts representing the functional annotation of stress-induced ROI-DMRs in relation to genes in the reference chicken genome. The left pie represents ROI-DMRs identified in the BR experiment and the right pie represents ROI-DMRs found in the SW experiment. The middle pie chart shows the ROI-DMRs overlapping between lineages.

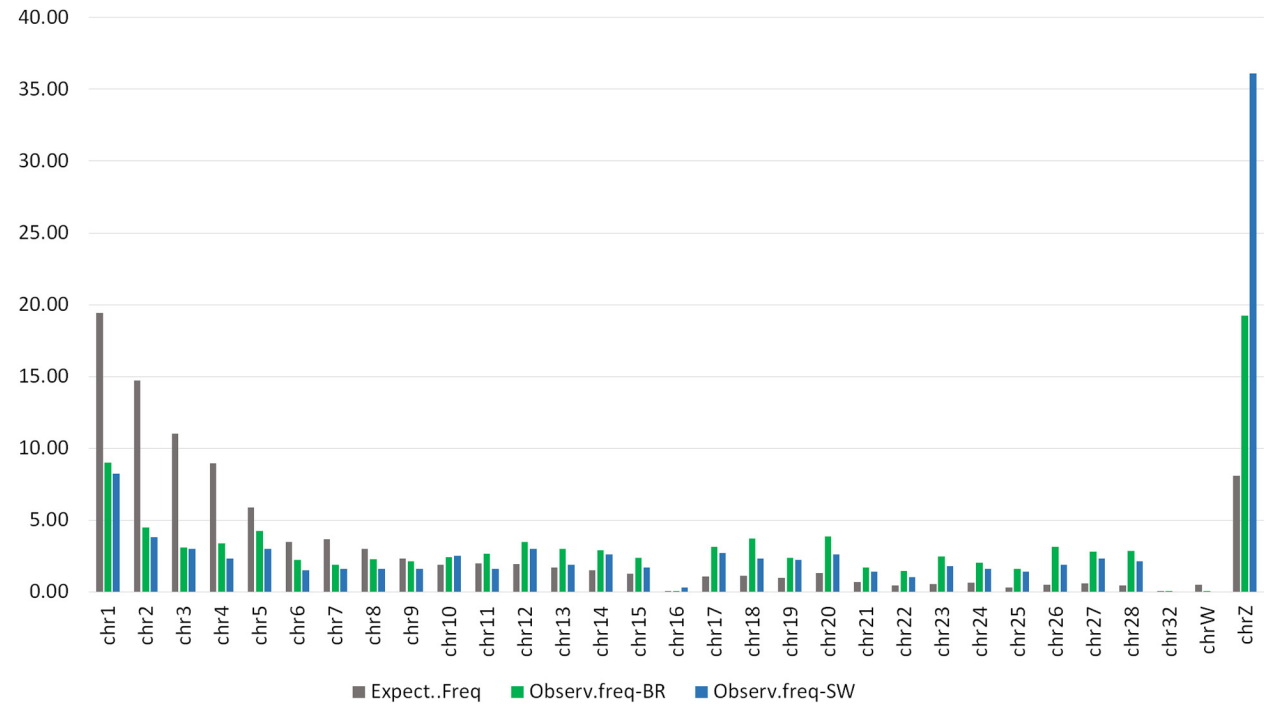



**FIGURE 5 |** Distribution expectancy of random 100,000 windows of 237 ± 184 bps across the *Gallus gallus* chromosomes compared with the observed distribution of 5,058 and 994 peaks called between the S and C groups of the BR and SW populations, respectively (ROI).

Next, we performed pathway gene enrichment analysis using ROI-DMR related genes. We identified 285 and 162 enriched pathways for BR and SW, respectively (**Supplementary Spreadsheet 4**). Considering an entities ratio of 0.05, which was calculated from the number of genes from a DMR-responsive gene list over the total number of genes involved in a particular canonical pathway, we found 47 pathways identifiers in common between the lineages. The pathway analysis considers the connectivity among molecules, which is represented by pathway steps. This information provides a better indication of the proportion of pathways in common between the analyzed data. All these 47 common pathways exhibit steps in common

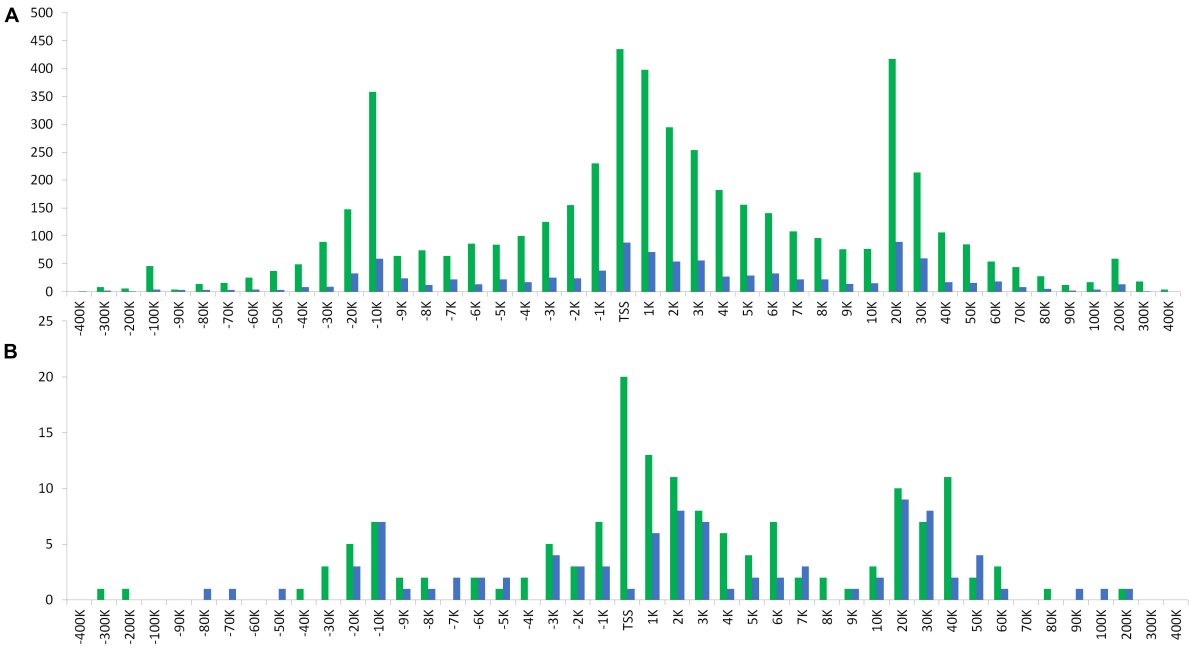



**FIGURE 6 |** Distribution of **(A)** the ROI peaks and, **(B)** the ROI-DMRs for each analyzed population (BR and SW) in relation to the nearest TSS location.

with other pathway identifiers (ratio > 0.072) (Croft et al., 2011). From these, we selected two pathways as being of special interest: cardiac conduction (FDR = 0.08) from the pathways obtained with the SW DMRs list, and Laminin interactions (FDR = 0.05) from the pathways obtained with the BR DMR list (**Table 6** and **Supplementary Spreadsheet 4**).

## DISCUSSION

The present study compared the RBC methylome of chickens subjected to social isolation to controls across different biomes to detect whether a common stress-related epigenetic profile (in DNA methylation) could be identified. For this, the RBC methylomic differences among lineages from different breeding programs and biomes were investigated. We performed a combined GBS + MeDIPs approach (Pértille et al., 2017a) to interrogate a reduced fraction of the RBC methylome of each individual in a pool of barcoded DNA samples. For the analysis, we used two approaches: in the first approach, a DMR call across 100 bp windows (named ADJW) was used, while in the second, pre-determined windows were used for the DMR call based on previous peak calling between the treatments (named ROI). In addition, the reduced genome of BR individuals was sequenced using the GBS approach (Pértille et al., 2016) for analysis of the genetic background.

The observation of differential methylation between treatments in specific genomic regions can sometimes be caused by confounding factors unrelated to differential immunoprecipitation (Lentini et al., 2018). To correct for this, we compared the relative differences in coverage of the inputs before immunoprecipitation. We did not identify sequencing coverage effects that interfered with the proper identification of DMRs.

Due to the massive omics data generated by NGS approaches, it is quite challenging to choose the appropriate statistic aiming to convert the data gathered into biologically relevant information. For epigenetic data, for example, commonly used software employed for obtaining DMR between treatments rely on *t*-statistics (Smyth, 2005; Luo et al., 2018), followed by statistical corrections for multiple tests. However, there is no consensus to date on which set of statistics would be the most appropriated (Korthauer et al., 2019). Many researchers have chosen to be more flexible regarding the statistical analysis, by accepting false positives but carrying out *a posteriori* analyses to integrate biological evidence into the statistics (Hoops et al., 2006; Mi et al., 2013; Croft et al., 2014; Krämer et al., 2014). In the present study, we investigated DMRs emerging from different p-value thresholds between S and C within each lineage (i.e., BR and SW). This was performed using the two above mentioned different approaches.

An interesting general parameter was that the distance among ROI-DMRs identified between the S and C groups (in both BR and SW populations) presented a multi-modal distribution with an exponential growth of the distances from 1–2 K to 20 K, 200 K, and up to 10 M. This is an unexpected pattern that deserves further investigation. We also analyzed the distance of ROI-DMRs in relation to the closest TSS and identified a trimodal distribution of the distances. Interestingly, in both populations one of the peaks of this trimodal distribution was located at the

**TABLE 5 |** Descriptive statistics and gene annotation DMRs found with ADJW and ROI ($P \leq 0.05$) that overlap between BR and SW populations (S vs. C groups).

| Test | Lineage | Location | Width | CpG | % of CpG | LogFC | *P*-value | FDR *p*-value | Position regarding gene | Gene symbol | ENSEMBL name | Gene strand |
|---|---|---|---|---|---|---|---|---|---|---|---|---|
| ADJW | BR | chr11:19110301-19110400 | 100 | 5 | 5% | 1 | 1.61E-02 | 1.00E+00 | Intron/5 prime UTR | DBNDD1/CDH1 | ENSGALG00000000528/ ENSGALG00000000608 | −1 |
| | SW | | | | | −2.4 | 4.14E-02 | 1.00E+00 | Upstream gene | URAH/ CDH1 | ENSGALG00000000549/ ENSGALG00000000608 | −1 |
| | BR | chr20:49501-49600 | 100 | 6 | 6% | −1.3 | 9.27E-03 | 1.00E+00 | Intergenic | – | – | – |
| | SW | | | | | −4.4 | 4.18E-05 | 2.03E-01 | | | | |
| ROI | BR | chr2:256975-257649 | 675 | 25 | 4% | 0.8 | 3.31E-02 | 1.00E+00 | Intron | – | ENSGALG00000031276 | −1 |
| | SW | chr2:256386-257357 | 972 | 41 | 4% | 3.5 | 4.35E-02 | 4.80E-01 | | | | |

*/ DMRs commonly related to more than one gene.*

TSS, while the other two peaks were located at −10 and +20 Kbps from the TSS, (**Figure 6**). These distributions were consistent across chromosome types (autosomal or sexual).

The most frequent DMR peaks identified in this study were located around a gene TSS (**Figure 6**). This finding may have important functional consequences, since methylation levels in TSS are reported to be highly predictive of gene expression activity (Teschendorff and Relton, 2018). The peak found 10 Kbps upstream of the TSS suggests the presence of TFBS. Although studies, in general, focus on promoter-proximal regulatory regions, the influence of TF binding distant to TSS (even as far as >20 kb) to gene expression is also of relevance (McCord et al., 2011). The dynamic binding of transcription factors to TFBS is known to be affected by DNA methylation, but the specific ways this interaction occurs is still a matter of investigation (Héberlé and Bardet, 2019). Another peak identified was spread between 20 and 40 Kbps downstream of the TSS. This corresponds to terminal or downstream regions in genes. Downstream gene regions are associated with complex genetic networks in living cells, mainly at the protein regulation and degradation level (Moriya et al., 2014). The downstream boundary is also near to the downstream core promoter element (DPE), which has a particularly important role in transcription regulation by RNA polymerase II (Kadonaga, 2002).

The observation of specific peaks with a high presence of ROI-DMRs in relation to the TSS and the fact that these peaks were located in regions of potential regulation by transcription factors prompted us to investigate the possibility that these peaks could be enriched for a specific TFBS. The following TFBS motifs were highly present (>50%) in these ROI-DMRs: Tfcp2l1 and Esrrb in all ROI-DMR peaks, RELA in all but the TSS BR peak, KLF4 in the 20–40 kb downstream and TSS SW peaks, and Zfx in the 10 kb upstream and TSS BR peaks. Of particular interest is the fact that nearly 100% of these ROI-DMRs had hits against the Tfcp2l1 motif. Thus, some sequence variations of the Tfcp2l1 TFBS motif that contain CpGs could be transversal indicators of DNA methylation changes in relation to stress. Interestingly, recent research shows, in mouse and humans, that Esrrb and Klf4 are regulatory targets of Tfcp2l1 (Wang et al., 2019). Our results suggest that these effects could be mediated by DNA methylation. These are interesting findings that deserve further investigation, particularly in relation to the role of these transcription factors in the stress response.

Most of the ROI-DMRs identified in this study were located in intronic regions (36%), followed by downstream to genes (28.5%), intergenic regions (21.5%), upstream to genes (7%), and coding sequences (7%). Exon–intron boundaries have a well characterized role in guiding the splicing machinery (Schwartz and Ast, 2010). DMRs between exons, splice sites, and flanking-intronic regions are reported to be involved in the regulation of alternative splicing (Lev Maor et al., 2015). Moreover, it is known that methylation in regulatory regions (e.g., promoters) are usually associated with transcriptional repression, while in gene bodies, DNA methylation is associated with high levels of gene expression (Jones, 1999; Meissner et al., 2008; Deaton and Bird, 2011). Indeed, independent of the threshold used, most of our DMRs (including the ones overlapping between lineages)

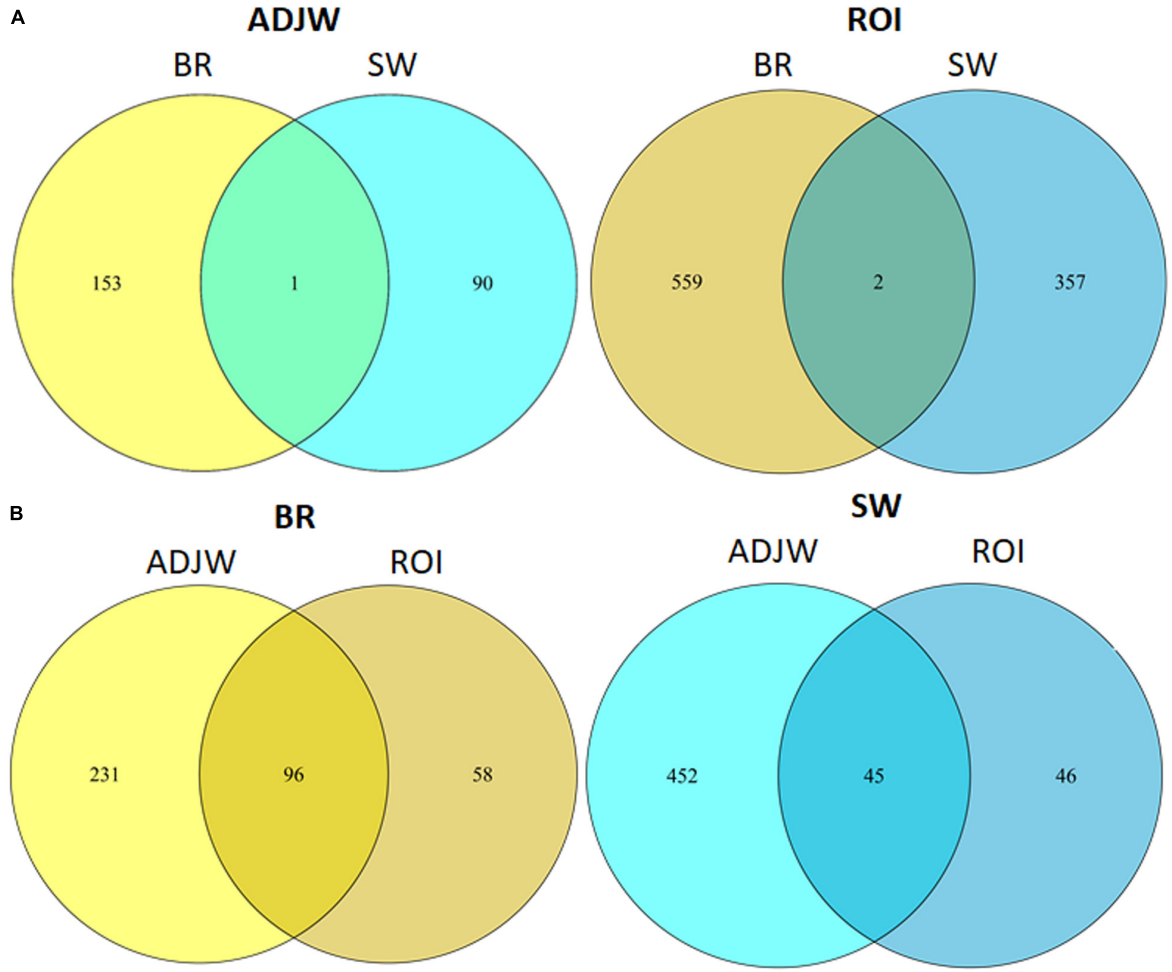



**FIGURE 7 |** Venn diagram showing the number of ROI-DMRs overlapping between **(A)** lineages within each DMR detection method employed, and **(B)** DMR detection methods employed within each lineage.

**TABLE 6 |** Pathways overlapping between BR and SW lineages after pathway enrichment performed with Reactome in each population using $p < 0.05$ DMRs.

| Lineage | DMR location | Related gene | GENE NAME | Consequence | Pathway | |
|---|---|---|---|---|---|---|
| | | | | | Identifier | Name |
| BR | 12:11592836-11593728 | ENSGALG00000006802 | *LAMB2* | Coding sequence, intron | R-GGA-3000157 | Laminin interactions |
| SW | 7:6634619-6634980 | ENSGALG00000038311 | *COL18A1* | Intron | | |
| BR | chr1:61077944-61078198 | ENSGALG00000036964 | *Novel gene* | Intron | R-GGA-5576891 | Cardiac conduction |
| SW | chr26:1304953-1305335 | ENSGALG00000000329 | *AHCYL1* | Coding sequence, intron | | |

*Functional annotation of the entities used to identify these pathways are also shown.*

were primarily located in intronic regions, followed by down- and upstream gene regions, and coding sequences (exons) (**Figure 4**). Up- and downstream gene regions contain insulator elements that "protect" genes from inappropriate signals emanating from neighboring genes (Blackwood, 1998).

Differentially methylated regions were preferentially located in microchromosomes and in ChrZ in both lineages studied (**Figure 5**). ROI-DMRs in the sex ChrZ were present at a rate 2.38× (BR) and 4.47× (SW) higher than randomly expected. Therefore, this strongly suggests that ChrZ is a hotspot of DMRs induced by stress in RBCs. Ten ROI-DMRs were identified in the ChrZ of the BR population, while 13 ROI-DMRs were identified in the ChrZ of the SW population ($P \leq 0.05$). Most of these DMRs were located within intronic regions of novel genes. Studies have shown an important role for sex chromosomes in the stress response (Seney et al., 2013). In humans, the sex chromosome is reported to be involved in regulating the expression of mood-related genes (Seney et al., 2013), and in mice the Y

chromosome has been shown to affect several neurobehavioral traits (Sluyter et al., 1999).

In relation to specific DMRs that could be putative markers of stress, we identified 7 DMRs in the BR and 4 DMRs in the SW lineages when using a stringent threshold ($P \leq 0.0005$) (**Table 3**). The only DMR that passed FDR correction ($\leq$0.05) in both ROI and ADJW analysis was identified in the BR population. This DMR is located in Chr28 and 1,994 bps upstream the TSS of the *ADAMTSL5* gene, at its promotor region. In addition, this DMR is located downstream ($\leq$3 kb) of the *THOP1* gene *ADAMTSL5* (thrombospondin type-1 domain-containing protein 6), is involved in the degradation of the extracellular matrix, has antiangiogenic properties, and plays an important role in inflammatory processes. Hypermethylation of the *ADAMTSL5* gene is associated with chemoresistance to acute lymphoblastic leukemia in humans (Abdullah et al., 2017). *THOP* (thimet oligopeptidase 1) is important in metabolism regulation, being broadly expressed in testis (Pineau et al., 1999). *THOP1* codes a kinase protein that uses zinc as a cofactor in humans (Gene ID: 7064). One of the mechanisms of downregulation of this gene is suggested to be hypermethylation of its promoter region (Nomoto et al., 2014). In our study, this region downstream of the *THOP1* gene was hypermethylated in the stressed group. Two significant DMRs ($P \leq 0.0005$) were identified in ChrZ (ROI: chrZ: 7,337,093–7,337,617 and ADJW: chrZ: 70,400,401–70,400,700). One of them was in an intergenic position in SW animals and the other was located in an intron of the *UBE2R2* gene in BR animals. The *UBE2R2* gene is related to protein ubiquitination of many processes (R4GIV8_CHICK), and is reported to be one of the 14 Z-linked zebra-finch genes that has likely diverged from the Galliform lineage (Itoh et al., 2006).

We compared the DMRs obtained across our two experiments to find common DMRs emerging after social isolation stress between lineages. We were able to identify 3 DMRs ($P \leq 0.05$, see **Figure 7** and **Table 5**) overlapping between the BR and SW individuals. These overlapping DMRs were located on Chr2, 11, and 20 and in intronic (ENSGALG00000031276, *DBNND1* and *CDH1* genes), upstream (*URAH* and *CDH1* genes), and intergenic regions in these chromosomes, respectively. The genes associated to these DMRs are involved in cancer diseases in vertebrates. Downregulation or inactivation of the *CDH1* gene is involved in cancer progression and metastasis (Beavon, 2000). Interestingly, its regulation is dependent on many mechanisms (Acs et al., 2001) including germline mutations (Guilford et al., 1998; Pharoah et al., 2001) and promotor hypermethylation (Yoshiura et al., 1995; Stevenson et al., 2010). The *URAH* gene is associated with hepatomegaly and hepatocellular carcinoma in mice. The *ArfGAT* gene (ENSGALG00000031276) is part of the Arf family of proteins, which are involved in cancer progression, through cell–cell adhesion, integrin internalization and recycling, and actin cytoskeleton remodeling (Casalou et al., 2016). These genes can be considered strong candidates for future studies aiming at diagnosing long-term stress in the production environment by tracking epigenetic changes in RBCs of chickens.

Using subsets of gene-related DMRs ($P \leq 0.05$) we performed gene enrichment analyses in SW and BR lineages. We selected two overlapping pathways found between these lineages to be discussed: "Laminin interactions" (R-HSA-3000157), which describes the action of multi-domain trimeric basement membrane proteins contributing to the structure of the extracellular matrix, thereby influencing the behavior of associated cells, such as adhesion, differentiation, migration, phenotype stability, and resistance to anoikic (Domogatskaya et al., 2012); and "cardiac conduction" (R-GGA-5576891), which involves the mechanism of the normal sequence of contraction of atria and ventricles of the heart activated by a groups of cardiac cells. The genes participating in these common pathways are mostly related to cancer and other diseases in vertebrates. Mutations in the *LAMB2* gene cause autosomal recessive Pierson syndrome, a congenital nephrotic disorder syndrome that culminates in ocular and neurologic abnormalities (Matejas et al., 2010). The *COL18A1* gene is associated with neovascularization and vascular permeability in atherosclerosis in mice (Moulton et al., 2004) and is also reported to inhibit angiogenesis and tumor growth (Arvanitidis and Karsdal, 2016). The *AHCYL1* gene is a estrogen-stimulated gene expressed in the chicken oviduct affecting growth, development, and calcium metabolism of the mature oviduct of hens (Jeong et al., 2012b). *AHCYL1* expression is associated with ovarian carcinogenesis as an oncogene in chickens, however, has a paradoxical effect as a tumor suppressor in human epithelial ovarian cancer (Jeong et al., 2012a).

These findings are relevant for the future identification of epigenetic markers of stress in RBCs, a tissue that is subjected to systemic hormonal fluctuations caused by a centrally produced stress response. Curiously, all levels of analyses performed in this study showed that basically all genes related to stress-responsive DMRs in RBCs (caused by the environmental effect) have already been studied and related to abnormalities or disorders. These abnormalities are often considered to be inherited or represent idiopathic etiologies but are not generally associated with epigenetic alterations caused by detrimental exposures such as long-term stress.

## CONCLUSION

This paper describes potential candidate genes for stress diagnosis across layer populations of chickens reared in different biomes. With a $P \leq 0.05$ we found 4 genes related to 3 DMRs observed in both populations analyzed here. Among the gene-related DMRs obtained, we also found 4 genes related to the top two biological pathways enrichedin both BR and SW populations. These DMRs were within or nearby ($3 \leq$ kb far) genes. In addition, we provide a robust list of DMRs related to an experimental condition that is well known to generate stress response and consequently, compromise the animals' health. Interestingly, the sexual ChrZ had a DMR rate higher than randomly expected, indicating that this chromosome is a strong candidate for screening for epigenetic changes caused by stress. The biological functions of the genes associated to the DMRs found in our study, and their related enriched pathways, are relevant for the function of the tissue investigated (RBC). Our results suggest that most of the identified DMRs are enriched near TSS, DPE, and specific TFBS. These DMRs could be tested more

extensively as markers for long-term stress diagnosis in order to monitor good practices in real life animal production setups.

## DATA AVAILABILITY STATEMENT

The datasets generated for this study can be found in the ENA, http://www.ebi.ac.uk/ena/data/view/PRJEB34868.

## ETHICS STATEMENT

All animal experimental protocols employed in the present study were performed in accordance with international guidelines for animal welfare. In Brazil, the study was approved by the resolution #008/2017 from the Embrapa Swine and Poultry Ethics Committee on Animal Utilization (CEUA) following the National Council for the Control of Animal Experimentation (CONCEA). In Sweden the study was under the license #50-13 from the Regional Committee for Scientific Research on Animals from Linköping, Sweden.

## AUTHOR CONTRIBUTIONS

FP analyzed the data and wrote the manuscript with the valuable help of CG-B and MP. PJ and CG-B were responsible for the experiments design in Sweden, while LC, ML, and FP were responsible for the experiments design at the Brazilian facilities. AI and ML were responsible for conducting the field experiments carried out in Brazil, while MS conducted the experiments in the Swedish facilities, which included tissue sampling and DNA extraction. MS, AF, SR, and AI carried out the lab work for sequencing library prep. LC, ML, PJ, and CG-B provided the lab and office infrastructure. LC, ML, CG-B, and PJ provided overall supervision for the research activities. The final version of the manuscript was produced by FP and CG-B. All authors reviewed the final drafts and approved the last version of the manuscript.

## FUNDING

The authors greatly appreciate funding from the Brazilian Agricultural Research Corporation (Embrapa) project #11.15.02.003.05.03, the São Paulo Research Foundation (FAPESP) thematic project #2014/08704-0 to LLC, the European Research Council (ERC) advanced grant #322206 'GeneWell' to PJ, and the Swedish Research Council for Sustainable Development (FORMAS) grants #2018-01074 and #2017-00946 to CG-B. FP appreciates funding from FAPESP projects #2016/20440-3 and #2018/13600-0. ML and LC thank the National Council for Scientific and Technological Development (CNPq) for research fellowships. The authors acknowledge the support from the National Genomics Infrastructure in Stockholm funded by the Science for Life Laboratory, the Knut and Alice Wallenberg Foundation, and the Swedish Research Council. Likewise, the authors appreciate the computational resources provided by the SNIC/Uppsala Multidisciplinary Center for Advanced Computational Science, for assistance with massive parallel sequencing and for access to the UPPMAX computational infrastructure.

## ACKNOWLEDGMENTS

Sincere thanks to Marcio Gilberto Saatkamp for his essential contribution in conducting the experiments at the Brazilian facility. The authors are grateful for the infrastructure support from the University of São Paulo, Linköping University, and the Embrapa Swine and Poultry National Research Center.

## SUPPLEMENTARY MATERIAL

The Supplementary Material for this article can be found online at: https://www.frontiersin.org/articles/10.3389/fgene.2020.508809/full#supplementary-material

## REFERENCES

Abdullah, M., Choo, C. W., Alias, H., Abdul Rahman, E. J., Mohd Ibrahim, H., Jamal, R., et al. (2017). ADAMTSL5 and CDH11: putative epigenetic markers for therapeutic resistance in acute lymphoblastic leukemia. *Hematology* 22, 386–391. doi: 10.1080/10245332.2017.1299417

Acs, G., Lawton, T. J., Rebbeck, T. R., LiVolsi, V. A., and Zhang, P. J. (2001). Differential Expression of E-Cadherin in Lobular and Ductal Neoplasms of the Breast and Its Biologic and Diagnostic Implications. *Am. J. Clin. Pathol.* 115, 85–98. doi: 10.1309/FDHX-L92R-BATQ-2GE0

Andrews, S. (2010). *FASTQC. A Quality Control Tool for High Throughput Sequence Data*. Available online at: http://www.bioinformatics.babraham.ac.uk/projects/fastqc (accessed November 26, 2017).

Arvanitidis, A., and Karsdal, M. A. (2016). *Biochemistry of Collagens, Laminins and Elastin*. Netherland: Elsevier, 97–99.

Beavon, I. R. . (2000). The E-cadherin-catenin complex in tumour metastasis. *Eur. J. Cancer* 36, 1607–1620. doi: 10.1016/S0959-8049(00)00158-1

Bélteky, J., Agnvall, B., Bektic, L., Höglund, A., Jensen, P., and Guerrero-Bosagna, C. (2018). Epigenetics and early domestication: differences in hypothalamic DNA methylation between red junglefowl divergently selected for high or low fear of humans. *Genet. Sel. Evol.* 50:13. doi: 10.1186/s12711-018-0384-z

Berk, S. A., McGettrick, J. R., Hansen, W. K., and Breuner, C. W. (2016). Methodological considerations for measuring glucocorticoid metabolites in feathers. *Conserv. Physiol.* 4:cow020. doi: 10.1093/conphys/cow020

Blackwood, E. M. (1998). Going the Distance: A Current View of Enhancer Action. *Science* 281, 60–63. doi: 10.1126/science.281.5373.60

Broos, S., Soete, A., Hooghe, B., Moran, R., van Roy, F., and De Bleser, P. (2013). PhysBinder: improving the prediction of transcription factor binding sites by flexible inclusion of biophysical properties. *Nucl. Acids Res.* 41, W531–W534. doi: 10.1093/nar/gkt288

Cao, Y., Jin, H.-G., Ma, H.-H., and Zhao, Z.-H. (2017). Comparative analysis on genome-wide DNA methylation in longissimus dorsi muscle between Small Tailed Han and Dorper×Small Tailed Han crossbred sheep. *Asian Austr. J. Anim. Sci.* 30, 1529–1539. doi: 10.5713/ajas.17.0154

Capra, E., Toschi, P., Del Corvo, M., Lazzari, B., Scapolo, P. A., Loi, P., et al. (2017). Genome-Wide Epigenetic Characterization of Tissues from Three Germ Layers Isolated from Sheep Fetuses. *Front. Genet.* 8:115. doi: 10.3389/fgene.2017.00115

Casalou, C., Faustino, A., and Barral, D. C. (2016). Arf proteins in cancer cell migration. *Small GTPases* 7, 270–282. doi: 10.1080/21541248.2016.1228792

Catchen, J. M., Amores, A., Hohenlohe, P., Cresko, W., and Postlethwait, J. H. (2011). Stacks: Building and Genotyping Loci De Novo From Short-Read Sequences. *G3 Amp* 58, 171–182. doi: 10.1534/g3.111.000240

Cavalcante, R. G., Qin, T., and Sartor, M. A. (2019). *Novel Bioinformatics Methods for Toxicoepigenetics Toxicoepigenetics*. Netherland: Elsevier, 265–288. doi: 10.1016/B978-0-12-812433-8.00012-5

Choi, M., Lee, J., Le, M. T., Nguyen, D. T., Park, S., Soundrarajan, N., et al. (2015). Genome-wide analysis of DNA methylation in pigs using reduced representation bisulfite sequencing. *DNA Res.* 22, 343–355. doi: 10.1093/dnares/dsv017

Croft, D., Mundo, A. F., Haw, R., Milacic, M., Weiser, J., Wu, G., et al. (2014). The Reactome pathway knowledgebase. *Nucl. Acids Res.* 42, D472-D477. doi: 10.1093/nar/gkt1102

Croft, D., O'Kelly, G., Wu, G., Haw, R., Gillespie, M., Matthews, L., et al. (2011). Reactome: a database of reactions, pathways and biological processes. *Nucl. Acids Res.* 39, D691-D697. doi: 10.1093/nar/gkq1018

Deaton, A. M., and Bird, A. (2011). CpG islands and the regulation of transcription. *Genes Dev.* 25, 1010–1022. doi: 10.1101/gad.2037511

Denham, J., Marques, F. Z., Bruns, E. L., O'Brien, B. J., and Charchar, F. J. (2016). Epigenetic changes in leukocytes after 8 weeks of resistance exercise training. *Eur. J. Appl. Physiol.* 116, 1245–1253. doi: 10.1007/s00421-016-3382-2

Diez-Silva, M., Dao, M., Han, J., Lim, C.-T., and Suresh, S. (2010). Shape and Biomechanical Characteristics of Human Red Blood Cells in Health and Disease. *MRS Bull.* 35, 382–388.

Dolinoy, D. C., Huang, D., and Jirtle, R. L. (2007). Maternal nutrient supplementation counteracts bisphenol A-induced DNA hypomethylation in early development. *Proc. Natl. Acad. Sci.* 104, 13056–13061. doi: 10.1073/pnas.0703739104

Domogatskaya, A., Rodin, S., and Tryggvason, K. (2012). Functional Diversity of Laminins. *Annu. Rev. Cell Dev. Biol.* 28, 523–553. doi: 10.1146/annurev-cellbio-101011-155750

Eberhart, D. E., and Washburn, K. W. (1993). Assessing the Effects of the Naked Neck Gene on Chronic Heat Stress Resistance in Two Genetic Populations. *Poult. Sci.* 72, 1391–1399. doi: 10.3382/ps.0721391

Elshire, R. J., Glaubitz, J. C., Sun, Q., Poland, J. A., Kawamoto, K., Buckler, E. S., et al. (2011). A Robust, Simple Genotyping-by-Sequencing (GBS) Approach for High Diversity Species. *PLoS One* 6:e19379. doi: 10.1371/journal.pone.0019379

Fagiolini, M., Jensen, C. L., and Champagne, F. A. (2009). Epigenetic influences on brain development and plasticity. *Curr. Opin. Neurobiol.* 19, 207–212. doi: 10.1016/j.conb.2009.05.009

Fallahsharoudi, A., de Kock, N., Johnsson, M., Ubhayasekera, S. J. K. A., Bergquist, J., Wright, D., et al. (2015). Domestication Effects on Stress Induced Steroid Secretion and Adrenal Gene Expression in Chickens. *Sci. Rep.* 5:15345. doi: 10.1038/srep15345

Fang, X., Zhao, Z., Yu, H., Li, G., Jiang, P., Yang, Y., et al. (2017). Comparative genome-wide methylation analysis of longissimus dorsi muscles between Japanese black (Wagyu) and Chinese Red Steppes cattle. *PLoS One* 12:e0182492. doi: 10.1371/journal.pone.0182492

Feil, R., and Fraga, M. F. (2012). Epigenetics and the environment: emerging patterns and implications. *Nat. Rev. Genet.* 13, 97–109. doi: 10.1038/nrg3142

Feng, J., Liu, T., Qin, B., Zhang, Y., and Liu, X. S. (2012). Identifying ChIP-seq enrichment using MACS. *Nat. Protoc.* 7, 1728–1740. doi: 10.1038/nprot.2012.101

Frésard, L., Morisson, M., Brun, J.-M., Collin, A., Pain, B., Minvielle, F., et al. (2013). Epigenetics and phenotypic variability: some interesting insights from birds. *Genet. Sel. Evol.* 45:16. doi: 10.1186/1297-9686-45-16

Fulton, J. E. (2006). Avian Genetic Stock Preservation: An Industry Perspective. *Poult. Sci.* 85, 227–231. doi: 10.1093/ps/85.2.227

Gao, F., Zhang, J., Jiang, P., Gong, D., Wang, J.-W., Xia, Y., et al. (2014). Marked methylation changes in intestinal genes during the perinatal period of preterm neonates. *BMC Genom.* 15:716. doi: 10.1186/1471-2164-15-716

Glaubitz, J. C., Casstevens, T. M., Lu, F., Harriman, J., Elshire, R. J., Sun, Q., et al. (2014). TASSEL-GBS: a high capacity genotyping by sequencing analysis pipeline. *PLoS One* 9:e90346. doi: 10.1371/journal.pone.0090346

Goerlich, V. C., Nätt, D., Elfwing, M., Macdonald, B., and Jensen, P. (2012). Transgenerational effects of early experience on behavioral, hormonal and gene expression responses to acute stress in the precocial chicken. *Horm. Behav.* 61, 711–718. doi: 10.1016/j.yhbeh.2012.03.006

Guerrero-Bosagna, C. M., Sabat, P., Valdovinos, F. S., Valladares, L. E., and Clark, S. J. (2008). Epigenetic and phenotypic changes result from a continuous pre and post natal dietary exposure to phytoestrogens in an experimental population of mice. *BMC Physiol.* 8:17. doi: 10.1186/1472-6793-8-17

Guerrero-Bosagna, C., and Jensen, P. (2015). Optimized method for methylated DNA immuno-precipitation. *MethodsX* 2, 432–439. doi: 10.1016/j.mex.2015.10.006

Guerrero-Bosagna, C., and Skinner, M. K. (2012). Environmentally induced epigenetic transgenerational inheritance of phenotype and disease. *Mol. Cell. Endocrinol.* 354, 3–8. doi: 10.1016/j.mce.2011.10.004

Guerrero-Bosagna, C., Pértille, F., Gomez, Y., Rezaei, S., Gebhardt, S., Vögeli, S., et al. (2020). DNA methylation variation in the brain of laying hens in relation to differential behavioral patterns. *Comp. Biochem. Physiol. Part D Genom. Proteom.* 35:100700. doi: 10.1016/j.cbd.2020.100700

Guilford, P., Hopkins, J., Harraway, J., McLeod, M., McLeod, N., Harawira, P., et al. (1998). E-cadherin germline mutations in familial gastric cancer. *Nature* 392, 402–405. doi: 10.1038/32918

Habermann, F. A., Cremer, M., Walter, J., Kreth, G., von Hase, J., Bauer, K., et al. (2001). Arrangements of macro- and microchromosomes in chicken cells. *Chromosome Res.* 9, 569–584. doi: 10.1023/A:1012447318535

Han, M. V, and Zmasek, C. M. (2009). phyloXML: XML for evolutionary biology and comparative genomics. *BMC Bioinform.* 10:356. doi: 10.1186/1471-2105-10-356

Héberlé, É., and Bardet, A. F. (2019). Sensitivity of transcription factors to DNA methylation. *Essays Biochem.* 63, 727–741. doi: 10.1042/EBC20190033

Heimbürge, S., Kanitz, E., and Otten, W. (2019). The use of hair cortisol for the assessment of stress in animals. *Gen. Comp. Endocrinol.* 270, 10–17. doi: 10.1016/j.ygcen.2018.09.016

Henry, J. P. (1993). Psychological and physiological responses to stress: the right hemisphere and the hypothalamo-pituitary-adrenal axis, an inquiry into problems of human bonding. *Integr. Physiol. Behav. Sci.* 28, 369–87.

Hoops, S., Sahle, S., Gauges, R., Lee, C., Pahle, J., Simus, N., et al. (2006). COPASI–a COmplex PAthway SImulator. *Bioinformatics* 22, 3067–3074. doi: 10.1093/bioinformatics/btl485

Ishibashi, M., Akiyoshi, H., Iseri, T., and Ohashi, F. (2013). Skin conductance reflects drug-induced changes in blood levels of cortisol, adrenaline and noradrenaline in dogs. *J. Vet. Med. Sci.* 75, 809–813. doi: 10.1292/jvms.12-0478

Itoh, Y., Kampf, K., and Arnold, A. P. (2006). Comparison of the chicken and zebra finch Z chromosomes shows evolutionary rearrangements. *Chromosom. Res.* 14, 805–815. doi: 10.1007/s10577-006-1082-1

Jeong, W., Kim, H. S., Kim, Y. B., Kim, M. A., Lim, W., Kim, J., et al. (2012a). Paradoxical expression of AHCYL1 affecting ovarian carcinogenesis between chickens and women. *Exp. Biol. Med.* 237, 758–767. doi: 10.1258/ebm.2012.011433

Jeong, W., Kim, J., Ahn, S. E., Lee, S. I., Bazer, F. W., Han, J. Y., et al. (2012b). AHCYL1 Is Mediated by Estrogen-Induced ERK1/2 MAPK Cell Signaling and MicroRNA Regulation to Effect Functional Aspects of the Avian Oviduct. *PLoS One* 7:e49204. doi: 10.1371/journal.pone.0049204

Jones, P. A. (1999). The DNA methylation paradox. *Trends Genet.* 15, 34–7. .

Kadonaga, J. T. (2002). The DPE, a core promoter element for transcription by RNA polymerase II. *Exp. Mol. Med.* 34, 259–264. doi: 10.1038/emm.2002.36

Kain, K. H., Miller, J. W. I., Jones-Paris, C. R., Thomason, R. T., Lewis, J. D., Bader, D. M., et al. (2014). The chick embryo as an expanding experimental model for cancer and cardiovascular research. *Dev. Dyn.* 243, 216–228. doi: 10.1002/dvdy.24093

Kile, M. L., Andres Houseman, E., Baccarelli, A. A., Quamruzzaman, Q., Rahman, M., Mostofa, G., et al. (2014). Effect of prenatal arsenic exposure on DNA methylation and leukocyte subpopulations in cord blood. *Epigenetics* 9, 774–782. doi: 10.4161/epi.28153

Korthauer, K., Kimes, P. K., Duvallet, C., Reyes, A., Subramanian, A., Teng, M., et al. (2019). A practical guide to methods controlling false discoveries in computational biology. *Genome Biol.* 20:118. doi: 10.1186/s13059-019-1716-1

Krämer, A., Green, J., Pollard, J., and Tugendreich, S. (2014). Causal analysis approaches in Ingenuity Pathway Analysis. *Bioinformatics* 30, 523–530. doi: 10.1093/bioinformatics/btt703

Langmead, B., and Salzberg, S. L. (2012). Fast gapped-read alignment with Bowtie 2. *Nat. Methods* 9, 357–359. doi: 10.1038/nmeth.1923

Lentini, A., Lagerwall, C., Vikingsson, S., Mjoseng, H. K., Douvlataniotis, K., Vogt, H., et al. (2018). A reassessment of DNA-immunoprecipitation-based genomic profiling. *Nat. Methods* 15, 499–504. doi: 10.1038/s41592-018-0038-7

Lev Maor, G., Yearim, A., and Ast, G. (2015). The alternative role of DNA methylation in splicing regulation. *Trends Genet.* 31, 274–280. doi: 10.1016/j.tig.2015.03.002

Li, H., Handsaker, B., Wysoker, A., Fennell, T., Ruan, J., Homer, N., et al. (2009). The sequence alignment/map format and SAMtools. *Bioinformatics* 25, 2078–2079. doi: 10.1093/bioinformatics/btp352

Lienhard, M., Grimm, C., Morkel, M., Herwig, R., and Chavez, L. (2014). MEDIPS: genome-wide differential coverage analysis of sequencing data derived from DNA enrichment experiments. *Bioinformatics* 30, 284–286. doi: 10.1093/bioinformatics/btt650

Luo, C., Hajkova, P., and Ecker, J. R. (2018). Dynamic DNA methylation: In the right place at the right time. *Science* 361, 1336–1340. doi: 10.1126/science.aat6806

Matejas, V., Hinkes, B., Alkandari, F., Al-Gazali, L., Annexstad, E., Aytac, M. B., et al. (2010). Mutations in the human laminin β2 (LAMB2) gene and the associated phenotypic spectruma. *Hum. Mutat.* 31, 992–1002. doi: 10.1002/humu.21304

McCord, R. P., Zhou, V. W., Yuh, T., and Bulyk, M. L. (2011). Distant cis-regulatory elements in human skeletal muscle differentiation. *Genomics* 98, 401–411. doi: 10.1016/j.ygeno.2011.08.003

McLaren, W., Pritchard, B., Rios, D., Chen, Y., Flicek, P., and Cunningham, F. (2010). Deriving the consequences of genomic variants with the Ensembl API and SNP Effect Predictor. *Bioinformatics* 26, 2069–2070. doi: 10.1093/bioinformatics/btq330

Meissner, A., Mikkelsen, T. S., Gu, H., Wernig, M., Hanna, J., Sivachenko, A., et al. (2008). Genome-scale DNA methylation maps of pluripotent and differentiated cells. *Nature* 454, 766–770. doi: 10.1038/nature07107

Meluzzi, A., Fabbri, C., Folegatti, E., and Sirri, F. (2008). Survey of chicken rearing conditions in Italy: effects of litter quality and stocking density on productivity, foot dermatitis and carcase injuries. *Br. Poult. Sci.* 49, 257–264. doi: 10.1080/00071660802094156

Mi, H., Muruganujan, A., Casagrande, J. T., and Thomas, P. D. (2013). Large-scale gene function analysis with the PANTHER classification system. *Nat. Protoc.* 8, 1551–1566. doi: 10.1038/nprot.2013.092

Moriya, T., Yamamura, M., and Kiga, D. (2014). Effects of downstream genes on synthetic genetic circuits. *BMC Syst. Biol.* 8:S4. doi: 10.1186/1752-0509-8-S4-S4

Moulton, K. S., Olsen, B. R., Sonn, S., Fukai, N., Zurakowski, D., and Zeng, X. (2004). Loss of Collagen XVIII Enhances Neovascularization and Vascular Permeability in Atherosclerosis. *Circulation* 110, 1330–1336. doi: 10.1161/01.CIR.0000140720.79015.3C

Mueller, B. U., Martin, K. J., Dreyer, W., Bezold, L. I., and Mahoney, D. H. (2006). Prolonged QT interval in pediatric sickle cell disease. *Pediatr. Blood Cancer* 47, 831–833. doi: 10.1002/pbc.20539

Müller, S., Lehnert, K., Seibel, H., Driver, J., Ronnenberg, K., Teilmann, J., et al. (2013). Evaluation of immune and stress status in harbour porpoises (Phocoena phocoena): can hormones and mRNA expression levels serve as indicators to assess stress? *BMC Vet. Res.* 9:145. doi: 10.1186/1746-6148-9-145

Niazi, U., Geyer, K. K., Vickers, M. J., Hoffmann, K. F., and Swain, M. T. (2016). DISMISS: detection of stranded methylation in MeDIP-Seq data. *BMC Bioinformatics* 17:295. doi: 10.1186/s12859-016-1158-7

Nomoto, S., Hishida, M., Inokawa, Y., Takano, N., Kanda, M., Nishikawa, Y., et al. (2014). Expression Analysis of THOP1 in Background Liver, a Prognostic Predictive Factor in Hepatocellular Carcinoma, Extracted by Multiarray Analysis. *Ann. Surg. Oncol.* 21, 443–450. doi: 10.1245/s10434-014-3581-1

O'Neill, J. S., and Reddy, A. B. (2011). Circadian clocks in human red blood cells. *Nature* 469, 498–503. doi: 10.1038/nature09702

Peeters, M., Sulon, J., Beckers, J.-F., Ledoux, D., and Vandenheede, M. (2011). Comparison between blood serum and salivary cortisol concentrations in horses using an adrenocorticotropic hormone challenge. *Equine Vet. J.* 43, 487–493. doi: 10.1111/j.2042-3306.2010.00294.x

Pértille, F., Brantsæter, M., Nordgreen, J., and Coutinho, L. L. (2017a). DNA methylation profiles in red blood cells of adult hens correlate to their rearing conditions. *J. Exp. Biol.* 220, 3579–3587. doi: 10.1242/jeb.157891

Pértille, F., Da Silva, V. H., Johansson, A. M., Lindström, T., Wright, D., Coutinho, L. L., et al. (2019). Mutation dynamics of CpG dinucleotides during a recent event of vertebrate diversification. *Epigenetics* 14, 1–23. doi: 10.1080/15592294.2019.1609868

Pértille, F., Guerrero-Bosagna, C., Silva, V. H. da, Boschiero, C., Nunes, J. de R. da S., Ledur, M. C., et al. (2016). High-throughput and Cost-effective Chicken Genotyping Using Next-Generation Sequencing. *Sci. Rep.* 6:26929. doi: 10.1038/srep26929

Pértille, F., Moreira, G. C. M., Zanella, R., Nunes, J. de R. da S., Boschiero, C., Rovadoscki, G. A., et al. (2017b). Genome-wide association study for performance traits in chickens using genotype by sequencing approach. *Sci. Rep.* 7:41748. doi: 10.1038/srep41748

Pharoah, P. D. P., Guilford, P., and Caldas, C. (2001). Incidence of gastric cancer and breast cancer in CDH1 (E-cadherin) mutation carriers from hereditary diffuse gastric cancer families. *Gastroenterology* 121, 1348–1353. doi: 10.1053/gast.2001.29611

Pineau, C., McCool, S., Glucksman, M. J., Jégou, B., and Pierotti, A. R. (1999). Distribution of thimet oligopeptidase (E.C. 3.4.24.15) in human and rat testes. *J. Cell Sci.* 112, 3455–62.

Poland, J. A, Brown, P. J., Sorrells, M. E., and Jannink, J.-L. (2012). Development of high-density genetic maps for barley and wheat using a novel two-enzyme genotyping-by-sequencing approach. *PLoS One* 7:e32253. doi: 10.1371/journal.pone.0032253

Provencal, N., Suderman, M. J., Guillemin, C., Massart, R., Ruggiero, A., Wang, D., et al. (2012). The Signature of Maternal Rearing in the Methylome in Rhesus Macaque Prefrontal Cortex and T Cells. *J. Neurosci.* 32, 15626–15642. doi: 10.1523/JNEUROSCI.1470-12.2012

Richard A. Stein, D. L. D. (2012). Epigenetics: A Fascinating Field with Profound Research, Clinical, & Public Health Implications. *Am. Biol. Teach.* 74, 213–223. doi: 10.1525/abt.2012.74.4.3

Robinson, M. D., and Oshlack, A. (2010). A scaling normalization method for differential expression analysis of RNA-seq data. *Genome Biol.* 11:R25. doi: 10.1186/gb-2010-11-3-r25

Sandercock, D. A., Hunter, R. R., Nute, G. R., Mitchell, M. A., and Hocking, P. M. (2001). Acute Heat Stress-Induced Alterations in Blood Acid-Base Status and Skeletal Muscle Membrane Integrity in Broiler Chickens at Two Ages: Implications for Meat Quality. *Poult. Sci.* 80, 418–425. doi: 10.1093/ps/80.4.418

Schwartz, S., and Ast, G. (2010). Chromatin density and splicing destiny: on the cross-talk between chromatin structure and splicing. *EMBO J.* 29, 1629–1636. doi: 10.1038/emboj.2010.71

Seney, M. L., Ekong, K. I., Ding, Y., Tseng, G. C., and Sibille, E. (2013). Sex chromosome complement regulates expression of mood-related genes. *Biol. Sex Differ.* 4:20. doi: 10.1186/2042-6410-4-20

Sevane, N., Martínez, R., and Bruford, M. W. (2019). Genome-wide differential DNA methylation in tropically adapted Creole cattle and their Iberian ancestors. *Anim. Genet.* 50, 15–26. doi: 10.1111/age.12731

Skinner, M. K., Manikkam, M., and Guerrero-Bosagna, C. (2010). Epigenetic transgenerational actions of environmental factors in disease etiology. *Trends Endocrinol. Metab.* 21, 214–222. doi: 10.1016/j.tem.2009.12.007

Sluyter, F., Korte, S., Van Baal, G. C., De Ruiter, A. J., and Van Oortmerssen, G. (1999). Y Chromosomal and Sex Effects on the Behavioral Stress Response in the Defensive Burying Test in Wild House Mice. *Physiol. Behav.* 67, 579–585. doi: 10.1016/S0031-9384(99)00101-8

Smyth, G. K. (2005). "limma: Linear Models for Microarray Data," *Bioinformatics and Computational Biology Solutions Using R and Bioconductor*, eds R Gentleman, Carey V.J. Huber W. Irizarry R.A. Dudoit S. (New York: Springer-Verlag), 397–420.

Stevenson, W. S., Hyland, C. D., Zhang, J.-G., Morgan, P. O., Willson, T. A., Gill, A., et al. (2010). Deficiency of 5-hydroxyisourate hydrolase causes hepatomegaly and hepatocellular carcinoma in mice. *Proc. Natl. Acad. Sci.* 107, 16625–16630. doi: 10.1073/pnas.1010390107

Su, J., Wang, Y., Xing, X., Liu, J., and Zhang, Y. (2014). Genome-wide analysis of DNA methylation in bovine placentas. *BMC Genomics* 15:12. doi: 10.1186/1471-2164-15-12

Susiarjo, M., Sasson, I., Mesaros, C., and Bartolomei, M. S. (2013). Bisphenol A Exposure Disrupts Genomic Imprinting in the Mouse. *PLoS Genet.* 9:e1003401. doi: 10.1371/journal.pgen.1003401

Teschendorff, A. E., and Relton, C. L. (2018). Statistical and integrative system-level analysis of DNA methylation data. *Nat. Rev. Genet.* 19, 129–147. doi: 10.1038/nrg.2017.86

Wang, D., Szyf, M., Benkelfat, C., Provenal, N., Turecki, G., Caramaschi, D., et al. (2012). Peripheral SLC6A4 DNA methylation is associated with in vivo measures of human brain serotonin synthesis and childhood physical aggression. *PLoS One* 7, 3–10. doi: 10.1371/journal.pone.0039501

Wang, X., and Kadarmideen, H. N. (2019). Genome−wide DNA methylation analysis using next−generation sequencing to reveal candidate genes responsible for boar taint in pigs. *Anim. Genet.* 50, 644–659. doi: 10.1111/age.12842

Wang, X., and Kadarmideen, H. N. (2020). Characterization of Global DNA Methylation in Different Gene Regions Reveals Candidate Biomarkers in Pigs with High and Low Levels of Boar Taint. *Vet. Sci.* 7:77. doi: 10.3390/vetsci7020077

Wang, X., Wang, X., Zhang, S., Sun, H., Li, S., Ding, H., et al. (2019). The transcription factor TFCP2L1 induces expression of distinct target genes and promotes self-renewal of mouse and human embryonic stem cells. *J. Biol. Chem.* 294, 6007–6016. doi: 10.1074/jbc.RA118.006341

Xanthopoulos, A., Giamouzis, G., Melidonis, A., Kitai, T., Paraskevopoulou, E., Paraskevopoulou, P., et al. (2017). Red blood cell distribution width as a prognostic marker in patients with heart failure and diabetes mellitus. *Cardiovasc. Diabetol.* 16:81. doi: 10.1186/s12933-017-0563-1

Yanagita, K., Shiraishi, J., Kawakami, S.-I., and Bungo, T. (2011). Time Course Changes in the Blood Parameters and the Expression of Diencephalic CRH and AVT mRNA Due to Acute Isolation Stress in Chicks. *J. Poult. Sci.* 48, 125–129. doi: 10.2141/jpsa.010120

Yoshiura, K., Kanai, Y., Ochiai, A., Shimoyama, Y., Sugimura, T., and Hirohashi, S. (1995). Silencing of the E-cadherin invasion-suppressor gene by CpG methylation in human carcinomas. *Proc. Natl. Acad. Sci.* 92, 7416–7419. doi: 10.1073/pnas.92.16.7416

Yu, G., Wang, L.-G., and He, Q.-Y. (2015). ChIPseeker: an R/Bioconductor package for ChIP peak annotation, comparison and visualization. *Bioinformatics* 31, 2382–2383. doi: 10.1093/bioinformatics/btv145

Yuan, X.-L., Zhang, Z., Li, B., Gao, N., Zhang, H., Sangild, P. T., et al. (2017). Genome-wide DNA methylation analysis of the porcine hypothalamus-pituitary-ovary axis. *Sci. Rep.* 7:4277. doi: 10.1038/s41598-017-04603-x

Zhang, X., Zhang, S., Ma, L., Jiang, E., Xu, H., Chen, R., et al. (2017). Reduced representation bisulfite sequencing (RRBS) of dairy goat mammary glands reveals DNA methylation profiles of integrated genome-wide and critical milk-related genes. *Oncotarget* 8, 115326–115344. doi: 10.18632/oncotarget.23260

Zhang, Y., Li, F., Feng, X., Yang, H., Zhu, A., Pang, J., et al. (2017). Genome-wide analysis of DNA Methylation profiles on sheep ovaries associated with prolificacy using whole-genome Bisulfite sequencing. *BMC Genomics* 18:759. doi: 10.1186/s12864-017-4068-9

Zhang, Y., Liu, T., Meyer, C. A., Eeckhoute, J., Johnson, D. S., Bernstein, B. E., et al. (2008). Model-based Analysis of ChIP-Seq (MACS). *Genome Biol.* 9:R137. doi: 10.1186/gb-2008-9-9-r137

Zhou, Y., Connor, E. E., Bickhart, D. M., Li, C., Baldwin, R. L., Schroeder, S. G., et al. (2018). Comparative whole genome DNA methylation profiling of cattle sperm and somatic tissues reveals striking hypomethylated patterns in sperm. *Gigascience* 7:giy039. doi: 10.1093/gigascience/giy039

Zulkifli, I. (2013). Review of human-animal interactions and their impact on animal productivity and welfare. *J. Anim. Sci. Biotechnol.* 4:25. doi: 10.1186/2049-1891-4-25

**Conflict of Interest:** The authors declare that the research was conducted in the absence of any commercial or financial relationships that could be construed as a potential conflict of interest.

*Copyright © 2020 Pértille, Ibelli, Sharif, Poleti, Fröhlich, Rezaei, Ledur, Jensen, Guerrero-Bosagna and Coutinho. This is an open-access article distributed under the terms of the Creative Commons Attribution License (CC BY). The use, distribution or reproduction in other forums is permitted, provided the original author(s) and the copyright owner(s) are credited and that the original publication in this journal is cited, in accordance with accepted academic practice. No use, distribution or reproduction is permitted which does not comply with these terms.*

frontiers in Genetics

ORIGINAL RESEARCH
published: 03 November 2020
doi: 10.3389/fgene.2020.562855

# Whole Transcriptome Analysis Identifies the Taxonomic Status of a New Chinese Native Cattle Breed and Reveals Genes Related to Body Size

*Xiao-Dong Zheng[1,2,3,4,5†], Jin Cheng[1,2†], Wen-Juan Qin[1,2,6], Nyamsuren Balsai[1,2], Xuan-Jian Shang[1,2], Meng-Ting Zhang[1,2] and Hong-Quan Chen[1,2,6*]*

[1] School of Animal Science and Technology, Anhui Agricultural University, Hefei, China, [2] Key Laboratory of Anhui Local Livestock and Poultry Genetic Resources Conservation and Biobreeding, Hefei, China, [3] Department of Dermatology, The First Affiliated Hospital of Anhui Medical University, Hefei, China, [4] Key Laboratory of Dermatology (Anhui Medical University), Ministry of Education, Hefei, China, [5] Key Laboratory of Major Autoimmune Diseases, Hefei, China, [6] International Immunization Center, Anhui Agricultural University, Hefei, China

Wandong (WD) cattle has recently been identified as a new Chinese native cattle breed by the National Commission for Livestock and Poultry Genetic Resources. The population size of this breed is less than 10,000. WD cattle and Dabieshan (DB) cattle are sympatric but are raised in different ecological environments, on mountains and plains, respectively, and the body sizes of these two breeds are markedly different. Blood samples were obtained from 8 adult female WD cattle and 7 adult female DB cattle (24 months old). The total RNA was extracted from leukocyte cells, and sequencing experiments were conducted on the Illumina HiSeq$^{TM}$ 4000 platform. After the removal of one outlier sample from the WD cattle breed as determined by principal component analysis (PCA), phylogenetic and population structure analyses indicated that WD and DB cattle formed a distinct Central China cattle group and showed evidence of hybridization between *Bos. taurus* and *Bos. indicus*. The immune-regulator CD48 ($P$ = 1.3E-6) was associated with breed-specific traits according to loss-of-function variant enrichment analysis. In addition, 113 differentially expressed genes were identified between the two breeds, many of which are associated with the regulation of body growth, which is the major difference between the two breeds. This study showed that WD cattle belong to the group of hybrids between *Bos. Taurus* and *Bos. indicus*, and one novel gene associated with breed traits and multiple differentially expressed genes between these two closely related breeds was identified. The results provide insights into the genetic mechanisms that underlie economically important traits, such as body size, in cattle.

**Keywords: whole transcriptome analysis, enrichment analysis, agricultural traits, taxonomic status, native cattle**

OPEN ACCESS

***Edited by:***
*George E. Liu, United States Department of Agriculture, United States*

***Reviewed by:***
*Lingyang Xu, Chinese Academy of Agricultural Sciences, China*
*Filippo Biscarini, National Research Council (CNR), Italy*

***Correspondence:**
*Hong-Quan Chen*
*chqchq@ahau.edu.cn*

*† These authors have contributed equally to this work*

***Specialty section:***
*This article was submitted to Livestock Genomics, a section of the journal Frontiers in Genetics*

***Received:*** *16 May 2020*
***Accepted:*** *11 September 2020*
***Published:*** *03 November 2020*

***Citation:***
*Zheng X-D, Cheng J, Qin W-J, Balsai N, Shang X-J, Zhang M-T and Chen H-Q (2020) Whole Transcriptome Analysis Identifies the Taxonomic Status of a New Chinese Native Cattle Breed and Reveals Genes Related to Body Size. Front. Genet. 11:562855. doi: 10.3389/fgene.2020.562855*

## INTRODUCTION

As key providers of milk, meat, leather and labor, cattle are one of the most important livestock species worldwide and have been domesticated since the early Neolithic period (Loftus et al., 1994, 1999; Beja-Pereira et al., 2006). More than 1000 cattle breeds have been identified around the world (Leroy et al., 2016), and 57 indigenous cattle breeds have originated from and been domesticated

in China, as described in the State Catalog of Livestock and Poultry Genetic Resource 2008. Extant domesticated cattle have been categorized by many researchers into two major geographic taxa: humpless taurine (*Bos. taurus*) and humped indicine (*Bos. indicus*) (Hiendleder et al., 2008; Gibbs et al., 2009; Canavez et al., 2012; Porto-Neto et al., 2013). Recent studies have indicated that cattle breeds from Central China show reliable evidence of having originated from hybridization between *Bos. taurus* and *Bos. indicus* (Lai et al., 2006; Lei et al., 2006; Mei et al., 2017; Chen et al., 2018).

Chinese cattle breeds vary in their intrinsic characteristics and are important genetic resources. However, there is pressure on the genetic diversity of cattle, and the worldwide extinction of some (local) cattle breeds is a major concern (Pariset et al., 2010; Biscarini et al., 2015). An interesting example is provided by the Wandong (WD) cattle breed, which was recently identified in Fengyang county, Anhui Province, by the National Commission for Livestock and Poultry Genetic Resources. WD cattle were domesticated in the watershed region between the Yangtze River and Huai River approximately 500 years ago and mainly exhibit two kinds of hair colors, yellow and brown. WD is one of the best breeds reared in China; it is characterized by a medium size and high-quality meat production that can reach the level of "3A plus" identified by the National Committee on Livestock and Poultry Genetic Resources. Additionally, it is one of the breeds that can be raised in the ecological environment in hilly areas with poor land and little rainfall. However, according to the statistics department data, the total breed population of WD cattle has declined alarmingly rapidly from more than 100,000 heads in the 1990s to less than 10,000 heads recently. Therefore, there is an urgent need to protect this precious genetic resource.

Dabieshan (DB) cattle were mainly domesticated in the eastern Dabie Mountains. These animals are small in size and suitable for farming in the mountains. Currently, the total breed population of DB cattle is more than 200,000 heads. The large population and purity of its genetic resources make DB cattle one of the best local livestock breeds for population genetic studies. Companies that raise cattle in this area mainly intend to maintain pure genetic resources. Therefore, it is rare for DB cattle to be in contact with other breeds. In the absence of gene flow, adaptive variants and linked variants through hitchhiking are expected to quickly increase in frequency within isolated populations (Rettelbach et al., 2019) and may evolve into differentiation islands through positive selection. In addition, genetic drift or purifying selection [background selection (BGS)] will reduce the population genomic diversity when a population is not large enough and will increase the number of differentiation islands between different populations (Burri et al., 2015). A gradual increase in the number of differentiation islands may have resulted in the evolution of this unique breed, which is able to adapt to mountainous environments.

In this study, we performed whole-genome RNA sequencing on these two phenotypically diverse domestic Chinese cattle breeds. By combining the obtained whole-genome RNA sequence data and whole-genome sequence data from 11 additional representative taurine and indicine breeds, we explored the taxonomic status of the WD cattle breed in more detail. Since loss-of-function variant association studies are considered extensions of genome wide association studies (Lu et al., 2017; Wen et al., 2018), we also investigated genes and corresponding variants that are associated with agriculturally important traits, such as size, through gene-level loss-of-function (LOF) variant enrichment analysis, which has proven to be efficient in detecting evidence of linkage in whole-genome sequencing data (Artomov et al., 2017; He et al., 2019; Yang et al., 2020). The aims of our analyses were to provide new insights into the population stratification of worldwide domestic cattle breeds and explore the relationship between genetic variants and agricultural traits.

# MATERIALS AND METHODS

Animal experiments were executed according to the Institutional Animal Care and Use Committee (IACUC) guidelines under current approved protocols at Anhui Agricultural University.

## Sampling and Public Data Collection

Blood samples were obtained from 8 adult female WD cattle and 7 adult female DB cattle (24 months old) (**Figure 1**). WD cattle were fed and maintained under the same management conditions at the Daming Agriculture and Animal Technology Development Co., Ltd., which is located in FengYang county (Anhui Province) and has been designated as a WD cattle genetic resource conservation farm, while the DB cattle came from another conservation farm and were fed and maintained at the Anhui Wanjia Modern Agriculture Co., Ltd., Taihu County, Anhui Province.

We collected whole-genome RNAseq data from Qinchuan cattle (QC, $n$ = 4, GSE47653), one of the most common local cattle breeds. In addition, whole-genome sequence data from 8 local Iran cattle (PRJEB6119) and 25 local Uganda cattle (PRJEB7061) were downloaded from the European Variation Archive[1] website (details in **Supplementary Table 5**).

## RNA Extraction and cDNA Library Construction

The total RNA was extracted from plasma leukocyte cells extracted from samples collected from the jugular vein of each individual using TRIzol reagent (Life Technologies, United States) according to the manufacturer's instructions. A TruSeq RNA Sample Preparation Kit (Illumina, United States) was used to purify the RNA and synthesize first- and second-strand cDNA. The quality was monitored with a NanoDrop ND-1000 spectrophotometer. The concentration of each sample was more than 50 pg/L, the amount of total RNA was more than 400 pg, and the RNA integrity number (RIN) was higher than 7.0. Then, an Agilent Bioanalyzer 2100 (Agilent Technology, United States) was used to determine the library fragment size distribution and assess whether it was suitable for computational analysis.

[1] https://www.ebi.ac.uk/eva/

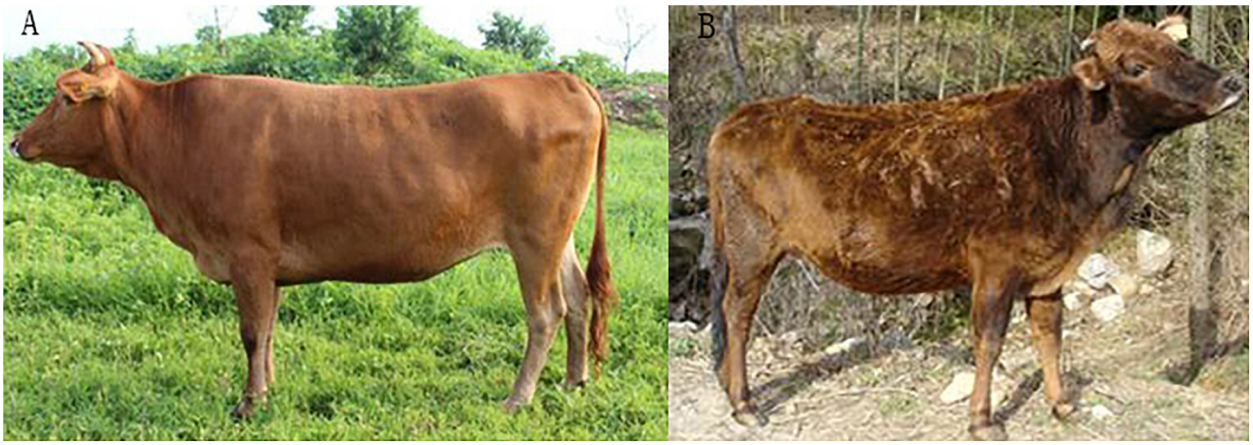



**FIGURE 1 |** WD cattle and DB cattle. WD cattle **(A)** and DB cattle **(B)** were fed and maintained at the Daming Agriculture and Animal Technology Development Co., Ltd., FengYang County, Anhui Province, and the Anhui Wanjia Modern Agriculture Co., Ltd., Taihu County, Anhui Province, respectively.

## High-Throughput Sequencing and Variant Calling

Sequence experiments were conducted by the Beijing Genomics Institute (BGI, Shenzhen, China) using the Illumina HiSeq™ 4000 platform. Single reads (50 bp) obtained from sequencing were checked by FastQC (v0.11.5)[2], and adapter sequences were removed with Trimmomatic (V0.36) (Bolger et al., 2014). Genome index files were generated by STAR (Dobin et al., 2013) using the gene annotation information GTF file (UCD1.2.95) and the *Bos. taurus* genome fast file (UMD3.1/bosTau6) (Zimin et al., 2009). Then, whole-transcriptome alignment was performed to obtain all splicing sites the first time. Thereafter, we used the STAR in the two-pass mode to rebuild the genomic index to obtain better alignments around novel splice junctions, and the clean reads were realigned to the *Bos. taurus* genome with Picard to mark duplicates with the default parameters. Variant calling was performed according to the best practices using the GATK HaplotypeCaller module (Van der Auwera et al., 2013) with the following quality control parameters: QualByDepth (QD) set to less than 2.0 and FisherStrand (FS) set to more than 30. ANNOVAR (Wang et al., 2010) was used to annotate variants relative to RefSeq annotations (UMD3.1).

## Phylogenetic and Population Structure Analyses

We obtained the PLINK genotype data format files by using the PLINK 1.9 "–vcf" command with the "–a2-allele" parameter, which will force the VCF (variant call format, generated by GATK program) file reference alleles to be set to A2. After that, the program of "convert" will calculate the number of copies of reference alleles per marker per individual (1 means one copy of the reference allele, 2 means two copies of the reference allele, and 9 means missing data) according to the PLINK SNP file. Principal component analysis was carried out with the overlapping common variants between the local data and the obtained public dataset to identify outlier samples using the smartPCA program of the EIGENSOFT (Patterson et al., 2006) package. A phylogenetic tree was constructed by using the neighbor-joining method in the program PHYLIP v3.695[3], and the distance matrices (1 minus the identity-by-state value) were calculated using PLINK 1.07 (Purcell et al., 2007). The population structure was further inferred using ADMIXTURE (Alexander et al., 2009) with the kinship (K) set from 2 to 7.

## Whole-Genome Association Study

To identify genetic differentiation between these two typical cattle breeds, we performed single-variant analysis using Fisher's exact test in PLINK with all variants passing quality control and calculated the genomic inflation based on the *P*-value distribution by the median chi-squared statistic (Yang et al., 2011). Thereafter, we performed multiple-variant testing with selected variants annotated as LOF variants (such as frame shift insertions, frame shift deletions, no frame shift insertions, no frame shift deletions, non-synonymous SNVs, stop gains, stop losses). Genes with two or more LOF variants were preserved to perform gene-level enrichment analysis. Three independent gene-based analysis methods, the Burden test, the sequence kernel association test (SKAT), and the optimal sequencing kernel association test (SKATO), were applied using the R package SKAT program (Wu et al., 2010, 2011), and one additional chi-squared test was performed with an in-house script.

## Differential Gene Expression Analysis

Clean reads in the RNA-seq data were mapped to the *Bos. taurus* genome (UMD3.1) using STAR aligner with the TranscriptomeSAM option. The output BAM files were processed using RSEM (Li and Dewey, 2011) to investigate gene expression levels. An in-house script was used to generate an expression matrix with transcripts per kilobase of exon

[2]http://www.bioinformatics.babraham.ac.uk/projects/fastqc/

[3]http://evolution.genetics.washington.edu/phylip.html

model per million mapped read (TPM) values, which were obtained from the RSEM output gene abundance results. Based on a normal distribution and using log reads count values, a generalized linear model implemented in the R package limma (V 3.37.4) was used to assess differentially expressed genes (DEGs) using the empirical Bayes-moderated t statistics method (eBays). Differentially expressed genes with raw *p*-values lower than 0.05 and log2-fold changes larger than 334 (a mean value of the absolute value of the log2-fold change plus 2 multiple standard deviations of the absolute value of the log2-fold change) were considered significant. The R package ggplot2 (V3.1.0) was used to construct the volcano plot. To speculate about the potential biological processes related to bovine agricultural traits in which DEGs are involved, we performed the analysis of Gene Ontology (GO) and Kyoto Encyclopedia of Genes and Genomes (KEGG) pathways with the R package clusterProfiler (Yu et al., 2012).

# RESULTS

## Alignments and Variant Identification

Fifteen samples from two cattle breeds (WD and DB) were sequenced using RNA-seq technology, generating an average of 24,135,850 raw sequencing reads, from which 23,893,462 clean reads remained after the filtering of low quality reads, and 21,054,824 uniquely mapped reads were finally obtained, with an average genome mapping ratio of 87.23 (**Supplementary Table 1**). A total of 724,998 single-nucleotide polymorphisms (SNPs) and 44,883 small insertions and deletions (InDels) were detected. A total of 20,819 variants were defined as LOF variants. After the removal of multiallelic variants (MNPs-multiple nucleotide polymorphisms, InDels), 20,575 variants remained. Then, variants (SNPs or InDels) with >90% call rates where each variant was uniquely located in one particular gene were retained. Additionally, the retained genes should have no less than LOF variants. Finally, we obtained 12,670 variants located in 2,720 genes for the subsequent gene-level enrichment analysis.

## Population Genetic Structure

Whole-genome RNA-seq data from four pooled QC cattle were aligned with data from fifteen local cattle that were subjected to the variant calling procedure described above. More than one million variants were detected. Two additional datasets were obtained, whole-genome sequence data from nine breeds from Uganda (25 individuals; 29,133,488 variants) and one breed from Iran (8 individuals; 19,999,624 variants). A total of 425,728 autosomal variants from these three datasets and were used for the population structure analysis.

Principal component analysis (PCA) demonstrated a clear genetic structure, with the samples from local Chinese cattle clustering together except for one sample, WD1, which was removed from the subsequent analysis (**Figure 2**). The same population affinities were recovered in phylogenetic trees constructed via the neighbor-joining (NJ) method (**Figure 3**). ADMIXTURE analysis also recapitulated these findings. To choose the best value for K, we set $K = 2$ to $K = 7$. When $K = 2$ or 3, we obtained the smallest cross-validation error (**Supplementary Figure 1**). Using these parameters we observed three geographically distributed ancestral components, labeled Middle East, Central China and Africa components (**Figure 4**). We noted that the QC, WD and DB breeds from three separate geographical regions formed a distinct Central China group. All cattle breeds from other regions (the Middle East and Africa) showed evidence of hybridization between *Bos. taurus* and *Bos. indicus*.

## Single Variant Association

Seven of the DB and seven of the WD cattle (one outlying sample was removed on the basis of PCA) were adult females (2 years old). It was obvious that the body size was significantly different between the two breeds (**Table 1**). To investigate the genetic linkage of this agricultural trait, we used 751,939 autosomal variants obtained from whole-genome RNA-seq of the two breeds, after performing quality control by excluding SNPs with a call rate of <90%, a minor allele frequency (MAF) <0.01, and Hardy–Weinberg equilibrium (HWE) in both cohorts <5e-8. The remaining 318,568 variants were employed to perform the whole-genome association analysis, and the distribution of –log10 *P*-values across all *B. taurus* autosomes used for the agricultural trait association of WD and DB cattle are shown in **Supplementary Figure 2**. After correction for the genomic inflation factor ($\lambda_{gc} = 2.2742$), there was no single variant showing evidence of a whole-genome significant association.

## Statistical Tests of the Robust Genes

We performed multiple-variant testing with the rare variants through SKAT analysis in R. Although the quantile-quantile plot of SKAT, SKATO and Burden *P*-values suggested that there was only moderate genomic inflation or systematic bias in this study (**Supplementary Figure 3**), no gene could pass the Bonferroni correction *P*-value threshold ($P < 1.84e\text{-}5$, 0.05/2720). However, there were 87 genes with gene-based association *P*-values (P_skat, P_skato, and P_burden) of less than 0.05.

We further counted the minor allele numbers of these genes to fill the cross tabulation and performed the chi-squared test. With no evidence of genomic inflation ($\lambda gc = 0.1172$), we observed a study-wide significant association for the CD48 gene (P_Chi = 1.3E-6, OR = 0.049, 95% CI = 0.011–0.209) and obtained suggestive evidence for an additional three genes (P_Chi < 1e-4) (**Figure 5**). Finally, there were 30 genes with a *P*-value of less than 0.05 according to four types of gene-level enrichment analysis methods (**Table 2**).

## Differential Gene Expression

Based on the eBays method, genes with associated *P*-values of less than 0.05 and fold changes greater than 334 were considered as significant. Compared with WD cattle, 86 genes that were upregulated and 27 genes that were downregulated in DB cattle showed significant changes in transcript abundance. After false discovery rate (FDR, Benjamini–Hochberg method) correction, 64 genes were observed to be upregulated, and 21 genes were observed to be downregulated (**Supplementary Table 2**).

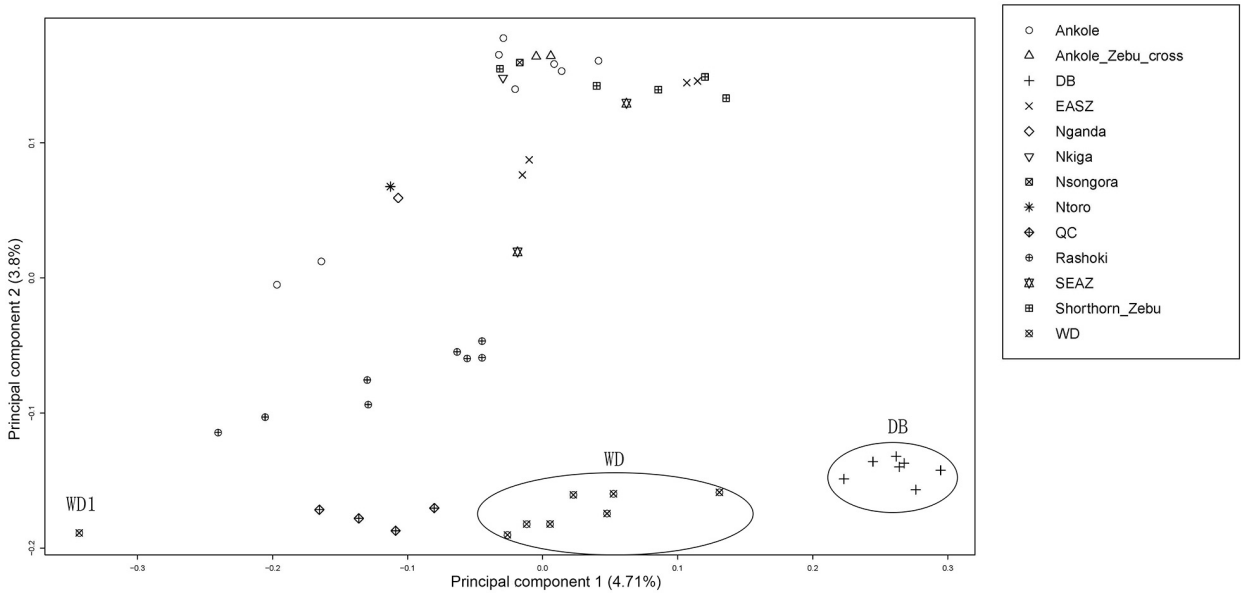



**FIGURE 2 |** Principal component analysis of 11 cattle breeds. Principal component analysis (PCA) of 11 worldwide distributed cattle breeds.

A total of 113 DEGs are included in the volcano plot (**Supplementary Figure 4**).

## Gene Ontology (GO) Annotation for DEGs and LOF Genes

In total, 151 GO terms were assigned to 130 DEGs, and 134 terms were significantly enriched (Benjamini–Hochberg adjusted $P < 0.05$). Among these terms, 99 corresponded to biological processes, 28 to cellular components, and 10 to molecular functions (**Supplementary Table 3**). There were 28 GO terms assigned to the 30 LOF genes, all of which corresponded to cellular components. Only one GO term (GO:0031094) exhibited a *P*-value of less than 0.05 (**Supplementary Table 4**) which was involved in the regulation of the platelet dense tubular network (GO:0031094, p_adjust = 9.56e-3). including one suggested F2R gene identified by LOF enrichment analysis.

# DISCUSSION

The findings of this study confirmed and extended the results of previous studies (Mei et al., 2017; Chen et al., 2018). The observed phylogenetic and population structure indicates that these Central Chinese cattle breeds formed an exclusive genetic group. The PCA provided similar results, and PC2 tended to separate populations sampled in Africa and those from the Middle East and Central China. Consistent with the geographic distance, the combination of PC1 and PC2 places the Middle Eastern cattle breed Rashoki between the African and Central Chinese cattle breeds. These data show that WD and DB cattle breeds present extremely low heterozygosity (∼0.2 and 0.18, respectively), while the QC, Rashoki cattle and African cattle breeds all exhibit intermediate heterozygosity (∼0.34–0.38), similar to a previous study of African taurine and indicine breeds (Orozco-terWengel et al., 2015). In contrast to other Central Chinese cattle breeds, WD cattle and DB cattle are raised in isolated environments, on the plains between the Huai and Yangtze rivers and in the mountains, respectively. The relatively less gene flow in these two breeds results in lower heterozygosity and a higher inbreeding coefficient than in other Central Chinese breeds. Additionally, WD cattle recently faced an extinction crisis in which the herd was reduced to six thousand head in 2011.

It remains unclear how genetic changes gradually accumulated in the genome and how these diverging breeds evolved. Reduced gene flow may speed up speciation, leading to large regions around divergently selected trait loci that are protected from recombination between genomic regions containing different locally adapted alleles (Via and West, 2008). The speciation process of restricted recombination caused the retention of these locally adapted variants and linked neutral variants in the distinct population genomes via extensive hitchhiking, probably causing the original ancestor to evolve into these two breeds that are able to adapt to different environments.

The greatest differences in the physical phenotypes of these two breeds are their body size and adaptation to different environments. There are many genes that have been reported to be associated with the economic traits of cattle (Li et al., 2010; Pausch et al., 2017; Raza et al., 2018; Sun et al., 2018; Cheng et al., 2020). In particular, genes such as MYLK4 (Zheng et al., 2019), CRTC3 (Wu et al., 2018), LEPR (Guo et al., 2008), and LHX4 (Ren et al., 2010) have been reported to be associated with the growth traits of Chinese cattle breeds. As body size is one the most important economic/growth traits for the modern breeding industry, it is valuable to investigate the genetic dynamics of this trait.

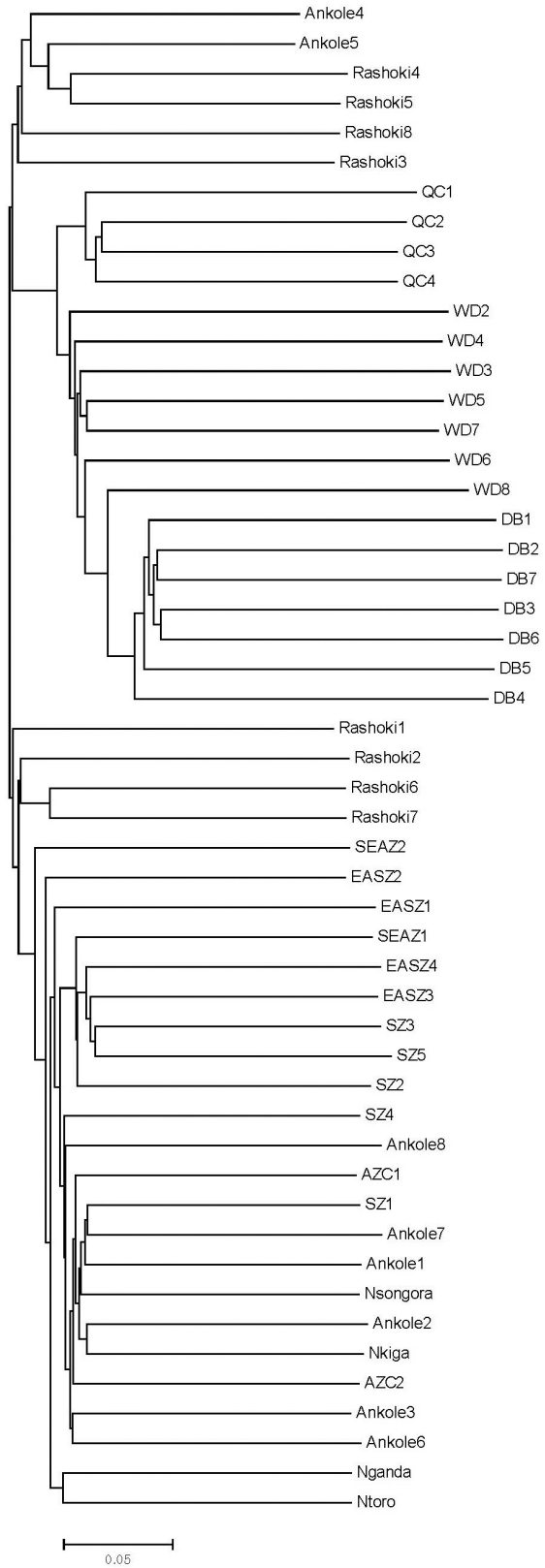



**FIGURE 3 |** Phylogenetic tree of 11 cattle breeds. The neighbor-joining (NJ) phylogenetic tree constructed using whole-genome autosome SNP data.

In this study, variant association analysis indicated the existence of moderate genomic inflation between these two cattle breeds, and no associated SNPs were detected. Therefore, based on advantages in detecting associations such as higher efficiency (greater detection power, and lower criteria for multiple testing) (Chen and Wang, 2019), a gene-based association strategy was used to identify physical traits associated with specific genes. Three gene-based methods (SKAT, SKATO, and Burden) showed there was moderate genomic inflation and that no gene could pass the threshold of the Bonferroni correction *P*-value. However, the chi-squared tests showed no evidence of genomic inflation at the gene level ($\lambda_{gc}$ = 0.1172), and a novel gene, CD48, was found to be significantly associated with the differences in the traits of these two breeds, even after Bonferroni correction. Additionally, three genes with a suggestive association were found: ESPNL (espin-like), PRCP (prolylcarboxypeptidase) and F2R (coagulation factor II thrombin receptor) (P_Chi < 1e-4).

The encoded CD48 protein is located on the surface of lymphocytes and other immune cells and participates in activation and differentiation pathways in these cells. PRCP encodes a member of the peptidase S28 family of serine exopeptidases, which can cleave C-terminal amino acids linked to proline in peptides such as angiotensin II and has been reported to be associated with leanness, cell proliferation and blood pressure regulation. One study showed that PRCP depletion reduces cell proliferation (Adams et al., 2013). F2R is an important member of the GPCR family that is highly expressed in osteoclasts. Another study demonstrated that F2r responds to RANKL (receptor activator of nuclear factor-κB ligand) stimulation to attenuate osteoclastogenesis by inhibiting both the F2r-Akt and F2r-NFκB signaling pathways, which leads to a reduction in the expression of osteoclast genes (Zhang et al., 2020).

Differential gene expression analysis identified 86 genes that were upregulated in DB cattle compared to WD cattle (**Supplementary Table 2**). Unexpectedly, more than 50 genes were related to the ribosomal unit and endoplasmic reticulum. Ribosomal proteins are essential for protein translation, and specific ribosomal proteins have been shown to play an essential role in tumorigenesis, immune signaling, and development. The targeted deletion of RPL29 (ribosomal protein L29) in mice showed that animals are viable but are up to 50% smaller than their control littermates at weaning age (Kirn-Safran et al., 2007). On the other hand, 27 genes were upregulated in WD cattle compared to DB cattle, most of which were related to immunoreactions, transcription factors, signal transduction and metabolism. Interestingly, one upregulated gene (TLN1, *P* = 8.13E-6) was involved in the spreading and migration of osteoclasts, which may be correlated with the LOF enrichment results. Among these genes, the transforming growth factor gene (TGFB1) was significantly upregulated in WD cattle (*P* = 8.65E-7). TGFB1 has been reported to be a key regulator of feed efficiency in beef cattle, and motif discovery analysis showed that most genes co-expressed with TGFB1 were enriched

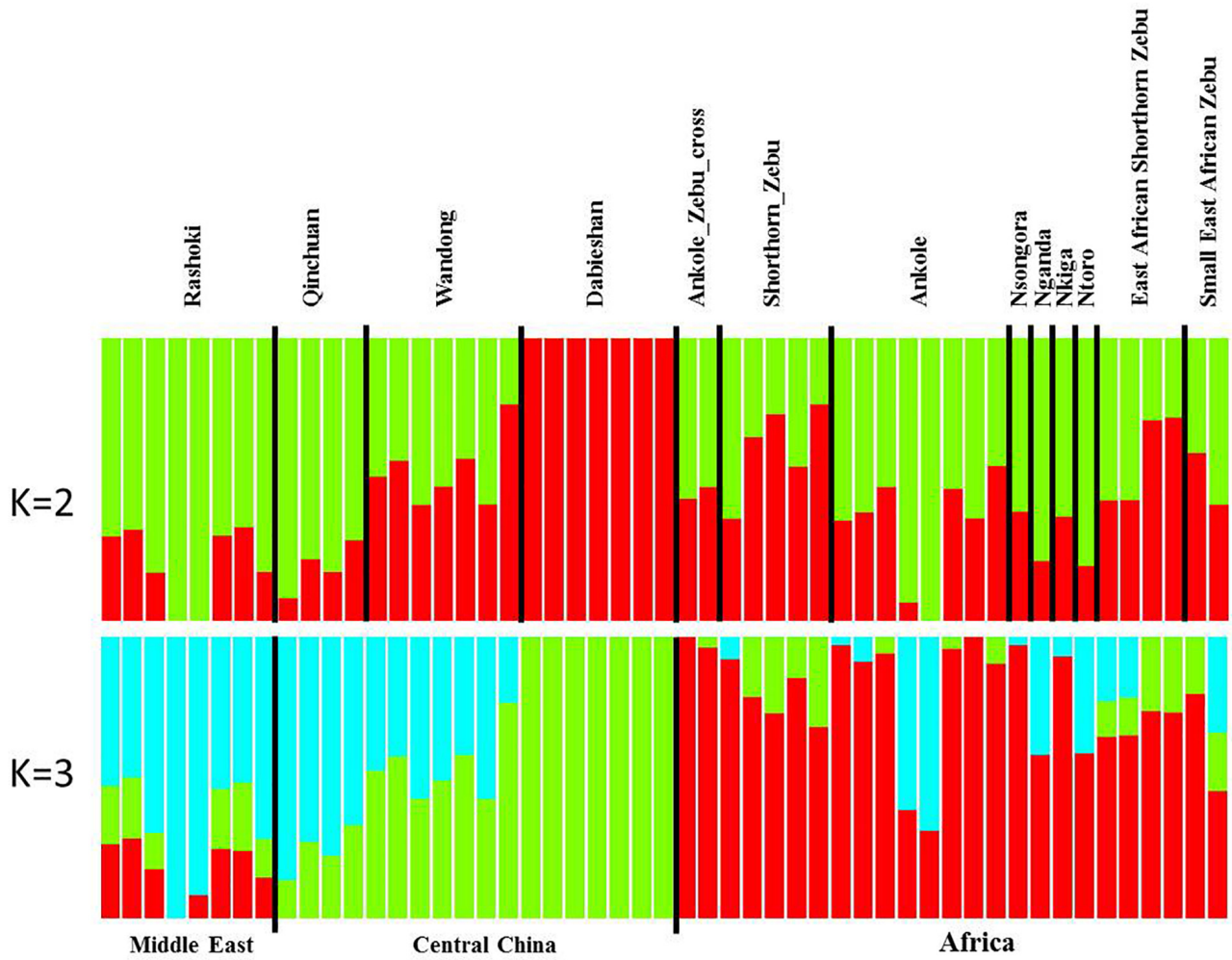



**FIGURE 4 |** Genetic structure of 11 cattle breeds. Model-based clustering of cattle breeds using ADMIXTURE with $K = 2$ and $K = 3$. Breeds are arranged by geographic regions and labeled with the name of each breed.

**TABLE 1 |** Agricultural traits of two typical cattle breeds.

| Agricultural traits | breed | N | Min | Max | Mean | SD | 95% CI |
|---|---|---|---|---|---|---|---|
| Height at withers (cm) | WD | 7 | 124.7 | 130.4 | 127.17 | 2.2 | 126.34–128 |
| Body length (cm) | WD | 7 | 140.7 | 151.6 | 146.03 | 4.02 | 144.51–147.55 |
| Bust size (cm) | WD | 7 | 170.5 | 179.3 | 174.26 | 3.32 | 173.01–175.51 |
| Weight (kg) | WD | 7 | 379.1 | 437.2 | 410.2 | 23.67 | 401.25–419.15 |
| Height at withers (cm) | DB | 7 | 110.6 | 119.3 | 115.31 | 3.31 | 114.06–116.56 |
| Body length (cm) | DB | 7 | 122.9 | 129.5 | 125.87 | 2.11 | 125.07–126.67 |
| Bust size (cm) | DB | 7 | 153.2 | 160.2 | 156.39 | 2.39 | 155.49–157.29 |
| Weight (kg) | DB | 7 | 280.6 | 293.7 | 284.87 | 4.43 | 283.2–286.54 |

*N, number of cattle; SD, standard deviation; CI, confidence interval.*

for binding sites related to master regulators of muscle differentiation (Alexandre et al., 2019). Furthermore, a large meta-analysis of human data including 46 genome-wide association (GWA) studies of 133,635 individuals, also highlighted a role of TGFB2 in the TGF-beta signaling pathway in regulating human height (Lango Allen et al., 2010). Searches in the Online Mendelian Inheritance in Man (OMIM) database by using the search keywords "short stature," "overgrowth," "skeletal dysplasia," and "brachydactyly" revealed gene records of TGFBR1 and TGFBR2 (receptors of TGFB1 and TGFB2) and many ribosomal protein genes, consistent with our data.

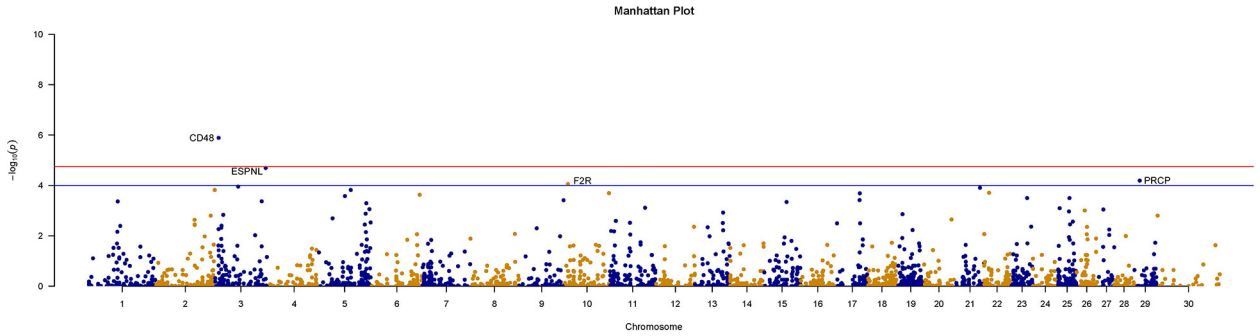



**FIGURE 5 |** Manhattan plots of size-associated genomic variants based on the chi-squared test. Manhattan plots of -log10 (*p*-values) for two breeds based on the gene level LOF variant count chi-squared test method. The red horizontal line indicates the study-wide significance level following the Bonferroni correction for the gene-based method [-log10 (0.05/2720)], and the blue horizontal line indicates the suggestive significance level.

**TABLE 2 |** 51 genes with *P*-values of less than 0.05 according to four independent gene-level LOF variant enrichment analysis methods.

| Gene | N.Marker | A1 | A2 | B1 | B2 | OR (95% CI) | P_Chi | P_skat | P_skato | P_burden |
|---|---|---|---|---|---|---|---|---|---|---|
| CD48 | 10 | 2 | 138 | 32 | 108 | 0.049 (0.011–0.209) | 1.3E-06 | 0.029818 | 0.007941 | 0.007113 |
| ESPNL | 4 | 18 | 38 | 44 | 12 | 0.129 (0.055–0.302) | 2.04E-05 | 0.013621 | 0.006 | 0.003257 |
| PRCP | 8 | 34 | 78 | 69 | 43 | 0.272 (0.156–0.473) | 6.47E-05 | 0.024092 | 0.024114 | 0.024528 |
| F2R | 8 | 1 | 111 | 22 | 90 | 0.037 (0.005–0.279) | 8.83E-05 | 0.004401 | 0.004521 | 0.000835 |
| TCTN1 | 9 | 2 | 124 | 23 | 103 | 0.072 (0.017–0.314) | 0.000207 | 0.041766 | 0.02924 | 0.026316 |
| HPS1 | 13 | 19 | 163 | 49 | 133 | 0.316 (0.178–0.563) | 0.000995 | 0.035728 | 0.004116 | 0.003033 |
| VPS72 | 3 | 12 | 30 | 30 | 12 | 0.16 (0.062–0.412) | 0.001485 | 0.021421 | 0.020794 | 0.020457 |
| GPATCH3 | 2 | 16 | 12 | 28 | 0 | Null | 0.001598 | 0.01049 | 0.01049 | 0.01049 |
| RPAP3 | 4 | 6 | 50 | 24 | 32 | 0.16 (0.059–0.434) | 0.002042 | 0.046709 | 0.016822 | 0.017364 |
| TTC27 | 7 | 2 | 96 | 18 | 80 | 0.093 (0.021–0.411) | 0.002578 | 0.013399 | 0.013399 | 0.013399 |
| TBL2 | 4 | 5 | 51 | 22 | 34 | 0.152 (0.052–0.439) | 0.002767 | 0.041708 | 0.037379 | 0.036504 |
| ALG12 | 8 | 28 | 84 | 55 | 57 | 0.345 (0.196–0.608) | 0.002969 | 0.013395 | 0.013414 | 0.048094 |
| NIF3L1 | 4 | 4 | 52 | 20 | 36 | 0.138 (0.044–0.439) | 0.003543 | 0.007855 | 0.013035 | 0.012078 |
| CLK1 | 2 | 3 | 25 | 16 | 12 | 0.09 (0.022–0.369) | 0.003736 | 0.00129 | 0.002294 | 0.002294 |
| LY86 | 5 | 0 | 70 | 12 | 58 | Null | 0.004374 | 0.01049 | 0.01049 | 0.01049 |
| HSPA14 | 4 | 1 | 55 | 14 | 42 | 0.055 (0.007–0.431) | 0.004617 | 0.029138 | 0.006702 | 0.006702 |
| SMYD5 | 2 | 9 | 19 | 22 | 6 | 0.129 (0.039–0.43) | 0.006692 | 0.036717 | 0.036866 | 0.038031 |
| HCLS1 | 2 | 1 | 27 | 12 | 16 | 0.049 (0.006–0.416) | 0.006978 | 0.006702 | 0.006702 | 0.006702 |
| MAK16 | 3 | 3 | 39 | 16 | 26 | 0.125 (0.033–0.472) | 0.00933 | 0.016705 | 0.004503 | 0.004503 |
| TMEM242 | 3 | 9 | 33 | 24 | 18 | 0.205 (0.079–0.533) | 0.010545 | 0.021164 | 0.025414 | 0.030723 |
| NDUFB4 | 4 | 0 | 56 | 9 | 47 | Null | 0.020472 | 0.034965 | 0.01049 | 0.01049 |
| TREM1 | 8 | 2 | 110 | 14 | 98 | 0.127 (0.028–0.574) | 0.021371 | 0.041363 | 0.041363 | 0.020973 |
| ARG2 | 2 | 0 | 28 | 8 | 20 | Null | 0.025172 | 0.034965 | 0.034965 | 0.034965 |
| UMPS | 3 | 3 | 39 | 14 | 28 | 0.154 (0.04–0.586) | 0.030324 | 0.016628 | 0.007454 | 0.007454 |
| SLC35A5 | 3 | 3 | 39 | 14 | 28 | 0.154 (0.04–0.586) | 0.030324 | 0.011943 | 0.010195 | 0.010195 |
| RPIA | 3 | 0 | 42 | 8 | 34 | Null | 0.031466 | 0.01049 | 0.01049 | 0.01049 |
| VAMP5 | 2 | 4 | 24 | 14 | 14 | 0.167 (0.046–0.607) | 0.042298 | 0.037557 | 0.013045 | 0.013045 |
| PRR5 | 4 | 2 | 54 | 12 | 44 | 0.136 (0.029–0.639) | 0.042755 | 0.043415 | 0.031177 | 0.033217 |
| ATP2A2 | 2 | 0 | 28 | 7 | 21 | Null | 0.046012 | 0.034965 | 0.034965 | 0.034965 |
| TMEM19 | 2 | 0 | 28 | 7 | 21 | Null | 0.046012 | 0.034965 | 0.034965 | 0.034965 |

*N.Marker, the SNP number involved in genes; A1, minor allele count of WD cattle; A2, major allele count of WD cattle; B1, minor allele count of DB cattle; B2, major allele count of DB cattle; OR (95% CI), odds ratio value of the chi-squared test, 95% confidence interval; P_Chi, gene-level chi-squared test P-value; P_skat, gene-based test SKAT P value; P_skato, gene-based test SKATO P-value; P_burden, gene-based test Burden P-value.*

## CONCLUSION

In summary, we performed a whole-transcriptome study for WD and DB cattle. By using publicly available global cattle data, phylogenetic and PCA analyses indicated that these Central Chinese cattle breeds formed exclusive genetic groups even within breeds of hybrid *Bos. taurus* × *Bos. indicus* cattle, and these results are consistent with the results of previous studies (Yu et al., 1999; Mei et al., 2017; Chen et al., 2018), which confirmed that these two local Chinese breeds originated from hybridization between *Bos. taurus* and *Bos. indicus*. LOF variant enrichment analysis identified one novel gene, CD48, and three genes with a suggestive association. Among these genes, F2R responds to RANKL stimulation to attenuate osteoclastogenesis, and the PRCP gene has been reported to be involved in cell growth and angiogenesis. Differential gene expression analysis showed that many ribosomal protein genes are upregulated in DB cattle, and many transcription factors and metabolism-related genes are upregulated in WD cattle. All of these genes are connected with the economic trait of body size. However, further large-scale studies are needed to understand the roles of these genes and to identify robust phenotype-associated genes/mutations with a large effect size. Our results indicate that whole-genome RNA_seq experiments are an efficient approach for investigating population genetic diversity and the genetic architecture of complex traits in mammals.

## DATA AVAILABILITY STATEMENT

The datasets presented in this study can be found in online repositories. The names of the repository/repositories and accession number(s) can be found in the article/ **Supplementary Material**.

## ETHICS STATEMENT

The animal study was reviewed and approved by the Anhui Agricultural University.

## AUTHOR CONTRIBUTIONS

X-DZ carried out the data, statistical, and other analyses and wrote the original draft. JC carried out the original investigation and design of the project, sample collection, and project administration. W-JQ, NB, X-JS, and M-TZ carried out the investigation and formal analysis. H-QC carried out the conceptualization, funding acquisition, methodology, project administration, supervision, and writing, review, and editing of the manuscript with input from all other authors. All authors contributed to the article and approved the submitted version.

## FUNDING

This study was financially supported by the National Natural Science Foundation of China (NSFC) (grant number 31272402).

## ACKNOWLEDGMENTS

We thank the Daming Agriculture and Animal Technology Development Co., Ltd., and the Anhui Wanjia Modern Agriculture Co., Ltd., for sample collection from WD and DB cattle. We are also grateful to Prof. Martin F. Bachmann for his editorial help in the preparation of this manuscript.

## SUPPLEMENTARY MATERIAL

The Supplementary Material for this article can be found online at: https://www.frontiersin.org/articles/10.3389/fgene.2020.562855/full#supplementary-material

**Supplementary Figure 1 |** ADMIXTURE cross-validation plot. ADMIXTURE cross-validation plot for the whole-genome autosome dataset of 11 worldwide cattle breeds set at $K = 2$ through 7.

**Supplementary Figure 2 |** Manhattan plots of *P*-values based on the single-variant association test. Manhattan plots of -log10 (*p*-values) for two breeds based on the single-variant association test. The red horizontal line indicates the genome-wide significance level from Bonferroni correction [-log10 (5e-8)] for the single-marker analysis, and the blue horizontal line indicates the suggestive significance level [-log10 (1e-5)].

**Supplementary Figure 3 |** Quantile-quantile plots of *P*-values. The observed negative logarithms of the *P*-values obtained using three types of gene-based methods for the two breeds are plotted against their expected values under the null hypothesis of no association.

**Supplementary Figure 4 |** Volcano plot of DEGs for the two cattle breeds. DEG expression profiling [with transcripts per kilo-base of exon model per million mapped reads (TPM) values] was constructed for the two breeds. Red plots represent genes that are significantly upregulated, and green plots represent genes that are significantly downregulated.

## REFERENCES

Adams, G. N., Stavrou, E. X., Fang, C., Merkulova, A., Alaiti, M. A., Nakajima, K., et al. (2013). Prolylcarboxypeptidase promotes angiogenesis and vascular repair. *Blood* 122, 1522–1531. doi: 10.1182/blood-2012-10-460360

Alexander, D. H., Novembre, J., and Lange, K. (2009). Fast model-based estimation of ancestry in unrelated individuals. *Genome Res.* 19, 1655–1664. doi: 10.1101/gr.094052.109

Alexandre, P. A., Naval-Sanchez, M., Porto-Neto, L. R., Ferraz, J. B. S., Reverter, A., and Fukumasu, H. (2019). Systems Biology Reveals NR2F6 and TGFB1 as Key Regulators of Feed Efficiency in Beef Cattle. *Front. Genet.* 10:230. doi: 10.3389/fgene.2019.00230

Artomov, M., Stratigos, A. J., Kim, I., Kumar, R., Lauss, M., Reddy, B. Y., et al. (2017). Rare Variant, Gene-Based Association Study of Hereditary Melanoma Using Whole-Exome Sequencing. *J Natl. Cancer Inst.* 109:djx083 doi: 10.1093/jnci/djx083

Beja-Pereira, A., Caramelli, D., Lalueza-Fox, C., Vernesi, C., Ferrand, N., Casoli, A., et al. (2006). The origin of European cattle: evidence from modern and ancient DNA. *Proc. Natl. Acad. Sci. U S A.* 103, 8113–8118. doi: 10.1073/pnas.0509210103

Biscarini, F., Nicolazzi, E. L., Stella, A., Boettcher, P. J., and Gandini, G. (2015). Challenges and opportunities in genetic improvement of local livestock breeds. *Front. Genet.* 6:33. doi: 10.3389/fgene.2015.00033

Bolger, A. M., Lohse, M., and Usadel, B. (2014). Trimmomatic: a flexible trimmer for Illumina sequence data. *Bioinformatics* 30, 2114–2120. doi: 10.1093/bioinformatics/btu170

Burri, R., Nater, A., Kawakami, T., Mugal, C. F., Olason, P. I., Smeds, L., et al. (2015). Linked selection and recombination rate variation drive the evolution of the genomic landscape of differentiation across the speciation continuum of Ficedula flycatchers. *Genome Res.* 25, 1656–1665. doi: 10.1101/gr.196485.115

Canavez, F. C., Luche, D. D., Stothard, P., Leite, K. R., Sousa-Canavez, J. M., Plastow, G., et al. (2012). Genome sequence and assembly of Bos indicus. *J. Hered.* 103, 342–348. doi: 10.1093/jhered/esr153

Chen, N., Cai, Y., Chen, Q., Li, R., Wang, K., Huang, Y., et al. (2018). Whole-genome resequencing reveals world-wide ancestry and adaptive introgression events of domesticated cattle in East Asia. *Nat. Commun.* 9:2337. doi: 10.1038/s41467-018-04737-0

Chen, Z., and Wang, K. (2019). Gene-based sequential burden association test. *Stat. Med.* 38, 2353–2363. doi: 10.1002/sim.8111

Cheng, J., Qin, W. J., Balsaia, N., Shang, X. J., Zhang, M. T., and Chen, H. Q. (2020). Transcriptional activity of FIGLA, NEUROG2, and EGR1 transcription factors associated with polymorphisms in the proximal regulatory region of GPR54 gene in cattle. *Anim. Reprod. Sci.* 218:106506. doi: 10.1016/j.anireprosci.2020.106506

Dobin, A., Davis, C. A., Schlesinger, F., Drenkow, J., Zaleski, C., Jha, S., et al. (2013). STAR: ultrafast universal RNA-seq aligner. *Bioinformatics* 29, 15–21. doi: 10.1093/bioinformatics/bts635

Gibbs, R. A., Taylor, J. F., Van Tassell, C. P., Barendse, W., Eversole, K. A., Gill, C. A., et al. (2009). Genome-wide survey of SNP variation uncovers the genetic structure of cattle breeds. *Science* 324, 528–532. doi: 10.1126/science.1167936

Guo, Y., Chen, H., Lan, X., Zhang, B., Pan, C., Zhang, L., et al. (2008). Novel SNPs of the bovine LEPR gene and their association with growth traits. *Biochem. Genet.* 46, 828–834. doi: 10.1007/s10528-008-9197-z

He, K. Y., Li, X., Kelly, T. N., Liang, J., Cade, B. E., Assimes, T. L., et al. (2019). Leveraging linkage evidence to identify low-frequency and rare variants on 16p13 associated with blood pressure using TOPMed whole genome sequencing data. *Hum. Genet.* 138, 199–210. doi: 10.1007/s00439-019-01975-0

Hiendleder, S., Lewalski, H., and Janke, A. (2008). Complete mitochondrial genomes of *Bos taurus* and Bos indicus provide new insights into intra-species variation, taxonomy and domestication. *Cytogenet. Genome Res.* 120, 150–156. doi: 10.1159/000118756

Kirn-Safran, C. B., Oristian, D. S., Focht, R. J., Parker, S. G., Vivian, J. L., and Carson, D. D. (2007). Global growth deficiencies in mice lacking the ribosomal protein HIP/RPL29. *Dev. Dyn.* 236, 447–460. doi: 10.1002/dvdy.21046

Lai, S. J., Liu, Y. P., Liu, Y. X., Li, X. W., and Yao, Y. G. (2006). Genetic diversity and origin of Chinese cattle revealed by mtDNA D-loop sequence variation. *Mol. Phylogenet. Evol.* 38, 146–154. doi: 10.1016/j.ympev.2005.06.013

Lango Allen, H., Estrada, K., Lettre, G., Berndt, S. I., Weedon, M. N., Rivadeneira, F., et al. (2010). Hundreds of variants clustered in genomic loci and biological pathways affect human height. *Nature* 467, 832–838. doi: 10.1038/nature09410

Lei, C. Z., Chen, H., Zhang, H. C., Cai, X., Liu, R. Y., Luo, L. Y., et al. (2006). Origin and phylogeographical structure of Chinese cattle. *Anim. Genet.* 37, 579–582. doi: 10.1111/j.1365-2052.2006.01524.x

Leroy, G., Baumung, R., Boettcher, P., Scherf, B., and Hoffmann, I. (2016). Review: Sustainability of crossbreeding in developing countries; definitely not like crossing a meadow. *Animal* 10, 262–273. doi: 10.1017/S175173111500213X

Li, B., and Dewey, C. N. (2011). RSEM: accurate transcript quantification from RNA-Seq data with or without a reference genome. *BMC Bioinformatics* 12:323. doi: 10.1186/1471-2105-12-323

Li, F., Chen, H., Lei, C. Z., Ren, G., Wang, J., Li, Z. J., et al. (2010). Novel SNPs of the bovine GAD1/gad67 gene and their association with growth traits in three native Chinese cattle breeds. *Mol. Biol. Rep.* 37, 501–505. doi: 10.1007/s11033-009-9699-8

Loftus, R. T., Ertugrul, O., Harba, A. H., El-Barody, M. A., MacHugh, D. E., Park, S. D., et al. (1999). A microsatellite survey of cattle from a centre of origin: the Near East. *Mol. Ecol.* 8, 2015–2022. doi: 10.1046/j.1365-294x.1999.00805.x

Loftus, R. T., MacHugh, D. E., Bradley, D. G., Sharp, P. M., and Cunningham, P. (1994). Evidence for two independent domestications of cattle. *Proc. Natl. Acad. Sci. U S A.* 91, 2757–2761. doi: 10.1073/pnas.91.7.2757

Lu, X., Peloso, G. M., Liu, D. J., Wu, Y., Zhang, H., Zhou, W., et al. (2017). Exome chip meta-analysis identifies novel loci and East Asian-specific coding variants that contribute to lipid levels and coronary artery disease. *Nat. Genet.* 49, 1722–1730. doi: 10.1038/ng.3978

Mei, C., Wang, H., Liao, Q., Wang, L., Cheng, G., Zhao, C., et al. (2017). Genetic architecture and selection of Chinese cattle revealed by whole genome resequencing. *Mol. Biol. Evol.* 35, 688–699. doi: 10.1093/molbev/msx322

Orozco-terWengel, P., Barbato, M., Nicolazzi, E., Biscarini, F., Milanesi, M., Davies, W., et al. (2015). Revisiting demographic processes in cattle with genome-wide population genetic analysis. *Front. Genet.* 6:191. doi: 10.3389/fgene.2015.00191

Pariset, L., Mariotti, M., Nardone, A., Soysal, M. I., Ozkan, E., Williams, J. L., et al. (2010). Relationships between Podolic cattle breeds assessed by single nucleotide polymorphisms (SNPs) genotyping. *J. Anim. Breed Genet.* 127, 481–488. doi: 10.1111/j.1439-0388.2010.00868.x

Patterson, N., Price, A. L., and Reich, D. (2006). Population structure and eigenanalysis. *PLoS Genet.* 2:e190. doi: 10.1371/journal.pgen.0020190

Pausch, H., Emmerling, R., Gredler-Grandl, B., Fries, R., Daetwyler, H. D., and Goddard, M. E. (2017). Meta-analysis of sequence-based association studies across three cattle breeds reveals 25 QTL for fat and protein percentages in milk at nucleotide resolution. *BMC Genomics* 18:853. doi: 10.1186/s12864-017-4263-8

Porto-Neto, L. R., Sonstegard, T. S., Liu, G. E., Bickhart, D. M., Da Silva, M. V., Machado, M. A., et al. (2013). Genomic divergence of zebu and taurine cattle identified through high-density SNP genotyping. *BMC Genomics* 14:876. doi: 10.1186/1471-2164-14-876

Purcell, S., Neale, B., Todd-Brown, K., Thomas, L., Ferreira, M. A., Bender, D., et al. (2007). PLINK: a tool set for whole-genome association and population-based linkage analyses. *Am. J. Hum. Genet.* 81, 559–575. doi: 10.1086/519795

Raza, S. H. A., Gui, L., Khan, R., Schreurs, N. M., Xiaoyu, W., Wu, S., et al. (2018). Association between FASN gene polymorphisms ultrasound carcass traits and intramuscular fat in Qinchuan cattle. *Gene* 645, 55–59. doi: 10.1016/j.gene.2017.12.034

Ren, G., Chen, H., Zhang, L. Z., Lan, X. Y., Wei, T. B., Li, M. J., et al. (2010). A coding SNP of LHX4 gene is associated with body weight and body length in bovine. *Mol. Biol. Rep.* 37, 417–422. doi: 10.1007/s11033-009-9486-6

Rettelbach, A., Nater, A., and Ellegren, H. (2019). How Linked Selection Shapes the Diversity Landscape in Ficedula Flycatchers. *Genetics* 212, 277–285. doi: 10.1534/genetics.119.301991

Sun, Y., Liu, K., Huang, Y., Lan, X., and Chen, H. (2018). Differential expression of FOXO1 during development and myoblast differentiation of Qinchuan cattle and its association analysis with growth traits. *Sci. China Life Sci.* 61, 826–835. doi: 10.1007/s11427-017-9205-1

Van der Auwera, G. A., Carneiro, M. O., Hartl, C., Poplin, R., Del Angel, G., Levy-Moonshine, A., et al. (2013). From FastQ data to high confidence variant calls: the Genome Analysis Toolkit best practices pipeline. *Curr. Protoc. Bioinform.* 43, 11.10.1-11.10.33. doi: 10.1002/0471250953.bi1110s43

Via, S., and West, J. (2008). The genetic mosaic suggests a new role for hitchhiking in ecological speciation. *Mol. Ecol.* 17, 4334–4345. doi: 10.1111/j.1365-294X.2008.03921.x

Wang, K., Li, M., and Hakonarson, H. (2010). ANNOVAR: functional annotation of genetic variants from high-throughput sequencing data. *Nucl. Acids Res.* 38:e164. doi: 10.1093/nar/gkq603

Wen, L., Zhu, C., Zhu, Z., Yang, C., Zheng, X., Liu, L., et al. (2018). Exome-wide association study identifies four novel loci for systemic lupus erythematosus in Han Chinese population. *Ann. Rheum. Dis.* 77:417. doi: 10.1136/annrheumdis-2017-211823

Wu, M. C., Kraft, P., Epstein, M. P., Taylor, D. M., Chanock, S. J., Hunter, D. J., et al. (2010). Powerful SNP-set analysis for case-control genome-wide association studies. *Am. J. Hum. Genet.* 86, 929–942. doi: 10.1016/j.ajhg.2010.05.002

Wu, M. C., Lee, S., Cai, T., Li, Y., Boehnke, M., and Lin, X. (2011). Rare-variant association testing for sequencing data with the sequence kernel association test. *Am. J. Hum. Genet.* 89, 82–93. doi: 10.1016/j.ajhg.2011.05.029

Wu, S., Ning, Y., Raza, S. H. A., Zhang, C., Zhang, L., Cheng, G., et al. (2018). Genetic variants and haplotype combination in the bovine CRTC3 affected conformation traits in two Chinese native cattle breeds (*Bos Taurus*). *Genomics* 111, 1736–1744. doi: 10.1016/j.ygeno.2018.11.028

Yang, C., Chen, M., Huang, H., Li, X., Qian, D., Hong, X., et al. (2020). Exome-Wide Rare Loss-of-Function Variant Enrichment Study of 21,347 Han Chinese Individuals Identifies Four Susceptibility Genes for Psoriasis. *J. Invest. Dermatol.* 140, 799–805e791.

Yang, J., Weedon, M. N., Purcell, S., Lettre, G., Estrada, K., Willer, C. J., et al. (2011). Genomic inflation factors under polygenic inheritance. *Eur. J. Hum. Genet.* 19, 807–812. doi: 10.1038/ejhg.2011.39

Yu, G., Wang, L. G., Han, Y., and He, Q. Y. (2012). clusterProfiler: an R package for comparing biological themes among gene clusters. *OMICS* 16, 284–287. doi: 10.1089/omi.2011.0118

Yu, Y., Nie, L., He, Z. Q., Wen, J. K., Jian, C. S., and Zhang, Y. P. (1999). Mitochondrial DNA variation in cattle of south China: origin and introgression. *Anim. Genet.* 30, 245–250. doi: 10.1046/j.1365-2052.1999.00483.x

Zhang, Y., Wang, H., Zhu, G., Qian, A., and Chen, W. (2020). F2r negatively regulates osteoclastogenesis through inhibiting the Akt and NFkappaB signaling pathways. *Int. J. Biol. Sci.* 16, 1629–1639. doi: 10.7150/ijbs.41867

Zheng, L., Zhang, G. M., Dong, Y. P., Wen, Y. F., Dong, D., Lei, C. Z., et al. (2019). Genetic Variant of MYLK4 Gene and its Association with Growth Traits in Chinese Cattle. *Anim. Biotechnol.* 30, 30–35. doi: 10.1080/10495398.2018.1426594

Zimin, A. V., Delcher, A. L., Florea, L., Kelley, D. R., Schatz, M. C., Puiu, D., et al. (2009). A whole-genome assembly of the domestic cow. *Bos taurus*. *Genome Biol.* 10:R42. doi: 10.1186/gb-2009-10-4-r42

**Conflict of Interest:** The authors declare that the research was conducted in the absence of any commercial or financial relationships that could be construed as a potential conflict of interest.

*Copyright © 2020 Zheng, Cheng, Qin, Balsai, Shang, Zhang and Chen. This is an open-access article distributed under the terms of the Creative Commons Attribution License (CC BY). The use, distribution or reproduction in other forums is permitted, provided the original author(s) and the copyright owner(s) are credited and that the original publication in this journal is cited, in accordance with accepted academic practice. No use, distribution or reproduction is permitted which does not comply with these terms.*

frontiers in Genetics

ORIGINAL RESEARCH
published: 23 December 2020
doi: 10.3389/fgene.2020.616960

# Genetic Determinism Exists for the Global DNA Methylation Rate in Sheep

*Dominique Hazard*, Florence Plisson-Petit, Carole Moreno-Romieux, Stéphane Fabre and Laurence Drouilhet*

*GenPhySE, Université de Toulouse, INRAE, ENVT, Castanet Tolosan, France*

Recent studies showed that epigenetic marks, including DNA methylation, influence production and adaptive traits in plants and animals. So far, most studies dealing with genetics and epigenetics considered DNA methylation sites independently. However, the genetic basis of the global DNA methylation rate (GDMR) remains unknown. The main objective of the present study was to investigate genetic determinism of GDMR in sheep. The experiment was conducted on 1,047 Romane sheep allocated into 10 half-sib families. After weaning, all the lambs were phenotyped for global GDMR in blood as well as for production and adaptive traits. GDMR was measured by LUminometric Methylation Analysis (LUMA) using a pyrosequencing approach. Association analyses were conducted on some of the lambs ($n$ = 775) genotyped by using the Illumina OvineSNP50 BeadChip. Blood GDMR varied among the animals (average 70.7 ± 6.0%). Female lambs had significantly higher GDMR than male lambs. Inter-individual variability of blood GDMR had an additive genetic component and heritability was moderate ($h^2$ = 0.20 ± 0.05). No significant genetic correlation was found between GDMR and growth or carcass traits, birthcoat, or social behaviors. Association analyses revealed 28 QTLs associated with blood GDMR. Seven genomic regions on chromosomes 1, 5, 11, 17, 24, and 26 were of most interest due to either high significant associations with GDMR or to the relevance of genes located close to the QTLs. QTL effects were moderate. Genomic regions associated with GDMR harbored several genes not yet described as being involved in DNA methylation, but some are already known to play an active role in gene expression. In addition, some candidate genes, *CHD1*, *NCO3A, KDM8, KAT7*, and *KAT6A* have previously been described to be involved in epigenetic modifications. In conclusion, the results of the present study indicate that blood GDMR in domestic sheep is under polygenic influence and provide new insights into DNA methylation genetic determinism.

**Keywords: epigenetics, blood, heritability, genetic correlation, QTL**

OPEN ACCESS

***Edited by:***
*Eveline M. Ibeagha-Awemu, Agriculture and Agri-Food Canada (AAFC), Canada*

***Reviewed by:***
*Hans D. Daetwyler, La Trobe University, Australia*
*Matthew L. Spangler, University of Nebraska-Lincoln, United States*

****Correspondence:***
*Dominique Hazard*
*dominique.hazard@inrae.fr*

***Specialty section:***
*This article was submitted to Livestock Genomics, a section of the journal Frontiers in Genetics*

***Received:*** *13 October 2020*
***Accepted:*** *07 December 2020*
***Published:*** *23 December 2020*

***Citation:***
*Hazard D, Plisson-Petit F, Moreno-Romieux C, Fabre S and Drouilhet L (2020) Genetic Determinism Exists for the Global DNA Methylation Rate in Sheep. Front. Genet. 11:616960. doi: 10.3389/fgene.2020.616960*

## INTRODUCTION

Genetic selection in several livestock species has recently progressed to include heritable DNA polymorphisms (i.e., genomic selection) for the improvement of production traits (Goddard et al., 2010). However, recent studies also showed that non-genetic information responsible for phenotypic differences between animals can also be inherited across generations (Johannes et al., 2008; Danchin et al., 2011). One such non-genetic inherited piece of information

concerns epigenetic marks. Epigenetic modifications include biochemical modifications of DNA (methylation) or proteins tied to DNA (methylation and acetylation of histone proteins). These epigenetics processes act in an interrelated way to influence gene expression and hence phenotype in response to environmental conditions, thereby demonstrating that the eukaryotic genome can respond dynamically to changes in the environment to which every individual is exposed (Geiman and Robertson, 2002).

One of the key mechanisms in the regulation of gene expression in mammals is cytosine methylation at CpG dinucleotides, the most common DNA modification in eukaryotes. The importance of epigenetics in mammals and plants has been demonstrated in several studies and epigenetics contribute to the inheritance of traits of interest. In plants, DNA methylation in several differentially methylated regions was shown to explain 60–90% of the heritability of complex traits (Cortijo et al., 2014). In humans, DNA methylation explained 7–11% of the body mass index while SNP explained 5–8% of the same trait (Dick et al., 2014). In livestock, current studies aim to identify epi-loci underlying traits of agronomical interest. For instance, in sheep, genome-wide analysis of DNA methylation profiles has already revealed numerous epi-loci associated with prolificacy or body size (Cao et al., 2015; Zhang et al., 2017). Epigenetic sources of inheritance are not currently taken into consideration in selection strategies in livestock production but these studies could help identify the origin of variability of production traits and later on, improve genetic progress.

Taking into account variations in epigenetic marks may enable better modeling of phenotypic variation and improving the precision of genetic evaluation of traits and breeds. In addition, taking epigenetic events into account may help not only understand but also improve adaptive processes in both plants and mammals. Particular epigenetic recombinant inbred lines of *Arabidopsis thaliana* showed highly variable DNA methylation, while being genetically very similar (Latzel et al., 2013). Using these plant model lines, it was demonstrated an important role of epigenetics in adaptive process facing saline conditions for example (Kooke et al., 2015). Moreover, evolutionary studies showed that epigenetic inheritance may be important for natural selection and transmission of advantageous traits, for a review (see Donohue, 2014). Recent advances in epigenetic studies in natural populations addressed how epigenetic inheritance may influence adaptive evolution by focusing on epigenetic stability and inheritance itself as a potentially evolving trait (Herman et al., 2014; Schlichting and Wund, 2014). These articles brought into focus the genetic and ecological basis of epigenetic stability and raised a number of questions including "is the stability of epigenetic marks heritable?"

Turck and Coupland (2014) showed that DNA methylation has the potential to be mitotically and meiotically stable, whereas histone modification is involved in environmentally induced epigenetic regulation that may be reversible. These authors hypothesized that both the degree of DNA methylation and the stability of environmentally induced changes in gene expression via histone modification are associated with changes in the DNA sequence that can cause heritable variation in epigenetic regulation. New scientific questions arise concerning the relationship between genetics and epigenetics as part of the improvement of livestock species and their adaptation to changing production systems. In the present study, we used a complementary approach to those used in existing studies by considering the global methylation of genomic DNA as a novel quantitative phenotype to provide essential information on the processes involved in epigenetic inheritance. DNA methylation in differentially methylated regions representing a very small proportion of genomic DNA global methylation, we hypothesized that the stable fraction of DNA methylation is genetically determined and can be inherited across generations. To test this hypothesis, we quantified the global DNA methylation rate in blood samples collected from domestic sheep. Sheep not only has the advantage of being a species of agronomical interest, but also represents an interesting animal model to study adaptive processes. The aim of the present study was to estimate the genetic component of the global DNA methylation rate and to identify the genomic loci underlying the phenotype.

# MATERIALS AND METHODS

## Animals and Management

The experimental animals were Romane lambs, a fixed crossbreed between Romanov x Berrichon du Cher (Ricordeau et al., 1992). Data collected from a total of 1,047 male and female lambs over a period of 5 years were used in this study. The lambs originated from 10 rams, each ram was used for only 1 year. All the animals were born in April, identified at birth using electronic ear tags, and reared outdoors with their dams under extensive conditions in the experimental "la Fage" farm on 280 ha of rangeland (Causse du Larzac, Roquefort sur Soulzon, South of France). The farming system, management and environment characteristics are detailed in Gonzalez-Garcia et al. (2014). The lambs were weighed regularly from lambing to weaning to estimate average daily gain. All the lambs were weaned at 85 $\pm$ 4 days of age. Two weeks after weaning, experimental lambs were individually exposed to two behavioral tests. Tests of each animal were all performed on the same day, with a total of around 35 lambs tested per day on 10–11 consecutive test-days per year. After the behavioral tests (i.e., approximately 1 month after weaning), lambs were blood sampled for genotyping and determination of the global DNA methylation rate.

## Global DNA Methylation Rate

The global DNA methylation rate (GDMR) was measured from whole blood samples taken from sheep. Genomic DNA was extracted from the blood samples using a high-salt extraction method (Roussot et al., 2003). Methylation analyses were performed using the LUMA assay (Karimi et al., 2006a,b). Briefly, this method relies on the use of methylation-sensitive and –insensitive restriction endonucleases: *Hpa*II and *Msp*I, respectively. The target sequence for both enzymes is CCGG, *Hpa*II is not able to cut if the internal cytosine is methylated ($C^mCGG$), whereas *Msp*I cuts the restriction site whatever the methylation status. Moreover, *Eco*RI (recognition site: GAATTC)

was used as an internal control for normalization of DNA amount. For each sample, DNA was independently digested by *Eco*RI + *Hpa*II and *Eco*RI + *Msp*I restriction enzymes (New England Biolabs) and then analyzed using a Q24 Pyromark sequencer and Q24 1.0.10 software (Qiagen). The dispensation order for nucleotides was GTGTCACATGTGTG. Methylation rate was calculated from peak heights as [1 − [(*Hpa*II(G)/ *Eco*RI_Hpa(T))/(*Msp*I(G)/ *Eco*RI_Msp(T))] × 100]. The same internal control DNA sample was used for each pyrosequencing run. Finally, considering complete digestions, GDMR integrates data from nearly six million CCGG sites detected *in silico* on sheep reference genome OAR v3.1.

## Behavioral Traits

Two behavioral tests were used to evaluate sociability for conspecifics and reaction to a human. A complete description of the devices and test procedure used for behavioral measurements are given in Hazard et al. (2016). Briefly, the arena test (AT) aimed to evaluate sociability for conspecifics in three successive phases: (1) attraction for conspecifics with visual contact (Arena test phase 1, AT1), (2) reactivity to social separation from conspecifics by preventing visual contact between the tested lamb and conspecifics (Arena test phase 2, AT2), and (3) attraction for conspecifics in presence of a motionless human standing in front of conspecifics (Arena test phase 3, AT3). The variables used were the frequency of low-pitched bleats (i.e., the lamb bleated with its mouth closed) recorded during AT1 (AT1-LBLEAT), and the frequency of high-pitched bleats (i.e., the lamb bleated with its mouth open) recorded during AT2 (AT2-HBLEAT). Locomotor activity was assessed by measuring the number of zones crossed during AT2 (AT2-LOCOM). Vigilance postures (i.e., animal motionless, head in an upright position, and ears perpendicular to the head) were measured during AT2 (AT2-VIGIL). The time spent in each virtual zone was recorded and the ewe's proximity score to conspecifics during AT3 (AT3-PROX) was calculated by weighting the time spent in each zone.

The corridor test (CT) aimed to evaluate the reaction to a human. The second phase of the CT was used to evaluate the lamb's reaction to a walking human. The mean distance between the tested lamb and the walking human was recorded (CT2-DIST).

## Zootechnical Traits

At birth, the type of lamb birthcoat was graded on a scale of one to nine based on composition and structure of the coat, i.e., grade 1, single wooly coat with no halo- or coarse hair, hair length < 10 mm; grade 9, double hairy coat (coarse hair mixed with fine down) > 25 mm in length. Further details on this trait are provided in Allain et al. (2014). Lambs were weighed at birth (birth weight, kg) and weaning (weaning weight, kg). Lambs were also weighed regularly from lambing to weaning to estimate average daily gain. Growth rates (i.e., average daily gain, ADG, in g) were estimated in all lambs from birth to 30, from 30 to 60 and from 60 to 90 days of age (called ADG0-30, ADG30-60, ADG60-90, respectively). In addition, some carcass traits were measured at slaughter only for males, including dressing yield (DY, percentage), conformation score (CONF, score 0–6), compactness (COMP) (i.e., width/length ratio of the carcass, percentage), external fat score (FAT Score, score 0–9), and back fat depth at the 12th rib (FAT depth, mm).

## Statistical Analysis

Analyses of variance were performed to assess the significant fixed effects affecting each measured trait. The tested effects were sex (male or female), born and reared litter size, age of the dam, age and weight of the lambs and year of measurement. The litter size effect was classified according to the number of lambs born and suckled (class 1, ewes lambing and suckling singletons; class 2, ewes lambing twins but suckling only one lamb; class 3, ewes lambing and suckling twins; and class 4, ewes lambing and suckling more than two lambs). The age of the dam effect included ewes that were one, two, and three or more than 3 years old (classes 1, 2, and 3, respectively). The year of measurement effect covered the 5 years over which data were collected. The GLM procedures of the SAS® software (SAS Institute Inc, 1999) were applied to the variables to test the fixed effects and first order interactions. The factors of variation showing significant effect (i.e., $P < 0.05$) on the considered trait were included in subsequent genetic analyses. The fixed effects considered depended on the trait. In addition, for the GDMR trait, we investigated differences between lamb families by testing a family effect (10 classes), nested in the year effect, according to the GLM procedure describe above. This was only used for GDMR because the genetic variability of the other traits included in the present study has already been described (Bibé et al., 2002; Allain et al., 2014; Hazard et al., 2014).

## Genetic Analyses

The (co)variance components of each trait were estimated by restricted maximum likelihood applied to an animal model using ASREML 3.0 software (Gilmour et al., 2009). For each trait, the model included the appropriate fixed effects (i.e., sex, born and reared litter size, age of the dam, year of measurement) and a direct additive genetic effect of the animal considered as random effect. For some traits analyzed, a litter or a dam permanent environmental effect was added as random effect in the model based on present results or the results of previous studies that described an appropriate model for the trait concerned (Bibé et al., 2002; Allain et al., 2014; Hazard et al., 2014). For GDMR, weight and growth traits, the dam was considered as a permanent environmental effect. For birthcoat, the animal's litter was considered as a permanent environmental effect. The following complete animal mixed model was fitted:

$$y = X\beta + Z_a a + W_c c + e \quad (1)$$

where $y$ is the vector of observations for the trait(s) being analyzed, β is the vector of appropriate fixed effects (sex of lambs, litter size born and suckled, age of the dam and year of measurement), $a$ is the vector of random genetic effects and $c$ is the vector of permanent environmental effects, when appropriate, with incidence matrices X, $Z_a$, and $W_c$, respectively, and e is the vector of residual effects. Univariate analyses were performed to estimate the variance of each trait. Bivariate analyses were performed to estimate the genetic correlations between the

GDMR and the other traits using the same model as that used in univariate analyses.

## Genomic Analyses

Genomic analyses were only done for the GDMR trait. Nine of the 10 families were used (i.e., family 10 was not genotyped). Among the 1,047 lambs phenotyped for GDMR, 800 lambs were genotyped (i.e., after filtering an individual call rate $\geq$ 98%) as well as their nine respective sires using the Illumina OvineSNP50 BeadChip (i.e., 54,241 SNPs). Outlier individuals were removed, and genomic analyses were performed using 775 phenotyped and genotyped lambs. SNP quality was checked as described by Hazard et al. (2014) (i.e., SNP call rates < 97%, a minor allele frequency < 1%, inconsistent for Hardy-Weinberg disequilibrium). Sex chromosomes were not included for analysis. Finally, 40,725 autosomal SNPs were retained for QTL analyses.

Genome wide association analysis was performed of the whole population genotyped using joint analysis considering simultaneously linkage association and linkage disequilibrium (LDLA) to take advantage of both family structure and linkage disequilibrium (Legarra and Fernando, 2009) using QTLMAP software (Gilbert et al., 2008). The LDLA method consisted in interval mapping and LDLA model considered the sire haplotypes effects of the LD model in addition to sire QTL effect. A haplotype size of four SNP was used, and when haplotype frequency was less than 1%, haplotypes were assigned to a rare haplotype group. The chromosome-wise *p*-values were estimated assuming that, conditional on the QTL position, the likelihood ratio test statistics followed a $\chi^2$-distribution with k degrees of freedom, k being the number of genetic effects (Piepho, 2001). In our study, k was equal to the number of haplotypes plus the number of families for LDLA. Genome-wise *p*-values were obtained by correcting for multiple testing assuming that the number of independent tests was equal to the number of chromosomes analyzed (i.e., 26 independent tests corresponding to the 26 autosomes) (Benjamini and Hochberg, 1995; Knott et al., 1998). Confidence intervals were determined using the "2-LOD drop-off" criterion and assuming 1 LOD = 4.61 LRT (Lynch and Walsh, 1998).

For each QTL, the confidence interval expanded by 2 Mb on each side was used to extract gene annotation by using the Biomart tool from Ensembl release 101 of the sheep reference genome OAR v3.1[1]. Functional annotations for epigenetic modifiers were extracted from dbEM[2] (Nanda et al., 2016) and from the review about epigenetic modifiers by Feinberg et al. (2016).

# RESULTS

## Phenotypes and Genetic Analyses

Descriptive statistics of GDMR are summarized in **Table 1**. The mean value of GDMR was 70.71% and the coefficient of variation was 8.40%. Analysis of the gender effect indicated that female lambs had higher GDMR than male lambs. Marked differences were observed between extreme values within a gender. Phenotypic variability of male lambs was higher than female lambs. No significant effects of litter size, age of the dam, age of the lamb and weight (at birth or at weaning) were found, but a significant effect of family (nested in the year effect) was found on GDMR. One family had a low GDMR at 66.60% (family 3) contrasting with four families having a higher GDMR ranging from 71.95 to 74.11% (families 1, 2, 7, and 8). Four families had intermediate GDMR ranging from 68.86 to 70.85% (families 4, 5, 6, 9, and 10). The difference between extreme families reached 1.25 SD. Differences in phenotypic variability were observed between families.

The estimated variance components of GDMR are listed in **Table 2**. The estimated heritability for GDMR was moderate ($0.20 \pm 0.05$) and the permanent environment effect of the dam was very low. The additive genetic coefficient of variation for GDMR was also low (3.5%).

Descriptive statistics and genetic parameters for additional traits recorded in the lambs used in the present study are reported in **Table 3**. Heritability estimates for behavioral, zootechnical and carcass traits were generally moderate to high ($0.20 \pm 0.05$ to $0.74 \pm 0.07$). Only low-pitched bleats and conformation score traits showed low heritability. No genetic correlation was found between GDMR and behavioral, birthcoat or zootechnical traits.

## Genomic Analyses

The significant QTLs found using LDLA and reaching genome-wide (GW) or chromosome-wide (CW) significance thresholds are reported in **Table 4** and **Figure 1**. Four haplotype-trait associations reached the GW significance thresholds and 16 haplotype-trait associations reached the 1% CW significance threshold. Eight significant associations reaching the 5% CW threshold were also detected. Associations found in LDLA mapped to 14 chromosomes. The four associations that reached the GW threshold of significance localized on chromosomes 1 (OAR1, 13.20 and 179.50 Mb) and 17 (OAR17, 40.14 and 55.54 Mb). Associations reaching the 1% CW significance threshold were mapped on chromosomes OAR3, 5, 13, 14, 16, 17, 18, 21, 23, 24, and 26. Effects of QTLs found in LDLA ranged from 0.68 to 3.20% of the total phenotypic variance of GDMR.

By crossing information from sheep reference genome annotation (OAR v3.1), the database of epigenetic modifiers (dbEM, (Nanda et al., 2016) and those reported by Feinberg et al. (2016), we highlighted *CHD1, NCO3A, KDM8, KAT7*, and *KATA6* as the most obvious candidate genes from each QTL (+2 Mb each side of the confidence interval), likely to play a role in the GDMR variation (**Table 4**).

# DISCUSSION

The global DNA methylation rate measured by LUMA reached 70% in sheep blood. This result is consistent with global DNA methylation percentages reported in human blood analyzed by LUMA (for a review, see Soriano-Tarraga et al., 2013). The

[1]http://www.ensembl.org

[2]http://crdd.osdd.net/raghava/dbem

**TABLE 1 |** Number of records, mean (± SD), minimum, maximum, quartiles, and least squares means for global DNA methylation rate in the whole population and for each sex and each family.

| | | Number of lambs | Mean (±SD) | Min | Max | Q1 | Q3 | *P*-value | LSMeans |
|---|---|---|---|---|---|---|---|---|---|
| Population | | 1047 | 70.71 (5.97) | 23.08 | 87.94 | 68.72 | 74.24 | | |
| Sex | Male | 426 | 68.75 (7.21) | 23.08 | 80.63 | 66.54 | 72.60 | *** | 69.12 |
| | Female | 621 | 72.05 (4.47) | 40.61 | 87.94 | 70.01 | 74.85 | | 72.17 |
| Family (year) | 1 | 93 | 73.40 (4.37) | 55.82 | 81.28 | 71.17 | 76.81 | *** | 73.05 |
| | 2 | 77 | 74.73 (3.55) | 60.56 | 80.79 | 72.82 | 77.21 | | 74.11 |
| | 3 | 116 | 66.94 (8.15) | 27.04 | 75.34 | 65.34 | 71.46 | | 66.63 |
| | 4 | 91 | 71.27 (6.7) | 23.08 | 79.85 | 69.83 | 75.05 | | 70.85 |
| | 5 | 115 | 68.95 (4.95) | 37.96 | 77.06 | 66.24 | 72.05 | | 68.86 |
| | 6 | 117 | 69.40 (5.62) | 43.39 | 87.94 | 66.82 | 72.18 | | 69.29 |
| | 7 | 101 | 73.00 (3.89) | 55.01 | 77.89 | 71.30 | 75.87 | | 72.57 |
| | 8 | 108 | 72.20 (3.31) | 61.02 | 78.83 | 70.52 | 74.43 | | 71.95 |
| | 9 | 123 | 69.92 (5.60) | 41.62 | 79.56 | 68.65 | 73.03 | | 69.81 |
| | 10 | 106 | 69.64 (6.73) | 28.03 | 77.22 | 68.19 | 73.32 | | 69.33 |

****P-value < 0.001. Min, minimum; max, maximum; Q1, first quartile; Q3, third quartile; LSMeans, least squares means; Family effect was nested in the year effect.*

**TABLE 2 |** Estimates of heritability, repeatability, permanent and residual effects (±S.E.) for the global DNA methylation rate.

| | | Component | | | Repeatability ($r^2$) | Total $\sigma_p^2$ |
|---|---|---|---|---|---|---|
| | *n* | Genetic ($h^2$) | Permanent ($m^2$) | Residual ($e^2$) | | |
| GDMR | 1,047 | 0.20 ± 0.05 | 0.02 ± 0.03 | 0.78 ± 0.05 | 0.22 ± 0.05 | 31.3 ± 1.5 |

*$h^2$, $m^2$, $e^2$, proportion of total phenotypic variance attributed to additive genetic, permanent, and residual effects, respectively, Total $\sigma_p^2$, total phenotypic variance; $r^2 = h^2 + m^2$; n, number of animals.*

**TABLE 3 |** Number of records, mean (±SD), estimates of heritability, and permanent environmental effects for behavioral, zootechnical and carcass traits, and genetic correlations between these traits and the global DNA methylation rate.

| | *n* | Mean (±SD) | $h^2$ | $p^2$ | $r_g$ |
|---|---|---|---|---|---|
| AT1-LBLEAT | 1,047 | 0.28 (0.28) | 0.17 (0.07) | ne | <0.05 (<0.01) |
| AT2-HBLEAT | 1,047 | 2.91 (1.39) | 0.46 (0.07) | ne | 0.05 (0.03) |
| AT2-LOCOM | 1,017 | 19.44 (8.5) | 0.26 (0.07) | ne | <0.05 (<0.01) |
| AT2-VIGIL | 1,017 | 20.68 (9.81) | 0.32 (0.07) | ne | <0.05 (<0.01) |
| AT3-PROX | 990 | 26.26 (16.89) | 0.27 (0.06) | ne | <0.05 (<0.01) |
| CT2-DIST | 1,047 | 5.37 (1.14) | 0.20 (0.06) | ne | <0.05 (<0.01) |
| Birthcoat (score 0–9) | 1,032 | 6.06 (3.38) | 0.74 (0.07) | 0.15 (0.04) | <0.05 (<0.01) |
| Birth weight (kg) | 1,047 | 3. 9 (0.8) | 0.26 (0.09) | 0.27 (0.05) | <0.05 (<0.01) |
| Weaning weight (kg) | 1,043 | 23.3 (4.2) | 0.36 (0.09) | 0.20 (0.04) | <0.05 (<0.01) |
| ADG0-30 (g) | 1,047 | 360.3 (73.04) | 0.30 (0.08) | 0.24 (0.04) | <0.05 (<0.01) |
| ADG30-60 (g) | 1,047 | 227.4 (50.5) | 0.34 (0.08) | 0.06 (0.04) | <0.05 (<0.01) |
| ADG60-90 (g) | 1,046 | 216.0 (58.0) | 0.32 (0.07) | 0.10 (0.04) | <0.05 (<0.01) |
| DY (%) | 386 | 42.07 (2.19) | 0.41 (0.15) | ne | <0.05 (<0.01) |
| CONF (score 0–6) | 390 | 3.44 (0.8) | 0.09 (0.08) | ne | <0.05 (<0.01) |
| COMP (%) | 388 | 32.26 (1.46) | 0.58 (0.20) | ne | <0.05 (<0.01) |
| FAT score (score 0–9) | 390 | 5.07 (1.39) | 0.22 (0.12) | ne | <0.05 (<0.01) |
| FAT depth (mm) | 389 | 1.87 (1.36) | 0.36 (0.13) | ne | <0.05 (<0.01) |

*AT1/2/3, arena test phase 1/2/3; CT2, corridor test phase2; LBLEAT, low bleats; HBLEAT, high bleats; LOCOM, locomotion; VIGIL, vigilance behavior; PROX, proximity score; DIST, mean distance between tested animal and a human; ADG, average daily gain; DY, dressing yield; CONF, conformation score; COMP, compactness. $h^2$, $p^2$, proportion of total phenotypic variance attributed to additive genetic or permanent environmental effects, respectively, $r_g$, genetic correlations; standard errors are in parentheses; ne, not estimated.*

value of GDMR in the present study is also in the range of calculated DNA methylation either using the global CpG methylation rate (50–55%) measured by reduced representation bisulfite sequencing (RRBS) in sheep muscle (Couldrey et al., 2014) or the total methyl content measured by high performance liquid chromatography reported in somatic tissues (80%) in

**TABLE 4 |** List of QTLs detected in joint analysis (linkage disequilibrium linkage analysis) associated with the global DNA methylation rate.

| Chr. | Significance | level[a] | QTL effect (%)[b] | Confidence interval (Mb) | Flanking markers[c] | | Annotated protein coding genes within confidence interval | Epigenetic modifier candidate |
|---|---|---|---|---|---|---|---|---|
| 1 | **GW** | * | 2.48 | 13.1–13.4 | OAR1_13033760.1 | s62110.1 | RRAGC, GJA9, RHDB | |
| 1 | CW | * | 2.75 | 69.3–69.5 | OAR1_74015424.1 | OAR1_74065628.1 | MTF2 | |
| 1 | CW | * | 3.0 | 138.0–138.3 | OAR1_149183890.1 | OAR1_149346875.1 | – | |
| 1 | **GW** | * | 2.4 | 179.4–179.6 | OAR1_193623565.1 | OAR1_193664187.1 | – | |
| 2 | CW | * | 1.44 | 199.7–199.9 | OAR2_211501156.1 | OAR2_211573792.1 | – | |
| 3 | CW | ** | 1.0 | 114.5–114.7 | OAR3_122117752.1 | OAR3_122207054.1 | – | |
| 5 | CW | ** | 0.83 | 96.6–96.9 | OAR5_105186382.1 | OAR5_105374983.1 | – | CHD1 |
| 11 | CW | * | 2.95 | 10.5–10.9 | s74938.1 | OAR11_10495137.1 | MAD13, INTS2, BRIP1 | |
| 11 | CW | * | 0.85 | 37.4–37.6 | OAR11_39854191.1 | OAR11_39948154.1 | HOXB1/2/3/4/5/6/7/9 | KAT7 |
| 13 | CW | * | 2.9 | 17.8–18.5 | OAR13_20537279.1 | OAR13_20578061.1 | PARD3 | |
| 13 | CW | * | 2.7 | 32.1–32.3 | OAR13_35499997.1 | OAR13_35648372.1 | NSUN6, EPC1 | |
| 13 | CW | ** | 1.17 | 74.5–74.7 | s65442.1 | s62908.1 | CDH22, SLC35C2, ELMO2 | NCOA3 |
| 14 | CW | ** | 2.45 | 7.7–7.9 | s16689.1 | OAR14_8081413.1 | CMIP, PLCG2, SNORA70 | |
| 14 | CW | ** | 2.06 | 10.7–10.9 | s26487.1 | s43948.1 | – | |
| 14 | CW | ** | 2.77 | 14.8–15.2 | OAR14_15219778.1 | OAR14_15268863.1 | GTP2, DNAJA2, NETO2, ITFG1 | |
| 14 | CW | ** | 2.85 | 17.5–18.3 | s22016.1 | s31525.1 | ZNF423, CNEP1R1, HEATR3, TENT4B, ADCY7, BRD7 | |
| 16 | CW | ** | 2.38 | 4.5–4.8 | OAR16_4698169.1 | OAR16_4737110_X.1 | DUSP1, ERGIC1, RPL26L1, ATP6V0E1 | |
| 17 | CW | ** | 2.7 | 26.7–26.9 | OAR17_29456634.1 | s52728.1 | – | |
| 17 | **GW** | *** | 2.71 | 40.0–40.2 | OAR17_43310387.1 | OAR17_43356226.1 | PPID, ETFDH, C4orf46, RXFP1 | |
| 17 | **GW** | * | 2.8 | 55.4–55.6 | OAR17_60522910.1 | s57641.1 | CCDC60 | |
| 18 | CW | ** | 1.68 | 6.6–6.8 | OAR18_6256173.1 | s37275.1 | TTC23, SYNM | |
| 21 | CW | ** | 0.80 | 3.7–4.1 | OAR21_4678890.1 | s05427.1 | – | |
| 23 | CW | ** | 0.68 | 8.3–8.5 | OAR23_9159961.1 | OAR23_9204273.1 | – | |
| 23 | CW | ** | 2.7 | 34.4–34.6 | OAR23_36433223.1 | s07796.1 | GATA6 | |
| 24 | CW | * | 2.5 | 7.4–7.7 | OAR24_8719574.1 | s03253.1 | TMEM114, METTL22, ABAT, TMEM186, PMM2, CARHSP1 | |
| 24 | CW | ** | 3.2 | 23.6–24.0 | s12637.1 | OAR24_26210500.1 | – | KDM8 |
| 24 | CW | ** | 1.08 | 32.6–33.0 | s64882.1 | s17643.1 | RCC1L, NCF1, GTF2IRD1, CLIP2 | |
| 26 | CW | ** | 2.0 | 33.4–33.6 | OAR26_38152631.1 | OAR26_38251830.1 | ADAM18, IDO1, IDO2 | KAT6A |

*Significant QTLs reaching the chromosome-wide or the genome-wide thresholds are listed. [a]*$p < 5\%$; **$p < 1\%$; ***$p < 0.1\%$. [b]Percentage of phenotypic variance explained by the haplotype with the most effect (absolute value). [c]SNPs flanking the QTL with significant association. CW, chromosome wide; GW, genome wide; Position and genes are based on the reference genome Oar_v3.1.*

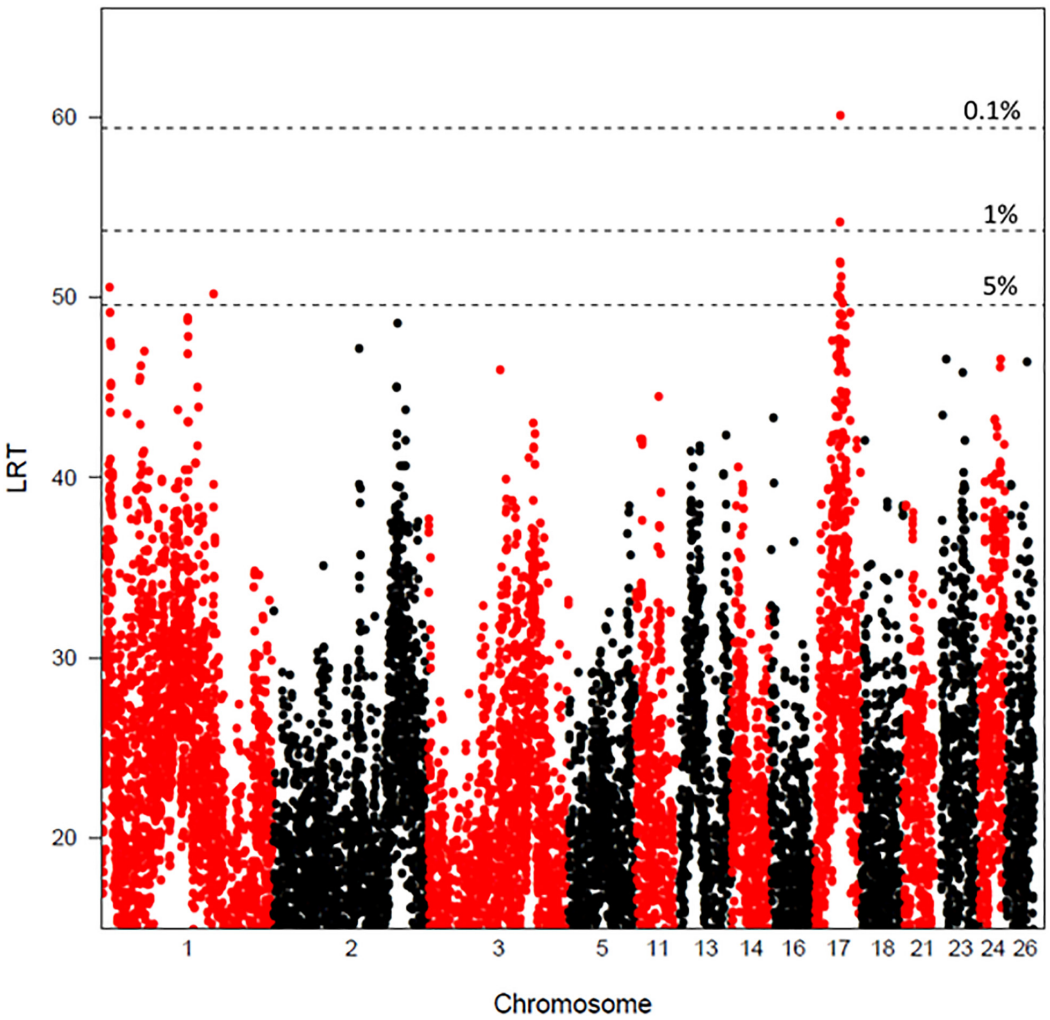



**FIGURE 1 |** Chromosome plots of the likelihood ratio test values obtained for global DNA methylation rate by LDLA analysis. The likelihood ratio test (LRT) is plotted against SNP haplotype positions (four consecutive SNPs) for chromosomes 1, 2, 3, 5, 11, 13, 14, 16, 17, 18, 21, 23, 24, and 26. The horizontal lines indicate the 5, 1, and 0.1% genome wide thresholds. One percent chromosome wide thresholds were OAR3, 47.6; OAR5, 37.4; OAR13, 42.6; OAR14, 35.9; OAR16, 38.7; OAR17, 42.3; OAR18, 40.6; OAR21, 37.3; OAR23, 45.7; OAR24, 42.8, and OAR26, 47.1. 5% chromosome wide thresholds were OAR1, 45.5; OAR2, 45.0; OAR11, 41.3; OAR13, 38.3; OAR24, 38.4.

humans (Ehrlich et al., 1982). The large range observed for DNA methylation rate across the genome is likely due to the methods used for quantification of DNA methylation and/or the tissues studied. Indeed, in their review, Soriano-Tarraga et al. (2013) reported that variation in global DNA methylation in human blood analyzed by LUMA ranged from 52 to 78% depending on the DNA isolation method used. In addition, Doherty and Couldrey (2014) reported that RRBS libraries are biased because they contain promoter regions which have high CG content known to be largely devoid of DNA methylation. Consequently, RRBS libraries are expected to display lower methylation on average across genome than unbiased libraries.

Variability was observed for the GDMR phenotype recorded in this study. Part of this variability originated from differences between male and female lambs. Sex differences in the methylome have already been reported in humans. In human liver, females displayed higher average DNA methylation in the X-chromosome whereas males presented higher DNA methylation in autosomes in this tissue (García-Calzón et al., 2018). Genome-wide sex differences in locus-specific DNA methylation across autosomes have also been reported in other human tissues such as blood (Singmann et al., 2015). In the present study, the positions of DNA methylation across genome were unknown, so we are unable to conclude whether gender difference in DNA methylation found in lambs was of similar magnitude on the X-chromosome and autosomes. In addition, it should be kept in mind that we investigated DNA methylation in young lambs (4 months of age), not in adult sheep. A study investigating gender differences in DNA methylation in human blood at birth reported that CpG located on autosomes, as well as DMR, were hypermethylated in girls compared to boys (Yousefi et al., 2015). Because gender differences in DNA methylation

across autosomes in human blood varied between newborns and adults, we cannot exclude that a sex by age interaction could affect DNA methylation in sheep blood.

We hypothesized that GDMR has a genetic component in sheep. The variance component decomposition analysis of GDMR revealed moderate heritability (20%). To our knowledge, this is the first heritability estimate for GDMR in livestock species. Estimation of heritability of DNA methylation levels in human whole blood at thousands of sites has shown that heritability estimates vary across the genome but is on average 20%, consistently with our estimate in sheep blood (van Dongen et al., 2016). Additional studies in humans also indicated that the average twin based heritability of DNA methylation across genome-wide CpGs varied between 5 and 19% depending on the tissue (i.e., $h^2$ = 5, 7, and 12% in placenta, human umbilical vascular endothelial cells and cord blood mononuclear cells from newborns twins, respectively, $h^2$ = 18% in peripheral blood lymphocytes from adolescent twins [Gordon et al., 2012; McRae et al., 2014]). Interestingly, Shah et al. (2014) reported that DNA methylation in whole blood remained stable over the human lifetime, as indicated by the high correlation (0.68) between DNA methylation repeatability in older people (median age 70–90) and heritability estimated in teenagers.

Genetic relationships between GDMR and production or adaptive traits were also investigated in the present study. We did not find any relationship between GDMR and production or adaptive traits in domestic sheep. Our results contrasted with the negative correlation between total DNA methylation level and daily growth rate in fish embryos (Ou et al., 2019). To our knowledge, no published works provide evidence of a relationship between GDMR in blood and the specific adaptive traits used in the present study (social behaviors and birthcoat). Some relationships would be expected, since several studies suggested epigenetic influence on adaptive processes in mammals (Massicotte et al., 2011; Lea et al., 2016). Nevertheless, only a few adaptive traits were explored in this study and we cannot exclude the possibility that such relationships exist for other adaptive traits or in older animals. Additionally, regardless of the absence of relationships between GDMR and adaptive traits in our study, we cannot exclude, by considering individually DNA methylation sites, to find epi-loci associated with production or adaptive traits investigated in the present study. Indeed, epi-loci have previously been reported to be associated with animal behaviors (Champagne and Curley, 2009; Roth, 2013; Verhulst et al., 2016; Seebacher and Krause, 2019).

Even if the greater attention paid to epigenetics in farm animals has led to an increasing number of GWA epigenetic studies, genomic studies of DNA methylation rate had remained to be performed. In our study, we were particularly interested in detecting QTLs for GDMR in domestic sheep. The QTL analysis for GDMR resulted in mapping 28 QTLs on 14 chromosomes, with four regions (on OAR1 and OAR17) reaching the genome wide level of significance. Each detected QTL explained less than 3% of the phenotypic variance. Our experimental design enabled to reach a power of 90% for the detection of a QTL explaining 8% of the phenotypic variance while the power was 20% for a QTL that explains 1% of phenotypic variance (Luo, 1998). Consequently, the undetected QTLs likely had a limited effect on GDMR. Thus, the low proportion of variance explained by each QTL supports the hypothesis that GDMR in domestic sheep is under polygenic influence and unlikely under the control of a major gene. Nevertheless, several QTLs mapped in the present study could probably act in combination to account for substantial genetic variation of GDMR.

To better understand the underlying molecular mechanisms associated with these QTLs, we looked for possible overlapping between the location of the identified QTLs (confidence interval enlarged by 2 Mb each side) and the location of annotated genes relevant to epigenetics. Despite the large number of genes located close to the QTL regions identified, only few genes seem relevant as epigenetic modifiers through their action on methylation or acetylation processes on DNA or histones. Indeed, by crossing the list of positional genes in enlarged QTL regions with that of known epigenetic modifiers either from the dbEM database (Nanda et al., 2016) or those listed in Feinberg et al. (2016), only *CHD1, KDM8, NCO3A, KAT7*, and *KATA6* appeared as the most obvious candidate genes. *CHD1* gene encodes the chromodomain-helicase-DNA-binding protein 1 (OAR5: 95.4 Mb), that functions as substrate recognition component of the transcription regulatory histone acetylation complex SAGA. Mutations in *CHD1* are frequently associated with prostate cancers (Berger et al., 2011). Functional analyses have shown that CHD1 was involved in transient DNA methylation and several loci were hypermethylated in *CHD1* deleted strains of Neurospora crassa (Belden et al., 2011). KDM8 (Lysin demethylase 8 or Jumonji C domain-containing demethylase 5, JDMD5; OAR24: 24.8 Mb) is a histone H3 demethylase with specificity for Lys-36. This demethylase promotes homologous recombination (Amendola et al., 2017), cell proliferation (Hsia et al., 2010) and protects from nerve demyelination (Fuhrmann et al., 2018). Interestingly, a second gene encoding an important histone lysine demethylase, *KDM2B* (Lysine-specific demethylase 2B, OAR17: 53.23 Mb), was found close to one of the enlarged QTL regions (OAR17: 55.4–55.6 Mb). In this region, we also identified *SETD1B* gene (Histone-lysine N-methyltransferase SETD1B, 53.06 Mb) which encodes a component of a histone methyltransferase complex that specifically methylates Lys-4 of histone H3 and is responsible for the epigenetic control of chromatin structure and gene expression. A specific hypermethylation signature was associated with loss of function mutations in the *SETD1B* gene (Krzyzewska et al., 2019). The *NCOA3* gene (nuclear receptor coactivator 3; OAR13: 32.0 Mb) encodes a nuclear receptor coactivator with histone acetyltransferase activity. It particularly interacts with other transcriptional activators such p300/CBP-associated factor and CREB binding protein (CREBBP) as part of a multi-subunit coactivation complex. The *CREBBP* gene, also located near a significant QTL position (OAR 24: 3.1 Mb) has been recently reported to be involved in the crosstalk between DNA methylation and histone acetylation

(Zhang et al., 2020). Finally, two lysine acetyltransferase coding genes of the MYST family, *KAT6A* (lysine acetyltransferase 6A, also named *MOZ*, OAR26: 35.3 Mb) and *KAT7* (lysine acetyltransferase 7, also named *HBO1*, OAR11: 36.4 Mb) has been reported to play a key role in acetylation of lysine residues in histone H3 and/or H4 (Kitabayashi et al., 2001). Interestingly, KDM8, NCOA3 and KAT7 act as androgen or estrogen receptor co-regulators (Sharma et al., 2000; Vija et al., 2013; Wagner et al., 2013; Wang et al., 2019). Polymorphisms that alter the function of these genes could explain that female lambs had higher GDMR than male lambs.

The level and state of histone acetylation regulated by histone acetyl transferase enzymes are widely reported to be an epigenetic regulation of gene expression (Kouzarides, 2007). Therefore, we cannot exclude the possibility that global DNA methylation in sheep is associated with histone acetylation, since relationships between DNA methylation and histone de-acetylation have already been described (Geiman and Robertson, 2002; Vaissière et al., 2008). Several other coding genes, located close to QTLs we identified, have been reported to be involved in the regulation of transcription or regulation of chromatin architecture. Although no scientific evidence has suggested their involvement in DNA methylation to date, these genes could mediate this process through their active role in the coregulatory complexes that associate epigenetic modifiers to modulate transcription.

## CONCLUSION

Inter-individual variability in global DNA methylation rate in blood has an additive genetic component in sheep and heritability was moderate ($h^2 = 0.20 \pm 0.05$). This opens the way for a possible genetic selection of this trait and create experimental divergent lines to investigate further the relationship between GDMR and adaptive traits as already evidenced in plants (Johannes et al., 2009; Kooke and Keurentjes, 2015). Moreover, this work reported the first SNP-based QTL detection study for GDMR as a quantitative trait in livestock species. The evidence of 28 QTLs associated with blood GDMR, each explaining a small proportion of the phenotypic variance (between 1 and 3%), most likely indicated a polygenic determinism of this trait. The further identification of genes and their polymorphisms underlying the global DNA methylation rate assessed in our study will paves the way for a deeper understanding the genetic component of such a trait.

## DATA AVAILABILITY STATEMENT

The raw data supporting the conclusions of this article will be made available by the authors, without undue reservation.

## ETHICS STATEMENT

The animal study was reviewed and approved by the Local ethics committee SCIENCE ET SANTE ANIMALES N°115 (Ecole Nationale Vétérinaire de Toulouse).

## AUTHOR CONTRIBUTIONS

DH, LD, CM-R, and SF conceived and designed the genetic experimental design and were involved in planning the study. FP-P was in charge of the phenotyping of GDMR. DH performed statistical and genetic analyses. DH, LD, SF, FP-P, and CM-R analyzed and interpreted the results. DH drafted the manuscript. LD, SF, and CM-R helped in writing, reviewing, and editing the final manuscript. All authors have read and approved the final manuscript.

## FUNDING

This study was granted by the INRAE metaprogram SELGEN (GENEPIGEN project), particularly for the phenotyping of GDMR. Genotyping was funded by ANR and APIS-GENE organizations in the frame of SheepSNPQTL project (ANR-08-GENM-039). The INRAE Division of Animal Genetics supported computational facilities and experimental costs for the production of the animals and the collection of behavioral, zootechnical and carcass traits.

## ACKNOWLEDGMENTS

We are indebted to Paul Autran for the management of the experimental farm, Didier Foulquié and Fabien Carrière for managing the experimental flock, for animal care as well as for their active role in collecting experimental data. We also thank Alain Boissy and Eric Delval (INRAE UMR Herbivores) for their involvement in behavioral experiments, and Dominique François for his involvement in the management of animal breeding.

## REFERENCES

Allain, D., Foulquié, D., Autran, P., Francois, D., and Bouix, J. (2014). Importance of birthcoat for lamb survival and growth in the romane sheep breed extensively managed on rangelands. *J. Anim. Sci.* 92, 54–63. doi: 10.2527/jas.2013-6660

Amendola, P. G., Zaghet, N., Ramalho, J. J., Johansen, J. V., Boxem, M., and Salcini, A. E. (2017). JMJD-5/KDM8 regulates H3K36me2 and is required for late steps of homologous recombination and genome integrity. *PLoS Genet.* 13:e1006632. doi: 10.1371/journal.pgen.1006632

Belden, W. J., Lewis, Z. A., Selker, E. U., Loros, J. J., and Dunlap, J. C. (2011). CHD1 remodels chromatin and influences transient DNA methylation at the clock gene frequency. *PLoS Genet.* 7:e1002166. doi: 10.1371/journal.pgen.1002166

Benjamini, Y., and Hochberg, Y. (1995). Controlling the false discovery rate - a pratical and powerful approach to multiple testing. *J. R. Stat. Soc. Ser. B Methodol.* 57, 289–300. doi: 10.1111/j.2517-6161.1995.tb02031.x

Berger, M. F., Lawrence, M. S., Demichelis, F., Drier, Y., Cibulskis, K., Sivachenko, A. Y., et al. (2011). The genomic complexity of primary human prostate cancer. *Nature* 470, 214–220. doi: 10.1038/nature09744

Bibé, B., Brunel, J., Bourdillon, Y., Laradoux, D., Gordy, M., Weisbecker, J., et al. (2002). "Genetic parameters of growth and carcass quality of lambs at the French progeny-test station Berrytest," in *Proceedings of the 7th World Congress on Genetics Applied to Livestock Production*, (Montpellier).

Cao, J. X., Wei, C. H., Liu, D. M., Wang, H. H., Wu, M. M., Xie, Z. Y., et al. (2015). DNA methylation Landscape of body size variation in sheep. *Sci. Rep.* 5:13950. doi: 10.1038/srep13950

Champagne, F. A., and Curley, J. P. (2009). Epigenetic mechanisms mediating the long-term effects of maternal care on development. *Neurosci. Biobehav. Rev.* 33, 593–600. doi: 10.1016/j.neubiorev.2007.10.009

Cortijo, S., Wardenaar, R., Colomé-Tatché, M., Gilly, A., Etcheverry, M., Labadie, K., et al. (2014). Mapping the epigenetic basis of complex traits. *Science* 343, 1145–1148. doi: 10.1126/science.1248127

Couldrey, C., Brauning, R., Bracegirdle, J., Maclean, P., Henderson, H. V., and McEwan, J. C. (2014). Genome-wide DNA methylation patterns and transcription analysis in sheep muscle. *PLoS One* 9:101853. doi: 10.1371/journal.pone.0101853

Danchin, E., Charmantier, A., Champagne, F. A., Mesoudi, A., Pujol, B., and Blanchet, S. (2011). Beyond DNA: integrating inclusive inheritance into an extended theory of evolution. *Nat. Rev. Genet.* 12, 475–486. doi: 10.1038/nrg3028

Dick, K. J., Nelson, C. P., Tsaprouni, L., Sandling, J. K., Aïssi, D., Wahl, S., et al. (2014). DNA methylation and body-mass index: a genome-wide analysis. *Lancet* 383, 1990–1998. doi: 10.1016/s0140-6736(13)62674-62674

Doherty, R., and Couldrey, C. (2014). Exploring genorne wide bisulfite sequencing for DNA rnethylation analysis in livestock: a technical assessment. *Front. Genet.* 5:126. doi: 10.3389/fgene.2014.00126

Donohue, K. (2014). THE epigenetics of adaptation: focusing on epigenetic stability as an evolving trait. *Evolution* 68, 617–619. doi: 10.1111/evo.12347

Ehrlich, M., Gama-Sosa, M. A., Huang, L.-H., Midgett, R. M., Kuo, K. C., McCune, R. A., et al. (1982). Amount and distribution of 5-methylcytosine in human DNA from different types of tissues or cells. *Nucleic Acids Res.* 10, 2709–2721. doi: 10.1093/nar/10.8.2709

Feinberg, A. P., Koldobskiy, M. A., and Gondor, A. (2016). Epigenetic modulators, modifiers and mediators in cancer aetiology and progression. *Nat. Rev. Genet.* 17, 284–299. doi: 10.1038/nrg.2016.13

Fuhrmann, D., Mernberger, M., Nist, A., Stiewe, T., and Elsasser, H. P. (2018). Miz1 controls schwann cell proliferation via H3K36(me2) demethylase Kdm8 to prevent peripheral nerve demyelination. *J. Neurosci.* 38, 858–877. doi: 10.1523/jneurosci.0843-17.2017

García-Calzón, S., Perfilyev, A., de Mello, V. D., Pihlajamäki, J., and Ling, C. (2018). Sex differences in the methylome and transcriptome of the human liver and circulating HDL-cholesterol levels. *J. Clin. Endocrinol. Metab.* 103, 4395–4408. doi: 10.1210/jc.2018-2423

Geiman, T. M., and Robertson, K. D. (2002). Chromatin remodeling, histone modifications, and DNA methylation—how does it all fit together? *J. Cell. Biochem.* 87, 117–125. doi: 10.1002/jcb.10286

Gilbert, H., Le Roy, P., Moreno, C., Robelin, D., and Elsen, J. M. (2008). QTLMAP, a software for QTL detection in outbred populations. *Ann. Hum. Genet.* 72, 694–694.

Gilmour, A. R., Gogel, B. J., Cullis, B. R., and Thompson, R. (2009). *ASReml User Guide Release 3.0*. Hemel Hempstead: VSN International Ltd.

Goddard, M. E., Hayes, B. J., and Meuwissen, T. H. E. (2010). Genomic selection in livestock populations. *Genet. Res.* 92, 413–421. doi: 10.1017/S0016672310000613

Gonzalez-Garcia, E., de Figuereido, V. G., Foulquie, D., Jousserand, E., Autran, P., Camous, S., et al. (2014). Circannual body reserve dynamics and metabolic profile changes in Romane ewes grazing on rangelands. *Domest. Anim. Endocrinol.* 46, 37–48. doi: 10.1016/j.domaniend.2013.10.002

Gordon, L., Joo, J. E., Powel, J. E., Ollikainen, M., Novakovic, B., Li, X., et al. (2012). Neonatal DNA methylation profile in human twins is specified by a complex interplay between intrauterine environmental and genetic factors, subject to tissue-specific influence. *Genome Res.* 22, 1395–1406. doi: 10.1101/gr.136598.111

Hazard, D., Bouix, J., Chassier, M., Delval, E., Foulquie, D., Fassier, T., et al. (2016). Genotype by environment interactions for behavioral reactivity in sheep. *J. Anim. Sci.* 94, 1459–1471. doi: 10.2527/jas2015-0277

Hazard, D., Moreno, C., Foulquié, D., Delval, E., François, D., Bouix, J., et al. (2014). Identification of QTLs for behavioral reactivity to social separation and humans in sheep using the OvineSNP50 BeadChip. *BMC Genom.* 15:778. doi: 10.1186/1471-2164-15-778

Herman, J. J., Spencer, H. G., Donohue, K., and Sultan, S. E. (2014). How stable 'should' epigenetic modifications be? Insights from adaptive plasticity and bet hedging. *Evolution* 68, 632–643. doi: 10.1111/evo.12324

Hsia, D. A., Tepper, C. G., Pochampalli, M. R., Hsia, E. Y. C., Izumiya, C., Huerta, S. B., et al. (2010). KDM8, a H3K36me2 histone demethylase that acts in the cyclin A1 coding region to regulate cancer cell proliferation. *Proc. Natl. Acad. Sci. U. S. A.* 107, 9671–9676. doi: 10.1073/pnas.1000401107

Johannes, F., Colot, V., and Jansen, R. C. (2008). Epigenome dynamics: a quantitative genetics perspective. *Nat. Rev. Genet.* 9, 883–890. doi: 10.1038/nrg2467

Johannes, F., Porcher, E., Teixeira, F. K., Saliba-Colombani, V., Simon, M., Agier, N., et al. (2009). Assessing the impact of transgenerational epigenetic variation on complex traits. *PLoS Genet.* 5:e1000530. doi: 10.1371/journal.pgen.1000530

Karimi, M., Johansson, S., and Ekstrom, T. J. (2006a). Using LUMA A luminometric-based assay for global DNA-methylation. *Epigenetics* 1, 45–48.

Karimi, M., Johansson, S., Stach, D., Corcoran, M., Grander, D., Schalling, M., et al. (2006b). LUMA (LUminometric methylation assay) - a high throughput method to the analysis of genomic DNA methylation. *Exp. Cell Res.* 312, 1989–1995. doi: 10.1016/j.yexcr.2006.03.006

Kitabayashi, I., Aikawa, Y., Nguyen, L. A., Yokoyama, A., and Ohki, M. (2001). Activation of AML1-mediated transcription by MOZ and inhibition by the MOZ–CBP fusion protein. *EMBO J.* 20, 7184–7196. doi: 10.1093/emboj/20.24.7184

Knott, S. A., Marklund, L., Haley, C. S., Andersson, K., Davies, W., Ellegren, H., et al. (1998). Multiple marker mapping of quantitative trait loci in a cross between outbred wild boar and large white pigs. *Genetics* 149, 1069–1080.

Kooke, R., Johannes, F., Wardenaar, R., Becker, F., Etcheverry, M., Colot, V., et al. (2015). Epigenetic basis of morphological variation and phenotypic plasticity in *Arabidopsis thaliana*. *Plant Cell* 27, 337–348. doi: 10.1105/tpc.114.133025

Kooke, R., and Keurentjes, J. J. B. (2015). Epigenetic variation contributes to environmental adaptation of *Arabidopsis thaliana*. *Plant Signal. Behav.* 10:e1057368. doi: 10.1080/15592324.2015.1057368

Kouzarides, T. (2007). Chromatin modifications and their function. *Cell* 128, 693–705. doi: 10.1016/j.cell.2007.02.005

Krzyzewska, I. M., Maas, S. M., Henneman, P., Lip, K. V. D., Venema, A., Baranano, K., et al. (2019). A genome-wide DNA methylation signature for SETD1B-related syndrome. *Clin. Epigenet.* 11:156. doi: 10.1186/s13148-019-0749-743

Latzel, V., Allan, E., Silveira, A. B., Colot, V., Fischer, M., and Bossdorf, O. (2013). Epigenetic diversity increases the productivity and stability of plant populations. *Nat. Commun.* 4:2875. doi: 10.1038/ncomms3875

Lea, A. J., Altmann, J., Alberts, S. C., and Tung, J. (2016). Resource base influences genome-wide DNA methylation levels in wild baboons (*Papio cynocephalus*). *Mol. Ecol.* 25, 1681–1696. doi: 10.1111/mec.13436

Legarra, A., and Fernando, R. L. (2009). Linear models for joint association and linkage QTL mapping. *Genet. Sel. Evol.* 41:43. doi: 10.1186/1297-9686-41-43

Luo, Z. W. (1998). Detecting linkage disequilibrium between a polymorphic marker locus and a trait locus in natural populations. *Heredity* 80, 198–208. doi: 10.1046/j.1365-2540.1998.00275.x

Lynch, M., and Walsh, B. (1998). *Genetics and Analysis of Quantitative Traits*. Sunderland, MA: Sinauer Associates.

Massicotte, R., Whitelaw, E., and Angers, B. (2011). DNA methylation: a source of random variation in natural populations. *Epigenetics* 6, 421–427. doi: 10.4161/epi.6.4.14532

McRae, A. F., Powell, J. E., Henders, A. K., Bowdler, L., Hemani, G., Shah, S., et al. (2014). Contribution of genetic variation to transgenerational inheritance of DNA methylation. *Genome Biol.* 15:R73. doi: 10.1186/gb-2014-15-5-r73

Nanda, J. S., Kumar, R., and Raghava, G. P. S. (2016). DbEM: a database of epigenetic modifiers curated from cancerous and normal genomes. *Sci. Rep.* 6:19340. doi: 10.1038/srep19340

Ou, M., Mao, H. H., Luo, Q., Zhao, J., Liu, H. Y., Zhu, X. P., et al. (2019). The DNA methylation level is associated with the superior growth of the hybrid fry in snakehead fish (*Channa argus* x *Channa maculata*). *Gene* 703, 125–133. doi: 10.1016/j.gene.2019.03.072

Piepho, H. P. (2001). A quick method for computing approximate thresholds for quantitative trait loci detection. *Genetics* 157, 425–432.

Ricordeau, G., Tchamitchian, L., Brunel, J., Nguyen, T., and François, D. (1992). La race ovine INRA 401: un exemple de souche synthétique. *INRA Produ. Anim.* 5, 255–262. doi: 10.20870/productions-animales.1992.5.hs.4300

Roth, T. L. (2013). Epigenetic mechanisms in the development of behavior: advances, challenges, and future promises of a new field. *Dev. Psychopathol.* 25(4 Pt 2), 1279–1291. doi: 10.1017/S0954579413000618

Roussot, O., Feve, K., Plisson-Petit, F., Pitel, F., Faure, J. M., Beaumont, C., et al. (2003). AFLP linkage map of the Japanese quail *Coturnix japonica*. *Genet. Sel. Evol.* 35, 559–572. doi: 10.1186/1297-9686-35-6-559

SAS Institute Inc (1999). *SAS/STAT§ User's Guide, Version 8*. Cary, NC: SAS Institute Inc.

Schlichting, C. D., and Wund, M. A. (2014). Phenotypic plasticity and epigenetic marking: an assessment of evidence for genetic accommodation. *Evolution* 68, 656–672. doi: 10.1111/evo.12348

Seebacher, F., and Krause, J. (2019). Epigenetics of social behaviour. *Trends Ecol. Evol.* 34, 818–830. doi: 10.1016/j.tree.2019.04.017

Shah, S., McRae, A. F., Marioni, R. E., Harris, S. E., Gibson, J., Henders, A. K., et al. (2014). Genetic and environmental exposures constrain epigenetic drift over the human life course. *Genome Res.* 24, 1725–1733. doi: 10.1101/gr.176933.114

Sharma, M., Zarnegar, M., Li, X. Y., Lim, B., and Sun, Z. J. (2000). Androgen receptor interacts with a novel MYST protein, HBO1. *J. Biol. Chem.* 275, 35200–35208. doi: 10.1074/jbc.M004838200

Singmann, P., Shem-Tov, D., Wahl, S., Grallert, H., Fiorito, G., Shin, S.-Y., et al. (2015). Characterization of whole-genome autosomal differences of DNA methylation between men and women. *Epigenetics Chromatin* 8:43. doi: 10.1186/s13072-015-0035-33

Soriano-Tarraga, C., Jimenez-Conde, J., Giralt-Steinhauer, E., Ois, A., Rodriguez-Campello, A., Cuadrado-Godia, E., et al. (2013). DNA isolation method is a source of global DNA methylation variability measured with LUMA. experimental analysis and a systematic review. *PLoS One* 8:e60750. doi: 10.1371/journal.pone.0060750

Turck, F., and Coupland, G. (2014). Natural variation in epigenetic gene regulation and its effects on plant developmental traits. *Evolution* 68, 620–631. doi: 10.1111/evo.12286

Vaissière, T., Sawan, C., and Herceg, Z. (2008). Epigenetic interplay between histone modifications and DNA methylation in gene silencing. *Mutat. Res. Rev. Mut. Res.* 659, 40–48. doi: 10.1016/j.mrrev.2008.02.004

van Dongen, J., Nivard, M. G., Willemsen, G., Hottenga, J. J., Helmer, Q., Dolan, C. V., et al. (2016). Genetic and environmental influences interact with age and sex in shaping the human methylome. *Nat. Commun.* 7:11115. doi: 10.1038/ncomms11115

Verhulst, E. C., Mateman, A. C., Zwier, M. V., Caro, S. P., Verhoeven, K. J. F., and van Oers, K. (2016). Evidence from pyrosequencing indicates that natural variation in animal personality is associated with DRD4 DNA methylation. *Mol. Ecol.* 25, 1801–1811. doi: 10.1111/mec.13519

Vija, L., Meduri, G., Comperat, E., Vasiliu, V., Izard, V., Ferlicot, S., et al. (2013). Expression and characterization of androgen receptor coregulators, SRC-2 and HBO1, during human testis ontogenesis and in androgen signaling deficient patients. *Mol. Cell. Endocrinol.* 375, 140–148. doi: 10.1016/j.mce.2013.05.004

Wagner, M., Koslowski, M., Paret, C., Schmidt, M., Tureci, O., and Sahin, U. (2013). NCOA3 is a selective co-activator of estrogen receptor alpha-mediated transactivation of PLAC1 in MCF-7 breast cancer cells. *BMC Cancer* 13:570. doi: 10.1186/1471-2407-13-570

Wang, H. J., Pochampalli, M., Wang, L. Y., Zou, J. X., Li, P. S., Hsu, S. C., et al. (2019). KDM8/JMJD5 as a dual coactivator of AR and PKM2 integrates AR/EZH2 network and tumor metabolism in CRPC. *Oncogene* 38, 17–32. doi: 10.1038/s41388-018-0414-x

Yousefi, P., Huen, K., Davé, V., Barcellos, L., Eskenazi, B., and Holland, N. (2015). Sex differences in DNA methylation assessed by 450 K BeadChip in newborns. *BMC Genom.* 16:911. doi: 10.1186/s12864-015-2034-y

Zhang, B. L., Gu, X. H., Han, X., Gao, Q., Liu, J., Guo, T. W., et al. (2020). Crosstalk between DNA methylation and histone acetylation triggers GDNF high transcription in glioblastoma cells. *Clin. Epigenet.* 12:47. doi: 10.1186/s13148-020-00835-833

Zhang, Y. L., Li, F. Z., Feng, X., Yang, H., Zhu, A. X., Pang, J., et al. (2017). Genome-wide analysis of DNA Methylation profiles on sheep ovaries associated with prolificacy using whole-genome Bisulfite sequencing. *BMC Genom.* 18:759. doi: 10.1186/s12864-017-4068-4069

**Conflict of Interest:** The authors declare that the research was conducted in the absence of any commercial or financial relationships that could be construed as a potential conflict of interest.

*Copyright © 2020 Hazard, Plisson-Petit, Moreno-Romieux, Fabre and Drouilhet. This is an open-access article distributed under the terms of the Creative Commons Attribution License (CC BY). The use, distribution or reproduction in other forums is permitted, provided the original author(s) and the copyright owner(s) are credited and that the original publication in this journal is cited, in accordance with accepted academic practice. No use, distribution or reproduction is permitted which does not comply with these terms.*

frontiers in Genetics

ORIGINAL RESEARCH
published: 11 January 2021
doi: 10.3389/fgene.2020.574167

# Dysregulated H3K27 Acetylation Is Implicated in Fatty Liver Hemorrhagic Syndrome in Chickens

*Yaling Zhu[1,2,3], Qingjie Zeng[1], Fang Li[2], Haoshu Fang[2,3], Zhimin Zhou[1], Tao Jiang[1], Chao Yin[1], Qing Wei[1], Yujie Wang[1], Jiming Ruan[1]* and Jianzhen Huang[1]**

[1] College of Animal Science and Technology, Jiangxi Agricultural University, Nanchang, China, [2] Department of Pathophysiology, Anhui Medical University, Hefei, China, [3] Laboratory Animal Research Center, College of Basic Medical Science, Anhui Medical University, Hefei, China

Epigenetic regulation of gene expression has been reported in the pathogenesis of metabolic disorders such as diabetes and liver steatosis in humans. However, the molecular mechanisms of fatty liver hemorrhagic syndrome (FLHS) in chickens have been rarely studied. H3K27ac chromatin immunoprecipitation coupled with high-throughput sequencing and high-throughput RNA sequencing was performed to compare genome-wide H3K27ac profiles and transcriptomes of liver tissue between healthy and FLHS chickens. In total, 1,321 differential H3K27ac regions and 443 differentially expressed genes were identified (| log2Fold change| $\geq$ 1 and *P*-value $\leq$ 0.05) between the two groups. Binding motifs for transcription factors involved in immune processes and metabolic homeostasis were enriched among those differential H3K27ac regions. Differential H3K27ac peaks were associated with multiple known FLHS risk genes, involved in lipid and energy metabolism (*PCK1*, *APOA1*, *ANGPTL4*, and *FABP1*) and the immune system (*FGF7*, *PDGFRA*, and *KIT*). Previous studies and our current results suggested that the high-energy, low-protein (HELP) diet might have an impact on histone modification and chromatin structure, leading to the dysregulation of candidate genes and the peroxisome proliferator-activated receptor (PPAR) signaling pathway, which causes excessive accumulation of fat in the liver tissue and induces the development of FLHS. These findings highlight that epigenetic modifications contribute to the regulation of gene expression and play a central regulatory role in FLHS. The PPAR signaling pathway and other genes implicated in FLHS are of great importance for the development of novel and specific therapies for FLHS-susceptible commercial laying hens.

**Keywords: fatty liver hemorrhagic syndrome, ChIP-seq, RNA-seq, H3K27ac, chicken**

OPEN ACCESS

***Edited by:***
*Helene Kiefer,*
*INRA Centre Jouy-en-Josas, France*

***Reviewed by:***
*Vincent Coustham,*
*INRA Centre Val de Loire, France*
*James Ronald Davie,*
*University of Manitoba, Canada*
*Tasnim Beacon,*
*University of Manitoba, Canada, in collaboration with reviewer JD*

****Correspondence:***
*Jiming Ruan*
*rjm903@163.com*
*Jianzhen Huang*
*hjzh0722@aliyun.com*

***Specialty section:***
*This article was submitted to Epigenomics and Epigenetics, a section of the journal Frontiers in Genetics*

***Received:*** *19 June 2020*
***Accepted:*** *23 November 2020*
***Published:*** *11 January 2021*

***Citation:***
*Zhu Y, Zeng Q, Li F, Fang H, Zhou Z, Jiang T, Yin C, Wei Q, Wang Y, Ruan J and Huang J (2021) Dysregulated H3K27 Acetylation Is Implicated in Fatty Liver Hemorrhagic Syndrome in Chickens. Front. Genet. 11:574167. doi: 10.3389/fgene.2020.574167*

## INTRODUCTION

Fatty liver hemorrhagic syndrome (FLHS) is a lipid metabolism disorder, which is characterized by a dramatic drop in egg production and increased mortality of commercial laying hens, in turn causing considerable economic losses (Hansen and Walzem, 1993; Trott et al., 2014; Rozenboim et al., 2016). Several factors have been reported to contribute to the development of FLHS, including

heredity, environment, nutrition, toxic substances, and hormones (Schuman et al., 2000; Li et al., 2013). Among these, nutrition is considered the main cause of FLHS in the modern poultry industry, and 97% of affected chickens have large fat depots (Trott et al., 2014). Despite of the progress made in understanding the risk factors that contribute to FLHS, the epigenetic mechanism via which nutrition drives FLHS susceptibility remain elusive, and adaptive changes in epigenetic and transcriptional regulation play an important role in the phenotypic adaptation of cells to the environment (Corradin and Scacheri, 2014; Lee et al., 2014; Nammo et al., 2018).

Many reports support the notion that epigenomic dysregulation may influence transcriptional output and signaling pathways, providing a mechanistic basis for investigating its involvement in various common diseases, such as non-alcoholic fatty liver (NAFLD), diabetes, Alzheimer's diseases, and others (Ling and Groop, 2009; Lee et al., 2014; Marzi et al., 2018; Nammo et al., 2018). For example, Lee et al. (2014) found that epigenetic manipulation through the metabolic pathway of one-carbon metabolism slows the progression of NAFLD. Ling and Groop (2009) suggested that genome-wide technologies for studying the gene expression and genetic variations in patients with type 2 diabetes have revealed a variety of new diabetes-related genes. Marzi et al. (2018) reported that differentially acetylated peaks were enriched for disease-related pathways and associated genes, a change which was involved in the development of amyloid-β and tau pathology in sporadic late-onset AD. To date, however, no systematic study has examined the regulatory modifications of FLHS in chicken.

H3K27ac, an epigenetic marker of active enhancers and promoters, is strongly associated with transcription factor binding and gene expression. Genome-wide H3K27ac profiles provide valuable information not only for annotating variants but also for understanding disease in both humans and animals (Creyghton et al., 2010; Marzi et al., 2018). Herein, we carried out chromatin immunoprecipitation combined with high-throughput sequencing (ChIP-Seq) for the H3K27ac marker and RNA sequencing to analyze the genome-wide H3K27ac profiles and liver transcriptomes of high-energy, low-protein (HELP) diet-induced FLHS chicken models and healthy birds with the aim of identifying transcription factor binding motifs, candidate genes, and pathways functionally related to FLHS.

# MATERIALS AND METHODS

## Ethics and Consent

All the animals are raised in compliance with the care and use guidelines of experimental animals established by the Ministry of Agriculture of China. This study was approved by the Ethics Committee of Jiangxi Agricultural University and Anhui Medical University.

## Experimental Animals and Tissue Collection

To study the transcriptional programs and epigenomes of liver tissues from healthy and FLHS chickens, we first chose 90 healthy 155-day-old Hy-Line Brown layers with an average body weight of 1.5 kg. After 7 days of accommodation at temperature of 28°C, layers were randomly assigned as experimental and control groups, so that each group had 45 layers divided between three replicates (15 layers per replicate). Layers in the control group were fed a standard diet (Baker and Han, 1994), and those of the experimental group were fed a HELP diet (**Supplementary Table 1**). Then, we randomly dissected livers from three experimental and three control chickens at about 8 weeks of age, following the standardized sample collection protocols of the FAANG Project[1] for following RNA-seq and ChIP-seq.

Phenotypic values are presented as mean ± standard deviation ($M \pm SD$). Statistical comparisons of phenotypic values between the experimental and control groups were carried out using the Student's *t*-test. Statistical differences were considered significant at $P \leq 0.05$ and highly significant at $P \leq 0.01$.

## Histopathological Examination

We dissected fresh liver samples and fixed them in 10% neutral buffered formalin. Samples were then routinely embedded in paraffin and stained with hematoxylin and eosin (H&E) as previously reported (Cinti, 2001). We used an optical microscope to observe stained sections and Image-Pro Plus 6.0 software to calculate the diameters of stained adipocytes.

## RNA Sequencing and Analysis of Differential Gene Expression

Total RNA was extracted from liver tissue using the TRIzol reagent (Invitrogen, United States). Extracted RNA was then used to construct cDNA libraries using the NEBNext® Ultra™ Directional RNA Library Prep Kit for Illumina® (NEB, United States). On a HiSeq 4000 platform (Illumina) by Novogene (United States), 150-bp reads (paired-end) were generated at a depth of approximately 46.2 million reads (**Supplementary Table 2**).

We mapped filtered reads to the chicken reference genome Gallus_gallus-6.0 (Ensembl) using STAR-2.5.3a (Dobin et al., 2013). The featureCounts software (Liao et al., 2014) was used with "gene" as the feature and in strand-unaware mode. Lowly expressed genes (when the counts across 90% samples are lower than 2) were then removed, since those are usually more vulnerable to measurement errors as reported in our previous study (Zhu et al., 2020). The fragments per kilobase of transcript sequence per millions base pairs (FPKM) algorithm was used to normalize the expression of each gene. Differential expression analysis was performed using the DESeq2 R package (Love et al., 2014), and the resulting *P*-value was adjusted using Benjamini and Hochberg's approach for controlling false discovery rates (Zhu et al., 2020). Bioinformatics analyses were performed in R version 3.5.1[2].

[1] https://www.faang.org

[2] https://www.r-project.org/

## Differential ChIP-Seq Analysis of H3K27-Acetylated Regions

Chromatin immunoprecipitation samples, from the same samples used in RNA-seq, were prepared using the SimpleChIP® Plus Enzymatic Chromatin IP Kit (Magnetic Beads, 9005) with 500 μg chromatin and 5 μg anti-H3K27ac antibody (Active motif, 39133), following protocols from https://www.encodeproject.org/about/experiment-guidelines/ and https://www.animalgenome.org/community/FAANG. The dissected tissues are treated with 37% formaldehyde to cross-link proteins covalently to DNA. This is followed by cell disruption and sonication to shear the chromatin to a target size of 100–300 bp (Nord et al., 2013). After protease and RNAse treatment, DNA was purified, and real-time quantitative polymerase chain reaction (RT-PCR) was performed. Chromatin immunoprecipitation (ChIP) and input library construction and sequencing procedures were carried out according to Illumina protocols with minor modifications (Illumina, San Diego, CA, United States) to obtain approximately 35.5 million reads per library (**Supplementary Table 2**).

Trimmed clean reads were mapped to the chicken reference genome Gallus_gallus-6.0 (Ensembl) using the Burrows–Wheeler Aligner (BWA) (Abuin et al., 2015), allowing two mismatches. After that, a Model-based Analysis for ChIP-Seq version 2.1.0 (MACS 2.1.0) peak caller was used to determine H3K27ac-enriched regions by setting the *q*-value threshold as 1e-5 (Zhang et al., 2008). Peak files were then sorted and analyzed for intersections using bedtools version 2.27.0 (Quinlan and Hall, 2010). Peak regions were intersected for all peaks across data sets, with a distance of less than 1 kb between summits (defined as the base position with the highest coverage within the peak region) used as the merge criteria, following similar steps set by a previous report (Nord et al., 2013). **Table 1** shows a summary of statistics for all ChIP-seq data sets.

The PeakAnalyzer[3] tool was used to scan the chicken genome and identify functional elements, proximal or distal to the transcript start site (Salmon-Divon et al., 2010). H3K27ac-enriched merged regions were considered distal putative enhancers if region boundaries were at a distance of over 1 kb from the transcription start site (TSS) following the similar discipline set by the previous report (Shen et al., 2012). Hypergeometric Optimization of Motif EnRichment (HOMER) (Heinz et al., 2010), a suite of tools for ChIP-Seq data analysis and motif discovery, was adopted to understand H3K27ac enrichment of distal and proximal regions across the genome and identify the transcription factor (TF) binding motifs associated with FLHS in chickens by running the command findMotifsGenome.pl.

To identify FLHS-associated differentially acetylated regions between healthy and FLHS chickens (**Figure 4C**), we followed a protocol set by previous reports (Nord et al., 2013) and quantified peak coverage based on read counts from the BAM files for peak read depth using the samtools (version 1.2) "bedcov" utility (Li et al., 2009). Empirical coverage was estimated by comparing coverage within 20-bp bins across one megabase of mappable chicken reference genome (Ensembl) sequence. ChIP and input sample coverage were normalized by total mapped read count and peak length, and input coverage was subtracted from ChIP coverage to limit the effects of fragmentation bias. We then used the DESeq2 R package (Love et al., 2014) to obtain differential H3K27ac regions between healthy and FLHS samples according to the normalized peak coverage. Regions with a *P*-value of less than 0.05 and $|\log2\text{foldchange}| \geq 1$ were considered as differential peaks.

## Identification of the Candidate Target Genes Regulated by Differential H3K27ac Peaks

To predict candidate targets regulated by differential H3K27ac peaks, we computed the correlation between the normalized counting reads of each differential peak and gene expression level (normalized as FPKM) within the same chromosomes (Takahashi et al., 2015). Correlated peak–gene pair was defined with Pearson correlation coefficient higher than 0.8 and *P*-value lower than 0.01. Then, we selected top 100 poorly and highly acetylated peak-associated genes by ordering both Cor and *P*-value first and then screen out the top 100 peak-associated genes for further functional enrichment analyses.

## Gene Ontology and Pathway Enrichment Analyses

Functional enrichment analyses were separately conducted for significantly hyper- and hypo-acetylated peaks ($P$-value $\leq 0.05$). We then used DAVID[4] (Bindea et al., 2009), PANTHER[5] (Mi et al., 2013), and KEGG[6] (a database resource for understanding high-level functions and utilities of the biological system) to identify overrepresented GO terms and pathways of the differentially expressed genes (DEGs), accompanied by H3K27ac changes in the same direction. GO terms with a corrected *P*-value of less than 0.05 were considered significantly enriched by DEGs.

## ChIP-qPCR and RT-PCR Validation

ChIP DNA was prepared using the SimpleChIP® Plus Enzymatic Chromatin IP Kit (Magnetic Beads, 9005) with

[3]https://www.bioinformatics.org/peakanalyzer/

**TABLE 1 |** Effect of fatty liver hemorrhagic syndrome on liver index, hepatic triglyceride, and hepatic total cholesterol in chickens[1].

| Parameters[2] | Control | Experimental |
|---|---|---|
| Liver index (‰) | $14.12 \pm 0.70^{A}$ | $20.03 \pm 0.68^{B}$ |
| Hepatic TG (mmol/g) | $4.22 \pm 0.29^{A}$ | $9.44 \pm 0.43^{B}$ |
| Hepatic TC (mmol/g) | $1.64 \pm 0.15^{A}$ | $3.30 \pm 0.31^{B}$ |

*[1]Values are presented as the mean ± SD ($n \geq 10$). Values with different capital letter superscripts mean highly significant difference between different groups ($P \leq 0.01$). [2]Liver index (‰) = humid weight of liver/body weight; TG, triglyceride; TC, total cholesterol.*

[4]https://david-d.ncifcrf.gov/

[5]http://www.pantherdb.org/

[6]http://www.genome.jp/kegg/

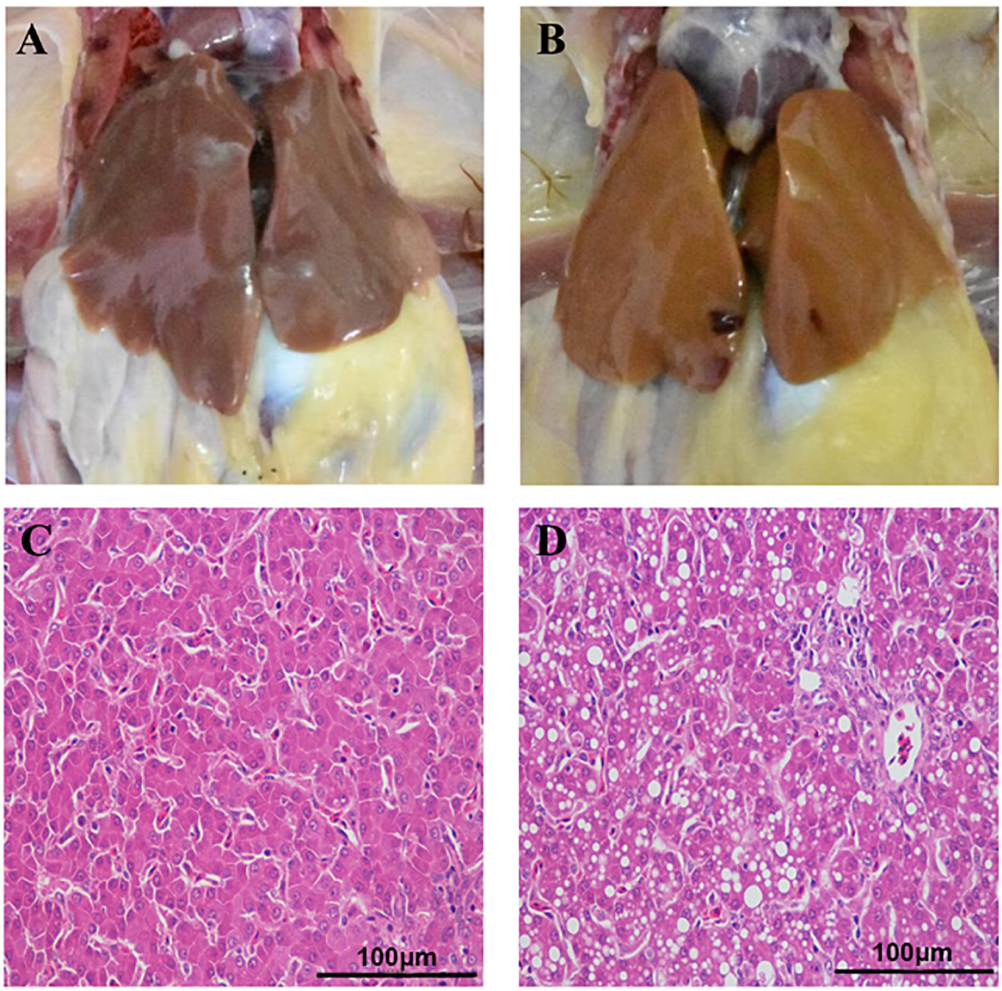



**FIGURE 1 |** Anatomical and histopathological images of the liver in chickens. **(A)** Liver tissue of healthy chickens. **(B)** Liver tissue of FLHS chickens. **(C)** Histopathological section of the liver from the healthy group. **(D)** Histopathological section of the liver of the FLHS group. Scale bars = 100 μm.

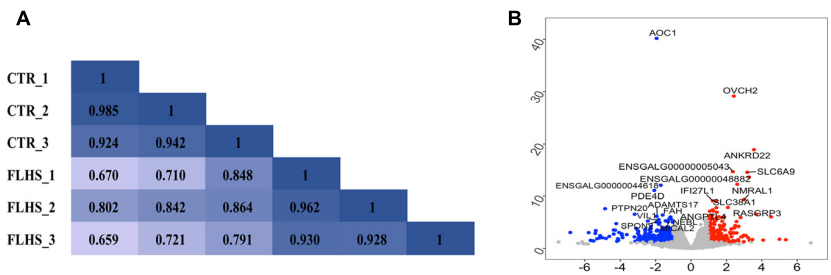



**FIGURE 2 |** Distinct transcriptional signature between healthy and FLHS chickens. **(A)** Pearson correlation coefficient for each pair of biological replicates in RNA-Seq. **(B)** Volcano plot of top significant differentially expressed genes between healthy and FLHS chickens. The red and blue dot indicates upregulated gene and downregulated gene, respectively.

500 μg chromatin from the same six samples used in RNA-seq and 5 μg anti-H3K27ac antibody (Active motif, 39133), following protocols from https://www.encodeproject.org/about/experiment-guidelines/ and https://www.animalgenome.org/community/FAANG. We adopted ChIP-qPCR to quantify ChIP DNA concentrations from samples in real time by analyzing fluorescent signal intensities that are proportional to the amount of amplicon after completing the ChIP assay and sample purification. Then, we firstly calculated the percent of input for each ChIP: %Input = $2^{[-\Delta\ Ct\ (normalized ChIP)]}$, then

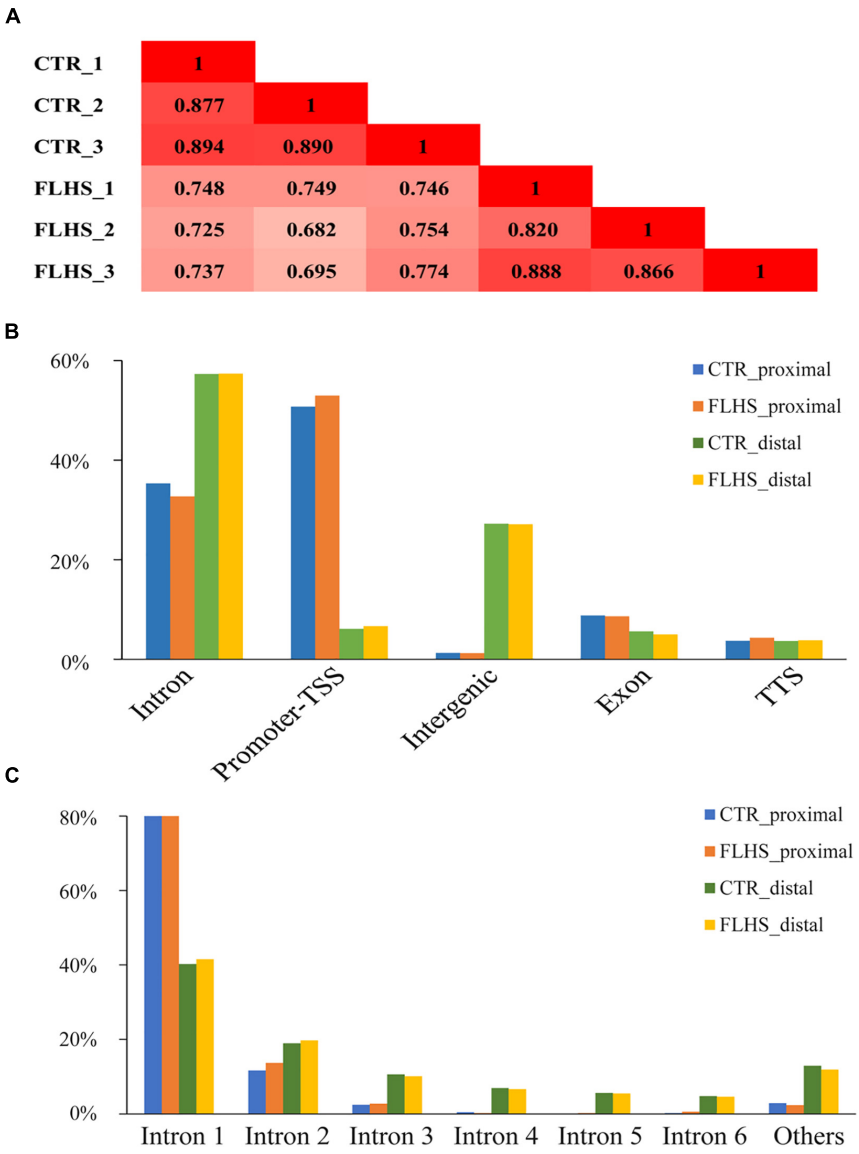



**FIGURE 3 |** Mapping *in vivo* H3K27ac mark across genomic features via ChIP-Seq. **(A)** Pearson correlation coefficient for each pair of biological replicates in ChIP-Seq. **(B)** Breakdown on proximal and distal enrichment across genome in the healthy and FLHS. **(C)** The distribution of the H3K27ac peaks among each intron.

normalized the positive locus ΔCt values to negative locus (ΔΔCt) by subtracting the ΔCt value obtained for the positive locus from the ΔCt value for negative locus: ($\Delta\Delta Ct = \Delta Ct_{positive} - \Delta Ct_{negative}$), and finally, we calculated the fold enrichment of the positive locus sequence in ChIP DNA over the negative locus: fold enrichment = $2^{\Delta\ \Delta\ Ct}$.

RNA was reverse-transcribed into first-strand cDNA with Moloney Murine Leukemia Virus transcriptase (Promega, United States) and oligo (dT) (TaKaRa, Japan) using 2 μg of total RNA. The mRNA expression level of *PCK1*, *APOA1*, *FGF7*, and *KIT* genes were quantified by real-time PCR using a LightCycler 480 instrument with the LightCycler 480 SYBR Green I Master Mix (Roche, United States). For RT-PCR amplification, cDNA was pre-denatured at 95°C for 10 min, followed by 40 cycles of 95°C for 30 s and 60°C for 1 min. The relative expression level of the target gene was normalized to that of the housekeeping gene β-actin by the $2^{-\Delta\ \Delta\ CT}$ method.

## RESULTS

### Pathological and Histopathological Differences Between the Liver Tissues From the FLHS and Normal Individuals

Fatty liver hemorrhagic syndrome-affected chickens had large, friable, and soft livers in contrast to healthy hens (**Figure 1A**), and the color varied from yellow to orange (**Figure 1B**), which is consistent with previous reports (Spurlock and Savage, 1993;

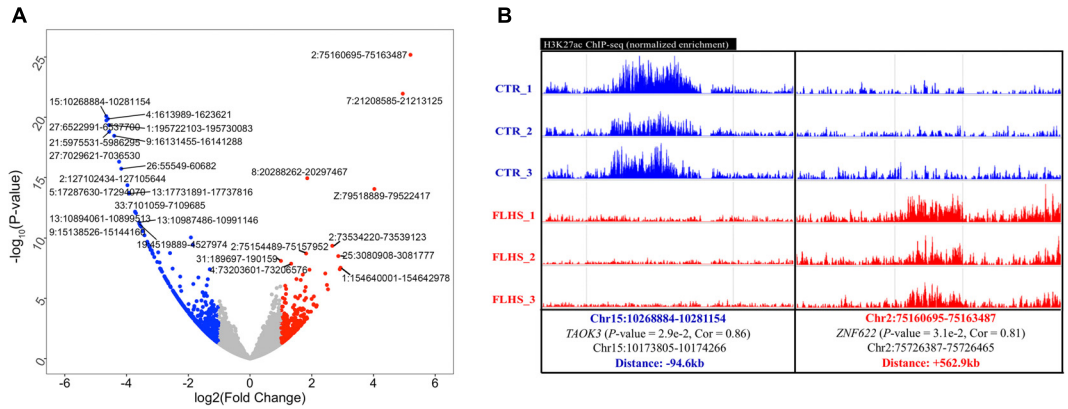



**FIGURE 4 |** Differential H3K27ac peaks associated with FLHS in the liver. **(A)** Top 10 significant differential H3K27ac peaks between healthy and FLHS chickens. **(B)** Representative validation of differential peaks exhibiting distinct activity of the H3K27ac signal across healthy and FLHS chickens.

Rozenboim et al., 2016; Zhu et al., 2020). Similar to the results we previously published (Zhu et al., 2020), there was no statistical difference in body weight between hens of the two groups, but the liver index of the FLHS group was significantly ($P \leq 0.01$) higher than that of the healthy group (**Table 1**). Further, the concentrations of hepatic triglycerides (TG) and total cholesterol (TC) were much higher ($P \leq 0.01$) than in healthy individuals (**Table 1**). In addition, as H&E staining showed, the hepatocytes in the healthy group displayed regular hepatic sinusoids and normal hepatic cords (**Figure 1C**). However, the histology of the livers in the FLHS group demonstrated liver lesions, with micro-vesicular steatosis (a lot of hepatocytes containing vacuoles of variable sizes, i.e., fat droplets) (**Figure 1D**).

## Transcriptomic Differences Between the Healthy and FLHS Chickens

To reveal the global relationship between the liver epigenome and transcriptome in healthy and FLHS chickens, we firstly used RNA-Seq and obtained about 46.2 million (37.9∼53.8M) 150-bp paired-end reads for each sample. On average, 43.8 million (36.3∼50.5M) unique reads per sample were mapped to the chicken reference genome, and only ∼2 million were classified as improper pairs (**Supplementary Table 2**). A reasonable explanation of the amount of improperly mapped reads is the poor quality of the chicken genome assembly. We then investigated sample heterogeneity between healthy and FLHS samples by calculating Pearson correlation coefficients between the biological replicates. As shown in **Figure 2A**, the correlation coefficients between samples within each group (control or FLHS) were higher than those between groups, suggestive of the high biological reproducibility of our RNA-Seq data to be used for further analyses.

To identify differentially expressed genes between the healthy and FLHS chickens, we adopted the R package DESeq2 (Love et al., 2014) for read count normalization and DEG identification. In total, 443 DEGs were identified with a $|\log2\ (\text{fold change})| \geq 1$ and an adjusted $P$-value $\leq 0.05$ (**Supplementary Figure 1**). Among these DEGs, 151 were upregulated and 292 were downregulated in FLHS chickens compared to healthy hens. The top 10 upregulated and downregulated genes are indicated in **Figure 2B**, including *OVCH2* (Wang and Ma, 2019), *ANKRD22* (Yin et al., 2017), *ENSGALG00000005043* (Moreira et al., 2018), *SLC6A9* (Alfadhel et al., 2016), *NMRAL1* (Garciandia and Suarez, 2013), *RASGRP3* (Oh-hora et al., 2003), *SLC38A1* (Kondoh et al., 2007), *ANGPTL4* (La Paglia et al., 2017; Singh et al., 2018), *AOC1* (Iffiu-Soltesz et al., 2010), *PDE4D* (Yun et al., 2016), *ADAMTS17* (Mead and Apte, 2018), *VIL1* (Xieraili et al., 2012; Roy et al., 2018), *FAH* (Grompe, 2017), and *SPON2* (Zhang Y. L. et al., 2018), which have been reported as involved in the regulation of inflammatory processes and lipid metabolism (**Table 2**).

## Genome-Wide Profiling of H3K27ac Mark in the Healthy and FLHS Chickens

To examine the genome-wide *cis*-regulatory profiles of healthy and FLHS chickens, we adopted the H3K27ac epigenetic mark, a histone modification associated with active enhancers and promoters (Creyghton et al., 2010; Rada-Iglesias et al., 2011). We generated high-quality H3K27ac ChIP-seq data using postmortem liver tissues dissected from three healthy and three FLHS chickens (**Supplementary Figure 2**). For each ChIP or input sample, 35.5 million (29.4∼49.4M) 50-bp single-end reads were obtained. On average, 32.2 million (26.5∼44.9M) reads per sample were uniquely mapped to the chicken reference genome Gallus_gallus-6.0 (Ensembl) via BWA (Abuin et al., 2015; **Supplementary Table 2**). We then calculated Pearson's correlation coefficients between samples to examine the reproducibility of our ChIP-seq assays. Pearson's correlation analysis indicated that samples were clustered closely by treatment (control or FLHS), confirming high biological reproducibility data for further functional analysis (**Figure 3A**).

We identified peaks using MACS2 to determine H3K27ac enrichment loci across the genome ($q$-value = 1e-5) (Zhang et al., 2008). Following a protocol set by previous reports (Nord et al., 2013; Villar et al., 2015), we separated the H3K27ac-enriched regions into putative distal peaks, defined as regions positioned at least 1-kb away from known TSSs, and proximal regions that

**TABLE 2 |** The top 10 up- and downregulated genes identified by RNA-Seq in FLHS chickens.

| Genes | log2FoldChange | *P*-value | *P*-adj | Regulation | Functions |
|---|---|---|---|---|---|
| *OVCH2* | 2.42 | 7.3E-30 | 5.4E-26 | Up | Metabolism and transportation of amino acids |
| *ANKRD22* | 3.56 | 1.2E-19 | 6.0E-16 | Up | Inflammatory response and apoptosis |
| *ENSGALG00000005043* | 2.36 | 1.9E-15 | 7.1E-12 | Up | Cholesterol homeostasis and lipid metabolic process |
| *SLC6A9* | 3.17 | 2.5E-15 | 7.4E-12 | Up | Neurotransmitter and amino acid transport |
| *ENSGALG00000048882* | 2.61 | 5.3E-13 | 1.1E-09 | Up | / |
| *NMRAL1* | 2.99 | 4.5E-10 | 6.7E-07 | Up | Immune response and apoptosis |
| *IFI27L1* | 1.23 | 7.3E-10 | 9.8E-07 | Up | Apoptotic process |
| *RASGRP3* | 2.08 | 1.4E-08 | 1.6E-05 | Up | Ras protein signal transduction and immune response |
| *SLC38A1* | 1.43 | 1.6E-08 | 1.6E-05 | Up | Amino acid transporter and energy metabolism |
| *ANGPTL4* | 1.25 | 6.6E-08 | 5.8E-05 | Up | Glucose and lipid metabolism |
| *AOC1* | −1.94 | 6.6E-41 | 9.8E-37 | Down | Lipid metabolism |
| *ENSGALG00000044618* | −1.71 | 7.9E-13 | 1.5E-09 | Down | / |
| *PDE4D* | −2.07 | 8.0E-12 | 1.3E-08 | Down | Phosphodiesterase activity and inflammatory response |
| *ADAMTS17* | −1.94 | 7.0E-07 | 4.0E-04 | Down | Body fat distribution and metallopeptidase activity |
| *VIL1* | −1.83 | 3.0E-06 | 1.1E-03 | Down | Inflammatory response |
| *FAH* | −1.44 | 5.1E-06 | 1.5E-03 | Down | Immune response and type II diabetes mellitus |
| *PTPN20* | −2.44 | 5.9E-06 | 1.7E-03 | Down | Proliferation, differentiation, migration, and survival |
| *MICAL2* | −1.38 | 6.1E-06 | 1.7E-03 | Down | Cell differentiation and migration and angiogenesis |
| *NEBL* | −1.29 | 8.0E-06 | 2.1E-03 | Down | Organelle organization and tropomyosin binding |
| *SPON2* | −1.96 | 8.9E-06 | 2.3E-03 | Down | Immune responses |

were within 1 kb of or overlapped TSSs. **Supplementary Figure 2** shows a schematic overview of the analysis. In total, we identified 34,424 high-confidence H3K27ac peaks, including 2,045 regions that were proximal to known TSSs and 32,379 distal regions. We then used the HOMER software (Heinz et al., 2010) to understand the enrichment of putative distal and proximal peaks in each of the two groups. The larger proportion of putative distal peaks fell into intron (∼57.3% in controls and ∼57.4% in FLHS) and intergenic chromosomal regions (∼27.2% in controls and ∼27.1% in FLHS), while putative proximal peaks were mostly located in the promoter TSS region (∼50.8% in controls and ∼53.0% in FLHS) (**Figure 3B**), which was in agreement with the fact that putative proximal peaks were more likely to overlap with transcript start sites and promoters (Villar et al., 2015). In contrast, distal peaks had a tendency to fall into intron regions. In addition, both in controls and the FLHS group, a larger proportion of H3K27ac peaks overlapped with the first intron of corresponding genes (∼81.3% of the proximal and ∼40.9% of the distal) (**Figure 3C**), suggestive of the important regulatory role of sequences located in the first intron of genes. Taken together, these results revealed the landscape of H3K27ac modifications and the proximal and distal *cis*-regulatory element distribution of these regions.

## FLHS-Associated Differential H3K27ac Peaks in the Liver

We adopted the DESeq2 R package (Love et al., 2014) to obtain differential H3K27ac regions between healthy and FLHS samples. A total of 1,321 (4.1%) of the 32,379 peaks were characterized as FLHS-associated differential acetylation with a $|\log2\text{ (fold change)}| \geq 1$ and a $P$-value $\leq 0.05$ (**Supplementary Figure 3**). Further, a significant enrichment of hypo-acetylated FLHS-associated peaks (894 or 2.8%) compared to hyper-acetylated FLHS-associated peaks (427 or 1.3%) was observed. The top 10 poorly and highly acetylated peaks are labeled in **Figure 4A** and **Supplementary Table 3**. To further validate the differential H3K27ac peaks between FLHS chickens and controls, we obtained the normalized signal of locations and putative associated target genes (**Figure 4B** and **Supplementary Figure 4**). For instance, an enhancer (Chr15:10268884-10281154) with higher H3K27ac enrichment in the control was related to *TAOK3* ($P$-value = 2.9e-2, Cor = 0.86), a gene associated with immune processes (Hammad et al., 2017). In contrast, a region (Chr2: 75160695-75163487) with increased hyper-acetylation in FLHS was identified near *ZNF622*, consistent with the known role of this gene in hepatic steatosis (Wu et al., 2018b). Together, these results reveal the widespread dysregulation of histone acetylation in the liver of FLHS chickens. In addition, we found that the distance between the differential peaks and associated genes were 94.6 and 562.9 kb (**Supplementary Figure 4**), respectively, which confirmed the enhancers are distal regulatory elements and may "skip" neighboring genes to regulate more "physically distant" ones (Andersson et al., 2014).

## Correlations in Activity Profiles Link Differential H3K27ac Peaks to Target Genes

In order to assess the association between epigenetic changes and transcript levels, we integrated ChIP-Seq and RNA-Seq data and computed the correlation between activities of differential peaks and abundance of nearby transcripts within a 1-Mb region (Takahashi et al., 2015). We identified 4,204 significant peak–gene correlations with a Cor (peak–gene correlation) $\geq 0.8$ and a $P$-value $\leq 0.01$, including 438 and 3,764 correlations

in the control and FLHS groups, respectively (**Figure 5**). Intriguingly, we also found that the number of negative peak–gene correlations was larger than that of positive peak–gene correlations for FLHS hyper-acetylated peaks (**Supplementary Figure 5A**). Compared to FLHS hypo-acetylated peak–genes (**Supplementary Figure 5B**), the frequency of peak–gene correlations within a region of 100 kb of the hyper-acetylated peaks was higher than beyond this region, showing that the frequency of both positive and negative correlations decayed with distance (**Supplementary Figure 5C**). In addition, the average distance between the peak and associated genes was 455.7 kb, which confirmed the active enhancer properties of H3K27ac, namely, that it can regulate genes without distance restrictions and may "skip" neighboring genes to regulate more "physically distant" ones (Creyghton et al., 2010; Pennacchio et al., 2013; Andersson et al., 2014; Marzi et al., 2018).

## TF Binding Motif Analysis of Differential H3K27ac Peaks

As TF binding motifs play an essential role in triggering epigenetic reprogramming, they may be abundant in regulatory regions that undergo epigenetic changes due to environmental stimuli (Kheradpour and Kellis, 2014; Nammo et al., 2018). Herein, we adopted HOMER[7] to characterize the sequence motifs for DNA-binding proteins in differentially enriched H3K27ac regions in FLHS samples compared to controls. In total, 922 known TF binding motifs were enriched by differential H3K27ac peaks between healthy and FLHS chickens. Of those, 10 significantly enriched motifs ($P$-value $\leq$ 0.01) are listed in **Table 3**, including those for ERG, FOXA1, GABPA, FLI1, ETV1, PHA-4, ELF1, FOXO1, ETS1, and ETV2, factors reported to be involved in the regulation of inflammatory processes and metabolic homeostasis. Among them, ERG (Schafer et al., 2015), GABPA (Yuan et al., 2018), FLI1 (Chen et al., 2018), ETV1 (Baena et al., 2013; Heeg et al., 2016), ELF1 (Seifert et al., 2019), and ETS1 (Zhang Y. et al., 2018) are transcription factors associated with the immune system. Together, these results suggest that DNA-binding proteins involved in FLHS-induced epigenomic regulation are mainly transcription factors associated with the immune system and metabolic homeostasis. This observation is in accordance with the fact that transcription factors can serve as direct transcriptional activators and induce epigenetic changes in regulatory regions of the genome (Sugiaman-Trapman, 2018).

## Functional Enrichment of Differentially Expressed Genes That Were Accompanied by H3K27ac Changes

To conduct functional enrichment analysis of acetylic variation, we further identified the top 100 poorly and highly acetylated

[7]http://homer.ucsd.edu/homer/motif/motifDatabase.html

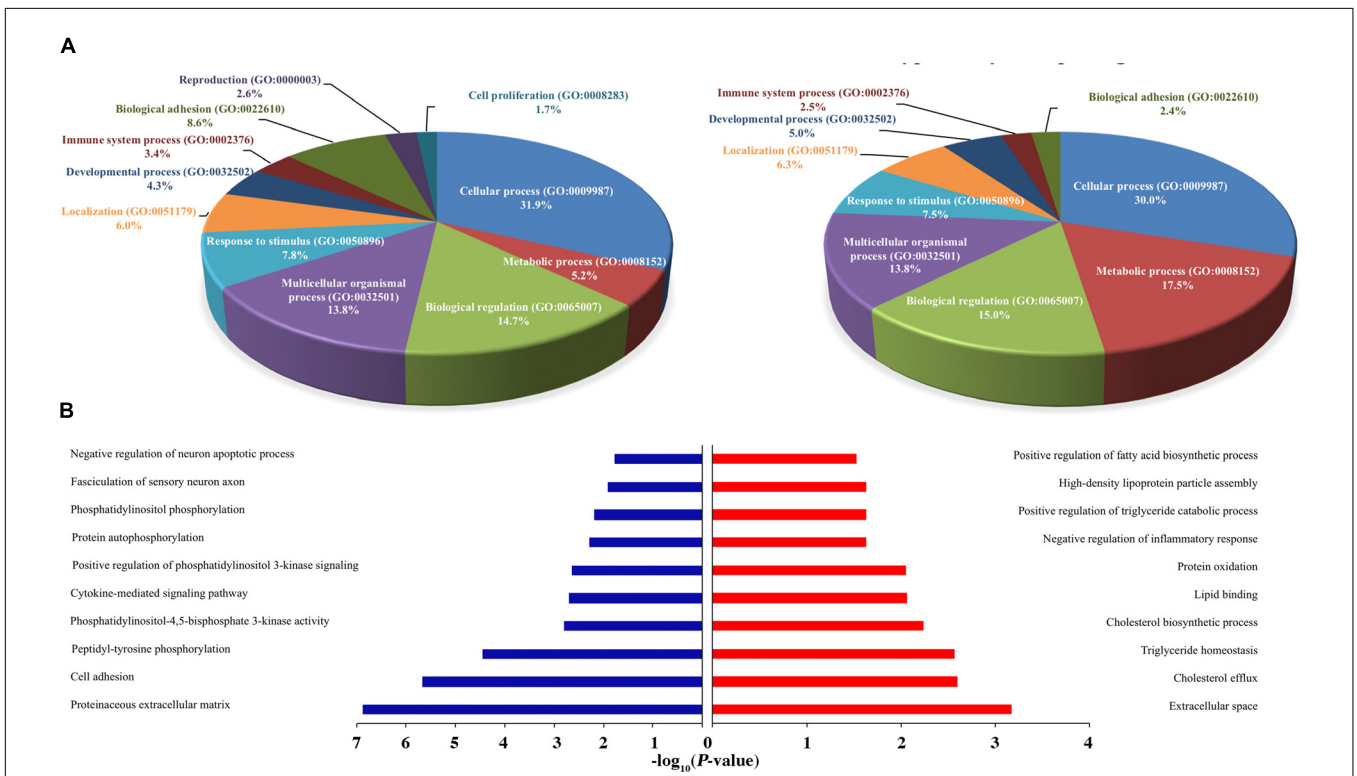



**FIGURE 5 |** Functional annotation of H3K27ac ChIP-Seq and RNA-Seq between healthy and FLHS groups. **(A)** Functional enrichment of biological processes of putative target genes associated with differentially poorly and highly acetylated peaks. **(B)** Regulation terms of putative target genes of differentially poorly and highly acetylated peaks.

**TABLE 3 |** The enriched TF binding motifs of FLHS differential H3K27ac peaks.

| Rank | Name | Motif | *P*-value | *q*-value | # Target Sequences with Motif | % of Targets Sequences with Motif | Function |
|---|---|---|---|---|---|---|---|
| 1 | ERG |  | 1.0E-04 | 1.3E-02 | 227 | 17.18% | Angiogenesis, inflammation, and apoptosis |
| 2 | FOXA1 |  | 1.0E-04 | 1.3E-02 | 206 | 15.59% | Metabolism and glucose homeostasis |
| 3 | GABPA |  | 1.0E-04 | 2.1E-02 | 118 | 8.93% | Mitochondrial function, innate and acquired immunity |
| 4 | FLI1 |  | 1.0E-03 | 3.2E-02 | 146 | 11.05% | Development of pre-T cell lymphoblastic leukemia/lymphoma |
| 5 | ETV1 |  | 1.0E-03 | 3.2E-02 | 178 | 13.47% | Cell proliferation, apoptosis, and differentiation |
| 6 | PHA-4 |  | 1.0E-03 | 3.7E-02 | 500 | 37.85% | Excessive lipid accumulation, energy metabolism |
| 7 | ELF1 |  | 1.0E-03 | 3.7E-02 | 59 | 4.47% | Antiviral immune response |
| 8 | FOXO1 |  | 1.0E-03 | 4.5E-02 | 293 | 22.18% | Metabolism regulation, disease prevention |
| 9 | ETS1 |  | 1.0E-03 | 4.5E-02 | 145 | 10.98% | Immune homeostasis |
| 10 | ETV2 |  | 1.0E-03 | 4.7E-02 | 125 | 9.46% | Hematopoiesis and vasculogenesis |

peak-associated genes, revealing overall increases and decreases in *cis*-regulatory activity, respectively (Please see section "Materials and Methods" for more details). We then used PANTHER (see text footnote 5) to understand the relevant biological processes of these differential peak-associated target genes. Remarkably, genes were overrepresented in multiple biological processes, such as "Cellular process (GO: 0009987)," "Metabolic process (GO: 0008152)," "Biological regulation (GO: 0065007)," "Response to stimulus (GO: 0050896)," and "Immune system process (GO: 0002376)," indicating that differentially acetylated peaks may trigger the expression of genes associated with these processes during the development of FHLS in chickens. Interestingly, FLHS hyper-acetylated peak-associated genes were more enriched in metabolic process, accounting for 17.5% compared to 5.2% for hypo-acetylated peak-associated genes (**Figure 5A**). For immune system processes, hypo-acetylated peak-associated genes (3.4%) were slightly more than FLHS hyper-acetylated peak-associated genes (2.5%). These results suggested that upregulated peak-associated genes may be more involved in metabolic processes, while downregulated peak-associated genes were more linked to other cellular processes, including immune processes. To further search for significantly overrepresented gene ontology terms associated with poorly and highly acetylated peak-associated genes, functional annotation was also performed using DAVID (see text footnote 4). Terms for the regulation of cholesterol and lipid metabolic processes were significantly enriched ($P$-value $\leq$ 0.01, **Figure 5B**) in the FLHS group, in consistence with results of the PANTHER-based analysis (**Figure 5A**).

## Overrepresented Pathways of Differential Peak–Genes

We tried to better understand pathways that were overrepresented by all differential peak-associated genes between control and FLHS chickens by using DAVID (see text footnote 4) and the KEGG database (see text footnote 6). In total, five significant pathways [peroxisome proliferator-activated receptor (PPAR) signaling pathway, fat digestion and absorption, PI3K-Akt signaling pathway, Rap1 signaling pathway, and the MAPK signaling pathway] were enriched ($P$-value $\leq$ 0.05) (**Table 4**), including peak-associated genes *PCK1* (Chr20:11003689-11003961) (Millward et al., 2010), *APOA1* (Chr24:5089487-5090379) (Li et al., 2018), *ANGPTL4* (Chr28:1779594-1787257) (Oteng et al., 2019), *FABP1* (Chr4:86731254-86735175) (Rodriguez Sawicki et al., 2017), *NTRK2* (ChrZ:41171358-41171800) (Geibel et al., 2014), *FGF7* (Chr10:11491528-11493116) (Itoh et al., 2016), *PDGFRA* (Chr4:65059385-65060498) (Awuah et al., 2013), and *KIT* (Chr4:65997303-65998627) (Rice et al., 2018), which are related to lipid metabolism, glucose homeostasis, and immune processes (**Table 5**). Of note, the most significantly enriched pathway, the PPAR signaling pathway, has three branches: PPARα, PPARβ/δ, and PPARγ, which are involved in the regulation of peroxisome proliferation, hepato-carcinogenesis, fatty acid metabolism, lipid homeostasis, adipocyte differentiation, and glucose metabolism (**Supplementary Figure 6**). Among those, PPARα is a nutrient sensor, which allows for the adaptation to fatty acid catabolism, lipogenesis, and ketone body synthesis in response to feeding and starvation in rodent models during systemic inflammation, atherosclerosis, and non-alcoholic steatohepatitis (NASH) (Pawlak et al., 2015). PPARβ/δ is a ligand-activated transcription factor, involved in the regulation of lipid metabolism, glucose homeostasis, and insulin sensitivity (Zarei et al., 2017). PPARγ signaling has also been implicated in the control of lipid homeostasis, macrophage function, and immunity through insulin-sensitive activation, lipid storage, metabolic regulation, and inflammatory mediators termed adipokines (Tontonoz and Spiegelman, 2008). Taken together, targeting the PPAR signaling pathway may improve insulin sensitivity, prevent lipid accumulation, and reduce liver damage during FLHS inflammatory attacks in chickens.

## ChIP-qPCR and RT-PCR Validation of Peak-Associated Target Genes

To test the interested genes enriched in pathways that related with lipid metabolic, glucose homeostasis, and immune processes, we further performed ChIP-qPCR and RT-PCR to test the enrichment and mRNA expression levels of *PCK1*, *APOA1*,

**TABLE 4 |** Top canonical pathways that are enriched by differentially peak–genes between FLHS-affected and non-affected chickens.

| ID | Pathways | *P*-value | Associated peak–genes | Regulated | Function |
|---|---|---|---|---|---|
| hsa03320 | PPAR signaling pathway | 3.58E-03 | *APOA1*, *FABP1*, *PCK1*, and *ANGPTL4* | Up | It involved in several physiological processes including modulation of cellular differentiation; development; metabolism of carbohydrates, lipids, and proteins; and tumorigenesis |
| hsa04975 | Fat digestion and absorption | 1.40E-02 | *APOA4*, *APOA1*, and *FABP1* | Up | It is essential in the prevention of a calorie balance disorder and improving the pathological conditions of metabolic syndrome through improvement of obesity |
| hsa04151 | PI3K-Akt signaling pathway | 1.59E-02 | *LAMA4*, *FGF7*, *PDGFRA*, *PDGFD*, and *KIT* | Down | It is critical in restricting pro-inflammatory and promoting anti-inflammatory responses in TLR-stimulated macrophages and has been considered as a negative regulator of TLR and NF-κB signaling in macrophages |
| hsa04015 | Rap1 signaling pathway | 2.18E-02 | *FGF7*, *PDGFRA*, *PDGFD*, and *KIT* | Down | It plays a dominant role in the control of cell–cell and cell–matrix interactions by regulating the function of integrins and other adhesion molecules in various cell types. Rap1 also regulates MAP kinase (MAPK) activity in a manner highly dependent on the context of cell types |
| hsa04010 | MAPK signaling pathway | 3.53E-02 | *FGF7*, *NTF3*, *NTRK2*, and *PDGFRA* | Down | It is essential in regulating many cellular processes including inflammation, cell stress response, cell differentiation, cell division, cell proliferation, metabolism, motility, and apoptosis |

**TABLE 5 |** Interested genes enriched in pathways which related with lipid metabolic, glucose homeostasis, and immune processes, etc.

| Gene | Symbol | FoldChange | *P*-value | H3K27ac peak | Correlation | Regulated | Function |
|---|---|---|---|---|---|---|---|
| *PCK1* | Phosphoenolpyruvate carboxykinase 1 | 7.90 | 4.9E-02 | Chr20:11003689-11003961 | 0.890 | Up | This gene is a main control point for the regulation of gluconeogenesis and the expression can be regulated by insulin, glucocorticoids, glucagon, cAMP, and diet |
| *APOA1* | Apolipoprotein A1 | 3.09 | 2.9E-02 | Chr24:5089487-5090379 | 0.887 | Up | The encoded preproprotein promotes cholesterol efflux from tissues to the liver for excretion and is a cofactor for lecithin cholesterol acyltransferase (LCAT), an enzyme responsible for the formation of most plasma cholesteryl esters |
| *ANGPTL4* | Angiopoietin-like 4 | 2.38 | 6.6E-08 | Chr28:1779594-1787257 | 0.983 | Up | This gene encodes a glycosylated, which functions as a serum hormone that regulates glucose homeostasis, lipid metabolism, and insulin sensitivity |
| *FABP1* | Fatty acid binding protein 1 | 2.04 | 1.7E-03 | Chr4:86731254-86735175 | 0.929 | Up | This gene encodes the fatty acid binding protein found in the liver and plays an essential role in fatty acid uptake, transport, and metabolism |
| *NTRK2* | Neurotrophic receptor tyrosine kinase 2 | 7.21 | 1.1E-02 | ChrZ:41171358-41171800 | 0.902 | Down | This gene encodes a member of the neurotrophic tyrosine receptor kinase (NTRK) family and associates with obesity and mood disorders |
| *FGF7* | Fibroblast growth factor 7 | 5.55 | 2.0E-02 | Chr10:11491528-11493116 | 0.974 | Down | The protein encoded by this gene is a member of the fibroblast growth factor (FGF) family and involves in a variety of biological processes, including embryonic development, cell growth, morphogenesis, tissue repair, tumor growth, and invasion |
| *PDGFRA* | Platelet-derived growth factor receptor alpha | 2.85 | 9.4E-04 | Chr4:65059385-65060498 | 0.864 | Down | This gene plays a role in organ development, wound healing, and tumor progression |
| *KIT* | Receptor tyrosine kinase | 2.48 | 3.7E-02 | Chr4:65997303-65998627 | 0.892 | Down | It encodes a tyrosine kinase receptor and is part of signaling pathways that control multiple cellular processes, including cell proliferation, survival, and migration |

*ANGPTL4*, *FABP1*, and *KIT* genes in FLHS pathological chickens relative to control individuals. The ChIP-qPCR fold enrichment of *PCK1*, *APOA1*, *ANGPTL4*, and *FABP1* was significantly increased ($P \leq 0.05$) in the FLHS samples (**Figures 6A–D**), in accordance with the mRNA expression level (**Figures 6F–I**), while *KIT* peak was significantly decreased ($P \leq 0.05$) (**Figure 6E**), which is also consistent with our RNA-seq result (**Figure 6J**).

## DISCUSSION

In this study, we describe the alterations of acetylic variation and the transcriptome landscape resulting from a standard and a high-energy, low-protein (HELP) diet. Intriguingly, as metabolic disorders such as obesity and liver steatosis often stem from the dysregulation of lipid homeostasis and immune pathways (Steinberg, 2007; Gurzov et al., 2016), our study also revealed

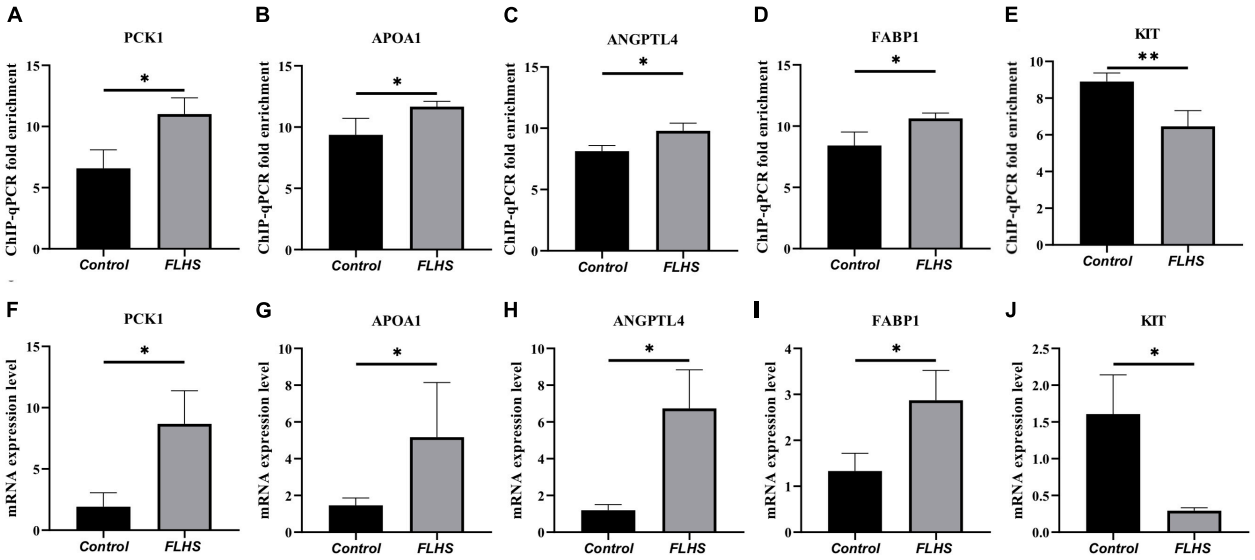



**FIGURE 6 |** ChIP-qPCR and RT-PCR validation of peak-associated target genes. **(A–E)** ChIP-qPCR fold enrichment of *PCK1*, *APOA1*, *ANGPTL4*, *FABP1*, and *KIT* genes in FLHS pathological chickens relative to control individuals. **(F–J)** The mRNA expression levels of *PCK1*, *APOA1*, *ANGPTL4*, *FABP1*, and *KIT* genes in FLHS pathological chickens relative to control individuals. Expression levels were determined as the fold change in $2^{-\Delta\Delta Ct}$ levels relative to the control group with median expression set to 1. Significance was assessed by *t*-test, $^{*}P \leq 0.05$, $^{**}P \leq 0.01$.

that differentially acetylated peaks were involved in the regulation of a number of genes enriched in lipid metabolism, glucose homeostasis, and immune biological processes, including *PCK1*, *APOA1*, *ANGPTL4*, *FABP1*, *NTRK2*, *FGF7*, *PDGFRA*, and *KIT*. To the best of our knowledge, this is the first study to investigate the variation of H3K27ac marks in FLHS in chickens. Further, apart from identifying candidate genes and molecular pathways, we also provide a framework for future genome-wide studies of this modification.

In addition, our analyses revealed that diet-induced FLHS resulted in genome-wide epigenetic alterations and enrichment of TF binding motifs in H3K27ac regions, including the binding motifs for ERG, FOXA1, GABPA, FLI1, ETV1, PHA-4, ELF1, FOXO1, ETS1, and ETV2, which are factors reported to be involved in immune system processes and metabolic homeostasis in FLHS chickens, in accordance with the results of the functional enrichment analysis of candidate differentially expressed genes. For example, ERG, a transcription factor of the ETS family, plays key roles in the regulation of cell proliferation, differentiation, inflammation, and apoptosis (Schafer et al., 2015). PHA-4 (Panowski et al., 2007; Wu et al., 2018a), FOXA1 (Swinstead et al., 2016; Xing et al., 2018; Zhou et al., 2020), and FOXO1 (Xing et al., 2018) are transcription factors related to metabolic homeostasis. Wu et al. have revealed that PHA-4/FoxA functions as a sensor of nucleolar stress. The complex binds and transactivates the expression of the lipogenic genes, promoting subsequent lipid accumulation (Panowski et al., 2007; Wu et al., 2018a). Xing et al. (2018) discovered that Forkhead box transcription factor O1 (FOXO1) plays a role in response to cellular stimulation and maintenance of tissue homeostasis. This observation further confirmed the fact that TF motifs act as transcriptional activators and play a vital role in regulating transcriptional programs that control cellular behavior and disease phenotypes (Corradin and Scacheri, 2014; Sugiaman-Trapman, 2018).

Given its close relationship with transcriptional activation through transcription factor binding, we highlighted target genes of FLHS-associated variation in H3K27ac. Most significantly enriched were the PPAR signaling pathways, which act as regulators of lipid and lipoprotein metabolism and glucose homeostasis. Based on the biological functions of candidate genes (**Table 5**) and previous studies of PPAR signaling, we proposed a model of the involvement of H3K27ac in the epigenetic regulation mechanism of FLHS in laying hens (**Figure 7**). In this model, the HELP diet may have an impact on histone modification of H3K27ac and chromatin structure, leading to the dysregulation of candidate genes related to lipid and energy metabolism (*PCK1*, *APOA1*, *ANGPTL4*, and *FABP1*), the immune system (*FGF7*, *PDGFRA*, and *KIT*), and PPAR signaling, which causes the excessive accumulation of fat in liver tissue and induces the formation of FLHS, supportive of the notion that changes in epigenetic modifications and transcriptional regulation are essential for phenotypic adaptation to environmental stimuli (Ling and Groop, 2009; Corradin and Scacheri, 2014; Carrer et al., 2017; Siersbaek et al., 2017; Marzi et al., 2018; Jahan et al., 2020). Thus, better understanding of the PPAR pathways and the functional roles of candidate genes in the context of FLHS are of great value and may enable us to develop new and specific therapies for FLHS-susceptible commercial laying hens.

It is important to note that the current study had a number of limitations. First, the number of tested samples was relatively small. In light of this, we have observed substantial differences between healthy and FLHS cases, including FLHS-associated regulatory alterations in genes and pathways that are known to

play a role in the development of FLHS. Differential acetylated peaks of controls and FLHS chickens showed clear clustering, which implies that samples were mainly distinguished by a common molecular pathology of lipid homeostasis, energy metabolism, and immune function. In addition, the results of our TF binding motif analyses and functional enrichment analyses of genes associated with differentially acetylated peaks were in consistence with previous observations from larger numbers of samples. Second, H3K27ac, while a typical modification that regulates genomic function, can only provide relatively limited information about transcriptional activity (Kimura, 2013; Nammo et al., 2018). We found the differences in a number of genes annotated to differentially acetylated peaks and revealed their associated signaling pathways, supporting the notion that dysregulation of H3K27 acetylation and the PPAR signaling pathway are involved in the excessive accumulation of fat in liver tissue and the onset of lipid metabolic disorders (Chinetti et al., 2000; Beacon et al., 2020). Nevertheless, further experiments are still required to confirm the model and candidate genes.

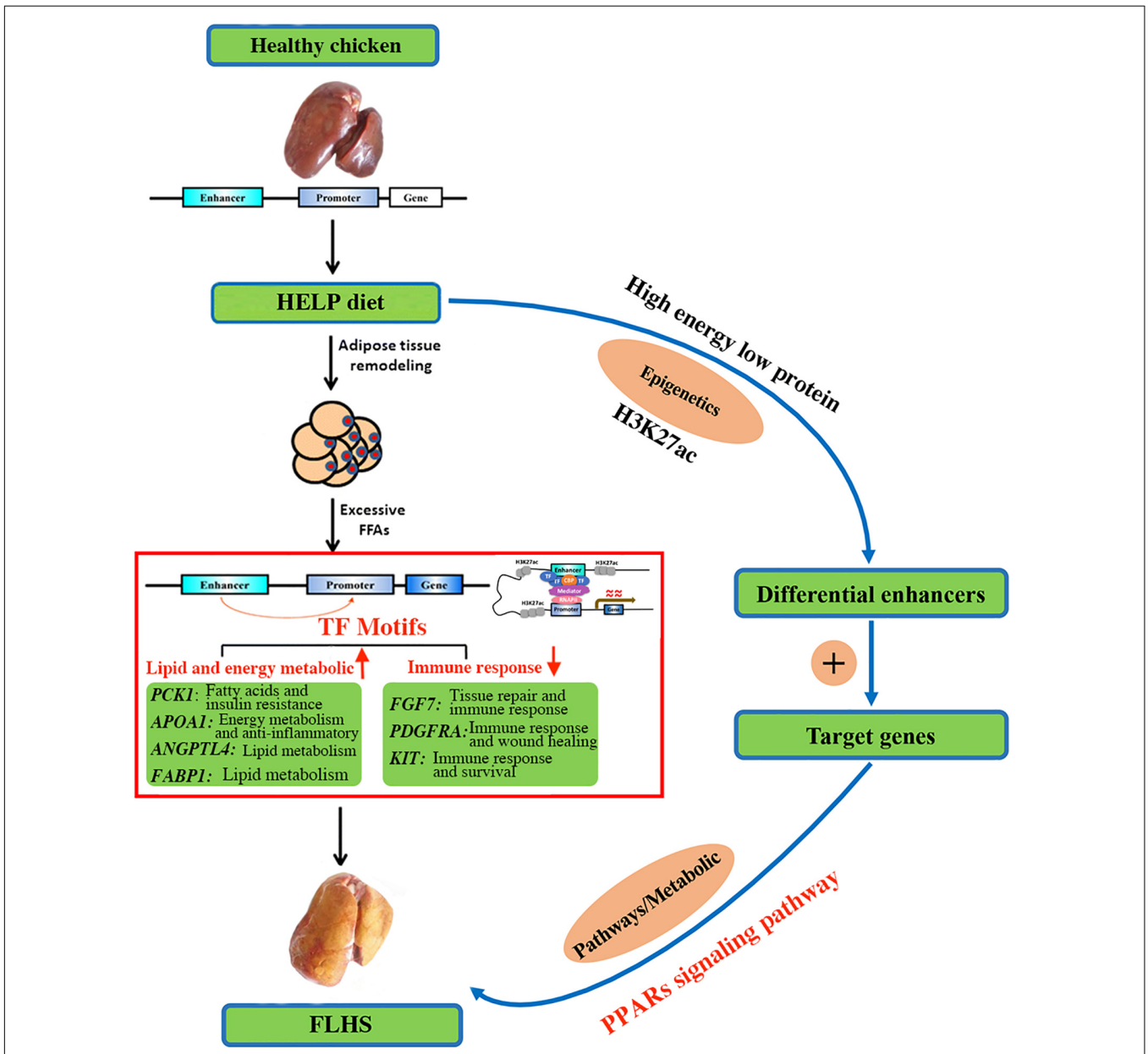



**FIGURE 7 |** A proposed model on the epigenetic regulation mechanisms of histone H3K27 acetylation causing the FLHS in laying hens. Mediated by histone-modifying enzyme, HELP could have an impact on histone modification of H3K27ac and chromatin structure, leading to the dysregulation of genes related to lipid and energy metabolism (*PCK1*, *APOA1*, *ANGPTL4*, and *FABP1*) and immune response (*FGF7*, *PDGFRA*, and *KIT*), and PPAR signaling pathway, which may cause the excessive accumulation of fat in liver tissue and induce the development of the FLHS.

This study provided evidence for the widespread H3K27ac dysregulation in the liver of FLHS-affected chickens and the enrichment of TF binding sequence motifs in response to disease. Notably, we identified that FLHS-associated variations in H3K27ac marks were associated with multiple known FLHS risk genes involved in lipid and energy metabolism (*PCK1*, *APOA1*, *ANGPTL4*, and *FABP1*) and immune function (*FGF7*, *PDGFRA*, and *KIT*). Further, we observed that the PPAR signaling pathway was the most significantly enriched in FLHS. In addition, we present a framework for integrating genome-wide studies of histone modifications and transcriptional regulation, both critical for the phenotypic adaptation to environmental stimuli, in the study of lipid metabolism disorders.

## CONCLUSION

This study provided evidence for widespread acetylic variation in the liver of FLHS-affected chickens and enrichment of sequence motifs showing changes in response to disease. Notably, we identified that FLHS-regulatory variable H3K27ac was associated with multiple known FLHS risk genes, which robustly associated with lipid and energy metabolism (*PCK1*, *APOA1*, *ANGPTL4*, and *FABP1*) and immune system (*FGF7*, *PDGFRA*, and *KIT*), and discovered the most significantly enriched signaling pathway of PPARs. We also presented a framework for genome-wide studies of histone modifications in lipid metabolic disorders, by integrating our data with results obtained from transcriptional regulation, which are both essential for phenotypic adaptation to environments.

## DATA AVAILABILITY STATEMENT

The RNA-Seq and ChIP-Seq data of healthy and FLHS individuals analyzed for this study can be found at GSA (https://bigd.big.ac.cn/gsa/browse/CRA002527).

## ETHICS STATEMENT

The animal study was reviewed and approved by the Jiangxi Agricultural University and Anhui Medical University. Written informed consent was obtained from the owners for the participation of their animals in this study.

## AUTHOR CONTRIBUTIONS

JH and JR conceived and designed the experiments. QZ, ZZ, CY, and YW performed the experiments. YZ, QZ, TJ, and FL analyzed the data. YZ, JH, and JR wrote and revised the manuscript. All authors read and approved the final manuscript.

## FUNDING

This work was supported by the National Natural Science Foundation of China (31960690 and 31460648) and Anhui Medical University high level introduction of talent research start-up fund (XJ201925).

## ACKNOWLEDGMENTS

We are grateful to colleagues in College of Animal Science and Technology, Jiangxi Agricultural University for sample collection.

## SUPPLEMENTARY MATERIAL

The Supplementary Material for this article can be found online at: https://www.frontiersin.org/articles/10.3389/fgene.2020.574167/full#supplementary-material

## REFERENCES

Abuin, J. M., Pichel, J. C., Pena, T. F., and Amigo, J. (2015). BigBWA: approaching the burrows-wheeler aligner to big data technologies. *Bioinformatics* 31, 4003–4005. doi: 10.1093/bioinformatics/btv506

Alfadhel, M., Nashabat, M., Qahtani, H. A., Alfares, A., Mutairi, F. A., Shaalan, H. A., et al. (2016). Mutation in SLC6A9 encoding a glycine transporter causes a novel form of non-ketotic hyperglycinemia in humans. *Hum. Genet.* 135, 1263–1268. doi: 10.1007/s00439-016-1719-x

Andersson, R., Gebhard, C., Miguel-Escalada, I., Hoof, I., Bornholdt, J., Boyd, M., et al. (2014). An atlas of active enhancers across human cell types and tissues. *Nature* 507, 455–461. doi: 10.1038/nature12787

Awuah, P. K., Nejak-Bowen, K. N., and Monga, S. P. (2013). Role and regulation of PDGFRalpha signaling in liver development and regeneration. *Am. J. Pathol.* 182, 1648–1658. doi: 10.1016/j.ajpath.2013.01.047

Baena, E., Shao, Z., Linn, D. E., Glass, K., Hamblen, M. J., Fujiwara, Y., et al. (2013). ETV1 directs androgen metabolism and confers aggressive prostate cancer in targeted mice and patients. *Genes Dev.* 27, 683–698. doi: 10.1101/gad.211011.112

Baker, D. H., and Han, Y. (1994). Ideal amino acid profile for chicks during the first three weeks posthatching. *Poult. Sci.* 73, 1441–1447.

Beacon, T. H., Xu, W., and Davie, J. R. (2020). Genomic landscape of transcriptionally active histone arginine methylation marks, H3R2me2s and H4R3me2a, relative to nucleosome depleted regions. *Gene* 742:144593. doi: 10.1016/j.gene.2020.144593

Bindea, G., Mlecnik, B., Hackl, H., Charoentong, P., Tosolini, M., Kirilovsky, A., et al. (2009). ClueGO: a cytoscape plug-in to decipher functionally grouped gene ontology and pathway annotation networks. *Bioinformatics* 25, 1091–1093. doi: 10.1093/bioinformatics/btp101

Carrer, A., Parris, J. L., Trefely, S., Henry, R. A., Montgomery, D. C., Torres, A., et al. (2017). Impact of a high-fat diet on tissue Acyl-CoA and histone acetylation levels. *J. Biol. Chem.* 292, 3312–3322. doi: 10.1074/jbc.M116.750620

Chen, N., Zhao, G., Yan, X., Lv, Z., Yin, H., Zhang, S., et al. (2018). A novel FLI1 exonic circular RNA promotes metastasis in breast cancer by coordinately regulating TET1 and DNMT1. *Genome Biol.* 19:218. doi: 10.1186/s13059-018-1594-y

Chinetti, G., Fruchart, J.-C., and Staels, B. (2000). Peroxisome proliferator-activated receptors (PPARs)-nuclear receptors at the crossroads between lipid metabolism and inflammation. *Inflamm. Res.* 49, 497–505.

Cinti, S. (2001). The adipose organ: morphological perspectives of adipose tissues. *Proc. Nutr. Soc.* 60, 319–328. doi: 10.1079/pns200192

Corradin, O., and Scacheri, P. C. (2014). Enhancer variants-evaluating functions in common disease. *Genome Med.* 6:85. doi: 10.1186/s13073-014-0085-3

Creyghton, M. P., Cheng, A. W., Welstead, G. G., Kooistra, T., Carey, B. W., Steine, E. J., et al. (2010). Histone H3K27ac separates active from poised enhancers and predicts developmental state. *Proc. Natl. Acad. Sci. U.S.A.* 107, 21931–21936. doi: 10.1073/pnas.1016071107

Dobin, A., Davis, C. A., Schlesinger, F., Drenkow, J., Zaleski, C., Jha, S., et al. (2013). STAR: ultrafast universal RNA-seq aligner. *Bioinformatics* 29, 15–21. doi: 10.1093/bioinformatics/bts635

Garciandia, A., and Suarez, T. (2013). The NMRA/NMRAL1 homologue PadA modulates the expression of extracellular cAMP relay genes during aggregation in *Dictyostelium discoideum*. *Dev. Biol.* 381, 411–422. doi: 10.1016/j.ydbio.2013.06.013

Geibel, M., Badurek, S., Horn, J. M., Vatanashevanopakorn, C., Koudelka, J., Wunderlich, C. M., et al. (2014). Ablation of TrkB signalling in CCK neurons results in hypercortisolism and obesity. *Nat. Commun.* 5:3427. doi: 10.1038/ncomms4427

Grompe, M. (2017). Fah knockout animals as models for therapeutic liver repopulation. *Adv. Exp. Med. Biol.* 959, 215–230. doi: 10.1007/978-3-319-55780-9_20

Gurzov, E. N., Stanley, W. J., Pappas, E. G., Thomas, H. E., and Gough, D. J. (2016). The JAK/STAT pathway in obesity and diabetes. *FEBS J.* 283, 3002–3015. doi: 10.1111/febs.13709

Hammad, H., Vanderkerken, M., Pouliot, P., Deswarte, K., Toussaint, W., Vergote, K., et al. (2017). Transitional B cells commit to marginal zone B cell fate by Taok3-mediated surface expression of ADAM10. *Nat. Immunol.* 18, 313–320. doi: 10.1038/ni.3657

Hansen, R. J., and Walzem, R. L. (1993). Avian fatty liver hemorrhagic syndrome: A comparative review. *Adv. Vet. Sci. Comp. Med.* 37, 451–468.

Heeg, S., Das, K. K., Reichert, M., Bakir, B., Takano, S., Caspers, J., et al. (2016). ETS-Transcription factor ETV1 regulates stromal expansion and metastasis in pancreatic cancer. *Gastroenterology* 151, 540–553.e514. doi: 10.1053/j.gastro.2016.06.005

Heinz, S., Benner, C., Spann, N., Bertolino, E., Lin, Y. C., Laslo, P., et al. (2010). Simple combinations of lineage-determining transcription factors prime cis-regulatory elements required for macrophage and B cell identities. *Mol. Cell* 38, 576–589. doi: 10.1016/j.molcel.2010.05.004

Iffiu-Soltesz, Z., Wanecq, E., Prevot, D., Gres, S., and Carpene, C. (2010). Histamine oxidation in mouse adipose tissue is controlled by the AOC3 gene-encoded amine oxidase. *Inflamm. Res.* 59(Suppl. 2), S227–S229. doi: 10.1007/s00011-009-0129-0

Itoh, N., Nakayama, Y., and Konishi, M. (2016). Roles of FGFs as paracrine or endocrine signals in liver development, health, and disease. *Front. Cell Dev. Biol.* 4:30. doi: 10.3389/fcell.2016.00030

Jahan, S., Beacon, T. H., Xu, W., and Davie, J. R. (2020). A typical chromatin structure of immune-related genes expressed in chicken erythrocytes. *Biochem. Cell Biol.* 98, 171–177. doi: 10.1139/bcb-2019-0107

Kheradpour, P., and Kellis, M. (2014). Systematic discovery and characterization of regulatory motifs in ENCODE TF binding experiments. *Nucleic Acids Res.* 42, 2976–2987. doi: 10.1093/nar/gkt1249

Kimura, H. (2013). Histone modifications for human epigenome analysis. *J. Hum. Genet.* 58, 439–445. doi: 10.1038/jhg.2013.66

Kondoh, N., Imazeki, N., Arai, M., Hada, A., Hatsuse, K., Tsuo, H. A. M., et al. (2007). Activation of a system A amino acid transporter, ATA1SLC38A1, in human hepatocellular carcinoma and preneoplastic liver tissues. *Intern. J. Oncol.* 31, 81–87. doi: 10.3892/ijo.31.1.81

La Paglia, L., Listi, A., Caruso, S., Amodeo, V., Passiglia, F., Bazan, V., et al. (2017). Potential role of ANGPTL4 in the cross talk between metabolism and cancer through PPAR signaling pathway. *PPAR Res.* 2017:8187235. doi: 10.1155/2017/8187235

Lee, J. H., Friso, S., and Choi, S. W. (2014). Epigenetic mechanisms underlying the link between non-alcoholic fatty liver diseases and nutrition. *Nutrients* 6, 3303–3325. doi: 10.3390/nu6083303

Li, C. X., Chen, L. L., Li, X. C., Ng, K. T., Yang, X. X., Lo, C. M., et al. (2018). ApoA-1 accelerates regeneration of small-for-size fatty liver graft after transplantation. *Life Sci.* 215, 128–135. doi: 10.1016/j.lfs.2018.10.053

Li, H., Handsaker, B., Wysoker, A., Fennell, T., Ruan, J., Homer, N., et al. (2009). The sequence alignment/Map format and SAMtools. *Bioinformatics* 25, 2078–2079. doi: 10.1093/bioinformatics/btp352

Li, J., Zhao, X. L., Yuan, Y. C., Gilbert, E. R., Wang, Y., Liu, Y. P., et al. (2013). Dietary lysine affects chickens from local Chinese pure lines and their reciprocal crosses. *Poult. Sci.* 92, 1683–1689. doi: 10.3382/ps.2012-02865

Liao, Y., Smyth, G. K., and Shi, W. (2014). featureCounts: an efficient general purpose program for assigning sequence reads to genomic features. *Bioinformatics* 30, 923–930. doi: 10.1093/bioinformatics/btt656

Ling, C., and Groop, L. (2009). Epigenetics: a molecular link between environmental factors and type 2 diabetes. *Diabetes* 58, 2718–2725. doi: 10.2337/db09-1003

Love, M. I., Huber, W., and Anders, S. (2014). Moderated estimation of fold change and dispersion for RNA-seq data with DESeq2. *Genome Biol.* 15:550. doi: 10.1186/s13059-014-0550-8

Marzi, S. J., Leung, S. K., Ribarska, T., Hannon, E., Smith, A. R., Pishva, E., et al. (2018). A histone acetylome-wide association study of Alzheimer's disease identifies disease-associated H3K27ac differences in the entorhinal cortex. *Nat. Neurosci.* 21, 1618–1627. doi: 10.1038/s41593-018-0253-7

Mead, T. J., and Apte, S. S. (2018). ADAMTS proteins in human disorders. *Matrix Biol.* 7, 225–239. doi: 10.1016/j.matbio.2018.06.002

Mi, H., Muruganujan, A., and Thomas, P. D. (2013). PANTHER in 2013: modeling the evolution of gene function, and other gene attributes, in the context of phylogenetic trees. *Nucleic Acids Res.* 41, D377–D386. doi: 10.1093/nar/gks1118

Millward, C. A., Desantis, D., Hsieh, C. W., Heaney, J. D., Pisano, S., Olswang, Y., et al. (2010). Phosphoenolpyruvate carboxykinase (Pck1) helps regulate the triglyceride/fatty acid cycle and development of insulin resistance in mice. *J. Lipid Res.* 51, 1452–1463. doi: 10.1194/jlr.M005363

Moreira, G. C. M., Boschiero, C., Cesar, A. S. M., Reecy, J. M., Godoy, T. F., Trevisoli, P. A., et al. (2018). A genome-wide association study reveals novel genomic regions and positional candidate genes for fat deposition in broiler chickens. *BMC Genom.* 19:374. doi: 10.1186/s12864-018-4779-6

Nammo, T., Udagawa, H., Funahashi, N., Kawaguchi, M., Uebanso, T., Hiramoto, M., et al. (2018). Genome-wide profiling of histone H3K27 acetylation featured fatty acid signalling in pancreatic beta cells in diet-induced obesity in mice. *Diabetologia* 61, 2608–2620. doi: 10.1007/s00125-018-4735-7

Nord, A. S., Blow, M. J., Attanasio, C., Akiyama, J. A., Holt, A., Hosseini, R., et al. (2013). Rapid and pervasive changes in genome-wide enhancer usage during mammalian development. *Cell* 155, 1521–1531. doi: 10.1016/j.cell.2013.11.033

Oh-hora, M., Johmura, S., Hashimoto, A., Hikida, M., and Kurosaki, T. (2003). Requirement for Ras guanine nucleotide releasing protein 3 in coupling phospholipase C-gamma2 to Ras in B cell receptor signaling. *J. Exp. Med.* 198, 1841–1851. doi: 10.1084/jem.20031547

Oteng, A. B., Ruppert, P. M. M., Boutens, L., Dijk, W., van Dierendonck, X., Olivecrona, G., et al. (2019). Characterization of ANGPTL4 function in macrophages and adipocytes using Angptl4-knockout and Angptl4-hypomorphic mice. *J. Lipid Res.* 60, 1741–1754. doi: 10.1194/jlr.M094128

Panowski, S. H., Wolff, S., Aguilaniu, H., Durieux, J., and Dillin, A. (2007). PHA-4/Foxa mediates diet-restriction- induced longevity of *C. elegans*. *Nature* 447, 550–555. doi: 10.1038/nature05837

Pawlak, M., Lefebvre, P., and Staels, B. (2015). Molecular mechanism of PPARalpha action and its impact on lipid metabolism, inflammation and fibrosis in non-alcoholic fatty liver disease. *J. Hepatol.* 62, 720–733. doi: 10.1016/j.jhep.2014.10.039

Pennacchio, L. A., Bickmore, W., Dean, A., Nobrega, M. A., and Bejerano, G. (2013). Enhancers: five essential questions. *Nat. Rev. Genet.* 14, 288–295. doi: 10.1038/nrg3458

Quinlan, A. R., and Hall, I. M. (2010). BEDTools: a flexible suite of utilities for comparing genomic features. *Bioinformatics* 26, 841–842. doi: 10.1093/bioinformatics/btq033

Rada-Iglesias, A., Bajpai, R., Swigut, T., Brugmann, S. A., Flynn, R. A., and Wysocka, J. (2011). A unique chromatin signature uncovers early developmental enhancers in humans. *Nature* 470, 279–283. doi: 10.1038/nature09692

Rice, C. M., Davies, L. C., Subleski, J. J., Maio, N., Gonzalez-Cotto, M., Andrews, C., et al. (2018). Tumour-elicited neutrophils engage mitochondrial metabolism to circumvent nutrient limitations and maintain immune suppression. *Nat. Commun.* 9:5099. doi: 10.1038/s41467-018-07505-2

Rodriguez Sawicki, L., Bottasso Arias, N. M., Scaglia, N., Falomir Lockhart, L. J., Franchini, G. R., Storch, J., et al. (2017). FABP1 knockdown in human enterocytes impairs proliferation and alters lipid metabolism. *Biochim. Biophys. Acta Mol. Cell Biol. Lipids* 1862, 1587–1594. doi: 10.1016/j.bbalip.2017.09.006

Roy, S., Esmaeilniakooshkghazi, A., Patnaik, S., Wang, Y., George, S. P., Ahrorov, A., et al. (2018). Villin-1 and gelsolin regulate changes in Actin dynamics that affect cell survival signaling pathways and intestinal inflammation. *Gastroenterology* 154, 1405–1420.e1402. doi: 10.1053/j.gastro.2017.12.016

Rozenboim, I., Mahato, J., Cohen, N. A., and Tirosh, O. (2016). Low protein and high-energy diet: a possible natural cause of fatty liver hemorrhagic syndrome in caged White Leghorn laying hens. *Poult. Sci.* 95, 612–621. doi: 10.3382/ps/pev367

Salmon-Divon, M., Dvinge, H., Tammoja, K., and Bertone, P. (2010). PeakAnalyzer: genome-wide annotation of chromatin binding and modification loci. *BMC Bioinform.* 11:415. doi: 10.1186/1471-2105-11-415

Schafer, E. S., Margolin, J., Poplack, D. G., and Rabin, K. R. (2015). Molecular genetics of acute Lymphoblastic leukemia. *Mol. Basis Cancer* 152, 395–406. doi: 10.1016/B978-1-4557-4066-6.00026-3

Schuman, B. E., Squires, E. J., and Leeson, S. (2000). Effect of dietary flaxseed, flax oil and n-3 fatty acid supplement on hepatic and plasma characteristics relevant to fatty liver haemorrhagic syndrome in laying hens. *Br. Poult. Sci.* 41, 465–472. doi: 10.1080/713654970

Seifert, L. L., Si, C., Saha, D., Sadic, M., de Vries, M., Ballentine, S., et al. (2019). The ETS transcription factor ELF1 regulates a broadly antiviral program distinct from the type I interferon response. *PLoS Pathog.* 15:e1007634. doi: 10.1371/journal.ppat.1007634

Shen, Y., Yue, F., McCleary, D. F., Ye, Z., Edsall, L., Kuan, S., et al. (2012). A map of the cis-regulatory sequences in the mouse genome. *Nature* 488, 116–120. doi: 10.1038/nature11243

Siersbaek, M., Varticovski, L., Yang, S., Baek, S., Nielsen, R., Mandrup, S., et al. (2017). High fat diet-induced changes of mouse hepatic transcription and enhancer activity can be reversed by subsequent weight loss. *Sci. Rep.* 7:40220. doi: 10.1038/srep40220

Singh, A. K., Aryal, B., Chaube, B., Rotllan, N., Varela, L., Horvath, T. L., et al. (2018). Brown adipose tissue derived ANGPTL4 controls glucose and lipid metabolism and regulates thermogenesis. *Mol. Metab.* 11, 59–69. doi: 10.1016/j.molmet.2018.03.011

Spurlock, M. E., and Savage, J. E. (1993). Effect of dietary protein and selected antioxidants on fatty liver hemorrhagic syndrome induced in japanese quail. *Poul. Sci.* 72, 2095–2105. doi: 10.3382/ps.0722095

Steinberg, G. R. (2007). Inflammation in obesity is the common link between defects in fatty acid metabolism and insulin resistance. *Cell Cycle* 6, 888–894. doi: 10.4161/cc.6.8.4135

Sugiaman-Trapman, D. (2018). *The Role of RFX Transcription Factors in Neurons and in the Human Brain*. Sweden: Karolinska Institutet.

Swinstead, E. E., Miranda, T. B., Paakinaho, V., Baek, S., Goldstein, I., Hawkins, M., et al. (2016). Steroid receptors reprogram FoxA1 occupancy through dynamic chromatin transitions. *Cell* 165, 593–605. doi: 10.1016/j.cell.2016.02.067

Takahashi, J. S., Kumar, V., Nakashe, P., Koike, N., Huang, H. C., Green, C. B., et al. (2015). ChIP-seq and RNA-seq methods to study circadian control of transcription in mammals. *Methods Enzymol.* 551, 285–321. doi: 10.1016/bs.mie.2014.10.059

Tontonoz, P., and Spiegelman, B. M. (2008). Fat and beyond: the diverse biology of PPARgamma. *Annu. Rev. Biochem.* 77, 289–312. doi: 10.1146/annurev.biochem.77.061307.091829

Trott, K. A., Giannitti, F., Rimoldi, G., Hill, A., Woods, L., Barr, B., et al. (2014). Fatty liver hemorrhagic syndrome in the backyard chicken: a retrospective histopathologic case series. *Vet. Pathol.* 51, 787–795. doi: 10.1177/0300985813503569

Villar, D., Berthelot, C., Aldridge, S., Rayner, T. F., Lukk, M., Pignatelli, M., et al. (2015). Enhancer evolution across 20 mammalian species. *Cell* 160, 554–566. doi: 10.1016/j.cell.2015.01.006

Wang, C., and Ma, W. (2019). Hypothalamic and pituitary transcriptome profiling using RNA-sequencing in high-yielding and low-yielding laying hens. *Sci. Rep.* 9:10285. doi: 10.1038/s41598-019-46807-3

Wu, J., Jiang, X., Li, Y., Zhu, T., Zhang, J., Zhang, Z., et al. (2018a). PHA-4/FoxA senses nucleolar stress to regulate lipid accumulation in *Caenorhabditis elegans*. *Nat. Commun.* 9:1195. doi: 10.1038/s41467-018-03531-2

Wu, J., Zhang, R., Shen, F., Yang, R., DaZhou, L., Cao, H., et al. (2018b). Altered DNA methylation sites in peripheral blood leukocytes from patients with simple steatosis and nonalcoholic Steatohepatitis (NASH). *Med. Sci. Monit.* 24, 6946–6967. doi: 10.12659/MSM.909747

Xieraili, M., Yasen, M., Mogushi, K., Obulhasim, G., Mayinuer, A., Aihara, A., et al. (2012). Villin 1 is a predictive factor for the recurrence of high serum alpha-fetoprotein-associated hepatocellular carcinoma after hepatectomy. *Cancer Sci.* 103, 1493–1501. doi: 10.1111/j.1349-7006.2012.02315.x

Xing, Y. Q., Li, A., Yang, Y., Li, X. X., Zhang, L. N., and Guo, H. C. (2018). The regulation of FOXO1 and its role in disease progression. *Life Sci.* 193, 124–131. doi: 10.1016/j.lfs.2017.11.030

Yin, J., Fu, W., Dai, L., Jiang, Z., Liao, H., Chen, W., et al. (2017). ANKRD22 promotes progression of non-small cell lung cancer through transcriptional up-regulation of E2F1. *Sci. Rep.* 7:4430. doi: 10.1038/s41598-017-04818-y

Yuan, X., Mu, N., Wang, N., Li, K., Cheng, G., Zhang, L., et al. (2018). GABPA inhibits invasion/metastasis in papillary thyroid carcinoma by regulating DICER1 expression. *Oncogene* 38, 965–979. doi: 10.1038/s41388-018-0483-x

Yun, S., Budatha, M., Dahlman, J. E., Coon, B. G., Cameron, R. T., Langer, R., et al. (2016). Interaction between integrin alpha5 and PDE4D regulates endothelial inflammatory signalling. *Nat. Cell Biol.* 18, 1043–1053. doi: 10.1038/ncb3405

Zarei, M., Barroso, E., Palomer, X., Dai, J., Rada, P., Quesada-López, T., et al. (2017). Hepatic regulation of VLDL receptor by PPARβ/δ and FGF21 modulates non-alcoholic fatty liver disease. *Mol. Metab.* 8, 117–131. doi: 10.1016/j.molmet.2017.12.008

Zhang, Y., Liu, T., Meyer, C. A., Eeckhoute, J., Johnson, D. S., Bernstein, B. E., et al. (2008). Model-based analysis of ChIP-Seq (MACS). *Genome Biol.* 9:r137. doi: 10.1186/gb-2008-9-9-r137

Zhang, Y., Wu, J., Ye, M., Wang, B., Sheng, J., Shi, B., et al. (2018). ETS1 is associated with cisplatin resistance through IKKα/NF-κB pathway in cell line MDA-MB-231. *Cancer Cell Intern.* 18:86. doi: 10.1186/s12935-018-0581-4

Zhang, Y. L., Li, Q., Yang, X. M., Fang, F., Li, J., Wang, Y. H., et al. (2018). SPON2 Promotes M1-like macrophage recruitment and inhibits Hepatocellular carcinoma metastasis by distinct integrin-Rho GTPase-Hippo pathways. *Cancer Res.* 78, 2305–2317. doi: 10.1158/0008-5472.CAN-17-2867

Zhou, S., Hawley, J. R., Soares, F., Grillo, G., Teng, M., Madani Tonekaboni, S. A., et al. (2020). Noncoding mutations target cis-regulatory elements of the FOXA1 plexus in prostate cancer. *Nat. Commun.* 11:441. doi: 10.1038/s41467-020-14318-9

Zhu, Y., Mao, H., Peng, G., Zeng, Q., Ruan, J., and Huang, J. (2020). Effect of JAK-STAT pathway in regulation of fatty liver hemorrhagic syndrome in chickens. *AJAS* 33. doi: 10.5713/ajas.19.0874

**Conflict of Interest:** The authors declare that the research was conducted in the absence of any commercial or financial relationships that could be construed as a potential conflict of interest.

*Copyright © 2021 Zhu, Zeng, Li, Fang, Zhou, Jiang, Yin, Wei, Wang, Ruan and Huang. This is an open-access article distributed under the terms of the Creative Commons Attribution License (CC BY). The use, distribution or reproduction in other forums is permitted, provided the original author(s) and the copyright owner(s) are credited and that the original publication in this journal is cited, in accordance with accepted academic practice. No use, distribution or reproduction is permitted which does not comply with these terms.*

frontiers in Genetics

BRIEF RESEARCH REPORT
published: 05 February 2021
doi: 10.3389/fgene.2021.633564

# Weaning Induces Stress-Dependent DNA Methylation and Transcriptional Changes in Piglet PBMCs

*Ryan J. Corbett[1], Andrea M. Luttman[1], Kaitlin E. Wurtz[2], Janice M. Siegford[2], Nancy E. Raney[2], Laura M. Ford[2] and Catherine W. Ernst[2]**

[1] Genetics and Genome Sciences Graduate Program, Michigan State University, East Lansing, MI, United States,
[2] Department of Animal Science, Michigan State University, East Lansing, MI, United States

Changes to the epigenome, including those to DNA methylation, have been proposed as mechanisms by which stress can induce long-term physiological changes in livestock species. Pig weaning is associated with dietary and social stress, both of which elicit an immune response and changes to the hypothalamic–pituitary–adrenal (HPA) axis. While differential methylation following stress has been assessed in model organisms, it remains poorly understood how the pig methylome is altered by stressors in production settings. We quantified changes in CpG methylation and transcript abundance in piglet peripheral blood mononuclear cells (PBMCs) following weaning and also assessed differential patterns in pigs exhibiting high and low stress response as measured by cortisol concentration and lesion scores. Blood was collected from nine gilt piglets 24 h before and after weaning, and whole-genome bisulfite sequencing (WGBS) and RNA-sequencing were performed on six and nine animals, respectively, at both time points. We identified 2,674 differentially methylated regions (DMRs) that were enriched within promoters of genes associated with lymphocyte stimulation and transcriptional regulation. Stress groups displayed unique differential methylation and expression patterns associated with activation and suppression of T cell immunity in low and high stress animals, respectively. Differential methylation was strongly associated with differential expression; specifically, upregulated genes were enriched among hypomethylated genes. We observed post-weaning hypermethylation of the glucocorticoid receptor (*NR3C1*) promoter and a significant decrease in *NR3C1* expression ($n = 9$, $p = 6.1 \times 10^{-3}$). Our results indicate that weaning-associated stress elicits genome-wide methylation changes associated with differential gene expression, reduced T cell activation, and an altered HPA axis response.

**Keywords: epigenetics, DNA methylation, pig, weaning, gene expression, *NR3C1***

OPEN ACCESS

***Edited by:***
*Stephanie McKay,*
*University of Vermont, United States*

***Reviewed by:***
*Elisabetta Giuffra,*
*Institut National de Recherche pour l'Agriculture, l'Alimentation et l'Environnement (INRAE), France*
*David Greg Riley,*
*Texas A&M University, United States*

****Correspondence:***
*Catherine W. Ernst*
*ernstc@msu.edu*

***Specialty section:***
*This article was submitted to Livestock Genomics, a section of the journal Frontiers in Genetics*

***Received:*** *25 November 2020*
***Accepted:*** *14 January 2021*
***Published:*** *05 February 2021*

***Citation:***
*Corbett RJ, Luttman AM, Wurtz KE, Siegford JM, Raney NE, Ford LM and Ernst CW (2021) Weaning Induces Stress-Dependent DNA Methylation and Transcriptional Changes in Piglet PBMCs. Front. Genet. 12:633564. doi: 10.3389/fgene.2021.633564*

## INTRODUCTION

Livestock animals experience numerous stressors throughout their lifetime that result in short- and long-term effects on physiology and performance (Yahav and Hurwitz, 1996; Geverink et al., 1998; Molenaar et al., 2011; Li et al., 2017; Johnson et al., 2018). Weaning represents a period of dietary and social stress in pig production systems with acute effects on digestive physiology and

immune response (Lallès et al., 2004). In addition to direct effects of weaning, piglets are exposed to unfamiliar individuals in nursery pens, which results in aggressive encounters and skin lesion development (Wurtz et al., 2017). Overall, blood lymphocyte concentrations have been shown to be significantly reduced in weaned pigs (Kick et al., 2012), and additional psychosocial stress experienced during weaning has been associated with lower concentrations of T cell subpopulations (Tuchscherer et al., 2009). One reliable indicator of stress response following pig weaning and mixing is lesion counts, as this measure has been shown to be associated with aggressive behavior, hypothalamic–pituitary–adrenal axis (HPA) activity, and risk of infection, as well as negatively associated with immunocompetence (Fernandez et al., 1994; Morrow-Tesch et al., 1994; Turner et al., 2006, 2009). Weaning stress can have long-term consequences on gut health and disease susceptibility (reviewed in Moeser et al., 2017), yet the molecular mechanisms underlying these relationships remain poorly characterized. It has been proposed that epigenetic mechanisms may link stress from environmental stimuli to lasting changes in gene expression and physiology (Tzschentke and Basta, 2002; González-Recio et al., 2015).

DNA methylation is an epigenetic modification involving the enzymatic addition of a methyl group to the 5-carbon of cytosine rings, producing 5-methylcytosine. Methylation occurs almost exclusively at CpG dinucleotides in mammals and has context-specific associations with gene expression. In gene promoters and intronic enhancers, methylation generally functions to decrease levels of transcription through the alteration of transcription factor binding sites or the recruitment of transcriptional repressors (Bird and Wolffe, 1999; Varley et al., 2013; Greenberg and Bourc'his, 2019). Numerous studies have assessed DNA methylation patterns in peripheral blood mononuclear cells (PBMCs), as these can be repeatedly obtained from the same subjects and provide indications of alteration in stress response pathways; for instance, human studies have found increased levels of stress exposure to be associated with increased glucocorticoid receptor (*NR3C1*) methylation and decreased *NR3C1* expression in blood (Oberlander et al., 2008; Perroud et al., 2011; González Ramírez et al., 2020). DNA methylation studies have been performed in pig tissues in response to different stressors (Hao et al., 2016; Wang et al., 2017). However, assessment of DNA methylation in the pig in response to natural production stressors has not been extensively studied nor has the association between differential methylation and gene expression.

In the current study, we sought to identify differentially methylated regions (DMRs) and differentially expressed genes (DEGs) associated with weaning. We also assessed differential methylation and expression separately in pigs exhibiting high and low levels of weaning stress as determined by changes in serum cortisol concentration and post-weaning lesion counts. Lastly, we looked specifically at the effect of weaning on *NR3C1* methylation and expression as an indicator of alterations in the HPA axis response.

# MATERIALS AND METHODS

## Sample Collection

Blood was sampled from nine crossbred gilts (four and five from two litters) weaned at 28–29 days of age. At weaning, littermates were separated into nursery pens containing six gilts of various litters. Samples were collected 24 h before and 24 h after weaning, and body lesions were counted immediately before and 24 h after weaning by the same trained counter (Wurtz et al., 2017). Blood was collected from each animal per time point in Vacutainer whole blood collection tubes with no additive (Becton Dickinson) for serum isolation and Vacutainer tubes containing freeze-dried sodium heparin (VWR) for PBMC isolation. PBMCs were isolated from each animal at both time points following centrifugation in ACCUSPIN$^{TM}$ System-Histopaque-1077® tubes (Sigma-Aldrich) according to manufacturer's instructions. Serum cortisol concentrations were measured using the DetectX Cortisol Enzyme Immunoassay from Serum and Plasma Kit (Arbor Assays). Optical density was measured at 450 nm using a microplate reader, and readings were converted into ng/ml concentrations using Arbor Assays software. We assessed changes in serum cortisol concentration and post-weaning lesion counts as phenotypic measurements of stress response. High stress (HS) and low stress (LS) animals were visually selected as those at the extremes of the two-dimensional plot of the two phenotypes and further subjected to DNA methylation analyses (**Supplementary Figure 1**).

## Nucleic Acid Isolation and Sequencing

DNA was isolated from six pre- and six post-weaning PBMC samples using the PureLink Genomic DNA Kit. Prior to library preparation, DNA samples were spiked with unmethylated lambda phage DNA (5 ng lambda DNA/1 μg sample DNA) to assess sodium bisulfite conversion. DNA was sodium bisulfite converted using the Zymo EZ DNA Methylation-Gold Kit. Eight of the 12 libraries were prepared using the Kapa Hyper Prep DNA Kit (Roche), and the remaining four libraries were prepared using the Swift Biosciences Accel-NGS Methyl-Seq Library Kit. WGBS was performed on an Illumina HiSeq 4000 instrument in 2 × 150 PE format at an average depth of 18X per sample.

Peripheral blood mononuclear cell RNA from all animals at both time points was isolated using the miRNeasy Mini Kit (Qiagen). For eight of the 18 RNA samples, ribosomal RNA (rRNA) was depleted using the Illumina Ribo-Zero Gold Kit; the remaining RNA samples were subject to rRNA and globin RNA depletion using Illumina Ribo-Zero Plus Kit. All sequencing libraries were prepared using the Illumina TruSeq Total RNA Library Preparation Kit. RNA-sequencing (RNA-seq) was performed on an Illumina HiSeq 4000 instrument in 2 × 150 PE format.

## WGBS Bioinformatics

Whole-genome bisulfite sequencing reads were trimmed using Trimmomatic (Bolger et al., 2014) to remove low-quality

bases and reads (parameters: LEADING:25 TRAILING:25 AVGQUAL:20 MINLEN:30). Libraries prepared using the Roche kit were subject to the removal of the first six bases from forward and reverse reads (HEADCROP:6), while libraries prepared using the Swift Biosciences kit were subject to removal of the first 10 bases from forward reads and first 15 bases from reverse reads (HEADCROP:10/15) per the manufacturer's instructions.

Trimmed reads were aligned to the *Sus scrofa* reference genome (v11.1) using Bismark v0.18.1 (Krueger and Andrews, 2011). The genome_preparation command with default parameters was used to create a bowtie2 index of an *in silico* bisulfite-converted reference genome, after which the alignment was performed using the Bismark command (parameters: –maxins 1000 –score_min L,0,-0.6 –unmapped). Reads that were unpaired following trimming were merged with unmapped forward reads and remapped as single-end reads using the same parameters. We assessed sodium bisulfite conversion efficiency of samples by mapping reads to a lambda genome bowtie2 index with default parameters. Among reads aligning to the lambda genome, the percentage of methylated cytosines was subtracted from 100 to calculate bisulfite conversion efficiency. Due to sub-optimal conversion in some samples, we ran Bismark's filter_non_conversion command with default parameters to remove reads that contained $\geq$3 consecutive methylated non-CpG cytosines. Conversion rates were $\geq$99.5% in all libraries following this filtering. Remaining reads were deduplicated using Bismark's deduplicate_bismark command with default parameters, and the methylation_extractor command was used to calculate methylation rates at all CpGs in the *S. scrofa* genome using default parameters.

Differential methylation analysis between stages was performed using the *methylKit* R package v.1.6.3 (Akalin et al., 2012). For each sample, we discarded CpGs in the 99.5th percentile of coverage to exclude potential PCR duplicates. CpGs within 1 kb non-overlapping windows were consolidated, and average CpG methylation rates were calculated. Only regions with coverage of at least 20 reads in $\geq$4 samples per treatment were retained for further analysis. Logistic regression models were fitted for each region accounting for the fixed effects of library prep and animal within library prep, and random effect of litter to test if stage (post- versus pre-weaning) had a significant effect on the log odds ratio of regional CpG methylation rate. DMRs were classified as those with methylation difference $>$10% and FDR $<$ 0.05. Separate post-weaning differential methylation analyses were also run for LS and HS animals using the same methods.

Differentially methylated regions were annotated with respect to their overlap with gene features to identify differentially methylated genes (DMGs). Genes were classified as promoter- or gene body-DMGs if they contained a DMR in their promoter [2 kb up- or downstream of transcription start site (TSS)] or gene body, respectively. DMRs not overlapping a gene were classified as intergenic. DMG lists were submitted for gene set enrichment analysis (GSEA) using GOrilla software (Eden et al., 2009).

## RNA-Sequencing Bioinformatics

RNA-sequencing reads were trimmed of adapters and low-quality bases using Trimmomatic (HEADCROP:10 LEADING:25 TRAILING:25 AVGQUAL:20 MINLEN:30).

Trimmed reads were aligned to the *S. scrofa* reference genome using TopHat2 (Kim et al., 2013) (parameter: –library-type "fr-firststrand"), and gene counts were obtained using HTSeq-count (Anders et al., 2015) (parameters: -m intersection-non-empty -i gene_id -t exon -s reverse).

Differential expression analyses were performed using the *DESeq2* R package (Love et al., 2011). A negative binomial model was fitted that tested for the effect of stage and corrected for the effects of litter, library preparation, and animal within library preparation. DEGs were classified as those with FDR $<$ 0.05, regardless of log2-fold change. DEGs were submitted for GSEA using GOrilla to identify enriched GO terms. Four separate *DEseq2* analyses were performed for: (1) all animals ($n$ = 9/stage), (2) HS animals and (3) LS animals ($n$ = 3/stage), and (4) animals with WGBS data ($n$ = 6/stage).

## Assessment of NR3C1 Methylation and Expression

We assessed *NR3C1* promoters for regional and site-specific methylation differences, and PBMC *NR3C1* transcript abundance was measured by RNA-seq and RT-qPCR. Total RNA was reverse transcribed using the High Capacity cDNA Reverse Transcription Kit (Applied Biosystems). *B2M* and *GAPDH* were used as reference genes due to their reported stable expression in PBMCs (Cinar et al., 2013; Wang et al., 2014). Assays were performed in triplicate on a StepOnePlus Real-time PCR Instrument (Applied Biosystems) using 5 μl cDNA (50 ng total), 1 μl TaqMan Gene Expression Assay (Applied Biosystems Assay Nos. Ss03378868_u1, Ss03374854_g1, and Ss03391154_m1 for *NR3C1*, *B2M*, and *GAPDH*, respectively), 10 μl TaqMan Fast Advanced Mastermix (Applied Biosystems), and 4 μl water. Reaction conditions were 50°C for 2 min and 95°C for 2 min, followed by 40 cycles of 95°C for 1 s and 60°C for 20 s. Delta Cts (dCts) were obtained for each sample by subtracting the geometric mean of the reference gene Cts from the *NR3C1* Ct, and a paired $t$-test was performed to assess the significance of stage on dCts. Fold change in abundance at post- versus pre-weaning was calculated using the $2^{-\Delta\Delta Ct}$ method.

# RESULTS

## Serum Cortisol and Lesion Count Measurements Identify Low- and High-Stress Animals Following Weaning

We measured serum cortisol concentrations and skin lesion counts before and after weaning in nine gilts in order to assess differential stress response. Percent change in serum cortisol concentration was significantly positively correlated with post-weaning lesion counts ($r$ = 0.70, $p$ = 0.036; **Supplementary Figure 1**). We designated the three animals exhibiting the lowest and highest values of these parameters as LS (two gilts from litter

98 and one from litter 102) and HS (one gilt from litter 98 and two from litter 102), respectively.

## Weaning Differential Methylation Is Associated With Lymphocyte Immune Response Genes

We obtained 128–194M WGBS reads across samples, of which 86–89% uniquely aligned to the *S. scrofa* reference genome (**Supplementary Table 1**). We achieved sufficient coverage to assess differential methylation post- versus pre-weaning at 972,067 1 kb regions. We observed clustering of samples based on litter (data not shown) and thus corrected for this as a random effect in our differential methylation analysis. We identified 2,674 DMRs between stages when considering all animals, of which 1,363 DMRs were hypermethylated and 1,311 DMRs were hypomethylated post-weaning (**Figure 1A** and **Supplementary Tables 2,3**). We annotated DMRs along with all tested regions to gene features and observed a 3.4-fold and 2.1-fold overrepresentation of hyper- and hypo-DMRs in gene promoters, respectively (**Figure 1B**). Conversely, there was a depletion of DMRs in gene bodies and intergenic regions.

We also assessed post- versus pre-weaning differential methylation separately in LS and HS animals and identified unique patterns between groups. HS animals possessed a greater number of DMRs overall (9,945 vs. 6,141); however, while HS animals had roughly the same number of hyper- and hypo-DMRs (4,938 and 5,007, respectively), LS animals had a greater proportion of hypo-DMRs ($n$ = 3,473) relative to hyper-DMRs ($n$ = 2,668). Similar to DMRs among all animals, HS hyper-DMRs were more overrepresented in promoters than were HS hypo-DMRs (**Figure 1A**), while LS hyper- and hypo-DMRs were overrepresented in promoters at similar magnitudes. These results indicate that differential methylation at weaning is strongly associated with gene promoters and suggest that the proportions of hyper- and hypo-DMRs are dependent on stress level.

To determine if differential methylation influences genes involved in similar biological processes, we submitted DMGs for enrichment analysis (**Table 1**). Among all animals, promoter-DMGs were enriched for T cell- and plasma cell-specific processes. Genes hypermethylated in their promoters included interleukin 2 receptor alpha (*IL2RA*) and LIM domain only 1 (*LMO1*), whereas hypomethylated genes included several involved in T cell proliferation (*CD3E* and *TNFSF14*) and apoptosis (*LGALS1*). While hypermethylated gene body-DMGs were not enriched for specific processes related to immunity, we identified several such processes enriched among hypomethylated DMGs including "Positive regulation of lymphocyte differentiation" and "B cell receptor signaling pathway."

We also identified shared and unique enriched GO terms among DMGs in LS and HS animals (**Supplementary Table 4**). In both groups, post-weaning promoter hypomethylation was enriched in genes involved in leukocyte differentiation and activation (**Supplementary Tables 4A,E**). Post-weaning hypomethylated genes in the LS group were also enriched for T cell-related processes ("alpha-beta T cell receptor complex" and "regulation of gamma-delta T cell activation"). Conversely, terms related to T cells ("alpha-beta T cell activation" and "T cell differentiation") were enriched among hypermethylated genes in the HS group (**Supplementary Table 4F**). As gene hypomethylation is generally associated with gene activation, these data suggest that weaning stress level is negatively associated with T cell activity in part through differences in DNA

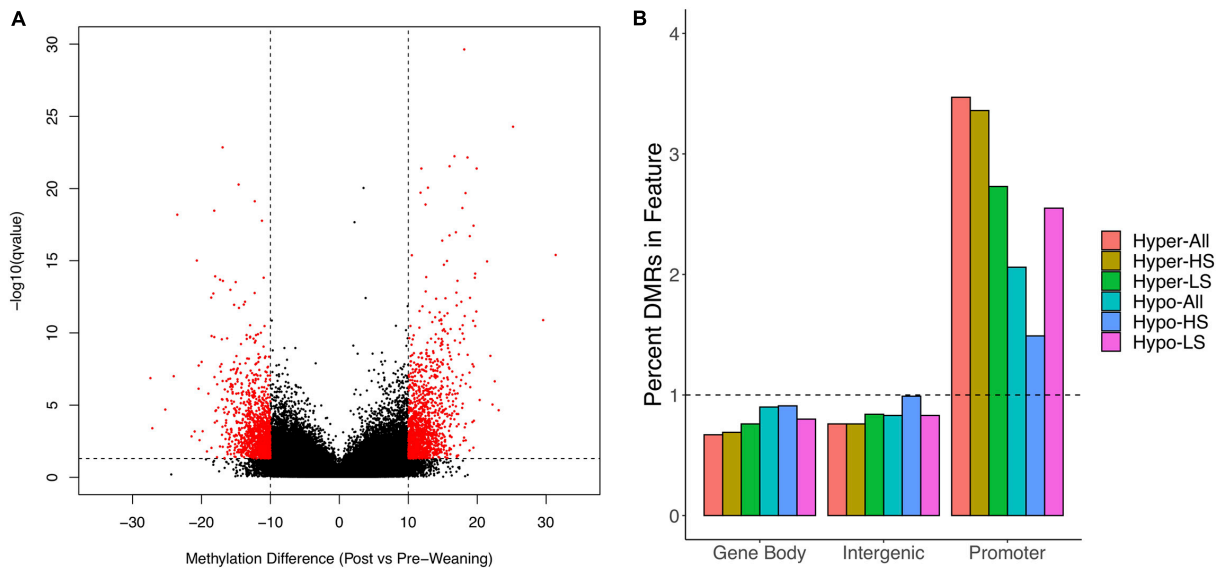



**FIGURE 1 |** Differential methylation in post- versus pre-weaning PBMCs. **(A)** Volcano plot of methylation difference against –log10 ($q$-value). Red dots indicate significant differentially methylated regions (DMRs). **(B)** Enrichment of hypomethylated and hypermethylated DMRs for All, HS, and LS pigs in gene features. Horizontal line indicates expected relative proportion of DMRs in feature if no enrichment (i.e., 1). HS, high stress; LS, low stress.

**TABLE 1 |** Enriched GO terms among promoter- and gene body-DMGs.

| GO term | Enrichment | *P*-value | Genes |
|---|---|---|---|
| **Hypermethylated promoter-DMGs** | | | |
| Catecholamine secretion | 34.05 | 8.60E-04 | *MECP2, NISCH* |
| Regulation of T cell homeostatic proliferation | 34.05 | 8.60E-04 | *IL2RA, LMO1* |
| **Hypomethylated promoter-DMGs** | | | |
| T cell costimulation | 7.44 | 5.30E-04 | *PTPN6, TNFSF14, LGALS1, CD3E, PIK3R1* |
| Lymphocyte costimulation | 7.28 | 5.8E-04 | |
| Plasma cell differentiation | 43.66 | 6.98E-04 | *LGALS1, ITM2A* |
| **Hypomethylated gene body-DMGs** | | | |
| Positive regulation of lymphocyte differentiation | 3.62 | 2.07E-04 | *PIK3R6, RASGRP1, IL4R, TOX, ZBTB7B, IL2RA, IL12RB1, PTPRC, INPP5D, ZMIZ1, RUNX1* |
| Regulation of response to stimulus | 1.28 | 2.68E-04 | 157 genes |
| Positive regulation of leukocyte differentiation | 2.92 | 3.06E-04 | *PIK3R6, IL4R, TOX, IL2RA, TRIB1, IL12RB1, GNAS, INPP5D, RUNX1, RASGRP1, ZBTB46, ZBTB7B, PTPRC, ZMIZ1* |
| Positive regulation of hemopoiesis | 2.68 | 3.11E-04 | *PIK3R6, IL4R, TOX, IL2RA, TRIB1, IL12RB1, GNAS, INPP5D, RUNX1, RASGRP1, ZBTB46, ZBTB7B, PTPRC, ZMIZ1, STAT3, ETS1* |
| Immune response-activating cells surface receptor signaling pathway | 2.31 | 4.34E-04 | *VAV3, ELMO2, ICAM2, MAPK1, BLK, INPP5D, PSMB7, MYO1G, CYFIP2, ACTB, LCP2, PRKCB, BTRC, EIF2B2, MYO1C, NFATC2, PTPRC, ARPC1B, CD247, PDE4B* |
| B cell receptor signaling pathway | 5.50 | 6.17E-04 | *VAV3, ELMO2, ICAM2, MAPK1, BLK, PTPRC, NFATC2* |

methylation. To further test this hypothesis, we assessed T cell co-receptor genes for post-weaning differential methylation in both stress groups. We identified opposing differential methylation in these genes between stress groups (**Table 2**). Regions in *CD3E*, *CD3D*, *CD3G*, and *CD4* were hypomethylated post-weaning in the LS group but not DM in the HS group, while a *CD8B* region was hypermethylated post-weaning in the HS group and not DM in the LS group.

## Weaning Differential Gene Expression Is Associated With Differential Gene Methylation

We assessed PBMC gene expression in nine gilts via RNA-seq and obtained 62–108M reads per sample (**Supplementary Table 5**). We identified 13,580 expressed genes and 1,480 DEGs between stages (**Supplementary Table 6**; 721 upregulated and 759 downregulated post-weaning). Numerous GO terms were enriched among upregulated genes, the most significant of which were related to immune, inflammatory, and stress response (**Supplementary Table 7A**). Downregulated genes were enriched for terms related to transcriptional and post-transcriptional regulation (**Supplementary Table 7B**).

Differential expression analysis was also performed on LS and HS animals separately. A larger number of weaning DEGs were identified in the LS group (134 upregulated and 42 downregulated post-weaning) compared to the HS group (49 genes upregulated and 13 downregulated). DEGs were submitted for GSEA, and only upregulated genes contained enriched GO terms. There were numerous terms enriched among both sets of upregulated genes (e.g., "Inflammatory response" and "Positive regulation of cytokine production"), but unique GO terms were also enriched (**Supplementary Tables 7C,D**). LS upregulated genes were enriched for terms related to viral response, type I interferon signaling, and NIK/NF-κB signaling. HS upregulated genes were enriched for terms related to apoptosis and negative regulation of CD4-positive, alpha-beta T cell proliferation and activation.

To determine the degree of overlap between DEGs and DMGs, we identified DEGs between stages in the same six animals for which methylation data were generated. There was a total of 387 DEGs (275 upregulated and 112 downregulated), and these were significantly enriched among DMGs (**Supplementary Figure 2**). Twenty-eight DEGs were also promoter-DMGs, and there was particular enrichment for upregulated genes among hypomethylated promoter-DMGs ($p = 3.56 \times 10^{-3}$; **Supplementary Figure 2A**). Additionally, 29 DEGs were also gene body-DM, and there was again enrichment for upregulated genes among hypomethylated gene body-DMGs ($p = 0.021$; **Supplementary Figure 2B**). There is thus evidence that differential methylation is strongly associated with differential expression in post-weaning piglet PBMCs, and specifically that hypomethylation is associated with increased gene expression.

Because T cell co-receptor genes exhibited unique differential methylation patterns between stress groups, we determined the extent to which such patterns associated with differential expression between HS and LS animals. *CD8B*, which was gene body-hypermethylated only in the HS group post-weaning, was also significantly downregulated in the HS group (**Table 2**; log2FC = −1.67) but not in the LS group (log2FC = −0.25). *CD4* exhibited post-weaning promoter hypomethylation in the LS group but not in the HS group and exhibited more decreased expression in the HS group (log2FC = −0.387) although this difference was not statistically significant. Changes in the expression of genes with associated differences in regional methylation suggest that such regions may harbor regulatory elements that dictate stress-dependent T cell gene expression.

## *NR3C1* Differential Methylation and Expression Is Indicative of Altered HPA Axis Response

We did not observe significant regional differences in CpG methylation associated with weaning in either of the two *NR3C1* promoters in the pig genome. We thus assessed

**TABLE 2 |** Weaning differential methylation and expression of T cell co-receptor genes.

| Gene | DMR location | Gene feature | Methylation difference (post vs. pre) | | | Log2 fold change (post vs. pre-weaning) | | |
|---|---|---|---|---|---|---|---|---|
| | | | All | LS | HS | All | LS | HS |
| *CD3E* | 9:45620001-45621000 | Promoter | −9.13 | −13.17 | −6.02 | 0.076 | 0.064 | 0.024 |
| | 9:45621001-45622000 | Promoter | **−16.43*** | **−19.64** | **−17.50** | | | |
| | 9:45624001-45625000 | Gene body | −6.63 | **−13.63** | 2.98 | | | |
| *CD3D* | 9:45645001-45646000 | Promoter | −5.08 | **−18.71** | 2.95 | **0.273** | 0.165 | 0.081 |
| *CD3G* | | | | | | −0.460 | −0.528 | −0.588 |
| *CD4* | 5:63916001-63917000 | Promoter | −5.39 | **−17.70** | 6.06 | −0.122 | −0.143 | −0.387 |
| *CD8A* | – | – | – | – | – | **−0.311** | −0.079 | −0.59 |
| *CD8B* | 3:57970001-57971000 | Promoter | **16.50** | **15.17** | **17.49** | **−0.80** | −0.251 | **−1.67** |
| | 3:57988001-57989000 | Gene body | 11.93 | −0.81 | **20.57** | | | |

*Boldface indicates significant differential methylation/expression.*

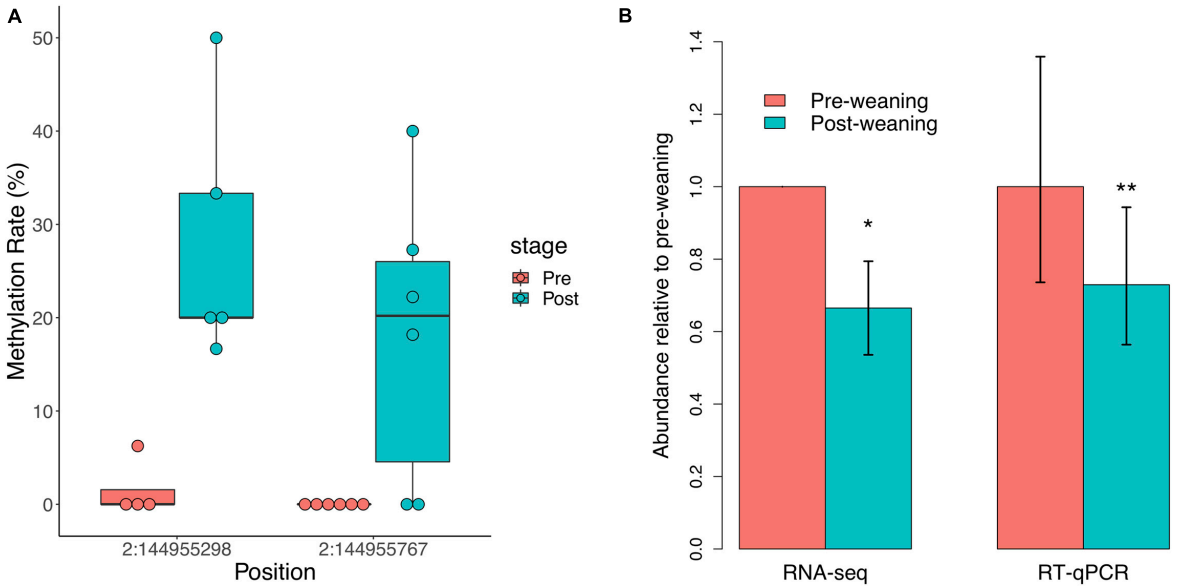



**FIGURE 2 |** Glucocorticoid receptor (*NR3C1*) gene methylation and expression in response to weaning. **(A)** Two CpG sites in the *NR3C1* promoter (797 and 328 bp downstream of TSS) are significantly hypermethylated post-weaning ($n$ = 6 animals/stage). **(B)** NR3C1 transcript abundance is significantly reduced post-weaning, as measured by RNA-sequencing and RT-qPCR ($n$ = 9 animals/stage). *= < 0.05, **= < 0.01.

individual CpG methylation differences and identified two differentially methylated CpGs (DMCs), both of which were hypermethylated post-weaning (**Figure 2A**). These DMCs lie 797 and 328 bp downstream of the first *NR3C1* TSS and exhibited 17 and 21% increases in methylation post-weaning, respectively. We observed a corresponding decrease in *NR3C1* transcript abundance via RNA-seq (**Figure 2B**; log2FC = −0.588, $p = 0.026$), which was also validated via RT-qPCR (log2FC = −0.455, $p = 6.1 \times 10^{-3}$). These results recapitulate findings in human and mouse studies that stress exposure is associated with *NR3C1* promoter hypermethylation and decreased expression in peripheral tissues.

## DISCUSSION

This study has identified epigenetic alterations in pigs as a response to weaning stress by assessing DNA methylation patterns in piglet PBMCs prior to and after weaning and mixing with unfamiliar individuals. By selecting animals displaying extremes in post-weaning serum cortisol change and skin lesion counts, we were able to assess not only the overall effect of weaning on DNA methylation in PBMCs but also how responses varied depending on stress level. PBMCs are a valuable peripheral cell type to study in the context of weaning for numerous reasons; first, they consist primarily of monocytes and lymphocytes whose activity, proliferation, and differentiation has been shown to be significantly altered by weaning-associated stress (Blecha et al., 1983; Niekamp et al., 2007; Kick et al., 2012). Furthermore, PBMC expression and methylation of genes involved in the HPA axis—namely *NR3C1*—have been shown to be suitable "surrogates" for measurement of gene activity in neuronal tissues (González Ramírez et al., 2020).

We observed global CpG methylation rates in piglet PBMCs between 79.1 and 82.9%. A high proportion of

variation in DNA methylation could be attributed to litter, which emphasized the need to correct for this variable when assessing for weaning-specific differential methylation patterns. The presence of 2,674 DMRs between stages indicates that weaning-associated changes in DNA methylation were present at many genomic loci. Additionally, we observed unique differential methylation patterns between LS and HS animals, with HS animals possessing more DMRs but LS animals having a greater proportion of hypomethylated regions. Previous studies in livestock species have identified differential methylation patterns in stressed versus non-stressed animals. Hao et al. (2016) identified thousands of DMRs in *longissimus dorsi* muscle of heat-stressed versus control pigs within genes involved in energy metabolism, stress response, and calcium signaling. Multiple studies have identified differential lymphocyte DNA methylation associated with prenatal transportation stress in Brahman bulls and heifers (Littlejohn et al., 2018; Baker et al., 2020; Cilkiz et al., 2020) and identified thousands of DM loci enriched in stress and immune response genes. Our results indicate that weaning stress also alters DNA methylation patterns in pig immune cells—particularly within gene promoters—and that the magnitude and direction of such alterations may be dependent on the level of stress experienced.

When considering all animals, post-weaning differential methylation impacted genes involved in immune cell processes. *IL2RA* exhibited hypermethylation in post-weaning PBMCs; this gene has previously been shown to possess extensive promoter hypomethylation in activated CD4+ T cells (Belot et al., 2018), suggesting that the opposite state observed here may suppress such activation. Clear differences were observed when assessing GO enrichment among LS and HS DMGs. Particularly, LS animals exhibited hypomethylation of genes involved in T cell activation and differentiation, while HS animals exhibited hypermethylation of genes involved in these processes. Overall, expression patterns were consistent with the differential methylation observed in LS and HS animals in terms of impacted biological processes. Upregulated HS genes were enriched for GO terms related to T cell apoptosis and negative regulation of CD4+ T cell proliferation, and these were not observed among the LS upregulated genes. Previous studies have shown CD4+ T cell concentrations to be the most significantly reduced following periods of psychosocial and weaning stress (Tuchscherer et al., 2009). Our data suggest that differential gene regulation by DNA methylation may play a role in a reduced T cell response with increasing levels of stress. This was particularly evident when assessing differential methylation and expression by stress group among T cell co-receptor genes. Many of these genes exhibited post-weaning differential methylation patterns indicative of lower gene activation in the HS group compared to the LS group, and *CD8B* also exhibited significantly lower expression post-weaning only in the HS group. *CD8B* encodes a subunit of the CD8 co-receptor in cytotoxic T cells. Studies have shown that corticosterone injections decrease CD8+ T cell concentrations in humans (Nair et al., 2007; Ashcraft et al., 2008) and that in pigs cytotoxic T cell concentrations decrease following weaning (Kick et al., 2012). Our methylation analyses have identified a DMR in the gene body of *CD8B* that may act in regulating *CD8B* expression, particularly in response to weaning stress and cortisol levels.

Lastly, we observed significant post-weaning hypermethylation in CpGs in the *NR3C1* promoter and a corresponding decrease in expression. The glucocorticoid receptor not only functions as an inducer of cortisol-mediated transcription in peripheral tissues but also regulates the HPA axis response in a negative feedback loop (de Kloet et al., 1998). *NR3C1* hypermethylation and downregulation in the hypothalamus has often been an indicator of stress vulnerability, and recent studies have shown comparable patterns in PBMCs (Oberlander et al., 2008; Perroud et al., 2011). Our data show that pigs exhibit similar patterns of *NR3C1* hypermethylation and downregulation in response to weaning stress. However, we did not observe significant differences in post-weaning *NR3C1* methylation and expression between LS and HS pigs, potentially due to our limited sample size in this study.

## CONCLUSION

In summary, we have elucidated epigenetic patterns of acute weaning-associated stress response in pigs. Future studies should seek to assess patterns of methylation and expression in PBMCs at later periods following weaning to assess long-term effects of weaning stress on pig immunity and performance. Additionally, assessment of other tissues involved in the HPA axis would provide a more direct measurement of stress response that could be compared to regulation and expression of genes in peripheral tissues. Continued analysis of genes undergoing stress-dependent gene regulation and expression may reveal biomarkers that are predictive of pig stress resilience.

## DATA AVAILABILITY STATEMENT

The datasets presented in this study can be found in online repositories. The names of the repository/repositories and accession number(s) can be found below: https://www.ncbi.nlm.nih.gov/, PRJNA632582.

## ETHICS STATEMENT

The animal study was reviewed and approved by the Michigan State University Institutional Animal Care and Use Committee AUF# 04/17-062-00.

## AUTHOR CONTRIBUTIONS

CE and JS designed the experiment. RC, KW, and CE collected the blood samples. KW performed the lesion scoring. RC and

NR performed the nucleic acid isolation and immunoassays. RC and AL analyzed the phenotypic and sequencing data. LF performed the RT-qPCR and analyzed the results. RC wrote the manuscript. All authors read, edited, and approved the manuscript.

## FUNDING

This study was made possible by the financial support of the Michigan Alliance for Animal Agriculture (M-AAA; proposal #AA17-29). RC was funded by a USDA NIFA National Needs Training Grant (#2015-38420-23697) and a NIFA EWD Predoctoral Fellowship (#2019-67011-29619).

## ACKNOWLEDGMENTS

The authors wish to thank Kevin Turner and the MSU Swine Teaching and Research Center for rearing and caring of the animals, and for their assistance with blood sample collection, as well as the MSU Genomics Core for their technical and sequencing support.

## SUPPLEMENTARY MATERIAL

The Supplementary Material for this article can be found online at: https://www.frontiersin.org/articles/10.3389/fgene.2021.633564/full#supplementary-material

## REFERENCES

Akalin, A., Kormaksson, M., Li, S., Garrett-Bakelman, F. E., Figueroa, M. E., Melnick, A., et al. (2012). MethylKit: a comprehensive R package for the analysis of genome-wide DNA methylation profiles. *Genome Biol.* 13:R87. doi: 10.1186/gb-2012-13-10-R87

Anders, S., Pyl, P. T., and Huber, W. (2015). HTSeq–a Python framework to work with high-throughput sequencing data. *Bioinformatics* 31, 166–169. doi: 10.1093/bioinformatics/btu638

Ashcraft, K. A., Hunzeker, J., and Bonneau, R. H. (2008). Psychological stress impairs the local CD8+ T cell response to mucosal HSV-1 infection and allows for increased pathogenicity via a glucocorticoid receptor-mediated mechanism. *Psychoneuroendocrinology* 33, 951–963. doi: 10.1016/j.psyneuen.2008.04.010

Baker, E. C., Cilkiz, K. Z., Riggs, P. K., Littlejohn, B. P., Long, C. R., Welsh, T. H., et al. (2020). Effect of prenatal transportation stress on DNA methylation in Brahman heifers. *Livest. Sci.* 240:104116. doi: 10.1016/j.livsci.2020.104116

Belot, M. P., Castell, A. L., Le Fur, S., and Bougnères, P. (2018). Dynamic demethylation of the IL2RA promoter during in vitro CD4+ T cell activation in association with IL2RA expression. *Epigenetics* 13, 459–472. doi: 10.1080/15592294.2018.1469893

Bird, A. P., and Wolffe, A. P. (1999). Methylation-induced repression-belts, braces, and chromatin. *Cell* 99, 451–454. doi: 10.1016/S0092-8674(00)81532-9

Blecha, F., Pollmann, D. S., and Nichols, D. A. (1983). Weaning pigs at an early age decreases cellular immunity. *J. Anim. Sci.* 56, 396–400. doi: 10.2527/jas1983.562396x

Bolger, A. M., Lohse, M., and Usadel, B. (2014). Trimmomatic: A flexible trimmer for Illumina sequence data. *Bioinformatics* 30, 2114–2120. doi: 10.1093/bioinformatics/btu170

Cilkiz, K. Z., Baker, E. C., Riggs, P. K., Littlejohn, B. P., Long, C. R., Welsh, T. H., et al. (2020). Genome-wide DNA methylation alteration in prenatally stressed Brahman heifer calves with the advancement of age. *Epigenetics* 2020, 1–18. doi: 10.1080/15592294.2020.1805694

Cinar, M. U., Islam, M. A., Pröll, M., Kocamis, H., Tholen, E., Tesfaye, D., et al. (2013). Evaluation of suitable reference genes for gene expression studies in porcine PBMCs in response to LPS and LTA. *BMC Res. Notes* 6:56. doi: 10.1186/1756-0500-6-56

de Kloet, E. R., Vreugdenhil, E., Oitzl, M. S., and Joëls, M. (1998). Brain Corticosteroid Receptor Balance in Health and Disease 1. *Endocr. Rev.* 19, 269–301. doi: 10.1210/edrv.19.3.0331

Eden, E., Navon, R., Steinfeld, I., Lipson, D., and Yakhini, Z. (2009). GOrilla: A tool for discovery and visualization of enriched GO terms in ranked gene lists. *BMC Bioinformatics* 10:48. doi: 10.1186/1471-2105-10-48

Fernandez, X., Meunier-Salaün, M. C., and Mormede, P. (1994). Agonistic behavior, plasma stress hormones, and metabolites in response to dyadic encounters in domestic pigs: Interrelationships and effect of dominance status. *Physiol. Behav.* 56, 841–847. doi: 10.1016/0031-9384(94)90313-1

Geverink, N. A., Kappers, A., Van De Burgwal, J. A., Lambooij, E., Blokhuis, H. J., and Wiegant, V. M. (1998). Effects of Regular Moving and Handling on the Behavioral and Physiological Responses of Pigs to Preslaughter Treatment and Consequences for Subsequent Meat Quality. *J. Anim. Sci.* 76, 2080–2085. doi: 10.2527/1998.7682080x

González Ramírez, C., Villavicencio Queijeiro, A., Jiménez Morales, S., Bárcenas López, D., Hidalgo Miranda, A., Ruiz Chow, A., et al. (2020). The NR3C1 gene expression is a potential surrogate biomarker for risk and diagnosis of posttraumatic stress disorder. *Psychiatry Res.* 284:112797. doi: 10.1016/j.psychres.2020.112797

González-Recio, O., Toro, M. A., and Bach, A. (2015). Past, present, and future of epigenetics applied to livestock breeding. *Front. Genet.* 6:305. doi: 10.3389/fgene.2015.00305

Greenberg, M. V. C., and Bourc'his, D. (2019). The diverse roles of DNA methylation in mammalian development and disease. *Nat. Rev. Mol. Cell Biol.* 20, 590–607. doi: 10.1038/s41580-019-0159-6

Hao, Y., Cui, Y., and Gu, X. (2016). Genome-wide DNA methylation profiles changes associated with constant heat stress in pigs as measured by bisulfite sequencing. *Sci. Rep.* 6:27507. doi: 10.1038/srep27507

Johnson, J. S., Aardsma, M. A., Duttlinger, A. W., and Kpodo, K. R. (2018). Early life thermal stress: Impact on future thermotolerance, stress response, behavior, and intestinal morphology in piglets exposed to a heat stress challenge during simulated transport. *J. Anim. Sci.* 96, 1640–1653. doi: 10.1093/jas/sky107

Kick, A. R., Tompkins, M. B., Flowers, W. L., Whisnant, C. S., and Almond, G. W. (2012). Effects of stress associated with weaning on the adaptive immune system in pigs1. *J. Anim. Sci.* 90, 649–656. doi: 10.2527/jas.2010-3470

Kim, D., Pertea, G., Trapnell, C., Pimentel, H., Kelley, R., and Salzberg, S. L. (2013). TopHat2: accurate alignment of transcriptomes in the presence of insertions, deletions and gene fusions. *Genome Biol.* 14:R36. doi: 10.1186/gb-2013-14-4-r36

Krueger, F., and Andrews, S. R. (2011). Bismark: a flexible aligner and methylation caller for Bisulfite-Seq applications. *Bioinformatics* 27, 1571–1572. doi: 10.1093/bioinformatics/btr167

Lallès, J. P., Boudry, G., Favier, C., Le Floc'h, N., Luron, I., Montagne, L., et al. (2004). Gut function and dysfunction in young pigs: Physiology. *Anim. Res.* 53, 301–316. doi: 10.1051/animres:2004018

Li, Y., Song, Z., Kerr, K. A., and Moeser, A. J. (2017). Chronic social stress in pigs impairs intestinal barrier and nutrient transporter function, and alters neuro-immune mediator and receptor expression. *PLoS One* 12:171617. doi: 10.1371/journal.pone.0171617

Littlejohn, B. P., Price, D. M., Neuendorff, D. A., Carroll, J. A., Vann, R. C., Riggs, P. K., et al. (2018). Prenatal transportation stress alters genome-wide DNA methylation in suckling Brahman bull calves. *J. Anim. Sci.* 96, 5075–5099. doi: 10.1093/jas/sky350

Love, M. I., Huber, W., and Anders, S. (2011). Moderated estimation of fold change and dispersion for RNA-seq data with DESeq2. *Genome Biol.* 15:8. doi: 10.1186/s13059-014-0550-8

Moeser, A. J., Pohl, C. S., and Rajput, M. (2017). Weaning stress and gastrointestinal barrier development: Implications for lifelong gut health in pigs. *Anim. Nutr.* 3, 313–321. doi: 10.1016/j.aninu.2017.06.003

Molenaar, R., Hulet, R., Meijerhof, R., Maatjens, C. M., Kemp, B., and Van den Brand, H. (2011). High eggshell temperatures during incubation decrease

growth performance and increase the incidence of ascites in broiler chickens. *Poult. Sci.* 90, 624–632. doi: 10.3382/ps.2010-00970

Morrow-Tesch, J. L., McGlone, J. J., and Salak-Johnson, J. L. (1994). Heat and Social Stress Effects on Pig Immune Measures. *J. Anim. Sci.* 72, 2599–2609.

Nair, A., Hunzeker, J., and Bonneau, R. H. (2007). Modulation of microglia and CD8+ T cell activation during the development of stress-induced herpes simplex virus type-1 encephalitis. *Brain Behav. Immun.* 21, 791–806. doi: 10.1016/j.bbi.2007.01.005

Niekamp, S. R., Sutherland, M. A., Dahl, G. E., and Salak-Johnson, J. L. (2007). Immune responses of piglets to weaning stress: Impacts of photoperiod. *J. Anim. Sci.* 85, 93–100. doi: 10.2527/jas.2006-153

Oberlander, T. F., Weinberg, J., Papsdorf, M., Grunau, R., Misri, S., and Devlin, A. M. (2008). Prenatal exposure to maternal depression, neonatal methylation of human glucocorticoid receptor gene (NR3C1) and infant cortisol stress responses. *Epigenetics* 3, 97–106. doi: 10.4161/epi.3.2.6034

Perroud, N., Paoloni-Giacobino, A., Prada, P., Olié, E., Salzmann, A., Nicastro, R., et al. (2011). Increased methylation of glucocorticoid receptor gene (NR3C1) in adults with a history of childhood maltreatment: A link with the severity and type of trauma. *Transl. Psychiatry* 1:60. doi: 10.1038/tp.2011.60

Tuchscherer, M., Kanitz, E., Puppe, B., Tuchscherer, A., and Viergutz, T. (2009). Changes in endocrine and immune responses of neonatal pigs exposed to a psychosocial stressor. *Res. Vet. Sci.* 87, 380–388. doi: 10.1016/j.rvsc.2009.04.010

Turner, S. P., Roehe, R., D'Eath, R. B., Ison, S. H., Farish, M., Jack, M. C., et al. (2009). Genetic validation of postmixing skin injuries in pigs as an indicator of aggressiveness and the relationship with injuries under more stable social conditions. *J. Anim. Sci.* 87, 3076–3082. doi: 10.2527/jas.2008-1558

Turner, S. P., White, I. M. S., Brotherstone, S., Farnworth, M. J., Knap, P. W., Penny, P., et al. (2006). Heritability of post-mixing aggressiveness in grower-stage pigs and its relationship with production traits. *Anim. Sci.* 82, 615–620. doi: 10.1079/ASC200678

Tzschentke, B., and Basta, D. (2002). Early development of neuronal hypothalamic thermosensitivity in birds: influence of epigenetic temperature adaptation. *Comp. Biochem. Physiol. Part A Mol. Integr. Physiol.* 131, 825–832. doi: 10.1016/S1095-6433(02)00020-X

Varley, K. E., Gertz, J., Bowling, K. M., Parker, S. L., Reddy, T. E., Pauli-Behn, F., et al. (2013). Dynamic DNA methylation across diverse human cell lines and tissues. *Genome Res.* 23, 555–567. doi: 10.1101/gr.147942.112

Wang, H., Wang, J., Ning, C., Zheng, X., Fu, J., Wang, A., et al. (2017). Genome-wide DNA methylation and transcriptome analyses reveal genes involved in immune responses of pig peripheral blood mononuclear cells to poly I:C. *Sci. Rep.* 7:9709. doi: 10.1038/s41598-017-10648-9

Wang, J., Wang, Y., Wang, H., Hao, X., Wu, Y., and Guo, J. (2014). Selection of reference genes for gene expression studies in porcine whole blood and peripheral blood mononuclear cells under polyinosinic:Polycytidylic acid stimulation. *Asian Austral. J. Anim. Sci.* 27, 471–478. doi: 10.5713/ajas.2013.13471

Wurtz, K. E., Siegford, J. M., Bates, R. O., Ernst, C. W., and Steibel, J. P. (2017). Estimation of genetic parameters for lesion scores and growth traits in group-housed pigs1. *J. Anim. Sci.* 95, 4310–4317. doi: 10.2527/jas2017.1757

Yahav, S., and Hurwitz, S. (1996). Induction of thermotolerance in male broiler chickens by temperature conditioning at an early age. *Poult Sci.* 75, 402–406. doi: 10.3382/ps.0750402

**Conflict of Interest:** The authors declare that the research was conducted in the absence of any commercial or financial relationships that could be construed as a potential conflict of interest.

*Copyright © 2021 Corbett, Luttman, Wurtz, Siegford, Raney, Ford and Ernst. This is an open-access article distributed under the terms of the Creative Commons Attribution License (CC BY). The use, distribution or reproduction in other forums is permitted, provided the original author(s) and the copyright owner(s) are credited and that the original publication in this journal is cited, in accordance with accepted academic practice. No use, distribution or reproduction is permitted which does not comply with these terms.*

frontiers in Genetics

REVIEW
published: 23 February 2021
doi: 10.3389/fgene.2020.613636

# Impacts of Epigenetic Processes on the Health and Productivity of Livestock

*Mengqi Wang*[1,2] *and Eveline M. Ibeagha-Awemu*[1]*

[1] *Agriculture and Agri-Food Canada, Sherbrooke Research and Development Centre, Sherbrooke, QC, Canada,*
[2] *Department of Animal Science, Laval University, Quebec, QC, Canada*

The dynamic changes in the epigenome resulting from the intricate interactions of genetic and environmental factors play crucial roles in individual growth and development. Numerous studies in plants, rodents, and humans have provided evidence of the regulatory roles of epigenetic processes in health and disease. There is increasing pressure to increase livestock production in light of increasing food needs of an expanding human population and environment challenges, but there is limited related epigenetic data on livestock to complement genomic information and support advances in improvement breeding and health management. This review examines the recent discoveries on epigenetic processes due to DNA methylation, histone modification, and chromatin remodeling and their impacts on health and production traits in farm animals, including bovine, swine, sheep, goat, and poultry species. Most of the reports focused on epigenome profiling at the genome-wide or specific genic regions in response to developmental processes, environmental stressors, nutrition, and disease pathogens. The bulk of available data mainly characterized the epigenetic markers in tissues/organs or in relation to traits and detection of epigenetic regulatory mechanisms underlying livestock phenotype diversity. However, available data is inadequate to support gainful exploitation of epigenetic processes for improved animal health and productivity management. Increased research effort, which is vital to elucidate how epigenetic mechanisms affect the health and productivity of livestock, is currently limited due to several factors including lack of adequate analytical tools. In this review, we (1) summarize available evidence of the impacts of epigenetic processes on livestock production and health traits, (2) discuss the application of epigenetics data in livestock production, and (3) present gaps in livestock epigenetics research. Knowledge of the epigenetic factors influencing livestock health and productivity is vital for the management and improvement of livestock productivity.

**Keywords: DNA methylation and histone modification, epigenetics biomarker, application of epigenetics data, growth and development, livestock, productivity, health and disease**

OPEN ACCESS

***Edited by:***
*Nick V. L. Serão,*
*Iowa State University, United States*

***Reviewed by:***
*Christopher K. Tuggle,*
*Iowa State University, United States*
*Marcela Maria De Souza,*
*Iowa State University, United States*

****Correspondence:***
*Eveline M. Ibeagha-Awemu*
*eveline.ibeagha-awemu@canada.ca*

***Specialty section:***
*This article was submitted to Livestock Genomics, a section of the journal Frontiers in Genetics*

***Received:*** *02 October 2020*
***Accepted:*** *21 December 2020*
***Published:*** *23 February 2021*

***Citation:***
*Wang M and Ibeagha-Awemu EM (2021) Impacts of Epigenetic Processes on the Health and Productivity of Livestock. Front. Genet. 11:613636. doi: 10.3389/fgene.2020.613636*

## INTRODUCTION

Increasing animal food demand by an ever-expanding human population as well as the challenges of global climate change is a clarion call for the sustainable development of the food animal industry, with the expectation of increased supply of high-quality animal proteins with minimal environmental impacts. In response, recent research efforts are geared towards developing different approaches to improve livestock production efficiency, decrease production cost, and develop environmentally friendly livestock production systems (Capper and Bauman, 2013; Scott, 2018). In recent years, the application of modern technologies including advanced sequencing technologies, genotype analysis, and genome profiling has promoted important changes in livestock genetic breeding programs and gains in important livestock traits like milk yield/quality in dairy cattle and goat, meat quality in beef cattle and swine, egg yield/quality in chickens, etc. Continued technological advances have further promoted the implementation of genomic selection in livestock production (Georges et al., 2019; Gurgul et al., 2019). Sequence analysis of livestock genomes uncovered the general molecular and regulatory mechanisms of the coding and non-coding genome underlying production and health traits, which have supported advances in trait improvement (Kamath et al., 2016; Do et al., 2017a; Wara et al., 2019). These factors still fall short of accounting for the optimal level of variation that is required to achieve continued improvements in livestock health and productivity. The epigenome, which responds to internal and external environmental cues, is less explored but contains additional levels of variation that could be exploited for livestock trait improvement.

Epigenetics is defined as the study of heritable molecular modifications responsible for the regulation of genome activities and gene expression, resulting in phenotypic differences without alterations to the basic DNA sequence (Nicoglou and Merlin, 2017; Greally, 2018). Epigenetic processes, which include DNA methylation, histone modification, chromatin remodeling, and non-coding RNA (ncRNA) regulation, regulate gene expression and, thus, play significant roles in genome function and stability (Bird, 2002; Kouzarides, 2007; Morris and Mattick, 2014; Do and Ibeagha-Awemu, 2017). The epigenome, which encompasses these epigenetic processes, is dynamic during the whole lifetime

**Abbreviations:** 5hmC, 5-hydroxymethylcytosine; 5mC, 5-methylcytosine; *ABCA1*, subfamily A, member 1; *ABCA7*, subfamily A, member 7; *ABCG1*, ATP binding cassette subfamily G member 1; *ACACA*, acetyl-coenzyme A carboxylase alpha; *ACC*, acetyl-CoA carboxylase; *ACOX2*, acyl-CoA oxidase 2; *ACSL1*, acyl-CoA synthetase long chain family member 1; *ACSS2*, acyl-CoA synthetase short-chain family member 2; *ADAMTS3*, ADAM metallopeptidase with thrombospondin type 1 motif 3; *Akt*, serine/threonine protein kinase Akt; ATAC, Ada-Two-A-Containing complex; BAF, BRM/BRG1-associated factor complexes; *BTK*, Bruton tyrosine kinase; *BPI*, bactericidal/permeability-increasing protein; BVDV, bovine viral diarrhea virus; *CACNA1S*, calcium voltage-gated channel subunit alpha1 S; *CACNG6*: calcium voltage-gated channel auxiliary subunit gamma 6; *CAPN10*, calpain 10; *LOC101896713*, caspase-3; *CASP8*, caspase-8; *CAV1*, caveolin-1; *CD4*, CD4 molecule; *CKS1B*, CDC28 protein kinase regulatory subunit 1B; *COL6A1*, collagen type VI alpha 1 chain; CpG, cytosine-phosphate-guanosine; *CRYL1*, crystallin lambda 1; *CSF1*, colony stimulating factor 1; *CSN1S1*, alpha s1 casein; *CTCF*, CCCTC-binding factor; *CXCL14*, C-X-C motif chemokine ligand 14; *DICER1*, dicer 1, ribonuclease III; *DLK1*, delta like non-canonical Notch ligand 1; DMC, differentially methylated cytosines; DMG, differentially methylated gene; DMR, differentially methylated region; *DNMTs*, DNA methyltransferases; *DNMT1*, DNA methyltransferase 1; *DNMT2*, DNA methyltransferase 2; *DNMT3A*, DNA methyltransferase 3 A; *DNMT3B*, DNA methyltransferase 3 B; *DNMT3C*, DNA methyltransferase 3 C; *DNMT3L*, DNA methyltransferase 3 L; *E. coli*, *Escherichia coli*; *E2F2*, E2F transcription factor 2; *EEF1D*, eukaryotic translation elongation factor 1 delta; *EFNB2*, ephrin B2; *EGFR*, epidermal growth factor receptor; *EHMT2*, euchromatic histone lysine methyltransferase 2; *ElF5*, E74-like factor 5; *ENPP3*, ectonucleotide pyrophosphatase/phosphodiesterase 3; *EPO*, erythropoietin; *ERα*, estrogen receptor 1 (alpha); EWAS, epigenome-wide association studies; *FADS6*, fatty acid desaturase 6; *FASN*, fatty acid synthase; *FAT-1*, FAT atypical cadherin 1; *FATP1*, fatty acid transport protein 1; *FDFT1*, farnesyl-diphosphate farnesyltransferase 1; *FTO*, fat mass- and obesity-associated protein; *GALK1*, galactokinase 1; *GLUT1*, glucose transporter 1; *GR*, glucocorticoid receptor; *GSTP1*, glutathione S-transferase Pi 1; *GSTT1L*, glutathione S-transferase theta 1-like; GWAS, genomic-wide association studies; H3K27ac, the acetylation at the 27th lysine residue of the histone H3 protein; H3K26me3, the trimethylation at the 26th lysine residue of the histone H3 protein; H3K27me3, the trimethylation at the 27th lysine residue of the histone H3 protein; H3K36me3, the trimethylation at the 36th lysine residue of the histone H3 protein; H3K4me1, the monomethylation at the fourth lysine residue of the histone H3 protein; H3K4me3, the trimethylation at the fourth lysine residue of the histone H3 protein; H4K12ac, the acetylation at the 12th lysine residue of the histone H4 protein; *HDAC2*, histone deacetylase 2; *HDAC3*, histone deacetylase 3; *HDAC6*, histone deacetylase 6; *HIF-1α*, hypoxia-inducible factor 1 subunit alpha; *HIF-3α*, hypoxia-inducible factor 3 subunit alpha; *HOTAIR*, HOX transcript antisense RNA; *HOXC8*, homeobox C8; *HP*, haptoglobin; *HSD17B2*, hydroxysteroid 17-beta dehydrogenase 2; *IDH2*, isocitrate dehydrogenase (NADP(+)) 2; IGF1, insulin-like growth factor 1; *IGF2*, insulin-like growth factor 2; *IGF2R*, insulin-like growth factor 2 receptor; *IGFBP4*, insulin-like growth factor binding protein 4; *IL-10*, interleukin-10; *IL-1β*, interleukin-1 beta; *IL−6*, interleukin−6; *IL-6R*, interleukin-6 receptor; *IL−8*, interleukin−8; *IL-1R2*, interleukin 1 receptor type 2; *iNOS2*, inducible nitric oxide synthase 2; *INS*, insulin; *KAT2A*, lysine acetyltransferase 2A; Kcnq1, potassium voltage-gated channel subfamily Q member 1; *KCNQ3*, potassium voltage-gated channel subfamily Q member 3; *LBP*, lipopolysaccharide binding protein; LPS, bacterial lipopolysaccharide; *MAPRE1*, microtubule associated protein RP/EB family member 1; MBD, methyl-binding domain; *MBD1*, methyl binding domain 1; MDBK, Madin–Darby bovine kidney; MeCP1, methyl-CpG binding protein 1; MeCP2, methyl-CpG binding protein 2; Met, methionine; *MTTP*, microsomal triglyceride transfer protein; *MUSTN1*, musculoskeletal, embryonic nuclear protein 1; *MYB*, myb proto-oncogene protein; *NCKAP5*, NCK-associated protein 5; ncRNA, non-coding RNA; NDV, Newcastle disease virus; *NPY*, neuropeptide Y; *NR4A1*, nuclear receptor subfamily 4 group A member 1; *NRF1*, nuclear respiratory factor 1; *NTN1*, netrin 1; NuRD, nucleosome remodeling and deacetylation complex; *OAS1*, 2′–5′-oligoadenylate synthetase 1; *OAS2*, 2′–5′-oligoadenylate synthetase 2; *PACSNI1*, protein kinase C and casein kinase substrate in neurons 1; *PCK1*, phosphoenolpyruvate carboxykinase 1; *PEMT*, phosphatidylethanolamine N-methyltransferase; PHF14, PHD Finger Protein 14; *PITX1*, paired-like homeodomain transcription factor 1; *POMC*, proopiomelanocortin; *PPARG2*, peroxisome proliferator-activated receptor gamma; *PPARα*, peroxisome proliferator-activated receptor alpha; *PPARδ*, peroxisome proliferator-activated receptor delta; PPARγ, peroxisome proliferator-activated receptor gamma; PRRSV, porcine reproductive and respiratory syndrome virus; *PTX3*, pentraxin 3RRBS: reduced representation bisulfite sequencing; RSC, remodel the structure of chromatin; *RXRα*, retinoid X receptor alpha; *RYR1*, ryanodine receptor 1; *S6K1*, ribosomal protein S6 kinase 1; *S. aureus*, *Staphylococcus aureus*; *SAA3*, serum amyloid A 3; *SALL4*, spalt-like transcription factor 4; *SCD1*, stearoyl-CoA desaturase 1; *SDF4*, stromal cell derived factor 4; *SEPT9*, Septin 9; *SIN3A*, SIN3 transcription regulator family member A; *SIRT2*, sirtuin 2; *SIRT4*, sirtuin 4; *SIX1*, SIX homeobox 1; SNP, single nucleotide polymorphisms; *SNX25*, sorting nexin 25; *SREBF1*, sterol regulatory element binding transcription factor 1; *SREBP1*, sterol regulatory element binding protein 1; *SRXN1*, sulfiredoxin 1; *SS18*, SS18 subunit of BAF chromatin remodeling complex; SWI/SNF, switch/sucrose non-fermentable complexes; *TCF7L2*, type 2 diabetes gene; TET, ten-eleven translocation methylcytosine dioxygenases; *TGFB3*, transforming growth factor beta 3; *TLR-4*, toll-like receptor 4; *TMEM8C*, transmembrane protein 8c;*TNFα*, tumor necrosis factor α; *TNF*, tumor necrosis factor; *TNFSF8*, TNF superfamily member 8; TSS, transcriptional start sites; *UCP3*, uncoupling protein 3; VTGII, vitellogenin 2; WGBS, whole-genome bisulfite sequencing; WHO, United Nations World Health Organization.

and is significantly associated with the interaction between genetic activities and environmental stimulation (Bernstein et al., 2007; Monk et al., 2019). Sufficient evidence from epigenetics-related studies in humans and animals have demonstrated the distinctive roles of epigenetic mechanisms in various biological processes, such as growth, development, metabolism, and health (Ibeagha-Awemu and Zhao, 2015; Paiva et al., 2019). The occurrence of epigenetic mechanisms with important roles at specific key times of development or pathological conditions may be key to further exploration of the intricacies of diseases. In addition, the awareness and use of epigenetic mechanisms could be advantageous to the understanding of quantitative traits and in achieving advancements in the improvement of livestock productivity and disease resistance (Ibeagha-Awemu and Zhao, 2015; Ibeagha-Awemu and Khatib, 2017; Banta and Richards, 2018; Panzeri and Pospisilik, 2018). The important contribution of epigenetic processes to phenotypic outcome in livestock is beginning to attract attention implying that the impacts of these processes may soon find application in advancing livestock productivity and health (Doherty et al., 2014; Goddard and Whitelaw, 2014; Meirelles et al., 2014; Ibeagha-Awemu and Zhao, 2015; Triantaphyllopoulos et al., 2016; Ibeagha-Awemu and Khatib, 2017; Yakovlev, 2018; Paiva et al., 2019). This review has been categorized into sections that concentrate on discussing the epigenetics processes and impacts on gene regulation; evidence of the impacts of epigenetic regulatory mechanisms underlying productivity and health in different species of livestock animals, such as bovine, swine, sheep, goat, poultry, and other species; application of epigenetics data in livestock production; and research gaps and future perspectives. Evidence of epigenetic impacts on livestock reproduction and epigenetic alterations due to assisted reproduction technologies have been addressed in several recent reviews (Weksberg et al., 2007; Das et al., 2017; Franco, 2017; Khezri et al., 2020; Rivera, 2020; Wang et al., 2020e) and will not be discussed here.

## EPIGENETIC PROCESSES AND IMPACTS ON GENE REGULATION

### DNA Methylation

DNA methylation is thus far the most stable and characterized epigenetic modification in most mammalian genomes. DNA methylation principally occurs in the fifth carbon of cytosine residues (addition of a methyl or hydroxymethyl group, denoted as 5mC or 5hmC, respectively) in DNA sequence and mostly at cytosine-phosphate-guanosine (CpG) dinucleotides and to a lesser extent at cytosine-phosphate-adenosine (CpA), cytosine-phosphate-thymine (CpT), and cytosine-phosphate-cytosine (CpC) dinucleotides. The formation of DNA methylation patterns is catalyzed by the activities of a class of enzymes known as DNA methyltransferases (DNMTs). While DNMT3A and DNMT3B are responsible for the establishment of DNA methylation patterns during embryonic development or in response to environmental challenges, DNMT1 maintains DNA methylation during cell division (Edwards et al., 2017; Luo et al., 2018; Schmitz et al., 2019). DNMT3L, which acts as a co-factor of DNMT3A and DNMT3B during *de novo* DNA methylation, is required for mammalian genome imprinting (Hanna and Kelsey, 2014; Basu, 2016; Veland et al., 2019). There are other DNMTs which act in different biological processes. For example, DNMT3C is responsible for the silencing of young retrotransposons (Barau et al., 2016), while DNMT2 plays active roles in RNA methylation and the expression of small ncRNAs (Raddatz et al., 2013; Jeltsch et al., 2017; Zhang et al., 2018b). However, when established DNA methylation is not maintained, the process of passive or active demethylation sets in. Passive demethylation is through the activities of TET (ten–eleven translocation methylcytosine dioxygenases) proteins (e.g., TET1, TET2, and TET3) which mediate the oxidation of 5mC to produce 5-hydroxymethylcytosine (5hmC), 5-formylcytosine (5fC), and 5-carboxylcytosine (5caC; He et al., 2011; Wu and Zhang, 2017). Active demethylation is when replication-dependent dilution of 5hmC, 5fC, and 5caC or thymine DNA glycosylase (TDG)-mediated excision of 5fC and 5caC is coupled with base excision repair (Wu and Zhang, 2017). Other TET–TDG-independent mechanisms are also proposed to mediate active DNA demethylation (Wu and Zhang, 2010, 2014; Bochtler et al., 2017).

The impact of DNA methylation on gene expression is associated with its genome distribution. CpG-rich regions (also known as CpG islands) are frequently distributed in the promoter regions (usually extends to 5′UTR) and usually non-methylated, whereby its abnormal methylation may cause the repression of corresponding transcription and gene silencing (Deaton and Bird, 2011; Smith et al., 2020). About 72% of promoters are within CpG islands and nearly unmethylated, and their activities might be regulated by DNA methylation (Saxonov et al., 2006; Deaton and Bird, 2011). Promoter CpG islands have differential susceptibility to methylation during normal development or during disease progression (e.g., carcinogenesis), which might be influenced by intrinsic sequence properties (Feltus et al., 2006). Most promoter CpG islands (usually unmethylated) escape from *de novo* methylation during all developmental stages, and the activity of promoters with intermediate to high CpG content was negatively correlated with their DNA methylation status (Weber et al., 2007). However, there are still a small number of methylated CpG islands in gene promoters, such as at germline imprinting control regions, or on the inactive X chromosome in female somatic cells (Proudhon et al., 2012). DNA methylation could perturb gene expression activities through direct inhibition of transcription factor (TF) binding or indirect mediation by methyl-binding domain (MBD) proteins that recruit chromatin-modifying activities to methylated DNA (Razin and Kantor, 2005; Zhu et al., 2016; Yin et al., 2017; Greenberg and Bourc'his, 2019). It has been noted that TFs are likely to induce local epigenetic remodeling (Wapinski et al., 2013). DNA methylation in recognition sequences of some TFs was revealed to alter their binding specificity (Zhu et al., 2016). It was reported that DNA methylation of target sequences diminished the binding activity of numerous TFs in the human genome, whereas some TFs of the extended homeodomain family preferred CpG methylated sequences (Yin et al., 2017). The identification of MBDs, such as methyl-CpG binding protein 1 (MeCP1) and

methyl-CpG binding protein 2 (MeCP2), revealed that DNA methylation is connected with chromatin structure and gene expression. Except for binding to CpG-rich heterochromatin, some MBDs contain a transcriptional repressor complex that may induce histone deacetylation and chromatin remodeling, contributing to gene silencing (Razin and Kantor, 2005; Greenberg and Bourc'his, 2019).

DNA methylation is also found in the gene body, especially in introns, and is prone to high levels of methylation (Maunakea et al., 2010). DNA methylation in gene body is highly conserved across eukaryotes and has been positively correlated with transcription (Lister et al., 2009; Varley et al., 2013), indicating potential functions other than gene silencing. Two hypotheses underlying the function of DNA methylation in gene bodies have been suggested (Greenberg and Bourc'his, 2019). On the one hand, DNA methylation enriched at exons influences splicing and gene expression (Gelfman et al., 2013; Yang et al., 2014; Shayevitch et al., 2018). DNA methylation was found to facilitate exon exclusion by preventing CCCTC-binding factor (CTCF) binding or contribute to exon inclusion by recruitment of MeCP2 or splicing factors (Shukla et al., 2011; Maunakea et al., 2013; Yearim et al., 2015). However, these mechanisms could only explain a small portion of alternative splicing events. On the other hand, gene body DNA methylation suppresses intragenic promoters consistent with the possible role of DNA methylation as a transcriptional repressor. It was reported that binding of ADD domain to H3K36me3 released the inhibition of DNMT3 enzymes thereby promoting the establishment of *de novo* DNA methylation and, consequently, inhibition of cryptic promoters (Carrozza et al., 2005; Greenberg and Bourc'his, 2019). Indeed, methylation of CpG island in gene body suppressed promoter activity, and altered methylation contributed to the regulation of transcription initiation in a tissue- and cell-type-specific mechanism in mammals (Maunakea et al., 2010). Compared with its well-established repressive function at regulatory elements (such as the promoter region), less is known about DNA methylation regulation and function(s) at intergenic regions. Intergenic regions are mainly populated by regulatory ncRNA genes and other regulatory elements yet to be described, and the DNA methylation at these regions potentially regulates these factors. Downstream regions of genes contain miRNA binding sites, which may interact with DNA methylation and regulate gene expression. For example, the interaction between piwi RNA and DNA methylation is dedicated to silencing transposable elements in the germline (Manakov et al., 2015; Barau et al., 2016).

## Histone Modifications

Histone modification is another important epigenetic mechanism with significant impacts on chromatin regulation and regulation of transcription processes (Adamczyk, 2019). Histones are a family of proteins (H1/H5, H2A, H2B, H3, and H4) that park and order the DNA molecule into structural units called nucleosomes. The N-terminal tails of histones are subjected to various posttranscriptional or posttranslational modifications with more than 100 forms (e.g., lysine acetylation, lysine methylation, ubiquitination, serine/threonine phosphorylation, crotonylation, sumoylation, etc.) with varying effects on transcriptional activities described (Kouzarides, 2007; Zhao and Shilatifard, 2019; Roma-Rodrigues et al., 2020). Histone acetylation and methylation frequently occurs in the lysine of the N-terminal tails resulting from the interaction of associated enzymes or factors (Srivastava et al., 2016). Histone acetyltransferases are responsible for histone acetylation, which play important roles in releasing chromatin structure (histone–DNA interaction) and promoting transcriptional activities, while histone deacetylases cause deacetylation to repress gene expression (Dose et al., 2011; Schmauss, 2017). Similarly, the dynamic changes of histone methylation, which are generally classified into tri-, di-, and monomethylation of lysine residues and the monomethylation of arginine residues, are regulated by histone methyltransferases and demethylases (Ye et al., 2017). The impact of histone methylation on transcriptional activity is complex and depends on both modified residues and the state of methylation (Jambhekar et al., 2019). Additionally, histone phosphorylation, ubiquitylation, and ADP ribosylation are involved in the regulation of DNA damage and transcriptional activities (Liu C. et al., 2017; Alhamwe et al., 2018; Shanmugam et al., 2018).

## Chromatin Remodeling

Chromatin structure dynamics always correspond with the instructive gene expression pattern for cellular differentiation and lineage specification during development (Kishi and Gotoh, 2018; Quan et al., 2020). In addition to the covalent modification of DNA and histone, the remodeling of nucleosome is another important determinant of chromatin structure. Nucleosome formation, which is crucial for the compaction of genomic DNA into chromatin, has intrinsic dynamic properties regulated by chromatin remodeling complexes to ensure genomic DNA functions in chromatin (Zhou C. Y. et al., 2016; Kobayashi and Kurumizaka, 2019). Increasingly, reports of copious chromatin remodeling complexes and their essential regulatory potentials related to transcription activities and gene expression during development and disease processes have emerged (Bhattacharjee et al., 2016; Kim and Kaang, 2017; Stachowiak et al., 2020). Adenosine triphosphate (ATP)-dependent chromatin remodeling complexes are particularly known to utilize the energy derived from ATP hydrolysis to change nucleosome structure and consequently regulate DNA accessibility to TFs (Hota and Bruneau, 2016). As one representative of ATP-dependent complexes, BRM/BRG1-associated factor (BAF) complexes, also known as SWI/SNF (switch/sucrose non-fermentable) complexes, have various roles in gene activation and repression during mammalian development and in the development of disease (Clapier et al., 2017; Alfert et al., 2019; Hota et al., 2019). BAF complexes consist of over 15 different subunits with varied roles at different stages of mammalian development, including embryogenesis, neural development, cardiovascular development, skeletal muscle development, immune cell development, etc. (Hota and Bruneau, 2016; Nguyen et al., 2016; Sokpor et al., 2017; Sun et al., 2018). Homologous to the BAF complex, the RSC (remodel structure of chromatin) remodeling complex is an abundant and fundamental nuclear protein complex with

important roles in transcriptional and other cellular processes, including initiation and elongation of transcription as well as replication, segregation, and chromosome repair (Klein-Brill et al., 2019; Ye et al., 2019). The RSC complex can partially disrupt histone–DNA interaction by stable binding to nucleosomes or enhancer elements and can also disassemble or slide nucleosome through a DNA-sequence-dependent system, that is required for nucleosome-free region formation by removing nucleosome from upstream of transcription start sites (TSSs; Spain et al., 2014; Lorch and Kornberg, 2017; Kubik et al., 2018). Besides, nucleosome remodeling and deacetylation (NuRD) complex (highly conserved in mammals), initially defined as a transcriptional repressor, has been reported to link histone modifications to nucleosome remodeling and interaction with numerous TFs (Feng and Zhang, 2003; Liang et al., 2017). Genome-wide data revealed the presence of the NuRD complex at all active enhancers and promoters in diverse cells, and also that NuRD could deposit histone modifications at enhancers and promoters of active genes and thereby trigger their repression (Miller et al., 2016; Yang et al., 2016a; Bornelöv et al., 2018).

## Non-coding RNA Regulation

In addition to these classic epigenetic processes (DNA methylation, histone modification, and chromatin remodeling), ncRNAs also play important regulatory roles in gene expression and chromatin modification impacting livestock production and health (Do et al., 2017a; Benmoussa et al., 2020). ncRNAs are a class of RNA species that mediate their functions as RNA (are not translated into proteins) and generally regulate gene expression at the transcriptional and posttranscriptional levels. ncRNAs with epigenetic-related functions interfere with transcription, mRNA stability, or translation and include small interfering RNA (siRNA), piwi-interacting RNA (piRNA), microRNA (miRNA), and long non-coding RNA (lncRNA; Kaikkonen et al., 2011; Wei et al., 2017). For example, some miRNAs regulated by *DNMT1* are involved in the regulation of mammary gland development and lactation in dairy cattle (Do et al., 2017b; Melnik and Schmitz, 2017a). The binding of miRNA to a specific target, resulting in degradation or blockage of mRNA transcription, may induce a feedback modification related to DNA methylation (Lamouille et al., 2014). Besides, ncRNAs have been found to be involved in the regulation of epigenetic alterations in both DNA and histones (Sabin et al., 2013). Furthermore, it is speculated that some transcripts initiating from gene body CpG islands are regulated by ncRNAs whose presence or absence affects the expression of the associated protein-coding genes or nearby genes (Mercer et al., 2009). For example, AIR is a ncRNA that initiates at a CpG island within intron 2 of *IGF2R* and is essential for silencing of the paternal allele (Sleutels et al., 2002). Similarly, analysis of a CpG island in intron 10 of the imprinted *KCNQ1* gene identified it as the origin of a non-coding transcript (KCNQ1OT1) that is required for imprinting of several genes within this domain (Mancini-DiNardo et al., 2006). ncRNA regulation impacts on livestock productivity will not be discussed in this review as it has been adequately covered in the literature and in recent reviews (Do and Ibeagha-Awemu, 2017; Wara et al., 2019; Kosinska-Selbi et al., 2020).

# EVIDENCE OF THE IMPACTS OF EPIGENETIC PROCESSES ON LIVESTOCK PRODUCTION AND HEALTH

## Epigenetic Impacts on Livestock Reproduction, Growth, and Development

Dynamic epigenetic modifications are essential for normal growth and development through involvement in numerous biological processes, especially in response to environmental stimulus (Del Corvo et al., 2020; Thompson et al., 2020). The identification of epigenomic patterns in different tissues helps in the further understanding of epigenetic regulatory roles in livestock development and health. The impacts of epigenetic regulatory processes on livestock production in response to different impact factors or the exposome and the phenotypic outcomes are summarized in **Figure 1**. The important regulatory roles and impacts of epigenetic processes on placental and embryo development of livestock have been discussed in detail in many excellent reviews (Das et al., 2017; Franco, 2017; Hwang et al., 2017).

The genomic DNA methylation profiles of several tissues in multiple livestock species including cattle, chicken, swine, goat, sheep, etc. have been characterized (Korkmaz and Kerr, 2017; Lee K. H. et al., 2017; Zhang Y. et al., 2017; McKay et al., 2018; Sevane et al., 2019; Liu et al., 2020; Wang et al., 2020b). DNA methylation pattern screening in embryo at different embryonic stages of development, especially at the early stage when two major epigenetic reprogramming occur, indicated important regulatory roles of DNA methylation in embryo viability and fetus development relating to various metabolic and differentiation processes (Ispada et al., 2018; Salilew-Wondim et al., 2018; Duan et al., 2019; Cao P. et al., 2020; Ivanova et al., 2020). DNA methylation changes were found to partly explain the poor performance of offspring caused by maternal stressors, such as heat stress, metabolic disorder, and negative energy balance (Desmet et al., 2016; Akbarinejad et al., 2017). Differentially methylated cytosines (DMCs) in the liver from calves under maternal heat stress or cooling treatment (fans and water soakers) were found in genes involved in immune function, cell cycle, development, and enzyme activity, while DMCs in mammary gland tissues were enriched in biological functions, including protein binding, phosphorylation, enzyme and cell activation, and cell signaling (Skibiel et al., 2018). It was observed recently that sperm DNA methylome was characterized by generally low methylation levels compared with somatic tissue DNA methylome (Perrier et al., 2018; Zhou et al., 2018). Moreover, dysregulation of DNA methylation in sperm (Kropp et al., 2017; Perrier et al., 2018; Fang et al., 2019b) and histone modifications, including histone acetylation and methylation (Kutchy et al., 2017, 2018), were found to impact male fertility and related traits. For instance, sperm whole-genome bisulfite sequence (WGBS) data from high- and low-fertile bulls indicated high methylation differences (1,765 DMCs) and 10 candidate genes for the prediction of bull fertility (Gross et al., 2020). Another sperm WGBS dataset from 28 bulls further classified the

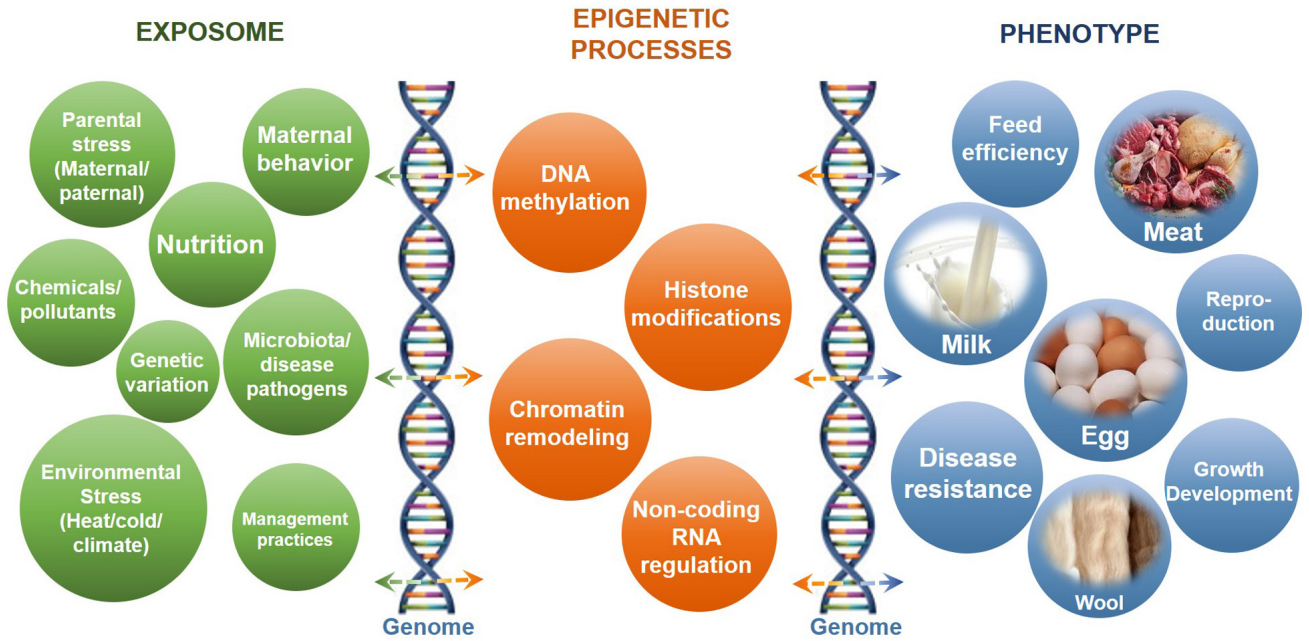



**FIGURE 1 |** The impacts of epigenetic regulatory processes on livestock production in response to different impact factors or the exposome. Shown are the common impact factors or exposome **(left)** that interact with epigenetic processes **(center)** and the genome (vertical DNA helix structures) to influence phenotypic outcome **(right)**.

sperm methylome into conversed, variable, and highly variable methylated regions (Liu S. et al., 2019). The highly variable methylated regions associated significantly with reproduction traits and were enriched for glycosyltransferase genes that are crucial for spermatogenesis and fertilization, while the variable methylated regions were co-localized with genes with functions in sperm motility (Liu S. et al., 2019). In addition, methylation analysis of high and low motile bull sperm populations found methylation variations in genes involved in chromatin remodeling and repetitive element activities in pericentric regions, which is indicative of crucial epigenetic regulatory functions in sperm functionality and fertility (Capra et al., 2019). Methylation alteration was also predicted as one potential epigenetic regulatory mechanism underlying sperm fertility differences caused by age and other stressors such as heat or oxidative stress (Lambert et al., 2018; Rahman et al., 2018; Wyck et al., 2018; Takeda et al., 2019). Moreover, epigenomic profiling of somatic tissues such as the liver, brain, and mammary gland tissues revealed that epigenetic modifications impact bovine development, health, and productivity (Zhou Y. et al., 2016; Kweh et al., 2019; Wang et al., 2020c). For example, DNA methylation is involved in the regulation of *SIRT6* promoter activity during bovine adipocyte differentiation (Hong et al., 2018).

Analysis of epigenetic processes in different porcine tissues, including tooth, brain, small intestine, and longissimus dorsi muscle, indicated their significant regulatory roles during the growth and development of pigs (Su et al., 2016; Larsen et al., 2018). The DNA methylation patterns of porcine tooth germ from different developmental stages (embryonic day 50 and day 60) revealed 2,469 differentially methylated genes (DMGs), including 104 DMGs with potential key regulatory roles in porcine tooth development (Su et al., 2016). Using the whole-genome DNA methylation approach to profile DNA methylation of porcine longissimus dorsi muscles from heat-stressed and non-stressed pigs, Hao and colleagues identified 57,147 differentially methylated regions (DMRs) and corresponding DMGs ($n$ = 1,422) with functions in energy and lipid metabolism, cellular defense, and stress responses, indicating the roles of DNA methylation in heat stress processes (Hao et al., 2016). The expressions of *DNMT1*, *DNMT3A*, and *DNMT3B* were found to decrease in brain tissues during the middle stage of gestation, indicating the potential of DNA methylation to regulate brain development of piglets (Larsen et al., 2018). Daily oral boluses of broad-spectrum antibiotics after preterm birth decreased bacterial density, diversity, and fermentation and altered the DNA methylation profile in the small intestine, which is indicative of the influence of epigenetic process on bacterial colonization of preterm neonate's intestine (Pan et al., 2018). Furthermore, transcriptional N6-methyladenosine ($m^6A$) profiling in porcine liver at different ages (0 day, 21 days, and 2 years) demonstrated that $m^6A$ modified about 33% of transcribed genes with roles in the regulation of growth and development and metabolic and protein catabolic processes implying that $m^6A$ methylation may be vital for the regulation of nutrient metabolism in porcine liver (He et al., 2017). Moreover, abundant $m^6A$ modifications were identified in granulosa

cells, which are crucial for follicle development with potential associations with steroidogenesis and folliculogenesis in pigs (Cao Z. et al., 2020).

DNA methylation and histone modification patterns have been characterized in various chicken strains in recent years, indicating the potential roles of epigenetic processes in the development and evolution of chicken (Li et al., 2015; Sarah-Anne et al., 2017). Epigenetic analysis of various tissues including the brain, retina, cornea, liver, and muscle strongly revealed the involvement of DNA methylation in the growth and development of chicken (Liu et al., 2016, Liu Z. et al., 2019; Lee I. et al., 2017). For example, DNA methylation profiles of broilers and layers at different embryonic stages revealed lower methylation levels in broilers, and enriched gene ontology terms related to muscle development by corresponding genes suggest a potential contribution of DNA methylation to embryonic muscle development (Liu Z. et al., 2019). *ACC* and *MTTP* showed abundant expression and were negatively correlated with lower DNA methylation at their promoter regions in the liver of chickens with fatty liver syndrome, linking DNA methylation to fat metabolism (Liu et al., 2016). The global DNA methylation profiling of strongly and weakly inbred chickens identified various DMRs and DMGs enriched in reproduction pathways, indicating the regulatory roles of DNA methylation in the repressed development of the reproduction system of inbred chickens (Han et al., 2020). Besides, chicken erythrocyte epigenome analysis identified more than 100 highly transcribed genes located in dynamical highly acetylated, salt-soluble chromatin domains, which were associated with H3K4me3 and H3K27ac, and also produced distinct antisense transcripts (Jahan et al., 2016). Results of comparing histone H1 subtypes between five avian species (chicken, gray partridge, quail, duck, and pheasant) indicated the potential involvement of histone modification in chromatin structure and function in the development of poultry (Kowalski and Pałyga, 2017).

In addition to the main livestock species discussed above, some epigenetics-related data have been reported in other livestock species. For instance, DNA methylation was predicted to be an age-dependent process in domestic horses (Andraszek et al., 2016). Different from the generally methylated mammalian genomes, honeybees have unique methylation patterns that concentrate in gene bodies and are associated with gene expression (Wedd and Maleszka, 2016; Harris et al., 2019). DNA methylation is involved in the learning and memory processes of honeybees, crucial traits for honey production (Li et al., 2017). Besides, epigenetic modifications, including DNA methylation, histone methylation, and phosphorylation, represent new possible mechanisms of sex and caste determination process in honeybees (Cardoso-Júnior et al., 2017; Yagound et al., 2019). Moreover, WGBS data showed differential methylation levels between honeybee queen larvae and worker larvae as well as 38 DMGs with functions in specific organ differentiation, morphology, reproduction, and vision differentiation during caste determination (Wang et al., 2020a). Furthermore, the identification of allele-specific DNA methylation patterns in honeybees provided a relatively reliable theory of genomic imprinting underlying parent-of-organ effects caused by reciprocal crosses (Remnant et al., 2016).

## Epigenetic Regulation in Response to Nutritional Stimulus

Nutrition represents the principal environmental determinant of an individual's growth and development. In order to enhance livestock health and welfare, reduce production cost, and adapt to global warming, efforts have been concentrated on adjusting nutritional supplements to livestock animals and their related impacts (McGuffey, 2017; Bobeck, 2020). Growing evidence supports the notion that permanent alterations in the epigenome of germline cells or embryos could be transferred to offspring, referred to as intergeneration or transgenerational epigenetic inheritance (Heard and Martienssen, 2014; Miska and Ferguson-Smith, 2016). It is well accepted that nutrition-induced epigenetic alterations can be heritable; however, the underlying mechanism is still controversial. On one side, epigenetic changes caused by consistent nutritional stimulus were identified in somatic tissues, indicating an undefined indirect mechanism of inheritance (Xue et al., 2016). On the other side, continuous stimulus as a result of the effects of nutritional factors on health and diseases of livestock could be transmitted between generations through altered epigenetic state of germline cells (Ideraabdullah and Zeisel, 2018). For example, the excessively high or excessive lack of nutrition (hyper-/hyponutrition, respectively) or nutrition component deficiencies could lead to epigenetic alterations (DNA methylation, histone modifications, and ncRNAs) in germ cells and transmission to subsequent generations (Guo T. et al., 2020). A number of studies, both *in vivo* and *in vitro*, showed that nutritional stimulus, including methionine, choline, and energy restriction, could induce epigenetic modifications causing the alteration of gene expression (Murdoch et al., 2016; Chavatte-Palmer et al., 2018; Elolimy et al., 2019). Data on the epigenetic modifications in response to nutritional stimulus in livestock are summarized in **Table 1**.

DNA methylation modifications in response to nutritional stimulus or environmental changes may cause alteration in production performance or disease susceptibility (Jang and Serra, 2014; Block and El-Osta, 2017; Maugeri and Barchitta, 2020). The interaction between changes in feed composition and epigenetic regulatory mechanisms has been reported. Liver tissues of methionine (Met)-supplemented Holsteins were found to have lower general DNA methylation levels compared with that of Holsteins without Met supplementation (Osorio et al., 2016). In the same study, the overall gene expression levels of *PPARα* and its target genes were upregulated in Met-supplemented Holsteins, which was related to improved metabolism and immune functions (Osorio et al., 2016). Additionally, differential expression of *ADAMTS3* and *ENPP3* genes (have roles related to the biosynthesis and regulation of glycosyltransferase activity, respectively) between grass-fed and grain-fed Angus cattle were associated with the methylation abundance of corresponding DMRs (Li Y. et al., 2019). Meanwhile, DNA methylation was involved in the regulation of altered gene expression in response to high-concentrate diets resulting in the downregulation of

**TABLE 1 |** Epigenetic alterations in response to nutritional stimulus in livestock.

| Parameter | Breed | Organ | Epigenetic alteration | *Potential epigenetic marker genes | References |
|---|---|---|---|---|---|
| **Cattle** | | | | | |
| Methionine supplementation throughout the peripartal period | Holstein cows | Liver | Global DNA methylation was lower, promoter methylation of *PPARA* was higher | *PPARA* | Osorio et al., 2016 |
| Grass-fed and grain-fed | Angus cattle | Rumen tissue | 217 DMRs | *ADAMTS3*, *ENPP3* | Li Y. et al., 2019 |
| High- vs low-concentrate corn straw (HCS/LCS) and low-concentrate mixed forage diet | Chinese Holstein cows | Mammary tissue | H3 acetylation reduced in HCS. Methylation of *STAT5A* reduced in HCS. Methylation of *SCD* increased in HCS | *STAT5A* | Dong et al., 2014 |
| High- vs low-concentrate diet | Holstein cows | Liver | Chromatin loosening at the promoter region | *TLR4*, *LBP*, *HP*, *SAA3* | Chang et al., 2015 |
| Methyl donor supplementation of pregnant animals | Holstein cows and calves | Blood | More than 2,000 DMG between offspring | *CEND1*, *VSIG2*, *B3GNT8*, etc. | Bach et al., 2017 |
| 85 vs 140% feed restriction | Angus–Simmental crossbred cows | *Longissimus dorsi* and *semitendinosus* muscles | One DMR (contains 23 to 24 CpGs) in *IGF2* | *IGF2* | Paradis et al., 2017 |
| Butyrate treatment | Holstein cows | Rumen primary epithelial cells from 2-week-old bull calves | Increased genome coverage (%) of CTCF, H3K27me3, and H3K4me3 and decreased coverage of H3K27ac, H3K4me1, and ATAC | Weak enhancers and flanking active transcriptional start sites | Fang et al., 2019a |
| **Swine** | | | | | |
| Restricted diet | Pig | Endometrium and embryos | Altered DNA methylation of selected genes | *ACP5*, *RGS12*, *EDNRB*, *TLR3*, *ADIPOR2*, *DNMT1* | Zglejc-Waszak et al., 2019 |
| Vitamin C supplementation | Pig | Oocyte | Methylation erasure on 5mC, $m^6A$, and H3K27me3, but establishment of H3K4me3 and H3K36me3 | *TET2*, *DNMT3B*, *HIF-1α*, *HIF-2α*, *TET3*, *METTL14*, *KDM5b*, and *EED* | Yu et al., 2018 |
| Omega-3 fatty acid supplementation | Piglet | Leukocyte | One hypomethylated DMR in chromosome 4, two hypermethylated DMRs in chromosomes 4 and 12 | *RUNX1T1* | Boddicker et al., 2016 |
| Maternal bisphenol A and methyl donor supplementation | Piglets from Landrace × Yorkshire sows | Piglet intestinal samples | Altered DNA methylation level of *PEPT1* in jejunum of offspring | *PEPT1*, *DNMT3a*, *LCT*, *DNMT1*, *MTHFR* | Liu H. et al., 2017 |
| Maternal methyl donor dietary supplementation | Piglets from White × Landrace sows | Liver samples from piglets | Increased methylation at the promoter of *IGF-1* in the methyl donor group | *IGF−1* | Jin C. et al., 2018 |
| Maternal betaine supplementation | Piglets from Landrace × Yorkshire sows | Liver samples from piglets | DNA hypermethylation and enriched H3K27me3 on the promoter region | *GALK1* | Cai et al., 2017 |
| **Poultry** | | | | | |
| Maternal genistein supplementation | Laying broiler breeder hens | Liver from pullets | Induced H3K36me3 and H4K12ac at the *PPARD* promoter | *PPARD* | Lv et al., 2019 |

*(Continued)*

**TABLE 1 |** Continued

| Parameter | Breed | Organ | Epigenetic alteration | *Potential epigenetic marker genes | References |
|---|---|---|---|---|---|
| Prenatal betaine supplementation | Juvenile chicken | Liver from juvenile chicken | Increased CpG methylation at promoter regions | *LXR* and *CYP27A1* | Hu et al., 2017b |
| Maternal betaine supplementation | Rugao Yellow chicken breeder hens | Hypothalamus of F1 cockerels | Modification of promoter CpG methylation | *DNMT1*, *BHMT SREBP-1*, *SREBP-2*, and *APO-A1* | Idriss et al., 2018 |
| Maternal betaine supplementation | Rugao yellow-feathered laying hens | Blood from pullets | Hypomethylated promoter regions of steroidogenic genes | *AHCYL*, *GNMT1*, and *BHMT* | Abobaker et al., 2019 |
| Methionine and betaine supplementation | Geese | Liver | Altered DNA methylation of *LOC106032502* | *LOC106032502* | Yang et al., 2018 |

**Potential epigenetic marker genes: These are genes harboring differentially methylated CpG sites or regions; vs, versus; DMR, differential methylated region; DMG, differential methylated gene; DMC, differential methylated CpG; HCS, high-concentrate corn straw; LCS, low-concentrate corn straw; CTCF, CCCTC-binding factor; ATAC, Ada-Two-A-Containing complex; H3K27me3, the trimethylation at the 27th lysine residue of the histone H3 protein; H3K4me3, the trimethylation at the fourth lysine residue of the histone H3 protein; H3K27ac, the acetylation at the 27th lysine residue of the histone H3 protein; H3K4me1, the monomethylation at the fourth lysine residue of the histone H3 protein; H3K36me3, the trimethylation at the 36th lysine residue of the histone H3 protein; H4K12ac, the acetylation at the 12th lysine residue of the histone H4 protein.*

immune-related genes (*TLR-4*, *LBP*, *HP*, and *SAA3*) in mammary and liver tissues of cows (Dong et al., 2014; Chang et al., 2015; Xu et al., 2018). In addition to DNA methylation, other epigenetic modifications have been reported to respond to nutritional stimulus. Histone H3 acetylation was significantly reduced in mammary gland tissue and also correlated negatively with lipopolysaccharide (LPS) concentrations in the mammary arterial blood of Chinese Holstein cows fed a high-concentrate corn straw diet (Dong et al., 2014). Linseed oil supplementation of Holstein cows in mid lactation, which resulted in 30% reduction of milk fat yield, significantly repressed the expression of histone acetylases (*HDAC2*, *HDAC3*, *SIRT2*, and *KAT2A*) and histone methyltransferase (*EHMT2*), suggesting potential epigenetic regulation of milk fatty acid synthesis (Li and Ibeagha-Awemu, 2017). Additionally, chromatin loosening was found to contribute to the upregulation of some immune-related genes in the liver of dairy cows in response to a high-concentrate diet (Chang et al., 2015). Furthermore, butyrate treatment of rumen epithelial cells revealed increased genome coverage (percentage) of CTCF, H3K27me3, and H3K4me3, but decreased coverage of H3K27ac, H3K4me1, and ATAC (Fang et al., 2019a). In the same study, 15 distinct chromatin states were defined according to the combination of identified epigenomic markers in genomic regions, which revealed that weak enhancers flanking active transcriptional start sites could be possible mechanisms underlying gene expression regulation by epigenomic markers (Fang et al., 2019a).

Nutritional supplementation during pregnancy caused epigenetic alterations in the fetus with long-term influences on the development and productivity of the offspring. Embryos (at 6.5 days) of dairy cows showed lower DNA methylation level in response to Met supplementation during the preimplantation period, which probably enhanced its survival capacity (Acosta et al., 2016). The supplementation of methyl donors to Holstein dams during pregnancy significantly altered the methylome of their offspring, and the DMCs affected the expression of genes involved in various biological processes, such as immune function, regulation of cell growth, and kinase activity (Bach et al., 2017). Maternal methyl donor supplementation was also found to alter the hepatic metabolism program of calves by maintaining Met homeostasis, DNA methylation, energy metabolism, etc., which potentially contributed to better nutrient utilization efficiency of calves and promoted their growth and development performance (Alharthi et al., 2019). Moreover, energy restriction significantly impacted the DNA methylation level of a DMR in *IGF2* in fetal longissimus dorsi of beef cattle, where *IGF2* expression was negatively associated with fetus weight in Angus–Simmental crossbred cows (Paradis et al., 2017). Furthermore, offsprings' weight was affected by their mothers' high-fat diet (offspring were obese), and individual differences of obesity were potentially regulated by epigenetic modifications (Keleher et al., 2018; Glendining and Jasoni, 2019). Also, 5hmC and 5mC were found to be negatively and positively correlated with body weight in offspring, respectively, and altered CpG methylation in the proopiomelanocortin (*POMC*) promoter region induced histone modification through binding of MBD1 to 5mC, which reduced *POMC* expression (Marco et al., 2016). Furthermore, it was reported that changes in diet during pregnancy can also influence the reproduction ability of female offspring, which may be regulated by epigenetic modifications (Noya et al., 2019; Shah and Chauhan, 2019).

In pigs, dietary changes, such as feed restriction and vitamin C supplemental feeding, were reported to induce modifications of DNA methylation during development of porcine germline cell and embryo (Yu et al., 2018; Zglejc-Waszak et al., 2019). Prenatal and postnatal dietary omega-3 fatty acid supplementation resulted in altered global DNA methylation patterns and probable implication in the growth and inflammatory processes of piglets (Boddicker et al., 2016). In addition, supplementation of methyl donors during gestation could improve intestinal digestion and absorption and the growth rate of offspring piglets, and these attributes were associated with DNA methylation modifications

in specific genes and their corresponding regulated expression (Liu H. et al., 2017; Jin C. et al., 2018). Furthermore, repressed expression of *GALK1* gene by DNA hypermethylation and histone trimethylation in the liver was associated with low serum concentration of galactose in neonatal pigs in response to betaine-supplemental feeding of sows (Cai et al., 2017).

Epigenetic modifications have been reported to regulate the impacts of parental feed additive supplementation on offspring pullets. For example, histones H3K36me3 and H4K12ac in the promoter region of *PPAR*δ gene were involved in the regulation of altered lipid metabolism and growth performance following maternal genistein supplementation (Lv et al., 2019). Betaine is a frequently used supplement in the chicken industry, and its impact on intercellular metabolism is probably influenced by DNA methylation (Hu et al., 2017a). DNA methylation alteration was found to regulate gene expression related to cholesterol and corticosteroid synthesis of offspring pullets in response to maternal betaine supplementation (Hu et al., 2017b; Idriss et al., 2018; Abobaker et al., 2019). Additionally, DNA methylation was associated with the regulation of transcriptional regulatory network in response to dietary methionine and betaine supplementation in goose (Yang et al., 2018).

## Epigenetic Regulation of Livestock Products

### Milk

Milk production is the most important economic trait of the bovine dairy industry, which is affected by multitudinous factors including genetics, nutrition, health, farm management, and environmental conditions (Pragna et al., 2017; Waterman et al., 2017; Sørensen et al., 2018). As summarized in **Table 2**, epigenetic modifications have been identified as important regulatory mechanisms of milk production in dairy cows and other livestock species (Singh et al., 2010, 2011; Ibeagha-Awemu and Zhao, 2015). Significant differences of global DNA methylation levels in blood were reported between lactating dairy cows with high and low milk yield, indicating the association between milk yield and DNA methylation (Dechow and Liu, 2018; Wang H. et al., 2019). Particularly, abnormal DNA methylation around the STAT5-binding enhancer in the αS1-casein promoter negatively regulated αS1-casein synthesis in milk during lactation, which could be affected by foreign stimulus, such as mastitis and daily milking times (Platenburg et al., 1996; Vanselow et al., 2006; Nguyen et al., 2014). Additionally, the DNA methylation of *EEF1D*, a gene strongly related to milk production, regulates its spatial expression (Liu X. et al., 2017). Meanwhile, differential DNA methylation levels of milk-related genes (e.g., *PPAR*α, *RXR*α, and *NPY*) in the mammary glands of dairy goats at dry and lactation periods indicated important regulatory roles of DNA methylation in goat lactation (Zhang X. et al., 2017). Moreover, inhibition of miR-145 expression impaired fatty acid synthesis in goat milk by increased methylation levels of some lipid-related genes (*FASN*, *SCD1*, *PPARG*, and *SREBF1*) (Wang et al., 2017b). In addition, higher promoter DNA methylation of *ACACA* and *SCD* downregulated their expression and were associated with decreased milk fat of dairy goats in response to a high grain diet (Tian et al., 2017).

Interesting reports of how DNA methylation interacts with miRNA expression and function to regulate milk production have emerged. MiR-152 and miR-29s and their respective target genes *DNMT1*, and *DNMT3A*, and *DNMT3B* are inversely expressed during lactation (Bian et al., 2015; Melnik et al., 2016). For example, miR-148a and miR-152 as well as miRNA-29s impact bovine mammary gland epithelial cell activities and milk synthesis by reducing the mRNA expression levels of *DNMT1* as well as *DNMT3A* and *DNMT3B*, respectively (Wang et al., 2014; Melnik and Schmitz, 2017a; Liang et al., 2018). Specifically, over- or forced expression of miR-152 resulted in marked reduction of DNMT1 expression (both mRNA and protein), decrease in global DNA methylation levels, increase in the expression of two lactation-related genes (*AKT* and *PPAR*γ), and enhanced viability and multiplication capacity of mammary epithelial cells (Wang et al., 2014). These effects were reversed by inhibition of miR-152 expression (Wang et al., 2014). Similarly, inhibition of miR-29s triggered global DNA hypermethylation and increased methylation levels of the promoters of some important lactation-related genes, such as *CSN1S1*, *EIF5*, *SREBP1*, *PPAR*γ, and *GLUT1*, and consequently decreased the secretion of triglycerides, lactose, and lactoprotein by cow mammary gland epithelial cells (Bian et al., 2015). MiRNAs targeting *DNMTs* were also found to decrease the methylation of core CpG islands at the promoter regions of genes (such as *FTO*, *INS*, *IGF1*, *CAV1*, etc.) involved in the activation or regulation of various genes with roles in metabolism and milk synthesis (Melnik and Schmitz, 2017b). Conversely, induced methylation at the 5′ terminal of miR-183 inhibited its expression, consequently affecting milk lipid metabolism of dairy cows (Jiao et al., 2020). Furthermore, milk exosomes, regarded as epigenetic regulators that transfer specific regulatory molecules to consumers, regulate the expression of *DNMTs* and affect human health, especially milk allergy (Melnik et al., 2016; Paparo et al., 2016; Melnik and Schmitz, 2017b).

### Meat

DNA methylation is one of the most studied epigenetic mechanisms involved in the regulation of gene expression related to muscle development (**Table 2**; Baik et al., 2014; Gotoh, 2015; Chen Z. et al., 2019). The genome-wide DNA methylation profiles of longissimus dorsi muscles from different breeds of sheep provided insight on the epigenetic regulatory mechanisms modulating the expression of genes involved in the regulation of muscle development, such as *DLK1*, *NR4A1*, *TGFB3*, *ACSL1*, *RYR1*, *ACOX2*, *PPARG2*, *NTN1*, and *MAPRE1* (Couldrey et al., 2014; Cao et al., 2017; Fan et al., 2020). Meanwhile, a number of DMRs on genes associated with important biological processes such as lipid translocation and lipid transport were identified in latissimus dorsi muscle from different breeds of beef cattle with diverse meat quality traits (Fang et al., 2017). For instance, DNA methylation profiling in relation to beef tenderness in Angus cattle revealed 7,215 DMRs between tender and tough beef (Zhao et al., 2020). The DMRs were significantly enriched in ATP binding cassette subfamily and myosin-related genes,

**TABLE 2 |** Alteration of epigenetic markers in relation to livestock production traits.

| Parameter | Breed | Organ | Epigenetic alteration | Production trait | Model and references |
|---|---|---|---|---|---|
| **Milk** | | | | | |
| High and low milk yield | Holstein cows | Peripheral blood mononuclear cells | 72 DMRs between high and low milk yield, 252 DMRs across herd environments | Milk yield | Dechow and Liu, 2018 |
| High and low milk yield | Holstein cows | Jugular venous blood | DNA methylation rates in the lower-yield cows were significantly higher than those in the higher-yield animals | Milk and protein yield | Wang L. et al., 2019 |
| Experimentally induced mastitis by *E. coli* and *S. aureus* | Holstein cows | Liver and mammary gland tissues | Remethylation of upstream promoter of *CSN1S1* gene in response to *E. coli* infection | α*S1*-casein synthesis | Vanselow et al., 2006 |
| Once/twice daily milking | Holstein cows | Liver and mammary gland tissue | Altered methylation of four CpG within the distal upstream regulatory region of the *CSN1S1* gene | Milk production (yield and milking frequency) | Nguyen et al., 2014 |
| Different lactation stages | Holstein cows | Blood | DNA methylation of *EEF1D* was lower in the dry period than the early stage of lactation | Milk production | Liu X. et al., 2017 |
| Different lactation stages | Xinong Saanen goats | Mammary gland tissue | Methylation levels of 95 and 54 genes in the lactation period were up- or downregulated, respectively, relative to the dry period | Milk production | Zhang X. et al., 2017 |
| Different lactation stages | Xinong Saanen goats | Mammary gland tissue | Inhibition of miR−145 increased methylation levels of *FASN*, *SCD1*, *PPARG*, and *SREBF1* | Milk fat synthesis | Wang et al., 2017b |
| High- and low-concentrate diet feeding | Guanzhong goats | Mammary gland tissue | Increased DNA methylation level in the promoter regions of the *ACACA* and *SCD* genes | Milk fat production and composition | Tian et al., 2017 |
| **Meat** | | | | | |
| Two sheep breeds differing in meat production ability | Small-tailed Han and Dorper × small-tailed Han crossbred sheep | *Longissimus dorsi* muscles | 808 DMRs and global loss of DNA methylation in the DMRs in the crossbred sheep, 12 potential DMGs | Meat production | Cao et al., 2017 |
| Two cattle breeds exhibiting different meat production ability | Japanese black and Chinese Red Steppes cattle | *Longissimus dorsi* muscles | 23,150 DMRs identified, 331 DMRs correlated negatively with expression of DE genes, 21 DMRs located in promoter regions | Muscle development and related meat quality traits | Fang et al., 2017 |
| Divergent beef tenderness | Angus beef | *Longissimus dorsi* muscles | DNA methylation profiles related to beef tenderness, and 7215 DMRs between tender and tough beef | Beef tenderness | Zhao et al., 2020 |
| Three cattle breeds differing in meat production abilities | Simmental, Yunling, and Wenshan cattle | *Longissimus dorsi* muscles | 18 DM and DE genes between Simmental and Wenshan cattle, 14 DM and DE genes between Simmental and Yunling cattle, 28 DM genes between Wenshan and Yunling cattle | Meat quality | Chen Z. et al., 2019 |
| Three growth stages | Polled yak | *Longissimus dorsi* muscles | 1,344, 822, and 420 genes with DM CCGG sites and 2,282, 3,056, and 537 genes with DM CCWGG sites between 6-month-old vs 90-day-old, 6-month-old vs 3-year-old, and 3-year-old vs 90-day-old fetuses, respectively | Muscle development and growth | Ma et al., 2019 |

*(Continued)*

**TABLE 2 |** Alteration of epigenetic markers in relation to livestock production traits.

| Parameter | Breed | Organ | Epigenetic alteration | Production trait | Model and references |
|---|---|---|---|---|---|
| Feed restriction | Angus–Simmental crossbred cows | *Longissimus dorsi* and *semitendinosus* muscle | One DMR in *IGF2* | Muscle function | Paradis et al., 2017 |
| Fetal and adult cattle | Qinchuan cattle | *Longissimus dorsi* muscles | Three DMCs in the core promoter region of *SIX1*, histone H4 and E2F2 bind to *SLX1* | Muscle development | Wei et al., 2018 |
| Obese, lean, and miniature pig breeds | Tongcheng, Landrace, and Wuzhishan pigs | Blood leukocytes | 2,807, 2,969, and 5,547 DMGs in the Tongcheng vs Landrace, Tongcheng vs Wuzhishan, and Landrace vs Wuzhishan comparisons, respectively | Fat-related phenotype variance | Yang et al., 2016b |
| Obese and lean type pig breeds | Landrace pigs and Rongchang pigs | Backfat | 483 DMRs in the promoter regions | Fat deposition and fatty acid composition | Zhang S. et al., 2016 |
| Castrated and non-castrated pigs | Male Huainan pigs | Liver and adipose tissues | *GHR* methylation rate in the liver of castrated and non-castrated pigs were 93.33% and 0, respectively | Castration-induced fat deposition | Wang et al., 2017e |
| Pig breeds differing in metabolic characters | Duroc and Pietrain | *Longissimus dorsi* muscles | More than 2,000 DMCs | Muscle metabolism | Ponsuksili et al., 2019 |
| Three pig breeds differing in fatness traits | Polish Large White, Duroc and Pietrain | Subcutaneous fat, visceral fat, and *longissimus dorsi* muscle | H3K9ac and H3K4me3 correlated to the expression level of selected genes | Adipose tissue accumulation | Kociucka et al., 2017 |
| Highest and lowest pH among littermates | Duroc | *Longissimus dorsi* muscle | 3,468 DMRs, including 44 and 21 protein-coding genes with hyper- and hypomethylation regions in their gene bodies | Postmortem energy metabolism and pH | Park et al., 2019 |
| High and low boar taint | Pigs | Testis | 32 DE genes with DMCs | Boar taint | Wang and Kadarmideen, 2019a,c |
| Different growth stages | Gushi hens | Breast muscle | 2,714 DMRs and 378 DMGs | Intramuscular fat deposition and water-holding capacity | Zhang M. et al., 2017 |
| Different feed conditions and breeds | Daninghe and Qingjiaoma chickens | Breast muscle | 46 CpG sites and 3 CpG islands in *UCP3*, different methylation levels of *UCP* and *FATP1* between groups | Breast muscle (intramuscular fat content) | Gao et al., 2015, 2017 |
| **Egg** | | | | | |
| Before and after reproductive maturation | Hy-Line Brown commercial female chickens | Ovaries | Increased methylation of two CpG sites in ERα; increased H3K27ac and decreased H3K36me3 related to increased ERα mRNA transcript | Reproductively mature, egg production | Guo M. et al., 2020 |
| Betaine supplementation | Laying hens | Liver | Hypomethylation of promoter in *GR* | Egg production | Omer et al., 2018, 2020 |
| **Wool** | | | | | |
| Different generations of cashmere goats | Cashmere goats | Skin | 336 hyper- and 753 hypomethylated 5mC, corresponding to 214 hyper- and 560 hypomethylated genes | Cashmere traits | Dai et al., 2019 |
| Anagen and telogen stages | Cashmere goats | Skin | 1,311 DMRs corresponding to 493 DMGs (269 hyper- and 224 hypomethylated DMGs) | Hair cycling and cashmere growth | Li et al., 2018 |
| Coarse type and fine type cashmere | Cashmere goats | Skin | 9,085 DM N6-methyladenosine sites | Cashmere fiber growth | Wang et al., 2020f |
| Cashmere goats and other goat species | Cashmere goats | Skin | Altered methylation degree of *HOXC8* exon 1 | Cashmere fiber growth | Bai et al., 2017 |
| Anagen and telogen stages | Cashmere goats | Skin | Altered promoter methylation of *HOTAIR* gene | Cashmere fiber growth | Jiao et al., 2019 |

*DM, differentially methylated; DE, differentially expressed; DMR, differential methylated region; DMG, differential methylated gene; DMC, differential methylated CpG; H3K9ac, histone H3 lysine 9 acetylation; H3K4me3, trimethylation at the fourth lysine residue of histone H3 protein; H3K27ac, acetylation at the 27th lysine residue of histone H3 protein; H3K36me3, trimethylation at the 36th lysine residue of histone H3 protein.*

including *ABCA1*, *ABCA7*, and *ABCG1*, with roles in beef tenderness and fatty acid metabolism (Zhao et al., 2020). Besides, demethylation of a DMR in the *SIRT4* promoter promoted its transcriptional activity through *CMYB* mediation or inhibited its transcriptional activity through *NRF1* mediation, thereby shedding light on the role of an epigenetic process in the transcriptional regulation of the expression of *SIRT4* during bovine adipocyte differentiation (Hong et al., 2019). In addition, important genes with DMRs, including *TMEM8C*, *IGF2*, *FASN*, *CACNA1S*, *FADS6*, and *MUSTN1*, were significantly associated with differences in muscle development and meat quality in several cattle (beef) breeds (Chen Z. et al., 2019; Ma et al., 2019). The methylation level of *IGF2*, which negatively correlated with its expression, was found to change more in longissimus dorsi muscle than in semitendinosus muscle in response to feed restriction (Paradis et al., 2017). Besides, differential expression of some important DNA methylation genes (*DNMT3A*, *DNMT3B*, and *DNMT1*) were significantly associated with meat and carcass quality traits such as carcass weight, flank thickness, and chuck short rib score in Wagyu × Limousin × Fuzhou yellow crossbred beef cattle (Guo et al., 2012; Liu et al., 2015). DNA methylation in the core promoter region of *SIX1* gene in muscle tissues was potentially regulated by histone H4 and *E2F2* and shown to impact muscle development in Qinchuan cattle (Wei et al., 2018). Expression and splicing quantitative trait loci mapping analyses for meat quality traits in longissimus dorsi muscle found that the expression of *PHF14*, an important epigenetic regulator of organ development, was influenced by multigenic effects (Leal-Gutiérrez et al., 2020). The PHF14 protein has many plant homeodomain fingers that are able to recognize specific epigenetic markers on histone tails and thus regulate gene expression, indicating its important roles in skeletal muscle growth and development.

Meat quality is also a trait of high interest in the pig industry. Genome-wide DNA methylation analysis identified numerous DMRs and DMGs between obese and lean pigs, revealing vital roles of DNA methylation in lipogenesis in pigs (Yang et al., 2016b). Specifically, the back fat of Landrace pigs (leaner) had higher global DNA methylation level than the fatty Rongchang pigs, indicating that some identified DMRs may affect lipid metabolism (Zhang S. et al., 2016). Altered methylation in lipid metabolism-related genes was also identified in diverse tissues from different pig breeds (Wang et al., 2017e; Ponsuksili et al., 2019). Additionally, histone modifications were found to affect adipose tissue accumulation by regulating corresponding gene expression (Kociucka et al., 2017). Moreover, DNA methylation pattern scanning revealed its potential involvement in other meat quality traits, such as pH, meat color, and carcasses' traits (Te Pas et al., 2017; Park et al., 2019). Boar taint, an unpleasant odor that affects pork acceptability, was found to be regulated by epigenetic processes. Genome-wide methylation analysis of the testis of pigs with high, medium, and low boar taint associated DMCs and candidate genes with pig reproduction (e.g., *DICER1*, *PCK1*, *SS18*, and *TGFB3*) and boar taint (e.g., *CAPN10*, *FTO*, *HSD17B2*, *IGF2*, *SALL4*, *FASN*, *PEMT*, *CRYL1*, *DNMT3A*, and *EGFR*) thereby revealing important regulatory roles of DNA methylation in boar taint formation (Wang and Kadarmideen, 2019a,b).

In chickens, DNA methylation was reported as one of the regulatory mechanisms modulating crucial meat traits such as intramuscular fat deposition and skeletal muscle development (Zhang M. et al., 2017, Zhang et al., 2020). The whole-genome DNA methylation profiles of later laying-period hen and juvenile hens with differential intramuscular fat deposition and water-holding capacities identified 378 DMRs related to muscle development (Zhang M. et al., 2017). Further research indicated that DNA methylation affected the intramuscular fat deposition by regulating the expression of some key genes, such as *ABCA1*, *COL6A1*, and *GSTT1L* (Zhang M. et al., 2017, Zhang et al., 2020). Moreover, different breeds or feed condition significantly affected the methylation levels of *UCP3* and *FATP1* genes in chicken breast muscle, which enhanced the reliability of these genes as important candidate genes of intramuscular fat deposition in chicken meat (Gao et al., 2015, 2017). The alterations of epigenetic markers in relation to livestock products (milk, meat, egg, and wool) are summarized in **Table 2**.

## Egg

Egg laying in poultry relies on the reproductive maturation of the ovaries, where epigenetic mechanisms play important regulatory roles (He et al., 2018). Epigenetic modifications in *ER*α were identified during ovarian development and maturation, whereby higher DNA methylation rates in specific CpG sites, higher histone H3K27ac, and lower H3K36me3 associated the abundance of *ER*α expression with important roles in egg laying (Guo M. et al., 2020). In addition, changes in DNA methylation were identified in response to betaine supplementation and were associated with improved egg laying performance in hens (Xing and Jiang, 2012). Supplemental betaine potentially caused hypomethylation of the promoter of *GR*, followed by enhanced expression of *GR* and *GR/ER*α interaction (contributed to increase *VTGII* expression in the liver), which partly supported improved egg production in betaine-supplemented laying hens (Omer et al., 2018). Furthermore, promoter region methylation could be the possible regulatory mechanism underlying altered expression of liver lipid synthesis and transport-related genes in response to betaine supplementation, which supported the synthesis and release of yolk precursor substances in the liver and consequently promoted egg laying performance (Omer et al., 2020).

## Wool

Wool is an economic product of high regard with increasing value in the goat industry, but the limited yield of cashmere wool (or cashmere) was recently speculated to be potentially regulated by epigenetic modifications (Wang et al., 2017f, 2020d). DNA methylation and histone acetylation were found to actively contribute to the regulation of goat fetal fibroblast cells, which is critical for cashmere production (Wang et al., 2017f; Palazzese et al., 2018). Recently, DNA methylation was associated to the genetic stability of cashmere traits between generations of cashmere goats (Dai et al., 2019). Besides, genome-wide scanning revealed potential regulatory roles of DNA methylation and RNA

m$^6$A methylation in the growth and development of cashmere fibers in cashmere goats (Li et al., 2018; Wang et al., 2020f). Moreover, epigenetic modifications of some specific genes were reported to affect cashmere traits. For instance, methylation of *HOXC8* is involved in regulating the growth of cashmere fiber in cashmere goat (Bai et al., 2017). Promoter methylation of *HOTAIR* gene and related suppressed expression were found to regulate the reconstruction of secondary hair follicles in cashmere goat (Jiao et al., 2019). Furthermore, crucial regulatory roles for DNA methylation in wool fiber development and transformation of fur with special characters and production purpose, such as curly wool with beautiful white color or high-quality brush hair, have been observed (Qiang et al., 2018; Xiao et al., 2019).

## Epigenetic Regulation of Livestock Health

### Epigenetic Regulation of Livestock Response to Environmental Stress

Environmental stressors including heat stress, pathogens, dietary changes, etc. are the greatest determinants of individual health and productivity. As summarized in **Table 3**, epigenetic alterations in response to environmental stressors have been reported in livestock animals. Heat stress has negative impacts on animal production and health, which may continue to be of great concern due to increasing global temperatures. The important roles of DNA and histone methylation on heat-shock proteins under heat stress and heat acclimation and their involvement in host response to heat stress were summarized recently (Wu et al., 2020a). Heat stress, potentially regulated by epigenetic modifications, such as DNA methylation, DNA hydroxymethylation, and histone modifications, was reported to significantly affect bovine embryonic development and fertility (Mendes et al., 2017; de Barros and Paula-Lopes, 2018; Diaz et al., 2019; Sun et al., 2019). Epigenetic regulation was associated with the effects of betaine on heat stress reduction in poultry (Nayak et al., 2016; Saeed et al., 2017). In addition, DNA methylation and histone H3K27me3 and H3K4me3 changes were identified to partly regulate the adaption of chickens to embryonic thermal manipulation, which is crucial for improving their thermal adaptability to heat stress in postnatal life (Kisliouk et al., 2017; Vinoth et al., 2018; David et al., 2019). DMRs and associated genes with roles in energy and lipid metabolism, cellular defense, and stress responses were identified in longissimus dorsi muscles of heat-stressed pigs indicative of roles of epigenetic regulation of pig muscle development, meat quality, and heat stress processes in pigs (Hao et al., 2016). Increased m$^6$A RNA methylation level and increased expression levels of m$^6$A-related enzymes and heat stress proteins were observed in the liver of sheep after heat stress, indicating involvement of m$^6$A in the regulation of host response to heat stress (Lu et al., 2019).

Hypoxic stress is an important environmental stressor affecting porcine growth, especially in high-altitude regions. Genome-wide DNA methylation profiles of porcine tissues from pigs raised in regions of different altitudes revealed important regulatory roles of DNA methylation in porcine hypoxia adaptation (Jin L. et al., 2018; Zhang et al., 2019). For example, some DMGs identified in heart tissues of Tibetan pigs from high- and low-altitude regions were significantly enriched in hypoxia-inducible factor (HIF) 1 signaling pathway suggesting impact on hypoxia-related processes (Zhang et al., 2019). Particularly, DNA methylation mediated the expression of *SIN3A* and *CACNG6* in longissimus dorsi muscle of Tibetan pigs during low-altitude acclimation (Jin L. et al., 2018). Moreover, methylation changes in hypoxia genes, such as higher methylation levels in *HIF-1α*, *HIF-3α*, and *EPO* and lower methylation level in *HIF-1*, were identified in the heart, liver, lungs, kidney, muscle, and brain tissues of plateau goat and sheep, suggesting the involvement of epigenetic regulatory mechanisms of hypoxia resistance of plateau animals (Wang et al., 2017g).

In cattle, maternal stress due to transportation was identified as a potential factor that induced methylome changes in Brahman bull calves, whereby thousands of hyper- and hypomethylated CpG sites were identified compared with non-transported control calves (Littlejohn et al., 2018). The methylome changes were through increased DNA methylation sites at promoter regions of genes enriched in pathways related to behavior, stress response, metabolism, and immune response, which induced the repression of their transcriptional activities (Littlejohn et al., 2018). In goat, lowered global DNA methylation level was thought to be involved in upregulated activity of caspase-3 and caspase-8 enzymes, increased expression of inflammatory cytokines (*IL-10*, *IL-1*β, and *iNOS2*) and activation of TLR-4 and NF-κB pathways in response to chronic stress induced by long-term application of low doses of dexamethasone in colonic epithelium of goats (Cai et al., 2019).

### Epigenetic Regulation of Livestock Immune Response to Disease Pathogens

Epigenetic modifications are known to significantly affect the dynamic regulation of immune responses to infection and other stressors (Emam et al., 2019; Safi-Stibler and Gabory, 2019). Studies on DNA methylation and the immune response have described the methylation of immune-related genes and the global DNA methylation patterns in response to varied disease pathogens (**Table 3**). For example, DNA methylation was found to directly affect gene expression in CD4+ T cells during an infection of *Mycobacterium bovis* in cattle (Doherty et al., 2016). The promoter region of miR-29b showed significant decreased methylation level in Madin–Darby bovine kidney (MDBK) cell line infected with bovine viral diarrhea virus (BVDV; Fu et al., 2017). Moreover, silencing of *DNMT1* expression in MDBK significantly decreased miR-29b promoter methylation and upregulated its expression, as well as repressed BVDV replication, supporting the interaction between DNA methylation and miRNA in the regulation of livestock health (Fu et al., 2017). Bacterial LPS stimulation of endometrial cells resulted in increased expression of immune-related genes (*IL-6* and *IL-8*), which was enhanced by the inhibition of DNA methylation (Wang et al., 2018). In bovine mammary epithelial cells, altered methylome (mainly hypermethylation) in response to lower doses of LPS (1–10 EU/ml) impacted the expression of genes (e.g., *ACACA*, *ACSS2*, and *S6K1*) related to milk production (lipid and amino acid metabolism), while

**TABLE 3 |** Epigenetic changes impacting livestock health.

| Stimulus or disease | Breed | Organ | Epigenetic alteration | References |
|---|---|---|---|---|
| **Environment stress** | | | | |
| Heat stress (embryonic thermal manipulation) | Chicken; PB-2 and NN lines | Brain tissue (hypothalamus) | Altered methylation at *HSPs* | Kisliouk et al., 2017; Vinoth et al., 2018 |
| Heat stress (embryonic thermal manipulation) | Broiler chickens | Hypothalamus and muscle tissues | 785 H3K4me3 and 148 H3K27me3 differential peaks in the hypothalamus | David et al., 2019 |
| Heat stress | Male DLY pigs | *Longissimus dorsi* muscles | 57,147 DMRs corresponding to 1,422 DMGs | Hao et al., 2016 |
| Heat stress | Hu sheep | Liver | Increased $m^6A$ on RNA of HSPs | Lu et al., 2019 |
| Hypoxic stress (high and low altitude) | Tibetan pigs | *Longissimus dorsi* muscles | DMRs mainly involved in starch and sucrose metabolism | Jin L. et al., 2018 |
| Hypoxic stress (different species and high/low altitude) | Tibetan and Yorkshire pigs | Heart | 6,829, 11,997, 2,828, and 1,286 DMRs between TH vs YH, TL vs YL, TH vs TL, and YH vs YL | Zhang et al., 2019 |
| Hypoxic stress (different species and highest plateau) | Tibetan goat, Tibetan sheep, Chuanzhong goat, and small-tailed Han sheep | Various tissues, including the heart, liver, lungs, kidney, muscle, and brain | Higher methylation in *HIF-1α*, *HIF-3α*, and *EPO.* Lower methylation rate in *FIH-1* | Wang et al., 2017g |
| Prenatal (transportation stress) | Brahman cows and their offspring | Blood | 7,407 hyper- and 8,721 hypomethylated CpG sites, including 1,205 DMCs located within promoter regions | Littlejohn et al., 2018 |
| **Disease** | | | | |
| *Mycobacterium bovis* infection | Holstein–Friesian cattle | CD4 + T cells | Genome-wide DNA methylation profile revealed 760 DMRs | Doherty et al., 2016 |
| *Mycobacterium bovis* infection | *In vitro* | Alveolar macrophages | H3K4me3 is more prevalent in chromatin, at a genome-wide level in the infected group | Hall et al., 2019 |
| Johne's disease | Holstein cows | Ileum and ileum lymph node | 2,000 DMCs and 205 DMRs in the ileum, 6,394 DMCs and 3,946 DMRs in ileum lymph node in response to *Mycobacterium avium* spp. *paratuberculosis* | Ibeagha-Awemu et al., 2020a,b |
| Clinical mastitis | Holstein cattle | Blood | Altered methylation of *CD4* | Wang et al., 2013; Usman et al., 2016 |
| Clinical mastitis | Holstein cows | Mammary glands | Changed DNA methylation-regulated *IL6R* transcription | Zhang et al., 2018a |
| *E. coil*- and *S. aureus*-induced mastitis | Holstein cows | Mammary glands, peripheral blood | Genome-wide DNA methylation profile revealed a plethora of DMRs | Song et al., 2016; Sajjanar et al., 2019; Ju et al., 2020; Wang et al., 2020c; Wu et al., 2020b |
| *E. coil*-induced mastitis | Holstein cows | Lymphocytes | H3K27me3 levels in silent genes were higher in subclinical *S. aureus* mastitis cattle than in healthy cows | He et al., 2016 |
| LPS challenge | Cows | Endometrial cells | Decreased methylation of specific CpG sites at IL-6; increased expression level of *IL-6*, *IL-8*, and *DNMTs* | Wang et al., 2018 |
| LPS challenge | *In vitro* | Mammary epithelial cell | High LPS dose induced hypomethylation of immune-related genes, while low LPS dose induced hypermethylation of lactation-related genes | Chen J. et al., 2019 |
| BVDV | *In vitro* | Madin–Darby bovine kidney cell | *DNMT1* silencing induced decreased methylation level of miR-29b and repressed BVDV replication | Fu et al., 2017 |

*(Continued)*

**TABLE 3 |** Continued

| Stimulus or disease | Breed | Organ | Epigenetic alteration | References |
|---|---|---|---|---|
| Subacute ruminal acidosis | Dairy goat | Liver | Reduced promoter methylation level of *LOC101896713* and *CASP8* | Chang et al., 2018 |
| Scrapie | Sheep | Thalamus | 8,907 DMRs | Hernaiz et al., 2019 |
| Poly I:C stimulation | Dapulian and Landrace pigs | Peripheral blood mononuclear cell | 5,827 DMRs and 70 DM and DE genes | Wang et al., 2017c |
| Bacteria colonization in intestine | Danish Landrace × Large White × Duroc pigs | Distal small intestine | Changed genome-wide DNA methylation related to the expression of immune genes | Pan et al., 2018, 2020 |
| *E. coli* challenge | Sows | Mammary epithelial cells | 561 and 898 DMCs at 3 and 24 h after *E. coli* challenge | Sajjanar et al., 2019 |
| Porcine epidemic diarrhea virus | Large White piglets | Jejunum | Higher H3K4me3 enrichment and expression levels of some antiviral genes in the infected group | Wang H. et al., 2019 |
| PRRSV | Transgenic pigs | serum and lung tissues | *HDAC6* overexpression enhances resistance to PRRSV infection | Lu et al., 2017 |
| H5N1 influenza virus | BWEL-SPF chicken | Spleen, thymus, and bursa of Fabricius | Significantly upregulated total DNA methylation levels in the thymus and bursa of the infected group | Zhang Y. et al., 2016 |
| *Salmonella enterica* infection | Domestic chickens | Blood | 879 DMRs including 135 DMRs in the promoter regions | Wang et al., 2017a |
| Marek's disease | Two specific pathogen-free inbred lines of White Leghorn | Bursa of Fabricius | Different H3K27me3 markers associated with immune-related genes | Mitra et al., 2015; Song, 2016 |
| NDV infection under heat stress condition | Fayoumi and Leghorn | Bursa | Greater differences in histone modification (H3K27ac and H3K4me1) levels in Leghorns than Fayoumis, associated genes enriched in biological processes gene ontology terms related to cell cycle and receptor signaling of lymphocytes | Chanthavixay et al., 2020b |

*H3K4me3, trimethylation at the fourth lysine residue of histone H3 protein; H3K27me3, trimethylation at the 27th lysine residue of histone H3 protein; DMR, differential methylated region; DMG, differential methylated gene; HSP, heat-shock protein; DMC, differential methylated CpG; TH, Tibetan pigs grown in the highland; TL, Tibetan pigs grown in the lowland; YH, Yorkshire pigs grown in the highland; YL, Yorkshire pigs grown in the lowland; E. coil, Escherichia coli; S. aureus, Staphylococcus aureus; LPS, lipopolysaccharide; BVDV, bovine viral diarrhea virus; PRRSV, porcine reproductive and respiratory syndrome virus; DM, differentially methylated, DE, differentially expressed; NDV, Newcastle disease virus; H3K27ac, acetylation at the 27th lysine residue of histone H3 protein; H3K4me1, the monomethylation at the fourth lysine residue of the histone H3 protein.*

high LPS doses (>10 EU/ml) induced hypomethylation of genes in immune response pathways (Chen J. et al., 2019). DNA methylation was reported to regulate the expression of *IL-6R* rather than genetic mutations in response to mastitic pathogen (Zhang et al., 2018a). Moreover, the co-stimulation of bovine mammary epithelial cells with LPS, peptidoglycan (PGN), and lipoteichoic acid (LTA) significantly increased DNA hypomethylation compared with LPS stimulation, indicating that the additive effects of co-stimulation decreased methylation levels resulting in increased transcriptome changes and inflammatory responses (Wu et al., 2020c). The hypermethylation of the *CD4* promoter was reported to repress its gene expression in Holstein cows with clinical mastitis (Wang et al., 2013; Usman et al., 2016). Recently, *NCKAP5* and transposon *MTD* were found to be differentially methylated in a mouse model of mastitis, indicating their potential effects on the development of *Staphylococcus aureus* mastitis and their potential as epigenetic markers of *S. aureus* mastitis (Di Wang et al., 2020). Furthermore, a plethora of DMRs were identified in bovine mammary gland tissues in response to mastitis caused by different pathogens, including *Escherichia coil* and *S. aureus*, revealing crucial regulatory roles of DNA methylation in mammary immunity during mastitis (Sajjanar et al., 2019; Wu et al., 2020b). Moreover, genome-wide DNA methylation alteration in the format of $C^mCGG$ was significantly related to the immune response to *S. aureus*-induced mastitis, and several genes including *IL-6R*, *TNF*, *BTK*, *IL-1R2*, and *TNFSF8* were identified as potential epigenetic markers of *S. aureus* mastitis (Wang et al., 2020c). DMRs were also identified in peripheral blood from mastitis-infected cattle, further demonstrating the importance of DNA methylation in host immune response (Song et al., 2016; Ju et al., 2020).

In addition to DNA methylation, histone modifications also contribute to mammary gland immunity (Silva et al., 2018; Wu et al., 2020b). For example, inhibition of histone deacetylase increased the expression of β-defensin and possibly improved host resistance to intramammary infections (Kweh et al., 2019). Besides, H3K27me3 in the upstream region of key genes like *IL-10*, *PTX3*, etc. regulated their expression in bovine lymphocytes in response to *S. aureus* mastitis (He et al., 2016). Recently, integration of chromatin immunoprecipitation sequencing (ChIP-seq), RNA sequencing, and miRNA sequencing data from *M. bovis*-infected macrophage revealed that bovine alveolar macrophage transcriptional reprogramming arises through discrepant distribution of H3K4me3 and RNA polymerase

II at key immune genes (Hall et al., 2019). However, no differences were found between the methylomes of healthy and *M. bovis*-infected bovine alveolar macrophage 24 h post infection suggesting that DNA methylation may be less involved in the early host response to *M. bovis* (O'Doherty et al., 2019).

In dairy goats, reduced promoter methylation contributed to the regulated expression of key genes related to inflammation and apoptosis in the liver during subacute ruminal acidosis induced by high-concentrate diets (Chang et al., 2018). Additionally, abnormal DNA methylation levels of genes with roles in signaling and transportation and their involvement in the pathogenesis of scrapie were identified in sheep with scrapie compared with healthy controls (Hernaiz et al., 2019). Dynamic DNA methylation changes have also been reported to impact porcine immune responses by regulating the expression of immune-related genes. A high number of DMRs showing inverse association with gene expression were identified in peripheral blood mononuclear cells in response to poly I:C stimulation, as well as 70 differently methylated and expressed genes with related functions in the regulation of the immune system and leukocyte activation (Wang et al., 2017c). Differential gene expression in response to poly I:C and LPS stimulation was also reported to be significantly associated with H3K27ac alteration at active regulatory regions enriched for TF binding motifs of TFs with roles in the inflammation response (Herrera-Uribe et al., 2020). In addition, involvement of DNA methylation in the regulation of the expression of intestinal immune metabolism-related genes during bacteria colonization immediately after birth and the subsequent influence on newborn intestinal immune development has been reported (Pan et al., 2018, 2020). Promoter methylation level of *BPI* gene in Yorkshire, Sutai, and Meishan pigs was negatively associated with its gene expression and contributed to intestinal immunity and disease susceptibility (Wang et al., 2017d). Promoter methylation in *PACSNI1* repressed its expression and indirectly promoted the production of *IL−6*, *IL−8*, and *TNFα*, indicating its potential to mediate porcine response to disease pathogens (Feng et al., 2019). In addition to regulatory roles in porcine immune responses, epigenetic mechanisms, including DNA methylation and histone modifications, were frequently observed to play roles in porcine diseases. *E. coli*-induced DNA methylation alteration in the form of DMCs in porcine mammary epithelial cells was mapped to the regulatory regions of immune-related genes, such as *SDF4*, *SRXN1*, *CSF1*, and *CXCL14* (Sajjanar et al., 2019). A total of 1,885 H3K4me3 associated with 1,723 genes were identified in the jejunum of piglets with porcine epidemic diarrhea virus, revealing a positive correlation between higher H3K4me3 deposition and increased expression levels of some antiviral genes, including *AS1*, *OAS2*, *EFNB2*, and *CKS1B* (Wang H. et al., 2019). The overexpression of *HDAC6* enhanced host resistance to porcine reproductive and respiratory syndrome virus (PRRSV) infection, resulting in repressed PRRSV production *in vitro* and lower viral load in the lung and less clinical symptoms *in vivo* (Lu et al., 2017).

Epigenetic modifications also play important regulatory roles in the immune response of chickens. The whole genome-wide DNA methylation patterns of lungs from two chicken lines differing in genetic resistance to multiple pathogens revealed many immune-related gene ontology terms enriched by genes within DMRs, suggesting DNA methylation as a possible regulatory mechanism underlying the immune response differences (Li et al., 2015). A dynamic unstable chromatin structure with nucleosome-free regions, that intermingled with H3K4me3- and H3K27ac-modified nucleosomes, was identified in the body of some genes participating in the innate immune response of chickens (Jahan et al., 2019). Also, 5hmC was associated with B-cell death during the immune response to infectious bursal disease virus infection in chickens (Ciccone et al., 2017). In addition, DNA methylation, histone modifications, and other epigenetic signatures were reported during the immune response to diverse infectious diseases in chickens. The global DNA methylation level of immune organs, including thymus and bursa, was significantly upregulated in chickens with avian influenza virus infection (Zhang Y. et al., 2016). The blood methylome showed slightly higher methylation levels around the transcription start and termination sites in *Salmonella enterica*-infected chickens than healthy controls, and the differentially methylated peaks in the promoter regions were vastly correlated with immune-related genes (Wang et al., 2017a). Marek's disease virus induced various temporal chromatin signatures to bursa of Fabricius chickens at different stages of Marek's disease development, and the differential H3K27me3 was significantly enriched in pathways related to the immune response (Mitra et al., 2015; Song, 2016). The response of two genetically distinct highly inbred layer chicken lines (Leghorns and Fayoumis) to Newcastle disease virus (DNV) infection while under heat stress revealed greater differences in histone modification (H3K27ac and H3K4me1) levels in Leghorns than Fayoumis, and the associated genes were enriched in biological processes gene ontology terms related to cell cycle and receptor signaling of lymphocytes, thereby revealing the possible cellular mechanisms underlying the development of genetic variation in NDV resistance (Chanthavixay et al., 2020a). Furthermore, epigenetic reprogramming in the form of histone trimethylation and acetylation is possibly involved in the regulation of gene expression related to improved innate immune system conditioning following vaccination of laying hens (Kang et al., 2019a,b).

# APPLICATION OF EPIGENETICS DATA IN LIVESTOCK PRODUCTION

## Epigenetics Biomarkers in Health Management

A biomarker is a factor or distinctive property or character that can be measured and evaluated as an indicator or gauge of normal biological and pathological processes. The Food and Agricultural Organization defines a biomarker as any substance, structure, or process which impacts or predicts the incidence of disease or its consequences, and could be quantified (World Health Organization [WHO], 2001). Biomarkers are classified into

many specific types, including diagnostic, prognostic, predictive, therapy monitoring, and risk biomarkers (Bock, 2009). For clinical application, biomarkers are expected to be specific, sensitive, and stable and could be validated in abundant samples by different labs (Mishra and Verma, 2010).

According to the properties of biomarkers, an epigenetic biomarker is defined as any epigenetic mark or changed epigenetic mechanism that is measurable in different tissues or body fluids and can delineate a disease condition (detection), predict the outcome of disease (prognostic biomarker) or response to therapy or treatment (predictive biomarker) or a monitor of treatment response (therapy monitoring biomarker), or forecast the risk of future disease development (risk biomarker) (García-Giménez et al., 2016). Since epigenetic markers respond to different types of internal (e.g., maternal environment, etc.) and external environmental cues (e.g., nutrition, management practices, disease pathogens, etc.) as directed by the underlying genetic composition during a lifetime, epigenetic biomarkers may represent the evolution of individual phenotype variations and can contribute to improved disease and production management. In addition, the dynamic changes due to extra- or intraenvironmental cellular conditions and disease progression or evolution in response to environmental factors are one advantage of epigenetic biomarkers when compared with stable (not changing) genetic biomarkers based on gene sequence (García-Giménez et al., 2016). Association of genetic biomarkers to phenotypes is often inconsistent across studies, while epigenetic markers are promising substitutes for the timely diagnosis and monitoring of diseases (Rahat et al., 2020). Furthermore, epigenetic markers being tissue specific reflect the pattern of disease progression (Zeng et al., 2019). Moreover, epigenetic markers, especially methylated DNA and miRNA, have high stability in a variety of samples (e.g., tissues, blood, urine, plasma, milk, etc.) and are stable over a range of conditions. Also, a higher spontaneous epimutation rate (three orders of magnitude) than genetic mutation rate in *Arabidopsis thaliana* has been reported (Schmitz et al., 2011), implying a higher spontaneous mutation rate and availability of more raw materials for genetic improvement due to epimutations than genetic or nucleotide mutations. An epimutation, which is different from DNA mutation, is generally defined as a heritable change in gene activity that is linked to gain or loss of DNA methylation or modifications of chromatin (Oey and Whitelaw, 2014). Epimutations have been further separated into primary (occurs in the absence of DNA sequence change) and secondary (occurs secondary to a DNA mutation in a *cis*- or *trans*-acting factor) categories (Horsthemke, 2006). Moreover, epimutations have been described as constitutional, meaning that they are derived from the germline and consequently should be present in all of the tissues of an individual or somatic (arise in cells in somatic tissues) (Hitchins and Ward, 2009). Evidence of how epimutations induced by endocrine disrupting chemicals impact gene expression, potentially leading to the development of heritable disease conditions in humans have been summarized recently (Lehle and Mccarrey, 2020).

To enable application, biomarkers must be characterized and validated. In farm animals, however, epigenetic research is still at the exploratory level, compared with extensive work in humans and model organisms that has enabled the detection of epigenetic biomarkers and application in various conditions. In humans, epigenome-wide association studies (EWAS) have facilitated the identification of epigenetic biomarkers and their association with phenotype of complex traits, such as human longevity, disease predisposition, diseases, etc. (Abbring et al., 2019; Szymczak et al., 2020). Besides, growing EWAS evidence supports the application of epigenetic biomarkers in human disease diagnosis and treatment (Birney et al., 2016; Carnero-Montoro and Alarcón-Riquelme, 2018; Edris et al., 2019). Various epigenetic biomarkers have been identified for different diseases, such as tumors, colorectal cancer, cardiovascular diseases, etc., revealing their potential use in prognostic, prediction, and even treatment (Kamińska et al., 2019; Soler-Botija et al., 2019; Jung et al., 2020). A DNA methylation assay based on *SEPT9* was the first Food and Drug Administration (FDA)-approved cancer test based on DNA methylation and showed high sensitivity (71.1–95.6%) and specificity (81.5–99%) to colorectal cancer, the leading cause of cancer deaths (Tanić and Beck, 2017). In addition, a *GSTP1* methylation assay based on a hypermethylated CpG island in the promoter of *GSTP1* and frequently reported in tumor tissues from prostate cancer patients is under clinical test to improve the detection sensitivity, specificity, and accuracy of early prostate cancer diagnosis (Martignano et al., 2016; Markou et al., 2017). Recently, the discovery of epigenetic drugs promoted the further development of sensitive epigenetic biomarkers for predicting or dealing with disease evaluation (Sistare and DeGeorge, 2007). For instance, DNMT inhibitors, including 5-azacytidine and 5-aza-2'-deoxycytidine, were approved by the FDA and demonstrated to be highly efficient in the treatment of hematological malignancies (Kantarjian et al., 2012; Adès et al., 2013). DNMT inhibitors (azacitidine and decitabine) were reported to significantly improve the survival of patients with myelodysplastic syndromes; however, only about 50% of patients showed good clinical responses that were measurable or visible after 4–6 months of treatment (Lee et al., 2013). To deal with the silent 4–6-month stage, predictive epigenetic biomarkers would have great clinical value to reduce the possible effects of ineffective treatments that may cause side effects, unnecessary cost, and time wastage (Treppendahl et al., 2016).

As discussed in the sections above, diverse alterations of epigenetic markers have been revealed to be significantly associated with livestock health, suggesting their potential as epigenetic biomarkers that could be used for diagnostic, prognostic, predictive, or therapy monitoring. Moreover, environmental factors, such as living or farm environment, feed quality/quantity, pathogens, parental stress, environmental stress, chemicals, etc., directly affect livestock productivity, and these effects captured through epigenetic markers can be included in animal health management. For example, dynamic alterations of epigenetic mechanisms in response to parental nourishment and environmental factors or perturbations, especially at the stage of embryo development during pregnancy,

have been demonstrated (Dean et al., 2005; Luo et al., 2018), and their identification and consideration during critical stages of offspring development could lead to healthier pregnancies by including them in farm management strategies. In addition, the identification of possible epigenetic biomarkers underlying these effects could contribute to the evaluation of health and productivity of offspring early in life paving the way for early intervention. Epigenetics biomarkers could be particularly suitable for the detection and management of chronic, silent (no obvious clinical symptoms) livestock diseases, such as metabolic disorders, porcine muscular degenerative disease, chronic mastitis, subacute ruminal acidosis, and paratuberculosis.

## Epigenetic Biomarkers for Breeding Purposes

The contribution of epigenetic modifications to livestock phenotype variation, supported by growing evidence, is gaining importance and supports the potential application of epigenetic biomarkers, especially DNA methylation in livestock breeding programs (González-Recio et al., 2015; Ibeagha-Awemu and Zhao, 2015; Triantaphyllopoulos et al., 2016; Ibeagha-Awemu and Khatib, 2017; Paiva et al., 2019). The potential usefulness of epigenetic biomarkers in livestock breeding is further emphasized by the fact that phenotypic expression is not only a reflection of an individual's DNA composition or sequence but also a reflection of how the genome is copied and regulated by the epigenome taking into account both past and present environmental influences or information (Ibeagha-Awemu and Khatib, 2017). Furthermore, epigenetic inheritance (also known as non-genetic inheritance or transgenerational epigenetic effects) refers to any modification in offspring phenotype that is due to the transmission of factors other than DNA sequence information from parents or ancestors (Bonduriansky and Day, 2009). Epigenetic inheritance has been reported to play crucial roles in phenotypic variation during one's own and offspring development (Triantaphyllopoulos et al., 2016; Nilsson et al., 2018). Therefore, epigenetic inheritance, including intragenerational and transgenerational inheritance, underscores the notion that individual phenotype modifications could at least partly result from the environmental effects on founder generations during key developmental stages of germline cells (Skinner, 2011; Nilsson et al., 2018; Skinner et al., 2018). Therefore, the transmission of epigenetic biomarkers, such as DNA methylation, histone modifications, and ncRNAs, between generations plays a part in epigenetic inheritance in livestock animals (Feeney et al., 2014; Triantaphyllopoulos et al., 2016; Thompson et al., 2020). The current genetic data used for livestock breeding could only explain a portion of phenotypic variance or trait heritability, and supplementing genetic data with epigenetic biomarkers could improve the prediction accuracy of breeding values (González-Recio et al., 2015; Ibeagha-Awemu and Khatib, 2017; Yakovlev, 2018).

As discussed in the sections above, epigenetic variations ranging from single sites to epigenome-wide maps and their regulatory mechanisms of gene expression have been reported in different tissues of several mammalian species (Ibeagha-Awemu and Zhao, 2015; Chavatte-Palmer et al., 2018; Ahmad et al., 2019; Morales-Nebreda et al., 2019; Choi et al., 2020). Furthermore, association between single nucleotide polymorphisms (SNPs) and differential DNA methylation has been reported, indicating that methylation alteration leads to variable expression of related genes and thereby phenotype determination (Banovich et al., 2014; Imgenberg-Kreuz et al., 2018). The alteration of CpG sites caused by SNP suggested one possible mechanism that SNP impacts gene expression by the altered epigenetic patterns, thereby suggesting the possible application of epigenetic biomarkers in livestock improvement breeding (Zhi et al., 2013; Maldonado et al., 2019). However, data to support the exploration and application of epigenetic biomarkers in livestock breeding is currently limited. For instance, data on the contribution of epigenetic alterations to the heritability of livestock health and production traits are not available. Moreover, statistical methods are urgently needed to support quantification of the exact contribution of epigenetic biomarkers to phenotype variation. It was proposed recently that the effects of genetic and non-genetic inheritance should be dissected and considered in the estimation of trait heritability (Danchin et al., 2011). Therefore, the animal or mixed-effects models or statistical approaches that support the simultaneous evaluation of several variance components can be expanded to include the non-genetic or epigenetic components of variation for the purpose of livestock breeding (Tal et al., 2010; Ibeagha-Awemu and Khatib, 2017). Thence, the relationship between DNA methylation biomarkers with production traits, identified through EWAS, could be included in the development of new breeding methods to enable quantification of the epigenetic contribution to the prediction of breeding values.

# RESEARCH GAPS AND FUTURE PERSPECTIVES

## Develop Tools for Livestock Epigenetic Research

Next-generation sequencing methods, such as WGBS, reduced representation bisulfite sequencing (RRBS), ChIP-Seq, etc., have supported the profiling of epigenetic markers at a genome-wide scale in livestock species. However, only a limited number of samples can be profiled at a time due to the cost associated with using these technologies. Furthermore, data generated on a limited number of samples is not adequate for use in improvement management/breeding. Therefore, less expensive tools that support application in a large number of samples are needed to support the application of epigenetic information in livestock production. In humans for example, array-based DNA methylation arrays have been developed to support EWAS and for further application in disease diagnosis and treatment (Birney et al., 2016; Carnero-Montoro and Alarcón-Riquelme, 2018). The Infinium® HumanMethylation450 BeadChip methylation array (450K) is popularly used to detect methylation changes at 450,000 CpG sites in the human epigenome, and was recently updated to Infinium MethylationEPIC BeadChip array (850K) with doubled coverage (over 850,000 CpG sites) of methylation

sites (Sandoval et al., 2011; Moran et al., 2016). The high accuracy and reliability of DNA methylation measurement and association with biological traits, in hundreds to thousands of samples based on arrays, promoted the wide application of DNA methylation in EWAS in humans (Li M. et al., 2019). The lack of commercially available epigenome analysis assays severely restricts the application of EWAS for uncovering the epigenetic biomarkers associated with livestock health and production traits. The development of epigenome-wide arrays for epigenetic pattern identification in large samples becomes a prerequisite for the application of epigenetic biomarkers in livestock breeding and production management. Therefore, there is an urgent need for the development of livestock-specific assays based on epigenetic mechanisms (especially DNA methylation) with high reliability and commercial availability. Besides, livestock epigenetics research is developing with the potential to improve the reliability and accuracy of breeding values estimation with possible application in livestock management, breeding, and selection.

Genome editing technologies which have been successfully used to modify livestock phenotype through the introduction of useful alleles for heat tolerance, disease resistance (e.g., tuberculosis, mastitis, bovine respiratory disease), production (e.g., production of male-only offspring, myostatin gene knockout), elimination of allergens (e.g., beta-lactoglobulin gene knockout), and welfare (e.g., introduction of polled or hornlessness) into livestock populations [reviewed by Mueller et al. (2019); Van Eenennaam (2019), and Bishop and Van Eenennaam (2020)] hold great promise for furthering the application of epigenetic modifications in livestock improvement. Moreover, application of epigenetic editing at specific loci of interest epitomizes an innovative procedure that might selectively and heritably alter gene expression (Vojta et al., 2016).

## Expand Epigenetic Exploration in Livestock Organs and Tissues Under Varying Conditions

As demonstrated in the sections above, epigenetic markers contribute to livestock phenotype variation. Moreover, the epigenome responds to the exposome (nutrition, pathogens, chemicals, maternal behavior, parental environment, climatic conditions, environment, management practices, etc.) in a tissue- and cell-specific manner. With current advances in sequencing and data management technologies, the possibility for genome-wide analysis of epigenetic modifications in specific livestock tissues in response to the exposome is enormous. However, compared with human and model organisms, epigenetic studies in livestock is less developed. Many possible reasons have been advanced to explain this, including limited available funding, research tools and epigenetic research activities on livestock, insufficient recognition of the contribution of epigenetic variation to livestock phenotype diversity, and limited involvement of a considerable number of research professionals in livestock epigenetic research (Ibeagha-Awemu and Zhao, 2015). Efforts of the international consortium on functional annotation of animal genomes (FAANG Project, www.faang.org) and various genome-wide DNA methylation or histone modifications profiling (mentioned in the sections above) have reported epigenetic variation in diverse but limited tissues of livestock species (Foissac et al., 2019; Halstead et al., 2020). Therefore, more efforts are needed to explore the epigenetic variations and biomarkers in different livestock organs/tissues under varying conditions and their contribution to phenotypic expression. Furthermore, monitoring of the dynamic changes of epigenetic markers in response to environmental factors, such as nutritional changes and diseases, could be used to develop new health and disease detection and prediction tools.

## Recognize Epigenetic Contribution to Livestock Phenotype Diversity

Even with mounting evidence supporting the contribution of epigenetic modifications to livestock phenotype variation, there is limited recognition and exploitation of the contribution of epigenetic biomarkers to phenotype variation in livestock management and breeding. Development of advanced statistical methods is required to enhance the understanding of how epigenetic markers interact with genetic factors to influence phenotype diversity of production and health traits in livestock. Furthermore, potential epigenetic regulation has been explored only in a handful of traits and conditions. Moreover, most recent investigations paid attention to the epigenetic modifications in response to single factors, but majority of livestock traits are modulated by the interaction of multiple factors, therefore deserving holistic approaches. Therefore, identification of the epigenetic contributions to livestock traits under the influence of multiple factors is needed and will bring added value for the utilization of epigenetic biomarkers in livestock management. Moreover, limited studies have focused on the linkage between epigenetic modifications and developmental outcomes. Thus, in-depth exploration linking epigenetics and related physiologic responses may further our understanding of the mechanisms underlying livestock productivity and health.

## Examine, Document, and Exploit Epigenetic Inheritance in Livestock

Among the epigenetic studies carried out in livestock, a limited number focused on epigenetic inherence and epigenetic transgenerational biomarkers detection (Triantaphyllopoulos et al., 2016). A major challenge in the examination of epigenetic inherence and its potential application in livestock breeding is the ability to trace epigenetic variations between generations. Accumulating evidence indicates that environmentally induced epigenetic biomarkers could be acquired and used to form transgenerational memory that is partly responsible for environmentally induced heritable traits (Heijmans et al., 2008; Daxinger and Whitelaw, 2010). As summarized in **Tables 1–3**, many factors, such as pathogens, nutrition, etc., are associated with epigenetic alterations during individual development, especially in germline cells. It has been reported that environmentally induced epigenetic transgenerational inherence of DNA methylation changes in sperm promoted

genome instability such as changes of copy number variations in next generations (Skinner et al., 2015). However, the effects of environmental variables on offspring still cannot be fully and directly estimated. The stochastic changes of epigenetic biomarkers act as potential intermedium between environmental variables and related phenotypic variation. In addition, stochastic epigenetic changes can generate tissue- or cell-specific epigenetic variability over time without changes in DNA sequence, contributing to explain the phenotypic variation that cannot be explained by genetic mechanisms (Petronis, 2010). Therefore, recognition of the significance of transgenerational epigenetic inheritance for animal breeding purposes will also facilitate further exploration of currently identified epigenetic effects and their applications in livestock production (Feeney et al., 2014).

## Explore Potential Applications of Epigenetic Biomarkers in Livestock Production and Health

With the development of livestock epigenetic research, reliable epigenetic biomarkers related to productivity and health could be identified and used in livestock management (Franco, 2017; Lin et al., 2019). For example, epigenetic biomarkers in embryo biopsies, placenta, or newborn blood could be discovered and used to develop predictive biomarkers for future phenotypes of interest later in life. Moreover, epigenetic biomarkers in sperm could be used for the selection of sires and sperm quality. Possible monitoring of dynamic epigenetic biomarkers during individual development has potential for use to predict responses to environmental exposure and stressors before observable phenotypic changes. Epigenetic biomarkers could be used to improve the efficiency of different diets, disease diagnosis, and treatments and determine cost-saving avenues (time and money) for precision livestock management.

# CONCLUSION

This review summarized recent epigenetic reports in livestock and discussed the potential application of epigenetic processes in livestock productivity and health management. The wealth of epigenetic modification data constantly being discovered in livestock has the potential to contribute to enhanced livestock productivity and health. A better understanding of epigenetic modifications, such as DNA methylation, is expected to compliment information on genome processes, including molecular, cellular, biological, and immune responses, and provide deeper insights on how they interact to define phenotypic outcome. Given the high dependence of humans on foods of animal origin and the need to protect the environment, information on epigenetic regulatory processes has the potential to support the development of strategies for increased productivity of livestock animals with minimal environmental impacts. With regard to livestock reproduction, development, growth, productivity, product quality, health, and the immune response, the role of epigenetics and the underlying mechanisms remains to be fully clarified. Knowledge of epigenetic impacts on livestock health can potentially support the development of strategies to lower disease incidence and increase disease resistance in livestock. It also can increase the suitability and efficiency of diagnostic measures, control approaches, such as vaccination, and treatments. To promote the successful application of epigenetics information in livestock management and improvement, more studies and tools are needed to examine the epigenetic effects and to develop strategies for implementation. However, the current comprehension and exploration of epigenetic mechanisms and their potentials in livestock health and production management is far from complete. More studies are therefore needed to get a better understanding of the epigenetic mechanisms underlying phenotypic variation in livestock production and health.

# AUTHOR CONTRIBUTIONS

EI-A conceptualized the study and obtained funding. MW and EI-A made substantial, direct, and intellectual contribution to the work and approved it for publication.

# FUNDING

Funding for this study was provided by Agriculture and Agri-Food Canada.

# REFERENCES

Abbring, S., Wolf, J., Ayechu-Muruzabal, V., Diks, M. A., Alashkar Alhamwe, B., Alhamdan, F., et al. (2019). Raw cow's milk reduces allergic symptoms in a murine model for food allergy—a potential role for epigenetic modifications. *Nutrients* 11:1721. doi: 10.3390/nu11081721

Abobaker, H., Hu, Y., Omer, N. A., Hou, Z., Idriss, A. A., and Zhao, R. (2019). Maternal betaine suppresses adrenal expression of cholesterol trafficking genes and decreases plasma corticosterone concentration in offspring pullets. *J. Anim. Sci. Biotechnol.* 10:87.

Acosta, D., Denicol, A., Tribulo, P., Rivelli, M., Skenandore, C., Zhou, Z., et al. (2016). Effects of rumen-protected methionine and choline supplementation on the preimplantation embryo in Holstein cows. *Theriogenology* 85, 1669–1679. doi: 10.1016/j.theriogenology.2016.01.024

Adamczyk, S. (2019). *Role of Chromatin Structure in Regulating Transcription*. Doctoral dissertation, Oakland: Oakland University.

Adès, L., Sekeres, M. A., Wolfromm, A., Teichman, M. L., Tiu, R. V., Itzykson, R., et al. (2013). Predictive factors of response and survival among chronic myelomonocytic leukemia patients treated with azacitidine. *Leuk. Res.* 37, 609–613. doi: 10.1016/j.leukres.2013.01.004

Ahmad, S. F., Shanaz, S., Kumar, A., Dar, A. H., Mohmad, A., and Bhushan, B. (2019). Crosstalk of epigenetics with biological rhythmicity in animal kingdom. *Biol. Rhythm Res.* 1–9. doi: 10.1080/09291016.2019.1607218

Akbarinejad, V., Gharagozlou, F., and Vojgani, M. (2017). Temporal effect of maternal heat stress during gestation on the fertility and anti-Müllerian hormone concentration of offspring in bovine. *Theriogenology* 99, 69–78. doi: 10.1016/j.theriogenology.2017.05.018

Alfert, A., Moreno, N., and Kerl, K. (2019). The BAF complex in development and disease. *Epigenetics Chromatin* 12:19.

Alhamwe, B. A., Khalaila, R., Wolf, J., von Bülow, V., Harb, H., Alhamdan, F., et al. (2018). Histone modifications and their role in epigenetics of atopy and allergic diseases. *Allergy Asthma Clin. Immunol.* 14:39.

Alharthi, A., Coleman, D., Liang, Y., Batistel, F., Elolimy, A., Yambao, R., et al. (2019). Hepatic 1-carbon metabolism enzyme activity, intermediate metabolites, and growth in neonatal Holstein dairy calves are altered by maternal supply of methionine during late pregnancy. *J. Dairy Sci.* 102, 10291–10303. doi: 10.3168/jds.2019-16562

Andraszek, K., Gryzińska, M., Danielewicz, A., Batkowska, J., and Smalec, E. (2016). Age-dependent stability of nucleoli and global DNA methylation level in spermatocytes of the domestic horse (*Equus caballus*). *Can. J. Anim. Sci.* 96, 215–220. doi: 10.1139/cjas-2015-0076

Bach, A., Aris, A., and Guasch, I. (2017). Consequences of supplying methyl donors during pregnancy on the methylome of the offspring from lactating and non-lactating dairy cattle. *PLoS One* 12:e0189581. doi: 10.1371/journal.pone.0189581

Bai, W. L., Wang, J. J., Yin, R. H., Dang, Y. L., Wang, Z. Y., Zhu, Y. B., et al. (2017). Molecular characterization of HOXC8 gene and methylation status analysis of its exon 1 associated with the length of cashmere fiber in liaoning cashmere goat. *Genetica* 145, 115–126. doi: 10.1007/s10709-017-9950-5

Baik, M., Vu, T., Piao, M., and Kang, H. (2014). Association of DNA methylation levels with tissue-specific expression of adipogenic and lipogenic genes in longissimus dorsi muscle of Korean cattle. *Asian-Australas. J. Anim. Sci.* 27, 1493–1498. doi: 10.5713/ajas.2014.14283

Banovich, N. E., Lan, X., McVicker, G., Van de Geijn, B., Degner, J. F., Blischak, J. D., et al. (2014). Methylation QTLs are associated with coordinated changes in transcription factor binding, histone modifications, and gene expression levels. *PLoS Genet.* 10:e1004663. doi: 10.1371/journal.pgen.1004663

Banta, J. A., and Richards, C. L. (2018). Quantitative epigenetics and evolution. *Heredity* 121, 210–224. doi: 10.1038/s41437-018-0114-x

Barau, J., Teissandier, A., Zamudio, N., Roy, S., Nalesso, V., Hérault, Y., et al. (2016). The DNA methyltransferase DNMT3C protects male germ cells from transposon activity. *Science* 354, 909–912. doi: 10.1126/science.aah5143

Basu, A. (2016). *Role of DNMT3L in Development*. Manipal: Manipal University.

Benmoussa, A., Laugier, J., Beauparlant, C. J., Lambert, M., Droit, A., and Provost, P. (2020). Complexity of the microRNA transcriptome of cow milk and milk-derived extracellular vesicles isolated via differential ultracentrifugation. *J. Dairy Sci.* 103, 16–29. doi: 10.3168/jds.2019-16880

Bernstein, B. E., Meissner, A., and Lander, E. S. (2007). The mammalian epigenome. *Cell* 128, 669–681. doi: 10.1016/j.cell.2007.01.033

Bhattacharjee, D., Shenoy, S., and Bairy, K. L. (2016). DNA methylation and chromatin remodeling: the blueprint of cancer epigenetics. *Scientifica* 2016:e6072357.

Bian, Y., Lei, Y., Wang, C., Wang, J., Wang, L., Liu, L., et al. (2015). Epigenetic regulation of miR-29s affects the lactation activity of dairy cow mammary epithelial cells. *J. Cell. Physiol.* 230, 2152–2163. doi: 10.1002/jcp.24944

Bird, A. (2002). DNA methylation patterns and epigenetic memory. *Genes Dev.* 16, 6–21. doi: 10.1101/gad.947102

Birney, E., Smith, G. D., and Greally, J. M. (2016). Epigenome-wide association studies and the interpretation of disease-omics. *PLoS Genet.* 12:e1006105. doi: 10.1371/journal.pgen.1006105

Bishop, T. F., and Van Eenennaam, A. L. (2020). Genome editing approaches to augment livestock breeding programs. *J. Exp. Biol.* 223(Suppl. 1), jeb207159. doi: 10.1242/jeb.207159

Block, T., and El-Osta, A. (2017). Epigenetic programming, early life nutrition and the risk of metabolic disease. *Atherosclerosis* 266, 31–40. doi: 10.1016/j.atherosclerosis.2017.09.003

Bobeck, E. A. (2020). Functional nutrition in livestock and companion animals to modulate the immune response. *J. Anim. Sci.* 98:skaa035.

Bochtler, M., Kolano, A., and Xu, G. L. (2017). DNA demethylation pathways: additional players and regulators. *Bioessays* 39, 1–13.

Bock, C. (2009). Epigenetic biomarker development. *Epigenomics* 1, 99–110. doi: 10.2217/epi.09.6

Boddicker, R., Koltes, J., Fritz-Waters, E., Koesterke, L., Weeks, N., Yin, T., et al. (2016). Genome-wide methylation profile following prenatal and postnatal dietary omega-3 fatty acid supplementation in pigs. *Anim. Genet.* 47, 658–671. doi: 10.1111/age.12468

Bonduriansky, R., and Day, T. (2009). Nongenetic inheritance and its evolutionary implications. *Annu. Rev. Ecol. Evol. Syst.* 40, 103–125. doi: 10.1146/annurev.ecolsys.39.110707.173441

Bornelöv, S., Reynolds, N., Xenophontos, M., Gharbi, S., Johnstone, E., Floyd, R., et al. (2018). The nucleosome remodeling and deacetylation complex modulates chromatin structure at sites of active transcription to fine-tune gene expression. *Mol. Cell.* 71, 56–72. doi: 10.1016/j.molcel.2018.06.003

Cai, D., Yuan, M., Liu, H., Han, Z., Pan, S., Yang, Y., et al. (2017). Epigenetic and SP1-mediated regulation is involved in the repression of galactokinase 1 gene in the liver of neonatal piglets born to betaine-supplemented sows. *Eur. J. Nutr.* 56, 1899–1909. doi: 10.1007/s00394-016-1232-y

Cai, L., Hua, C., Geng, Y., Chen, Q., Niu, L., Tao, S., et al. (2019). Chronic dexamethasone exposure activates the TLR4-Mediated inflammation pathway and induces epithelial apoptosis in the goat colon. *Biochem. Biophys. Res. Commun.* 518, 7–13. doi: 10.1016/j.bbrc.2019.07.071

Cao, P., Li, H., Zuo, Y., and Nashun, B. (2020). Characterization of DNA methylation patterns and mining of epigenetic markers during genomic reprogramming in SCNT embryos. *Front. Cell Dev. Biol.* 8:570107. doi: 10.3389/fcell.2020.570107

Cao, Z., Zhang, D., Wang, Y., Tong, X., Avalos, L. F. C., Khan, I. M., et al. (2020). Identification and functional annotation of m6A methylation modification in granulosa cells during antral follicle development in pigs. *Anim. Reprod. Sci.* 29:106510. doi: 10.1016/j.anireprosci.2020.106510

Cao, Y., Jin, H.-G., Ma, H.-H., and Zhao, Z.-H. (2017). Comparative analysis on genome-wide DNA methylation in longissimus dorsi muscle between small tailed han and dorper× small tailed han crossbred sheep. *Asian-Australas. J. Anim. Sci.* 30, 1529–1539. doi: 10.5713/ajas.17.0154

Capper, J. L., and Bauman, D. E. (2013). The role of productivity in improving the environmental sustainability of ruminant production systems. *Annu. Rev. Anim. Biosci.* 1, 469–489. doi: 10.1146/annurev-animal-031412-103727

Capra, E., Lazzari, B., Turri, F., Cremonesi, P., Portela, A. M. R., Ajmone-Marsan, P., et al. (2019). Epigenetic analysis of high and low motile sperm populations reveals methylation variation in satellite regions within the pericentromeric position and in genes functionally related to sperm DNA organization and maintenance in *Bos taurus*. *BMC Genomics* 20:940. doi: 10.1186/s12864-019-6317-6

Cardoso-Júnior, C. A., Fujimura, P. T., Santos-Júnior, C. D., Borges, N. A., Ueira-Vieira, C., Hartfelder, K., et al. (2017). Epigenetic modifications and their relation to caste and sex determination and adult division of labor in the stingless bee Melipona scutellaris. *Genet. Mol. Biol.* 40, 61–68. doi: 10.1590/1678-4685-gmb-2016-0242

Carnero-Montoro, E., and Alarcón-Riquelme, M. E. (2018). Epigenome-wide association studies for systemic autoimmune diseases: the road behind and the road ahead. *Clin. Immunol.* 196, 21–33. doi: 10.1016/j.clim.2018.03.014

Carrozza, M. J., Li, B., Florens, L., Suganuma, T., Swanson, S. K., Lee, K. K., et al. (2005). Histone H3 methylation by Set2 directs deacetylation of coding regions by Rpd3S to suppress spurious intragenic transcription. *Cell* 123, 581–592. doi: 10.1016/j.cell.2005.10.023

Chang, G., Liu, X., Ma, N., Yan, J., Dai, H., Roy, A. C., et al. (2018). Dietary addition of sodium butyrate contributes to attenuated feeding-induced hepatocyte apoptosis in dairy goats. *J. Agric. Food Chem.* 66, 9995–10002. doi: 10.1021/acs.jafc.8b03526

Chang, G., Zhang, K., Xu, T., Jin, D., Guo, J., Zhuang, S., et al. (2015). Epigenetic mechanisms contribute to the expression of immune related genes in the livers of dairy cows fed a high concentrate diet. *PLoS One* 10:e0123942. doi: 10.1371/journal.pone.0123942

Chanthavixay, G., Kern, C., Wang, Y., Saelao, P., Lamont, S. J., Gallardo, R. A., et al. (2020a). Integrated transcriptome and histone modification analysis reveals NDV infection under heat stress affects bursa development and proliferation in susceptible chicken line. *Front. Genet.* 11:567812. doi: 10.3389/fgene.2020.567812

Chanthavixay, G., Kern, C., Wang, Y., Saelao, P., Lamont, S. J., Gallardo, R. A., et al. (2020b). Integrated transcriptome and histone modification analysis reveals NDV infection under heat stress affects bursa development and proliferation in susceptible chicken line. *Front. Genet.* 11:1176.

Chavatte-Palmer, P., Velazquez, M., Jammes, H., and Duranthon, V. (2018). Epigenetics, developmental programming and nutrition in herbivores. *Animal* 12, s363–s371.

Chen, J., Wu, Y., Sun, Y., Dong, X., Wang, Z., Zhang, Z., et al. (2019). Bacterial lipopolysaccharide induced alterations of genome-wide DNA methylation and promoter methylation of lactation-related genes in bovine mammary epithelial cells. *Toxins* 11:298. doi: 10.3390/toxins11050298

Chen, Z., Chu, S., Xu, X., Jiang, J., Wang, W., Shen, H., et al. (2019). Analysis of longissimus muscle quality characteristics and associations with DNA methylation status in cattle. *Genes Genomics* 41, 1147–1163. doi: 10.1007/s13258-019-00844-4

Choi, J., Lyons, D. B., Kim, M. Y., Moore, J. D., and Zilberman, D. (2020). DNA Methylation and Histone H1 Jointly Repress Transposable Elements and Aberrant Intragenic Transcripts. *Mol. Cell.* 77, 310–323. doi: 10.1016/j.molcel.2019.10.011

Ciccone, N. A., Smith, L. P., Mwangi, W., Boyd, A., Broadbent, A. J., Smith, A. L., et al. (2017). Early pathogenesis during infectious bursal disease in susceptible chickens is associated with changes in B cell genomic methylation and loss of genome integrity. *Dev. Comp. Immunol.* 73, 169–174. doi: 10.1016/j.dci.2017.03.014

Clapier, C. R., Iwasa, J., Cairns, B. R., and Peterson, C. L. (2017). Mechanisms of action and regulation of ATP-dependent chromatin-remodelling complexes. *Nat. Rev. Mol. Cell Biol.* 18, 407–422. doi: 10.1038/nrm.2017.26

Couldrey, C., Brauning, R., Bracegirdle, J., Maclean, P., Henderson, H. V., and McEwan, J. C. (2014). Genome-wide DNA methylation patterns and transcription analysis in sheep muscle. *PLoS One* 9:e101853. doi: 10.1371/journal.pone.0101853

Dai, B., Zhang, M., Yuan, J.-L., Ren, L.-Q., Han, X.-Y., and Liu, D.-J. (2019). Integrative analysis of methylation and transcriptional profiles to reveal the genetic stability of cashmere traits in the Tβ4 overexpression of cashmere goats. *Animals* 9:1002. doi: 10.3390/ani9121002

Danchin, É, Charmantier, A., Champagne, F. A., Mesoudi, A., Pujol, B., and Blanchet, S. (2011). Beyond DNA: integrating inclusive inheritance into an extended theory of evolution. *Nat. Rev. Genet.* 12, 475–486. doi: 10.1038/nrg3028

Das, L., Parbin, S., Pradhan, N., Kausar, C., and Patra, S. K. (2017). Epigenetics of reproductive infertility. *Front. Biosci.* 9:509–535. doi: 10.2741/s497

David, S.-A., Vitorino Carvalho, A., Gimonnet, C., Brionne, A., Hennequet-Antier, C., Piégu, B., et al. (2019). Thermal manipulation during embryogenesis impacts H3K4me3 and H3K27me3 histone marks in chicken hypothalamus. *Front. Genet.* 10:1207. doi: 10.3389/fgene.2019.01207

Daxinger, L., and Whitelaw, E. (2010). Transgenerational epigenetic inheritance: more questions than answers. *Genome Res.* 20, 1623–1628. doi: 10.1101/gr.106138.110

de Barros, F. R. O., and Paula-Lopes, F. F. (2018). Cellular and epigenetic changes induced by heat stress in bovine preimplantation embryos. *Mol. Reprod. Dev.* 85, 810–820. doi: 10.1002/mrd.23040

Dean, W., Lucifero, D., and Santos, F. (2005). DNA methylation in mammalian development and disease. *Birth Defects Res.* 75, 98–111.

Deaton, A. M., and Bird, A. (2011). CpG islands and the regulation of transcription. *Genes Dev.* 25, 1010–1022. doi: 10.1101/gad.2037511

Dechow, C. D., and Liu, W.-S. (2018). DNA methylation patterns in peripheral blood mononuclear cells from holstein cattle with variable milk yield. *BMC Genomics* 19:744. doi: 10.1186/s12864-018-5124-9

Del Corvo, M., Bongiorni, S., Stefanon, B., Sgorlon, S., Valentini, A., Ajmone Marsan, P., et al. (2020). Genome-wide DNA methylation and gene expression profiles in cows subjected to different stress level as assessed by cortisol in milk. *Genes* 11:850. doi: 10.3390/genes11080850

Desmet, K. J., Van Hoeck, V., Gagné, D., Fournier, E., Thakur, A., O'doherty, A., et al. (2016). Exposure of bovine oocytes and embryos to elevated non-esterified fatty acid concentrations: integration of epigenetic and transcriptomic signatures in resultant blastocysts. *BMC Genomics* 17:1004. doi: 10.1186/s12864-016-3366-y

Di Wang, Y. W., Shi, L., Khan, M. Z., Fan, L., Wang, Y., and Yu, Y. (2020). Genome-wide DNA methylation pattern in a mouse model reveals two novel genes associated with *Staphylococcus aureus* mastitis. *Asian-Australas. J. Anim. Sci.* 33, 203–211. doi: 10.5713/ajas.18.0858

Diaz, F., Gutierrez, E., Foster, B., Hardin, P., and Bondioli, K. (2019). 114 Effect of in vivo heat stress on DNA methylation and DNA hydroxymethylation of bovine oocytes. *Reprod. Fertil. Dev.* 31:183. doi: 10.1071/rdv31n1ab114

Do, D. N., Dudemaine, P.-L., Fomenky, B., and Ibeagha-Awemu, E. M. (2017a). *Transcriptome Analysis of Non-Coding RNAs in Livestock Species: Elucidating the Ambiguity. Applications of RNA-Seq and Omics Strategies: From Microorganisms to Human Health*. London: IntechOpen, 103.

Do, D. N., Li, R., Dudemaine, P.-L., and Ibeagha-Awemu, E. M. (2017b). MicroRNA roles in signalling during lactation: an insight from differential expression, time course and pathway analyses of deep sequence data. *Sci. Rep.* 7:44605.

Do, D. N., and Ibeagha-Awemu, E. M. (2017). *Non-Coding RNA Roles in Ruminant Mammary Gland Development and Lactation*. London: IntechOpen, 55–81.

Doherty, R., Farrelly, C. O., and Meade, K. G. (2014). Comparative epigenetics: relevance to the regulation of production and health traits in cattle. *Anim. Genet.* 45, 3–14. doi: 10.1111/age.12140

Doherty, R., Whiston, R., Cormican, P., Finlay, E. K., Couldrey, C., Brady, C., et al. (2016). The CD4+ T cell methylome contributes to a distinct CD4+ T cell transcriptional signature in *Mycobacterium bovis*-infected cattle. *Sci. Rep.* 6:31014.

Dong, G., Qiu, M., Ao, C., Zhou, J., Wang, X., Zhang, Z., et al. (2014). Feeding a high-concentrate corn straw diet induced epigenetic alterations in the mammary tissue of dairy cows. *PLoS One* 9:e107659. doi: 10.1371/journal.pone.0107659

Dose, A., Liokatis, S., Theillet, F.-X., Selenko, P., and Schwarzer, D. (2011). NMR profiling of histone deacetylase and acetyl-transferase activities in real time. *ACS Chem. Biol.* 6, 419–424. doi: 10.1021/cb1003866

Duan, J., Jiang, Z., Alqahtani, F., Mandoiu, I., Hong, D., Zheng, X., et al. (2019). Methylome dynamics of bovine gametes and in vivo early embryos. *Front. Genet.* 10:512. doi: 10.3389/fgene.2019.00512

Edris, A., den Dekker, H. T., Melén, E., and Lahousse, L. (2019). Epigenome-wide association studies in asthma: A systematic review. *Clin. Exp. Allergy* 49, 953–968. doi: 10.1111/cea.13403

Edwards, J. R., Yarychkivska, O., Boulard, M., and Bestor, T. H. (2017). DNA methylation and DNA methyltransferases. *Epigenetics Chromatin* 10:23.

Elolimy, A., Vailati-Riboni, M., Liang, Y., and Loor, J. J. (2019). Cellular mechanisms and epigenetic changes: role of nutrition in livestock. *Vet. Clin. Food Anim. Pract.* 35, 249–263.

Emam, M., Livernois, A., Paibomesai, M., Atalla, H., and Mallard, B. (2019). Genetic and epigenetic regulation of immune response and resistance to infectious diseases in domestic ruminants. *Vet. Clin. Food Anim. Pract.* 35, 405–429. doi: 10.1016/j.cvfa.2019.07.002

Fan, Y., Liang, Y., Deng, K., Zhang, Z., Zhang, G., Zhang, Y., et al. (2020). Analysis of DNA methylation profiles during sheep skeletal muscle development using whole-genome bisulfite sequencing. *BMC Genomics* 21:327. doi: 10.1186/s12864-020-6751-5

Fang, L., Liu, S., Liu, M., Kang, X., Lin, S., Li, B., et al. (2019a). Functional annotation of the cattle genome through systematic discovery and characterization of chromatin states and butyrate-induced variations. *BMC Biol.* 17:68. doi: 10.1186/s12915-019-0687-8

Fang, L., Zhou, Y., Liu, S., Jiang, J., Bickhart, D. M., Null, D. J., et al. (2019b). Integrating signals from sperm methylome analysis and genome-wide association study for a better understanding of male fertility in cattle. *Epigenomes* 3:10. doi: 10.3390/epigenomes3020010

Fang, X., Zhao, Z., Yu, H., Li, G., Jiang, P., Yang, Y., et al. (2017). Comparative genome-wide methylation analysis of longissimus dorsi muscles between Japanese black (Wagyu) and Chinese Red Steppes cattle. *PLoS One* 12:e0182492. doi: 10.1371/journal.pone.0182492

Feeney, A., Nilsson, E., and Skinner, M. K. (2014). Epigenetics and transgenerational inheritance in domesticated farm animals. *J. Anim. Sci. Biotechnol.* 5:48. doi: 10.1186/2049-1891-5-48

Feltus, F. A., Lee, E. K., Costello, J. F., Plass, C., and Vertino, P. M. (2006). DNA motifs associated with aberrant CpG island methylation. *Genomics* 87, 572–579. doi: 10.1016/j.ygeno.2005.12.016

Feng, Q., and Zhang, Y. (2003). "The NuRD complex: linking histone modification to nucleosome remodeling," in *Protein Complexes that Modify Chromatin. Current Topics in Microbiology and Immunology*, Vol. 274, ed. J. L. Workman (Berlin: Springer), 269–290. doi: 10.1007/978-3-642-55747-7_10

Feng, W., Zhou, L., Wang, H., Hu, Z., Wang, X., Fu, J., et al. (2019). Functional analysis of DNA methylation of the PACSIN1 promoter in pig peripheral blood mononuclear cells. *J. Cell. Biochem.* 120, 10118–10127. doi: 10.1002/jcb.28295

Foissac, S., Djebali, S., Munyard, K., Vialaneix, N., Rau, A., Muret, K., et al. (2019). Multi-species annotation of transcriptome and chromatin structure in domesticated animals. *BMC Biol.* 17:108. doi: 10.1186/s12915-019-0726-5

Franco, M. M. (2017). Epigenetics in genetic improvement and animal reproduction. *Arch. Latinoam. Producción Anim.* 25, 75–80.

Fu, Q., Shi, H., and Chen, C. (2017). Roles of bta-miR-29b promoter regions DNA methylation in regulating miR-29b expression and bovine viral diarrhea virus NADL replication in MDBK cells. *Arch. Virol.* 162, 401–408. doi: 10.1007/s00705-016-3107-1

Gao, G., Wang, H., Zhao, X., Li, Q., Li, J., Li, Q., et al. (2015). Feeding conditions and breed affect the level of DNA methylation of the mitochondrial uncoupling protein 3 gene in chicken breast muscle. *J. Anim. Sci.* 93, 1522–1534. doi: 10.2527/jas.2014-8431

Gao, G., Wang, H., Zhao, X., Li, Q., Wang, C., Li, J., et al. (2017). Effect of feeding conditions on the methylation status of Fatp1 gene in chicken breast muscle. *Braz. J. Poult. Sci.* 19, 55–58. doi: 10.1590/1806-9061-2016-0367

García-Giménez, J. L., Ushijima, T., and Tollefsbol, T. O. (2016). "Epigenetic biomarkers: new findings, perspectives, and future directions in diagnostics," in *Epigenetic Biomarkers and Diagnostics*, ed. J. L. García-Giménez (Amsterdam: Elsevier), 1–18. doi: 10.1016/b978-0-12-801899-6.00001-2

Gelfman, S., Cohen, N., Yearim, A., and Ast, G. (2013). DNA-methylation effect on cotranscriptional splicing is dependent on GC architecture of the exon–intron structure. *Genome Res.* 23, 789–799. doi: 10.1101/gr.143503.112

Georges, M., Charlier, C., and Hayes, B. (2019). Harnessing genomic information for livestock improvement. *Nat. Rev. Genet.* 20, 135–156. doi: 10.1038/s41576-018-0082-2

Glendining, K. A., and Jasoni, C. L. (2019). Maternal high fat diet-induced obesity modifies histone binding and expression of oxtr in offspring hippocampus in a sex-specific manner. *Int. J. Mol. Sci.* 20:329. doi: 10.3390/ijms20020329

Goddard, M. E., and Whitelaw, E. (2014). The use of epigenetic phenomena for the improvement of sheep and cattle. *Front. Genet.* 5:247. doi: 10.3389/fgene.2014.00247

González-Recio, O., Toro, M. A., and Bach, A. (2015). Past, present and future of epigenetics applied to livestock breeding. *Front. Genet.* 6:305. doi: 10.3389/fgene.2015.00305

Gotoh, T. (2015). Potential of the application of epigenetics in animal production. *Anim. Prod. Sci.* 55, 145–158. doi: 10.1071/an14467

Greally, J. M. (2018). A user's guide to the ambiguous word'epigenetics'. *Nat. Rev. Mol. Cell Biol.* 19, 207–208. doi: 10.1038/nrm.2017.135

Greenberg, M. V., and Bourc'his, D. (2019). The diverse roles of DNA methylation in mammalian development and disease. *Nat. Rev. Mol. Cell Biol.* 20, 590–607. doi: 10.1038/s41580-019-0159-6

Gross, N., Peñagaricano, F., and Khatib, H. (2020). Integration of whole-genome DNA methylation data with RNA sequencing data to identify markers for bull fertility. *Anim. Genet.* 51, 502–510. doi: 10.1111/age.12941

Guo, M., Chen, Y., Chen, Q., Guo, X., Yuan, Z., Kang, L., et al. (2020). Epigenetic changes associated with increased estrogen receptor alpha mRNA transcript abundance during reproductive maturation in chicken ovaries. *Anim. Reprod. Sci.* 214:106287. doi: 10.1016/j.anireprosci.2020.106287

Guo, T., Luo, F., and Lin, Q. (2020). You are affected by what your parents eat: Diet, epigenetics, transgeneration and intergeneration. *Trends Food Sci. Technol.* 100, 248–261. doi: 10.1016/j.tifs.2020.04.021

Guo, X., Liu, X., Xu, X., Wu, M., Zhang, X., Li, Q., et al. (2012). The expression levels of DNMT3a/3b and their relationship with meat quality in beef cattle. *Mol. Biol. Rep.* 39, 5473–5479. doi: 10.1007/s11033-011-1349-2

Gurgul, A., Miksza-Cybulska, A., Szmatoła, T., Jasielczuk, I., Piestrzyńska-Kajtoch, A., Fornal, A., et al. (2019). Genotyping-by-sequencing performance in selected livestock species. *Genomics* 111, 186–195. doi: 10.1016/j.ygeno.2018.02.002

Hall, T. J., Vernimmen, D., Browne, J. A., Mullen, M. P., Gordon, S. V., MacHugh, D. E., et al. (2019). Alveolar macrophage chromatin is modified to orchestrate host response to *Mycobacterium bovis* infection. *Front. Genet.* 10:e01386. doi: 10.3389/fgene.2019.01386

Halstead, M. M., Kern, C., Saelao, P., Wang, Y., Chanthavixay, G., Medrano, J. F., et al. (2020). A comparative analysis of chromatin accessibility in cattle, pig, and mouse tissues. *BMC Genomics* 21:698. doi: 10.1186/s12864-020-07078-9

Han, W., Xue, Q., Li, G., Yin, J., Zhang, H., Zhu, Y., et al. (2020). Genome-wide analysis of the role of DNA methylation in inbreeding depression of reproduction in Langshan chicken. *Genomics* 112, 2677–2687. doi: 10.1016/j.ygeno.2020.02.007

Hanna, C., and Kelsey, G. (2014). The specification of imprints in mammals. *Heredity* 113, 176–183. doi: 10.1038/hdy.2014.54

Hao, Y., Cui, Y., and Gu, X. (2016). Genome-wide DNA methylation profiles changes associated with constant heat stress in pigs as measured by bisulfite sequencing. *Sci. Rep.* 6:27507.

Harris, K. D., Lloyd, J. P., Domb, K., Zilberman, D., and Zemach, A. (2019). DNA methylation is maintained with high fidelity in the honey bee germline and exhibits global non-functional fluctuations during somatic development. *Epigenetics Chromatin* 12:62.

He, S., Wang, H., Liu, R., He, M., Che, T., Jin, L., et al. (2017). mRNA N6-methyladenosine methylation of postnatal liver development in pig. *PLoS One* 12:e0173421. doi: 10.1371/journal.pone.0173421

He, Y., Song, M., Zhang, Y., Li, X., Song, J., Zhang, Y., et al. (2016). Whole-genome regulation analysis of histone H3 lysin 27 trimethylation in subclinical mastitis cows infected by *Staphylococcus aureus*. *BMC Genomics* 17:565. doi: 10.1186/s12864-016-2947-0

He, Y., Zuo, Q., Edwards, J., Zhao, K., Lei, J., Cai, W., et al. (2018). DNA methylation and regulatory elements during chicken germline stem cell differentiation. *Stem Cell Rep.* 10, 1793–1806. doi: 10.1016/j.stemcr.2018.03.018

He, Y.-F., Li, B.-Z., Li, Z., Liu, P., Wang, Y., Tang, Q., et al. (2011). Tet-mediated formation of 5-carboxylcytosine and its excision by TDG in mammalian DNA. *Science* 333, 1303–1307. doi: 10.1126/science.1210944

Heard, E., and Martienssen, R. A. (2014). Transgenerational epigenetic inheritance: myths and mechanisms. *Cell* 157, 95–109. doi: 10.1016/j.cell.2014.02.045

Heijmans, B. T., Tobi, E. W., Stein, A. D., Putter, H., Blauw, G. J., Susser, E. S., et al. (2008). Persistent epigenetic differences associated with prenatal exposure to famine in humans. *Proc. Natl. Acad. Sci. U.S.A.* 105, 17046–17049. doi: 10.1073/pnas.0806560105

Hernaiz, A., Sentre, S., Bolea, R., López-Pérez, O., Sanz, A., Zaragoza, P., et al. (2019). "Epigenetic changes in the central nervous system of sheep naturally infected with scrapie," in *Proceedings of the 18th Jornadas Sobre Producción Animal, Zaragoza, España, 7 y 8 de mayo de 2019*, Zaragoza, 507–509.

Herrera-Uribe, J., Liu, H., Byrne, K. A., Bond, Z. F., Loving, C. L., and Tuggle, C. K. (2020). Changes in H3K27ac at gene regulatory regions in porcine alveolar macrophages following LPS or PolyIC exposure. *Front. Genet.* 11:817. doi: 10.3389/fgene.2020.00817

Hitchins, M. P. and Ward, R. L. (2009). Constitutional (germline) *MLH1* epimutation as an aetiological mechanism for hereditary non-polyposis colorectal cancer. *J. Med. Genet.* 46, 793–802. doi: 10.1136/jmg.2009.068122

Hong, J., Wang, X., Mei, C., Wang, H., and Zan, L. (2019). DNA methylation and transcription factors competitively regulate SIRT4 promoter activity in bovine adipocytes: roles of NRF1 and CMYB. *DNA Cell Biol.* 38, 63–75. doi: 10.1089/dna.2018.4454

Hong, J.-Y., Mei, C.-G., Li, S.-J., Wang, H.-B., Zhao, C.-P., and Zan, L.-S. (2018). Coordinate regulation by transcription factors and DNA methylation in the core promoter region of SIRT6 in bovine adipocytes. *Arch. Biochem. Biophys.* 659, 1–12. doi: 10.1016/j.abb.2018.09.018

Horsthemke, B. (2006). Epimutations in human disease. *Curr. Top. Microbiol. Immunol.* 310, 45–59. doi: 10.1007/3-540-31181-5_4

Hota, S. K., and Bruneau, B. G. (2016). ATP-dependent chromatin remodeling during mammalian development. *Development* 143, 2882–2897. doi: 10.1242/dev.128892

Hota, S. K., Johnson, J. R., Verschueren, E., Thomas, R., Blotnick, A. M., Zhu, Y., et al. (2019). Dynamic BAF chromatin remodeling complex subunit inclusion promotes temporally distinct gene expression programs in cardiogenesis. *Development* 146:dev174086. doi: 10.1242/dev.174086

Hu, Y., Sun, Q., Liu, J., Jia, Y., Cai, D., Idriss, A. A., et al. (2017a). In ovo injection of betaine alleviates corticosterone-induced fatty liver in chickens through epigenetic modifications. *Sci. Rep.* 7:40251.

Hu, Y., Sun, Q., Zong, Y., Liu, J., Idriss, A. A., Omer, N. A., et al. (2017b). Prenatal betaine exposure alleviates corticosterone-induced inhibition of CYP27A1 expression in the liver of juvenile chickens associated with its promoter DNA methylation. *Gen. Comp. Endocrinol.* 246, 241–248. doi: 10.1016/j.ygcen.2016.12.014

Hwang, J. H., An, S. M., Kwon, S., Park, D. H., Kim, T. W., Kang, D. G., et al. (2017). DNA methylation patterns and gene expression associated with litter size in Berkshire pig placenta. *PLoS One* 12:e0184539. doi: 10.1371/journal.pone.0184539

Ibeagha-Awemu, E. M., Bhattarai, S., Dudemaine, P.-L., Wang, M., Mckay, S. D., Zhao, X., et al. (2020a). 63 DNA methylome wide profile associates differentially methylated loci and regions with cow's ileal lymph node response to Mycobacterium avium subsp. paratuberculosis. *J. Anim. Sci.* 98, 39–40. doi: 10.1093/jas/skaa278.071

Ibeagha-Awemu, E. M., Bhattarai, S., Dudemaine, P.-L., Wang, M., Mckay, S. D., Zhao, X., et al. (2020b). PSVIII-15 Genome wide DNA methylation analysis reveals role of DNA methylation in cow's ileal response to Mycobacterium avium subsp. paratuberculosis. *J. Anim. Sci.* 98, 260–261. doi: 10.1093/jas/skaa278.471

Ibeagha-Awemu, E. M., and Khatib, H. (2017). "Epigenetics of livestock breeding," in *Handbook of Epigenetics*, 2nd Edn, Chap. 29. ed. T. O. Tollefsbol (Cambridge: Academic Press), 441–463.

Ibeagha-Awemu, E. M., and Zhao, X. (2015). Epigenetic marks: regulators of livestock phenotypes and conceivable sources of missing variation in livestock improvement programs. *Front. Genet.* 6:302. doi: 10.3389/fgene.2015.00302

Ideraabdullah, F. Y., and Zeisel, S. H. (2018). Dietary modulation of the epigenome. *Physiol. Rev.* 98, 667–695. doi: 10.1152/physrev.00010.2017

Idriss, A. A., Hu, Y., Hou, Z., Hu, Y., Sun, Q., Omer, N. A., et al. (2018). Dietary betaine supplementation in hens modulates hypothalamic expression of cholesterol metabolic genes in F1 cockerels through modification of DNA methylation. *Comp. Biochem. Physiol. B Biochem. Mol. Biol.* 217, 14–20. doi: 10.1016/j.cbpb.2017.12.001

Imgenberg-Kreuz, J., Almlöf, J. C., Leonard, D., Alexsson, A., Nordmark, G., Eloranta, M.-L., et al. (2018). DNA methylation mapping identifies gene regulatory effects in patients with systemic lupus erythematosus. *Ann. Rheum. Dis.* 77, 736–743. doi: 10.1136/annrheumdis-2017-212379

Ispada, J., De Lima, C. B., Sirard, M.-A., Fontes, P. K., Nogueira, M. F. G., Annes, K., et al. (2018). Genome-wide screening of DNA methylation in bovine blastocysts with different kinetics of development. *Epigenetics Chromatin* 11:1.

Ivanova, E., Canovas, S., Garcia-Martínez, S., Romar, R., Lopes, J. S., Rizos, D., et al. (2020). DNA methylation changes during preimplantation development reveal inter-species differences and reprogramming events at imprinted genes. *Clin. Epigenetics* 12:64.

Jahan, S., Beacon, T. H., Xu, W., and Davie, J. R. (2019). Atypical chromatin structure of immune-related genes expressed in chicken erythrocytes. *Biochem. Cell Biol.* 98, 171–177. doi: 10.1139/bcb-2019-0107

Jahan, S., Xu, W., He, S., Gonzalez, C., Delcuve, G. P., and Davie, J. R. (2016). The chicken erythrocyte epigenome. *Epigenetics Chromatin* 9:19.

Jambhekar, A., Dhall, A., and Shi, Y. (2019). Roles and regulation of histone methylation in animal development. *Nat. Rev. Mol. Cell Biol.* 20, 625–641. doi: 10.1038/s41580-019-0151-1

Jang, H., and Serra, C. (2014). Nutrition, epigenetics, and diseases. *Clin. Nutr. Res.* 3, 1–8. doi: 10.1007/978-3-319-31143-2_66-1

Jeltsch, A., Ehrenhofer-Murray, A., Jurkowski, T. P., Lyko, F., Reuter, G., Ankri, S., et al. (2017). Mechanism and biological role of Dnmt2 in nucleic acid methylation. *RNA Biol.* 14, 1108–1123. doi: 10.1080/15476286.2016.1191737

Jiao, P., Yuan, Y., Zhang, M., Sun, Y., Wei, C., Xie, X., et al. (2020). PRL/microRNA-183/IRS1 pathway regulates milk fat metabolism in cow mammary epithelial cells. *Genes* 11:196. doi: 10.3390/genes11020196

Jiao, Q., Yin, R. H., Zhao, S. J., Wang, Z. Y., Zhu, Y. B., Wang, W., et al. (2019). Identification and molecular analysis of a lncRNA-HOTAIR transcript from secondary hair follicle of cashmere goat reveal integrated regulatory network with the expression regulated potentially by its promoter methylation. *Gene* 688, 182–192. doi: 10.1016/j.gene.2018.11.084

Jin, C., Zhuo, Y., Wang, J., Zhao, Y., Xuan, Y., Mou, D., et al. (2018). Methyl donors dietary supplementation to gestating sows diet improves the growth rate of offspring and is associating with changes in expression and DNA methylation of insulin-like growth factor-1 gene. *J. Anim. Physiol. Anim. Nutr.* 102, 1340–1350. doi: 10.1111/jpn.12933

Jin, L., Mao, K., Li, J., Huang, W., Che, T., Fu, Y., et al. (2018). Genome-wide profiling of gene expression and DNA methylation provides insight into low-altitude acclimation in Tibetan pigs. *Gene* 642, 522–532. doi: 10.1016/j.gene.2017.11.074

Ju, Z., Jiang, Q., Wang, J., Wang, X., Yang, C., Sun, Y., et al. (2020). Genome-wide methylation and transcriptome of blood neutrophils reveal the roles of DNA methylation in affecting transcription of protein-coding genes and miRNAs in *E. coli*-infected mastitis cows. *BMC Genomics* 21:102. doi: 10.1186/s12864-020-6526-z

Jung, G., Hernández-Illán, E., Moreira, L., Balaguer, F., and Goel, A. (2020). Epigenetics of colorectal cancer: biomarker and therapeutic potential. *Nat. Rev. Gastroenterol. Hepatol.* 17, 111–130. doi: 10.1038/s41575-019-0230-y

Kaikkonen, M. U., Lam, M. T., and Glass, C. K. (2011). Non-coding RNAs as regulators of gene expression and epigenetics. *Cardiovasc. Res.* 90, 430–440. doi: 10.1093/cvr/cvr097

Kamath, P. L., Foster, J. T., Drees, K. P., Luikart, G., Quance, C., Anderson, N. J., et al. (2016). Genomics reveals historic and contemporary transmission dynamics of a bacterial disease among wildlife and livestock. *Nat. Commun.* 7:11448.

Kamińska, K., Nalejska, E., Kubiak, M., Wojtysiak, J., Żołna, Ł, Kowalewski, J., et al. (2019). Prognostic and predictive epigenetic biomarkers in oncology. *Mol. Diagn. Ther.* 23, 83–95. doi: 10.1007/s40291-018-0371-7

Kang, Y., Nii, T., Isobe, N., and Yoshimura, Y. (2019a). Effects of *Salmonella* enteritidis vaccination on the expression of innate immune molecules and histone modifications in the follicular theca of laying hens. *J. Poult. Sci.* 56, 298–307. doi: 10.2141/jpsa.0190034

Kang, Y., Nii, T., Isobe, N., and Yoshimura, Y. (2019b). Effects of the routine multiple vaccinations on the expression of innate immune molecules and induction of histone modification in ovarian cells of layer chicks. *Poult. Sci.* 98, 5127–5136. doi: 10.3382/ps/pez214

Kantarjian, H. M., Thomas, X. G., Dmoszynska, A., Wierzbowska, A., Mazur, G., Mayer, J., et al. (2012). Multicenter, randomized, open-label, phase III trial of decitabine versus patient choice, with physician advice, of either supportive care or low-dose cytarabine for the treatment of older patients with newly diagnosed acute myeloid leukemia. *J. Clin. Oncol.* 30:2670. doi: 10.1200/jco.2011.38.9429

Keleher, M. R., Zaidi, R., Shah, S., Oakley, M. E., Pavlatos, C., El Idrissi, S., et al. (2018). Maternal high-fat diet associated with altered gene expression, DNA methylation, and obesity risk in mouse offspring. *PLoS One* 13:e0192606. doi: 10.1371/journal.pone.0192606

Khezri, A., Narud, B., Stenseth, E.-B., Zeremichael, T. T., Myromslien, F. D., Wilson, R. C., et al. (2020). Sperm DNA hypomethylation proximal to reproduction pathway genes in maturing elite Norwegian Red bulls. *Front. Genet.* 11:922. doi: 10.3389/fgene.2020.00922

Kim, S., and Kaang, B.-K. (2017). Epigenetic regulation and chromatin remodeling in learning and memory. *Exp. Mol. Med.* 49:e281. doi: 10.1038/emm.2016.140

Kishi, Y., and Gotoh, Y. (2018). Regulation of chromatin structure during neural development. *Front. Neurosci.* 12:874. doi: 10.3389/fnins.2018.00874

Kisliouk, T., Cramer, T., and Meiri, N. (2017). Methyl CpG level at distal part of heat-shock protein promoter HSP 70 exhibits epigenetic memory for heat stress by modulating recruitment of POU 2F1-associated nucleosome-remodeling deacetylase (Nu RD) complex. *J. Neurochem.* 141, 358–372. doi: 10.1111/jnc.14014

Klein-Brill, A., Joseph-Strauss, D., Appleboim, A., and Friedman, N. (2019). Dynamics of chromatin and transcription during transient depletion of the RSC chromatin remodeling complex. *Cell Rep.* 26, 279–292. doi: 10.1016/j.celrep.2018.12.020

Kobayashi, W., and Kurumizaka, H. (2019). Structural transition of the nucleosome during chromatin remodeling and transcription. *Curr. Opin. Struct. Biol.* 59, 107–114. doi: 10.1016/j.sbi.2019.07.011

Kociucka, B., Stachecka, J., Szydlowski, M., and Szczerbal, I. (2017). Rapid communication: the correlation between histone modifications and expression of key genes involved in accumulation of adipose tissue in the pig. *J. Anim. Sci.* 95, 4514–4519. doi: 10.2527/jas2017.2010

Korkmaz, F. T., and Kerr, D. E. (2017). Genome-wide methylation analysis reveals differentially methylated loci that are associated with an age-dependent increase in bovine fibroblast response to LPS. *BMC Genomics* 18:405. doi: 10.1186/s12864-017-3796-1

Kosinska-Selbi, B., Mielczarek, M., and Szyda, J. (2020). Long non-coding RNA in livestock. *Animal* 10, 2003–2013.

Kouzarides, T. (2007). Chromatin modifications and their function. *Cell* 128, 693–705. doi: 10.1016/j.cell.2007.02.005

Kowalski, A., and Pałyga, J. (2017). Distribution of non-allelic histone H1 subtypes in five avian species. *Ann. Anim. Sci.* 17, 385–398. doi: 10.1515/aoas-2016-0063

Kropp, J., Carrillo, J. A., Namous, H., Daniels, A., Salih, S. M., Song, J., et al. (2017). Male fertility status is associated with DNA methylation signatures in sperm and transcriptomic profiles of bovine preimplantation embryos. *BMC Genomics* 18:280. doi: 10.1186/s12864-017-3673-y

Kubik, S., O'Duibhir, E., de Jonge, W. J., Mattarocci, S., Albert, B., Falcone, J.-L., et al. (2018). Sequence-directed action of RSC remodeler and general regulatory factors modulates+ 1 nucleosome position to facilitate transcription. *Mol. Cell.* 71, 89–102. doi: 10.1016/j.molcel.2018.05.030

Kutchy, N., Menezes, E., Chiappetta, A., Tan, W., Wills, R., Kaya, A., et al. (2018). Acetylation and methylation of sperm histone 3 lysine 27 (H3K27ac and H3K27me3) are associated with bull fertility. *Andrologia* 50:e12915. doi: 10.1111/and.12915

Kutchy, N. A., Velho, A., Menezes, E. S., Jacobsen, M., Thibaudeau, G., Wills, R. W., et al. (2017). Testis specific histone 2B is associated with sperm chromatin dynamics and bull fertility-a pilot study. *Reprod. Biol. Endocrinol.* 15:59.

Kweh, M. F., Merriman, K. E., and Nelson, C. D. (2019). Inhibition of DNA methyltransferase and histone deacetylase increases β-defensin expression but not the effects of lipopolysaccharide or 1, 25-dihydroxyvitamin D3 in bovine mammary epithelial cells. *J. Dairy Sci.* 102, 5706–5712. doi: 10.3168/jds.2018-16141

Lambert, S., Blondin, P., Vigneault, C., Labrecque, R., Dufort, I., and Sirard, M.-A. (2018). Spermatozoa DNA methylation patterns differ due to peripubertal age in bulls. *Theriogenology* 106, 21–29. doi: 10.1016/j.theriogenology.2017.10.006

Lamouille, S., Xu, J., and Derynck, R. (2014). Molecular mechanisms of epithelial–mesenchymal transition. *Nat. Rev. Mol. Cell Biol.* 15:178.

Larsen, K., Kristensen, K. K., and Callesen, H. (2018). DNA methyltransferases and tRNA methyltransferase DNMT2 in developing pig brain-expression and promoter methylation. *Gene Rep.* 11, 42–51. doi: 10.1016/j.genrep.2018.02.003

Leal-Gutiérrez, J. D., Elzo, M. A., and Mateescu, R. G. (2020). Identification of eQTLs and sQTLs associated with meat quality in beef. *BMC Genomics* 21:104. doi: 10.1186/s12864-020-6520-5

Lee, I., Rasoul, B. A., Holub, A. S., Lejeune, A., Enke, R. A., and Timp, W. (2017). Whole genome DNA methylation sequencing of the chicken retina, cornea and brain. *Sci. Data* 4:170148.

Lee, K. H., Song, Y., O'Sullivan, M., Pereira, G., Loh, R., and Zhang, G. B. (2017). The implications of DNA methylation on food allergy. *Int. Arch. Allergy Immunol.* 173, 183–192. doi: 10.1159/000479513

Lee, Y. G., Kim, I., Yoon, S. S., Park, S., Cheong, J. W., Min, Y. H., et al. (2013). Comparative analysis between azacitidine and decitabine for the treatment of myelodysplastic syndromes. *Br. J. Haematol.* 161, 339–347.

Lehle, J. D., and Mccarrey, J. R. (2020). Differential susceptibility to endocrine disruptor-induced epimutagenesis. *Environ. Epigenet.* 6:dvaa016. doi: 10.1093/eep/dvaa016

Li, C., Li, Y., Zhou, G., Gao, Y., Ma, S., Chen, Y., et al. (2018). Whole-genome bisulfite sequencing of goat skins identifies signatures associated with hair cycling. *BMC Genomics* 19:638. doi: 10.1186/s12864-018-5002-5

Li, J., Li, R., Wang, Y., Hu, X., Zhao, Y., Li, L., et al. (2015). Genome-wide DNA methylome variation in two genetically distinct chicken lines using MethylC-seq. *BMC Genomics* 16:851. doi: 10.1186/s12864-015-2098-8

Li, M., Zou, D., Li, Z., Gao, R., Sang, J., Zhang, Y., et al. (2019). EWAS atlas: a curated knowledgebase of epigenome-wide association studies. *Nucleic Acids Res.* 47, D983–D988.

Li, Y., Carrillo, J. A., Ding, Y., He, Y., Zhao, C., Liu, J., et al. (2019). DNA methylation, microRNA expression profiles and their relationships with transcriptome in grass-fed and grain-fed angus cattle rumen tissue. *PLoS One* 14:e0214559. doi: 10.1371/journal.pone.0214559

Li, R., and Ibeagha-Awemu, E. M. (2017). Altered gene expression of epigenetic modifying enzymes in response to dietary supplementation with linseed oil. *J. Dairy Res.* 84:119. doi: 10.1017/s002202991700022x

Li, Y., Zhang, L.-Z., Yi, Y., Hu, W.-W., Guo, Y.-H., Zeng, Z.-J., et al. (2017). Genome-wide DNA methylation changes associated with olfactory learning and memory in Apis mellifera. *Sci. Rep.* 7:17017.

Liang, S., Nie, Z.-W., Guo, J., Niu, Y.-J., Shin, K.-T., Ock, S. A., et al. (2018). Overexpression of microRNA-29b decreases expression of DNA methyltransferases and improves quality of the blastocysts derived from somatic cell nuclear transfer in cattle. *Microsc. Microanal.* 24, 29–37. doi: 10.1017/s1431927618000016

Liang, Z., Brown, K. E., Carroll, T., Taylor, B., Vidal, I. F., Hendrich, B., et al. (2017). A high-resolution map of transcriptional repression. *Elife* 6:e22767.

Lin, S., Fang, L., Liu, G. E., and Li, C.-J. (2019). *Epigenetics and Heritable Phenotypic Variations in Livestock*. Amsterdam: Elsevier, 283–313.

Lister, R., Pelizzola, M., Dowen, R. H., Hawkins, R. D., Hon, G., Tonti-Filippini, J., et al. (2009). Human DNA methylomes at base resolution show widespread epigenomic differences. *Nature* 462, 315–322. doi: 10.1038/nature08514

Littlejohn, B. P., Price, D. M., Neuendorff, D. A., Carroll, J. A., Vann, R. C., Riggs, P. K., et al. (2018). Prenatal transportation stress alters genome-wide DNA methylation in suckling Brahman bull calves. *J. Anim. Sci.* 96, 5075–5099. doi: 10.1093/jas/sky350

Liu, C., Vyas, A., Kassab, M. A., Singh, A. K., and Yu, X. (2017). The role of poly ADP-ribosylation in the first wave of DNA damage response. *Nucleic Acids Res.* 45, 8129–8141. doi: 10.1093/nar/gkx565

Liu, H., Wang, J., Mou, D., Che, L., Fang, Z., Feng, B., et al. (2017). Maternal methyl donor supplementation during gestation counteracts the bisphenol a-induced impairment of intestinal morphology, disaccharidase activity, and nutrient transporters gene expression in newborn and weaning pigs. *Nutrients* 9:423. doi: 10.3390/nu9050423

Liu, X., Yang, J., Zhang, Q., and Jiang, L. (2017). Regulation of DNA methylation on EEF1D and RPL8 expression in cattle. *Genetica* 145, 387–395. doi: 10.1007/s10709-017-9974-x

Liu, S., Fang, L., Zhou, Y., Santos, D. J., Xiang, R., Daetwyler, H. D., et al. (2019). Analyses of inter-individual variations of sperm DNA methylation and their potential implications in cattle. *BMC Genomics* 20:888. doi: 10.1186/s12864-019-6228-6

Liu, Z., Han, S., Shen, X., Wang, Y., Cui, C., He, H., et al. (2019). The landscape of DNA methylation associated with the transcriptomic network in layers and broilers generates insight into embryonic muscle development in chicken. *Int. J. Biol. Sci.* 15, 1404–1418. doi: 10.7150/ijbs.35073

Liu, S., Yu, Y., Zhang, S., Cole, J. B., Tenesa, A., Wang, T., et al. (2020). Epigenomics and genotype-phenotype association analyses reveal conserved genetic architecture of complex traits in cattle and human. *BMC Biol.* 18:80. doi: 10.1186/s12915-020-00792-6

Liu, X., Usman, T., Wang, Y., Wang, Z., Xu, X., Wu, M., et al. (2015). Polymorphisms in epigenetic and meat quality related genes in fourteen cattle breeds and association with beef quality and carcass traits. *Asian-Australas. J. Anim. Sci.* 28, 467–475. doi: 10.5713/ajas.13.0837

Liu, Z., Li, Q., Liu, R., Zhao, G., Zhang, Y., Zheng, M., et al. (2016). Expression and methylation of microsomal triglyceride transfer protein and acetyl-CoA carboxylase are associated with fatty liver syndrome in chicken. *Poult. Sci.* 95, 1387–1395. doi: 10.3382/ps/pew040

Lorch, Y., and Kornberg, R. D. (2017). Chromatin-remodeling for transcription. *Q. Rev. Biophys.* 50:e5.

Lu, T., Song, Z., Li, Q., Li, Z., Wang, M., Liu, L., et al. (2017). Overexpression of histone deacetylase 6 enhances resistance to porcine reproductive and respiratory syndrome virus in pigs. *PLoS One* 12:e0169317. doi: 10.1371/journal.pone.0169317

Lu, Z., Ma, Y., Li, Q., Liu, E., Jin, M., Zhang, L., et al. (2019). The role of N 6-methyladenosine RNA methylation in the heat stress response of sheep (*Ovis aries*). *Cell Stress Chaperones* 24, 333–342. doi: 10.1007/s12192-018-00965-x

Luo, C., Hajkova, P., and Ecker, J. R. (2018). Dynamic DNA methylation: In the right place at the right time. *Science* 361, 1336–1340. doi: 10.1126/science.aat6806

Lv, Z., Fan, H., Song, B., Li, G., Liu, D., and Guo, Y. (2019). Supplementing genistein for breeder hens alters the fatty acid metabolism and growth performance of offsprings by epigenetic modification. *Oxid. Med. Cell. Longev.* 2019:e9214209.

Ma, X., Jia, C., Chu, M., Fu, D., Lei, Q., Ding, X., et al. (2019). Transcriptome and DNA methylation analyses of the molecular mechanisms underlying with longissimus dorsi muscles at different stages of development in the polled Yak. *Genes* 10:970. doi: 10.3390/genes10120970

Maldonado, M. B., de Rezende Neto, N. B., Nagamatsu, S. T., Carazzolle, M. F., Hoff, J. L., Whitacre, L. K., et al. (2019). Identification of bovine CpG SNPs as potential targets for epigenetic regulation via DNA methylation. *PLoS One* 14:e0222329. doi: 10.1371/journal.pone.0222329

Manakov, S. A., Pezic, D., Marinov, G. K., Pastor, W. A., Sachidanandam, R., and Aravin, A. A. (2015). MIWI2 and MILI have differential effects on piRNA biogenesis and DNA methylation. *Cell Rep.* 12, 1234–1243. doi: 10.1016/j.celrep.2015.07.036

Mancini-DiNardo, D., Steele, S. J., Levorse, J. M., Ingram, R. S., and Tilghman, S. M. (2006). Elongation of the Kcnq1ot1 transcript is required for genomic imprinting of neighboring genes. *Genes Dev.* 20, 1268–1282. doi: 10.1101/gad.1416906

Marco, A., Kisliouk, T., Tabachnik, T., Weller, A., and Meiri, N. (2016). DNA CpG methylation (5mC) and its derivative (5hmC) alter histone post translational modifications at the POMC promoter, affecting the impact of perinatal diet on leanness and obesity of the offspring. *Diabetes* 65, 2258–2267. doi: 10.2337/db15-1608

Markou, A. N., Paraskevopoulos, P., Lazaridou, M., Chen, S., Kroneis, T., Świerczewska, M., et al. (2017). *GSTP1 Promoter Methylation in In-Vivo Isolated CTCs from High-Risk Prostate Cancer Patients*. Washington, DC: American Association for Cancer Research.

Martignano, F., Gurioli, G., Salvi, S., Calistri, D., Costantini, M., Gunelli, R., et al. (2016). GSTP1 methylation and protein expression in prostate cancer: diagnostic implications. *Dis. Markers* 2016:e4358292.

Maugeri, A., and Barchitta, M. (2020). How dietary factors affect DNA methylation: lesson from epidemiological studies. *Medicina* 56:374. doi: 10.3390/medicina56080374

Maunakea, A. K., Chepelev, I., Cui, K., and Zhao, K. (2013). Intragenic DNA methylation modulates alternative splicing by recruiting MeCP2 to promote exon recognition. *Cell Res.* 23, 1256–1269. doi: 10.1038/cr.2013.110

Maunakea, A. K., Nagarajan, R. P., Bilenky, M., Ballinger, T. J., D'Souza, C., Fouse, S. D., et al. (2010). Conserved role of intragenic DNA methylation in regulating alternative promoters. *Nature* 466, 253–257. doi: 10.1038/nature09165

McGuffey, R. (2017). A 100-year review: metabolic modifiers in dairy cattle nutrition. *J. Dairy Sci.* 100, 10113–10142. doi: 10.3168/jds.2017-12987

McKay, S., Betancourt, F., Bhattarai, S., Buttolph, T., White, S., Lachance, H., et al. (2018). 115 Profiling conservation of DNA methylation in cattle. *J. Anim. Sci.* 96(Suppl._3), 370–370. doi: 10.1093/jas/sky404.812

Meirelles, F. V., Bressan, F. F., Smith, L. C., Perecin, F., Chiaratti, M. R., and Ferraz, J. B. S. (2014). Cytoplasmatic inheritance, epigenetics and reprogramming DNA as tools in animal breeding. *Livest. Sci.* 166, 199–205. doi: 10.1016/j.livsci.2014.05.024

Melnik, B. C., John, S. M., and Schmitz, G. (2016). Milk: an epigenetic inducer of FoxP3 expression. *J. Allergy Clin. Immunol.* 138, 937–938. doi: 10.1016/j.jaci.2016.04.039

Melnik, B. C., and Schmitz, G. (2017a). DNA methyltransferase 1-targeting miRNA-148a of dairy milk: a potential bioactive modifier of the human epigenome. *Funct. Foods Health Dis.* 7, 671–687. doi: 10.31989/ffhd.v7i9.379

Melnik, B. C., and Schmitz, G. (2017b). Milk's role as an epigenetic regulator in health and disease. *Diseases* 5:12. doi: 10.3390/diseases5010012

Mendes, V., Dias, R., Souza, J., Souza, E., Quintao, C., Batista, R., et al. (2017). 184 effect of histone deacetylase inhibitor on development of embryos derived from heat-shocked bovine oocytes. *Reprod. Fertil. Dev.* 29, 200–201. doi: 10.1071/rdv29n1ab184

Mercer, T. R., Dinger, M. E., and Mattick, J. S. (2009). Long non-coding RNAs: insights into functions. *Nat. Rev. Genet.* 10, 155–159.

Miller, A., Ralser, M., Kloet, S. L., Loos, R., Nishinakamura, R., Bertone, P., et al. (2016). Sall4 controls differentiation of pluripotent cells independently of the Nucleosome Remodelling and Deacetylation (NuRD) complex. *Development* 143, 3074–3084. doi: 10.1242/dev.139113

Mishra, A., and Verma, M. (2010). Cancer biomarkers: are we ready for the prime time? *Cancers* 2, 190–208. doi: 10.3390/cancers2010190

Miska, E. A., and Ferguson-Smith, A. C. (2016). Transgenerational inheritance: Models and mechanisms of non–DNA sequence–based inheritance. *Science* 354, 59–63. doi: 10.1126/science.aaf4945

Mitra, A., Luo, J., He, Y., Gu, Y., Zhang, H., Zhao, K., et al. (2015). Histone modifications induced by MDV infection at early cytolytic and latency phases. *BMC Genomics* 16:311. doi: 10.1186/s12864-015-1492-6

Monk, D., Mackay, D. J., Eggermann, T., Maher, E. R., and Riccio, A. (2019). Genomic imprinting disorders: lessons on how genome, epigenome and environment interact. *Nat. Rev. Genet.* 20, 235–248. doi: 10.1038/s41576-018-0092-0

Morales-Nebreda, L., McLafferty, F. S., and Singer, B. D. (2019). DNA methylation as a transcriptional regulator of the immune system. *Transl. Res.* 204, 1–18. doi: 10.1016/j.trsl.2018.08.001

Moran, S., Arribas, C., and Esteller, M. (2016). Validation of a DNA methylation microarray for 850,000 CpG sites of the human genome enriched in enhancer sequences. *Epigenomics* 8, 389–399. doi: 10.2217/epi.15.114

Morris, K. V., and Mattick, J. S. (2014). The rise of regulatory RNA. *Nat. Rev. Genet.* 15, 423–437. doi: 10.1038/nrg3722

Mueller, M., Cole, J., Sonstegard, T., and Van Eenennaam, A. (2019). Comparison of gene editing versus conventional breeding to introgress the POLLED allele into the US dairy cattle population. *J. Dairy Sci.* 102, 4215–4226. doi: 10.3168/jds.2018-15892

Murdoch, B. M., Murdoch, G. K., Greenwood, S., and McKay, S. (2016). Nutritional influence on epigenetic marks and effect on livestock production. *Front. Genet.* 7:182. doi: 10.3389/fgene.2016.00182

Nayak, N., Bhanja, S., Ahmad, S. F., Mehra, M., Goel, A., Sahu, A. R., et al. (2016). Role of epigenetic modifications in improving the thermo-tolerance, growth and immuno-competence in poultry: current status and future applications. *Indian J. Poul. Sci.* 51, 1–9. doi: 10.5958/0974-8180.2016.00015.5

Nguyen, H., Sokpor, G., Pham, L., Rosenbusch, J., Stoykova, A., Staiger, J. F., et al. (2016). Epigenetic regulation by BAF (mSWI/SNF) chromatin remodeling complexes is indispensable for embryonic development. *Cell Cycle* 15, 1317–1324. doi: 10.1080/15384101.2016.1160984

Nguyen, M., Boutinaud, M., Pétridou, B., Gabory, A., Pannetier, M., Chat, S., et al. (2014). DNA methylation and transcription in a distal region upstream from the bovine AlphaS1 casein gene after once or twice daily milking. *PLoS One* 9:e111556. doi: 10.1371/journal.pone.0111556

Nicoglou, A., and Merlin, F. (2017). Epigenetics: A way to bridge the gap between biological fields. *Stud. Hist. Philos. Sci. C* 66, 73–82. doi: 10.1016/j.shpsc.2017.10.002

Nilsson, E. E., Sadler-Riggleman, I., and Skinner, M. K. (2018). Environmentally induced epigenetic transgenerational inheritance of disease. *Environ. Epigenet.* 4:dvy016.

Noya, A., Casasús, I., Ferrer, J., and Sanz, A. (2019). Effects of developmental programming caused by maternal nutrient intake on postnatal performance of beef heifers and their calves. *Animals* 9:1072. doi: 10.3390/ani9121072

O'Doherty, A. M., Rue-Albrecht, K. C., Magee, D. A., Ahting, S., Irwin, R. E., Hall, T. J., et al. (2019). The bovine alveolar macrophage DNA methylome is resilient to infection with *Mycobacterium bovis*. *Sci. Rep.* 9:1510. doi: 10.1038/s41598-018-37618-z

Oey, H., and Whitelaw, E. (2014). On the meaning of the word 'epimutation'. *Trends Genet.* 30, 519–520. doi: 10.1016/j.tig.2014.08.005

Omer, N. A., Hu, Y., Hu, Y., Idriss, A. A., Abobaker, H., Hou, Z., et al. (2018). Dietary betaine activates hepatic VTGII expression in laying hens associated with hypomethylation of GR gene promoter and enhanced GR expression. *J. Anim. Sci. Biotechnol.* 9:2.

Omer, N. A., Hu, Y., Idriss, A. A., Abobaker, H., Hou, Z., Yang, S., et al. (2020). Dietary betaine improves egg-laying rate in hens through hypomethylation and glucocorticoid receptor–mediated activation of hepatic lipogenesis-related genes. *Poult. Sci.* 99, 3121–3132. doi: 10.1016/j.psj.2020.01.017

Osorio, J., Jacometo, C., Zhou, Z., Luchini, D., Cardoso, F., and Loor, J. J. (2016). Hepatic global DNA and peroxisome proliferator-activated receptor alpha promoter methylation are altered in peripartal dairy cows fed rumen-protected methionine. *J. Dairy Sci.* 99, 234–244. doi: 10.3168/jds.2015-10157

Paiva, J., Resende, M., Resende, R., Oliveira, H., Silva, H., Caetano, G., et al. (2019). Epigenetics: mechanisms, inheritance and implications in animal breeding. *Arch. Zootec.* 68, 304–311.

Palazzese, L., Czernik, M., Iuso, D., Toschi, P., and Loi, P. (2018). Nuclear quiescence and histone hyper-acetylation jointly improve protamine-mediated nuclear remodeling in sheep fibroblasts. *PLoS One* 13:e0193954. doi: 10.1371/journal.pone.0193954

Pan, X., Gong, D., Nguyen, D. N., Zhang, X., Hu, Q., Lu, H., et al. (2018). Early microbial colonization affects DNA methylation of genes related to intestinal immunity and metabolism in preterm pigs. *DNA Res.* 25, 287–296. doi: 10.1093/dnares/dsy001

Pan, X., Thymann, T., Gao, F., and Sangild, P. T. (2020). Rapid gut adaptation to preterm birth involves feeding-related DNA methylation reprogramming of intestinal genes in pigs. *Front. Immunol.* 11:565. doi: 10.3389/fimmu.2020.00565

Panzeri, I., and Pospisilik, J. A. (2018). Epigenetic control of variation and stochasticity in metabolic disease. *Mol. Metab.* 14, 26–38. doi: 10.1016/j.molmet.2018.05.010

Paparo, L., Nocerino, R., Cosenza, L., Aitoro, R., D'Argenio, V., Del Monaco, V., et al. (2016). Epigenetic features of FoxP3 in children with cow's milk allergy. *Clin. Epigenetics* 8:86.

Paradis, F., Wood, K. M., Swanson, K. C., Miller, S. P., McBride, B. W., and Fitzsimmons, C. (2017). Maternal nutrient restriction in mid-to-late gestation influences fetal mRNA expression in muscle tissues in beef cattle. *BMC Genomics* 18:632. doi: 10.1186/s12864-017-4051-5

Park, H., Seo, K.-S., Lee, M., and Seo, S. (2019). Identification of meat quality-related differentially methylated regions in the DNA of the longissimus dorsi muscle in pig. *Anim. Biotechnol.* 31, 189–194. doi: 10.1080/10495398.2019.1604378

Perrier, J.-P., Sellem, E., Prézelin, A., Gasselin, M., Jouneau, L., Piumi, F., et al. (2018). A multi-scale analysis of bull sperm methylome revealed both species peculiarities and conserved tissue-specific features. *BMC Genomics* 19:404. doi: 10.1186/s12864-018-4764-0

Petronis, A. (2010). Epigenetics as a unifying principle in the aetiology of complex traits and diseases. *Nature* 465, 721–727. doi: 10.1038/nature09230

Platenburg, G. J., Vollebregt, E. J., Karatzas, C. N., Kootwijk, E. P., De Boer, H. A., and Strijker, R. (1996). Mammary gland-specific hypomethylation ofHpa II sites flanking the bovine αS1-casein gene. *Transgenic Res.* 5, 421–431. doi: 10.1007/bf01980207

Ponsuksili, S., Trakooljul, N., Basavaraj, S., Hadlich, F., Murani, E., and Wimmers, K. (2019). Epigenome-wide skeletal muscle DNA methylation profiles at the background of distinct metabolic types and ryanodine receptor variation in pigs. *BMC Genomics* 20:492. doi: 10.1186/s12864-019-5880-1

Pragna, P., Archana, P., Aleena, J., Sejian, V., Krishnan, G., Bagath, M., et al. (2017). Heat stress and dairy cow: impact on both milk yield and composition. *Int. J. Dairy Sci.* 12, 1–11. doi: 10.3923/ijds.2017.1.11

Proudhon, C., Duffié, R., Ajjan, S., Cowley, M., Iranzo, J., Carbajosa, G., et al. (2012). Protection against de novo methylation is instrumental in maintaining parent-of-origin methylation inherited from the gametes. *Mol. Cell.* 47, 909–920. doi: 10.1016/j.molcel.2012.07.010

Qiang, W., Guo, H., Li, Y., Shi, J., Yin, X., and Qu, J. (2018). Methylation analysis of CMTM3 and DUSP1 gene promoters in high-quality brush hair in the yangtze river delta white goat. *Gene* 668, 166–173. doi: 10.1016/j.gene.2018.05.031

Quan, H., Yang, Y., Liu, S., Tian, H., Xue, Y., and Gao, Y. Q. (2020). Chromatin structure changes during various processes from a DNA sequence view. *Curr. Opin. Struct. Biol.* 62, 1–8. doi: 10.1016/j.sbi.2019.10.010

Raddatz, G., Guzzardo, P. M., Olova, N., Fantappié, M. R., Rampp, M., Schaefer, M., et al. (2013). Dnmt2-dependent methylomes lack defined DNA methylation patterns. *Proc. Natl. Acad. Sci. U.S.A.* 110, 8627–8631. doi: 10.1073/pnas.1306723110

Rahat, B., Ali, T., Sapehia, D., Mahajan, A., and Kaur, J. (2020). Circulating cell-free nucleic acids as epigenetic biomarkers in precision medicine. *Front. Genet.* 11:844. doi: 10.3389/fgene.2020.00844

Rahman, M. B., Schellander, K., Luceño, N. L., and Van Soom, A. (2018). Heat stress responses in spermatozoa: Mechanisms and consequences for cattle fertility. *Theriogenology* 113, 102–112. doi: 10.1016/j.theriogenology.2018.02.012

Razin, A., and Kantor, B. (2005). DNA methylation in epigenetic control of gene expression. *Prog. Mol. Subcell. Biol.* 38, 151–167. doi: 10.1007/3-540-27310-7_6

Remnant, E. J., Ashe, A., Young, P. E., Buchmann, G., Beekman, M., Allsopp, M. H., et al. (2016). Parent-of-origin effects on genome-wide DNA methylation in the Cape honey bee (*Apis mellifera* capensis) may be confounded by allele-specific methylation. *BMC Genomics* 17:226. doi: 10.1186/s12864-016-2506-8

Rivera, R. M. (2020). Consequences of assisted reproductive techniques on the embryonic epigenome in cattle. *Reprod. Fertil. Dev.* 32, 65–81. doi: 10.1071/rd19276

Roma-Rodrigues, C., Rivas-García, L., Baptista, P. V., and Fernandes, A. R. (2020). Gene therapy in cancer treatment: why go nano? *Pharmaceutics* 12:233. doi: 10.3390/pharmaceutics12030233

Sabin, L. R., Delás, M. J., and Hannon, G. J. (2013). Dogma derailed: the many influences of RNA on the genome. *Mol. Cell.* 49, 783–794. doi: 10.1016/j.molcel.2013.02.010

Saeed, M., Babazadeh, D., Naveed, M., Arain, M. A., Hassan, F. U., and Chao, S. (2017). Reconsidering betaine as a natural anti-heat stress agent in poultry industry: a review. *Trop. Anim. Health Prod.* 49, 1329–1338. doi: 10.1007/s11250-017-1355-z

Safi-Stibler, S., and Gabory, A. (2019). *Epigenetics and the Developmental Origins of Health and Disease: Parental Environment Signalling to the Epigenome, Critical Time Windows and Sculpting the Adult Phenotype*. Amsterdam: Elsevier.

Sajjanar, B., Trakooljul, N., Wimmers, K., and Ponsuksili, S. (2019). DNA methylation analysis of porcine mammary epithelial cells reveals differentially methylated loci associated with immune response against *Escherichia coli* challenge. *BMC Genomics* 20:623. doi: 10.1186/s12864-019-5976-7

Salilew-Wondim, D., Saeed-Zidane, M., Hoelker, M., Gebremedhn, S., Poirier, M., Pandey, H. O., et al. (2018). Genome-wide DNA methylation patterns of bovine blastocysts derived from in vivo embryos subjected to in vitro culture before, during or after embryonic genome activation. *BMC Genomics* 19:424. doi: 10.1186/s12864-018-4826-3

Sandoval, J., Heyn, H., Moran, S., Serra-Musach, J., Pujana, M. A., Bibikova, M., et al. (2011). Validation of a DNA methylation microarray for 450,000 CpG sites in the human genome. *Epigenetics* 6, 692–702. doi: 10.4161/epi.6.6.16196

Sarah-Anne, D., Mersch, M., Foissac, S., Collin, A., Pitel, F., and Coustham, V. (2017). Genome-wide epigenetic studies in chicken: a review. *Epigenomes* 1:20. doi: 10.3390/epigenomes1030020

Saxonov, S., Berg, P., and Brutlag, D. L. (2006). A genome-wide analysis of CpG dinucleotides in the human genome distinguishes two distinct classes of promoters. *Proc. Natl. Acad. Sci. U.S.A.* 103, 1412–1417. doi: 10.1073/pnas.0510310103

Schmauss, C. (2017). The roles of class I histone deacetylases (HDACs) in memory, learning, and executive cognitive functions: a review. *Neurosci. Biobehav. Rev.* 83, 63–71. doi: 10.1016/j.neubiorev.2017.10.004

Schmitz, R. J., Lewis, Z. A., and Goll, M. G. (2019). DNA methylation: shared and divergent features across eukaryotes. *Trends Genet.* 35, 818–827. doi: 10.1016/j.tig.2019.07.007

Schmitz, R. J., Schultz, M. D., Lewsey, M. G., O'Malley, R. C., Urich, M. A., Libiger, O., et al. (2011). Transgenerational epigenetic instability is a source of novel methylation variants. *Science* 334, 369–373. doi: 10.1126/science.1212959

Scott, C. (2018). Sustainably sourced junk food? Big food and the challenge of sustainable diets. *Glob. Environ. Polit.* 18, 93–113. doi: 10.1162/glep_a_00458

Sevane, N., Martínez, R., and Bruford, M. W. (2019). Genome-wide differential DNA methylation in tropically adapted Creole cattle and their Iberian ancestors. *Anim. Genet.* 50, 15–26. doi: 10.1111/age.12731

Shah, S. M., and Chauhan, M. S. (2019). Modern biotechnological tools for enhancing reproductive efficiency in livestock. *Indian J. Genet.* 79(1 Suppl. 241), 249.

Shanmugam, M. K., Arfuso, F., Arumugam, S., Chinnathambi, A., Jinsong, B., Warrier, S., et al. (2018). Role of novel histone modifications in cancer. *Oncotarget* 9, 11414–11426.

Shayevitch, R., Askayo, D., Keydar, I., and Ast, G. (2018). The importance of DNA methylation of exons on alternative splicing. *RNA* 24, 1351–1362. doi: 10.1261/rna.064865.117

Shukla, S., Kavak, E., Gregory, M., Imashimizu, M., Shutinoski, B., Kashlev, M., et al. (2011). CTCF-promoted RNA polymerase II pausing links DNA methylation to splicing. *Nature* 479, 74–79. doi: 10.1038/nature10442

Silva, L. G., Ferguson, B. S., Avila, A. S., and Faciola, A. P. (2018). Sodium propionate and sodium butyrate effects on histone deacetylase (HDAC) activity, histone acetylation, and inflammatory gene expression in bovine mammary epithelial cells. *J. Anim. Sci.* 96, 5244–5252.

Singh, K., Erdman, R. A., Swanson, K. M., Molenaar, A. J., Maqbool, N. J., Wheeler, T. T., et al. (2010). Epigenetic regulation of milk production in dairy cows. *J. Mammary Gland. Biol. Neoplasia* 15, 101–112.

Singh, K., Molenaar, A., Swanson, K., Gudex, B., Arias, J., Erdman, R., et al. (2011). Epigenetics: a possible role in acute and transgenerational regulation of dairy cow milk production. *Animal* 6, 375–381. doi: 10.1017/s1751731111002564

Sistare, F., and DeGeorge, J. (2007). Preclinical predictors of clinical safety: opportunities for improvement. *Clin. Pharmacol. Ther.* 82, 210–214. doi: 10.1038/sj.clpt.6100243

Skibiel, A., Peñagaricano, F., Amorín, R., Ahmed, B., Dahl, G., and Laporta, J. (2018). In utero heat stress alters the offspring epigenome. *Sci. Rep.* 8:14609.

Skinner, M. K. (2011). Environmental epigenetic transgenerational inheritance and somatic epigenetic mitotic stability. *Epigenetics* 6, 838–842. doi: 10.4161/epi.6.7.16537

Skinner, M. K., Guerrero-Bosagna, C., and Haque, M. M. (2015). Environmentally induced epigenetic transgenerational inheritance of sperm epimutations promote genetic mutations. *Epigenetics* 10, 762–771. doi: 10.1080/15592294.2015.1062207

Skinner, M. K., Maamar, M. B., Sadler-Riggleman, I., Beck, D., Nilsson, E., McBirney, M., et al. (2018). Alterations in sperm DNA methylation, non-coding RNA and histone retention associate with DDT-induced epigenetic transgenerational inheritance of disease. *Epigenetics Chromatin* 11, 1–24. doi: 10.1080/15592294.2020.1853319

Sleutels, F., Zwart, R., and Barlow, D. P. (2002). The non-coding Air RNA is required for silencing autosomal imprinted genes. *Nature* 415, 810–813. doi: 10.1038/415810a

Smith, J., Sen, S., Weeks, R. J., Eccles, M. R., and Chatterjee, A. (2020). Promoter DNA hypermethylation and paradoxical gene activation. *Trends Cancer* 6, 392–406. doi: 10.1016/j.trecan.2020.02.007

Sokpor, G., Xie, Y., Rosenbusch, J., and Tuoc, T. (2017). Chromatin remodeling BAF (SWI/SNF) complexes in neural development and disorders. *Front. Mol. Neurosci.* 10:243. doi: 10.3389/fnmol.2017.00243

Soler-Botija, C., Gálvez-Montón, C., and Bayes Genis, A. (2019). Epigenetic biomarkers in cardiovascular diseases. *Front. Genet.* 10:950. doi: 10.3389/fgene.2019.00950

Song, J. (2016). Genome-wide assessment of inbred chicken lines indicates epigenetics signatures of resistance to Marek's disease. *J. Anim. Sci.* 94:47. doi: 10.2527/jas2016.94supplement447x

Song, M., He, Y., Zhou, H., Zhang, Y., Li, X., and Yu, Y. (2016). Combined analysis of DNA methylome and transcriptome reveal novel candidate genes with susceptibility to bovine *Staphylococcus aureus* subclinical mastitis. *Sci. Rep.* 6:29390.

Sørensen, J. T., Winckler, C., Wallenbeck, A., Spengler, A., Knierim, U., Kargo, M., et al. (2018). *Improving Animal Health and Welfare in Organic Cattle Milk Production through Breeding and Management*. Aarhus: Aarhus University.

Spain, M. M., Ansari, S. A., Pathak, R., Palumbo, M. J., Morse, R. H., and Govind, C. K. (2014). The RSC complex localizes to coding sequences to regulate Pol II and histone occupancy. *Mol. Cell.* 56, 653–666. doi: 10.1016/j.molcel.2014.10.002

Srivastava, R., Singh, U. M., and Dubey, N. K. (2016). Histone Modifications by different histone modifiers: insights into histone writers and erasers during chromatin modification. *J. Biol. Sci. Med.* 2, 45–54.

Stachowiak, M., Szymanski, M., Ornoch, A., Jancewicz, I., Rusetska, N., Chrzan, A., et al. (2020). SWI/SNF chromatin remodeling complex and glucose metabolism are deregulated in advanced bladder cancer. *IUBMB Life* 72, 1175–1188. doi: 10.1002/iub.2254

Su, Y., Fan, Z., Wu, X., Li, Y., Wang, F., Zhang, C., et al. (2016). Genome-wide DNA methylation profile of developing deciduous tooth germ in miniature pigs. *BMC Genomics* 17:134. doi: 10.1186/s12864-016-2485-9

Sun, X., Hota, S. K., Zhou, Y.-Q., Novak, S., Miguel-Perez, D., Christodoulou, D., et al. (2018). Cardiac-enriched BAF chromatin-remodeling complex subunit Baf60c regulates gene expression programs essential for heart development and function. *Biol. Open* 7:bio029512. doi: 10.1242/bio.029512

Sun, X., Li, J., Fu, L., Jiang, J., Zhao, J., and Wang, G. (2019). The epigenetic modification in mammals under heat stress. *World J. Vet. Sci.* 1:1005.

Szymczak, S., Dose, J., Torres, G. G., Heinsen, F.-A., Venkatesh, G., Datlinger, P., et al. (2020). DNA methylation QTL analysis identifies new regulators of human longevity. *Hum. Mol. Genet.* 29, 1154–1167. doi: 10.1093/hmg/ddaa033

Takeda, K., Kobayashi, E., Nishino, K., Imai, A., Adachi, H., Hoshino, Y., et al. (2019). Age-related changes in DNA methylation levels at CpG sites in bull spermatozoa and in vitro fertilization-derived blastocyst-stage embryos revealed by combined bisulfite restriction analysis. *J. Reprod. Dev.* 65, 305–312. doi: 10.1262/jrd.2018-146

Tal, O., Kisdi, E., and Jablonka, E. (2010). Epigenetic contribution to covariance between relatives. *Genetics* 184, 1037–1050. doi: 10.1534/genetics.109.112466

Tanić, M., and Beck, S. (2017). Epigenome-wide association studies for cancer biomarker discovery in circulating cell-free DNA: technical advances and challenges. *Curr. Opin. Genet. Dev.* 42, 48–55. doi: 10.1016/j.gde.2017.01.017

Te Pas, M. F., Lebret, B., and Oksbjerg, N. (2017). Measurable biomarkers linked to meat quality from different pig production systems. *Arch. Tierz.* 60, 271–283. doi: 10.5194/aab-60-271-2017

Thompson, R. P., Nilsson, E., and Skinner, M. K. (2020). Environmental epigenetics and epigenetic inheritance in domestic farm animals. *Anim. Reprod. Sci.* 220:106316. doi: 10.1016/j.anireprosci.2020.106316

Tian, P., Luo, Y., Li, X., Tian, J., Tao, S., Hua, C., et al. (2017). Negative effects of long-term feeding of high-grain diets to lactating goats on milk fat production and composition by regulating gene expression and DNA methylation in the mammary gland. *J. Anim. Sci. Biotechnol.* 8:74.

Treppendahl, M. B., Kristensen, L. S., and Grønbæk, K. (2016). Chapter 5 – Biomarkers and methodologies for monitoring epigenetic drug effects in cancer," in *Epigenetic Biomarkers and Diagnostics*, ed. J. L. García-Giménez (Boston, MA: Academic Press), 91–118. doi: 10.1016/B978-0-12-801899-6.00005-X

Triantaphyllopoulos, K. A., Ikonomopoulos, I., and Bannister, A. J. (2016). Epigenetics and inheritance of phenotype variation in livestock. *Epigenetics Chromatin* 9:31.

Usman, T., Yu, Y., and Wang, Y. (2016). CD4 promoter hyper methylation is associated with lower gene expression in clinical mastitis cows and vice versa in the healthy controls. *J. Anim. Sci.* 94, 38–38. doi: 10.2527/jas2016.94supplement438x

Van Eenennaam, A. L. (2019). Application of genome editing in farm animals: Cattle. *Transgenic Res.* 28, 93–100. doi: 10.1007/s11248-019-00141-6

Vanselow, J., Yang, W., Herrmann, J., Zerbe, H., Schuberth, H.-J., Petzl, W., et al. (2006). DNA-remethylation around a STAT5-binding enhancer in the αS1-casein promoter is associated with abrupt shutdown of αS1-casein synthesis during acute mastitis. *J. Mol. Endocrinol.* 37, 463–477. doi: 10.1677/jme.1.02131

Varley, K. E., Gertz, J., Bowling, K. M., Parker, S. L., Reddy, T. E., Pauli-Behn, F., et al. (2013). Dynamic DNA methylation across diverse human cell lines and tissues. *Genome Res.* 23, 555–567. doi: 10.1101/gr.147942.112

Veland, N., Lu, Y., Hardikar, S., Gaddis, S., Zeng, Y., Liu, B., et al. (2019). DNMT3L facilitates DNA methylation partly by maintaining DNMT3A stability in mouse embryonic stem cells. *Nucleic Acids Res.* 47, 152–167. doi: 10.1093/nar/gky947

Vinoth, A., Thirunalasundari, T., Shanmugam, M., Uthrakumar, A., Suji, S., and Rajkumar, U. (2018). Evaluation of DNA methylation and mRNA expression of heat shock proteins in thermal manipulated chicken. *Cell Stress Chaperones* 23, 235–252. doi: 10.1007/s12192-017-0837-2

Vojta, A., Dobrinić, P., Tadić, V., Bočkor, L., Korać, P., Julg, B., et al. (2016). Repurposing the CRISPR-Cas9 system for targeted DNA methylation. *Nucleic Acids Res.* 44, 5615–5628. doi: 10.1093/nar/gkw159

Wang, F., Li, J., Li, Q., Liu, R., Zheng, M., Wang, Q., et al. (2017a). Changes of host DNA methylation in domestic chickens infected with *Salmonella enterica*. *J. Genet.* 96, 545–550. doi: 10.1007/s12041-017-0818-3

Wang, H., Shi, H., Luo, J., Yi, Y., Yao, D., Zhang, X., et al. (2017b). MiR-145 regulates lipogenesis in goat mammary cells via targeting INSIG1 and epigenetic regulation of lipid-related genes. *J. Cell. Physiol.* 232, 1030–1040. doi: 10.1002/jcp.25499

Wang, H., Wang, J., Ning, C., Zheng, X., Fu, J., Wang, A., et al. (2017c). Genome-wide DNA methylation and transcriptome analyses reveal genes involved in immune responses of pig peripheral blood mononuclear cells to poly I: C. *Sci. Rep.* 7:9709.

Wang, H., Wu, J., Wu, S., Wu, S., and Bao, W. (2017d). DNA methylation differences of the BPI promoter among pig breeds and the regulation of gene expression. *RSC Adv.* 7, 48025–48030. doi: 10.1039/c7ra05549h

Wang, J., Chen, J., Zhang, J., Gao, B., Bai, X., Lan, Y., et al. (2017e). Castration-induced changes in the expression profiles and promoter methylation of the GHR gene in Huainan male pigs. *Anim. Sci. J.* 88, 1113–1119. doi: 10.1111/asj.12739

Wang, X., Wang, Z., Wang, Q., Wang, H., Liang, H., and Liu, D. (2017f). Epigenetic modification differences between fetal fibroblast cells and mesenchymal stem cells of the Arbas Cashmere goat. *Res. Vet. Sci.* 114, 363–369. doi: 10.1016/j.rvsc.2017.07.007

Wang, Y., Luo, M., Jiang, M., Lin, Y., and Zhu, J. (2017g). Comparative analysis of tissue expression and methylation reveals the crucial hypoxia genes in hypoxia-resistant animals. *Can. J. Anim. Sci.* 98, 204–212.

Wang, H., Liu, Z., Wang, Y., Ma, L., Zhang, W., and Xu, B. (2020a). Genome-wide differential DNA methylation in reproductive, morphological, and visual system differences between queen bee and worker Bee (*Apis mellifera*). *Front. Genet.* 11:770. doi: 10.3389/fgene.2020.00770

Wang, M., Feng, S., Ma, G., Miao, Y., Zuo, B., Ruan, J., et al. (2020b). Whole-genome methylation analysis reveals epigenetic variation in cloned and donor pigs. *Front. Genet.* 11:23. doi: 10.3389/fgene.2020.00023

Wang, M., Liang, Y., Ibeagha-awemu, M. E., Li, M., Zhang, H., Chen, Z., et al. (2020c). Genome-wide DNA methylation analysis of mammary gland tissues from Chinese holstein cows with *Staphylococcus aureus* induced mastitis. *Front. Genet.* 19:1295.

Wang, S., Li, F., Liu, J., Zhang, Y., Zheng, Y., Ge, W., et al. (2020d). Integrative analysis of methylome and transcriptome reveals the regulatory mechanisms of hair follicle morphogenesis in cashmere goat. *Cells* 9:969. doi: 10.3390/cells9040969

Wang, X., Qu, J., Li, J., He, H., Liu, Z., and Huan, Y. (2020e). Epigenetic reprogramming during somatic cell nuclear transfer: recent progress and future directions. *Front. Genet.* 11:205. doi: 10.3389/fgene.2020.00205

Wang, Y., Zheng, Y., Guo, D., Zhang, X., Guo, S., Hui, T., et al. (2020f). m6A methylation analysis of differentially expressed genes in skin tissues of coarse and fine type liaoning cashmere goats. *Front. Genet.* 10:1318. doi: 10.3389/fgene.2019.01318

Wang, H., Yang, L., Qu, H., Feng, H., Wu, S., and Bao, W. (2019). Global mapping of H3K4 trimethylation (H3K4me3) and transcriptome analysis reveal genes involved in the response to epidemic diarrhea virus infections in pigs. *Animals* 9:523. doi: 10.3390/ani9080523

Wang, L., Sun, H., Guan, L., and Liu, J. (2019). Relationship of blood DNA methylation rate and milk performance in dairy cows. *J. Dairy Sci.* 102, 5208–5211. doi: 10.3168/jds.2018-15869

Wang, J., Bian, Y., Wang, Z., Li, D., Wang, C., Li, Q., et al. (2014). MicroRNA-152 regulates DNA methyltransferase 1 and is involved in the development and lactation of mammary glands in dairy cows. *PLoS One* 9:e101358. doi: 10.1371/journal.pone.0101358

Wang, J., Yan, X., Nesengani, L. T., Ding, H., Yang, L., and Lu, W. (2018). LPS-induces IL-6 and IL-8 gene expression in bovine endometrial cells "through DNA methylation". *Gene* 677, 266–272. doi: 10.1016/j.gene.2018.07.074

Wang, X., Zhang, Y., He, Y. H., Ma, P. P., Fan, L. J., Wang, Y. C., et al. (2013). Aberrant promoter methylation of the CD4 gene in peripheral blood cells of mastitic dairy cows. *Genet. Mol. Res.* 12, 6228–6239. doi: 10.4238/2013.december.4.10

Wang, X., and Kadarmideen, H. (2019a). Genome-wide DNA methylation analysis using next-generation sequencing to reveal candidate genes responsible for boar taint in pigs. *Anim. Genet.* 50, 644–659. doi: 10.1111/age.12842

Wang, X., and Kadarmideen, H. (2019b). "Genome-wide DNA methylation profiles of pig testis reveal epigenetic markers/genes for boar taint," in *Proceedings of the 70th Annual Meeting of the European Federation of Animal Science*, (Rome: EAAP).

Wang, X., and Kadarmideen, H. N. (2019c). An epigenome-wide DNA methylation map of testis in pigs for study of complex traits. *Front. Genet.* 10:405. doi: 10.3389/fgene.2019.00405

Wapinski, O. L., Vierbuchen, T., Qu, K., Lee, Q. Y., Chanda, S., Fuentes, D. R., et al. (2013). Hierarchical mechanisms for direct reprogramming of fibroblasts to neurons. *Cell* 155, 621–635. doi: 10.1016/j.cell.2013.09.028

Wara, A. B., Chhotaray, S., Shafi, B. U. D., Panda, S., Tarang, M., Yosuf, S., et al. (2019). Role of miRNA signatures in health and productivity of livestock. *Int. J. Curr. Microbiol. App. Sci.* 8, 727–738. doi: 10.20546/ijcmas.2019.804.079

Waterman, R., Geary, T., Petersen, M., and MacNeil, M. (2017). Effects of reduced in utero and post-weaning nutrition on milk yield and composition in primiparous beef cows. *Animal* 11, 84–90. doi: 10.1017/s1751731116001257

Weber, M., Hellmann, I., Stadler, M. B., Ramos, L., Pääbo, S., Rebhan, M., et al. (2007). Distribution, silencing potential and evolutionary impact of promoter DNA methylation in the human genome. *Nat. Genet.* 39, 457–466. doi: 10.1038/ng1990

Wedd, L., and Maleszka, R. (2016). DNA methylation and gene regulation in honeybees: from genome-wide analyses to obligatory epialleles. *Adv. Exp. Med. Biol.* 45, 193–211. doi: 10.1007/978-3-319-43624-1_9

Wei, D., Li, A., Zhao, C., Wang, H., Mei, C., Khan, R., et al. (2018). Transcriptional regulation by CpG sites methylation in the core promoter region of the bovine SIX1 gene: roles of histone H4 and E2F2. *Int. J. Mol. Sci.* 19:213. doi: 10.3390/ijms19010213

Wei, J.-W., Huang, K., Yang, C., and Kang, C.-S. (2017). Non-coding RNAs as regulators in epigenetics. *Oncol. Rep.* 37, 3–9.

Weksberg, R., Shuman, C., Wilkins-Haug, L., Mann, M., Croughan, M., Stewart, D., et al. (2007). Workshop report: evaluation of genetic and epigenetic risks associated with assisted reproductive technologies and infertility. *Fertil. Steril.* 88, 27–31. doi: 10.1016/j.fertnstert.2006.11.114

World Health Organization [WHO] (2001). *Biomarkers in Risk Assessment: Validity and Vlidation-Environmental Health Criteria 222*. Geneva: WHO.

Wu, H., and Zhang, Y. (2014). Reversing DNA methylation: mechanisms, genomics, and biological functions. *Cell* 156, 45–68. doi: 10.1016/j.cell.2013.12.019

Wu, J., Zhang, W., and Li, C. (2020a). Recent advances in genetic and epigenetic modulation of animal exposure to high temperature. *Front. Genet.* 11:e653. doi: 10.3389/fgene.2020.00653

Wu, Y., Chen, J., Sun, Y., Dong, X., Wang, Z., Chen, J., et al. (2020b). PGN and LTA from *Staphylococcus aureus* induced inflammation and decreased lactation through regulating DNA methylation and histone H3 acetylation in bovine mammary epithelial cells. *Toxins* 12:238. doi: 10.3390/toxins12040238

Wu, Y., Sun, Y., Dong, X., Chen, J., Wang, Z., Chen, J., et al. (2020c). The synergism of PGN, LTA and LPS in inducing transcriptome changes, inflammatory responses and a decrease in lactation as well as the associated epigenetic mechanisms in bovine mammary epithelial cells. *Toxins* 12:387. doi: 10.3390/toxins12060387

Wu, S. C., and Zhang, Y. (2010). Active DNA demethylation: many roads lead to Rome. *Nat. Rev. Mol. Cell Biol.* 11, 607–620. doi: 10.1038/nrm2950

Wu, X., and Zhang, Y. (2017). TET-mediated active DNA demethylation: mechanism, function and beyond. *Nat. Rev. Genet.* 18:517. doi: 10.1038/nrg.2017.33

Wyck, S., Herrera, C., Requena, C. E., Bittner, L., Hajkova, P., Bollwein, H., et al. (2018). Oxidative stress in sperm affects the epigenetic reprogramming in early embryonic development. *Epigenetics Chromatin* 11:60.

Xiao, P., Zhong, T., Liu, Z., Ding, Y., Guan, W., He, X., et al. (2019). Integrated analysis of methylome and transcriptome changes reveals the underlying regulatory signatures driving the curly wool transformation in Chinese Zhongwei goat. *Front. Genet.* 10:1263. doi: 10.3389/fgene.2019.01263

Xing, J., and Jiang, Y. (2012). Effect of dietary betaine supplementation on mRNA level of lipogenesis genes and on promoter CpG methylation of fatty acid synthase (FAS) gene in laying hens. *Afr. J. Biotechnol.* 11, 6633–6640.

Xu, T., Seyfert, H., and Shen, X. (2018). Epigenetic mechanisms contribute to decrease stearoyl-CoA desaturase 1 expression in the liver of dairy cows after prolonged feeding of high-concentrate diet. *J. Dairy Sci.* 101, 2506–2518. doi: 10.3168/jds.2017-12878

Xue, J., Schoenrock, S. A., Valdar, W., Tarantino, L. M., and Ideraabdullah, F. Y. (2016). Maternal vitamin D depletion alters DNA methylation at imprinted loci in multiple generations. *Clin. Epigenetics* 8:107.

Yagound, B., Smith, N. M., Buchmann, G., Oldroyd, B. P., and Remnant, E. J. (2019). Unique DNA methylation profiles are associated with cis-variation in honey bees. *Genome Biol. Evol.* 11, 2517–2530. doi: 10.1093/gbe/evz177

Yakovlev, A. (2018). Epigenetic effects in livestock breeding. *Russ. J. Genet.* 54, 897–909. doi: 10.1134/s1022795418080148

Yang, X., Han, H., De Carvalho, D. D., Lay, F. D., Jones, P. A., and Liang, G. (2014). Gene body methylation can alter gene expression and is a therapeutic target in cancer. *Cancer Cell* 26, 577–590. doi: 10.1016/j.ccr.2014.07.028

Yang, Y., Yamada, T., Hill, K. K., Hemberg, M., Reddy, N. C., Cho, H. Y., et al. (2016a). Chromatin remodeling inactivates activity genes and regulates neural coding. *Science* 353, 300–305. doi: 10.1126/science.aad4225

Yang, Y., Zhou, R., Mu, Y., Hou, X., Tang, Z., and Li, K. (2016b). Genome-wide analysis of DNA methylation in obese, lean, and miniature pig breeds. *Sci. Rep.* 6:30160.

Yang, Z., Yang, H., Gong, D., Rose, S., Pirgozliev, V., Chen, X., et al. (2018). Transcriptome analysis of hepatic gene expression and DNA methylation in

methionine-and betaine-supplemented geese (*Anser cygnoides* domesticus). *Poult. Sci.* 97, 3463–3477. doi: 10.3382/ps/pey242

Ye, J., Wu, W., Li, Y., and Li, L. (2017). Influences of the gut microbiota on DNA methylation and histone modification. *Dig. Dis. Sci.* 62, 1155–1164. doi: 10.1007/s10620-017-4538-6

Ye, Y., Wu, H., Chen, K., Clapier, C. R., Verma, N., Zhang, W., et al. (2019). Structure of the RSC complex bound to the nucleosome. *Science* 366, 838–843.

Yearim, A., Gelfman, S., Shayevitch, R., Melcer, S., Glaich, O., Mallm, J.-P., et al. (2015). HP1 is involved in regulating the global impact of DNA methylation on alternative splicing. *Cell Rep.* 10, 1122–1134. doi: 10.1016/j.celrep.2015.01.038

Yin, Y., Morgunova, E., Jolma, A., Kaasinen, E., Sahu, B., Khund-Sayeed, S., et al. (2017). Impact of cytosine methylation on DNA binding specificities of human transcription factors. *Science* 356:eaaj2239. doi: 10.1126/science.aaj2239

Yu, X.-X., Liu, Y.-H., Liu, X.-M., Wang, P.-C., Liu, S., Miao, J.-K., et al. (2018). Ascorbic acid induces global epigenetic reprogramming to promote meiotic maturation and developmental competence of porcine oocytes. *Sci. Rep.* 8:6132.

Zeng, C., Stroup, E. K., Zhang, Z., Chiu, B. C.-H., and Zhang, W. (2019). Towards precision medicine: advances in 5-hydroxymethylcytosine cancer biomarker discovery in liquid biopsy. *Cancer Commun.* 39:12. doi: 10.1186/s40880-019-0356-x

Zglejc-Waszak, K., Waszkiewicz, E., and Franczak, A. (2019). Periconceptional undernutrition affects the levels of DNA methylation in the peri-implantation pig endometrium and in embryos. *Theriogenology* 123, 185–193. doi: 10.1016/j.theriogenology.2018.10.002

Zhang, B., Ban, D., Gou, X., Zhang, Y., Yang, L., Chamba, Y., et al. (2019). Genome-wide DNA methylation profiles in Tibetan and Yorkshire pigs under high-altitude hypoxia. *J. Anim. Sci. Biotechnol.* 10:25.

Zhang, M., Li, D., Zhai, Y., Wang, Z., Ma, X., Zhang, D., et al. (2020). The landscape of DNA methylation associated with the transcriptomic network of intramuscular adipocytes generates insight into intramuscular fat deposition in chicken. *Front. Cell Dev. Biol.* 8:206. doi: 10.3389/fcell.2020.00206

Zhang, M., Yan, F.-B., Li, F., Jiang, K.-R., Li, D.-H., Han, R.-L., et al. (2017). Genome-wide DNA methylation profiles reveal novel candidate genes associated with meat quality at different age stages in hens. *Sci. Rep.* 7:45564.

Zhang, X., Zhang, S., Ma, L., Jiang, E., Xu, H., Chen, R., et al. (2017). Reduced representation bisulfite sequencing (RRBS) of dairy goat mammary glands reveals DNA methylation profiles of integrated genome-wide and critical milk-related genes. *Oncotarget* 8, 115326–115344. doi: 10.18632/oncotarget.23260

Zhang, Y., Li, F., Feng, X., Yang, H., Zhu, A., Pang, J., et al. (2017). Genome-wide analysis of DNA Methylation profiles on sheep ovaries associated with prolificacy using whole-genome Bisulfite sequencing. *BMC Genomics* 18:759. doi: 10.1186/s12864-017-4068-9

Zhang, S., Shen, L., Xia, Y., Yang, Q., Li, X., Tang, G., et al. (2016). DNA methylation landscape of fat deposits and fatty acid composition in obese and lean pigs. *Sci. Rep.* 6:35063.

Zhang, Y., Meng, J., Gao, Y., Zhang, J., Niu, S., Yu, X., et al. (2016). Changes in methylation of genomic DNA from chicken immune organs in response to H5N1 influenza virus infection. *Genet. Mol. Res.* 15:e15037382.

Zhang, Y., Wang, X., Jiang, Q., Hao, H., Ju, Z., Yang, C., et al. (2018a). DNA methylation rather than single nucleotide polymorphisms regulates the production of an aberrant splice variant of IL6R in mastitic cows. *Cell Stress Chaperones* 23, 617–628. doi: 10.1007/s12192-017-0871-0

Zhang, Y., Zhang, X., Shi, J., Tuorto, F., Li, X., Liu, Y., et al. (2018b). Dnmt2 mediates intergenerational transmission of paternally acquired metabolic disorders through sperm small non-coding RNAs. *Nat. Cell Biol.* 20, 535–540. doi: 10.1038/s41556-018-0087-2

Zhao, C., Ji, G., Carrillo, J. A., Li, Y., Tian, F., Baldwin, R. L., et al. (2020). The profiling of DNA methylation and its regulation on divergent tenderness in angus beef cattle. *Front. Genet.* 11:939. doi: 10.3389/fgene.2020.00939

Zhao, Z., and Shilatifard, A. (2019). Epigenetic modifications of histones in cancer. *Genome Biol.* 20:245.

Zhi, D., Aslibekyan, S., Irvin, M. R., Claas, S. A., Borecki, I. B., Ordovas, J. M., et al. (2013). SNPs located at CpG sites modulate genome-epigenome interaction. *Epigenetics* 8, 802–806. doi: 10.4161/epi.25501

Zhou, C. Y., Johnson, S. L., Gamarra, N. I., and Narlikar, G. J. (2016). Mechanisms of ATP-dependent chromatin remodeling motors. *Annu. Rev. Biophys.* 45, 153–181. doi: 10.1146/annurev-biophys-051013-022819

Zhou, Y., Xu, L., Bickhart, D. M., Schroeder, S. G., Connor, E. E., Alexander, L. J., et al. (2016). Reduced representation bisulphite sequencing of ten bovine somatic tissues reveals DNA methylation patterns and their impacts on gene expression. *BMC Genomics* 17:779. doi: 10.1186/s12864-016-3116-1

Zhou, Y., Connor, E. E., Bickhart, D. M., Li, C., Baldwin, R. L., Schroeder, S. G., et al. (2018). Comparative whole genome DNA methylation profiling of cattle sperm and somatic tissues reveals striking hypomethylated patterns in sperm. *GigaScience* 7:giy039.

Zhu, H., Wang, G., and Qian, J. (2016). Transcription factors as readers and effectors of DNA methylation. *Nat. Rev. Genet.* 17, 551–565. doi: 10.1038/nrg.2016.83

**Conflict of Interest:** The authors declare that the research was conducted in the absence of any commercial or financial relationships that could be construed as a potential conflict of interest.

*Copyright © 2021 Her Majesty the Queen in Right of Canada, as represented by the Minister of Agriculture and Agri-Food Canada for the contribution of Mengqi Wang and Eveline M. Ibeagha-Awemu. This is an open-access article distributed under the terms of the Creative Commons Attribution License (CC BY). The use, distribution or reproduction in other forums is permitted, provided the original author(s) and the copyright owner(s) are credited and that the original publication in this journal is cited, in accordance with accepted academic practice. No use, distribution or reproduction is permitted which does not comply with these terms.*

frontiers in Genetics

REVIEW
published: 03 March 2021
doi: 10.3389/fgene.2021.557934

# The Epigenetics of Gametes and Early Embryos and Potential Long-Range Consequences in Livestock Species—Filling in the Picture With Epigenomic Analyses

*Linkai Zhu*[1], *Sadie L. Marjani*[2]* *and Zongliang Jiang*[1]*

[1] AgCenter, School of Animal Sciences, Louisiana State University, Baton Rouge, LA, United States, [2] Department of Biology, Central Connecticut State University, New Britain, CT, United States

OPEN ACCESS

**Edited by:**
Stephanie McKay,
University of Vermont, United States

**Reviewed by:**
Giovanni Chillemi,
University of Tuscia, Italy
George E. Liu,
Agricultural Research Service (USDA), United States

***Correspondence:**
Sadie L. Marjani
sadie.marjani@ccsu.edu
Zongliang Jiang
zjiang@agcenter.lsu.edu

**Specialty section:**
This article was submitted to Livestock Genomics, a section of the journal Frontiers in Genetics

**Received:** 30 April 2020
**Accepted:** 04 February 2021
**Published:** 03 March 2021

**Citation:**
Zhu L, Marjani SL and Jiang Z (2021) The Epigenetics of Gametes and Early Embryos and Potential Long-Range Consequences in Livestock Species—Filling in the Picture With Epigenomic Analyses. Front. Genet. 12:557934. doi: 10.3389/fgene.2021.557934

The epigenome is dynamic and forged by epigenetic mechanisms, such as DNA methylation, histone modifications, chromatin remodeling, and non-coding RNA species. Increasing lines of evidence support the concept that certain acquired traits are derived from environmental exposure during early embryonic and fetal development, i.e., fetal programming, and can even be "memorized" in the germline as epigenetic information and transmitted to future generations. Advances in technology are now driving the global profiling and precise editing of germline and embryonic epigenomes, thereby improving our understanding of epigenetic regulation and inheritance. These achievements open new avenues for the development of technologies or potential management interventions to counteract adverse conditions or improve performance in livestock species. In this article, we review the epigenetic analyses (DNA methylation, histone modification, chromatin remodeling, and non-coding RNAs) of germ cells and embryos in mammalian livestock species (cattle, sheep, goats, and pigs) and the epigenetic determinants of gamete and embryo viability. We also discuss the effects of parental environmental exposures on the epigenetics of gametes and the early embryo, and evidence for transgenerational inheritance in livestock.

**Keywords: epigenetics, sperm, oocytes, embryos, cattle, sheep, goats, pigs**

## INTRODUCTION

The epigenome carries information encoded by DNA methylation, chromatin configuration, histone modifications, and non-coding RNAs. Drastic epigenome reprogramming occurs during gametogenesis and early embryogenesis, leading to the reset of the epigenetic modifications and the conversion of differentiated gametes into a totipotent embryo. The dynamics of this epigenome reprogramming have been extensively studied in rodent models and humans with fewer studies focused on domestic species. Deficiencies in epigenetic remodeling during this time

can cause severe developmental defects, especially in domestic species where assisted reproductive technologies (ARTs) are widely used for research and accelerating genetic selection from genetically superior animals (Sutcliffe et al., 2006). Abnormalities in embryos, fetuses, placentas, and offspring created *in vitro* are thought to be due to improper establishment and/or maintenance of the epigenetic modifications formed during this window (Li et al., 2005; Fernandez-Gonzalez et al., 2010).

Dramatic phenotypic differences have been established and stabilized between livestock breeds by decades and sometimes centuries of selective breeding. These differences include growth rate, presence or absence of horns, muscle characteristics, milk production, heat tolerance, fertility and many others. In some cases, these phenotypic differences can be clearly defined as allelic variations between breeds and are inherited as genetic traits. However, there is phenotypic variation that is not due to underlying sequence differences. In cattle, for example, 32–80% (depending on the trait) of the additive genetic variance can be attributed to genetic variation (e.g., single nucleotide polymorphisms, substitutions) (Haile-Mariam et al., 2013). Thus, there is a missing heritability component (Yang et al., 2010). Furthermore, the interaction of the genotype with environmentally susceptible epigenetic modifications contributes to phenotypic variability and is important to analyze. In many species, there is evidence that environmentally induced epigenetic modifications can persist in future generations serving as a "memory" of past experiences (Daxinger and Whitelaw, 2012; Heard and Martienssen, 2014). Many correlative studies in animal models, such as rats, mice, and even in humans, have suggested various epigenetic factors (e.g., DNA methylation, histone modification, and small RNAs) in germ cells may carry these memories, reviewed in Daxinger and Whitelaw (2012), Heard and Martienssen (2014), Chen et al. (2016b), and Zhang et al. (2019). Numerous studies have looked at the effects of parental environmental exposures on livestock development and production. However, a more limited number of studies in domestic animals have examined the epigenetic mechanisms/modifications responsible, and even fewer have sought to identify transgenerational inheritance.

The development of epigenomic technologies is facilitating the global profiling of germline and embryonic epigenomes, and rapidly improving our understanding of epigenetic regulation and inheritance in a number of species. These achievements provide new areas for the development of promising technologies, or potential management modifications that can neutralize adverse conditions or even improve the performance of livestock. In this review, we outline the current epigenetic characterization of germ cells and embryos in livestock species. We avoid extensive discussion of the epigenetic analysis in model organisms, such as rodents, which have been comprehensively reviewed elsewhere (Smith and Meissner, 2013; Lee et al., 2014; Xu and Xie, 2018; Greenberg and Bourc'his, 2019; Wen and Tang, 2019). We will also discuss studies in livestock species that analyze parental, environmentally induced epigenetics in gametes, the embryo and fetus, and evidence of transgenerational inheritance.

# EPIGENETIC REPROGRAMMING DURING EARLY EMBRYO DEVELOPMENT IN LIVESTOCK SPECIES

## DNA Cytosine Methylation

5-methylcytocine methylation (5mC) is an important epigenetic modification. It plays essential roles in mammalian development as it is crucial in regulating gene expression, genomic imprinting, silencing of repetitive DNA, differentiation, and X chromosome inactivation (Li et al., 1993; Bird, 2002; Jaenisch and Bird, 2003; Hackett et al., 2013). 5mC can conceal gene regulatory regions and recruit transcriptional repressors and/or chromatin modifiers/remodelers, and therefore is mostly involved in gene silencing (Schultz et al., 2015). However, 5mC has been implicated in transactivation if distributed within the gene body as seen in bovine oocytes and placental tissues (Schroeder et al., 2015). TET enzymes can modify 5mC to 5hmC, 5fC, 5caC, which can be considered as epigenetic modifications in their own right (Inoue and Zhang, 2011; Inoue et al., 2011; Wossidlo et al., 2011). Full characterization of these modifications in early embryos is lacking in livestock species.

DNA methylation is relatively stable in differentiated somatic cells, but highly dynamic during the development of primordial germ cell (PGCs) and preimplantation embryos when global DNA methylation patterns are reprogrammed (Saadeh and Schulz, 2014). In the mammalian embryos studied to date, the first reprogramming event takes place post-fertilization and involves widespread and swift demethylation of the paternal genome, followed by a progressive drop in global DNA methylation of the maternal genome as cleavage progresses (Smith et al., 2012, 2014; Guo et al., 2014; Gao et al., 2017; Jiang et al., 2018; Duan et al., 2019). This nadir is followed by global *de novo* methylation (Mayer et al., 2000; Oswald et al., 2000; Santos et al., 2002; Smith et al., 2012; Gao et al., 2017; Jiang et al., 2018; Duan et al., 2019). The second wave of mammalian DNA methylation reprogramming takes place in PGCs where global demethylation and erasure occurs and imprints are formed based on the sex of the fetus (Popp et al., 2010; Guibert et al., 2012; Hackett et al., 2013; Hill et al., 2018).

Most of what is known about the dynamics of 5mC methylation during preimplantation development in domestic species was revealed by immunostaining (Dean et al., 2001; Beaujean et al., 2004; Park et al., 2007; Deshmukh et al., 2011; Dobbs et al., 2013). While immunostaining provides important overall methylation dynamics, it does not provide specific sequence information of the methylated/de-methylated regions. The more sequence-based approach of a DNA methylation microarray was used to analyzed blastocyst stage embryos in porcine (Bonk et al., 2008) and bovine (Salilew-Wondim et al., 2015, 2018; Ispada et al., 2018). Although considerably more specific than immunostaining, microarrays are limited by the finite number of probes used in their construction and do not provide high-level single-nucleotide resolution of methylation status. Numerous studies have also been performed to evaluate the methylation level of selected candidate genes and regulatory regions in bovine and porcine oocytes and embryos (Gebert et al.,

2009; Niemann et al., 2010; Heinzmann et al., 2011; Dobbs et al., 2013; Zhao et al., 2013; O'Doherty et al., 2015; Mattern et al., 2016; Urrego et al., 2017).

Using reduced representative bisulfite sequencing (RRBS), we were the first to report methylome dynamics at single-base resolution in bovine *in vivo* preimplantation embryos (Jiang et al., 2018). It has also been used to assess methylation patterns in many bovine tissues, including the uterus and testes (Zhou et al., 2016). RRBS preferentially selects CpG-rich regions, such as CpG islands, while CpG shores are usually under-represented (Doherty and Couldrey, 2014). These shore regions are known to play important roles in tissue differentiation (Doi et al., 2009). Recently, the development of single-cell whole genome bisulfite sequencing (WGBS) allowed for the reliable and affordable revelation of potentially all CpG sites in a single oocyte or embryo (Smallwood et al., 2014). It also allows for interrogation of 5mC in non-CpG contexts, which are preferentially enriched in oocytes, embryos and stem cells (Lister et al., 2009; Tomizawa et al., 2011) and not clearly mapped in many livestock species. We adopted the WGBS method to further characterize stage-specific genome-wide DNA methylation in bovine sperm, immature oocytes, oocytes matured *in vivo* and *in vitro*, as well as *in vivo* developed single embryos at the 2-, 4-, 8-, and 16-cell stages (Duan et al., 2019). Both studies indicated that the major wave of genome-wide demethylation was completed by the 8-cell stage in bovine embryos. Sequencing-based analyses have profiled the demethylation during preimplantation development in mice (Smallwood et al., 2011; Smith et al., 2012), and primates (Gao et al., 2017) including humans (Guo et al., 2014; Smith et al., 2014). The timing of the major wave of genome-wide demethylation differs from what was observed in bovine embryos, for example, the most marked demethylation occurred at the zygote stage in mice (Smith et al., 2012), at the 2-cell stage in rhesus monkeys (Gao et al., 2017), and at the 4-cell stage in humans (Smith et al., 2012; Guo et al., 2014).

Our analysis also found that sperm and oocytes were differentially methylated in numerous regions (DMRs), which were primarily intergenic, suggesting that these non-coding regions may play important roles in gamete specification. DMRs were also identified between *in vivo* and *in vitro* matured oocytes, reinforcing environmental effects on epigenetic modifications (further discussion of this later). Overall, these characterizations are critical to understanding the epigenetic reprogramming and regulation that occurs during normal, bovine embryonic development *in vivo*, and to providing insight into the epigenetic alterations that occur during *in vitro* maturation (IVM) of oocytes and culture (IVC) of embryos after *in vitro* fertilization (IVF). Importantly, bovine embryos, which are more like human embryos than mouse embryos are in terms of gene expression profiles and developmental timing (Jiang et al., 2014), can serve as a great model for understanding early human development, especially since human *in vivo* embryos are not available for research.

## DNA $N^6$-Adenine Methylation

It was widely accepted that 5mC was the only form of DNA methylation in mammalian genomes and that the other modifications were absent, such as $N^6$-adenine methylation ($N^6$-mA), which is predominantly found in prokaryotes and a limited number of eukaryotes (Heyn and Esteller, 2015). The role $N^6$-mA plays in gene regulation and epigenetic remodeling remains essentially uncharted. With the development of next generation sequencing technologies, $N^6$-mA was found to be present in several eukaryotes, including *C. elegans* (Greer et al., 2015), green algae (Fu et al., 2015), and Drosophila (Zhang et al., 2015). With the advent of more sensitive detection techniques, $N^6$-mA has been more recently identified in *Xenopus laevis* (Koziol et al., 2016), and mammals, i.e., in mouse kidney (Koziol et al., 2016), and embryonic stem cells (ECSs) (Wu T. P. et al., 2016), porcine gametes and embryos (Liu J. et al., 2016), human glioblastoma (Xie et al., 2018), and mouse trophoblast lineages (Li et al., 2020). In pigs, mass spectrometry analysis showed that the $N^6$-mA/A ratio in oocytes (0.09%) was ∼6 times higher than that in sperm. This ratio rose to ∼0.17% from the four-cell to the morula stage and then decreased to 0.05% at the blastocyst stage. However, only a low level of $N^6$-mA was observed in genomic DNA of various adult porcine tissues. These results were also confirmed by immunostaining, which further supports the presence of $N^6$-mA in porcine early embryos (Liu J. et al., 2016). These findings defy the prevalent theory of 5mC as the only form of DNA methylation in the mammalian genome and suggest that $N^6$-mA is conserved and may be important during early development and differentiation (Li et al., 2020). In addition, $N^6$-mA in mammals appears to be a repressor of gene expression, that unlike 5mC, is independent of CpG islands and thus would have increased sequence flexibility. The specificity and dynamics of $N^6$-mA establishment and removal will be crucial for understanding its role in gametes and embryos.

## Chromatin Remodeling

Accessible chromatin delineates regulatory sequences, such as promoters, enhancers, and locus-control regions. Early mammalian embryos experience extensive chromatin remodeling and proper regulation of chromatin state is essential for transcription and preimplantation development (Burton and Torres-Padilla, 2014). However, it has been difficult to explore global chromatin landscape and its dynamics in gametes and early embryos due to the amount of DNA typically required for such analyses. Recently, low input or single-cell assays to profile chromatin remodeling have been developed [DNase-seq, an assay for transposase-accessible chromatin (ATAC-seq), nucleosome occupancy and methylome analysis (NOMe-seq), and 5C-seq or Hi-C] reviewed by Xu and Xie (2018).

These methods have interrogated chromatin configuration from different angles in gametes and early embryos. The dynamics of chromatin accessibility in gametes and early embryos in mice and humans have been extensively analyzed (Lu et al., 2016; Wu J. et al., 2016; Guo et al., 2017; Inoue et al., 2017; Jachowicz et al., 2017; Jung et al., 2017; Wu et al., 2018; Liu L. et al., 2019). Unsurprisingly, these studies have revealed highly active chromatin landscapes during early development. As one would expect, generally, chromatin was more accessible in embryos after embryonic genome activation (EGA). Interestingly, Guo et al. (2017)

reported a more oscillating chromatin state, with chromatin accessibility increasing from gametes to zygotes, followed by a decrease after the late zygote stage, before increasing again in the four-cell embryo. Additionally, by integrating chromatin accessibility with the transcriptome in early embryos, a regulatory network was constructed, and this identified the transcription factors associated with preimplantation development and lineage specification (Wu J. et al., 2016).

Distinct chromatin organizations in gametes and preimplantation embryos have been revealed using the Hi-C approach (Battulin et al., 2015; Du et al., 2017; Flyamer et al., 2017; Jung et al., 2017; Ke et al., 2017). Topologically Associating Domains (TADs) and chromatin compartments in sperm appear to be largely like those in other mammalian cells, such as embryonic stem cells or somatic cells (Battulin et al., 2015; Jung et al., 2017). In oocytes, TADs are present in GV oocytes, but are not observed in MII oocytes (Ke et al., 2017), which makes sense given the transcriptional inactivity at this stage. The re-establishment of TADs after fertilization is slower compared with that observed in somatic cells after division and coincides with EGA (Du et al., 2017; Ke et al., 2017). Allele-specific chromatin architecture was also observed during mammalian embryogenesis. In zygotes, chromatin compartments appear to be absent or faint in the maternal pronucleus, but are evident in the paternal genome (Du et al., 2017; Flyamer et al., 2017; Ke et al., 2017). The 3D chromatin structure across consecutive stages of mouse somatic cell nuclear transfer (SCNT) embryos was also examined using a low-input Hi-C (Chen et al., 2020). This work identified defects in the cloned embryos, specifically stronger TAD boundaries and abnormal interactions between super-enhancers and promoters. Importantly, this research sheds even more light on what is required for successful nuclear reprogramming during SCNT (Chen et al., 2020).

Integrating these datasets from mouse and human gametes and embryos provides a widespread view of the chromatin configuration changes during early embryogenesis. However, the chromatin reorganization in livestock gametes and embryos remains largely unknown. Following our recent efforts to characterize the DNA methylomes of bovine early embryos (Jiang et al., 2018; Duan et al., 2019), we profiled the accessible chromatin in bovine oocytes and early embryos using ATAC-seq (Ming et al., 2020). We generated a high-resolution map of accessible chromatin in bovine oocytes and embryos at the 2-, 4-, 8-cell, morula, blastocyst and elongating stages. We identified distinct gene network programs and transcription factors that differ between *in vivo* and *in vitro* derived blastocysts, which may serve as biomarkers of embryo viability. We also performed an integrative analysis of the transcriptome, DNA methylome and chromatin dynamics and exposed the essential components of the regulatory network controlling bovine early embryonic development. The comprehensive dataset we established will further the understanding of the epigenetic reprogramming that takes place during early bovine embryogenesis. Another characterization of the accessible chromatin in early bovine embryos using the same ATAC-seq approach was recently published (Halstead et al., 2020). Similar to the findings in humans and mice (Lu et al., 2016; Wu J. et al., 2016; Wu et al., 2018), both studies suggest that cattle embryos experience progressive chromatin accessibility during cleavage, which is consistent with the transcriptional activation of the embryonic genome. Interestingly, Halstead et al. (2020) identified a conserved set of maternal factors in mice, cattle and humans that were involved in regulating chromatin remodeling prior to EGA. They also found that the open chromatin regions set during EGA were enriched for homeobox motifs. Overall, open chromatin patterns had significant similarities between cattle and human embryos, providing further evidence that cattle embryos are a good model for human preimplantation development.

## Histone Modifications

Histone modifications are essential for regulating gene expression. Post-translational modifications (PTMs) of histone tails can directly alter the spatial arrangement of nucleosomes on the DNA and the higher-order chromatin structure. Importantly, they can also affect the recruitment of other proteins and complexes onto the chromatin (Kouzarides, 2007). Therefore, the accessibility of chromatin to transcription factors and the subsequent gene expression pattern can be controlled by histone PTMs (Venkatesh and Workman, 2015). Interestingly, histone PTMs can be passed to progeny through gametes (Skvortsova et al., 2018). Conventionally, chromatin immunoprecipitation with high-throughput sequencing (ChIP-seq), which is widely used to survey histone PTMs, requires millions of cells to get high-quality libraries. Modification and improvement of the ChIP-seq methodology and the analysis pipeline [CUT&RUN (Skene and Henikoff, 2017)] has made it possible to retrieve high quality and reproducible data from single cells, reviewed in Xu and Xie (2018). Therefore, it is now feasible to reveal the genome-wide distribution of histone PTMs in gametes and preimplantation embryos.

The reprogramming of histone modifications during early embryo development has been well-established in mice (Dahl et al., 2016; Liu X. et al., 2016; Zhang B. et al., 2016; Zheng et al., 2016; Inoue et al., 2017; Hanna et al., 2018). Both H3K4me3 and H3K27me3 display widespread distal domains in mouse oocytes, which can be inherited in early embryos and regulate zygotic gene expression (Dahl et al., 2016; Zhang B. et al., 2016; Zheng et al., 2016; Inoue et al., 2017). During gametogenesis, distinct histone modifications are established in females and males (Zheng et al., 2016). After fertilization, maternal H3K4me3 from the oocyte is inherited by early embryos, before it is removed upon the start of EGA at the late two-cell stage. By contrast, sperm H3K4me3 and H3K27me3 are quickly removed after fertilization. This is then followed by re-establishment of low-level broad domains across the genome (Zhang B. et al., 2016). Most recently, the remodeling of histone modifications in human early embryo development was reported (Xia et al., 2019). Unlike what is observed in the mouse, the activating mark, H3K4me3, occurs as strong peaks at promoters in human GV oocytes. After fertilization, zygotes displayed widespread H3K4me3 patterns (Xia et al., 2019).

Dynamic changes in histone modifications in gametes and embryos have been widely reported using immunofluorescence in different livestock species, including bovine and porcine (Lepikhov et al., 2008; Ross et al., 2008; Canovas et al., 2012;

Herrmann et al., 2013; Diao et al., 2014; Huang et al., 2015; Xie et al., 2016; Chung et al., 2017; Liu et al., 2018). Recently, Org et al. (2019) published the first genome-wide localization of histone H3K4me3 and H3K27me3 in the inner cell mass (ICM) and trophectoderm (TE) of bovine blastocysts. By linking histone PTM profiling and gene expression, this study revealed similar levels of H3K4me3 and H3K27me3 in both up- and down-regulated genes, respectively, in the ICM. In the TE, however, higher levels of H3K4me3 around promoter regions and lower levels of H3K27me3 across the whole gene region were observed in upregulated genes. The authors suggested that together these two histone modifications exert proactive epigenetic regulation in the TE, but not in the ICM (Org et al., 2019). However, it is important to note that locus specific localization of histone modifications has not been investigated across preimplantation embryo development in livestock species to date.

During epigenetic remodeling of bovine embryos, the enzymes that are responsible for the methylation of H3K9me2, H3K9me3, H3K4me2, H3K4me3, and H3K27me3 are known; they include EHMT1/2, SUV39H1/H2, SETDB1, EZH2, and SMYD3 (McGraw et al., 2007; Ross et al., 2008; Golding et al., 2015; Bai et al., 2016; Zhang et al., 2016b). The expression of enzymes responsible for removal of the methylation from H3K4, H3K9, H3K27 were also characterized in bovine early embryos (Glanzner et al., 2018). KDM6B (JMJD3) is involved in the erasure of H3K27me3 during embryo cleavage. Knockdown of *KDM6B* in bovine oocytes resulted in compromised EGA and reduced development to the blastocyst stage (Canovas et al., 2012; Chung et al., 2017). Likewise, knockdown of *SMYD3*, a H3K4 methyltransferase, in bovine *in vitro* matured oocytes negatively impacted embryo development at the 8-cell stage and beyond and resulted in decreased *NANOG* expression in oocytes, but increased expression in early embryos (Bai et al., 2016).

In porcine embryos, H3K4me2/3 is actively demethylated to the monomethylated form (H3K4me1) from 4-cell to blastocyst stage by lysine-specific histone demethylase 5B (KDM5B, also known as JARID1B or PLU-1), whose expression is elevated during this time frame. Demethylation of H3K4me3 is suggested to be important in maintaining proper H3K4me3 (permissive)/H3K27me3 (repressive) ratio during porcine blastocyst formation (Huang et al., 2015), which is consistent with select genes (e.g., members of homeobox family, etc.) being silenced for proper lineage specification during differentiation (Bernstein et al., 2006). The elaborate balance between H3K4me3 and H3K27me3 is also controlled by KDM6B, which is a H3K27me3 demethylase. *KDM6B* knockout alters gene expression at the 8-cell stage and hampers bovine blastocyst formation (Chung et al., 2017).

## Non-coding RNAs

As sequencing technologies advance, we learn that up to 90% of the eukaryotic genome is transcribed to some extent, while messenger RNAs (mRNAs), which are protein-coding, only account for 1–2% of the total RNA population (Ponting and Belgard, 2010). The remaining "non-coding" RNAs can be classified into "housekeeping" RNAs (e.g., ribosomal RNA, rRNA; transfer RNA, tRNA; small nuclear RNA, snRNA; small nucleolar RNA, snoRNA), and "regulatory" RNAs (e.g., small non-coding RNA, sncRNA; long non-coding RNA, lncRNAs) that are involved in modulating gene expression (Kim and Sung, 2012).

In mammals, the "regulatory" ncRNAs have been found to be actively involved in gametogenesis and early embryo development. PIWI-interacting RNAs (piRNAs) and associated PIWI proteins are rarely found in somatic cells, while they are enriched in male germ cells and comprise the majority of sncRNAs present during spermatogenesis in mice (Deng and Lin, 2002; Kuramochi-Miyagawa et al., 2004). It has been shown that piRNAs are indispensable for spermatogenesis and fertility in mice (Fu and Wang, 2014) probably through their role in the repression of transposons (Carmell et al., 2007), where piRNAs facilitate the *de novo* methylation of transposon-encoding genes, therefore preventing their accumulation (Kuramochi-Miyagawa et al., 2008; De Fazio et al., 2011; Siomi et al., 2011).

It has also been established in mice that besides piRNA populations, miRNAs and siRNAs are also present during spermatogenesis and show stage-specific transcription (Hayashi et al., 2008; Song et al., 2011). Nonetheless, our understanding of miRNA and siRNA functionality of germ cells is rather limited compared to what is known about piRNAs. In mice, disruption of sncRNA biogenesis is associated with defective primordial germ cell proliferation, meiotic progression, spermatid condensation/elongation, and elimination of spermatocytes (Maatouk et al., 2008; Romero et al., 2011; Song et al., 2011; Greenlee et al., 2012; Wu et al., 2012; Zimmermann et al., 2014; Modzelewski et al., 2015). Other roles of sncRNAs in murine spermatogenesis, e.g., heterochromatin formation, transcriptional silencing and DNA damage repair, have been reviewed elsewhere (Hilz et al., 2016). Compared with their role in males, miRNAs and piRNAs seem to be non-essential in later stages of oogenesis and in early embryos, at least in mice (Suh et al., 2010; Hilz et al., 2016). Recent studies suggest that this aspect of the functionality of sncRNAs in mice might be the exception in mammals. For example, studies show that PIWI proteins and piRNAs are present in human, macaque and bovine ovaries, indicating their role of transposon repression in oocytes (Roovers et al., 2015). Of note, PIWIL3, one of the four PIWI proteins in most eutherian mammals, is only found in oocytes and not in the testis in bovine, while this copy is completely lost in mice (Roovers et al., 2015). Thus, it appears that sncRNA functions in gametogenesis diverged during evolution.

Our understanding of ncRNAs during gametogenesis and embryo development in livestock species mainly comes from quantitative RT-PCR analyses (Tesfaye et al., 2009; Tscherner et al., 2014; Gilchrist et al., 2016; Berg and Pfeffer, 2018). However, comprehensive profiling of ncRNAs has been conducted in bovine (Gilchrist et al., 2016; Pasquariello et al., 2017; Cuthbert et al., 2019), porcine (Yang et al., 2012; Zhong et al., 2018), and caprine (Deng et al., 2018; Ling et al., 2019) with high-throughput sequencing-based technology. In cattle, miRNA abundance is elevated at 8-cell stage when the major EGA occurs. Of note, the upregulated miRNAs were predicted to target genes involved in cell development, cell division, Wnt signaling and pluripotency, etc. (Cuthbert et al., 2019). In contrast, piRNAs

were found in bovine oocytes and blastocysts, but not in 8-cell stage embryos. The shift of sncRNA abundance at 8-cell stage alludes to an important role in activating the bovine embryonic genome (Cuthbert et al., 2019). In porcine, lncRNAs have been involved in oocyte maturation, transcriptional regulation of EGA, first lineage segregation and somatic reprogramming to pluripotency (Yang et al., 2012; Zhong et al., 2018). Interestingly, many of the sncRNAs are mapped to annotated repetitive elements (e.g., SINEs and LINEs) in the pig genome, indicating the regulatory function of these elements during early embryo development (Yang et al., 2012). In goats, 5,160 differentially expressed lncRNAs were identified across developmental stages; the extensive association of lncRNA target genes with other key regulatory genes indicates that lncRNAs are indispensable in embryonic development (Ling et al., 2019). However, the functional characterization of sncRNAs during early embryo development and gametogenesis is still limited in livestock species, so how sncRNAs contribute to the overall epigenetic regulation that takes place during this time is unclear.

Overall, epigenome reprogramming is extensively characterized in the mouse, and most recently, in humans. Recent epigenomic studies building on advances in ultra-low input chromatin profiling methods will help to integrate the DNA methylome, chromatin states, histone modifications and non-coding RNAs during early embryo development in livestock. As discussed, research in these areas is emerging on a large scale. It would be very interesting to combine all available datasets to determine the conserved and divergent epigenome reprogramming programs during early embryo development across different mammalian species. Most importantly, it is critical to determine how the different epigenetic mechanisms regulate the transcriptional program, and how different epigenomic reprogramming events interact with each other to secure successful development.

# EPIGENETIC DETERMINANTS OF GAMETE AND EMBRYO VIABILITY

## Epigenetics and Oocyte Viability

Success in *in vitro* embryo production (IVP) relies on successful oocyte collection and optimal oocyte quality (Baruselli et al., 2012). However, manipulation of oocytes by superovulation, IVM, oocyte cryopreservation, etc. influences oocyte competency, largely through the introduction of epigenetic abnormalities. Additionally, environmental stressors can reduce oocyte competence even further. The effects of aging on oocyte quality and associated epigenetic changes have been documented and extensively reviewed in humans (Ge et al., 2015). There is growing interest to identify the epigenetic signatures of gametes, and investigate the key molecular drivers that are perturbed at susceptibility loci leading to aberrant gametes in livestock.

Superovulation and oocyte pick up (OPU) have been widely used in bovine IVP programs to increase the number of oocytes from elite animals for assisted reproduction. As observed in human and mouse studies, superovulation can induce aberrant epigenetic profiles and alter gene expression in oocytes and embryos (Khoueiry et al., 2008; Fauque, 2013). In cattle, oocytes retrieved with or without stimulation showed significantly different expression of genes regulating the cell cycle; overall, more than 50% of the genes studied were upregulated after gonadotropin treatment (Chu et al., 2012). Differential DNA methylation of imprinted loci was also detected in oocytes collected from women and mice after superovulation (Shi and Haaf, 2002; Sato et al., 2007). Limited studies have been carried out on the epigenetic landscape of oocytes retrieved from hormonally primed cows. In one study, divergent DNA methylation patterns were found only in satellite sequences, but not in developmentally important, non-imprinted genes (e.g., *SLC2A1, PRDX1, ZAR*) after FSH and IGF1 treatment (Diederich et al., 2012). To determine the ultimate effect of exogenous hormone on oocyte competence and embryo quality, comprehensive epigenomic studies are needed; however, this is limited by the ability to collect enough naturally ovulated oocytes to serve as proper controls.

Oocyte maturation is relatively efficient *in vitro*, especially in cattle and swine, and is now widely used to generate source material for ARTs and gene editing both for agricultural and basic research applications. However, it is well-established that *in vivo* derived oocytes are much more developmentally competent and capable of normal development at higher rates than those *in vitro* matured (Leibfried-Rutledge et al., 1987; Reik and Maher, 1997; Rizos et al., 2002). In cattle, genome-wide methylation patterns during oocyte maturation *in vivo* and *vitro* have been comprehensively investigated (Jiang et al., 2018; Duan et al., 2019). Global DNA methylation of oocytes appears to be stable during the *in vitro* maturation process; *in vitro* maturation maintained GV oocyte-levels of methylation. Whereas, *in vivo* maturation increased DNA methylation levels in both RRBS and WGBS studies (Jiang et al., 2018; Duan et al., 2019). Interestingly, a significant increase in DNA methylation level was found in *in vivo* matured oocytes compared to *in vitro* matured ones in our RRBS study (Jiang et al., 2018), which only detected the clustered CGs that are mainly located within CpG islands (CGI). However, only a minor increase in DNA methylation level was observed after *in vivo* maturation (Duan et al., 2019), which is consistent with mouse studies (Kono et al., 1996; Smallwood et al., 2011) and most recently found in humans as well (Ye et al., 2020). A total of 801 DMRs associated with 68 genes, were found differentially methylated between *in vivo* and *in vitro* matured oocytes. Interestingly, many of these have not been characterized for their roles in maturation, making them good candidates for gene-specific epigenetic modification studies (Duan et al., 2019). These observations provide the underlying mechanism for the abnormal gene expression and reduced embryo and fetal development when oocytes are matured *in vitro*. Interestingly, imprinted loci (e.g., *H19/IGF2, PEG3, SNRPN*), in which epigenetic aberrations are commonly found in imprinting defects in human, mouse and bovine embryos, showed no or only minor methylation alteration between *in vivo* and *in vitro* matured bovine oocytes. However, their mRNA expression levels were changed when matured *in vitro* (Duan et al., 2019), indicating that regulatory mechanisms other

than DNA methylation may affect these loci and subsequent oocyte competence and developmental potential of embryos (Heinzmann et al., 2011).

IVM culture conditions influence oocyte competence. For example, when a defined maturation medium with three cytokines (FGF2, LIF, and IGF1) dubbed "FLI medium," was used, researchers saw improved nuclear maturation of oocytes derived from immature porcine ovaries and a significant increase in blastocyst rate (Yuan et al., 2017). The introduction of simulated physiological oocyte maturation (SPOM) has substantially improved bovine embryo development *in vitro* (Albuz et al., 2010). Many factors in the culture medium have been identified to be involved in epigenetic signature alteration of *in vitro* matured oocytes, including non-esterified fatty acids (NEFA) (Desmet et al., 2016). In contrast to the changes in DNA methylation during *in vitro* maturation that we previously discussed, histone modifications have shown more dynamic changes. H3K9me2, which is strongly associated with transcription repression and acts as a DNA methylation protector (Nakamura et al., 2012), is present from the GV stage until the end of the maturation period, while H4K12ac, which is associated with active promoters, declines drastically after the break down of the germinal vesicle (Racedo et al., 2009). Unlike DNA methylation, genome-wide histone modification dynamics are not available during *in vitro* maturation, thus ChIP-Seq analyses are necessary to understand the effects of this process.

Oocyte cryopreservation is another routine procedure in IVP. It has been established that vitrification affects cellular structures of oocytes and the developmental potential of embryos (Khalili et al., 2017). Chen H. et al. (2016) showed that DNA methylation and H3K9me3 levels are reduced in the bovine oocytes after vitrification, leading to a drastic decline in blastocyst rate. Given the fact that DNA methylation and H3K9me3 are usually associated with gene silencing and heterochromatin formation (Becker et al., 2016), lower abundance of these two epigenetic modifications indicates a permissive and more relaxed chromatin state. This may lead to aberrant epigenetic regulation and expression of imprinted genes (Chen H. et al., 2016). In another study evaluating the effect of different freezing protocols on DNA methylation levels of bovine oocytes, opposing results were obtained depending on the method, with decreased global DNA methylation in slow freezing and DMSO groups, and elevated DNA methylation with the propylene glycol protocol (Hu et al., 2012). Advanced sequencing-based methods will provide more locus-specific information, and are therefore more instructive in directing future studies and possible protocol modifications.

## Epigenetic Modifications Associated With Sperm Fertility in Livestock Species

Male fertility is critical for livestock reproduction, and is mostly influenced by environmental, management and epigenetic factors. There is a growing interest to develop potent epigenomic biomarkers for bull fertility via a systematic approach by compiling epigenomic datasets and associations with reliable phenotypic data.

It has been proposed that sperm-borne factors (proteins, mRNAs, DNA methylation, histone modification, and miRNAs) are associated with fertility and are indispensable for early embryo development (Ostermeier et al., 2004; Yuan et al., 2016). The current knowledge in humans about the different epigenetic signals in sperm that are responsive to environment and evidence of sperm-borne epigenetic factors is well-reviewed in Donkin and Barres (2018). In cattle, studies using sperm samples from low and high fertility bulls have suggested various sperm factors associated with bull fertility, including sperm proteomics, gene expression, sperm protamine status, macromolecules, metabolomics, superoxide dismutase, and amino acids of seminal plasma (Peddinti et al., 2008; Feugang et al., 2010; Govindaraju et al., 2012a; De Oliveira et al., 2013; Dogan et al., 2015; Grant et al., 2015; Kaya and Memili, 2016; Kutchy et al., 2017, 2019; Velho et al., 2018, 2019; Viana et al., 2018; Menezes et al., 2019; Ugur et al., 2019; Memili et al., 2020).

Epigenetic modifications are reported to be associated with sperm fertility, although the mechanisms governing this process remain unclear. For example, acetylation and methylation of H3K27 (H3K27ac and H3K27me3) in sperm has been correlated with bull fertility (Kutchy et al., 2018). Furthermore, inadequate histone replacement in sperm coincides with reduced fertility in bulls (Dogan et al., 2015). Genome-wide H3K4me2 and H3K27me3 profiles were also analyzed in the sperm of water buffalo bulls with divergent fertility. When comparing buffalo sperm from bulls with high fertility and sub-fertility, a total of 84 genes associated with H3K4me2 and 80 genes associated with H3K27me3 were differentially enriched (Verma et al., 2015).

MicroRNAs can also influence male fertility by regulating gene expression (Govindaraju et al., 2012b). Sperm miR-15a and miR-29b have been reported to be associated with bull fertility (Menezes et al., 2020). When researchers looked at small RNAs in sperm with low and high motility from a single bull by RNA-sequencing, they found altered miRNA and piRNA expression (Capra et al., 2017). The characterization of the epigenome in high and low motility bovine sperm also had methylation variations that affected genes involved chromatin organization (Capra et al., 2019). Profiles of the bull sperm small non-coding RNAs across breeds was most recently characterized and showed that miRNAs make up about 20% of the RNA population. This study also increased the list of known miRNAs in bovine sperm considerably (Sellem et al., 2020).

Recent studies using RRBS and WGBS have fully characterized the bull sperm methylome and identified partially methylated domains and hypomethylated regions unique to sperm when compared to somatic tissues (Perrier et al., 2018; Zhou et al., 2018, 2020; Fang et al., 2019). Additionally, assessment of the DNA methylation of spermatozoa between high and low fertility bulls revealed 76 DMRs (Kropp et al., 2017). These studies provide initial steps toward understanding the roles of small non-coding RNAs and methylation in sperm and fertility.

Due to the inability to conduct *in vitro* spermatogenesis in livestock species, sperm usually experience less environmental stressors than oocytes. For example, stresses during IVM, including oxygen tension, temperature fluctuation, media composition and osmotic stress, could cause epigenetic

alternations in oocytes (El Hajj and Haaf, 2013; Osman et al., 2018). In domestic species, since the establishment of epigenetic modifications has finished before sperm are retrieved and treated for IVP, the chance is much higher that epigenetic defects in the sperm genome come from perturbation during *in vivo* spermatogenesis rather than sperm handling procedures (Urrego et al., 2014). However, adverse conditions may be present in the testis and lead to male infertility by disrupting epigenetic regulation as has been observed in humans (Rajanahally et al., 2019; Sadler-Riggleman et al., 2019). Reactive oxygen species (ROS)-induced oxidative stress is known to cause DNA damage in sperm in mammals (Schieber and Chandel, 2014). A recent study indicates that ROS can also affect the epigenetic reprogramming of sperm after fertilization (Wyck et al., 2018). The AID-TDG mediated base excision repair (BER) pathway has been found to be pivotal for active demethylation of the paternal genome (Kohli and Zhang, 2013). However, in the presence of a DNA lesion, XRCC1, a protein involved in the last step of BER, is recruited to repair the damaged DNA instead of functioning in demethylation; this led to aberrant active demethylation in the male pronucleus of bovine zygotes (Wyck et al., 2018).

## Epigenetics and Embryo Competence

ARTs are widely used to treat human infertility and improve animal production (Sjunnesson, 2019). IVP embryos are also widely used for research and have increasingly become sources of blastocyst transfer in cattle. Moreover, the production of cloned, transgenic and genome-edited animals relies on the *in vitro* production of embryos. More importantly, *in vitro* production of embryos has allowed the elucidation of many important biochemical and molecular processes that occur throughout oocyte maturation, fertilization, and at the different stages of preimplantation embryo development. There is concern that ARTs contribute to developmental failure and long-term epigenetic alterations in the offspring. Environmental perturbations experienced during *in vitro* embryo production can lead to imprinting diseases in humans (Sutcliffe et al., 2006) and large offspring syndrome (LOS) in ruminants (Young et al., 1998; Chen et al., 2013). The underlying mechanisms are largely unknown at present, but alterations in gene expression and epigenetic modifications, largely DNA methylation, during this critical period are thought to be involved in LOS (Wrenzycki and Niemann, 2003; Li et al., 2005; Sutcliffe et al., 2006; Fernandez-Gonzalez et al., 2010). Epigenetic reprogramming also can occur aberrantly in cloned (SCNT) embryos and the incomplete reprogramming of the differentiated somatic cell DNA may contribute to the low efficiency of cloning (Dean et al., 2001). Abnormal epigenetic regulation in cloned embryos has also been discussed (Yang et al., 2007). A comprehensive study comparing both global gene expression patterns and the epigenome of IVP, SCNT-derived livestock embryos to *in vivo* counterparts would be very interesting.

A number of studies have reported that the *in vitro* environment during IVM, IVP and SCNT significantly alters DNA methylation in the embryos in a locus-specific manner (Bourc'his et al., 2001; Dean et al., 2001; Kang et al., 2002; Han et al., 2003; Niemann et al., 2010; Reis e Silva et al., 2012; Smith et al., 2015; Sirard, 2017; Zhao et al., 2020). In bovine SCNT blastocysts, methylation analysis of 41 amplicons associated with 25 developmentally important genes on 15 different chromosomes (a total of 1,079 CpG sites) showed reduced levels of methylation (Niemann et al., 2010). Embryos derived by IVF and SCNT show epigenetic anomalies in DMRs controlling the expression of some imprinted genes, including *SNRPN, H19/IGF2*, and *IGF2R* (Smith et al., 2015). In another study using immunostaining analysis, DNA methylation reprogramming in bovine preimplantation embryos from SCNT and IVF was compared. The results showed that global DNA methylation followed a typical pattern of demethylation and remethylation in IVF preimplantation embryos; however, the genome remained hypermethylated in SCNT preimplantation embryos (Zhang et al., 2016a). Interestingly, the aberrant methylation of satellite 1 regions in bovine SCNT embryos was corrected as embryo development and differentiation takes places (Sawai et al., 2010). By using EmbryoGENE DNA Methylation Array, Salilew-Wondim et al. identified altered DNA methylation in blastocysts collected *in vivo* after being subjected to various time periods of *in vitro* culture, clearly indicating that *in vitro* culture conditions perturb the epigenetic profiles of preimplantation embryos (Salilew-Wondim et al., 2015, 2018). Most recently, the WGBS technique was used to analyze the methylation patterns of bovine blastocysts derived from *in vivo*, IVF, or IVF with vitrified oocytes and revealed a large number of DMRs that may contribute to the differences in quality between *in vitro* and *in vivo* derived embryos (Zhao et al., 2020). In porcine embryos, the DNA methylation level was increased in *in vitro* embryos compared to *in vivo* ones suggesting the adverse effect of *in vitro* culture on the DNA methylome (Deshmukh et al., 2011). SCNT embryos also had higher DNA methylation levels compared to their fertilized counterparts in sheep (Beaujean et al., 2004). In sheep LOS models, reduced expression of *IGF2R* but not *IGF2* [whose overexpression due to loss of imprinting status is postulated in human fetal overgrowth syndromes (Reik and Maher, 1997)] was caused by loss of methylation on the second intron DMR (Young et al., 2001).

Histone modifications, specifically histone methylation, was also shown to be a key epigenetic barrier to epigenetic reprogramming in SCNT embryos (Matoba et al., 2014). In bovine, immunofluorescence analysis revealed that the acetylation and methylation levels of H3K9ac, H3K18ac, H4K5ac, H4K8ac, H3K4me3, and H3K9me2 were abnormally increased in the SCNT embryos from the zygote to the 8-cell stage, while H4K8ac and H4K5ac were abnormal when compared with the IVF controls. After EGA, the distribution and the pattern of the histone modifications were similar in both SCNT and IVF embryos (Wu et al., 2011). The hypermethylation of H3K9 was also observed in SCNT embryos and associated with DNA hypermethylation; in addition, an association between the epigenetic modifications and the developmental potential of cloned embryos was established (Santos et al., 2003). In porcine, global hypermethylation of H3K27me3 was observed in early cloned embryos compared with IVF embryos (Xie et al., 2016). Cao et al. (2015) compared multiple histone methylation modifications, including transcriptionally repressive

(H3K9me2, H3K9me3, H3K27me2, H3K27me3, H4K20me2, and H4K20me3) and active modifications (H3K4me2, H3K4me3, H3K36me2, H3K36me3, H3K79me2, and H3K79me3) between porcine SCNT and IVF embryos at different developmental stages. Histone methylation exhibited stage-specific abnormal patterns in SCNT embryos (Cao et al., 2015). IVP may also change the localization of histone PTMs systematically, separate from SCNT. Between *in vivo* and *in vitro* derived bovine embryos, histone modifying enzymes (e.g., PRMT5, KDM5B, KAT8, HDAC1, and HAT1, etc.) were differentially expressed during preimplantation development (Duan et al., 2019). It has been theorized that the low efficiency of SCNT embryo development rate results, in part, from the divergent DNA methylation and histone modification status between terminally differentiated somatic cells and mature spermatozoa (Peat and Reik, 2012; Jin et al., 2017).

A number of studies have defined precise approaches to remove epigenetic barriers and improve the efficiency of SCNT. In the mouse, treatment with histone deacetylase inhibitors (Kishigami et al., 2006, 2007; Van Thuan et al., 2009), the overexpression of H3K9me3 demethylase *Kdm4b/4d* (Matoba et al., 2014; Liu W. et al., 2016), the correction of abnormal DNA remethylation (Gao et al., 2018) or the deletion of *Xist* on the active X chromosome (Inoue et al., 2010) can significantly improve the developmental potential of SCNT embryos. This significant body of work provides considerable evidence that aberrant epigenetic modifications are the major barriers to complete reprogramming of the donor cell during SCNT.

In porcine, GSK126 and GSK-J4, two small molecule inhibitors of H3K27me3 methylase (EZH2) and demethylases (UTX/JMJD3), were used to improve the developmental efficiency of cloned embryos by reducing the H3K27me3 level (GSK126) (Xie et al., 2016). However, GSK-J4 treatment increased the H3K27me3 level in cloned embryos and decreased the cloned embryo development (Xie et al., 2016). Another study showed that BIX-01294 (a specific inhibitor of histone-lysine methyltransferase of H3K9) enhanced the developmental competence of porcine SCNT embryos (Huang et al., 2016). In addition, use of histone deacetylase inhibitors (e.g., trichostatin A) in the SCNT protocol has been shown to improve both *in vitro* and *in vivo* developmental competence in pigs (Zhao et al., 2010). In bovine, it has been reported that inhibiting H3K9 methyltransferases (SUV39H1) or injecting H3K9 demethylases (KDM4E) in SCNT embryos could improve blastocyst rates similar to what was observed in mice (Zhang et al., 2017; Liu et al., 2018).

Establishing proper epigenetic modifications during gametogenesis and embryogenesis is an important aspect in reproduction and embryo biotechnology. The reprogramming process may be influenced by external and internal factors that result in improper epigenetic changes in germ cells and embryos. Therefore, a combination of epigenetic and other factors could be responsible for the decreased developmental competence of oocytes matured *in vitro* and/or embryos produced *in vitro*. Further comprehensive epigenetic studies are required to compare embryos produced with different ARTs in a stage specific manner using high-throughput sequencing approaches. Also, a full mechanistic description of the many facets of epigenetic reprogramming during this developmental timeframe is needed. Understanding the epigenetic mechanisms is essential to gain insights into normal molecular regulation and correlate it with unperturbed embryonic and fetal development. This would also help to improve ART success and develop new approaches to improve the fertility of animals.

## THE EFFECTS OF PARENTAL ENVIRONMENTAL EXPOSURE ON EPIGENETICS AND REPRODUCTION PHENOTYPES

Animal models, such as rats and mice, have been used extensively to study correlations between epigenetics and disease and there is emerging research in this area using livestock. Considerable work has been focused on studying developmental origins of adult health and disease since it was hypothesized over 30 years ago (Barker, 1990, 1995). Epidemiological studies in humans have shown that parental malnutrition can affect offspring much later in life and extend into the next generation (Heijmans et al., 2008; Pembrey et al., 2014; Eriksen et al., 2017). As a notable example, mothers who were pregnant during the Nazi imposed food crisis in the Netherlands in 1944, also known as the Dutch Hunger Winter, had children with a wide range of health problems as adults, including type II diabetes, obesity, cancer, cardiovascular disease and schizophrenia (Heijmans et al., 2008). Higher body weight was also observed in the next generation in adulthood (Painter et al., 2008; Veenendaal et al., 2013). Tobi et al. (2014) used reduced representation bisulfite sequencing to examine DNA from whole blood in individuals that experienced the Dutch Hunger Winter *in utero* compared with siblings born before or after the period. They found 181 differentially methylated regions in exposed individuals compared to their siblings. The regions were enriched for genes involved in early development (Tobi et al., 2014). The fact that the authors could detect differences more than 60 years after the event emphasizes the nature of epigenetic mechanisms and the importance of epigenetic reprogramming during early development.

Nutrient intake is one of the most direct influences of environment on phenotype. The interaction between nutrition and reproduction has important implications for fertility, especially in cows (Martin et al., 2010). In cattle, prenatal, early post-natal and juvenile nutritional scenarios impact reproductive activity of females later in life; thus, there is the potential for strategic nutritional management during these critical times to program reproduction (Funston et al., 2010). Nutrition is important for epigenetics. For example, nutrients like folate, choline, b-vitamins (B2, B6, B12), and methionine are methyl donors to *S*-adenosylmethionine (SAM), which is the substrate used by DNA and histone methyltransferases in the one-carbon metabolism pathway, reviewed in Clare et al. (2019). Research in both cattle and sheep has shown that maternal diet (supplemented with methyl-donors) during the peri-conception period and/or pregnancy can alter DNA methylation in embryos

and in analyzed fetal tissues (Sinclair et al., 2007; Lan et al., 2013; Acosta et al., 2016).

A lot of the fetal programming work conducted in livestock species has been focused on nutrient restriction during pregnancy and its impacts on reproductive function, behavior and growth, reviewed in Ashworth et al. (2009) and Sinclair et al. (2016). In pigs, studies have found significant effects of maternal malnutrition on offspring gene expression, growth, and metabolism to name a few (Leibfried-Rutledge et al., 1987; Barker, 1990; Li et al., 1993; Gonzalez-Bulnes et al., 2014; Ji et al., 2017; Franczak et al., 2018). For instance, Franczak et al. (2018) found over 450 highly differentially expressed genes (>5 fold and mostly up-regulated) between day 15 and 16 pig embryos from gilts fed a normal control diet and gilts fed a restricted diet during fertilization and early preimplantation development (days 0–9). In sheep and goats, calorie restriction during pregnancy resulted in aberrant imprinted (*IGF2, PHLDA2, DIRS3, SLC22A18*) (Duan et al., 2018) (*IGF2R*) (Williams-Wyss et al., 2014) and epigenetic regulator (*TET1, MBD2*) gene expression, respectively, in the tissues of late gestation fetuses (Li et al., 2018). Nutrient restriction during the peri-conception period in sheep also resulted in reduced methylation and increased H3K9 acetylation in the promoters of the hypothalamic genes proopiomelanocortin and the glucocorticoid receptor in fetuses, indicating the role of maternal malnutrition's programming of metabolic and stress response issues later in life (Stevens et al., 2010; Begum et al., 2012). Very recent work by Toschi et al. (2020) in sheep found that maternal peri-conceptional (−14/+28 days) nutrient restriction can also affect the sperm methylome of offspring. Using RRBS analysis, the authors identified 244 DMRs in the sperm of offspring that experienced poor nutrition *in utero* compared with control rams. They also found reduced sperm motility, abnormal chromatin structure and a reduction in the ability to produce blastocysts in this treatment group. Interestingly, folic acid supplementation during the restriction period also created many DMRs, but this treatment rescued the blastocyst rate (Toschi et al., 2020). This result supports the concept of using management interventions to offset epigenetic perturbations and improve reproductive outcomes.

The previously discussed work outlines research that induced nutrient restriction during peri-conception or pregnancy; however, recent work has focused on understanding the epigenetic impacts of post-partum negative energy balance on oocyte methylation in high-producing dairy cows. O'Doherty et al. (2014) looked at imprinted gene methylation during the early, mid and late post-partum periods and found highly variable methylation levels across the time points for several genes. A follow up IVM experiment found specific effects of non-esterified fatty acids (NEFAs) and NEFAs + SAM on the methylation of *PLAGL1* (O'Doherty et al., 2014). Recent work expanded on this candidate gene analysis and used WGBS to examine the effects of negative energy balance on the epigenome of *in vivo* oocytes collected at early (∼37 days post-partum) and mid (∼65 days post-partum) time points vs. oocytes from heifers (Poirier et al., 2020). The oocytes collected during the early negative energy balance period displayed significant methylation variation within the group (3 replicate pools of oocytes); they also had lower methylation levels overall compared with the mid post-partum and control oocytes. These two factors combined led to the identification of a vast amount of DMRs unique to the early group, many of which were associated with genes involved in key metabolic processes. It is also of interest that a large majority of the imprinted gene bodies analyzed had higher methylation levels in the early post-partum oocytes compared with the other groups. One region, a uniquely differentially methylated CpG island in the early post-partum group specifically mapped to the imprinted gene, *MEST*. Oocytes collected at the mid post-partum time point were much more similar to control oocytes (in overall methylation level and number of DMRs), indicating a degree of recovery when the cows returned to positive energy status (Poirier et al., 2020). Taken together, this work indicates that nutritional stress can impact the methylome of developing gametes, which likely has impacts for gamete viability and developmental potential.

In humans and rodents, studies have shown that paternal nutritional status is associated with metabolic disruptions in the offspring (Chen et al., 2016a). Malnutrition affects sperm viability in males of various species. In rodents, malnourished fathers produce developmentally delayed and metabolically compromised embryos; the conceptuses also have altered placental development (Carone et al., 2010). The effects of paternal malnutrition on the reproductive physiology of adult offspring have also been observed. In mice, two generations of progeny from fathers who ingested a low-protein diet during the preconception period had abnormalities in their reproductive organs (Carone et al., 2010). In female offspring of malnourished fathers, oocyte meiotic competence was reduced, expression of glucose transporters in ovaries and cumulus cells was altered, and reproductive ability was compromised, as seen by lower fertilization and cleavage rates as well as embryos with delayed development (Ashworth et al., 2009). In cattle production systems, bulls are commonly placed on high-energy rations during development to result in a high rate of weight gain (Allen et al., 2017). Energy expenditure during the breeding season commonly results in weight loss in bulls, especially in bulls that have not reached their mature body weight and are still undergoing post-pubertal reproductive maturation (Cardoso et al., 2014). Undernutrition can also occur in pastures or range-based systems, due to normal seasonal variation in nutrient availability (Hills et al., 2015). Therefore, metabolic scenarios related to weight loss and undernutrition could affect seminal parameters and influence epigenetic transmission of traits. These events support the role of sires in the nutritional programming of reproductive function.

Bull fertility is a critical factor dictating economic potential in cattle production systems. Fertility is affected by several factors, including management, nutrition, disease, stress, age, and genetics. A decline in bull fertility affects the conception rate of herds, resulting in decreased production and therefore decreased profit. The ability to confidently predict male fertility would be a boon to the livestock industry. For example, fertility differences among different breeds and even individual bulls within same breed have been well-documented (Den Daas et al., 1998; Dejarnette, 2005). It has been shown that sperm

molecular differences between individuals are associated with specific phenotypes of bull infertility (Dogan et al., 2015). The "omics" approaches, such as genomics, transcriptomics, proteomics, metabolomics and epigenomics, have been used to ascertain molecular determinants of bull fertility (Feugang et al., 2010; De Oliveira et al., 2013; Kumar et al., 2015; Bromfield, 2016; Westfalewicz et al., 2017; Velho et al., 2018; Menezes et al., 2020). For example, recent work using RNA-seq examined sperm-derived RNAs in pre-EGA bovine embryos and found 65 differentially expressed RNAs in embryos fertilized with sperm from bulls with low and high fertility (Gross et al., 2019). Analyses of inter-individual variations in bull sperm DNA methylation found a number of DMRs with significant associations with reproduction traits like sperm motility, further supporting the notion that epigenetic information can be harnessed to improve production (Liu S. et al., 2019). Despite abundant research, vast gaps in the knowledge base exist, including specific functional genomic signatures coupled with epigenetic profiles in different bull breeds, as well as mechanisms for their involvement in fertility.

In the livestock industry, selected sires have greater opportunities for breeding, in comparison to females. A small number of sires may be able to "nutritionally" program reproduction in a significant number of female progeny. Thus, assessing the impact of paternal nutrition on reproductive function and the potential heritability of acquired traits merits investigation as a viable strategy to mitigate problems with infertility and subfertility.

## TRANSGENERATIONAL EPIGENETIC INHERITANCE IN LIVESTOCK SPECIES

Dramatic phenotypic differences have been established and stabilized between livestock breeds. There are two different models of phenotypic polymorphism: (1) differences between breeds where dramatic phenotypic differences exist due to decades of selective breeding; and (2) environmentally induced phenotypic differences, specifically those induced by nutritional status. There is significant evidence in mammals that individuals can acquire environmentally induced epigenetic modifications that can be passed transgenerationally, reviewed in Daxinger and Whitelaw (2012), Heard and Martienssen (2014), Chen et al. (2016b), and Zhang et al. (2019). In the case of transgenerational inheritance, it is the founder individual that experiences the environmentally induced epigenetic perturbation and this is passed down via gametes to subsequent generations that have never experienced direct exposure. For true transgenerational inheritance when a gestating female has faced the perturbing event, the aberrant epigenetic pattern must persist to the third generation (F3) (Jirtle and Skinner, 2007). This is because the embryo or fetus' primordial germ cells or gametes (which will form the F2 generation) will also potentially be exposed during their development. In males and non-pregnant females, epigenetic persistence to the F2 generation is sufficient (Skinner, 2008). Thus, it becomes clear the difficulties involved in conducting strong transgenerational epigenetic inheritance studies in livestock species, specifically the cost and complexities associated with performing a study across several generations in species with long generation intervals.

There has been some multigenerational research in dairy cattle that showed the granddam's prenatal environment influenced milk production of daughters and granddaughters (Gonzalez-Recio et al., 2012; Gudex et al., 2014). However, since the analysis started with pregnant females, the F2 generation was exposed, and so the work cannot be categorized as transgenerational in nature. Nonetheless, a transgenerational study with epigenetic analysis has been done in swine. Braunschweig et al. (2012) examined Swiss Large White F2 animals to identify effects of a methyl-donor enriched diet fed to founder boars. They found differences in carcass traits (the control diet progeny tended to be fatter with a trend of decreased shoulder muscle percentage) and gene expression in the liver (64 DEGs), muscle (79 DEGs), and kidney (53 DEGs) of pigs whose grandsires had the experimental diet vs. pigs that descended from control diet fed pigs. The authors examined the DNA methylation pattern of the promoter region of a few selected genes and found reduced methylation of the promoter for the gene iodotyrosine deiodinase in the livers of the experimental progeny; the methylation level was correlated with gene expression level. While this study is limited by the number of F2 pigs analyzed (8 for each group) and the lack of a genome-wide epigenetic analysis, it is the first attempt to examine transgenerational inheritance in a livestock species (Braunschweig et al., 2012).

There is even compelling evidence for transgenerational inheritance in humans. Among the epidemiological human examples, the detailed analysis of the copious historical data from Överkalix, Sweden demonstrates the effects of famine during pre-pubescence in both girls and boys on subsequent grandchildren's health and longevity (Bygren et al., 2001, 2014; Pembrey et al., 2006; Kaati et al., 2007). Physiological challenges (severe nutrient restriction and stress) to grandparents were linked with health issues in the following generations.

We now appreciate that phenotypic complexity goes beyond Mendelian genetics. It is critical that we continue intensive research in this area to fully characterize the epigenetic (and other) mechanisms involved. Furthermore, despite the difficulties inherent in transgenerational studies, it is imperative to expedite this research in livestock species. It will provide a better understanding of the underlying mechanisms controlling phenotype, animal reproduction and health, and the potential means to induce and/or counteract epigenetic modifications for several generations.

### Searching for Epigenetic Factors That Transmit Acquired Phenotypes

The processes by which environmental information is coded and transmitted inter-generationally via the germline remains unclear. Correlative studies in mammals have suggested that DNA methylation, histone modification and small RNA could contribute to intergenerational inheritance of

environment-induced phenotypes. Particularly, evidence from laboratory rodents that these parental environment induced traits could be "memorized" in sperm and transmitted to the future generations, implicating sperm-mediated epigenetic inheritance, reviewed in Chen et al. (2016b) and Zhang et al. (2019). Recently developed technologies in the field of omics including genome-wide high throughput sequencing, dynamic imaging of genomic loci, quantitative proteomics and computational analyses have allowed insight into some of these processes (Gomez et al., 2013; Doherty and Couldrey, 2014; Small et al., 2014).

DNA methylation is a solid candidate for epigenetic inheritance in animals because of its relative stability and our understanding of the mechanisms of its deposition and erasure (Bestor, 2000; Jurkowska et al., 2011). Insights from genome-wide methylome studies suggest that a considerable fraction of the mammalian genome might evade the DNA demethylation that occurs normally during preimplantation and PGC reprogramming (Hackett et al., 2013; Guo et al., 2014; Smith et al., 2014; Tang et al., 2015). These escapee modifications could then be transmitted to future generations. In addition, we know that some regions (e.g., imprinted genes) have to be protected from embryonic epigenetic reprogramming and that perturbations can result in differences in DNA methylation (Barlow and Bartolomei, 2014). It has been shown that sperm DNA methylation is altered by various environmental exposures in mice, and it contributes to transgenerational epigenetic inheritance (Radford et al., 2014). Recent work points toward the possible mechanism for transmitting paternal environmental exposures to the next generation, via sperm DNA methylation, ncRNAs and histone retention (Ben Maamar et al., 2020). Additionally, age-related methylation changes are well-documented in human sperm; more recent studies shed light on this in bulls as well (Lambert et al., 2018; Takeda et al., 2019; Khezri et al., 2020; Wu et al., 2020a). Histone modifications have also been implicated in transgenerational epigenetic inheritance (Siklenka et al., 2015). Several studies have established the histone modification mediating epigenetic memory of the germline in *C. elegans* (Rechtsteiner et al., 2010; Gaydos et al., 2014). This major mechanism of epigenetic inheritance has been intensively reviewed (Skvortsova et al., 2018).

Among the epigenetic mechanisms, sncRNAs appear to play a pivotal role in mediating environmental information transmission through sperm in mammals, reviewed in Chen et al. (2016b) and Zhang et al. (2019). Several sncRNAs can be altered in the spermatozoa from obese and/or diabetic men, male mice and rats. Altered sperm sncRNAs, such as miRNA and tsRNA, have been observed following paternal exposure to diet change or stress (Fullston et al., 2013; Gapp et al., 2014; Chen et al., 2016a; Zhang et al., 2018). Injection of sperm RNA from exposed males (e.g., unhealthy diet, mental stress) has been demonstrated to efficiently induce transgenerational inheritance in mammals (Rassoulzadegan et al., 2006; Wagner et al., 2008; Grandjean et al., 2009; Rodgers et al., 2015; Chen et al., 2016a), suggesting sperm RNA is an active epigenetic modulator of offspring phenotypes. In addition, several RNA modifications such as $m^5C$, $m^2G$ have been found to be enriched in the sperm tsRNA and are sensitive to diet changes (Chen et al., 2016a; Zhang et al., 2018). These sperm RNA modifications could alter RNA structure and thus the interactions between RNA, DNA and proteins, leading to potentially greater consequences and wide-ranging effects (Zhang et al., 2018). Wu et al. (2020b) identified distinct differences in sperm-borne miRNAs from bulls of different ages, several of which targeted genes expressed in early embryos. This newly appreciated role of the sperm as RNA-based carriers of hereditary information provides a promising angle with which to understand aging and the etiology of environmentally induced disease beyond the initial exposure.

While epigenetic information can certainly be transmitted between generations, there is a shortage of research in livestock species thus far. A significant challenge to be met in this research area will be to track epigenetic information from one generation to another in cattle, pigs, sheep and goats. Given the effects of environment and aging on epigenetic modifications, future studies need to be carefully designed. This type of research will be made increasingly possible with the continued complete characterization of epigenetics during livestock early embryo development.

## Potential Application of Epigenetic Information in Livestock Production

Aside from understanding the nature of the epigenetic code with regard to programming offspring phenotypes, perhaps an equally important mission is to control offspring health and production by harnessing this epigenetic information.

First, it is possible that a reliable epigenetic "code" exists, which if interpreted, may allow us to predict future phenotypes with accuracy; this prospect is very exciting. This has obvious implications for male reproduction. For example, bulls can breed a large number of cows each breeding season, and this relatively large reproductive opportunity amplifies the impact of environmental scenarios in a few individuals on the future performance of many progeny. If artificial insemination or other ARTs are used, the potential to acquire abnormal phenotypes due to age or nutrition stress in the sire, for example, can be compounded with the perturbations caused by the ART, thus elevating the spread of the undesirable epigenetic modifications in the offspring. The ability to counteract these effects would be very beneficial to producers and researchers.

Second, epigenetic codes could be used as clinical biomarkers of gamete and embryo viability. Improvement of pregnancy rates with *in vitro* produced embryos is a critical problem that needs to be addressed in economically valuable livestock species. The efficiency of producing viable embryos and the development of such embryos after transferring them to recipients is inferior to their *in vivo* derived counterparts, especially in cattle (Thompson, 1997; Diskin and Morris, 2008; Diskin et al., 2011, 2016). In addition, the offspring can have a high incidence of abnormalities, including large offspring syndrome (LOS), severe placental abnormalities, respiratory problems, prolonged gestation, and dystocia (Young et al., 1998; Yang et al., 2007).

Future studies are needed to fully elucidate how epigenetics contributes to these abnormalities, which would therefore help us develop new approaches to improve ARTs and more closely mimic *in vivo* profiles. This would improve gamete quality and embryo viability.

Third, phenotypic polymorphism between cattle breeds may be reflected in the gametes as epigenetic codes and represent a potential opportunity to introgress phenotypic differences from one breed to another by "epigenetic engineering." Recently genome editing tools, such as CRISPR-Cas9 or TALENs, have been utilized to introduce an allele from one breed into the genome of a dramatically different breed. For example, the polled allele from the Angus breed was edited into the Holstein genome resulting in a naturally polled Holstein (Carlson et al., 2016; Young et al., 2020). Additionally, an allelic variation for the long version of the prolactin receptor (the "slick" allele) from the Senepol breed (heat tolerant breed) was introduced into the Angus breed (meat producing breed) using genome editing technology (Bastiaansen et al., 2018). Like genome editing, there is also the power of epigenome editing. Here, a deactivated Cas9 protein can be used to haul epigenetic modifier cargo (such as DNMT3a, TET3, KDM6B, HAT, etc.) to targeted regions in the genome, turning genes on or off as desired (Gomez et al., 2019).

Fourth, livestock species offer clear advantages to study epigenetic inheritance. For example, the use of the livestock will allow us to readily profile semen parameters such as sperm concentration, total sperm per ejaculate and progressive motility, as well as epigenetic modifications in the sperm in a consecutive manner in each animal, although the heterogeneity of the sperm epigenome would need to be examined. This would represent an advantage over rodent models and may represent a better model for understanding the dynamic changes in humans.

## CONCLUDING REMARKS

Our understanding of the different layers of epigenomic regulation during gametogenesis and embryogenesis in livestock species is incomplete. Advances in low-input genomic and epigenomic sequencing technologies are now driving the global comprehensive profiling of germline and embryonic epigenomes, thereby improving our understanding of epigenetic regulation in normal development and assessing the impacts of ARTs and other environmental stressors on gametes and embryos. Also, a more complete understanding of inter- and transgenerational epigenetic inheritance in mammals will encourage further research into how experiences can be encoded by epigenetics; this knowledge can lead to application in livestock production and health. Finally, the development of precise editing or modulation of germline and embryonic epigenomes will enable the design of strategies to counteract adverse conditions or to program production performance in livestock. Such strategies for epigenetically programming performance would constitute a significant change with the potential for long-ranging effects in the livestock industry.

## AUTHOR CONTRIBUTIONS

All authors listed have made a substantial, direct and intellectual contribution to the work, and approved it for publication.

## FUNDING

This work was supported by a USDA-NIFA grant (2019-67016-29863), a USDA-NIFA W4171 grant, a NIH Eunice Kennedy Shriver National Institute of Child Health and Human Development Grant (1R01HD102533), and the Audubon Center for Research of Endangered Species grant (1920R0447).

## REFERENCES

Acosta, D. A. V., Denicol, A. C., Tribulo, P., Rivelli, M. I., Skenandore, C., Zhou, Z., et al. (2016). Effects of rumen-protected methionine and choline supplementation on the preimplantation embryo in Holstein cows. *Theriogenology* 85, 1669–1679. doi: 10.1016/j.theriogenology.2016.01.024

Albuz, F. K., Sasseville, M., Lane, M., Armstrong, D. T., Thompson, J. G., and Gilchrist, R. B. (2010). Simulated physiological oocyte maturation (SPOM): a novel *in vitro* maturation system that substantially improves embryo yield and pregnancy outcomes. *Hum. Reprod.* 25, 2999–3011. doi: 10.1093/humrep/deq246

Allen, C. C., Tedeschi, L. O., Keisler, D. H., Cardoso, R. C., Alves, B. R. C., Amstalden, M., et al. (2017). Interaction of dietary energy source and body weight gain during the juvenile period on metabolic endocrine status and age at puberty in beef heifers. *J. Anim. Sci.* 95, 2080–2088. doi: 10.2527/jas.2016.1002

Ashworth, C. J., Toma, L. M., and Hunter, M. G. (2009). Nutritional effects on oocyte and embryo development in mammals: implications for reproductive efficiency and environmental sustainability. *Philos. Trans. R. Soc. Lond B Biol. Sci.* 364, 3351–3361. doi: 10.1098/rstb.2009.0184

Bai, H., Li, Y., Gao, H., Dong, Y., Han, P., and Yu, H. (2016). Histone methyltransferase SMYD3 regulates the expression of transcriptional factors during bovine oocyte maturation and early embryonic development. *Cytotechnology* 68, 849–859. doi: 10.1007/s10616-014-9838-5

Barker, D. J. (1990). The fetal and infant origins of adult disease. *BMJ* 301:1111. doi: 10.1136/bmj.301.6761.1111

Barker, D. J. (1995). The fetal and infant origins of disease. *Eur. J. Clin. Invest.* 25, 457–463. doi: 10.1111/j.1365-2362.1995.tb01730.x

Barlow, D. P., and Bartolomei, M. S. (2014). Genomic imprinting in mammals. *Cold Spring Harb. Perspect. Biol.* 6:a018382. doi: 10.1101/cshperspect.a018382

Baruselli, P. S., Sa Filho, M. F., Ferreira, R. M., Sales, J. N., Gimenes, L. U., Vieira, L. M., et al. (2012). Manipulation of follicle development to ensure optimal oocyte quality and conception rates in cattle. *Reprod. Domest. Anim.* 47(Suppl. 4), 134–141. doi: 10.1111/j.1439-0531.2012.02067.x

Bastiaansen, J. W. M., Bovenhuis, H., Groenen, M. A. M., Megens, H. J., and Mulder, H.A. (2018). The impact of genome editing on the introduction of monogenic traits in livestock. *Genet. Sel. Evol.* 50:18. doi: 10.1186/s12711-018-0389-7

Battulin, N., Fishman, V. S., Mazur, A. M., Pomaznoy, M., Khabarova, A. A., Afonnikov, D. A., et al. (2015). Comparison of the three-dimensional organization of sperm and fibroblast genomes using the Hi-C approach. *Genome Biol.* 16:77. doi: 10.1186/s13059-015-0642-0

Beaujean, N., Taylor, J., Gardner, J., Wilmut, I., Meehan, R., and Young, L. (2004). Effect of limited DNA methylation reprogramming in the normal sheep embryo on somatic cell nuclear transfer. *Biol. Reprod.* 71, 185–193. doi: 10.1095/biolreprod.103.026559

Becker, J. S., Nicetto, D., and Zaret, K. S. (2016). H3K9me3-Dependent Heterochromatin: Barrier to Cell Fate Changes. *Trends Genet.* 32, 29–41. doi: 10.1016/j.tig.2015.11.001

Begum, G., Stevens, A., Smith, E. B., Connor, K., Challis, J. R., Bloomfield, F., et al. (2012). Epigenetic changes in fetal hypothalamic energy regulating pathways are associated with maternal undernutrition and twinning. *FASEB J.* 26, 1694–1703. doi: 10.1096/fj.11-198762

Ben Maamar, M., Beck, D., Nilsson, E., Mccarrey, J. R., and Skinner, M. K. (2020). Developmental origins of transgenerational sperm histone retention following ancestral exposures. *Dev. Biol.* 465, 31–45. doi: 10.1016/j.ydbio.2020.06.008

Berg, D. K., and Pfeffer, P. L. (2018). MicroRNA expression in bovine preimplantation embryos. *Reprod. Fertil. Dev.* 30, 546–554. doi: 10.1071/RD17101

Bernstein, B. E., Mikkelsen, T. S., Xie, X., Kamal, M., Huebert, D. J., Cuff, J., et al. (2006). A bivalent chromatin structure marks key developmental genes in embryonic stem cells. *Cell* 125, 315–326. doi: 10.1016/j.cell.2006.02.041

Bestor, T. H. (2000). The DNA methyltransferases of mammals. *Hum. Mol. Genet.* 9, 2395–2402. doi: 10.1093/hmg/9.16.2395

Bird, A. (2002). DNA methylation patterns and epigenetic memory. *Genes Dev.* 16, 6–21. doi: 10.1101/gad.947102

Bonk, A. J., Li, R., Lai, L., Hao, Y., Liu, Z., Samuel, M., et al. (2008). Aberrant DNA methylation in porcine *in vitro*-, parthenogenetic-, and somatic cell nuclear transfer-produced blastocysts. *Mol. Reprod. Dev.* 75, 250–264. doi: 10.1002/mrd.20786

Bourc'his, D., Le Bourhis, D., Patin, D., Niveleau, A., Comizzoli, P., Renard, J. P., et al. (2001). Delayed and incomplete reprogramming of chromosome methylation patterns in bovine cloned embryos. *Curr. Biol.* 11, 1542–1546. doi: 10.1016/S0960-9822(01)00480-8

Braunschweig, M., Jagannathan, V., Gutzwiller, A., and Bee, G. (2012). Investigations on transgenerational epigenetic response down the male line in F2 pigs. *PLoS ONE* 7:e30583. doi: 10.1371/journal.pone.0030583

Bromfield, J. J. (2016). A role for seminal plasma in modulating pregnancy outcomes in domestic species. *Reproduction* 152, R223–R232. doi: 10.1530/REP-16-0313

Burton, A., and Torres-Padilla, M. E. (2014). Chromatin dynamics in the regulation of cell fate allocation during early embryogenesis. *Nat. Rev. Mol. Cell Biol.* 15, 723–734. doi: 10.1038/nrm3885

Bygren, L. O., Kaati, G., and Edvinsson, S. (2001). Longevity determined by paternal ancestors' nutrition during their slow growth period. *Acta Biotheor.* 49, 53–59. doi: 10.1023/A:1010241825519

Bygren, L. O., Tinghog, P., Carstensen, J., Edvinsson, S., Kaati, G., Pembrey, M. E., et al. (2014). Change in paternal grandmothers' early food supply influenced cardiovascular mortality of the female grandchildren. *BMC Genet.* 15:12. doi: 10.1186/1471-2156-15-12

Canovas, S., Cibelli, J. B., and Ross, P. J. (2012). Jumonji domain-containing protein 3 regulates histone 3 lysine 27 methylation during bovine preimplantation development. *Proc. Natl. Acad. Sci. U.S.A.* 109, 2400–2405. doi: 10.1073/pnas.1119112109

Cao, Z., Li, Y., Chen, Z., Wang, H., Zhang, M., Zhou, N., et al. (2015). Genome-wide dynamic profiling of histone methylation during nuclear transfer-mediated porcine somatic cell reprogramming. *PLoS ONE* 10:e0144897. doi: 10.1371/journal.pone.0144897

Capra, E., Lazzari, B., Turri, F., Cremonesi, P., Portela, A. M. R., Ajmone-Marsan, P., et al. (2019). Epigenetic analysis of high and low motile sperm populations reveals methylation variation in satellite regions within the pericentromeric position and in genes functionally related to sperm DNA organization and maintenance in Bos taurus. *BMC Genomics* 20:940. doi: 10.1186/s12864-019-6317-6

Capra, E., Turri, F., Lazzari, B., Cremonesi, P., Gliozzi, T. M., Fojadelli, I., et al. (2017). Small RNA sequencing of cryopreserved semen from single bull revealed altered miRNAs and piRNAs expression between High- and Low-motile sperm populations. *BMC Genomics* 18:14. doi: 10.1186/s12864-016-3394-7

Cardoso, R. C., Alves, B. R., Prezotto, L. D., Thorson, J. F., Tedeschi, L. O., Keisler, D. H., et al. (2014). Use of a stair-step compensatory gain nutritional regimen to program the onset of puberty in beef heifers. *J. Anim. Sci.* 92, 2942–2949. doi: 10.2527/jas.2014-7713

Carlson, D. F., Lancto, C. A., Zang, B., Kim, E. S., Walton, M., Oldeschulte, D., et al. (2016). Production of hornless dairy cattle from genome-edited cell lines. *Nat. Biotechnol.* 34, 479–481. doi: 10.1038/nbt.3560

Carmell, M. A., Girard, A., Van De Kant, H. J., Bourc'his, D., Bestor, T. H., De Rooij, D. G., et al. (2007). MIWI2 is essential for spermatogenesis and repression of transposons in the mouse male germline. *Dev. Cell* 12, 503–514. doi: 10.1016/j.devcel.2007.03.001

Carone, B. R., Fauquier, L., Habib, N., Shea, J. M., Hart, C. E., Li, R., et al. (2010). Paternally induced transgenerational environmental reprogramming of metabolic gene expression in mammals. *Cell* 143, 1084–1096. doi: 10.1016/j.cell.2010.12.008

Chen, H., Zhang, L., Deng, T., Zou, P., Wang, Y., Quan, F., et al. (2016). Effects of oocyte vitrification on epigenetic status in early bovine embryos. *Theriogenology* 86, 868–878. doi: 10.1016/j.theriogenology.2016.03.008

Chen, M., Zhu, Q., Li, C., Kou, X., Zhao, Y., Li, Y., et al. (2020). Chromatin architecture reorganization in murine somatic cell nuclear transfer embryos. *Nat. Commun.* 11:1813. doi: 10.1038/s41467-020-15607-z

Chen, Q., Yan, M., Cao, Z., Li, X., Zhang, Y., Shi, J., et al. (2016a). Sperm tsRNAs contribute to intergenerational inheritance of an acquired metabolic disorder. *Science* 351, 397–400. doi: 10.1126/science.aad7977

Chen, Q., Yan, W., and Duan, E. (2016b). Epigenetic inheritance of acquired traits through sperm RNAs and sperm RNA modifications. *Nat. Rev. Genet.* 17, 733–743. doi: 10.1038/nrg.2016.106

Chen, Z., Robbins, K. M., Wells, K. D., and Rivera, R. M. (2013). Large offspring syndrome: a bovine model for the human loss-of-imprinting overgrowth syndrome Beckwith-Wiedemann. *Epigenetics* 8, 591–601. doi: 10.4161/epi.24655

Chu, T., Dufort, I., and Sirard, M. A. (2012). Effect of ovarian stimulation on oocyte gene expression in cattle. *Theriogenology* 77, 1928–1938. doi: 10.1016/j.theriogenology.2012.01.015

Chung, N., Bogliotti, Y. S., Ding, W., Vilarino, M., Takahashi, K., Chitwood, J. L., et al. (2017). Active H3K27me3 demethylation by KDM6B is required for normal development of bovine preimplantation embryos. *Epigenetics* 12, 1048–1056. doi: 10.1080/15592294.2017.1403693

Clare, C. E., Brassington, A. H., Kwong, W. Y., and Sinclair, K. D. (2019). One-carbon metabolism: linking nutritional biochemistry to epigenetic programming of long-term development. *Annu. Rev. Anim. Biosci.* 7, 263–287. doi: 10.1146/annurev-animal-020518-115206

Cuthbert, J. M., Russell, S. J., White, K. L., and Benninghoff, A. D. (2019). The maternal-to-zygotic transition in bovine *in vitro*-fertilized embryos is associated with marked changes in small non-coding RNAsdagger. *Biol. Reprod.* 100, 331–350. doi: 10.1093/biolre/ioy190

Dahl, J. A., Jung, I., Aanes, H., Greggains, G. D., Manaf, A., Lerdrup, M., et al. (2016). Broad histone H3K4me3 domains in mouse oocytes modulate maternal-to-zygotic transition. *Nature* 537, 548–552. doi: 10.1038/nature19360

Daxinger, L., and Whitelaw, E. (2012). Understanding transgenerational epigenetic inheritance via the gametes in mammals. *Nat. Rev. Genet.* 13, 153–162. doi: 10.1038/nrg3188

De Fazio, S., Bartonicek, N., Di Giacomo, M., Abreu-Goodger, C., Sankar, A., Funaya, C., et al. (2011). The endonuclease activity of Mili fuels piRNA amplification that silences LINE1 elements. *Nature* 480, 259–263. doi: 10.1038/nature10547

De Oliveira, R. V., Dogan, S., Belser, L. E., Kaya, A., Topper, E., Moura, A., et al. (2013). Molecular morphology and function of bull spermatozoa linked to histones and associated with fertility. *Reproduction* 146, 263–272. doi: 10.1530/REP-12-0399

Dean, W., Santos, F., Stojkovic, M., Zakhartchenko, V., Walter, J., Wolf, E., et al. (2001). Conservation of methylation reprogramming in mammalian development: aberrant reprogramming in cloned embryos. *Proc. Natl. Acad. Sci. U.S.A.* 98, 13734–13738. doi: 10.1073/pnas.241522698

Dejarnette, J. M. (2005). The effect of semen quality on reproductive efficiency. *Vet. Clin. North Am. Food Anim. Pract.* 21, 409–418. doi: 10.1016/j.cvfa.2005.02.011

Den Daas, J. H., De Jong, G., Lansbergen, L. M., and Van Wagtendonk-De Leeuw, A. M. (1998). The relationship between the number of spermatozoa inseminated and the reproductive efficiency of individual dairy bulls. *J. Dairy Sci.* 81, 1714–1723. doi: 10.3168/jds.S0022-0302(98)75739-X

Deng, M., Liu, Z., Ren, C., Zhang, G., Pang, J., Zhang, Y., et al. (2018). Long noncoding RNAs exchange during zygotic genome activation in goat. *Biol. Reprod.* 99, 707–717. doi: 10.1093/biolre/ioy118

Deng, W., and Lin, H. (2002). miwi, a murine homolog of piwi, encodes a cytoplasmic protein essential for spermatogenesis. *Dev. Cell* 2, 819–830. doi: 10.1016/S1534-5807(02)00165-X

Deshmukh, R. S., Ostrup, O., Ostrup, E., Vejlsted, M., Niemann, H., Lucas-Hahn, A., et al. (2011). DNA methylation in porcine preimplantation embryos developed *in vivo* and produced by *in vitro* fertilization, parthenogenetic activation and somatic cell nuclear transfer. *Epigenetics* 6, 177–187. doi: 10.4161/epi.6.2.13519

Desmet, K. L., Van Hoeck, V., Gagne, D., Fournier, E., Thakur, A., O'doherty, A. M., et al. (2016). Exposure of bovine oocytes and embryos to elevated non-esterified fatty acid concentrations: integration of epigenetic and transcriptomic signatures in resultant blastocysts. *BMC Genomics* 17:1004. doi: 10.1186/s12864-016-3366-y

Diao, Y. F., Oqani, R. K., Li, X. X., Lin, T., Kang, J. W., and Jin, D. I. (2014). Changes in histone H3 lysine 36 methylation in porcine oocytes and preimplantation embryos. *PLoS ONE* 9:e100205. doi: 10.1371/journal.pone.0100205

Diederich, M., Hansmann, T., Heinzmann, J., Barg-Kues, B., Herrmann, D., Aldag, P., et al. (2012). DNA methylation and mRNA expression profiles in bovine oocytes derived from prepubertal and adult donors. *Reproduction* 144, 319–330. doi: 10.1530/REP-12-0134

Diskin, M. G., and Morris, D. G. (2008). Embryonic and early foetal losses in cattle and other ruminants. *Reprod. Domest. Anim.* 43(Suppl. 2), 260–267. doi: 10.1111/j.1439-0531.2008.01171.x

Diskin, M. G., Parr, M. H., and Morris, D. G. (2011). Embryo death in cattle: an update. *Reprod. Fertil. Dev.* 24, 244–251. doi: 10.1071/RD11914

Diskin, M. G., Waters, S. M., Parr, M. H., and Kenny, D. A. (2016). Pregnancy losses in cattle: potential for improvement. *Reprod. Fertil. Dev.* 28, 83–93. doi: 10.1071/RD15366

Dobbs, K. B., Rodriguez, M., Sudano, M. J., Ortega, M. S., and Hansen, P. J. (2013). Dynamics of DNA methylation during early development of the preimplantation bovine embryo. *PLoS ONE* 8:e66230. doi: 10.1371/journal.pone.0066230

Dogan, S., Vargovic, P., Oliveira, R., Belser, L. E., Kaya, A., Moura, A., et al. (2015). Sperm protamine-status correlates to the fertility of breeding bulls. *Biol. Reprod.* 92:92. doi: 10.1095/biolreprod.114.124255

Doherty, R., and Couldrey, C. (2014). Exploring genome wide bisulfite sequencing for DNA methylation analysis in livestock: a technical assessment. *Front. Genet.* 5:126. doi: 10.3389/fgene.2014.00126

Doi, A., Park, I. H., Wen, B., Murakami, P., Aryee, M. J., Irizarry, R., et al. (2009). Differential methylation of tissue- and cancer-specific CpG island shores distinguishes human induced pluripotent stem cells, embryonic stem cells and fibroblasts. *Nat. Genet.* 41, 1350–1353. doi: 10.1038/ng.471

Donkin, I., and Barres, R. (2018). Sperm epigenetics and influence of environmental factors. *Mol. Metab.* 14, 1–11. doi: 10.1016/j.molmet.2018.02.006

Du, Z., Zheng, H., Huang, B., Ma, R., Wu, J., Zhang, X., et al. (2017). Allelic reprogramming of 3D chromatin architecture during early mammalian development. *Nature* 547, 232–235. doi: 10.1038/nature23263

Duan, J. E., Jiang, Z. C., Alqahtani, F., Mandoiu, I., Dong, H., Zheng, X., et al. (2019). Methylome dynamics of bovine gametes and *in vivo* early embryos. *Front. Genet.* 10:512. doi: 10.3389/fgene.2019.00512

Duan, J. E., Zhang, M., Flock, K., Seesi, S. A., Mandoiu, I., Jones, A., et al. (2018). Effects of maternal nutrition on the expression of genomic imprinted genes in ovine fetuses. *Epigenetics* 13, 793–807. doi: 10.1080/15592294.2018.1503489

El Hajj, N., and Haaf, T. (2013). Epigenetic disturbances in *in vitro* cultured gametes and embryos: implications for human assisted reproduction. *Fertil. Steril.* 99, 632–641. doi: 10.1016/j.fertnstert.2012.12.044

Eriksen, K. G., Radford, E. J., Silver, M. J., Fulford, A. J. C., Wegmuller, R., and Prentice, A. M. (2017). Influence of intergenerational *in utero* parental energy and nutrient restriction on offspring growth in rural Gambia. *FASEB J.* 31, 4928–4934. doi: 10.1096/fj.201700017R

Fang, L., Zhou, Y., Liu, S., Jiang, J., Bickhart, D. M., Null, D. J., et al. (2019). Comparative analyses of sperm DNA methylomes among human, mouse and cattle provide insights into epigenomic evolution and complex traits. *Epigenetics* 14, 260–276. doi: 10.1080/15592294.2019.1582217

Fauque, P. (2013). Ovulation induction and epigenetic anomalies. *Fertil. Steril.* 99, 616–623. doi: 10.1016/j.fertnstert.2012.12.047

Fernandez-Gonzalez, R., Ramirez, M. A., Pericuesta, E., Calle, A., and Gutierrez-Adan, A. (2010). Histone modifications at the blastocyst Axin1(Fu) locus mark the heritability of *in vitro* culture-induced epigenetic alterations in mice. *Biol. Reprod.* 83, 720–727. doi: 10.1095/biolreprod.110.084715

Feugang, J. M., Rodriguez-Osorio, N., Kaya, A., Wang, H., Page, G., Ostermeier, G. C., et al. (2010). Transcriptome analysis of bull spermatozoa: implications for male fertility. *Reprod. Biomed. Online* 21, 312–324. doi: 10.1016/j.rbmo.2010.06.022

Flyamer, I. M., Gassler, J., Imakaev, M., Brandao, H. B., Ulianov, S. V., Abdennur, N., et al. (2017). Single-nucleus Hi-C reveals unique chromatin reorganization at oocyte-to-zygote transition. *Nature* 544, 110–114. doi: 10.1038/nature21711

Franczak, A., Zglejc-Waszak, K., Martyniak, M., Waszkiewicz, E. M., and Kotwica, G. (2018). Peri-conceptional nutritional restriction alters transcriptomic profile in the peri-implantation pig embryos. *Anim. Reprod. Sci.* 197, 305–316. doi: 10.1016/j.anireprosci.2018.08.045

Fu, Q., and Wang, P. J. (2014). Mammalian piRNAs: biogenesis, function, and mysteries. *Spermatogenesis* 4:e27889. doi: 10.4161/spmg.27889

Fu, Y., Luo, G. Z., Chen, K., Deng, X., Yu, M., Han, D., et al. (2015). N6-methyldeoxyadenosine marks active transcription start sites in Chlamydomonas. *Cell* 161, 879–892. doi: 10.1016/j.cell.2015.04.010

Fullston, T., Ohlsson Teague, E. M., Palmer, N. O., Deblasio, M. J., Mitchell, M., Corbett, M., et al. (2013). Paternal obesity initiates metabolic disturbances in two generations of mice with incomplete penetrance to the F2 generation and alters the transcriptional profile of testis and sperm microRNA content. *FASEB J.* 27, 4226–4243. doi: 10.1096/fj.12-224048

Funston, R. N., Larson, D. M., and Vonnahme, K. A. (2010). Effects of maternal nutrition on conceptus growth and offspring performance: implications for beef cattle production. *J. Anim. Sci.* 88, E205–215. doi: 10.2527/jas.2009-2351

Gao, F., Niu, Y., Sun, Y. E., Lu, H., Chen, Y., Li, S., et al. (2017). *De novo* DNA methylation during monkey pre-implantation embryogenesis. *Cell Res.* 27, 526–539. doi: 10.1038/cr.2017.25

Gao, R., Wang, C., Gao, Y., Xiu, W., Chen, J., Kou, X., et al. (2018). Inhibition of Aberrant DNA Re-methylation improves post-implantation development of somatic cell nuclear transfer embryos. *Cell Stem Cell* 23, 426–435.e425. doi: 10.1016/j.stem.2018.07.017

Gapp, K., Jawaid, A., Sarkies, P., Bohacek, J., Pelczar, P., Prados, J., et al. (2014). Implication of sperm RNAs in transgenerational inheritance of the effects of early trauma in mice. *Nat. Neurosci.* 17, 667–669. doi: 10.1038/nn.3695

Gaydos, L. J., Wang, W., and Strome, S. (2014). Gene repression. H3K27me and PRC2 transmit a memory of repression across generations and during development. *Science* 345, 1515–1518. doi: 10.1126/science.1255023

Ge, Z. J., Schatten, H., Zhang, C. L., and Sun, Q. Y. (2015). Oocyte ageing and epigenetics. *Reproduction* 149, R103–114. doi: 10.1530/REP-14-0242

Gebert, C., Wrenzycki, C., Herrmann, D., Groger, D., Thiel, J., Reinhardt, R., et al. (2009). DNA methylation in the IGF2 intragenic DMR is re-established in a sex-specific manner in bovine blastocysts after somatic cloning. *Genomics* 94, 63–69. doi: 10.1016/j.ygeno.2009.03.004

Gilchrist, G. C., Tscherner, A., Nalpathamkalam, T., Merico, D., and Lamarre, J. (2016). MicroRNA expression during bovine oocyte maturation and fertilization. *Int. J. Mol. Sci.* 17:396. doi: 10.3390/ijms17030396

Glanzner, W. G., Rissi, V. B., De Macedo, M. P., Mujica, L. K. S., Gutierrez, K., Bridi, A., et al. (2018). Histone 3 lysine 4, 9, and 27 demethylases expression profile in fertilized and cloned bovine and porcine embryos. *Biol. Reprod.* 98, 742–751. doi: 10.1093/biolre/ioy054

Golding, M. C., Snyder, M., Williamson, G. L., Veazey, K. J., Peoples, M., Pryor, J. H., et al. (2015). Histone-lysine N-methyltransferase SETDB1 is required for development of the bovine blastocyst. *Theriogenology* 84, 1411–1422. doi: 10.1016/j.theriogenology.2015.07.028

Gomez, D., Shankman, L. S., Nguyen, A. T., and Owens, G. K. (2013). Detection of histone modifications at specific gene loci in single cells in histological sections. *Nat. Methods* 10, 171–177. doi: 10.1038/nmeth.2332

Gomez, J. A., Beitnere, U., and Segal, D. J. (2019). Live-animal epigenome editing: convergence of novel techniques. *Trends Genet.* 35, 527–541. doi: 10.1016/j.tig.2019.04.007

Gonzalez-Bulnes, A., Astiz, S., Ovilo, C., Lopez-Bote, C. J., Sanchez-Sanchez, R., Perez-Solana, M. L., et al. (2014). Early-postnatal changes in adiposity and

lipids profile by transgenerational developmental programming in swine with obesity/leptin resistance. *J. Endocrinol.* 223, M17–29. doi: 10.1530/JOE-14-0217

Gonzalez-Recio, O., Ugarte, E., and Bach, A. (2012). Trans-generational effect of maternal lactation during pregnancy: a Holstein cow model. *PLoS ONE* 7:e51816. doi: 10.1371/journal.pone.0051816

Govindaraju, A., Dogan, S., Rodriguez-Osorio, N., Grant, K., Kaya, A., and Memili, E. (2012a). Delivering value from sperm proteomics for fertility. *Cell Tissue Res.* 349, 783–793. doi: 10.1007/s00441-012-1452-2

Govindaraju, A., Uzun, A., Robertson, L., Atli, M. O., Kaya, A., Topper, E., et al. (2012b). Dynamics of microRNAs in bull spermatozoa. *Reprod. Biol. Endocrinol.* 10:82. doi: 10.1186/1477-7827-10-82

Grandjean, V., Gounon, P., Wagner, N., Martin, L., Wagner, K. D., Bernex, F., et al. (2009). The miR-124-Sox9 paramutation: RNA-mediated epigenetic control of embryonic and adult growth. *Development* 136, 3647–3655. doi: 10.1242/dev.041061

Grant, K. E., De Oliveira, R. V., Hennington, B. S., Govindaraju, A., Perkins, A., Stokes, J., et al. (2015). Sperm superoxide dismutase is associated with bull fertility. *Reprod. Fertil. Dev.* 28, 1405–1413. doi: 10.1071/RD14399

Greenberg, M. V. C., and Bourc'his, D. (2019). The diverse roles of DNA methylation in mammalian development and disease. *Nat. Rev. Mol. Cell Biol.* 20, 590–607. doi: 10.1038/s41580-019-0159-6

Greenlee, A. R., Shiao, M. S., Snyder, E., Buaas, F. W., Gu, T., Stearns, T. M., et al. (2012). Deregulated sex chromosome gene expression with male germ cell-specific loss of Dicer1. *PLoS ONE* 7:e46359. doi: 10.1371/journal.pone.0046359

Greer, E. L., Blanco, M. A., Gu, L., Sendinc, E., Liu, J., Aristizabal-Corrales, D., et al. (2015). DNA Methylation on N6-Adenine in C. elegans. *Cell* 161, 868–878. doi: 10.1016/j.cell.2015.04.005

Gross, N., Strillacci, M. G., Penagaricano, F., and Khatib, H. (2019). Characterization and functional roles of paternal RNAs in 2-4 cell bovine embryos. *Sci. Rep.* 9:20347. doi: 10.1038/s41598-019-55868-3

Gudex, B., Johnson, D., and Singh, K. (2014). Prenatal maternal and possible transgenerational epigenetic effects on milk production. *PLoS ONE* 9:e98928. doi: 10.1371/journal.pone.0098928

Guibert, S., Forne, T., and Weber, M. (2012). Global profiling of DNA methylation erasure in mouse primordial germ cells. *Genome Res* 22, 633–641. doi: 10.1101/gr.130997.111

Guo, F., Li, L., Li, J., Wu, X., Hu, B., Zhu, P., et al. (2017). Single-cell multi-omics sequencing of mouse early embryos and embryonic stem cells. *Cell Res* 27, 967–988. doi: 10.1038/cr.2017.82

Guo, H., Zhu, P., Yan, L., Li, R., Hu, B., Lian, Y., et al. (2014). The DNA methylation landscape of human early embryos. *Nature* 511, 606–610. doi: 10.1038/nature13544

Hackett, J. A., Sengupta, R., Zylicz, J. J., Murakami, K., Lee, C., Down, T. A., et al. (2013). Germline DNA demethylation dynamics and imprint erasure through 5-hydroxymethylcytosine. *Science* 339, 448–452. doi: 10.1126/science.1229277

Haile-Mariam, M., Nieuwhof, G. J., Beard, K. T., Konstatinov, K. V., and Hayes, B. J. (2013). Comparison of heritabilities of dairy traits in Australian Holstein-Friesian cattle from genomic and pedigree data and implications for genomic evaluations. *J. Anim. Breed. Genet.* 130, 20–31. doi: 10.1111/j.1439-0388.2012.01001.x

Halstead, M. M., Ma, X., Zhou, C., Schultz, R. M., and Ross, P. J. (2020). Chromatin remodeling in bovine embryos indicates species-specific regulation of genome activation. *Nat. Commun.* 11:4654. doi: 10.1038/s41467-020-18508-3

Han, Y. M., Kang, Y. K., Koo, D. B., and Lee, K. K. (2003). Nuclear reprogramming of cloned embryos produced *in vitro*. *Theriogenology* 59, 33–44. doi: 10.1016/S0093-691X(02)01271-2

Hanna, C. W., Taudt, A., Huang, J., Gahurova, L., Kranz, A., Andrews, S., et al. (2018). MLL2 conveys transcription-independent H3K4 trimethylation in oocytes. *Nat. Struct. Mol. Biol.* 25, 73–82. doi: 10.1038/s41594-017-0013-5

Hayashi, K., Chuva De Sousa Lopes, S. M., Kaneda, M., Tang, F., Hajkova, P., Lao, K., et al. (2008). MicroRNA biogenesis is required for mouse primordial germ cell development and spermatogenesis. *PLoS ONE* 3:e1738. doi: 10.1371/journal.pone.0001738

Heard, E., and Martienssen, R. A. (2014). Transgenerational epigenetic inheritance: myths and mechanisms. *Cell* 157, 95–109. doi: 10.1016/j.cell.2014.02.045

Heijmans, B. T., Tobi, E. W., Stein, A. D., Putter, H., Blauw, G. J., Susser, E. S., et al. (2008). Persistent epigenetic differences associated with prenatal exposure to famine in humans. *Proc. Natl. Acad. Sci. U.S.A.* 105, 17046–17049. doi: 10.1073/pnas.0806560105

Heinzmann, J., Hansmann, T., Herrmann, D., Wrenzycki, C., Zechner, U., Haaf, T., et al. (2011). Epigenetic profile of developmentally important genes in bovine oocytes. *Mol. Reprod. Dev.* 78, 188–201. doi: 10.1002/mrd.21281

Herrmann, D., Dahl, J. A., Lucas-Hahn, A., Collas, P., and Niemann, H. (2013). Histone modifications and mRNA expression in the inner cell mass and trophectoderm of bovine blastocysts. *Epigenetics* 8, 281–289. doi: 10.4161/epi.23899

Heyn, H., and Esteller, M. (2015). An adenine code for DNA: a second life for N6-Methyladenine. *Cell* 161, 710–713. doi: 10.1016/j.cell.2015.04.021

Hill, P. W. S., Leitch, H. G., Requena, C. E., Sun, Z., Amouroux, R., Roman-Trufero, M., et al. (2018). Epigenetic reprogramming enables the transition from primordial germ cell to gonocyte. *Nature* 555, 392–396. doi: 10.1038/nature25964

Hills, J. L., Wales, W. J., Dunshea, F. R., Garcia, S. C., and Roche, J. R. (2015). Invited review: an evaluation of the likely effects of individualized feeding of concentrate supplements to pasture-based dairy cows. *J. Dairy Sci.* 98, 1363–1401. doi: 10.3168/jds.2014-8475

Hilz, S., Modzelewski, A. J., Cohen, P. E., and Grimson, A. (2016). The roles of microRNAs and siRNAs in mammalian spermatogenesis. *Development* 143, 3061–3073. doi: 10.1242/dev.136721

Hu, W., Marchesi, D., Qiao, J., and Feng, H. L. (2012). Effect of slow freeze versus vitrification on the oocyte: an animal model. *Fertil. Steril.* 98, 752–760.e753. doi: 10.1016/j.fertnstert.2012.05.037

Huang, J., Zhang, H., Wang, X., Dobbs, K. B., Yao, J., Qin, G., et al. (2015). Impairment of preimplantation porcine embryo development by histone demethylase KDM5B knockdown through disturbance of bivalent H3K4me3-H3K27me3 modifications. *Biol. Reprod.* 92:72. doi: 10.1095/biolreprod.114.122762

Huang, J., Zhang, H., Yao, J., Qin, G., Wang, F., Wang, X., et al. (2016). BIX-01294 increases pig cloning efficiency by improving epigenetic reprogramming of somatic cell nuclei. *Reproduction* 151, 39–49. doi: 10.1530/REP-15-0460

Inoue, A., Jiang, L., Lu, F., Suzuki, T., and Zhang, Y. (2017). Maternal H3K27me3 controls DNA methylation-independent imprinting. *Nature* 547, 419–424. doi: 10.1038/nature23262

Inoue, A., Shen, L., Dai, Q., He, C., and Zhang, Y. (2011). Generation and replication-dependent dilution of 5fC and 5caC during mouse preimplantation development. *Cell Res.* 21, 1670–1676. doi: 10.1038/cr.2011.189

Inoue, A., and Zhang, Y. (2011). Replication-dependent loss of 5-hydroxymethylcytosine in mouse preimplantation embryos. *Science* 334:194. doi: 10.1126/science.1212483

Inoue, K., Kohda, T., Sugimoto, M., Sado, T., Ogonuki, N., Matoba, S., et al. (2010). Impeding Xist expression from the active X chromosome improves mouse somatic cell nuclear transfer. *Science* 330, 496–499. doi: 10.1126/science.1194174

Ispada, J., De Lima, C. B., Sirard, M. A., Fontes, P. K., Nogueira, M. F. G., Annes, K., et al. (2018). Genome-wide screening of DNA methylation in bovine blastocysts with different kinetics of development. *Epigenetics Chromatin* 11:1. doi: 10.1186/s13072-017-0171-z

Jachowicz, J. W., Bing, X., Pontabry, J., Boskovic, A., Rando, O. J., and Torres-Padilla, M. E. (2017). LINE-1 activation after fertilization regulates global chromatin accessibility in the early mouse embryo. *Nat. Genet.* 49, 1502–1510. doi: 10.1038/ng.3945

Jaenisch, R., and Bird, A. (2003). Epigenetic regulation of gene expression: how the genome integrates intrinsic and environmental signals. *Nat. Genet.* 33, 245–254. doi: 10.1038/ng1089

Ji, Y., Wu, Z., Dai, Z., Wang, X., Li, J., Wang, B., et al. (2017). Fetal and neonatal programming of postnatal growth and feed efficiency in swine. *J. Anim. Sci. Biotechnol.* 8:42. doi: 10.1186/s40104-017-0173-5

Jiang, Z., Lin, J., Dong, H., Zheng, X., Marjani, S. L., Duan, J., et al. (2018). DNA methylomes of bovine gametes and *in vivo* produced preimplantation embryos. *Biol. Reprod.* 99, 949–959. doi: 10.1093/biolre/ioy138

Jiang, Z., Sun, J., Dong, H., Luo, O., Zheng, X., Obergfell, C., et al. (2014). Transcriptional profiles of bovine *in vivo* pre-implantation development. *BMC Genomics* 15:756. doi: 10.1186/1471-2164-15-756

Jin, L., Guo, Q., Zhu, H. Y., Xing, X. X., Zhang, G. L., Xuan, M. F., et al. (2017). Quisinostat treatment improves histone acetylation and developmental

competence of porcine somatic cell nuclear transfer embryos. *Mol. Reprod. Dev.* 84, 340–346. doi: 10.1002/mrd.22787

Jirtle, R. L., and Skinner, M. K. (2007). Environmental epigenomics and disease susceptibility. *Nat. Rev. Genet.* 8, 253–262. doi: 10.1038/nrg2045

Jung, Y. H., Sauria, M. E. G., Lyu, X., Cheema, M. S., Ausio, J., Taylor, J., et al. (2017). Chromatin states in mouse sperm correlate with embryonic and adult regulatory landscapes. *Cell Rep.* 18, 1366–1382. doi: 10.1016/j.celrep.2017.01.034

Jurkowska, R. Z., Jurkowski, T. P., and Jeltsch, A. (2011). Structure and function of mammalian DNA methyltransferases. *Chembiochem* 12, 206–222. doi: 10.1002/cbic.201000195

Kaati, G., Bygren, L. O., Pembrey, M., and Sjostrom, M. (2007). Transgenerational response to nutrition, early life circumstances and longevity. *Eur. J. Hum. Genet.* 15, 784–790. doi: 10.1038/sj.ejhg.5201832

Kang, Y. K., Park, J. S., Koo, D. B., Choi, Y. H., Kim, S. U., Lee, K. K., et al. (2002). Limited demethylation leaves mosaic-type methylation states in cloned bovine pre-implantation embryos. *EMBO J.* 21, 1092–1100. doi: 10.1093/emboj/21.5.1092

Kaya, A., and Memili, E. (2016). Sperm macromolecules associated with bull fertility. *Anim. Reprod. Sci.* 169, 88–94. doi: 10.1016/j.anireprosci.2016.02.015

Ke, Y., Xu, Y., Chen, X., Feng, S., Liu, Z., Sun, Y., et al. (2017). 3D Chromatin structures of mature gametes and structural reprogramming during mammalian embryogenesis. *Cell* 170, 367–381.e320. doi: 10.1016/j.cell.2017.06.029

Khalili, M. A., Shahedi, A., Ashourzadeh, S., Nottola, S. A., Macchiarelli, G., and Palmerini, M. G. (2017). Vitrification of human immature oocytes before and after *in vitro* maturation: a review. *J. Assist. Reprod. Genet.* 34, 1413–1426. doi: 10.1007/s10815-017-1005-4

Khezri, A., Narud, B., Stenseth, E. B., Zeremichael, T. T., Myromslien, F. D., Wilson, R. C., et al. (2020). Sperm DNA hypomethylation proximal to reproduction pathway genes in maturing elite norwegian red bulls. *Front. Genet.* 11:922. doi: 10.3389/fgene.2020.00922

Khoueiry, R., Ibala-Rhomdane, S., Mery, L., Blachere, T., Guerin, J. F., Lornage, J., et al. (2008). Dynamic CpG methylation of the KCNQ1OT1 gene during maturation of human oocytes. *J. Med. Genet.* 45, 583–588. doi: 10.1136/jmg.2008.057943

Kim, E. D., and Sung, S. (2012). Long noncoding RNA: unveiling hidden layer of gene regulatory networks. *Trends Plant Sci.* 17, 16–21. doi: 10.1016/j.tplants.2011.10.008

Kishigami, S., Bui, H. T., Wakayama, S., Tokunaga, K., Van Thuan, N., Hikichi, T., et al. (2007). Successful mouse cloning of an outbred strain by trichostatin A treatment after somatic nuclear transfer. *J. Reprod. Dev.* 53, 165–170. doi: 10.1262/jrd.18098

Kishigami, S., Mizutani, E., Ohta, H., Hikichi, T., Thuan, N. V., Wakayama, S., et al. (2006). Significant improvement of mouse cloning technique by treatment with trichostatin A after somatic nuclear transfer. *Biochem. Biophys. Res. Commun.* 340, 183–189. doi: 10.1016/j.bbrc.2005.11.164

Kohli, R. M., and Zhang, Y. (2013). TET enzymes, TDG and the dynamics of DNA demethylation. *Nature* 502, 472–479. doi: 10.1038/nature12750

Kono, T., Obata, Y., Yoshimzu, T., Nakahara, T., and Carroll, J. (1996). Epigenetic modifications during oocyte growth correlates with extended parthenogenetic development in the mouse. *Nat. Genet.* 13, 91–94. doi: 10.1038/ng0596-91

Kouzarides, T. (2007). Chromatin modifications and their function. *Cell* 128, 693–705. doi: 10.1016/j.cell.2007.02.005

Koziol, M. J., Bradshaw, C. R., Allen, G. E., Costa, A. S. H., Frezza, C., and Gurdon, J. B. (2016). Identification of methylated deoxyadenosines in vertebrates reveals diversity in DNA modifications. *Nat. Struct. Mol. Biol.* 23, 24–30. doi: 10.1038/nsmb.3145

Kropp, J., Carrillo, J. A., Namous, H., Daniels, A., Salih, S. M., Song, J., et al. (2017). Male fertility status is associated with DNA methylation signatures in sperm and transcriptomic profiles of bovine preimplantation embryos. *BMC Genomics* 18:280. doi: 10.1186/s12864-017-3673-y

Kumar, A., Kroetsch, T., Blondin, P., and Anzar, M. (2015). Fertility-associated metabolites in bull seminal plasma and blood serum: 1H nuclear magnetic resonance analysis. *Mol. Reprod. Dev.* 82, 123–131. doi: 10.1002/mrd.22450

Kuramochi-Miyagawa, S., Kimura, T., Ijiri, T. W., Isobe, T., Asada, N., Fujita, Y., et al. (2004). Mili, a mammalian member of piwi family gene, is essential for spermatogenesis. *Development* 131, 839–849. doi: 10.1242/dev.00973

Kuramochi-Miyagawa, S., Watanabe, T., Gotoh, K., Totoki, Y., Toyoda, A., Ikawa, M., et al. (2008). DNA methylation of retrotransposon genes is regulated by Piwi family members MILI and MIWI2 in murine fetal testes. *Genes Dev.* 22, 908–917. doi: 10.1101/gad.1640708

Kutchy, N. A., Menezes, E. S. B., Chiappetta, A., Tan, W., Wills, R. W., Kaya, A., et al. (2018). Acetylation and methylation of sperm histone 3 lysine 27 (H3K27ac and H3K27me3) are associated with bull fertility. *Andrologia* 50:e12915. doi: 10.1111/and.12915

Kutchy, N. A., Menezes, E. S. B., Ugur, M. R., Ul Husna, A., Eldebaky, H., Evans, H. C., et al. (2019). Sperm cellular and nuclear dynamics associated with bull fertility. *Anim. Reprod. Sci.* 211:106203. doi: 10.1016/j.anireprosci.2019.106203

Kutchy, N. A., Velho, A., Menezes, E. S. B., Jacobsen, M., Thibaudeau, G., Wills, R. W., et al. (2017). Testis specific histone 2B is associated with sperm chromatin dynamics and bull fertility-a pilot study. *Reprod. Biol. Endocrinol.* 15:59. doi: 10.1186/s12958-017-0274-1

Lambert, S., Blondin, P., Vigneault, C., Labrecque, R., Dufort, I., and Sirard, M. A. (2018). Spermatozoa DNA methylation patterns differ due to peripubertal age in bulls. *Theriogenology* 106, 21–29. doi: 10.1016/j.theriogenology.2017.10.006

Lan, X., Cretney, E. C., Kropp, J., Khateeb, K., Berg, M. A., Penagaricano, F., et al. (2013). Maternal diet during pregnancy induces gene expression and DNA methylation changes in fetal tissues in sheep. *Front. Genet.* 4:49. doi: 10.3389/fgene.2013.00049

Lee, H. J., Hore, T. A., and Reik, W. (2014). Reprogramming the methylome: erasing memory and creating diversity. *Cell Stem Cell* 14, 710–719. doi: 10.1016/j.stem.2014.05.008

Leibfried-Rutledge, M. L., Critser, E. S., Eyestone, W. H., Northey, D. L., and First, N. L. (1987). Development potential of bovine oocytes matured *in vitro* or *in vivo*. *Biol. Reprod.* 36, 376–383. doi: 10.1095/biolreprod36.2.376

Lepikhov, K., Zakhartchenko, V., Hao, R., Yang, F., Wrenzycki, C., Niemann, H., et al. (2008). Evidence for conserved DNA and histone H3 methylation reprogramming in mouse, bovine and rabbit zygotes. *Epigenetics Chromatin* 1:8. doi: 10.1186/1756-8935-1-8

Li, E., Beard, C., and Jaenisch, R. (1993). Role for DNA methylation in genomic imprinting. *Nature* 366, 362–365. doi: 10.1038/366362a0

Li, T., Vu, T. H., Ulaner, G. A., Littman, E., Ling, J. Q., Chen, H. L., et al. (2005). IVF results in *de novo* DNA methylation and histone methylation at an Igf2-H19 imprinting epigenetic switch. *Mol. Hum. Reprod.* 11, 631–640. doi: 10.1093/molehr/gah230

Li, X., Yan, Q., Tang, S., Tan, Z., Fitzsimmons, C. J., and Yi, K. (2018). Effects of maternal feed intake restriction during pregnancy on the expression of growth regulation, imprinting and epigenetic transcription-related genes in foetal goats. *Anim. Reprod. Sci.* 198, 90–98. doi: 10.1016/j.anireprosci.2018.09.005

Li, Z., Zhao, S., Nelakanti, R. V., Lin, K., Wu, T. P., Alderman, M. H. III., et al. (2020). N(6)-methyladenine in DNA antagonizes SATB1 in early development. *Nature* 583, 625–630. doi: 10.1038/s41586-020-2500-9

Ling, Y. H., Zheng, Q., Li, Y. S., Sui, M. H., Wu, H., Zhang, Y. H., et al. (2019). Identification of lncRNAs by RNA sequencing analysis during *in vivo* pre-implantation developmental transformation in the goat. *Front. Genet.* 10:1040. doi: 10.3389/fgene.2019.01040

Lister, R., Pelizzola, M., Dowen, R. H., Hawkins, R. D., Hon, G., Tonti-Filippini, J., et al. (2009). Human DNA methylomes at base resolution show widespread epigenomic differences. *Nature* 462, 315–322. doi: 10.1038/nature 08514

Liu, J., Zhu, Y., Luo, G. Z., Wang, X., Yue, Y., Wang, X., et al. (2016). Abundant DNA 6mA methylation during early embryogenesis of zebrafish and pig. *Nat. Commun.* 7:13052. doi: 10.1038/ncomms13052

Liu, L., Leng, L., Liu, C., Lu, C., Yuan, Y., Wu, L., et al. (2019). An integrated chromatin accessibility and transcriptome landscape of human pre-implantation embryos. *Nat. Commun.* 10:364. doi: 10.1038/s41467-018-08244-0

Liu, S., Fang, L., Zhou, Y., Santos, D. J. A., Xiang, R., Daetwyler, H. D., et al. (2019). Analyses of inter-individual variations of sperm DNA methylation and their potential implications in cattle. *BMC Genomics* 20:888. doi: 10.1186/s12864-019-6228-6

Liu, W., Liu, X., Wang, C., Gao, Y., Gao, R., Kou, X., et al. (2016). Identification of key factors conquering developmental arrest of somatic cell cloned embryos by combining embryo biopsy and single-cell sequencing. *Cell Discov.* 2:16010. doi: 10.1038/celldisc.2016.10

Liu, X., Wang, C., Liu, W., Li, J., Li, C., Kou, X., et al. (2016). Distinct features of H3K4me3 and H3K27me3 chromatin domains in pre-implantation embryos. *Nature* 537, 558–562. doi: 10.1038/nature19362

Liu, X., Wang, Y., Gao, Y., Su, J., Zhang, J., Xing, X., et al. (2018). H3K9 demethylase KDM4E is an epigenetic regulator for bovine embryonic development and a defective factor for nuclear reprogramming. *Development* 145:dev158261. doi: 10.1242/dev.158261

Lu, F., Liu, Y., Inoue, A., Suzuki, T., Zhao, K., and Zhang, Y. (2016). Establishing chromatin regulatory landscape during mouse preimplantation development. *Cell* 165, 1375–1388. doi: 10.1016/j.cell.2016.05.050

Maatouk, D. M., Loveland, K. L., Mcmanus, M. T., Moore, K., and Harfe, B. D. (2008). Dicer1 is required for differentiation of the mouse male germline. *Biol. Reprod.* 79, 696–703. doi: 10.1095/biolreprod.108.067827

Martin, G. B., Blache, D., Miller, D. W., and Vercoe, P. E. (2010). Interactions between nutrition and reproduction in the management of the mature male ruminant. *Animal* 4, 1214–1226. doi: 10.1017/S1751731109991674

Matoba, S., Liu, Y., Lu, F., Iwabuchi, K. A., Shen, L., Inoue, A., et al. (2014). Embryonic development following somatic cell nuclear transfer impeded by persisting histone methylation. *Cell* 159, 884–895. doi: 10.1016/j.cell.2014.09.055

Mattern, F., Herrmann, D., Heinzmann, J., Hadeler, K. G., Bernal-Ulloa, S. M., Haaf, T., et al. (2016). DNA methylation and mRNA expression of developmentally important genes in bovine oocytes collected from donors of different age categories. *Mol. Reprod. Dev.* 83, 802–814. doi: 10.1002/mrd.22692

Mayer, W., Niveleau, A., Walter, J., Fundele, R., and Haaf, T. (2000). Demethylation of the zygotic paternal genome. *Nature* 403, 501–502. doi: 10.1038/35000656

McGraw, S., Vigneault, C., and Sirard, M. A. (2007). Temporal expression of factors involved in chromatin remodeling and in gene regulation during early bovine *in vitro* embryo development. *Reproduction* 133, 597–608. doi: 10.1530/REP-06-0251

Memili, E., Moura, A. A., and Kaya, A. (2020). Metabolomes of sperm and seminal plasma associated with bull fertility. *Anim. Reprod. Sci.* 220:106355. doi: 10.1016/j.anireprosci.2020.106355

Menezes, E. B., Velho, A. L. C., Santos, F., Dinh, T., Kaya, A., Topper, E., et al. (2019). Uncovering sperm metabolome to discover biomarkers for bull fertility. *BMC Genomics* 20:714. doi: 10.1186/s12864-019-6074-6

Menezes, E. S. B., Badial, P. R., El Debaky, H., Husna, A. U., Ugur, M. R., Kaya, A., et al. (2020). Sperm miR-15a and miR-29b are associated with bull fertility. *Andrologia* 52:e13412. doi: 10.1111/and.13412

Ming, H., Sun, J., Pasquariello, R., Herrick, J. R., Yuan, Y., Gutierrez, E., et al. (2020). 2 The landscape of accessible chromatin in bovine oocytes and early embryos. *Reprod. Fertil. Dev.* 32:125. doi: 10.1071/RDv32n2Ab2

Modzelewski, A. J., Hilz, S., Crate, E. A., Schweidenback, C. T., Fogarty, E. A., Grenier, J. K., et al. (2015). Dgcr8 and Dicer are essential for sex chromosome integrity during meiosis in males. *J. Cell Sci.* 128, 2314–2327. doi: 10.1242/jcs.167148

Nakamura, T., Liu, Y. J., Nakashima, H., Umehara, H., Inoue, K., Matoba, S., et al. (2012). PGC7 binds histone H3K9me2 to protect against conversion of 5mC to 5hmC in early embryos. *Nature* 486, 415–419. doi: 10.1038/nature11093

Niemann, H., Carnwath, J. W., Herrmann, D., Wieczorek, G., Lemme, E., Lucas-Hahn, A., et al. (2010). DNA methylation patterns reflect epigenetic reprogramming in bovine embryos. *Cell. Reprogram* 12, 33–42. doi: 10.1089/cell.2009.0063

O'Doherty, A. M., Magee, D. A., O'shea, L. C., Forde, N., Beltman, M. E., Mamo, S., et al. (2015). DNA methylation dynamics at imprinted genes during bovine pre-implantation embryo development. *BMC Dev. Biol.* 15:13. doi: 10.1186/s12861-015-0060-2

O'Doherty, A. M., O'gorman, A., Al Naib, A., Brennan, L., Daly, E., Duffy, P., et al. (2014). Negative energy balance affects imprint stability in oocytes recovered from postpartum dairy cows. *Genomics* 104, 177–185. doi: 10.1016/j.ygeno.2014.07.006

Org, T., Hensen, K., Kreevan, R., Mark, E., Sarv, O., Andreson, R., et al. (2019). Genome-wide histone modification profiling of inner cell mass and trophectoderm of bovine blastocysts by RAT-ChIP. *PLoS ONE* 14:e0225801. doi: 10.1371/journal.pone.0225801

Osman, E., Franasiak, J., and Scott, R. (2018). Oocyte and Embryo Manipulation and Epigenetics. *Semin. Reprod. Med.* 36, e1–e9. doi: 10.1055/s-0039-1688801

Ostermeier, G. C., Miller, D., Huntriss, J. D., Diamond, M. P., and Krawetz, S. A. (2004). Reproductive biology: delivering spermatozoan RNA to the oocyte. *Nature* 429:154. doi: 10.1038/429154a

Oswald, J., Engemann, S., Lane, N., Mayer, W., Olek, A., Fundele, R., et al. (2000). Active demethylation of the paternal genome in the mouse zygote. *Curr. Biol.* 10, 475–478. doi: 10.1016/S0960-9822(00)00448-6

Painter, R. C., Osmond, C., Gluckman, P., Hanson, M., Phillips, D. I., and Roseboom, T. J. (2008). Transgenerational effects of prenatal exposure to the Dutch famine on neonatal adiposity and health in later life. *BJOG* 115, 1243–1249. doi: 10.1111/j.1471-0528.2008.01822.x

Park, J. S., Jeong, Y. S., Shin, S. T., Lee, K. K., and Kang, Y. K. (2007). Dynamic DNA methylation reprogramming: active demethylation and immediate remethylation in the male pronucleus of bovine zygotes. *Dev. Dyn.* 236, 2523–2533. doi: 10.1002/dvdy.21278

Pasquariello, R., Fernandez-Fuertes, B., Strozzi, F., Pizzi, F., Mazza, R., Lonergan, P., et al. (2017). Profiling bovine blastocyst microRNAs using deep sequencing. *Reprod. Fertil. Dev.* 29, 1545–1555. doi: 10.1071/RD16110

Peat, J. R., and Reik, W. (2012). Incomplete methylation reprogramming in SCNT embryos. *Nat. Genet.* 44, 965–966. doi: 10.1038/ng.2393

Peddinti, D., Nanduri, B., Kaya, A., Feugang, J. M., Burgess, S. C., and Memili, E. (2008). Comprehensive proteomic analysis of bovine spermatozoa of varying fertility rates and identification of biomarkers associated with fertility. *BMC Syst. Biol.* 2:19. doi: 10.1186/1752-0509-2-19

Pembrey, M., Saffery, R., Bygren, L. O., Network in Epigenetic, E., and Network in Epigenetic, E. (2014). Human transgenerational responses to early-life experience: potential impact on development, health and biomedical research. *J. Med. Genet.* 51, 563–572. doi: 10.1136/jmedgenet-2014-102577

Pembrey, M. E., Bygren, L. O., Kaati, G., Edvinsson, S., Northstone, K., Sjostrom, M., et al. (2006). Sex-specific, male-line transgenerational responses in humans. *Eur. J. Hum. Genet.* 14, 159–166. doi: 10.1038/sj.ejhg.5201538

Perrier, J. P., Sellem, E., Prezelin, A., Gasselin, M., Jouneau, L., Piumi, F., et al. (2018). A multi-scale analysis of bull sperm methylome revealed both species peculiarities and conserved tissue-specific features. *BMC Genomics* 19:404. doi: 10.1186/s12864-018-4764-0

Poirier, M., Tesfaye, D., Hailay, T., Salilew-Wondim, D., Gebremedhn, S., Rings, F., et al. (2020). Metabolism-associated genome-wide epigenetic changes in bovine oocytes during early lactation. *Sci. Rep.* 10:2345. doi: 10.1038/s41598-020-59410-8

Ponting, C. P., and Belgard, T. G. (2010). Transcribed dark matter: meaning or myth? *Hum. Mol. Genet.* 19, R162–168. doi: 10.1093/hmg/ddq362

Popp, C., Dean, W., Feng, S., Cokus, S. J., Andrews, S., Pellegrini, M., et al. (2010). Genome-wide erasure of DNA methylation in mouse primordial germ cells is affected by AID deficiency. *Nature* 463, 1101–1105. doi: 10.1038/nature08829

Racedo, S. E., Wrenzycki, C., Lepikhov, K., Salamone, D., Walter, J., and Niemann, H. (2009). Epigenetic modifications and related mRNA expression during bovine oocyte *in vitro* maturation. *Reprod. Fertil. Dev.* 21, 738–748. doi: 10.1071/RD09039

Radford, E. J., Ito, M., Shi, H., Corish, J. A., Yamazawa, K., Isganaitis, E., et al. (2014). *In utero* effects. *In utero* undernourishment perturbs the adult sperm methylome and intergenerational metabolism. *Science* 345:1255903. doi: 10.1126/science.1255903

Rajanahally, S., Raheem, O., Rogers, M., Brisbane, W., Ostrowski, K., Lendvay, T., et al. (2019). The relationship between cannabis and male infertility, sexual health, and neoplasm: a systematic review. *Andrology* 7, 139–147. doi: 10.1111/andr.12585

Rassoulzadegan, M., Grandjean, V., Gounon, P., Vincent, S., Gillot, I., and Cuzin, F. (2006). RNA-mediated non-mendelian inheritance of an epigenetic change in the mouse. *Nature* 441, 469–474. doi: 10.1038/nature04674

Rechtsteiner, A., Ercan, S., Takasaki, T., Phippen, T. M., Egelhofer, T. A., Wang, W., et al. (2010). The histone H3K36 methyltransferase MES-4 acts epigenetically to transmit the memory of germline gene expression to progeny. *PLoS Genet.* 6:e1001091. doi: 10.1371/journal.pgen.1001091

Reik, W., and Maher, E. R. (1997). Imprinting in clusters: lessons from Beckwith-Wiedemann syndrome. *Trends Genet.* 13, 330–334. doi: 10.1016/S0168-9525(97)01200-6

Reis e Silva, A. R., Bruno, C., Fleurot, R., Daniel, N., Archilla, C., Peynot, N., et al. (2012). Alteration of DNA demethylation dynamics by *in vitro*

culture conditions in rabbit pre-implantation embryos. *Epigenetics* 7, 440–446. doi: 10.4161/epi.19563

Rizos, D., Ward, F., Duffy, P., Boland, M. P., and Lonergan, P. (2002). Consequences of bovine oocyte maturation, fertilization or early embryo development *in vitro* versus *in vivo*: implications for blastocyst yield and blastocyst quality. *Mol. Reprod. Dev.* 61, 234–248. doi: 10.1002/mrd.1153

Rodgers, A. B., Morgan, C. P., Leu, N. A., and Bale, T. L. (2015). Transgenerational epigenetic programming via sperm microRNA recapitulates effects of paternal stress. *Proc. Natl. Acad. Sci. U.S.A.* 112, 13699–13704. doi: 10.1073/pnas.1508347112

Romero, Y., Meikar, O., Papaioannou, M. D., Conne, B., Grey, C., Weier, M., et al. (2011). Dicer1 depletion in male germ cells leads to infertility due to cumulative meiotic and spermiogenic defects. *PLoS ONE* 6:e25241. doi: 10.1371/journal.pone.0025241

Roovers, E. F., Rosenkranz, D., Mahdipour, M., Han, C. T., He, N., Chuva De Sousa Lopes, S. M., et al. (2015). Piwi proteins and piRNAs in mammalian oocytes and early embryos. *Cell Rep.* 10, 2069–2082. doi: 10.1016/j.celrep.2015.02.062

Ross, P. J., Ragina, N. P., Rodriguez, R. M., Iager, A. E., Siripattarapravat, K., Lopez-Corrales, N., et al. (2008). Polycomb gene expression and histone H3 lysine 27 trimethylation changes during bovine preimplantation development. *Reproduction* 136, 777–785. doi: 10.1530/REP-08-0045

Saadeh, H., and Schulz, R. (2014). Protection of CpG islands against *de novo* DNA methylation during oogenesis is associated with the recognition site of E2f1 and E2f2. *Epigenetics Chromatin* 7:26. doi: 10.1186/1756-8935-7-26

Sadler-Riggleman, I., Klukovich, R., Nilsson, E., Beck, D., Xie, Y., Yan, W., et al. (2019). Epigenetic transgenerational inheritance of testis pathology and Sertoli cell epimutations: generational origins of male infertility. *Environ. Epigenet.* 5:dvz013. doi: 10.1093/eep/dvz013

Salilew-Wondim, D., Fournier, E., Hoelker, M., Saeed-Zidane, M., Tholen, E., Looft, C., et al. (2015). Genome-Wide DNA methylation patterns of bovine blastocysts developed *in vivo* from embryos completed different stages of development *in vitro*. *PLoS ONE* 10:e0140467. doi: 10.1371/journal.pone.0140467

Salilew-Wondim, D., Saeed-Zidane, M., Hoelker, M., Gebremedhn, S., Poirier, M., Pandey, H. O., et al. (2018). Genome-wide DNA methylation patterns of bovine blastocysts derived from *in vivo* embryos subjected to *in vitro* culture before, during or after embryonic genome activation. *BMC Genomics* 19:424. doi: 10.1186/s12864-018-4826-3

Santos, F., Hendrich, B., Reik, W., and Dean, W. (2002). Dynamic reprogramming of DNA methylation in the early mouse embryo. *Dev. Biol.* 241, 172–182. doi: 10.1006/dbio.2001.0501

Santos, F., Zakhartchenko, V., Stojkovic, M., Peters, A., Jenuwein, T., Wolf, E., et al. (2003). Epigenetic marking correlates with developmental potential in cloned bovine preimplantation embryos. *Curr. Biol.* 13, 1116–1121. doi: 10.1016/S0960-9822(03)00419-6

Sato, A., Otsu, E., Negishi, H., Utsunomiya, T., and Arima, T. (2007). Aberrant DNA methylation of imprinted loci in superovulated oocytes. *Hum. Reprod.* 22, 26–35. doi: 10.1093/humrep/del316

Sawai, K., Takahashi, M., Moriyasu, S., Hirayama, H., Minamihashi, A., Hashizume, T., et al. (2010). Changes in the DNA methylation status of bovine embryos from the blastocyst to elongated stage derived from somatic cell nuclear transfer. *Cell. Reprogram* 12, 15–22. doi: 10.1089/cell.2009.0039

Schieber, M., and Chandel, N. S. (2014). ROS function in redox signaling and oxidative stress. *Curr. Biol.* 24, R453–462. doi: 10.1016/j.cub.2014.03.034

Schroeder, D. I., Jayashankar, K., Douglas, K. C., Thirkill, T. L., York, D., Dickinson, P. J., et al. (2015). Early developmental and evolutionary origins of gene body DNA methylation patterns in mammalian placentas. *PLoS Genet.* 11:e1005442. doi: 10.1371/journal.pgen.1005442

Schultz, M. D., He, Y., Whitaker, J. W., Hariharan, M., Mukamel, E. A., Leung, D., et al. (2015). Human body epigenome maps reveal noncanonical DNA methylation variation. *Nature* 523:212. doi: 10.1038/nature14465

Sellem, E., Marthey, S., Rau, A., Jouneau, L., Bonnet, A., Perrier, J. P., et al. (2020). A comprehensive overview of bull sperm-borne small non-coding RNAs and their diversity across breeds. *Epigenetics Chromatin* 13:19. doi: 10.1186/s13072-020-00340-0

Shi, W., and Haaf, T. (2002). Aberrant methylation patterns at the two-cell stage as an indicator of early developmental failure. *Mol. Reprod. Dev.* 63, 329–334. doi: 10.1002/mrd.90016

Siklenka, K., Erkek, S., Godmann, M., Lambrot, R., Mcgraw, S., Lafleur, C., et al. (2015). Disruption of histone methylation in developing sperm impairs offspring health transgenerationally. *Science* 350:aab2006. doi: 10.1126/science.aab2006

Sinclair, K. D., Allegrucci, C., Singh, R., Gardner, D. S., Sebastian, S., Bispham, J., et al. (2007). DNA methylation, insulin resistance, and blood pressure in offspring determined by maternal periconceptional B vitamin and methionine status. *Proc. Natl. Acad. Sci. U.S.A.* 104, 19351–19356. doi: 10.1073/pnas.0707258104

Sinclair, K. D., Rutherford, K. M., Wallace, J. M., Brameld, J. M., Stoger, R., Alberio, R., et al. (2016). Epigenetics and developmental programming of welfare and production traits in farm animals. *Reprod. Fertil. Dev.* 28, 1443–1478. doi: 10.1071/RD16102

Siomi, M. C., Sato, K., Pezic, D., and Aravin, A. A. (2011). PIWI-interacting small RNAs: the vanguard of genome defence. *Nat. Rev. Mol. Cell Biol.* 12, 246–258. doi: 10.1038/nrm3089

Sirard, M. A. (2017). The influence of *in vitro* fertilization and embryo culture on the embryo epigenetic constituents and the possible consequences in the bovine model. *J. Dev. Orig. Health Dis.* 8, 411–417. doi: 10.1017/S2040174417000125

Sjunnesson, Y. (2019). *In vitro* fertilisation in domestic mammals—a brief overview. *Ups. J. Med. Sci.* 1–9. doi: 10.1080/03009734.2019.1697911

Skene, P. J., and Henikoff, S. (2017). An efficient targeted nuclease strategy for high-resolution mapping of DNA binding sites. *Elife* 6:e21856. doi: 10.7554/eLife.21856

Skinner, M. K. (2008). What is an epigenetic transgenerational phenotype? F3 or F2. *Reprod. Toxicol.* 25, 2–6. doi: 10.1016/j.reprotox.2007.09.001

Skvortsova, K., Iovino, N., and Bogdanovic, O. (2018). Functions and mechanisms of epigenetic inheritance in animals. *Nat. Rev. Mol. Cell Biol.* 19, 774–790. doi: 10.1038/s41580-018-0074-2

Small, E. C., Xi, L., Wang, J. P., Widom, J., and Licht, J. D. (2014). Single-cell nucleosome mapping reveals the molecular basis of gene expression heterogeneity. *Proc. Natl. Acad. Sci. U.S.A.* 111, E2462–2471. doi: 10.1073/pnas.1400517111

Smallwood, S. A., Lee, H. J., Angermueller, C., Krueger, F., Saadeh, H., Peat, J., et al. (2014). Single-cell genome-wide bisulfite sequencing for assessing epigenetic heterogeneity. *Nat. Methods* 11, 817–820. doi: 10.1038/nmeth.3035

Smallwood, S. A., Tomizawa, S., Krueger, F., Ruf, N., Carli, N., Segonds-Pichon, A., et al. (2011). Dynamic CpG island methylation landscape in oocytes and preimplantation embryos. *Nat. Genet.* 43, 811–814. doi: 10.1038/ng.864

Smith, L. C., Therrien, J., Filion, F., Bressan, F., and Meirelles, F. V. (2015). Epigenetic consequences of artificial reproductive technologies to the bovine imprinted genes SNRPN, H19/IGF2, and IGF2R. *Front. Genet.* 6:58. doi: 10.3389/fgene.2015.00058

Smith, Z. D., Chan, M. M., Humm, K. C., Karnik, R., Mekhoubad, S., Regev, A., et al. (2014). DNA methylation dynamics of the human preimplantation embryo. *Nature* 511, 611–615. doi: 10.1038/nature13581

Smith, Z. D., Chan, M. M., Mikkelsen, T. S., Gu, H., Gnirke, A., Regev, A., et al. (2012). A unique regulatory phase of DNA methylation in the early mammalian embryo. *Nature* 484, 339–344. doi: 10.1038/nature10960

Smith, Z. D., and Meissner, A. (2013). DNA methylation: roles in mammalian development. *Nat. Rev. Genet.* 14, 204–220. doi: 10.1038/nrg3354

Song, R., Hennig, G. W., Wu, Q., Jose, C., Zheng, H., and Yan, W. (2011). Male germ cells express abundant endogenous siRNAs. *Proc. Natl. Acad. Sci. U.S.A.* 108, 13159–13164. doi: 10.1073/pnas.1108567108

Stevens, A., Begum, G., Cook, A., Connor, K., Rumball, C., Oliver, M., et al. (2010). Epigenetic changes in the hypothalamic proopiomelanocortin and glucocorticoid receptor genes in the ovine fetus after periconceptional undernutrition. *Endocrinology* 151, 3652–3664. doi: 10.1210/en.2010-0094

Suh, N., Baehner, L., Moltzahn, F., Melton, C., Shenoy, A., Chen, J., et al. (2010). MicroRNA function is globally suppressed in mouse oocytes and early embryos. *Curr. Biol.* 20, 271–277. doi: 10.1016/j.cub.2009.12.044

Sutcliffe, A. G., Peters, C. J., Bowdin, S., Temple, K., Reardon, W., Wilson, L., et al. (2006). Assisted reproductive therapies and imprinting disorders–a preliminary British survey. *Hum. Reprod.* 21, 1009–1011. doi: 10.1093/humrep/dei405

Takeda, K., Kobayashi, E., Nishino, K., Imai, A., Adachi, H., Hoshino, Y., et al. (2019). Age-related changes in DNA methylation levels at CpG sites in bull spermatozoa and *in vitro* fertilization-derived blastocyst-stage embryos revealed by combined bisulfite

restriction analysis. *J. Reprod. Dev.* 65, 305–312. doi: 10.1262/jrd.2018-146

Tang, W. W., Dietmann, S., Irie, N., Leitch, H. G., Floros, V. I., Bradshaw, C. R., et al. (2015). A unique gene regulatory network resets the human germline epigenome for development. *Cell* 161, 1453–1467. doi: 10.1016/j.cell.2015.04.053

Tesfaye, D., Worku, D., Rings, F., Phatsara, C., Tholen, E., Schellander, K., et al. (2009). Identification and expression profiling of microRNAs during bovine oocyte maturation using heterologous approach. *Mol. Reprod. Dev.* 76, 665–677. doi: 10.1002/mrd.21005

Thompson, J. G. (1997). Comparison between *in vivo*-derived and *in vitro*-produced pre-elongation embryos from domestic ruminants. *Reprod. Fertil. Dev.* 9, 341–354. doi: 10.1071/R96079

Tobi, E. W., Goeman, J. J., Monajemi, R., Gu, H., Putter, H., Zhang, Y., et al. (2014). DNA methylation signatures link prenatal famine exposure to growth and metabolism. *Nat. Commun.* 5:5592. doi: 10.1038/ncomms6592

Tomizawa, S., Kobayashi, H., Watanabe, T., Andrews, S., Hata, K., Kelsey, G., et al. (2011). Dynamic stage-specific changes in imprinted differentially methylated regions during early mammalian development and prevalence of non-CpG methylation in oocytes. *Development* 138, 811–820. doi: 10.1242/dev.061416

Toschi, P., Capra, E., Anzalone, D. A., Lazzari, B., Turri, F., Pizzi, F., et al. (2020). Maternal peri-conceptional undernourishment perturbs offspring sperm methylome. *Reproduction* 159, 513–523. doi: 10.1530/REP-19-0549

Tscherner, A., Gilchrist, G., Smith, N., Blondin, P., Gillis, D., and Lamarre, J. (2014). MicroRNA-34 family expression in bovine gametes and preimplantation embryos. *Reprod. Biol. Endocrinol.* 12:85. doi: 10.1186/1477-7827-12-85

Ugur, M. R., Dinh, T., Hitit, M., Kaya, A., Topper, E., Didion, B., et al. (2019). Amino acids of seminal plasma associated with freezability of bull sperm. *Front Cell Dev Biol.* 7:347. doi: 10.3389/fcell.2019.00347

Urrego, R., Bernal-Ulloa, S. M., Chavarria, N. A., Herrera-Puerta, E., Lucas-Hahn, A., Herrmann, D., et al. (2017). Satellite DNA methylation status and expression of selected genes in Bos indicus blastocysts produced *in vivo* and *in vitro*. *Zygote* 25, 131–140. doi: 10.1017/S096719941600040X

Urrego, R., Rodriguez-Osorio, N., and Niemann, H. (2014). Epigenetic disorders and altered gene expression after use of Assisted Reproductive Technologies in domestic cattle. *Epigenetics* 9, 803–815. doi: 10.4161/epi.28711

Van Thuan, N., Bui, H. T., Kim, J. H., Hikichi, T., Wakayama, S., Kishigami, S., et al. (2009). The histone deacetylase inhibitor scriptaid enhances nascent mRNA production and rescues full-term development in cloned inbred mice. *Reproduction* 138, 309–317. doi: 10.1530/REP-08-0299

Veenendaal, M. V., Painter, R. C., De Rooij, S. R., Bossuyt, P. M., Van Der Post, J. A., Gluckman, P. D., et al. (2013). Transgenerational effects of prenatal exposure to the 1944-45 Dutch famine. *BJOG* 120, 548–553. doi: 10.1111/1471-0528.12136

Velho, A., Wang, H., Koenig, L., Grant, K. E., Menezes, E. S., Kaya, A., et al. (2019). Expression dynamics of Integrin Subunit Beta 5 in bovine gametes and embryos imply functions in male fertility and early embryonic development. *Andrologia* 51:e13305. doi: 10.1111/and.13305

Velho, A. L. C., Menezes, E., Dinh, T., Kaya, A., Topper, E., Moura, A. A., et al. (2018). Metabolomic markers of fertility in bull seminal plasma. *PLoS ONE* 13:e0195279. doi: 10.1371/journal.pone.0195279

Venkatesh, S., and Workman, J. L. (2015). Histone exchange, chromatin structure and the regulation of transcription. *Nat. Rev. Mol. Cell Biol.* 16, 178–189. doi: 10.1038/nrm3941

Verma, A., Rajput, S., Kumar, S., De, S., Chakravarty, A. K., Kumar, R., et al. (2015). Differential histone modification status of spermatozoa in relation to fertility of buffalo bulls. *J. Cell. Biochem.* 116, 743–753. doi: 10.1002/jcb.25029

Viana, A. G. A., Martins, A. M. A., Pontes, A. H., Fontes, W., Castro, M. S., Ricart, C., et al. (2018). Proteomic landscape of seminal plasma associated with dairy bull fertility. *Sci. Rep.* 8:16323. doi: 10.1038/s41598-018-34152-w

Wagner, K. D., Wagner, N., Ghanbarian, H., Grandjean, V., Gounon, P., Cuzin, F., et al. (2008). RNA induction and inheritance of epigenetic cardiac hypertrophy in the mouse. *Dev. Cell* 14, 962–969. doi: 10.1016/j.devcel.2008.03.009

Wen, L., and Tang, F. (2019). Human Germline Cell Development: from the Perspective of Single-Cell Sequencing. *Mol. Cell* 76, 320–328. doi: 10.1016/j.molcel.2019.08.025

Westfalewicz, B., Dietrich, M. A., Mostek, A., Partyka, A., Bielas, W., Nizanski, W., et al. (2017). Analysis of bull (Bos taurus) seminal vesicle fluid proteome in relation to seminal plasma proteome. *J. Dairy Sci.* 100, 2282–2298. doi: 10.3168/jds.2016-11866

Williams-Wyss, O., Zhang, S., Maclaughlin, S. M., Kleemann, D., Walker, S. K., Suter, C. M., et al. (2014). Embryo number and periconceptional undernutrition in the sheep have differential effects on adrenal epigenotype, growth, and development. *Am. J. Physiol. Endocrinol. Metab.* 307, E141–150. doi: 10.1152/ajpendo.00051.2012

Wossidlo, M., Nakamura, T., Lepikhov, K., Marques, C. J., Zakhartchenko, V., Boiani, M., et al. (2011). 5-Hydroxymethylcytosine in the mammalian zygote is linked with epigenetic reprogramming. *Nat. Commun.* 2:241. doi: 10.1038/ncomms1240

Wrenzycki, C., and Niemann, H. (2003). Epigenetic reprogramming in early embryonic development: effects of *in-vitro* production and somatic nuclear transfer. *Reprod. Biomed. Online* 7, 649–656. doi: 10.1016/S1472-6483(10)62087-1

Wu, C., Blondin, P., Vigneault, C., Labrecque, R., and Sirard, M. A. (2020a). The age of the bull influences the transcriptome and epigenome of blastocysts produced by IVF. *Theriogenology* 144, 122–131. doi: 10.1016/j.theriogenology.2019.12.020

Wu, C., Blondin, P., Vigneault, C., Labrecque, R., and Sirard, M. A. (2020b). Sperm miRNAs- potential mediators of bull age and early embryo development. *BMC Genomics* 21:798. doi: 10.1186/s12864-020-07206-5

Wu, J., Huang, B., Chen, H., Yin, Q., Liu, Y., Xiang, Y., et al. (2016). The landscape of accessible chromatin in mammalian preimplantation embryos. *Nature* 534, 652–657. doi: 10.1038/nature18606

Wu, J., Xu, J., Liu, B., Yao, G., Wang, P., Lin, Z., et al. (2018). Chromatin analysis in human early development reveals epigenetic transition during ZGA. *Nature* 557, 256–260. doi: 10.1038/s41586-018-0080-8

Wu, Q., Song, R., Ortogero, N., Zheng, H., Evanoff, R., Small, C. L., et al. (2012). The RNase III enzyme DROSHA is essential for microRNA production and spermatogenesis. *J. Biol. Chem.* 287, 25173–25190. doi: 10.1074/jbc.M112.362053

Wu, T. P., Wang, T., Seetin, M. G., Lai, Y., Zhu, S., Lin, K., et al. (2016). DNA methylation on N(6)-adenine in mammalian embryonic stem cells. *Nature* 532, 329–333. doi: 10.1038/nature17640

Wu, X., Li, Y., Xue, L., Wang, L., Yue, Y., Li, K., et al. (2011). Multiple histone site epigenetic modifications in nuclear transfer and *in vitro* fertilized bovine embryos. *Zygote* 19, 31–45. doi: 10.1017/S0967199410000328

Wyck, S., Herrera, C., Requena, C. E., Bittner, L., Hajkova, P., Bollwein, H., et al. (2018). Oxidative stress in sperm affects the epigenetic reprogramming in early embryonic development. *Epigenetics Chromatin* 11:60. doi: 10.1186/s13072-018-0224-y

Xia, W., Xu, J., Yu, G., Yao, G., Xu, K., Ma, X., et al. (2019). Resetting histone modifications during human parental-to-zygotic transition. *Science* 365, 353–360. doi: 10.1126/science.aaw5118

Xie, B., Zhang, H., Wei, R., Li, Q., Weng, X., Kong, Q., et al. (2016). Histone H3 lysine 27 trimethylation acts as an epigenetic barrier in porcine nuclear reprogramming. *Reproduction* 151, 9–16. doi: 10.1530/REP-15-0338

Xie, Q., Wu, T. P., Gimple, R. C., Li, Z., Prager, B. C., Wu, Q., et al. (2018). N(6)-methyladenine DNA Modification in Glioblastoma. *Cell* 175, 1228–1243.e1220. doi: 10.1016/j.cell.2018.10.006

Xu, Q., and Xie, W. (2018). Epigenome in early mammalian development: inheritance, reprogramming and establishment. *Trends Cell Biol.* 28, 237–253. doi: 10.1016/j.tcb.2017.10.008

Yang, C. X., Du, Z. Q., Wright, E. C., Rothschild, M. F., Prather, R. S., and Ross, J. W. (2012). Small RNA profile of the cumulus-oocyte complex and early embryos in the pig. *Biol. Reprod.* 87:117. doi: 10.1095/biolreprod.111.096669

Yang, J., Benyamin, B., Mcevoy, B. P., Gordon, S., Henders, A. K., Nyholt, D. R., et al. (2010). Common SNPs explain a large proportion of the heritability for human height. *Nat. Genet.* 42, 565–569. doi: 10.1038/ng.608

Yang, X., Smith, S. L., Tian, X. C., Lewin, H. A., Renard, J. P., and Wakayama, T. (2007). Nuclear reprogramming of cloned embryos and its implications for therapeutic cloning. *Nat. Genet.* 39, 295–302. doi: 10.1038/ng1973

Ye, M., Yang, Z. Y., Zhang, Y., Xing, Y. X., Xie, Q. G., Zhou, J. H., et al. (2020). Single-cell multiomic analysis of *in vivo* and *in vitro* matured human oocytes. *Hum. Reprod.* 35, 886–900. doi: 10.1093/humrep/deaa044

Young, A. E., Mansour, T. A., Mcnabb, B. R., Owen, J. R., Trott, J. F., Brown, C. T., et al. (2020). Author correction: genomic and phenotypic analyses

of six offspring of a genome-edited hornless bull. *Nat. Biotechnol.* 38:245. doi: 10.1038/s41587-020-0423-5

Young, L. E., Fernandes, K., Mcevoy, T. G., Butterwith, S. C., Gutierrez, C. G., Carolan, C., et al. (2001). Epigenetic change in IGF2R is associated with fetal overgrowth after sheep embryo culture. *Nat. Genet.* 27, 153–154. doi: 10.1038/84769

Young, L. E., Sinclair, K. D., and Wilmut, I. (1998). Large offspring syndrome in cattle and sheep. *Rev. Reprod.* 3, 155–163. doi: 10.1530/ror.0.0030155

Yuan, S., Schuster, A., Tang, C., Yu, T., Ortogero, N., Bao, J., et al. (2016). Sperm-borne miRNAs and endo-siRNAs are important for fertilization and preimplantation embryonic development. *Development* 143, 635–647. doi: 10.1242/dev.131755

Yuan, Y., Spate, L. D., Redel, B. K., Tian, Y., Zhou, J., Prather, R. S., et al. (2017). Quadrupling efficiency in production of genetically modified pigs through improved oocyte maturation. *Proc. Natl. Acad. Sci. U.S.A.* 114, E5796–E5804. doi: 10.1073/pnas.1703998114

Zhang, B., Zheng, H., Huang, B., Li, W., Xiang, Y., Peng, X., et al. (2016). Allelic reprogramming of the histone modification H3K4me3 in early mammalian development. *Nature* 537, 553–557. doi: 10.1038/nature19361

Zhang, G., Huang, H., Liu, D., Cheng, Y., Liu, X., Zhang, W., et al. (2015). N6-methyladenine DNA modification in Drosophila. *Cell* 161, 893–906. doi: 10.1016/j.cell.2015.04.018

Zhang, J., Qu, P., Zhou, C., Liu, X., Ma, X., Wang, M., et al. (2017). MicroRNA-125b is a key epigenetic regulatory factor that promotes nuclear transfer reprogramming. *J. Biol. Chem.* 292, 15916–15926. doi: 10.1074/jbc.M117.796771

Zhang, S., Chen, X., Wang, F., An, X., Tang, B., Zhang, X., et al. (2016a). Aberrant DNA methylation reprogramming in bovine SCNT preimplantation embryos. *Sci. Rep.* 6:30345. doi: 10.1038/srep30345

Zhang, S., Wang, F., Fan, C., Tang, B., Zhang, X., and Li, Z. (2016b). Dynamic changes of histone H3 lysine 9 following trimethylation in bovine oocytes and pre-implantation embryos. *Biotechnol. Lett.* 38, 395–402. doi: 10.1007/s10529-015-2001-3

Zhang, Y., Shi, J., Rassoulzadegan, M., Tuorto, F., and Chen, Q. (2019). Sperm RNA code programmes the metabolic health of offspring. *Nat. Rev. Endocrinol.* 15, 489–498. doi: 10.1038/s41574-019-0226-2

Zhang, Y., Zhang, X., Shi, J., Tuorto, F., Li, X., Liu, Y., et al. (2018). Dnmt2 mediates intergenerational transmission of paternally acquired metabolic disorders through sperm small non-coding RNAs. *Nat. Cell Biol.* 20, 535–540. doi: 10.1038/s41556-018-0087-2

Zhao, J., Hao, Y., Ross, J. W., Spate, L. D., Walters, E. M., Samuel, M. S., et al. (2010). Histone deacetylase inhibitors improve *in vitro* and *in vivo* developmental competence of somatic cell nuclear transfer porcine embryos. *Cell. Reprogram* 12, 75–83. doi: 10.1089/cell.2009.0038

Zhao, M. T., Rivera, R. M., and Prather, R. S. (2013). Locus-specific DNA methylation reprogramming during early porcine embryogenesis. *Biol. Reprod.* 88:48. doi: 10.1095/biolreprod.112.104471

Zhao, Y. H., Wang, J. J., Zhang, P. P., Hao, H. S., Pang, Y. W., Wang, H.-Y., et al. (2020). Oocyte IVM or vitrification significantly impairs DNA methylation patterns in blastocysts as analysed by single-cell whole-genome methylation sequencing. *Reprod. Fertil. Dev.* 32:676–689. doi: 10.1071/RD19234

Zheng, H., Huang, B., Zhang, B., Xiang, Y., Du, Z., Xu, Q., et al. (2016). Resetting epigenetic memory by reprogramming of histone modifications in mammals. *Mol. Cell* 63, 1066–1079. doi: 10.1016/j.molcel.2016.08.032

Zhong, L., Mu, H., Wen, B., Zhang, W., Wei, Q., Gao, G., et al. (2018). Long non-coding RNAs involved in the regulatory network during porcine pre-implantation embryonic development and iPSC induction. *Sci. Rep.* 8:6649. doi: 10.1038/s41598-018-24863-5

Zhou, Y., Connor, E. E., Bickhart, D. M., Li, C., Baldwin, R. L., Schroeder, S. G., et al. (2018). Comparative whole genome DNA methylation profiling of cattle sperm and somatic tissues reveals striking hypomethylated patterns in sperm. *Gigascience* 7:giy039. doi: 10.1093/gigascience/giy039

Zhou, Y., Liu, S., Hu, Y., Fang, L., Gao, Y., Xia, H., et al. (2020). Comparative whole genome DNA methylation profiling across cattle tissues reveals global and tissue-specific methylation patterns. *BMC Biol.* 18:85. doi: 10.1186/s12915-020-00793-5

Zhou, Y., Xu, L., Bickhart, D. M., Abdel Hay, E. H., Schroeder, S. G., Connor, E. E., et al. (2016). Reduced representation bisulphite sequencing of ten bovine somatic tissues reveals DNA methylation patterns and their impacts on gene expression. *BMC Genomics* 17:779. doi: 10.1186/s12864-016-3116-1

Zimmermann, C., Romero, Y., Warnefors, M., Bilican, A., Borel, C., Smith, L. B., et al. (2014). Germ cell-specific targeting of DICER or DGCR8 reveals a novel role for endo-siRNAs in the progression of mammalian spermatogenesis and male fertility. *PLoS ONE* 9:e107023. doi: 10.1371/journal.pone.0107023

**Conflict of Interest:** The authors declare that the research was conducted in the absence of any commercial or financial relationships that could be construed as a potential conflict of interest.

*Copyright © 2021 Zhu, Marjani and Jiang. This is an open-access article distributed under the terms of the Creative Commons Attribution License (CC BY). The use, distribution or reproduction in other forums is permitted, provided the original author(s) and the copyright owner(s) are credited and that the original publication in this journal is cited, in accordance with accepted academic practice. No use, distribution or reproduction is permitted which does not comply with these terms.*

frontiers in Genetics

ORIGINAL RESEARCH
published: 19 March 2021
doi: 10.3389/fgene.2021.630290

# Environmentally Driven Color Variation in the Pearl Oyster *Pinctada margaritifera* var. *cumingii* (Linnaeus, 1758) Is Associated With Differential Methylation of CpGs in Pigment- and Biomineralization-Related Genes

*Pierre-Louis Stenger[1,2], Chin-Long Ky[1,2], Céline M. O. Reisser[1,3], Céline Cosseau[4], Christoph Grunau[4], Mickaël Mege[1,5], Serge Planes[6] and Jeremie Vidal-Dupiol[2]**

[1] IFREMER, UMR 241 Écosystèmes Insulaires Océaniens, Labex Corail, Centre du Pacifique, Tahiti, French Polynesia, [2] IHPE, Université de Montpellier, CNRS, IFREMER, Université de Perpignan Via Domitia, Montpellier, France, [3] MARBEC, Université de Montpellier, CNRS, IFREMER, IRD, Montpellier, France, [4] IHPE, Université de Montpellier, CNRS, IFREMER, Université de Perpignan Via Domitia, Perpignan, France, [5] IFREMER, PDG-RBE-SGMM-LGPMM, La Tremblade, France, [6] EPHE-UPVD-CNRS, USR 3278 CRIOBE, Labex Corail, PSL Research University, Université de Perpignan, Perpignan, France

OPEN ACCESS

**Edited by:**
Stephanie McKay,
University of Vermont, United States

**Reviewed by:**
Silvio Zaina,
University of Guanajuato, Mexico
Yu Jiao,
Guangdong Ocean University, China

***Correspondence:**
Jeremie Vidal-Dupiol
jeremie.vidal.dupiol@ifremer.fr

**Specialty section:**
This article was submitted to Epigenomics and Epigenetics, a section of the journal Frontiers in Genetics

**Received:** 17 November 2020
**Accepted:** 19 February 2021
**Published:** 19 March 2021

**Citation:**
Stenger P-L, Ky C-L, Reisser CMO, Cosseau C, Grunau C, Mege M, Planes S and Vidal-Dupiol J (2021) Environmentally Driven Color Variation in the Pearl Oyster Pinctada margaritifera var. cumingii (Linnaeus, 1758) Is Associated With Differential Methylation of CpGs in Pigment- and Biomineralization-Related Genes. Front. Genet. 12:630290. doi: 10.3389/fgene.2021.630290

Today, it is common knowledge that environmental factors can change the color of many animals. Studies have shown that the molecular mechanisms underlying such modifications could involve epigenetic factors. Since 2013, the pearl oyster *Pinctada margaritifera* var. *cumingii* has become a biological model for questions on color expression and variation in Mollusca. A previous study reported color plasticity in response to water depth variation, specifically a general darkening of the nacre color at greater depth. However, the molecular mechanisms behind this plasticity are still unknown. In this paper, we investigate the possible implication of epigenetic factors controlling shell color variation through a depth variation experiment associated with a DNA methylation study performed at the whole genome level with a constant genetic background. Our results revealed six genes presenting differentially methylated CpGs in response to the environmental change, among which four are linked to pigmentation processes or regulations (*GART*, *ABCC1*, *MAPKAP1*, and *GRL101*), especially those leading to darker phenotypes. Interestingly, the genes *perlucin* and *MGAT1*, both involved in the biomineralization process (deposition of aragonite and calcite crystals), also showed differential methylation, suggesting that a possible difference in the physical/spatial organization of the crystals could cause darkening (iridescence or transparency modification of the biomineral). These findings are of great interest for the pearl production industry, since wholly black pearls and their opposite, the palest pearls, command a higher value on several markets. They also open the route of epigenetic improvement as a new means for pearl production improvement.

**Keywords: pearl oyster, environmental pressure, depth, color change, pigmentation, DNA methylation, methylome characterization**

## INTRODUCTION

Pearls have captivated and amazed human civilization since 7500 BP (Charpentier et al., 2012) and have formed the basis for economic development of several tropical countries. French Polynesia started to trade pearls with Europeans at the end of the 18th century (Southgate and Lucas, 2011) and has been an industrial producer since 1964 (Le Pennec, 2010). Today, cultured pearl farming represents the second economic resource of the country, just behind tourism (Ky et al., 2019). However, since 2001, an unprecedented economic crisis has endangered the French Polynesian pearl farming sector due to the overproduction of low quality pearls (Bouzerand, 2018). To remediate to this socio-economic crisis, the policy of producing "less but better" was adopted in 2013 (Ky et al., 2013). Since then, production has focused on obtaining cultured pearls with high market value, by selecting traits such as pearl color.

Two individuals are needed to produce a pearl, a donor and a recipient oyster. The sacrificed donor is used to provide a piece of mantle (the biomineralizing graft) which is placed, together with a small marble of nacre, into the gonad of the recipient oyster. Donor oysters are selected for their inner-shell color, since the color of a cultured pearl is determined by that of the donor oyster (Ky et al., 2013). Recipient oysters are selected for their vigor. The Polynesian black-lipped pearl oyster, *Pinctada margaritifera* var. *cumingii* (Linnaeus, 1758) is the pearl oyster species showing the largest range of inner shell color (Ky et al., 2013, 2017), therefore offering a wide range of pearl colors and shades, like dark, pastel, silver, peacock, red, golden, green, blue, and even rainbow (Ky et al., 2014; Stenger et al., 2019). Moreover, the color of this bivalve has both a structural (iridescence; Liu et al., 1999) and a biological (pigments; Iwahashi and Akamatsu, 1994) basis. While the genetic determination of this color has been partly demonstrated (Ky et al., 2013, 2017), several environmental factors are also known to affect the shell color (Joubert et al., 2014; Le Pabic et al., 2016; Le Moullac et al., 2018), such as the depth at which an oyster is grown (Stenger et al., 2019). In this latter work, authors demonstrated that the transplantation of oysters from the sub-surface (−4 m) to the bottom of the lagoon (−30 m) significantly darkens the inner shell color compared with oysters maintained at the sub-surface. This induced phenotype was persistent through time ("enduring"), even after the oysters were returned to shallow water, which would seem to indicate an epigenetic control mechanism rather than a direct environmental influence acting on the darkening of the shell color (Stenger et al., 2019).

Since the first definition of epigenetic by Waddington in the late 1930s, epigenetic received many definitions (Nicoglou and Merlin, 2017). In this work we have selected the definition proposed by Russo et al. (1996), e.g., *"epigenetic is the study of mitotically and/or meiotically heritable changes in gene function that cannot be explained by changes in DNA sequence"* (Russo et al., 1996). Mechanistically, this memory function is based on changes in chromatin structure, such as non-coding RNA and/or histone modifications and/or DNA methylation. Here, we use the term epigenetics to describe any changes in DNA methylation that occur upon environmental cues. Coloration mediates an organism's relationship with their environment in important ways including anti-predator defenses, social signaling, thermoregulation, or protection (Cuthill et al., 2017). Several species are known to change their coloration more than once in their lifetime in response to environmental triggers to reach an optimal phenotype in a new environment. To increase their camouflage the arctic hare *Lepus arcticus* (Ross, 1819), the ermine *Mustela erminea* (Linnaeus, 1758), and the ptarmigan *Lagopus muta* (Montin, 1776) changed their coat color from brown or gray in the summer to white in the winter (Zimova et al., 2018). These changes are known to be induced by temperature, photoperiod, and/or food rarefaction (Zimova et al., 2018). The corresponding changes in color expression could be brought by epigenetic processes (Hu and Barrett, 2017) like in mouses (Dolinoy, 2008). Indeed, the most striking example of color change in mammals rely on the environmentally induced differential DNA methylation of the intracisternal A-particle gene located upstream of the agouti locus (Dolinoy et al., 2006; Dolinoy, 2008). In Mollusca, a few epigenetic studies have been made, especially on color expression and variation. To date, Feng et al. (2018) provided a catalog of long non-coding RNA (lncRNA) expressed in the mantle of the Pacific oyster *Crassostrea gigas* (Thunberg, 1793). These authors suggested that these lncRNAs may affect the expression of pigment-related genes such as tyrosinase-like proteins, dopamine, beta-monooxygenase, chorion peroxidase, or cytochrome P450 2U1, thus leading to different shell color phenotypes. More recently, the same group (Feng et al., 2020) have studied the role of microRNAs in the regulation of the shell color of *Crassostrea gigas*. In this study, four miRNAs (lgi-miR-315, lgi-miR-96b, lgi-miR-317, and lgi-miR-153) were found closely associated with shell color along with the regulation of Cytochrome P450 2U1, Tyrosinase-like protein 2 and 3. The authors concluded that lgi-miR-317, its targeted mRNA encoding peroxidase, and the lncRNA TCONS_00951105 might play a key role in shell melanin synthesis.

Because color phenotype is important for the pearl market and the phenotypic plasticity of this trait is associated with the putative involvement of epigenetic mechanisms, the study of these mechanisms opens a new avenue for improvement in the pearl industry with, for example, the development of epi-markers for environmentally induced color variation testing. As a first step in exploring a possible interaction between epigenetic mechanisms and color variation, we designed a depth variation experiment to induce environmentally driven color variation. In order to disentangle the genetic factors from the epigenetic ones influencing color variation, a non-lethal sampling design was used enabling us to monitor changes in DNA methylation over time and depth within the same individuals (constant genotypes). DNA methylation was studied at the whole genome scale by whole-genome bisulfite sequencing and provided evidence for an epigenetic control of pearl oyster color variation. This approach enabled us to find any differences in DNA methylation in pearl oysters after a period at increased depth and, when this occurred, to examine whether genes related to pigmentation and/or biomineralization processes were affected by such changes. Results of this kind could allow the pearl industry to turn to more sustainable production strategies.

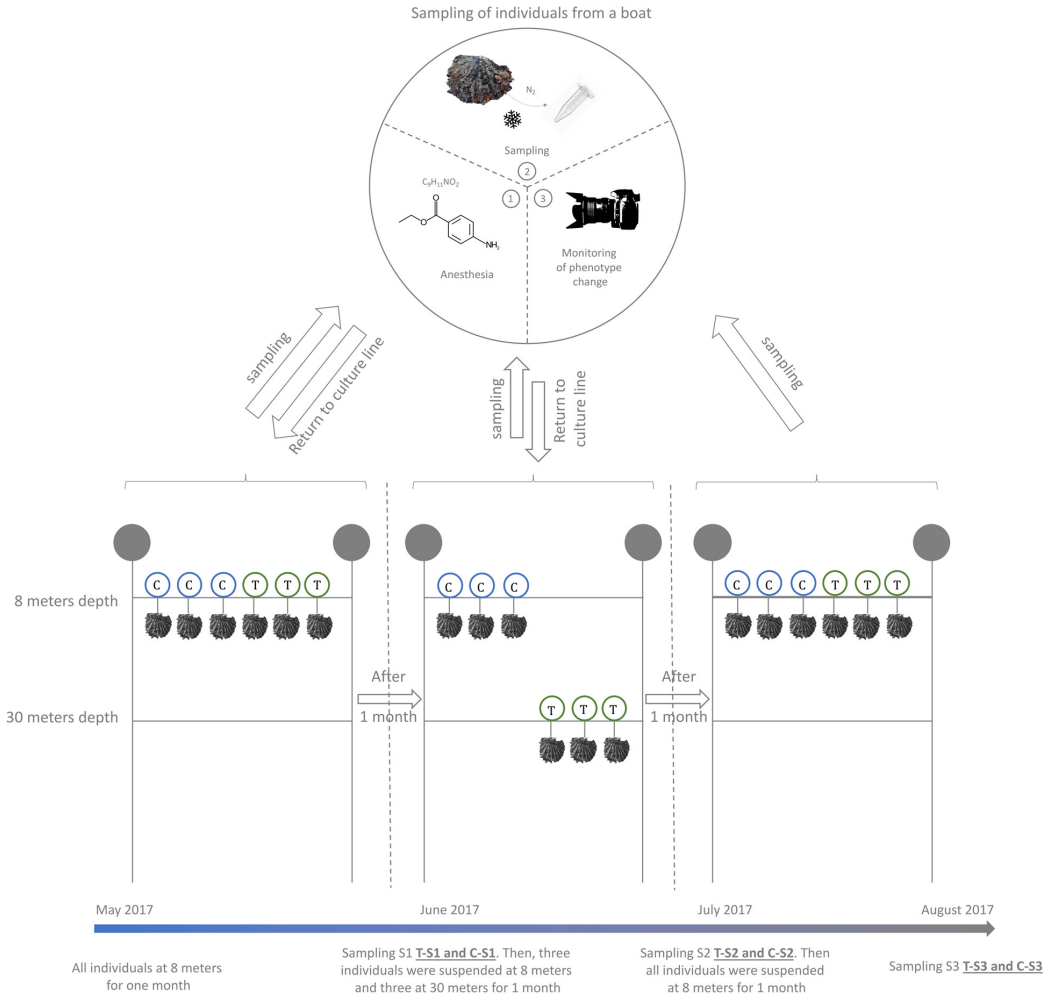



**FIGURE 1 |** Design of the Yo-Yo experiment. Six *P. margaritifera* individuals were used for this experiment. Three individuals were maintained at a depth of 8 m during the whole experiment and were used as a control (C – in blue circles). The three other individuals were subjected to depth variation treatment (T – in green circles). A non-lethal sampling of mantle tissue was made every month at the time of the depth change.

# MATERIALS AND METHODS

## Biological Material and the Yo-Yo Experiment

In order to trigger an environmentally driven color change of the inner shell of *P. margaritifera*, we set up an *in situ* "yo-yo" experiment (May to August 2017) (**Figure 1**). Six individuals of 4 years of age (approximately 14 cm height) originating from three different families (two individuals per family Stenger et al., in press) were used. These six individuals were first maintained at 8 m depth for 1 month (May 2017). Then, three of them (1 from each family) were selected and transferred to 30 m depth (treatment) for environmental pressure while the three others were left at 8 m (control). This exposure was maintained for 1 month (June 2017). Then, the three pearl oysters that had been placed at 30 m were transferred back to 8 m depth for a final month of exposure (July 2017). During each transfer, a piece of mantle (the biomineralizing tissue responsible for the inner shell coloration) was sampled by a non-lethal method: (i) oysters were anesthetized in 20 L seawater containing 200 mL benzocaine at 120 g/L 96° ethanol under air aeration; (ii) they opened their valves under the effect of the benzocaine, a 5 $mm^3$ fragment of the mantle was carefully sampled with tweezers and scissors; (iii) the sample was flash frozen in liquid nitrogen. Alongside the sampling of the mantle, the color of the inner shell of each individual (control and treatment) was filmed with a mini photo studio for color variation analysis. This mini standardized photo studio was composed of a tripod supporting a Nikon D3100 reflex camera equipped with a Nikon 18-55VR lens. This set up was used to film the reflection of the inner shell color on a small mirror (spatula). To assess constant exposition to light, all films were made under a blackout drape with three white LED lamps.

## Color Variation Analysis

For each sample, ten screenshots from the films were randomly captured and analyzed for color variation. Color was quantified

and qualified using the R package *ImaginR* V.2 (Stenger, 2017) as previously described (Stenger et al., 2019). A Shapiro test (stats v3.5.0 R package) was used to assess the normal distribution of the data. The average saturation and darkness for each sample were calculated from all ten screenshots, and a Wilcoxon test (*stats v3.5.0* R package based on Hollander et al., 1973 and Royston, 1995) was used to test for any difference between the groups.

## DNA Extraction and BS-seq

DNA was extracted with the QIAamp DNA Mini Kit (QIAGEN®, Cat No./ID: 51306) following manufacturer's recommendations, with the addition of two steps: (i) a RNase A treatment to remove RNA and (ii) after overnight digestion the addition of 50 µL of a saturated KCl solution (34 g KCl/100 g $H_2O$) and a centrifugation at 14,000*g* for 15 min to remove the mucopolysaccharides (Sokolov, 2000). DNA quality and quantity were assessed with a NanoDrop™ 2000 and 1.2% agarose gel electrophoresis. Bisulfite-conversion, library construction, and sequencing (2 × 150 bp) were performed by Genome Québec (MPS Canada) on an Illumina HiSeq X.

## Bioinformatics Pipeline

Analyses were performed on the Ifremer Datarmor cluster[1]. Raw read quality was assessed with FastQC (Andrews, 2010; **Supplementary Table 1**). Reads were cleaned and adaptors removed with Trimmomatic (Bolger et al., 2014) (V. 0.36 – illuminaclip 2:30:10; leading 28, trailing 28, and minlen 40). Bismark aligner (Krueger and Andrews, 2011) (V. 0.19) was used to map reads on the draft genome of *P. margaritifera* (Reisser et al., 2020) using the following parameters: multi-seed length of 30 bp, 0 mismatches, default minimum alignment score function. Deduplication was done with Deduplicate_bismark (Krueger and Andrews, 2011). Bed files for methylome characterization were obtained with Bismark_methylation_extractor (Krueger and Andrews, 2011). All scripts are provided on GitHub (PLStenger/Pearl_Oyster_Colour_BS_Seq/00_scripts). Raw reads are available through the NCBI Sequence Read Archive (SRA, BioProject PRJNA663978, BioSample SAMN16191417 to SAMN16191446).

## Methylation Calling, Methylome Characterization, and Differential Methylation Analysis

The R package *Methylkit* (Akalin et al., 2012) (V. 1.11.0) was used for methylation calling in CpG, CHH, and CHG contexts using a minimum coverage of 10, directly from BAM files with *processBismarkAln*. *Methylkit* was also used for methylation characterization in the CpG, CHH, and CHG contexts, as well as for the coverage calculation and clustering analysis (ward clustering correlation distance method). The average gene methylation was calculated with DeepTools V. 3.3.0 (Ramírez et al., 2014). The gene body methylation rate (GBMR), corresponding to the CpG methylation rate, was calculated with the map function from bedtools V. 2.27.1 (Quinlan and Hall, 2010).

[1]https://wwz.ifremer.fr/pcdm/Equipement

The mantle' gene expression data used for methylation/gene expression correlation analysis came from individuals studied in Stenger et al., in press (SRA BioProject PRJNA521849). Briefly, RNA sequencing was done using high quality RNA extracted from twelve individuals. Library construction and sequencing was performed (Paired–end 100-bp; Illumina® HiSeq® 4000) by Génome Québec (MPS Canada). Read quality check and trimming were done as described in the section "Bioinformatics Pipeline." Cleaned reads were paired-mapped against the *P. margaritifera* draft genome with TopHat (V1.4.0) (Trapnell et al., 2012). Cufflinks (V2.2.1.0) and Cuffmerge (V2.2.1.0) were used to assemble and merge the transcriptome produced for each library, respectively (Trapnell et al., 2012). HTSeq-count (V0.6.1) (Anders et al., 2015) was used to count read-mapped per transcript. The average of the twelve count files was computed and the RPKM method was used for gene expression data normalization as previously done in Wang et al., 2014.

To identify the effect of the depth treatment, differentially methylated CpGs (DMCpGs) were identified with the *getMethylDiff* function of the R package *Methylkit*, with difference >25% and $q$ value < 0.05 for CpG positions between depth treatment and control oysters at each sampling time.

## Functional Analysis of Differentially Methylated Genes

An annotation file was obtained following the first three steps of https://github.com/enormandeau/go_enrichment, completed with PLASTX (Nguyen and Lavenier, 2009) against UniProt-Swiss-Prot and TrEMBL ($e$-value at $1 \times 10^{-3}$). A protein domain search was then performed with InterProScan. Finally, Gene Ontology terms were assigned with Blast2GO by combining information from the two annotation files (Conesa et al., 2005).

GOATOOLS (Klopfenstein et al., 2018) was used to test for enrichment of GO terms in a selected set of genes (significantly differentially methylated, lowly and highly methylated), using a Fisher's exact test. Histograms showing the GO terms enrichment of were generated with the *ggplot2* R package (Wickham and Chang, 2019) (V. 2.2.1).

# RESULTS

## Depth Variation Induces Significant Darkening

The color variation analysis with the *ImaginR* package detected no significant modification of hue, saturation or darkness among the controls during the 3 months of the "yo-yo" experiment (pairwise Wilcoxon tests with $P$ values > 0.05). Among the samples subjected to the treatment, no significant change occurred for hue or saturation during the 3 months of the experiment. However, a significant difference in darkness (pairwise Wilcoxon tests with $P$ values < $1.10e^{-5}$) was detected, with an increase in the darkness value during the month at 30 m depth. This increase was still visible and significant after the oysters were returned to 8 m depth for 1 month (pairwise Wilcoxon tests with $P$ values < $1.10e^{-5}$; **Table 1**).

Raw data are available for download using the following links (screenshots: https://figshare.com/articles/dataset/ImaginR_raw_data_screenshots_zip/14049983; videos: https://figshare.com/articles/dataset/ImaginR_raw_data_videos_zip/14049986).

## Read Processing and Read Mapping to the Reference Genome

For the control, Illumina sequencing produced averages of 105,505,318 (±1,514,514; $n$ = 3), 103,770,226 (±5,087,254; $n$ = 3), and 103,490,158 (±5,509,306; $n$ = 3) raw sequence reads for sampling times 1, 2, and 3, respectively. For the depth treatment, averages of 98,184,541 (±6,186,502; $n$ = 3), 104,727,236 (±6,141,350; $n$ = 3), and 113,132,278 (±4,306,828; $n$ = 3) raw sequence reads were produced for sampling times 1, 2, and 3, respectively. After cleaning and filtering, averages of 101,575,689 (±1,584,202), 100,159,677 (±5,076,306), and 100,073,964 (±5,415,409) reads were kept for the control, and 94,669,211 (±5,877,099), 101,048,705 (±6,094,775), and 109,246,931 (±4,195,331) for the depth treatment, for the three successive sampling times, respectively. Filtered reads were mapped on the reference genome with Bismark and showed similar mapping rates for all samples (∼32.1%) (**Supplementary Table 2**). PCR duplicates were removed and represented, on average, 0.059% (±0.002) of the total reads.

## Characterization of the *P. margaritifera* Mantle Methylome

Methylation in the *P. margaritifera* mantle displayed a mosaic pattern with an enrichment in the gene showing a CpG methylation rate of 22.81% in introns, 17.32% in exons, and an average of 18.26% in gene body (**Figures 2A,B**). A slight enrichment in the 3 kbps upstream (12.67%) and downstream (16.58%) of genes (**Figures 2A,B**) is also found. The whole genome CpG methylation rate is equal to 11.53% on average.

The fractionation of gene body methylation rate (**Figure 2C**) shows a bimodal distribution characterized by two peaks. This distribution enables the classification of genes into two sets: the "lowly" methylated genes (0.00–0.19% methylation – rank 0–0.2 and marked as "1" **Figure 2C**) and the "highly" methylated genes (0.50–40.12% of methylation; 40.12% is the maximum methylation found in a gene in these data – rank 0.5–1 and marked as "2" **Figure 2C**). The enrichment analysis performed on the lowly methylated genes showed an overrepresentation of GO terms involved in reproductive process functions, such as "oocyte maturation" (GO:0001556), "primary sex determination" (GO:0007539), "male meiosis I" (GO:0007141), etc., cellular signaling, such as "negative regulation or cellular response to drug" (GO:0048523), "negative regulation of phospholipid metabolic process" (GO:0071072), etc., and "androgen receptor signaling pathway" (GO:0030521). In the highly methylated genes set, the enrichment analysis showed an overrepresentation of GO terms involved in housekeeping functions, such as "mRNA regulation" (GO:0043488), "mRNA splice site regulation" (GO:0006376), "ribosomal small unit assembly" (GO:0000028), "transcription-dependent tethering of RNA polymerase II" (GO:0000972), "DNA amplification" (GO:0006277), etc (**Supplementary Figure 1**).

To test for a correlation between the GBMR and the level of gene expression, the distribution of gene body methylation levels was represented according to gene expression rank (in RPKM). This distribution revealed that moderately expressed genes (100–1000 RPKM) have higher methylation levels than lowly (>100 RPKM) or highly (<1000) expressed ones in *P. margaritifera* (**Figure 2D**).

**TABLE 1 |** Darkness values obtained with the *ImaginR* R package analysis.

| Conditions | Individual | Time 1 | Time 2 | Time 3 |
|---|---|---|---|---|
| **Control** | #1 | 0.600000 | 0.596078 | 0.629804 |
| | #2 | 0.646275 | 0.653595 | 0.650000 |
| | #3 | 0.455462 | 0.522876 | 0.455556 |
| **Depth treatment** | #4 | 0.775686 | 0.387451 | 0.375686 |
| | #5 | 0.866231 | 0.437909 | 0.513726 |
| | #6 | 0.845378 | 0.326797 | 0.419608 |
| | | *P* values<1.10e$^{-5}$ | | |
| | | *P* values<1.10e$^{-5}$ | | |

*Only P. margaritifera individuals from the depth treatment group showed significant differences (pairwise Wilcoxon tests with P values < 1.10e$^{-5}$ ***) between sampling times 1 and 2, and sampling times 1 and 3. Sampling times 1, 2, and 3 correspond to June, July and August 2017, respectively, as explained in* ***Figure 1****.*

## Methylation Calling and Differential Methylation Analysis

Methylation calling showed that the Cytosine methylation level was in average of 16.5% [12.0% in the CpG context, 0.9% in the CHG context, 1.0% in the CHH context, and 2.6% in another context (CN or CHN); **Supplementary Figure 2**]. Similarities between the methylation patterns of each sample were analyzed by a clustering approach (ward clustering correlation distance method). This showed that samples clustered first by treatment (depth vs. control), then by genotype (i.e., individuals) and, for the control only, by sampling time (**Figure 3**).

For the differential methylation analysis, triplicates were made according to treatment (depth and control), and nine pairwise comparisons were made in order to identify and disentangle the different effects (**Figure 4**). Time effect was quantified by the differential methylation analysis performed among the control individuals (C; three different genotypes), but between the sampling times (S; three samples per genotype). This led us to perform three comparisons (C-S1 vs. C-S2, C-S2 vs. C-S3, and C-S1 vs. C-S3). Overall, time effect was associated with non-redundant (not visible in other conditions) hyper- or hypomethylations of 60 and 111 CpGs, respectively. Neither hyper- nor hypomethylation were detected in CHG or CHH contexts.

The cumulative effect of depth variation and time was quantified by differential methylation analysis performed among the individuals in the depth treatment (T; three different genotypes), but between the sampling times (S; three samples per genotype). As previously, this led us to make three pairwise comparisons (T-S1 vs. T-S2, T-S2 vs. T-S3, and T-S1 vs. T-S3).

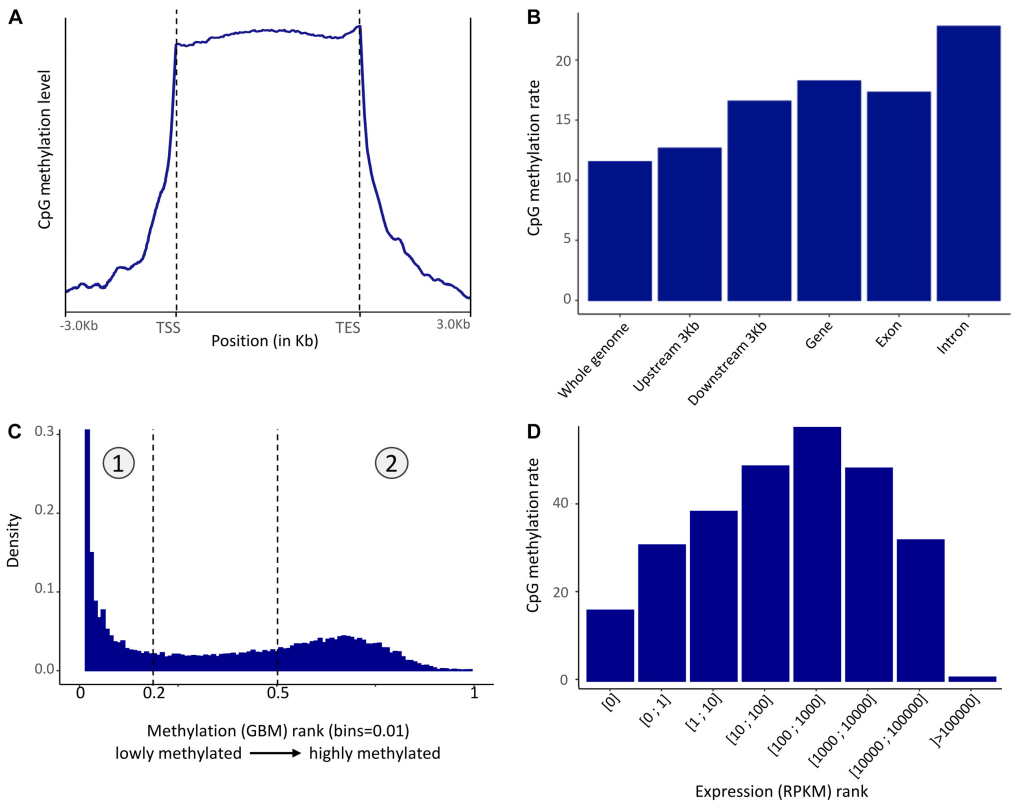



**FIGURE 2 | (A)** Pattern of methylation level in the mantle of *P. margaritifera* (TSS, Transcription Start Site; TES, Transcription End Site) reported on a metagene. **(B)** Distribution of methylated CpG in different genomic regions. **(C)** Distribution of methylated CpG across genes ranked according to methylation level. The left part (1) is composed of lowly methylated genes while the right part (2) is composed of highly methylated genes. **(D)** CpG methylation rate averaged across rank of gene expression.

In total, 71 non-redundant hyper- and 76 non-redundant hypomethylations were identified, all in the CpG context.

The cumulative effect of depth variation and genotype was quantified by differential methylation analysis performed between treatments (depth treatment vs. control; three genotypes per condition) at the three-sampling times (T-S1 vs. C-S1, T-S2 vs. C-S2, and T-S3 vs. C-S3). These analyses revealed that: (i) in the CpG context, 2087 non-redundant cytosines were hypermethylated while 2935 non-redundant cytosines were hypomethylated; (ii) in the CHG context, 12 non-redundant cytosines were hypermethylated and 16 were hypomethylated; (iii) in the CHH context, three non-redundant cytosines were hypermethylated and three were hypomethylated.

Finally, to extract the effect of the depth variation only, we subtracted the time effect from the cumulative effect of depth and time (comparison among treatments, but between the sampling times). To do so, positions presenting differential methylation in response to the time effect were considered as non-significant when they were also differentially methylated in the cumulative effect of depth and time. None of the CpGs that were differentially methylated for the time effect were also differentially methylated for the depth variation and time effect. All the 71 hyper- and 76 hypomethylations previously identified were therefore kept for subsequent analysis.

## Enrichment Analysis and Exploration of Genes With Differentially Methylated Positions

To correlate changes in DNA methylation with changes in pigmentation, we first performed an enrichment analysis and looked for biological processes and molecular functions linked to pigmentation. As a second step, we then individually screened the genes displaying DMCpGs and searched the literature for their putative involvement in pigmentation. DMCpG that were located outside of the gene body were not considered (92 DMCpGs). Genes encoding proteins of unknown function were present in the set of genes containing DMCpGs, but the lack of functional annotation prevented us from proposing a mechanism that could explain their involvement in the phenotypic changes that occurred, although we cannot exclude that they may have a role in this phenomenon.

### C-S1 vs. C-S2 vs. C-S3 Comparison

The GO categories significantly enriched in control conditions in relation to time were not associated with pigmentation. They were, however, associated with a seasonal effect, shown by an enrichment in GO terms linked to growth and reproduction (**Supplementary Figure 2**). The methylation information for

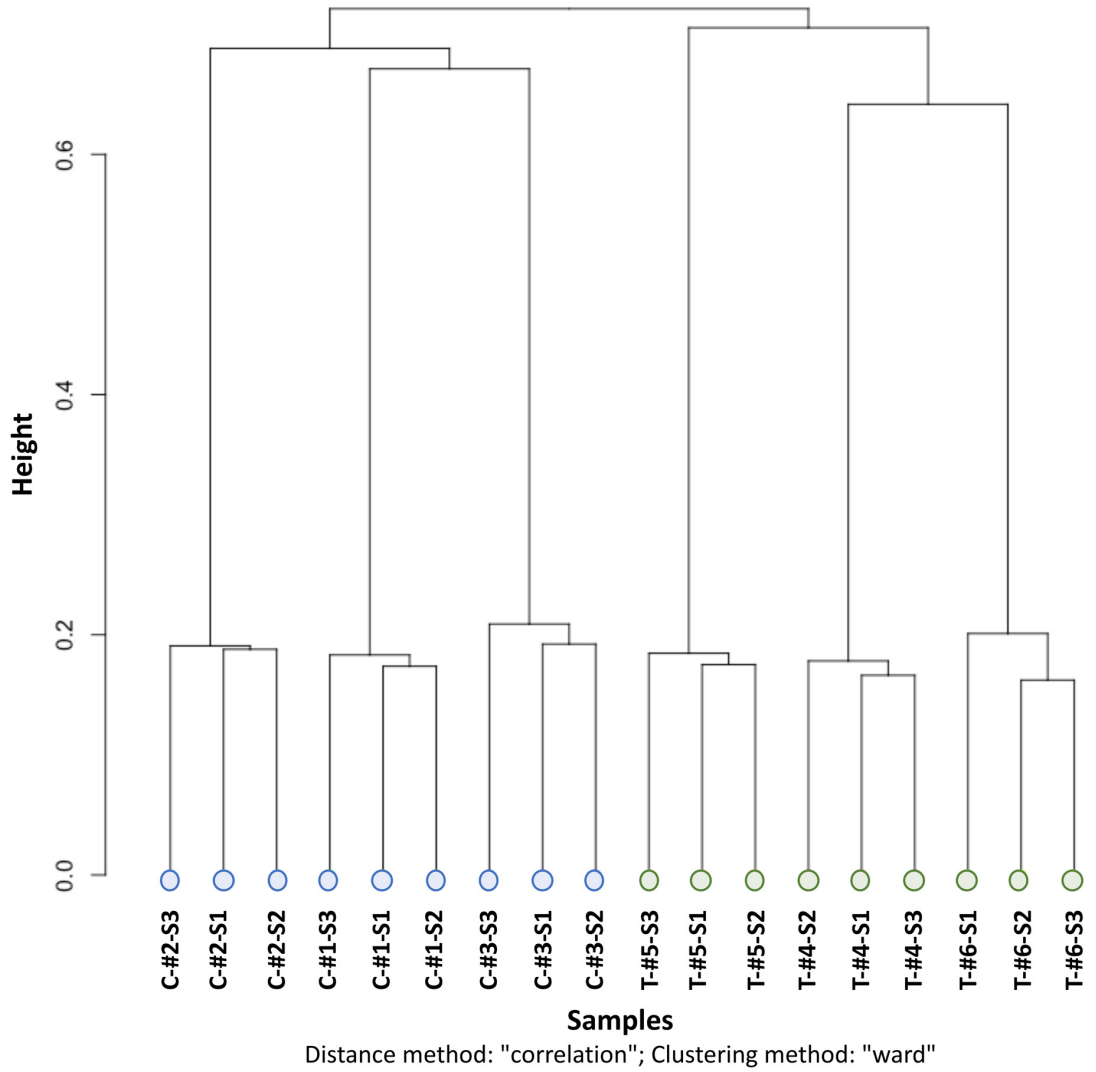



**FIGURE 3 |** CpG methylation clustering with the distance method "correlation" and clustering method "ward" from the clusterSamples function of the R package *Methylkit*. C, control individual (in blue); T, depth treatment individual (in green); #, label of the individual number; S1, sampling time 1; S2, sampling time 2; S3, sampling time 3.

all these genes and for all comparisons are provided in **Supplementary Table 3**.

### T-S1 (1 Month at 8 m Depth) vs. T-S2 (1 Month at 8 m Depth Followed by 1 Month at 30 m Depth)

Gene ontology (GO) terms enrichment analysis performed for biological process category showed an enrichment of several GO terms associated with pigmentation (**Figure 5**): "pigment metabolic process" (GO:0042440), "pteridine-containing compound metabolic process" (GO:0042558, Frost and Malacinski, 1979), and "folic acid-containing compound biosynthetic process" (GO:0009396, Katz et al., 1987). For the molecular function category, additional GO terms linked to pigmentation processes were enriched: "UDP-glycosyltransferase activity" (GO:0008194, Vajro et al., 1995), "hydroxymethyl-formyl- and related transferase activity" (GO:0016742, Moreau et al., 2012), "alpha-1,3-mannosyl-glycoprotein 2-beta-N-acetylglucosaminyltransferase activity" (GO:0003827, Zhai et al., 2016), "phosphoribosylglycinamide formyltransferase activity" (GO:0004644), and "acetylglucosaminyltransferase activity" (GO:0016262, Chakraborty et al., 1999; Shin et al., 2015).

At the gene level (**Table 2**), three candidate genes were identified that had hypermethylated CpGs after the month at −30 m. The first encodes a trifunctional purine biosynthetic protein adenosine-3 (*GART*), the second an alpha-1,3-mannosyl-glycoprotein-2-beta-n-acetylglucosaminyltransferase (*MGAT1*), and the third a multidrug resistance-associated protein (*ABCC1*). *GART* is known to be involved in the synthesis of purines (purine synthesis pathway) and expression disturbances of this gene can modify the production of two pigments: melanin and pheomelanin (Amsterdam et al., 2004; Ng et al., 2009).

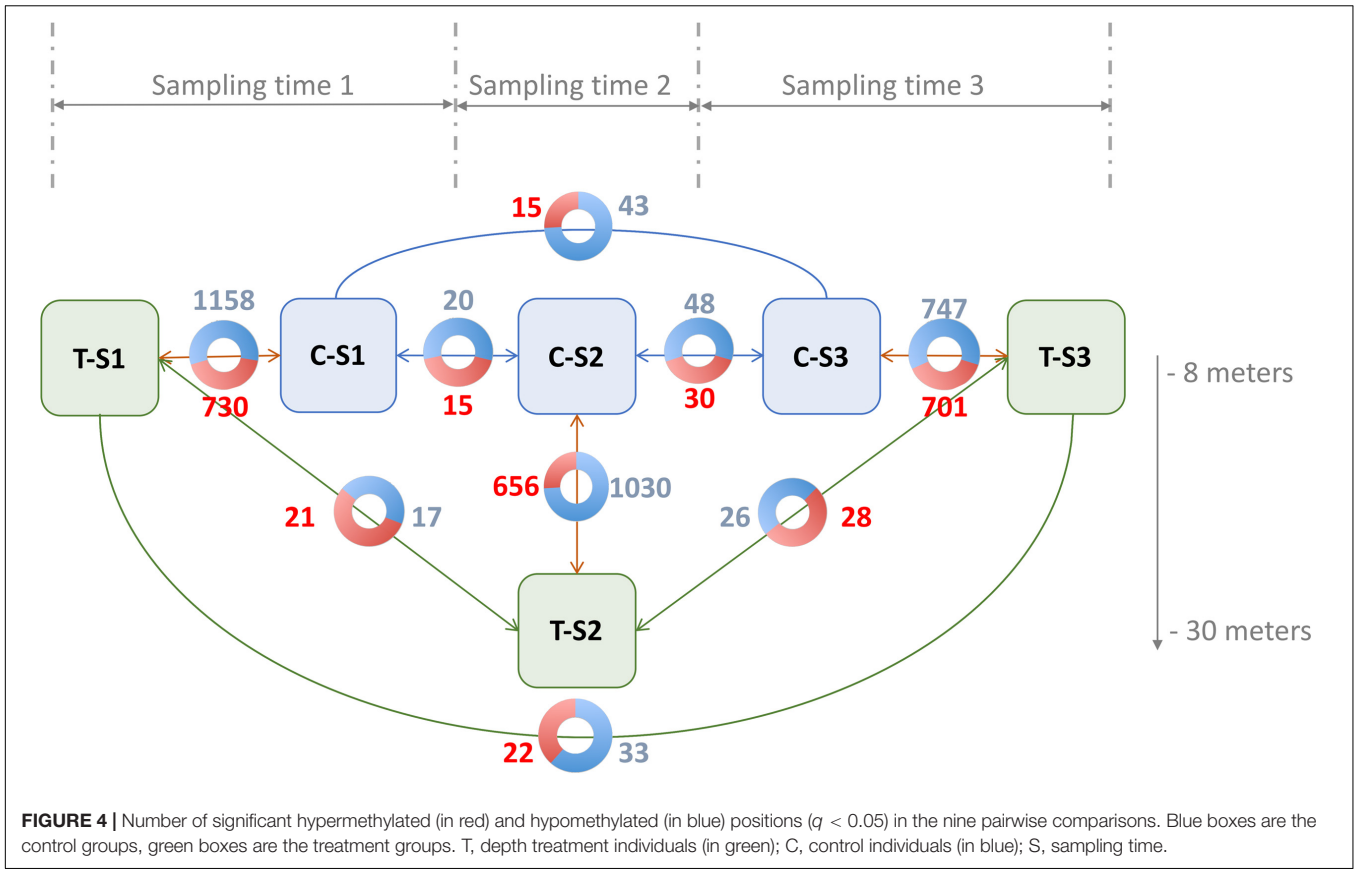



**FIGURE 4 |** Number of significant hypermethylated (in red) and hypomethylated (in blue) positions ($q < 0.05$) in the nine pairwise comparisons. Blue boxes are the control groups, green boxes are the treatment groups. T, depth treatment individuals (in green); C, control individuals (in blue); S, sampling time.

MGAT1 is involved in the glycan synthesis pathway, and is known to be essential for shell formation in the *Pinctada* genus (Takakura et al., 2008). Finally, the *ABBC1* gene encodes an active transporter of glutathione-S-transferase (Homolya et al., 2003; Fernandes and Gattass, 2009; Rocha et al., 2014), an enzyme regulating the balance of eumelanin/pheomelanin production (Sonthalia et al., 2016).

### T-S2 (1 Month at 8 m Depth Followed by 1 Month at 30 m Depth) vs. T-S3 (1 Month at 8 m, 1 Month at 30 m, and 1 Month Back at 8 m)

GO term enrichment analysis highlighted enrichment for several GO terms associated with pigmentation (**Figure 6**): "L-ornithine transmembrane transporter" (GO:0000064) for the biological process category; and "ornithine transport" (GO:0015822), "lysine transport" (GO:0015819), "L-amino acid transport" (GO:0015807), "basic amino acid transmembrane transporter activity" (GO:0015171), "L-amino acid transmembrane transporter activity" (GO:0015179), and "xenobiotic transporter activity" (GO:0015238) for the molecular function category.

At the gene level, 15 genes displaying DMCpGs were deemed good candidates to partly explain the phenotypic changes observed. Among the hypomethylated genes, we found those for a cationic amino acid transporter 2 (*SLC7A2*), a multidrug-associated protein (also present in the T-S1 vs. T-S2 comparison), and a coiled-coil domain-containing protein 79 (*CCDC79*). SLC7A2 is involved in the transport of arginine, lysine, and ornithine. A high number of the proteins found in the mineralized structure of *P. margaritifera* are known to be enriched in arginine and lysine, such as MSP-1, MSP-2, Aspein, Prismlain-14, and MSI60 (Addadi et al., 2006; Joubert et al., 2010; Gueguen et al., 2013). According to the NCBI GenPept database, CCDC79 can bind ion calcium, like the product of the *MGAT1* gene (see above). Among the hypermethylated genes, we found those for a G-protein coupled receptor (*GRL101*), a target of rapamycin complex 2 subunit (*MAPKAP1*), an enolase (*enolase-4*), sodium/potassium/calcium exchanger 1 and a perlucin-like protein. MAPKAP1 (TOR signaling pathway) promotes dark epithelial pigmentation (Liu et al., 2017), GRL101 (rhodopsin signaling pathway) is an ortholog of the pigment dispersing factor (Tanaka et al., 2014), and enolase (glycolysis/gluconeogenesis pathway) is a biomarker of vitiligo, a human pigmentation disorder affecting melanocytes (Hamid et al., 2015). Perlucin is a well-known matrix protein found in the nacreous layer of the pearl oyster shell (Joubert et al., 2010) with a function in the biomineralization process.

We also identified several GO terms with a less important role in pigmentation, like "TOR signaling" (GO:0031929), "TORC2 signaling" (GO:0038203), "glycolytic process" (GO:0006096), and "compound eye development" (GO:0048749) for the biological process GO category; and "calcium, potassium: sodium antiporter activity" (GO:0005432), "alkali metal ion binding" (GO:0031420), and "mannose binding" (GO:0005537) for the molecular function GO category.

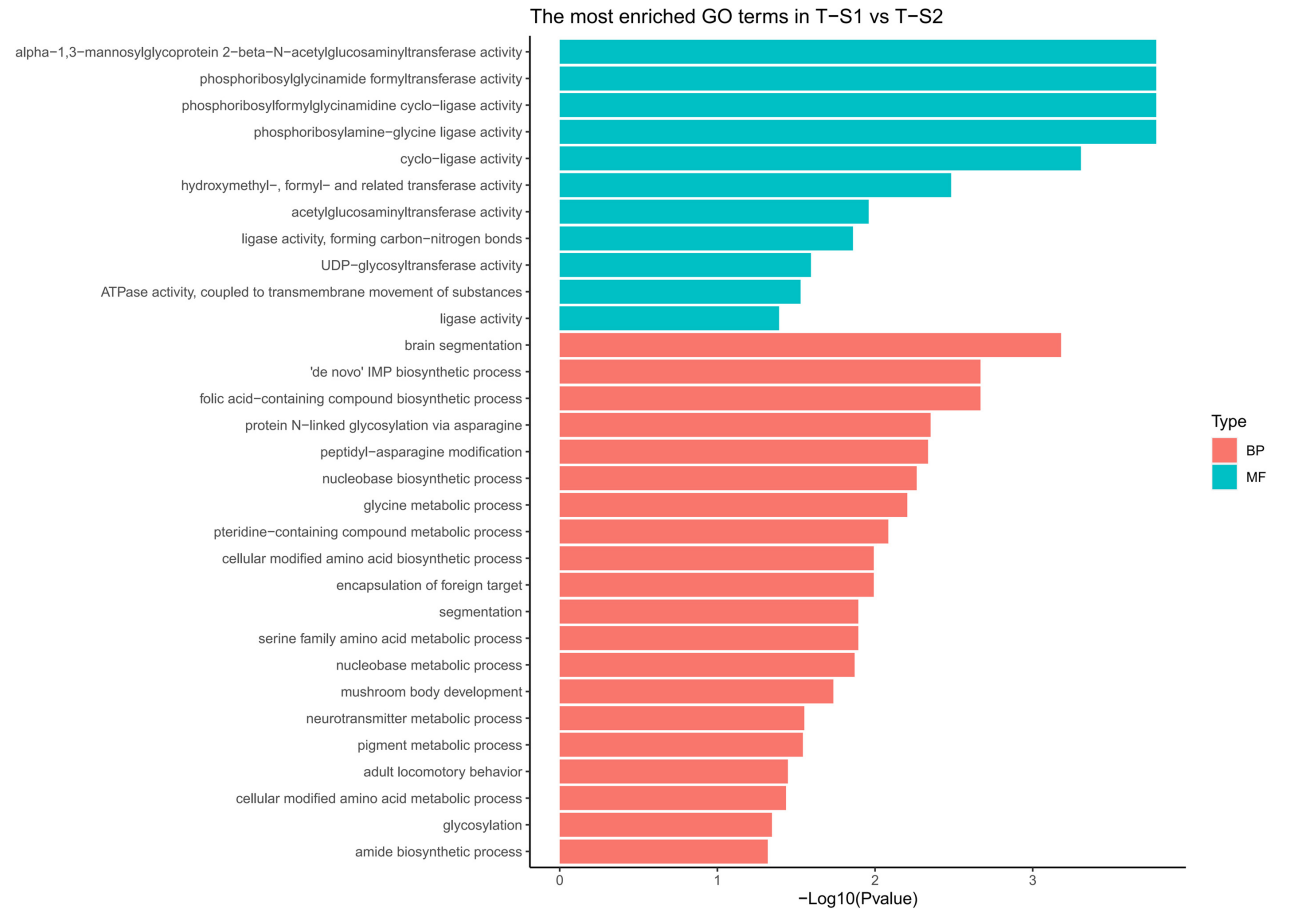



**FIGURE 5 |** Histograms of the enriched biological processes (BP) and molecular functions (MF) from the genes with differentially methylated positions in individuals from the depth treatment samplings in T-S1 vs. T-S2 (T-S1, T-S2 = depth treatment at sampling times 1 and 2, respectively).

### T-S1 (1 Month at 8 m Depth) vs. T-S3 (1 Month at 8 m, 1 Month at 30 m, and 1 Month Back at 8 m)

As the previous enrichment analyses revealed, significant enrichment of several GO categories correlated with pigmentation were identified like in the T-S2 vs. T-S3 pairwise comparison (**Figure 7**): "L-ornithine transmembrane transporter" (GO:0000064) for the biological process GO category; and "ornithine transport" (GO:0015822), "lysine transport" (GO:0015819), "L-amino acid transport" (GO:0015807), "basic amino acid transmembrane transporter activity" (GO:0015171), "L-amino acid transmembrane transporter activity" (GO:0015179), and "xenobiotic transporter activity" (GO:0015238) for molecular function GO category.

At the gene level, only the *GPI-anchor transamidase gene* could be linked to the pigmentation process (among other pathways) since it is involved in a human disorder characterized by altered dermal pigmentation (Ng and Freeze, 2014).

We also identified several GO terms with a less important role in pigmentation, such as the "drug transmembrane transport" (GO:0006855) for the biological process GO category; and "attachment of GPI anchor to protein" (GO:0016255), "regulation of TOR signaling" (GO:0032006), and "protein glycosylation" (GO:0006486) for the molecular function GO category.

## DISCUSSION

Pearl farming, the second economic resource of French Polynesia, has been suffering a major economic crisis since 2001. To address this problem, stakeholders, together with pearl farmers and scientists, are developing an ambitious plan to reduce the volume of pearl production, but to increase pearl quality. This objective could be reached through one of the most economically interesting traits of *Pinctada margaritifera*: its ability to express the largest range of inner shell color (and thus pearl color) of any pearl-producing species worldwide (Ky et al., 2014; Stenger et al., 2019). Indeed, producing unique, highly valuable, pearls displaying a palette of phenotypes ranging from very dark to very pale colors constitutes an efficient way to diversify the production and appeal to different markets. Selection of donor oysters based on color phenotype was started a few years ago (Ky et al., 2013). However, the possibility of acting directly on the selected

**TABLE 2 |** All significantly differentially methylated positions (*q* value < 0.05) for treatment comparisons.

| Scaffold name | Scaffold size | Position | Genomic element | *q*value | Diff_M | Gene annotation name | |
|---|---|---|---|---|---|---|---|
| scaffold11 | 453194 | 35819 | UPSTREAM | 0.0282 | −17.46 | —NA— | Depth treatment: time 1 *vs* time 2 |
| scaffold11 | 453194 | 35847 | UPSTREAM | 0.0282 | −21.46 | | |
| scaffold11282 | 54383 | 4058 | GENE_mRNA | 0.0354 | 31.90 | trifunctional purine biosynthetic protein adenosine-3-like isoform X1 | |
| scaffold1133 | 336669 | 153064 | UPSTREAM | 0.0133 | 24.13 | —NA— | |
| scaffold1625 | 401360 | 350179 | GENE_mRNA | 0.0284 | 20.83 | alpha-1,3-mannosyl-glycoprotein 2-beta-N-acetylglucosaminyltransferase isoform X3 | |
| scaffold2357 | 95418 | 29644 | GENE_mRNA | 0.0284 | 29.22 | multidrug resistance-associated protein 1-like isoform X1 | |
| scaffold2357 | 95418 | 29691 | GENE_mRNA | 0.0284 | 31.77 | | |
| scaffold3816 | 161365 | 94615 | UPSTREAM | 0.0284 | −31.61 | —NA— | |
| scaffold4468 | 144975 | 29587 | DOWNSTREAM | 0.0470 | 20.43 | PREDICTED: uncharacterized protein LOC109618538 | |
| scaffold4716 | 65370 | 6520 | EXON_CDS | 0.0284 | 27.45 | —NA— | |
| scaffold5609 | 111224 | 54055 | UPSTREAM | 0.0257 | −24.59 | —NA— | |
| scaffold10 | 363274 | 309202 | EXON_CDS | 0.0201 | −15.97 | —NA— | Depth treatment: time 2 *vs* time 3 |
| scaffold10423 | 31023 | 17485 | GENE_mRNA | 0.0406 | −14.58 | cationic amino acid transporter 2-like isoform X1 | |
| scaffold11822 | 47775 | 21990 | GENE_mRNA | 0.0186 | 27.95 | uncharacterized protein LOC111108810 | |
| scaffold1371 | 144177 | 54477 | GENE_mRNA | 0.0433 | 16.39 | G-protein coupled receptor GRL101-like | |
| scaffold18 | 585035 | 250513 | GENE_mRNA | 0.0361 | 30.71 | target of rapamycin complex 2 subunit MAPKAP1-like | |
| scaffold2163 | 271214 | 87225 | DOWNSTREAM | 0.0433 | 28.72 | PREDICTED: uncharacterized protein LOC105344672 | |
| scaffold2357 | 95418 | 29691 | GENE_mRNA | 0.0261 | −29.94 | multidrug resistance-associated protein 1-like isoform X1 | |
| scaffold236 | 195829 | 77424 | GENE_mRNA | 0.0216 | 25.97 | enolase 4-like isoform X3 | |
| scaffold2576 | 104445 | 84826 | GENE_mRNA | 0.0026 | −38.55 | Coiled-coil domain-containing protein 79 | |
| scaffold2582 | 91290 | 78204 | GENE_mRNA | 0.0133 | 41.28 | sodium/potassium/calcium exchanger 1-like | |
| scaffold2582 | 91290 | 78245 | GENE_mRNA | 0.0099 | 43.74 | | |
| scaffold381 | 319941 | 276927 | DOWNSTREAM | 0.0433 | 17.94 | —NA— | |
| scaffold5757 | 154693 | 48096 | GENE_mRNA | 0.0406 | 15.15 | perlucin-like protein | |
| scaffold5757 | 154693 | 48114 | GENE_mRNA | 0.0336 | 19.65 | | |
| scaffold592 | 283515 | 144263 | GENE_mRNA | 0.0261 | 31.63 | PREDICTED: uncharacterized protein LOC105317977 isoform X11 | |
| scaffold6243 | 82815 | 59659 | GENE_mRNA | 0.0409 | 38.89 | RNA polymerase II-associated protein 3-like isoform X2 | |
| scaffold720 | 228729 | 148045 | GENE_mRNA | 0.0186 | −28.81 | DNA-directed RNA polymerase I subunit RPA2-like | |
| scaffold10423 | 31023 | 17485 | GENE_mRNA | 0.0318 | −15.74 | cationic amino acid transporter 2-like isoform X1 | Depth treatment: time 1 *vs* time 3 |
| scaffold10423 | 31023 | 17511 | GENE_mRNA | 0.0199 | −19.43 | | |
| scaffold10423 | 31023 | 17518 | GENE_mRNA | 0.0326 | −17.08 | | |
| scaffold10423 | 31023 | 17520 | GENE_mRNA | 0.0129 | −19.70 | | |
| scaffold11 | 453194 | 35819 | UPSTREAM | 0.0198 | −17.46 | —NA— | |
| scaffold1133 | 336669 | 153064 | UPSTREAM | 0.0320 | 19.98 | —NA— | |
| scaffold1657 | 298101 | 43346 | GENE_mRNA | 0.0127 | −24.93 | kinesin-like protein KIF2A | |
| scaffold2163 | 271214 | 87184 | DOWNSTREAM | 0.0207 | −26.20 | PREDICTED: uncharacterized protein LOC105344672 | |
| scaffold2163 | 271214 | 87224 | DOWNSTREAM | 0.0153 | −27.03 | | |
| scaffold273 | 459813 | 427122 | GENE_mRNA | 0.0334 | −16.66 | NACHT and WD repeat domain-containing protein 2-like isoform X2 | |
| scaffold273 | 459813 | 427125 | GENE_mRNA | 0.0326 | −16.14 | | |

*(Continued)*

**TABLE 2 |** Continued

| Scaffold name | Scaffold size | Position | Genomic element | *q*value | Diff_M | Gene annotation name |
|---|---|---|---|---|---|---|
| scaffold273 | 459813 | 427294 | GENE_mRNA | 0.0256 | −20.97 | |
| scaffold3199 | 215908 | 10021 | UPSTREAM | 0.0318 | 30.03 | —NA— |
| scaffold4848 | 64103 | 14806 | GENE_mRNA | 0.0261 | −35.91 | GPI-anchor transamidase-like |
| scaffold6242 | 215376 | 126991 | GENE_mRNA | 0.0164 | −22.59 | SH3 and cysteine-rich domain-containing protein 3 |
| scaffold734 | 224438 | 4180 | UPSTREAM | 0.0079 | 16.63 | polypeptide N-acetylgalactosaminyltransferase 5-like |
| scaffold734 | 224438 | 4185 | UPSTREAM | 0.0153 | 14.74 | |

*Scaffold name: scaffold number; Scaffold size: scaffold size; Position: position of the significantly differentially methylated positions on this scaffold; Genomic element: the genomic feature containing the DNA methylation change; q value: q value; Diff-M: the differential methylation level obtained using the Methylkit R package; Gene annotation name: Gene annotation according to the nr and swiss-prot blast top hit. Blue shading (negative values) indicates hypomethylation of the position and red shading (positive values) hypermethylation; darker shading indicates a stronger degree of hypomethylation of hypermethylation, respectively. The last column indicates in which comparison the significantly different methylated positions were found.*

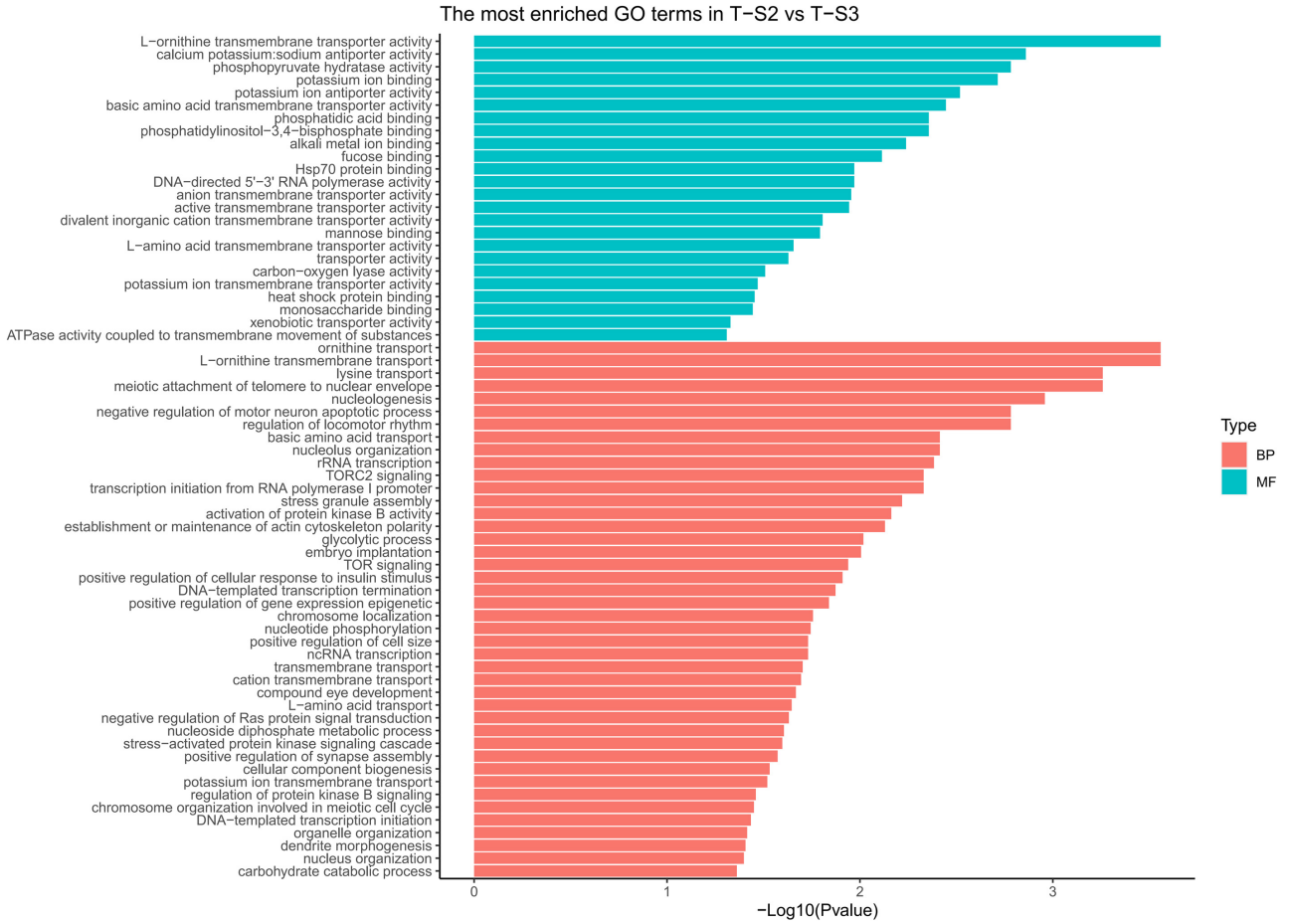



**FIGURE 6 |** Histograms of the enriched biological processes (BP) and molecular functions (MF) from the genes with differentially methylated positions in individuals from the depth treatment samplings in T-S2 vs. T-S3 (T-S2, T-S3 = depth treatment at sampling times 2 and 3, respectively).

oysters to enhance their color and quality as donors is also an attractive method for improving pearl quality. For this, a better understanding of the interactions between the phenotype and gene expression correlated with environmental conditions is essential (Gavery and Roberts, 2017), and would allow the development of epigenetic marker-assisted selection or, more generally, epigenetics-assisted cultural practices.

As a first step to understanding the mechanisms behind this environmentally induced color variation, we applied an environmental forcing (culture-depth variation) known to affect

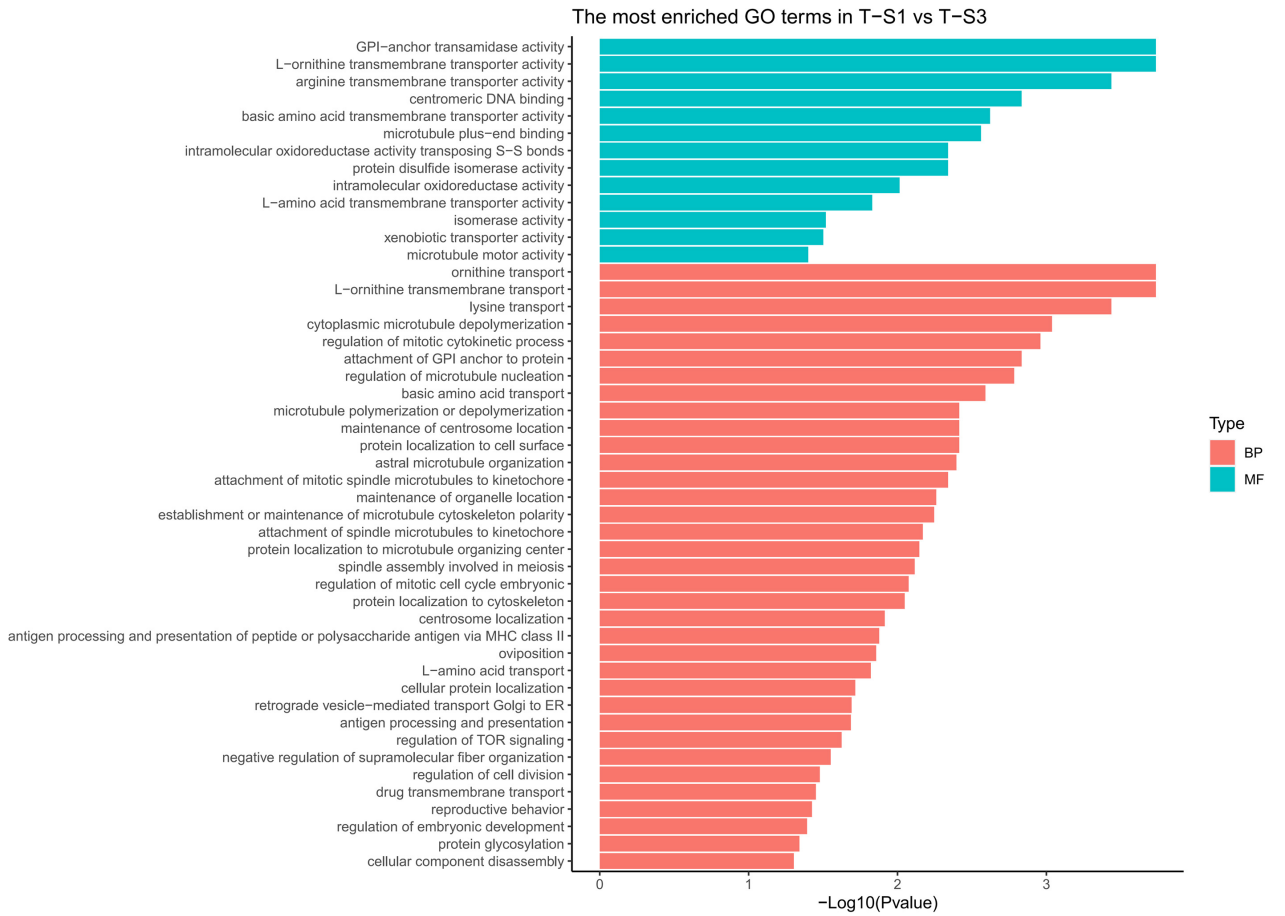



**FIGURE 7 |** Histograms of the enriched biological processes (BP) and molecular functions (MF) from the genes with differentially methylated positions in individuals from the depth treatment samplings in T-S1 vs. T-S3 (T-S1, T-S3 = depth treatment at sampling times 1 and 3, respectively).

pearl and inner-shell darkness (Stenger et al., 2019), and studied, under constant genotype, the DNA methylation changes induced. In addition to providing the first description of a pearl oyster methylome, our analyses identified specific methylation changes that affected candidate genes involved in the expression of shell and pearl color darkness. These genes were involved in both pigmentation (biological coloring mechanisms) and iridescence (physical coloring mechanisms based on the differential organization of biomineral crystals).

## The First Methylome of the *Pterioidea* Super-Family Shows Similar Characteristics to Other Invertebrate Methylomes

The present study provides to our knowledge the first methylome of a member of the *Pterioidea* super-family. The whole-genome bisulfite sequencing (WGBS-seq) of the pearl oyster mantle tissues revealed that its methylome is of the mosaic type and similar in many ways to what is classically described in some other invertebrates. Indeed, *P. margaritifera* mainly displays cytosine methylation in the CpG context, as already described in *Crassostrea gigas* (Thunberg, 1793) by Gavery and Roberts (2013) and in *Biomphalaria glabrata* (Say, 1818) by Adema et al. (2017). Likewise, differential methylation was also mainly identified in the CpG context, as in Wang et al. (2014) who reported that more than 99% of DNA methylation changes were restricted to the CpG context in *C. gigas*. The pattern of methylation we obtained occurred essentially in the gene bodies, with some accretion upstream and downstream of the gene, as described for mosaic methylation in other mollusks (Sarda et al., 2012; Wang et al., 2014; Rondon et al., 2017). These features of a short, but densely methylated region (corresponding to the genes), interspersed by long unmethylated regions (intergenic) are characteristic of the mosaic pattern of DNA methylation (Gavery and Roberts, 2013), which shows the typical bimodal distribution generally met in invertebrates. The lowly methylated genes were involved in the reproductive process, cellular signaling, and environmentally responsive functions. The low methylation of genes involved in the response to environmental changes is something reported in many different invertebrates (Sarda et al., 2012), but the presence of functions associated with reproduction is less common. It may be explained by the tissue used to produce this methylome, the mantle, which is a tissue not involved in reproduction

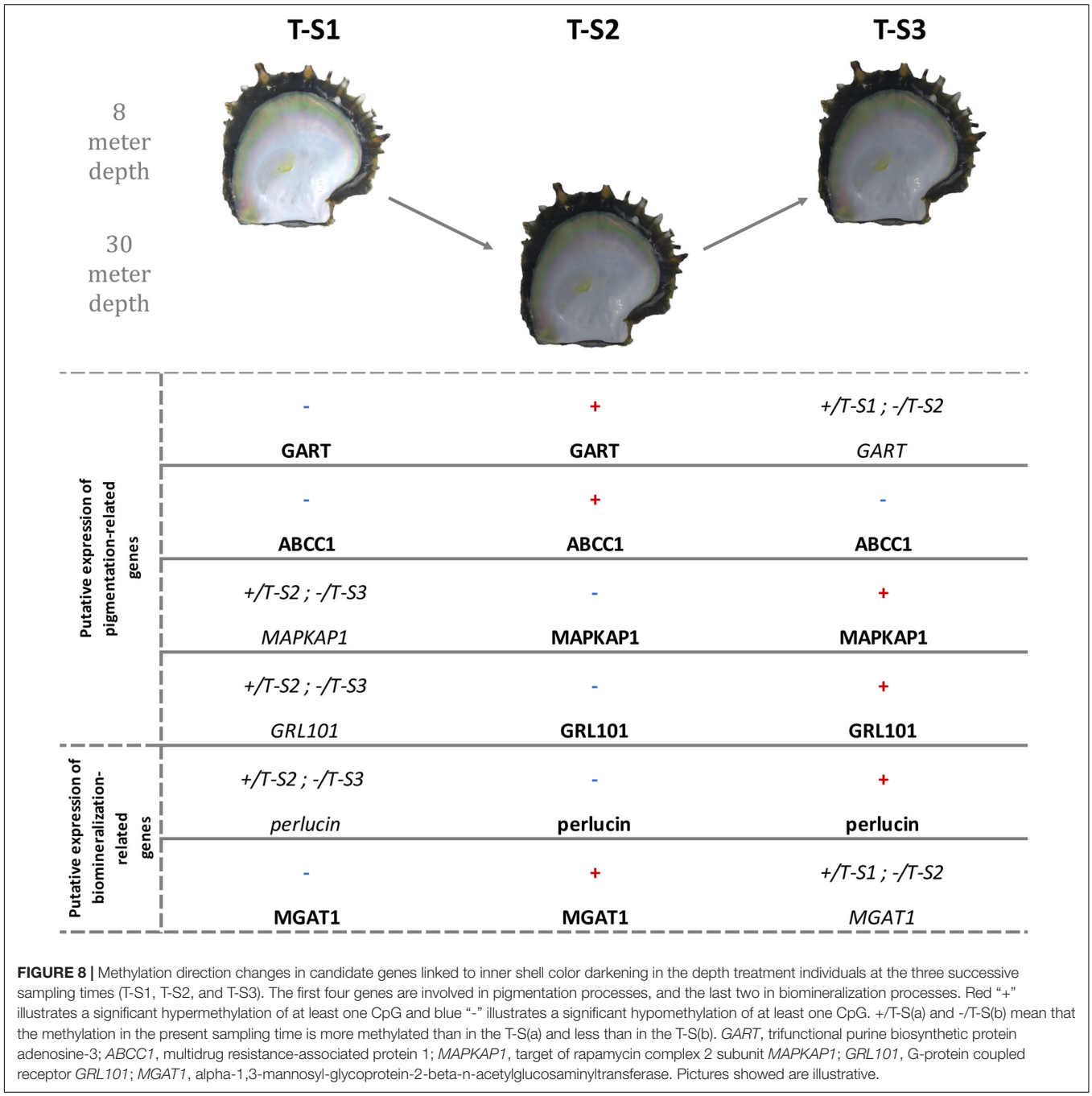



**FIGURE 8 |** Methylation direction changes in candidate genes linked to inner shell color darkening in the depth treatment individuals at the three successive sampling times (T-S1, T-S2, and T-S3). The first four genes are involved in pigmentation processes, and the last two in biomineralization processes. Red "+" illustrates a significant hypermethylation of at least one CpG and blue "-" illustrates a significant hypomethylation of at least one CpG. +/T-S(a) and -/T-S(b) mean that the methylation in the present sampling time is more methylated than in the T-S(a) and less than in the T-S(b). *GART*, trifunctional purine biosynthetic protein adenosine-3; *ABCC1*, multidrug resistance-associated protein 1; *MAPKAP1*, target of rapamycin complex 2 subunit *MAPKAP1*; *GRL101*, G-protein coupled receptor *GRL101*; *MGAT1*, alpha-1,3-mannosyl-glycoprotein-2-beta-n-acetylglucosaminyltransferase. Pictures showed are illustrative.

(see correlation between methylation levels and gene expression **Figure 2D**). The genes identified in highly methylated regions were essentially involved in housekeeping functions (Gavery and Roberts, 2013; Olson and Roberts, 2014; Wang et al., 2014). When comparing the gene body methylation rate with the gene expression level, we demonstrated that moderately methylated genes have higher expression levels than lowly or highly methylated ones. This result is consistent with other studies (Feng et al., 2010; Xiang et al., 2010; Zemach et al., 2010) and strengthens the emerging hypothesis that, in invertebrates, gene expression and gene body methylation functions as a negative feedback loop in which gene expression increases with gene methylation until reaching a tipping point where additional methylation decreases transcription (Dixon et al., 2018).

## Environmentally Induced DNA Methylation Changes and Their Link With Pigmentation

Among the DNA methylation changes that occurred during our experiment, several occurred in genes known to be involved in pigmentation pathways. Among these, the pteridine pathway

was recently identified as a key player in the expression of the yellow color phenotype in *P. margaritifera* (Stenger et al., in press). Indeed, different derivates of pteridine can lead to the production of sepiapterin and xanthopterins, two yellow pigments (Ng et al., 2009). The folic acid pathway is also significantly affected by DNA methylation changes. Although its involvement in molluscan pigmentation is unknown, folic acid deficiency is linked to melanosis (e.g., melanin overproduction) in mammals, which results in a black pigmentation (Sharp et al., 1980). Since the implication of melanin in pearl oyster pigmentation has previously been identified (Lemer et al., 2015), an epigenetically driven modification of gene expression in the folic-acid pathway could be associated with the darkening color phenotypes expressed in response to an increase in depth.

At the gene level, *GART*, a hypermethylated gene included in three enriched GO categories (**Figure 8**), encodes a trifunctional purine biosynthetic protein, adenosine-3. This protein is involved in the *de novo* purine synthesis pathway (Amsterdam et al., 2004) and is composed of three subunits (a phosphoribosylglycinamide formyltransferase, a phosphoribosylglycinamide synthetase, and a phosphoribosylaminoimidazole synthetase). Biochemically, it catalyzes steps 2, 3, and 5 of inosine monophosphate (IMP) synthesis (Amsterdam et al., 2004; Ng et al., 2009). IMP is one of the precursors initiating the pterin and the Raper-Manson pathways, two pathways leading to pigmentation in *P. margaritifera* (Stenger et al., in press). Ng et al. (2009) have shown that mutations in *GART* are associated with pigmentation defects in juvenile zebrafish *Danio rerio* (Buchanan-Hamilton, 1822) due to disturbances of the pterin and Rapper-Mason pathways. Wild-type zebrafish are mainly yellow with black spots, while Δ-GART juveniles are entirely black (Ng et al., 2009). We can, therefore, hypothesize that methylation changes in the *GART* gene may affect its expression, subsequently affecting the pterin and Rapper-Mason pathways and leading to a darkening of the shell.

The gene for multidrug resistance-associated protein 1 (*ABCC1*) presented two hypermethylated positions after the period at 30 m, a methylation state that reverted after the return to 8 m. *ABCC1* is known to mediate ATP-dependent transport of glutathione and glutathione conjugates (Homolya et al., 2003). In a previous study it was proposed that glutathione plays an essential role in the expression of the yellow and black pigments (Stenger et al., in press). Glutathione-S-transferase (GST) activity is central in regulating the production of the yellow pheomelanin and black eumelanin pigments through the Raper-Manson pathway (Sonthalia et al., 2016). Methylation changes in the *ABCC1* gene could therefore promote variation in the quantity of glutathione available and modify the regulation of the production of pheomelanin and eumelanin. An overproduction of eumelanin may explain the observed darkening of the shell.

*GRL101* presented a hypermethylated response to the return to 8 m. According to Tanaka et al. (2014), this gene is an ortholog of the pigment dispersing factor, a gene responsible for changes in the concentration of chromatophoral pigment in response to darkness (Rao and Riehm, 1993). In crustaceans, it was proposed that color variation due to changing light conditions was caused by the dispersion of retinal chromatophore pigments linked with the activation of *GRL101* (Rao and Riehm, 1993; Auerswald et al., 2008). The methylation change of *GRL101*, the similarities between the environmental triggers (a decrease of light) activating *GRL101* in other organisms, and the phenotypes resulting from this activation argue in favor of the involvement of *GRL101* in *P. margaritifera* color variation.

The *GPI-anchor transamidase-like* gene was hypomethylated after the return to 8 m depth. According to Ng and Freeze (2014), a mutation of the *GPI-anchor transamidase* genes is involved in a human disorder characterized by an altered dermal pigmentation (Ng and Freeze, 2014). This was later confirmed by RNAi experiments targeting GPI-anchor transamidase transcripts and resulting in a hyper-pigmented dark swellings in the maize anthracnose fungus *Colletotrichum graminicola* (G.W. Wilson 1914) (Oliveira-Garcia and Deising, 2016).

*Enolase-4* is another candidate gene displaying hypomethylation at 30 m. Enolases are metalloenzymes involved in glycolysis and glycogen storage. One study reported a correlation between enolase activity and pigmentation: Hamid et al. (2015) showed that patients with vitiligo (a pigmentation disorder affecting melanocytes and inhibiting pigment synthesis) synthesize antibodies directed against enolases. Since their discovery, enolases have been used as biomarkers for the diagnosis, treatment, and monitoring of vitiligo (Hamid et al., 2015). The causes of this pathology are still unclear, although both genetic and environmental factors seem to be involved (Hamid et al., 2015). In the case of the pearl oyster, the hypomethylation of the enolase gene at 30 m may be associated with a change of expression inducing a darker phenotype.

The last of the genes subject to methylation change (hypermethylation after the last period at 8 m) and displaying a functional link with pigmentation is the target of rapamycin complex 2 subunit (*MAPKAP1*). This gene is involved in the TORC2 and TOR signaling pathways. The activation of these signaling pathways is known to promote a dark epithelial pigmentation due to the proliferation and the migration of retinal pigmentation epithelial cells (RPE cells) (Liu et al., 2017).

Among the six genes displaying a functional link with the pigmentation process or its regulation, four (*GART*, *ABCC1*, *MAPKAP1*, and *GRL101*) were associated with the expression of darker phenotypes, while the two others were associated with pigmentation disorders. Further experiments will be necessary to confirm and define their role, such as gene expression quantification, RNAi, and, once possible, genome editing, and epigenetic engineering. Thus, our results provide the first step toward this new research field.

## Biomineralization and Pearl Darkness

In addition to a darkening of the coloration (Stenger et al., 2019), previous experiments have shown that a variation in depth also affects the shape and size of the aragonite tablets of the shell of *P. margaritifera* (Rousseau and Rollion-Bard, 2012). Aragonite tablets are the structural unit of nacre, the $CaCO_3$ polymorph that constitutes the inner-shell of pearl oyster and the pearl itself (Rousseau and Rollion-Bard, 2012). Variation in the organization of these aragonite tablets can induce a change in color and luster (brightness) due to a change in the physical iridescence

(Liu et al., 1999; Wang et al., 2008). Although not yet demonstrated, it is suspected that pigments contributing to nacre color are constituents of the intra-lamellar silk-fibroin gel that is localized between aragonite tablets (Addadi et al., 2006). Variation in the size of these tablets could therefore lead to a variation in the quantity of pigments that can be viewed through the last biomineralized aragonite layers. Interestingly, among the genes displaying methylation changes in response to a variation in water depth, two are well-known actors of the biomineralization processes of the nacreous layer: *perlucin* (Joubert et al., 2010) and *MGAT1* (Takakura et al., 2008).

Perlucin is a protein found in the shell organic matrix of several Mollusca, including *P. margaritifera* (Weiss et al., 2000; Blank et al., 2003; Marie et al., 2013; Joubert et al., 2014). Experiments with purified Mollusca perlucin have suggested its involvement in calcium carbonate precipitation by favoring nucleation, crystallization and crystal growth control (Weiss et al., 2000). A variation in its expression can therefore have a huge effect on aragonite tablet size and organization (Rousseau and Rollion-Bard, 2012) and may thus modify the iridescence and transparency properties of the top aragonite layers (Rousseau and Rollion-Bard, 2012).

*MGAT1* is a gene whose product initiates carbohydrate formation and is essential for the conversion of high-mannose to hybrid and complex N-glycans. This protein is involved in the protein glycosylation pathway, which is part of Protein modification. Interestingly, Takakura et al. (2008) identified an acidic N-glycan post-translationally attached to nacrein in *Pinctada fucata* that allows calcium binding. Moreover, nacrein is one of the main proteins found in the nacreous part of the shell (Rousseau and Rollion-Bard, 2012). So, although the *MGAT1* gene plays no role in crystal formation, a possible link affecting nacrein formation can still be found. Future proteomics studies will be necessary to better uncover the role of *MGAT1* in *P. margaritifera* shell coloration.

### Epigenetics and Pearl Culture

As previously reported, the yo-yo experiment resulted in a general darkening of the inner shell of *P. margaritifera* in response to an increase in depth (Stenger et al., 2019), an environmentally induced phenotype that was maintained even after a return to the control depth (8 m). Such an enduring phenotypic response could be considered as good evidence of the involvement of epigenetic control (Sutherland and Costa, 2003; Harris et al., 2012; Bräutigam et al., 2013). The maintenance of this phenotype was previously documented in this species cultured for pearl production, and can last for over 18 months (Stenger et al., 2019). In another biological model, maize, stress-induced hypermethylation of *P-pr* (Richards, 2006; Lukens and Zhan, 2007) was associated with a reduced pigmentation that lasted in some cases for the entire life of an individual, and could even be transmitted to the next generation (Richards, 2006; Bossdorf et al., 2008). Such effects could offer huge benefits for pearl farming. First, this long-lasting effect suggests that farmers could better control their production through dedicated conditioning of recipient and/or donor oysters. Additionally, the transgenerational effect described for maize, although not yet tested for pearl oysters, suggests that epigenetic marker-assisted selection could be envisioned. Such an approach may offer the possibility of selecting phenotypes of interest without the associated risk of eroding genetic diversity and/or the integration into natural populations of spat produced by farmed oysters (Reisser et al., 2020).

## DATA AVAILABILITY STATEMENT

The datasets generated for this study can be found on the NCBI (BioProject PRJNA663978). Scripts used are provided on GitHub (PLStenger/Pearl_Oyster_Colour_BS_Seq/00_scripts).

## AUTHOR CONTRIBUTIONS

JV-D, P-LS, SP, and C-LK designed the study. P-LS and MM performed the experiments. P-LS, CC, and CG analyzed the data. P-LS and JV-D drafted the manuscript. Funding was obtained by CL-K, SP, and JV-D. All authors approved the manuscript.

## FUNDING

This study was supported by grants from the "Direction des Ressources Marines," through the AmeliGEN project (# 10065/MEI/DRMM). P-LS's Ph.D. was funded by AmeliGEN and the Pacific Doctoral School (EDP) (ED 469). This study was performed within the framework of the "Laboratoire d'Excellence (LABEX)" TULIP (ANR-10-LABX-41) and CORAIL (ANR-10-LABEX).

## ACKNOWLEDGMENTS

The authors would like to thank the Regahiga Pearl Farm (Mangareva Island, Gambier Archipelago, French Polynesia) for providing the pearl oysters used in this study.

## SUPPLEMENTARY MATERIAL

The Supplementary Material for this article can be found online at: https://www.frontiersin.org/articles/10.3389/fgene.2021.630290/full#supplementary-material

**Supplementary Figure 1 |** Treemaps of biological processes obtained from the GO terms significantly enriched from the lowly methylated genes **(A)** (data from **Figure 2C** – "1" part) and the highly methylated genes **(B)** (data from **Figure 2C** – "2" part).

**Supplementary Figure 2 |** Treemaps of biological processes and molecular functions obtained from the GO terms significantly enriched from the genes with differentially methylated positions in control individuals (C-S1, control in time 1; C-S2, control in time 2; C-S3, control in time 3).

**Supplementary Table 1 |** FastQC results for raw and trimmed data.

**Supplementary Table 2 |** Average values by category (control/depth treatment) and sampling time for: the number of read pairs, paired-end alignments, mapping efficiency, number of duplicated alignments removed after mapping, the number of C in sequences, the number of C in percentage in CpG,

CHG, CHH or in unknown contexts, and the basic statistics of the gene body methylation rate (GBM – on the 54408 genes of the reference genome).

**Supplementary Table 3 |** All significantly differentially methylated positions (*q* value < 0.05) for the controls. Scaffold name: scaffold number; Scaffold size: scaffold size; Position: position of the significantly differentially methylated positions on this scaffold; Genomic element: the genomic feature containing the DNA methylation change; *q* value: *q* value; Diff-M: the differential methylation level obtained using the *Methylkit R* package; Gene annotation name: Gene annotation according to the nr and swiss-prot blast top hit. Blue shading (negative values) indicates hypomethylation of the position and red shading (positive values) hypermethylation; darker shading indicates a stronger degree of hypomethylation of hypermethylation, respectively. The last column indicates in which comparison the significantly different methylated positions were found.

## REFERENCES


Addadi, L., Joester, D., Nudelman, F., and Weiner, S. (2006). Mollusk shell formation: a source of new concepts for understanding biomineralization processes. *Chemistry* 12, 980–987. doi: 10.1002/chem.200500980

Adema, C. M., Hillier, L. D. W., Jones, C. S., Loker, E. S., Knight, M., Minx, P., et al. (2017). Whole genome analysis of a schistosomiasis-transmitting freshwater snail. *Nat. Commun.* 8:15451. doi: 10.1038/ncomms15451

Akalin, A., Kormaksson, M., Li, S., Garrett-Bakelman, F. E., Figueroa, M. E., Melnick, A., et al. (2012). MethylKit: a comprehensive R package for the analysis of genome-wide DNA methylation profiles. *Genome Biol.* 13:R87. doi: 10.1186/gb-2012-13-10-R87

Amsterdam, A., Nissen, R. M., Sun, Z., Swindell, E. C., Farrington, S., and Hopkins, N. (2004). Identification of 315 genes essential for early zebrafish development. *Proc. Natl. Acad. Sci. U.S.A.* 101, 12792–12797. doi: 10.1073/pnas.0403929101

Anders, S., Pyl, P. T., and Huber, W. (2015). Genome analysis HTSeq — a Python framework to work with high-throughput sequencing data. *Bioinformatics* 31, 166–169. doi: 10.1093/bioinformatics/btu638

Andrews, S. (2010). *FastQC: A Quality Control Tool for High Throughput Sequence Data*. Cambridge: Babraham Bioinforma.

Auerswald, L., Freier, U., Lopata, A., and Meyer, B. (2008). Physiological and morphological colour change in Antarctic krill, *Euphausia superba*: a field study in the Lazarev Sea. *J. Exp. Biol.* 211, 3850–3858. doi: 10.1242/jeb.024232

Blank, S., Arnoldi, M., Khoshnavaz, S., Treccani, L., Kuntz, M., Mann, K., et al. (2003). The nacre protein perlucin nucleates growth of calcium carbonate crystals. *J. Microsc.* 212(Pt 3), 280–291. doi: 10.1111/j.1365-2818.2003.01263.x

Bolger, A. M., Lohse, M., and Usadel, B. (2014). Genome analysis trimmomatic: a flexible trimmer for illumina sequence data. *Bioinformatics* 30, 2114–2120. doi: 10.1093/bioinformatics/btu170

Bossdorf, O., Richards, C. L., and Pigliucci, M. (2008). Epigenetics for ecologists. *Ecol. Lett.* 11, 106–115. doi: 10.1111/j.1461-0248.2007.01130.x

Bouzerand, E. (2018). *Points Forts de la Polynésie Française – Bilan – La Perle en 2016*. Papeete: Institu de la Statistique de la Polynésia française.

Bräutigam, K., Vining, K. J., Lafon-Placette, C., Fossdal, C. G., Mirouze, M., Marcos, J. G., et al. (2013). Epigenetic regulation of adaptive responses of forest tree species to the environment. *Ecol. Evol.* 3, 399–415. doi: 10.1002/ece3.461

Chakraborty, A. K., Funasaka, Y., Ichihashi, M., Sodi, S., Bhattacharya, M., and Pawelek, J. (1999). Upregulation of mRNA for the melanocortin-1 receptor but not for melanogenic proteins in macrophage x melanoma fusion hybrids exhibiting increased melanogenic and metastatic potential. *Pigment Cell Res.* 12, 355–366. doi: 10.1111/j.1600-0749.1999.tb00519.x

Charpentier, V., Phillips, C. S., and Méry, S. (2012). Pearl fishing in the ancient world: 7500 BP. *Arab. Archaeol. Epigr.* 23, 1–6. doi: 10.1111/j.1600-0471.2011.00351.x

Conesa, A., Götz, S., García-gómez, J. M., Terol, J., Talón, M., Genómica, D., et al. (2005). Blast2GO: a universal tool for annotation, visualization and analysis in functional genomics research. *BMC Bioinformatics* 21:3674–3676. doi: 10.1093/bioinformatics/bti610

Cuthill, I. C., Allen, W. L., Arbuckle, K., Caspers, B., Chaplin, G., Hauber, M. E., et al. (2017). The biology of color. *Science* 357:eaan0221. doi: 10.1126/science.aan0221

Dixon, G., Liao, Y., Bay, L. K., and Matz, M. V. (2018). Role of gene body methylation in acclimatization and adaptation in a basal metazoan. *Proc. Natl. Acad. Sci. U.S.A.* 115, 13342–13346. doi: 10.1073/pnas.1813749115

Dolinoy, D. C. (2008). The agouti mouse model: an epigenetic biosensor for nutritional and environmental alterations on the fetal epigenome. *Nutr. Rev.* 66, 7–11. doi: 10.1111/j.1753-4887.2008.00056.x

Dolinoy, D. C., Weidman, J. R., Waterland, R. A., and Jirtle, R. L. (2006). Maternal genistein alters coat color and protects Avy mouse offspring from obesity by modifying the fetal epigenome. *Environ. Health Perspect.* 114, 567–572. doi: 10.1289/ehp.8700

Feng, D., Li, Q., Yu, H., Kong, L., and Du, S. (2018). Transcriptional profiling of long non-coding RNAs in mantle of *Crassostrea gigas* and their association with shell pigmentation. *Sci. Rep.* 8:1436. doi: 10.1038/s41598-018-19950-6

Feng, D., Li, Q., Yu, H., Liu, S., Kong, L., and Du, S. (2020). Integrated analysis of microRNA and mRNA expression profiles in *Crassostrea gigas* to reveal functional miRNA and miRNA-targets regulating shell pigmentation. *Sci. Rep.* 10:20238. doi: 10.1038/s41598-020-77181-0

Feng, S., Cokus, S. J., Zhang, X., Chen, P. Y., Bostick, M., Goll, M. G., et al. (2010). Conservation and divergence of methylation patterning in plants and animals. *Proc. Natl. Acad. Sci. U.S.A.* 107, 8689–8694. doi: 10.1073/pnas.1002720107

Fernandes, J., and Gattass, C. R. (2009). Topological polar surface area defines substrate transport by multidrug resistance associated protein 1 (MRP1/ABCC1). *J. Med. Chem.* 52, 1214–1218. doi: 10.1021/jm801389m

Frost, S. K., and Malacinski, G. M. (1979). The developmental genetics of pigment mutants in the Mexican axolotl. *Dev. Genet.* 1, 271–294. doi: 10.1002/dvg.1020010402

Gavery, M. R., and Roberts, S. B. (2013). Predominant intragenic methylation is associated with gene expression characteristics in a bivalve mollusc. *PeerJ* 2013, 1–15. doi: 10.7717/peerj.215

Gavery, M. R., and Roberts, S. B. (2017). Epigenetic considerations in aquaculture. *PeerJ* 5:e4147. doi: 10.7717/peerj.4147

Gueguen, Y., Montagnani, C., Joubert, C., Marie, B., Belliard, C., Tayale, A., et al. (2013). "Characterization of molecular processes involved in the pearl formation in *Pinctada margaritifera* for the sustainable development of pearl farming industry in French Polynesia," in *Recent Advances in Pearl Research–Proceedings of the International Symposium on Pearl Research 2011*, eds S. Watabe, K. Maeyama, and H. Nagasawa (Setagaya: TERRAPUB), 183–193.

Hamid, K. M., Bitsue, Z. K., and Mirshafiey, A. (2015). Autoantibodies profile in vitiligo. *J. Pigment. Disord.* 2, 1–5. doi: 10.4172/2376-0427.1000187

Harris, K. D. M., Bartlett, N. J., and Lloyd, V. K. (2012). *Daphnia* as an emerging epigenetic model organism. *Genet. Res. Int.* 2012, 1–8. doi: 10.1155/2012/147892

Hollander, M., Wolfe, D. A., and Chicken, E. (1973). "The one-way layout," in *Nonparametric Statistical Methods*, 3rd Edn, eds John Wiley & sons (New York, NY: John Wiley and Sons), 202–288.

Homolya, L., Váradi, A., and Sarkadi, B. (2003). Multidrug resistance-associated proteins: export pumps for conjugates with glutathione, glucuronate or sulfate. *BioFactors* 17, 103–114. doi: 10.1002/biof.5520170111

Hu, J., and Barrett, R. D. H. (2017). Epigenetics in natural animal populations. *J. Evol. Biol.* 30, 1612–1632. doi: 10.1111/jeb.13130

Iwahashi, Y., and Akamatsu, S. (1994). Porphyrin pigment in Black-Lip pearls and Its application to pearl identification. *Fish. Sci.* 60, 69–71. doi: 10.2331/fishsci.60.69

Joubert, C., Linard, C., Le Moullac, G., Soyez, C., Saulnier, D., Teaniniuraitemoana, V., et al. (2014). Temperature and food influence shell growth and mantle gene expression of shell matrix proteins in the pearl oyster *Pinctada margaritifera*. *PLoS One* 9:e103944. doi: 10.1371/journal.pone.0103944

Joubert, C., Piquemal, D., Marie, B., Manchon, L., Pierrat, F., Zanella-Cléon, I., et al. (2010). Transcriptome and proteome analysis of *Pinctada margaritifera* calcifying mantle and shell: focus on biomineralization. *BMC Genomics* 11:613. doi: 10.1186/1471-2164-11-613

Katz, M. L., Drea, C. M., and Robison, W. G. Jr. (1987). Dietary vitamins A and E influence retinyl ester composition and content of the retinal pigment epithelium. *Biochim. Biophys. Acta* 924, 432–441.

Klopfenstein, D. V., Zhang, L., Pedersen, B. S., Ramírez, F., Vesztrocy, A. W., Naldi, A., et al. (2018). GOATOOLS: a python library for gene ontology analyses. *Sci. Rep.* 8:10872. doi: 10.1038/s41598-018-28948-z

Krueger, F., and Andrews, S. R. (2011). Bismark: a flexible aligner and methylation caller for Bisulfite-Seq applications. *Bioinformatics* 27, 1571–1572. doi: 10.1093/bioinformatics/btr167

Ky, C. L., Broustal, F., Potin, D., and Lo, C. (2019). The pearl oyster (*Pinctada margaritifera*) aquaculture in French Polynesia and the indirect impact of long-distance transfers and collection-culture site combinations on pearl quality traits. *Aquac. Rep.* 13:100182. doi: 10.1016/j.aqrep.2019.100182

Ky, C.-L., Blay, C., Sham-Koua, M., Lo, C., and Cabral, P. (2014). Indirect improvement of pearl grade and shape in farmed *Pinctada margaritifera* by donor "oyster" selection for green pearls. *Aquaculture* 432, 154–162. doi: 10.1016/j.aquaculture.2014.05.002

Ky, C.-L., Blay, C., Sham-Koua, M., Vanaa, V., Lo, C., and Cabral, P. (2013). Family effect on cultured pearl quality in black-lipped pearl oyster *Pinctada margaritifera* and insights for genetic improvement. *Aquat. Living Resour.* 26, 133–145. doi: 10.1051/alr/2013055

Ky, C.-L., Le Pabic, L., Sham Koua, M., Nicolas, M., Seiji, N., and Devaux, D. (2017). Is pearl colour produced from *Pinctada margaritifera* predictable through shell phenotypes and rearing environments selections? *Aquaculture* 48, 1041–1057. doi: 10.1111/are.12947

Le Moullac, G., Schuck, L., Chabrier, S., Belliard, C., Lyonnard, P., Broustal, F., et al. (2018). Influence of temperature and pearl rotation on biomineralization in the pearl oyster, *Pinctada margaritifera*. *J. Exp. Biol.* 221:jeb186858. doi: 10.1242/jeb.186858

Le Pabic, L., Parrad, S., Sham Koua, M., Nakasai, S., Saulnier, D., Devaux, D., et al. (2016). Culture site dependence on pearl size realization in *Pinctada margaritifera* in relation to recipient oyster growth and mantle graft biomineralization gene expression using the same donor phenotype. *Estuar. Coast. Shelf Sci.* 182, 294–303. doi: 10.1016/j.ecss.2016.03.009

Le Pennec, M. (2010). *Huître Perlière et Perle de Tahiti*. Puna'auia: Université de la Polynésie française.

Lemer, S., Saulnier, D., Gueguen, Y., and Planes, S. (2015). Identification of genes associated with shell color in the black-lipped pearl oyster, *Pinctada margaritifera*. *BMC Genomics* 16:568. doi: 10.1186/s12864-015-1776-x

Liu, Y., Chen, Z., Cheng, H., Chen, J., and Qian, J. (2017). Gremlin promotes retinal pigmentation epithelial (RPE) cellproliferation, migration and VEGF production via activating VEGFR2-Akt-mTORC2 signaling. *Oncotarget* 8, 979–987.

Liu, Y., Shigley, J., and Hurwit, K. (1999). Iridescent color of a shell of the mollusk *Pinctada margaritifera* caused by diffraction. *Opt. Express* 4, 177–182. doi: 10.1364/OE.4.000177

Lukens, L. N., and Zhan, S. (2007). The plant genome's methylation status and response to stress: implications for plant improvement. *Curr. Opin. Plant Biol.* 10, 317–322. doi: 10.1016/j.pbi.2007.04.012

Marie, B., Joubert, C., Tayalé, A., and Zanella-cléon, I. (2013). Different secretory repertoires control the biomineralization processes of prism and nacre deposition of the pearl oyster shell. *Proc. Natl. Acad. Sci. U.S.A.* 109, 20986–20991. doi: 10.1073/pnas.1210552109

Moreau, C., Ambrose, M. J., Turner, L., Hill, L., Noel Ellis, T. H., and Hofer, J. M. I. (2012). The b gene of pea encodes a defective flavonoid 3',5'-hydroxylase, and confers pink flower color. *Plant Physiol.* 159, 759–768. doi: 10.1104/pp.112.197517

Ng, A., Uribe, R. A., Yieh, L., Nuckels, R., and Gross, J. M. (2009). Zebrafish mutations in gart and paics identify crucial roles for de novo purine synthesis in vertebrate pigmentation and ocular development. *Development* 136, 2601–2611. doi: 10.1242/dev.038315

Ng, B. G., and Freeze, H. H. (2014). Human genetic disorders involving glycosylphosphatidylinositol (GPI) anchors and glycosphingolipids (GSL). *J. Inherit. Metab. Dis.* 38, 171–178. doi: 10.1007/s10545-014-9752-1

Nguyen, V. H., and Lavenier, D. (2009). PLAST: parallel local alignment search tool for database comparison. *BMC Bioinformatics* 10:329. doi: 10.1186/1471-2105-10-329

Nicoglou, A., and Merlin, F. (2017). Epigenetics: a way to bridge the gap between biological fields. *Stud. Hist. Philos. Sci. Part C Stud. Hist. Philos. Biol. Biomed. Sci.* 66, 73–82. doi: 10.1016/j.shpsc.2017.10.002

Oliveira-Garcia, E., and Deising, H. B. (2016). The glycosylphosphatidylinositol anchor biosynthesis genes GPI12, GAA1, and GPI8 are essential for cell-wall integrity and pathogenicity of the maize anthracnose fungus *Colletotrichum graminicola*. *Mol. Plant Microbe Interact.* 29, 889–901. doi: 10.1094/MPMI-09-16-0175-R

Olson, C. E., and Roberts, S. B. (2014). Genome-wide profiling of DNA methylation and gene expression in *Crassostrea gigas* male gametes. *Front. Physiol.* 5:224. doi: 10.3389/fphys.2014.00224

Quinlan, A. R., and Hall, I. M. (2010). BEDTools: a flexible suite of utilities for comparing genomic features. *Bioinformatics* 26, 841–842. doi: 10.1093/bioinformatics/btq033

Ramírez, F., Dündar, F., Diehl, S., Grüning, B. A., and Manke, T. (2014). DeepTools: a flexible platform for exploring deep-sequencing data. *Nucleic Acids Res.* 42, W187–W191. doi: 10.1093/nar/gku365

Rao, K. R., and Riehm, J. P. (1993). Pigment-dispersing hormones. *Ann. N. Y. Acad. Sci.* 680, 78–88.

Reisser, C. M. O., Gendre, R., Le, Chupeau, C., Lo-Yat, A., Planes, S., et al. (2020). Population connectivity and genetic assessment of exploited and natural populations of pearl oysters within a French polynesian atoll lagoon. *Genes (Basel).* 11, 1–16. doi: 10.3390/genes11040426

Richards, E. J. (2006). Inherited epigenetic variation—revisiting soft inheritance. *Nat. Rev. Genet.* 7, 395–402. doi: 10.1038/nrg1834

Rocha, G. D. G., Oliveira, R. R., Kaplan, M. A. C., and Gattass, C. R. (2014). 3β-Acetyl tormentic acid reverts MRP1/ABCC1 mediated cancer resistance through modulation of intracellular levels of GSH and inhibition of GST activity. *Eur. J. Pharmacol.* 741, 140–149. doi: 10.1016/j.ejphar.2014.07.054

Rondon, R., Grunau, C., Fallet, M., Charlemagne, N., Sussarellu, R., Chaparro, C., et al. (2017). Effects of a parental exposure to diuron on Pacific oyster spat methylome. *Environ. Epigenetics* 3, 1–13. doi: 10.1093/eep/dvx004

Rousseau, M., and Rollion-Bard, C. (2012). Influence of the depth on the shape and thickness of nacre tablets of *Pinctada margaritifera* pearl oyster, and on oxygen isotopic composition. *Minerals* 2, 55–64. doi: 10.3390/min2010055

Royston, P. (1995). Remark AS R94: a remark on algorithm AS 181: the W-test for normality. *J. R. Stat. Soc. Ser. C Appl. Stat.* 44, 547–551. doi: 10.2307/2986146

Russo, V. E., Martienssen, R. A., and Riggs, A. D. (1996). *Epigenetic Mechanisms of Gene Regulation*. Cold Spring Harbor, NY: Cold Spring Harbor Laboratory Press.

Sarda, S., Zeng, J., Hunt, B. G., and Yi, S. V. (2012). The evolution of invertebrate gene body methylation. *Mol. Biol. Evol.* 29, 1907–1916. doi: 10.1093/molbev/mss062

Sharp, J. R., Insalaco, S. J., and Johnson, L. F. (1980). "Melanosis" of the duodenum associated with a gastric ulcer and folic acid deficiency. *Gastroenterology* 78, 366–369. doi: 10.1016/0016-5085(80)90590-9

Shin, D. H., Cho, M., Choi, M. G., Das, P. K., Lee, S. K., Choi, S. B., et al. (2015). Identification of genes that may regulate the expression of the transcription factor production of anthocyanin pigment 1 (PAP1)/MYB75 involved in *Arabidopsis* anthocyanin biosynthesis. *Plant Cell Rep.* 34, 805–815. doi: 10.1007/s00299-015-1743-7

Sokolov, E. P. (2000). An improved method for DNA isolation from mucopolysaccharide-rich molluscan tissues. *J. Molluscan Stud.* 66, 573–575. doi: 10.1093/mollus/66.4.573

Sonthalia, S., Daulatabad, D., and Sarkar, R. (2016). Glutathione as a skin whitening agent: facts, myths, evidence and controversies. *Indian J. Dermatol.* 82, 262. doi: 10.4103/0378-6323.179088

Southgate, P., and Lucas, J. (2011). *The Pearl Oyster*. Amsterdam: Elsevier.

Stenger, P.-L. (2017). *Package ImaginR*. Available online at: https://cran.r-project.org/web/packages/ImaginR/ImaginR.pdf (accessed May 29, 2017).

Stenger, P.-L., Ky, C.-L., Reisser, C., Duboisset, J., and Dicko, H. (in press). Molecular pathways and pigments behind the colors of the pearl oyster *Pinctada margaritifera* var. *cumingii* (Linnaeus 1758). *Genes*.

Stenger, P.-L., Vidal-Dupiol, J., Reisser, C., Planes, S., and Ky, C. (2019). Colour plasticity in the shells and pearls of animal graft model *Pinctada margaritifera* through colour quantification with the HSV system. *Sci. Rep.* 75:20. doi: 10.1038/s41598-019-43777-4

Sutherland, J. E., and Costa, M. A. X. (2003). Epigenetics and the environment. *Ann. N. Y. Acad. Sci.* 983, 151–160.

Takakura, D., Norizuki, M., Ishikawa, F., and Samata, T. (2008). Isolation and characterization of the N-linked oligosaccharides in nacrein from

*Pinctada fucata*. *Mar. Biotechnol.* 10, 290–296. doi: 10.1007/s10126-007-9063-8

Tanaka, Y., Suetsugu, Y., Yamamoto, K., Noda, H., and Shinoda, T. (2014). Transcriptome analysis of neuropeptides and G-protein coupled receptors (GPCRs) for neuropeptides in the brown planthopper *Nilaparvata lugens*. *Peptides* 53, 125–133. doi: 10.1016/j.peptides.2013.07.027

Trapnell, C., Roberts, A., Goff, L., Pertea, G., Kim, D., Kelley, D. R., et al. (2012). Differential gene and transcript expression analysis of RNA-seq experiments with TopHat and Cufflinks. *Nat. Protoc.* 7, 562–578. doi: 10.1038/nprot.2012.016

Vajro, P., Thaler, M. M., and Blanckaert, N. (1995). Bile pigment composition and bilirubin esterification in the developing chick. *Pediatr. Res.* 38, 349–355. doi: 10.1203/00006450-199509000-00013

Wang, N., Lee, Y. H., and Lee, J. (2008). Recombinant perlucin nucleates the growth of calcium carbonate crystals: molecular cloning and characterization of perlucin from disk abalone, *Haliotis discus discus*. *Comp. Biochem. Physiol. B Biochem. Mol. Biol.* 149, 354–361. doi: 10.1016/j.cbpb.2007.10.007

Wang, X., Li, Q., Lian, J., Li, L., Jin, L., Cai, H., et al. (2014). Genome-wide and single-base resolution DNA methylomes of the Pacific oyster *Crassostrea gigas* provide insight into the evolution of invertebrate CpG methylation. *BMC Genomics* 15:1119. doi: 10.1186/1471-2164-15-1119

Weiss, I. M., Kaufmann, S., Mann, K., and Fritz, M. (2000). Purification and characterization of perlucin and perlustrin, two new proteins from the shell of the mollusc *Haliotis laevigata*. *Biochem. Biophys. Res. Commun.* 267, 17–21. doi: 10.1006/bbrc.1999.1907

Wickham, H., and Chang, W. (2019). *Package 'ggplot2.'*.

Xiang, H., Zhu, J., Chen, Q., Dai, F., Li, X., Li, M., et al. (2010). Single base-resolution methylome of the silkworm reveals a sparse epigenomic map. *Nat. Biotechnol.* 28, 516–520. doi: 10.1038/nbt.1626

Zemach, A., McDaniel, I. E., Silva, P., and Zilberman, D. (2010). Genome-wide evolutionary analysis of eukaryotic DNA methylation. *Science* 328, 916–919. doi: 10.1126/science.1186366

Zhai, S., Xia, X., and He, Z. (2016). Carotenoids in staple cereals: metabolism, regulation, and genetic manipulation. *Front. Plant Sci.* 7:1197. doi: 10.3389/fpls.2016.01197

Zimova, M., Hackländer, K., Good, J. M., Melo-Ferreira, J., Alves, P. C., and Mills, L. S. (2018). Function and underlying mechanisms of seasonal colour moulting in mammals and birds: what keeps them changing in a warming world? *Biol. Rev.* 93, 1478–1498. doi: 10.1111/brv.12405

**Conflict of Interest:** The authors declare that the research was conducted in the absence of any commercial or financial relationships that could be construed as a potential conflict of interest.

*Copyright © 2021 Stenger, Ky, Reisser, Cosseau, Grunau, Mege, Planes and Vidal-Dupiol. This is an open-access article distributed under the terms of the Creative Commons Attribution License (CC BY). The use, distribution or reproduction in other forums is permitted, provided the original author(s) and the copyright owner(s) are credited and that the original publication in this journal is cited, in accordance with accepted academic practice. No use, distribution or reproduction is permitted which does not comply with these terms.*

frontiers in Genetics

ORIGINAL RESEARCH
published: 28 May 2021
doi: 10.3389/fgene.2021.633132

# Methylome Patterns of Cattle Adaptation to Heat Stress

*Marcello Del Corvo[1,2]*, Barbara Lazzari[2], Emanuele Capra[2], Ludmilla Zavarez[3,4], Marco Milanesi[3,4], Yuri Tani Utsunomiya[3,4], Adam Taiti Harth Utsunomiya[3,4], Alessandra Stella[2], Guilherme de Paula Nogueira[3], Josè Fernando Garcia[3,4] and Paolo Ajmone-Marsan[1]*

[1] Department of Animal Science Food and Nutrition – DIANA, Nutrigenomics and Proteomics Research Centre – PRONUTRIGEN, and Biodiversity and Ancient DNA Research Centre, Università Cattolica del Sacro Cuore, Piacenza, Italy, [2] Istituto di Biologia e Biotecnologia Agraria, Consiglio Nazionale delle Ricerche IBBA CNR, Milan, Italy, [3] School of Veterinary Medicine, Araçatuba, Department of Production and Animal Health, São Paulo State University (unesp), Araçatuba, Brazil, [4] International Atomic Energy Agency, Collaborating Centre on Animal Genomics and Bioinformatics, Araçatuba, Brazil

Heat stress has a detrimental impact on cattle health, welfare and productivity by affecting gene expression, metabolism and immune response, but little is known on the epigenetic mechanisms mediating the effect of temperature at the cellular and organism level. In this study, we investigated genome-wide DNA methylation in blood samples collected from 5 bulls of the heat stress resilient Nellore breed and 5 bulls of the Angus that are more heat stress susceptible, exposed to the sun and high temperature-high humidity during the summer season of the Brazilian South-East region. The methylomes were analyzed during and after the exposure by Reduced Representation Bisulfite Sequencing, which provided genome-wide single-base resolution methylation profiles. Significant methylation changes between stressful and recovery periods were observed in 819 genes. Among these, 351 were only seen in Angus, 366 were specific to Nellore, and 102 showed significant changes in methylation patterns in both breeds. KEGG and Gene Ontology (GO) enrichment analyses showed that responses were breed-specific. Interestingly, in Nellore significant genes and pathways were mainly involved in stress responses and cellular defense and were under methylated during heat stress, whereas in Angus the response was less focused. These preliminary results suggest that heat challenge induces changes in methylation patterns in specific loci, which should be further scrutinized to assess their role in heat tolerance.

**Keywords: heat stress, epigenetics, DNA methylation, animals welfare, cattle, red blood cell**

OPEN ACCESS

***Edited by:***
*Helene Kiefer,*
*INRAE Centre Jouy-en-Josas, France*

***Reviewed by:***
*Geoffrey E. Dahl,*
*University of Florida, United States*
*Pasqualino Loi,*
*University of Teramo, Italy*

****Correspondence:***
*Marcello Del Corvo*
*marcello.delcorvo@ibba.cnr.it*

***Specialty section:***
*This article was submitted to Livestock Genomics, a section of the journal Frontiers in Genetics*

***Received:*** *24 November 2020*
***Accepted:*** *04 May 2021*
***Published:*** *28 May 2021*

***Citation:***
*Del Corvo M, Lazzari B, Capra E, Zavarez L, Milanesi M, Utsunomiya YT, Utsunomiya ATH, Stella A, Nogueira GP, Garcia JF and Ajmone-Marsan P (2021) Methylome Patterns of Cattle Adaptation to Heat Stress. Front. Genet. 12:633132. doi: 10.3389/fgene.2021.633132*

## INTRODUCTION

Rapid and unpredictable climate change and extreme climatic events (floods, drought, extreme temperatures) are increasing in frequency, which have an impact on agricultural productivity and affect food security. These changes are not only limited to tropical and subtropical regions but also affect more temperate regions (Rajaud and Noblet-Ducoudré, 2017). In the most vulnerable areas, management and breeding of livestock should address heat stress and decreasing water availability, while maintaining fitness and productivity in order to remain viable (Rojas-Downing et al., 2017). To satisfy the demand for animal products, which is increasing at a faster rate than human population growth, it is necessary for the livestock sector to respond to rapid changes in the climate.

Heat stressed animals are not able to adequately dissipate the excess of endogenous and exogenous heat to maintain the body thermal balance (Bernabucci et al., 2014). Heat stress is a primary stressor for high-producing dairy cows which have a high metabolic rate with associated endothermy, which results in heat-induced depression of milk production and growth (Cowley et al., 2015). Therefore, heat stress results in economic losses due to reduced production and reproduction performance (Aguilar et al., 2010; Nardone et al., 2010; Mehla et al., 2014; Biffani et al., 2016; Macciotta et al., 2017). Physiological changes are observed affecting the ability of the animal to cope with heat stress. For example, rectal temperature and respiration rate increase (Dikmen et al., 2015; Perano et al., 2015). Some of these reponses have a genetic component, moderate heritability and have been associated with genomic variants, e.g., several candidate genes have been identified for rectal temperature (Dikmen et al., 2013, 2015). Traditional phenotype-based selection for adaptation and fitness, while maintaining productivity, is difficult and slow as these traits are difficult to measure. For this reason, genomic information could accelerate the genetic progress for adaptation traits. SNP markers associated with heat tolerance have been detected in dairy cattle (Hayes et al., 2009; Dikmen et al., 2012, 2013), although few causative genes have been identified (reviewed in Collier et al., 2008). One of these, the prolactin receptor gene (*PRLR*), carries mutations having a major effect on heat tolerance (Littlejohn et al., 2014; Porto-Neto et al., 2018). This variant causes the SLICK phenotype which is easily detected as it confers animals a short and sleek coat (Olson et al., 2003; Dikmen et al., 2008). Holstein cattle into which a SLICK haplotype was introduced had superior thermoregulatory ability compared with wild-type Holsteins (Dikmen et al., 2014).

Little is known about the biology of adaptation, and even less about mechanisms that mediate changes in gene expression and metabolism in animals subjected to environmental stress. Technologies developed to sequence and characterize the human genome have paved the way for the routine sequencing of the genomes of agriculturally important species. In addition to the genome sequence, epigenetic features control gene expression and have attracted much attention in the last few years. At least four molecular systems are involved in the control of gene expression, including DNA methylation (Bernstein et al., 2007), non-coding RNAs (Mitchell et al., 2009), histone post-translational modifications (Strahl and Allis, 2000), and chromatin remodeling (Cosma et al., 2010). DNA methylation was the first identified and is currently the better-studied epigenetic regulatory mechanism of gene expression. In mammalian cells, DNA methylation mostly occurs at the cytosine of a CpG dinucleotide, and CpG islands, which are enriched for CpG dinucleotides, are frequently located in promoter regions at the 5′ of coding sequences.

There is still limited knowledge on the relationship between epigenetic patterns and phenotypic variation in livestock. Nevertheless, epigenetic effects on some trait have been described, e.g., growth is affected by epigenetic imprinting of IGF2 in pig (Van Laere et al., 2003), and epigenetic regulation of callipyge affects development in sheep (Georges et al., 2003; Vuocolo et al., 2007). Recent studies have characterized pig and chicken methylomes (Li et al., 2012; Nätt et al., 2012). An atlas of the porcine methylome identified that differentially methylated regions contain ∼80% of the known or candidate human obesity-related genes, 72% of which mapping in QTL regions that affect fatness and pork quality (Li et al., 2012). Nätt et al. (2012) suggested that the heritability of methylation in the chicken genome might play a role in adaptation and selection since they observed an over-representation of differentially methylated genes in selective sweep regions associated with domestication. This could mean that novel methylation patterns have been acquired by domestic animals during their selection history. In dairy cows, recent work has shed light on the role of epigenetics in the regulation of milk synthesis and mammary development (Singh et al., 2010). In the lactating cow, remethylation of the typically hypo-methylated casein gene promoter drastically reduces casein mRNA expression and milk protein synthesis during acute udder infection.

The association between DNA methylation patterns and heat stress has been suggested. For example exposure of male guinea pigs to chronic heat stress has been shown to alter DNA methylation patterns in the liver of both the F0 and F1 generations (Weyrich et al., 2016).

In the current paper, epigenomic responses to heat stress were investigated in indicine (*Bos indicus*) and taurine (*Bos taurus*) cattle. We hypothesize that, in addition to morphological traits determined by genetics (coat color, body size and conformation, large ears, loose skin, sweat gland size), the adaptation to heat and the better ability to cope with deleterious effects of a high temperature of the indicine Nellore compared to the taurine Angus breed is also associated with changes in DNA methylation patterns of specific regulatory genes and metabolic pathways. In the study reported here, cattle of these two breeds were exposed to the sun during the high temperature and high humidity season of the Brazilian South-East region and the physiological and epigenetic responses assessed.

# MATERIALS AND METHODS

## Animals Treatment and Experimental Design

A total of 25 Nellore (indicine heat-tolerant breed) and 25 Angus (taurine heat-susceptible breed) bullocks were included in the investigation. Animals were all healthy young males of about 15 months of age at the time of the investigation. We selected half-sibs animals within each breed to minimize genetic variation. Angus bullocks were purchased at 7 months of age in Uruguaiana (Rio Grande do Sul state, Brazil) and arrived at UNESP Aracatuba (Sao Paulo state, Brazil) experimental station (located at −21.186244 latitude and −50.439053 longitude) on June 13, 2015. Seven-month old Nellore bullocks were purchased in Dourados (Mato Grosso do Sul state, Brazil), kept at Agua Branca farm in Birigui (Sao Paulo, Brazil) until 10 months of age and moved to UNESP on September 2, 2015. Animals were kept at the experimental station of the Veterinary Faculty, Universidade Estadual Paulista – UNESP- Araçatuba Campus. A full description of the diet fed during the study is given

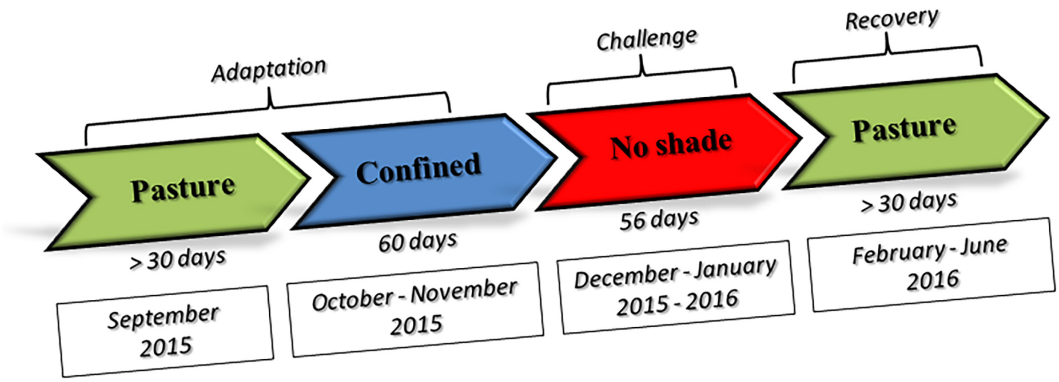



**FIGURE 1 |** Schematic representation of the experimental design.

in **Supplementary File 1**, while a schematic representation of experimental design is given in the **Figure 1**.

***Adaptation period***. On October 3, 2015, the steers were randomly assigned to 2 groups (1 Nellore and 1 Angus groups) of 12 or 13 animals and kept in two 200 square meter paddocks of which 100 square meters was covered by a shadowing net (80% sunblock) with regular access to pasture until December 3 (60 days). This period will be further referred to as pre-challenge adaptation period (PRE).

***Challenge.*** The experiment started on December 4, 2015, by removing the shadowing net from paddocks. Animal groups were therefore kept without shade until February 3, 2016 (56 days). This period is subsequently referred to as the experimental challenge period (EXP).

***Recovery period.*** On February 4th shadowing nets were replaced such that all animals were kept with shade available and were allowed access to pasture until slaughter at the end of June 2016. This period will be further referred to as post challenge recovery period (POST).

***Sampling.*** Nellore adaptation period terminated in November 2015, when the season was already hot and humid and animals were under moderate stres. Sampling was therefore planned at the beginning of February 2016, at peak heat stress period, and in the middle of June 2016, during the cool season, after full recovery from heat stress.

## Environmental Data Collection

Environmental data were collected hourly from June 1, 2015 to October 10, 2016 from CETESB meteorological station located in the UNESP campus, nearby the experimental site. Experimental variables collected were Temperature (T, in centigrades) and Humidity (H, in percentage). Missing data were imputed using the median among −10/ + 10 day data at the same time.

## DNA Isolation, Library Preparation and Sequencing

Blood (10 ml) was collected from the same 5 randomly selected Nellore (heat stress resilient) and 5 randomly selected Angus (heat stress susceptible) belonging to sun-exposed group, in two periods: in February 2016 (stressful/challenge period) and June 2016 (recovery period). We used QIAamp DNA Blood Midi Kit (Qiagen) procedures to extract DNA from whole blood. One μg input was used in the MSP1 digest by overnight incubation at 37°C, following manufacturer instruction. Libraries were prepared using the TruSeq® DNA PCR-Free Library Preparation Kit (Illumina) including a step of bisulfite treatment. Subsequently, ligated products corresponding to DNA fragments 150–400-bp long were converted with EpiTectBisulfite Kits (Qiagen) and finally, PCR amplified with KAPA HiFi Uracil + (KapaBiosystems) to obtain RRBS libraries. DNA with a known methylation level was used as a spike control, and all conversion rates were >99%, ranging from 99.11 to 99.53% (**Supplementary Table 1**). Twenty Reduced Representation Bisulfite Sequencing (RRBS) libraries were used for cluster generation and subsequent sequencing on Illumina HiSeq 2500 PE 2 × 50 bp (NXT-Dx Ghent, Belgium).[1]

## Environmental Indexes

From environmental data we obtained THI (*Temperature Humidity Index*), which considers temperature (T) and humidity (H) in a single index: (1.8 * T + 32) − [(0.55 − 0.0055 * H) * (1.8 * T - 26)] (Thom, 1959). Values above 75 were considered as moderate stress, above 85 as severe stress and over 90 as extreme stress (McDowell et al., 1976).

## Data Analysis

Preliminary quality control of raw reads was carried out with FastQC v0.11.9.[2] The FASTQ sequence reads were generated using the Illumina Casava pipeline 1.8.2. The quality and adapter trimming of Illumina raw sequenze was performed with Trim Galore v0.6.1[3] using a two-step approach, which allowed us to remove two additional bases containing a cytosine, which were artificially introduced in the end-repair step during the library preparation. Bismark software (version 0.22.3) (Krueger and Andrews, 2011) was used to align each bisulfite-treated read to the bovine reference genome (ARS-UCD1.2) with option-N

[1]http://www.nxt-dx.com/

[2]http://www.bioinformatics.babraham.ac.uk/projects/fastqc/

[3]http://www.bioinformatics.babraham.ac.uk/projects/trim_galore/

1 (maximum number of mismatches allowed). The reference genome was first transformed into a bisulfite-converted version (C-to-T and G-to-A conversions) and then indexed using bowtie2 software (Langmead and Salzberg, 2012). Sequence reads were also transformed into fully bisulfite-converted versions (C-to-T and G-to-A conversions) before they were aligned to similarly converted versions of the genome in a directional manner. Sequence reads that produced the best unique alignment from the two alignment processes (original top and bottom strand) were then compared to the normal genomic sequence, and the methylation state of all cytosine positions in the reads was inferred using the *Bismark_methylation_extractor* function. Read duplicates were marked and removed using Picard Tools v2.23.[4]

## Identification of Differentially Methylated Regions (DMRs) and Genes (DMGs)

DMRs were identified within the statistical environment R using the library methylKit (Akalin et al., 2012), which applies a sliding-window approach with a window of 1,000 bp and a step size of 500 bp. We first filtered out bases with less than 10 reads or more than the 99.9th percentile of coverage distribution. This step was done to ensure a good quality of the data and great confidence in the methylation percentage. Coverage values were then normalized by default and bases were merged in order to retain the ones that were covered in all samples. A logistic regression was then implemented to obtain *p* values. Specifically, in any given region methylKit models the methylation proportion $P_i$, for sample $i = 1,\ldots,n$ (where n is the number of animals) by the following logistic regression model:

$$\log(P_i/(1 - P_i)) = \beta_0 + \beta_1 * T_i$$

where $T_i$ denotes the treatment indicator for sample i, $T_i = 1$ if sample i is in the treatment group (stress period) and $T_i = 0$ if sample i is in control group (recovery period). The parameter $\beta_0$ denotes the log odds of the control group and $\beta_1$ the log oddsratio between the treatment and control group. Therefore, independent tests for all the regions of interest are run against the null hypothesis $H_0$: $\beta_1 = 0$. The null hypothesis is rejected when the logodds (and hence the methylation proportions) are different between the treatment and the control group and the region therefore classified as a DMR. *P* values were then adjusted to *q* values using the Sliding Linear Model (SLIM) method (Wang et al., 2011). We excluded covariates and over dispersion correction from the model since they showed not to provide significant changes to the results. DMRs were considered statistically significant if the *q* value was lower than 0.05, read coverage greater than 10 in all samples and methylation difference between groups at least 15%. When a DMR and a specific gene region overlapped, the corresponding gene was selected as the DMR-related gene, namely a differentially methylated gene (DMG). Gene features within DMGs were annotated by matching information available in the General Feature Format (GFF) file downloaded from the Ensembl database, release 101.[5] The promoter region was defined as an area 2-kb upstream of the transcription start sites.

## Gene Ontology and KEGG Enrichment Analysis of DMR-Related Genes

Gene Ontology (GO) and KEGG pathway enrichment analysis of DMGs were performed by *clusterProfiler*, an ontology-based R package able to automate the process of biological term classification and enrichment analysis of gene clusters and to provide a visualization module for displaying analysis results (Yu et al., 2012). GO terms and KEGG with *p* values of less than 0.01 and *q* values of less than 0.1 were considered significantly enriched by DMR-related genes.

# RESULTS

## Heat Stress Based on Environmental Parameters

The environmental conditions were analyzed and Temperature Humidity indices (THI), were calculated to evaluate the severity of heat challenge before during and after the experimental period (**Figure 2**).

## Global Mapping of DNA Methylation

A mean of 60 million raw reads were generated for Nellore samples and 67 million for Angus samples during challenge period and 89 million and 80 million, respectively during the recovery period. After removing low-quality reads, 57 and 64 million of clean reads for the experimental period and 85 and 76 million for the recovery period for Nellore and Angus respectively remained. In the two periods the average value of uniquely mapped reads covering the cattle genome corresponds to 43.18 and 43.82% in Nellore and 44.5 and 46.1% in Angus (**Table 1** and **Supplementary Table 1**).

## DNA Methylation Patterns

We observed an average genome-wide level of 66.26% CG, 0.44% CHG, and 0.32% CHH methylation (H = A, T or C) in Nellore during challenge and 66.8% CG, 0.5% CHG, and 0.34% CHH methylation during recovery. Values in Angus were 67.7% CG, 0.3% CHG, and 0.2% CHH methylation in the experimental period and 67.14% CG, 0.3% CHG, and 0.22% CHH methylation in the post challenge period (**Table 2**).

Over 66% of the CpG sites were methylated in both breeds during challenge and recovery periods. Heat stress effects did not significantly change DNA methylation of either the CpG and non-CpG sites in both breeds at a genome-wide level (**Table 2**).

## DNA Methylation Level in Different Genome Features

We investigated the DNA methylation level in five different genome features including promoters, 5′UTRs, exons, introns

[4]http://broadinstitute.github.io/picard

[5]http://ftp.ensembl.org/pub/release-101/gff3/bos_taurus/Bos_taurus.ARS-UCD1.2.101.gff3.gz

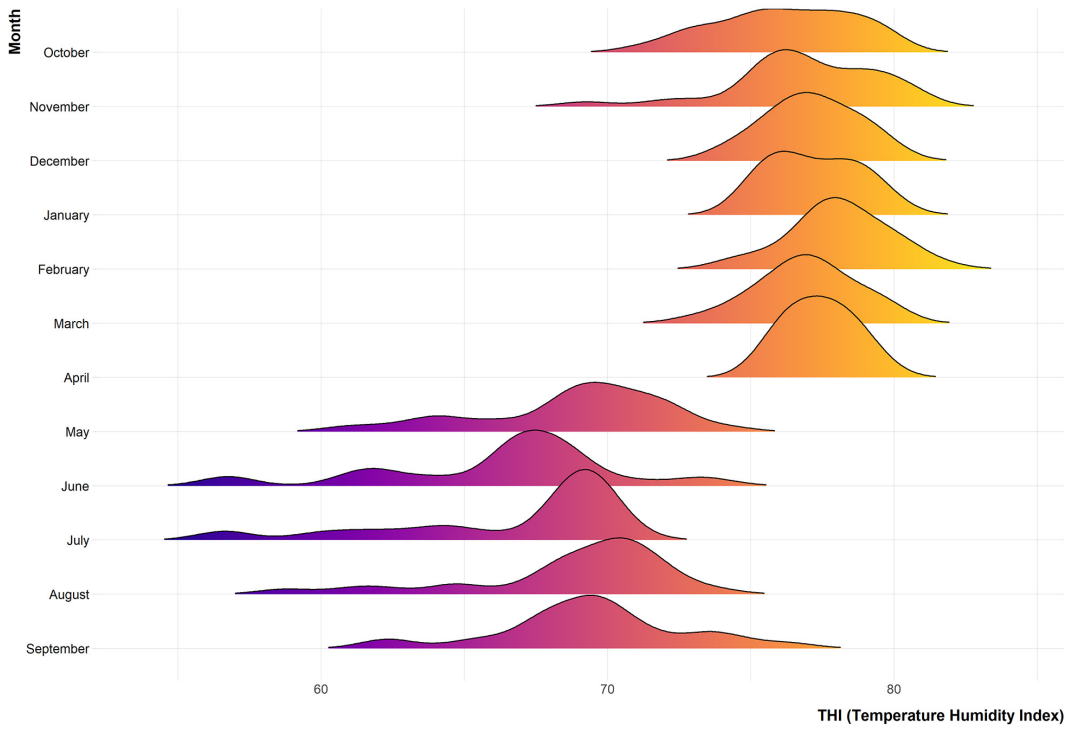



**FIGURE 2 |** Ridgeline plot showing distribution of daily average THI recorded at CETESB meteorological station located in the UNESP campus from October 2015 to September 2016.

**TABLE 1 |** Data generated by Reduced Representation Bisulfite Sequencing (RRBS).

| | Nellore | | Angus | |
|---|---|---|---|---|
| | **Challenge** | **Recovery** | **Challenge** | **Recovery** |
| Raw reads | 60,091,512 | 89,179,323 | 67,901,537 | 80,179,472 |
| Clean reads | 57,699,800 | 85,587,160 | 64,763,022 | 76,551,213 |
| Total mapped reads | 25,980,704 | 38,923,431 | 30,123,254 | 36,899,326 |
| Average mapping rate (%) | 43.18% | 43.82% | 44.5% | 46.1% |

**TABLE 2 |** Genome-wide percentage of methylated CG, CHG, and CHH in Nellore and Angus breed during challenge and recovery period.

| | Nellore | | Angus | |
|---|---|---|---|---|
| | **Challenge** | **Recovery** | **Challenge** | **Recovery** |
| mCG percent (%) | 66.26% | 66.8% | 67.7% | 67.14% |
| mCHG percent (%) | 0.44% | 0.5% | 0.3% | 0.3% |
| mCHH percent (%) | 0.32% | 0.34% | 0.2% | 0.22% |

and 3′UTRs, using a sliding window approach. In both breeds methylation level of CG dinucleotides showed a similar pattern during challenge and recovery periods. Promoter regions exhibited a higher variability compared with other features, with the maximum distance between the first and the third quartile. Exon, intron and 3′UTR regions showed the highest methylation level, while the 5′UTR had the lowest average level of methylation (**Supplementary Figure 1**).

## Differentially Methylated Regions (DMRs) and Related Genes (DMGs)

Principal component analysis (PCA) based on genome-wide DNA methylation clearly distinguished Angus from Nellore but not the two different periods (stress and recovery) (**Supplementary Figure 2**). Differential methylation analysis identified a total of 4662 DMRs. There were 2695 DMRs between Angus and Nellore that did not change between stress and recovery periods and therefore are related to breed differences rather than a response to heat. It is interesting to note that 62% of these were hyper-methylated and 38% hypo-methylated in Angus compared with Nellore, suggesting an overall higher level of metylation in Angus vs Nellore. A total of 1967 windows were differentially methylated in the stress period compared with the recovery period (**Supplementary Table 2**), 857 in Angus, 896 in Nellore of these only 214 were seen in both breeds, indicating that epigenetic signatures related to heat stress response and recovery are mostly breed specific (**Figure 3**).

Heat map analysis indicates that in Angus, a large proportion of methylated regions were maintained in both periods possibly indicating difficulty in recovering after a severe stress. Conversely, Nellore seems to respond to stress with

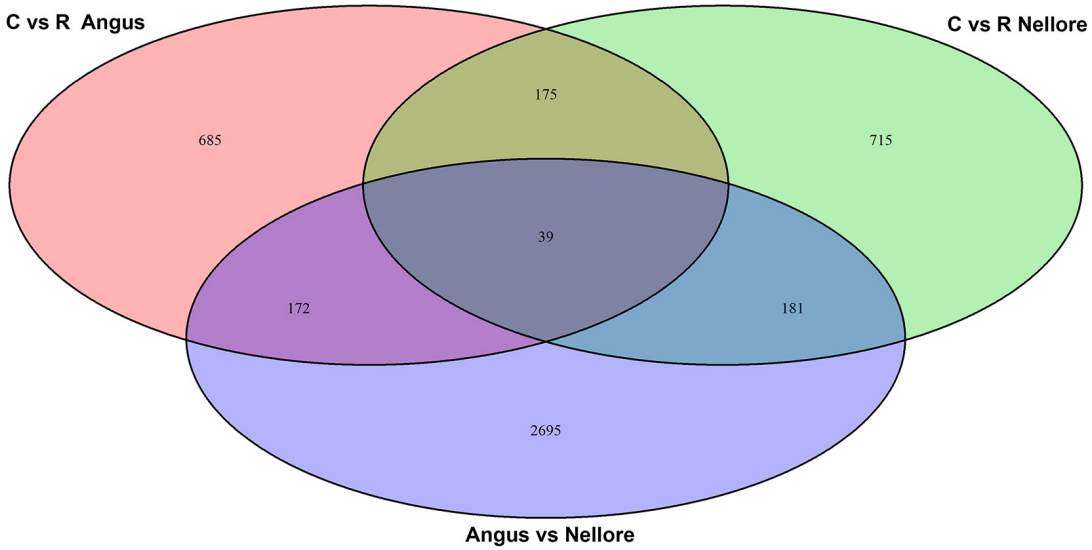



**FIGURE 3 |** Venn diagram of differentially methylated windows in Angus and Nellore (C, Challenge, R, Recovery).

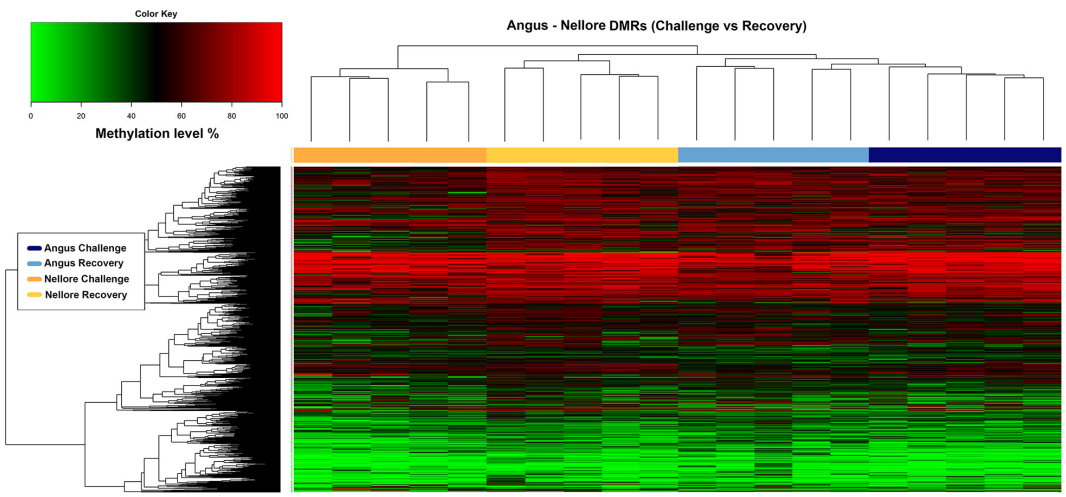



**FIGURE 4 |** Heatmap of methylation level (y axis) in Angus and Nellore populations (x axis) within 1967 DMRs. The blue and azure bars correspond to methylation level of Angus samples during challenge and recovery season and the orange and yellow bars correspond to methylation level of Nellore samples during challenge and recovery season respectively.

a demethylation of several key genomic regions during challenge (**Figure 4**).

The blue and azure bars correspond to methylation level of Angus samples during challenge and recovery season and the orange and yellow bars correspond to methylation level of Nellore samples during challenge and recovery season respectively.

We annotated all 1967 DMRs using the genomic location and the matching annotation information on the genome structure of the cattle genome. The 857 DMRs containing windows identified in Angus overlapped with 351 annotated genes (192 hyper-methylated and 159 hypo-methylated during stress), while in Nellore the 896 windows overlapped with 366 genes (85 hyper-methylated and 281 hypo-methylated during stress). Among these genes 39 were common between Angus and Nellore even though they mapped to different genomic regions. Furthermore the 214 DMRs that were shared between breeds overlapped with 102 genes (among these, 61% were hyper or hypo-methylated in both breeds, while 39% show an opposite trend). In both breeds more than 50% of the differentially methylated regions were located in introns, 31% in the exons, withless than 5% in each of 3′,5′ UTR and promoter regions.

## GO and KEGG Analysis of DMGs

Pathway enriched analysis was carried out to identify the metabolic and the immune system pathways affected and identify those that are relevant to a heat stress response. For each breed all DMGs detected were mapped to terms within the GO and

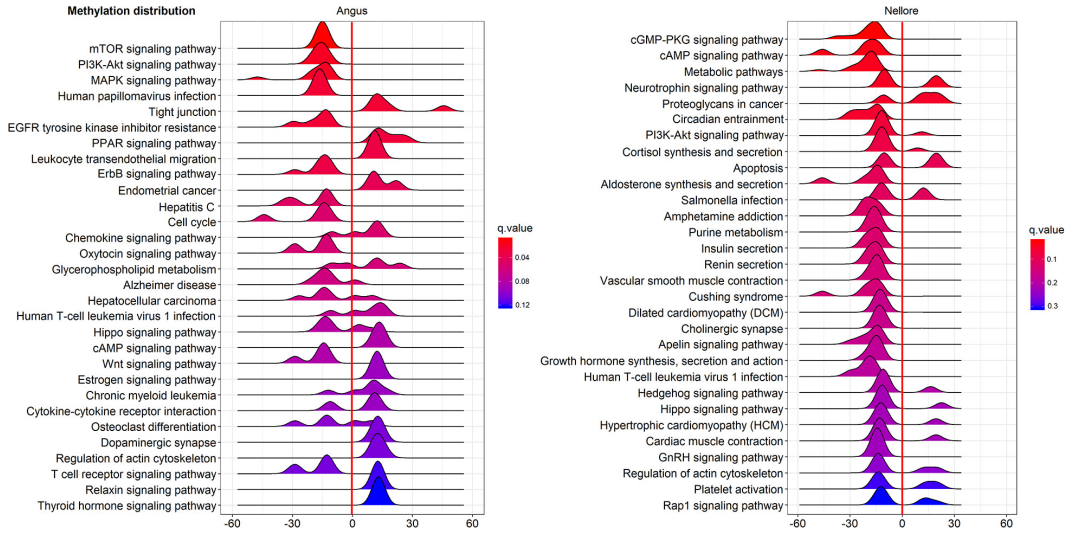



**FIGURE 5 |** KEGG analysis of DMGs in Angus (left side) and Nellore (right side) in challenge and recovery periods. Peak hight is proportial to the number of differentially methylated genes, color to *p* value. Negative values indicate hypo-methylation, positive values hyper-methylation during heat stress.

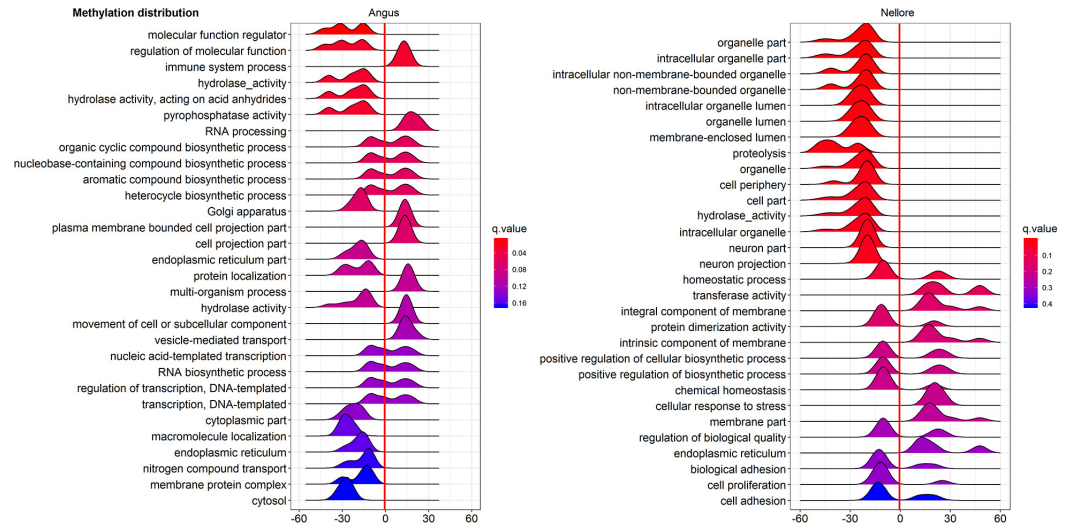



**FIGURE 6 |** Gene Ontology analysis of DMGs in Angus (left side) and Nellore (right side) in challenge and recovery periods. Peak hight is proportial to the number of differentially methylated genes, color to *p* value. Negative values indicate hypo-methylation, positive values hyper-methylation during heat stress.

the KEGG databases. Both breeds had a similar proportion of DMGs within GO pathways enriched: cellular process (Angus 184; 61.5%; Nellore 188; 62.7%); single-organism process (Angus 73; 24.4%; Nellore 68; 22.7%) and metabolic process (Angus 42; 14%; Nellore 44; 14.7%). KEGG analysis identified 77 pathways in Angus and 78 in Nellore. Among theme, 49 overlap between the two breeds, but a comparison between the top 30 pathways (**Figures 5**, **6**) showed only few cellular functions (a single one in GO enrichment analysis, phosphoric diester hydrolase activity) in common between breeds. It is also interesting to note that shared pathways are enriched only minimally by the same DMGs (32% in Angus and 30% in Nellore), and more than half of these presents opposite behavior, having higher methylation in the stress period and lower in the recovery period in one breed and the opposite in the other. This reflects again the specific response that we previously observed from the Venn diagram analysis.

## DISCUSSION

The tropical environment of the Brazilian Southeast region is characterized by high temperature and humidity and episodes of feed and water scarcity. Nellore cattle have greater resistance to such conditions, surviving, breeding and being productive in the tropics (Valente et al., 2015). In comparison Angus have difficulties adapting to extreme climatic conditions, failing to

thrive with tropical heat and humidity, and are susceptible to pathogen challenges. Animal homeostasis in different environments is maintained by modulating metabolic processes to counteract the deleterious effects of stressful conditions (Chovatiya and Medzhitov, 2014). Epigenetic signatures, such as DNA methylation, act as a mediator between changing environmental conditions and animal metabolic response to maintain homeostasis. The present work investigated: (i) changes in DNA methylation that occur in cattle under heat stress, compared with non-stressful conditions and; (ii) differences in methylation in response to heat stress observed in tolerant indicine Nellore versus non-tolerant taurine Angus cattle.

We analyzed genome-wide DNA methylation using the RRBS method. We extracted DNA from blood, as an easily accessible and highly informative indicator of animal response to environmental challenges. The main source of DNA was therefore obtained from white cells, even if we can't exclude a possible co-extraction of some circulating free DNA, that under stressful conditions may increase its usually low concentration in plasma (Cree et al., 2017; Henriksen et al., 2020). It has been shown that methylation levels at CpG sites in leukocytes are predictors of variability of CpG methylation or may at least partially be considered as proxies of epigenetic processes in other tissues (Ma et al., 2014; Braun et al., 2019; Del Corvo et al., 2020).

## Key Pathways Related to the Immune System and Metabolic Processes in Angus and Nellore

In the present study several KEGG gene-sets with differential methyation were identified both in Nellore and Angus breeds in response to heat stress. In Nellore we detected metabolic pathways, circadian entrainment, cGMP-PKG, cAMP and PI3K-Akt signaling pathways that were enriched in differentially methylated genes. Several of these pathways are related to the immune system and inflammatory response. Circadian entrainment pathway has emerged as an internal regulator with the potential to impact disease (Scheiermann et al., 2013). Furthermore, a previous study demonstrated that signaling pathways (cGMP-PKG, cAMP and PI3K-Akt) might form a network with genes related to immuno regulatory mechanisms (Zaccolo and Movsesian, 2007; Wehbi and Taskén, 2016).

In the current study we observed gene enrichment in KEGG metabolic pathways in blood that are known to be involved in heat stress response in other tissues (Rhoads et al., 2010). In particular, pathways for hormone synthesis and/or secretion (cortisol, aldosterone, insulin, renin, growth hormone, GnRH; **Figure 6**) were all enriched in hypo-methylated genes. Blood cells have been previosly shown to be indicative of methylation status of other tissues in human (Ma et al., 2014). This characteristic is to be further confirmed, however, it would be remarkable, as blood is an easily accessible tissue.

In Angus patterns of response were detected from pathway analysis, that would not have been detectable in a single gene analysis. Several KEGG pathways were enriched in DMGs during heat exposure, including signaling networks, such as MAPK, mTOR, ErbB, PI3k/AKT and pathways related to hepatitis C and other viral infections that can be stimulated in response to heat stress (Danaher et al., 1999). A study of rat skeletal muscle demonstrated that genes in mTOR and PI3k/AKT pathways are activated by a temperature increase (Yoshihara et al., 2013). The ErbB signaling pathway plays a role upstream of MAPK signaling, which affects lipid metabolism (Zhang et al., 2017). Heat stress affects the regulation of lipolysis and the rate-limiting enzymes of lipogenesis (Faylon et al., 2015). In addition, the MAPK pathway is a downstream target of ErbB receptors, which are mediators of cell proliferation, differentiation, apoptosis, and cell motility (Holbro and Hynes, 2004).

Furthermore phosphoric diester hydrolase activity, the only GO pathway shared by both breeds as shown by enrichment analysis, seems to be activated by differentially methylated genes in liver and mammary gland of bull calves in another study as a consequence of maternal conditions of heat stress (Skibiel et al., 2018).

## Key Differentially Methylated Genes Related to the Immune System and Inflammatory Response in Angus and Nellore

We identified several genes involved in the biological processes significant for the immune system and inflammatory response. Among them fatty acid elongase 5 (*ELOVL5)*, F2R like thrombin or trypsin receptor 3 (*F2RL3)*, fatty acid desaturase 1 (*FADS1)*, mitogen-activated protein kinase kinasekinase 1 (*MAP3K1)*, phosphodiesterase 5A (*PDE5A)*, netrin 1 (*NTN1)*, RAS p21 protein activator 3 (*RASA3)* and peroxiredoxin 1 (*PRDX)* were identified in Nellore. Genes linked to immune defense were in DMRs between stress and recovery periods also in Angus. These included autophagy related 16 like 2 (*ATG16L2)*, calcium voltage-gated channel subunit alpha1 C (*CACNA1C)*and growth arrest and DNA damage inducible alpha (*GADD45A)*. These genes are expressed in blood cells and have been shown to be differentially methylated also in the brain and are linked to nervous system functions.

In the present study, DMGs identified in Nellore were mainly hypo-methylated in the heat stress period, including in prometer regions, suggesting a pro-active response of this breed to the challenge, to maintain homeostasis.

For example, F2R like thrombin or trypsin receptor 3 (*F2RL3)* encodes the thrombin protease-activated receptor-4 *(PAR-4)*, which is expressed on the surface of various body tissues, including circulating leukocytes (Xu et al., 1998; Vergnolle et al., 2002). The activation of PAR-4 is involved in leukocyte recruitment, as well as in the regulation of vascular endothelial cell activity (Vergnolle et al., 2002; Kataoka et al., 2003; Leger et al., 2006; Gomides et al., 2012). These pathophysiological events are considered to be the early steps of the vascular inflammatory reaction (Vergnolle et al., 2002; Steinhoff et al., 2005; Leger et al., 2006). Sibbons et al. (2018) showed that in peripheral blood mononuclear cells (PBMCs), the up-regulation of enzymes coded by the fatty acid elongase 5 *(ELOVL5)* and fatty acid desaturase 1 (*FADS1)* genes increases the synthesis of n-3 PUFA. Polyunsaturated fatty acids (PUFAs) play key roles in the immune response by acting as substrates for the synthesis of lipid second messengers, including eicosanoids, implicated

in cell activation, and for cell membrane biosynthesis. In the present study, these two genes were hypo-methylated during the challenge period, possibly indicating an increase in gene expression. Interestingly, supplementation of PUFAs to the diet can protect animals from the deleterious effects of heat stress on bull sperms by improving quality and motility parameters of fresh semen (Gholami et al., 2011).

A mitogen-activated protein kinase (*MAP3K-1*) which is member of family of serine/threonine kinases (Pham et al., 2013) was in a region that was hypo-methylated in Nellore during the heat stress period. MAPK signaling is important for T lymphocyte development, homeostasis, and effector responses (von Boehmer, 1990; Kronenberg and Gapin, 2002). Among these, natural killer T cells (NKT) constitute a unique T cell population of the immune system (Kronenberg and Gapin, 2007). In mice, it was demonstrated that a deletion of MAP3K-1 leads to an increased NKT cell infiltration into the liver and a higher degree of liver damage (Suddason et al., 2016). It is therefore not surprising that in Nellore this gene is involved in heat response, since it has been widely documented in cattle that acute thermal stress decreases the number of helper T cells and increases the number of NK cells (Nagai and Iriki, 2001).

Phosphodiesterase 5A (*PDE5A)* encodes a cGMP-specific phosphodiesterase involved in cell signaling, protein binding, phosphorylation, cell activation and cGMP binding was found to be hypo-methylated in Nellore during heat stress. A hypo-methylated window located within an intronic region of this gene has been described in the above mentioned work of Skibiel et al. (2018), where DNA methylation of bull calves and heifers has been measured after gestation under maternal conditions of heat stress. In the present study another intronic region of the same gene was also hypo-methylated.

Both RAS p21 protein activator 3 (*RASA3)* and netrin 1 (*NTN1)* were hypo-methylated in Nellore during heat stress. RASA3 encodes for an enzyme member of the GAP1 family of GTPase-activating proteins. This gene is highly expressed in peripheral blood mononuclear cells during activation of the immune system cells and the inflammatory reaction (Wu et al., 2018). NTN1 is a neuroimmune guidance protein expressed in vascular endothelial cells that regulates inflammatory cell recruitment (Ly et al., 2005; Boneschansker et al., 2016). In human, a significant increase in core body temperature during heat stress is associated with a worsening of cognitive functions of people coping with mental illness (Hämäläinen et al., 2012). Differential methylation of both NTN1 and RASA3 has been reported in blood mononuclear cells of patients affected by the neurodegenerative disease, multiple sclerosis (MS), a disease known to be influenced by high body temperature (Flensner et al., 2011). This suggests that epigenetic regulation of NTN1 and RASA3 may be involved in homoeostatic changes of specific nervous system functions due to heat stress. Multiple sclerosis is associated with systemic sclerosis (SSc) (Pelidou et al., 2007). A recent methylome and transcriptome study carried out in blood cells of patients affected by systemic sclerosis detected five DMGs that were hypo-methylated in heat challenged Nellore in the present study: inositol polyphosphate-5-phosphatase A (*INPP5A)*, Spi-1 proto-oncogene (*SPI1)*, transcription factor 3 (*TCF3)*, in addition to F2RL3 and MAP3K1 (Zhu et al., 2018). This suggest a link between the increase of body temperature and changes in the nervous system, through regulation of inflammatory processes.

Heat stress induced oxidative stress (Altan et al., 2003; Mujahid et al., 2005; Lin et al., 2006) can damage cellular macromolecules and interfere with cell signaling pathways. Peroxiredoxin1 (*PRDX1*) encodes a member of the peroxiredoxin family, which acts as a peroxidase as well as a chaperone to protect proteins from oxidative damage (Nassour et al., 2016) and plays key roles in innate immunity and inflammation (Knoops et al., 2016). The effect of heat stress on *in vitro* bovine granulosa cells resulted in incresed expression of PRDX1 in response to oxidative stress and to re-establish cellular homeostasis (Alemu et al., 2018). PRDX1 was hypo-methylation within intronic regions during the challenge period in Nellore.

The level of methylation of Angus samples was higher than those of Nellore, more than half of the significant DMGs were hyper-methylated in the promoter regions during heat stress and therefore gene expression of these genes was likely to be reduced in response to the challenge. This may be associated with the greater vulnerability of this breed to heat stress compared to the Nellore (Bagath et al., 2019). Some of the DMGs were associated with the immune system and were hyper-methylated during heat stress. Autophagy related 16 like 2 (*ATG16L2)* showed opposite behavior in the two breeds, having higher methylation in the stress period and lower in the recovery period in Angus and the opposite in Nellore. ATG16L2 codes for a protein which plays a role in autophagy (Ishibashi et al., 2011). It was observed that heat stress in pig populations leads to a suppression of autophagy and autophagosomal degradation, which results in the persistence of damaged mitochondria in cells that in turn leads to a dysfunctional intracellular environment (Brownstein et al., 2017). These authors reported a decrease in the autophagy related gene transcripts, which is consistent with our results that show a hyper-methylation in the gene body of ATG16L2. This gene has also been shown to be differentially methylated in blood mononuclear cells of patients affected by multiple sclerosis compared with controls (Kulakova et al., 2016).

Calcium voltage-gated channel subunit alpha1 C (*CACNA1C),* hyper-methylated in Angus during the heat stress period, belongs to a gene family coding for calcium channels. These channels transport positively charged calcium ions that play a key role in the cell's ability to generate and transmit electrical signals (Liao et al., 2005). Calcium signaling is essential for T cell activation, tolerance of self-antigens, and homeostasis (Lewis, 2001). In lymphocytes, it has been shown that a signaling cascade leads to an increase of intracellular free calcium that in turn activate immune receptors (Fracchia et al., 2013). White blood cells of mice exposed to acute stress conditions, such as sleep deprivation, progressively loose intracellular Ca2 + and deplete endoplasmic reticulum (ER) reserves, resulting in an impaired immune response (Lungato et al., 2012). Genetic variations in CACNA1C are associated with multiple forms of neuropsychiatric diseases linked to stress and anxiety (Lee et al., 2016).

Growth arrest and DNA damage inducible alpha (*GADD45A)* was hyper-methylated in Angus during the challenge. Under

various stress types, GADD45A maintains genomic integrity in many cell types by surveillance of a DNA-damage (Zhan, 2005) and promoting cell death, cell cycle arrest, and DNA repair (Moskalev et al., 2012). Increased mRNA levels of GADD45A have been reported in hematopoietic stem cells (HSCs), that are required for the continuous regeneration of the blood and the immune system and regulate stress responses (Orkin and Zon, 2008).

Changes in MAPK signaling, a pathway significantly enriched in DMGs in Angus during heat stress, are correlated with defects in innate immune responses of neutrophils and macrophages lacking GADD45 family members (Salerno et al., 2010).

## CONCLUSION

In summary, the present study describes DNA methylation profiles in blood samples of Nellore and Angus steers exposed to the sun during the high temperature season of the Brazilian summer. We detected regions that were differentially methylated that have been previously been associated with activation of immune responses and counteracting the effect of heat stress. Methylation analysis identified specific breed patterns with different methylation responses to stress and recovery. The Nellore appears to actively respond to high temperature by reducing methylation of several key genes and pathways associated with heat response. Angus, however, increases the methylation levels in genes in some of the few pathways that are common between breeds. Further research is also needed to explore the function of demethylation of non-CpG dinucleotides, to improve our knowledge about the biological significance of changes seen as a response to stress.

## DATA AVAILABILITY STATEMENT

The datasets presented in this study can be found in online repositories. The names of the repository/repositories and accession number(s) can be found below: https://www.ncbi.nlm.nih.gov/geo/query/acc.cgi?acc=GSE161113, GSE161113.

## ETHICS STATEMENT

The animal study was reviewed and approved by CEUA (Ethics Committee on the Use of Animals) of the Universidade Estadual Paulista (FOA n° 2014-01445). Written informed consent was obtained from the owners for the participation of their animals in this study.

## AUTHOR CONTRIBUTIONS

GN, JG, and PA-M conceived and designed the study. LZ, MM, AU, and GN performed the experiments. EC performed the DNA extraction, libraries preparation, and sequencing. MD and BL analyzed the data. MD, BL, YU, AS, GN, and PA-M prepared the manuscript. All authors reviewed and approved the final manuscript.

## FUNDING

This research was supported by the São Paulo Research Foundation (FAPESP).

## SUPPLEMENTARY MATERIAL

The Supplementary Material for this article can be found online at: https://www.frontiersin.org/articles/10.3389/fgene.2021.633132/full#supplementary-material

**Supplementary Figure 1 |** DNA methylation levels of different functional regions in Angus and Nellore and in challenge and recovery periods.

**Supplementary Figure 2 |** Principal component analysis (PCA) based on genome-wide DNA methylation in Angus and Nellore and in challenge (C) and recovery (R) periods.

**Supplementary Table 1 |** Sequencing summary.

**Supplementary Table 2 |** Differentially methylated regions and genes between challenge and recovery period in Angus and Nellore breeds (q value = 0.05). Sheet 1: shared regions between Angus and Nellore. Sheet 2: Angus unique regions. Sheet 3: Nellore unique regions.

**Supplementary File 1 |** Details on animals treatment and diet.

## REFERENCES

Aguilar, I., Misztal, I., and Tsuruta, S. (2010). Short communication: genetic trends of milk yield under heat stress for US Holsteins. *J. Dairy Sci.* 93, 1754–1758. doi: 10.3168/jds.2009-2756

Akalin, A., Kormaksson, M., Li, S., Garrett-Bakelman, F. E., Figueroa, M. E., Melnick, A., et al. (2012). methylKit: a comprehensive R package for the analysis of genome-wide DNA methylation profiles. *Genome Biol.* 13:R87. doi: 10.1186/gb-2012-13-10-r87

Alemu, T. W., Pandey, H. O., Salilew Wondim, D., Gebremedhn, S., Neuhof, C., Tholen, E., et al. (2018). Oxidative and endoplasmic reticulum stress defense mechanisms of bovine granulosa cells exposed to heat stress. *Theriogenology* 110, 130–141. doi: 10.1016/j.theriogenology.2017.12.042

Altan, Ö, Pabuccuoglu, A., Altan, A., Konyalioglu, S., and Bayraktar, H. (2003). Effect of heat stress on oxidative stress, lipid peroxidation and some stress parameters in broilers. *Brit. Poult. Sci.* 44, 545–550. doi: 10.1080/00071660310001618334

Bagath, M., Krishnanan, G., Devaraj, C., Rashamol, V. P., Pragna, P., Lees, A. M., et al. (2019). The impact of heat stress on the immune system in dairy cattle: a review. *Res. Vet. Sci.* 126, 94–102. doi: 10.1016/j.rvsc.2019.08.011

Bernabucci, U., Biffani, S., Buggiotti, L., Vitali, A., Lacetera, N., and Nardone, A. (2014). The effects of heat stress in Italian Holstein dairy cattle. *J. Dairy Sci.* 97, 471–486. doi: 10.3168/jds.2013-6611

Bernstein, E., Goldberg, A. D., and Allis, C. D. (2007). Epigenetics: a landscape takes shape. *Cell* 128, 635–638. doi: 10.1016/j.cell.2007.02.006

Biffani, S., Bernabucci, U., Vitali, A., Lacetera, N., and Nardone, A. (2016). Short communication: effect of heat stress on nonreturn rate of Italian Holstein cows. *J. Dairy Sci.* 99, 5837–5843. doi: 10.3168/jds.2015-10491

Boneschansker, L., Nakayama, H., Eisenga, M., Wedel, J., Klagsbrun, M., Irimia, D., et al. (2016). Netrin-1 augments chemokinesis in CD4+ T cells in vitro

and elicits a proinflammatory response in vivo. *J. Immunol.* 197, 1389–1398. doi: 10.4049/jimmunol.1502432

Braun, P. R., Han, S., Hing, B., Nagahama, Y., Gaul, L. N., Heinzman, J. T., et al. (2019). Genome-wide DNA methylation comparison between live human brain and peripheral tissues within individuals. *Transl. Psychiatry* 9:47.

Brownstein, A. J., Ganesan, S., Summers, C. M., Pearce, S., Hale, B. J., Ross, J. W., et al. (2017). Heat stress causes dysfunctional autophagy in oxidative skeletal muscle. *Physiol. Rep.* 5:e13317. doi: 10.14814/phy2.13317

Chovatiya, R., and Medzhitov, R. (2014). Stress, inflammation, and defense of homeostasis. *Mol. Cell* 54, 281–288. doi: 10.1016/j.molcel.2014.03.030

Collier, R. J., Collier, J. L., Rhoads, R. P., and Baumgard, L. H. (2008). Invited review: genes involved in the bovine heat stress response. *J. Dairy Sci.* 91, 445–454. doi: 10.3168/jds.2007-0540

Cosma, M. P., Tanaka, T., and Nasmyth, K. (2010). Ordered recruitment of transcription and chromatin remodeling factors to a cell cycle- and developmentally regulated promoter. *Cell* 97, 299–311. doi: 10.1016/s0092-8674(00)80740-0

Cowley, S., Whittaker, K., Malone, M., Donetto, S., Grigulis, A., and Maben, J. (2015). Why health visiting? Examining the potential public health benefits from health visiting practice within a universal service: a narrative review of the literature. *Int. J. Nurs. Stud.* 52, 465–480. doi: 10.1016/j.ijnurstu.2014.07.013

Cree, I. A., Uttley, L., Buckley Woods, H., Kikuchi, H., Reiman, A., Harnan, S., et al. (2017). The evidence base for circulating tumour DNA blood-based biomarkers for the early detection of cancer: a systematic mapping review. *BMC Cancer* 17:697. doi: 10.1186/s12885-017-3693-7

Danaher, R. J., Jacob, R. J., Chorak, M. D., Freeman, C. S., and Miller, C. S. (1999). Heat stress activates production of herpes simplex virus type 1 from quiescently infected neurally differentiated PC12 cells. *J. Neurovirol.* 5, 374–383. doi: 10.3109/13550289909029478

Del Corvo, M., Bongiorni, S., Stefanon, B., Sgorlon, S., Valentini, A., Ajmone Marsan, P., et al. (2020). Genome-wide DNA methylation and gene expression profiles in cows subjected to different stress level as assessed by cortisol in milk. *Genes* 11:850. doi: 10.3390/genes11080850

Dikmen, S., Alava, E., Pontes, E., Fear, J. M., Dikmen, B. Y., Olson, T. A., et al. (2008). Differences in thermoregulatory ability between slick-haired and wild-type lactating Holstein cows in response to acute heat stress. *J. Dairy Sci.* 91, 3395–3402. doi: 10.3168/jds.2008-1072

Dikmen, S., Cole, J. B., Null, D. J., and Hansen, P. J. (2012). Heritability of rectal temperature and genetic correlations with production and reproduction traits in dairy cattle. *J. Dairy Sci.* 95, 3401–3405. doi: 10.3168/jds.2011-4306

Dikmen, S., Cole, J. B., Null, D. J., and Hansen, P. J. (2013). Genome-wide association mapping for identification of quantitative trait loci for rectal temperature during heat stress in Holstein cattle. *PLoS One* 8:e69202. doi: 10.1371/journal.pone.0069202

Dikmen, S., Khan, F. A., Huson, H. J., Sonstegard, T. S., Moss, J. I., Dahl, G. E., et al. (2014). The SLICK hair locus derived from Senepol cattle confers thermotolerance to intensively managed lactating Holstein cows. *J. Dairy Sci.* 97, 5508–5552. doi: 10.3168/jds.2014-8087

Dikmen, S., Wang, X. Z., Ortega, M. S., Cole, J. B., Null, D. J., and Hansen, P. J. (2015). Single nucleotide polymorphisms associated with thermoregulation in lactating dairy cows exposed to heat stress. *J. Anim. Breed. Genet.* 132, 409–419. doi: 10.1111/jbg.12176

Faylon, M. P., Baumgard, L. H., Rhoads, R. P., and Spurlock, D. M. (2015). Effects of acute heat stress on lipid metabolism of bovine primary adipocytes. *J. Dairy Sci.* 98, 8732–8740. doi: 10.3168/jds.2015-9692

Flensner, G., Ek, A. C., Söderhamn, O., and Landtblom, A. M. (2011). Sensitivity to heat in MS patients: a factor strongly influencing symptomology–an explorative survey. *BMC Neurol.* 11:27. doi: 10.1186/1471-2377-11-27

Fracchia, K. M., Pai, C. Y., and Walsh, C. M. (2013). Modulation of T cell metabolism and function through calcium signaling. *Front. Immunol.* 4:324. doi: 10.3389/fimmu.2013.00324

Georges, M., Charlier, C., and Cockett, N. (2003). The callipyge locus: evidence for the trans interaction of reciprocally imprinted genes. *Trends Genet.* 19, 248–252. doi: 10.1016/s0168-9525(03)00082-9

Gholami, H., Chamani, M., Towhidi, A., and Fazeli, M. H. (2011). Improvement of semen quality in Holstein bulls during heat stress by dietary supplementation of omega-3 fatty acids. *Int. J. Fertil. Steril.* 4, 160–167.

Gomides, L. F., Duarte, I. D., Ferreira, R. G., Perez, A. C., Francischi, J. N., and Klein, A. (2012). Proteinase-activated receptor-4 plays a major role in the recruitment of neutrophils induced by trypsin or carrageenan during pleurisy in mice. *Pharmacology* 89, 275–282. doi: 10.1159/000337378

Hämäläinen, P., Ikonen, A., Romberg, A., Helenius, H., and Ruutiainen, J. (2012). The effects of heat stress on cognition in persons with multiple sclerosis. *Mult. Scler.* 18, 489–497. doi: 10.1177/1352458511422926

Hayes, B. J., Bowman, P. J., Chamberlain, A. J., Savin, K., van Tassell, C. P., Sonstegard, T. S., et al. (2009). A validated genome wide association study to breed cattle adapted to an environment altered by climate change. *PLoS One* 4:e6676. doi: 10.1371/journal.pone.0006676

Henriksen, T. V., Reinert, T., Christensen, E., Sethi, H., Birkenkamp-Demtröder, K., Gögenur, M., et al. (2020). The effect of surgical trauma on circulating free DNA levels in cancer patients-implications for studies of circulating tumor DNA. *Mol. Oncol.* 14, 1670–1679. doi: 10.1002/1878-0261.12729

Holbro, T., and Hynes, N. E. (2004). ErbB receptors: directing key signaling networks throughout life. *Annu. Rev. Pharmacol. Toxicol.* 44, 195–217. doi: 10.1146/annurev.pharmtox.44.101802.121440

Ishibashi, K., Fujita, N., Kanno, E., Omori, H., Yoshimori, T., Itoh, T., et al. (2011). Atg16L2, a novel isoform of mammalian Atg16L that is not essential for canonical autophagy despite forming an Atg12–5-16L2 complex. *Autophagy* 7, 1500–1513. doi: 10.4161/auto.7.12.18025

Kataoka, H., Hamilton, J. R., McKemy, D. D., Camerer, E., Zheng, Y. W., Cheng, A., et al. (2003). Protease-activated receptors 1 and 4 mediate thrombin signaling in endothelial cells. *Blood* 102, 3224–3231. doi: 10.1182/blood-2003-04-1130

Knoops, B., Argyropoulou, V., Becker, S., Ferté, L., and Kuznetsova, O. (2016). Multiple roles of peroxiredoxins in inflammation. *Mol. Cells* 39, 60–64. doi: 10.14348/molcells.2016.2341

Kronenberg, M., and Gapin, L. (2002). The unconventional lifestyle of NKT cells. *Nat. Rev. Immunol.* 2, 557–568. doi: 10.1038/nri854

Kronenberg, M., and Gapin, L. (2007). Natural killer T cells: know thyself. *Proc. Natl. Acad. Sci. U.S.A.* 104, 5713–5714. doi: 10.1073/pnas.0701493104

Krueger, F., and Andrews, S. R. (2011). Bismark: a flexible aligner and methylation caller for Bisulfite-Seq applications. *Bioinformatics* 27, 1571–1572. doi: 10.1093/bioinformatics/btr167

Kulakova, O. G., Kabilov, M. R., Danilova, L. V., Popova, E. V., Baturina, O. A., Tsareva, E. Y., et al. (2016). Whole-genome DNA methylation analysis of peripheral blood mononuclear cells in multiple sclerosis patients with different disease courses. *Acta Naturae* 8, 103–110. doi: 10.32607/20758251-2016-8-3-103-110

Langmead, B., and Salzberg, S. L. (2012). Fast gapped-read alignment with Bowtie 2. *Nat. Methods* 9, 357–359. doi: 10.1038/nmeth.1923

Lee, A. S., De Jesús-Cortés, H., Kabir, Z. D., Knobbe, W., Orr, M., Burgdorf, C., et al. (2016). The Neuropsychiatric disease-associated gene cacna1c mediates survival of young hippocampal neurons. *eNeuro* 3:ENEURO.0006-16.2016. doi: 10.1523/ENEURO.0006-16.2016

Leger, A. J., Covic, L., and Kuliopulos, A. (2006). Protease-activated receptors in cardiovascular diseases. *Circulation* 114, 1070–1077. doi: 10.1161/circulationaha.105.574830

Lewis, R. S. (2001). Calcium signaling mechanisms in T lymphocytes. *Annu. Rev. Immunol.* 19, 497–521.

Li, M., Wu, H., Luo, Z., Xia, Y., Guan, J., Wang, T., et al. (2012). An atlas of DNA methylomes in porcine adipose and muscle tissues. *Nat. Commun.* 3:850. doi: 10.1038/ncomms1854

Liao, P., Yong, T. F., Liang, M. C., Yue, D. T., and Soong, T. W. (2005). Splicing for alternative structures of Cav1.2 Ca2+ channels in cardiac and smooth muscles. *Cardiovasc. Res.* 68, 197–203. Epub. 2005 Jul 27. Review., doi: 10.1016/j.cardiores.2005.06.024

Lin, H., Decuypere, E., and Buyse, J. (2006). Acute heat stress induces oxidative stress in broiler chickens. *Comp. Biochem. Physiol. A Mol. Integr. Physiol.* 144, 11–17. doi: 10.1016/j.cbpa.2006.01.032

Littlejohn, M. D., Henty, K. M., Tiplady, K., Johnson, T., Harland, C., Lopdell, T., et al. (2014). Functionally reciprocal mutations of the prolactin signalling pathway define hairy and slick cattle. *Nat. Commun.* 5:5861. doi: 10.1038/ncomms6861

Lungato, L., Gazarini, M. L., Paredes-Gamero, E. J., Tersariol, I. L., Tufik, S., D'Almeida, V., et al. (2012). Sleep deprivation impairs calcium signaling

in mouse splenocytes and leads to a decreased immune response. *Biochim. Biophys. Acta* 1820, 1997–2006. doi: 10.1016/j.bbagen.2012.09.010

Ly, N. P., Komatsuzaki, K., Fraser, I. P., Tseng, A. A., Prodhan, P., Moore, K. J., et al. (2005). Netrin-1 inhibits leukocyte migration in vitro and in vivo. *Proc. Natl. Acad. Sci. U.S.A.* 102, 14729–14734. doi: 10.1073/pnas.0506233102

Ma, B., Wilker, E. H., Willis-Owen, S. A., Byun, H. M., Wong, K. C., Motta, V., et al. (2014). Predicting DNA methylation level across human tissues. *Nucleic Acids Res.* 42, 3515–3528. doi: 10.1093/nar/gkt1380

Macciotta, N. P. P., Biffani, S., Bernabucci, U., Lacetera, N., Vitali, A., Ajmone-Marsan, P., et al. (2017). Derivation and genome-wide association study of a principal component-based measure of heat tolerance in dairy cattle. *J. Dairy Sci.* 100, 4683–4697. doi: 10.3168/jds.2016-12249

McDowell, R. E., Hooven, N. W., and Camoens, J. K. (1976). Effect of climate on performance of Holsteins in first lactation. *J. Dairy Sci.* 59, 965–973. doi: 10.3168/jds.S0022-0302(76)84305-6

Mehla, K., Magotra, A., Choudhary, J., Singh, A. K., Mohanty, A. K., Upadhyay, R. C., et al. (2014). Genome-wide analysis of the heat stress response in Zebu (Sahiwal) cattle. *Gene* 533, 500–507. doi: 10.1016/j.gene.2013.09.051

Mitchell, G., Amit, I., Garber, M., French, C., Lin, M. F., Feldser, D., et al. (2009). Chromatin signature reveals over a thousand highly conserved large non-coding RNAs in mammals. *Nature* 458, 223–227. doi: 10.1038/nature07672

Moskalev, A. A., Smit-McBride, Z., Shaposhnikov, M. V., Plyusnina, E. N., Zhavoronkov, A., Budovsky, A., et al. (2012). Gadd45 proteins: relevance to aging, longevity and age-related pathologies. *Ageing Res. Rev.* 11, 51–66. doi: 10.1016/j.arr.2011.09.003

Mujahid, A., Yoshiki, Y., Akiba, Y., and Toyomizu, M. (2005). Superoxide radical production in chicken skeletal muscle induced by acute heat stress. *Poult. Sci.* 84, 307–314. doi: 10.1093/ps/84.2.307

Nagai, M., and Iriki, M. (2001). "Changes in immune activities by heat stress," in *Thermotherapy for Neoplasia, Inflammation, and Pain*, eds M. Kosaka, T. Sugahara, K. L. Schmidt, and E. Simon (Tokyo: Springer), 266–270 doi: 10.1007/978-4-431-67035-3_30

Nardone, A., Ronchi, B., Lacetera, N., Ranieri, M. S., and Bernabucci, U. (2010). Effects of climate changes on animal production and sustainability of livestock systems. *Livest. Sci.* 130, 57–69. doi: 10.1016/j.livsci.2010.02.011

Nassour, H., Wang, Z., Saad, A., Papaluca, A., Brosseau, N., Affar el, B., et al. (2016). Peroxiredoxin 1 interacts with and blocks the redox factor APE1 from activating interleukin-8 expression. *Sci. Rep.* 6:29389. doi: 10.1038/srep29389

Nätt, D., Rubin, C.-J., Wright, D., Johnsson, M., Beltéky, J., Andersson, L., et al. (2012). Heritable genome-wide variation of gene expression and promoter methylation between wild and domesticated chickens. *BMC Genomics* 13:59. doi: 10.1186/1471-2164-13-59

Olson, T. A., Lucena, C., Chase, C. C. Jr., and Hammond, A. C. (2003). Evidence of a major gene influencing hair length and heat tolerance in *Bos taurus* cattle. *J. Anim. Sci.* 81, 80–90. doi: 10.2527/2003.81180x

Orkin, S. H., and Zon, L. I. (2008). Hematopoiesis: an evolving paradigm for stem cell biology. *Cell* 132, 631–644. doi: 10.1016/j.cell.2008.01.025

Pelidou, S. H., Tsifetaki, N., Giannopoulos, S., Deretzi, G., Voulgari, P., Kyritsis, A., et al. (2007). Multiple sclerosis associated with systemic sclerosis. *Rheumatol. Int.* 27, 771–773.

Perano, K. M., Usack, J. G., Angenent, L. T., and Gebremedhin, K. G. (2015). Production and physiological responses of heat-stressed lactating dairy cattle to conductive cooling. *J. Dairy Sci.* 98, 5252–5261. doi: 10.3168/jds.2014-8784

Pham, T. T., Angus, S. P., and Johnson, G. L. (2013). MAP3K1: genomic alterations in cancer and function in promoting cell survival or apoptosis. *Genes Cancer* 4, 419–426. doi: 10.1177/1947601913513950

Porto-Neto, L. R., Bickhart, D. M., Landaeta-Hernandez, A. J., Utsunomiya, Y. T., Pagan, M., Jimenez, E., et al. (2018). Convergent evolution of Slick coat in cattle through truncation mutations in the prolactin receptor. *Front. Genet.* 9:57. doi: 10.3389/fgene.2018.00057

Rajaud, A., and Noblet-Ducoudré, N. (2017). Tropical semi-arid regions expanding over temperate latitudes under climate change. *Clim. Change* 144, 703–719. doi: 10.1007/s10584-017-2052-7

Rhoads, M. L., Kim, J. W., Collier, R. J., Crooker, B. A., Boisclair, Y. R., Baumgard, L. H., et al. (2010). Effects of heat stress and nutrition on lactating Holstein cows: II. *J. Dairy Sci.* 93, 170–179. doi: 10.3168/jds.2009-2469

Rojas-Downing, M. M., Nejadhashemi, P. A., Timothy, H., and Woznicki, S. A. (2017). Climate change and livestock: impacts, adaptation, and mitigation. *Clim. Risk. Manag.* 16, 145–163.

Salerno, D., Tront, S. J., Hoffman, B., and Liebermann, D. (2010). Deficiency in stress response Gadd45a and Gadd45b alters MAPK kinase signaling leading to functional defects in innate immune responses of neutrophils and macrophages in vitro and in vivo. *Blood* 116:927. doi: 10.1182/blood.v116.21.927.927

Scheiermann, C., Kunisaki, Y., and Frenette, P. S. (2013). Circadian control of the immune system. *Nat. Rev. Immunol.* 13, 190–198. doi: 10.1038/nri3386

Sibbons, C. M., Irvine, N. A., Pérez-Mojica, J. E., Calder, P. C., Lillycrop, K. A., Fielding, B. A., et al. (2018). Polyunsaturated fatty acid biosynthesis involving Δ8 desaturation and differential dna methylation of *FADS2* regulates proliferation of human peripheral blood mononuclear cells. *Front. Immunol.* 9:432. doi: 10.3389/fimmu.2018.00432

Singh, K., Erdman, R. A., Swanson, K. M., Molenaar, A. J., Maqbool, N. J., Wheeler, T. T., et al. (2010). Epigenetic regulation of milk production in dairy cows. *J. Mammary Gland Biol. Neoplasia* 15, 101–112. doi: 10.1007/s10911-010-9164-2

Skibiel, A. L., Peñagaricano, F., Amorín, R., Ahmed, B. M., Dahl, G. E., Laporta, J., et al. (2018). In utero heat stress alters the offspring epigenome. *Sci. Rep.* 8:14609. doi: 10.1038/s41598-018-32975-1

Steinhoff, M., Buddenkotte, J., Shpacovitch, V., Rattenholl, A., Moormann, C., Vergnolle, N., et al. (2005). Proteinase-activated receptors: transducers of proteinase-mediated signaling in inflammation and immune response. *Endocr. Rev.* 26, 1–43. doi: 10.1210/er.2003-0025

Strahl, B. D., and Allis, C. D. (2000). The language of covalent histone modifications. *Nature* 403, 41–45. doi: 10.1038/47412

Suddason, T., Anwar, S., Charlaftis, N., and Gallagher, E. T. - (2016). Cell-specific deletion of Map3k1 reveals the critical role for Mekk1 and Jnks in Cdkn1b-dependent proliferative expansion. *Cell Rep.* 14, 449–457. doi: 10.1016/j.celrep.2015.12.047

Thom, E. C. (1959). The discomfort index. *Weatherwise* 12, 57–59. doi: 10.1080/00431672.1959.9926960

Valente, T. S., Sant'Anna, A. C., Baldi, F., Albuquerque, L. G., and da Costa, M. J. (2015). Genetic association between temperament and sexual precocity indicator traits in Nellore cattle. *J. Appl. Genet.* 56, 349–354. doi: 10.1007/s13353-014-0259-0

Van Laere, A. S., Nguyen, M., Braunschweig, M., Nezer, C., Collette, C., Moreau, L., et al. (2003). A regulatory mutation in IGF2 causes a major QTL effect on muscle growth in the pig. *Nature* 425, 832–836. doi: 10.1038/nature02064

Vergnolle, N., Derian, C. K., D'Andrea, M. R., Steinhoff, M., and Andrade-Gordon, P. (2002). Characterization of thrombin-induced leukocyte rolling and adherence: a potential proinflammatory role for proteinase-activated receptor-4. *J. Immunol.* 169, 1467–1473. doi: 10.4049/jimmunol.169.3.1467

von Boehmer, H. (1990). Developmental biology of T cells in T cell-receptor transgenic mice. *Annu. Rev. Immunol.* 8, 531–556. doi: 10.1146/annurev.iy.08.040190.002531

Vuocolo, T., Byrne, K., White, J., McWilliam, S., Reverter, A., Cockett, N. E., et al. (2007). Identification of a gene network contributing to hypertrophy in callipyge skeletal muscle. *Physiol. Genomics* 28, 253–272. doi: 10.1152/physiolgenomics.00121.2006

Wang, H., Tuominen, L. K., and Tsai, C. (2011). SLIM: a sliding linear model for estimating the proportion of true null hypotheses in datasets with dependence structures. *Bioinformatics* 27, 225–231. doi: 10.1093/bioinformatics/btq650

Wehbi, V. L., and Taskén, K. (2016). Molecular mechanisms for cAMP-mediated immunoregulation in T cells–role of anchored protein kinase a signaling units. *Front. Immunol.* 7:222. doi: 10.3389/fimmu.2016.00222

Weyrich, A., Benz, S., Karl, S., Jeschek, M., Jewgenow, K., and Fickel, J. (2016). Paternal heat exposure causes DNA methylation and gene expression changes of Stat3 in Wild guinea pig sons. *Ecol. Evol.* 6, 2657–2666. doi: 10.1002/ece3.1993

Wu, B., Zhang, S., Guo, Z., Wang, G., Zhang, G., Xie, L., et al. (2018). RAS P21 protein activator 3 (RASA3) specifically promotes pathogenic T helper 17 cell generation by repressing T-helper-2-cell-biased programs. *Immunity* 49, 886–898.e5. doi: 10.1016/j.immuni.2018.09.004

Xu, W. F., Andersen, H., Whitmore, T. E., Presnell, S. R., Yee, D. P., Ching, A., et al. (1998). Cloning and characterization of human protease-activated receptor 4. *Proc. Natl. Acad. Sci. U.S.A.* 95, 6642–6646.

Yoshihara, T., Naito, H., Kakigi, R., Ichinoseki-Sekine, N., Ogura, Y., Sugiura, T., et al. (2013). Heat stress activates the Akt/mTOR signalling pathway in rat skeletal muscle. *Acta Physiol.* 207, 416–426. doi: 10.1111/apha.12040

Yu, G., Wang, L., Han, Y., and He, Q. (2012). clusterProfiler: an R package for comparing biological themes among gene clusters. *OMICS* 16, 284–287. doi: 10.1089/omi.2011.0118

Zaccolo, M., and Movsesian, M. A. (2007). cAMP and cGMP signaling cross-talk. *Circ. Res.* 100, 1569–1578. doi: 10.1161/circresaha.106.144501

Zhan, Q. (2005). Gadd45a, a p53- and BRCA1-regulated stress protein, in cellular response to DNA damage. *Mutat. Res.* 569, 133–143. doi: 10.1016/j.mrfmmm.2004.06.055

Zhang, J., Song, F., Zhao, X., Jiang, H., Wu, X., Wang, B., et al. (2017). EGFR modulates monounsaturated fatty acid synthesis through phosphorylation of SCD1 in lung cancer. *Mol. Cancer* 16:127. doi: 10.1186/s12943-017-0704-x

Zhu, H., Zhu, C., Mi, W., Chen, T., Zhao, H., Zuo, X., et al. (2018). Integration of genome-wide DNA methylation and transcription uncovered aberrant methylation-regulated genes and pathways in the peripheral blood mononuclear cells of systemic sclerosis. *Int. J. Rheumatol.* 2018:7342472. doi: 10.1155/2018/7342472

**Conflict of Interest:** The authors declare that the research was conducted in the absence of any commercial or financial relationships that could be construed as a potential conflict of interest.

*Copyright © 2021 Del Corvo, Lazzari, Capra, Zavarez, Milanesi, Utsunomiya, Utsunomiya, Stella, de Paula Nogueira, Garcia and Ajmone-Marsan. This is an open-access article distributed under the terms of the Creative Commons Attribution License (CC BY). The use, distribution or reproduction in other forums is permitted, provided the original author(s) and the copyright owner(s) are credited and that the original publication in this journal is cited, in accordance with accepted academic practice. No use, distribution or reproduction is permitted which does not comply with these terms.*

frontiers in Genetics

ORIGINAL RESEARCH
published: 19 October 2021
doi: 10.3389/fgene.2021.689748

# Comprehensive Analysis of Transcriptome-wide m$^6$A Methylome Upon *Clostridium perfringens* Beta2 Toxin Exposure in Porcine Intestinal Epithelial Cells by m$^6$A Sequencing

*Juanli Zhang*[1], *Qiaoli Yang*[1], *Jiaojiao Yang*[1], *Xiaoli Gao*[1], *Ruirui Luo*[1], *Xiaoyu Huang*[1], *Zunqiang Yan*[1], *Pengfei Wang*[1], *Wei Wang*[1], *Kaihui Xie*[1], *Bo Zhang*[1] *and Shuangbao Gun*[1,2]*

[1]*College of Animal Science and Technology, Gansu Agricultural University, Lanzhou, China,* [2]*Gansu Research Center for Swine Production Engineering and Technology, Lanzhou, China*

OPEN ACCESS

**Edited by:**
*George E. Liu, Agricultural Research Service (USDA), United States*

**Reviewed by:**
*Narendra Singh, Stowers Institute for Medical Research, United States*
*Eveline M Ibeagha-Awemu, Agriculture and Agri-Food Canada (AAFC), Canada*

***Correspondence:**
*Shuangbao Gun*
*gunsbao056@126.com*

**Specialty section:**
*This article was submitted to Epigenomics and Epigenetics, a section of the journal Frontiers in Genetics*

**Received:** *01 April 2021*
**Accepted:** *30 September 2021*
**Published:** *19 October 2021*

**Citation:**
*Zhang J, Yang Q, Yang J, Gao X, Luo R, Huang X, Yan Z, Wang P, Wang W, Xie K, Zhang B and Gun S (2021) Comprehensive Analysis of Transcriptome-wide m$^6$A Methylome Upon* Clostridium perfringens *Beta2 Toxin Exposure in Porcine Intestinal Epithelial Cells by m$^6$A Sequencing. Front. Genet. 12:689748. doi: 10.3389/fgene.2021.689748*

Piglet diarrhea is a swine disease responsible for serious economic impacts in the pig industry. *Clostridium perfringens* beta2 toxin (CPB2), which is a major toxin of *C. perfringens* type C, may cause intestinal diseases in many domestic animals. N$^6$-methyladenosine (m$^6$A) RNA methylation plays critical roles in many immune and inflammatory diseases in livestock and other animals. However, the role of m$^6$A methylation in porcine intestinal epithelial (IPEC-J2) cells exposed to CPB2 has not been studied. To address this issue, we treated IPEC-J2 cells with CPB2 toxin and then quantified methylation-related enzyme expression by RT-qPCR and assessed the m$^6$A methylation status of the samples by colorimetric N$^6$-methyladenosine quantification. The results showed that the methylation enzymes changed to varying degrees while the m$^6$A methylation level increased ($p < 0.01$). On this basis, we performed N$^6$-methyladenosine sequencing (m$^6$A-seq) and RNA sequencing (RNA-seq) to examine the detailed m$^6$A modifications and gene expression of the IPEC-J2 cells following CPB2 toxin exposure. Our results indicated that 1,448 m$^6$A modification sites, including 437 up-regulated and 1,011 down-regulated, differed significantly between CPB2 toxin exposed cells and non-exposed cells ($p < 0.05$). KEGG pathway analysis results showed that m$^6$A peaks up-regulated genes ($n = 394$) were mainly enriched in cancer, Cushing syndrome and Wnt signaling pathways, while m$^6$A peaks down-regulated genes ($n = 920$) were mainly associated with apoptosis, small cell lung cancer, and the herpes simplex virus 1 infection signaling pathway. Furthermore, gene expression (RNA-seq data) analysis identified 1,636 differentially expressed genes (DEGs), of which 1,094 were up-regulated and 542 were down-regulated in the toxin exposed group compared with the control group. In addition, the down-regulated genes were involved in the Hippo and Wnt signaling pathways. Interestingly, the combined results of m$^6$A-seq and RNA-seq identified genes with up-regulated m$^6$A peaks but with down-regulated expression, here referred to as "hyper-down" genes ($n = 18$), which were mainly enriched in the Wnt signaling pathway. Therefore, we speculate that the genes in the Wnt signaling pathway may be modified by m$^6$A methylation in CPB2-induced IPEC-J2 cells. These findings

provide new insights enabling further exploration of the mechanisms underlying piglet diarrhea caused by CPB2 toxin.

**Keywords: m$^6$A-seq, RNA-seq, beta2 toxin, M$^6$A modification, porcine intestinal epithelial cells**

## INTRODUCTION

*Clostridium perfringens*, which is one of the most important zoonotic pathogens (Immerseel et al., 2005), can cause severe bleeding ulcers and mucosal necrosis of the small intestine in humans and animals. It can produce four main toxins (α, β, ε, ι), according to which it is divided into five types: A, B, C, D, and E (Garcia et al., 2012). The *C. perfringens* beta2 (CPB2) toxin was first discovered in the supernatant of a culture *of C. perfringens* type C by Gibert et al. (1997). Its protein molecular weight is 28 kDa, with an isoelectric point of 5.4–5.5, and it is associated with gastrointestinal diseases in livestock caused by *C. perfringens*. The effect of CPB2 toxin on intestinal membrane epithelial cells indicates that it is strongly cytotoxic. When a low concentration of the toxin is introduced into these cells, the cells become rounded and damaged (Gibert et al., 1997). However, the mechanism by which CPB2 toxin induces diarrhea in animals (especially pigs) is still unclear and should be further studied.

N$^6$-methyladenosine (m$^6$A) modification is pervasive within mRNA and plays important regulatory roles in various biological processes (Meyer et al., 2012). In mammalian species, about one-third of mRNAs are modified by m$^6$A (average of three to five m$^6$A modifications in each mRNA), and many m$^6$A sites are evolutionarily conserved between humans and mice (Huang et al., 2020). Dominissini et al. (2012) used m$^6$A-specific antibodies to enrich fragments containing m$^6$A and to identify the expression of m$^6$A in whole transcripts of humans and mice by a high-throughput sequencing method (MeRIP-seq). m$^6$A is mainly located near the termination codons and 3′UTRs of mRNA, and can influence pre-mRNA splicing (Zhao et al., 2014; Xiao et al., 2016), RNA structure (Liu et al., 2015), nuclear mRNA (Fustin et al., 2013), miRNA maturation (Alarcón et al., 2015), mRNA stability (Huang et al., 2018), chromosome inactivation (Patil et al., 2016), mRNA translation (Shi et al., 2017), and even RNA degradation (Zhu et al., 2014).

m$^6$A modification plays very important roles in various immune and inflammatory responses to bacterial infection, such as the inflammatory response of human dental pulp cells (HDPCs) induced by lipopolysaccharide (LPS) (Feng et al., 2018) and the response of porcine small intestinal epithelial (IPEC-J2) cells to *Escherichia coli* K88 infection (Zong et al., 2018). In addition, Wu et al. (2020) found that deletion of YTH domain family 2 (YTHDF2) in the m$^6$A reader promotes the demethylation of histone H3 lysine-27 trimethylation (H3K27me3) modifications, which in turn increases proinflammatory cytokine levels. However, the role of m$^6$A modification in IPEC-J2 cells exposed to CPB2 remains unclear. Therefore, to better understand m$^6$A modification in response to CPB2 toxin exposure, we performed N$^6$-methyladenosine sequencing (m$^6$A-seq) and RNA sequencing (RNA-seq) to investigate differentially methylated genes (DMGs) and differentially expressed genes (DEGs) in IPEC-J2 cells that were exposed to CPB2. Our results provide a theoretical basis for further research into the molecular mechanisms of m$^6$A modification in IPEC-J2 cells exposed to CPB2.

## MATERIALS AND METHODS

### CPB2 Toxin Extraction and Purification

The extraction and purification of CPB2 toxin were performed according to the method described by Luo et al. (2020). Briefly, a recombinant plasmid containing the CPB2 gene was successfully constructed and transformed into *E. coli* BL21 competent cells. Then, a single colony was selected, placed in medium containing kanamycin and incubated for 2.5 h at 37°C and 220 rpm. When the optical density (OD) reached 0.5–0.8, 1 mM isopropyl β-D-1-thiogalactopyranoside (IPTG, Solarbio, Beijing, China) was added to induce the bacteria at 16°C for 12 h. The precipitates were collected and suspended in 20 mM Tris-HCl buffer (pH 8.0), sonicated on ice, and purified by using High-Affinity Ni-Charged Resin FF (GenScript, Nanjing, China). The resin was washed with 10 mM imidazole lysis buffer and then eluted with 250 and 500 mM imidazole. Recombinant protein expression was detected by 12% alkyl sulfate-polyacrylamide gel electrophoresis (SDS-PAGE). Next, 10 mL of protein sample was loaded into a membrane and purified by dialysis against 1 × PBS (pH 7.6) for 24 h, then concentrated with PEG6000 for 40 min. Finally, Endotoxin Erasol (Genscript, Nanjing, China) was used to remove endotoxins.

### Cell Culture

IPEC-J2 cells were provided by the Beijing Beina Chuanglian Institute of Biotechnology (Beijing, China) and cultured in 90% Dulbecco's modified Eagle's medium (DMEM, HyClone, Logan, United States) with 10% fetal bovine serum (FBS, HyClone), penicillin (100 U/mL), and streptomycin (100 μg/mL) at 37°C in a 5% $CO_2$ atmosphere. The medium was changed every 2 days, and the cells were passaged by trypsinization at 80–90% confluency.

### CPB2 Toxin Treatment of Cells and Total m$^6$A Measurement

IPEC-J2 cells were seeded in 6-well plates at a density of $1\times10^5$ cells/mL and cultured overnight (24 h). Then, cells in three wells were each treated with 20 μg/mL CPB2 (treatment group) while cells in the other three wells were not exposed to toxin (control group) (Gao et al., 2020; Luo et al., 2020). Total RNA was extracted by using TRIzol reagent according to the manufacturer's instructions (Invitrogen, Carlsbad,

**TABLE 1 |** Primer sequences for RT-qPCR and MeRIP-qPCR.

| Gene | Primer sequence (5′-3′) | Product length (bp) | Accession no |
|---|---|---|---|
| *METTL3* | F: CCACTTCTGGTGGCCCTAAG<br>R: CGCCAGATCAGAAAGGTGGT | 104 | XM_003128580.5 |
| *METTL14* | F: GAGATTGCAGCTCCTCGATCA<br>R: CCCCACTTGCGTAAACACAC | 89 | XM_003129231.6 |
| *WTAP* | F: GCGGGAATAAGGCCTCCAAC<br>R: TGTGAGTGGCGTGTGAGAGA | 136 | XM_005659114.3 |
| *FTO* | F: GCATGGCTGCTTATTTCGGG<br>R: TGCATCAGAGCCCTTCACTG | 154 | NM_001112692.1 |
| *ALKBH5* | F: CCAGTTCAAGCCTATCCGGG<br>R: ATCCACTGAGCACAGTCACG | 80 | XM_021067995.1 |
| *YTHDF1* | F: ATCGCCTCCTACAAGCACTC<br>R: CTGTTTGCTCCGATTCTGCC | 111 | XM_021078236.1 |
| *YTHDF2* | F: GGACAACTGAGCAACGGAGA<br>R: GCTGAGAAGTCAATCCCGCT | 131 | XM_005665152.3 |
| *YTHDF3* | F: CAACCAATAGTGTGCCCCCA<br>R: TGGGTTGGTGGAGCCTTTAC | 214 | XM_021089309.1 |
| *YTHDC1* | F: TGAGAATGTGTCCCTTGCCA<br>R: CACCTCCCAGCATCTTAGCAT | 230 | XM_021101402.1 |
| *YTHDC2* | F: GAAGTGATGGATGGGAGCGA<br>R: ATATCACCACCACCTCGTGC | 142 | XM_021084629.1 |
| *EGR1* | F: GGACATGGCGACAACCTTTT<br>R: TCCCACCTAAGAGGAACCCT | 139 | XM_003123974.6 |
| *MYC* | F: TCAGAAAAAGACGTGCTGCG<br>R: AGTTCCTCCCTCCAATAGGTCA | 102 | NM_001005154.1 |
| *FZD7* | F: CAAGTTCGGCTTCCAATGGC<br>R: CATGTAGGGCGCTGTAGGAT | 148 | XM_013984388.2 |
| *WNT9A* | F: GGAGAAGAACTGCGAGAGCAT<br>R: GTATAGACCTCCTCACGCTGG | 141 | XM_003123611.5 |
| *FOSL1* | F: CCCCAGTGGAAGTGGTTCAG<br>R: GAAGTCTCGGAACATGCCCT | 137 | XM_003122519.3 |
| *ITGA9* | F: AAGACAGTTGGGACTGGGTC<br>R: AGTGGGGCCTCCGAAAAATC | 141 | XM_021071659.1 |
| *IL2RA* | F: GCAACCATGCAGCCAATCAT<br>R: GGCTTCTTACTGCCCTTGGT | 161 | XM_021064060.1 |
| *TLR2* | F:GGAGCCTTAGAAGTAGAGTTTG<br>R: TGTCTCCACATTACCGAGGG | 102 | NM_213761.1 |
| *FZD5* | F: TCGTGAGGCCATTACTGGGA<br>R: TTTCGGCTTCTCAAATGCGG | 94 | XM_0056722133.3 |
| *WNT11* | F: CATGCGCTTCGCTTCCACTT<br>R: TCGGCTTCCTTTGATGTCCTG | 87 | XM_013979149.2 |
| *GAPDH* | F: AGTATGATTCCACCCACGGC<br>R: TACGTAGCACCAGCATCACC | 139 | XM_021091114.1 |

United States), and the m$^6$A content was detected with an m$^6$A RNA methylation quantification kit (Epigentek, Farmingdale, United States). Specifically, RNA purity was confirmed according to the following ratios: A260/A280 > 1.9 and A260/A230 > 1.7. In each reaction, the RNA (200 ng) samples were treated with an m$^6$A antibody, and detection was performed based on the manufacturer's instructions. Finally, the absorbance values were measured at 450 nm.

## Real-Time Quantitative PCR (RT-qPCR)

RNA (800 ng) from each sample was employed to synthesize cDNA by using a reverse transcription kit (Accurate Biotechnology, Changsha, China). Thereafter, a SYBR® Green Premix Pro Taq HS qPCR Kit (Accurate Biotechnology) and a LightCycler 480II apparatus (Roche, Basel, Switzerland) were used to perform RT-qPCR. The sequences of the primers used in this study are presented in **Table 1**; *GAPDH* served as an internal control. The relative levels of DEGs were determined by the $2^{-\Delta\Delta Ct}$ method (Livak and Schmittgen, 2001).

## m$^6$A-Seq and RNA-Seq Library Construction

First, RNA was extracted, and the RNA purity and integrity were analyzed. Total RNA was extracted from IPEC-J2 cells (see *CPB2 toxin treatment of cells and total m6A measurement*) by using TRIzol reagent (Invitrogen, Carlsbad, United States) and then quantified with a NanoDrop ND-1000 instrument (NanoDrop, Wilmington, United States). A Bioanalyzer 2100 system (Agilent, Santa Clara, United States) was used to evaluate the integrity of RNA according to the criterion of an RNA integrity number (RIN) > 7.0. RNA integrity was further confirmed by denaturing agarose gel electrophoresis. Second, the input (RNA-seq) library and the immunoprecipitation (IP) (m$^6$A-seq) library were

constructed. Briefly, an Epicenter Ribo-Zero Gold Kit (Illumina, San Diego, United States) was applied to digest and remove ribosomal RNA (rRNA) from the total RNA. A Magnesium RNA Fragmentation Module (NEB, Ipswich, United States) was used to fragment the RNA into 150-nucleotide-long fragments at 86°C for 7 min. The obtained RNA fragments were then divided into two portions. One portion was used to directly construct a conventional transcriptome sequencing library, which was retained as the input RNA, while the other portion was enriched by an m$^6$A-specific antibody (Synaptic Systems, Gottingen, Germany) and was retained as IP RNA. Thereafter, the IP RNA and input RNA were reverse-transcribed to cDNA by SuperScript™ II Reverse transcriptase (Invitrogen, Carlsbad, United States). The second strand of DNA was then synthesized, and adapters were added to the blunt ends of each strand (each adapter contained a T-base overhang for ligating the adapter to the A-tailed fragmented DNA) by using *E. coli* DNA polymerase I (NEB, Ipswich, United States), RNase H (NEB, Ipswich, United States) and a dUTP Solution (Thermo Fisher, San Jose, United States). Then, the two strands were digested with the enzyme UDG (NEB), after which PCR was conducted with the following program: predenaturation at 95°C for 3 min; eight cycles of 15 s at 98°C, 15 s at 60°C (annealing), and 30 s at 72°C (extension); and a final extension at 72°C for 5 min. The average insert size for the final cDNA library was 300 ± 50 bp. Finally, the Illumina NovaSeq™ 6000 platform (Illumina, San Diego, United States) was used to carry out double-ended sequencing according to its standard operating procedures in PE150 sequencing mode by LC Bio Technology Co., Ltd., Hangzhou, China.

## Bioinformatic Analysis of m$^6$A-Seq and RNA-Seq

Data quality control. We handled the raw data reads of the IP and input samples by using Fastp software (https://github.com/OpenGene/fastp). In this process, the reads showing adaptor contamination, presenting an N ratio >5%, and containing low-quality sequences were removed. Finally, clean reads were obtained (Chen et al., 2018; Wang et al., 2021; Zhao et al., 2021).

Peak identification and differential peak analysis. HISAT2 software (Kim et al., 2015) (http://daehwankimlab.github.io/hisat2) was used to map reads to the *Sus scrofa* 11.1 reference genome (ftp://ftp.ensembl.org/pub/release-96/fasta/sus_scrofa/dna/). The mapped reads of the IP and input samples were employed for differential peak analysis by using the R package exomePeak (https://bioconductor.org/packages/exomePeak) (Meng et al., 2014; Wang et al., 2021). The peaks were visualized with IGV software (http://www.igv.org) (Robinson et al., 2017; Yang et al., 2020). We annotated the peaks by using ChIPseeker (https://bioconductor.org/packages/ChIPseeker) (Yu et al., 2015). Finally, a motif analysis was performed with the MEME2 (http://meme-suite.org) (Bailey et al., 2009) and HOMER (http://homer.ucsd.edu/homer/motif) (Heinz et al., 2010) softwares.

DMGs and DEGs analysis. StringTie (https://ccb.jhu.edu/software/stringtie) was used to determine the expression levels of all the mRNA transcripts from the input libraries by calculating their fragments per kilobase of transcript per million mapped reads (FPKM) values (total exon fragments/mapped reads [millions] × exon length [kb]) (Pertea et al., 2015), and the R package edgeR (https://bioconductor.org/packages/edgeR) was used to analyze the DEGs (Robinson et al., 2010). Gene Ontology (GO) and Kyoto Encyclopedia of Genes and Genomes (KEGG) analyses were performed with Database for Annotation, Visualization and Integrated Discovery by using OmicStudio tools (https://www.omicstudio.cn/tool) (Chen et al., 2020; Zhou et al., 2020).

## M$^6$A IP (MeRIP) Followed RT-qPCR (MeRIP-qPCR)

RNA (1,000 ng/μL) samples from the control and CPB2 groups (300 μL each sample) were subjected to m$^6$A IP using the GenSeq® m$^6$A MeRIP Kit (GenSeq Inc., Shanghai, China) according to the manufacturer's protocol (Wang et al., 2020a; Hou et al., 2021). Briefly, the RNA was fragmented into smaller pieces of 200 nt by using an RNA fragmentation reagent and then divided into 3 and 297 μL. 3 μL was directly reverse-transcribed into cDNA (input), while the 297 μL was enriched with an m$^6$A antibody and then reverse-transcribed into cDNA (IP) after purification. Finally, RT-qPCR was performed for detection.

## Statistical Analyses

All experimental procedures were performed at least three times. The m$^6$A peaks were filtered according to two criteria: enrichment ≥2 and a $p$-value < 0.05. The differential peaks and DEGs were screened in the CPB2 group vs the control group according to a |log2 (fold change)| >0.585 and a $p$-value < 0.05. The RT-qPCR and MeRIP-qPCR data were analyzed by using the SPSS v.21 and GraphPad Prism v.8.0 software programs. The mean ± standard deviation (SD) was used to describe the data, and statistically significant differences are denoted with one asterisk (*) for $p < 0.05$ or two asterisks (**) for $p < 0.01$.

# RESULTS

## Detection of Methylation-Related Enzyme Expression and m$^6$A Levels

To investigate the effect of m$^6$A modification in CPB2-induced IPEC-J2 cells, the mRNA expression levels of methylation-related enzymes and the total m$^6$A content of the control and CPB2 groups were detected by RT-qPCR and with an m$^6$A RNA methylation quantification kit, respectively. As shown in **Figures 1A,B**, the expression levels of *METTL3*, *ALKBH5*, and *YTHDF3* were increased dramatically ($p < 0.01$), while those of *METTL14*, *FTO*, and *YTHDC2* were decreased significantly in the CPB2 toxin group relative to the control group ($p < 0.01$); *WTAP* and *YTHDC1* levels were also decreased ($p < 0.05$), but *YTHDF1* and *YTHDF2* levels were not changed ($p > 0.05$) (**Figure 1A**). In addition, the total m$^6$A level was obviously increased in the CPB2 group ($p < 0.01$, **Figure 1B**). These results suggested that

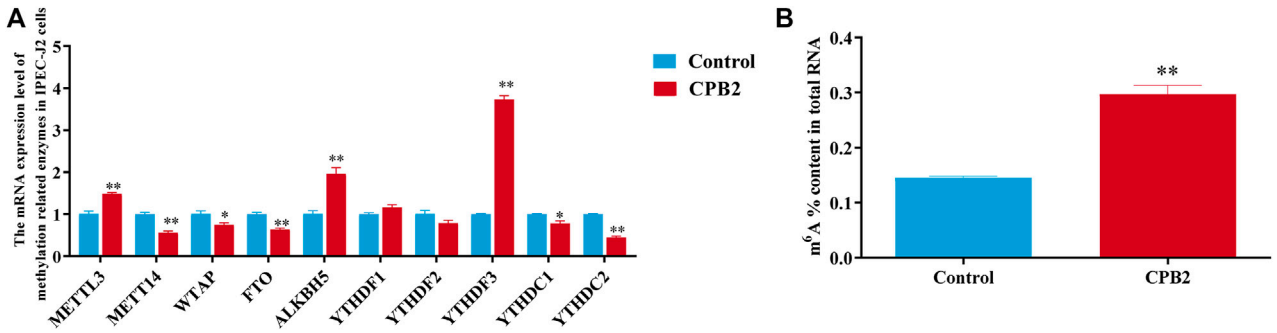



**FIGURE 1 |** Evaluation of the expression levels of methylase-related enzymes and m$^6$A levels under 20 μg/mL CPB2 treatment. **(A)** qPCR analysis of the expression of methylation-related enzymes after 24 h of cells exposure to 20 μg/ml CPB2 toxin. **(B)** Determination of m$^6$A levels in IPEC-J2 cells after treating with 20 μg/mL CPB2 for 24 h.

**TABLE 2 |** Sequence statistics and quality control.

| Sample ID | Raw reads | Valid reads | Valid% | Q20% | Q30% | GC% |
|---|---|---|---|---|---|---|
| Control1_IP | 85,492,316 | 82,300,032 | 87.19 | 96.52 | 90.94 | 52.87 |
| Control2_IP | 87,774,992 | 84,673,108 | 88.09 | 96.52 | 90.97 | 53.28 |
| Control3_IP | 86,612,186 | 83,480,924 | 87.76 | 96.33 | 90.59 | 53.39 |
| CPB2_1_IP | 90,242,216 | 86,944,982 | 87.8 | 96.56 | 91.01 | 52.96 |
| CPB2_2_IP | 86,934,932 | 83,429,868 | 86.82 | 96.39 | 90.78 | 53.41 |
| CPB2_3_IP | 89,642,446 | 86,070,422 | 86.79 | 96.41 | 90.77 | 53.99 |
| Control1_input | 97,586,308 | 93,048,292 | 84.9 | 96.54 | 91.09 | 55.12 |
| Control2_input | 96,994,146 | 92,000,280 | 84.62 | 96.53 | 91.09 | 55.3 |
| Control3_input | 93,495,320 | 88,512,112 | 84.2 | 96.3 | 90.67 | 55.92 |
| CPB2_1_input | 95,043,768 | 90,159,134 | 84.15 | 96.58 | 91.17 | 55.18 |
| CPB2_2_input | 97,478,686 | 91,769,152 | 83.24 | 96.37 | 90.85 | 55.73 |
| CPB2_3_input | 92,752,804 | 88,474,096 | 84.76 | 96.46 | 90.95 | 55.71 |

differences in m$^6$A methylation modifications may exist between the control group and the CPB2 group.

## Sequence Statistics and Quality Control

To further explore the biological process of m$^6$A modification in IPEC-J2 cells exposed to CPB2 toxin, three samples each from the control and CPB2 groups were collected for m$^6$A sequencing. Two types of libraries corresponding to the control group and CPB2 group were further constructed and designated the IP libraries (m$^6$A-seq) and the input libraries (RNA-seq), respectively. For the IP libraries, a total of 89,642,446–90,242,216 raw reads were obtained for the CPB2 group, while 85,492,316–87,774,992 raw reads were obtained for the control group (**Table 2**). For the input libraries, there were 92,752,804–97,478,686 raw reads for the CPB2 group and 93,495,320–97,586,308 raw reads for the control group (**Table 2**). The percentages of clean (valid) reads for the control group and the CPB2 group were greater than 86.79% in the IP libraries and 83.24% in the input libraries. For all libraries, the Q20 and Q30 values were at least 90% (**Table 2** and **Supplementary Table S1**). In addition, clean reads whose ribosome sequences were removed were compared with the porcine reference genome. The results showed that the clean reads were mainly aligned to exon regions, introns, and intergenic regions, and the proportions of exons exceeded 60% in the control and CPB2 groups (**Supplementary Figure S1**; **Table S2**).

## Peak Distributions of m$^6$A Modifications in the Whole Genome

After the full-range peak calling results of the porcine reference genome were scanned, a Poisson distribution model was used to check the reads of the candidate peak regions and to calculate the *p*-values of given peak regions. In this experiment, we were able to distinguish the differences in these peaks (i.e., enrichment ≥2, $p < 0.05$) and identify the peaks in the IP libraries, whose results were compared with those of the input libraries. We found that the numbers of peaks in the control group vs the CPB2 group were 20,533 and 19,241, respectively (**Supplementary Table S3**). Additionally, 18,695 peaks were the same between the control group and the CPB2 group, accounting for 90% of all detected peaks (**Figure 2A**). Furthermore, we analyzed the distributions of peaks on the pig chromosomes in the CPB2 group and control group. Interestingly, there were more peaks on chromosomes 1, 2, 3, 6, 12, 13, and 14 than on other chromosomes, and the most peaks were distributed on chromosome 6 (**Figures 2B,C**, **Supplementary Table S4**). Then, we analyzed the distributions of peaks in gene functional elements in both groups. The results showed that the m$^6$A peaks in the control

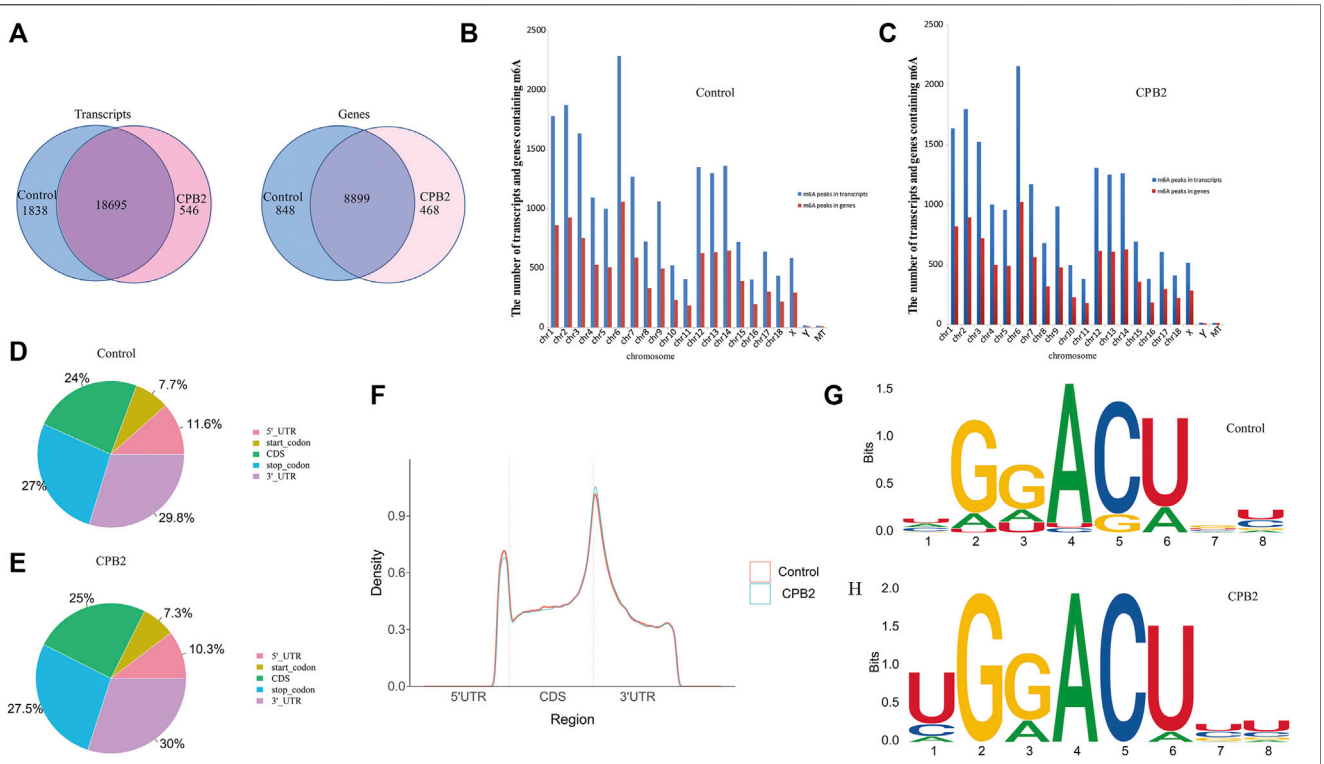



**FIGURE 2 |** Peak Distribution. **(A)** m$^6$A peaks distributions in the control group and CPB2 group among mRNA transcripts (left) and genes (right). **(B)** Numbers of m$^6$A peaks in the mRNA transcripts and genes of chromosomes in the control group. **(C)** Numbers of m$^6$A peaks in the mRNA transcripts and genes of chromosomes in the CPB2 group. **(D)** Distributions of m$^6$A peaks in different gene functional elements (5′UTR, 3′UTR, 1st exon, and other exons) in the control group. **(E)** Distributions of m$^6$A peaks in different gene functional elements (5′UTR, 3′UTR, 1st exon, and other exons) in the CPB2 group. **(F)** Density distributions of m$^6$A peaks in different gene functional elements (5′UTR, CDS, and 3′UTR) in the control group and CPB2 group. **(G, H)** Motif sites in the control (top) and CPB2 groups (bottom).

group and CPB2 group were mainly enriched in the 3′UTRs and stop codon regions (**Figures 2D,E**, **Figure 2F**). Next, HOMER and MEME2 softwares were employed to identify the most reliable motifs in the peak regions, which identified the GGACU motif in the control group and the UGGACU motif in the CPB2 group (**Figures 2G,H**).

## Differential m$^6$A Peaks Between the CPB2 and Control Groups

To analyze the distributions of m$^6$A peaks among the different chromosomes, genes, and mRNA transcripts in the CPB2 and control groups, we scanned the differential peaks and found 1,448 differential m$^6$A peaks. Among these peaks, we found 437 significantly upregulated peaks in 394 genes (here referred to as differentially methylated genes, DMGs) and 1,011 significantly downregulated peaks in 920 genes (**Figure 3A** and **Supplementary Table S5**). The top 20 altered m$^6$A peaks represented the 10 most upregulated genes and the 10 most downregulated genes (**Table 3** and **Supplementary Table S5**). Furthermore, relative to the control group (excluding the peaks showing no significant difference on the mitochondrial chromosome), the CPB2 group exhibited differential peaks distributed on other chromosomes; there were more downregulated peaks than upregulated peaks, and the peaks were most abundant on chromosome 6 (**Figure 3B** and **Supplementary Table S6**). We also counted the peaks distributed in genes and found that many genes contained one peak, which accounted for 46.7% (184/394) of the DMGs with upregulated peaks and 48.9% (452/920) DMGs with downregulated (**Figure 3C** and **Supplementary Table S7**). In analyzing the number of differential peaks among all mRNA transcripts, we found that the majority of mRNA transcripts in the whole genome showed one peak, while a few mRNA transcripts showed two or more differential peaks (**Figure 3D** and **Supplementary Table S7**). In addition, we calculated the densities of m$^6$A modifications among mRNA molecules and found that the gene fragments containing more m$^6$A peaks were longer (**Figure 3E**).

## GO and KEGG Analysis of Genes Presenting Differential m$^6$A Peaks (DMGs)

To investigate the biological processes associated with m$^6$A modification in IPEC-J2 cells in response to CPB2 infection, we analyzed the functions of DMGs presenting upregulated m6A peaks (n = 437) or downregulated peaks (n = 1,011) according to GO terms and KEGG signaling pathways. The GO results were divided into three categories: the biological process (BP), cellular component (CC), and molecular function (MF) categories. The

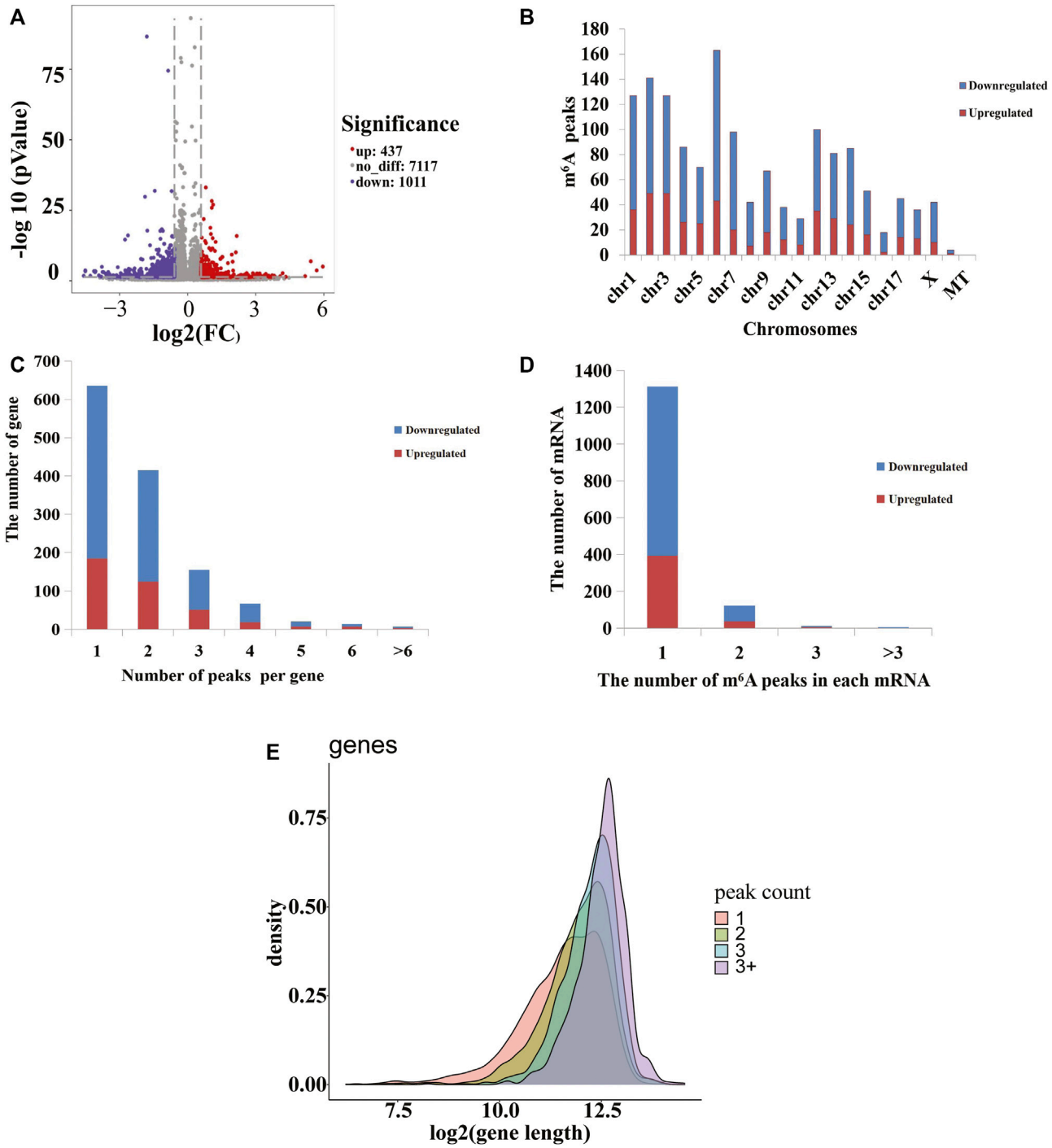



**FIGURE 3 |** m6A peaks in the control and CPB2 groups. **(A)** Significantly different m$^6$A peaks in the CPB2 group vs the control group. **(B)** Significant differences in the distributions of m$^6$A peaks on pig chromosomes. **(C)** Distributions of differential m$^6$A peaks in per gene. **(D)** Distributions of differential m$^6$A peaks in per mRNA. **(E)** Distributions of peaks with different sizes.

top 10 BP, CC, and MF terms that were enriched for genes with upregulated and downregulated m$^6$A peaks are shown in **Figures 4A,B**. For the KEGG pathway analysis, we display the top 10 enriched KEGG pathways based on their *p*-values. The results showed that genes with upregulated m$^6$A peaks were mainly enriched in cancer signaling pathways (20 genes), the Cushing syndrome signaling pathway (9 genes), and the Wnt signaling pathway (9 genes) (**Figure 4C** and **Supplementary Table S5**), while genes with downregulated m$^6$A peaks were mainly enriched in the apoptosis pathway (15 genes), the small cell lung cancer

**TABLE 3 |** Top 10 significantly upregulated and top 10 significantly downregulated m$^6$A peaks (CPB2 vs control).

| Chromosome | Peak start | Peak end | Gene ID | Gene name | Regulation | *p*-value | Log2 (fold change) | Peak region |
|---|---|---|---|---|---|---|---|---|
| chr12 | 41,074,651 | 41,075,895 | ENSSSCG00000031620 | ENSSSCG00000031620 | up | 8.91E-06 | 5.95 | 3′UTR |
| chr3 | 10,755,262 | 10,755,381 | ENSSSCG00000023004 | FZD9 | up | 0.00020417 | 5.68 | CDS |
| chr18 | 6,382,439 | 6,383,066 | ENSSSCG00000033909 | ENSSSCG00000033909 | up | 1.20E-07 | 5.42 | CDS |
| chr9 | 121,457,341 | 121,457,431 | ENSSSCG00000033352 | FAM163A | up | 0.02238721 | 5.17 | 3′UTR |
| chr10 | 28,509,561 | 28,509,920 | ENSSSCG00000033321 | GAS1 | up | 0.03890451 | 4.32 | CDS |
| chr15 | 140,319,882 | 140,320,272 | ENSSSCG00000034101 | D2HGDH | up | 0.00194984 | 4.18 | CDS |
| chr2 | 70,622,697 | 70,622,965 | ENSSSCG00000013607 | ENSSSCG00000013607 | up | 0.02570396 | 4.07 | 5′UTR |
| chr3 | 113,558,282 | 113,558,342 | ENSSSCG00000029413 | DNMT3A | up | 0.01659587 | 3.81 | CDS |
| chr4 | 98,093,837 | 98,093,896 | ENSSSCG00000006634 | TNFAIP8L2 | up | 0.03311311 | 3.81 | 3′UTR |
| chr8 | 12,807,001 | 12,807,091 | ENSSSCG00000008747 | NCAPG | up | 0.01202264 | 3.72 | 3′UTR |
| chrY | 25,251,102 | 25,252,331 | ENSSSCG00000034853 | ENSSSCG00000034853 | down | 0 | -10.1 | 3′UTR |
| chr6 | 54,469,817 | 54,469,877 | ENSSSCG00000038579 | DKKL1 | down | 0.01737801 | -4.58 | 3′UTR |
| chr4 | 97,240,279 | 97,240,459 | ENSSSCG00000006610 | S100A11 | down | 0.00019953 | -4.51 | 3′UTR |
| chr7 | 52,922,051 | 52,922,196 | ENSSSCG00000035897 | ENSSSCG00000035897 | down | 0.00041687 | -4.51 | CDS |
| chr7 | 23,655,139 | 23,655,378 | ENSSSCG00000001400 | DDX39B | down | 0.01659587 | -4.29 | 3′UTR |
| chr7 | 36,352,159 | 36,352,488 | ENSSSCG00000038553 | TSPO2 | down | 0.00038905 | -4.13 | 3′UTR |
| chr4 | 99,142,708 | 99,142,917 | ENSSSCG00000006666 | SV2A | down | 0.00091201 | -4.08 | 5′UTR |
| chrX | 58,487,996 | 58,488,554 | ENSSSCG00000011830 | ENSSSCG00000011830 | down | 0.00039811 | -4.06 | CDS |
| chrY | 25,253,141 | 25,253,380 | ENSSSCG00000034853 | ENSSSCG00000034853 | down | 0.01230269 | -3.91 | 3′UTR |
| chr6 | 159,511,892 | 159,511,981 | ENSSSCG00000027119 | SELRC1 | down | 0.03311311 | -3.81 | 5′UTR |

signaling pathway (11 genes) and the herpes simplex virus 1 infection signaling pathway (27 genes) (**Figure 4D** and **Supplementary Table S5**).

## DEGs (RNA-Seq Data) Following CPB2 Treatment of IPEC-J2 Cells

We used RNA-seq data (the m$^6$A-seq input library) to analyze DEGs after treating IPEC-J2 cells with CPB2 (**Figures 5A,B**, **Supplementary Table S8**). In total, 1,636 DEGs were detected in the CPB2 group relative to the control group, among which 1,094 DEGs were upregulated and 542 DEGs were downregulated. We list the top 20 most significantly upregulated genes and downregulated genes in tables (10 of each; **Table 4**, **Supplementary Table S8**), and the top 10 GO terms and top 10 KEGG pathways of the DEGs are displayed in **Figure 5C**, **Figure 5D**, and **Supplementary Table S8**. Both upregulated and downregulated genes were involved in the regulation of transcription, DNA templates, and signal transduction as well as the positive regulation of transcription by RNA polymerase in the BP category. The upregulated genes also participated in immune and inflammatory responses. The KEGG results indicated that upregulated genes were enriched predominantly in pathways related to influenza A cytokine-cytokine receptor interaction, cell adhesion molecules (CAMs), *Staphylococcus aureus* infection, NOD-like receptors, chemokines and TNF signaling pathways. The downregulated genes were involved in pathways related to Hippo signaling, Wnt signaling, terpenoid backbone biosynthesis, proteoglycans in cancer, melanogenesis, bladder cancer, transcriptional misregulation in cancer, basal cell carcinoma, glycolysis/gluconeogenesis, and TGF-beta signaling.

## Combined m$^6$A-Seq and RNA-Seq Analysis

To further explore the functional significance of m$^6$A modification in IPEC-J2 cells in response to CPB2, we investigated whether m$^6$A methylation was the basis of the observed expression differences. For this purpose, m$^6$A-seq data and RNA-seq data were used to detect DMGs and DEGs. Thereafter, combined m$^6$A-seq and RNA-seq analysis divided a total of 192 genes into four main groups (**Figure 6A** and **Supplementary Table S9**): a group of 52 hypermethylated and upregulated genes (hyper-up genes), a group of 47 hypomethylated and downregulated genes (hypo-down genes), a group of 18 hypermethylated and downregulated genes (hyper-down genes) and a group of 75 hypomethylated and upregulated genes (hypo-up genes). The 18 hyper-down genes, 52 hyper-up genes and 75 hypo-up genes were further investigated by KEGG analysis, which revealed that the top 10 enriched KEGG pathways among the hyper-down genes were mainly related to glycolysis/gluconeogenesis; neomycin, kanamycin, gentamicin biosynthesis and Wnt signaling pathways (**Figure 6B** and **Supplementary Table S9**). In contrast, the hyper-up genes were mainly enriched in the CAMs signaling pathway (**Figure 6C** and **Supplementary Table S9**). In addition, the 75 hypo-up genes were mainly enriched in signaling pathways such as the FoxO, Hippo, and basal cell carcinoma pathways (**Figure 6D** and **Supplementary Table S9**).

## Validation of DEGs and DMGs by qPCR and MeRIP-qPCR

To verify the m$^6$A-seq and RNA-seq data, we randomly selected 10 DEGs (*EGR1*, *MYC*, *FZD7*, *WNT9A*, *FOSL1*, *ITGA9*, *IL2RA*, *TLR2*, *FZD5*, and *WNT11*) and checked the reliability of the RNA-seq data by RT-qPCR. According to the combined m$^6$A-seq

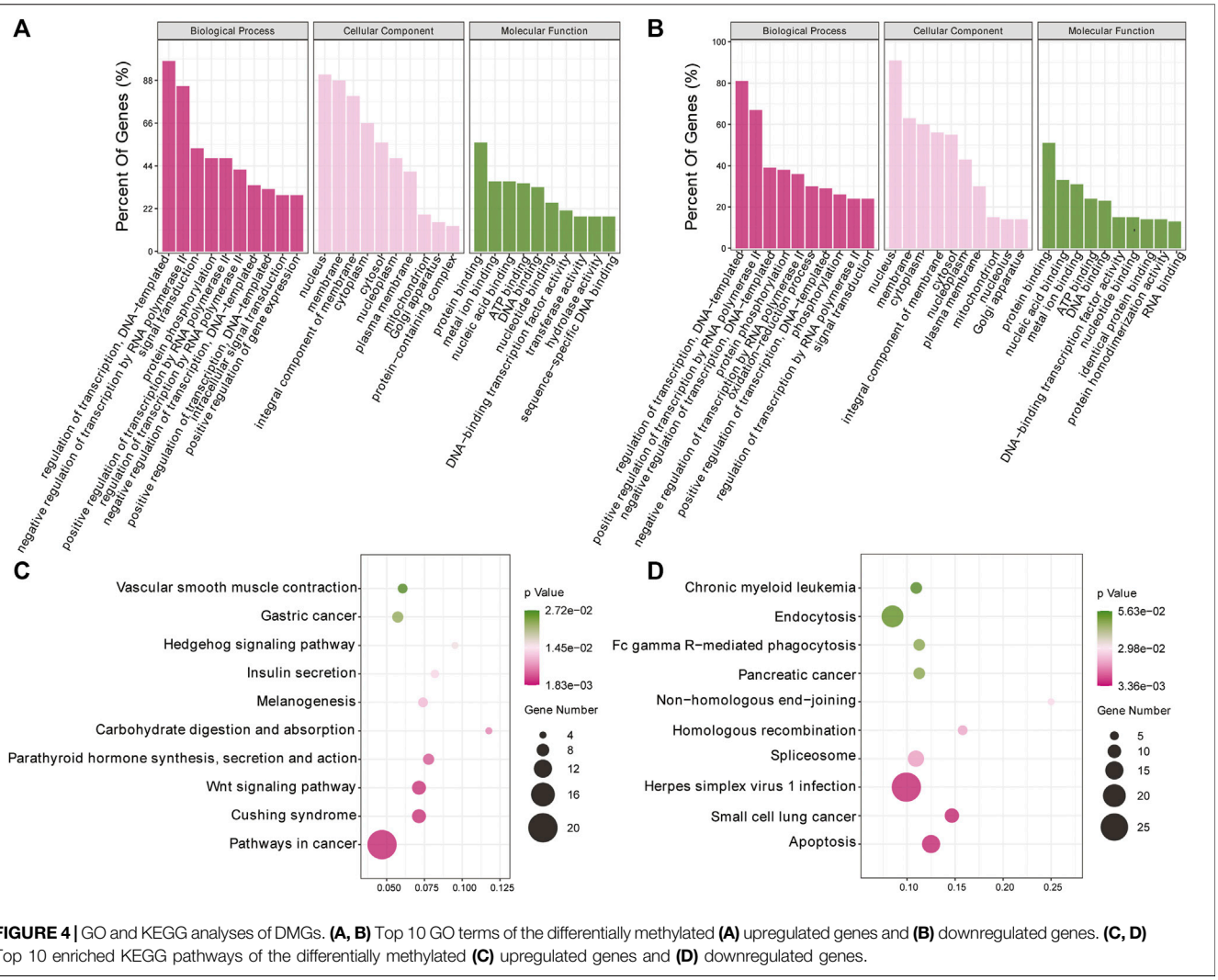



**FIGURE 4 |** GO and KEGG analyses of DMGs. **(A, B)** Top 10 GO terms of the differentially methylated **(A)** upregulated genes and **(B)** downregulated genes. **(C, D)** Top 10 enriched KEGG pathways of the differentially methylated **(C)** upregulated genes and **(D)** downregulated genes.

and RNA-seq analysis results, three DMGs (*WNT9A*, *FOSL1*, and *WNT11*) were selected for the MeRIP-qPCR assay. The RT-qPCR and MeRIP-qPCR results (**Figures 7A,B**) were consistent with the RNA-seq and m$^6$A-seq results, thus confirming the reliability of the results of our m$^6$A-seq experiment.

## DISCUSSION

Similar to DNA and protein modifications, m$^6$A modification is a dynamically reversible posttranscriptional change that mainly regulates mRNA expression, splicing, structure, stability, lifespan, and degradation as well as RNA modification during translation (Fu et al., 2014; Adhikari et al., 2016). This modification plays roles in bacterial and viral infections, intestinal diseases, and host immune responses (Sebastian-delaCruz et al., 2020; Wu et al., 2020). Feng et al. (2018) demonstrated that the expression levels of m$^6$A and *METTL3* were upregulated in HDPCs stimulated by LPS. Similarly, in another study, both the m$^6$A levels and the mRNA expression of *WTAP* increased when THP-1 cells were treated with heat-killed *Salmonella typhimurium* (HKST) (Wu et al., 2020). However, Zong et al. found that when IPEC-J2 cells were infected with *E. coli* K88, the methylation level of m$^6$A was significantly reduced, while the expression of m$^6$A reader proteins (*YTHDF1* and *YTHDF2*) were markedly increased, and the expression of the methyltransferase *METTL3* and the demethylase *FTO* were not changed; moreover, *E. coli* K88 infection was shown to cause intestinal inflammation and to impair lipid transport in the *YTHDF1*-dependent m$^6$A pathway in IPEC-J2 cells (Zong et al., 2018). In this experiment, we detected the mRNA expression of methylation-related enzymes and the overall level of m$^6$A methylation, and the results demonstrated that the mRNA expression levels of the methyltransferases *METTL3*, *METTL14*, and *WTAP* and the demethylases *FTO* and *ALKBH5* were altered, while the overall m$^6$A level was increased significantly. Therefore, we speculate that the m$^6$A methylation modification may be involved in the CPB2-induced inflammatory response of IPEC-J2 cells.

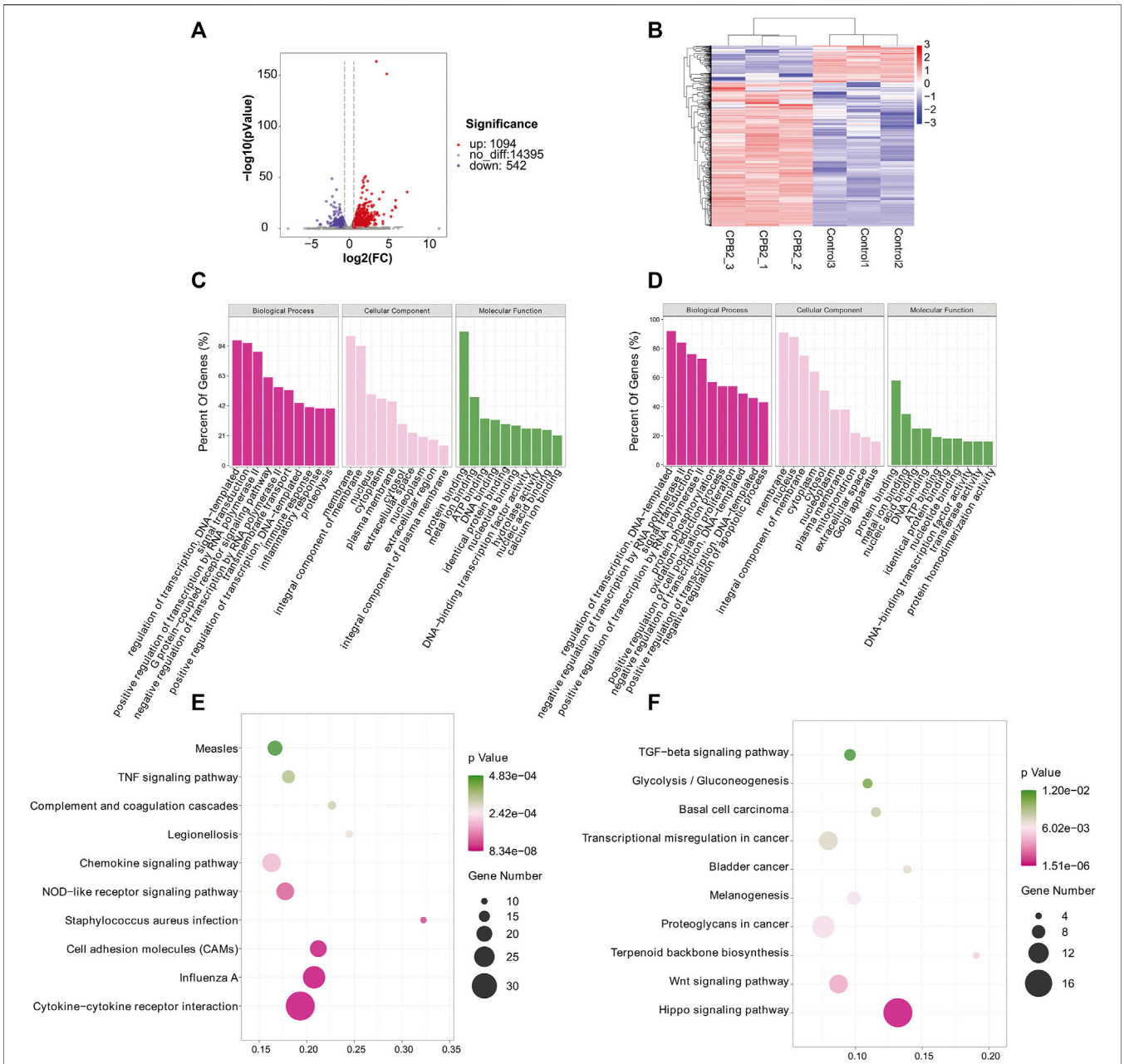



**FIGURE 5 |** GO and KEGG analyses of DEGs. **(A)** Volcano plot showing the differential gene expression in the CPB2 and control groups. **(B)** Heatmap showing the overall expression patterns of DEGs in three CPB2 individuals and three control individuals. Red indicates upregulated DEGs, and blue indicates downregulated DEGs. **(C, D)** Top 10 GO terms of the (C) upregulated and (D) downregulated DEGs. **(E, F)** Top 10 KEGG pathways enriched for the (E) upregulated and (F) downregulated DEGs.

In this study, we found 18,695 peaks that were the same in the CPB2 and control groups, which accounted for 90% of all the peaks. This indicated that most of the peaks corresponded to functions that maintained the physiological homeostasis of the organism. In mouse tissues and human cells, m$^6$A has been shown to be located mainly near stop codons and 3′UTRs (Dominissini et al., 2012; Meyer et al., 2012). We analyzed the distributions of m$^6$A peaks in different gene functional elements and found that m$^6$A peaks were indeed mainly distributed in 3′UTRs and stop codon regions. These findings are consistent with those of Wang et al. (2020b) and prove that m$^6$A motif enrichment is more common in 3′UTRs than in other regions. The 3′UTR regulates the stability, localization, expression, and translation of mRNA. Multiple RNA-binding proteins bind in this region to perform regulatory functions and regulate protein–protein interactions (Mayr, 2018). The m6A methylation recognition proteins, YTHDF1 and YTHDF2, mainly recognize the m$^6$A motifs of 3′UTRs and alter the

**TABLE 4 |** Top 10 upregulated and top 10 downregulated DEGs (CPB2 vs control).

| Gene name | Locus | Regulation | Fold change | *p*-value |
|---|---|---|---|---|
| OLFM4 | chr11:26,350,032–26,375,740 | up | 164.4964353 | 1.90719E-36 |
| CCL17 | chr6:19,345,764–19,348,965 | up | 60.09315203 | 4.09127E-21 |
| HHATL | chr13:26,205,616–26,219,937 | up | 59.85677737 | 1.96714E-28 |
| GC | chr8:68,326,287–68,364,937 | up | 57.73376422 | 3.20932E-22 |
| PRICKLE2 | chr13:45,620,368–45,789,113 | up | 43.95440161 | 1.42386E-18 |
| C3 | chr2:72,431,163–72,471,564 | up | 27.30318327 | 3.2955E-152 |
| SLFN11 | chr12:39,986,366–39,992,685 | up | 21.62979927 | 1.75657E-14 |
| ADORA2A | chr14:49,468,862–49,487,628 | up | 14.17608216 | 1.33747E-29 |
| PCP4L1 | chr4:89,186,937–89,212,840 | up | 13.8161881 | 2.28515E-13 |
| CCL22 | chr6:19,296,637–19,302,737 | up | 11.84724721 | 1.74685E-16 |
| ZSCAN26 | chrX:45,772,497–45,798,482 | down | 0.137483812 | 3.34197E-27 |
| ZFAND1 | chr15:32,408,854–32,475,979 | down | 0.151873654 | 2.66575E-07 |
| ITGA1 | chr6:47,643,560–47,657,784 | down | 0.161195423 | 9.01136E-06 |
| OCA2 | chr7:22,114,800–22,133,148 | down | 0.18087438 | 1.64436E-12 |
| NAB2 | chr4:54,908,876–54,931,825 | down | 0.195968666 | 1.13013E-05 |
| ZMAT2 | chr16:32,185,484–32,295,491 | down | 0.19937155 | 0.012466794 |
| ANKRD61 | chr15:56,657,598–56,869,920 | down | 0.199594035 | 0.003131712 |
| SPRY4 | chr5:22,400,548–22,410,479 | down | 0.203847311 | 1.0527E-10 |
| EGR1 | chr2:142,411,086–142,417,154 | down | 0.209337433 | 9.52077E-24 |
| MFAP3 | chr3:5,097,791–5,117,889 | down | 0.210674837 | 3.27485E-06 |

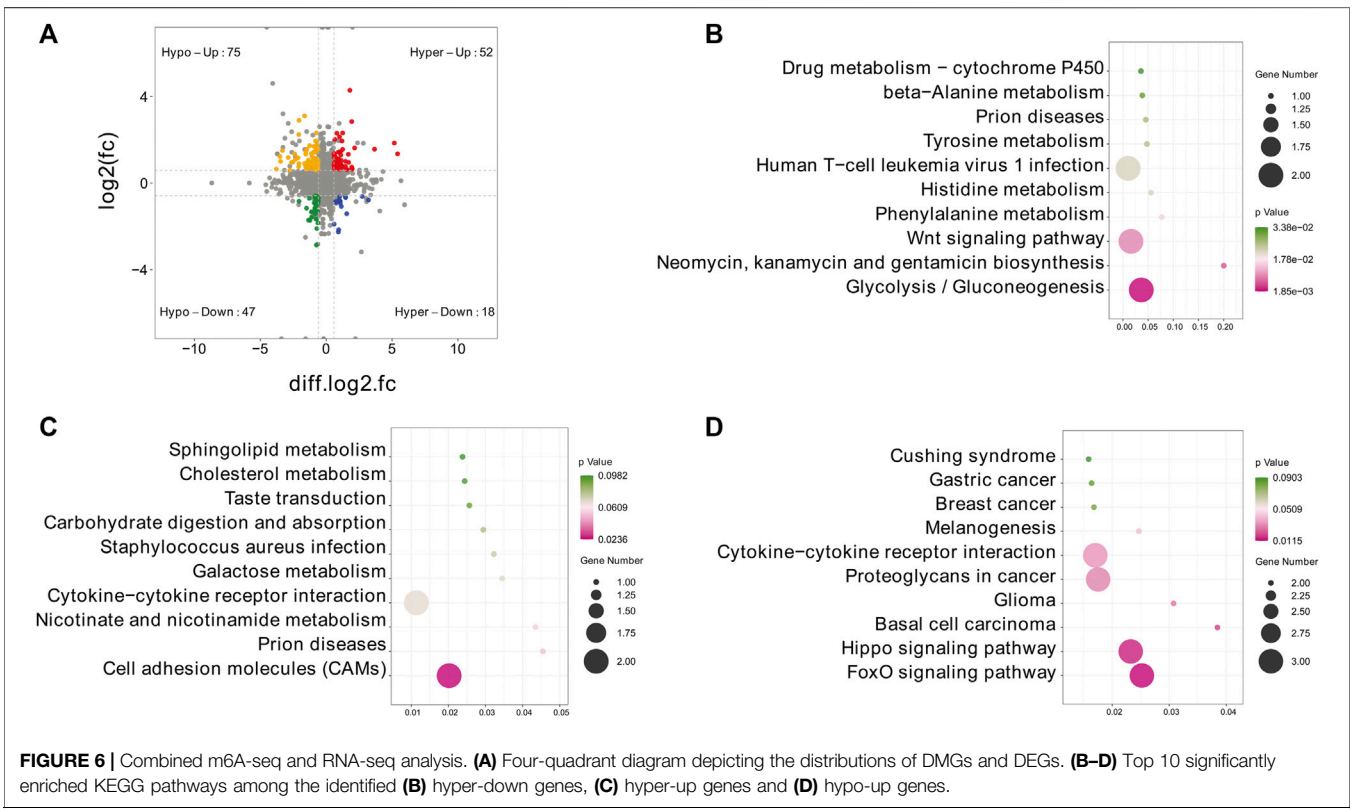



**FIGURE 6 |** Combined m6A-seq and RNA-seq analysis. **(A)** Four-quadrant diagram depicting the distributions of DMGs and DEGs. **(B–D)** Top 10 significantly enriched KEGG pathways among the identified **(B)** hyper-down genes, **(C)** hyper-up genes and **(D)** hypo-up genes.

translation efficiency and degradation rate of m$^6$A-modified RNA (Wang et al., 2015; Chen et al., 2018). A conserved m$^6$A motif sequence, gg (R: G, A, U; R: G, A; H: U, A, C), was recently reported (Han et al., 2019). Our results revealed conserved m$^6$A motifs of GGACU and UGGACU in the control and CPB2 groups, respectively, similar to the findings of Han et al. (2019). These results suggest that these motifs may be recognized by certain proteins and play important roles in IPEC-J2 cells in response to CPB2.

Relative to the control group, the CPB2 group exhibited 1,448 differential peaks (437 upregulated and 1,011 downregulated). The DMGs with upregulated peaks were mainly enriched in cancer

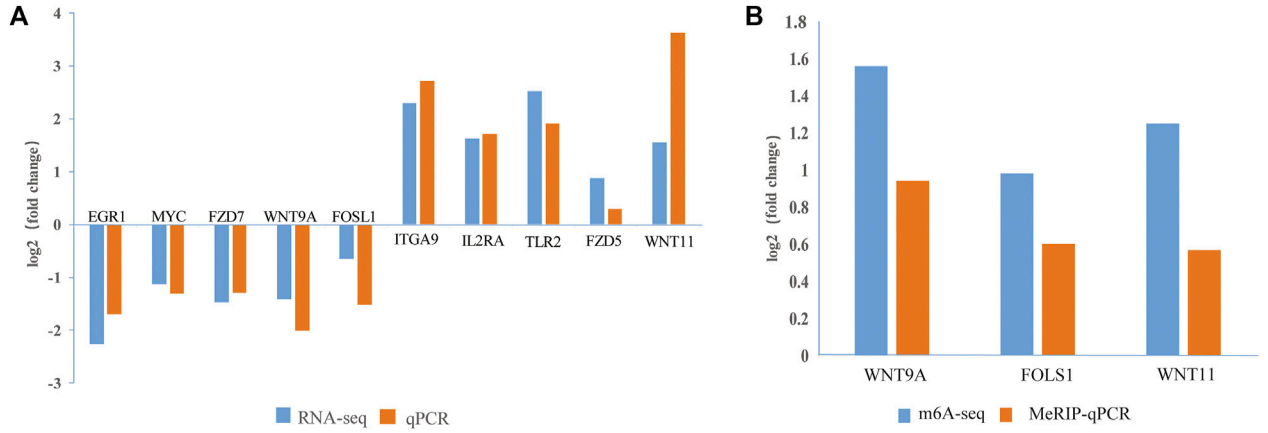



**FIGURE 7 |** Verification of DEGs and DMGs. **(A)** The expression levels of 10 genes were verified by qPCR and RNA-seq. **(B)** The m$^6$A methylation modifications of three genes were verified by MeRIP-qPCR and m$^6$A-seq. The fold changes are expressed as the ratios of gene expression in CPB2-treated vs control samples. The blue and orange bars indicate the RNA-seq and m$^6$A-seq or qRT-PCR and MeRIP-qPCR results, respectively.

signaling pathways, the Cushing syndrome signaling pathway and the Wnt signaling pathway. Interestingly, some of these genes appeared simultaneously in many signaling pathways. For example, *WNT11*, *WNT9A*, and *FZD9* were all enriched in cancer signaling pathways, the Cushing syndrome signaling pathway, and the Wnt signaling pathway. These three genes encode the main ligands and receptors that regulate the activation and deactivation of the Wnt signaling pathway. The Wnt signaling pathway impacts intestinal balance, self-renewal, and malignant transformation (Liu et al., 2011). The *WNT11* gene is a novel important contributor to intestinal homeostasis and host defense and participates in the protection of host intestinal cells by blocking the invasion of pathogenic bacteria, inhibiting inflammation, and inhibiting apoptosis (Liu et al., 2011). In addition, some studies have indicated that *WNT11* regulates the development of the heart and kidneys via an atypical Wnt signaling pathway and inhibits the inflammation of intestinal epithelial cells (Pandur et al., 2002; Majumdar et al., 2003; Liu et al., 2011). *WNT9A* is considered to act as a tumor suppressor gene in relation to the development of colorectal cancer (Ali et al., 2016). Intriguingly, according to the GO and KEGG analyses, we found that the DMGs and DEGs were almost always significantly enriched in the Wnt signaling pathway., Therefore, we propose that m$^6$A modification is involved in the inflammatory response induced by CPB2 in IPEC-J2 cells and that it may modulate this inflammatory response by influencing the gene expression of the Wnt signaling pathway.

## CONCLUSION

In this study, we analyzed how m$^6$A methylation is modified in CPB2-induced IPEC-J2 cells. The results suggest that m$^6$A methylation may play a role in the Wnt signaling pathway in CPB2-induced IPEC-J2 cells and exert anti-inflammatory or proinflammatory effects on intestinal diseases. These findings provide a basis for further research into the functions of m$^6$A methylation modifications in CPB2 toxin-induced piglet diarrhea.

## DATA AVAILABILITY STATEMENT

Our data are deposited in the G E O repository, the accession number: GSE167267. We have published our data on October 5, 2021. The link for data disclosure is as follows: https://www.ncbi.nlm.nih.gov/geo/query/acc.cgi?acc=GSE167267.

## AUTHOR CONTRIBUTIONS

JZ, QY, ZY, and SG conceived the project; JZ, JY, RL, XG, XH, and PW designed most experiments; WW, KX, XG, RL, and BZ performed data analyses; JZ, JY, WW, KX, RL and XG performed the experiments; and JZ wrote the paper with suggestions from SG.

## FUNDING

This work was supported by Education Science and Technology Innovation Project of Gansu Province (GSSYLXM-02), the National Natural Science Foundation of China (31960646), the Youth Science and Technology Fund Program of Gansu Province (20JR5RA005) and the Education Department of Gansu Province: Excellent Graduate student "Innovation Star" project 2021CXZX-351.

## ACKNOWLEDGMENTS

We thank LC-BIO Biotech Ltd. (Hangzhou, China) for supporting the high-throughput sequencing instrument.

## SUPPLEMENTARY MATERIAL

The Supplementary Material for this article can be found online at: https://www.frontiersin.org/articles/10.3389/fgene.2021.689748/full#supplementary-material.

## REFERENCES


Adhikari, S., Xiao, W., Zhao, Y.-L., and Yang, Y.-G. (2016). m6A: Signaling for mRNA Splicing. *RNA Biol.* 13 (9), 756–759. doi:10.1080/15476286.2016.1201628

Alarcón, C. R., Goodarzi, H., Lee, H., Liu, X., Tavazoie, S., and Tavazoie, S. F. (2015). HNRNPA2B1 Is a Mediator of m6A-dependent Nuclear RNA Processing Events. *Cell* 162 (6), 1299–1308. doi:10.1016/j.cell.2015.08.011

Ali, I., Medegan, B., and Braun, D. (2016). WNT9A Induction Linked to Suppression of Human Colorectal Cancer Cell Proliferation. *Ijms* 17 (4), 495–506. doi:10.3390/ijms17040495

Bailey, T. L., Boden, M., Buske, F. A., Frith, M., Grant, C. E., Clementi, L., et al. (2009). MEME SUITE: Tools for Motif Discovery and Searching. *Nucleic Acids Res.* 37, W202–W208. doi:10.1093/nar/gkp335

Chen, J., Zhang, Z., Lei, Z., Shimizu, K., Yao, P., Su, Z., et al. (2020). Occurrence and Distribution of Antibiotic Resistance Genes in the Coastal Sediments of Effluent-Receiving Areas of WWTPs, China. *Bioresour. Tech. Rep.* 11 (100511), 100511–100517. doi:10.1016/j.biteb.2020.100511

Chen, S., Zhou, Y., Chen, Y., and Gu, J. (2018). Fastp: an Ultra-fast All-In-One FASTQ Preprocessor. *Bioinformatics* 34 (17), i884–i890. doi:10.1093/bioinformatics/bty560

Dominissini, D., Moshitch-Moshkovitz, S., Schwartz, S., Salmon-Divon, M., Ungar, L., Osenberg, S., et al. (2012). Topology of the Human and Mouse m6A RNA Methylomes Revealed by m6A-Seq. *Nature* 485 (7397), 201–206. doi:10.1038/nature11112

Feng, Z., Li, Q., Meng, R., Yi, B., and Xu, Q. (2018). METTL 3 Regulates Alternative Splicing of MyD88 upon the Lipopolysaccharide-induced Inflammatory Response in Human Dental Pulp Cells. *J. Cel. Mol. Med.* 22 (5), 2558–2568. doi:10.1111/jcmm.13491

Fu, Y., Dominissini, D., Rechavi, G., and He, C. (2014). Gene Expression Regulation Mediated through Reversible m6A RNA Methylation. *Nat. Rev. Genet.* 15 (5), 293–306. doi:10.1038/nrg3724

Fustin, J.-M., Doi, M., Yamaguchi, Y., Hida, H., Nishimura, S., Yoshida, M., et al. (2013). RNA-methylation-dependent RNA Processing Controls the Speed of the Circadian Clock. *Cell* 155, 793–806. doi:10.1016/j.cell.2013.10.026

Gao, X., Yang, Q., Huang, X., Yan, Z., Zhang, S., Luo, R., et al. (2020). Effects of *Clostridium perfringens* Beta2 Toxin on Apoptosis, Inflammation, and Barrier Function of Intestinal Porcine Epithelial Cells. *Microb. Pathogenesis* 147, 104379. doi:10.1016/j.micpath.2020.104379

Garcia, J. P., Beingesser, J., Fisher, D. J., Sayeed, S., McClane, B. A., Posthaus, H., et al. (2012). The Effect of *Clostridium perfringens* Type C Strain CN3685 and its Isogenic Beta Toxin Null Mutant in Goats. *Vet. Microbiol.* 157 (3-4), 412–419. doi:10.1016/j.vetmic.2012.01.005

Gibert, M., Jolivet-Renaud, C., and Popoff, M. R. (1997). Beta2 Toxin, a Novel Toxin Produced by *Clostridium perfringens*. *Gene* 203 (1), 65–73. doi:10.1016/s0378-1119(97)00493-9

Han, D., Liu, J., Chen, C., Dong, L., Liu, Y., Chang, R., et al. (2019). Anti-tumour Immunity Controlled through mRNA m6A Methylation and YTHDF1 in Dendritic Cells. *Nature* 566 (7743), 270–274. doi:10.1038/s41586-019-0916-x

Heinz, S., Benner, C., Spann, N., Bertolino, E., Lin, Y. C., Laslo, P., et al. (2010). Simple Combinations of Lineage-Determining Transcription Factors Prime Cis-Regulatory Elements Required for Macrophage and B Cell Identities. *Mol. Cel* 38, 576–589. doi:10.1016/j.molcel.2010.05.004

Hou, G., Zhao, X., Li, L., Yang, Q., Liu, X., Huang, C., et al. (2021). SUMOylation of YTHDF2 Promotes mRNA Degradation and Cancer Progression by Increasing its Binding Affinity with m6A-Modified mRNAs. *Nucleic Acids Res.* 49 (5), 2859–2877. doi:10.1093/nar/gkab065

Huang, H., Weng, H., and Chen, J. (2020). m6A Modification in Coding and Non-coding RNAs: Roles and Therapeutic Implications in Cancer. *Cancer Cell* 37 (3), 270–288. doi:10.1016/j.ccell.2020.02.004

Huang, H., Weng, H., Sun, W., Qin, X., Shi, H., Wu, H., et al. (2018). Recognition of RNA N6-Methyladenosine by IGF2BP Proteins Enhances mRNA Stability and Translation. *Nat. Cel Biol* 20 (3), 285–295. doi:10.1038/s41556-018-0045-z

Immerseel, F. V., Buck, J. D., Pasmans, F., Huyghebaert, G., Haesebrouck, F., and Ducatelle, R. (2004). Clostridium Perfringensin Poultry: an Emerging Threat for Animal and Public Health. *Avian Pathol.* 33 (6), 537–549. doi:10.1080/03079450400013162

Kim, D., Langmead, B., and Salzberg, S. L. (2015). HISAT: a Fast Spliced Aligner with Low Memory Requirements. *Nat. Methods* 12 (4), 357–360. doi:10.1038/nmeth.3317

Liu, N., Dai, Q., Zheng, G., He, C., Parisien, M., and Pan, T. (2015). N6-methyladenosine-dependent RNA Structural Switches Regulate RNA-Protein Interactions. *Nature* 518 (7540), 560–564. doi:10.1038/nature14234

Liu, X., Wu, S., Xia, Y., Li, X. E., Xia, Y., Zhou, Z. D., et al. (2011). Wingless Homolog Wnt11 Suppresses Bacterial Invasion and Inflammation in Intestinal Epithelial Cells. *Am. J. Physiology-Gastrointestinal Liver Physiol.* 301 (6), G992–G1003. doi:10.1152/ajpgi.00080.2011

Livak, K. J., and Schmittgen, T. D. (2001). Analysis of Relative Gene Expression Data Using Real-Time Quantitative PCR and the 2−ΔΔCT Method. *Methods* 25 (4), 402–408. doi:10.1006/meth.2001.1262

Luo, R., Yang, Q., Huang, X., Yan, Z., Gao, X., Wang, W., et al. (2020). *Clostridium perfringens* Beta2 Toxin Induced *In Vitro* Oxidative Damage and its Toxic Assessment in Porcine Small Intestinal Epithelial Cell Lines. *Gene* 759, 144999. doi:10.1016/j.gene.2020.144999

Majumdar, A., Vainio, S., Kispert, A., McMahon, J., and McMahon, A. P. (2003). Wnt11andRet/Gdnfpathways Cooperate in Regulating Ureteric Branching during Metanephric Kidney Development. *Development* 130, 3175–3185. doi:10.1242/dev.00520

Mayr, C. (2018). What Are 3′ UTRs Doing? *Cold Spring Harb Perspect. Biol.* 11 (4), a034728–15. doi:10.1101/cshperspect.a034728

Meng, J., Lu, Z., Liu, H., Zhang, L., Zhang, S., Chen, Y., et al. (2014). A Protocol for RNA Methylation Differential Analysis with MeRIP-Seq Data and exomePeak R/Bioconductor Package. *Methods* 69 (3), 274–281. doi:10.1016/j.ymeth.2014.06.008

Meyer, K. D., Saletore, Y., Zumbo, P., Elemento, O., Mason, C. E., and Jaffrey, S. R. (2012). Comprehensive Analysis of mRNA Methylation Reveals Enrichment in 3′ UTRs and Near Stop Codons. *Cell* 149 (7), 1635–1646. doi:10.1016/j.cell.2012.05.003

Pandur, P., Läsche, M., Eisenberg, L. M., and Kühl, M. (2002). Wnt-11 Activation of a Non-canonical Wnt Signalling Pathway Is Required for Cardiogenesis. *Nature* 418, 636–641. doi:10.1038/nature00921

Patil, D. P., Chen, C.-K., Pickering, B. F., Chow, A., Jackson, C., Guttman, M., et al. (2016). m6A RNA Methylation Promotes XIST-Mediated Transcriptional Repression. *Nature* 537 (7620), 369–373. doi:10.1038/nature19342

Pertea, M., Pertea, G. M., Antonescu, C. M., Chang, T.-C., Mendell, J. T., and Salzberg, S. L. (2015). StringTie Enables Improved Reconstruction of a Transcriptome from RNA-Seq Reads. *Nat. Biotechnol.* 33 (3), 290–295. doi:10.1038/nbt.3122

Robinson, J. T., Thorvaldsdóttir, H., Wenger, A. M., Zehir, A., and Mesirov, J. P. (2017). Variant Review with the Integrative Genomics Viewer. *Cancer Res.* 77 (21), e31–e34. doi:10.1158/0008-5472.CAN-17-0337

Robinson, M. D., Mccarthy, D. J., and Smyth, G. K. (2010). edgeR: a Bioconductor Package for Differential Expression Analysis of Digital Gene Expression Data. *Bioinformatics* 26 (1), 139–140. doi:10.1093/bioinformatics/btp616

Sebastian-delaCruz, M., Olazagoitia-Garmendia, A., Gonzalez-Moro, I., Santin, I., Garcia-Etxebarria, K., and Castellanos-Rubio, A. (2020). Implication of m6A mRNA Methylation in Susceptibility to Inflammatory Bowel Disease. *Epigenomes* 4, 16. doi:10.3390/epigenomes4030016

Shi, H., Wang, X., Lu, Z., Zhao, B. S., Ma, H., Hsu, P. J., et al. (2017). YTHDF3 Facilitates Translation and Decay of N6-Methyladenosine-Modified RNA. *Cell Res* 27 (3), 315–328. doi:10.1038/cr.2017.15

Wang, X., Zhao, B. S., Roundtree, I. A., Lu, Z., Han, D., Ma, H., et al. (2015). N6-methyladenosine Modulates Messenger RNA Translation Efficiency. *Cell* 161 (6), 1388–1399. doi:10.1016/j.cell.2015.05.014

Wang, Y., Sun, J., Lin, Z., Zhang, W., Wang, S., Wang, W., et al. (2020b). m6A mRNA Methylation Controls Functional Maturation in Neonatal Murine β-Cells. *Diabetes* 69 (8), 1708–1722. doi:10.2337/db19-0906

Wang, Y., Zhang, L., Ren, H., Ma, L., Guo, J., Mao, D., et al. (2021). Role of Hakai in m$^6$A Modifycation Pathway in Drosophila. *Nat. Commun.* 12 (1), 1–15. doi:10.1038/s41467-021-22424-51

Wang, Y., Zheng, Y., Guo, D., Zhang, X., Guo, S., Hui, T., et al. (2020a). m6A Methylation Analysis of Differentially Expressed Genes in Skin Tissues of Coarse and Fine Type Liaoning Cashmere Goats. *Front. Genet.* 10, 1318. doi:10.3389/fgene.2019.01318

Wu, C., Chen, W., He, J., Jin, S., Liu, Y., Yi, Y., et al. (2020). Interplay of m6A and H3K27 Trimethylation Restrains Inflammation during Bacterial Infection. *Sci. Adv.* 6 (34), eaba0647. doi:10.1126/sciadv.aba0647

Xiao, W., Adhikari, S., Dahal, U., Chen, Y.-S., Hao, Y.-J., Sun, B.-F., et al. (2016). Nuclear M 6 A Reader YTHDC1 Regulates mRNA Splicing. *Mol. Cel* 61 (4), 507–519. doi:10.1016/j.molcel.2016.01.012

Yang, J., Liu, J., Zhao, S., and Tian, F. (2020). N6-methyladenosine Mettl3 Modulates the Proliferation and Apoptosis of Lens Epithelial Cells in Diabetic Cataract. *Mol. Ther. - Nucleic Acids* 20, 111–116. doi:10.1016/j.omtn.2020.02.002

Yu, G., Wang, L.-G., and He, Q.-Y. (2015). ChIPseeker: an R/Bioconductor Package for ChIP Peak Annotation, Comparison and Visualization. *Bioinformatics* 31 (14), 2382–2383. doi:10.1093/bioinformatics/btv145

Zhao, T., Wang, J., Wu, Y., Han, L., Chen, J., Wei, Y., et al. (2021). Increased m6A Modification of RNA Methylation Related to the Inhibition of Demethylase FTO Contributes to MEHP-Induced Leydig Cell Injury☆. *Environ. Pollut.* 268 (115627), 115627–115637. doi:10.1016/j.envpol.2020.115627

Zhao, X., Yang, Y., Sun, B.-F., Shi, Y., Yang, X., Xiao, W., et al. (2014). FTO-dependent Demethylation of N6-Methyladenosine Regulates mRNA Splicing and Is Required for Adipogenesis. *Cel Res* 24 (12), 1403–1419. doi:10.1038/cr.2014.151

Zhou, Y., Liu, J., Lei, Q., Han, H., Liu, W., Cunwei, T., et al. (2020). Transcriptome Analysis of the Chicken Follicular Theca Cells with miR-135a-5p Suppressed. *G3 (Bethesda)* 10 (11), 4071–4081. doi:10.1534/g3.120.401701

Zhu, T., Roundtree, I. A., Wang, P., Wang, X., Wang, L., Sun, C., et al. (2014). Crystal Structure of the YTH Domain of YTHDF2 Reveals Mechanism for Recognition of N6-Methyladenosine. *Cel Res* 24 (12), 1493–1496. doi:10.1038/cr.2014.152

Zong, X., Zhao, J., Wang, H., and Wang, Y. (2018). PSXIV-41 Intestinal Inflammatory Impairs Lipid Transport via m6A-dependent Pathyway. *J. Anim. Sci.* 96, 41–42. doi:10.1093/jas/sky404.093

**Conflict of Interest:** The authors declare that the research was conducted in the absence of any commercial or financial relationships that could be construed as a potential conflict of interest.

**Publisher's Note:** All claims expressed in this article are solely those of the authors and do not necessarily represent those of their affiliated organizations, or those of the publisher, the editors and the reviewers. Any product that may be evaluated in this article, or claim that may be made by its manufacturer, is not guaranteed or endorsed by the publisher.

*Copyright © 2021 Zhang, Yang, Yang, Gao, Luo, Huang, Yan, Wang, Wang, Xie, Zhang and Gun. This is an open-access article distributed under the terms of the Creative Commons Attribution License (CC BY). The use, distribution or reproduction in other forums is permitted, provided the original author(s) and the copyright owner(s) are credited and that the original publication in this journal is cited, in accordance with accepted academic practice. No use, distribution or reproduction is permitted which does not comply with these terms.*

frontiers in Cell and Developmental Biology

ORIGINAL RESEARCH
published: 03 December 2021
doi: 10.3389/fcell.2021.689067

# Integrated Study of Transcriptome-wide m$^6$A Methylome Reveals Novel Insights Into the Character and Function of m$^6$A Methylation During Yak Adipocyte Differentiation

*Yongfeng Zhang[1,2], Chunnian Liang[1], Xiaoyun Wu[1], Jie Pei[1], Xian Guo[1], Min Chu[1], Xuezhi Ding[1], Pengjia Bao[1], Qudratullah Kalwar[1] and Ping Yan[1,2]**

[1]Key Laboratory of Yak Breeding Engineering Gansu Province, Lanzhou Institute of Husbandry and Pharmaceutical Sciences, Chinese Academy of Agricultural Sciences, Lanzhou, China, [2]State Key Laboratory of Grassland Agro-Ecosystems, College of Pastoral Agriculture Science and Technology, Lanzhou University, Lanzhou, China

OPEN ACCESS

**Edited by:**
Stephanie McKay,
University of Vermont, United States

**Reviewed by:**
Narendra Singh,
Stowers Institute for Medical Research, United States
Xiaojian Shao,
National Research Council Canada (NRC-CNRC), Canada

***Correspondence:**
Ping Yan
pingyanlz@163.com

**Specialty section:**
This article was submitted to Epigenomics and Epigenetics, a section of the journal Frontiers in Cell and Developmental Biology

**Received:** 31 March 2021
**Accepted:** 01 November 2021
**Published:** 03 December 2021

**Citation:**
Zhang Y, Liang C, Wu X, Pei J, Guo X, Chu M, Ding X, Bao P, Kalwar Q and Yan P (2021) Integrated Study of Transcriptome-wide m$^6$A Methylome Reveals Novel Insights Into the Character and Function of m$^6$A Methylation During Yak Adipocyte Differentiation. Front. Cell Dev. Biol. 9:689067. doi: 10.3389/fcell.2021.689067

Yak (*Bos grunniens*) is considered an iconic symbol of Tibet and high altitude, but they suffer from malnutrition during the cold season that challenges the metabolism of energy. Adipocytes perform a crucial role in maintaining the energy balance, and adipocyte differentiation is a complex process involving multiple changes in the expression of genes. $N^6$-methyladenosine (m$^6$A) plays a dynamic role in post-transcription gene expression regulation as the most widespread mRNA modification of the higher eukaryotes. However, currently there is no research existing on the m$^6$A transcriptome-wide map of bovine animals and their potential biological functions in adipocyte differentiation. Therefore, we performed methylated RNA immunoprecipitation sequencing (MeRIP-seq) and RNA sequencing (RNA-seq) to determine the distinctions in m$^6$A methylation and gene expression during yak adipocyte differentiation. In yak adipocyte and preadipocyte the content of m$^6$A and m$^6$A-associated enzymes was substantially different. In the two groups, a total of 14,710 m$^6$A peaks and 13,388 m$^6$A peaks were identified. For the most part, m$^6$A peaks were enriched in stop codons, 3′-untranslated regions, and coding regions with consensus motifs of GGACU. The functional enrichment exploration displayed that differentially methylated genes participated in some of the pathways associated with adipogenic metabolism, and several candidate genes (*KLF9*, *FOXO1*, *ZNF395*, and *UHRF1*) were involved in these pathways. In addition to that, there was a positive association between m$^6$A abundance and levels of gene expression, which displayed that m$^6$A may play a vital role in modulating gene expression during yak adipocyte differentiation. Further, in the adipocyte group, several methylation gene protein expression levels were significantly higher than in preadipocytes. In short, it can be concluded that the current study provides a comprehensive explanation of the m$^6$A features in the yak transcriptome, offering in-depth insights into m$^6$A topology and

associated molecular mechanisms underlying bovine adipocyte differentiation, which might be helpful for further understanding its mechanisms.

**Keywords: yak, adipocyte, N6-methyladenosine, MeRIP-seq, regulatory mechanism**

## INTRODUCTION

$N^6$-methyladenosine ($m^6A$) was first discovered in the 1970s as the most prevalent internal modification of polyadenylated mRNAs and long noncoding RNAs (lncRNAs) in higher eukaryotes (Desrosiers et al., 1974; Perry and Kelley, 1974; Adams and Cory, 1975; Furuichi et al., 1975; Lavi and Shatkin, 1975; Wei and Moss, 1975). The modification of $m^6A$ methylation is mounted by a series of $m^6A$ methyltransferases labeled as writers: methyltransferases such as 3 and 14 (METTL3 and METTL14), Wilms Tumor 1-associated protein (WTAP), VIRMA, vir-Like $m^6A$ methyltransferase associated (KIAA1429), RNA binding motif protein 15 (RBM15), and zinc finger CCCH domain 13 (ZC3H13) (Bokar et al., 1997; Agarwala et al., 2012; Liu et al., 2014; Ping et al., 2014; Schwartz et al., 2014; Patil et al., 2016; Knuckles et al., 2018; Wen et al., 2018). Besides this, $m^6A$ demethylases eliminate methylation from RNAs to enable a delicately dynamic equilibrium modification and are named erasers: fat mass and obesity-associated protein (FTO) and α-ketoglutarate-dependent dioxygenase alkB homolog 5 (ALKBH5) (Jia et al., 2011; Zheng et al., 2013). Further, specific proteins, including the YTH domain family (YTHDF1-3) and IGF2BPs (IGF2BP1-3) (Dominissini et al., 2012; Luo and Tong, 2014; Wang et al., 2014; Wang et al., 2015), were identified as a category of proteins called readers that recognize the information of RNA methylation modifications and engage in downstream mRNA translation, degradation, microRNA binding, and RNA-protein interactions (Liu and Pan, 2016; Roundtree I. A. et al., 2017; Nachtergaele and He, 2017; Zhao et al., 2017). Notably, two independent studies established an $m^6A$ RNA immunoprecipitation accompanied with high-throughput sequencing (MeRIP-seq) and subsequently identified the first $N^6$-methyladenosine modification map to methylomes with a resolution of 100-nucleotides (Dominissini et al., 2012; Meyer et al., 2012). Meanwhile, MeRIP-seq has been used to identify the $m^6A$ profile in humans and mice. These results reveal that $m^6A$ is predominantly located close to stop codons, 3′-untranslated regions (3′-UTRs), and also in long internal exons and transcription start sites, suggesting that $m^6A$ plays a crucial role in the post-transcriptional regulation of gene expression. These innovative studies reflect that the construction of transcriptome-wide $m^6A$ methylome profiles is of great importance to further investigate the characteristics and functions of such modification.

Currently, $m^6A$ modifications are reported in several areas of RNA metabolism, such as RNA localization, transport, splicing, stability, and translation (Liu and Pan, 2016; Roundtree I. A. et al., 2017; Nachtergaele and He, 2017; Zhao et al., 2017). Previous studies describe that $m^6A$ modification of mRNA plays an important biological function in controlling cellular metabolic processes, and it is reportedly involved in determining mammalian embryonic stem cell fate (Batista et al., 2014), regulating the initiation and differentiation of meiosis in murine spermatogonial stem cells (Xu et al., 2017), and maintaining the myogenic potential of proliferating skeletal muscle progenitors (Kudou et al., 2017). In particular, FTO facilitates the differentiation of mouse preadipocytes by regulating alternative splicing of pre-mRNAs for genes associated with adipogenesis (Zhao et al., 2014). Zhong et al. report that knockdown of METTL3 or YTHDF2 *in vitro* enhanced the stability and expression of peroxisome proliferator-activator receptor alpha (PPARα) mRNA, leading to decreased lipid accumulation in a hepatocellular carcinoma cell line (HepG2) (Zhong et al., 2018). Besides this, a recent study reveals that RNA $m^6A$ modification has a potential function in the deposition of porcine adipose tissue (Tao et al., 2017), and the modification of $m^6A$ on the mRNA of mitochondrial carrier homology 2 (MTCH2) promotes the differentiation of pig intermuscular preadipocytes (Jiang et al., 2019). Thus, we assume that $m^6A$ modification may also refer to bovine adipocyte differentiation according to the notable functions of $m^6A$ modification described above. However, our knowledge about the relationship between $m^6A$ modification and bovine adipocyte differentiation is still scarce.

The yak is the major bovine livestock breed on the Qinghai-Tibet Plateau and is the only large ruminant domestic species that enables daily necessities, such as meat, milk, wool, skins, fuel, and economic benefits, for local herders (Long et al., 1999; Dong et al., 2006). On the Qinghai-Tibet Plateau, domestic yaks mainly grow on natural pastures under typical grazing conditions (Long et al., 2008). Owing to seasonal variations in forage, yaks must constantly undergo insufficient feeding during the harsh winter season (October–May), which leads to the large seasonal weight changes and a circular rhythm of "live in summer, weighty in autumn, thin in winter, and dead in spring" (Shikui et al., 2003). Consequently, the subcutaneous adipose layer of yak accumulates rapidly in summer and early autumn to provide essential energy requirements and withstand severe cold through selective fat catabolism during the cold season (Ding et al., 2012). The distinctive metabolic pattern makes the yak a fascinating model for studying adipose metabolism in plateau domestic animals. Adipocytes are a major component of adipose tissue and are considered to be the cornerstone of metabolic homeostasis regulation throughout the body (Ali et al., 2013). Therefore, it is necessary to assay $m^6A$ sites at the transcriptome-wide level to identify the potential biological functions of RNA $m^6A$ modification during yak adipocyte differentiation.

In the present study, we initially isolated preadipocytes from yak adipose tissue and differentiated them into mature adipocytes successfully. We obtained the first transcriptome-wide $m^6A$

methylome profile in yak by MeRIP-seq and elucidated the features of $m^6A$ modification during yak adipocyte differentiation. We found that the different $m^6A$ RNA modifications between yak preadipocytes and mature adipocytes have potential regulatory roles in gene expression and pathways related to adipose energy metabolism. This study explores the role of $m^6A$ modification in bovine adipose metabolism and complements $m^6A$ studies in plateau domestic livestock, which may be a breakthrough point for exploring energy metabolism in yaks.

# MATERIALS AND METHODS

## Ethics Statement

Animal treatment during research was carried out in complete accordance with the protocols and guidelines for animal ethics of the People's Republic of China, and all operations were approved by the Animal Administration and Ethics Committee of Lanzhou Institute of Husbandry and Pharmaceutical Sciences, Chinese Academy of Agricultural Sciences (Permit No. SYXK-2014–0002).

## Preadipocyte Isolation

The Datong Yak Breeding Center (Datong County, Qinghai, China) provided three healthy 3-day-old Datong yaks. The night before slaughter, yaks were not fed. On the next morning, the yaks were humanely sacrificed by the way of electrical stunned (90 V, 10 s, and 50 Hz) at a commercial slaughter facility and exsanguinated as necessary to ameliorate the suffering, according to standard approved industry protocols. The subcutaneous adipose tissue was harvested according to the protocols and guidelines for animal ethics of the People's Republic of China. Primary yak preadipocytes were cultured from subcutaneous adipose tissue according to our previous study (Zhang Y. et al., 2018; Zhang et al., 2020). Briefly, the subcutaneous fat tissue was flushed with penicillin (200 U/mL) and streptomycin (200 U/mL) added to the phosphate saline buffer (HyClone, Thermo Fisher Scientific, Carlsbad, CA, United States). After that, they were finely minced into about 1 $mm^3$ piece in an aseptic setting. The segments were digested by Type I collagenase in a continuously agitated water bath at 37°C for 60–90 min. With a 40-μm nylon mesh film, indigestible material was screened, and the filtrate was resuspended for 5 min at 1400 g. The sediment was subsequently incubated at room temperature for 10 min with the erythrocyte lysis buffer (0.154 M NH4Cl, 10 mM $KHCO_3$, 0.1 mM EDTA). The cells were then filtered with 200-μm nylon mesh film and rinsed twice with a serum-free medium. After 5 min of centrifugation at 1400 g, preadipocytes were harvested and solubilized in the growth media, including DMEM-F12 (Hyclone, UT, United States) supplemented with 10% fetal bovine serum (FBS, Gibco, MA, United States).

## Adipogenic Differentiation and Staining of Oil Red O

The adipogenic differentiation was performed according to our previous study (Zhang Y. et al., 2018; Zhang et al., 2020). Preadipocyte was induced for 2 days by adipogenic compounds composed of 3-isobutyl-methylxanthine (MIX) (Sigma, MO, United States), dexamethasone (Sigma, MO, United States), rosiglitazone (Sigma, MO, United States), and insulin (Sigma, MO, United States) after cell confluence approached 70% in growth media. The medium was replaced after 2 days with DMEM-F12 containing 10% FBS, penicillin (200 U/mL), streptomycin (200 U/mL), and 5 ng/ml of insulin and updated with cycles of 2 days until day 12. The cells were usually flushed twice with PBS and set for 1 h in 4% formalin. Cells were then reacted at room temperature for 30 min with a saturated solution of Oil Red O. Then, cells were rinsed three times with sterile water, and photographs were acquired from light microscopy.

## Quantitative Real-Time PCR

Total RNAs were extracted using TRIzol reagent (Invitrogen, CA, United States) from *in vitro* cultured yak preadipocytes and differentiated adipocytes (three biological replicates for each condition). Concentration and quality were further evaluated using denaturing gel electrophoresis and spectroscopy (Thermo, Waltham, MA, United States). Reverse transcription of mRNA was conducted using commercial kits (Takara, Japan) according to the manufacturer's protocols. Real-time RT-PCR was accomplished in a CFX Link Real-Time PCR Detection System, and 10 μl volume of reaction consisting of 5 μl 2xSYBR Premix Ex Taq II, 0.4 μl primers (10 μM), and 0.8 μl cDNA. The reaction condition was as follows: denaturation for 30 s at 95°C followed by 35 additional cycles for 15 s at 94°C, annealing for the 30 s at 72°C. A melting procedure with a heating rate of 0.5°C/10 s was performed to create melting curves ranging from 95°C. The gene expression levels were estimated using the $2^{-\Delta\Delta Ct}$. **Supplementary Table S1** lists the sequences used for the primers.

## Measuring the $m^6A$ Content

The overall content of mRNA $m^6A$ was measured by a methylation quantification kit of EpiQuik RNA (Epigentek, P-9005, NY, United States). In short, a standard curve was constructed at concentrations of 0.01–0.5 ng/μl by positive control. The equivalent RNA solution (1–8 μl) and negative control were applied to the strip wells. The plate was wrapped with parafilm, incubating for 1.5 h at 37°C. Then, the wells were washed three times and added to the 1:1000 diluted capture antibody at room temperature for 1 h. After washing thrice, the detection antibody (1:2000 dilution) and enhancer solution were applied to every well incubated at room temperature for 30 min. After five washes, detection solutions were placed on each well and incubated for 10 min at room temperature to protect from light. Finally, a stop solution was applied to each well and absorbance read with a microplate reader at 450 nm.

## MeRIP-Seq and mRNA Sequencing

According to the manufacturer's protocol, the total RNA was extracted using Trizol reagent (Invitrogen, CA, United States). A Bioanalyzer 2100 and RNA 6000 Nano LabChip Kit (Agilent, CA, United States) with RIN number >7.0 were used to evaluate the total RNA quality and quantity. Nearly over 200 μg total RNA

was performed to isolate Poly (A) mRNA through magnetic beads (Invitrogen) attached to poly-T oligo. After purifying, poly (A) mRNA fractions are broken into 100-nt-long oligonucleotides using a Magnesium RNA Fragmentation Module (NEB, cat.E6150, United States) under 86°C for 7 min. Then, the fragmentation of broken RNA was incubated in immunoprecipitation (IP) buffer (50 mM Tris-HCl, 750 mM NaCl, and 0.5% Igepal CA-630) supplied with BSA (0.5–1 μg/μl) for 2 h at 4°C with $m^6A$-specific antibody (No. 202003, Synaptic Systems, Germany). Subsequently, the above mixture was incubated with protein-A beads (Thermo Fisher Scientific, MA, United States) and eluted with elution buffer (1 × IP buffer and 6.7 mM $m^6A$). The eluted RNA was extracted by TRIzol reagent (Thermo Fisher Scientific) according to the manufacturer. Then, IP RNA and untreated input control fragment RNA were reverse-transcribed to create the cDNA by SuperScript™ II Reverse Transcriptase (Invitrogen, cat. 1896649, CA, United States), which was then used to synthesize U-labeled second-stranded DNAs with *E. coli* DNA polymerase I (NEB, cat.M0209, MA, United States), RNase H (NEB, cat.M0297, MA, United States), and dUTP Solution (Thermo Fisher, cat. R0133, MA, United States). Besides this, the A-base was added to the blunt ends of each strand and prepared for linkage to the indexed adapters. Each adapter holds a T-base overhang to link the adapter to the A-tailed fragmented DNA. Single- or dual-index adapters were linked to the fragments, and size selection was performed with AMPureXP beads. After the heat-labile UDG enzyme (NEB, cat. M0280, MA, United States) treatment of the U-labeled second-stranded DNA, the ligated products are amplified with PCR by the following conditions: initial denaturation at 95°C for 3 min, eight denaturation cycles at 98°C for 15 s, annealing at 60°C for 15 s, extension at 72°C for 30 s, and then final extension at 72°C for 5 min. The average insert size of the paired-end libraries was ~100 ± 50 bp. Finally, the $m^6A$-seq libraries were performed with Tru Standard mRNA Sample Prep Kit (Illumina) along with the published protocol (Huse et al., 2003). The 2 × 150 bp paired-end sequenced (PE150) on Illumina Novaseq™ 6000 (LC-Bio Technology CO., Ltd., Hangzhou, China) in accordance with the vendor's recommended protocol.

## Sequencing Data Analysis

First of all, in-house perl scripts and Cutadapt (Martin, 2011) were performed to eliminate the reads containing contaminants of the adapter, bases of low quality, and indeterminate. Meanwhile, the quality of the sequence was validated using fastp. The reads were mapped to the *Bos_mutus* genome (Version: BosGru_v2.0) by HISAT2 (Kim et al., 2015) with default parameters. Using R package exomePeak (Meng et al., 2014) identify the $m^6A$ peaks from mapped reads of IP and input libraries with bed or bam format to configure for viewing on IGV software (http://www.igv.org/) or the UCSC genome browser. The parameters of the exomePeak R package are as follows: "PEAK_CUTOFF_PVALUE = 0.05, PEAK_CUTOFF_FDR = NA, FRAGMENT_LENGTH = 100." The examination was performed using the Poisson distribution model, and a $p$-value < 0.05 was considered as a peak. *De novo* and defined motifs were identified by MEME (Bailey et al., 2009) and HOMER (Heinz et al., 2010), accompanied by perl scripts in the house seeking the motif concerning peak. Called peaks were annotated using ChIPseeker (Yu et al., 2015) by intersection with gene architecture. The difference peaks were identified using the exomePeak R package with parameters $p$-value < 0.05 and | log2 (fold change)| ≥ 1. StringTie (Pertea et al., 2015) calculated the expression level of all mRNAs from input libraries, which normalized with FPKM {FPKM = [total exon fragments/mapped reads (millions)]}. The differentially expressed mRNAs were collected by R package edgeR (Robinson et al., 2010) with the |log2 (fold change)| > 1 and $p$-value < 0.05. GO seq R package was performed on the Gene Ontology (GO, http://www.geneontology.org/) enrichment analysis for the differentially expressed genes (Young et al., 2010). The Kyoto Encyclopedia of Genes and Genomes (KEGG, http://www.genome.jp/kegg/) database is a major resource for learning high-level functions and utilities of biological systems. The statistical enrichment tests for genes of differential expression in the KEGG pathways were used in the KOBAS software (Xie et al., 2011).

## Western Blotting

Proteins were extracted from preadipocytes and adipocytes. After detecting the total protein concentration, the protein was denatured at 95°C for 5 min with a protein loading of 50 μg. Subsequently, SDS-PAGE electrophoresis was performed with 10% of the isolate gel and 4% of the concentrate gel, and electrophoresis at 40 V for 25 min in the concentrate gel and 100 V for 80 min in the isolate gel. Then, the protein was transferred to the PVDF membrane and immersed in the closure solution at 37°C for 1.5 h. Then, it was incubated in monoclonal rabbit anti-ENTPD1, anti-USP2, and anti-PGAM2 (1:1000; Abcam, Cambridge, United Kingdom) and monoclonal mouse anti-β-actin (1:5,000; Beyotime, Shanghai, China). Finally, the membranes were incubated for 1.5 h at 37°C by adding an HRP-labeled goat secondary antibody and images captured using a Chemi Doc System (Bio-Rad, Hercules, CA). Grayscale values of proteins were evaluated by ImageJ (https://imagej.nih.gov/ij/).

## Statistical Analysis

The SPSS 22 software package was used to evaluate statistics. A one-way test of variance assessed the significance of the differences between all of the groups. Statistically significant was the degree of probability * $p$ < 0.05;** $p$ < 0.01. Values are shown as mean ± SEM.

# RESULTS

## The Yak Preadipocyte Induced Differentiation and Global $m^6A$ Quantification

The results of Oil Red O show that the visibility of lipid droplets in adipocytes increased significantly at day 12 compared to day 0 after induction with adipogenic agents (**Figures 1A,B**, **Supplementary Figure S1**). Meanwhile, the expression of

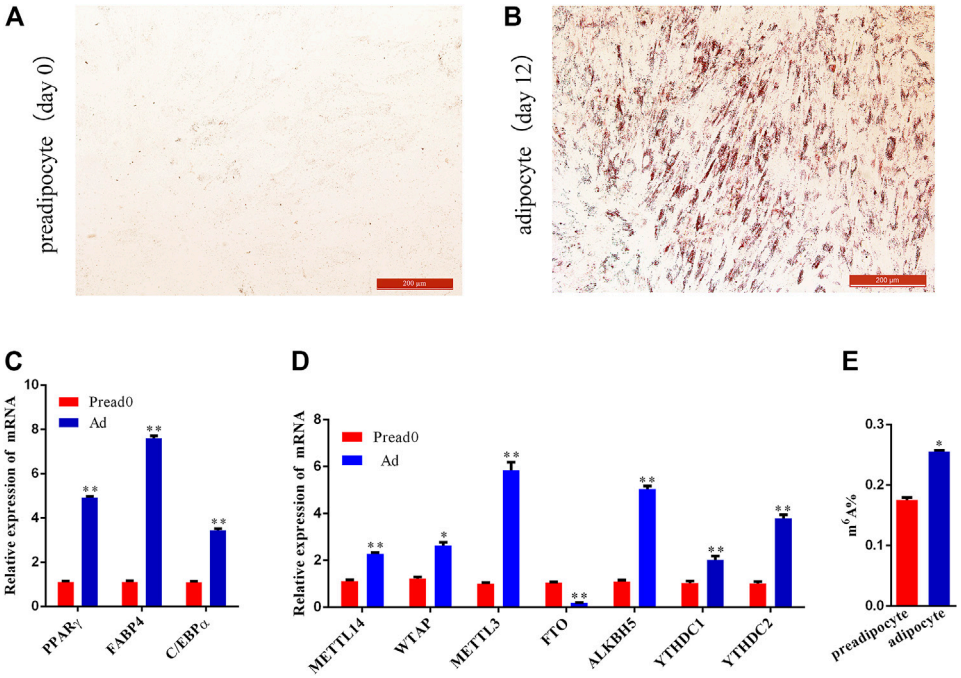



**FIGURE 1 |** Preadipocyte-induced differentiation and detection of m$^6$A level between preadipocyte and adipocyte. **(A,B)** Preadipocytes and adipocytes dyed with Oil red O. **(C)** Relative expression of *PPARγ*, *C/EBPα*, and *FABP4* between preadipocyte (day 0) and adipocyte (day 12). **(D)** The mRNA expression level of methyltransferases (*METTL14*, *WTAP*, and *METTL3*), demethylases (*FTO* and *ALKBH5*) and m$^6$A-binding proteins (*YTHDC1*and *YTHDC2*). **(E)** m$^6$A abundance between the preadipocytes and adipocytes. (SEM, * $p < 0.05$;** $p < 0.01$).

adipocyte differentiation-specific marker genes (*PPARγ*, *C/EBPα*, and *FABP4*) was significantly elevated on day 12 (adipocyte) compared with day 0 (preadipocyte) (**Figure 1C**), suggesting preadipocyte full differentiation into adipocyte. Subsequently, to overview the m$^6$A methylation during yak adipocyte differentiation, the expression of RNA methylation-related genes was contrasted by quantitative real-time PCR (qRT-PCR) detected, including *METTL3*, *WTAP*, *METTL14*, *FTO*, *ALKBH5*, and *YTHDC1/2*. Comparing the group of preadipocytes (Pread0) and adipocytes (Ad), the findings show that the expression level of methyltransferases (*METTL14*, *WTAP*, and *METTL3*) and *ALKBH5* were dramatically upregulated, whereas *FTO* was substantially downregulated, and m$^6$A-binding proteins (*YTHDC1* and *YTHDC2*) were drastically upregulated (**Figure 1D**). Furthermore, the content of m$^6$A in the group of adipocytes was significantly higher compared with the preadipocyte group (**Figure 1E**). Thereby, we hypothesized that, during yak adipocyte differentiation, the difference of m$^6$A methylation may exist, which was furtherly discovered using MeRIP-seq.

## Transcriptome-wide m$^6$A-Seq Reveals Global m$^6$A Modification Patterns During Yak Adipocyte Differentiation

The yak adipocyte and preadipocyte of three biological replicates were used for transcriptome-wide m$^6$A-sequencing (m$^6$A-seq) and RNA-sequencing (RNA-seq) assays. In total, 12 libraries were sequenced, comprising three replicates of preadipocyte and adipocyte for input and MeRIP samples (**Supplementary Table S2**). With each MeRIP library, an average of 9.22 Giga base-pair (Gb) of high-quality data was produced, and 9.49 Gb per input library (RNA-seq data set). Then, we eliminated reads containing adapter pollutants, low quality, and indeterminate bases, an average of 7.17 and 7.11 Gb obtained from per MeRIP and input libraries, respectively. The valid data were mapped to the *Bos_mutus* genome (Version: BosGru_v2.0) using HISAT2. The proportions of mapped reads ranged from 87.96 to 96.57%, correspondingly (**Supplementary Table S2**). The RNA species of transcripts included mRNA (19,916), misc_RNA (386), ncRNA (262), pseudogene (916), and tRNA(179) (**Supplementary Figure S2**). In the yak Ad group, R package exomePeak found a total of 14,710 m$^6$A peaks, containing transcripts of 9633 genes. Likewise, 13,388 m$^6$A peaks were found in the Pread0 group corresponding to transcripts of 9142 genes (**Figures 2A,B**). In addition, 5848 peaks were consistently observed in the two groups, and 3964 genes within the groups were modified by m$^6$A. Compared with the Pread0 group, the Ad group had 9226 new peaks occurring with the absence of 7904 peaks, reflecting the significant difference between Pread0 and Ad groups in global m$^6$A modification trends (**Figures 2A–C**). m$^6$A methylomes were ulteriorly mapped by HOMER software to define whether RRACH motifs (R represents purine; A is m$^6$A; and H is U, A, or C) were ubiquitous in our detected m$^6$A. The results of the enrichment analysis in both groups show that the consensus motifs of m$^6$A RRACH were GGACU (**Figure 2D**) accorded with

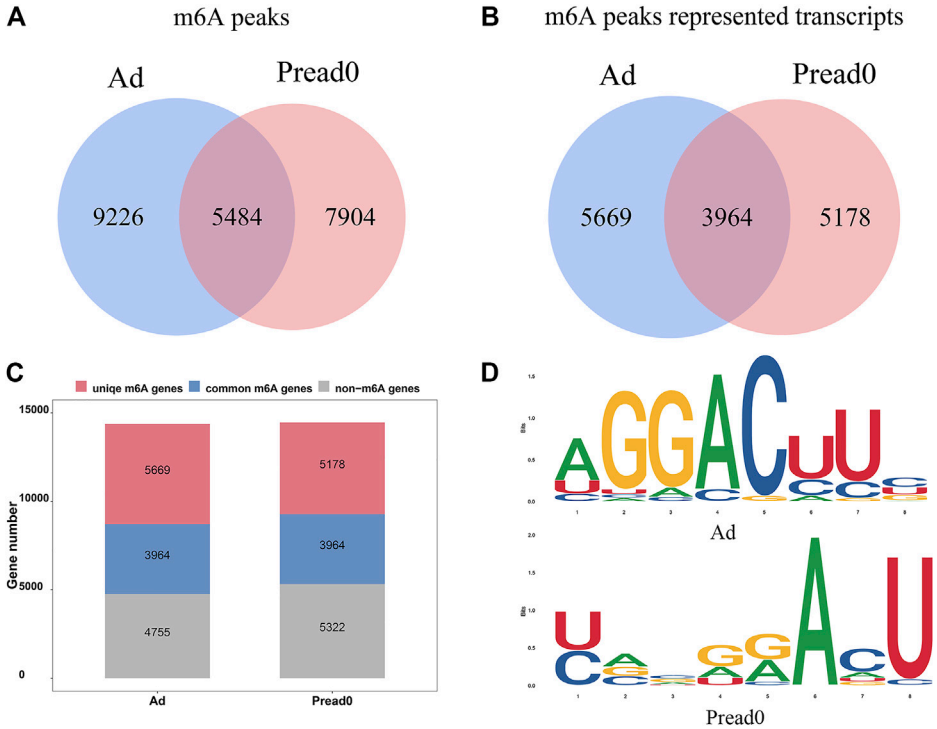



**FIGURE 2 |** m$^6$A-seq transcriptome-wide and m$^6$A peak analysis. **(A)** Number of common and specific m$^6$A peaks in groups of preadipocyte and adipocyte. **(B)** Venn diagram showing the m$^6$A peaks for transcripts of two group. **(C)** Profile of m$^6$A-modified genes discovered in m$^6$A-seq. **(D)** The motifs enriched from m$^6$A peaks identified from the groups of adipocyte and preadipocyte.

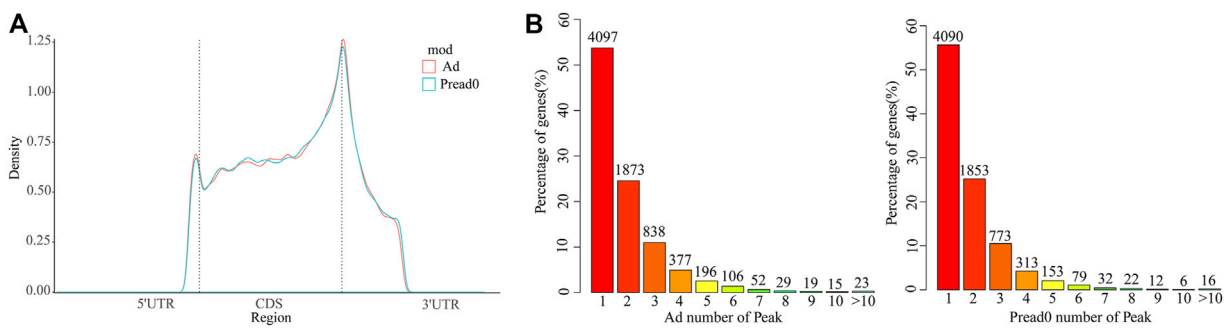



**FIGURE 3 |** m$^6$A methylome distributed on yak transcripts. **(A)** m$^6$A peaks enriched with transcripts. Transcript is separated into three parts comprising 5′ untranslated region, coding sequence and 3′ untranslated region. **(B)** Proportion of genes possessing m$^6$A peaks with different numbers.

previous studies, which strengthens the credibility of the m$^6$A peaks and confirms the presence of a prevailing methylated modification mechanism.

## Analysis of m$^6$A Modification Distribution in Yak Transcriptome

We analyzed metagene models of m$^6$A peaks in the global transcriptome to identify the differential distribution of m$^6$A in transcripts. Our findings indicated that m$^6$A peaks were predominantly enriched in the coding sequence (CDS) near the start and stop codons and approach the beginning of the 3′ untranslated region (3′UTRs) in Ad and Pread0 (**Figure 3A**), which contrast to the pattern found in mice and chickens (Luo et al., 2019; Cheng et al., 2021). Subsequently, to systematically calculate the enrichment, we investigated nonoverlapping transcript segments per m$^6$A peak with 5′UTR, CDS, and 3′UTR (**Supplementary Figure S3A**), in which most of them were abundant in CDS. Interestingly, m$^6$A peak relative increased at 5′UTR and CDS region in Ad compared with Pread 0 and decreased in 3′UTR region. Afterward, we explored the distribution of m$^6$A modified peaks with each gene, finding

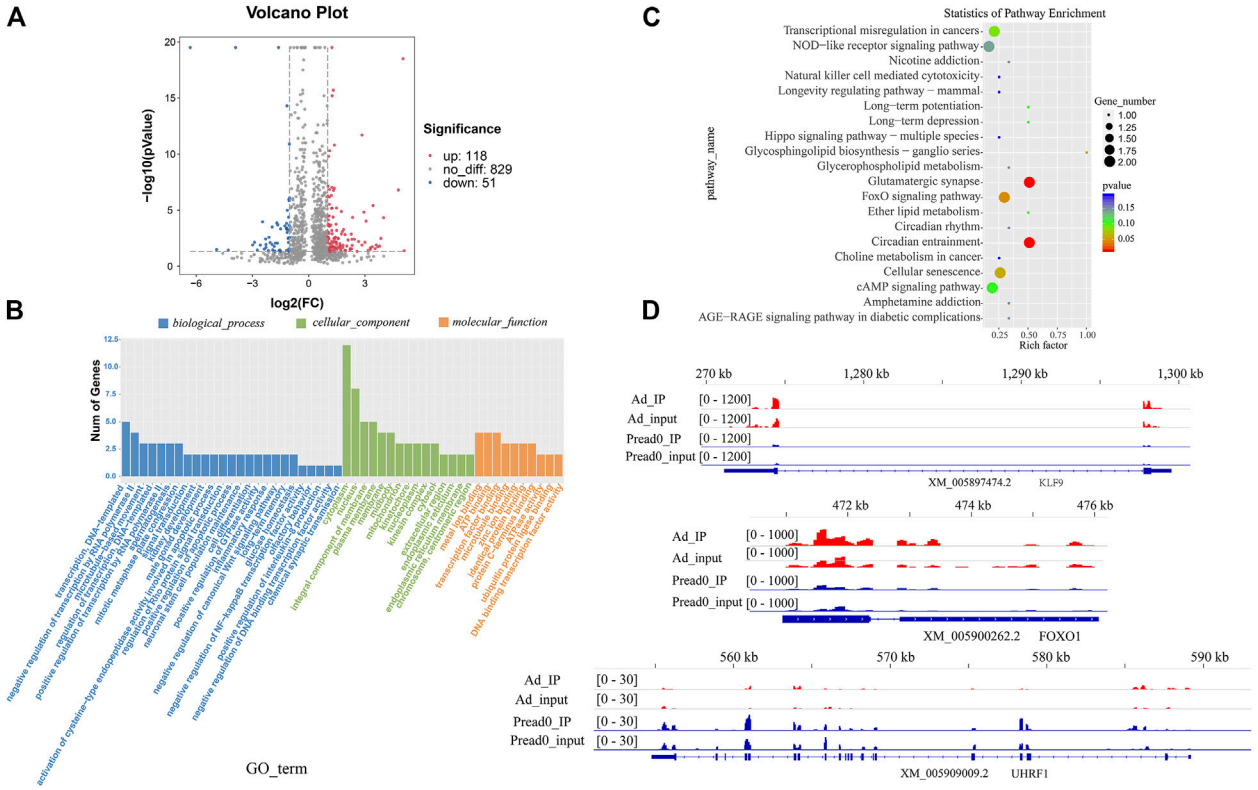



**FIGURE 4 |** The alteration of global m$^6$A modification in adipocyte compared with preadipocyte. **(A)** Volcano plots showing different m$^6$A peaks (fold change ≥2 and $p < 0.05$) between preadipocyte and adipocyte. **(B)** GO terms of genes with differential m$^6$A peaks between preadipocyte and adipocyte. **(C)** The top 20 markedly enriched pathways for the genes of differential peaks between preadipocyte and adipocyte. **(D)** The abundance of m$^6$A on *KLF9*, *FOXO1*, and *UHRF1* mRNA transcripts observed by m$^6$A-seq in preadipocyte and adipocyte. Blue boxes represent exons; blue lines represent introns.

that almost 60% of methylated genes hold only one m$^6$A peak, and most genes contain one to three m$^6$A peaks (**Figure 2B**). Furthermore, we investigated the relationship between m$^6$A peak number and gene length. The results show a global trend that the longer gene length has more m$^6$A peaks (**Supplementary Figure S3B**).

## Analysis of the GO and KEGG Pathways of Differentially Methylated Genes

The comparison was performed for the abundance of m$^6$A peaks between preadipocytes and adipocytes. These findings exposed that 118 markedly hypermethylated m$^6$A peaks and 51 substantially hypomethylated peaks were obtained (|log2 (fold change)| > 1, $p < 0.05$) (**Figure 4A**). The residual peaks of the m$^6$A were viewed as unaltered peaks. Moreover, differentially methylated m$^6$A peaks represented genes investigated by GO and KEGG pathway analysis, revealing the biological significance of m$^6$A methylation during yak adipocyte differentiation. GO analysis revealed that differentially methylated genes were mainly implicated with DNA-templated and regulation of transcription by RNA polymerase II (ontology: biological process), cytoplasm, nucleus and integral component of membrane (ontology: cellular component), and transcription factor and microtubule binding (ontology: molecular function) (**Figure 4B**, **Supplementary File S1**). Meanwhile, the top 20 biological enrichment of KEGG pathways indicated that the genes differently methylated were substantially related to the adipogenic metabolism regulation pathways, NOD-like receptor signaling pathway, FoxO signaling pathway, Ether lipid metabolism, cAMP signaling pathway, and Hippo signaling pathway (**Figure 4C**; **Supplementary File S2**). These results reveal that several genes related to lipid metabolism were modified by m$^6$A methylation during yak adipocyte differentiation. Furthermore, the genes (*KLF9*, *FOXO1*, and *UHRF1*) differentially methylated sites were analyzed by Integrative Genomics Viewer (IGV) software (**Figure 4D**), located in 5′UTRs, exons, and 3′UTRs. In the 5′UTR region of *KLF9*, the m$^6$A site was hypermethylated in the adipocyte group compared with the control group, and its mRNA expression was upregulated. In the 3′UTR region of *FOXO1*, the m$^6$A site was hypomethylated in the adipocyte group compared with the control group, and its mRNA expression was upregulated. In the exon region of *UHRF1*, the m$^6$A site was hypermethylated in the adipocyte group

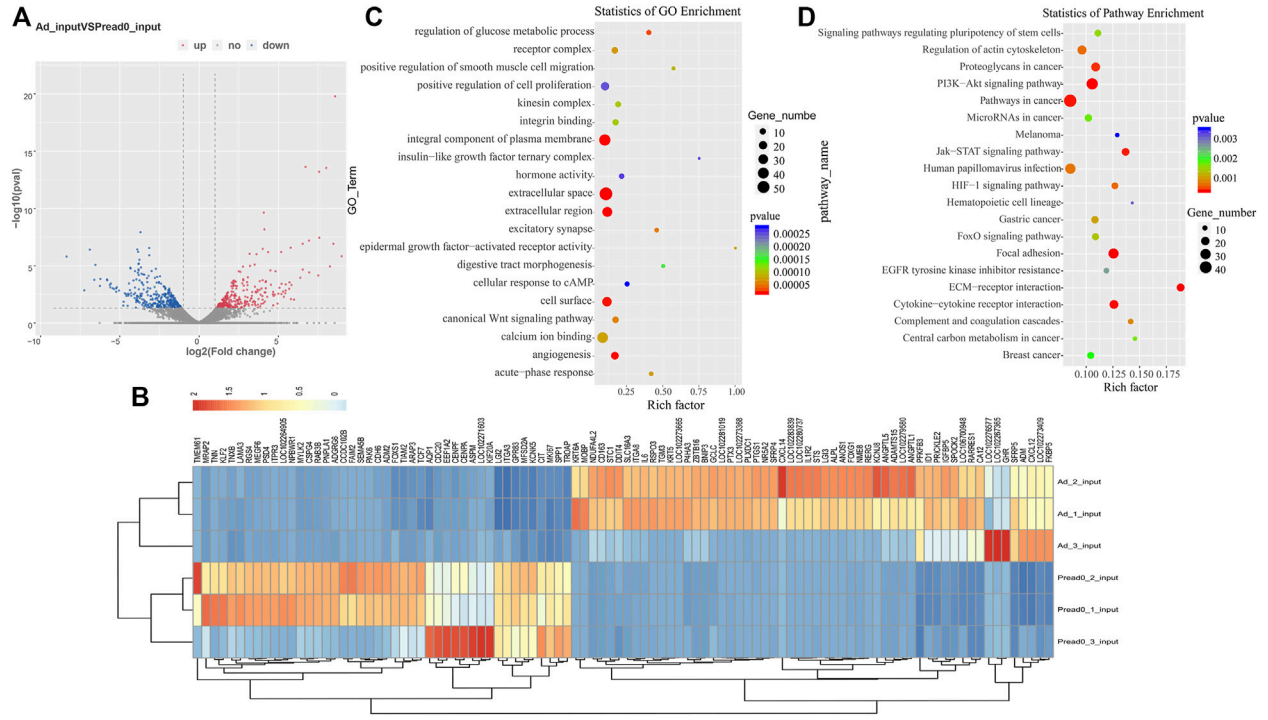



**FIGURE 5 |** RNA-seq analysis of genes differentially expressed between preadipocyte and adipocyte. **(A)** Volcano plots illustrating the differentially expressed genes. **(B)** Clustered heat map for comparing preadipocyte and adipocyte with the top 100 most differentially expressed genes. **(C)** The top 20 significantly GO enrichment terms for significantly differentially expressed genes. **(D)** The top 20 enriched pathways of dramatically differentially expressed genes.

compared with the control group, and its mRNA expression was downregulated (**Supplementary File S3**). The different m$^6$A methylation levels of these genes may affect their expression.

## RNA-Seq Identification of Genes Differentially Expressed in Both Groups

An analysis of the RNA-seq data set (m$^6$A-seq input library) displayed that the trends of global mRNA expression between preadipocyte and adipocyte were considerably different. There were 648 significantly different mRNAs, including 300 upregulated and 348 downregulated (|log2 (fold change)| > 1, $p < 0.05$) as shown in **Figure 5A**. Then, we conducted a clustered heat map to further explore the potential roles of the genes (**Figure 5B**; **Supplementary File S4**). Furthermore, GO ontology and KEGG pathway were performed to analyze the differentially expressed genes. As **Figure 5C**; **Supplementary File S5** display, the top 20 most notable functional annotations include regulation of glucose metabolic process, canonical Wnt signaling pathway, positive regulation of cell proliferation, and insulin-like growth factor ternary complex, which influence adipocyte differentiation. Meanwhile, the pathway exploration revealed that signaling pathways regulating pluripotency of stem cells, ECM-receptor interaction, PI3K-Akt signaling pathway, and FoxO signaling pathway were significantly enriched (**Figure 5D**; **Supplementary File S6**), revealing that differentially expressed genes potentially participated in adipogenic metabolism.

## Conjoint Analysis of RIP-Seq and RNA-Seq Data With Both Groups

We found an interesting relationship of differentially methylated m$^6$A peaks and gene expression patterns in preadipocytes and adipocytes through cross-analysis of the m$^6$A-seq and RNA-seq results, in which a positive correlation existed in differentially methylated m$^6$A peaks and gene expression levels (**Figure 6A**). Otherwise, all genes were segregated into mainly four types: eight hypermethylated and upregulated genes termed “hyper-up”; seven hypomethylated and downregulated genes termed “hypo-down”; 12 hypermethylated while downregulated genes termed “hyper-down”; and two hypomethylated while upregulated genes termed “hypo-up” (**Figure 6B**). There were slightly more hyper-up and hypo-down than hyper-down and hypo-up. **Table 1** lists the expression of genes that were significantly differently (|log2 (fold change)| > 1, $p$<.05), comprising significantly differently methylated peaks. Then, both groups were evaluated for the overall expression levels of the m$^6$A-methylated and non-m$^6$A-methylated transcripts (**Figure 6C**); the expression of methylated transcripts was higher than that of nonmethylated transcripts. These suggest that, in yak adipocyte differentiation, m$^6$A modifications appear to have a positive association with mRNA expression.

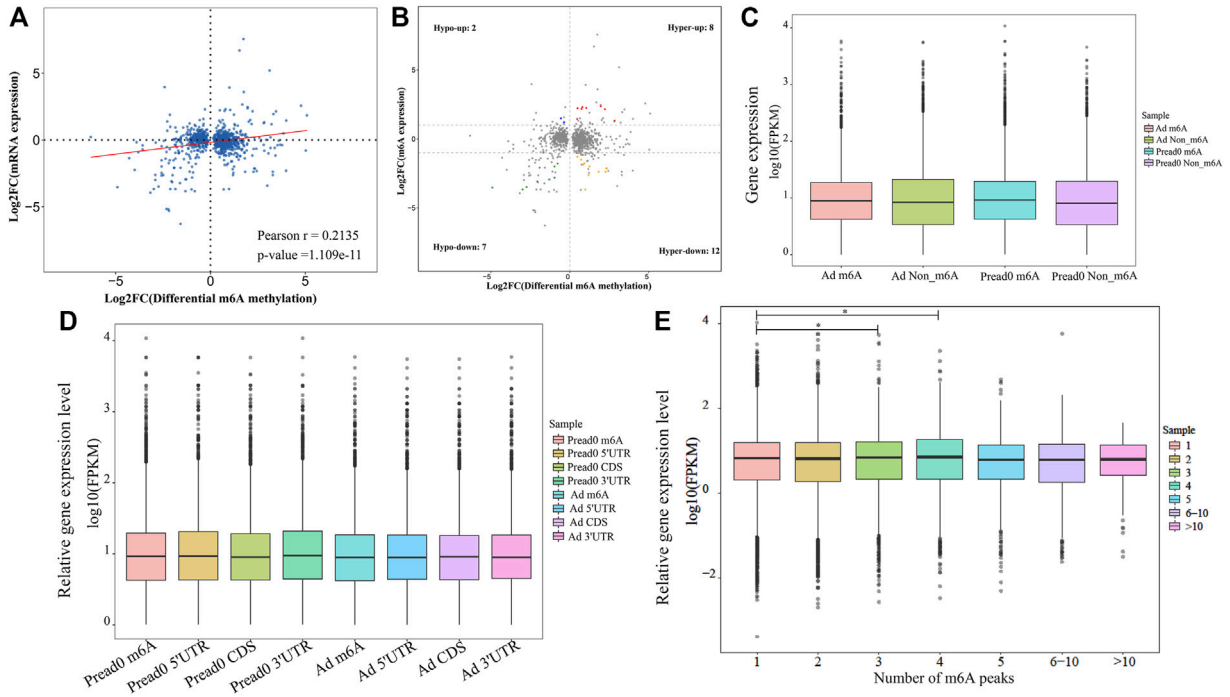



**FIGURE 6 |** Conjoint analysis of differentially methylated genes and differentially expressed genes. **(A)** Dot plot of $Log_2$ fold change (FC) (mRNA expression) versus $Log_2$ FC (differential $m^6A$ methylation) revealing a positive association between total $m^6A$ methylation and level of mRNA expression (Pearson $r = 0.2135$; $p$-value = 1.109e-11). **(B)** Four-quadrant plot showing differentially expressed genes with differentially methylated $m^6A$ peaks. **(C)** The holistic expression levels of the transcripts with $m^6A$-methylated and non-$m^6A$-methylated in different groups. **(D)** For all $m^6A$ peaks, the position of $m^6A$ peaks for RNA transcripts and gene relative expression level. **(E)** Relative mRNA transcript expression level with different number of $m^6A$ peaks. *$p < 0.05$ compared with the $m^6A$ peak = 1.

Furthermore, we were wondering if the position of $m^6A$ peaks on RNA transcripts or the number of $m^6A$ peaks per transcript is correlated with the levels of gene expression. Based on $m^6A$ modification sites, RNA transcripts were classified into subgroups. As shown in (**Figure 6D**), $m^6A$ modifications of RNA transcripts in CDS, 5′UTR or 3′UTR do not differ with gene expression. Through studying $m^6A$-modified sites and relative expression levels of genes, revealing that the genes have three or four modified sites appears to be more abundant in contrast with other $m^6A$-modified sites (**Figure 6E**). Furthermore, we implemented qRT-PCR to confirm the expression of differentially methylated genes between adipocyte and preadipocyte. The mRNA expression pattern was consistent with the RNA-seq data (**Supplementary Figure S4A–B**), which confirms the validity of our transcriptome results.

## Differentially Methylation Modification is Linked to the Translation of Genes

Previous research indicates that RNA methylation plays an essential role in the translation of mRNA. Therefore, to reveal the influence of RNA methylation on mRNA translation, we explored the metagene with significant differences for methylation and nonsignificant differences in gene expression during yak preadipocyte differentiation. There were 155 genes with significant differences in methylation, and nonsignificant differences in expression existed in preadipocytes and adipocytes (**Figure 7A**; **Supplementary File S7**). To predict the function of these genes, GO and KEGG analyses were performed. These genes are mainly allocated to organism development, DNA binding, canonical Wnt signaling pathway, citrate cycle (TCA cycle), and calcium signaling pathway (**Supplementary Figure S5A–B**; **Supplementary Files S8, S9**). Therefore, the candidate genes were selected from the top 10 genes (**Table 2**) with the peck fold change for Western blot. Interestingly, the protein expression levels (ENTPD1, USP2, and PGAM2) were substantially higher in the adipocyte than the preadipocyte group (**Figure 7B,C**). The findings indicate that RNA methylation not only may regulate mRNA expression, but also effect mRNA translation during yak preadipocyte differentiation.

# DISCUSSION

The harsh environment of the Qinghai-Tibet Plateau encourages the yak to develop a special mechanism for energy metabolism. As an organ for energy metabolism, adipose tissue plays a crucial role in this process. To date, it is found that epigenetic regulation is engaged in various biological processes, including embryo development, stem cell self-renewal, DNA damage response, primary miRNA processing, and energy metabolism (Wu and Sun, 2006; Shi and Wu, 2009; Donohoe and Bultman, 2012; Li

**TABLE 1 |** List of 28 genes with significant changes in m$^6$A and mRNA transcript abundance in yak adipocyte as compared with preadipocytes.

| Gene name | Pattern | m$^6$A level change | | | | mRNA level change | |
|---|---|---|---|---|---|---|---|
| | | Peak region | Peak start | Peak end | diff.p | log2(fc) | *p*-value |
| QPRT | Hyper-up | Exon | 491048 | 491299 | 0.03 | 2.30 | 0.00 |
| BCL2L11 | Hyper-up | 5′ UTR | 1175002 | 1175378 | 0.03 | 2.15 | 0.04 |
| PER1 | Hyper-up | 3′ UTR | 235431 | 236437 | 0.02 | 2.22 | 0.00 |
| KLHL29 | Hyper-up | 3′ UTR | 4950507 | 4950957 | 0.02 | 1.44 | 0.02 |
| KLF9 | Hyper-up | 5′ UTR | 1298633 | 1299052 | 0.01 | 2.18 | 0.00 |
| ZNF395 | Hyper-up | 3′ UTR | 730872 | 731331 | 0.01 | 2.25 | 0.00 |
| ZNF608 | Hyper-up | Exon | 980374 | 980553 | 0.04 | 2.38 | 0.00 |
| MTERF4 | Hyper-up | 3′ UTR | 726115 | 726234 | 0.01 | 1.32 | 0.02 |
| CD247 | Hypo-down | 3′ UTR | 33979 | 34575 | 0.01 | −1.78 | 0.02 |
| SLCO5A1 | Hypo-down | Exon | 1066324 | 1066623 | 0.01 | −2.00 | 0.01 |
| AFAP1L2 | Hypo-down | Exon | 854,733 | 856,548 | 0.04 | −3.48 | 0.02 |
| CENPF | Hypo-down | Exon | 1363460 | 1363640 | 0.01 | −3.67 | 0.00 |
| USP43 | Hypo-down | 3′ UTR | 129792 | 130001 | 0.01 | −3.08 | 0.00 |
| ARHGEF28 | Hypo-down | Exon | 175098 | 178009 | 0.01 | −2.81 | 0.00 |
| ARAP3 | Hypo-down | Exon | 442290 | 442350 | 0.03 | −3.53 | 0.00 |
| PHF19 | Hyper-down | 3′ UTR | 273548 | 273938 | 0.00 | −1.29 | 0.04 |
| ADAMTSL1 | Hyper-down | 3′ UTR | 142570 | 142929 | 0.00 | −1.99 | 0.01 |
| PLD3 | Hyper-down | 3′ UTR | 118422 | 118482 | 0.01 | −1.16 | 0.05 |
| CDCA8 | Hyper-down | 3′ UTR | 4260517 | 4260782 | 0.01 | −2.38 | 0.04 |
| PLEKHA6 | Hyper-down | Exon | 333151 | 338353 | 0.01 | −1.76 | 0.02 |
| SHANK1 | Hyper-down | Exon | 403394 | 404020 | 0.01 | −2.14 | 0.00 |
| SHANK1 | Hyper-down | Exon | 406035 | 406274 | 0.01 | −2.14 | 0.00 |
| CENPF | Hyper-down | Exon | 1341226 | 1357574 | 0.01 | −3.67 | 0.00 |
| B4GALNT1 | Hyper-down | 3′ UTR | 320399 | 320607 | 0.01 | −2.38 | 0.04 |
| TEAD4 | Hyper-down | 3′ UTR | 240855 | 242598 | 0.01 | −1.50 | 0.03 |
| RHBDF2 | Hyper-down | 3′ UTR | 274815 | 275085 | 0.03 | −1.86 | 0.02 |
| UHRF1 | Hyper-down | Exon | 560816 | 563952 | 0.02 | −2.62 | 0.01 |
| FOXO1 | Hypo-up | 3′ UTR | 475509 | 475778 | 0.01 | 1.21 | 0.05 |
| LOC102267107 | Hypo-up | 3′ UTR | 311297 | 311596 | 0.01 | 1.49 | 0.02 |

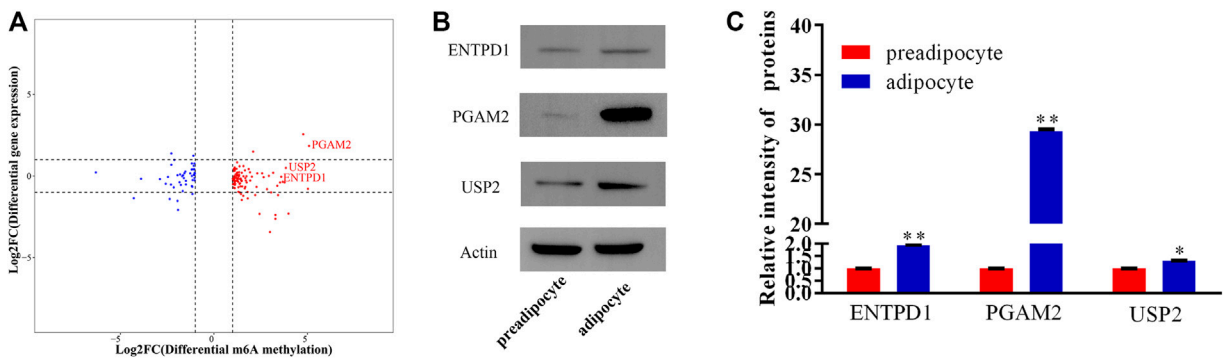



**FIGURE 7 |** The analysis of genes with significant differences in methylation and non-significant differences expression during yak adipocytes differentiation. **(A)** Four quadrant plot showing the genes with significant differences in methylation and non-significant differences expression. **(B,C)** The proteins of USP2, ENTPD1, and PGAM2 were expressed in preadipocytes and adipocytes (SEM, * $p < 0.05$;** $p < 0.01$).

et al., 2013; Wang et al., 2013). In recent years, as the most extensive and plentiful internal modification on mRNAs, m$^6$A modification is a major focus in the area of epigenetic regulation (Niu et al., 2013). Furthermore, the potential roles of m$^6$A modification in most domestic animals, and especially for adipogenic differentiation, remained largely unknown. For the first time, our study establishes a comprehensive transcriptome-wide pattern of m$^6$A modification in yak preadipocyte and adipocyte using MeRIP-Seq technology to explore the function of m$^6$A modification in bovine adipogenic differentiation. Our findings show that yak mRNA m$^6$A sites were primarily located in CDS, 5′UTRs and 3′UTRs, and the distribution semblable with

**TABLE 2 |** List of 10 genes with significant difference in m$^6$A and nonsignificant difference expression in yak adipocyte as compared with preadipocyte.

| Gene name | m$^6$A level | | | | | mRNA level | |
|---|---|---|---|---|---|---|---|
| | Peak region | Peak start | Peak end | diff.log2.fc | diff.p | log2(fc) | *p*-value |
| PGAM2 | Exon | 437745 | 438043 | 5.09 | 0.04 | 1.85 | 1 |
| LOC102285565 | 5′UTR | 38451 | 38681 | 5.03 | 0.00 | −0.78 | 0.44 |
| LOC102280847 | 5′UTR | 101406 | 101799 | 4.78 | 0.00 | 2.57 | 0.28 |
| NRARP | Exon | 501948 | 502122 | 3.99 | 0.00 | −2.30 | 1 |
| USP2 | Exon | 2422394 | 2422633 | 3.85 | 0.00 | 0.50 | 0.62 |
| LOC102284166 | 5′UTR | 252439 | 252618 | 3.78 | 0.02 | −0.38 | 0.57 |
| GPR135 | Exon | 30403 | 30553 | 3.68 | 0.02 | −0.35 | 1 |
| ENTPD1 | 5′UTR | 638635 | 638694 | 3.60 | 0.01 | −0.04 | 1.00 |
| PRR22 | Exon | 80,040 | 80129 | 3.54 | 0.03 | −0.39 | 0.76 |
| ZFPM1 | Exon | 1465574 | 1465753 | 3.43 | 0.00 | −1.16 | 0.24 |

humans and mice (Dominissini et al., 2012; Meyer et al., 2012), suggesting that, in mammalian transcriptomes, the overall distribution of m$^6$A sites is similar. Besides this, Luo et al. reveal that m$^6$A modifications were also enriched near the start codons of Arabidopsis (Luo et al., 2014). Thus, the distribution of m$^6$A modification has various forms in different species. The m$^6$A located at mRNA 5′UTR and 3′UTR of yak differ from mice and chickens (Luo et al., 2019; Cheng et al., 2021). We found m$^6$A more enrichment in 3′UTR compared with 5′UTR, which contrasts with other mammals (Luo et al., 2019; Wang et al., 2019). The high-level of m$^6$A methylation located in 3′UTR may be associated with mRNA stability, selective polyadenylation, signaling transport, and translocation (Shen et al., 2016; Yue et al., 2018). In addition, the m$^6$A modification on the 3′UTR plays a regulatory element role for protein translation by recruiting specific factors to these m$^6$A sites for RNA transport or protein synthesis (Niu et al., 2013; Wang et al., 2014). This may be one of the reasons causing a potential positive correlation between the degree of m$^6$A methylation and transcript levels. Otherwise, the current study finds an m$^6$A peak relatively increased at mRNA 5′UTR in Ad compared with Pread 0. The m$^6$A located at mRNA 5′UTR can improve its cap-independent translation under heat shock (Meyer et al., 2015; Zhou et al., 2015). This indicates that the higher m$^6$A signal at 5′UTR may promote mRNA translation during yak preadipocyte differentiation. Further, in our study, approximately 80% of the methylated transcripts included one or two m$^6$A peaks, and about 20% of the methylated transcripts included three or more than three m$^6$A peaks. The ratio is higher than in humans (5.5%) (Dominissini et al., 2012), pigs (10%) (Wang et al., 2018), chickens (5%) (Cheng et al., 2021), and mice (10%) (Luo et al., 2019). This phenomenon may be due to the more rapid rate of lipid metabolism in yaks, which is consistent with a previous study that cells and tissues with greater proliferation and differentiation capacity may require higher levels of m$^6$A methylation to adapt to faster growth and development (Tao et al., 2017). According to previous studies, the consistent motif pattern of "RRACH" was over-represented in the m$^6$A motif sequence area (Harper et al., 1990; Dominissini et al., 2012; Meyer et al., 2012). Accordingly, in comparison with previous studies (Dominissini et al., 2012; Meyer et al., 2012), the consensus motif GGACU sequence in the yak transcriptome was appropriately identified, revealing that RNA adenosine methylation was conserved in mammals.

Earlier studies indicate that m$^6$A modification is closely related to gene expression (Meyer et al., 2012; Fu et al., 2014; Yue et al., 2015; Chen et al., 2020). Jean-Michel Fustin et al. report that *METTL3* depletion inhibited the export mRNA (Jean-Michel et al., 2013), and Guanqun Zheng et al. report that depletion of *ALKBH5* increased the export of mRNA to the cytoplasm (Zheng et al., 2013), suggesting m$^6$A promotes the export of mRNA and modulates gene expression (Zhao et al., 2017). In HeLa cells, YTHDC1 was discovered to interact with SRSF3 and nuclear RNA export factor 1 (NXF1) to promote the export of m$^6$A-modified mRNA out of the nucleus (Roundtree IA. et al., 2017). These results indicate a potential positive association between the degree of m$^6$A methylation and the transcript level. In the present study, the genes *METTL3*, *WTAP*, *METTL14*, *FTO*, *ALKBH5*, and *YTHDC1/2* were dramatically upregulated in adipocytes than the preadipocytes, and the majority of modified m$^6$A genes were expressed at a medium level with a positive relationship in gene expression and m$^6$A methylated modification. Our findings are in agreement with Chen et al., who reveal that m$^6$A modifications tend to have a positive correlation with mRNA expression in clear cell renal cell carcinoma (Chen et al., 2020). These findings show that m$^6$A methylation affects gene expression by controlling post-transcription regulation. The m$^6$A-reader protein-containing YTH structural domain 2 (YTHDC2) can preferentially bind m$^6$A within the consensus motif and improve the translation efficiency of mRNA (Yang et al., 2018). Interestingly, *YTHDC2* was significantly upregulated during yak preadipocyte differentiation. Therefore, we speculate that m$^6$A methylation modification not only influences mRNA expression but also may regulate mRNA translation during yak preadipocyte differentiation. Consequently, the genes with significant differences in methylation and nonsignificant differences in expression were detected in this study. Intriguingly, the results of Western blot revealed that the expression of ectonucleotidases CD39 (ENTPD1), ubiquitin-specific protease-2 (USP2), and phosphoglycerate mutase 2 (PGAM2) were significantly elevated in adipocytes compared with preadipocytes. Previous studies report that USP2 can influence the stabilization of fatty acid synthase (FAS), and 3,3′-diindolylmethane inhibits

adipogenesis in preadipocytes by targeting USP2 activity (Graner et al., 2004; Yang et al., 2017). Enjyoji et al. reveal that entpd1-deficient mice have impaired glucose tolerance, reduced insulin sensitivity, and significantly elevated plasma insulin levels (Enjyoji et al., 2008). PGAM2 plays an important role in glycolysis, muscle growth and development, and organism physiological balance (Qiu et al., 2008; Mikawa et al., 2021). Accordingly, it is logical to conclude that $m^6A$ methylation modification exerts an essential role through affecting the translation of mRNA during yak preadipocyte differentiation. Nevertheless, further study is needed to verify the conjecture.

GO analysis explored the differentially methylated genes, which participated in the transcript regulation with a variety of transcription factors by RNA polymerase II. For example, FOXO1 identified as a Forkhead transcription factor controlling the differentiation of adipocytes (Nakae et al., 2003) and many members of the ZNF family considered as the crucial eukaryotic transcription factors involved in adipogenic metabolism (Wei et al., 2013), indicating $m^6A$ methylation participates in lipid metabolism. The KEGG pathway analysis revealed that the signaling pathway of differentially methylated genes is closely related to adipose metabolisms, such as the FoxO signaling pathway, Ether lipid metabolism, Glycerophospholipid metabolism, and Hippo signaling pathway-multiple species. In particular, *FOXO1* was further found to be involved in the FoxO signaling pathway, which demonstrated the importance of adipocyte differentiation (Nakae et al., 2003). As a TEA domain family transcription factor, *TEAD4* was selected from Hippo signaling pathway-multiple species, which recruits the cofactors VGLL4 and CtBP2 to inhibit murine adipogenesis (Zhang W. et al., 2018). To summarize the above findings, we concluded that activating the FoxO and Hippo signaling pathways through $m^6A$ methylated gene may perform a key function during the differentiation of yak adipocytes.

Integrated analysis of $m^6A$-seq and mRNA-seq data exposed that 28 significant change genes exist in the adipocyte group with differently methylated $m^6A$ sites compared with preadipocyte. Several of the genes are confirmed to regulate adipose metabolism and adipogenic differentiation, such as *ZNF395*, *KLF9*, *TEAD4*, *FOXO1*, and *UHRF1*. *ZNF395*, the mRNA of which is hypermethylated and the expression upregulated in the adipocyte group compared with the preadipocyte group. As a member of the C2H-type Zinc finger proteins, *ZNF395* is classified as Papillomavirus-binding factor and Huntington disease gene regulatory region binding protein 2 (Tanaka et al., 2004). Experiments of loss and gain function demonstrate that *ZNF395* interacts with *PPARG2* to modulate the transcriptional regulatory pathway that may be necessary for preadipocyte differentiation (Hasegawa et al., 2013). Besides this, previous literature reports that mesenchymal stem cells were cotransduced with *ZNF395* and *PPARG2* enhanced the endogenous expression of *PPARG2* and *C/EBPα*, which are necessary for adipocyte differentiation (Sichtig et al., 2007; Hasegawa et al., 2013). In addition to that, it is reported that Krüppel-like factor 9 (*KLF9*), deemed to be the basic transcription element-binding protein-1 (BTEB1), could transactivate *PPARγ2* to regulate adipogenesis in the 3T3-L1 cell line (Pei et al., 2011). Besides this, Kimura Hiroko et al. find that *KLF9* triggered the early stage of adipogenesis by promoting the *C/EBPβ* gene expression in 3T3-L1 cells (Kimura and Fujimori, 2014). Ubiquitin-like with PHD and RING finger domains 1 (*UHRF1*) is widely documented to promote cell proliferation. Additionally, a study revealed that *UHRF1* facilitates the proliferation of human adipose-derived stem cells and represses adipogenesis via inhibiting peroxisome proliferator-activated receptor $\gamma$ (Chen et al., 2019). These findings suggest that $m^6A$ modifications may perform an essential role during yak adipocyte differentiation.

## CONCLUSION

Current findings display that the $m^6A$ profiles and distribution patterns in the yak transcriptome. Besides this, functional enrichment analysis of differentially methylated genes reveal that several candidate genes participated in lipid metabolic pathways, suggesting that $m^6A$ methylation modifications are involved in the modulation of yak preadipocyte differentiation. Furthermore, we also explore the correlation between $m^6A$ methylation and the level of gene expression or mRNA translation, indicating a potential regulatory mechanism for $m^6A$ in adipocyte differentiation. These results provide additional knowledge of $m^6A$ methylation in adipose tissues, and it set the foundation for further understanding its possible roles and regulatory mechanisms, which could be helpful for exploration the yak adaptive mechanism in the harsh environment.

## DATA AVAILABILITY STATEMENT

The data was submitted to the data base of the Sequence Read Archive (SRA). The appropriate number for accession is PRJNA649748.

## ETHICS STATEMENT

The animal study was reviewed and approved by the Animal Administration and Ethics Committee of Lanzhou Institute of Husbandry and Pharmaceutical Sciences, Chinese Academy of Agricultural Sciences. Written informed consent was obtained from the owners for the participation of their animals in this study.

## AUTHOR CONTRIBUTIONS

The experiments were conceived and designed by YZ and PY. The experiments were performed by YZ. The experiments were assisted with JP, XW, XG, MC, PB, XD, CL. The paper was written by YZ and revised by QK. All authors have read and agreed to the published version of the article.

## FUNDING

The National Natural Science Foundation of China (31972561), The Agricultural Science and Technology

Innovation Program (CAASASTIP-2014-LIHPS-01) and The National Beef Cattle Industry Technology & System (CARS-37). The National Natural Science Foundation of China (31972561) supplied sequencing funding and laboratory verification cost, the Agricultural Science and Technology Innovation Program (CAASASTIP-2014-LIHPS-01) and the National Beef Cattle Industry Technology & System (CARS-37) supplied the source of experimental animals. The funding bodies played no role in the design of the study and collection, analysis, and interpretation of data and in writing the article.

## ACKNOWLEDGMENTS

We thank the Key laboratory of yak Breeding Engineering Gansu Province for experimental condition.

## SUPPLEMENTARY MATERIAL

The Supplementary Material for this article can be found online at: https://www.frontiersin.org/articles/10.3389/fcell.2021.689067/full#supplementary-material

## REFERENCES

Adams, J. M., and Cory, S. (1975). Modified Nucleosides and Bizarre 5′-termini in Mouse Myeloma mRNA. *Nature* 255 (5503), 28–33. doi:10.1038/255028a0

Agarwala, S. D., Blitzblau, H. G., Hochwagen, A., and Fink, G. R. (2012). RNA Methylation by the MIS Complex Regulates a Cell Fate Decision in Yeast. *Plos Genet.* 8 (6), e1002732. doi:10.1371/journal.pgen.1002732

Ali, A. T., Hochfeld, W. E., Myburgh, R., and Pepper, M. S. (2013). Adipocyte and Adipogenesis. *Eur. J. Cel Biol.* 92 (6-7), 229–236. doi:10.1016/j.ejcb.2013.06.001

Bailey, T. L., Boden, M., Buske, F. A., Frith, M., Grant, C. E., Clementi, L., et al. (2009). MEME SUITE: Tools for Motif Discovery and Searching. *Nucleic Acids Res.* 37 (Suppl. l_2), W202–W208. doi:10.1093/nar/gkp335

Batista, P. J., Molinie, B., Wang, J., Qu, K., Zhang, J., Li, L., et al. (2014). m6A RNA Modification Controls Cell Fate Transition in Mammalian Embryonic Stem Cells. *Cell stem cell* 15 (6), 707–719. doi:10.1016/j.stem.2014.09.019

Bokar, J. A., Shambaugh, M. E., Polayes, D., Matera, A. G., and Rottman, F. M. (1997). Purification and cDNA Cloning of the AdoMet-Binding Subunit of the Human mRNA (N6-Adenosine)-Methyltransferase. *Rna* 3 (11), 1233–1247.

Chen, K., Guo, Z., Luo, Y., Yuan, J., and Mo, Z. (2019). UHRF1 Promotes Proliferation of Human Adipose-Derived Stem Cells and Suppresses Adipogenesis via Inhibiting Peroxisome Proliferator-Activated Receptor γ. *Biomed. Research International.* 2019, 9456847 doi:10.1155/2019/9456847

Chen, Y., Zhou, C., Sun, Y., He, X., and Xue, D. (2020). m6A RNA Modification Modulates Gene Expression and Cancer-Related Pathways in clear Cell Renal Cell Carcinoma. *Epigenomics* 12 (2), 87–99. doi:10.2217/epi-2019-0182

Cheng, B., Leng, L., Li, Z., Wang, W., Jing, Y., Li, Y., et al. (2021). Profiling of RNA N6-Methyladenosine Methylation Reveals the Critical Role of m6A in Chicken Adipose Deposition. *Front. Cel Dev. Biol.* 9, 590468. doi:10.3389/fcell.2021.590468

Desrosiers, R., Friderici, K., and Rottman, F. (1974). Identification of Methylated Nucleosides in Messenger RNA from Novikoff Hepatoma Cells. *Proc. Natl. Acad. Sci.* 71 (10), 3971–3975. doi:10.1073/pnas.71.10.3971

Ding, X. Z., Guo, X., Yan, P., Liang, C. N., Bao, P. J., and Chu, M. (2012). Seasonal and Nutrients Intake Regulation of Lipoprotein Lipase (LPL) Activity in Grazing Yak (Bos Grunniens) in the Alpine Regions Around Qinghai Lake. *Livestock Sci.* 143 (1), 29–34. doi:10.1016/j.livsci.2011.08.004

Dominissini, D., Moshitch-Moshkovitz, S., Schwartz, S., Salmon-Divon, M., Ungar, L., Osenberg, S., et al. (2012). Topology of the Human and Mouse m6A RNA Methylomes Revealed by m6A-Seq. *Nature* 485 (7397), 201–206. doi:10.1038/nature11112

Dong, Q., Zhao, X., Ma, Y., Xu, S., and Li, Q. (2006). Live-weight Gain, Apparent Digestibility, and Economic Benefits of Yaks Fed Different Diets during winter on the Tibetan Plateau. *Livestock Sci.* 101 (1-3), 199–207. doi:10.1016/j.livprodsci.2005.11.009

Donohoe, D. R., and Bultman, S. J. (2012). Metaboloepigenetics: Interrelationships between Energy Metabolism and Epigenetic Control of Gene Expression. *J. Cel. Physiol.* 227 (9), 3169–3177. doi:10.1002/jcp.24054

Enjyoji, K., Kotani, K., Thukral, C., Blumel, B., Sun, X., Wu, Y., et al. (2008). Deletion of Cd39/entpd1 Results in Hepatic Insulin Resistance. *Diabetes* 57 (9), 2311–2320. doi:10.2337/db07-1265

Fu, Y., Dominissini, D., Rechavi, G., and He, C. (2014). Gene Expression Regulation Mediated through Reversible m6A RNA Methylation. *Nat. Rev. Genet.* 15 (5), 293–306. doi:10.1038/nrg3724

Furuichi, Y., Morgan, M., Shatkin, A. J., Jelinek, W., Salditt-Georgieff, M., and Darnell, J. E. (1975). Methylated, Blocked 5 Termini in HeLa Cell mRNA. *Proc. Natl. Acad. Sci.* 72 (5), 1904–1908. doi:10.1073/pnas.72.5.1904

Graner, E., Tang, D., Rossi, S., Baron, A., Migita, T., Weinstein, L. J., et al. (2004). The Isopeptidase USP2a Regulates the Stability of Fatty Acid Synthase in Prostate Cancer. *Cancer cell* 5 (3), 253–261. doi:10.1016/s1535-6108(04)00055-8

Harper, J. E., Miceli, S. M., Roberts, R. J., and Manley, J. L. (1990). Sequence Specificity of the Human mRNA N6-Adenosine Methylasein Vitro. *Nucl. Acids Res.* 18 (19), 5735–5741. doi:10.1093/nar/18.19.5735

Hasegawa, R., Tomaru, Y., de Hoon, M., Suzuki, H., Hayashizaki, Y., and Shin, J. W. (2013). Identification of ZNF395 as a Novel Modulator of Adipogenesis. *Exp. Cel. Res.* 319 (3), 68–76. doi:10.1016/j.yexcr.2012.11.003

Heinz, S., Benner, C., Spann, N., Bertolino, E., Lin, Y. C., Laslo, P., et al. (2010). Simple Combinations of Lineage-Determining Transcription Factors Prime Cis-Regulatory Elements Required for Macrophage and B Cell Identities. *Mol. Cel.* 38 (4), 576–589. doi:10.1016/j.molcel.2010.05.004

Huse, J. T., Byant, D., Yang, Y., Pijak, D. S., D'Souza, I., Lah, J. J., et al. (2003). Endoproteolysis of αβ-Secretase (αβ-Site Amyloid Precursor Protein-Cleaving Enzyme) within its Catalytic Domain. *J. Biol. Chem.* 278 (19), 17141–17149. doi:10.1074/jbc.m213303200

Jean-Michel, F., Masao, D., Yoshiaki, Y., Hayashi, H., Shinichi, N., Minoru, Y., et al. (2013). RNA-Methylation-Dependent RNA Processing Controls the Speed of the Circadian Clock. *Cell* 155 (4), 793–806. doi:10.1016/j.cell.2013.10.026

Jia, G., Fu, Y., Zhao, X., Dai, Q., Zheng, G., Yang, Y., et al. (2011). N6-methyladenosine in Nuclear RNA Is a Major Substrate of the Obesity-Associated FTO. *Nat. Chem. Biol.* 7 (12), 885–887. doi:10.1038/nchembio.687

Jiang, Q., Sun, B., Liu, Q., Cai, M., Wu, R., Wang, F., et al. (2019). MTCH2 Promotes Adipogenesis in Intramuscular Preadipocytes via an M 6 A-YTHDF1-dependent Mechanism. *FASEB j.* 33 (2), 2971–2981. doi:10.1096/fj.201801393RRR

Kim, D., Langmead, B., and Salzberg, S. L. (2015). HISAT: a Fast Spliced Aligner with Low Memory Requirements. *Nat. Methods* 12 (4), 357–360. doi:10.1038/nmeth.3317

Kimura, H., and Fujimori, K. (2014). Activation of Early Phase of Adipogenesis through Krüppel-like Factor KLF9-Mediated, Enhanced Expression of CCAAT/enhancer-binding Protein β in 3T3-L1 Cells. *Gene* 534 (2), 169–176. doi:10.1016/j.gene.2013.10.065

Knuckles, P., Lence, T., Haussmann, I. U., Jacob, D., Kreim, N., Carl, S. H., et al. (2018). Zc3h13/Flacc Is Required for Adenosine Methylation by Bridging the mRNA-Binding Factor Rbm15/Spenito to the m6A Machinery Component Wtap/Fl(2)d. *Genes Dev.* 32 (5-6), 415–429. doi:10.1101/gad.309146.117

Kudou, K., Komatsu, T., Nogami, J., Maehara, K., Harada, A., Saeki, H., et al. (2017). The Requirement of Mettl3-Promoted MyoD mRNA Maintenance in Proliferative Myoblasts for Skeletal Muscle Differentiation. *Open Biol.* 7 (9), 170119. doi:10.1098/rsob.170119

Lavi, S., and Shatkin, A. J. (1975). Methylated Simian Virus 40-specific RNA from Nuclei and Cytoplasm of Infected BSC-1 Cells. *Proc. Natl. Acad. Sci.* 72 (6), 2012–2016. doi:10.1073/pnas.72.6.2012

Li, D.-Q., Nair, S. S., and Kumar, R. (2013). The MORC Family. *Epigenetics* 8 (7), 685–693. doi:10.4161/epi.24976

Liu, J., Yue, Y., Han, D., Wang, X., Fu, Y., Zhang, L., et al. (2014). A METTL3-METTL14 Complex Mediates Mammalian Nuclear RNA N6-Adenosine Methylation. *Nat. Chem. Biol.* 10 (2), 93–95. doi:10.1038/nchembio.1432

Liu, N., and Pan, T. (2016). N6-methyladenosine-encoded Epitranscriptomics. *Nat. Struct. Mol. Biol.* 23 (2), 98–102. doi:10.1038/nsmb.3162

Long, R. J., Apori, S. O., Castro, F. B., and Ørskov, E. R. (1999). Feed Value of Native Forages of the Tibetan Plateau of China. *Anim. Feed Sci. Techn.* 80(2), 101–113. doi:10.1016/S0377-8401(99)00057-7

Long, R. J., Ding, L. M., Shang, Z. H., and Guo, X. H. (2008). The Yak Grazing System on the Qinghai-Tibetan Plateau and its Status. *Rangel. J.* 30 (2), 241–246. doi:10.1071/RJ08012

Luo, G.-Z., MacQueen, A., Zheng, G., Duan, H., Dore, L. C., Lu, Z., et al. (2014). Unique Features of the m6A Methylome in Arabidopsis thaliana. *Nat. Commun.* 5, 5630. doi:10.1038/ncomms6630

Luo, S., and Tong, L. (2014). Molecular Basis for the Recognition of Methylated Adenines in RNA by the Eukaryotic YTH Domain. *Proc. Natl. Acad. Sci.* 111 (38), 13834–13839. doi:10.1073/pnas.1412742111

Luo, Z., Zhang, Z., Tai, L., Zhang, L., Sun, Z., and Zhou, L. (2019). Comprehensive Analysis of Differences of N6-Methyladenosine RNA Methylomes between High-Fat-Fed and normal Mouse Livers. *Epigenomics* 11 (11), 1267–1282. doi:10.2217/epi-2019-0009

Martin, M. (2011). Cutadapt Removes Adapter Sequences from High-Throughput Sequencing Reads. *EMBnet j.* 17 (1), 10–12. doi:10.14806/ej.17.1.200

Meng, J., Lu, Z., Liu, H., Zhang, L., Zhang, S., Chen, Y., et al. (2014). A Protocol for RNA Methylation Differential Analysis with MeRIP-Seq Data and exomePeak R/Bioconductor Package. *Methods* 69 (3), 274–281. doi:10.1016/j.ymeth.2014.06.008

Meyer, K. D., Patil, D. P., Zhou, J., Zinoviev, A., Skabkin, M. A., Elemento, O., et al. (2015). 5′ UTR m6A Promotes Cap-independent Translation. *Cell* 163 (4), 999–1010. doi:10.1016/j.cell.2015.10.012

Meyer, K. D., Saletore, Y., Zumbo, P., Elemento, O., Mason, C. E., and Jaffrey, S. R. (2012). Comprehensive Analysis of mRNA Methylation Reveals Enrichment in 3′ UTRs and Near Stop Codons. *Cell* 149 (7), 1635–1646. doi:10.1016/j.cell.2012.05.003

Mikawa, T., Shibata, E., Shimada, M., Ito, K., Ito, T., Kanda, H., et al. (2021). Characterization of Genetically Modified Mice for Phosphoglycerate Mutase, a Vitally-Essential Enzyme in Glycolysis. *Plos one* 16 (4), e0250856. doi:10.1371/journal.pone.0250856

Nachtergaele, S., and He, C. (2017). The Emerging Biology of RNA post-transcriptional Modifications. *RNA Biol.* 14 (2), 156–163. doi:10.1080/15476286.2016.1267096

Nakae, J., Kitamura, T., Kitamura, Y., Biggs, W. H., III, Arden, K. C., and Accili, D. (2003). The Forkhead Transcription Factor Foxo1 Regulates Adipocyte Differentiation. *Dev. Cel.* 4 (1), 119–129. doi:10.1016/s1534-5807(02)00401-x

Niu, Y., Zhao, X., Wu, Y.-S., Li, M.-M., Wang, X.-J., and Yang, Y.-G. (2013). N6-methyl-adenosine (m6A) in RNA: an Old Modification with a Novel Epigenetic Function. *Genomics, Proteomics & Bioinformatics* 11 (1), 8–17. doi:10.1016/j.gpb.2012.12.002

Patil, D. P., Chen, C.-K., Pickering, B. F., Chow, A., Jackson, C., Guttman, M., et al. (2016). m6A RNA Methylation Promotes XIST-Mediated Transcriptional Repression. *Nature* 537 (7620), 369–373. doi:10.1038/nature19342

Pei, H., Yao, Y., Yang, Y., Liao, K., and Wu, J.-R. (2011). Krüppel-like Factor KLF9 Regulates PPARγ Transactivation at the Middle Stage of Adipogenesis. *Cell Death Differ* 18 (2), 315–327. doi:10.1038/cdd.2010.100

Perry, R. P., and Kelley, D. E. (1974). Existence of Methylated Messenger RNA in Mouse L Cells. *Cell* 1 (1), 37–42. doi:10.1016/0092-8674(74)90153-6

Pertea, M., Pertea, G. M., Antonescu, C. M., Chang, T.-C., Mendell, J. T., and Salzberg, S. L. (2015). StringTie Enables Improved Reconstruction of a Transcriptome from RNA-Seq Reads. *Nat. Biotechnol.* 33 (3), 290–295. doi:10.1038/nbt.3122

Ping, X.-L., Sun, B.-F., Wang, L., Xiao, W., Yang, X., Wang, W.-J., et al. (2014). Mammalian WTAP Is a Regulatory Subunit of the RNA N6-Methyladenosine Methyltransferase. *Cell Res* 24 (2), 177–189. doi:10.1038/cr.2014.3

Qiu, H., Zhao, S., Xu, X., Yerle, M., and Liu, B. (2008). Assignment and Expression Patterns of Porcine Muscle-specific Isoform of Phosphoglycerate Mutase Gene. *J. Genet. genomics* 35 (5), 257–260. doi:10.1016/s1673-8527(08)60036-3

Robinson, M. D., McCarthy, D. J., and Smyth, G. K. (2010). edgeR: a Bioconductor Package for Differential Expression Analysis of Digital Gene Expression Data. *Bioinformatics* 26 (1), 139–140. doi:10.1093/bioinformatics/btp616

Roundtree, I. A., Luo, G. Z., Zhang, Z., Wang, X., Zhou, T., Cui, Y., et al. (2017b). YTHDC1 Mediates Nuclear export of N6-Methyladenosine Methylated mRNAs. *Elife* 6, e31311. doi:10.7554/eLife.31311

Roundtree, I. A., Evans, M. E., Pan, T., and He, C. (2017a). Dynamic RNA Modifications in Gene Expression Regulation. *Cell* 169 (7), 1187–1200. doi:10.1016/j.cell.2017.05.045

Schwartz, S., Mumbach, M. R., Jovanovic, M., Wang, T., Maciag, K., Bushkin, G. G., et al. (2014). Perturbation of m6A Writers Reveals Two Distinct Classes of mRNA Methylation at Internal and 5′ Sites. *Cel Rep.* 8 (1), 284–296. doi:10.1016/j.celrep.2014.05.048

Shen, L., Liang, Z., Gu, X., Chen, Y., Teo, Z. W. N., Hou, X., et al. (2016). N 6 -Methyladenosine RNA Modification Regulates Shoot Stem Cell Fate in Arabidopsis. *Dev. Cel.* 38 (2), 186–200. doi:10.1016/j.devcel.2016.06.008

Shi, L., and Wu, J. (2009). Epigenetic Regulation in Mammalian Preimplantation Embryo Development. *Reprod. Biol. Endocrinol.* 7 (1), 59. doi:10.1186/1477-7827-7-59

Shikui, D., Ruijun, L., Muyi, K., Xiaogeng, P., and Yanjun, G. (2003). Effect of Urea Multinutritional Molasses Block Supplementation on Liveweight Change of Yak Calves and Productive and Reproductive Performances of Yak Cows. *Can. J. Anim. Sci.* 83 (1), 141–145. doi:10.4141/a01-097

Sichtig, N., Körfer, N., and Steger, G. (2007). Papillomavirus Binding Factor Binds to SAP30 and Represses Transcription via Recruitment of the HDAC1 Co-repressor Complex. *Arch. Biochem. Biophys.* 467 (1), 67–75. doi:10.1016/j.abb.2007.08.015

Tanaka, K., Shouguchi-Miyata, J., Miyamoto, N., and Ikeda, J.-E. (2004). Novel Nuclear Shuttle Proteins, HDBP1 and HDBP2, Bind to Neuronal Cell-specific Cis-Regulatory Element in the Promoter for the Human Huntington's Disease Gene. *J. Biol. Chem.* 279 (8), 7275–7286. doi:10.1074/jbc.m310726200

Tao, X., Chen, J., Jiang, Y., Wei, Y., Chen, Y., Xu, H., et al. (2017). Transcriptome-wide N 6 -methyladenosine Methylome Profiling of Porcine Muscle and Adipose Tissues Reveals a Potential Mechanism for Transcriptional Regulation and Differential Methylation Pattern. *BMC Genomics* 18 (1), 336. doi:10.1186/s12864-017-3719-1

Wang, X., Lu, Z., Gomez, A., Hon, G. C., Yue, Y., Han, D., et al. (2014). N6-methyladenosine-dependent Regulation of Messenger RNA Stability. *Nature* 505 (7481), 117–120. doi:10.1038/nature12730

Wang, X., Sun, B., Jiang, Q., Wu, R., Cai, M., Yao, Y., et al. (2018). mRNA m6A Plays Opposite Role in Regulating UCP2 and PNPLA2 Protein Expression in Adipocytes. *Int. J. Obes.* 42 (11), 1912–1924. doi:10.1038/s41366-018-0027-z

Wang, X., Zhao, B. S., Roundtree, I. A., Lu, Z., Han, D., Ma, H., et al. (2015). N6-methyladenosine Modulates Messenger RNA Translation Efficiency. *Cell* 161 (6), 1388–1399. doi:10.1016/j.cell.2015.05.014

Wang, Y., Zheng, Y., Guo, D., Zhang, X., Guo, S., Hui, T., et al. (2019). m6A Methylation Analysis of Differentially Expressed Genes in Skin Tissues of Coarse and Fine Type Liaoning Cashmere Goats. *Front. Genet.* 10, 1318. doi:10.3389/fgene.2019.01318

Wang, Z., Yao, H., Lin, S., Zhu, X., Shen, Z., Lu, G., et al. (2013). Transcriptional and Epigenetic Regulation of Human microRNAs. *Cancer Lett.* 331 (1), 1–10. doi:10.1016/j.canlet.2012.12.006

Wei, C. M., and Moss, B. (1975). Methylated Nucleotides Block 5'-terminus of Vaccinia Virus Messenger RNA. *Proc. Natl. Acad. Sci.* 72 (1), 318–322. doi:10.1073/pnas.72.1.318

Wei, S., Zhang, L., Zhou, X., Du, M., Jiang, Z., Hausman, G. J., et al. (2013). Emerging Roles of Zinc finger Proteins in Regulating Adipogenesis. *Cell. Mol. Life Sci.* 70 (23), 4569–4584. doi:10.1007/s00018-013-1395-0

Wen, J., Lv, R., Ma, H., Shen, H., He, C., Wang, J., et al. (2018). Zc3h13 Regulates Nuclear RNA m6A Methylation and Mouse Embryonic Stem Cell Self-Renewal. *Mol. Cel.* 69 (6), 1028–1038. doi:10.1016/j.molcel.2018.02.015

Wu, H., and Sun, Y. E. (2006). Epigenetic Regulation of Stem Cell Differentiation. *Pediatr. Res.* 59 (4), 21R–5R. doi:10.1203/01.pdr.0000203565.76028.2a

Xie, C., Mao, X., Huang, J., Ding, Y., Wu, J., Dong, S., et al. (2011). KOBAS 2.0: a Web Server for Annotation and Identification of Enriched Pathways and Diseases. *Nucleic Acids Res.* 39 (Web Server issue), W316–W322. doi:10.1093/nar/gkr483

Xu, K., Yang, Y., Feng, G.-H., Sun, B.-F., Chen, J.-Q., Li, Y.-F., et al. (2017). Mettl3-mediated m6A Regulates Spermatogonial Differentiation and Meiosis Initiation. *Cel Res* 27 (9), 1100–1114. doi:10.1038/cr.2017.100

Yang, H., Seo, S. G., Shin, S. H., Min, S., Kang, M. J., Yoo, R., et al. (2017). 3,3'-Diindolylmethane Suppresses High-Fat Diet-Induced Obesity through Inhibiting Adipogenesis of Pre-adipocytes by Targeting USP2 Activity. *Mol. Nutr. Food Res.* 61 (10), 1700119. doi:10.1002/mnfr.201700119

Yang, Y., Hsu, P. J., Chen, Y.-S., and Yang, Y.-G. (2018). Dynamic Transcriptomic m6A Decoration: Writers, Erasers, Readers and Functions in RNA Metabolism. *Cel Res* 28 (6), 616–624. doi:10.1038/s41422-018-0040-8

Young, M. D., Wakefield, M. J., Smyth, G. K., and Oshlack, A. (2010). Gene Ontology Analysis for RNA-Seq: Accounting for Selection Bias. *Genome Biol.* 11 (2), R14. doi:10.1186/gb-2010-11-2-r14

Yu, G., Wang, L.-G., and He, Q.-Y. (2015). ChIPseeker: an R/Bioconductor Package for ChIP Peak Annotation, Comparison and Visualization. *Bioinformatics* 31 (14), 2382–2383. doi:10.1093/bioinformatics/btv145

Yue, Y., Liu, J., Cui, X., Cao, J., Luo, G., Zhang, Z., et al. (2018). VIRMA Mediates Preferential m6A mRNA Methylation in 3'UTR and Near Stop Codon and Associates with Alternative Polyadenylation. *Cell Discov* 4 (1), 10–17. doi:10.1038/s41421-018-0019-0

Yue, Y., Liu, J., and He, C. (2015). RNAN6-methyladenosine Methylation in post-transcriptional Gene Expression Regulation. *Genes Dev.* 29 (13), 1343–1355. doi:10.1101/gad.262766.115

Zhang, W., Xu, J., Li, J., Guo, T., Jiang, D., Feng, X., et al. (2018a). The TEA Domain Family Transcription Factor TEAD4 Represses Murine Adipogenesis by Recruiting the Cofactors VGLL4 and CtBP2 into a Transcriptional Complex. *J. Biol. Chem.* 293 (44), 17119–17134. doi:10.1074/jbc.ra118.003608

Zhang, Y., Guo, X., Pei, J., Chu, M., Ding, X., Wu, X., et al. (2020). CircRNA Expression Profile during Yak Adipocyte Differentiation and Screen Potential circRNAs for Adipocyte Differentiation. *Genes* 11 (4), 414. doi:10.3390/genes11040414

Zhang, Y., Wu, X., Liang, C., Bao, P., Ding, X., Chu, M., et al. (2018b). MicroRNA-200a Regulates Adipocyte Differentiation in the Domestic Yak Bos Grunniens. *Gene* 650, 41–48. doi:10.1016/j.gene.2018.01.054

Zhao, B. S., Roundtree, I. A., and He, C. (2017). Post-transcriptional Gene Regulation by mRNA Modifications. *Nat. Rev. Mol. Cel Biol* 18 (1), 31–42. doi:10.1038/nrm.2016.132

Zhao, X., Yang, Y., Sun, B.-F., Shi, Y., Yang, X., Xiao, W., et al. (2014). FTO-dependent Demethylation of N6-Methyladenosine Regulates mRNA Splicing and Is Required for Adipogenesis. *Cel Res* 24 (12), 1403–1419. doi:10.1038/cr.2014.151

Zheng, G., Dahl, J. A., Niu, Y., Fedorcsak, P., Huang, C.-M., Li, C. J., et al. (2013). ALKBH5 Is a Mammalian RNA Demethylase that Impacts RNA Metabolism and Mouse Fertility. *Mol. Cel* 49 (1), 18–29. doi:10.1016/j.molcel.2012.10.015

Zhong, X., Yu, J., Frazier, K., Weng, X., Li, Y., Cham, C. M., et al. (2018). Circadian Clock Regulation of Hepatic Lipid Metabolism by Modulation of m6A mRNA Methylation. *Cel Rep.* 25 (7), 1816–1828. doi:10.1016/j.celrep.2018.10.068

Zhou, J., Wan, J., Gao, X., Zhang, X., Jaffrey, S. R., and Qian, S.-B. (2015). Dynamic m6A mRNA Methylation Directs Translational Control of Heat Shock Response. *Nature* 526 (7574), 591–594. doi:10.1038/nature15377

**Conflict of Interest:** The authors declare that the research was conducted in the absence of any commercial or financial relationships that could be construed as a potential conflict of interest.

**Publisher's Note:** All claims expressed in this article are solely those of the authors and do not necessarily represent those of their affiliated organizations, or those of the publisher, the editors and the reviewers. Any product that may be evaluated in this article, or claim that may be made by its manufacturer, is not guaranteed or endorsed by the publisher.

*Copyright © 2021 Zhang, Liang, Wu, Pei, Guo, Chu, Ding, Bao, Kalwar and Yan. This is an open-access article distributed under the terms of the Creative Commons Attribution License (CC BY). The use, distribution or reproduction in other forums is permitted, provided the original author(s) and the copyright owner(s) are credited and that the original publication in this journal is cited, in accordance with accepted academic practice. No use, distribution or reproduction is permitted which does not comply with these terms.*

frontiers in Genetics

ORIGINAL RESEARCH
published: 21 December 2021
doi: 10.3389/fgene.2021.797490

# Whole Genome Methylation Analysis Reveals Role of DNA Methylation in Cow's Ileal and Ileal Lymph Node Responses to *Mycobacterium avium* subsp. *paratuberculosis* Infection

*Eveline M. Ibeagha-Awemu[1]*, Nathalie Bissonnette[1]*, Suraj Bhattarai[2], Mengqi Wang[1], Pier-Luc Dudemaine[1], Stephanie McKay[2] and Xin Zhao[3]*

[1]Sherbrooke Research and Development Centre, Agriculture and Agri-Food Canada, Sherbrooke, QC, Canada, [2]Department of Animal and Veterinary Sciences, University of Vermont, Burlington, VT, United States, [3]Department of Animal Science, McGill University, Ste-Anne-Be-Bellevue, QC, Canada

OPEN ACCESS

**Edited by:**
*Dhirendra Kumar, National Institute of Environmental Health Sciences (NIEHS), United States*

**Reviewed by:**
*Yufeng Qin, Nanjing Medical University, China*
*Satish Sati, University of Pennsylvania, United States*

***Correspondence:**
*Eveline M. Ibeagha-Awemu*
*Eveline.ibeagha-awemu@agr.gc.ca*
*Nathalie Bissonnette*
*nathalie.bissonnette@agr.gc.ca*

**Specialty section:**
*This article was submitted to Epigenomics and Epigenetics, a section of the journal Frontiers in Genetics*

**Received:** *18 October 2021*
**Accepted:** *22 November 2021*
**Published:** *21 December 2021*

**Citation:**
*Ibeagha-Awemu EM, Bissonnette N, Bhattarai S, Wang M, Dudemaine P-L, McKay S and Zhao X (2021) Whole Genome Methylation Analysis Reveals Role of DNA Methylation in Cow's Ileal and Ileal Lymph Node Responses to* Mycobacterium avium *subsp.* paratuberculosis *Infection. Front. Genet. 12:797490. doi: 10.3389/fgene.2021.797490*

Johne's Disease (JD), caused by *Mycobacterium avium subsp paratuberculosis* (MAP), is an incurable disease of ruminants and other animal species and is characterized by an imbalance of gut immunity. The role of MAP infection on the epigenetic modeling of gut immunity during the progression of JD is still unknown. This study investigated the DNA methylation patterns in ileal (IL) and ileal lymph node (ILLN) tissues from cows diagnosed with persistent subclinical MAP infection over a one to 4 years period. DNA samples from IL and ILLN tissues from cows negative (MAPneg) ($n$ = 3) or positive for MAP infection (MAPinf) ($n$ = 4) were subjected to whole genome bisulfite sequencing. A total of 11,263 and 62,459 differentially methylated cytosines (DMCs), and 1259 and 8086 differentially methylated regions (DMRs) (FDR<0.1) were found between MAPinf and MAPneg IL and ILLN tissues, respectively. The DMRs were found on 394 genes (denoted DMR genes) in the IL and on 1305 genes in the ILLN. DMR genes with hypermethylated promoters/5′UTR [3 (IL) and 88 (ILLN)] or hypomethylated promoters/5′UTR [10 (IL) and 25 (ILLN)] and having multiple functions including response to stimulus/immune response (*BLK, BTC, CCL21, AVPR1A, CHRNG, GABRA4, TDGF1*), cellular processes (*H2AC20, TEX101, GLA, NCKAP5L, RBM27, SLC18A1, H2AC20BARHL2, NLGN3, SUV39H1, GABRA4, PPA1, UBE2D2*) and metabolic processes (*GSTO2, H2AC20, SUV39H1, PPA1, UBE2D2*) are potential DNA methylation candidate genes of MAP infection. The ILLN DMR genes were enriched for more biological process (BP) gene ontology (GO) terms ($n$ = 374), most of which were related to cellular processes (27.6%), biological regulation (16.6%), metabolic processes (15.4%) and response to stimulus/immune response (8.2%) compared to 75 BP GO terms (related to cellular processes, metabolic processes and transport, and system development) enriched for IL DMR genes. ILLN DMR genes were enriched for more pathways ($n$ = 47) including 13 disease pathways compared with 36 enriched pathways, including 7 disease/immune pathways for IL DMR genes. In conclusion, the results show tissue specific responses to MAP infection with more epigenetic changes (DMCs and DMRs) in the ILLN than in the IL tissue, suggesting

that the ILLN and immune processes were more responsive to regulation by methylation of DNA relative to IL tissue. Our data is the first to demonstrate a potential role for DNA methylation in the pathogenesis of MAP infection in dairy cattle.

**Keywords: DNA methylation, Johne's disease, *Mycobacterium avim* subsp. *paratuberculosis*, dairy cow, ileum and ileum lymph node, differentially methylated cytosines and differentially methylated regions**

## INTRODUCTION

Infection with *Mycobacterium avium* subsp. *paratuberculosis* (MAP), the causative agent of Johne's disease (JD) of bovine and other ruminants, is one of the major threats to cattle health and the economic profitability of the dairy industry (Whittington et al., 2019). JD is a long progressive and chronic enteric disease which progresses through three phases upon MAP infection (silent, subclinical, and clinical/advanced stages) and is characterized by imbalance in gut immunity, and MAP's ability to escape host immune surveillance, and subvert host cell responses to ensure its intracellular survival and replication (Whitlock and Buergelt, 1996; Arsenault et al., 2014; Koets et al., 2015). Similar with other mycobacterial organisms, MAP infects and persists first in macrophages and is found in lymphatic tissues before inducing pathology in the gut or elsewhere, as a secondary process. MAP acquired propensity to infect macrophages helps it to exquisitely adapt and survive in an aggressive host immune response environment. The long-term subclinical period (2–5 years) between the infection period (phase I) and the clinical period (phase III) of JD provides an opportunity for MAP to adapt its environment for its survival. It is known that, pathogenic mycobacteria, including the *Mycobacterium avium* complex pathogens, respond to host immune responses with counterattack strategies, notably to escape the maturation of phagolysosomes of the phagocytotic cells, which function to destroy them (Liu and Modlin, 2008). The involvement of epigenetic mechanisms in the regulation of MAP survival in the host has been proposed (Ariel et al., 2020), requiring further investigations. Furthermore, reported potential connection between JD and human diseases like Crohn's disease (CD) and arthritis rheumatoid (Over et al., 2011; Mcnees et al., 2015; Timms et al., 2016; Bo et al., 2020) emphasizes the importance of controlling JD. In addition, the effect of JD on animals, the environment and the economy highlights the need for deeper understanding of the host cellular processes that are perturbed or manipulated by MAP, in order to develop robust disease control strategies.

Several recent reviews have documented the contribution of epigenetic regulation (DNA methylation, histone modifications and miRNA and lncRNA expression) to economically important livestock traits, including disease susceptibility and the immune response (Doherty et al., 2014; Ibeagha-Awemu and Zhao, 2015; Triantaphyllopoulos et al., 2016; Thompson et al., 2020; Wang and Ibeagha-Awemu, 2021). For instance, miRNAs have been found to regulate the autophagic response to eliminate intracellular *Mycobacterium* (Wang et al., 2013; Wang et al., 2020), modulate inflammatory signaling and to control pathogen survival and replication including *Mycobacterium tuberculosis* (Sharbati et al., 2011; Mehta and Liu, 2014). Moreover, altered expression of miRNAs during bacterial (mycobacteria, salmonellae and listeriae) invasion of host cells have been shown to affect immune signalling pathways including apoptosis and autophagy related pathways (Sharbati et al., 2011; Hoeke et al., 2013; Pawar et al., 2016; Zur Bruegge et al., 2017). Meanwhile, DNA methylation, especially in CpG (cytosine-phosphate-guanosine) context, has been demonstrated for several cattle disease conditions caused by various pathogens, including *Mycobacterium bovis* (Doherty et al., 2016), etc. For example, the bovine $CD4^+$ T cells methylome comparison revealed 196 differentially methylated regions (DMRs) that directly contributed to differential gene expression including key inflammatory genes in $CD4^+$ cells isolated from *Mycobacterium bovis*-infected cows (Doherty et al., 2016). In addition, an *in vitro* study found that DNA methylation could regulate NLRP3 promoter activity and its gene expression, thereby implicating DNA methylation in NLRP3 inflammasome activation in response to *Mycobacterium tuberculosis* infection (Wei et al., 2016). Our recent studies reported that MAP impacted the expression of epigenetics genes (Ariel et al., 2019), the lncRNA pattern of macrophage, and the first host immune cell defense encountered while invading cows (Gupta et al., 2019; Marete et al., 2021b). Moreover, comparing the transcriptome landscape of macrophages and small intestinal tissues and draining lymph nodes from JD positive cows with JD negative cows, we observed modifications that show the apparent importance of immune and metabolic pathways hijacked by MAP to subvert the host immune system (Ariel et al., 2020; Ibeagha-Awemu et al., 2021) suggesting a role of epigenetic processes in host response to MAP infection. However, the effect of MAP on the bovine epigenome, specifically the DNA methylome remains unexplored. Considering that intracellular microbial infection can lead to alterations of the host DNA methylome; we hypothesize that epigenetics regulation would be among strategies used by MAP to establish a tolerant environment in infected cows. Therefore, this study used whole genome bisulfite sequencing (WGBS) technique to test the hypothesis that DNA methylation patterns of cow small intestinal tissues are altered during subclinical MAP infection.

## MATERIALS AND METHODS

### Experimental Animals

Animal selection and diagnosis of MAP status has been described in details in our recent publication (Ibeagha-Awemu et al., 2021). Briefly, animals were from companion studies (Ariel et al., 2020; Marete et al., 2021b; Marete et al., 2021c) which includes 23

commercial dairy farms (tie and free stall) positive for JD and located in the provinces of Québec and Ontario, Canada. Blood and fecal samples collected twice a year and over a period of one to 4 years were diagnosed for MAP status as described previously (Fock-Chow-Tho et al., 2017). Two different tests, Pourquier serum ELISA assay (IDEXX Laboratories, Markham, Ontario, Canada) and MAP fecal PCR were used to diagnosis for the presence of MAP. Cows positive for both serological and fecal tests were grouped as MAP-infected (MAPinf) ($n = 4$) while cows negative for both tests constituted the MAP-negative (MAPneg) or control group ($n = 5$). Mycobacterial fecal culture (Laboratoire d'épidémiosurveillance animale du Québec, Saint-Hyacinthe, Québec, Canada) was used to confirm live MAP excretion, as previously described (Arango-Sabogal et al., 2016). Animals ($n = 9$) were humanely euthanized by intra-venous administration of 5 mg detomidin and 120 ml euthansol, and ileal (IL) and ileal lymph node (ILLN) tissues without visible Peyer's patches were collected. Ileal tissue was taken at about 35 cm before the ileocecal valve and ILLN tissue was collected proximal to this point. Following collection of tissues, a third test, f57 real time qPCR was performed to confirm the presence or absence of MAP in the tissues according to our previous study (Ibeagha-Awemu et al., 2021). MAP was identified in tissues from all cows in the MAPinf group and its absence was demonstrated in all tissues from 3 cows out of 5 in MAPneg group (Ibeagha-Awemu et al., 2021). Only the 4 cows in MAPinf group and 3 cows in MAPneg group were further used.

## Acid Fast Staining

Tissue pieces about 3–4 $mm^2$, sampled for DNA methylation analysis were immediately embedded in OCT (Optimal cutting temperature compound) and stored in sealed containers at −80°C. Tissue sections (8 μm) were cut for acid fast staining at the Plateforme d'histologie et microscopie électronique, Faculté de médecine, Université de Sherbrooke.

## Library Preparation and Whole Genome Bisulfite Sequencing

Genomic DNA was isolated from IL and ILLN tissues using DNeasy Blood and Tissue Kit (Qiagen). DNA was quantified using the Quant-iT™ PicoGreen® dsDNA Assay Kit (Life Technologies) and bisulfite converted using the EZ DNA Methylation-Lightning Kit (Zymo). Libraries were generated using 200 ng DNA/sample and the NEBNext Ultra II DNA Library Prep Kit for Illumina (New England BioLabs) according to manufacturer's protocol, including CpG methylated pUC19 and unmethylated lambda phage spike-in controls. Size selection of libraries containing the desired insert size was achieved with SPRIselect beads (Beckman Coulter). Libraries were quantified using the Kapa Illumina GA with Revised Primers-SYBR Fast universal kit (Kapa Biosystems) and average size fragment was determined using a LabChip GX (PerkinElmer) instrument.

The libraries were normalized and pooled and then denatured in 0.05 N NaOH and neutralized using HT1 buffer. The pool was loaded at 225pM on an Illumina NovaSeq S4 lane using Xp protocol as per the manufacturer's recommendations. The run was performed for 2 × 150 cycles (paired-end mode). A phiX library was used as a control and mixed with libraries at 5% level. Base calling was performed with RTA v3. Bcl2fastq2 v2.20 software was used to demultiplex samples and to generate fastq reads. Sequencing was performed to achieve an average depth of 20× using the Illumina NovaSeq S4 system (Illumina, United States). WGBS library preparation and sequencing was performed by the Centre d'expertise et de services Génome Québec (https://cesgq.com/).

## Bioinformatics Processing of Whole Genome Bisulfite Sequencing Data

Initial quality control on raw reads to remove low quality reads (Phred score <20) and adaptor sequences was performed with TrimGalore v0.4.4 (Krueger, 2012) and CutAdapt v1.13 (Martin, 2011) programs using the default parameters. Read quality and metrics were visualised and curated using FastQC v0.11.3 (Andrews, 2010). The bovine reference genome, ARS-UCD1.2 was indexed using BSseeker2 -v2.1.7 (Guo et al., 2013). The cleaned data for each sample were then aligned to the indexed reference genome using bowtie2 aligner within BSseeker2 (Guo et al., 2013). Mapped reads were fixmated, sorted, and PCR duplicates removed with SAMtools-v1.7 (Li et al., 2009). The methylation level in each cytosine was then determined using BSseeker2 using the default parameters. Methylation data output included read coverage and percentage of methylated cytosines at each genomic cytosine position. Methylation sites in the context of CpG (cytosine-phosphate-guanosine) and non CpG (i.e. CHG or CHH where H denotes C (cytosine), A [adenosine) or T (thymine)] were extracted for each sample. Methylated cytosines were analysed in genic context including promoter (2000 bp upstream of the transcription start site), 5′UTR, exon, intron, 3′UTR and downstream region (2000 bp downstream of the transcription termination site) of genes, and in CpG island (CGI) context including regions surrounding CGIs such as CGI shores and CGI shelves. CGI shores included the 2 kb region upstream of the CpG island (CGI shore left) and 2 kb region downstream of the CpG island (CGI shore right). CGI shelves included the 2 kb region upstream of the CpG shore left (CpG shelf left) and 2 kb region downstream of the CpG shore right (CGI shelf right). Histograms of methylation sites, coverage and methylation distribution for all samples were performed with the R package methylKit -v1.12.0 (https://bioconductor.org/packages/release/bioc/html/methylKit.html) (Akalin et al., 2012). Moreover, the methylation levels of MAP-infected and negative IL or ILLN samples were merged and density plots generated according to chromosomes using the R package, Circlize (Gu et al., 2014) (https://cran.r-project.org/web/packages/circlize/index.html).

Based on CpG methylation, correlation analysis to determine the relationship between samples and principal component analysis to visualize sample clustering was also performed with methylKit. DNA methylation dynamic plots were generated with Beanplot program in R package (https://cran.r-project.org/web/packages/beanplot/) (Kampstra, 2008).

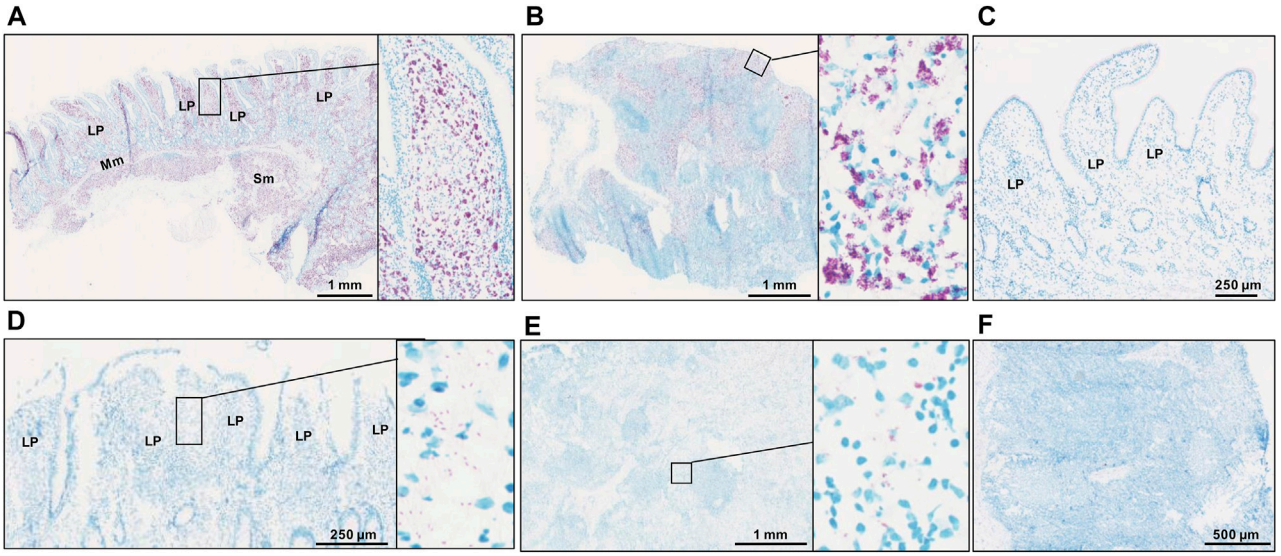



**FIGURE 1 |** Acid-fast staining for acid-fast bacteria in ileum **(A)** and ileum lymph node **(B)** from a MAP-infected cow with high copies of MAP, showing abundant acid-fast staining (purple color). Panels **(D)** (ileum) and **(E)** (ileum lymph node) are tissues from a MAP-infected cow with fewer copies of MAP, showing very sparse acid-fast staining. No evidence of acid fast bacteria was seen in ileum **(C)** and ileum lymph node **(F)** tissues of a MAP-negative cow. LP, lamina propria; Mm, muscularis mucosa; SM, submucosa.

## Differentially Methylated Cytosines and Regions, and Annotation

Methylated sites were compared between MAPinf and MAPneg groups with the Radmeth function of Methpipe -v3.4.3 (Song et al., 2013). The original *p* values generated from regression with the Radmeth were adjusted for multiple testing and combining significance in the bins of 1:200:1 which gave the false discovery rate (FDR) corrected *p* value. The annotation files for the genic region and CGIs were downloaded from the UCSC genome browser by selecting ARS-UCD1.2 assembly for Cow genome. Differentially methylated cytosines (DMCs) and differentially methylated regions (DMRs) were annotated within genic regions (promoter, 5′UTR, exon, intron, 3′UTR and downstream region) and in CGI context (CGIs, CGI shores and CGI shelves) with R package annotatr -v1.8.0 (Cavalcante and Sartor, 2017). Significantly differentially methylated cytosines and DMRs were defined as having Benjaminin and Hochberg (Benjamini and Hochberg, 1995) corrected false discovery rate (FDR) < 0.1. DMRs were further filtered for length (<1 kb) and including at least 3 CpG sites.

## Gene Ontology and Pathways Analysis

Genes harboring DMRs were subjected to functional enrichment analysis using ClueGO (http://apps.cytoscape.org/apps/cluego) (Bindea et al., 2009), which is an APP in Cytoscape (Shannon et al., 2003). Gene ontology (GO) terms and Kyoto Encyclopedia of Genes and Genomes (KEGG) pathways were adjusted with Benjamini-Hochberg correction FDR (Benjamini and Hochberg, 1995) and considered significantly enriched at FDR <0.05. GO terms were grouped in to biological processes (BP), molecular functions (MF) and cellular component (CC) categories. Enriched KEGG pathways were visualized with ClueGO.

# RESULTS

## MAP is Present in the Analyzed Tissues

Following the results of f57 qPCR demonstrating the presence of MAP in the MAPinf tissues and absence in the MAPneg tissues (Ibeagha-Awemu et al., 2021), we performed acid fast staining to visualize the distribution of MAP in the analyzed tissues. The result of acid fast staining showed abundant presence of acid fast bacteria (**Figures 1A,B**) or sparse-acid fast staining indicative of fewer acid fast bacteria (**Figures 1D,E**) in IL and ILLN tissues from two MAPinf cows. Meanwhile, no evidence of acid fast bacteria indicative of the absence of MAP was seen in IL and ILLN tissues from a MAPneg cow (**Figures 1C,F**). This result is consistent with the copy numbers of MAP detected by the method of f57 qPCR (Ibeagha-Awemu et al., 2021).

## Mapping Statistics

Genome-wide DNA methylation sequencing was conducted on IL and ILLN tissues from four cows positive for MAP infection and three cows negative for MAP infection at a depth of 25× and read length of 150 bp. A total of 2.02 B (billion) and 1.87 B clean reads (adaptor sequences, and reads with Phred score <20 removed) were obtained for IL and ILLN samples, respectively (**Supplementary Table S1**). Out of these numbers, 70.39% (IL) and 71.67% (ILLN) were uniquely aligned to the bovine reference genome. Mapping rate of bases (A, T, or C) ranged from 68.93 to 71.09% for IL samples and from 69.27 to 76.79% for ILLN samples of the seven cows. The average rate of methylated

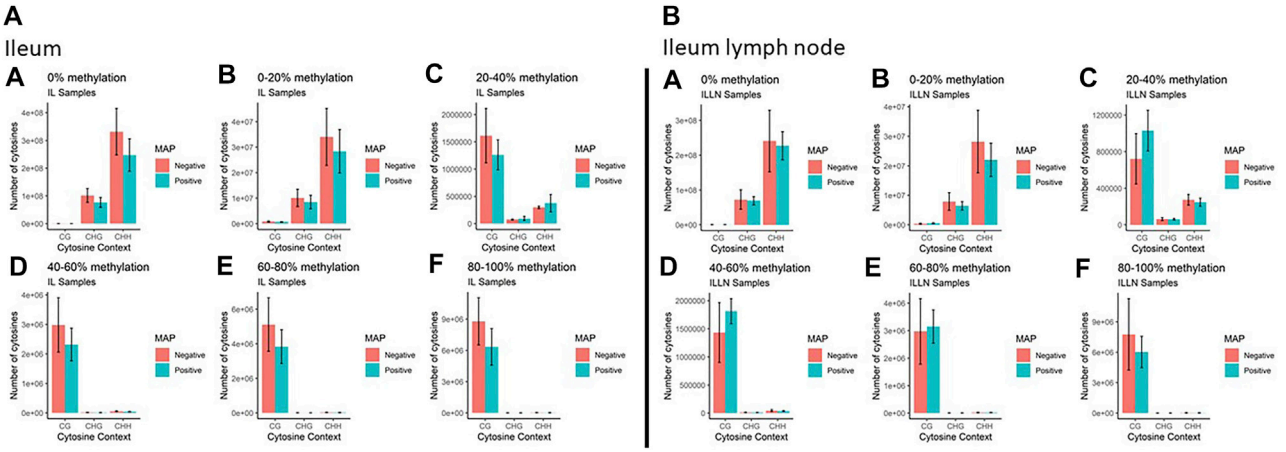



**FIGURE 2 |** The total number of cytosines present in CpG and non-CpG (CHG and CHH, where H = A, T or C) context along with the methylation levels in MAP-infected and MAP-negative **(A)** ileum (IL) and **(B)** IL lymph node (ILLN) samples. Moving from A to F in both IL and ILLN samples, the number of cytosines and percent methylation increases in CpG context whereas it decreases in non-CpG.

cytosines in CpG (or mCG), mCHG and mCHH contexts were 67.72, 0.89, 0.90, 71.34, 0.86 and 0.87% in IL and ILLN samples, respectively (**Supplementary Table S1**). Examination of the percentage of methylation in the various contexts indicated that, the number of cytosines and percent methylation increased in CpG context whereas it decreased in non-CpG context (**Figure 2**). Since methylation rates in the mCHG and mCHH contexts were very low, subsequent analyses were based on CpG context only.

## Global Mapping of DNA Methylation Status

A total of 44.5 million (M) (MAPinf) and 38.6 M (MAPneg), and 38.8 M (MAPinf) and 28.4 M (MAPneg) CpG sites with read coverage per base ≥10× were found in IL and ILLN samples respectively. Out of these, 15.7 M (including 1,342,23 sites in genic regions) and 12.3 M (including 1,246,608 sites in genic regions) methylated sites in IL and ILLN tissues of the seven cows, respectively were used to determine significantly differential methylation between MAPinf and MAPneg cows in each tissue. Pearson correlation was performed to understand the relationship between samples. As shown in **Supplementary Figure S1**, samples in both tissues were highly correlated with a Pearson correlation coefficient range from 0.70 to 0.79. Global chromosomal dynamics of methylated cytosine distribution in each group and tissue are shown in **Supplementary Figure S2**. To gain further insight into the methylation profiles, the extent of methylation levels at different genic regions was also analysed. Bean plots show that most of the CpG sites in the 5′UTR and promoter had low levels of methylation (mean of ~35 and ~48% in IL or ~47 and ~57% in ILLN, respectively), whereas, most of the CpG sites in other genic regions had higher levels of methylation (mean of >72% in both tissues) (**Supplementary Figures S3A,B**). Moreover, the mean level of methylation was slightly higher in the promoters and intron regions of IL MAPinf samples as compared to IL MAPneg samples. The converse was true for ILLN samples whereby the methylation rates were slightly lower in ILLN MAPinf samples as compared to ILLN MAPneg samples (**Supplementary Figures S3A,B**).

## Differentially Methylated Cytosines Between MAP-Infected and MAP-Negative Samples, and Distribution Patterns

A total of 11,263 and 62,459 significant DMCs (FDR<0.1) were found between MAPinf and MAPneg samples, including 1857 and 7703 in genic regions in IL and ILLN tissues, respectively (**Supplementary Tables S2A–D** and **Supplementary Figure S4**). Out of this number, 297 or 508, respectively were located in the promoter and 5′UTRs while highest numbers were located in intron regions. Chromosomal distribution of DMCs between MAPinf and MAPneg cows showed higher concentrations ($n$ > 500) on *Bos taurus* chromosomes (BTA) 1, 2, 3, 4, 5, 6, 7, 8, 9 and X and lowest numbers ($n$ < 100) on BTA 22, 28 and 29 in the IL (**Supplementary Table S2E**). Similarly, more significant DMCs (>3900) were located on BTA 1, 2, 3, 4, 5, 6, 7, 8, 9 and X and least numbers on BTA 25 ($n$ = 397), 28 (n = 429) and 29 ($n$ = 462) in ILLN samples (**Supplementary Table S2E**). A total of 835 DMCs, including 124 DMCs in genic regions, were common to both IL and ILLN tissues (**Supplementary Tables S2F,G**). The degree of methylation was further classified into hypermethylation (methylation difference (increase) between MAPinf and MAPneg samples is 25% or more), hypomethylation (methylation difference (decrease) between MAPinf and MAPneg samples is 25% or more) or none (neither hypermethylated or hypomethylated and having methylation difference < |25%|). In both tissues, a higher number of genic region DMCs were hypomethylated as compared to hypermethylation status (**Figures 3C,D**).

Distribution in CGI context indicated a higher number of significant DMCs in CGIs, CGI shores and shelves in IL (1697) as compared to 1529 in ILLN (**Figures 3E,F**, and **Supplementary Tables S3A,B**). Relative to CGIs, more DMCs were found in CGI

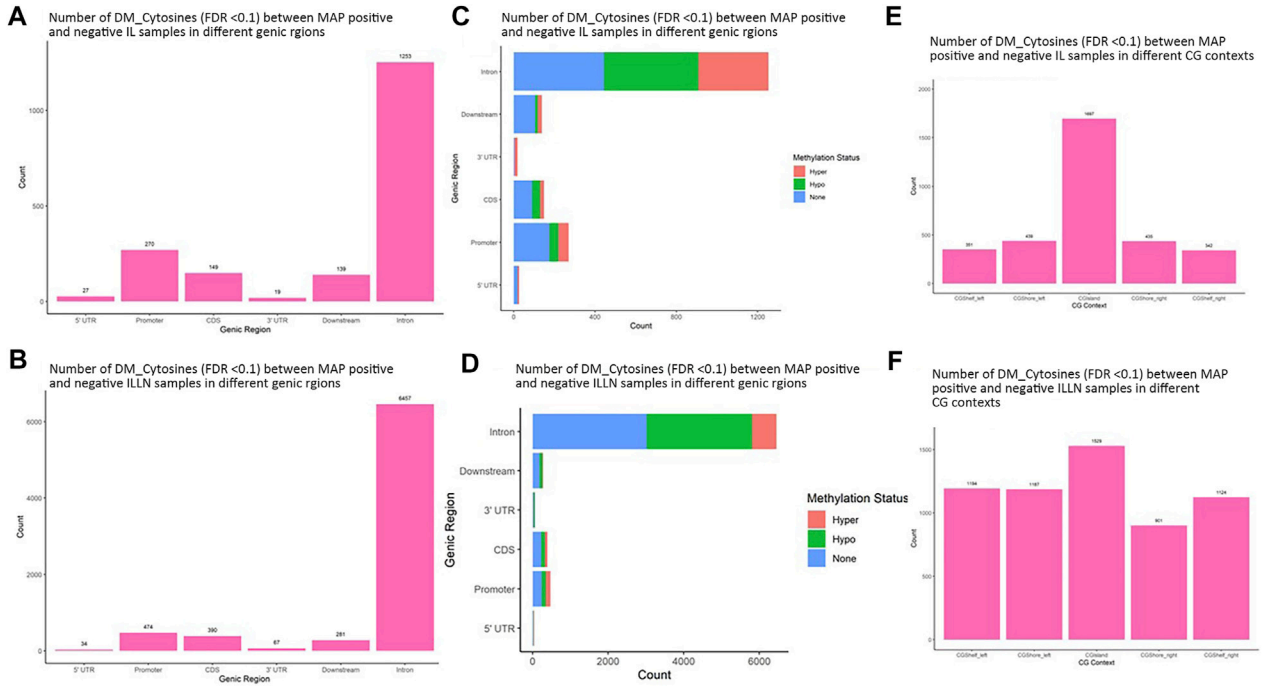



**FIGURE 3 |** Distribution of significantly differentially methylated cytosines (DMC) (FDR<0.1) in different genic regions between MAP-infected (MAPinf) and MAP-negative (MAPneg) **(A)** ileum (IL) and **(B)** IL lymph node (ILLN) tissues, and corresponding methylation status in **(D)** IL and **(C)** ILLN. A DMC was considered hypermethylated if it had a positive methylation difference ≥25% between MAPinf and MAPneg samples. Similarly, a DMC was hypomethylated if it had a negative methylation difference ≥25% between MAPinf and MAPneg samples. A DMC methylation status of none implies that the methylation difference was less than 25% in both scenarios. Distribution of differentially methylated cytosines in CG context in **(E)** IL and **(F)** ILLN tissues between MAPinf and MAPneg samples.

shores left and right than in CGI shelves left and right in IL, meanwhile, CGI shore left and CGI shelf left contained slightly higher numbers of DMCs than CGI shore right and CGI shelf right, respectively in ILLN (**Figures 3E,F** and **Supplementary Tables S3A,B**).

The DMCs were annotated to 503 genes in the IL, including to the promoters and or 5′UTRs of 54 genes (**Supplementary Table S2B**). In the IL, the most significant DMCs were found in the promoter regions of *TMEM15* (17 DMC sites, FDR from 5.89E-07 to 1.60E-04), *CDKN2C* (13 DMC sites, FDR from 2.46E-04 to 7.57E-04), CDS of *HSPA1A* (13 DMC sites, FDR = 1.49E-05 to 9.87E-04) and introns of *CD38* (2 DMC sites, FDR = 2.78E-05 to 0.0019), *CESP-1* (16 DMC site, FDR = 1.27E-04 to 0.004), *BCL2* (22 DMC sites, FDR from 1.45E-04 to 0.003), *NTRK3* (5 DMC sites, FDR from 4.65E-04 to 7.57E-04). A total of 89 genes harbored 6 to 89 DMCs, including bta-mir-2887–1 (89 DMC sites in downstream region), *HSPA1A* (48 sites in CDS), *PGAM1* (25 DMC sites in promoter), *BCL2* (22 DMC sites in intron), *TMEM15* (22 DMC sites in promoter), *CESP-1* (16 DMC sites in intron), *VPS37B* (16 DMC sites in intron), *BCL6* (15 DMCs in promoter) and *CD34* (15 DMCs in intron) (**Table 1**). Moreover, two genes harbored 14 (*TKTL1*) and 12 (*TOP3A*) DMC sites in their promoters, 5′UTRs and CDS.

In the ILLN, the significant DMCs were annotated to 1717 genes including in the promoters or 5′UTRs of 119 genes (**Supplementary Table S2D**). The most significant DMCs were found in the introns of *SOBP* (5 DMC sites, FDR from 1.33E-05 to 3.67E-05), *PDE5A* (8 DMC sites, FDR from 1.92E-05 to 0.0083), *PRDM5* (2 DMC sites, FDR = 1.54E-04), *ZNF553*, (14 DMC sites in downstream region, FDR from 2.41E-04 to 0.0091), *UBAC2* (4 DMC sites, FDR from 8.43E-04 to 0.0018), *RORB* (16 DMC sites, FDR from 0.0022 to 0.0049) and promoter of *RBM27* (9 DMC sites, FDR from 5.03E-04 to 0.0064). A total of 422 genes harbored 6 to 64 DMCs including *NLGN1* (64 DMC sites in intron), bta-mir-2887–1 (57 sites in downstream region), PDE5A (52 sites in intron), *PTPRK* (38 sites in intron), *TENM1* (37 sites in intron) and *EFNAS* (36 sites in 3′UTR and intron), etc. Moreover, about 36 genes harbored 6 to 21 DMC sites in their promoters including miR-387–1 (21 sites), *SUV39H1* (18 sites), *MSN* (17 sites), *OTUD5* (17 sites), *NR2E1* (16 sites), *TMEM15* (13 sites), etc.

## Differentially Methylated Regions Between MAP-Infected and MAP-Negative Samples, and Distribution Patterns

Significant DMRs were 1259 and 8086 (FDR<0.1) between MAPinf and MAPneg IL and ILLN samples, respectively (**Supplementary Tables S4A–D**). Chromosomal distribution indicated a higher number of DMRs (≥60 DMRs) on BTA 1, 2, 3, 4, 5, 6, 7, 8 and 9 in IL and on (≥400 DMRs) BTA 1, 2, 3, 4, 5, 6, 7, 8, 9 and X in ILLN while the least numbers were found on BTA 22 (n = 8), 28 (n = 12) and 29 (n = 11) in the IL and on BTA 25 ($n$ = 47), 28 ($n$ = 57) and 29 (n = 69) in the ILLN

**TABLE 1 |** Genes with hypermethylated or hypomethylated DMRs in their promoters or 5′UTRs in the ileum and ileum lymph node tissues of MAP-infected cows.

| Chr[a] | Start | End | MethyStatus[b] | MethDiff[c] | # CG[d] | Gene symbol and synonyms | Genic region | Function |
|---|---|---|---|---|---|---|---|---|
| **Ileum** | | | | | | | | |
| chr1 | 2767388 | 2767399 | Hyper | 0.4545 | 3 | C1H21orf62 | 5′ UTR | Not available |
| chr26 | 24841896 | 24841962 | Hyper | 0.2703 | 5 | GSTO2 | 5′ UTR | Involved in metabolic processes |
| chr1 | 83304091 | 83304285 | Hyper | 0.2926 | 14 | MAP6D1 | Promoter | Implicated in calmodulin binding |
| chr4 | 112058821 | 112059126 | Hyper | 0.2504 | 10 | EZH2 | Promoter | Involved in B cell differentiation, DNA methylation and histone H3K27 methylationetc. |
| chr6 | 102277355 | 102277489 | Hyper | 0.2670 | 6 | HSD17B11 | Promoter | Involved in androgen catabolic process and estrogen biosynthetic process |
| chr7 | 11812988 | 11813064 | Hyper | 0.3420 | 7 | MIR181D | Promoter | Supports mRNA binding and is involved in posttranscriptional gene silencing |
| chr8 | 60445670 | 60445682 | Hyper | 0.5972 | 3 | CCIN | Promoter | Roles in actin filament binding and protein binding. Involved in actin cytoskeleton organization, brain development, cell differentiation and spermatogenesis |
| chr19 | 42828468 | 42828675 | Hyper | 0.4820 | 11 | CCDC56; COA3 | Promoter | Roles in protein binding; involved in mitochondrial cytochrome c oxidase assembly and positive regulation of mitochondrial translation |
| chr7 | 50789736 | 50789822 | Hypo | −0.3279 | 10 | UBE2D2 | 5′ UTR | Involved in cellular processes, ubiquitin-protein ligase and metabolic processes |
| chr11 | 88020652 | 88021055 | Hypo | −0.3464 | 6 | ITGB1BP1 | 5′ UTR | Roles in GDP-dissociation inhibitor activity; integrin binding; protein kinase binding; and is involved in Notch signaling pathway, activation of protein kinase B activityetc. |
| chrX | 50803770 | 50803957 | Hypo | −0.2683 | 10 | GLA | 5′ UTR | Involved in cellular processes, galactosidase and metabolic processes |
| chr2 | 120178323 | 120178411 | Hypo | −0.2786 | 4 | CHRNG | Promoter | Implicated in response to stimulus and signalling |
| chr7 | 38857595 | 38857640 | Hypo | −0.4957 | 6 | RGS14 | Promoter | Roles in G-protein alpha-subunit binding, GDP-dissociation inhibitor activity, GTPase activating protein bindingetc. |
| chr11 | 29596293 | 29596466 | Hypo | −0.3359 | 4 | CALM2 | Promoter | Roles in N-terminal myristoylation domain binding, adenylate cyclase activator activity and disordered domain specific bindingetc. |
| chr13 | 61040934 | 61041114 | Hypo | −0.3170 | 5 | DEFB123 | Promoter | Involved in defense response to bacterium and the innate immune response |
| chr15 | 42380725 | 42380943 | Hypo | −0.3037 | 6 | ADM | Promoter | Involved in signal transduction |
| chr18 | 46457591 | 46457619 | Hypo | −0.3654 | 3 | TMEM149; IGFLR1 | Promoter | Involved in protein binding activities |
| chrX | 52808025 | 52808053 | Hypo | −0.4230 | 5 | MCART6; SLC25A53 | Promoter | Not available |
| **Ileum lymph node** | | | | | | | | |
| chr1 | 97612779 | 97612897 | Hyper | 0.4640 | 9 | TERC; TR | 5′ UTR | Involved in g-protein coupled receptor activity, response to stimulus and signalling |
| chrX | 18020880 | 18020987 | Hyper | 0.4435 | 10 | CCDC160 | 5′ UTR | Not available |
| chrX | 79493022 | 79493221 | Hyper | 0.37542 | 8 | NLGN3 | 5′ UTR | Roles in biological adhesion/regulation, cell adhesion, developmental process and signalling |
| chr1 | 66517241 | 66517269 | Hyper | 0.51326 | 3 | ILDR1 | Promoter | Roles in high-density lipoprotein particle receptor activity, protein binding; cellular response to leukemia inhibitory factor, endocytosis and positive regulation of peptide hormone secretion |
| chr3 | 20725467 | 20725535 | Hyper | 0.3824 | 5 | HIST2H2AC; H2AC20 | Promoter | Roles in cellular and metabolic processes |
| chr3 | 52530399 | 52530544 | Hyper | 0.2650 | 10 | BARHL2 | Promoter | Roles in cellular and metabolic processes |
| chr5 | 49488200 | 49488264 | Hyper | 0.3872 | 5 | C5H12orf66 | Promoter | Involved in cellular response to amino acid and glucose starvation, negative regulation of TORC1 signaling and protein localization to lysosome |
| chr5 | 50362472 | 50362729 | Hyper | 0.3306 | 8 | AVPR1A | Promoter | Roles in response to stimulus, signalling and cellular processes |
| chr6 | 25666563 | 25666667 | Hyper | 0.3021 | 5 | EIF4E | Promoter | Implicated in binding activities: DNA-binding, transcription factor binding, RNA 7-methylguanosine cap binding, RNA binding. Role in translation initiation factor activityetc. |
| chr6 | 65573034 | 65573154 | Hyper | 0.3145 | 6 | GABRA4 | Promoter | Roles in cellular processes, response to stimulus and signalling |

(Continued on following page)

**TABLE 1 |** (*Continued*) Genes with hypermethylated or hypomethylated DMRs in their promoters or 5′UTRs in the ileum and ileum lymph node tissues of MAP-infected cows.

| Chr[a] | Start | End | MethyStatus[b] | MethDiff[c] | # CG[d] | Gene symbol and synonyms | Genic region | Function |
|---|---|---|---|---|---|---|---|---|
| chr7 | 25117101 | 25117262 | Hyper | 0.2676 | 7 | SLC27A6 | Promoter | Implicated in arachidonate-CoA ligase activity, long-chain fatty acid transporter activity and long-chain fatty acid-CoA ligase activityetc. |
| chr7 | 43711718 | 43711816 | Hyper | 0.5535 | 4 | FAM174C; C7H19orf24 | Promoter | Not available |
| chr7 | 83617422 | 83617724 | Hyper | 0.2904 | 10 | HAPLN1; LP; CRTL1 | Promoter | Implicated in extracellular matrix structural constituent conferring compression resistance, hyaluronic acid binding, cell adhesion, central nervous system development, extracellular matrix organization and skeletal system development |
| chr8 | 6824520 | 6824567 | Hyper | 0.2727 | 9 | HPGD; PGDH | Promoter | Roles in cellular and metabolic processes |
| chr9 | 81419168 | 81419344 | Hyper | 0.3991 | 10 | PLAGL1; ZAC1 | Promoter | Implicated in DNA binding, DNA-binding transcription activator activity and metal ion bindingetc. |
| chr15 | 29699604 | 29699770 | Hyper | 0.3465 | 8 | MIZF; HINFP | Promoter | Implicated in DNA binding, DNA-binding transcription factor activity and chromatin bindingetc. |
| chr22 | 52872082 | 52872205 | Hyper | 0.4424 | 8 | TDGF1 | Promoter | Roles in cellular and developmental processes, response to stimulus and signalling |
| chr25 | 2375675 | 2375804 | Hyper | 0.3033 | 6 | PAQR4 | Promoter | Implicated in signaling receptor activity |
| chrX | 94769374 | 94769602 | Hyper | 0.2681 | 8 | MSN | Promoter | Implicated in actin and cell adhesion molecule binding, T cell aggregation, cytoskeleton organization and establishment of epithelial cell apical/basal polarityetc. |
| chr2 | 124527051 | 124527172 | Hypo | –0.3181 | 6 | EPB41 | 5′ UTR | Roles in 1-phosphatidylinositol binding, phosphoprotein binding and protein-containing complex assemblyetc. |
| chr4 | 105525926 | 105525975 | Hypo | –0.2783 | 4 | LOC780933 | 5′ UTR | Involved in endopeptidase activity, metal ion binding, digestion, and proteolysissetc. |
| chr16 | 12701415 | 12701500 | Hypo | –0.3002 | 4 | RGS1 | 5′ UTR | Involved in G-protein alpha-subunit binding, GTPase activator activity, calmodulin binding and the immune response |
| chr1 | 96451609 | 96451735 | Hypo | –0.4015 | 6 | SLC2A2 | Promoter | Implicated in D-glucose transmembrane transporter activity, fructose transmembrane transporter activity and in carbohydrate metabolic processetc. |
| chr1 | 115883148 | 115883250 | Hypo | –0.3184 | 5 | bta-mir-1246; MIR1246 | Promoter | Not available |
| chr2 | 91231696 | 91231897 | Hypo | –0.259 | 6 | WDR12 | Promoter | Implicated in protein binding, ribonucleoprotein complex binding and Notch signaling pathwayetc. |
| chr3 | 33247259 | 33247316 | Hypo | –0.4231 | 3 | MIR2285AS-3 | Promoter | Not available |
| chr4 | 44625402 | 44625552 | Hypo | –0.4710 | 3 | SLC26A5 | Promoter | Roles in anion:anion antiporter activity, bicarbonate transmembrane transporter activity and bicarbonate transportetc. |
| chr4 | 105504452 | 105504613 | Hypo | –0.3705 | 5 | TRYX3; PRSS58 | Promoter | Involved in serine-type endopeptidase activity and proteolysis |
| chr4 | 105804315 | 105804451 | Hypo | –0.3223 | 6 | LOC509513; TCRB | Promoter | Involved in signaling receptor activity, T cell mediated cytotoxicity directed against tumor cell target and in detection of tumor cell |
| chr5 | 25685792 | 25685855 | Hypo | –0.3334 | 3 | ZNF385A | Promoter | Implicated in DNA binding, mRNA 3′-UTR binding and RNA bindingetc. |
| chr5 | 30081038 | 30081161 | Hypo | –0.3327 | 4 | NCKAP5L | Promoter | Role in cellular processes |
| chr5 | 61699340 | 61699492 | Hypo | –0.2965 | 3 | bta-mir-1251; MIR1251 | Promoter | Role in gene silencing |
| chr6 | 89733241 | 89733396 | Hypo | –0.2832 | 3 | BTC | Promoter | Roles in cellular and metabolic processes, response to stimulus and signalling |
| chr6 | 116834070 | 116834098 | Hypo | –0.3655 | 3 | TMEM129 | Promoter | Implicated in metal ion binding, ubiquitin protein ligase activity and protein ubiquitination |
| chr7 | 57416113 | 57416446 | Hypo | –0.3427 | 10 | RBM27 | Promoter | Role in cellular process |
| chr8 | 7876115 | 7876240 | Hypo | –0.3657 | 4 | BLK | Promoter | Implicated in immune regulation, biological adhesion, biological regulation, cellular process, developmental process, metabolic process, response to stimulus and signalling |
| chr8 | 67283316 | 67283560 | Hypo | –0.3761 | 4 | SLC18A1 | Promoter | Implicated in cellular process and secondary carrier transporter activities |
| chr8 | 74789324 | 74789518 | Hypo | –0.2649 | 5 | DNAJA1 | Promoter | Involved in ATP binding, DNA damage response, detection of DNA damage and toxin transportetc. |

(Continued on following page)

**TABLE 1 |** (*Continued*) Genes with hypermethylated or hypomethylated DMRs in their promoters or 5′UTRs in the ileum and ileum lymph node tissues of MAP-infected cows.

| Chr[a] | Start | End | MethyStatus[b] | MethDiff[c] | # CG[d] | Gene symbol and synonyms | Genic region | Function |
|---|---|---|---|---|---|---|---|---|
| chr8 | 76081883 | 76081965 | Hypo | −0.3222 | 3 | CCL21 | Promoter | Roles in immune regulation, biological regulation, cellular process, metabolic process, response to stimulus and signalling |
| chr8 | 94567765 | 94567917 | Hypo | −0.2923 | 8 | NIPSNAP3A | Promoter | Involved in protein binding |
| chr18 | 51564992 | 51564998 | Hypo | −0.3296 | 3 | TEX101 | Promoter | Roles in cellular processes |
| chr23 | 28335000 | 28335166 | Hypo | −0.4334 | 4 | DHX16 | Promoter | Implicated in ATP binding, RNA binding and RNA splicingetc. |
| chr28 | 26458052 | 26458244 | Hypo | −0.3898 | 7 | PP; PPA1 | Promoter | Implicated in cellular and metabolic processes |
| chrX | 86776889 | 86777091 | Hypo | −0.3039 | 9 | SUV39H1 | Promoter | Implicated in cellular and metabolic processes |

[a]*Chr, chromosome.*
[b]*MethyStatus, methylation status, hyper = hyper methylated, hypo = hypomethylated.*
[c]*MethDiff, methylation difference between infected and non-infected tissues.*
[d]*#CG, number of CpG sites in each differentially methylated region.*

(**Supplementary Table S2E**). Out of the total number of DMRs, 426 (IL) and 2057 (ILLN) were found in genic regions (**Supplementary Tables S4B,D**). Distribution of DMRs in different genic regions indicated highest proportions in intronic regions and the least numbers in 5′UTR and 3′UTR in both issues (**Figures 4A,B**). Similarly, more hypermethylated and hypomethylated DMRs were found in the introns and least numbers in 5′UTR and 3′UTR in both issues (**Figures 4C,D**).

Distribution of DMRs in CGI context indicated a total number of 249 and 583 DMRs in the IL and ILLN, respectively (**Supplementary Tables S5A–B**, **Figures 4E,F**). Out of these, 89 and 102 DMRs were located within CGIs. Relative to these CGIs, 73 and 87 were located in CG shelf left and right, respectively in IL, while more DMRs (249 and 232) were found in CGI shelf left and right, respectively, in ILLN (**Figures 4E,F**).

The DMRs were annotated to 394 genes (here referred to as DMR genes) in the IL and to 1305 genes in the ILLN (**Supplementary Tables S4B,D**). Out of these, promoter and 5′UTR region DMRs were annotated to 43 genes in the IL including eight genes (*C1H21orf62, GST O 2, MAP6D1, EZH2, HSD17B11*, *bta-mir-181d, CCIN* and, *CCDC56*) with hypermethylated promoters and or 5′UTRs and 10 genes (*UBE2D2, ITGB1BP1, GLA, CHRNG, RGS14, CALM2, DEFB123, ADM, TMEM149, MCART6, SLC25A53*) with hypomethylated promoters or 5′UTRs (**Supplementary Table S4B** and **Table 1**). In the ILLN, DMRs were annotated to the promoters of 88 genes including, 19 genes with hypermethylated promoters and or 5′UTRs and 25 genes with hypomethylated promoters or 5′UTRs (**Supplementary Table S4D** and **Table 1**). Notable examples of genes with hypermethylated promoters or 5′UTRs included *TERC, EIF4E, PLAGL1*, CCDC160, ILDR1, HIST2H2AC, C5H12orf66, *FAM174C, TDGF1* etc., and with hypomethylated promoters or 5′UTRs included *SLC18A1, bta-mir-2285as-3, SLC2A2, SLC26A5, TRYX3, TMEM129, BLK, SLC18A1, CCL21, DHX16, PPA1,* etc. (**Table 1**). Browser screen shots of hypomethylated (*RGS14*) and hypermethylated (*TERC*) regions in two genes in the ILLN of MAPinf tissues are shown in **Figure 5**.

In order to understand the potential effects of methylation on the genes harboring DMRs, we examined their expression patterns in RNA-Seq data of the same samples (Ibeagha-Awemu et al., 2021). We found that, out of 394 and 1305 DMR genes in the IL and ILLN, respectively, 22 and 26, respectively, were also differentially expressed (FDR<0.1) at the mRNA level (**Table 2**).

## Functional Roles of Genes Harboring DMRs

To further determine the potential effects of cytosine methylation on the functions of genes, DMR genes were subjected to GO and pathways analysis. GO analysis of 394 DMR genes in the IL resulted in 75 BP, 11 MF and 19 CC GO terms (FDR<0.05) (**Supplementary Tables S6A–C**). Most of the enriched IL BP GO terms are related to cellular processes, metabolic processes, transport and system development while very few enriched terms (less than 1%) are related to disease and the immune process (**Supplementary Table S6A**). The most significant IL MF and CC GO terms were neurotransmitter receptor activity (FDR = 0.011) and synapse part (FDR = 0.006), respectively (**Supplementary Tables S6B,C**). A total of 36 KEGG pathways were enriched for IL DMR genes (**Supplementary Table S6D**) (**Figure 6**). The most enriched pathways included Gap junction (FDR = 0.009), Long-term depression (FDR = 0.009), Long-term potentiation (FDR = 0.011) and Sphingolipid signaling pathway (FDR = 0.011). Several disease and immune elated pathways were enriched for IL DMR genes, including C-type lectin receptor signaling pathway (FDR = 0.018), Inflammatory mediator regulation of TRP channels (FDR = 0.024), Cushing syndrome (FDR = 0.023); Hepatitis B (FDR = 0.037), Prostate cancer (FDR = 0.038), Non-small cell lung cancer (FDR = 0.037), Pancreatic cancer (FDR = 0.044), etc. Interestingly, some genes (n = 21) were enriched in many pathways, from 4 to 23 pathways (**Supplementary Table S6E**).

The 1305 ILLN DMR genes were enriched for 374 BP, 91 MF and 89 CC GO terms (**Supplementary Tables S7A–C**). Most of the enriched BP terms are related to cellular processes (27.6%), biological regulation (16.6%), metabolic processes (15.4%) and response to stimulus (8.2%) (**Supplementary Table S7A**). More disease/immune related BP GO terms were enriched (FDR <0.05) for ILLN DMR genes as compared to IL DMR genes. Cytoskeletal protein binding (FDR = 6.94E-07) and plasma membrane part (FDR = 4.36E-12) were the most significantly enriched MF and CC GO terms, respectively (**Supplementary Tables S7B,C**). Forty-seven

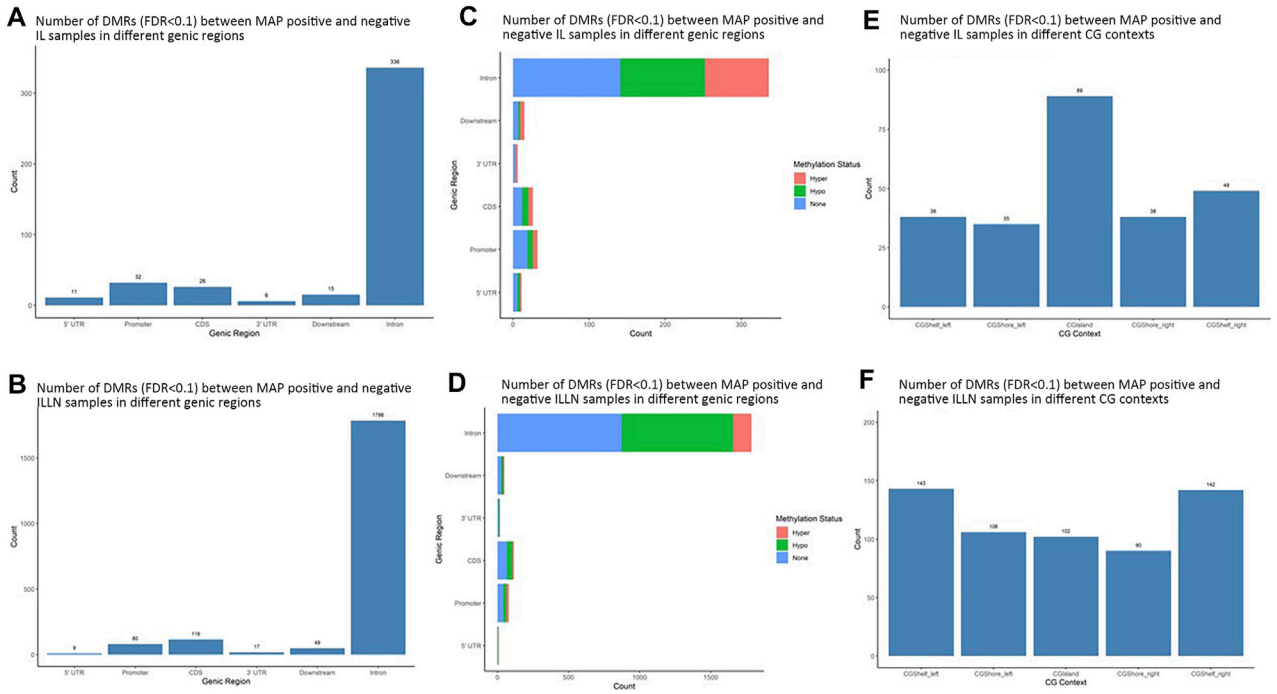



**FIGURE 4 |** Distribution of significantly differentially methylated regions (DMR) in different genic regions between MAP-infected (MAPinf) and MAP-negative (MAPneg) cows in **(A)** ileum (IL) and **(B)** IL lymph node (ILLN), and corresponding methylation status in **(D)** IL and **(C)** ILLN. A DMR was considered hypermethylated if it had a positve methylation difference ≥25% between MAPinf and MAPneg samples. Similarly, a DMR was hypomethylated if it had a decreased methylation difference ≥25% between MAPinf and MAPneg samples. A DMR methylation status of none implies that the methylation difference was less than 25% in both scenarios. Distribution of differentially methylated cytosines in CpG island context in **(E)** IL and **(F)** ILLN samples between MAPinf and MAPneg samples.

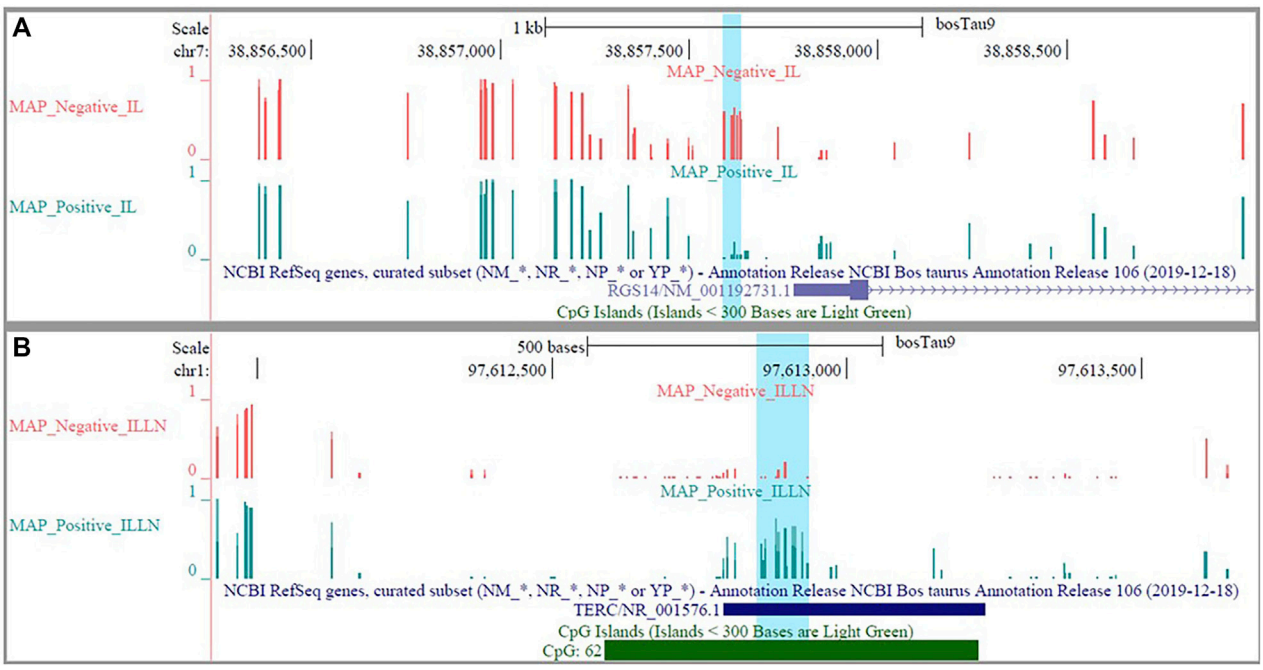



**FIGURE 5 |** Browser shots showing **(A)** a hypomethylated DMR in a CpG island in *RGS14* gene in IL MAP-infected compared with negative samples and **(B)** a hypermethylated DMR in a CpG island in *TERC* gene in ILLN MAP-infected compared with negative samples.

**TABLE 2 |** Select genes harboring differentially methylated regions and their gene (mRNA) expression patterns in the ileum and ileum lymph node of MAP-infected (MAPinf) compared to uninfected (MAPneg) cows.

| [b]Chr | Gene symbol | Differentially methylated region genes | | | | Gene | mRNA expression[a] | | | |
|---|---|---|---|---|---|---|---|---|---|---|
| | | [c]Met status | [d]#CpGs | [e]#DMRs | Genic region | | Base mean | L2FC[f] | p-value | Padj[g] |
| **Ileum** | | | | | | | | | | |
| chr21 | AMN | Hyper | 3 | 1 | Intron | AMN | 710.6131 | −1.5885 | 1.50E-07 | 4.99E-05 |
| chr26 | CPXM2 | Hyper, hypo | 8 | 2 | Intron | CPXM2 | 130.4401 | −2.3105 | 1.05E-06 | 0.0002 |
| chr23 | DEF6 | Hypo | 5 | 1 | Intron | DEF6 | 208.6724 | 0.7429 | 0.0052 | 0.0970 |
| chr3 | GBP4 | + | 3 | 1 | Intron | GBP4 | 994.8017 | 3.3463 | 0.0003 | 0.0139 |
| chr8 | HABP4 | Hypo, – | 6 | 2 | Intron | HABP4 | 460.2397 | −1.0853 | 0.0002 | 0.0097 |
| chr4 | IKZF1 | + | 3 | 1 | Intron | IKZF1 | 436.6308 | 1.0129 | 0.0017 | 0.0469 |
| chr15 | INSC | + | 3 | 1 | Intron | INSC | 30.7375 | -1.5367 | 0.0005 | 0.0209 |
| chr12 | LCP1 | + | 6 | 1 | Intron | LCP1 | 2878.195 | 1.5412 | 0.0007 | 0.0248 |
| chr19 | MGC137055 | – | 7 | 1 | Promoter | MGC127055 | 951.7676 | −1.3554 | 0.0003 | 0.0149 |
| chr28 | MTR | – | 4 | 1 | Intron | MTR | 441.8496 | −0.6786 | 0.0026 | 0.0634 |
| chr18 | PEPD; prolidase | Hypo | 4 | 1 | Intron | PEPD | 1994.9530 | −0.8194 | 0.0008 | 0.0276 |
| chr6 | PITX2 | Hypo | 4 | 1 | Intron | PITX2 | 29.8845 | −2.5165 | 0.0003 | 0.0138 |
| chr6 | PLAC8; PLAC8B | Hypo | 8 | 1 | Intron | PLAC8 | 234.1588 | 2.2503 | 0.0001 | 0.0070 |
| chr13 | PTPN1 | + | 3 | 1 | Intron | PTPN1 | 400.9077 | 0.8147 | 0.0002 | 0.0112 |
| chr8 | SLC1A1 | + | 5 | 1 | Downstream | SLC1A1 | 2182.2000 | −1.7007 | 0.0004 | 0.0176 |
| chr5 | STAB2; hare | – | 6 | 1 | Intron | STAB2 | 75.9034 | 3.5210 | 5.28E-05 | 0.0047 |
| chr2 | STAT1 | Hypo, – | 13 | 2 | CDS, intron | STAT1 | 8439.9450 | 1.4026 | 5.18E-05 | 0.0046 |
| chr13 | STK4 | – | 6 | 1 | Intron | STK4 | 634.3818 | 0.7495 | 0.0008 | 0.0283 |
| chr12 | TNLG7A; TNFSF13B | Hypo | 4 | 1 | Intron | TNLG7A | 99.1448 | 1.9854 | 0.0003 | 0.0147 |
| chr5 | TTLL1 | – | 3 | 1 | Intron | TTLL1 | 129.2584 | 1.1507 | 0.0013 | 0.0394 |
| chr9 | VNN2 | + | 4 | 1 | Intron | VNN2 | 254.2766 | 3.6994 | 1.19E-05 | 0.0017 |
| **Ileum lymph node** | | | | | | | | | | |
| chr3 | AK5 | – | 7 | 2 | Intron | AK5 | 11.1283 | −3.0134 | 0.0003 | 0.0438 |
| chr4 | AOAH | – | 6 | 1 | Intron | AOAH | 1144.6000 | 1.1055 | 3.61E-05 | 0.0114 |
| chr8 | CCL21 | Hypo | 3 | 1 | Promoter | CCL21 | 2962.0750 | −1.8148 | 0.0006 | 0.0595 |
| chr6 | CD38 | Hypo, – | 4 | 1 | Intron | CD38 | 1415.7860 | 0.5503 | 0.0002 | 0.0332 |
| chr5 | CNTN1 | Hypo, – | 11 | 3 | CDS, Intron | CNTN1 | 101.7895 | −1.7744 | 0.0001 | 0.0236 |
| chr1 | CXADR | Hypo | 4 | 1 | Intron | CXADR | 260.4728 | 1.9229 | 5.35E-06 | 0.0031 |
| chr8 | DMRT1 | None | 4 | 1 | Intron | DMBT1 | 2668.1770 | 1.2567 | 0.0004 | 0.0460 |
| chr8 | EBF2 | Hyper, Hypo | 10 | 2 | Intron, Intron | EBF2 | 17.5589 | −2.9054 | 0.0005 | 0.0545 |
| chr15 | ELMOD1 | + | 5 | 1 | Promoter | ELMOD1 | 9.7424 | −3.3565 | 8.91E-05 | 0.0209 |
| chr9 | FHL5 | – | 9 | 2 | Intron | FHL5 | 16.8634 | −2.2775 | 0.0003 | 0.0450 |
| chr3 | GADD45A | Hyper | 4 | 1 | CDS | GADD45A | 268.8654 | 1.2800 | 6.32E-05 | 0.0170 |
| chr2 | GALNT3 | – | 9 | 1 | CDS | GALNT3 | 306.6631 | −1.1925 | 2.07E-05 | 0.0084 |
| chr26 | GFRA1 | Hypo | 6 | 2 | Intron | GFRA1 | 229.3136 | −1.3818 | 7.97E-05 | 0.0200 |
| chr7 | GNG7 | Hypo | 6 | 1 | Intron | GNG7 | 370.6341 | 1.3462 | 3.23E-05 | 0.0105 |
| chr8 | GRIN3A | Hypo | 6 | 1 | Intron | GRIN3A | 22.4595 | −2.8343 | 0.0007 | 0.0664 |
| chr6 | LEF1 | + | 10 | 1 | Promoter | LEF1 | 1718.1730 | −1.3951 | 0.0010 | 0.0886 |
| chr6 | MTHFD2L | Hypo | 5 | 1 | Intron | MTHFD2L | 61.8015 | −1.5939 | 0.0003 | 0.0409 |
| chr9 | PRDM1 | – | 5 | 1 | Promoter | PRDM1 | 1057.196 | 0.9168 | 2.70E-07 | 0.0003 |
| chr22 | PRSS45 | – | 5 | 1 | Intron | PRSS45 | 17.6579 | −2.4531 | 2.77E-05 | 0.0096 |
| chr5 | PTPRQ | Hypo, +, – | 33 | 8 | Downstream, Introns | PTPRO | 79.2753 | 1.3915 | 1.92E-07 | 0.0002 |
| chr8 | SLC24A2 | Hypo | 9 | 3 | Intron | SLC24A2 | 28.5550 | −1.563 | 0.0012 | 0.0916 |
| chr3 | SPTA1 | + | 6 | 1 | Intron | SPTA1 | 27.9195 | −3.1868 | 0.0002 | 0.0336 |
| chr2 | STAT4 | – | 3 | 1 | Intron | STAT4 | 449.2908 | −1.1274 | 0.0011 | 0.0904 |
| chr9 | STXBP5 | Hypo | 3 | 1 | Intron | STXBP5 | 852.2494 | −0.6002 | 0.0006 | 0.0628 |
| chr9 | THEMIS | Hypo, - | 8 | 2 | CDS, intron | THEMIS | 975.8944 | −1.3937 | 0.0001 | 0.0229 |
| chr6 | UGT8 | Hypo | 3 | 1 | Intron | UGT8 | 77.1915 | −2.1056 | 1.76E-06 | 0.0012 |

[a]*mRNA, expression data is from Ibeagha-Awemu et al., 2021.*

[b]*Chr: chromosome.*

[c]*MethyStatus: methylation status, hyper = hyper methylated, hypo = hypomethylated, "+" = increased methylation level, "–" = decreased methylation level.*

[d]*#CpGs: number of CpG sites.*

[e]*#DMRs: number of differentially methylated regions.*

[f]*L2FC: Log2foldchange.*

[g]*Padj: p-values adjusted according to Benjaminin and Hochberg correction for false discovery rate.*

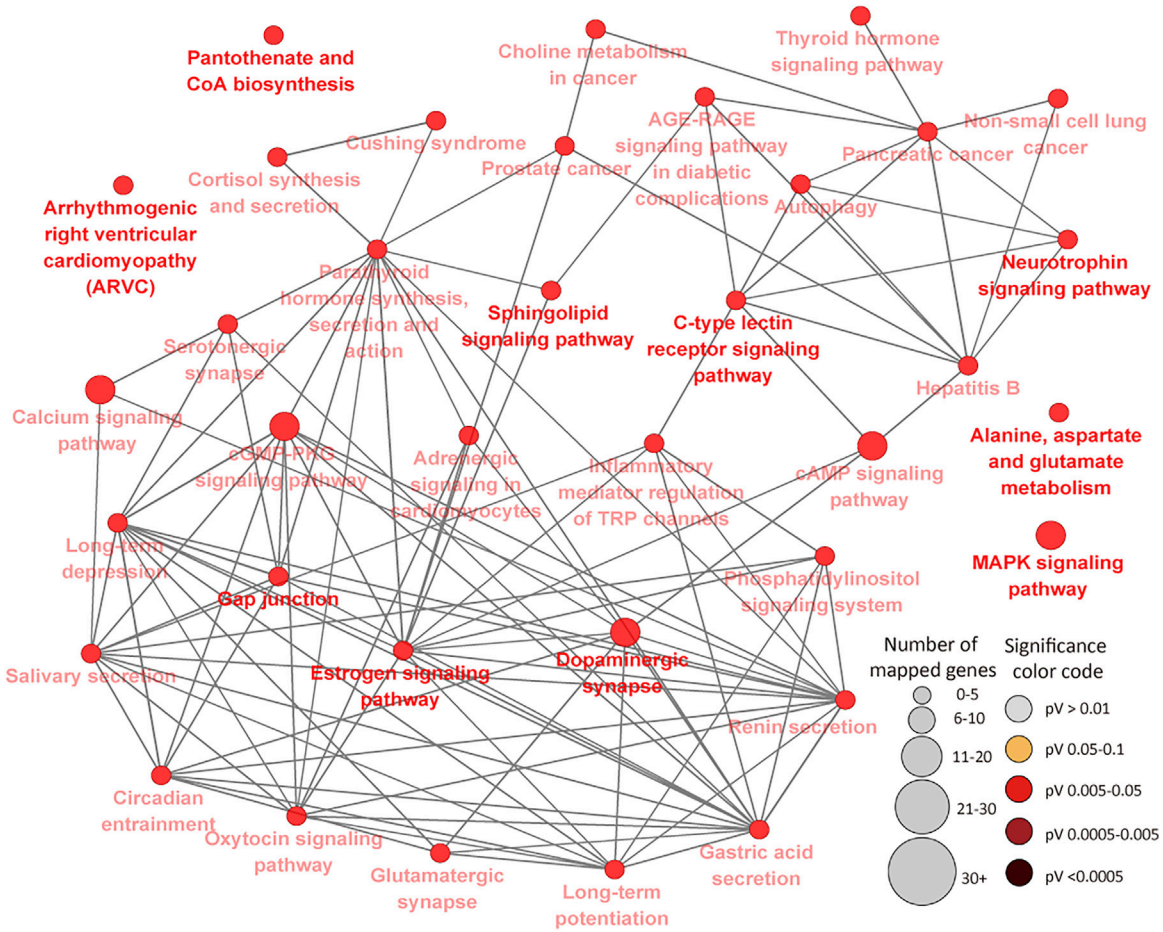



**FIGURE 6 |** KEGG Pathways enriched for ileal tissue differentially methylated region genes showing connections between pathways. Each node represents a pathway and the size (the larger the node, the higher the number of enriched genes) and color (the deeper the color, the more significant the enriched pathway is) of the node represents the number of enriched genes and level of significance, respectively. Straight lines connect pathways.

KEGG pathways were enriched for ILLN DMR genes including immune (e.g., Bacterial invasion of epithelial cells, Transcriptional misregulation in cancer, Cell adhesion molecules (CAMs), Inflammatory mediator regulation of TRP channels and Platelet activation, etc.) and disease (e.g., Cushing syndrome, pathways in cancer, Small cell lung cancer, Gastric cancer and Arrhythmogenic right ventricular cardiomyopathy (ARVC), etc.) related pathways (**Figure 7**; **Supplementary Table S7D**). Several metabolic pathways as well as cGMP-PKG signaling pathway were also enriched for ILLN DMR genes. A total of 63 genes were enriched in four to 28 pathways (**Supplementary Table S7E**).

A comparison of enriched pathways in both tissues indicated that 17 (FDR<0.05) pathways were commonly enriched for DMR genes in both tissues (**SupplementaryTable S6F**), including cGMP-PKG signaling pathway, MAPK signaling pathway, Oxytocin signaling pathway, Cushing syndrome, Arrhythmogenic right ventricular cardiomyopathy (ARVC) and Gastric acid secretion, etc. Furthermore, we compared the BP GO terms and pathways enriched for DMR genes with BP GO terms and pathways enriched for DE genes (Ibeagha-Awemu et al., 2021) in both tissues. Results indicated that 16 BP GO terms were commonly enriched for DMR genes and DE mRNAs in the IL, including regulation of cell migration, positive regulation of cell migration, negative regulation of growth, import into cell, positive regulation of B cell activation, regulation of mononuclear cell migration and lipid biosynthetic process, etc. (**Supplementary Table S6G**). Meanwhile, only C-type lectin receptor signaling pathway was commonly enriched for DMR genes and DE mRNAs in this tissue (IL) (**Supplementary Table S6H**). In the ILLN, only one BP GO term (regulation of B cell activation) was commonly enriched for DMR genes and DE genes (**Supplementary Table S7F**), while no KEGG pathway was commonly enriched.

## DISCUSSION

Several studies have shown that MAP alters the expression of genes, biological processes and pathways following MAP infection or during JD progression (Shin M. K. et al., 2015; Hempel et al., 2016; Alonso-Hearn et al., 2019; Ariel et al.,

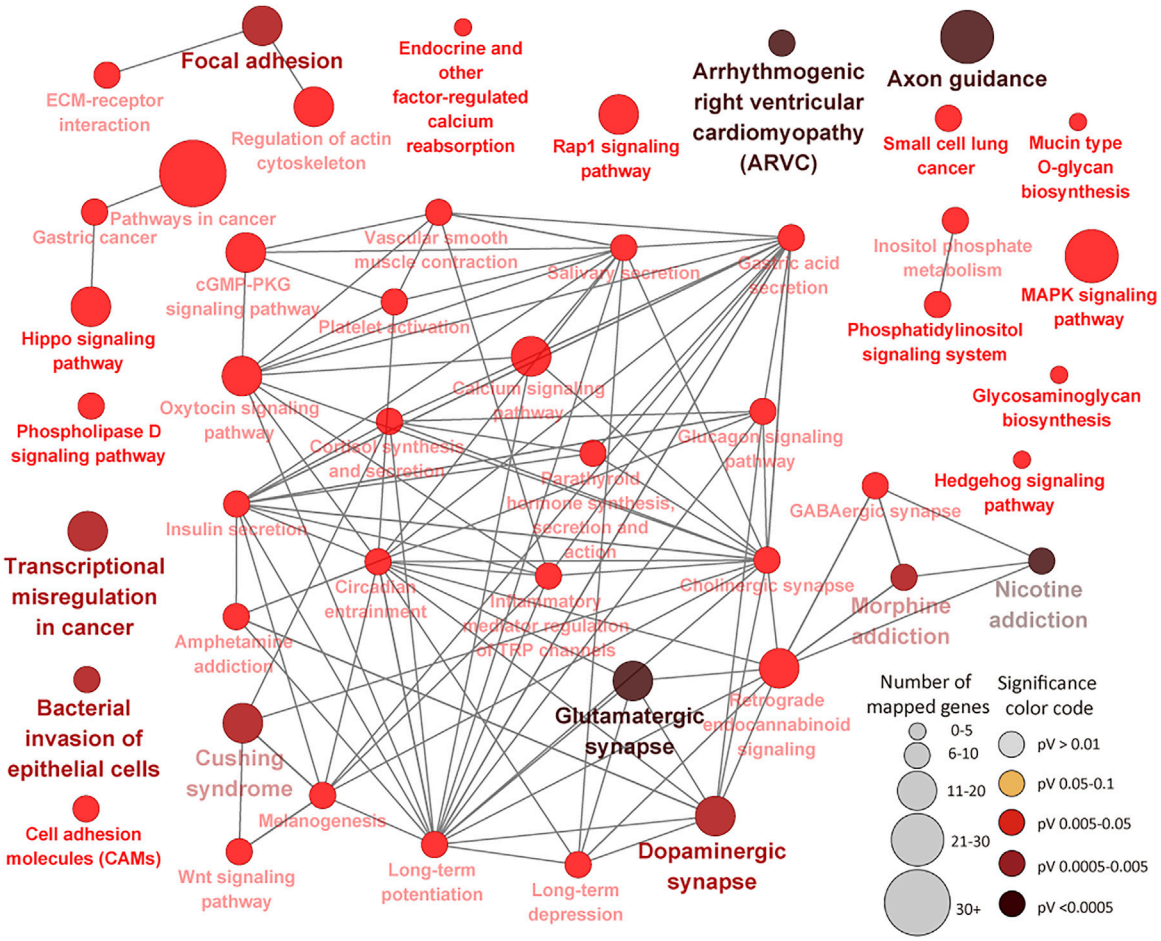



**FIGURE 7 |** KEGG Pathways enriched for ileal lymph node differentially methylated region genes showing connections between pathways. Each node represents a pathway and the size of the node represents the number of enriched genes (the larger the node, the higher the number of enriched genes) while the color intensity represents the level of significance (the deeper the color, the more significant the enriched pathway is). Straight lines connect pathways.

2020; Facciuolo et al., 2020; Ibeagha-Awemu et al., 2021). In addition, a few studies have reported the involvement of miRNAs in JD (Farrell et al., 2015; Gupta et al., 2018; Wang et al., 2019a; Wang et al., 2019b). Our recent studies suggested a possible role of epigenetic processes in the mRNA transcriptome response of bovine monocyte derived macrophages infected by MAP (Ariel et al., 2020; Marete et al., 2021a). Moreover, we observed that MAP initiated a heightened immune response in the IL as compared to a likely suppressed immune response in the ILLN tissues of cows with subclinical MAP infection, which could be underpinned by epigenetic processes (Ibeagha-Awemu et al., 2021). Thus, this study investigated the occurrence of epigenetic regulation through whole genome DNA methylation status analysis of ileal and ileal lymph node tissues in response to persistent MAP-infection in dairy cows.

Overall, DNA methylation data showed differential tissue responses to subclinical MAP infection between ileal and ileal lymph node tissues. More significant DMCs, DMRs and CGIs were recorded between MAPinf and MAPneg cows in the ILLN as compared to the IL. This suggests that, the DNA methylation state of cells in the ILLN were altered to a greater extent by the presence of MAP pathogen than in the IL. This observation corroborates data on differentially expressed mRNA transcriptome of the same samples which suggested a potentially suppressed immune state in the ILLN as compared to a heightened immune state of the IL (Ibeagha-Awemu et al., 2021). It seems that DNA methylation profile is a signature that distinguishes MAPinf status from MAPneg status. It has been revealed that disease-specific DNA methylation profiles of intestinal epithelial cells from the ascending colon could accurately separate Inflammatory bowel disease patients from healthy controls with a sensitivity of 75% while ileal methylation signatures were capable of distinguishing Crohn's disease from ulcerative colitis patients with a precision of 77% (Howell et al., 2018). Moreover, a participatory role of DNA methylation in the pathogenesis of MAP infection in cattle demonstrated by our data corroborates data from several studies showing aberrant changes of DNA methylation in Crohn's disease (similar pathology as JD) and other Inflammatory bowel disease conditions (Karatzas et al., 2014; Somineni et al., 2019; Zeng et al., 2019; Li Yim et al., 2020).

Generally, only a small proportion of significant DMCs and DMRs were annotated to genic regions, 15.4 and 33.84% in IL and 12.3 and 25.44% in ILLN, respectively, indicating that majority of DMCs that may paly a role in JD are located outside of protein coding genes. This observation is in line with results of numerous genome wide association studies which have associated more variants located outside of protein coding genes with cattle production and disease traits (Jiang et al., 2010; Wang et al., 2012; Ibeagha-Awemu et al., 2016). The functional role of the DMCs and DMRs in the intergenic regions are not yet known but their impact could be potential action in *cis* or *trans* to genes. Generally, the methylation levels in the regulatory regions (promoter and 5′UTR) of genes were lower as compared to other genic regions in both tissues. This result substantiates previous findings with the method of WGBS in cattle (Zhou et al., 2018; Duan et al., 2019). Meanwhile, higher numbers of DMCs and DMRs were recorded in the intron regions as compared to other genic regions in both tissues. It is generally acknowledged that DNA methylation in promoter regions provides a mechanism of regulation of gene expression. More hypomethylated and hypermethylated DMRs were identified in the promoter/5′UTRs of genes in the ILLN as compared to the IL (**Table 1**), suggesting potential effects of DNA methylation on gene expression, especially in the ILLN. Majority of the identified genes with hypo/hypermethylated DMRs in their promoters or 5′UTRs have roles in multiple processes like cellular and/or metabolic processes, and immune regulation/response to stimuli (e.g., *BARHL2, BLK, BTC, CCL21, GLA, CHRNG,H2AC20, GABRA4*, *PPA1, SLC18A1. PLAGL1, EIF4E, TDGF1,* etc.). Some of these genes have been associated with mycobacterial infections including JD and other human diseases. For example, *BARHL2*, a member of BarH family of homeodomain proteins is a transcriptional regulator and also known to impact cell fate specification, cell differentiation, survival and migration (Juraver-Geslin et al., 2011; Ding et al., 2012). Moreover, DNA methylation of *BARHL2* in exosomal DNA from gastric juice has been recognized as a predictive biomarker of gastric cancer (Yamamoto et al., 2016). *BLK,* a non-receptor tyrosine kinase involved in cell proliferation and differentiation has roles in B-cell receptor signaling and B-cell development. *BLK* was among highly downregulated genes following MAP infection in mice (Shin M.-K. et al., 2015). *CCL21* is a chemokine which functions in recruiting T cells and has been associated with inflammatory bowel disease in human (Kinchen et al., 2018) and JD in cattle (Ibeagha-Awemu et al., 2021). *H2AC20* gene encodes a replication-dependent histone that is a member of the histone H2A family and is associated with Riddle Syndrome and Xeroderma Pigmentosum Group E disease. *PPA1* like other inorganic pyrophosphatases is important for phosphate metabolism in cells. *SLC18A1, SLC27A6, SLC2A2, SLC25A53 and SLC26A5,* members of the solute carrier family have varied functions including participation in fatty acid/cholesterol transport, regulation of lymphocyte signalling and modulation of diverse metabolic pathways (Song et al., 2020). Gene expression data of the same samples indicated that 36 members of the solute carrier gene family were significantly regulated by the presence of MAP (Ibeagha-Awemu et al., 2021). It is known that MAP and other mycobacteria acquires and utilises host-derived fatty acids and cholesterol for their sustenance (Wilburn et al., 2018). For example, *SCL27A6* encodes FATP6, a member of the fatty acid transport protein family known to mediate the uptake of long chain fatty acids (Stahl et al., 2001). A recent study demonstrated involvement of *SCL27A6* in fatty acid transport into the mammary gland and how its overexpression alters fatty acid metabolism in the bovine mammary gland (Zhang et al., 2021). Therefore, alteration of the function of SCL27A6 and probably the other solute carriers due to DNA methylation may have consequences on pathogen survival during MAP infection. EIF4E expression has been reported as changed by MAP in Holstein cattle (Ibeagha-Awemu et al., 2021). *PLAGL1* functions as a suppressor of cell growth and its promoter methylation or deletion has been reported in cancerous cells (Peille et al., 2013; Li et al., 2014).

Results of functional analysis of IL and ILLN DMR genes further portrayed the potent effect of MAP on DNA methylation in the ILLN tissue as compared to IL tissue, whereby more GO terms and KEGG pathways were enriched for ILLN DMR genes as compared to IL DMR genes. In the IL, majority of enriched BP GO terms are related to cellular processes, metabolic processes, transport and system development processes suggesting that these processes were more sensitive to DNA methylation as opposed to only about 1% of BP GO terms being disease/immune related (e.g. regulation of mononuclear cell migration and positive regulation of B cell activation). Meanwhile, more immune/disease pathways and BP GO terms were enriched for ILLN DMR genes, suggesting that the immune response was sensitive to regulation by DNA methylation in this tissue. This result corroborates our recent findings of an activated immune state in the IL and a depressed immune response in the ILLN in response to MAP presence (Ibeagha-Awemu et al., 2021).

In the IL, it was interesting to note that 22 genes were enriched for 4 or more pathways, including *PLCB1* (23 pathways), *GNAI1* (22 pathways), *ITPR1* (21 pathways), *RAF1* (20 pathways), *CALM2* (16 pathways), *PIK3R3* (15 pathways), *MAPK10* (12 pathways), *CREB5* (10 pathways) and *BCL2* (9 pathways), etc., indicative of potentially important regulatory effects of DNA methylation of these genes and corresponding pathways during MAP infection. This is supported by the fact that some of them (genes and pathways) have been associated with JD in cattle and human diseases (e.g. cancer, tuberculosis, leishmaniasis, etc). For example, *GNAI1* and *GNAI3* were found to reduce colitis-associated tumorigenesis in mice through blocking of IL6 signaling and down-regulation of the expression of *GNAI2* (Li et al., 2019). Moreover, *GNAI1* was found as enriched in four pathways in human macrophages following infection by Leishmania (Fernandes et al., 2016). *ITPR1* which regulates important molecules like platelets in the innate and adaptive immune system was recently found in a quantitative trait loci (QTL) region for JD in Jersey cattle (Kiser et al., 2017). Furthermore, many identified GWAS (genome wide association study) associated genes or genes within QTL regions for JD like *PPFIBP1, ERGIC2, ITPR2, LEF1, DKK2, DEF6, CCDC91,* etc., (Gao et al., 2018; Mallikarjunappa et al.,

2018), presented different methylation status between MAPinf and MAPneg cows in this study, suggesting a possibility of mechanistic interactions between epigenetic and genetic signals in JD progression. *CALM2*, known to be involved in the regulation of a large number of enzymes and other proteins was reported as downregulated during MAP enteric colonization of ileal tissues of neonatal calves (Khare et al., 2012). Meanwhile, *CREB5* was among upregulated genes during tuberculosis infection in humans (Alam et al., 2019). Majority of the pathways enriched for IL DMR genes were highly interconnected (**Figure 6**) and notable ones like MARK Signalling pathway, C-type lectin receptor signaling pathway, Cushing syndrome, Inflammatory mediator regulation of TRP channels, cAMP signaling pathway have reported associations with JD and other mycobacterial infections (Rybaczyk et al., 2009; Ariel et al., 2020; Ibeagha-Awemu et al., 2021) or are being associated with JD for the first time.

Enrichment of more immune/disease related pathways for ILLN DMR genes as compared to IL DMR genes including notable pathways like Bacterial invasion of epithelial cells, Cushing syndrome, Transcriptional misregulation in cancer, Pathways in cancer, Inflammatory mediator regulation of TRP channels, Cell adhesion molecules (CAMs), Platelet activation, amongst others, emphases the involvement of DNA methylation in the immune response processes to MAP presence in this tissue. Many ILLN DMR genes ($n$ = 63) were enriched in four to 28 pathways suggesting central roles in JD. For example, the top ILLN pathways driving genes like *CACNA1A* (10 pathways), *CAMK2A* (14 pathways), *CAMK2D* (16 pathways), *CREB3L2* (10 pathways), *GNAQ* (24 pathways), *GSK3B* (10 pathways), *ITPR2* (19 pathways), *PLCB1* (28 pathways), *PPP3CA* (10 pathways), *PRKACB* (26 pathways), *PRKCB* (27 pathways), *ADCY1* (22 pathways), etc., are mainly involved in binding, catalytic and transporter activities. Apart from a reported role of *GSK3B* in the regulation of milk synthesis and proliferation *via* mTOR/S6K1 signaling pathway in dairy cow mammary gland epithelial cells (Zhang et al., 2014) or report that MAP fibronectin attachment protein (FAP) mediated dendritic cell $CD8^+$ T cell proliferation and cytotoxic T lymphocyte activity is *via GSK-3* (Noh et al., 2012), there are no reports of association of these genes with bovine JD. Considering that these genes are enriched in an appreciable number of immune/disease pathways during subclinical MAP infection, their roles in JD pathogenesis is worth investigating.

The Bacterial invasion of epithelial cells pathway (FDR = 0.002) and Focal adhesion pathway (FDR = 0.002) were among the top enriched pathways for ILLN DMR genes. The Focal adhesion pathway plays crucial roles in key biological processes such as cell motility, cell proliferation, cell differentiation, regulation of gene expression and cell survival, etc. Signalling events initiated by cell-matrix adhesions results in morphological alterations and modulation of gene expression. Activated focal adhesion kinase complexes with Src family kinases and other proteins to initiate multiple downstream signaling pathways to regulate diverse cellular functions, and are implicated in various human diseases including cancers (Zhao and Guan, 2011). Cell adhesion and Cell communication pathways have been linked to paratuberculosis in sheep (Gossner et al., 2017) and inflammatory bowel diseases (ulcerative and Crohn's disease) in humans and model animals (Ma et al., 2010; Brooks et al., 2017). Emergence of the Bacterial invasion of epithelial cells pathway as a top pathway in this study is not surprising knowing that MAP through various mechanisms internalizes in sub-epithelial macrophages where it effectively subverts host cell responses to promote intracellular survival and replication, and DNA methylation may be one of the regulating mechanisms. Although several pathways were commonly enriched in both tissues (e.g. cGMP-PKG signaling pathway, Cushing syndrome, Inflammatory mediator regulation of TRP channels, MAPK signaling pathway, Gastric acid secretion pathway, etc.), the majority of the implicated DMR genes where different between the two tissues (**Supplementary Tables S6D,F, S7D**), again attesting to the differential regulation of the two tissues by DNA methylation alteration.

Interestingly, comparison of the present data with mRNA-Seq data (Ibeagha-Awemu et al., 2021) of the same samples indicated that mostly BP GO terms in the IL (n = 16) were commonly enriched for IL DMR genes (this data) and genes expressed (mRNA-seq) in the IL tissues. Most of the terms are implicated in the movement of cells. Meanwhile in the ILLN only regulation of B cell activation BP GO term was commonly enriched for DMR genes and DE genes, while no KEGG pathway was commonly enriched. This is not surprising given that only a limited number of BP GO terms ($n$ = 10) and KEGG pathways ($n$ = 7.) were enriched for differentially expressed genes in this tissue (ILLN) (Ibeagha-Awemu et al., 2021). Given the high number of DMCs and DMRs identified in the ILLN and the lower number of DE genes identified in the same samples (Ibeagha-Awemu et al., 2021), it can be deduced that, the DNA methylation state of the cells, repressed the host cellular immune response to the presence of MAP, and therefore suggest a role for DNA methylation in the regulation of the host response to MAP infection. Moreover, comparison of the DNA methylation data with gene expression data of the same animals (**Table 2**) suggested that DNA methylation in other gene regions also potentially affected the expression of the corresponding genes. For example, the promoter methylation levels of three genes (*ELMOD1, LEF1* and *PRDM1*) and intron region methylation levels of 12 genes (*AMN, DEF6, PLAC8, STAB2, STAT1, STK4, TNFSF13B, AOAH, CD38, CXADR, GNG7* and *SPTA1*) were inversely related to gene expression. In most cases however, the state of DNA methylation was not inversely related to gene expression. This data suggests that JD development may be associated with anomalous methylation.

## CONCLUSION

This data is the first to demonstrate a participatory role of DNA methylation in the pathogenesis of MAP infection in dairy cattle. DNA methylation analysis demonstrated differential tissue responses to MAP infection with more DMCs and DMRs identified in ILLN tissues as compared to IL tissues of MAPinf compared to MAPneg cows, indicating that the ILLN was more impacted by regulation by DNA methylation as compared to IL tissue. Moreover, immune processes in the ILLN were more impacted by DNA methylation compared to the IL. Genes with hypermethylated (e.g. *GSTO2, CCDC56, TERC, NLGN3, H2AC20,*

*BARHL2, AVPR1A, EIF4E, GABRA4, PGDH, etc.)* or hypomethylated (e.g. *UBE2D2, ITGB1BP1, GLA, CHRNG, NCKAP5L, BTC, RBM27, BLK, SLC18A1, CCL21, TEX101, PPA1 and SUV39H1, etc.)* promoters as well as pathways driving DMR genes (e.g. *CACNA1A*, *CAMK2A*, *CAMK2D*, *CREB3L2*, *GNAQ, GSK3B*, *ITPR2*, *PLCB1*, *PPP3CA*, *PRKACB*, *PRKCB*, *ADCY1, etc.)* identified between MAPinf and MAPneg cows in this study could be potential biomarkers of MAP infection, which can support development of improved diagnostic and therapeutic solutions for JD management.

## DATA AVAILABILITY STATEMENT

The datasets presented in this study can be found in online repositories and in the article/**Supplementary Material**. The raw sequence reads generated for this study have been deposited in the NCBI Sequence Read Archive (SRA) under the BioProject ID PRJNA771921.

## ETHICS STATEMENT

The animal study was reviewed and approved by the Animal Care and Ethics Committee of Agriculture and Agri-Food Canada at the Sherbrooke Research and Development Center (AAFC-SRDC no. 466). Written informed consent for the use of animals was obtained from the farmers that participated in the study.

## AUTHOR CONTRIBUTIONS

Design of the study EI-A and NB; methodology, EI-A and SM; data curation and formal analysis, P-LD, SB, and MW; writing, EI-A; project administration and funding acquisition, NB; supervision of animal/tissue sampling and diagnosis, NB; supervision of laboratory and bioinformatics analyses, EI-A. All authors provided input in the interpretation of the results, have read and agreed to the published version of the manuscript.

## FUNDING

This research was supported by a contribution from the Dairy Research Cluster 3 (Dairy Farmers of Canada, Canadian Dairy Network and Agriculture, and Agri-Food Canada) under the Canadian Agricultural Partnership AgriScience Program (Project AAFC J-002095). Animal sampling, diagnosis, animal selection/ biopsies and some aspects of laboratory and bioinformatics analyses were supported by Projects AAFC J-000075, J-000079 and J-002223.

## ACKNOWLEDGMENTS

We appreciate the invaluable collaboration of the veterinarians and dairy producers in the Province of Quebec and the Centre d'expertise et de services Génome Québec for performing the WGBS library preparation and sequencing.

## SUPPLEMENTARY MATERIAL

The Supplementary Material for this article can be found online at: https://www.frontiersin.org/articles/10.3389/fgene.2021.797490/full#supplementary-material

## REFERENCES

Akalin, A., Kormaksson, M., Li, S., Garrett-Bakelman, F. E., Figueroa, M. E., Melnick, A., et al. (2012). methylKit: a Comprehensive R Package for the Analysis of Genome-wide DNA Methylation Profiles. *Genome Biol.* 13, R87. doi:10.1186/gb-2012-13-10-r87

Alam, A., Imam, N., Ahmed, M. M., Tazyeen, S., Tamkeen, N., Farooqui, A., et al. (2019). Identification and Classification of Differentially Expressed Genes and Network Meta-Analysis Reveals Potential Molecular Signatures Associated with Tuberculosis. *Front. Genet.* 10, 932. doi:10.3389/fgene.2019.00932

Alonso-Hearn, M., Canive, M., Blanco-Vazquez, C., Torremocha, R., Balseiro, A., Amado, J., et al. (2019). RNA-seq Analysis of Ileocecal Valve and Peripheral Blood from Holstein Cattle Infected with *Mycobacterium avium* subsp. paratuberculosis Revealed Dysregulation of the CXCL8/IL8 Signaling Pathway. *Sci. Rep.* 9, 14845. doi:10.1038/s41598-019-51328-0

Andrews, S. (2010). *FastQC: A Quality Control Tool for High Throughput Sequence Data*. Available at: https://www.bioinformatics.babraham.ac.uk/projects/fastqc/.

Arango-Sabogal, J. C., Côté, G., Paré, J., Labrecque, O., Roy, J. P., Buczinski, S., et al. (2016). Detection of *Mycobacterium avium* subsp. paratuberculosis in Tie-Stall Dairy Herds Using a Standardized Environmental Sampling Technique and Targeted Pooled Samples. *Can. J. Vet. Res.* 80, 175–182.

Ariel, O., Gendron, D., Dudemaine, P.-L., Gévry, N., Ibeagha-Awemu, E. M., and Bissonnette, N. (2020). Transcriptome Profiling of Bovine Macrophages Infected by *Mycobacterium avium* Spp. paratuberculosis Depicts Foam Cell and Innate Immune Tolerance Phenotypes. *Front. Immunol.* 10, 2874. doi:10.3389/fimmu.2019.02874

Ariel, O., Gendron, D., Dudemaine, P. L., Gévry, N., Ibeagha-Awemu, E. M., and Bissonnette, N. (2019). Transcriptome Profiling of Bovine Macrophages Infected by *Mycobacterium avium* subsp. paratuberculosis Depicts Foam Cell and Innate Immune Tolerance Phenotypes. *Front. Immunol.* 10, 2874. doi:10.3389/fimmu.2019.02874

Arsenault, R. J., Maattanen, P., Daigle, J., Potter, A., Griebel, P., and Napper, S. (2014). From Mouth to Macrophage: Mechanisms of Innate Immune Subversion by *Mycobacterium avium* subsp. paratuberculosis. *Vet. Res.* 45, 54. doi:10.1186/1297-9716-45-54

Benjamini, Y., and Hochberg, Y. (1995). Controlling the False Discovery Rate: A Practical and Powerful Approach to Multiple Testing. *J. R. Stat. Soc. Ser. B (Methodological)* 57, 289–300. doi:10.1111/j.2517-6161.1995.tb02031.x

Bindea, G., Mlecnik, B., Hackl, H., Charoentong, P., Tosolini, M., Kirilovsky, A., et al. (2009). ClueGO: a Cytoscape Plug-In to Decipher Functionally Grouped Gene Ontology and Pathway Annotation Networks. *Bioinformatics* 25, 1091–1093. doi:10.1093/bioinformatics/btp101

Bo, M., Jasemi, S., Uras, G., Erre, G. L., Passiu, G., and Sechi, L. A. (2020). Role of Infections in the Pathogenesis of Rheumatoid Arthritis: Focus on Mycobacteria. *Microorganisms* 8, 1459. doi:10.3390/microorganisms8101459

Brooks, J., Watson, A., and Korcsmaros, T. (2017). Omics Approaches to Identify Potential Biomarkers of Inflammatory Diseases in the Focal Adhesion

Complex. *Genomics, Proteomics & Bioinformatics* 15, 101–109. doi:10.1016/j.gpb.2016.12.003

Cavalcante, R. G., and Sartor, M. A. (2017). Annotatr: Genomic Regions in Context. *Bioinformatics (Oxford, England)* 33, 2381–2383. doi:10.1093/bioinformatics/btx183

Ding, Q., Joshi, P. S., Xie, Z.-H., Xiang, M., and Gan, L. (2012). BARHL2 Transcription Factor Regulates the Ipsilateral/contralateral Subtype Divergence in Postmitotic dI1 Neurons of the Developing Spinal Cord. *Proc. Natl. Acad. Sci.* 109, 1566–1571. doi:10.1073/pnas.1112392109

Dobson, B., O'brien, R., and Griffin, F. (2021). "The Search for Candidate Genes that Characterise Susceptibility or Resistance to *Mycobacterium avium* subsp. paratuberculosis,"in Proceedings of 11 International Colloquium on Paratuberculosis. Editors S. S. Nielsen and D. Bakker (Sydney, Australia: International Association For Paratuberculosis) 2001 Jul, 92–93.

Doherty, R., Farrelly, C. O., and Meade, K. G. (2014). Comparative Epigenetics: Relevance to the Regulation of Production and Health Traits in Cattle. *Anim. Genet.* 45, 3–14. doi:10.1111/age.12140

Doherty, R., Whiston, R., Cormican, P., Finlay, E. K., Couldrey, C., Brady, C., et al. (2016). The CD4+ T Cell Methylome Contributes to a Distinct CD4+ T Cell Transcriptional Signature in Mycobacterium Bovis-Infected Cattle. *Sci. Rep.* 6, 31014. doi:10.1038/srep31014

Duan, J. E., Jiang, Z. C., Alqahtani, F., Mandoiu, I., Dong, H., Zheng, X., et al. (2019). Methylome Dynamics of Bovine Gametes and *In Vivo* Early Embryos. *Front. Genet.* 10, 512. doi:10.3389/fgene.2019.00512

Facciuolo, A., Lee, A. H., Gonzalez Cano, P., Townsend, H. G. G., Falsafi, R., Gerdts, V., et al. (2020). Regional Dichotomy in Enteric Mucosal Immune Responses to a Persistent *Mycobacterium avium* subsp. paratuberculosis Infection. *Front. Immunol.* 11, 1020. doi:10.3389/fimmu.2020.01020

Farrell, D., Shaughnessy, R. G., Britton, L., Machugh, D. E., Markey, B., and Gordon, S. V. (2015). The Identification of Circulating MiRNA in Bovine Serum and Their Potential as Novel Biomarkers of Early *Mycobacterium avium* subsp paratuberculosis Infection. *PLoS One* 10, e0134310. doi:10.1371/journal.pone.0134310

Fernandes, M. C., Dillon, L. A., Belew, A. T., Bravo, H. C., Mosser, D. M., and El-Sayed, N. M. (2016). Dual Transcriptome Profiling of Leishmania-Infected Human Macrophages Reveals Distinct Reprogramming Signatures. *mBio* 7, e00027–00016. doi:10.1128/mBio.00027-16

Fock-Chow-Tho, D., Topp, E., Ibeagha-Awemu, E. A., and Bissonnette, N. (2017). Comparison of Commercial DNA Extraction Kits and Quantitative PCR Systems for Better Sensitivity in Detecting the Causative Agent of Paratuberculosis in Dairy Cow Fecal Samples. *J. Dairy Sci.* 100, 572–581. doi:10.3168/jds.2016-11384

Gao, Y., Jiang, J., Yang, S., Cao, J., Han, B., Wang, Y., et al. (2018). Genome-wide Association Study of *Mycobacterium avium* subsp. paratuberculosis Infection in Chinese Holstein. *BMC Genomics* 19, 972. doi:10.1186/s12864-018-5385-3

Gossner, A., Watkins, C., Chianini, F., and Hopkins, J. (2017). Pathways and Genes Associated with Immune Dysfunction in Sheep Paratuberculosis. *Sci. Rep.* 7, 46695. doi:10.1038/srep46695

Gu, Z., Gu, L., Eils, R., Schlesner, M., and Brors, B. (2014). Circlize Implements and Enhances Circular Visualization in R. *Bioinformatics* 30, 2811–2812. doi:10.1093/bioinformatics/btu393

Guo, W., Fiziev, P., Yan, W., Cokus, S., Sun, X., Zhang, M. Q., et al. (2013). BS-Seeker2: a Versatile Aligning Pipeline for Bisulfite Sequencing Data. *BMC Genomics* 14, 774. doi:10.1186/1471-2164-14-774

Gupta, P., Peter, S., Jung, M., Lewin, A., Hemmrich-Stanisak, G., Franke, A., et al. (2019). Analysis of Long Non-coding RNA and mRNA Expression in Bovine Macrophages Brings up Novel Aspects of *Mycobacterium avium* subsp. paratuberculosis Infections. *Sci. Rep.* 9, 1571. doi:10.1038/s41598-018-38141-x

Gupta, S. K., Maclean, P. H., Ganesh, S., Shu, D., Buddle, B. M., Wedlock, D. N., et al. (2018). Detection of microRNA in Cattle Serum and Their Potential Use to Diagnose Severity of Johne's Disease. *J. Dairy Sci.* 101, 10259–10270. doi:10.3168/jds.2018-14785

Hempel, R. J., Bannantine, J. P., and Stabel, J. R. (2016). Transcriptional Profiling of Ileocecal Valve of Holstein Dairy Cows Infected with *Mycobacterium avium* subsp. paratuberculosis. *PloS one* 11, e0153932. doi:10.1371/journal.pone.0153932

Hoeke, L., Sharbati, J., Pawar, K., Keller, A., Einspanier, R., and Sharbati, S. (2013). Intestinal *Salmonella typhimurium* Infection Leads to miR-29a Induced Caveolin 2 Regulation. *PLOS ONE* 8, e67300. doi:10.1371/journal.pone.0067300

Howell, K. J., Kraiczy, J., Nayak, K. M., Gasparetto, M., Ross, A., Lee, C., et al. (2018). DNA Methylation and Transcription Patterns in Intestinal Epithelial Cells from Pediatric Patients with Inflammatory Bowel Diseases Differentiate Disease Subtypes and Associate with Outcome. *Gastroenterology* 154, 585–598. doi:10.1053/j.gastro.2017.10.007

Ibeagha-Awemu, E. M., Bissonnette, N., Do, D. N., Dudemaine, P.-L., Wang, M., Facciuolo, A., et al. (2021). Regionally Distinct Immune and Metabolic Transcriptional Responses in the Bovine Small Intestine and Draining Lymph Nodes during a Subclinical *Mycobacterium avium* subsp. paratuberculosis Infection. *Front. Immunol.* 12, 760931. doi:10.3389/fimmu.2020.01020

Ibeagha-Awemu, E. M., Peters, S. O., Akwanji, K. A., Imumorin, I. G., and Zhao, X. (2016). High Density Genome Wide Genotyping-By-Sequencing and Association Identifies Common and Low Frequency SNPs, and Novel Candidate Genes Influencing Cow Milk Traits. *Sci. Rep.* 6, 31109. doi:10.1038/srep31109

Ibeagha-Awemu, E. M., and Zhao, X. (2015). Epigenetic marks: Regulators of Livestock Phenotypes and Conceivable Sources of Missing Variation in Livestock Improvement Programs. *Front. Genet.* 6, 302. doi:10.3389/fgene.2015.00302

Jiang, L., Liu, J., Sun, D., Ma, P., Ding, X., Yu, Y., et al. (2010). Genome Wide Association Studies for Milk Production Traits in Chinese Holstein Population. *PloS one* 5, e13661. doi:10.1371/journal.pone.0013661

Juraver-Geslin, H. A., Ausseil, J. J., Wassef, M., and Durand, B. C. (2011). Barhl2 Limits Growth of the Diencephalic Primordium through Caspase3 Inhibition of -catenin Activation. *Proc. Natl. Acad. Sci.* 108, 2288–2293. doi:10.1073/pnas.1014017108

Kampstra, P. (2008). Beanplot: A Boxplot Alternative for Visual Comparison of Distributions. *J. Stat. Softw.* 28, 1. doi:10.18637/jss.v028.c01

Karatzas, P. S., Gazouli, M., Safioleas, M., and Mantzaris, G. J. (2014). DNA Methylation Changes in Inflammatory Bowel Disease. *Ann. Gastroenterol.* 27, 125–132. doi:10.1093/ecco-jcc/jjv176

Khare, S., Lawhon, S. D., Drake, K. L., Nunes, J. E. S., Figueiredo, J. F., Rossetti, C. A., et al. (2012). Systems Biology Analysis of Gene Expression during *In Vivo Mycobacterium avium* Paratuberculosis Enteric Colonization Reveals Role for Immune Tolerance. *PLOS ONE* 7, e42127. doi:10.1371/journal.pone.0042127

Kinchen, J., Chen, H. H., Parikh, K., Antanaviciute, A., Jagielowicz, M., Fawkner-Corbett, D., et al. (2018). Structural Remodeling of the Human Colonic Mesenchyme in Inflammatory Bowel Disease. *Cell* 175, 372–386. e317. doi:10.1016/j.cell.2018.08.067

Kiser, J. N., White, S. N., Johnson, K. A., Hoff, J. L., Taylor, J. F., and Neibergs, H. L. (2017). Identification of Loci Associated with Susceptibility to *Mycobacterium avium* subsp. paratuberculosis (Map) Tissue Infection in Cattle. *J. Anim. Sci.* 95, 1080–1091. doi:10.2527/jas.2016.1152

Koets, A. P., Eda, S., and Sreevatsan, S. (2015). The within Host Dynamics of *Mycobacterium avium* subsp. paratuberculosis Infection in Cattle: where Time and Place Matter. *Vet. Res.* 46, 61. doi:10.1186/s13567-015-0185-0

Krueger, F. (2012). *Galore: A Wrapper Tool Around Cutadapt and FastQC to Consistently Apply Quality and Adapter Trimming to FastQ Files, with Some Extra Functionality for RRBS Data*. Available at: https://www.bioinformatics.babraham.ac.uk/projects/trim_galore/.

Li, H., Handsaker, B., Wysoker, A., Fennell, T., Ruan, J., Homer, N., et al.Genome Project Data Processing S; ubgroup (2009). The Sequence Alignment/Map Format and SAMtools. *Bioinformatics* 25, 2078–2079. doi:10.1093/bioinformatics/btp352

Li Yim, A. Y. F., Duijvis, N. W., Ghiboub, M., Sharp, C., Ferrero, E., Mannens, M. M. A. M., et al. (2020). Whole-genome DNA Methylation Profiling of CD14+ Monocytes Reveals Disease Status and Activity Differences in Crohn's Disease Patients. *J. Clin. Med.* 9, 1055. doi:10.3390/jcm9041055

Li, Z.-W., Sun, B., Gong, T., Guo, S., Zhang, J., Wang, J., et al. (2019). GNAI1 and GNAI3 Reduce Colitis-Associated Tumorigenesis in Mice by Blocking IL6 Signaling and Down-Regulating Expression of GNAI2. *Gastroenterology* 156, 2297–2312. doi:10.1053/j.gastro.2019.02.040

Li, Z., Ding, Y., Zhu, Y., Yin, M., Le, X., Wang, L., et al. (2014). Both gene Deletion and Promoter Hyper-Methylation Contribute to the Down-Regulation of ZAC/PLAGL1 Gene in Gastric Adenocarcinomas: a Case

Control Study. *Clin. Res. Hepatol. Gastroenterol.* 38, 744–750. doi:10.1016/j.clinre.2013.06.007

Liu, P. T., and Modlin, R. L. (2008). Human Macrophage Host Defense against *Mycobacterium tuberculosis*. *Curr. Opin. Immunol.* 20, 371–376. doi:10.1016/j.coi.2008.05.014

Ma, Y., Semba, S., Maemoto, A., Takeuchi, M., Kameshita, I., Ishida, A., et al. (2010). Oxazolone-induced Over-expression of Focal Adhesion Kinase in Colonic Epithelial Cells of Colitis Mouse Model. *FEBS Lett.* 584, 3949–3954. doi:10.1016/j.febslet.2010.07.054

Mallikarjunappa, S., Sargolzaei, M., Brito, L. F., Meade, K. G., Karrow, N. A., and Pant, S. D. (2018). Short Communication: Uncovering Quantitative Trait Loci Associated with Resistance to *Mycobacterium avium* subsp. paratuberculosis Infection in Holstein Cattle Using a High-Density Single Nucleotide Polymorphism Panel. *J. Dairy Sci.* 101, 7280–7286. doi:10.3168/jds.2018-14388

Marete, A., Ariel, O., Ibeagha-Awemu, E., and Bissonnette, N. (2021b). Identification of Long Non-coding RNA Isolated from Naturally Infected Macrophages and Associated with Bovine Johne's Disease in Canadian Holstein Using a Combination of Neural Networks and Logistic Regression. *Front. Vet. Sci.* 8, 639053. doi:10.3389/fvets.2021.639053

Marete, A., Ariel, O., Ibeagha-Awemu, E., and Bissonnette, N. (2021a). Identification of Long Non-coding RNA Isolated from Naturally Infected Macrophages and Associated with Bovine Johne's Disease in Canadian Holstein Using a Combination of Neural Networks and Logistic Regression. *Front. Vet. Sci.* 8, 639053. doi:10.3389/fvets.2021.639053

Marete, A., Schenkel, F., Kelton, D., Chesnais, J., Miglior, F., Ibeagha-Awemu, E., et al. (2021c). Sequence-based GWAS Identifies Candidate Genes for Susceptibility to MAP Infection in Canadian Holstein *Journal Of Genetics And Genomics* Submitted. *BMC Genomics*. 22. 162. doi:10.1186/s12864-021-07487-4

Martin, M. (2011). Cutadapt Removes Adapter Sequences from High-Throughput Sequencing Reads. *EMBnet j.* 17, 10–12. doi:10.14806/ej.17.1.200

Mcnees, A. L., Markesich, D., Zayyani, N. R., and Graham, D. Y. (2015). Mycobacterium Paratuberculosis as a Cause of Crohn's Disease. *Expert Rev. Gastroenterol. Hepatol.* 9, 1523–1534. doi:10.1586/17474124.2015.1093931

Mehta, M. D., and Liu, P. T. (2014). microRNAs in Mycobacterial Disease: Friend or Foe? *Front. Genet.* 5, 231. doi:10.3389/fgene.2014.00231

Noh, K. T., Shin, S. J., Son, K. H., Jung, I. D., Kang, H. K., Lee, S. J., et al. (2012). The Mycobacterium avium subsp. paratuberculosis fibronect in Attachment Protein, a Toll-like Receptor 4 Agonist, Enhances Dendritic Cell-Based Cancer Vaccine Potency. *Exp. Mol. Med.* 44, 340–349. doi:10.3858/emm.2012.44.5.038

Over, K., Crandall, P. G., O'Bryan, C. A., and Ricke, S. C. (2011). Current Perspectives onMycobacterium aviumsubsp.paratuberculosis,Johne's Disease, and Crohn's Disease: a Review. *Crit. Rev. Microbiol.* 37, 141–156. doi:10.3109/1040841x.2010.532480

Pawar, K., Sharbati, J., Einspanier, R., and Sharbati, S. (2016). Mycobacterium Bovis BCG Interferes with miR-3619-5p Control of Cathepsin S in the Process of Autophagy. *Front Cel Infect Microbiol* 6, 27. doi:10.3389/fcimb.2016.00027

Peille, A.-L., Brouste, V., Kauffmann, A., Lagarde, P., Le Morvan, V., Coindre, J.-M., et al. (2013). Prognostic Value of PLAGL1-specific CpG Site Methylation in Soft-Tissue Sarcomas. *PLoS One* 8, e80741. doi:10.1371/journal.pone.0080741

Rybaczyk, L., Rozmiarek, A., Circle, K., Grants, I., Needleman, B., Wunderlich, J. E., et al. (2009). New Bioinformatics Approach to Analyze Gene Expressions and Signaling Pathways Reveals Unique Purine Gene Dysregulation Profiles that Distinguish between CD and UC. *Inflamm. Bowel Dis.* 15, 971–984. doi:10.1002/ibd.20893

Shannon, P., Markiel, A., Ozier, O., Baliga, N. S., Wang, J. T., Ramage, D., et al. (2003). Cytoscape: a Software Environment for Integrated Models of Biomolecular Interaction Networks. *Genome Res.* 13, 2498–2504. doi:10.1101/gr.1239303

Sharbati, J., Lewin, A., Kutz-Lohroff, B., Kamal, E., Einspanier, R., and Sharbati, S. (2011). Integrated microRNA-mRNA-Analysis of Human Monocyte Derived Macrophages upon *Mycobacterium avium* Subsp. Hominissuis Infection. *PLoS One* 6, e20258. doi:10.1371/journal.pone.0020258

Shin, M.-K., Park, H., Shin, S. W., Jung, M., Lee, S.-H., Kim, D.-Y., et al. (2015a). Host Transcriptional Profiles and Immunopathologic Response Following *Mycobacterium avium* subsp. Paratuberculosis Infection in Mice. *PLOS ONE* 10, e0138770. doi:10.1371/journal.pone.0138770

Shin, M. K., Shin, S. W., Jung, M., Park, H., Park, H. E., and Yoo, H. S. (2015b). Host Gene Expression for *Mycobacterium avium* subsp. paratuberculosis Infection in Human THP-1 Macrophages. *Pathog. Dis.* 73, ftv031. doi:10.1093/femspd/ftv031

Somineni, H. K., Venkateswaran, S., Kilaru, V., Marigorta, U. M., Mo, A., Okou, D. T., et al. (2019). Blood-Derived DNA Methylation Signatures of Crohn's Disease and Severity of Intestinal Inflammation. *Gastroenterology* 156, 2254–2265. e2253. doi:10.1053/j.gastro.2019.01.270

Song, Q., Decato, B., Hong, E. E., Zhou, M., Fang, F., Qu, J., et al. (2013). A Reference Methylome Database and Analysis Pipeline to Facilitate Integrative and Comparative Epigenomics. *PloS one* 8, e81148. doi:10.1371/journal.pone.0081148

Song, W., Li, D., Tao, L., Luo, Q., and Chen, L. (2020). Solute Carrier Transporters: the Metabolic Gatekeepers of Immune Cells. *Acta Pharmaceutica Sinica B* 10, 61–78. doi:10.1016/j.apsb.2019.12.006

Stahl, A., Gimeno, R. E., Tartaglia, L. A., and Lodish, H. F. (2001). Fatty Acid Transport Proteins: a Current View of a Growing Family. *Trends Endocrinol. Metab.* 12, 266–273. doi:10.1016/s1043-2760(01)00427-1

Thompson, R. P., Nilsson, E., and Skinner, M. K. (2020). Environmental Epigenetics and Epigenetic Inheritance in Domestic Farm Animals. *Anim. Reprod. Sci.* 220, 106316. doi:10.1016/j.anireprosci.2020.106316

Timms, V. J., Daskalopoulos, G., Mitchell, H. M., and Neilan, B. A. (2016). The Association of *Mycobacterium avium* subsp. paratuberculosis with Inflammatory Bowel Disease. *PLOS ONE* 11, e0148731. doi:10.1371/journal.pone.0148731

Triantaphyllopoulos, K. A., Ikonomopoulos, I., and Bannister, A. J. (2016). Epigenetics and Inheritance of Phenotype Variation in Livestock. *Epigenetics & Chromatin* 9, 31. doi:10.1186/s13072-016-0081-5

Wang, J., Yang, K., Zhou, L., Wu, Y., Zhu, M., Lai, X., et al. (2013). MicroRNA-155 Promotes Autophagy to Eliminate Intracellular Mycobacteria by Targeting Rheb. *Plos Pathog.* 9, e1003697. doi:10.1371/journal.ppat.1003697

Wang, M., Bissonnette, N., Griebel, P., Dudemaine, P.-L., Do, D. N., and Ibeagha-Awemu, E. M. (2019a). PSVI-15 Transcriptome Analysis of Ileal Lymph Nodes Identifies Key microRNAs Affecting Disease Progression in Holstein Cows with Subclinical Johne's Disease. *J. Anim. Sci.* 97, 207–208. doi:10.1093/jas/skz258.426

Wang, M., Bissonnette, N., Griebel, P., Dudemaine, P.-L., Do, D. N., Mao, Y., et al. (2019b). PSVI-14 Differentially Expressed microRNAs with Potential Regulatory Roles in Ileum of Holstein Cows with Subclinical Johne's Disease. *J. Anim. Sci.* 97, 206–207. doi:10.1093/jas/skz258.425

Wang, M., and Ibeagha-Awemu, E. M. (2021). Impacts of Epigenetic Processes on the Health and Productivity of Livestock. *Front. Genet.* 11, 1812. doi:10.3389/fgene.2020.613636

Wang, X., Wurmser, C., Pausch, H., Jung, S., Reinhardt, F., Tetens, J., et al. (2012). Identification and Dissection of Four Major QTL Affecting Milk Fat Content in the German Holstein-Friesian Population. *PloS one* 7, e40711. doi:10.1371/journal.pone.0040711

Wang, Y., Chen, C., Xu, X.-D., Li, H., Cheng, M.-H., Liu, J., et al. (2020). Levels of miR-125a-5p Are Altered in Mycobacterium Avium-Infected Macrophages and Associate with the Triggering of an Autophagic Response. *Microbes Infect.* 22, 31–39. doi:10.1016/j.micinf.2019.07.002

Wei, M., Wang, L., Wu, T., Xi, J., Han, Y., Yang, X., et al. (2016). NLRP3 Activation Was Regulated by DNA Methylation Modification during *Mycobacterium tuberculosis* Infection. *Biomed. Res. Int.* 2016, 4323281. doi:10.1155/2016/4323281

Whitlock, R. H., and Buergelt, C. (1996). Preclinical and Clinical Manifestations of Paratuberculosis (Including Pathology). *Vet. Clin. North America: Food Anim. Pract.* 12, 345–356. doi:10.1016/s0749-0720(15)30410-2

Whittington, R., Donat, K., Weber, M. F., Kelton, D., Nielsen, S. S., Eisenberg, S., et al. (2019). Control of Paratuberculosis: Who, Why and How. A Review of 48 Countries. *BMC Vet. Res.* 15, 198. doi:10.1186/s12917-019-1943-4

Wilburn, K. M., Fieweger, R. A., and Vanderven, B. C. (2018). Cholesterol and Fatty Acids Grease the Wheels of *Mycobacterium tuberculosis* Pathogenesis. *Pathog. Dis.* 76, fty021. doi:10.1093/femspd/fty021

Yamamoto, H., Watanabe, Y., Oikawa, R., Morita, R., Yoshida, Y., Maehata, T., et al. (2016). BARHL2 Methylation Using Gastric Wash DNA or Gastric Juice Exosomal DNA Is a Useful Marker for Early Detection of Gastric Cancer in an *H. pylori* -Independent Manner. *Clin. Transl Gastroenterol.* 7, e184. doi:10.1038/ctg.2016.40

Zeng, Z., Mukherjee, A., and Zhang, H. (2019). From Genetics to Epigenetics, Roles of Epigenetics in Inflammatory Bowel Disease. *Front. Genet.* 10, 1017. doi:10.3389/fgene.2019.01017

Zhang, H., Shen, Z., Yang, Z., Jiang, H., Chu, S., Mao, Y., et al. (2021). Abundance of Solute Carrier Family 27 Member 6 (SLC27A6) in the Bovine Mammary Gland Alters Fatty Acid Metabolism. *Food Funct.* 12, 4909–4920. doi:10.1039/d0fo03289a

Zhang, X., Zhao, F., Si, Y., Huang, Y., Yu, C., Luo, C., et al. (2014). GSK3β Regulates Milk Synthesis in and Proliferation of Dairy Cow Mammary Epithelial Cells via the mTOR/S6K1 Signaling Pathway. *Molecules* 19, 9435–9452. doi:10.3390/molecules19079435

Zhao, X., and Guan, J.-L. (2011). Focal Adhesion Kinase and its Signaling Pathways in Cell Migration and Angiogenesis. *Adv. Drug Deliv. Rev.* 63, 610–615. doi:10.1016/j.addr.2010.11.001

Zhou, Y., Connor, E. E., Bickhart, D. M., Li, C., Baldwin, R. L., Schroeder, S. G., et al. (2018). Comparative Whole Genome DNA Methylation Profiling of Cattle Sperm and Somatic Tissues Reveals Striking Hypomethylated Patterns in Sperm. *GigaScience* 7, giy039. doi:10.1093/gigascience/giy039

Zur Bruegge, J., Einspanier, R., and Sharbati, S. (2017). A Long Journey Ahead: Long Non-coding RNAs in Bacterial Infections. *Front. Cel. Infect. Microbiol.* 7, 95. doi:10.3389/fcimb.2017.00095

**Conflict of Interest:** The authors declare that the research was conducted in the absence of any commercial or financial relationships that could be construed as a potential conflict of interest.

**Publisher's Note:** All claims expressed in this article are solely those of the authors and do not necessarily represent those of their affiliated organizations, or those of the publisher, the editors and the reviewers. Any product that may be evaluated in this article, or claim that may be made by its manufacturer, is not guaranteed or endorsed by the publisher.

*Copyright © 2021 Suraj Bhattarai, Stephanie McKay, Xin Zhao and Her Majesty the Queen in Right of Canada, as represented by the Minister of Agriculture and Agri-Food Canada for the contribution of Eveline M. Ibeagha-Awemu, Nathalie Bissonnette, Mengqi Wang and Pier-Luc Dudemaine. This is an open-access article distributed under the terms of the Creative Commons Attribution License (CC BY). The use, distribution or reproduction in other forums is permitted, provided the original author(s) and the copyright owner(s) are credited and that the original publication in this journal is cited, in accordance with accepted academic practice. No use, distribution or reproduction is permitted which does not comply with these terms.*

frontiers in Cell and Developmental Biology

ORIGINAL RESEARCH
published: 03 February 2022
doi: 10.3389/fcell.2022.820558

# Integrative Genome-Wide DNA Methylome and Transcriptome Analysis of Ovaries from Hu Sheep with High and Low Prolific

*Xiaolei Yao*[1,2], *Fengzhe Li*[1,2], *Zongyou Wei*[3], *M. A. El-Samahy*[1,2,4], *Xu Feng*[1,2], *Fan Yang*[1,2] *and Feng Wang*[1,2]*

[1]Hu Sheep Academy, Nanjing Agricultural University, Nanjing, China, [2]Jiangsu Livestock Embryo Engineering Laboratory, Nanjing Agricultural University, Nanjing, China, [3]Taicang Agricultural and Rural Science and Technology Service Center, and Graduate Workstation, Taicang, China, [4]Animal Production Research Institute, ARC, Ministry of Agriculture, Giza, Egypt

DNA methylation plays an important role in biological processes by affecting gene expression. However, how DNA methylation regulates phenotypic variation in Hu sheep remains unclear. Therefore, we generated genome-wide DNA methylation and transcriptomic profiles in the ovaries of Hu sheep with different prolificacies and genotypes (FecBB and FecB+). Results showed that ovary DNA methylome and transcriptome were significantly different between high prolificacy and low prolificacy Hu sheep. Comparative methylome analyses identified 10,644, 9,594, and 12,214 differentially methylated regions and 87, 1,121, and 2,375 genes, respectively, showing differential expression levels in three different comparison groups. Female reproduction-associated differentially methylated regions-related genes and differentially expressed genes were enriched, thereby the respective interaction networks were constructed. Furthermore, systematical integrative analyses revealed a negative correlation between DNA methylation around the transcriptional start site and gene expression levels, which was confirmed by testing the expression of integrin β2 subunit (ITGB2) and lysosome-associated protein transmembrane-4 beta (LAPTM4B) *in vivo* and *in vitro*. These findings demonstrated that DNA methylation influences the propensity for prolificacy by affecting gene expression in the ovaries, which may contribute to a greater understanding of the epigenome and transcriptome that will be useful for animal breeding.

**Keywords: DNA methylation, gene expression, ovary, prolificacy, Hu sheep**

OPEN ACCESS

***Edited by:***
*George E. Liu,*
*Agricultural Research Service (USDA), United States*

***Reviewed by:***
*Xiao Wang,*
*Konge Larsen ApS, Denmark*
*Mingxing Chu,*
*Institute of Animal Sciences (CAAS), China*
*Hui Li,*
*Guangxi University, China*

***Correspondence:**
*Feng Wang*
*caeet@njau.edu.cn*

***Specialty section:***
*This article was submitted to Epigenomics and Epigenetics, a section of the journal Frontiers in Cell and Developmental Biology*

***Received:*** *23 November 2021*
***Accepted:*** *14 January 2022*
***Published:*** *03 February 2022*

***Citation:***
*Yao X, Li F, Wei Z, El-Samahy MA, Feng X, Yang F and Wang F (2022) Integrative Genome-Wide DNA Methylome and Transcriptome Analysis of Ovaries from Hu Sheep with High and Low Prolific. Front. Cell Dev. Biol. 10:820558. doi: 10.3389/fcell.2022.820558*

## INTRODUCTION

Litter size is one of most important traits that determines the fecundity and reproductive efficiency of sheep bred for meat. In China, most sheep species are monotocous and seasonal estrus, although a few are polytocous. Compared with other sheep, Hu sheep is an excellent local breed in China, which is known for its high prolificacy and year-round estrus (Yue, 1996). Therefore, determining the molecular mechanisms associated with fecundity will help accelerate the breeding process of sheep with high prolificacy. Although the existing genetic studies have identified several genes with sheep fecundity, including GDF9, BMP15, and BMPR1B, the underlying genetic mechanisms remain largely unexplored (Chu et al., 2007; Polley et al., 2010; Farhadi et al., 2013; Wang et al., 2015). FecB

(mutation in BMPR1B) is one of the key genes associated with sheep prolificacy (Wang et al., 2015). Moreover, evidences revealed that sheep with the homozygous mutation (FecBB; BB) had the greater ovulation rates than those with the heterozygous mutation (FecB+; B+) or the wild-type genotype (++) (Fabre et al., 2006; Gootwine et al., 2008). Thus, Hu sheep with different prolificacies and genotypes (BB and B+) were selected as experimental subjects.

It is widely thought that ovarian dysfunction leads to infertility in mammals. One of the main functions of the ovaries is to produce mature oocytes and secrete reproductive hormones that are involved in the follicular development and ovulation. Therefore, studying the differences in regulatory mechanisms in the ovaries of sheep with different prolificacies may reveal the mechanisms behind the genetic regulation of little size traits.

DNA methylation is an epigenetic modification that regulates gene expression and serves as a key regulator of development (Fan et al., 2020; Yang et al., 2021), differentiation (Khavari et al., 2010), and other processes (Miyakuni et al., 2021). Recent studies have shifted their focus toward how DNA methylation regulates pubertal onset (Lomniczi et al., 2015; Yang et al., 2016; Yuan et al., 2019), estrus (An et al., 2018; Zhou et al., 2018), ovary (Wang et al., 2014; Yu et al., 2015; Sagvekar et al., 2019), oocyte (Mattern et al., 2017; Wei et al., 2019), and embryo development (Salilew-Wondim et al., 2015; Canovas et al., 2017), and reproductive diseases (Vazquez-Martinez et al., 2019; Cao et al., 2021; Zhong et al., 2021). In-depth studies pertaining on epigenetic modifications, such as DNA methylation, are facilitating improvement in animal breeding (Gonzalez-Recio et al., 2015). Several studies have reported the genome-wide methylation profiles associated with milk production-related phenotypes in dairy cows (Singh et al., 2012), and disease resistance in crops (Tirnaz and Batley, 2019), as well as litter size in goats and pigs (Hwang et al., 2017; Kang et al., 2021). Meanwhile, Miao et al. (2017) recently reported the DNA methylation patterns in the ovaries of Dorset sheep and Small Tail Han sheep. These studies have demonstrated that DNA methylation plays an important role in regulating fecundity.

DNA methylation and gene expression profiles have been previously studied in the ovaries of Hu sheep with different prolificacies (the BB genotype only) to elucidate the regulatory mechanisms involved in Hu sheep fecundity (Zhang et al., 2017; Feng et al., 2018). As an extension of this study, here we aimed to systematically investigate both genome-wide DNA methylation and gene expression profiles in the ovaries of Hu sheep with different prolificacies (high prolificacy, HP; low prolificacy, LP) and genotypes (BB and B+) by performing whole-genome bisulfite sequencing (WGBS) and RNA-sequencing (RNA-seq). Furthermore, an integrated analysis of DNA methylation and transcriptome was performed to reveal whether and how DNA methylation mediate prolificacy phenotypic variations by affecting gene expression.

# MATERIALS AND METHODS

## Animals and Sample Collection

We previously reported the details of the procedures for handling experimental animals and sample collection (Yao et al., 2021), which were approved by the Institutional Animal Ethics Committee of the Nanjing Agricultural University (SYXK 2011-0036). In brief, we firstly chose twenty non-pregnant ewes (2, 3 years old) based on their litter size numbers of three records, categorizing them as HP ewes (litter size = 3, $n = 4$) and LP ewes (litter size = 1, $n = 16$). Meanwhile, BMPR1B polymorphism genotyping of those ewes was detected as described previously (Yao et al., 2021). Finally, nine ewes were selected and divided into HPBB ($n = 3$), LPBB ($n = 3$) and LPB+ ($n = 3$) groups. All ewes were slaughtered during estrus and the ovarian samples were immediately collected and stored at −80°C for WGBS and RNA-seq.

## WGBS and RNA-seq

Genomic DNA and total RNA were extracted from ovarian tissue of the nine sheep using a Genomic DNA kit (Cat.#DP304-03,Tiangen, Beijing, China) and TRIzol reagent (Cat.# 15596-026; Invitrogen, Carlsbad, CA), respectively. The concentration and purity of isolated DNA and RNA were determined using NanDrop spectrophotometer (NanoDrop Technologies, Wilmington, DE, United States) and agarose gel electrophoresis. The preparation of nine genome-wide DNA methylation and transcriptome libraries and sequencing (WGBS and RNA-seq), respectively, were performed by Biomarker Technologies Corporation (Beijing, China). Notably, we previously reported the DNA methylation (Zhang et al., 2017) and mRNAs (Feng et al., 2018) profiles in ovaries of only HPBB and LPBB Hu sheep, and using the same described methods, we analyzed the WGBS and RNA-Seq data in this study, with some modifications. Briefly, the raw data were first filtered to remove low-quality reads, and the clean data were then aligned with the reference genome of sheep (Ovis aries v4.0).

Differential methylated regions (DMRs) were defined by the presence of at least three methylation sites in the region, and the difference in methylation levels was >0.2 (>0.3 for CG type) with *P*-value (Fisher's) < 0.05. Differentially expressed (DE) mRNAs were identified with the false discovery rate (FDR) < 0.05 and absolute value of $\log_2$ (fold change, FC) >1. Primarily, DMGs were detected through mapping the DMRs to genes based on their genomic location. In this study, we defined the genomic region from −3000 bp to the transcription start site (TSS) as the promoter region and from the TSS to the transcriptional termination site (TTS) as the gene body region. To visualize the overlapping gene sets, we generated venn diagrams using Venn diagram online tool (http://bioinformatics.psb.ugent.be/webtools/Venn/).

## Integrated Analysis

The correlation between gene expression and methylation was calculated using only differentially expressed genes (DEGs) and DMR-related genes (DMGs). For the global methylation around TSS regions (±2000 bp) and gene expression correlation analysis, the genes was divided into four groups according to their expression level: hightest, lowest, medium-high and medium-low. T visualize the relationship between methylation and gene expression, heatmaps were generated using the R package (heatmap).

## Functional Enrichment Analysis

Gene Ontology (GO) enrichment analyses of DMGs and DEGs were implemented by the Wallenius non-central hyper-geometric distribution in the GOseq R packages (Young et al., 2010). Kyoto Encyclopedia of Genes and Genomes (KEGG) analysis of DMGs and DEGs were evaluated using KOBAS software (Mao et al., 2005).

## Interaction Network Construction

The interaction network of DMGs and DEGs associated with female reproduction was analyzed using the STRING database (http://string-db.org/) and visualized with Cytoscape software (V3.4.0).

## Bisulfite Sequencing PCR

For BSP analysis, genomic DNA of ovaries from each groups was modified with sodium bisulfite using an EZ DNA Methylation-Direct Kit (Cat.#D5020; Zymo Research, Irvine, CA, United States). The PCR products were purified using a gel extraction kit (Cat.#DC301-01; Vazyme, Nanjing, China), then ligated and cloned into the pMD19-T vector (Cat.#6013; Takara, Osaka, Japan). Subsequently, ten positive clones of each sample were randomly selected for DNA sequencing. Data were analyzed and visualized using BIQ Analyzer software. BSP primers are listed in **Supplementary Table S1** and all operations were conducted according to the manufacturer's instructions.

## Cell Culture and Treatments

Hu sheep granulosa cells (GCs) were isolated from healthy follicles (2–5 mm) and cultured as our previously described (Yao et al., 2021). Briefly, GCs were seeded into different plates (6-well: $1 \times 10^6$ cells/well) in culture medium (Dulbecco's modified Eagle's medium/nutrient mixture F-12 supplemented with 10% fetal bovine serum, 2 mM L-glutamine, 100 IU/ml penicillin, and 100 μg/ml streptomycin) at 37°C and 5% $CO_2$. When the cultured GCs attained 60–70% confluence, the culture medium was replaced with new medium containing various concentrations (0, 1, 2, 5, 10, and 20 μM) of 5-Aza-deoxycytidine (5-Aza; Cat.#a3656; Sigma-Aldrich, United States), as a DNA methyltransferase inhibitor, and incubated for 48 h.

ITGB2 (integrin β2 subunit) knockdown was achieved using siRNAs, which were synthesized by GenePharma (Shanghai, China) and the sequences listed in **Supplementary Table S2**. After cultured GCs to 60–70% confluence, siRNA-NC and siRNA-ITGB2 were transfected into GCs with or without 10 μM 5-Aza for 48 h. Subsequently, all treated cells were collected for further analysis. All reagents used in cell culture were purchased from Life Technologies (Pleasanton CA, United States).

## Immunohistochemistry

Immunohistochemistry was performed following our previously described method (Yao et al., 2017). Rabbit anti-LAPTM4B (lysosome-associated protein transmembrane-4 beta; Cat.#18895 -1-AP; ProteinTech, Rosemont, IL, United States) were used as primary antibody. For negative control, the primary antibody was replaced with Tris-buffered saline. Digital images were examined using a light microscope (Nikon, Tokyo, Japan).

## Quantitative Reverse Transcriptase PCR

For qRT-PCR analysis, cDNA was synthesized using reverse transcription reagent kit with gDNA wiper (Cat.#R323-01; Vazyme, Nanjing, China). Subsequently, qRT-PCR was performed on an ABI 7500 Real-Time PCR System (Applied BioSystems, Carlsbad, CA, United States) using SYBR Green Master Mix (Cat.#Q711-02; Vazyme, Nanjing, China). Relative mRNA expression levels were quantified using $2^{-\Delta\Delta CT}$ method, with Glyceraldehyde 3-phosphate dehydrogenase (GAPDH) as the internal control. Primers were designed using the Primer 5.0 software and listed in **Supplementary Table S3**.

## Statistical Analysis

Data are presented as means ± SEM based on three independent experiments, with GraphPad Prism v7.0 (GraphPad Software, CA, United States). Statistical analyses were performed by the one-way analysis of variance followed by a post hoc test in the SPSS25.0 software package (Chicago, IL, United States). *P-values* < 0.05 were considered statistically significant.

# RESULTS

## Overview of Genome-Wide DNA Methylation Profiling in the Ovaries of Hu Sheep

To determine the effects of DNA methylation on the phenotypic variation of prolificacy, WGBS analysis was performed in the ovaries of HPBB, LPBB and LPB + groups of Hu sheep. After data filtering, each sample had approximately 210 million clean reads. Of mapped reads, 74.26, 73.94, and 66.65% in the HPBB, LPBB and LPB + groups, respectively, were used for subsequent analysis, with an average of 3.58% of methylated cytosine sites (**Supplementary Table S4**).

Global DNA methylation profiles indicated three contexts, CG, CHH, and CHG (where H is A, C, or T), existed in the ovaries of Hu sheep. The genomic methylation proportions of CG, CHG, and CHH contexts was respectively 72.23, 0.50 and 0.50% in the LPB + group, 69.60, 0.63 and 0.63% in the LPBB group, and 70.77, 0.70 and 0.66% in the HPBB group (**Figure 1A**). Among the three methylated contexts (CG, CHG and CHH), the methylated CG context represented 95.55, 95.20 and 95.06% in the LPB+, LPBB and HPBB groups, respectively (**Figure 1B**). In addition, the methylated level of CG context was mainly between 90 and 100%, whereas the methylated levels of CHG and CHH contexts apparently exhibited a more uniform distribution range from 10 to 30% (**Figure 1C**).

## Comparison of DMRs in the Ovaries of Hu Sheep with Different Prolificacies

The Model-Based Analysis of Bisulfite Sequencing package was used to identify DMRs and compare the DNA methylation

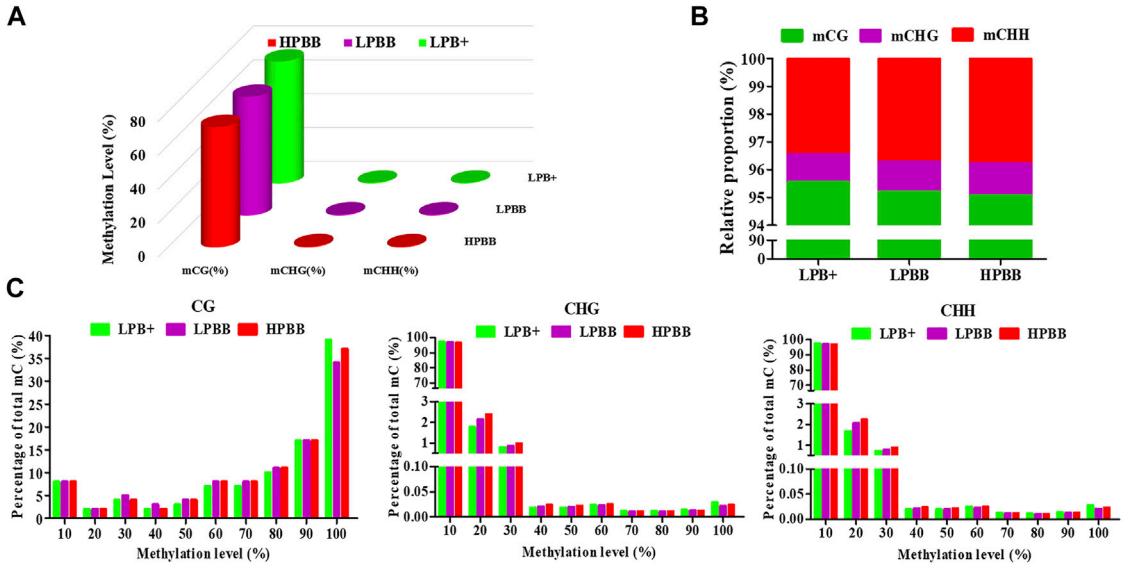



**FIGURE 1 |** DNA methylation levels and distribution in ovaries of Hu sheep with different prolificacies. **(A)** Genomic methylation levels of CG, CHG, and CHH in different groups. **(B)** Relative average proportions of CG, CHG, and CHH methylation contexts in ovaries among different groups. **(C)** The average methylation percentage (y-axis) for different methylation levels (x-axis) of CG, CHG, and CHH methylation in different groups.

profiles between the different groups. Overall, 10,644 DMRs (6,281 hyper-methylated and 4,363 hypo-methylated; 10,634 CG, 1 CHG and 9 CHH), 9,594 DMRs (4,359 hyper-methylated and 5,235 hypo-methylated; 9,583 CG, 2 CHG and 9 CHH) and 12,214 DMRs (4,562 hyper-methylated and 7,652 hypo-methylated; 12,199 CG, 1 CHG and 14 CHH) were identified in the LPBB vs. HPBB, LPB + vs. HPBB and LPB + vs. LPBB groups, respectively (**Figure 2A** and **Supplementary Tables S5–S7**). Moreover, the distribution of DMRs were mainly located at intergenic and intron regions (**Figures 2B–D**).

## Identification of DMGs and DEGs Among Different Comparison Groups

We identified 7,933 DMGs in the ovaries of the different comparison groups, of which 1,944 DMGs were common to all comparison groups (**Figure 3A** and **Supplementary Table S8**). Of these DMGs, 4,721 (3,393 hyper-methylated and 2,670 hypo-methylated), 4,426 (2,694 hyper-methylated and 2,951 hypo-methylated) and 5,152 (2,813 hyper-methylated and 3,812 hypo-methylated) were differentially methylated in the LPBB vs. HPBB, LPB + vs. HPBB and LPB + vs. LPBB groups, respectively (**Figure 3B**). Moreover, DMGs that exhibited DMRs in their promoter and gene body are shown in **Figures 3C–E**. The LPBB vs. HPBB, LPB + vs. HPBB and LPB + vs. LPBB groups contained 487, 404 and 528 genes, respectively, including both hyper- and hypo-methylated DMRs in their promoter and gene body.

There were 87 (19 up-regulated and 68 down-regulated), 1,121 (662 up-regulated and 459 down-regulated) and 2,375 (1,563 up-regulated and 812 down-regulated) DE mRNAs identified in the LPBB vs. HPBB, LPB + vs. HPBB and LPB + vs. LPBB groups, respectively (**Figures 4A–C**). Hierarchical clustering of the DE mRNAs (**Figures 4D–F**) revealed the expression patterns of the individuals for each comparison.

To confirm the reliability of the WGBS and RNA-seq data, four regions and seven genes were randomly selected for BSP and qRT-PCR, respectively. The results were consistent with the WGBS and RNA-seq data, suggesting that the WGBS and RNA-seq data were reliable for further study (**Figure 5**).

## Functional Enrichment and Interaction Network Construction

As previously mentioned, the majority of methylated cytosines were of the CG type; thus, we focused on DMGs of methylated CG for functional enrichment analysis. GO and KEGG analyses were performed to evaluate the functions of DMGs and DEGs in the ovaries of Hu sheep with different prolificacies. Across all comparisons, the DMGs were significantly enriched in the TGF-β and Wnt signaling pathways (**Supplementary Figure S1**). Furthermore, we selected the female reproduction associated DMGs (**Supplementary Tables S9–S11**) and DEGs (**Supplementary Tables S12–S14**) for functional enrichment and the interaction networks construction for each comparison (**Figure 6**). Interestingly, most of DMGs from all the comparison groups were enriched in the ovarian follicle development/rupture, BMP signaling pathway and ovulation GO terms, as well as the Wnt and TGF-β signaling pathways among all comparison groups (**Supplementary Figure S2**). Specifically, INHBA, TGFBR2 and SMAD7 genes of the TGF-β pathway and SFRP1, FZD1 and MAP3K7 genes of the Wnt

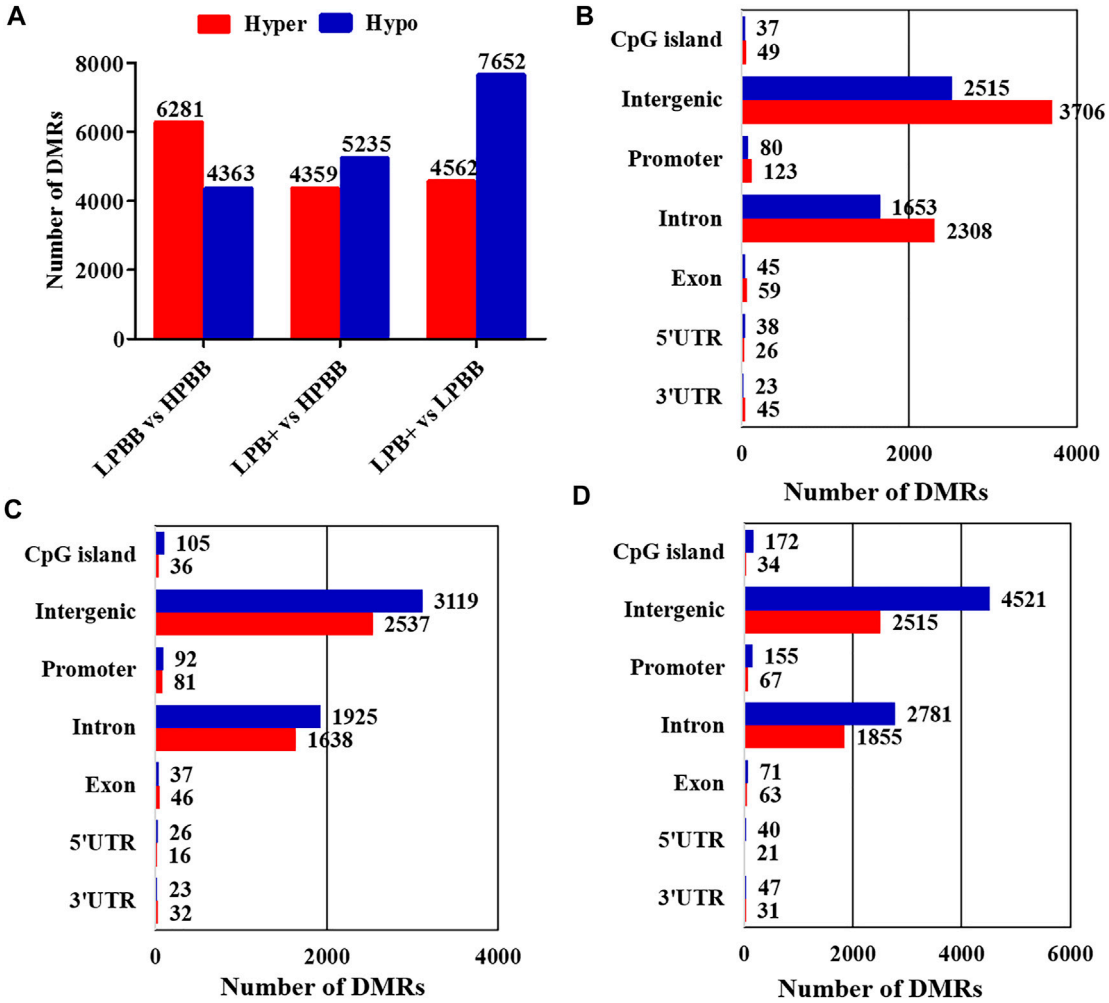



**FIGURE 2 |** Identification of DMRs in different groups. **(A)** The number of DMRs (hyper- and hypo-methylated) in different comparison groups. **(B,C)** The distribution of DMRs in different genomic elements in the **(B)** LPBB vs. HPBB, **(C)** LPB + vs. HPBB, and **(D)** LPB + vs. LPBB groups.

pathway were differentially methylated among all comparison groups.

Similarly, the female reproduction associated DEGs from the LPBB vs. HPBB group were enriched in the hormone biosynthetic process and embryo implantation in GO terms (**Supplementary Figure S3A**), ae well as the ovarian steroidogenesis, PI3K-Akt and Rap1 signaling pathways (**Supplementary Figure S3B**). Meanwhile, female reproduction associated DEGs from both the LPB + vs. HPBB and LPB + vs. LPBB groups were enriched in the female gonad and ovarian follicle development GO terms (**Supplementary Figures S3C,E**), as well as the ovarian steroidogenesis, PI3K-Akt, TGF-β and Wnt signaling pathways (**Supplementary Figures S3D,F**).

## Correlation Analysis Between DNA Methylation and Gene Expression

As shown in **Figures 7A–C**, a significant negative correlation was observed between DNA methylation level around the TSS and gene expression. In the LPBB vs. HPBB, LPB + vs. HPBB and LPB + vs. LPBB groups, we found that 13, 195 and 530 of the DMGs, respectively, associated with DEGs (**Figures 7D–F** and **Supplementary Tables S15–S17**). Moreover, the heatmap was constructed to visualize the relationship between DMGs and DEGs in the different comparison groups (**Figures 7G–I**). Many DMGs contained more than one DMR. For example, five DMRs in NDST4 were hyper-methylated and one DMR in NDST4 was hypo-methylated in the HPBB group compared to that in the LPBB group. In the LPBB vs. HPBB group, we identified 10 hyper-methylated genes with down-regulated expression levels in the HPBB group, including genes related to the Hippo (ITGB2), PI3K-Akt (SYK) and Rap1 (ITGB2) signaling pathways, while three genes were hypo-methylated and up-regulated in the HPBB group compared to that in the LPBB group (**Figure 7G** and **Supplementary Table S15**). In the LPB + vs. HPBB group, 77 genes were hyper-methylated and down-regulated in the HPBB group, and these genes were related to the regulation of the TGF-β (ID2), estrogen (LOC101114987)

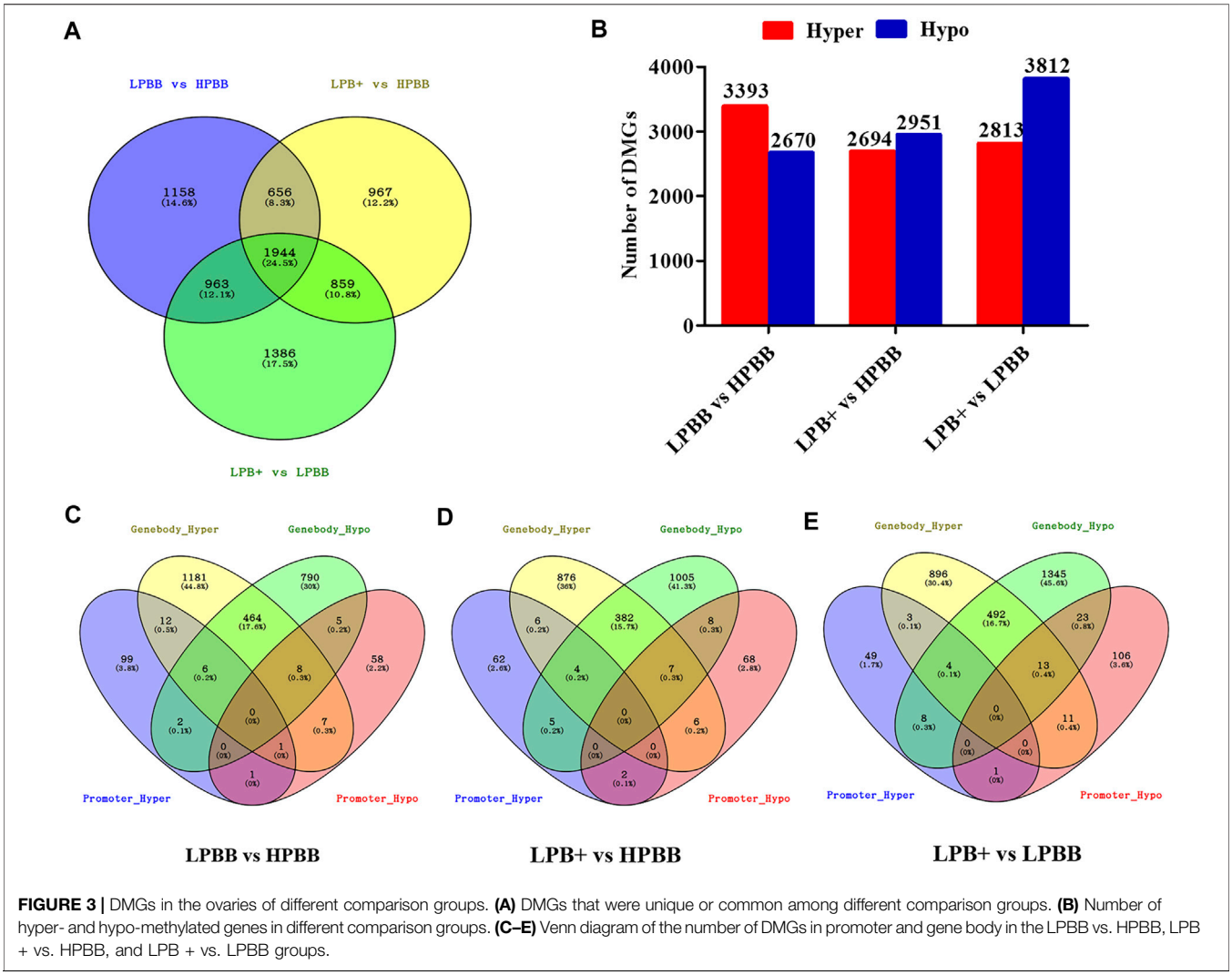



**FIGURE 3 |** DMGs in the ovaries of different comparison groups. **(A)** DMGs that were unique or common among different comparison groups. **(B)** Number of hyper- and hypo-methylated genes in different comparison groups. **(C–E)** Venn diagram of the number of DMGs in promoter and gene body in the LPBB vs. HPBB, LPB + vs. HPBB, and LPB + vs. LPBB groups.

and oocyte meiosis (LOC101112318 and PTTG1) signaling pathways. In contrast, 49 genes were hyper-methylated and down-regulated in the LPB + group, and these genes were related to the TGF-β (TGFBR2), PI3K-Akt (COL4A1, LOC101115805 and COL24A1), FoxO (TGFBR2 and FOXO3) and insulin (CBLB, PDE3A and RIMS2) signaling pathways (**Figure 7H** and **Supplementary Table S16**). In the LPB + vs. LPBB group, 153 genes were hyper-methylated and down-regulated in the LPBB group, and these genes were related to the PI3K-Akt (PRKAA2, FGF10, FGF12 and LOC101103187), TGF-β (ID2) and ovarian steroidogenesis (FSHR) pathways. We found that 201 genes were hypo-methylated and up-regulated in the LPBB group compared to that in the LPB + group, and these genes were related to the PI3K-Akt (COL24A1, TLR4, SYK, ITGAV, ITGA7, VWF, RELN, FLT4, KIT, SGK1, THBS2, COL4A1 and LOC101115805), TGF-β (CDKN2B and TGFBR2) and ovarian steroidogenesis (STAR and PRKX) pathways (**Figure 7I** and **Supplementary Table S17**). In addition, some genes exhibited coinciding methylation and expression patterns in three comparison groups (**Figures 7G–I** and **Supplementary Tables S15–S17**). Interestingly, we found that ITGB2 and LAPTM4B genes, which were hyper-methylated (DMRs in their promoter) and down-regulated in LPBB vs. HPBB group and both LPB + vs. HPBB and LPB + vs. LPBB group, respectively, to confirm the negative correlation between DNA methylation and gene expression.

## Integrative Analysis of ITGB2 and LAPTM4B Methylation and Expression

ITGB2 mRNA expression level in the LPBB group was significantly higher than that in the LPB+ and HPBB groups; with the expression being higher in the HPBB group than in the LPB + group (**Figure 8A**). LAPTM4B mRNA expression level in the LPB + group was significantly higher than that in the LPBB and HPBB groups (**Figure 8B**). These results were consistent with the RNA-seq data. Meanwhile, LAPTM4B protein was predominantly localized in the GCs of the antral follicle (**Figure 8C**).

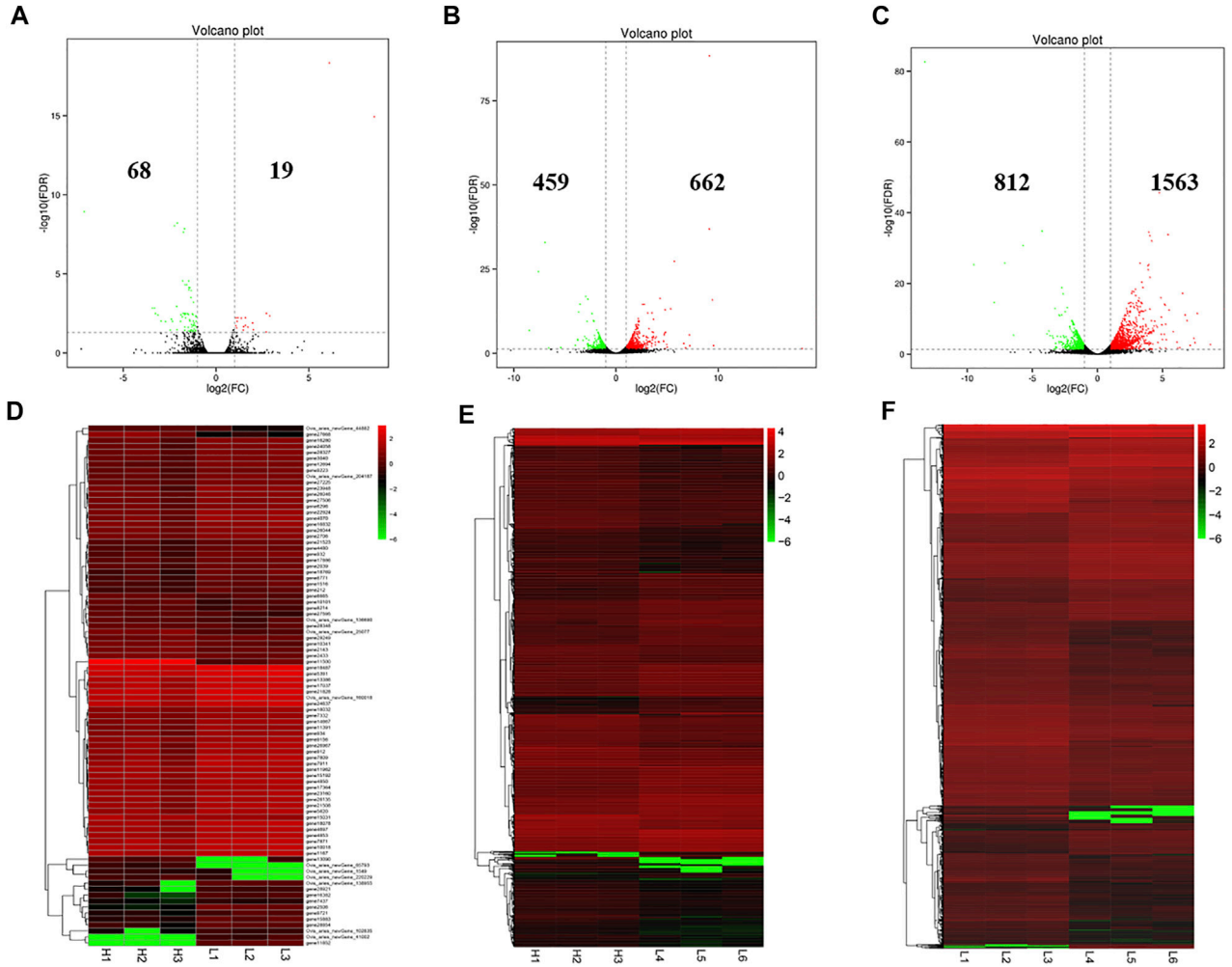



**FIGURE 4 |** Identification of DE mRNAs. **(A–C)** Volcano plot of DE mRNAs in each group. Red indicates up-regulation and green indicates down-regulation. **(D–F)** Hierarchical clustering of DE mRNAs in each group. **(A,D)**: LPBB vs. HPBB; (B and E): LPB + vs. HPBB; and **(C,F)**: LPB + vs. LPBB groups. HPBB (H1, H2, H3); LPBB (L1, L2, L3); LPB+ (L4, L5, L6).

Next, we evaluated the effect of 5-Aza on ITGB2 and LAPTM4B expression in cultured GCs, and the results showed that ITGB2 and LAPTM4B mRNA expression were significantly higher in the 5-Aza treatment group (**Figure 8D**). Moreover, following the treatment of GCs with 5-Aza, the methylation level of the LAPTM4B and ITGB2 promoter decreased compared to that of the control cells (**Figures 8E,F**). Additionally, the mRNA expression of ITGB2 was significantly decreased using siRNA-specific ITGB2 (**Figure 8G**), subsequently, we demonstrated that the treatment of 5-Aza inhibited ITGB2-specific siRNA-reduced ITGB2 expression in GCs (**Figure 8H**).

## DISCUSSION

Fecundity is an economically important trait in the sheep industry. Therefore, investigating the molecular mechanisms of sheep fecundity may assist in accelerating the breeding process. Herein, we systematically investigated the genome-wide DNA methylation and gene expression profiles in the ovaries of Hu sheep with different prolificacies and genotypes by WGBS and RNA-seq, respectively. Although it has been demonstrated that the homozygous mutation (BB) had the higher fecundity than the heterozygous mutation (B+) or wild-type (++), significant differences in prolificacy phenotypes were found in the same genotype (BB) of Hu sheep with under the same feeding conditions. Therefore, we conducted an integrated analysis of DNA methylation and gene expression patterns was performed to reveal the manner in which DNA methylation may regulate prolificacy by affecting gene expression.

WGBS revealed that approximately 3.58% of cytosine sites were methylated in the ovaries of Hu sheep, with the highest proportion of CG methylation context. This finding is corroborated by previous reports in other animals (Yuan et al., 2016; Hwang et al., 2017; Fan et al., 2020). Moreover, the DNA methylation of the CG context from the ovaries of Hu sheep exhibited significant hyper-methylation levels (90–100%), but CHH and CHG exhibited

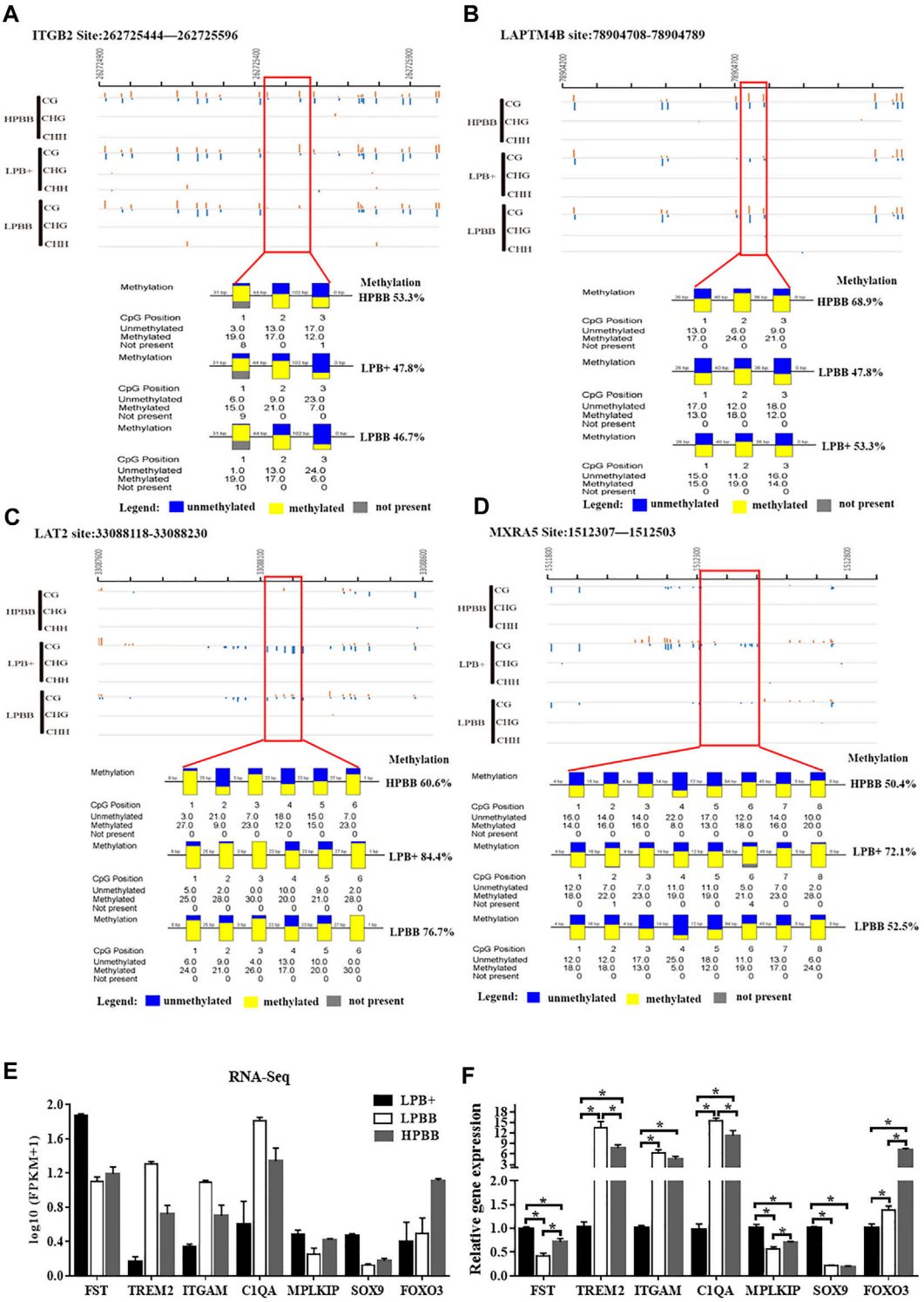



**FIGURE 5 |** Validation of WGBS and RNA-seq data by BSP and qRT-PCR, respectively. **(A,B)** A DMR across the different groups in the promoter of the ITGB2 and LAPTM4B from 262725444 to 262725596 and from 78904708 to 78904789, respectively. **(C)** A DMR across the three groups in the intron of LAT2 from 33088118 to 33088230. **(D)** A DMR across the three groups in the distal intergenic region of MXRA5 from 1512307 to 1512503. Each box corresponds to one CpG position in the genomic sequence. Blue indicates unmethylated and yellow indicates methylated. **(E)** Seven mRNAs were randomly selected from the RNA-seq data. RNA-seq data are presented as $\log_{10}$ (FPKM+1). FPKM: Fragments Per Kilobase of transcript per Million fragments mapped. **(F)** Validation of the DEGs using qRT-PCR.

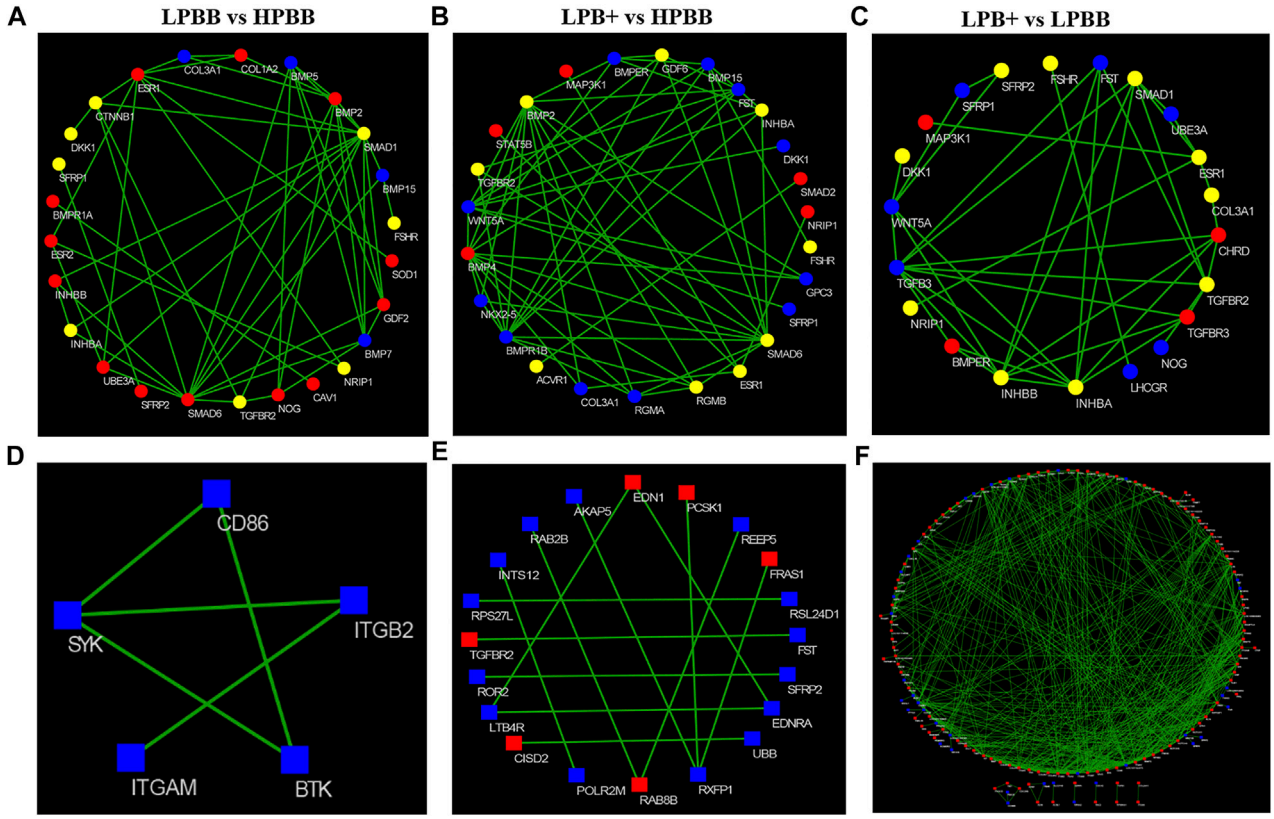



**FIGURE 6 |** Construction of the network of DMGs and DEGs related to female reproduction. **(A–C)** Red and blue colors represent strong-hyper and strong-hypo, respectively. Yellow color represents the coexisting strong-hyper and strong-hypo. **(D–F)** Red and blue colors represent up- and down-regulated, respectively. **(A,D)** LPBB vs. HPBB; (B and E) LPB + vs. HPBB; and **(C,F)** LPB + vs. LPBB groups.

hypo-methylation levels (10–30%), which is consistent with the results of a previous study in the ovaries of pigs (Yuan et al., 2016). These results suggest that the CG methylation was high-efficiently maintained in the ovaries of Hu sheep.

The majority of DMRs in the ovaries of Hu sheep exhibit a similar distribution to that observed in the ovaries or muscle of pigs and Hu sheep (Hwang et al., 2017; Yang et al., 2017; Fan et al., 2020), with the mainly located at the intergenic and intron elements. Accordingly, we identified numerous DMGs among the three comparison groups. As described above, focusing on the CG methylation context of DMGs, and we found that the common DMGs were significantly enriched in the TGF-β and Wnt signaling pathways, which have been confirmed to be involved in fecundity (Chu et al., 2007; Gao et al., 2020). For example, INHBA is associated with follicle development (Cui et al., 2020; Li et al., 2021), oocyte maturation (Tesfaye et al., 2009) and fecundity (Hiendleder et al., 1996; Yu et al., 2019). In the present study, INHBA was found to contain five distal intergenic DMRs, with four DMRs being hyper-methylated and one being hypo-methylated in the LPB + vs. HPBB group. Moreover, six DMRs (five distal intergenic and one intron) were identified in INHBA, of which five were hypo-methylated and one was hyper-methylated in the LPB + vs. LPBB group. FZD1 has been confirmed to regulate certain biological processes, including oocyte maturation, female fertility (Lapointe et al., 2012), embryonic development (Tribulo et al., 2017) and ovary development (Tepekoy et al., 2019). The methylation level of the 3′-UTR of FZD1 in the HPBB group was higher than that in the LPB + group. In addition, most DMGs were enriched in the ovulation and ovarian follicle development biological processes. These results supported the hypothesis that DNA methylation as a regulator of epigenetic modification could influence the prolificacy phenotype (Hwang et al., 2017; Miao et al., 2017; Zhang et al., 2017).

To understand how DNA methylation influences the prolificacy of Hu sheep, here, for the first time, we systematically analyzed and compared the genome-wide DNA methylation and transcriptome of ovaries from Hu sheep with different prolificacies and genotypes. The number of DMGs-DEGs in the LPBB vs. HPBB group was lower than that in both the LPB + vs. HPBB and LPB + vs. LPBB groups. This finding suggests that, although changes in DNA methylation may influence fecundity, the differences are mainly attributed to the genotype. The most significant results of this study showed that an inverse relationship was observed between DNA methylation and gene expression in the HPBB, LPBB, and LPB + groups, which is in agreement with the results of previous studies (Jadhao et al., 2017; Wang et al., 2017; Yang et al., 2017).

DNA methylation status in the promoter and gene body regions regulates gene expression by changing transcription efficiency or chromatin structure (Jones 2012; Yang et al.,

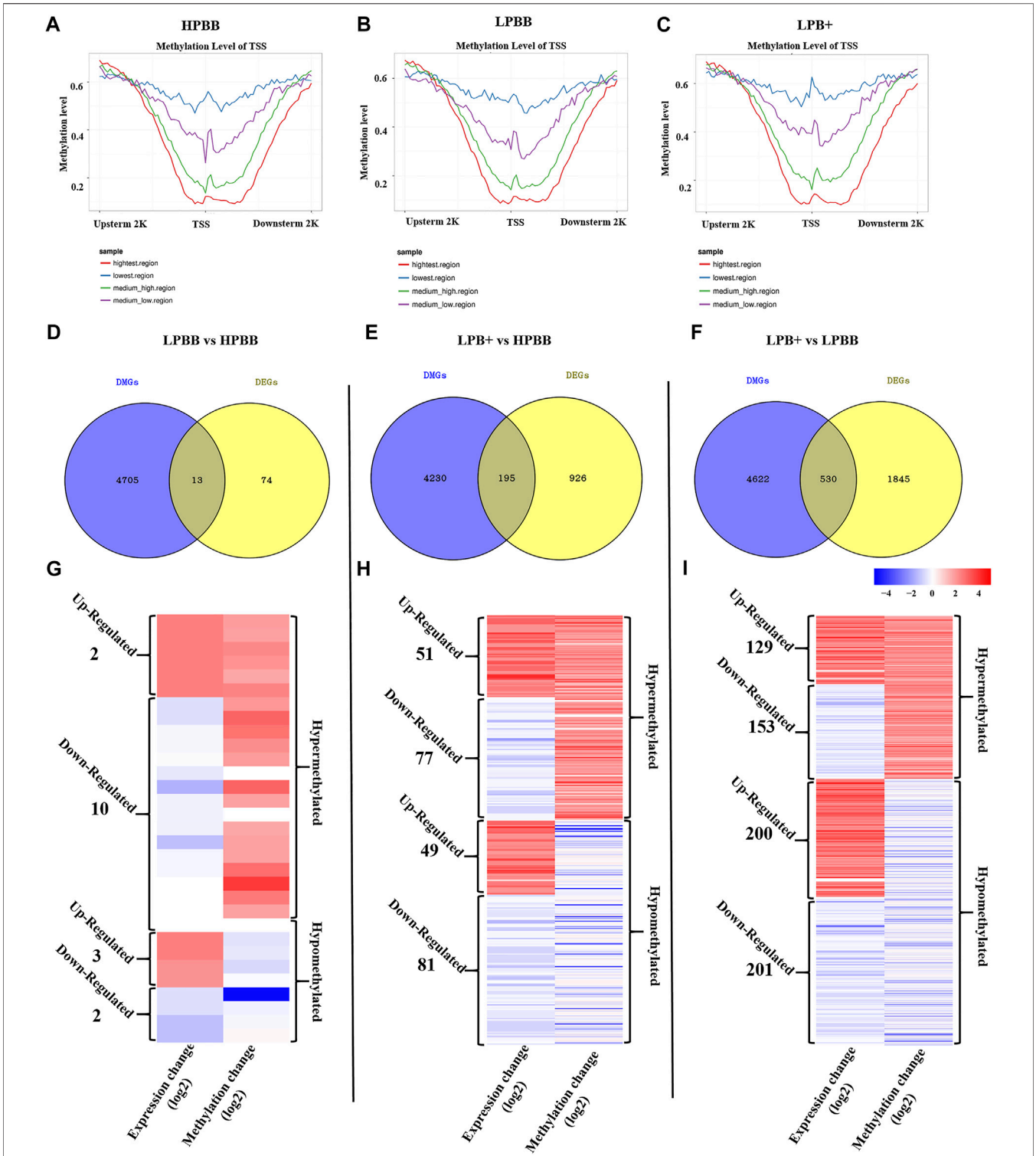



**FIGURE 7 |** Integrative analysis of the DNA methylome and transcriptome in the ovaries of different groups. **(A–C)** DNA methylation level distribution around TSS of four levels of gene expression in the different groups. **(D–F)** Venn diagram shows the common DMGs and DEGs. **(G–I)** Heatmap showing the differentially methylated levels and corresponding genes change in the different comparison groups.

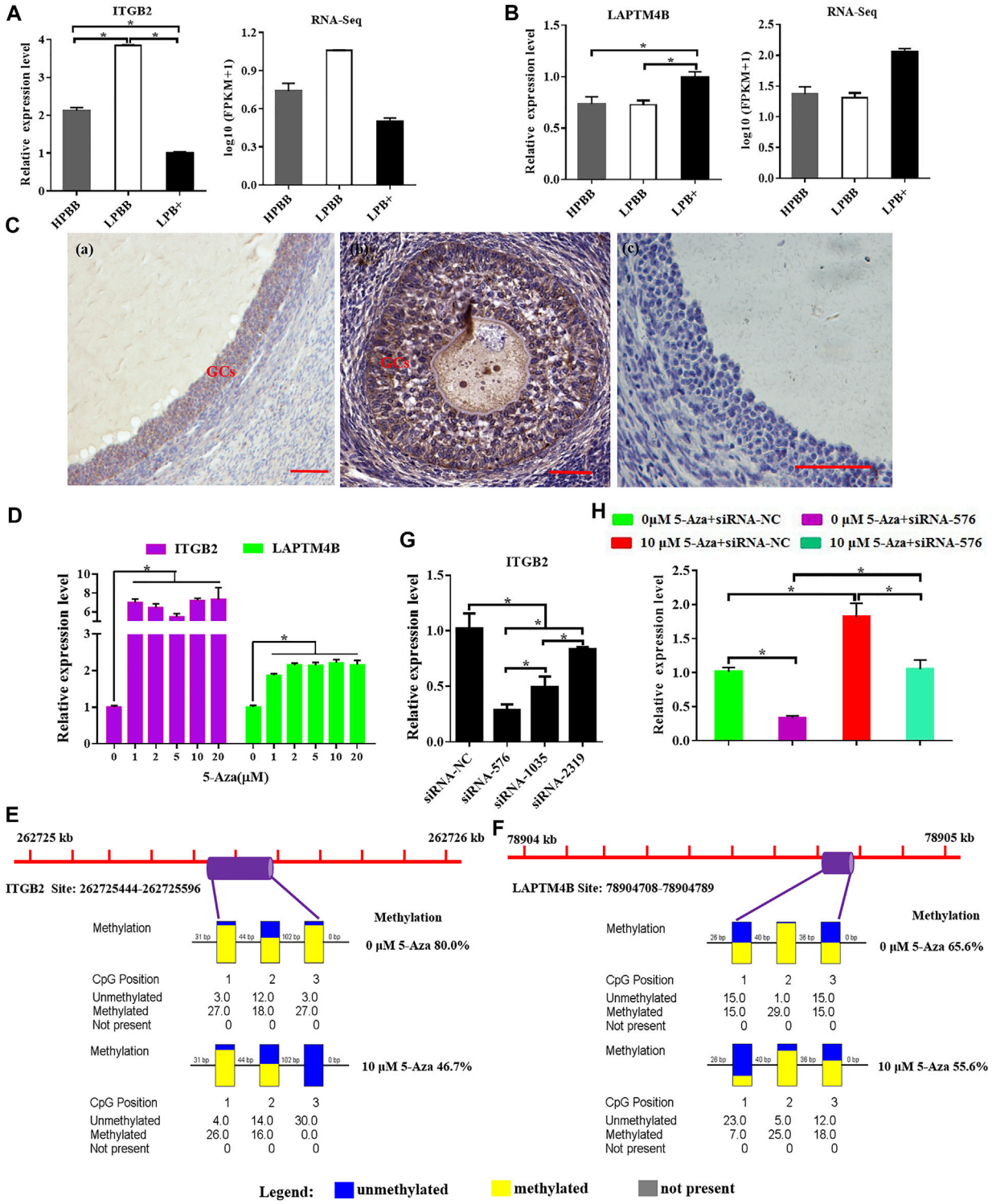



**FIGURE 8 |** Integrative analysis of methylation and expression levels of ITGB2 and LAPTM4B. **(A,B)** ITGB2 and LAPTM4B mRNA expression in the ovaries were detected by qRT-PCR. **(C)** Localization of LAPTM4B in the ovaries using immunohistochemistry. Scale bars = 50 μm. **(D)** ITGB2 and LAPTM4B mRNA expression levels in cultured GCs were detected after treatment with various concentrations (0, 1, 2, 5, 10, and 20 μM) of 5-Aza treatment. **(E,F)** Methylation levels of ITGB2 and LAPTM4B in cultured GCs after 10 μM 5-Aza treatment. **(G)** Suppression efficiency of ITGB2 was evaluated by qRT-PCR. **(H)** mRNA level of ITGB2 in cultured GCs stimulated by 5-Aza with or without siRNA-ITGB2.

2014). Therefore, we further selected the genes (ITGB2 and LAPTM4B) that exhibited inverse changes in DNA methylation and gene expression, and those with DMRs in the promoter or gene body for subsequent analyses. For example, the promoter region of ITGB2, an important regulator of embryo implantation (Guo et al., 2018), oocyte maturation (Antosik et al., 2016) and follicle development (Kisliouk et al., 2007; Antosik et al., 2016), was hyper-methylated in the HPBB group compared to that in the LPBB group; however, its expression was higher in the LPBB group than in the HPBB group. Meanwhile, ITGB2 expression level in atretic follicles was higher than in healthy follicles (Kisliouk et al., 2007). Up-regulated expression of ITGB2 in the LPBB group may be responsible for the increased number of atretic follicles. Previous studies have reported that LAPTM4B is expressed in the reproductive organs and reproductive diseases in bovine or human (Yang et al., 2008; Ndiaye et al., 2015; Meng et al., 2016). Ndiaye et al. (2015) reported that LAPTM4B expression was higher in large dominant follicles than in small antral follicles. The results of the present study showed that the LAPTM4B promoter was hyper-methylated and LAPTM4B expression was down-regulated in the HPBB group compared to that in the LPB + group. Moreover, the relationship between ITGB2 and LPATM4B expression and epigenetic modifications in the ovaries and cultured GCs were assessed, and the results showed an inverse relationships occurred for both. These findings may, to some extent, explain the significant differences in phenotypic variation among Hu sheep.

In summary, the present study systematically integrated DNA methylation and gene expression profiles in the ovaries of Hu sheep with different phenotypes and genotypes, indicating the potential mechanisms underlying on prolificacy phenotypic variation and providing new insights into the genetic mechanism responsible for the excellent fecundity of Hu sheep. As several factors, including physiological, environmental and diet, have been shown to affect phenotypic variation (Peaston and Whitelaw, 2006). Therefore, further studies are needed to fully understand the effects of epigenetic modification on the fecundity of Hu sheep, which may contribute to better reproductive efficiency.

## DATA AVAILABILITY STATEMENT

The raw data of transcriptome and DNA methylome have been deposited into the Sequence Read Archive database (https://www.ncbi.nlm.nih.gov/sra) under accession numbers are PRJNA681364 and PRJNA758179, respectively.

## ETHICS STATEMENT

The animal study was reviewed and approved by Institutional Animal Ethics Committee of the Nanjing Agricultural University (SYXK2011-0036).

## AUTHOR CONTRIBUTIONS

Bioinformatics analysis and methodology were performed by JY, XY, and FL. Investigation and resources were done by FW and ZW. Under the supervision of FW. Experiments validation were performed by XY and FY. Animal feeding and sample collection were done by FL, ZW, and XF. The original draft of the manuscript was written by XY. The manuscript was reviewed and edited by FW and ME-S.

## FUNDING

This work was supported by the National Natural Science Foundation of China (32002174; 31872357), Fundamental Research Funds for the Central Universities (KJQN202130), Jiangsu Agricultural Industry Technology System (JATS(2021) 141) and Jiangsu Planned Projects for Postdoctoral Research Funds (2021K254B).

## ACKNOWLEDGMENTS

We sincerely thank Jinyu Yang from the Biomarker Technologies Corporation for help in bioinformatic analysis.

## SUPPLEMENTARY MATERIAL

The Supplementary Material for this article can be found online at: https://www.frontiersin.org/articles/10.3389/fcell.2022.820558/full#supplementary-material

**Supplementary Figure S1 |** KEGG pathway enrichment analysis of DMGs. **(A)** LPBB vs. HPBB, **(B)** LPB+ vs. HPBB, and **(C)** LPB+ vs. LPBB groups.

**Supplementary Figure S2 |** GO and KEGG enrichment analysis of DMGs related to female reproduction. **(A)** LPBB vs. HPBB, **(B)** LPB+ vs. HPBB, and **(C)** LPB+ vs. LPBB groups.

**Supplementary Figure S3 |** GO and KEGG pathway enrichment analysis of DEGs related to female reproduction. **(A,B)** LPBB vs. HPBB, **(C,D)** LPB+ vs. HPBB, and **(E,F)** LPB+ vs. LPBB groups.

## REFERENCES

An, X., Ma, H., Han, P., Zhu, C., Cao, B., and Bai, Y. (2018). Genome-wide Differences in DNA Methylation Changes in Caprine Ovaries between Oestrous and Dioestrous Phases. *J. Anim. Sci Biotechnol* 9, 85. doi:10.1186/s40104-018-0301-x

Antosik, P., Jeseta, M., Kranc, W., Chachuła, A., Bryja, A., Budna, J., et al. (2016). Expression of Integrins and GDF9 mRNAs Is Associated with Ovarian Follicle Size and Donor Puberty Status in Pigs. *Med. Weter* 72, 750–754. doi:10.21521/mw.5601

Canovas, S., Ross, P. J., Kelsey, G., and Coy, P. (2017). DNA Methylation in Embryo Development: Epigenetic Impact of ART (Assisted Reproductive Technologies). *Bioessays* 39, 1700106. doi:10.1002/bies.201700106

Cao, P., Yang, W., Wang, P., Li, X., and Nashun, B. (2021). Characterization of DNA Methylation and Screening of Epigenetic Markers in Polycystic Ovary Syndrome. *Front. Cel Dev. Biol.* 9, 664843. doi:10.3389/fcell.2021.664843

Chu, M. X., Liu, Z. H., Jiao, C. L., He, Y. Q., Fang, L., Ye, S. C., et al. (2007). Mutations in BMPR-IB and BMP-15 Genes Are Associated with Litter Size in Small Tailed Han Sheep (Ovis aries)1. *J. Anim. Sci.* 85, 598–603. doi:10.2527/jas.2006-324

Cui, Z., Liu, L., Zhu, Q., Wang, Y., Yin, H., Li, D., et al. (2020). Inhibin A Regulates Follicular Development via Hormone Secretion and Granulosa Cell Behaviors in Laying Hens. *Cell Tissue Res* 381, 337–350. doi:10.1007/s00441-020-03207-8

Fabre, S., Pierre, A., Mulsant, P., Bodin, L., Di Pasquale, E., Persani, L., et al. (2006). Regulation of Ovulation Rate in Mammals: Contribution of Sheep Genetic Models. *Reprod. Biol. Endocrinol.* 4, 20. doi:10.1186/1477-7827-4-20

Fan, Y., Liang, Y., Deng, K., Zhang, Z., Zhang, G., Zhang, Y., et al. (2020). Analysis of DNA Methylation Profiles during Sheep Skeletal Muscle Development Using Whole-Genome Bisulfite Sequencing. *BMC genomics* 21, 327. doi:10.1186/s12864-020-6751-5

Fang, X., Zhao, Z., Yu, H., Li, G., Jiang, P., Yang, Y., et al. (2017). Comparative Genome-wide Methylation Analysis of Longissimus Dorsi Muscles between Japanese Black (Wagyu) and Chinese Red Steppes Cattle. *PloS one* 12, e0182492. doi:10.1371/journal.pone.0182492

Farhadi, A., Genualdo, V., Perucatti, A., Hafezian, S. H., Rahimi-Mianji, G., Lorenzi, L. D., et al. (2013). Comparative FISH Mapping of BMPR1B, BMP15 and GDF9 Fecundity Genes on Cattle, River buffalo, Sheep and Goat Chromosomes. *J. Genet.* 92, 595–597. doi:10.1007/s12041-013-0301-8

Feng, X., Li, F., Wang, F., Zhang, G., Pang, J., Ren, C., et al. (2018). Genome-wide Differential Expression Profiling of mRNAs and lncRNAs Associated with Prolificacy in Hu Sheep. *Biosci. Rep.* 38, BSR20171350. doi:10.1042/BSR20171350

Gao, X., Yao, X., Wang, Z., Li, X., Li, X., An, S., et al. (2020). Long Non-coding RNA366.2 Controls Endometrial Epithelial Cell Proliferation and Migration by Upregulating WNT6 as a ceRNA of miR-1576 in Sheep Uterus. *Biochim. Biophys. Acta (Bba) - Gene Regul. Mech.* 1863, 194606. doi:10.1016/j.bbagrm.2020.194606

González-Recio, O., Toro, M. A., and Bach, A. (2015). Past, Present, and Future of Epigenetics Applied to Livestock Breeding. *Front. Genet.* 6, 305. doi:10.3389/fgene.2015.00305

Gootwine, E., Reicher, S., and Rozov, A. (2008). Prolificacy and Lamb Survival at Birth in Awassi and Assaf Sheep Carrying the FecB (Booroola) Mutation. *Anim. Reprod. Sci.* 108, 402–411. doi:10.1016/10.1016/j.anireprosci.2007.09.009

Guo, F., Si, C., Zhou, M., Wang, J., Zhang, D., Leung, P. C. K., et al. (2018). Decreased PECAM1-Mediated TGF-β1 Expression in the Mid-secretory Endometrium in Women with Recurrent Implantation Failure. *Hum. Reprod.* 33, 832–843. doi:10.1093/humrep/dey022

Hiendleder, S., Leyhe, B., Jaeger, C., Erhardt, G., and Wassmuth, R. (1996). Molecular Characterization of Ovine α-, βA and βB-inhibin/activin Alleles. *J. Anim. Breed. Genet.* 113, 363–372. doi:10.1111/j.1439-0388.1996.tb00627.x

Hwang, J. H., An, S. M., Kwon, S., Park, D. H., Kim, T. W., Kang, D. G., et al. (2017). DNA Methylation Patterns and Gene Expression Associated with Litter Size in Berkshire Pig Placenta. *PloS one* 12, e0184539. doi:10.1371/journal.pone.0184539

Jones, P. A. (2012). Functions of DNA Methylation: Islands, Start Sites, Gene Bodies and beyond. *Nat. Rev. Genet.* 13, 484–492. doi:10.1038/nrg3230

Kang, B., Wang, J., Zhang, H., Shen, W., El-Mahdy Othman, O., Zhao, Y., et al. (2021). Genome-wide Profile in DNA Methylation in Goat Ovaries of Two Different Litter Size Populations. *J. Anim. Physiol. Anim. Nutr.*, 1–11. doi:10.1111/jpn.13600

Khavari, D. A., Sen, G. L., and Rinn, J. L. (2010). DNA Methylation and Epigenetic Control of Cellular Differentiation. *Cell cycle* 9, 3880–3883. doi:10.4161/cc.9.19.13385

Kisliouk, T., Friedman, A., Klipper, E., Zhou, Q.-Y., Schams, D., Alfaidy, N., et al. (2007). Expression Pattern of Prokineticin 1 and its Receptors in Bovine Ovaries during the Estrous Cycle: Involvement in Corpus Luteum Regression and Follicular Atresia. *Biol. Reprod.* 76, 749–758. doi:10.1095/biolreprod.106.054734

Lapointe, E., Boyer, A., Rico, C., Paquet, M., Franco, H. L., Gossen, J., et al. (2012). FZD1 Regulates Cumulus Expansion Genes and Is Required for Normal Female Fertility in Mice1. *Biol. Reprod.* 87, 104. doi:10.1095/biolreprod.112.102608

Li, Z., Wang, J., Zhao, Y., Ma, D., Zhao, M., Li, N., et al. (2021). scRNA-Seq of Ovarian Follicle Granulosa Cells from Different Fertility Goats Reveals Distinct Expression Patterns. *Reprod. Dom Anim.* 56, 801–811. doi:10.1111/rda.13920

Lomniczi, A., Wright, H., and Ojeda, S. R. (2015). Epigenetic Regulation of Female Puberty. *Front. Neuroendocrinology* 36, 90–107. doi:10.1016/j.yfrne.2014.08.003

Mao, X., Cai, T., Olyarchuk, J. G., and Wei, L. (2005). Automated Genome Annotation and Pathway Identification Using the KEGG Orthology (KO) as a Controlled Vocabulary. *Bioinformatics* 21, 3787–3793. doi:10.2307/159221510.1093/bioinformatics/bti430

Mattern, F., Heinzmann, J., Herrmann, D., Lucas-Hahn, A., Haaf, T., and Niemann, H. (2017). Gene-specific Profiling of DNA Methylation and mRNA Expression in Bovine Oocytes Derived from Follicles of Different Size Categories. *Reprod. Fertil. Dev.* 29, 2040–2051. doi:10.1071/RD16327

Meng, F., Chen, X., Song, H., Lou, G., and Fu, S. (2016). Lentivirus-mediated RNA Interference Targeting LAPTM4B Inhibits Human Ovarian Cancer Cell InvasionIn Vitro. *Chem. Biol. Drug Des.* 87, 121–130. doi:10.1111/cbdd.12632

Miao, X., Luo, Q., Zhao, H., and Qin, X. (2017). An Integrated Analysis of miRNAs and Methylated Genes Encoding mRNAs and lncRNAs in Sheep Breeds with Different Fecundity. *Front. Physiol.* 8, 1049. doi:10.3389/fphys.2017.01049

Miyakuni, K., Nishida, J., Koinuma, D., Nagae, G., Aburatani, H., Miyazono, K., et al. (2021). Genome-wide Analysis of DNA Methylation Identifies the Apoptosis-Related Gene UQCRH in Renal Cancer. *Mol. Oncol.* 16. doi:10.21203/rs.3.rs-147857/v1

Ndiaye, K., Carrière, P. D., Sirois, J., Silversides, D. W., and Lussier, J. G. (2015). Differential Expression of Lysosome-Associated Protein Transmembrane-4 Beta (LAPTM4B) in Granulosa Cells of Ovarian Follicles and in Other Bovine Tissues. *J. Ovarian Res.* 8, 12. doi:10.1186/s13048-015-0148-0

Peaston, A. E., and Whitelaw, E. (2006). Epigenetics and Phenotypic Variation in Mammals. *Mamm. Genome* 17, 365–374. doi:10.1007/s00335-005-0180-2

Polley, S., De, S., Brahma, B., Mukherjee, A., P.V., V., Batabyal, S., et al. (2010). Polymorphism of BMPR1B, BMP15 and GDF9 Fecundity Genes in Prolific Garole Sheep. *Trop. Anim. Health Prod.* 42, 985–993. doi:10.1007/s11250-009-9518-1

Sagvekar, P., Kumar, P., Mangoli, V., Desai, S., and Mukherjee, S. (2019). DNA Methylome Profiling of Granulosa Cells Reveals Altered Methylation in Genes Regulating Vital Ovarian Functions in Polycystic Ovary Syndrome. *Clin. Epigenet* 11, 61. doi:10.1186/s13148-019-0657-6

Salilew-Wondim, D., Fournier, E., Hoelker, M., Saeed-Zidane, M., Tholen, E., Looft, C., et al. (2015). Genome-Wide DNA Methylation Patterns of Bovine Blastocysts Developed *In Vivo* from Embryos Completed Different Stages of Development *In Vitro*. *PloS one* 10, e0140467. doi:10.1371/journal.pone.0140467

Singh, K., Molenaar, A. J., Swanson, K. M., Gudex, B., Arias, J. A., Erdman, R. A., et al. (2012). Epigenetics: a Possible Role in Acute and Transgenerational Regulation of Dairy Cow Milk Production. *Animal* 6, 375–381. doi:10.1017/S1751731111002564

Tepekoy, F., Uysal, F., Acar, N., Ustunel, I., and Akkoyunlu, G. (2019). The Effect of GnRH Antagonist Cetrorelix on Wnt Signaling Members in Pubertal and Adult Mouse Ovaries. *Histochem. Cel Biol* 152, 423–437. doi:10.1007/s00418-019-01817-0

Tesfaye, D., Ghanem, N., Carter, F., Fair, T., Sirard, M.-A., Hoelker, M., et al. (2009). Gene Expression Profile of Cumulus Cells Derived from Cumulus - Oocyte Complexes Matured Either *In Vivo* or *In Vitro*. *Reprod. Fertil. Dev.* 21, 451–461. doi:10.1071/rd08190

Tirnaz, S., and Batley, J. (2019). DNA Methylation: Toward Crop Disease Resistance Improvement. *Trends Plant Sci.* 24, 1137–1150. doi:10.1016/j.tplants.2019.08.007

Tribulo, P., Moss, J. I., Ozawa, M., Jiang, Z., Tian, X., and Hansen, P. J. (2017). WNT Regulation of Embryonic Development Likely Involves Pathways Independent of Nuclear CTNNB1. *Reproduction* 153, 405–419. doi:10.1530/REP-16-0610

Vázquez-Martínez, E. R., Gómez-Viais, Y. I., García-Gómez, E., Reyes-Mayoral, C., Reyes-Muñoz, E., Camacho-Arroyo, I., et al. (2019). DNA Methylation in the Pathogenesis of Polycystic Ovary Syndrome. *Reproduction* 158, R27–R40. doi:10.1530/REP-18-0449

Wang, H., Wang, J., Ning, C., Zheng, X., Fu, J., Wang, A., et al. (2017). Genome-wide DNA Methylation and Transcriptome Analyses Reveal Genes Involved in Immune Responses of Pig Peripheral Blood Mononuclear Cells to Poly I:C. *Sci. Rep.* 7, 9709. doi:10.1038/s41598-017-10648-9

Wang, W., Liu, S., Li, F., Pan, X., Li, C., Zhang, X., et al. (2015). Polymorphisms of the Ovine BMPR-IB, BMP-15 and FSHR and Their Associations with Litter Size in Two Chinese Indigenous Sheep Breeds. *Ijms* 16, 11385–11397. doi:10.3390/ijms160511385

Wang, X. X., Wei, J. Z., Jiao, J., Jiang, S. Y., Yu, D. H., and Li, D. (2014). Genome-wide DNA Methylation and Gene Expression Patterns Provide Insight into Polycystic Ovary Syndrome Development. *Oncotarget* 5, 6603–6610. doi:10.18632/oncotarget.2224

Wei, Y., Lang, J., Zhang, Q., Yang, C. R., Zhao, Z. A., Zhang, Y., et al. (2019). DNA Methylation Analysis and Editing in Single Mammalian Oocytes. *Proc. Natl. Acad. Sci. USA* 116, 9883–9892. doi:10.1073/pnas.1817703116

Yang, C., Ye, J., Li, X., Gao, X., Zhang, K., Luo, L., et al. (2016). DNA Methylation Patterns in the Hypothalamus of Female Pubertal Goats. *PloS one* 11, e0165327. doi:10.1371/journal.pone.0165327

Yang, X., Han, H., De Carvalho, D. D., Lay, F. D., Jones, P. A., and Liang, G. (2014). Gene Body Methylation Can Alter Gene Expression and Is a Therapeutic Target in Cancer. *Cancer cell* 26, 577–590. doi:10.1016/j.ccr.2014.07.028

Yang, Y., Yang, H., McNutt, M. A., Xiong, F., Nie, X., Li, L., et al. (2008). LAPTM4B Overexpression Is an Independent Prognostic Marker in Ovarian Carcinoma. *Oncol. Rep.* 20, 1077–1083. doi:10.3892/or_00000112

Yang, Y., Fan, X., Yan, J., Chen, M., Zhu, M., Tang, Y., et al. (2021). A Comprehensive Epigenome Atlas Reveals DNA Methylation Regulating Skeletal Muscle Development. *Nucleic Acids Res.* 49, 1313–1329. doi:10.1093/nar/gkaa1203

Yang, Y., Liang, G., Niu, G., Zhang, Y., Zhou, R., Wang, Y., et al. (2017). Comparative Analysis of DNA Methylome and Transcriptome of Skeletal Muscle in Lean-, Obese-, and Mini-type Pigs. *Sci. Rep.* 7, 39883. doi:10.1038/srep39883

Yao, X., Gao, X., Bao, Y., El-Samahy, M. A., Yang, J., Wang, Z., et al. (2021). lncRNA FDNCR Promotes Apoptosis of Granulosa Cells by Targeting the miR-543-3p/DCN/TGF-β Signaling Pathway in Hu Sheep. *Mol. Ther. - Nucleic Acids* 24, 223–240. doi:10.1016/j.omtn.2021.02.030

Yao, X., Yang, H., Zhang, Y., Ren, C., Nie, H., Fan, Y., et al. (2017). Characterization of GALNTL5 Gene Sequence and Expression in Ovine Testes and Sperm. *Theriogenology* 95, 54–61. doi:10.1016/j.theriogenology.2017.02.018

Young, M. D., Wakefield, M. J., Smyth, G. K., and Oshlack, A. (2010). Gene Ontology Analysis for RNA-Seq: Accounting for Selection Bias. *Genome Biol.* 11, R14. doi:10.1186/gb-2010-11-2-r14

Yu, D. Y., Wu, R. Z., Zhao, Y., Nie, Z. H., Wei, L., Wang, T. Y., et al. (2019). Polymorphisms of Four Candidate Genes and Their Correlations with Growth Traits in Blue Fox (Alopex lagopus). *Gene* 717, 143987. doi:10.1016/j.gene.2019.143987

Yu, Y. Y., Sun, C. X., Liu, Y. K., Li, Y., Wang, L., and Zhang, W. (2015). Genome-wide Screen of Ovary-specific DNA Methylation in Polycystic Ovary Syndrome. *Fertil. Sterility* 104, 145–153. doi:10.1016/j.fertnstert.2015.04.005

Yuan, X. L., Gao, N., Xing, Y., Zhang, H. B., Zhang, A. L., Liu, J., et al. (2016). Profiling the Genome-wide DNA Methylation Pattern of Porcine Ovaries Using Reduced Representation Bisulfite Sequencing. *Sci. Rep.* 6, 22138. doi:10.1038/srep22138

Yuan, X., Ye, S., Chen, Z., Pan, X., Huang, S., Li, Z., et al. (2019). Dynamic DNA Methylation of Ovaries during Pubertal Transition in Gilts. *BMC genomics* 20, 510. doi:10.1186/s12864-019-5884-x

Yue, G. H. (1996). Reproductive Characteristics of Chinese Hu Sheep. *Anim. Reprod. Sci.* 44, 223–230. doi:10.1016/0378-4320(96)01562-X

Zhang, Y., Li, F., Feng, X., Yang, H., Zhu, A., Pang, J., et al. (2017). Genome-wide Analysis of DNA Methylation Profiles on Sheep Ovaries Associated with Prolificacy Using Whole-Genome Bisulfite Sequencing. *BMC genomics* 18, 759. doi:10.1186/s12864-017-4068-9

Zhong, X., Jin, F., Huang, C., Du, M., Gao, M., and Wei, X. (2021). DNA Methylation of AMHRII and INSR Gene Is Associated with the Pathogenesis of Polycystic Ovary Syndrome (PCOS). *Thc* 29, 11–25. doi:10.3233/THC-218002

Zhou, X., Yang, S., Yan, F., He, K., and Zhao, A. (2018). Genome-wide DNA Methylation Profiles of Porcine Ovaries in Estrus and Proestrus. *Physiol. Genomics* 50, 714–723. doi:10.1152/physiolgenomics.00052.2017

**Conflict of Interest:** The authors declare that the research was conducted in the absence of any commercial or financial relationships that could be construed as a potential conflict of interest.

**Publisher's Note:** All claims expressed in this article are solely those of the authors and do not necessarily represent those of their affiliated organizations, or those of the publisher, the editors and the reviewers. Any product that may be evaluated in this article, or claim that may be made by its manufacturer, is not guaranteed or endorsed by the publisher.

*Copyright © 2022 Yao, Li, Wei, EI-Samahy, Feng, Yang and Wang. This is an open-access article distributed under the terms of the Creative Commons Attribution License (CC BY). The use, distribution or reproduction in other forums is permitted, provided the original author(s) and the copyright owner(s) are credited and that the original publication in this journal is cited, in accordance with accepted academic practice. No use, distribution or reproduction is permitted which does not comply with these terms.*

frontiers in Genetics

ORIGINAL RESEARCH
published: 11 March 2022
doi: 10.3389/fgene.2022.791283

# Variability in Global DNA Methylation Rate Across Tissues and Over Time in Sheep

*Laurence Drouilhet[1]*, Carole Moreno[1], Florence Plisson-Petit[1], Didier Marcon[2], Stéphane Fabre[1] and Dominique Hazard[1]*

[1]GenPhySE, Université de Toulouse, INRAE, ENVT, Castanet-Tolosan, France, [2]P3R, UE 0332, INRAE, Osmoy, France

Recent studies highlighted the influence of epigenetic marks in the variability of many complex traits, both in plants and animals. These studied focused only on specific sites of the genome having differentially methylated profiles among individuals and/or tissues. In contrast, we recently used the methylation rate of the entire genome as a unique measure considered as a novel quantitative phenotype in sheep. This phenotype named global DNA methylation rate (GDMR), measured by luminometric assay, integrates the methylation level of each CpG dinucleotide within the 6 million of CCGG sites along the ovine genome. GDMR measured in blood previously showed moderate heritability of 0.20 and provided evidence for a genetic determinism. The main objective of the present study was to better characterize the GDMR phenotype in various tissues and investigate its variability in several breeds of sheep reared in the same environment. GDMR was measured on blood samples collected monthly from 59 growing male and female lambs (24 Romane, 23 Blackbelly and 12 Charollais), between birth and 4 months of age. Blood GDMR was on average around 80% and was influenced by the sampling date ($p < 0.001$), the breed ($p = 0.002$) and the sex ($p = 0.002$). In addition, GDMR was determined in 12 somatic (frontal lobe, pituitary gland, heart, lung, sub cutaneous and perirenal adipose tissue, skeletal muscle, liver, spleen, adrenal gland, medulla and cortical kidney) and 6 reproductive tissues (ovary, oviduct, uterus, testis, epididymis and seminal vesicle). GDMR was on average 70% in somatic tissues but marked variation was observed depending on the tissue. The GDMR measured in blood was higher than that measured in other somatic tissues, and is not a good proxy of less accessible tissues. Female reproductive tissues had a 10% higher GDMR than male reproductive tissues. We demonstrated a significant influence of the breed on blood GDMR, certainly reflecting the influence of different genetic backgrounds. The effect of the breed on GDMR may be related to their specific abilities to adapt to and live in different conditions.

**Keywords: sheep, epigenetics, methylation, blood, tissues**

OPEN ACCESS

***Edited by:***
*Eveline M Ibeagha-Awemu, Agriculture and Agri-Food Canada (AAFC), Canada*

***Reviewed by:***
*Fenghua Lyu, China Agricultural University, China*
*Duy Ngoc Do, Dalhousie University, Canada*

****Correspondence:***
*Laurence Drouilhet*
*laurence.drouilhet@inrae.fr*

***Specialty section:***
*This article was submitted to Epigenomics and Epigenetics, a section of the journal Frontiers in Genetics*

***Received:*** *08 October 2021*
***Accepted:*** *08 February 2022*
***Published:*** *11 March 2022*

***Citation:***
*Drouilhet L, Moreno C, Plisson-Petit F, Marcon D, Fabre S and Hazard D (2022) Variability in Global DNA Methylation Rate Across Tissues and Over Time in Sheep. Front. Genet. 13:791283. doi: 10.3389/fgene.2022.791283*

## INTRODUCTION

Genetic improvement is widely used to increase animal production, health, and welfare in livestock systems. It is usually based on the use of phenotypes and pedigree data to estimate individual breeding values. DNA polymorphism data have recently started being used-depending on species and/or type of production-to estimate these values that characterize the landscape of genomic selection (Goddard et al., 2010). Variations in production traits are attributed to genetic determinism

plus environment effects and their interactions. Recent knowledge on the effects of the environment focuses on epigenetic phenomenon. Variations of epigenetic marks influence the expression of genes and hence phenotypes in response to environmental conditions, demonstrating that the eukaryotic genome responds dynamically to changes in the environment to which all individuals are exposed (Goddard and Whitelaw, 2014). For example in rats, reduced maternal care immediately after birth can alter the epigenetic state and expression of the glucocorticoid receptor gene, resulting in them becoming stressed adults (Weaver et al., 2004). In plants, epigenetic recombinant inbred lines of *Arabidopsis thaliana*, obtained by an initial cross of isogenic parents with different DNA methylation profiles, have provided a powerful tool to investigate the role and significance of epigenetic alteration in almost identical genetic backgrounds (Johannes et al., 2009; Latzel et al., 2013). Using these model plant lines, DNA hypomethylation of the whole genome was associated with lower resistance to increased saline environment (Kooke et al., 2015). It was also shown that multiple DNA methylation changes induced across the genome can be stably inherited over at least eight generations in the absence of selection, and that these changes are associated with substantial heritable variation in two complex traits, flowering time and plant height (Johannes et al., 2009). Therefore, new scientific questions arise about the relationship between genetics and epigenetics as part of livestock species improvement and their adaptation to changing production systems (Goddard and Whitelaw, 2014). Until now, epigenetic modifications induced by diet have been studied in a variety of livestock species (for a review, see Murdoch et al., 2016). In Scottish blackface ewes, the extent of periconceptional availability of nutrients was linked to the methionine-folate cycle altered DNA methylation and body fat content of offspring (Sinclair et al., 2007). However, studies in mammals (laboratory animal models, human or livestock) focus either on the methylation status of few candidate gene loci or on whole genome differentially methylated sites depending on the physiological or pathological questions raised needed to address. Thus, even with the use of genome bisulfite sequencing, the global methylation level of genomic DNA is never considered as a differential parameter between experimental conditions or individuals. In a recent study, we focused on global DNA methylation rate (GDMR) as a novel quantitative phenotype measured by pyrosequencing luminometric methylation assay (LUMA) in sheep (Hazard et al., 2020).

The LUMA technology considers the CpG located at the CCGG site recognized by methylation-independent MspI and methylation-sensitive HapII restriction enzymes (Karimi et al., 2006a; Karimi et al., 2006b). *In silico*, we counted around 6 million of CCGG sites on the ovine reference genome, which gives a reliable approximation of the methylated cytosine for CG of the entire genome. We showed that inter-individual variability in GDMR in blood had an additive genetic component in sheep with moderate heritability ($h^2$ = 0.20 ± 0.05). We then demonstrated the existence of genetic determinism of this particular epigenetic mark. Sheep are not only a species of agronomical interest but also represent an interesting animal model. Indeed, depending on the breed, sheep are reared in contrasted environments, sometimes in harsh conditions, thereby revealing their ability to adapt to and live in a wide range of conditions. Breeds of sheep also differ widely in their adaptive capacities depending on their origin and/or the production selection they undergo. Therefore, to better characterize the GDMR phenotype, we investigated variations in GDMR in the blood of several breeds of sheep reared in the same environment. We chose Romane (a stabilized composite breed between Romanov x Berrichon du Cher, Ricordeau et al., 1992) as representative of a rustic breed adapted to various temperate breeding conditions (intensive/indoors, extensive/outdoors), Charollais, a specialized breed for meat production (Huby et al., 2003) and Blackbelly as adapted to tropical environments with good resistance to parasitic gut worms (Sallé et al., 2012). The Romane and the Charollais breeds have common genetic components within the European northern sheep populations. However, among the French northern sheep populations, they appeared as the most divergent (Rochus et al., 2018). The Blackbelly breed originates from the Caribbean hair sheep breeds. Genome structural analysis of various sheep breed around the world clearly showed that Blackbelly breed is genetically different from the European breeds (Kijas et al., 2012; Spangler et al., 2017). In addition, to test whether the GDMR in the blood was representative of GDMR in other tissues, we searched for variations in GDMR in a large panel of ovine somatic and reproductive tissues.

# MATERIAL AND METHODS

## Ethics

The experiment was carried out in accordance with French national regulations for the use of animals for research purposes. The animals were bred at the INRAE experimental farm La Sapinière (Osmoy, France, experimental facility approval number C18–174–01). All the experiments were performed in accordance with the European Union Council directive (2010/63/UE) for the care and use of experimental animals for scientific purposes. Sampling procedures were approved by the local ethics committee C2EA-19 and authorized by the French Ministry of Higher Education, Research and Innovation (approval number: APAFIS#10243).

## Animals

In order to generate the experimental lambs, all the ewes (and thereafter lambs) from Romane, Blackbelly and Charolais breeds were reared at the same time within the same sheepfold of the experimental farm, but into separate pens according to breed. At the time of reproduction management, estrous cycle of ewes was synchronized by a male effect thanks to the presence of vasectomized males 15 days before the introduction of intact rams of the corresponding breed (two rams and 20 ewes per pen during 42 days). All ewes were managed the same manner according to their physiological status (before mating, gestation and suckling). We selected 49 least related experimental male and

female lambs (24 Romane, 23 Blackbelly and 12 Charollais), born in September 2017, identified at birth with electronic ear tags and reared indoors with their dam in similar conditions until weaning (**Supplementary Table S1**). From 15 days of age, in addition to maternal suckling, lambs had access to concentrate feed. Lambs were weaned around 64 days of age. At weaning, animals had free access to concentrate feed plus straw. After reaching a weight of 35 kg, each animal was fed 700 gr of feed concentrate per day plus 1.3 kg of hay per day.

## Samples

Blood samples were collected once a month (in the morning) from each animal ($n = 59$) from birth to 4 months of age ($n = 5$ blood samples/animal). A complete blood count (CBC) was performed on each fresh blood sample by the *Centre de recherches biologiques* (ERBC, Baugy, France, https://www.erbc-group.com/). The measured parameters were white blood cell count (neutrophil, eosinophil, basophil, lymphocyte and monocyte), red blood cell count, red cell volume, reticulocytes, hemoglobin, hematocrit, mean corpuscular volume, mean corpuscular hemoglobin, mean corpuscular hemoglobin concentration, platelet count and platelet volume. Whole blood genomic DNA coming from all nucleated blood cells was extracted for each sample to determine the global DNA methylation rate.

A subset of 15 Romane and 15 Blackbelly lambs was slaughtered at 5 months of age (**Supplementary Table S1**). Blood and 12 somatic tissues (frontal lobe, pituitary gland, heart, lung, sub cutaneous adipose tissue, perirenal adipose tissue, muscle, liver, spleen, adrenal gland, medulla kidney and cortical kidney) were sampled from each animal. Three additional reproductive tissues, specific to each sex (female: ovary, oviduct, uterus; male: testis, epididymis and seminal vesicle), were also collected (**Supplementary Table S2**). The CBC of the blood sample collected at 5 months of age was not performed.

## LUminometric Methylation Assay Analyses

The global DNA methylation level of whole blood samples or tissues of individuals was measured using the LUMA assay (Karimi et al., 2006a; Karimi et al., 2006b). Genomic DNA was extracted from blood samples using a high-salt extraction method (Roussot et al., 2003) and from tissue samples using NucleoSpin Tissue kit (Macherey Nagel). DNA was digested by EcoRI + HpaII or EcoRI + MspI restriction enzymes (New England Biolabs) and then analyzed using a Q24 Pyromark sequencer (Qiagen). MspI and HpaII have the same recognition site (CCGG), whereas HpaII is inhibited by the presence of a 5-methylcytosine. EcoRI (recognition site: GAATTC) was used as internal control for normalization. Runs were analyzed with PyroMark Q24 1.0.10 software (Qiagen). The dispensation order for nucleotides was GTGTCACATGTGTG. Methylation levels were calculated from peak heights as [1 − [(HpaII(G)/EcoRI_Hpa(T))/(MspI(G)/EcoRI_Msp(T))] × 100]. The same control sample was used in each pyrosequencing run; its coefficient of variation calculated from 86 measurements was 1.4%.

## Statistical Analysis

The fixed effects of breed, sex, litter size (singleton, twice or triplet), date of sampling, CBC and tissue were tested, when relevant, by mixed linear models using the MIXED procedure of SAS software (SAS, 2008). Only the fixed effects and their interactions for which $p < 0.05$ were considered as significant and retained in the different models presented below.

For global DNA methylation rate of the blood and the complete blood count, the equation was:

$$\mathrm{GDMR}_{ijk} \text{ or } \mathrm{CBC}_{ijk} = \mu + date_sampling_i + breed_j + sex_k + a_{ij_k} + e_{ijk}\,(model\,1) \quad (1)$$

with $date_sampling_i$ (5 levels), $breed_j$ (3 levels) and $sex_k$ (2 levels) as fixed effects, $a_{ijk}$ the animal repeated across sampling (as random effect), and $e_{ijk}$ the residual (as random effect). For the global DNA methylation rate of the blood considering the complete blood count, the equation was:

$$\mathrm{GDMR}_{ij} = \mu + \mathrm{CBC}_{ij} + breed_i + sex_j + a_{ij} + e_{ij}\ (model\,2) \quad (2)$$

with $CBC_{ij}$ as the covariable, with $breed_i$ (3 levels) and $sex_j$ (2 levels) as fixed effects, $a_{ij}$ the animal repeated across sampling (as a random effect), and $e_{ij}$ the residual (as a random effect). Model 3 was used to account for *GDMR* in tissues with the exception of tissues belonging to the reproductive tract:

$$\mathrm{GDMR}_{ij} = \mu + \mathrm{tissue}_i + sex_j + \mathrm{tissue}_i{}^{*}sex_j + a_{ij} + e_{ij}\ (model\,3) \quad (3)$$

with $\mathrm{tissue}_i$ (13 levels), $sex_j$ (2 levels), $a_{ij}$ the animal repeated across tissues (as a random effect), and $e_{ij}$ the residual (as a random effect). The effects of the age of the animal was tested but was not significant and therefore not retained in the model 3. Finally, for the GDMR of tissues belonging to the reproductive tract, the model 4 was:

$$\mathrm{GDMR}_{ij} = \mu + breed_i + tissue_j + a_{ij} + e_{ij}\ (model\,4) \quad (4)$$

with $breed_i$ (2 levels), $tissue_j$ (6 levels) and $a_{ij}$ the animal repeated across tissues (as a random effect) and $e_{ij}$ the residual (as a random effect).

Least squares means (LSMeans) for the fixed effects for each trait were obtained from these mixed linear models and were compared using Tukey test. LSMeans were considered significantly different with $p < 0.05$.

## Tissue-to-Tissue GDMR Correlation

Tissue-to-tissue GDMR correlations were estimated with the CORR procedure in SAS software (SAS, 2008), corresponding to Pearson correlation coefficients and the *p*-value associated.

# RESULTS

## Global DNA Methylation Rate of Blood

GDMR was measured in blood samples collected once a month from 59 lambs of three different breeds. The

**TABLE 1 |** Effects of sampling date, breed, and sex on blood GDMR.

| Effect | Level | LSMeans (SE) | *p*-value |
|---|---|---|---|
| Sampling date | Birth | 80.50$^{b}$ (0.24) | <0.0001 |
| | 1 month | 81.05$^{bc}$ (0.25) | |
| | 2 months | 79.76$^{a}$ (0.25) | |
| | 3 months | 81.01$^{bc}$ (0.25) | |
| | 4 months | 81.40$^{c}$ (0.25) | |
| Breed | Romane | 81.13$^{a}$ (0.17) | 0.002 |
| | Blackbelly | 80.24$^{b}$ (0.18) | |
| | Charollais | 80.87$^{ab}$ (0.26) | |
| Sex | male | 80.37$^{a}$ (0.18) | 0.002 |
| | female | 81.12$^{b}$ (0.15) | |

*Statistical model 1 was used. LSMeans: Least square means, SE: standard error. For each effect, values with different superscripts (a, b, c) were found to differ significantly ($p < 0.05$).*

sampling date, breed and sex were tested to explore GDMR variability using statistical model 1. The resulting $p$ values are listed in **Table 1**. GDMR was significantly influenced by the sampling date ($p < 0.001$), breed ($p = 0.002$) and sex ($p = 0.002$). GDMR was lowest around 2 months of age (**Figure 1A**). Average GDMR over time (LSmeans) was lower in Blackbelly lambs (80.24%) than in Romane lambs (81.13%), GDMR in Charollais was between the two. The difference between breeds was particularly marked at birth ($p = 0.02$, **Figure 1B**) and at around 2 months of age ($p = 0.05$, **Figure 1B**). In addition, female lambs showed higher overall GDMR than males (81.12 vs. 80.37%; $p = 0.002$, **Table 1**). This difference is markedly visible at birth ($p = 0.01$, **Figure 1C**) and 4 months of age ($p = 0.04$, **Figure 1C**). However, no correlation was found between the different GDMR over time, whether considering the raw data or the residuals of the mixed model (data not shown).

## Variability of the Complete Blood Count and its Influence on GDMR

A CBC was performed on fresh blood from each sample. Among the five consecutive blood samples, on average, lymphocytes (60.4% ± 11.6) and neutrophils (31.2% ± 10.5) were the two

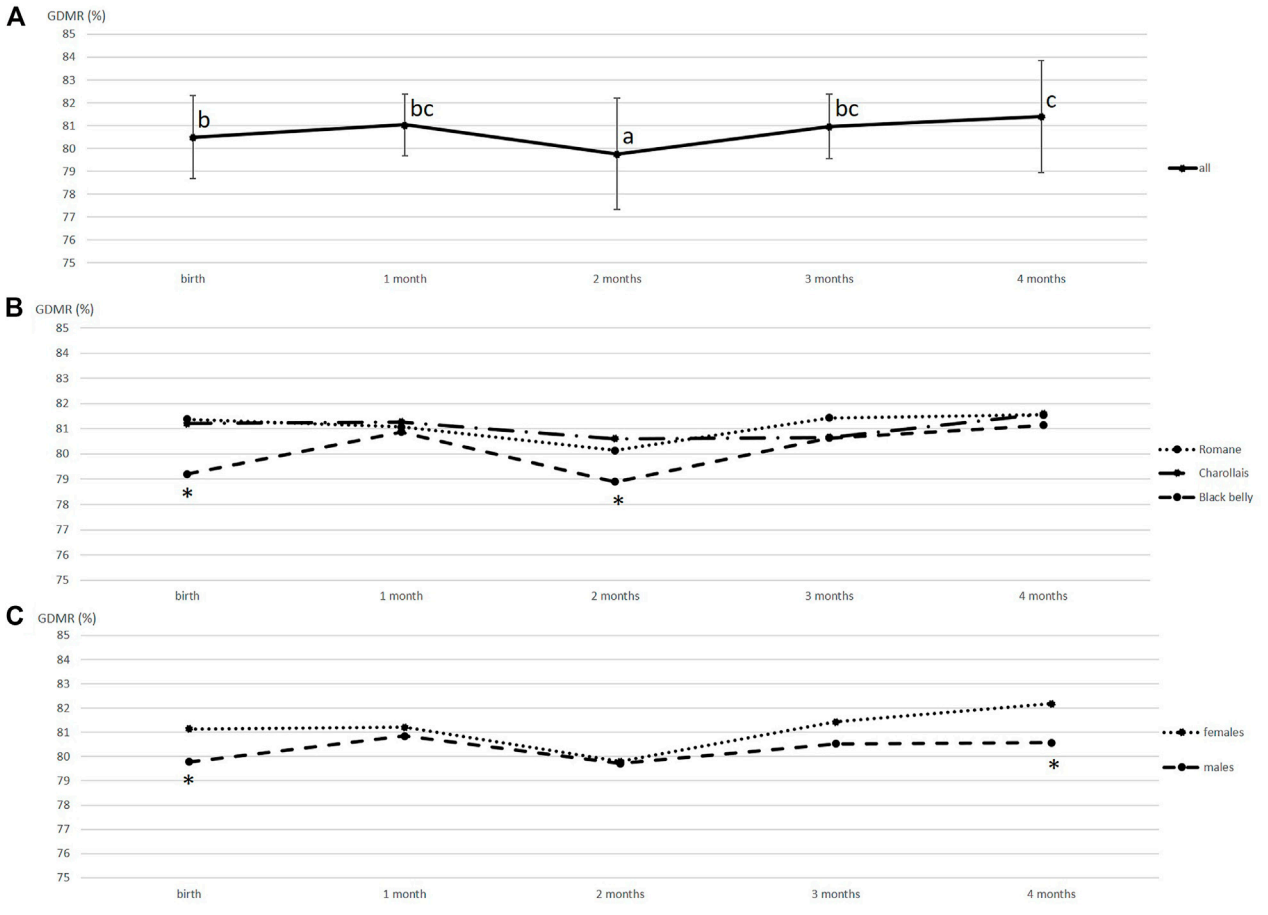



**FIGURE 1 |** Variations in the global methylation rate of blood DNA over time. **(A)** GDMR means were calculated for 59 animals, vertical bars represent standard deviation, values with different superscripts (a, b and c) were found to differ significantly ($p < 0.05$). **(B)** GDMR means were calculated for each breed, Charollais ($n = 12$), Romane ($n = 24$) and Blackbelly ($n = 23$). For each date, asterisks indicate that the Blackbelly value differs significantly ($p < 0.05$). **(C)** GDMR means calculated according to sex, 28 males and 31 females. For each date, asterisks indicate that the male and female values differ significantly ($p < 0.05$).

**TABLE 2 |** Proportion (%) of each nucleated cell type among the total white blood cells.

| (%) | Lymphocytes | Neutrophils | Monocytes | Eosinophils | Basophils |
|---|---|---|---|---|---|
| μ | 60.4 | 31.2 | 4.4 | 2.0 | 0.8 |
| SD | 11.6 | 10.5 | 2.8 | 1.6 | 0.3 |
| min | 4.9 | 7.4 | 0.2 | 0.3 | 0.2 |
| max | 84.8 | 72.3 | 34.6 | 10.3 | 2.5 |

*μ: average; SD, standard deviation; min: minimum; max, maximum.*

**TABLE 3 |** Effects of the sampling date, breed and the sex on the complete blood count.

| Blood component (Giga/L) | Effect | | | Breed LSMeans (SE) | | | Sex LSMeans (SE) | |
|---|---|---|---|---|---|---|---|---|
| | Sampling date | Breed | Sex | Romane | Blackbelly | Charollais | Male | Female |
| White blood cells | *** | *** | ns | $8.13^{a}$ (0.28) | $9.81^{b}$ (0.29) | $8.00^{a}$ (0.40) | ns | ns |
| Lymphocytes | *** | * | ns | $4.90^{a}$ (0.23) | $5.72^{b}$ (0.23) | $5.19^{ab}$ (0.32) | ns | ns |
| Neutrophils | *** | *** | * | $2.60^{a}$ (0.15) | $3.26^{b}$ (0.15) | $2.27^{a}$ (0.22) | $2.93^{a}$ (0.15) | $2.49^{b}$ (0.13) |
| Monocytes | *** | ns | ns | ns | ns | ns | ns | ns |
| Eosinophils | ** | *** | ns | $0.13^{a}$ (0.01) | $0.25^{b}$ (0.01) | $0.13^{a}$ (0.02) | ns | ns |
| Basophils | *** | *** | ns | $0.06^{a}$ (0.004) | $0.08^{b}$ (0.004) | $0.06^{a}$ (0.006) | ns | ns |

*Statistical model 1 was used. *: p < 0.05, **: p < 0.01, ***: p < 0.001. ns: not significant. Least square means (LSMeans) and the SE, of the breed and sex effects were estimated. For each effect, LSMeans, with different superscripts (a,b) were found to differ significantly (p < 0.05).*

**TABLE 4 |** Comparison of the models for analyses of GDMR of the blood.

| | Effect | | | | Bayesian information criterion (BIC) |
|---|---|---|---|---|---|
| | Sampling date | Neutrophil count | Breed | Sex | |
| Model 1 | <0.0001 | / | 0.002 | 0.002 | 1,182 |
| Model 2 | / | 0.02 | 0.01 | 0.008 | 1,187 |

most abundant cell types among the white blood cells (**Table 2**). For each cell type, we tested the effects of the sampling date, breed and sex (model 1). The associated *p*-values are listed in **Table 3**. All components of the CBC were significantly affected by the sampling date, and the breed effect was significant for all cell types except monocytes. The Blackbelly breed had more white blood cells than the Romane and Charollais breeds. Sex only affected the number of neutrophils ($p = 0.03$), which was higher in male than in female lambs.

Next, we considered CBC as a covariable in order to explain GDMR variability (model 2). Among all CBC components, the number of neutrophils was the only significant parameter. It was therefore retained in the model. The Bayesian information criterion (BIC) was used to select the statistical model that best described our data (**Table 4**). Model 1 had the lowest BIC, indicating that given the sampling date effect, this model fitted the data better than the model with the neutrophil count.

## Global DNA Methylation Rate of Somatic and Reproductive Tissues

Fifteen Blackbelly and 15 Romane lambs (representing 16 males and 14 females) were slaughtered at around 5 months of age to sample tissues. Samples of 13 different tissues (including a blood sample) were collected from both males and females. Three additional reproductive tissues, specific to each sex (testis, epididymis and seminal vesicle for males; ovary, oviduct and uterus for females), were also collected.

To explore the variability of GDMR among the somatic tissues collected, we tested the effects of the tissue, age, sex, breed, and possible interactions. The age of the animal and the breed effects were not significant and were not retained in model 3. As expected, we observed a strong effect of the type of tissue on GDMR ($p < 0.001$; **Figure 2**). In particular, the GDMR of five tissues differed significantly from each other. The highest level of GDMR was measured in blood, while the lowest levels were measured in adipose tissue, pituitary gland, cortical kidney, and liver, and the levels of GDMR levels in liver being extremely low (**Figure 2**). The average GDMR of the other tissues ranged from 67.69 to 72.46%. Among somatic tissues, lung presented the lowest variability (70.45% ± 1.81) and cortical kidney the highest (55.44% ± 7.77). The overall interaction between sex and tissue was close to significance ($p = 0.06$). This could be explained by a tendency to an effect of sex in adipose tissue ($p = 0.07$), and a highly significant impact of sex on the cortical kidney ($p = 0.0004$). Indeed, the GDMR of cortical kidney was 9% lower in females than in males (**Figure 3**).

Focusing on the reproductive tract, we found a strong tissue effect ($p < 0.0001$, model 4). Interestingly, GDMR did not differ significantly between tissues in females and GDMR of female tissues was 10% higher than GDMR in male tissues (**Figure 2**).

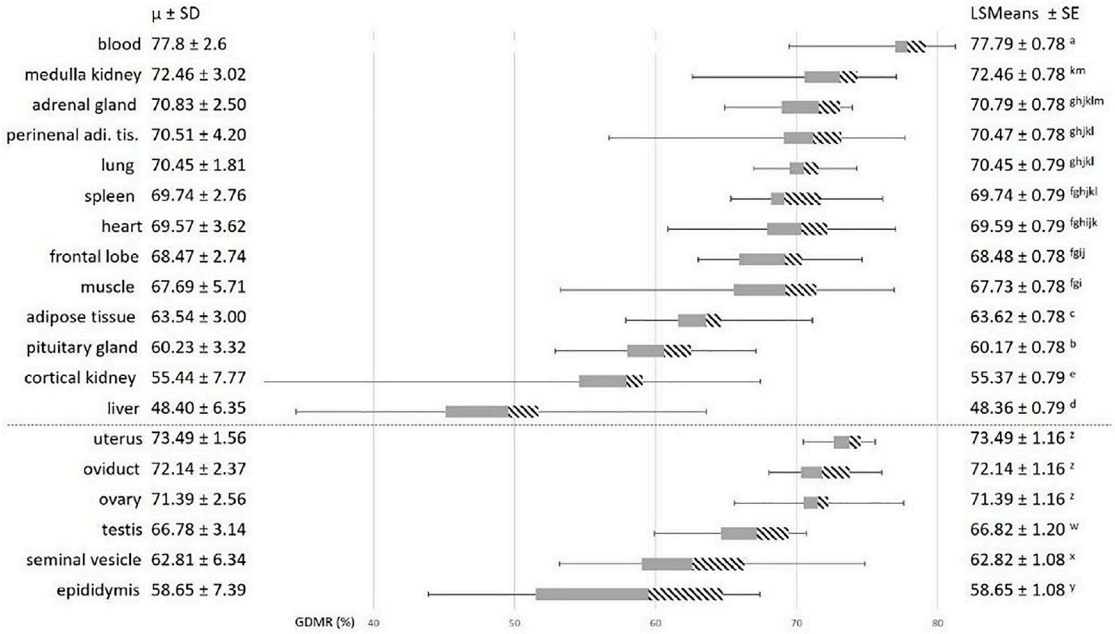



**FIGURE 2 |** Variability in global DNA methylation rate in somatic and reproductive tissues. Average GDMR was calculated for 30 animals, 16 males and 14 females, (15 Blackbelly and 15 Romane sheep). The grey bars represent the second quartile, the dashed bars represent the third quartile, and the horizontal lines on each side correspond to the first (on the left) and the fourth (on the right) quartiles. The tissues below the dotted line belong to female and male reproductive tracts. Statistical model 3 was used for the analysis of somatic tissues. For each effect, values with different superscripts (a to m) were found to be significantly different ($p < 0.05$). Statistical model 4 was used for the analysis of reproductive tissues. For each effect, values with different superscripts (y to z) were found to differ significantly ($p < 0.05$). perirenal adi. tis.: perirenal adipose tissue.

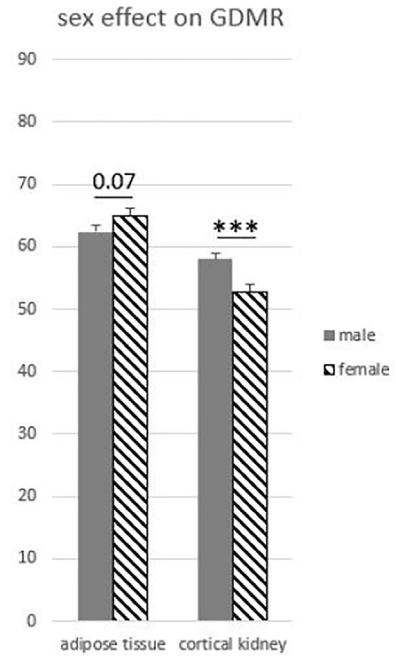



**FIGURE 3 |** Global DNA methylation rate influenced by sex in adipose and kidney tissues. Model 3 was used for statistical analysis. $^{***}p < 0.001$.

The GDMR of the female tissues was around 72% and quite homogenous (SD comprised between 1.56 and 2.56). In contrast, GDMR of male tissues was lower, ranging from 59 to 67% and more heterogeneous (SD comprised between 3.14 and 7.39) than that of females. Similar to the GDMR of blood, the overall GDMR of reproductive tissues was slightly lower in Blackbelly sheep than in Romane (breed effect, $p = 0.03$, model 4).

## Tissue-to-Tissue GDMR Correlation

At slaughter, using the GDMR dataset for 30 animals and 19 tissues (12 somatic tissues, three additional reproductive tissues specific to each sex and a blood sample), we looked for correlations of GDMR between tissues. The significant correlations ranged from −0.56 ($p = 0.04$) between ovary and adrenal gland, to 0.55 ($p = 0.03$) between medulla kidney and seminal vesicle (**Supplementary Table S3**). Using the blood previously sampled from birth to 4 months of age, the only significant strong correlation found was 0.63 between GDMR of ovary and GDMR of blood at 3 months of age ($p = 0.02$).

# DISCUSSION

In mammals, DNA methylation occurs almost exclusively in the symmetric CG context and is estimated to occur at ~70–80% of CG dinucleotides throughout the genome (Ehrlich et al., 1982). This

estimation is consistent with the average GDMR of 70% found in the present study for somatic tissues in sheep. Mapping studies indicate that highly methylated sequences include satellite DNAs, repetitive elements (including transposons and their inert relics), non-repetitive intergenic DNA, and exons of genes. Unlike in plants, DNA methylation in mammals covers most of the genome, the main exception being CpG islands. Indeed, the most striking feature of vertebrate DNA methylation patterns is the presence of CpG islands, that is, unmethylated GC-rich regions that possess high relative densities of CpG and are positioned at the 5′ ends of many human genes (Suzuki and Bird, 2008). Computational analysis of the human genome sequence predicts 29,000 CpG islands (Lander et al., 2001; Venter et al., 2001). Local 5mC depletion is a reliable signature of promoters and enhancers: CpG sites in promoter-associated CpG islands are often less than 10% methylated, whereas distal regulatory sequences such as enhancers are commonly marked by levels of 5mC ranging from 10 to 50% (Stadler et al., 2011).

As the LUMA technology quantifies the methylation rate of CpG located in the CCGG restriction site, the entire genome is scanned independently of the features of the DNA (repeated elements, genes, etc). Transposable elements make up 45% of the human genome (for a review, see Zhou W. et al., 2020). Therefore, the GDMR mainly represents the stable fraction of the DNA methylation of the genome. Indeed, the differentially methylated regions over cell development or organs represent only a small fraction of the CpG of the genome.

The time series analysis performed in the present study indicated that GDMR of the blood was influenced by the date of sampling, a possible combined effect of age and season, but only slight GDMR changes were observed over time and the average GDMR was around 80%. Aging has been reported to have a profound effect on DNA methylation in many tissues and cell types (Rakyan et al., 2010; Teschendorff et al., 2010; Horvath, 2013; Issa, 2014). In sheep, like in other species, an epigenetic clock has been described that is capable of estimating chronological age and of detecting accelerated rates of aging (Sugrue et al., 2021). However in our study, the time series only covered the first 6 months of life of the lambs and this was probably too short to detect a major effect of aging on GDMR. Therefore, the date of sampling effect is hypothesized to be more related to environmental changes as the circadian cycle or the season. To better understand this time effect, we explored the influence of the complete blood count over time on blood GDMR. Indeed, Dopico et al. (2015) showed the influence of the circadian cycle on the cellular composition of blood in humans. Additionally, Goldinger et al. (2015) suggested that temperature is a major factor driving seasonal variations of this blood composition. Similarly, we showed that the blood count was influenced by the date of sampling and thus probably by the season since the first blood sample was taken at the beginning of autumn and the last at the end of winter. However, among the counts of each type of white cell, GDMR of the blood was only influenced by the neutrophil count. As the model with the date of sampling statistically fit the data better than the model with the neutrophil count, we hypothesize that the effect of sampling date may include not only changes in blood count, but also additional environmental effects influenced by time that we were unable to identify and quantify.

We first hypothesized that blood GDMR may be representative of GDMR of somatic and reproductive tissues. In our study, GDMR of somatic tissues was on average 70%, but with marked variations depending on the tissue. The GDMR of blood was higher than that of somatic tissue (whatever the tissue considered). Even if significant, all the correlations were lower than 0.63 (highest value found between ovary and blood at 3 months) and thus were unlikely to reliably predict the GDMR of one tissue from the value of another one. Thus, the use of GDMR of blood as an indicator of GDMR in less accessible tissue is questionable. Variations in GDMR of blood (CV of 2.6% within or between animals) are probably too small in our experimental animals and too close to the CV of the assay (1.4%) to establish a correlation with the GDMR measured in another tissue. Nevertheless, the present findings in sheep are consistent with those obtained in different bovine somatic tissues. Most somatic tissue DNA samples in cattle had average methylation levels of 70–80% (Zhou Y. et al., 2020). To understand the variability of DNA methylation across cattle tissues and its regulation of gene expression, Zhou Y. et al. (2020) profiled the cattle DNA methylomes in 16 major tissues using the whole genome bisulfite sequencing (WGBS) method. However, it should be kept in mind that the GDMR values obtained by WGBS are often slightly higher than the values obtained using the LUMA technology. For example, in ovine muscle, Fan et al. (2020) analyzed the DNA methylation profiles in Hu sheep muscle (an endemic Chinese sheep breed) at two key developmental stages (110-days fetuses and two-year-old adults) using WGBS technology. They found genome-wide methylated cytosine (mC) levels for CG of 88.87 ± 0.67% in fetal samples and 85.33 ± 0.95% in adult samples. In our study using the same species but lambs of different ages, the GDMR measured in muscle was lower (67.69 ± 5.71%). In sheep ovaries, Zhang et al. (2017) found an overall genome-wide methylated cytosine level of 89.78% for CpG using WGBS, whereas we found a value of 71.39 ± 2.56% using the LUMA technology. Whereas WGBS accounts for all the CpG of the genome, the LUMA technology only considers the CpG located at the CCGG restriction site. In silico, we counted 5 994 593 CCGG sites on the ovine reference genome, which gives a reliable approximation of the methylated cytosine (mC) for CG of the entire genome but may explain the lower values found with the LUMA technology than with WGBS.

In the female tissues of the reproductive axis (ovary, uterus, and oviduct), GDMR was around 70% and corresponded to the average values obtained for the other somatic tissues. In contrast, the three male tissues (testis, epididymis, and seminal vesicle) had a lower average GDMR of around 60%. It would be interesting to compare this observation with the significant effect of sex in blood showing lower GDMR in males, but we found no similar data in the literature with which to compare our results to interpret the difference between sexes. Sex hormones could be involved in this phenomenon. In sheep, it has been shown that castration feminizes parts of the epigenome and delays epigenetic aging (Sugrue et al., 2021). Comparison of intact and castrated males would allow us to identify androgen-dependent age-associated methylation changes that affect known targets of sex hormone pathways and hormone binding transcription factors in castrated sheep. In rodents, a primary effect of gonadal steroids in the highly sexually-dimorphic preoptic area

(brain region) has been shown to reduce the activity of DNA methyltransferase (Dnmt), thereby decreasing DNA methylation and releasing masculinizing genes from epigenetic repression (Nugent et al., 2015). In this brain area, females had higher levels of methylation (measured by WGBS) with significantly more fully methylated CpG sites than males. In humans, the link between reproductive hormones and DNA methylation has also been described in hormonal therapy of cancer. Indeed, antiandrogen medication given to patient with prostate cancer increased *DNMT3A* and *DNMT3B* expression (Gravina et al., 2011). In the human endometrium, *DNMT* mRNA levels change during the menstrual cycle, and *DNMT3A* and *DNMT3B* mRNAs can be regulated by female sex steroid hormones in endometrial stromal cells (Yamagata et al., 2009). If sex hormones do indeed influence GDMR, a further study focusing on the time around puberty (starting from 6 months of age in sheep) would be interesting.

Investigation of GDMR of the blood in several breeds of sheep evidenced a breed specific effect mainly of the Blackbelly breed, consequently, to limit environmental effects, Blackbelly lambs were bred at the same time as Charollais and Romane lambs in the same environmental conditions. This significant influence of the breed on GDMR thus certainly reflects the influence of different genetic backgrounds. Indeed, Blackbelly sheep are well adapted to a semi-arid tropical environment (high temperature and humidity, but also to extended drought), in contrast to the Romane and Charollais breeds that are more adapted to temperate climates and different farming systems (free range, semi-free range, use of sheepfolds). The three breeds thus have different abilities to adapt to and survive in different conditions. In a previous study performed on around 700 Romane lambs reared outdoors (Hazard et al., 2020), the average GDMR of the blood was lower (around 70%) than the GDMR found in the present study (around 80%). The radically different farming system (entirely indoors vs. entirely outdoors) may partly explain the observed difference. As shown previously (Hazard et al., 2020), GDMR has a heritability of 0.20 ± 0.05 and could thus be genetically selected. DNA methylation is associated with repression of transposable elements and acts to limit their genotoxic potential. If GDMR is reduced by genetic selection, it could lead to instability of transposable elements in the genome. However, this genome plasticity could help animals adapt to changing production systems and environment. Kooke et al. (2015) showed that experimentally induced DNA hypomethylation of plants rendered them more sensitive to environmental variation and more flexible in their responses. Thus, the lower GDMR of the blood in lambs reared in extensive conditions than the GDMR level in indoor conditions may help improve sheep adaptation to a harsh environment.

## CONCLUSION

We explored the GDMR phenotype and investigated its variability in several tissues in different breeds of sheep reared in the same environment. The GDMR measured in blood was higher than that measured in somatic tissue whatever the tissue considered, and none of the significant correlations found was strong enough to predict a link between GDMR in different tissues. Thus, the use of GDMR of the blood as a proxy of GDMR in less accessible tissues is probably not appropriate. However, we evidenced a significant influence of the breed on GDMR, certainly reflecting the influence of different genetic backgrounds and raising questions about relationships between GDMR and the ability of these breeds of sheep to adapt to contrasting environments. Further studies will be conducted by creating genetically divergent lines for GDMR of the blood to investigate the consequences of high versus low levels of GDMR of the blood for several phenotypes including adaptive traits.

## DATA AVAILABILITY STATEMENT

The raw data supporting the conclusion of this article will be made available by the authors, without undue reservation.

## ETHICS STATEMENT

The animal study was reviewed and approved by local ethics committee C2EA-19 and authorized by the French Ministry of Higher Education, Research and Innovation (approval number: APAFIS#10243).

## AUTHOR CONTRIBUTIONS

LD, CM, SF and DH contributed to conception and design of the study. DM managed the animals breeding and tissues collection. FPP performed the LUMA analysis. LD performed the statistical analysis. LD wrote the first draft of the manuscript. All authors contributed to manuscript revision, read, and approved the submitted version

## SUPPLEMENTARY MATERIAL

The Supplementary Material for this article can be found online at: https://www.frontiersin.org/articles/10.3389/fgene.2022.791283/full#supplementary-material

## REFERENCES

Dopico, X. C., Evangelou, M., Ferreira, R. C., Guo, H., Pekalski, M. L., Smyth, D. J., et al. (2015). Widespread Seasonal Gene Expression Reveals Annual Differences in Human Immunity and Physiology. *Nat. Commun.* 6, 7000. doi:10.1038/ncomms8000

Ehrlich, M., Gama-Sosa, M. A., Huang, L.-H., Midgett, R. M., Kuo, K. C., McCune, R. A., et al. (1982). Amount and Distribution of 5-methylcytosine in Human DNA from Different Types of Tissues or Cells. *Nucl. Acids Res.* 10, 2709–2721. doi:10.1093/nar/10.8.2709

Fan, Y., Liang, Y., Deng, K., Zhang, Z., Zhang, G., Zhang, Y., et al. (2020). Analysis of DNA Methylation Profiles during Sheep Skeletal Muscle Development Using Whole-Genome Bisulfite Sequencing. *BMC Genomics* 21, 327. doi:10.1186/s12864-020-6751-5

Goddard, M. E., Hayes, B. J., and Meuwissen, T. H. E. (2010). Genomic Selection in Livestock Populations. *Genet. Res.* 92, 413–421. doi:10.1017/S0016672310000613

Goddard, M. E., and Whitelaw, E. (2014). The Use of Epigenetic Phenomena for the Improvement of Sheep and Cattle. *Front. Genet.* 5, 247. doi:10.3389/fgene.2014.00247

Goldinger, A., Shakhbazov, K., Henders, A. K., McRae, A. F., Montgomery, G. W., and Powell, J. E. (2015). Seasonal Effects on Gene Expression. *PLoS ONE* 10, e0126995. doi:10.1371/journal.pone.0126995

Gravina, G. L., Marampon, F., Piccolella, M., Motta, M., Ventura, L., Pomante, R., et al. (2011). Hormonal Therapy Promotes Hormone-Resistant Phenotype by Increasing DNMT Activity and Expression in Prostate Cancer Models. *Endocrinology* 152, 4550–4561. doi:10.1210/en.2011-1056

Hazard, D., Plisson-Petit, F., Moreno-Romieux, C., Fabre, S., and Drouilhet, L. (2020). Genetic Determinism Exists for the Global DNA Methylation Rate in Sheep. *Front. Genet.* 11, 1717. doi:10.3389/fgene.2020.616960

Horvath, S. (2013). DNA Methylation Age of Human Tissues and Cell Types. *Genome Biol.* 14, R115. doi:10.1186/gb-2013-14-10-r115

Issa, J.-P. (2014). Aging and Epigenetic Drift: a Vicious Cycle. *J. Clin. Invest.* 124, 24–29. doi:10.1172/JCI69735

Johannes, F., Porcher, E., Teixeira, F. K., Saliba-Colombani, V., Simon, M., Agier, N., et al. (2009). Assessing the Impact of Transgenerational Epigenetic Variation on Complex Traits. *Plos Genet.* 5, e1000530. doi:10.1371/journal.pgen.1000530

Karimi, M., Johansson, S., and Ekström, T. J. (2006a). Using LUMA: a Luminometric-Based Assay for Global DNA-Methylation. *Epigenetics* 1, 46–49. doi:10.4161/epi.1.1.2587

Karimi, M., Johansson, S., Stach, D., Corcoran, M., Grandér, D., Schalling, M., et al. (2006b). LUMA (LUminometric Methylation Assay)-A High Throughput Method to the Analysis of Genomic DNA Methylation. *Exp. Cel Res.* 312, 1989–1995. doi:10.1016/j.yexcr.2006.03.006

Kijas, J. W., Lenstra, J. A., Hayes, B., Boitard, S., Porto Neto, L. R., San Cristobal, M., et al. (2012). Genome-Wide Analysis of the World's Sheep Breeds Reveals High Levels of Historic Mixture and Strong Recent Selection. *Plos Biol.* 10, e1001258. doi:10.1371/journal.pbio.1001258

Kooke, R., Johannes, F., Wardenaar, R., Becker, F., Etcheverry, M., Colot, V., et al. (2015). Epigenetic Basis of Morphological Variation and Phenotypic Plasticity in *Arabidopsis thaliana*. *The Plant Cell* 27, 337–348. doi:10.1105/tpc.114.133025

Lander, E. S., Linton, L. M., Birren, B., Nusbaum, C., Zody, M. C., Baldwin, J., et al. (2001). Initial Sequencing and Analysis of the Human Genome. *Nature* 409, 860–921. doi:10.1038/35057062

Latzel, V., Allan, E., Bortolini Silveira, A., Colot, V., Fischer, M., and Bossdorf, O. (2013). Epigenetic Diversity Increases the Productivity and Stability of Plant Populations. *Nat. Commun.* 4, 2875. doi:10.1038/ncomms3875

Marie, H., Laurent, G., Sophie, M., De Hubert, R., Coralie, D.-B., and Verrier, É. (2003). Genetic Variability of Six French Meat Sheep Breeds in Relation to Their Genetic Management. *Genet. Sel Evol.* 35, 637. doi:10.1186/1297-9686-35-7-637

Murdoch, B. M., Murdoch, G. K., Greenwood, S., and McKay, S. (2016). Nutritional Influence on Epigenetic Marks and Effect on Livestock Production. *Front. Genet.* 7, 182. doi:10.3389/fgene.2016.00182

Nugent, B. M., Wright, C. L., Shetty, A. C., Hodes, G. E., Lenz, K. M., Mahurkar, A., et al. (2015). Brain Feminization Requires Active Repression of Masculinization via DNA Methylation. *Nat. Neurosci.* 18, 690–697. doi:10.1038/nn.3988

Rakyan, V. K., Down, T. A., Maslau, S., Andrew, T., Yang, T.-P., Beyan, H., et al. (2010). Human Aging-Associated DNA Hypermethylation Occurs Preferentially at Bivalent Chromatin Domains. *Genome Res.* 20, 434–439. doi:10.1101/gr.103101.109

Ricordeau, G., Tchamitchian, L., Brunel, J. C., Nguyen, T. C., and François, D. (1992). La gestion des populations : La race ovine INRA 401 : un exemple de souche synthétique. *INRA Prod. Anim.* 5, 255–262. doi:10.20870/productions-animales.1992.5.hs.4300

Rochus, C. M., Tortereau, F., Plisson-Petit, F., Restoux, G., Moreno-Romieux, C., Tosser-Klopp, G., et al. (2018). Revealing the Selection History of Adaptive Loci Using Genome-wide Scans for Selection: an Example from Domestic Sheep. *BMC Genomics* 19, 71. doi:10.1186/s12864-018-4447-x

Roussot, O., Feve, K., Plisson-Petit, F., Pitel, F., Faure, J.-M., Beaumont, C., et al. (2003). AFLP Linkage Map of the Japanese Quail Coturnix japonica. *Genet. Sel Evol.* 35, 559. doi:10.1186/1297-9686-35-6-559

Sallé, G., Jacquiet, P., Gruner, L., Cortet, J., Sauvé, C., Prévot, F., et al. (2012). A Genome Scan for QTL Affecting Resistance to Haemonchus contortus in Sheep1. *J. Anim. Sci.* 90, 4690–4705. doi:10.2527/jas.2012-5121

SAS (2008). *Statistical Analysis Systems Institute. Version 9.1*. Cary, North Carolina, USA: SAS Institute Inc.

Sinclair, K. D., Allegrucci, C., Singh, R., Gardner, D. S., Sebastian, S., Bispham, J., et al. (2007). DNA Methylation, Insulin Resistance, and Blood Pressure in Offspring Determined by Maternal Periconceptional B Vitamin and Methionine Status. *Proc. Natl. Acad. Sci.* 104, 19351–19356. doi:10.1073/pnas.0707258104

Spangler, G. L., Rosen, B. D., Ilori, M. B., Hanotte, O., Kim, E.-S., Sonstegard, T. S., et al. (2017). Whole Genome Structural Analysis of Caribbean Hair Sheep Reveals Quantitative Link to West African Ancestry. *PLoS ONE* 12, e0179021. doi:10.1371/journal.pone.0179021

Stadler, M. B., Murr, R., Burger, L., Ivanek, R., Lienert, F., Schöler, A., et al. (2011). DNA-binding Factors Shape the Mouse Methylome at Distal Regulatory Regions. *Nature* 480, 490–495. doi:10.1038/nature10716

Sugrue, V. J., Zoller, J. A., Narayan, P., Lu, A. T., Ortega-Recalde, O. J., Grant, M. J., et al. (2021). Castration Delays Epigenetic Aging and Feminizes DNA Methylation at Androgen-Regulated Loci. *eLife* 10, e64932. doi:10.7554/eLife.64932

Suzuki, M. M., and Bird, A. (2008). DNA Methylation Landscapes: Provocative Insights from Epigenomics. *Nat. Rev. Genet.* 9, 465–476. doi:10.1038/nrg2341

Teschendorff, A. E., Menon, U., Gentry-Maharaj, A., Ramus, S. J., Weisenberger, D. J., Shen, H., et al. (2010). Age-dependent DNA Methylation of Genes that Are Suppressed in Stem Cells Is a Hallmark of Cancer. *Genome Res.* 20, 440–446. doi:10.1101/gr.103606.109

Venter, J. C., Adams, M. D., Myers, E. W., Li, P. W., Mural, R. J., Sutton, G. G., et al. (2001). The Sequence of the Human Genome. *Science* 291, 1304–1351. doi:10.1126/science.1058040

Weaver, I. C. G., Cervoni, N., Champagne, F. A., D'Alessio, A. C., Sharma, S., Seckl, J. R., et al. (2004). Epigenetic Programming by Maternal Behavior. *Nat. Neurosci.* 7, 847–854. doi:10.1038/nn1276

Yamagata, Y., Asada, H., Tamura, I., Lee, L., Maekawa, R., Taniguchi, K., et al. (2009). DNA Methyltransferase Expression in the Human Endometrium: Down-Regulation by Progesterone and Estrogen. *Hum. Reprod.* 24, 1126–1132. doi:10.1093/humrep/dep015

Zhang, Y., Li, F., Feng, X., Yang, H., Zhu, A., Pang, J., et al. (2017). Genome-wide Analysis of DNA Methylation Profiles on Sheep Ovaries Associated with Prolificacy Using Whole-Genome Bisulfite Sequencing. *BMC Genomics* 18, 759. doi:10.1186/s12864-017-4068-9

Zhou, W., Liang, G., Molloy, P. L., and Jones, P. A. (2020). DNA Methylation Enables Transposable Element-Driven Genome Expansion. *Proc. Natl. Acad. Sci. USA* 117, 19359–19366. doi:10.1073/pnas.1921719117

Zhou, Y., Liu, S., Hu, Y., Fang, L., Gao, Y., Xia, H., et al. (2020). Comparative Whole Genome DNA Methylation Profiling across Cattle Tissues Reveals Global and Tissue-specific Methylation Patterns. *BMC Biol.* 18, 85. doi:10.1186/s12915-020-00793-5

**Conflict of Interest:** The authors declare that the research was conducted in the absence of any commercial or financial relationships that could be construed as a potential conflict of interest.

**Publisher's Note:** All claims expressed in this article are solely those of the authors and do not necessarily represent those of their affiliated organizations, or those of the publisher, the editors, and the reviewers. Any product that may be evaluated in this article, or claim that may be made by its manufacturer, is not guaranteed or endorsed by the publisher.

*Copyright © 2022 Drouilhet, Moreno, Plisson-Petit, Marcon, Fabre and Hazard. This is an open-access article distributed under the terms of the Creative Commons Attribution License (CC BY). The use, distribution or reproduction in other forums is permitted, provided the original author(s) and the copyright owner(s) are credited and that the original publication in this journal is cited, in accordance with accepted academic practice. No use, distribution or reproduction is permitted which does not comply with these terms.*

# Advantages of publishing in Frontiers

**OPEN ACCESS**
Articles are free to read for greatest visibility and readership

**FAST PUBLICATION**
Around 90 days from submission to decision

**HIGH QUALITY PEER-REVIEW**
Rigorous, collaborative, and constructive peer-review

**TRANSPARENT PEER-REVIEW**
Editors and reviewers acknowledged by name on published articles

**Frontiers**
Avenue du Tribunal-Fédéral 34
1005 Lausanne | Switzerland

**Visit us:** www.frontiersin.org
**Contact us:** frontiersin.org/about/contact

**REPRODUCIBILITY OF RESEARCH**
Support open data and methods to enhance research reproducibility

**DIGITAL PUBLISHING**
Articles designed for optimal readership across devices

**FOLLOW US**
@frontiersin

**IMPACT METRICS**
Advanced article metrics track visibility across digital media

**EXTENSIVE PROMOTION**
Marketing and promotion of impactful research

**LOOP RESEARCH NETWORK**
Our network increases your article's readership